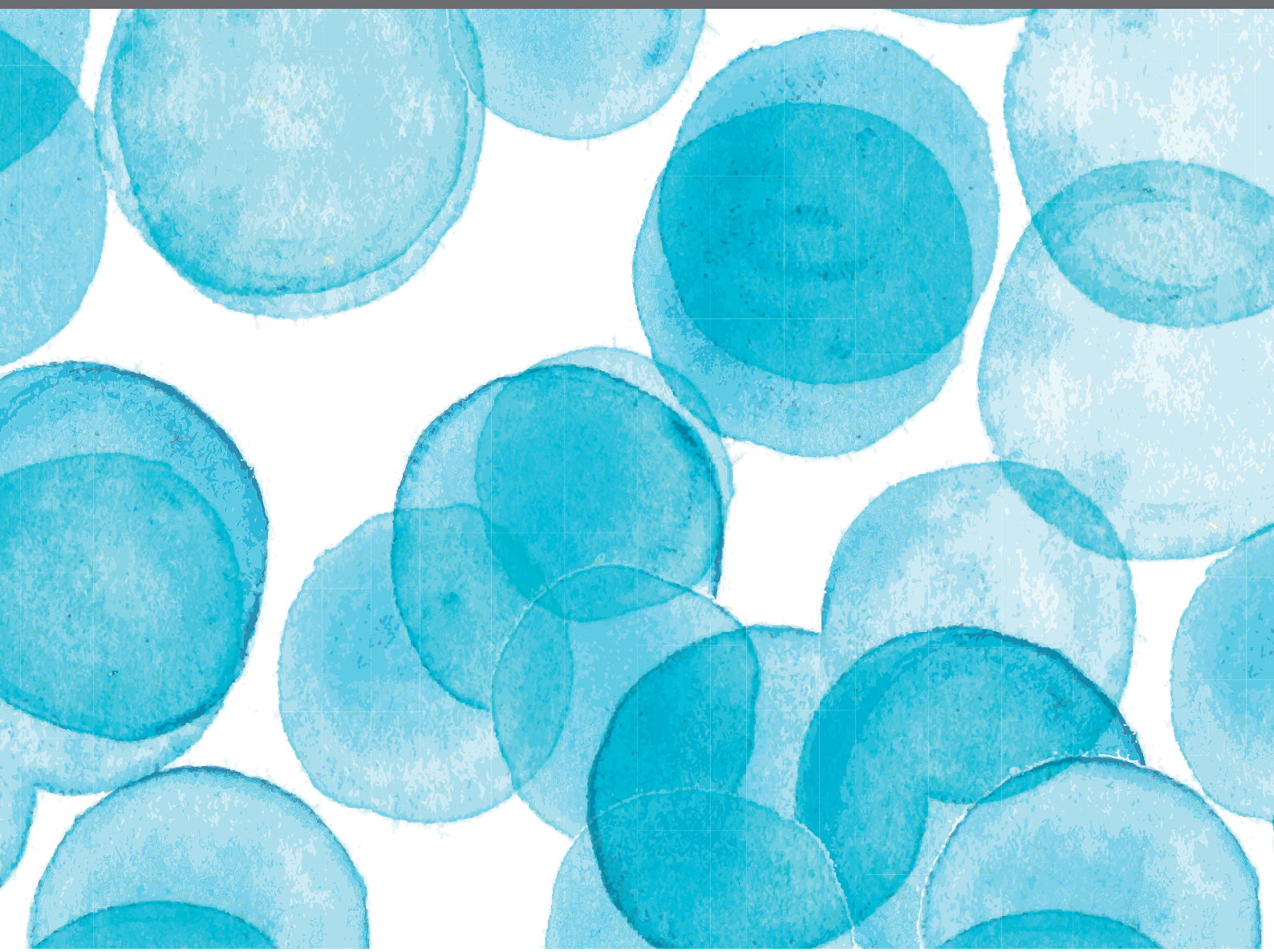
MICROBIAL SECONDARY METABOLITES: RECENT DEVELOPMENTS AND TECHNOLOGICAL CHALLENGES

EDITED BY: Bhim Pratap Singh, Mostafa E. Rateb, Susana Rodriguez-Couto, Maria de Lourdes Teixeira de Moraes Polizeli and Wen-Jun Li

PUBLISHED IN: Frontiers in Microbiology



frontiers Research Topics

Frontiers Copyright Statement

© Copyright 2007-2019 Frontiers Media SA. All rights reserved.

All content included on this site, such as text, graphics, logos, button icons, images, video/audio clips, downloads, data compilations and software, is the property of or is licensed to Frontiers Media SA ("Frontiers") or its licensees and/or subcontractors. The copyright in the text of individual articles is the property of their respective authors, subject to a license granted to Frontiers.

The compilation of articles constituting this e-book, wherever published, as well as the compilation of all other content on this site, is the exclusive property of Frontiers. For the conditions for downloading and copying of e-books from Frontiers' website, please see the Terms for Website Use. If purchasing Frontiers e-books from other websites or sources, the conditions of the website concerned apply.

Images and graphics not forming part of user-contributed materials may not be downloaded or copied without permission.

Individual articles may be downloaded and reproduced in accordance with the principles of the CC-BY licence subject to any copyright or other notices. They may not be re-sold as an e-book.

As author or other contributor you grant a CC-BY licence to others to reproduce your articles, including any graphics and third-party materials supplied by you, in accordance with the Conditions for Website Use and subject to any copyright notices which you include in connection with your articles and materials.

All copyright, and all rights therein, are protected by national and international copyright laws.

The above represents a summary only. For the full conditions see the Conditions for Authors and the Conditions for Website Use.

ISSN 1664-8714
ISBN 978-2-88945-901-8
DOI 10.3389/978-2-88945-901-8

About Frontiers

Frontiers is more than just an open-access publisher of scholarly articles: it is a pioneering approach to the world of academia, radically improving the way scholarly research is managed. The grand vision of Frontiers is a world where all people have an equal opportunity to seek, share and generate knowledge. Frontiers provides immediate and permanent online open access to all its publications, but this alone is not enough to realize our grand goals.

Frontiers Journal Series

The Frontiers Journal Series is a multi-tier and interdisciplinary set of open-access, online journals, promising a paradigm shift from the current review, selection and dissemination processes in academic publishing. All Frontiers journals are driven by researchers for researchers; therefore, they constitute a service to the scholarly community. At the same time, the Frontiers Journal Series operates on a revolutionary invention, the tiered publishing system, initially addressing specific communities of scholars, and gradually climbing up to broader public understanding, thus serving the interests of the lay society, too.

Dedication to Quality

Each Frontiers article is a landmark of the highest quality, thanks to genuinely collaborative interactions between authors and review editors, who include some of the world's best academicians. Research must be certified by peers before entering a stream of knowledge that may eventually reach the public - and shape society; therefore, Frontiers only applies the most rigorous and unbiased reviews.
Frontiers revolutionizes research publishing by freely delivering the most outstanding research, evaluated with no bias from both the academic and social point of view. By applying the most advanced information technologies, Frontiers is catapulting scholarly publishing into a new generation.

What are Frontiers Research Topics?

Frontiers Research Topics are very popular trademarks of the Frontiers Journals Series: they are collections of at least ten articles, all centered on a particular subject. With their unique mix of varied contributions from Original Research to Review Articles, Frontiers Research Topics unify the most influential researchers, the latest key findings and historical advances in a hot research area! Find out more on how to host your own Frontiers Research Topic or contribute to one as an author by contacting the Frontiers Editorial Office: researchtopics@frontiersin.org

MICROBIAL SECONDARY METABOLITES: RECENT DEVELOPMENTS AND TECHNOLOGICAL CHALLENGES

Topic Editors:
Bhim Pratap Singh, Mizoram University, India
Mostafa E. Rateb, University of the West of Scotland, Paisley, United Kingdom
Susana Rodriguez-Couto, IKERBASQUE, Bilbao, Spain
Maria de Lourdes Teixeira de Moraes Polizeli, FFCLRP, Universidade de São Paulo, Brazil
Wen-Jun Li, Sun Yat-Sen University, Guangzhou, China

Research on microbes plays an essential role in the improvement of biotechnological and biomedical areas. It has turned into a subject of expanding significance as new organisms and their related biomolecules are being characterized for several applications in health and agriculture. Microbial biomolecules confer the ability of microbes to cope with a range of adverse conditions. However, these biomolecules have several advantages over the plant origin, which makes them a suitable target in drug discovery and development. The reasons could be that microbial sources can be genetically engineered to enhance the production of desired natural production by large-scale fermentation. The interaction between microbes and their biotic and abiotic environment is fundamental to numerous processes taking place in the biosphere. The natural environments and hosts of these microorganisms are extremely diverse being reflected by the fact that microbes are widespread and occur in nearly every biological community on Earth. This metabolic versatility makes microbes interesting objects for a range of economically important biotechnological applications. Most of the biotechniques are established but inefficient genetic engineering strategies are still a bottleneck for selected microbe producing industrial scale biomolecules. Therefore, untapped microbial biodiversity and related metablomics, give a noteworthy wellspring of biologicals for the advancement of meds, immunizations, enhanced plants and for other natural applications. The present eBook volume contains articles on microbial secondary metabolites, microbial biosynthetic potential including biosynthetic gene expression, and metagenomics obtained from microorganism isolated unique from habitats like marine sources, endophytes, thermal springs, deserts, etc.

Citation: Singh, B. P., Rateb, M. E., Rodriguez-Couto, S., Polizeli, M. d. L. T. d. M., Li, W.-J., eds. (2019). Microbial Secondary Metabolites: Recent Developments and Technological Challenges. Lausanne: Frontiers Media.
doi: 10.3389/978-2-88945-901-8

Table of Contents

06 ***Editorial: Microbial Secondary Metabolites: Recent Developments and Technological Challenges***
Bhim Pratap Singh, Mostafa E. Rateb, Susana Rodriguez-Couto, Maria de Lourdes Teixeira de Moraes Polizeli and Wen-Jun Li

08 ***Production of the Bioactive Compounds Violacein and Indolmycin is Conditional in a* maeA *Mutant of* Pseudoalteromonas luteoviolacea *S4054 Lacking the Malic Enzyme***
Mariane S. Thøgersen, Marina W. Delpin, Jette Melchiorsen, Mogens Kilstrup, Maria Månsson, Boyke Bunk, Cathrin Spröer, Jörg Overmann, Kristian F. Nielsen and Lone Gram

19 ***Anti-rheumatoid Activity of Secondary Metabolites Produced by Endophytic* Chaetomium globosum**
Ahmed M. Abdel-Azeem, Sherif M. Zaki, Waleed F. Khalil, Noha A. Makhlouf and Lamiaa M. Farghaly

30 ***Integral use of Amaranth Starch to Obtain Cyclodextrin Glycosyltransferase, by* Bacillus megaterium*, to Produce* ß*-Cyclodextrin***
María Belem Arce-Vázquez, Edith Ponce-Alquicira, Ezequiel Delgado-Fornué, Ruth Pedroza-Islas, Gerardo Díaz-Godínez and J. Soriano-Santos

41 ***Functional Analysis of the Nitrogen Metabolite Repression Regulator Gene* nmrA *in* Aspergillus flavus**
Xiaoyun Han, Mengguang Qiu, Bin Wang, Wen-Bing Yin, Xinyi Nie, Qiuping Qin, Silin Ren, Kunlong Yang, Feng Zhang, Zhenhong Zhuang and Shihua Wang

53 ***Structural Elucidation and Molecular Docking of a Novel Antibiotic Compound From Cyanobacterium* Nostoc *sp. MGL001***
Niveshika, Ekta Verma, Arun K. Mishra, Angad K. Singh and Vinay K. Singh

68 ***Isolation, Screening, and Identification of Novel Isolates of Actinomycetes From India for Antimicrobial Applications***
Vineeta Singh, Shafiul Haque, Harshita Singh, Jyoti Verma, Kumari Vibha, Rajbir Singh, Arshad Jawed and C. K. M. Tripathi

77 ***Essential Oils: Sources of Antimicrobials and Food Preservatives***
Abhay K. Pandey, Pradeep Kumar, Pooja Singh, Nijendra N. Tripathi and Vivek K. Bajpai

91 ***Aflatoxins: A Global Concern for Food Safety, Human Health and Their Management***
Pradeep Kumar, Dipendra K. Mahato, Madhu Kamle, Tapan K. Mohanta and Sang G. Kang

101 ***Sigma Factor Regulated Cellular Response in a Non-solvent Producing* Clostridium beijerinckii *Degenerated Strain: A Comparative Transcriptome Analysis***
Yan Zhang, Shengyin Jiao, Jia Lv, Renjia Du, Xiaoni Yan, Caixia Wan, Ruijuan Zhang and Bei Han

113 *Antagonistic Activity and Mode of Action of Phenazine-1-Carboxylic Acid, Produced by Marine Bacterium* Pseudomonas aeruginosa *PA31x, Against* Vibrio anguillarum In vitro *and in a Zebrafish* In vivo *Model*
Linlin Zhang, Xueying Tian, Shan Kuang, Ge Liu, Chengsheng Zhang and Chaomin Sun

124 *Fungal Root Microbiome From Healthy and Brittle Leaf Diseased Date Palm Trees (*Phoenix dactylifera *L.) Reveals a Hidden Untapped Arsenal of Antibacterial and Broad Spectrum Antifungal Secondary Metabolites*
Fedia B. Mefteh, Amal Daoud, Ali Chenari Bouket, Faizah N. Alenezi, Lenka Luptakova, Mostafa E. Rateb, Adel Kadri, Neji Gharsallah and Lassaad Belbahri

142 *Cold Stress and Nitrogen Deficiency Affected Protein Expression of Psychrotrophic* Dyadobacter psychrophilus *B2 and* Pseudomonas jessenii *MP1*
Deep C. Suyal, Saurabh Kumar, Amit Yadav, Yogesh Shouche and Reeta Goel

148 *Cloning and Heterologous Expression of a Large-Sized Natural Product Biosynthetic Gene Cluster in* Streptomyces *Species*
Hee-Ju Nah, Hye-Rim Pyeon, Seung-Hoon Kang, Si-Sun Choi and Eung-Soo Kim

158 *Increased Biological Activity of* Aneurinibacillus migulanus *Strains Correlates With the Production of new Gramicidin Secondary Metabolites*
Faizah N. Alenezi, Imen Rekik, Ali Chenari Bouket, Lenka Luptakova, Hedda J. Weitz, Mostafa E. Rateb, Marcel Jaspars, Stephen Woodward and Lassaad Belbahri

169 *Discovery of Antimycin-Type Depsipeptides From a* wbl *Gene Mutant Strain of Deepsea-Derived* Streptomyces somaliensis *SCSIO ZH66 and Their Effects on Pro-Inflammatory Cytokine Production*
Huayue Li, Huiming Huang, Lukuan Hou, Jianhua Ju and Wenli Li

177 *The Biosynthetic Gene Cluster for Andrastin a in* Penicillium roqueforti
Juan F. Rojas-Aedo, Carlos Gil-Durán, Abdiel Del-Cid, Natalia Valdés, Pamela Álamos, Inmaculada Vaca, Ramón O. García-Rico, Gloria Levicán, Mario Tello and Renato Chávez

188 *Detection of Androgenic-Mutagenic Compounds and Potential Autochthonous Bacterial Communities During* In Situ *Bioremediation of Post-Methanated Distillery Sludge*
Ram Chandra and Vineet Kumar

206 *Optimum O_2:CH_4 Ratio Promotes the Synergy Between Aerobic Methanotrophs and Denitrifiers to Enhance Nitrogen Removal*
Jing Zhu, Xingkun Xu, Mengdong Yuan, Hanghang Wu, Zhuang Ma and Weixiang Wu

216 *Induction of Cryptic and Bioactive Metabolites Through Natural Dietary Components in an Endophytic Fungus* Colletotrichum gloeosporioides *(Penz.) Sacc.*
Vijay K. Sharma, Jitendra Kumar, Dheeraj K. Singh, Ashish Mishra, Satish K. Verma, Surendra K. Gond, Anuj Kumar, Namrata Singh and Ravindra N. Kharwar

225 *Fungal and Bacterial Pigments: Secondary Metabolites With Wide Applications*
Manik Prabhu Narsing Rao, Min Xiao and Wen-Jun Li

238 ***Identification, Bioactivity, and Productivity of Actinomycins From the Marine-Derived* Streptomyces heliomycini**
Dongyang Wang, Cong Wang, Pengyan Gui, Haishan Liu, Sameh M. H Khalaf, Elsayed A. Elsayed, Mohammed A. M. Wadaan, Wael N. Hozzein and Weiming Zhu

250 ***Dual Induction of new Microbial Secondary Metabolites by Fungal Bacterial Co-Cultivation***
Jennifer Wakefield, Hossam M. Hassan, Marcel Jaspars, Rainer Ebel and Mostafa E. Rateb

260 ***Fungal and Bacterial Diversity Isolated From* Aquilaria malaccensis *Tree and Soil, Induces Agarospirol Formation Within 3 Months After Artificial Infection***
Hemraj Chhipa and Nutan Kaushik

272 **In Vivo *Study of the Sorbicillinoid Gene Cluster in* Trichoderma reesei**
Christian Derntl, Fernando Guzmán-Chávez, Thiago M. Mello-de-Sousa, Hans-Jürgen Busse, Arnold J. M. Driessen, Robert L. Mach and Astrid R. Mach-Aigner

284 ***Marine Fungi: A Source of Potential Anticancer Compounds***
Sunil K. Deshmukh, Ved Prakash and Nihar Ranjan

frontiers in Microbiology

EDITORIAL
published: 26 April 2019
doi: 10.3389/fmicb.2019.00914

Editorial: Microbial Secondary Metabolites: Recent Developments and Technological Challenges

Bhim Pratap Singh[1], Mostafa E. Rateb[2], Susana Rodriguez-Couto[3], Maria de Lourdes Teixeira de Moraes Polizeli[4] and Wen-Jun Li[5]*

[1] Department of Biotechnology, Aizawl, Mizoram University, Aizawl, India, [2] School of Computing, Engineering and Physical Sciences, University of west of Scotland, Paisley, United Kingdom, [3] IKERBASQUE, Basque Foundation for Science, Bilbao, Spain, [4] Department of Biology, Faculty of Philosophy, Science and Letters of Ribeirão Preto, University of São Paulo, São Paulo, Brazil, [5] State Key Laboratory of Biocontrol and Guangdong Provincial Key Laboratory of Plant Resources, School of Life Sciences, Sun Yat-Sen University, Guangzhou, China

Keywords: microbial, secondary, metabolite, change, challenges

Editorial on the Research topic

Microbial Secondary Metabolites: Recent Developments and Technological Challenges

INTRODUCTION

Microbial secondary metabolites, like antibiotics, pigments, growth hormones, antitumor agents, and others, are not essential for the growth and development of microorganism, but they have shown a great potential for human and animal health (Ruiz et al., 2010). Among the microorganisms producing the above-mentioned compounds, bacteria, including actinobacteria, and fungi produce a diverse array of bioactive small molecules with significant potential to be used in medicine (O'Brien and Wright, 2011). These bioactive compounds are mainly produced by the activation of cryptic gene clusters which are not active under normal conditions and, thus, the expression of these clusters would be helpful in the exploitation of the chemical diversity of microorganisms (Pettit, 2011; Xu et al., 2019).

Although several reports on microbial secondary metabolites have been published in recent years (Passari et al., 2017; Zothanpuia et al., 2018; Overy et al., 2019), our understanding to enhance the production of bioactive secondary metabolites is still limited. The research topic "Microbial Secondary Metabolites: Recent Developments and Technological Challenges" comprises 25 articles covering important aspects on biodiversity, exploitation and utilization of microbial resources (terrestrial, marine, and endophytic) for the production of secondary metabolites together with their biological functions.

The current knowledge and potential of marine fungi for producing anticancer compounds has been reviewed (Deshmukh et al.) and the ability of the sea-derived *Streptomyces helimycini* for the production of actinomycins is presented (Zhu et al.). In a very interesting study, Wakefield et al. proved that the co-cultivation of fungi and bacteria led to the production of new secondary metabolites. There is a growing interest in looking for unique sources for the exploration of novel microbial populations having prospective to produce bioactive natural products. Thereby, the bacterial and fungal population obtained from *Aquilaria malaccensis* tree and soil enhanced the production of agarospirol within 3 months of artificial infection (Chhipa and Kaushik).

The present research topic includes four important research papers dealing with the production of bioactive secondary metabolites. Thus, a study by Alenezi et al. emphasized that the biological activity of *Aneurinibacillus migulans* isolates was directly correlated with the production of a new gramicidin.

OPEN ACCESS

Edited by:
Kian Mau Goh, University of Technology Malaysia, Malaysia

Reviewed by:
Navanietha Krishnaraj, National Institute of Technology, Durgapur, India

****Correspondence:***
Bhim Pratap Singh
bhimpratap@gmail.com

Specialty section:
This article was submitted to Microbiotechnology, Ecotoxicology and Bioremediation, a section of the journal Frontiers in Microbiology

Received: *15 February 2019*
Accepted: *10 April 2019*
Published: *26 April 2019*

Citation:
Singh BP, Rateb ME, Rodriguez-Couto S, Polizeli MdLTdM and Li W-J (2019) Editorial: Microbial Secondary Metabolites: Recent Developments and Technological Challenges. Front. Microbiol. 10:914. doi: 10.3389/fmicb.2019.00914

Narsing Rao et al. has focused on the importance of pigments originated from fungi and bacteria and their wide applications in health and industry. The article by Li et al. presented the production of somalimycin, a new antimycin-type depsipeptide, from a mutant of the deep-sea-derived *Streptomyces somaliensis*. Similarly, Thøgersen et al. demonstrated the production of the potentially antibacterial compounds violacein and indolmycin by a *mae*A mutant of the sea bacterium *Pseudoalteromonas luteoviolacea*.

A cluster of three articles gives emphasis to the biosynthetic gene clusters involved in microorganisms for the production of secondary metabolites. Hence, Derntl et al. demonstrated the role of genes, namely *sor*1, *sor*3, and *sor*4 of the orbicillinoid gene cluster and disclosed the function of *sor*4 which was not known. Another article by Rojas-Aedo et al. explained the role of the *adr* gene cluster involved in the biosynthesis of the potent antitumor compoundandrastin A in *Penicillium roqueforti*. In this article, the authors also have demonstrated that all the 10 genes of *adr* gene cluster were essential for the production of andrastin A. Lastly, Nah et al. reviewed the potential of the phylum Actinomycetes for natural production (NP) through biosynthetic gene clusters (BGC) heterologous expression systems as well as recent strategies specialized for the large-sized NP BGCs in *Streptomyces* heterologous hosts.

Other important candidates for the production of secondary metabolites are the endophytic microorganisms which were addressed by Mefteh et al. Thus, they presented that plants under biotic stress offered new and unique endophytes with diverse bioactivities as compared to healthy plants. Sharma et al. reported that the application of dietary components like grape skin and turmeric extracts enhanced the production of cryptic and bioactive metabolites, with anti-oxidant and antibacterial potential, by the endophytic fungus *Colletotrichum gloeosporioides*. Also, the endophytic fungi *Chaetomium globosum* isolated from Egyptian medicinal plants, proved to have anti-rheumatoid activity (Abdel-Azeem et al.).

In summary, the articles gathered in the research topic "Microbial Secondary Metabolites: recent development and Technological Challenges" explore the role of microorganisms from different sources showing biological activities. This will further enhance the present knowledge on the potential of microbial secondary metabolites in health and industry. One challenge which needs to be answered is the development of methods to understand the detailed mechanisms of cryptic genes and their relation to the production of bioactive compounds. Researchers also need to give more emphasis on the co-cultivation of different microorganisms having positive synergistic effect to produce novel bioactive molecules. We believe that this special issue gives some in-depth information about one of the important matters of the microbial world. Finally, our great thanks to all contributions, in total 165 authors, for the cohesive information in the form of reviews and research articles which have been compiled in this ebook. We strongly believe that the information compiled and presented in this ebook will be useful for the readers and will be the basis for the future investigation on "microbial secondary metabolites."

AUTHOR CONTRIBUTIONS

All authors mentioned have made significant contributions in the production of the editorial and have approved it for publication.

ACKNOWLEDGMENTS

We would like to thank all of the contributing authors and also the Frontiers team, for their constant efforts and support throughout in managing the research topic. BPS is thankful to the Department of Biotechnology, Ministry of Science and Technology for financial support in the form of DBT Unit of Excellence programme for NE (102/IFD/SAN/4290-4291/2016-2017).

REFERENCES

O'Brien, J., and Wright, G. D. (2011) An ecological perspective of microbial secondary metabolism. *Curr. Opin. Biotechnol.* 22, 552–558. doi: 10.1016/j.copbio.2011.03.010

Overy, D. P., Rämä, T., Oosterhuis, R., Walker, A. K., and Pang, K. L. (2019). The neglected marine fungi, sensu stricto, and their isolation for natural products' discovery. *Mar. Drugs* 17:E42. doi: 10.3390/md17010042

Passari, A. K., Mishra, V. K., Singh, G., Singh, P., Kumar, B., Gupta, V. K., et al. (2017). Insights into the functionality of endophytic actinobacteria with a focus on their biosynthetic potential and secondary metabolites production. *Sci. Rep.* 7:11809. doi: 10.1038/s41598-017-12235-4.

Pettit, R. K. (2011). Small-molecule elicitation of microbial secondary metabolites. *Microb. Biotechnol.* 4, 471–478. doi: 10.1111/j.1751-7915.2010.00196.x

Ruiz, B., Chávez, A., Forero, A., García-Huante, Y., Romero, A., Sánchez, M., et al. (2010) Production of microbial secondary metabolites: regulation by the carbon source. *Crit. Rev. Microbiol.* 36, 146–167. doi: 10.3109/10408410903489576

Xu, F., Wu, Y., Zhang, C., Davis, K. M., Moon, K., Bushin, L. B., et al. (2019) A genetics-free method for high-throughput discovery of cryptic microbial metabolites. *Nat. Chem. Biol.* 15, 161–168. doi: 10.1038/s41589-018-0193-2

Zothanpuia, Passari, A K, Leo, V. V., Kumar, B., Chnadra, P., Nayak, C., et al. (2018). Bioprospection of actinobacteria derived from freshwater sediments for their potential to produce antimicrobial compounds. *BMC Microb. Cell Fact.* 17:68. doi: 10.1186/s12934-018-0912-0

Conflict of Interest Statement: The authors declare that the research was conducted in the absence of any commercial or financial relationships that could be construed as a potential conflict of interest.

Copyright © 2019 Singh, Rateb, Rodriguez-Couto, Polizeli and Li. This is an open-access article distributed under the terms of the Creative Commons Attribution License (CC BY). The use, distribution or reproduction in other forums is permitted, provided the original author(s) and the copyright owner(s) are credited and that the original publication in this journal is cited, in accordance with accepted academic practice. No use, distribution or reproduction is permitted which does not comply with these terms.

frontiers in Microbiology

ORIGINAL RESEARCH
published: 16 September 2016
doi: 10.3389/fmicb.2016.01461

Production of the Bioactive Compounds Violacein and Indolmycin Is Conditional in a *maeA* Mutant of *Pseudoalteromonas luteoviolacea* S4054 Lacking the Malic Enzyme

*Mariane S. Thøgersen[1‡], Marina W. Delpin[1†‡], Jette Melchiorsen[1], Mogens Kilstrup[1], Maria Månsson[1†], Boyke Bunk[2], Cathrin Spröer[2], Jörg Overmann[2], Kristian F. Nielsen[1] and Lone Gram[1]**

[1] Department of Biotechnology and Biomedicine, Technical University of Denmark, Kongens Lyngby, Denmark, [2] Department of Microbial Ecology and Diversity Research, Leibniz Institute DSMZ–German Collection of Microorganisms and Cell Cultures – Partner Site Hannover-Braunschweig, German Centre for Infection Research, Braunschweig, Germany

It has previously been reported that some strains of the marine bacterium *Pseudoalteromonas luteoviolacea* produce the purple bioactive pigment violacein as well as the antibiotic compound indolmycin, hitherto only found in *Streptomyces*. The purpose of the present study was to determine the relative role of each of these two compounds as antibacterial compounds in *P. luteoviolacea* S4054. Using Tn*10* transposon mutagenesis, a mutant strain that was significantly reduced in violacein production in mannose-containing substrates was created. Full genome analyses revealed that the *vio*-biosynthetic gene cluster was not interrupted by the transposon; instead the insertion was located to the *maeA* gene encoding the malic enzyme. Supernatant of the mutant strain inhibited *Vibrio anguillarum* and *Staphylococcus aureus* in well diffusion assays and in MIC assays at the same level as the wild type strain. The mutant strain killed *V. anguillarum* in co-culture experiments as efficiently as the wild type. Using UHPLC-UV/Vis analyses, we quantified violacein and indolmycin, and the mutant strain only produced 7–10% the amount of violacein compared to the wild type strain. In contrast, the amount of indolmycin produced by the mutant strain was about 300% that of the wild type. Since inhibition of *V. anguillarum* and *S. aureus* by the mutant strain was similar to that of the wild type, it is concluded that violacein is not the major antibacterial compound in *P. luteoviolacea*. We furthermore propose that production of violacein and indolmycin may be metabolically linked and that yet unidentified antibacterial compound(s) may be play a role in the antibacterial activity of *P. luteoviolacea*.

Keywords: ***Pseudoalteromonas luteoviolacea*, indolmycin, violacein, conditional expression, antibacterial activity**

OPEN ACCESS

Edited by:
Mostafa Rateb,
University of the West of Scotland, UK

Reviewed by:
Blanca Barquera,
Rensselaer Polytechnic Institute, USA
Xuefeng Lu,
Qingdao Institute of Bioenergy and Bioprocess Technology (CAS), China

****Correspondence:***
Lone Gram
gram@bio.dtu.dk

[†]Present address:
Marina W. Delpin,
Flinders University, Adelaide, SA, Australia
Maria Månsson,
Chr. Hansen A/S, Hørsholm, Denmark

[‡]These authors have contributed equally to this work.

Specialty section:
This article was submitted to Microbial Physiology and Metabolism, a section of the journal Frontiers in Microbiology

Received: *14 July 2016*
Accepted: *01 September 2016*
Published: *16 September 2016*

Citation:
Thøgersen MS, Delpin MW, Melchiorsen J, Kilstrup M, Månsson M, Bunk B, Spröer C, Overmann J, Nielsen KF and Gram L (2016) Production of the Bioactive Compounds Violacein and Indolmycin Is Conditional in a maeA Mutant of Pseudoalteromonas luteoviolacea S4054 Lacking the Malic Enzyme. Front. Microbiol. 7:1461. doi: 10.3389/fmicb.2016.01461

INTRODUCTION

The production of bioactive secondary metabolites is an essential defense mechanism and/or competitive strategy for many bacterial species. Violacein, a purple bisindole metabolite, has been extensively studied and has been reported to be potently antibacterial, antiviral, anti-tumor, antiprotozoal, and antiparasitic (Balibar and Walsh, 2006; Durán et al., 2007). It is produced by members of the Beta- and Gamma-proteobacteria, and has enabled species to occupy new niches. The skin-dwelling *Janthinobacterium lividum*, for example, shares a mutualism with its amphibian host, synthesizing violacein that provides antifungal protection to its host (Brucker et al., 2008). In the marine environment, violacein-producing species of the *Pseudoalteromonas* genus have been isolated from marine sponges (Yang et al., 2007), from biofilms on bivalve shells (Gillan et al., 1998), and from other biotic surfaces such as the alga *Ulva australis* (Rao et al., 2007). These niches are typically high in bacterial density, however, it is not known if or how effective violacein is in mediating bacteria–bacteria-interactions.

The focus of this study is the purple marine bacterium *Pseudoalteromonas luteoviolacea* strain S4054, isolated from a seawater-immersed surface (Gram et al., 2010). Strains of *P. luteoviolacea* are distinctly purple due to the production of violacein (Gauthier, 1982; McCarthy et al., 1985) and have also been reported to synthesize an antimicrobial L-amino acid oxidase (Gómez et al., 2008), as well as the antibiotic compound pentabromopseudilin (Hanefeld et al., 1994). We previously detected violacein and pentabromopseudilin in strains of *P. luteoviolacea*, and we furthermore identified a non-violacein compound, indolmycin, from a culture of *P. luteoviolacea* S4054 where pentabromopseudilin was not detected (Månsson et al., 2010; Vynne et al., 2012). Both violacein and indolmycin are based on an indole scaffold, biosynthetically derived from L-tryptophan (Hurdle et al., 2004; Balibar and Walsh, 2006).

Indolmycin is a secondary metabolite with antibacterial properties which was first isolated from *Streptomyces griseus* (Hornemann et al., 1971). To date, indolmycin biosynthesis has not been reported in bacteria outside of the phylum Actinobacteria except for a few strains of *P. luteoviolacea* (Månsson et al., 2010; Vynne et al., 2011, 2012). Indolmycin acts as an antimicrobial compound due to its tryptophanyl-tRNA synthase inhibition activity (Werner et al., 1976), ceasing bacterial protein synthesis (Oliva et al., 2003). It is bacteriostatic against *Staphylococcus aureus*, and has been tested as a potential topical agent for use against both methicillin-resistant and vancomycin-intermediate *S. aureus* (Hurdle et al., 2004). However, indolmycin also has a bactericidal effect on Gram negative *Helicobacter pylori* (Kanamaru et al., 2001), and it has therefore been speculated that this compound has different modes of action on bacteria (Hurdle et al., 2004).

Vynne et al. (2011) clustered four strains of *Pseudoalteromonas luteoviolacea* based on the detection of their secondary metabolites by HPLC-UV/Vis. Two strains (S4054 with S4047) produced both violacein and indolmycin and two strains (S4060 with S2607) produced violacein and pentabromopseudilin (Vynne et al., 2011). Whilst violacein is difficult to dissolve in water and accumulates in the bacterial membrane (Konzen et al., 2006), both pentabromopseudilin and indolmycin are highly water soluble and may each serve the same role in the four strains. Månsson et al. (2016) analyzed the metabolome of 13 strains of *P. luteoviolacea*, and found a large variety in biochemical potential within each strain (Månsson et al., 2016). Also, a gene cluster consisting of 12 genes was identified as the potential indolmycin biosynthetic gene cluster. This adds to the nine genes identified by Du et al. (2015) encoding indolmycin in *Streptomyces griseus*, including two genes identified as homologues of the quorum sensing genes *luxI* and *luxR* which were not observed in *S. griseus* (Månsson et al., 2016).

In the present study, we sought to determine the importance of violacein in the antibacterial activity of *P. luteoviolacea* S4054. We initially attempted a targeted gene deletion approach but were unable to manipulate *P. luteoviolacea* in this manner and we therefore used a random mutagenesis approach, creating a mutant with negligible violacein production. Additionally, methodology was established to simultaneously quantify violacein and indolmycin against commercial standards to gain an accurate insight into the levels of each chemical compound being produced by *P. luteoviolacea* S4054 and mutant strains hereof.

MATERIALS AND METHODS

Bacterial Strains, Media, and Growth Conditions

Pseudoalteromonas luteoviolacea S4054 was isolated during the Danish research expedition "Galathea 3" (Gram et al., 2010). Strain S4054-2 is a spontaneous streptomycin resistant (Sm^R) mutant of S4054, which was isolated after overnight incubation at 25°C of strain S4054 on Marine Agar (MA; Difco 2216) supplemented with 200 $\mu g\ ml^{-1}$ streptomycin. Strain S4054-2-49 is a transposon (Tn) mutant generated from strain S4054-2, containing a single random insertion of miniTn*10:gfp:kan* (Stretton et al., 1998) in its genome. For broth cultures, all S4054-based strains were grown overnight at 25°C with shaking at 200 rpm. The liquid media used were: Marine Broth (MB; Difco 2216) and marine minimal medium (MMM) (Ostling et al., 1991) supplemented with 0.3% casamino acids (CAA; Difco 223050) and either 0.4% mannose or 0.4% glucose. Strain S4054-2 was furthermore supplemented with 200 $\mu g\ ml^{-1}$ streptomycin, and strain S4054-2-49 was supplemented with 200 $\mu g\ ml^{-1}$ streptomycin and 200 $\mu g\ ml^{-1}$ kanamycin. All carbon sources and chemicals used in this study were obtained from Sigma-Aldrich (Saint Louis, MO, USA) unless otherwise stated.

Target organisms for antibacterial susceptibility testing were *Vibrio anguillarum* 90-11-287 (Skov et al., 1995) and *V. anguillarum* NB10 (Milton et al., 1992) grown in MB or Tryptone Soy Broth (TSB; Oxoid CM129) or on MA or Tryptone Soy Agar (TSA; Oxoid CM131) and *Staphylococcus aureus* 8325 (Novick, 1967) grown in Luria Broth (LB) or on Luria Agar (LB agar) (Oxoid CM996B). All target strains were grown at 25°C. For co-cultivation experiments, we used a variant of *V. anguillarum* NB10 that was tagged with chloramphenicol resistance (Cm^R) by

insertion of plasmid pNQFlaC4-gfp27 (*cat, gfp*) into an intergenic region on the chromosome, *V. anguillarum* NB10 (Cm^R), kindly provided by D. Milton, University of Umeå.

Strains used for transposon mutagenesis were *Escherichia coli* DH5α(pNJ5000) and *E. coli* SM10λpir (pLOF::miniTn*10:gfp:kan*) (Stretton et al., 1998). *E. coli* strains were grown at 37°C on LB agar or in LB with shaking at 200 rpm. Streptomycin (200 μg ml^{-1}), kanamycin (200 μg ml^{-1}), tetracycline (10 μg ml^{-1}), and ampicillin (100 μg ml^{-1}) were used for selection.

To examine the conditional expression of violacein, Na-pyruvate and L-Tryptophan was added to the MMM medium containing CAA and mannose to a final concentration of 11 mg/ml and 1 mg/ml, respectively.

Transposon Mutagenesis and Selection of Mutants

A violacein-negative mutant of *P. luteoviolacea* was created by conjugation with an *E. coli* donor carrying the pLOF::miniTn*10:gfp:kan* plasmid. This plasmid is readily mobilized from *E. coli* to *P. luteoviolacea* but since the replication of the plasmid is dependent upon a non-conjugative helper plasmid (pNJ5000), stable kanamycin resistant (Km^R) transconjugants can only be obtained if the miniTn*10* transposes into the host chromosome (Stretton et al., 1998). Selection of Km^R *P. luteoviolacea* transposon mutants required that the *E. coli* donor cells could be selected against. Therefore a spontaneous Sm^R derivative of strain S4054 was selected on plates containing streptomycin. One such mutant, S4054-2 was shown to grow similar to the parental strain S4054 on marine agar (MA) as well as in MMM supplemented with casamino acids (CAA).

Triparental conjugation of *P. luteoviolacea* S4054-2, *E. coli* DH5α(pNJ5000), and *E. coli* SM10λpir (pLOF::miniTn*10:gfp:kan*) was performed on a HATF filter membrane (0.45 μm; Merck Millipore Co., Darmstadt, Germany) placed on MA supplemented with 0.4% glucose. Briefly, all three strains were grown for 18 h in their corresponding medium and optimal temperature. Fifty microliters of each strain were mixed and pipetted onto the HATF membrane. After overnight incubation at 25°C, growth on the filter was resuspended in 1 ml MB and 10 × 100 μl volumes were plated onto MA supplemented with streptomycin and kanamycin. After overnight incubation at 25°C, 50 colonies that grew were re-streaked onto MA supplemented with streptomycin and kanamycin. Mutant strains were selected based on reduced purple pigmentation as compared to strain S4054-2. Additionally, mutants were screened for green fluorescent protein (GFP) expression (using an Olympus BX50 microscope fitted with an epifluorescence filter; 488 nm excitation, 520 nm emission), indicative of the insertion of the promoterless *gfp* transposon in the correct orientation under the transcriptional control of the promoter of the interrupted gene.

To confirm the presence of the miniTn*10:gfp:kan* in strain S4054-2-49, a 1.3 kb region of the cassette was amplified by PCR with HotStarTaq DNA polymerase (Qiagen, Venlo, Netherlands), performed according to the manufacturer's instructions, using 0.2 μM of each primer kmseq-F and gfpsfiI-F (Stretton et al., 1998). PCR cycling conditions: 94°C for 3 min; (94°C for 30 s, 53°C for 30 s, 72°C for 60 s) × 30; 72°C for 10 min. PCR products were analysed and visualized by gel electrophoresis using 1% TAE agarose gels (Promega, Madison, WI, USA).

PacBio Library Preparation and Sequencing

To determine the site of the Tn insertion in strain S4054-2-49 and to detect other potentially random mutations that might affect the phenotypes of the mutant strains, *P. luteoviolacea* S4054, S4054-2, and S4054-2-49 were whole genome sequenced. Genomic DNA from the three strains was purified using the phenol/chloroform/isoamyl alcohol protocol described by Wilson (2001). SMRTbell® template library was prepared according to the instructions from Pacific Biosciences Inc. (Menlo Park, CA, USA) following the Procedure and Checklist – 20 kb Template Preparation Using BluePippin® Size-Selection System. Briefly, for preparation of 15 kb libraries 5 μg genomic DNA were end-repaired and ligated overnight to hairpin adapters applying components from the DNA/Polymerase Binding Kit P6 (Pacific Biosciences Inc.). Reactions were carried out according to the manufacturer's instructions. BluePippin® Size-Selection to 10 kb was performed according to the manufacturer's instructions (Sage Science, Beverly, MA, USA). Conditions for annealing of sequencing primers and binding of polymerase to purified SMRTbell® template were assessed with the Calculator in RS Remote (Pacific Biosciences Inc.). SMRT sequencing was carried out on the PacBio RSII (Pacific Biosciences Inc.) taking one 240-min movie for each SMRT cell. One SMRT cell per strain was run. In total, for strain S4054 87,476 reads (mean read length 9,065 bp), for strain S4054-2 74,109 reads (mean read length 9,226 bp), and for strain S4054-2-49 85,558 reads (mean read length 11,797 bp) were obtained.

Genome Assembly, Error Correction, and Annotation

Data from each SMRT Cell was assembled independently using the "RS_HGAP_Assembly.3" protocol included in SMRTPortal version 2.3.0 using default parameters. Each assembly revealed two circular chromosomes, but no plasmids. Validity of each assembly was checked using the "RS_Bridgemapper.1" protocol. Each replicon was circularized independently, particularly artificial redundancies at the ends of the contigs were removed and the two chromosomes were additionally adjusted to *dnaA* or *tus* as the first gene, respectively (Médigue et al., 2005). Finally, each genome was error-corrected by a mapping of Illumina reads onto finished genomes using BWA (Li and Durbin, 2009) with subsequent variant calling using VarScan (Koboldt et al., 2012). A consensus concordance of QV60 could be confirmed for all of the three genomes. Finally, all genomes were annotated using Prokka 1.8 (Seemann, 2014) and RAST (Aziz et al., 2008), and aligned using the genome alignment software MAUVE 2.4.0 (Darling et al., 2004). Single genes of interest were translated to amino acid sequences and aligned using CLC Main Workbench 7.6.4 and used in homology searches using

blastp (Basic Local Alignment Search Tool[1]). The genomes have been deposited in NCBI GenBank under Accession Numbers CP015411-CP015416.

The genomes were analyzed for putative biosynthetic gene clusters using AntiSMASH and the ClusterFinder algorithm (Medema et al., 2011; Weber et al., 2015).

Screening for Antibacterial Activity

The ability of *P. luteoviolacea* S4054, S4054-2, and S4054-2-49 to inhibit the growth of a target strain (*V. anguillarum* 90-11-287 and *S. aureus* 8325) seeded into agar substrates was tested as previously described (Hjelm et al., 2004; Gram et al., 2010). Briefly, the agar substrate contained 1.5% Instant Ocean (Aquarium Systems Inc., Sarrebourg, France), 0.3% CAA, 0.4% glucose and 1.2% agar (Oxoid Ltd., Hampshire, UK). For *S. aureus*, 1% peptone was added. Once cooled to 45°C and prior to pouring, 10 μl of target strain, which had been grown stagnant overnight at 25°C in its corresponding rich medium, was added to 20 ml agar substrate. For well diffusion agar assay, 5 mm diameter wells were punched into the agar surface and 50 μl of filter sterilized (0.2 μm filter; Merck Millipore Co.) culture supernatant was loaded into each well. The supernatants were produced by centrifugation and serial dilution of 24, 48, and 72 h cultures grown in MMM CAA mannose. After incubation, inhibition zones of the same size were identified for all three strains. Following 24 h incubation at 25°C, the diameter of the clearing zone produced due to inhibition of growth of the target strains from edge to edge of the zone, including the well, was measured. Each sample was tested in duplicate.

For minimum inhibition concentration (MIC) assay, target strains *V. anguillarum* 90-11-287 and *S. aureus* 8325 were cultured in MB and LB, respectively, and incubated stagnant at 25°C overnight. Strains S4054, S4054-2, and S4054-2-49 were cultured for 72 h at 25°C in MMM CAA mannose (no antibiotics), supernatants were sterile filtered (0.2 μm filters; Merck Millipore Co.), and tested in twofold dilutions in 100 μl target strain diluted to OD_{600} 0.01 in microtiter plates. Plates were incubated at 25°C overnight against *V. anguillarum* 90-11-287 and for 48 h against *S. aureus* 8325. All MICs were carried out with four replicates and repeated twice.

Vibrio anguillarum Competition Experiments

Vibrio anguillarum NB10 (Cm^R) was co-inoculated together with cultures of the *P. luteoviolacea* strains in MMM CAA mannose. All cultures were grown in a 50 ml volume of medium in a 250 ml Erlenmeyer flask in duplicate. Cultures of *V. anguillarum* NB10 (Cm^R) and S4054, S4054-2 or S4054-2-49 were grown separately overnight in TSB (NB10, Cm^R) and MMM CAA mannose (S4054 strains) and added to MMM CAA mannose to concentrations of 10^3 (NB10, Cm^R) and 10^6 (S4054 strains) cells ml^{-1}, respectively. Simultaneously, a MMM CAA mannose control culture was inoculated with 10^3 CFU ml^{-1} *V. anguillarum* NB10 (Cm^R). Samples were taken at regular intervals (0, 3, 6, 9, 12, and 24 h) and cell density was determined by dilution and surface plating. *Vibrio anguillarum* NB10 (Cm^R) from the competition experiment was counted on TSA plates with 4 μg ml^{-1} chloramphinicol incubated overnight at 30°C, since S4054 did not grow on TSA with chloramphenicol nor at 30°C. Strains S4054-2 and S4054-2-49 were selected for on MA with streptomycin and incubated at 25°C, since *V. anguillarum* NB10 (Cm^R) is streptomycin-sensitive.

Quantification of Violacein and Indolmycin

Extraction of violacein and indolmycin for quantitative studies was tested using propan-2-ol, methanol, ethanol, and acetonitrile. Acetonitrile created a two-phase system of variable size due to the media salts and could not be used. Methanol and ethanol had to be added at 5 and 2 times the sample volume, respectively, to extract the violacein quantitatively. This resulted in a lower concentration of the analytes in the mixture and also a need to inject more of the mixture to maintain a reasonable UHPLC (Ultra High-Performance Liquid Chromatography) peak shape for di-demethylindolmycin. Overall, propan-2-ol provided the most accurate extraction, so 5 ml of bacterial culture (fresh or thawed from −20°C storage) were prepared for the quantification of violacein, indolmycin, and indolmycin precursors by the addition of an equal volume of propan-2-ol.

The mixture was inverted until homogeneous and placed in an ultrasonication bath for 30 min. Tubes were centrifuged (4,000 × *g*, 15 min) to pellet the biomass (colorless) from the extracted violacein, indolmycin and related compounds in solution. Seven hundred and fifty microlitres of supernatant was transferred to an autosampler vial. UHPLC-UV/Vis analysis was performed on a Dionex RSLC Ultimate 3000 system (Sunnyvale, CA, USA) using a 150 mm × 2 mm i.d., 2.6 μm Kinetex C_{18} column (Phenomenex, Torrance, CA, USA), running at 800 μl min^{-1} and 60°C using a binary linear solvent system of water (A) and acetonitrile (B) (both buffered with 50 μl l^{-1} trifluoroacetic acid; TFA). The gradient program was: $t = 0$, 15% B; $t = 0.5$ min 25% B; $t = 6$ min 65% B; and $t = 7$ 100% B, keeping this for 1 min, then reverting to 15% in 1 min. A sample volume of 1.5 μl was injected.

Violacein (RT 2.76 min) was detected recording absorption at 578 ± 2 nm, and indolmycin (1.98 min), di-demethylindolmycin (RT 1.21 min), and the two mono-demethylindolmycin (1.60 and 1.64 min, integrated as one peak) by absorption at 219 ± 2 nm.

Quantification by external standard calibration using six different concentrations of violacein and indolmycin for the calibration (40, 20, 10, 5, 2, and 1 μM) resulted in a linear calibration curve with R^2 of 0.9999 and 0.9997, respectively. Extraction efficiency was tested by extracting various batches of samples three consecutive times, showing an extraction efficiency of >97%. The di- and mono-demethylindolmycins were quantified using the indolmycin calibration curve, since these compounds have the same

[1]http://blast.ncbi.nlm.nih.gov/Blast.cgi

chromophore and thus molar extinction coefficient. Detection limits were 1 μM for violacein, and 10, 5, and 1 μM for di-demethylindolmycin, mono-demethylindolmycin, and indolmycin, respectively.

Identification of Indolmycin-Related Compounds

Samples for HPLC-UV/MS analyses were prepared from 30 ml cultures in MB and MMM CAA glucose or mannose. The culture broth was extracted with Diaion HP20 (Sigma–Aldrich, St. Louis, MO, USA), which was subsequently filtered off and extracted with MeOH, while the pellet was extracted using ethyl acetate (EtOAc). Extracts of pellet and broth were pooled, filtered, and evaporated under N_2 until dry. Samples were re-dissolved in methanol (MeOH) and transferred to autosampler vials for HPLC-UV/MS analysis. HPLC-UV/MS samples were analyzed using an Agilent 1100 HPLC system with a diode array detector (Agilent Technologies, Waldbronn, Germany) coupled to an LCT TOF mass spectrometer (Micromass, Manchester, UK) using a Z-spray ESI source. A Phenomenex Luna II C_{18} column (50 mm × 2 mm, 3 μm) was used for separation, applying an acetonitrile-water (20 mM formic acid) 0.3 ml min^{-1} gradient (15–100%) over 20 min at 40°C.

Indolmycin (2.1 mg) and di-demethylindolmycin (1.7 mg) were isolated from a 1 l culture of S4054-2-49 in MMM CAA mannose by EtOAc extraction (2 × 500 ml). The EtOAc phase was dried with Na_2SO_4, filtered, and evaporated until dry. The crude extract was separated using a Luna II C_{18} column (250 × 10 mm, 5 μm; Phenomenex) on a Gilson 322 liquid chromatograph with a 215 liquid handler (BioLab, Risskov, Denmark), with an automatic fraction collector, applying a gradient from 20 to 100% acetonitrile in water (buffered with 50 ppm TFA) over 20 min (5 ml min^{-1}).

NMR spectra were recorded on a Varian Unity Inova 500 MHz spectrometer (Agilent) equipped with a 4 mm gHX Nano probe and with a spin rate of 2 kHz for all samples, using standard pulse sequences. The signals of the residual solvent protons and solvent carbons were used as internal references (δ_H 3.3 and δ_C 49.3 ppm for methanol-d_4).

Statistical Analyses

A two-sample two-tailed *t*-test (Zar, 1996) was used to compare the difference between two means of log transformed CFU ml^{-1} or concentrations of secondary metabolites.

RESULTS

Selection of Mutants with Impaired Violacein Production from a miniTn*10* Transposon Library of *P. luteoviolacea* S4054-2

Violacein producing bacteria are easily detected by their deep violet color. Initially, we attempted to construct a deletion mutant in either of the *vio*-genes, but all attempts on site-directed mutagenesis failed. Instead, a random transposon insertion library of mutants was constructed to select for violacein-negative mutants of the violacein producing, Sm^R *P. luteoviolacea* strain S4054-2. The Sm^R mutant used for conjugation behaved similarly to the wild type in growth and well diffusion agar assays. Whole genome sequencing revealed that the Sm resistance could be attributed to two single nucleotide polymorphisms (SNPs), both of which lead to non-synonymous amino acid exchange: One occurred in the *rpsL* gene which encodes the 30S ribosomal protein S12 and the other in the *rsmG* gene encoding the ribosomal RNA small subunit methyltransferase G (**Table 1**). Mutations in these two genes are known to confer streptomycin resistance in, e.g., *E. coli*, *Campylobacter coli*, and *Mycobacterium* spp. (Timms et al., 1992; Springer et al., 2001; Olkkola et al., 2010) and lead to antibiotic overproduction in *Streptomyces coelicolor* and several species of Actinomycetes (Nishimura et al., 2007; Tanaka et al., 2009). Therefore, we deduce that the acquired streptomycin resistance in strain S4054-2 is a result of either of these two mutations.

TABLE 1 | Mutations in *P. luteoviolacea* S4054 resulting in Sm^R strain S4054-2 and the *maeA* mutant S4054-2-49 based on WGS.

Strains	Type of mutation	Annotation of affected gene	Functional role	Effect of mutation
S4054 to S4054-2	A to G (aa: C to R, pos. 237)	*mreB*, Rod-shape determining protein MreB	Formation of the rod shape of cells	No phenotypic effect
	G to A (aa: P to S, pos. 91)	*rpsL*, 30S ribosomal protein S12	Confers streptomycin resistance in *E. coli*, high level	Streptomycin resistance
	C to T (aa: G to R, pos. 78)	*rsmG*, Ribosomal RNA small subunit methyltransferase G	Confers streptomycin resistance and antibiotic overproduction in Actinomycetes and Streptomycetes, low level	Streptomycin resistance and possibly indolmycin overproduction
S4054-2 to S4054-2-49	Insertion of Tn cassette	*maeA*, NAD-dependent malic enzyme	Conversion of malate to pyruvate	Interruption of *maeA*
	Insertion of 1 bp	*tonB*, Transport protein TonB	Cross-membrane uptake of specific substrates	Interruption of *tonB*

Further mutations appeared from the genome alignments, but could either be attributed to sequencing errors or occurred in regions that could not be annotated. Tn cassette, transposon cassette; aa, amino acid; pos., refers to the amino acid position in the annotated protein sequence.

Transposon mutagenesis of S4054-2 with *E. coli* DH5α/pLOF::miniTn*10:gfp:kan* resulted in a library of Sm^R and Km^R resistant S4054-2 *genX*::miniTn*10:gfp:kan* mutants, most of which were pigmented. Despite many repeated attempts only 50 mutants grew and one mutant S4054-2-49 showed a non-pigmented phenotype on MA plates containing streptomycin and kanamycin. PCR amplification of the *gfp-kan* junction in S4054-2-49 confirmed the presence of the miniTn*10:gfp:kan* and epifluorescence microscopy showed that the mutant, in contrast to S4054 and S4054-2, produced Gfp. Whole genome sequencing of S4054-2-49 showed that the miniTn*10* cassette had inserted into the *maeA* gene encoding a NAD-dependent malic enzyme that converts malate to pyruvate and CO_2. The insertion sequence was located between the N-terminal domain and the NAD-binding domain of *maeA*, interrupting the production of a functional malic enzyme (**Figure 1**).

Conditional Production of Violacein Pigmentation by the S4054-2 *maeA* Mutant

Selection of the *maeA* mutant was performed on solid MA medium, which contains sources of amino acids and vitamins (from peptone and yeast extract) as well as all required salts for S4054 to grow on. As detected during the selection of S4054-2-49 *maeA,* it showed a non-pigmented beige phenotype when grown on MA. After re-streaking the mutant, however, it was found that the colonies became purple after 2 days of growth at room temperature. This showed that the absence of the malic enzyme did not prevent the formation of violacein altogether, but rather delayed the production or redirected the metabolism away from violacein synthesis. Therefore we screened the mutant in a number of culturing conditions for the production of violacein pigment. The two parental strains, S4054 and S4054-2 (Sm^R), produced pigments under all conditions tested, but the *maeA* mutant failed to produce pigment in tubes containing liquid MMM medium supplemented with CAA and mannose. Interestingly, growth on MMM agar plates resulted in fully pigmented S4054-2-49 *maeA* colonies, which showed that either the mutant required high oxygen tension for violacein synthesis (provided on plates), or that the agar substrate provided a required compound for biosynthesis. Since violacein is derived from the amino acid tryptophan, the effect of L-tryptophan addition to liquid MA was tested. Addition of Na-pyruvate was also tested because the absence of the malic enzyme in the mutant could lower the pyruvate production. Tryptophan did not promote purple pigmentation, but instead resulted in a more yellowish tint. Addition of pyruvate or pyruvate + tryptophan also resulted in beige and yellowish cultures, with no visible trace of purple color.

Quantification of Violacein and Indolmycin in Wild Type and *maeA* Mutant

To obtain more quantitative evidence for the conditional production of violacein, we performed chemical analysis of 2-propanol extracts from culture samples after growth of S4054, S4054-2, and S4054-2-49 *maeA* mutant in liquid MMM CAA mannose medium. The *maeA* mutant was indeed deficient in violacein production as compared to the wild type (**Table 2**). The violacein concentration remained around 4 μM during 72 h of incubation in MMM CAA mannose, while the violacein concentration increased to 54 μM in the wild type culture, and to 80 μM in the S4054-2 Sm^R derivative.

During analysis of the mutant strains, a series of strong peaks was identified all of which were much higher than in the extracts from the wild type (**Figure 2**). The UHPLC-UV/MS profile of the Tn mutant S4054-2-49 *maeA* culture extract from MMM CAA mannose (**Figure 2C**) showed the expected

TABLE 2 | Antibacterial activity and mean violacein and indolmycin concentration (± standard error) produced by *P. luteoviolacea* S4054 and mutant strains in MMM CAA mannose.

Strain	Time (h)	Zone size of inhibition (mm)*		Violacein (μM)*	Indolmycin (μM)*
		V. anguillarum	*S. aureus*		
S4054	24	23	28	43 ± 9	36 ± 2
	48	27	35	50 ± 6	46 ± 2
	72	28	31	54 ± 9	56 ± 2
S4054-2	24	19	26	74 ± 17	21 ± 1
	48	26	31	74 ± 10	28 ± 3
	72	26	32	83 ± 13	44 ± 2
S4054-2-49	24	20	26	4.1 ± 0.1	107 ± 3
	48	23	29	3.8 ± 0.05	141 ± 0.3
	72	26	31	4.0 ± 0.1	165 ± 0.7

*Sampling time (h; indicative of hours post-inoculation of the culture) is indicated. *n = 2.*

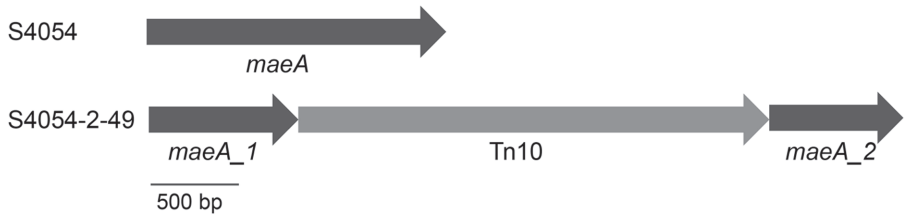


FIGURE 1 | Genetic arrangement of the Tn*10* insertion in the chromosome of *P. luteoviolacea* S4054-2. The Tn*10* cassette is located between the N-terminal domain (*maeA_1*) and the NAD-binding domain (*maeA_2*) of the NAD-dependent malic enzyme encoding gene *maeA*.

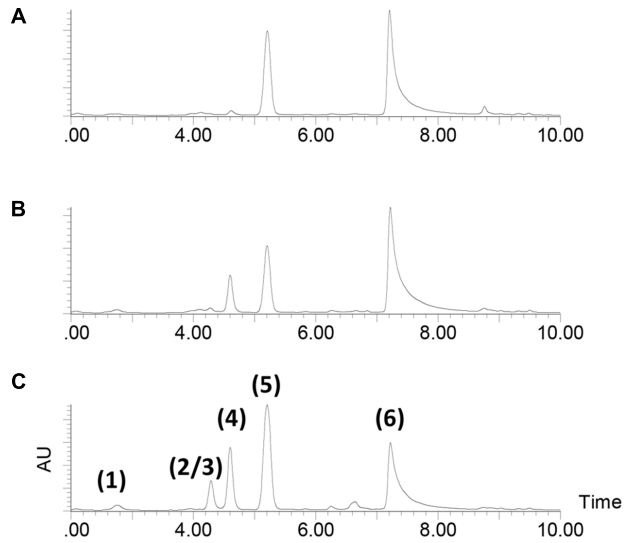


FIGURE 2 | HPLC-UV profiles of 72 h cultures grown in MMM CAA mannose. (A) wild type strain S4054, **(B)** streptomycin resistant mutant strain S4054-2, **(C)** transposon mutant strain S4054-2-49. The identity of the peaks were determined by LC-HRMS: (1) N,C-didemethyl-indolmycin, (2/3) mono-N/C-demethyl-indolmycin, (4) indolmycenic acid, (5) indolmycin, and (6) violacein.

peak for violacein (labeled 6 in **Figure 2C**) together with a series of compounds which could be identified as derivatives of indolmycin: di-demethylindolmycin (labeled 1 in **Figure 2C**), mono-N/C-demethylindolmycin (labeled 2 and 3), indolmycenic acid (labeled 4) (Hornemann et al., 1971), and indolmycin (labeled 5) (Speedie et al., 1975). Structures were validated by NMR for compounds 1, 5, and 6 (Månsson et al., 2010), while the remaining compounds were tentatively identified based on their retention time, accurate mass and the deduced molecular formulas together with their UV/Vis characteristics (**Figure 3**). Strains S4054 and S4054-2 produced the same compounds, but the ratios between the individual compounds were very different in all three strains (**Figures 2A,B**). Precise quantification showed that the concentration of indolmycin increased for both wild type and mutant strains, but that the final concentration in the *maeA* mutant was elevated 3.8-fold when compared to the level in the parental strain S4054-2. A stoichiometric calculation shows that the molar increase in indolmycin production is roughly 1.5-fold higher than the decrease in violacein production (1.2, 1.6, and 1.5, for 24, 48, and 72 h of growth, respectively), suggesting that the metabolism could have been rerouted in the *maeA* mutant.

Antibacterial Activity of Culture Supernatants from Wild Type and *maeA* Mutant

To test for the antibiotic activity of the three *P. luteoviolacea* strains, cell free extracts were produced to assay their inhibitory effect on the growth of *Vibrio anguillarum* and *Staphylococcus aureus*. Zones of 26-28 mm were found for *V. anguillarum* from 72 h-cultures while 31–32 mm inhibition zones were found for *S. aureus* (**Table 2**). Thus, the difference in violacein concentration in the cultures was not reflected in the size of the inhibition zones. MIC assays confirmed that the culture supernatants had identical levels of antibacterial activity with minimal inhibitory concentration at 32-fold and 128-fold dilutions against *V. anguillarum* and *S. aureus*, respectively (data not shown).

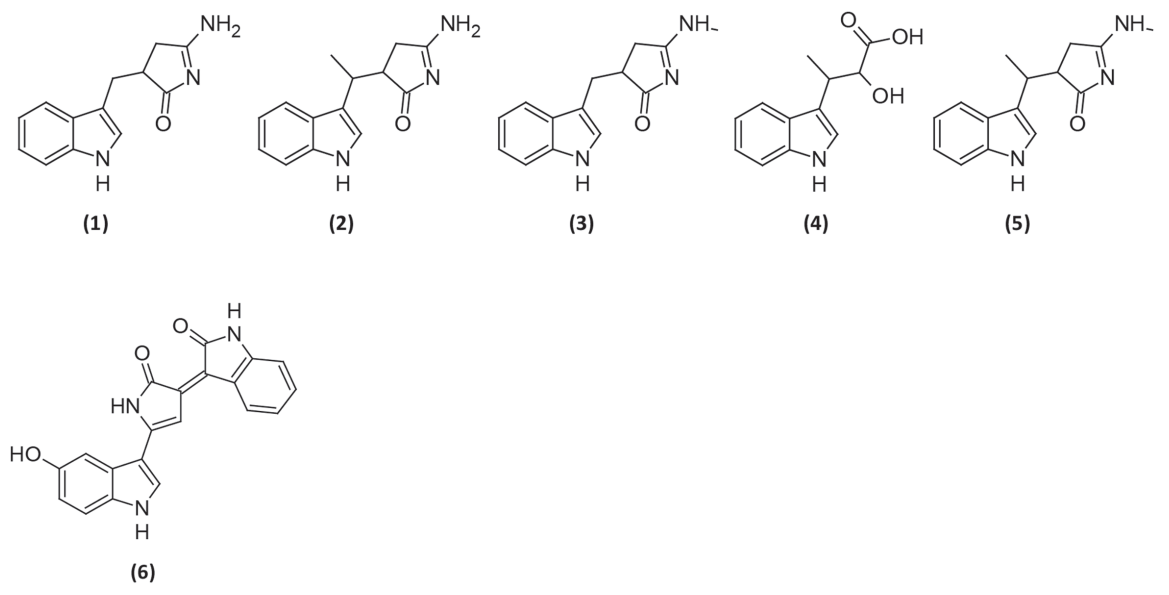


FIGURE 3 | Chemical structures of (1) N,C-didemethyl-indolmycin, (2/3) mono-N/C-demethyl-indolmycin, (4) indolmycenic acid, (5) indolmycin, and (6) violacein.

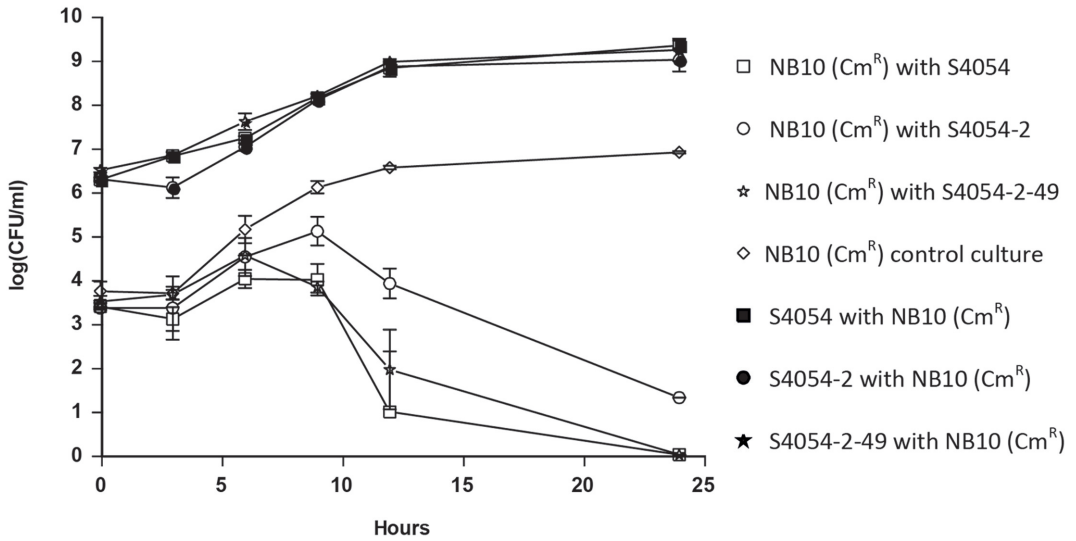


FIGURE 4 | Co-cultivation of *P. luteoviolacea* strains with *Vibrio anguillarum* NB10 (Cm^R). Colony forming units (CFU/ml) of *V. anguillarum* NB10 (Cm^R) (open symbols) after co-cultivation with S4054 wt (violacein, indolmycin), S4054-2 (violacein, indolmycin) or S4054-2-49 (violacein, indolmycin) as well as CFU/ ml of *P. luteoviolacea* S4054, S4054-2 or S4054-2-49 (black symbol) after co-cultivation with *V. anguillarum* NB10 (Cm^R) from 0 to 24 h. *Vibrio anguillarum* NB10 (Cm^R) control culture CFU/ml was also recorded during growth over 24 h.

Inhibition of *Vibrio anguillarum* by Co-culturing with *P. luteoviolacea* Wild Type and Mutant Strains

When *V. anguillarum* NB10 (Cm^R) was inoculated with S4054, S4054-2, or S4054-2 *maeA* in MMM CAA mannose at a ratio of approximately 1:1000 (10^3 and 10^6 cells ml^{-1} for *V. anguillarum* and *P. luteoviolacea*, respectively) the *Vibrio* strain was outcompeted after 25 h of growth (**Figure 4**). When *V. anguillarum* was grown alone, it showed a short exponential growth phase after a lag phase of 3 h, and grew to a cell density of almost 10^7 CFU ml^{-1}. Each of the three *P. luteoviolacea* strains had a similar growth pattern and grew to approximately 10^9 CFU ml^{-1} by 24 h (**Figure 4**). In co-cultures with *Pseudoalteromonas*, the *V. anguillarum* strains initially grew as in monocultures, but after 6 h where the *P. luteoviolacea* stains had grown to approximately 10^7 CFU ml^{-1}, the number of colony forming *V. anguillarum* cells started to level off. After 12 h where *P. luteoviolacea* entered stationary phase, most *V. anguillarum* cells had died, or were unable to form colonies. The bactericidal effect observed was not dependent on the production of violacein as there was no significant difference in *V. anguillarum* NB10 (Cm^R) cell numbers when grown together with S4054 ($P > 0.05$) or S4054-2-49 ($P > 0.05$).

DISCUSSION

Pseudoalteromonas luteoviolacea strain S4054 produces both violacein and indolmycin (Månsson et al., 2010). To the best of our knowledge, this is the only reported bacterial species that produce both violacein and indolmycin, leading us to investigate whether the synthesis of the two L-tryptophan derived bioactive compounds were interconnected. Transposon mutagenesis resulted in the isolation of a beige *maeA*::miniTn*10* mutant strain that exhibited a combination of reduced violacein and increased indolmycin production (**Table 2**). Culture supernatants from the *maeA* mutant, grown for 72 h, contained less than 10% of the violacein level present in culture

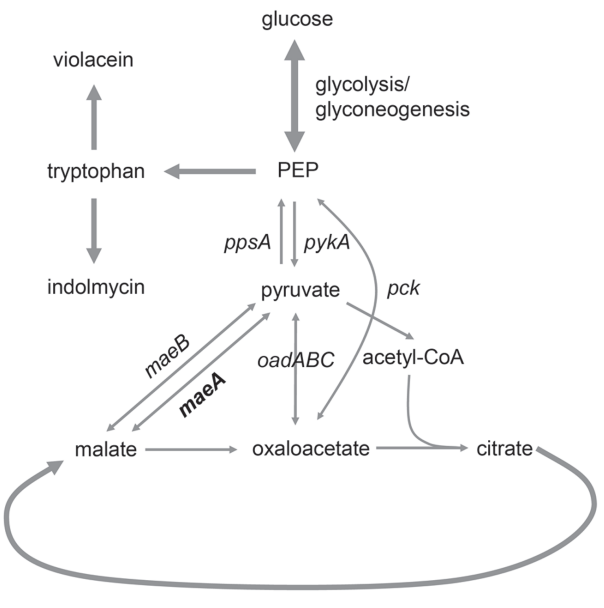


FIGURE 5 | Malic enzyme MaeA is catalyzing the conversion of malate into pyruvate, which is subsequently used for the production of tryptophan used for violacein and indolmycin biosynthesis.

supernatants from the wild type strain S4054 (**Table 2**). Konzen et al. (2006) proposed that violacein is located in the cell membrane of *C. violaceum* to protect the bacterial cell from oxidative stress. This function correlate well with our finding that violacein was only produced in the *maeA* mutant under high oxygen tensions. It is possible that the beige phenotype originating from the decreased violacein production in the mutant made it possible to detect stress induction of violacein genes by their pigmentation, while this induction would normally be hidden by the un-induced violacein production.

The malic enzyme, encoded by the *maeA* gene, catalyzes the conversion of malate into pyruvate and CO_2 (Kwon et al., 2007). When *P. luteoviolacea* grows on substrates that enter through the citric acid (TCA) cycle, its obligate respiratory energy metabolism is dependent upon replenishing reactions that can provide acetyl-CoA for the continuation of the cycle (**Figure 5**). According to the KEGG database (Kanehisa and Goto, 2000; Kanehisa et al., 2016), four enzymes are able to provide this function in *Pseudoalteromonas* species (data not shown): The malic enzymes MaeA and MaeB require NAD^+ or $NADP^+$ for reduction of malate to pyruvate and CO_2, respectively, while the phosphoenolpyruvate (PEP) carboxykinase (Pck) and the oxaloacetate decarboxylase (OadABC) are not redox enzymes. The replenishing enzymes are also needed for fueling the gluconeogenesis reactions needed for synthesis of amino acids, nucleotides, lipids, etc. Tryptophan synthesis which is needed for synthesis of both violacein and indolmycin is likely to be affected by the replenishment reactions as two molecules of PEP are consumed for every tryptophan molecule formed, in the AroH and AroA reactions, respectively (Kedar et al., 2007). Disruption of the *maeA* gene would prevent the use of NAD^+ to replenish pyruvate from malate and the mutant would rely on the remaining three reactions. Furthermore, the conversion of malate into pyruvate is the least thermodynamically favored reaction, but is the one that occurs in nature since the kinetic parameters of the malic enzyme have evolved to favor this direction (Murai et al., 1971; Stols and Donnelly, 1997). However, the opposite direction is actually thermodynamically favored (Goldberg et al., 1993), so with the MaeA encoding gene knocked out, pyruvate is converted into malate without the opposite reaction occurring. Violacein synthesis requires two molecules of tryptophan while indolmycin synthesis requires only one. Therefore the shift from violacein to indolmycin production would suggest that the *maeA* mutation had resulted in decreased tryptophan or PEP production. This appears highly illogical, so our hypothesis is that the conditional production of violacein in the *maeA* mutant is due to regulatory mechanisms controlling the replenishing reactions. Availability of redox co-enzymes, e.g., regeneration of NAD^+ in the respiratory chain, could also be important, as efficient aeration has been shown to be important for violacein production (Yang et al., 2007). At present the knowledge about these systems in *Pseudoalteromonas* species is too limited to make any conclusions about the exact nature of the cause.

With regard to their antimicrobial activity, culture supernatants from either wild type or *maeA* mutant inhibited the growth of Gram positive *S. aureus* and Gram negative *V. anguillarum* equally well (**Table 2**) in spite of the reduced violacein content in the *maeA* mutant. Since neither violacein nor indolmycin concentration correlated with the size of the inhibition zone, and since violacein is located in the cell membrane and therefore would not be present in our cell-free supernatants, we suggest that a yet unidentified compound could be responsible for the major part of the antimicrobial activity. This hypothesis is supported by the fact that the genome of *P. luteoviolacea* S4054 contains several putative biosynthetic gene clusters, most of which have not yet been assigned a specific function (Machado et al., 2015; Månsson et al., 2016). Out of a total of 36 putative antibiotic and secondary metabolite gene clusters determined by AntiSMASH (Medema et al., 2011; Weber et al., 2015), nine can be attributed a specific function, and a further nine can be attributed a hypothetical function, including production of indolmycin, and the remaining 18 can only be classified on a putative type of gene cluster level, primarily identified by the ClusterFinder algorithm (Weber et al., 2015)

AUTHOR CONTRIBUTIONS

MD and LG conceived the research, MD carried out transposon mutagenesis, plate inhibition assays, and co-culture inhibitions, MT and JM carried out MIC assays, MT, JM, and MK carried out substrate-dependent expression, MM and KN performed purification and quantification, BB, CS, and JO performed genome sequencing, assembly and annotation, MT carried out genome analysis, MT, MD, MK, and LG drafted the manuscript. All authors have read and approved the manuscript.

FUNDING

The research leading to these results has received funding from the Commission on Health, Food and Welfare under the Danish Council for Strategic Research and the MaCuMBA Project under the European Union's Seventh Framework Programme (FP7/2007-2013) under grant agreement no 311975. The publication reflects the views only of the author, and the European Union cannot be held responsible for any use which may be made of the information contained therein.

ACKNOWLEDGMENTS

The authors wish to thank Simone Severitt and Nicole Mrotzek for excellent technical assistance and Dr. Thomas Ostenfeld Larsen for valuable discussions. We would also like to thank Dr. Debra Milton, University of Umeå for providing the chromosomally tagged *Vibrio anguillarum* NB10. The present work was carried out as part of the Galathea 3 expedition under the auspices of the Danish Expedition Foundation. This is Galathea 3 contribution no. P118.

REFERENCES

Aziz, R. K., Bartels, D., Best, A. A., DeJongh, M., Disz, T., Edwards, R. A., et al. (2008). The RAST Server: rapid annotations using subsystems technology. *BMC Genomics* 9:75. doi: 10.1186/1471-2164-9-75

Balibar, C. J., and Walsh, C. T. (2006). In vitro biosynthesis of violacein from L-tryptophan by the enzymes VioA-E from *Chromobacterium violaceum*. *Biochemistry* 45, 15444–15457. doi: 10.1021/bi061998z

Brucker, R. M., Harris, R. N., Schwantes, C. R., Gallaher, T. N., Flaherty, D. C., Lam, B. A., et al. (2008). Amphibian chemical defense: antifungal metabolites of the microsymbiont *Janthinobacterium lividum* on the salamander *Plethodon cinereus*. *J. Chem. Ecol.* 34, 1422–1429. doi: 10.1007/s10886-008-9555-7

Darling, A. C. E., Mau, B., Blattner, F. R., and Perna, N. T. (2004). Mauve: multiple alignment of conserved genomic sequence with rearrangements. *Genome Res.* 14, 1394–1403. doi: 10.1101/gr.2289704

Du, Y.-L., Alkhalaf, L. M., and Ryan, K. S. (2015). In vitro reconstitution of indolmycin biosynthesis reveals the molecular basis of oxazolinone assembly. *Proc. Natl. Acad. Sci. U.S.A.* 112, 2717–2722. doi: 10.1073/pnas.1419964112

Durán, N., Justo, G. Z., Ferreira, C. V., Melo, P. S., Cordi, L., and Martins, D. (2007). Violacein: properties and biological activities. *Biotechnol. Appl. Biochem.* 48, 127–133. doi: 10.1042/BA20070115

Gauthier, M. J. (1982). Validation of the name *Alteromonas luteoviolacea*. *Int. J. Syst. Bacteriol.* 32, 82–86. doi: 10.1099/00207713-32-1-82

Gillan, D. C., Speksnijder, A. G. C. L., Zwart, G., and DeRidder, C. (1998). Genetic diversity of the biofilm covering *Montacuta ferruginosa* (Mollusca, Bivalvia) as evaluated by denaturing gradient gel electrophoresis analysis and cloning of PCR-amplified gene fragments coding for 16S rRNA. *Appl. Environ. Microbiol.* 64, 3464–3472.

Goldberg, R. N., Tewari, Y. B., Bell, D., and Fazio, K. (1993). Thermodynamics of enzyme catalyzed reactions: part 1. Oxidoreductases. *J. Phys. Chem. Ref. Data* 22, 515–582. doi: 10.1063/1.555939

Gómez, D., Espinosa, E., Bertazzo, M., Lucas-Elío, P., Solano, F., and Sanchez-Amat, A. (2008). The macromolecule with antimicrobial activity synthesized by *Pseudoalteromonas luteoviolacea* strains is an L-amino acid oxidase. *Appl. Microbiol. Biotechnol.* 79, 925–930. doi: 10.1007/s00253-008-1499-x

Gram, L., Melchiorsen, J., and Bruhn, J. B. (2010). Antibacterial activity of marine culturable bacteria collected from a global sampling of ocean surface waters and surface swabs of marine organisms. *Mar. Biotechnol.* 12, 439–451. doi: 10.1007/s10126-009-9233-y

Hanefeld, U., Floss, H. G., and Laatsch, H. (1994). Biosynthesis of the marine antibiotic pentabromopseudilin. 1. The benzene ring. *J. Org. Chem.* 59, 3604–3608. doi: 10.1021/jo00092a020

Hjelm, M., Bergh, O., Riaza, A., Nielsen, J., Melchiorsen, J., Jensen, S., et al. (2004). Selection and identification of autochthonous potential probiotic bacteria from turbot larvae (*Scophthalmus maximus*) rearing units. *Syst. Appl. Microbiol.* 27, 360–371. doi: 10.1078/0723-2020-00256

Hornemann, U., Hurley, L. H., Speedie, M. K., and Floss, H. G. (1971). The biosynthesis of indolmycin. *J. Am. Chem. Soc.* 93, 3028–3035. doi: 10.1021/ja00741a035

Hurdle, J. G., O'Neill, A. J., and Chopra, I. (2004). Anti-staphylococcal activity of indolmycin, a potential topical agent for control of staphylococcal infections. *J. Antimicrob. Chemother.* 54, 549–552. doi: 10.1093/jac/dkh352

Kanamaru, T., Nakano, Y., Toyoda, Y., Miyagawa, K. I., Tada, M., Kaisho, T., et al. (2001). In vitro and in vivo antibacterial activities of TAK-083, an agent for treatment of *Helicobacter pylori* infection. *Antimicrob. Agents Chemother.* 45, 2455–2459. doi: 10.1128/AAC.45.9.2455-2459.2001

Kanehisa, M., and Goto, S. (2000). KEGG: kyoto encyclopedia of genes and genomes. *Nucleic Acids Res.* 28, 27–30. doi: 10.1093/nar/28.1.27

Kanehisa, M., Sato, Y., Kawashima, M., Furumichi, M., and Tanabe, M. (2016). KEGG as a reference resource for gene and protein annotation. *Nucleic Acids Res.* 44, D457–D462. doi: 10.1093/nar/gkv1070

Kedar, P., Colah, R., and Shimizu, K. (2007). Proteomic investigation on the pyk-F gene knockout *Escherichia coli* for aromatic amino acid production. *Enzyme Microb. Technol.* 41, 455–465. doi: 10.1016/j.enzmictec.2007.03.018

Koboldt, D. C., Zhang, Q., Larson, D. E., Shen, D., McLellan, M. D., Lin, L., et al. (2012). VarScan 2: somatic mutation and copy number alteration discovery in cancer by exome sequencing. *Genome Res.* 22, 568–576. doi: 10.1101/gr.129684.111

Konzen, M., De Marco, D., Cordova, C. A., Vieira, T. O., Antônio, R. V., and Creczynski-Pasa, T. B. (2006). Antioxidant properties of violacein: possible relation on its biological function. *Bioorg. Med. Chem.* 14, 8307–8313. doi: 10.1016/j.bmc.2006.09.013

Kwon, Y. D., Kwon, O. H., Lee, H. S., and Kim, P. (2007). The effect of NADP-dependent malic enzyme expression and anaerobic C4 metabolism in *Escherichia coli* compared with other anaplerotic enzymes. *J. Appl. Microbiol.* 103, 2340–2345. doi: 10.1111/j.1365-2672.2007.03485.x

Li, H., and Durbin, R. (2009). Fast and accurate short read alignment with Burrows-Wheeler transform. *Bioinformatics* 25, 1754–1760. doi: 10.1093/bioinformatics/btp324

Machado, H., Sonnenschein, E. C., Melchiorsen, J., and Gram, L. (2015). Genome mining reveals unlocked bioactive potential of marine Gram-negative bacteria. *BMC Genomics* 16:158. doi: 10.1186/s12864-015-1365-z

Månsson, M., Phipps, R. K., Gram, L., Munro, M. H., Larsen, T. O., and Nielsen, K. F. (2010). Explorative solid-phase extraction (E-SPE) for accelerated microbial natural product discovery, dereplication, and purification. *J. Nat. Prod.* 73, 1126–1132. doi: 10.1021/np100151y

Månsson, M., Vynne, N. G., Klitgaard, A., Nybo, J. L., Melchiorsen, J., Nguyen, D. D., et al. (2016). An integrated metabolomic and genomic mining workflow to uncover the biosynthetic potential of bacteria. *mSystems* 1, 1–14. doi: 10.1128/mSystems.00028-15

McCarthy, S. A., Sakata, T., Kakimoto, D., and Johnson, R. M. (1985). Production and isolation of purple pigment by *Alteromonas luteoviolacea*. *Bull. Jpn. Soc. Sci. Fish* 51, 479–484. doi: 10.2331/suisan.51.479

Medema, M. H., Blin, K., Cimermancic, P., de Jager, V., Zakrzewski, P., Fischbach, M. A., et al. (2011). AntiSMASH: rapid identification, annotation and analysis of secondary metabolite biosynthesis gene clusters in bacterial and fungal genome sequences. *Nucleic Acids Res.* 39, 339–346. doi: 10.1093/nar/gkr466

Médigue, C., Krin, E., Pascal, G., Barbe, V., Bernsel, A., Bertin, P. N., et al. (2005). Coping with cold: the genome of the versatile marine Antarctica bacterium *Pseudoalteromonas haloplanktis* TAC125. *Genome Res.* 15, 1325–1335. doi: 10.1101/gr.4126905

Milton, D. L., Norqvist, A., and Wolf-Watz, H. (1992). Cloning of a metalloprotease gene involved in the virulence mechanism of *Vibrio anguillarum*. *J. Bacteriol.* 174, 7235–7244.

Murai, T., Tokushige, M., Nagai, J., and Katsuki, H. (1971). Physiological functions of NAD-and NADP-linked malic enzymes in *Escherichia coli*. *Biochem. Biophys. Res. Commun.* 43, 875–881. doi: 10.1016/0006-291X(71)90698-X

Nishimura, K., Hosaka, T., Tokuyama, S., Okamoto, S., and Ochi, K. (2007). Mutations in rsmG, encoding a 16S rRNA methyltransferase, result in low-level streptomycin resistance and antibiotic overproduction in *Streptomyces coelicolor* A3(2). *J. Bacteriol.* 189, 3876–3883. doi: 10.1128/JB.01776-06

Novick, R. (1967). Properties of a cryptic high-frequency transducing phage in *Staphylococcus aureus*. *Virology* 33, 155–166. doi: 10.1016/0042-6822(67)90105-5

Oliva, B., Miller, K., Caggiano, N., O'Neill, A. J., Cuny, G. D., Hoemann, M. Z., et al. (2003). Biological properties of novel antistaphylococcal quinoline-indole agents. *Antimicrob. Agents Chemother.* 47, 458–466. doi: 10.1128/AAC.47.2.458

Olkkola, S., Juntunen, P., Heiska, H., Hyytiäinen, H., and Hänninen, M. L. (2010). Mutations in the rpsL gene are involved in streptomycin resistance in *Campylobacter coli*. *Microb. Drug Resist.* 16, 105–110. doi: 10.1089/mdr.2009.0128

Ostling, J., Goodman, A., and Kjelleberg, S. (1991). Behaviour of IncP-1 plasmids and a miniMu transposon in a marine *Vibrio* sp.: isolation of starvation inducible lac operon fusions. *FEMS Microbiol. Ecol.* 86, 83–94. doi: 10.1111/j.1574-6941.1991.tb01740.x

Rao, D., Webb, J. S., Holmström, C., Case, R., Low, A., Steinberg, P., et al. (2007). Low densities of epiphytic bacteria from the marine alga *Ulva australis* inhibit settlement of fouling organisms. *Appl. Environ. Microbiol.* 73, 7844–7852. doi: 10.1128/AEM.01543-07

Seemann, T. (2014). Prokka: rapid prokaryotic genome annotation. *Bioinformatics* 30, 2068–2069. doi: 10.1093/bioinformatics/btu153

Skov, M. N., Pedersen, K., and Larsen, J. L. (1995). Comparison of pulsed-field gel electrophoresis, ribotyping, and plasmid profiling for typing of *Vibrio anguillarum* serovar O1. *Appl. Environ. Microbiol.* 61, 1540–1545.

Speedie, M. K., Hornemann, U., and Floss, H. G. (1975). Isolation and characterization of tryptophan transaminase and indolepyruvate C-methyltransferase. *J. Biol. Chem.* 250, 7819–7825.

Springer, B., Kidan, Y. G., Prammananan, T., Ellrott, K., Böttger, E. C., and Sander, P. (2001). Mechanisms of streptomycin resistance: selection of mutations in the 16S rRNA gene conferring resistance. *Antimicrob. Agents Chemother.* 45, 2877–2884. doi: 10.1128/AAC.45.10.2877

Stols, L., and Donnelly, M. I. (1997). Production of succinic acid through overexpression of NAD(+)-dependent malic enzyme in an *Escherichia coli* mutant. *Appl. Environ. Microbiol.* 63, 2695–2701.

Stretton, S., Techkarnjanaruk, S., McLennan, A. M., and Goodman, A. E. (1998). Use of green fluorescent protein to tag and investigate gene expression in marine bacteria. *Appl. Environ. Microbiol.* 64, 2554–2559.

Tanaka, Y., Komatsu, M., Okamoto, S., Tokuyama, S., Kaji, A., Ikeda, H., et al. (2009). Antibiotic overproduction by rpsL and rsmG mutants of various actinomycetes. *Appl. Environ. Microbiol.* 75, 4919–4922. doi: 10.1128/AEM.00681-09

Timms, A. R., Steingrimsdottir, H., Lehmann, A. R., and Bridges, B. A. (1992). Mutant sequences in the rpsL gene of *Escherichia coli* B/r: mechanistic implications for spontaneous and ultraviolet light mutagenesis. *Mol. Gen. Genet.* 232, 89–96. doi: 10.1007/BF00299141

Vynne, N. G., Månsson, M., and Gram, L. (2012). Gene sequence based clustering assists in dereplication of *Pseudoalteromonas luteoviolacea* strains with identical inhibitory activity and antibiotic production. *Mar. Drugs* 10, 1729–1740. doi: 10.3390/md10081729

Vynne, N. G., Månsson, M., Nielsen, K. F., and Gram, L. (2011). Bioactivity, chemical profiling, and 16S rRNA-based phylogeny of *Pseudoalteromonas* strains collected on a global research cruise. *Mar. Biotechnol.* 13, 1062–1073. doi: 10.1007/s10126-011-9369-4

Weber, T., Blin, K., Duddela, S., Krug, D., Kim, H. U., Bruccoleri, R., et al. (2015). antiSMASH 3.0 – a comprehensive resource for the genome mining of biosynthetic gene clusters. *Nucleic Acids Res.* 43, 1–7. doi: 10.1093/nar/gkv437

Werner, R. G., Thorpe, L. F., Reuter, W., and Nierhaus, K. H. (1976). Indolmycin inhibits prokaryotic tryptophanyl-tRNA ligase. *Eur. J. Biochem.* 68, 1–3. doi: 10.1111/j.1432-1033.1976.tb10758.x

Wilson, K. (2001). "Preparation of genomic DNA from bacteria." in *Current Protocols in Molecular Biology*, eds F. M. Ausubel, R. Brent, R. E. Kingston, D. D. Moore, J. A. Smith, J. G. Seidman, et al. (Hoboken, NJ: John Wiley & Sons, Inc), 2.4.1–2.4.2.

Yang, L. H., Xiong, H., Lee, O. O., Qi, S. H., and Qian, P. Y. (2007). Effect of agitation on violacein production in *Pseudoalteromonas luteoviolacea* isolated from a marine sponge. *Lett. Appl. Microbiol.* 44, 625–630. doi: 10.1111/j.1472-765X.2007.02125.x

Zar, J. H. (1996). *Biostatistical Analysis*. Englewood Cliffs, NJ: Prentice Hall Inc.

Conflict of Interest Statement: The authors declare that the research was conducted in the absence of any commercial or financial relationships that could be construed as a potential conflict of interest.

Copyright © 2016 Thøgersen, Delpin, Melchiorsen, Kilstrup, Månsson, Bunk, Spröer, Overmann, Nielsen and Gram. This is an open-access article distributed under the terms of the Creative Commons Attribution License (CC BY). The use, distribution or reproduction in other forums is permitted, provided the original author(s) or licensor are credited and that the original publication in this journal is cited, in accordance with accepted academic practice. No use, distribution or reproduction is permitted which does not comply with these terms.

frontiers in Microbiology

ORIGINAL RESEARCH
published: 20 September 2016
doi: 10.3389/fmicb.2016.01477

Anti-rheumatoid Activity of Secondary Metabolites Produced by Endophytic *Chaetomium globosum*

Ahmed M. Abdel-Azeem[1], Sherif M. Zaki[2], Waleed F. Khalil[3], Noha A. Makhlouf[4] and Lamiaa M. Farghaly[5]*

[1] Botany Department, Faculty of Science, Suez Canal University, Ismailia, Egypt, [2] Microbiology Department, Faculty of Science, Ain Shams University, Cairo, Egypt, [3] Pharmacology Department, Faculty of Veterinary Medicine, Suez Canal University, Ismailia, Egypt, [4] Histology Department, Faculty of Medicine, Ain Shams University, Cairo, Egypt, [5] Histology Department, Faculty of Medicine, Suez Canal University, Ismailia, Egypt

The aim of the present study was to investigate the anti-rheumatoid activity of secondary metabolites produced by endophytic mycobiota in Egypt. A total of 27 endophytic fungi were isolated from 10 dominant medicinal plant host species in Wadi Tala, Saint Katherine Protectorate, arid Sinai, Egypt. Of those taxa, seven isolates of *Chaetomium globosum* (CG1–CG7), being the most frequent taxon, were recovered from seven different host plants and screened for production of active anti-inflammatory metabolites. Isolates were cultivated on half – strength potato dextrose broth for 21 days at 28°C on a rotatory shaker at 180 rpm, and extracted in ethyl acetate and methanol, respectively. The probable inhibitory effects of both extracts against an adjuvant induced arthritis (AIA) rat model were examined and compared with the effects of methotrexate (MTX) as a standard disease-modifying anti-rheumatoid drug. Disease activity and mobility scoring of AIA, histopathology and transmission electron microscopy (TEM) were used to evaluate probable inhibitory roles. A significant reduction ($P < 0.05$) in the severity of arthritis was observed in both the methanolic extract of CG6 (MCG6) and MTX treatment groups 6 days after treatment commenced. The average arthritis score of the MCG6 treatment group was (10.7 ± 0.82) compared to (13.8 ± 0.98) in the positive control group. The mobility score of the MCG6 treatment group (1.50 ± 0.55) was significantly lower than that of the positive control group (3.33 ± 0.82). In contrast, the ethyl acetate extract of CG6 (EACG6) treatment group showed no improvements in arthritis and mobility scores in AIA model rats. Histopathology and TEM findings confirmed the observation. Isolate CG6 was subjected to sequencing for confirmation of phenotypic identification. The internal transcribed spacer (ITS) 1–5.8 s – ITS2 rDNA sequences obtained were compared with those deposited in the GenBank Database and registered with accession number KC811080 in the NCBI Database. The present study revealed that the methanol extract of endophytic fungus *C. globosum* (KC811080) recovered from maidenhair fern has an inhibitory effect on inflammation, histopathology and morphological features of rheumatoid arthritis in an AIA rat model.

Keywords: ***Chaetomium globosum,*** **adjuvant-induced arthritis, arid Sinai, fungarium, saint katherine protectorate**

OPEN ACCESS

Edited by:
Vijai Kumar Gupta, National University of Ireland, Galway, Ireland

Reviewed by:
Ram Prasad, Amity University, India
Venu Kamarthapu, New York University School of Medicine, USA

****Correspondence:***
Ahmed M. Abdel-Azeem
ahmed_abdelazeem@science.suez.edu.eg;
zemo3000@yahoo.com

Specialty section:
This article was submitted to Microbial Physiology and Metabolism, a section of the journal Frontiers in Microbiology

Received: *16 July 2016*
Accepted: *05 September 2016*
Published: *20 September 2016*

Citation:
Abdel-Azeem AM, Zaki SM, Khalil WF, Makhlouf NA and Farghaly LM (2016) Anti-rheumatoid Activity of Secondary Metabolites Produced by Endophytic Chaetomium globosum. Front. Microbiol. 7:1477. doi: 10.3389/fmicb.2016.01477

INTRODUCTION

Endophytic fungi are symbiotically associated biota of living plant tissues that induce symptomless disease to their hosts (Petrini, 1991) and are non-host specific (Cohen, 2006). Over last decade, scientists have focused their investigations on bio prospecting naturally occurring chemical compounds and biological material, especially in extreme diverse environments (Suryanarayanan et al., 2009; Abdel-Azeem et al., 2012; Mustafa et al., 2013; Salem and Abdel-Azeem, 2015). Medicinal plants and microbiota are the most consistent and generative sources of 'first-in-class' drugs (Newman and Cragg, 2007). Recently, remarkable pharmacological agents have been generated from endophytic fungi (Strobel and Daisy, 2003). More than 50% of previously unknown biologically active substances have been isolated from endophytes (Schulz et al., 2002). Endophytes have been the source of a number of bio-pharmacological compounds including those with antimicrobial, antitumor, anti-inflammatory, and antiviral activities (Aly et al., 2008; Liu et al., 2008; Souza et al., 2008). In Egypt, endophytic fungi from aquatic, halophilic, medicinal plants, and marine resources have been studied by various investigators (El-Morsy, 2000; Abdel-Motaal et al., 2010; Aly et al., 2011; Selim et al., 2011; Abdel-Monem et al., 2013; Salem and Abdel-Azeem, 2014).

Chaetomium Kunze is a cosmopolitan genus with about 100 accepted species (Kirk et al., 2008). In Egypt, 53 species and one variety of the genus *Chaetomium* have been recorded (Moustafa and Abdel-Azeem, 2005). *Chaetomium* has attracted the attention of researchers as an important genus in Ascomycota because of the variety of biological and biotechnological applications of its species in different areas, e.g., medical mycology (Zhang et al., 2010), biotechnology (Soni and Soni, 2010), and molecular studies (Aggarwal et al., 2008). To the best of our knowledge, more than 200 compounds, associated with unique and diverse structural types have been isolated and chemically identified from the genus *Chaetomium* (Fujimoto et al., 2004; Jiao et al., 2004; Bashyal et al., 2005; Kobayashi et al., 2005; Ding et al., 2006; Isham et al., 2007; Selim et al., 2014).

Rheumatoid arthritis is an autoimmune disease of humans that characterized by chronic inflammation of the synovial joints and erosive destruction of articular tissue due to progressive inflammation (Ngian, 2010). About 0.5–1% of the human population worldwide is affected by RA and 20–50 cases per 100,000 are recorded annually (Karmakar et al., 2010). MTX had become the principal drug used for the treatment of RA (Williams et al., 1985). MTX is an antifolate immunosuppressive drug that acts primarily on highly proliferating cells, during the synthesis (S)-phase of the cell cycle and inhibits neutrophil chemotaxis (Moreland et al., 1997). Treatment with MTX has been limited because of its toxicity and adverse side effects such as cytopenia, bloody vomit, diarrhea, nephrotoxicity and alopecia (Alarcon et al., 1989). Hence, the discovery of new drugs for the treatment of RA has become a major target of potentially considerable value.

New anti-inflammatory agents produced by fungi have been the focus of a few studies conducted by several investigators over the last two decades (Matsumoto et al., 1995; Chapuis et al., 2000; Lull et al., 2005; Schmidt et al., 2012). In order to fill-gaps in the research area of anti-inflammatory properties of fungal metabolites, we investigated the capability of endophytic mycobiota from wild medicinal host plants in the Saint Katherine Protectorate, Egypt, to produce anti-rheumatoid arthritis metabolites, and their probable inhibitory effects in an AIA rat model compared to the effects of MTX a standard disease-modifying anti-rheumatoid drug.

Abbreviations: AIA, adjuvant induced arthritis; ASFC, Arab society of fungal conservation; CFA, complete Freund's adjuvant; ITS, internal transcribed spacer; MTX, methotrexate; NC, negative control; NCBI, National Center for Biotechnology; PC, positive control; RA, rheumatoid arthritis; TEM, transmission electron microscope.

MATERIALS AND METHODS

Study Area and Sampling

Wadi Tala (1450–1670 m above sea level) is a rocky U-shaped valley, running from North to South, approximately 2.5 km west of Saint Katherine city. One hundred samples of the dominant plant species from ten localities namely: *Artemisia herba-alba* Asso; *Achillea fragrantissima* (Forssk) Sch.; *Capparis spinosa* L.; *Chiliadenus montanus* (Vahl) Brullo; *Echinops spinosissimus* Turra; *Origanum syriacum* L.; *Phlomis aurea* Decne; *Teucrium polium* L.; *Verbascum sinaiticum* Benth.; and *Adiantum capillus-veneris* L. were collected in sterilized polyethylene bags and transferred to the laboratory, where they were subsequently plated out. Samples were collected under permission of the Saint Katherine Protectorate for scientific purposes and no endangered species were involved in the study.

Isolation of Endophytic Mycobiota

A total of 1000 plates were used for the isolation of endophytic mycobiota (100 plates/plant). Pieces of stem and leaves (5 mm^2, four pieces in each plate) were surface sterilized and cut. The sections were washed three times in running water, immersed in 70% ethanol for 1–5 min, dipped in 5% NaOCl for 3–5 min, according to the plant thickness, and then dipped in 70% ethanol for 0.5 min (Fisher et al., 1993), before being plated on appropriate isolation media. For primary isolation, Czapek's yeast extract agar, supplemented with Rose bengal (1/1500), chloramphenicol (50 ppm), and Potato Dextrose Agar media were used.

Phenotypic Identification

Identification of the recovered endophytic fungal isolates was conducted up to the species level based on phenotypic means was and the relevant identification keys for: *Penicillium* (Raper and Thom, 1949; Pitt, 1980) *Aspergillus* (Klich, 2002); dematiaceous hyphomycetes (Ellis, 1971, 1976); *Fusarium* (Booth, 1971); miscellaneous fungi (Domsch et al., 2007); ascomycetes (Guarro et al., 2012) and *Chaetomium* (Doveri, 2013). The names of the authors of fungal taxa were abbreviated according to Kirk and Ansell (1992). The systematic arrangement of the recorded list follows the 10th edition of Ainsworth and Bisby's

Dictionary of the Fungi (Kirk et al., 2008). All name corrections, authorities, and taxonomic assignments of recorded species in the present study were checked against the Index Fungorum database.

Molecular Identification

Molecular identification of the promising isolate, *Chaetomium globosum* (CG6), was performed by comparing its ITS1 – 5.8S – ITS2 rDNA region sequence data with data on reference strains deposited in GenBank.

DNA Isolation

The Fungal isolate was grown on Potato dextrose agar and DNA was extracted according to the protocol provided in the Fermentas® Genomic DNA Purification Kit #K0512 (Thermo Fischer Scientific, Europe). Sufficient inoculum was suspended in 200 μL Tris-EDTA buffer (10 mM Tris-HCl, pH 8.0, 1 mM EDTA) in a 2.2 ml Eppendorf tube. The tubes of each sample were boiled for 3 min and then placed in ice water for 10 min. Lysis solution (400 μL) was added and the tubes were incubated at 65°C for 30 min, after which 600 μL of chloroform was added and the resulting solution carefully mixed. DNA was separated by centrifugation at 12000 rpm for 10 min at 4°C, and mixed with 800 μL of precipitation solution through several inversions at room temperature for 1 min. The tubes were then centrifuged at 12000 rpm for 10 min at 4°C. Pellets of DNA were dissolved in 100 μL of 1.2 M NaCl solution by gentle vortexing. Ice-cold isopropanol (500 μL) was added to the solution and each tube was incubated for 15 min at −20°C and then centrifuged at 12000 rpm for 10 min at 4°C. The DNA pellet was washed with 1 mL of ice-cold 70% ethanol, dried, and resuspended in sterile Tris-EDTA buffer.

Oligonucleotides

The oligonucleotide primers described by White et al. (1990) were used for amplification and sequencing of the ITS regions. ITS5 (5′-GGAAGTAAAAGTCGTAACAAGG-3′) AND ITS4 (5′-TCCTCCGCTTATTGATATGC-3′) (Bioneer Corporation, South Korea) were selected for the present study.

PCR and DNA Sequencing of the ITS1 – 5.8 s – ITS2 rDNA Region

Amplification reactions were carried out in 20 μL reaction mixtures containing 2.5 μL of each primer (10 pm), 2.5 μL of genomic DNA (5 μg/mL), and one PCR-Gold Master-Mix bead (Bio-ron, Germany). The bead contained buffers, dNTP, an enzyme, stabilizers, Tris-HCl, KCl, and MgCl2. A PCR Thermal Cycler (Techne®Genius – England) was used for amplification at the following settings: initial denaturation at 96°C for 5 min, 35 cycles of denaturation at 94°C for 30 s, annealing at 52°C for 30 s, extension at 72°C for 80 s, and a final extension at 72°C for 10 min. Products of the PCR reaction were sequenced directly using the Big-Dye terminator reagent kit and Taq polymerase in an automated DNA sequencer (Model 3100; PerkinEl-mer Inc/Applied Biosystems – Bioneer, South Korea), according to the manufacturer's protocol.

Nucleotide Accession Number

The nucleotide sequence data of the CG6 isolate of the present study was deposited in the NCBI GenBank nucleotide sequence database under accession number KC811080.

Extraction of Active Metabolites from Recovered *C. globosum* Isolates

Isolates of *C. globosum* under investigation (CG1–CG7) were grown on Oat Meal Agar at 28°C for 15 days. Each isolate was prepared by inoculation in 2 L Erlenmeyer flasks containing 1 L autoclaved potato dextrose broth and shaking at 180 rpm at 28°C for 21 days. The fermentation broth of each isolate was divided into two portions (2 L each) and filtered. Fresh mycelia were washed three times with distilled water and stored in a freezer. Two organic solvents, namely ethyl acetate and methanol, were used for extraction of active metabolites. The filtrate was divided into two portions (2 L each), and extracted three times with equal volumes of ethyl acetate and methanol, and collected separately. The frozen mycelia were ground and extracted three times in each solvent, and combined with organic extracts of the filtrate and evaporated until dry under reduced pressure according to the procedures outlined by Salem and Abdel-Azeem (2014). After evaporation, the dried extract was stored in away from light in a refrigerator until further use. For injection of rats, fresh prepared solution of solid metabolites was applied through re-suspension in sterile 10% Tween-80 in saline solution.

Animals, Induction of Adjuvant Induced Arthritis (AIA) Rat Model, and Treatments

Male Wistar albino rats (102) weighing 160–180 g were obtained from the Animal House Colony of the National Research Center of Egypt and divided into five groups (six rats each) after a week of acclimatization. The first group was the negative control group (NC) that was injected with saline and 10% Tween-80, instead of CFA and fungal extracts, respectively. All other groups were injected subcutaneously at the base of the tail with 100 μL CFA (Sigma-Aldrich, USA) to induce arthritis (Bendele, 2001). The second group was the positive control group (PC) that remained untreated but was administered 10% Tween-80 vehicle alone. The third and fourth groups (seven replicates each) were injected with methanol (MCG) and ethyl acetate (EACG) fungal extracts, respectively. The fifth group was treated with MTX (Orion Pharma, Espoo, Finland) as a standard disease-modifying anti-rheumatic-drug. All possible efforts were made to minimize animal suffering and reduce the number of rats used. The experimental protocol was approved by the Scientific Research Ethics Committee of the Faculty of Veterinary Medicine, Suez Canal University. After 14 days of CFA administration, clinical signs of arthritis were clearly evident and all treatments commenced at that time. Ethyl acetate and methanol fungal extracts were injected subcutaneously twice per week for 2 weeks at a dose of 10 and 30 μg extract/Kg BW., respectively, based on the finding of a pilot study conducting in

the veterinary pharmacology laboratory of Suez Canal University. Similarly, MTX was injected subcutaneously twice per week at a dose of 0.3 mg/Kg BW (Suzuki et al., 1997). The lowest doses that exhibited curative effects without apparent toxicity were selected for further analysis.

Assessing Swelling and Mobility Scoring

On the first day of treatment, swelling was assessed in the right hind paw via measurement of its mean thickness using a 0–10 mm electric caliper. Four definitions were used to score animal mobility according to the scale proposed by Ablin et al. (2010). The scores ranged from 0 to 4 as follows: 0 = normal, 1 = slightly impaired, 2 = major impairment, 3 = does not bear weight on paw, and 4 = no movement. Measurements and scoring of arthritis's were performed independently by two blinded technicians.

Histopathology Studies

Rats were sacrificed under light ether anesthesia and hind limbs were resected and fixed in 10% buffered formalin. Limbs were decalcified in 5% nitric acid, dehydrated, cleared, and embedded in paraffin for sectioning at a thickness of 5 μm. Sections were subsequently stained with hematoxylin and eosin (H & E; Bancroft and Stevens, 1996).

Transmission Electron Microscope Examination

Samples of skin, muscle, fatty tissues, and tendons from sacrificed rats were removed, trimmed of excessive subchondral bone, and cut into 1 mm^3 slabs. Fixation of cartilages, decalcification, rinsing, post-fixation, dehydration, embedding, sectioning, and ultra-sectioning were carried out. Ultra-thin sections were stained according to the methods outlined by Bancroft and Gamble (2008), using uranyl acetate and lead citrate. They were subsequently examined under a TEM (JEOL 1200 EX II, Japan) at the regional Mycology and Biotechnology center, AL-Azhar University, Egypt.

Data Analysis

Data of the treated groups were compared with those of the PC group (untreated AIA) to determine the significance of treatment efficacy. Data were subjected to the Bartlett's test (Bartlett, 1937; Winer et al., 1991), ANOVA, and Dunnett's multiple comparisons (Hsu, 1996). If unequal variances were obtained in the Bartlett's test, data were subjected to the non-parametric Kruskal–Wallis test for comparisons between treatments and the PC group (Daniel, 1990). Significance between groups was accepted when $P < 0.05$.

RESULTS

Species Composition

A total of 27 species, belonging to 19 genera of endophytic mycobiota, associated with 10 dominant plant species along Wadi Tala were recorded (**Table 1**). The results showed that teleomorphic Ascomycota were represented by four species (14.82%) and anamorphic Ascomycota by 23 species (85.18 %). *Aspergillus* (four species; 14.82%), *Chaetomium* (three species; 11.11%), *Alternaria* (three species; 11.11%), *Penicillium* (two species; 7.41%), and the remaining genera each represented by only one species were detected. Among all endophytic species recorded, *C. globosum* represented the most prevalent endophyte isolated (22.34% of the total number of isolates per plate) followed by *Alternaria alternata* (19.32%), *Nigrospora oryzae* (16.77%), and *Sarocladium strictum* (8.72%).

TABLE 1 | Total count, number of cases of isolation, and frequency of fungal taxa recovered.

Species	TC*	NCI**	% F***
Ascomycota (teleomorphic)			
Chaetomium bostrychodes Zopf	13	6	0.6
Ch. Globosum Kunze	333	112	11.2
Ch. piluliferum J. Daniels	17	5	0.5
Thielavia terricola (J.C. Gilman & E.V. Abbott) C.W. Emmons	30	4	0.4
Ascomycota (anamorphic)			
Acremonium rutilum W. Gams	130	55	5.5
Alternaria alternate (Fr.) Keissl.	288	250	25
A. atrum (Preuss) Woudenberg & Crous	12	4	0.4
A. tenuissima (Kunze) Wiltshire	27	6	0.6
Aspergillus candidus Link	6	3	0.3
A. flavus Link	35	14	1.4
A. niger Tiegh.	42	28	2.8
A. terreus Thom	17	5	0.5
Botryotrichum piluliferum Sacc. & Marchal	7	7	0.7
Cladosporium cladosporioides (Fresen.) de Vries	13	9	0.9
Curvularia lunata (Wakker) Boedijn	7	3	0.3
Drechslera spicifera (Bainier) Arx	90	45	4.5
Fusarium solani (Mart.) Sacc.	45	15	1.5
Nigrospora oryzae (Berk. & Broome) Petch	250	230	23
Penicillium chrysogenum Thom	19	5	0.5
Penicillium rubrum Stoll	3	2	0.2
Phoma herbarum Westend.	14	7	0.7
Sarocladium strictum (W. Gams) Summerb.	55	25	2.5
Stachybotrys chartarum (Ehrenb.) S. Hughes	5	3	0.3
Stemphylium botryosum Sacc.	7	3	0.3
Trichothecium roseum (Pers.) Link	5	3	0.3
Trichoderma pseudokoningii Rifai	12	3	0.3
Ulocladium botrytis Preuss	8	3	0.3
Total	1490		

**Colonies/Cut; **Number of Cases of Isolation; ***Frequency.*

Phenotypic Identification of *C. globosum* Isolates

Seven isolates of *C. globosum* were morphologically identified. Colonies showed a daily growth rate of 7–8 mm, with pale or olivaceous aerial mycelia, often with yellow, gray–green, green or red exudates. Ascomata mature within 7–9 days, measured 175–280 μm, and were olivaceous, gray–green or brown in reflected light, and tended to be superficial, spherical,

ovate or obovate, and ostiolate. The ascomatal wall was brown in color and composed of textura intricate. The cells were 2.0–3.5 μm in breadth, and the ascomatal hairs were numerous, typically unbranched, flexuous, undulate or coiled, often tapering, septate, brownish, 3–4.5 μm in breadth at the base, and up to 500 μm in length. The asci were clavate or slightly fusiform, stalked, evanescent, measured 30–40 × 11–16 μm, and contained eight ascospores. Ascospores were limoniform, typically biapiculate, bilaterally flattened, brownish when mature, thick-walled, contained numerous droplets, measured 9–12 × 8–10 × 6–8 μm, and featured an apical germ pore. Paraphyses were not observed.

Therapeutic Effects of Secondary Metabolites of *C. globosum* on Disease Activity and Mobility Scores

Severe arthritis was clearly evident in rats by day 14 after subcutaneous injection of CFA at the base of the tail, and persisted for more than 32 days. Treatment of AIA rats with the methanolic extract (MCG6) resulted in a significant reduction ($P < 0.05$) in severity of the arthritis score in comparison to the untreated PC. This curative effect was observed in both the MCG6 and MTX groups, 6 days after treatment commenced. The anti-arthritic effect of MCG6 increased gradually until the end of the experiment, 29 days post CFA administration (**Figure 1A**).

At 20 days post CFA administration, the average arthritis score of MCG6 treated rats was 10.7 ± 0.82 (mean ± standard deviation) compared to 13.8 ± 0.98 in PC rats. In contrast, the rats treated with ethyl acetate extract of CG6 (EACG6) showed no improvement in arthritis score through out the experimental period (no significant differences were observed between EACG6 and PC groups).

A significant reduction in the mobility score was observed following treatment with MCG6 indicating a clinical improvement in joint function. This reduction was significantly lower than that of PC rats on day 26 (1.50 ± 0.55 and 3.33 ± 0.82 for MCG6 and PC groups, respectively), and this significance

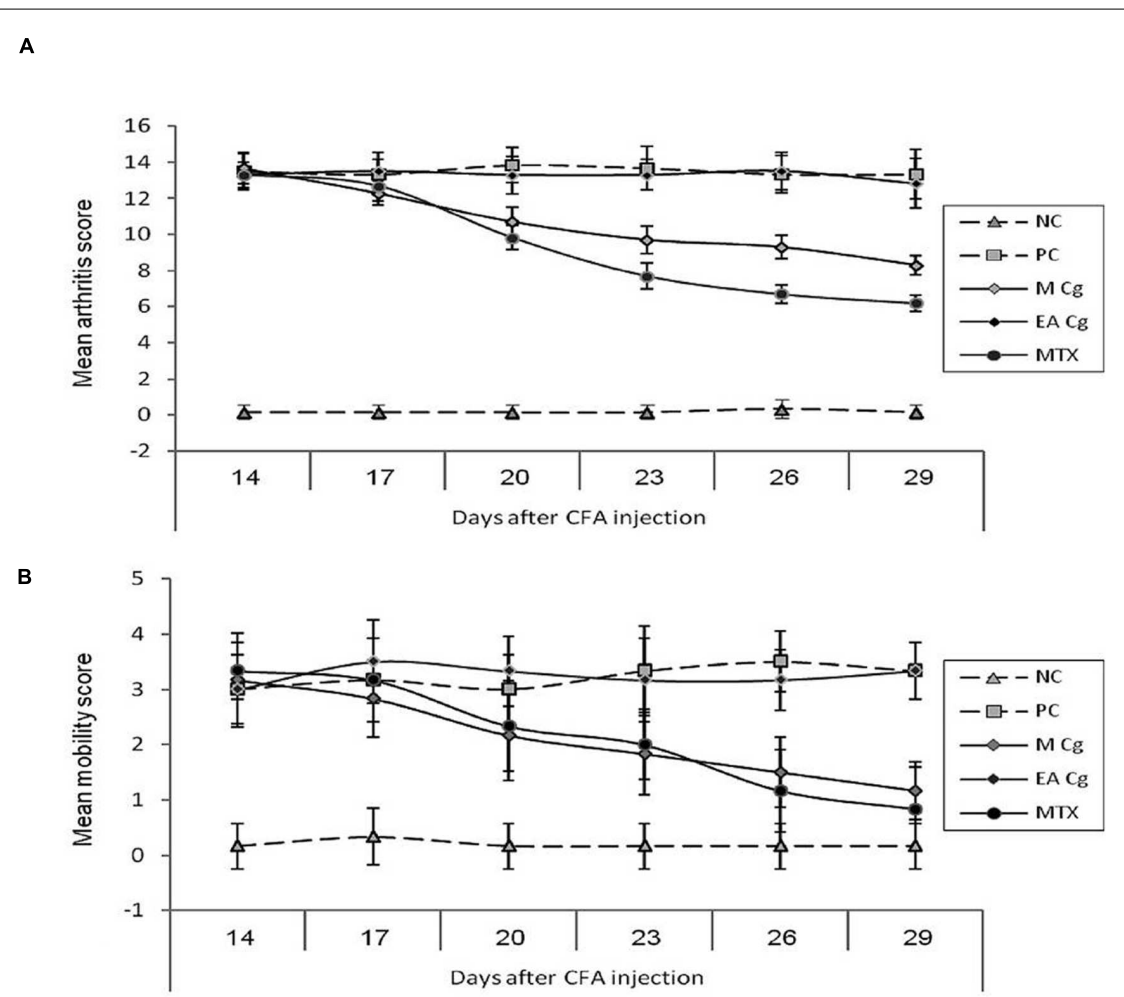


FIGURE 1 | Effect of *Chaetomium globosum* methanol (MCg) and ethyl acetate (EACg) extracts on the arithritis (graph A-mean arithritis score) and mobility scores (graph B-mean mobility score) after 14, 17, 20, 23, 26, and 29 days from arithritis induction. Mobility scale represented as 0 = normal, 1 = slightly impaired, 2 = major impairment, 3 = does not step on paw, and 4 = no movement.

persisted ($P < 0.05$) until the end of the treatment period at 29 days post CFA administration. The EACG6 group again showed no improvement in mobility scores and no significant differences were observed between the EACG6 and PC groups (**Figure 1B**).

Histopathology Findings

Sections of the control group that had been stained with (H & E) showed that the ankle joint was covered with typical hyaline cartilage (articular cartilage) on both surfaces, lacked a perichondrium and was separated by a joint cavity filled with articular fluid (**Figure 2**). Four zones were identified in the articular cartilage as follows: superficial tangential (with elongated chondrocytes and a long axis that was parallel to the surface), transitional (middle zone that contained scattered rounded chondrocytes), radial (with spherical chondrocytes arranged perpendicular to the surface), and calcified (that separated hyaline cartilage from the underlying subchondral bone) (**Figure 2A**).

The synovial membrane thickened and became infiltrated by inflammatory cells in the arthritic group. The thickened areas extended over, and penetrated deep into the articular cartilage, to form what is referred to as pannus and thereby, causing erosion and irregularity of the cartilage. The joint cavity was filled with exudation and inflammatory cells that included polymorphonuclear leukocytes, lymphocytes, and macrophages. The matrix of the nearby articular cartilage exhibited loss of basophilia (**Figure 2B**). Vascular synovium penetrated the cartilage and compressed the underlying bone. The chondrocytes were shrunken with darkened nuclei that were sometimes eccentric (**Figure 2C**).

The synovium was infiltrated with macrophages, lymphocytes, plasma cells, and fibroblast - like spindle cells that represented a mononuclear cellular inflammatory infiltrate. Plasma cells had eccentric nuclei and pink cytoplasm containing Russell bodies. As a prominent feature of the synovium was the presence of hyperplasia of spindle-shaped cells (**Figure 2D**).

The articular cartilage and bone beneath and beside the pannus were disrupted and areas of bone destruction were detected in the juxta-articular region (**Figure 3A**). The surface of the articular cartilage showed irregular textur, with surface erosions, and a loss of smooth contours (**Figure 3B**). The surrounding cartilage was characterized by a loss of basophilia in the matrix and degenerated chondrocytes. Many chondrocytes

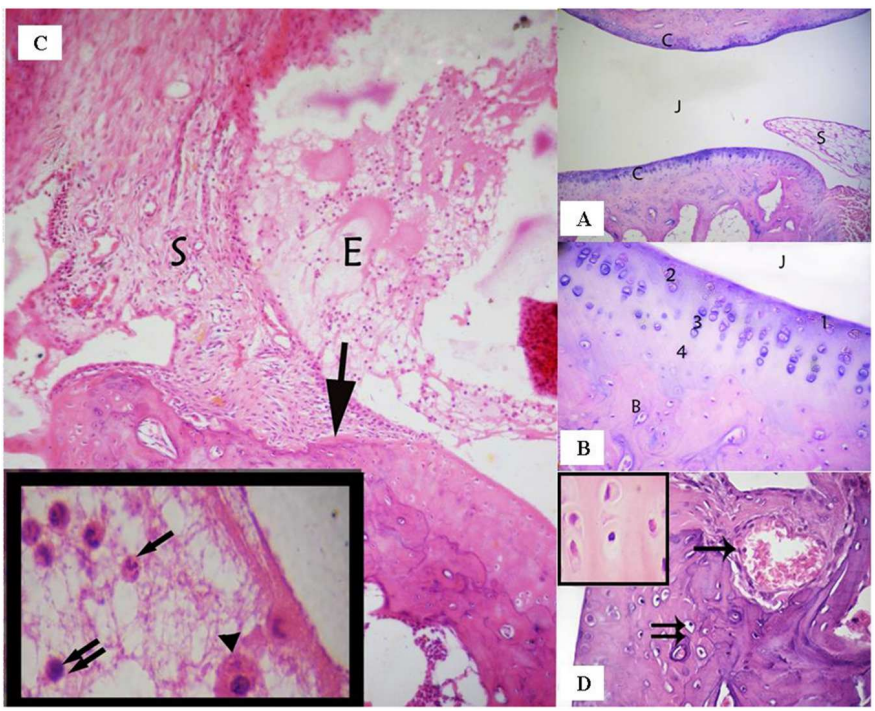


FIGURE 2 | (A) Ankle joint of the control group showing the articular cartilage **(C)**, the joint cavity (J), and the synovial membrane (S). (Control group, H & E, ×100). **(B)** Articular cartilage with its four zones: a superficial tangential zone (1), a transitional zone (2) that contained scattered chondrocytes, a radial zone (3) containing chondrocytes arranged perpendicular to the surface. A calcified zone (4) separating hyaline cartilage from the underlying subchondral bone **(B)**. (Control group, H & E, ×400). **(C)** A photomicrograph of the rheumatoid arthritis group showing infiltration of the synovial tissue (S) by inflammatory cells- that grows over the articular cartilage (↑) and causes its erosion and irregularity. The nearby articular cartilage has lost its basophilia. The joint cavity is filled with inflammatory cells and exudation (E). Inset: fluid filling the joint cavity contains fibrin deposits and many inflammatory cells, including polymorphonuclear leukocytes (↑), lymphocytes (↑↑), and macrophages (▲). (Arthritis group H & E, ×100, Inset ×1000). **(D)** A photomicrograph of arthritis group showing invasion of the cartilage matrix by fibrovascular synovial tissue that is compressing the underlying bone. Note: Blood vessels have invaded the cartilage matrix (↑). Notice also apoptotic chondrocytes (↑↑). Inset shows the acidophilic matrix of cartilaginous tissue and chondrocytes with darkened nuclei and shrunken cytoplasm; some chondrocytes have eccentric nuclei. (Arthritic group, H & E, ×400; Inset×1000).

appeared shrunken with acidophilic cytoplasm and pyknotic nuclei, vacuolated cytoplasm or darkened eccentric nuclei (**Figures 3C,D**). Various areas in the articular cartilage showed cell loss (**Figures 2D** and **3B**). The changes observed in the articular cartilage occurred peripherally and extended toward the center.

Examination of the MCG6 group showed that the ankle joint was covered by articular cartilage that was observed to be similar to that of the negative control group, except for the presence of some degenerated chondrocytes. The synovium was devoid of inflammatory cell infiltrates and the joint cavity was free of any exudates or inflammatory cells (**Figure 3C**).

Microscopic inspection of the EACG6 group showed that the synovium was hyperplastic and grew over the articular cartilage. The nearby cartilage exhibited an acidophilic matrix, some degenerated chondrocytes and areas of cell loss. The joint cavity showed an accumulation of cells and exudates without fibrin deposits (**Figure 3D**).

TEM Examination

Examination of TEM micrographs of the control group revealed that the chondrocytes had large vesicular nuclei, surrounded by faint cytoplasm with few organelles. The capsular or territorial zone that defines the matrix surrounding the cells, contained an abundance of randomly arranged collagen fibrils (**Figure 4A**). Degenerative changes were detected in the chondrocytes, including irregular contours, atrophied cell bodies, scanty cytoplasm, loss of cell processes, and dark irregular nuclei or vacuolated cytoplasm with many empty lacunae (**Figure 4B**). Examination of the MCG6 group revealed well-preserved chondrocytes with vesicular nuclei similar to those of the control group (**Figure 4C**). TEM studies of the EACG6 group showed shrunken chondrocytes with dark nuclei and apoptotic bodies. Many empty lacunae were also detected (**Figures 4D,E**).

Molecular Identification of the *C. globosum* (CG6) Isolate

The sequences of the ITS1–5.8 s–ITS2 rDNA region of the *C. globosum* (CG6) isolate were 510 bp in length. The NCBI database was accessed to identify the isolate using the BLAST homology search and the obtained ITS data. The ITS data of the isolated *C. globosum* (CG6) isolate was 99% identical to GenBank data of *C. globosum* (GenBank Accession Number JN209920).

DISCUSSION

Endophytic fungi represent an important factor in improving the drug discovery process, as they might consistently exhibit antimicrobial, anticancer, antiviral, and antioxidant

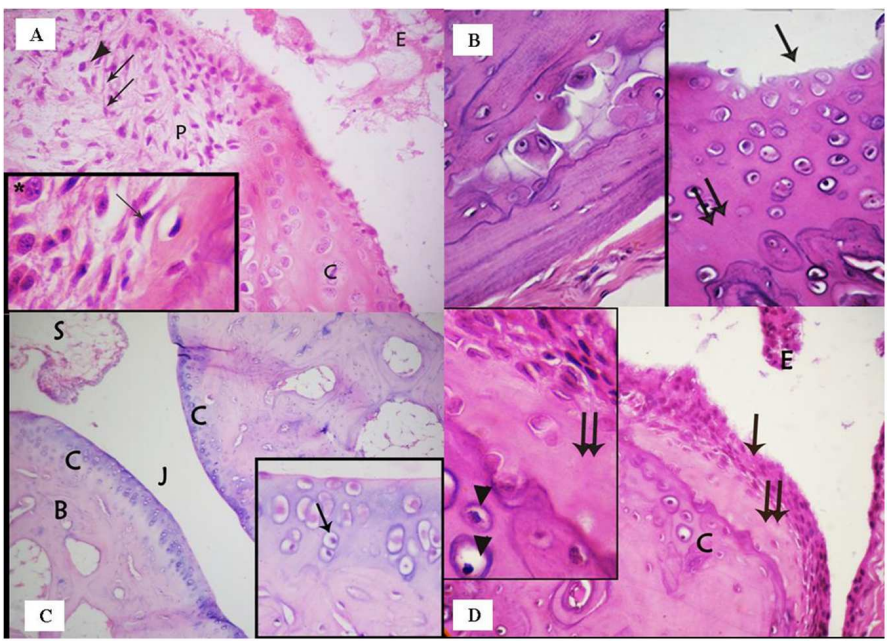


FIGURE 3 | (A) photomicrograph of the rheumatoid arthritis group showing infiltration of the synovial tissue by fibroblast – like spindle shaped cells (↑) and inflammatory cells, e.g., plasma cells (▲). Note that the nearby articular cartilage (C) has lost its basophilia. Notice also inflammatory cells and exudate (E) in the joint cavity. Inset: higher magnification of spindle shaped cells (↑) and plasma cells (*) in the synovium. (Arthritis group, H & E, ×400; Inset ×1000). **(B)** Photomicrograph of arthritis group showing: (a) areas of bone destruction within the bone matrix; (b) irregular surface of the articular cartilage with erosion on the surface (↑) and loss of its smooth contour. Note also areas of cell loss (↑↑). (Arthritis, H & E, ×400). **(C)** Photomicrograph of the ankle joint of the group treated with a methanolic extract of the fungus, showing the articular cartilage (C), the joint cavity (J), and synovial membrane (S). Few degenerated cells are evident (↑). (Methanolic extract group. H & E, ×100; Inset ×400). **(D)** Photomicrograph of the group treated with an ethanolic extract of the fungus showing the articular cartilage (C) covered by hyperplastic synovium (↑). The underlying cartilage has lost its basophilia and many chondrocytes appear degenerated. Inset: acidophilic matrix, area of cell loss (↑↑), and apoptotic chondrocytes (▲). (Ethyl acetate extract group, H & E, ×400; Inset×1000).

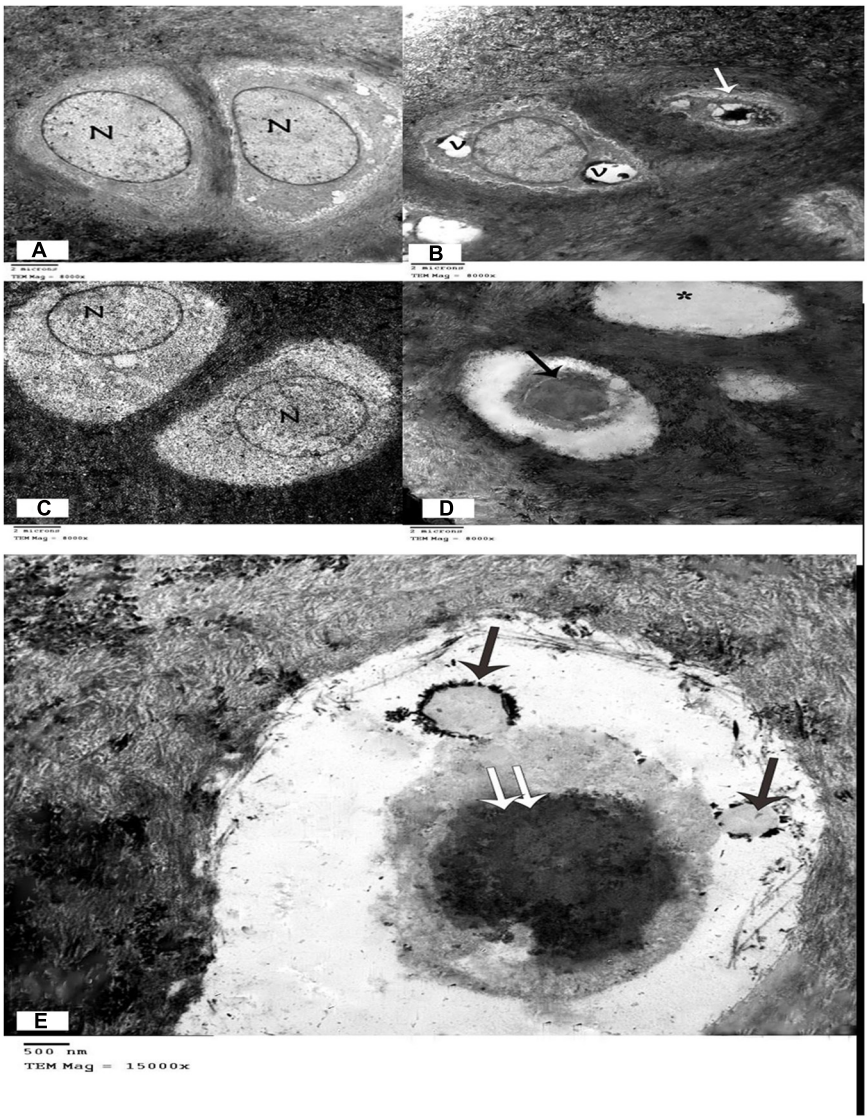


FIGURE 4 | (A) Electron micrograph showing two chondrocyte with lacunae. Vesicular nuclei (N), and cytoplasm with few organelles are evident. Chondrocytes are surrounded by a matrix full of collagen fibrils. (Control group, TEM, ×8000). **(B)** Electron micrograph of the arthritic group showing one chondrocyte with large vacuoles in the cytoplasm and another chondrocyte that appears shrunken with irregular contours, scanty cytoplasm, and a dark, irregular nucleus. (Arthritis group, TEM, ×8000). **(C)** Electron micrograph showing two chondrocytes within lacunae with vesicular nuclei and normal cytoplasm. (Group treated with methanolic extract of the fungus, TEM, ×8000). **(D)** Electron micrograph of the group treated with an ethyl acetate extract of the fungus, showing one shrunken chondrocyte with dark nucleus (↑), and empty lacuna (*). (Methanolic extract of the fungus group, TEM, ×8000). **(E)** Electron micrograph of the group treated with a methanolic extract of the fungus, showing apoptotic bodies (↑) in a shrunken chondrocyte with dark nucleus (↑↑). (Methanolic extract of the fungus group, TEM, ×15000).

activities (Strobel, 2002; Firáková et al., 2007; Debbab et al., 2011; Salem et al., 2013; Salem and Abdel-Azeem, 2014). Recently, anti-inflammatory and anti-thrombotic effects of a metabolite produced by Ascomycete fungal species were reported by Bollmann et al. (2015). Data of the present study regarding endophytic fungi showed that counts of fungal populations were relatively moderate. Similar observations of moderate fungal counts associated with medicinal plants from the Saint Katherine Protectorate have been recorded by several investigators (Selim et al., 2011, 2014; Abdel-Azeem and Salem, 2012). In comparison to endophytic taxa that have been previously isolated from the Saint Katherine Protectorate, our data indicates that some fungi are common to some species of medicinal plants, e.g., *C. globosum*, *Alternaria alternata,* and *Nigrospora oryzae*. These associations could be attributed to the chemical constituents of the plants. The ability of some of these plant species to live under water stress and the presence of various chemical compounds have been proven on endophytic actinomycetes by El-Shatoury et al. (2013) and on endophytic fungi in Saint Katherine Protectorate by Salem and Abdel-Azeem (2014). Tan and Zou (2001) reported that it is

possible to isolate hundreds of endophytic species from a single plant, with at least one of those species generally showing host specificity.

Rheumatoid arthritis is a severe, widespread disease that affects the joints of all age groups. Results of the present study showed a significant reduction ($P < 0.05$) in mobility scores and arthritic changes in both the MCG6- and MTX-treated AIA groups, in comparison to the PC group, whereas the EACG6 extract failed to either reduce or increase these scores. MTX was used as a first-line standard drug for the treatment of RA. The MCG6 dose administered in the present study (10 μg/Kg BW., twice weekly for 2 weeks) has for the first time been proven to significantly ameliorate histological features of the disease, joints inflammation, and severity of arthritis and improve motility as confirmed by histological and electron microscopic assessments. Joint exudates, inflammatory infiltration, pannus formation, synovial hyperplasia, cartilage degradation, and destruction of bone were all considerably reduced. Similarly, Gunatilaka (2006) stated that bioactive metabolites extracted from endophytes could be used as novel sources of antibiotics, immunosuppressants, antiparasitics, antioxidants, and anticancer agents. As RA is considered a reactive oxygen species (ROS)-linked disease (Valko et al., 2007), the beneficial effects of MCG6 might be due to its anti-oxidant properties that effectively combat the damage caused by ROS and oxygen – derived free radicals. Various types of biochemical compounds have been produced by *C. globosum*, including chaetoglobosins (cha; Zhang et al., 2010). Chaetoglobosins have anti-inflammatory properties and have been observed to significantly inhibit the production of tumor necrosis factor TNF-α, interleukin 6 (IL-6) and monocytes chemotactic protein-1 (MCP-1) (Dou et al., 2011). Hua et al. (2013) indicated that the cha-F metabolite has immunosuppressive properties that might prove useful in the control of dendritic cells associated with autoimmune and/or inflammatory diseases.

In the present study, the methanolic extract was found to be more effective than the ethyl acetate extract. Our results are consistent with those of Liu et al. (2007), who evaluated the antioxidant activity of the methanolic extract of endophytic *Xylaria* sp. isolated from *Ginkgo biloba*. The results indicated that in comparison to the ethyl acetate extract, the methanolic extract exhibited strong antioxidant activity, owing to the presence of phenolics and flavonoids. One host plant of *C. globosum* (CG6), *A. capillus-veneris,* contains many anti-inflammatory substances (Haider et al., 2013). The ability of this isolate (CG6) to produce anti-inflammatory substances could be attributed to its long period of co-evolution with *A. capillus-veneris*. This ability can also be expressed as the ability to produce the same or similar bioactive compounds as those produced by the host plants (Zhao et al., 2010, 2011).

CONCLUSION

In an AIA rat model that considered morphological, inflammatory, and histopathological features, metabolites of an endophytic native isolate of *C. globosum* (KC811080), recovered from maidenhair fern exhibit a direct inhibitory effects on RA. The present study highlights the remarkable use of fungal technology to produce potentially valuable products (anti-rheumatoid drugs), provides strong scientific evidence to the folkloric uses of this plant in the treatment of RA, and is interesting from a conservationist point of view, as isolated native endophytic taxa are maintained in the Fungarium of ASFC. We recommend further chemical studies to isolate the active principles of the extract of *C. globosum* evaluated in the present study.

AUTHOR CONTRIBUTIONS

All authors listed, have made substantial, direct, and intellectual contribution to the work, and approved it for publication.

ACKNOWLEDGMENTS

We deeply appreciate the kind assistance of Ms. Fatma M. Salem (Faculty of Science, Botany Department, Suez Canal University, Ismailia, Egypt) during sampling and isolation of endophytic fungi.

REFERENCES

Abdel-Azeem, A. M., and Salem, F. M. (2012). Biodiversity of Laccase producing fungi in Egypt. *Mycosphere* 3, 900–920.

Abdel-Azeem, A. M., Salem, F. M., Mohamed, H. M., Rashad, H. M., Mohamed, R. M., and Khalil, W. F. (2012). "Bioprospecting of Egyptian fungi for ecological and medical applications," in *Proceedings of the 8th Meeting on TWAS-ARO, Bibilotheca Alexandrina, December 30–31*. Available at: http://www.bibalex.gov.eg/CSSP/Presentations/Attachments/Fatma%20Salem/play.htm

Abdel-Monem, N. M., Abdel-Azeem, A. M., El-Ashry, E. H., Ghareeb, D. A., and Nabil-Adam, A. (2013). Pretreatment hepatoprotective effect of the marine fungus derived from sponge on hepatic toxicity induced by heavy metals in rats. *BioMed. Res. Int.* 2013:510879. doi: 10.1155/2013/510879

Abdel-Motaal, F. F., Nassar, M. S. M., El-Zayat, S. A., El-Sayed, M. A., and Ito, S. (2010). Antifungal activity of endophytic fungi isolated from Egyptian henbane (*Hyoscyamus muticus* L.). *Pak. J. Bot.* 42, 2883–2894.

Ablin, J. N., Entin-Meer, M., Aloush, V., Oren, S., Elkayam, O., George, J., et al. (2010). Protective effect of eotaxin-2 inhibition in adjuvant-induced arthritis. *Clin. Exp. Immunol.* 161, 276–283. doi: 10.1111/j.1365-2249.2010.04172.x

Aggarwal, R., Sharma, V., Kharbikar, L., and Renu, L. (2008). Molecular characterization of *Chaetomium* species using URP-PCR. *Genet. Mol. Biol.* 31, 943–946. doi: 10.1590/S1415-47572008005000014

Alarcon, G. S., Tracy, I. C., and Blackburn, WDJr (1989). Methotrexate in rheumatoid arthritis: toxic effects as the major factor in limiting long-term treatment. *Arthritis Rheum.* 32, 671–676. doi: 10.1002/anr.1780320603

Aly, A. H., Debbab, A., and Proksch, P. (2011). Fungal endophytes: unique plant inhabitants with great promises. *Appl. Microbiol. Biotechnol.* 90, 1829–1845. doi: 10.1007/s00253-011-3270-y

Aly, A. H., Edrada-Ebel, R., Wray, V., Muller, W. E. G., Kozytska, S., Hentschel, U., et al. (2008). Bioactive metabolites from the endophytic fungus *Ampelomyces* sp. isolated from the medicinal plant *Urospermum picroides*. *Phytochemistry* 69, 1716–1725. doi: 10.1016/j.phytochem.2008.02.013

Bancroft, J. D., and Gamble, M. (2008). *Theory and Practice of Histological Techniques*, 6th Edn. Philadelphia, PA: Churchill Livingstone.

Bancroft, J. D., and Stevens, A. L. (1996). *Theory and Practice of Histological techniques*, 4th Edn. Edinburgh: Churchill Livingstone.

Bartlett, M. S. (1937). Properties of sufficiency and statistical tests. *Proc. R. Soc. A* 160, 268–282. doi: 10.1098/rspa.1937.0109

Bashyal, B. P., Wijeratne, E. M., Faeth, S. H., and Gunatilaka, A. A. (2005). Globosumones A-C, cytotoxic orsellinic acid esters from the Sonoran desert endophytic fungus *Chaetomium globosum*. *J. Nat. Prod.* 68, 724–728. doi: 10.1021/np058014b

Bendele, A. (2001). Animal models of rheumatoid arthritis. *J Musculoskelet. Neuronal Interact.* 1, 377–385.

Bollmann, F., Jäckel, S., Schmidtke, L., Schrick, K., Reinhardt, C., Jurk, K., et al. (2015). Anti- Inflammatory and anti-thrombotic effects of the fungal metabolite galiellalactone in apolipoprotein e-deficient mice. *PLoS ONE* 10:e0130401. doi: 10.1371/journal.pone.0130401

Booth, C. (1971). *The Genus Fusarium*. Kew: Commonwealth Mycological Institute.

Chapuis, A. G., Rizzardi, G. P., D'Agostino, C., Attinger, A., Knabenhans, C., Fleury, S., et al. (2000). Effects of mycophenolic acid on human immunodeficiency virus infection in vitro and in vivo. *Nat. Med.* 6, 762–768. doi: 10.1038/77489

Cohen, S. D. (2006). Host selectivity and genetic variation of *Discula umbrinella* isolates from two oak species: analyses of intergenic spacer region sequences of ribosomal DNA. *Microb. Ecol.* 52, 463–469. doi: 10.1007/s00248-006-9073-5

Daniel, W. W. (1990). *Applied Nonparametric Statistics*, 2nd Edn. Boston, MA: PWS- Kent.

Debbab, A., Aly, A. H., and Proksch, P. (2011). Bioactive secondary metabolites from endophytes and associated marine derived fungi. *Fungal Divers.* 49, 1–12. doi: 10.1007/s13225-011-0114-0

Ding, G., Song, Y. C., Chen, J. R., Xu, C., Ge, H. M., Wang, X. T., et al. (2006). Chaetoglobosin U, a cytochalasan alkaloid from endophytic *Chaetomium globosum* IFB-E019. *J. Nat. Prod.* 69, 302–304.

Domsch, K. H., Gams, W., and Anderson, T. H. (2007). *Compendium of Soil Fungi*, 2nd Edn. Eching: IHW-Verlag & Verlagsbuchhandlung.

Dou, H., Song, Y., Liu, X., Gong, W., Li, E., Tan, R., et al. (2011). Chaetoglobosin Fex from the marine-derived endophytic fungus inhibits induction of inflammatory mediators via toll-like receptor 4 signaling in macrophages. *Biol. Pharm. Bull.* 34, 1864–1873. doi: 10.1248/bpb.34.1864

Doveri, F. (2013). An additional update on the genus *Chaetomium* with descriptions of two coprophilous species, new to Italy. *Mycosphere* 4, 820–846. doi: 10.5943/mycosphere/4/4/17

Ellis, M. B. (1971). *Dematiaceous Hyphomycetes*. Kew: Commonwealth Mycological Institute.

Ellis, M. B. (1976). *More Dematiaceous Hyphomycetes*. Kew: Commonwealth Mycological Institute.

El-Morsy, E. M. (2000). Fungi isolated from the endorhizosphere of halophytic plants from Red Sea Coast of Egypt. *Fungal Divers.* 5, 43–54.

El-Shatoury, S. A., El-Kraly, O. A., Trujillo, M. E., El-Kazzaz, W. M., El-Din, E. G., and Dewedar, A. (2013). Generic and functional diversity in endophytic actinomycetes from wild Compositae plant species at South Sinai - Egypt. *Res. Microbiol.* 2, 1–9. doi: 10.1016/j.resmic.2013.03.004

Firáková, S., Šturdíková, M., and Múčková, M. (2007). Bioactive secondary metabolites produced by microorganisms associated with plants. *Biologia* 62, 251–257. doi: 10.1016/j.ymben.2015.07.002

Fisher, P. J., Petrini, O., and Sutton, B. E. (1993). A comparative study of fungal endophytes in leaves, xylem and bark of Eucalyptus in Australia and England. *Sydowia* 45, 338–345.

Fujimoto, H., Sumino, M., Okuyama, E., and Ishibashi, M. (2004). Immunomodulatory constituents from an ascomycete, *Chaetomium seminudum*. *J. Nat. Prod.* 67, 98–102. doi: 10.1021/np0302201

Guarro, J., Gene, J., Stchigel, A. M., and Figueras, M. J. (2012). *Atlas of Soil Ascomycetes*. Holland: CBS-KNAW Fungal Biodiversity Centre.

Gunatilaka, A. A. L. (2006). Natural products from plant-associated microorganisms: distribution, structural diversity, bioactivity, and implications of their occurrence. *J. Nat. Prod*. 69, 509–526. doi: 10.1021/np058128n

Haider, S., Nazreen, S., Alam, M. M., Gupta, A., Hamid, H., and Alam, M. S. (2013). Anti-inflammatory and anti-nociceptive activities of two new triterpenoids from *Adiantum capillus-veneris* Linn. *J. Ethnopharmacol.* 138, 741–747. doi: 10.1080/14786419.2013.828292

Hsu, J. C. (1996). *Multiple Comparisons*. London: Chapman & Hall.

Hua, C., Yang, Y., Sun, L., Dou, H., Tan, R., and Hou, Y. (2013). Chaetoglobosin F, a small molecule compound, possesses immunomodulatory properties on bone marrow-derived dendritic cells via TLR9 signaling pathway. *Immunobiology* 218, 292–302. doi: 10.1016/j.imbio.2012.05.015

Isham, C. R., Tibodeau, J. D., Jin, W., Xu, R., Timm, M. M., and Bible, K. C. (2007). Chaetocin: a promising new antimyeloma agent with in vitro and in vivo activity mediated via imposition of oxidative stress. *Blood* 109, 2579–2588. doi: 10.1182/blood-2006-07-027326

Jiao, W., Feng, Y., Blunt, J. W., Cole, A. L., and Munro, M. H. (2004). Chaetoglobosins Q, R, and T, three further new metabolites from *Chaetomium globosum*. *J. Nat. Prod.* 67, 1722–1725.

Karmakar, S., Kay, J., and Gravallese, E. M. (2010). Bone damage in rheumatoid arthritis: mechanistic insights and approaches to prevention. *Rheum. Dis. Clin. North Am.* 36, 385–404. doi: 10.1016/j.rdc.2010.03.003

Kirk, P. M., and Ansell, A. E. (1992). *Authors of Fungal Names*. Kew: CAB International.

Kirk, P. M., Cannon, P. F., Minter, D. W., and Stalpers, J. A. (2008). *Ainsworth & Bisby's Dictionary of the Fungi*, 10th Edn. Wallingford, CT: CAB International.

Klich, M. A. (2002). *Identification of Common Aspergillus species*. Utrecht: Centralbureau voor Schimmelcultures.

Kobayashi, M., Kanasaki, R., Sato, I., Abe, F., Nitta, K., Ezaki, M., et al. (2005). FR207944, an antifungal antibiotic from *Chaetomium* sp. 217 I. Taxonomy, fermentation, and biological properties. *Biosci. Biotechnol. Biochem.* 69, 515–521. doi: 10.1271/bbb.69.515

Liu, X., Dong, M., Chen, X., Jiang, M., Lv, X., and Yan, G. (2007). Antioxidant activity and phenolics of an endophytic *Xylaria* sp. from Ginkgo biloba. *Food Chem.* 105, 548–554. doi: 10.1016/j.foodchem.2007.04.008

Liu, X., Dong, M., Chen, X., Jiang, M., Lv, X., and Zhou, J. (2008). Antimicrobial activity of an endophytic *Xylaria* sp.YX-28 and identification of its antimicrobial compound 7-amino- 4-methylcoumarin. *Appl. Microbiol. Biotechnol.* 78, 241–247. doi: 10.1007/s00253-007-1305-1

Lull, C., Wichers, H. J., and Savelkoul, H. F. J. (2005). Antiinflammatory and immunomodulating properties of fungal metabolites. *Mediators Inflamm.* 2005, 63–80. doi: 10.1155/MI.2005.63

Matsumoto, K., Tanaka, K., Matsutani, S., Sakazaki, R., Hinoo, H., Uotani, N., et al. (1995). Isolation and biological activity of thielocins: novel phospholipase A2 inhibitors produced by *Thielavia terricola* RF-143. *J. Antibiot.* 48, 106–112. doi: 10.7164/antibiotics.48.106

Moreland, L. W., Heck, L. W. Jr., and Koopman, W. J. (1997). Biologic agents for treating rheumatoid arthritis: concepts and progress. *Arthritis Rheum.* 40, 397–409. doi: 10.1002/art.1780400302

Moustafa, A. F., and Abdel-Azeem, A. M. (2005). The genus *Chaetomium* in Egypt. *El-Minia Sci. Bull.* 16, 235–256.

Mustafa, A. I., Abdel-Azeem, A. M., and Salem, F. M. (2013). "Surveying and exploitation of some taxa for extracellular biosynthesis of silver nanoparticles," in *Proceedings of the Third International Congress on Fungal Conservation*, Akyaka, 11–15.

Newman, D. J., and Cragg, G. M. (2007). Natural products as sources of new drugs over the last 25 years. *J. Nat. Prod.* 70, 461–477. doi: 10.1021/np068054v

Ngian, G. S. (2010). Rheumatoid arthritis. *Aust. Fam. Physician* 39, 626–628.

Petrini, O. (1991). "Fungal endophytes of tree leaves," in *Microbial Ecology of Leaves*, eds J. H. Andrews and S. S. Hirane (NewYork, NY: Springer), 179–197.

Pitt, J. I. (1980). *The Genus Penicillium and its Teleomorphic States Eupenicillium and Talaromyces*. London: Academic Press.

Raper, K. B., and Thom, C. A. (1949). *A Manual of the Penicillia*. Baltimore, MD: Williams & Wilkins.

Salem, F. M., and Abdel-Azeem, A. M. (2014). *Screening of Anticancer Metabolites Produced by Endophytic Fungi*. Saarbrücken: LAP LAMBERT Academic Publishing.

Salem, F. M., and Abdel-Azeem, A. M. (2015). "The influence of altitude on diversity of fungal endobionts of some medicinal plants in Egypt," in *Proceedings of the The Six International Conference of the ESES*, Ismailia.

Salem, F. M., Abdel-Azeem, A. M., Khalil, W. F., Zaki, S. M., and Saleh, S. Y. (2013). "Bioprospecting and conservation of Egyptian endophytic mycobiota:

taxa producing anticancer metabolites," in *Proceedings of the Third International Congress on Fungal Conservation*, Akyaka, 11–15.

Schmidt, N., Art, J., Forsch, I., Werner, A., Erkel, G., Jung, M., et al. (2012). The anti-inflammatory fungal compound (s)-curvularin reduces proinflammatory gene expression in an in vivo model of rheumatoid arthritis. *J. Pharmacol. Exp. Ther.* 343, 106–114. doi: 10.1124/jpet.112.192047

Schulz, B., Boyle, C., Draeger, S., Rommert, A. K., and Krohn, K. (2002). Endophytic fungi: a source of novel biologically active secondary metabolites. *Mycol. Res.* 106, 996–1004. doi: 10.1017/S0953756202006342

Selim, K. A., El-Beih, A. A., Abdel-Rahman, T. M., and El-Diwany, A. I. (2011). Biodiversity and antimicrobial activity of endophytes associated with Egyptian medicinal plants. *Mycosphere* 2, 669–678. doi: 10.5943/mycosphere/2/6/7

Selim, K. A., El-Beih, A. A., Abdel-Rahman, T. M., and El-Diwany, A. I. (2014). Biological evaluation of endophytic fungus, *Chaetomium globosum* JN711454, as potential candidate for improving drug discovery. *Cell Biochem. Biophys.* 68, 67–82. doi: 10.1007/s12013-013-9695-4

Soni, S. K., and Soni, R. (2010). Regulation of cellulase synthesis in *Chaetomium* erraticum. *BioResources* 5, 81–98.

Souza, A. D. L., Rodrigues-Filho, E., Souza, A. Q. L., Pereira, J. O., Calgarotto, A. K., Maso, V., et al. (2008). Koninginins, phospholipase A2 inhibitors from endophytic fungus *Trichoderma Koningii*. *Toxicon* 51, 240–250. doi: 10.1016/j.toxicon.2007.09.009

Strobel, G., and Daisy, B. (2003). Bioprospecting for microbial endophytes and their natural products. *Microbiol. Mol. Biol. Rev.* 67, 491–502. doi: 10.1128/MMBR.67.4.491-502.2003

Strobel, G. A. (2002). Rainforest endophytes and bioactive products. *Crit. Rev. Biotechnol.* 22, 315–333. doi: 10.1080/07388550290789531

Suryanarayanan, T. S., Thirunavukkarasu, N., Govindarajulu, M. B., Sasse, F., Jansen, R., and Murali, T. S. (2009). Fungal endophytes and bioprospecting. *Fungal Biol. Rev.* 23, 9–19. doi: 10.1016/j.fbr.2009.07.001

Suzuki, H., Hirano, N., Watanabe, C., and Tarumoto, Y. (1997). Carbon tetrachloride does not induce micronucleus in either mouse bone marro or peripheral blood. *Mutat. Res.* 394, 77–80. doi: 10.1016/S1383-5718(97)00128-9

Tan, R. X., and Zou, W. X. (2001). Endophytes: a rich source of functional metabolites. *Nat. Prod. Rep.* 18, 448–459. doi: 10.1039/b100918o

Valko, M., Leibfritz, D., Moncol, J., Cronin, M. T. D., Mazur, M., and Telser, J. (2007). Free radicals and antioxidants in normal physiological functions and human disease. *Int. J. Biochem. Cell Biol.* 39, 44–84. doi: 10.1016/j.biocel.2006.07.001

White, T., Bruns, T., Lee, S., and Taylor, J. (1990). "Amplification and direct sequencing of fungal ribososmal RNA genes for phylogenetics," in *PCR Protocols*, eds M. Innis, D. Gelfand, J. Sninsky, and T. White (New York, NY: Academic Press, Inc.), 315–322.

Williams, H. J., Willkens, R. F., Samuelson, C. O. Jr., Alarcon, G. S., Guttadauria, M., Yarboro, C., et al. (1985). Comparison of low-dose oral pulse methotrexate and placebo in the treatment of rheumatoid arthritis: a controlled clinical trial. *Arthritis Rheum.* 28, 721–730. doi: 10.1002/art.1780280702

Winer, B. J., Brown, D. R., and Michael, K. M. (1991). *Statistical Principles in Experimental Design*. New York, NY: McGraw-Hill Book Company.

Zhang, J., Ge, H. M., Jiao, R. H., Li, J., Peng, H., and Wang, Y. R. (2010). Cytotoxic chaetoglobosins from the endophyte *Chaetomium globosum*. *Planta Med.* 76, 1910–1914. doi: 10.1055/s-0030-1249936

Zhao, J., Shan, T., Mou, Y., and Zhou, L. (2011). Plant-derived bioactive compounds produced by endophytic fungi. *Mini Rev. Med. Chem.* 11, 159–168. doi: 10.2174/138955711794519492

Zhao, J., Zhou, L., Wang, J., Shan, T., Zhong, L., Liu, X., et al. (2010). "Endophytic fungi for producing bioactive compounds originally from their host plants," in *Current Research, Technology and Education Topics in Applied Microbiology Microbial Biotechnology*, ed. M. A. Vilas (Badajoz: Formatex Research Center), 567–576.

Conflict of Interest Statement: The authors declare that the research was conducted in the absence of any commercial or financial relationships that could be construed as a potential conflict of interest.

Copyright © 2016 Abdel-Azeem, Zaki, Khalil, Makhlouf and Farghaly. This is an open-access article distributed under the terms of the Creative Commons Attribution License (CC BY). The use, distribution or reproduction in other forums is permitted, provided the original author(s) or licensor are credited and that the original publication in this journal is cited, in accordance with accepted academic practice. No use, distribution or reproduction is permitted which does not comply with these terms.

frontiers in Microbiology

ORIGINAL RESEARCH
published: 23 September 2016
doi: 10.3389/fmicb.2016.01513

Integral Use of Amaranth Starch to Obtain Cyclodextrin Glycosyltransferase, by *Bacillus megaterium*, to Produce β-Cyclodextrin

María Belem Arce-Vázquez[1], Edith Ponce-Alquicira[1], Ezequiel Delgado-Fornué[2], Ruth Pedroza-Islas[3], Gerardo Díaz-Godínez[4] and J. Soriano-Santos[1]**

[1] Department of Biotechnology, Metropolitan Autonomus University, Mexico, Mexico, [2] Department of Wood, Cellulose and Paper, Biomaterials Research Center, University of Guadalajara, Jalisco, Mexico, [3] Department of Engineering and Chemistry, Iberoamericana University, Mexico, Mexico, [4] Laboratory of Biotechnology, Research Center for Biological Sciences, Autonomous University of Tlaxcala, Tlaxcala, México

OPEN ACCESS

Edited by:
Bhim Pratap Singh, Mizoram University, India

Reviewed by:
Ram Prasad, Amity University, India
Mukesh Kumar Yadav, Korea University, South Korea

***Correspondence:**
Gerardo Díaz-Godínez
diazgdo@hotmail.com
J. Soriano-Santos
jss@xanum.uam.mx

Specialty section:
This article was submitted to Microbiotechnology, Ecotoxicology and Bioremediation, a section of the journal Frontiers in Microbiology

Received: *18 July 2016*
Accepted: *09 September 2016*
Published: *23 September 2016*

Citation:
Arce-Vázquez MB, Ponce-Alquicira E, Delgado-Fornué E, Pedroza-Islas R, Díaz-Godínez G and Soriano-Santos J (2016) Integral Use of Amaranth Starch to Obtain Cyclodextrin Glycosyltransferase, by Bacillus megaterium, to Produce β-Cyclodextrin. Front. Microbiol. 7:1513. doi: 10.3389/fmicb.2016.01513

Cyclodextrin glycosyltransferase (CGTase) is an enzyme that produces cyclodextrins (CDs) from starch and related carbohydrates, producing a mixture of α-, β-, and γ-CDs in different amounts. CGTase production, mainly by *Bacillus* sp., depends on fermentation conditions such as pH, temperature, concentration of nutrients, carbon and nitrogen sources, among others. *Bacillus megaterium* CGTase produces those three types of CDs, however, β-CD should prevail. Although, waxy corn starch (CS) is used industrially to obtain CGTase and CDs because of its high amylopectin content, alternative sources such as amaranth starch (AS) could be used to accomplish those purposes. AS has high susceptibility to the amylolytic activity of CGTase because of its 80% amylopectin content. Therefore, the aim of this work was evaluate the AS as carbon source for CGTase production by *B. megaterium* in a submerged fermentation. Afterwards, the CGTase was purified partially and its activity to synthesize α-, β-, and γ-CDs was evaluated using 1% AS as substrate. *B. megaterium* produced a 66 kDa CGTase (Topt = 50°C; pHopt = 8.0), from the early exponential growth phase which lasted 36 h. The maximum CGTase specific activity (106.62 ± 8.33 U/mg protein) was obtained after 36 h of culture. CGTase obtained with a Km = 0.152 mM and a Vmax = 13.4 μM/min yielded 40.47% total CDs using AS which was roughly twice as much as that of corn starch (CS; 24.48%). High costs to produce CDs in the pharmaceutical and food industries might be reduced by using AS because of its higher α-, β- and γ-CDs production (12.81, 17.94, and 9.92%, respectively) in a shorter time than that needed for CS.

Keywords: amaranth starch, CGTase, cyclodextrin, submerged fermentation, *Bacillus megaterium*

INTRODUCTION

Cyclodextrins (CDs) are synthesized from starch and related carbohydrates such as amylose, amylopectin and maltooligosaccharide by cyclodextrin glycosyltransferase (CGTase, E.C.2.4.1.19) which is a bacterial extracellular enzyme (Ahmed and El-Refai, 2010). CGTase catalyzes the CDs formation from starch via inter- and intramolecular transglycosylation reactions, which include

cycization, disproportionation, coupling, and hydrolysis. CGTases usually produce a mixture of CDs, glucose, maltose, and other oligosaccharides with varying polymerisation degrees. The main natural CDs are α-, β-, and γ-CDs containing 6, 7, and 8 glucopyranose units, respectively. CDs have a unique structure of hydrophobic cavity of different diameter smaller than 0.6, 0.8, and 1.0 nm, respectively and hydrophylic surface. Furthermore, CDs are typical host molecules and may encapsulate a great variety of molecules to form crystalline inclusion complexes. The size/shape relationship and hydrogen bond interactions are vital for stability of the guest/host inclusion complex (Anselmi et al., 2008). Thus, the formation of the inclusion complexes modifies the physical and chemical properties of the host molecule, mostly in terms of water solubility. In this sense, CDs are important ingredients as molecular encapsulators for applications in food, cosmetic, and pharmaceutical industries (Sivakumar and Shakilabanu, 2013). For instance, topical application of ferulic acid (FA) may be useful for preventing skin cancer, but its application on the skin is limited by the poor stability of FA. The problem may be overcome by the use of CDs to form stable inclusion complexes to increase the stability of the active principle, and improve its solubility, bioavailability and delivery on the skin. Due to the importance of CDs and the derivatives, their safety and toxicological profiles have been reviewed. Oral administration of α-CD is, in general, well tolerated and is not associated with significant adverse effects. α-CD is not metabolized in the upper intestinal tract and its cleavage is only due to the intestinal flora of cecum and colon. β-CD has low aqueous solubility and side effects (e.g., nephrotoxicity), for this reason can be used orally because by this route is normally non-toxic. β-CD binds cholesterol, is absorbed in small scale (1–2%) in the upper intestinal tract after oral administration, and is less irritating than α-CD after intramuscular injection. β-CD is the most commonly used CD in pharmaceutical formulations, and thus, it is probably the most studied in humans. Comparing the toxicological profile of the three natural CDs, γ-CD seems to be the least toxic. But its complexes normally have limited solubility in aqueous solutions and tend to self-aggregate; therefore, its complexing abilities are limited compared to those of β-CD and some water-soluble β-CD derivatives (Sá Couto et al., 2015). A comparative analysis of more than 30 currently known CD containing pharmaceutical formulations shows that β-CD is the most commonly employed. The reason for this lies in the ease of its production and subsequent low price (more than 10,000 tons produced annually with an average bulk price of approximately 5 USD per kg). However, β-CD has some drawbacks, mainly its relatively poor aqueous solubility. Due to its, β-CD is unsuitable for parenteral administration. A universal solution to this problem was found in the substitution of multiple β-CD hydroxyls on both rims of the molecule resulting in a notably improved aqueous solubility (Kurkov and Loftsson, 2013).

CGTase is produced by bacteria, which can be found in various places such as soil, waste plantation, hot springs and even in deep sea mud. These bacteria are mostly *Bacillus* sp. However, *Klebsiella pneumoniae*, *Micrococcus luteus*, *Thermococcus* sp., *Brevibacterium* sp. and hyperthermophilic archaea are also reported as CGTase producers. The bacterial strain *Bacillus macerans* is the most frequently used source of the CGTase enzyme, but *B. megaterium* isolated from soil has also been utilized to optimize the CGTase production (Sivakumar and Shakilabanu, 2013). CGTase produced by *B. megaterium*, forms all three types of CDs, but the predominant product is β-CD (Pishtiyski et al., 2008). During the past 2 decades, 51 different CGTase crystal structures, isolated from bacteria, have been published. The 3D structures of CGTases from these sources are quite similar (>60%). According to the different CD specificities. α-, β-, or γ-CDs; CGTases are usually clasified into 3 subgroups (α-, β-, and γ-CGTases), which often have different CD specificities. *Paenibacillus macerans*, *Bacillus circulans*, *Alkaliphillic Bacillus* sp. and *Bacillus agaradhaerens* are commonly used to produce β-CD, because of it is catalyzed by a β-CGTase. Production of CGTase by *B. megaterium* and its optimized parameters are known, however, all CGTases produce α-, β-, and γ-CDs from starch in different ratios depending on the nature of CGTase and the reaction conditions (Han et al., 2014). Therefore, this study was also conducted to know the specificity of CGTase from *B. megaterium* as well as the CDs ratio that produced using amaranth starch (AS) as an alternative carbon source. Other strategy could be that used by Zhou et al. (2012), where they produce a recombinant α-CGTase by adapting its original α-CGTase gene to the codon usage of *B. megaterium* by systematic codon optimization. CGTase production can be improved by manipulating fermentation conditions such as pH, temperature, concentrations of nutrients and compositions of the production media (carbon and nitrogen sources). Sivakumar and Shakilabanu (2013) found that maltose was the best carbon source and yeast extract was the best nitrogen source for CGTase production using *B. megaterium*. Moreover, Ca^{2+} also influences the enzyme production. Optimization of culture conditions of CGTase production by *B. megaterium* NCR has been reported by Ahmed and El-Refai (2010). They found that fermentation time and K_2HPO_4 level were crucial factors in order to improve enzyme production process. Recently, the continuous operation has been chosen over the batch system, because it offers a greater process control, high productivity and an improvement of quality and yield. Thus, Rakmai and Cheirsilp (2016) have informed about a continuous production of β-CD by immobilized CGTase in mixed gel beads performed in a continuous stirred tank reactor and a packed bed reactor. Soluble corn starch (CS) has commonly been used as the substrate for CGTase production. Molecules of amylose and amilopectin (starch fractions) are organized into quasicrystalline macromolecular aggregates called starch granules. The size, shape, and structure of these granules vary substantially among botanical sources. The proportion of amylose and amylopectin in starches also vary with their source, but they usually fall in the range of 20–30% of amylose in normal cereral starch. Various types of starch can be used as substrate for CDs production, such as starch of potato and tapioca among others. Amylopectin gives higher yield of CDs because the reaction with CGTase begins at the non-reducing end of this branched molecule. Many efforts have been made to improve the production of CDs. For instance, to determine the optimal condition for β-CD production, it is essential

to understand the kinetics of the reaction. Until now, there have been several reports on factors affecting CD production by CGTases from several microorganisms. Some reports have focused on the kinetics of CGTase, but most of them have only focused on the effect of substrate concentation. The β-CD production by different sources of CGTase leads to a change in the kinetic behavior with impact on yield and productivity. The source of starch affect temperature for gelatinization, substrate concentration, enzyme concentration and reaction temperature on kinetics of β-CD production by CGTase (Cheirsilp et al., 2010).

Amaranth is a pseudo-cereal consumed mainly in Mexico and in Central and South America. Its starch content is around 58–66% and contain lysine at similar level to that of milk casein. AS is of a waxy or glutinous kind and consists of spherical, angular or poligonal granules with an exceptionally small size, ranging from 0.5 to 3 μm in diameter, which gives it high dispersibility. Amylose content in amaranth starch is exceptionally low, in the range 0–14%. Therefore, amaranth starch granules have high susceptibility to amylases because of their exceptionally high amylopectin content (Kong et al., 2009). Urban et al. (2012) used starch from *Amaranthus cruentus* to produce α-, β-, and γ-CDs by CGTase from *Paenibacillus macerans* CCM 2012. CGTase was obtained using soluble corn starch as substrate, by a 3-day cultivation in submerged fermentation (SmF) under aerobic conditions. However, the growth kinetic parameters of bacteria and enzyme activity at fermentation conditions were not evaluated. Hence, production of CGTase using AS as carbon source has not been assessed yet. Therefore, the aim of this work was, in the first part of the study, to characterize the CGTase production by *B. megaterium* in a SmF using starch of *Amaranthus hypochondriacus* L. as carbon source and CS was used as comparation. In the second part, CGTase obtained was used for study the production of CDs.

MATERIALS AND METHODS

Amaranth Starch

Grain of *Amaranthus hypochondriacus* L. of cultivar Revancha obtained from INIFAP-Campus Montecillo, Mexico was used in this research. Starch isolation from the amaranth grain was made by the alkaline method described by Villarreal et al. (2013). Briefly, the whole grain was milled using a Udy mil (Udy Corporation Fort Collins, Co, USA) until a flour was obtained. Flour (25 g) was steeped in a 1N NaOH (1:8) solution in a magnetic shaking heater at room temperature for 1 h. The mixture was then centrifuged at 3900 × g in a 420R Hettich equipment and the supernatant was kept to determine residual proteins. The precipitated solids were re-extracted until the protein content was less than 1 mg/mL. Then they were re-suspended in distilled water and adjusted pH to 7. Afterwards, they were washed and filtered with distilled water through a 74 μm opening stainless steel mesh. The retained fiber portion was milled, washed and filtered using distilled water. The resulted suspension was centrifuged, the supernatant discarded, as well as, the top layer of scrapped starch dark until an imperceptible dark layer was left. The resulting AS was oven dried at 60°C for 12 h and milled in a mortar and sieved in a 74 μm mesh. The moisture, ashes and crude protein of isolated from AS were determined in accordance with the Association of Official Analytical Chemists (AOAC, 2000) standardized techniques. The total starch content was determined by the method described by Holm et al. (1986). The protocol includes solubilizing the sample starch, converting it quantitatively to glucose and assaying the glucose with the glucose oxidase/peroxidase reagent. The glucose content in the sample was computed by least squares linear regression. The starch content was calculated on a dry matter basis according to the following formula:

$$\%\ starch = \frac{\mu g\ \text{glucose} \times 10^{-3} \times 25^{a)} \times 100\ (or\ less)^{a)} \times 0.9^{b)}}{\text{sample weight (mg dry basis)}} \times 100$$

where:

a) = dilution factors
b) = correction factor (glucose → glucan)

The yield and recovery of the starch obtained were estimated according to the following formulae:

$$\%\ yield = \frac{starch\ extracted\ (g)}{initial\ sample\ quantity\ (g)} \times 100$$

$$\%\ recovery = \frac{starch\ extracted\ (g)}{total\ starch\ sample\ (g)} \times 100$$

Amylose content was analyzed using an amylose/amylopectin Assay Kit (Megazyme, Ireland) based on concanavalin A (Con A) method. Briefly, starch samples were completely dispersed by heating in dimethyl sulphoxide. Lipids were removed by precipitating the starch in ethanol, recovering the precipitated starch. After dissolution of the precipitated sample in an acetate/salt solution, amylopectin was specifically precipitated by adding Con A and then it was removed by centrifugation. The amylose was enzymatically hydrolyzed at D-glucose, which was analyzed using glucose oxidase/peroxidase (glucose oxidase plus peroxidase and 4-aminoantipyrine (GOPOD)) reagent. The total starch amount, in a separate aliquot of the acetate/salt solution, was also hydrolyzed at D-glucose and was measured colorimetrically by glucose oxidase/peroxidase. The concentration of amylose in the starch sample was estimated as the ratio of absorbance of GOPOD at 510 nm of the supernatant of the precipitated sample with Con A, regard to the total starch sample.

The AS used in this study yielded 57.47 ± 0.28% with a recovery of 58.70 ± 0.18%. The proximal chemical analysis of amylaceous extract was (in g/100 g): moisture (8.07 ± 0.5), ashes (0.10 ± 0.0), and crude protein (0.06 ± 0.00). The $L*a*b$ color parameters of AS were measured using a Hunter Lab Color Flez EZ (Hunter Lab, USA) iluminante D65, 10°, and 125 inch diameter aperture (L = 96.21 ± 0.28, a = 0.067 ± 0.003 and b = 1.26 ± 0.06) being similar to other AS (Villarreal et al., 2013). The starch content of the amylaceous extract was 97.43 ± 1.54%., which had amylose (3.99 ± 0.12%) and amylopectin (96.01 ± 0.25%) content. These values were very similar to those displayed

by amylose and amylopectin in *A. cruentus* (5.4 and 94.6%, respectively; Kong et al., 2009; Villarreal et al., 2013). CS (total starch content = 99.0%; amylose content = 25.0%; amylopectin content = 75.0%; Sigma, Mexico) was used to compare the yields of CGTase and β-CD production.

Microorganism and Culture Media

CGTase was obtained using *B. megaterium* ATCC-10778. This bacterium was obtained from the strains collection of the School of Chemistry that belongs to the National Autonomous University of Mexico. The strain was spread on an agar plate with a medium that consisted of (g/L): meat-peptone broth 12.0, starch 10.0 and agar-agar 20.0. The pH of the medium was adjusted to 7.5. Plates were incubated at 37°C for 24 h. For inoculum preparation, the biomass from the agar plate was transferred to a 500 mL Erlenmeyer flask, with 50 mL of a medium at pH 7.0 that contained (g/L): starch 12.0, dextrose 10.0 and meat-peptone broth 5.0. The strain was cultivated at 37°C on a rotary shaker at 200 rpm for 24 h.

Fermentation Conditions for CGTase and Biomass Production

Biosynthesis of CGTase in SmF was carried out in a 1 L fermenter with 250 mL of sterile broth based on that used by Usharani et al. (2014), that contained the following (in g/L): AS (CS as control) (12.0), yeast extract (2.5), peptone (2.5), KH_2PO_4 (2.0), K_2HPO_4 (1.0) $MgSO_4$ (0.2). The medium was added with 0.5% (v/v) corn steep liquor. The medium pH was adjusted to 7.5. The fermenter was inoculated with 9.6×10^5 UFC of *B. megaterium*. The strain was incubated at 37°C at a constant agitation speed of 200 rpm for 96 h. Sample of 3 mL was taken every 12 h. The cells were centrifuged under cooling at 3500 × g for 15 min and in the supernatant, the CGTase activity was evaluated as well as, the content of protein and starch and pH were determined. Finally, the biomass was determined by dry weight.

Assay of biomass X = X(t) was done by using the Velhurst-Pearl or logistic equation:

$$\frac{dx}{dt} = \mu\left(1 - \frac{X}{X_{máx}}\right)X$$

Where μ is the maximal specific growth rate and X_{max} is the maximal (or equilibrium) biomass level achieved when dX/dt = 0 for X > 0. The solution of Velhurst-Pearl equation is as follows:

$$X = \frac{X_{max}}{1 + Ce^{-\mu t}}$$

Where, $C = (X_{max} - X_0)/X_0$, and $X = X_0$; the initial biomass value.

The estimation of kinetic parameters in the above equation was performed using a non-linear least square-fitting program "Solver" (Excel, Microsoft). The assessed kinetic parameters were: CGTase productivity ($P_E = E_{max}/t$) was evaluated by using the time of E_{max}. $Y_{E/X}$ is the yield of CGTase per unit of biomass produced, estimated as the relation between maximal CGTase activity (E_{max}) and X_{max}. CGTase productivity per unit of substrate ($Y_{E/S} = E_{max}/S$).

CGTase Activity Assay

The cyclization activity of CGTase was measured according to the phenolphthalein (PHP) method utilized by Costa et al. (2015). The β-CD production was assessed spectrophotometrically at 550 nm on the basis of its ability to form a colorless inclusion complex with PHP. Briefly, a reaction mixture of 1 mL containing 1% starch in 50 mM Tris-HCl buffer (pH 8) and 30 μL of crude enzyme were incubated at 40°C for 30 min. Then the reaction was stopped by a thermal shock. Afterwards 0.5 ml of reaction mixture was added with 1.2 mL of 3 mM PHP in 500 mM sodium carbonate buffer, pH 10.0. The amount of β-CD was determined by the absorbance decrease at 550 nm. One unit of the CGTase (U) was defined as the amount of enzyme that catalyzes the production of 1 μmol of β-CD per min under the assay conditions. A calibration curve was made using 80 to 800 μM β-CD. Finally, the specific activity of CGTase was expressed as U/mg protein.

The optimum pH and optimum temperature of CGTase were assessed according to More et al. (2012) with some modifications. A range of different pH values (3–10) at 40°C for 15 min were assayed by using 0.2 M citrate buffer (pH 3–4), 0.1 M acetate buffer (pH 5–6), 0.1 M phosphate buffer (pH 7), 0.05 M Tris-HCl buffer (pH 8) and 0.1 M borate-chloride buffer (pH 9-10). The aliquots were removed after incubation and assayed for the cyclization activity of CGTase. The effect of temperature on CGTase activity was evaluated in the range of 35–70°C in 50 mM Tris-HCl (pH 8) buffer. After incubation for 10 min, the cyclization activity was measured.

Partial Purification of CGTase Enzyme

The isolation of the CGTase was performed according to a previous method described by Gheetha and More (2010), with minor modifications. In the crude extract (SmF supernatant obtained after 36 h of culture), the fractional precipitation was performed by using ammonium sulfate (50, 75, and 80% w/v); then the enzyme was collected by centrifugation at 4000 × g for 20 min at 4°C. The precipitated protein was re-dissolved in 5 mM Tris-HCl buffer (pH 8.0). Then the precipitated residue was dialyzed using a membrane with a cut size of 6-8000 (Spectra / Por® Dialysis) against distilled water for 16 h. Afterwards, the water was changed every 2 h. Then 200 μl of enzyme crude was loaded onto a Sephadex G-200 column (1.4 × 29 cm) (Pharmacia, Uppsala, Sweden) using a Pharmacia LKB FPLC System (Uppsala, Sweden). The proteins were eluted by using the previous buffer at 0.2 mL/min. The 2 mL fractions were collected and monitored at 280 nm. The fractions with maximum absorbance were pooled and concentrated using a Sephadex G-50 column, equilibrated with 5 mM Tris-HCl buffer (pH 8.0). Then the fractions (2 mL) were collected in order to assess the enzymatic activity. The partially purified CGTase was confirmed by using a sodium dodecyl sulfate poly-acrylamide gel electrophoresis (SDS-PAGE). A protein molecular weight marker (Bio-Rad, Hercules, CA., USA) was used with the following: myosin 200 kDa; β-galactosidase 116.25 kDa; phosphorylase b 97.4 kDa; serum albumin 66.2 kDa; ovalbumin 45 kDa; carbonic anhydrase 31 kDa; trypsin inhibitor 21.5 kDa, lysozyme 14.4 kDa and aprotinin 6.5 kDa.

CGTase Kinetic Parameters

The parameters of CGTase were assessed through a Michaelis-Menten equation and the double reciprocal plot method by Lineweaver-Burk. Km and Vmax were determined with 10–100 mg/mL of AS in 50 mM Tris-HCl buffer (pH 8) at 50°C for up to 30 min. After incubation of the mixture reaction, the cyclization activity of CGTase was measured.

CD Production

The native AS isolated from grain of *A. hypochondriacus* L. was used to obtain β-CDs. Corn starch (CS) was also used as a positive control of the trial. The method carried out by Ibrahim et al. (2011), with some modifications, was used for the CDs formation. Briefly, starch gelatinization was performed at 50 and 70°C (for AS and CS, respectively) for 10 min in 50 mM glycine buffer (pH 8); then the reaction mixture was cooled to room temperature. Afterwards, CGTase partially purified (39 U/mL), previously obtained using AS as carbon source for *B. megaterium*, was reacted with 1% (w/v) substrate in glycine-NaOH buffer (pH 8) at 50°C for 12 h. The enzymatic reaction was stopped by boiling it for 10 min and after that, the reaction mixture was submerged in cold water for 10 min.

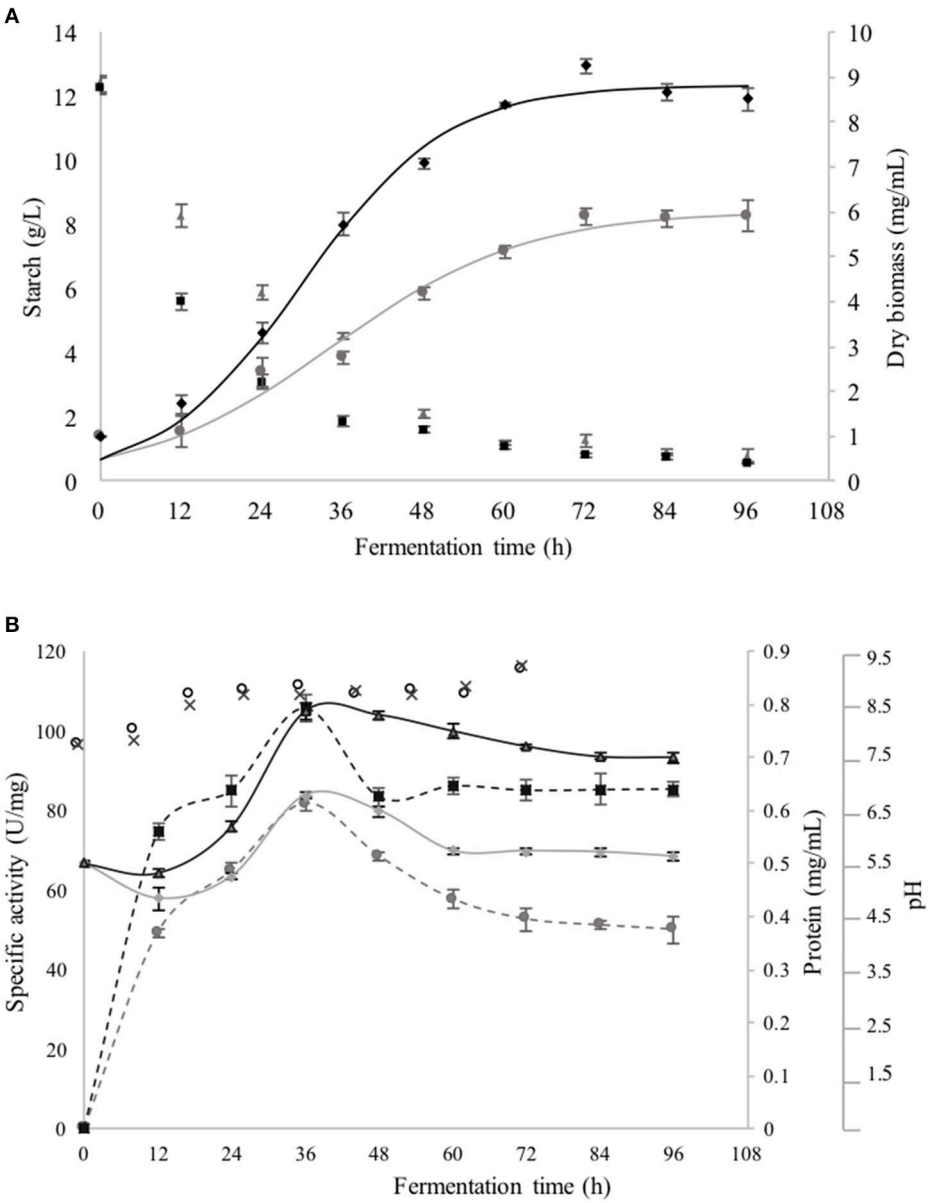


FIGURE 1 | (A) Growth curves of *Bacilus megaterium* grown in SmF using AS (♦) and CS (●) as carbon sources, as well as, the consumption of AS (■) and CS (▲). **(B)** Protein excreted in the broth with AS (—▲—) and CS (—♦—) as carbon sources; Specific activity of CGTase in the broth with AS (--■--) and CS (--●--) and pH of the broth with AS (x) and CS (○). The error bars on the graph represent the standard deviation of three different fermentation runs.

The CDs produced were measured by mass spectrometry (MS). The following settings were used: electrospray ionization (ESI) in positive mode. The dry gas (nitrogen) flow rate was set at 4.0 L/min and the dry heater operated at 180°C. The capillary voltage was set at 4500 V and the end plate offset at −500 V. Collision energy varied in the range of 25–30 eV. All ESI–MS experiments were performed on a MicrOTOFQII mass spectrometer equipped with an electrospray ion source (Bruker-Daltonics, Bremen, Germany). MS data were recorded in full scan mode (from 50 to 3000 m/z). Data processing was carried out with Chromeleon 6.8. Next the samples were introduced directly to the electrospray source of the MS using an LC pump and the mobile phase at a flow rate 3.0 μL/min. The mobile phase consisted of H_2O/ACN/FA (90:10:0.1, v/v/v) (A) and MeOH/ACN/FA (90:10:0.1, v/v/v) (B) in an A:B ratio of 90:10, v/v. HRMS (high resolution) measurements provided by a TOF analyzer in order to enable the processing of the elemental composition of the registered ions. The percentage of starch conversion (%) was defined as the weight percentage of initial substrate converted into total CDs (g β-CD/100 g starch).

Statistical Analysis

All experimental results were analyzed by one-way analysis of variance (ANOVA) and the Tukey's multiple comparison test ($p < 0.05$).

RESULTS

Growth Parameters of the *B. megaterium* Strain for CGTase Production

The kinetic growth parameters of *B. megaterium* in the SmF are presented in **Figures 1A,B**. Lag phase was practically negligible; the total growth time of *B. megaterium* was of 4 days (**Figure 1A**), the exponential phase was shorter when AS was used as substrate (36 h) compared to that observed with CS, which lasted 48 h. The value was significantly greater ($p < 0.05$) when AS was used as carbon source ($\mu = 0.094 \pm 0.001\,h^{-1}$) than that with CS (**Table 1**). After 72 h of fermentation, AS and CS contents were practically negligible ($p < 0.05$). Values of pH were very similar between cultures (initial pH was 7.5 in both cases and with the time rose to 8.5 for the first 24 h. It remained stable until 84 h of fermentation and finally reached pH 9.0 at the end) (**Figure 1B**). The time course production of CGTase in relation to the growth phases of *B. megaterium* is shown in **Figures 1A,B**. The enzyme synthesis using AS and CS as carbon source, began at the early exponential phase and the maximum CGTase specific activity was obtained after 36 h of cultivation, with spontaneous increase in cell biomass yield (**Figure 1A**). Thereafter, the CGTase activity gradually decreased with the prolongation of the fermentation periods up to 96 h. The shape of the curve of extracelular proteins was identical with that of CGTase specific activity. This activity obtained during the SmF, when AS was used at any time of the exponential phase, was roughly 25% greater than that observed when CS was utilized (**Figure 1B**). The maximum specific activity of CGTase obtained with AS as carbon source was higher (105.72 ± 8.33 U/mg protein) than that reported with CS (81.75 ± 3.2 U/mg protein).

TABLE 1 | Growth kinetic parameters of *Bacillus megaterium* in SmF for CGTase production.

Carbon source	μ (h^{-1})	$Y_{X/S}$ (gX/gS)	$Y_{E/X}$ (U/gX)	$Y_{E/S}$ (U/gS)
AS	$0.094 \pm 2.3 \times 10^{-3a}$	11.47[a]	9775[a]	44602[a]
CS	$0.075 \pm 4.4 \times 10^{-3b}$	4.66[b]	8689[a]	11355[b]

[a] *Data are the mean ± standard deviation of three replicates.*
[b] *Values that have the same superscript in a column do not differ significantly ($p < 0.05$).*

Table 1 shows that when AS was used as carbon source, the biomass and the CGTase, both reported per g of biomass were higher ($Y_{X/S} =$ 11.47 gX/ gS, $Y_{E/X} =$ 9775 U/gX, respectively) than those reported when was used the CS under the same fermentation conditions. The CGTase activity reported per g of AS was three times higher ($Y_{E/S} =$ 44602 U/g S) that the obtained per g of CS ($Y_{E/S} =$ 11355 U/g S). This proves that AS is a good alternative carbon source to obtain a higher yield of CGTase.

CGTase Characterization

The active fraction used for the biochemical characterization of the enzyme was located between fractions number 23 and 30 obtained from the gel filtration Sephadex G-200 column (**Figure 2A**). These fractions were gathered, concentrated by ultrafiltration and loaded on a Sephadex G-50 column. The fractions between 10 and 30 displayed CGTase activity (**Figure 2B**). The enzyme could be sufficiently purified in two steps (**Table 2**) with a recovery of 10.25% of activity and 40.32-fold purification for the specific enzymatic activity of 3946 U/mg. SDS-PAGE gel electrophoresis showed the presence of a single protein with an apparent molecular weight (Mr) ca 66 kDa (**Figure 2C**) accompanied by some minor proteins. The CGTase activity was measured at 40°C using the standard assay method by varying the pH values from 3.0 to 10.0. The optimum pH of the purified CGTase was 8.0 (**Figure 3A**) for the enzyme produced using both AS and CS. **Figure 3A** shows that the CGTase retained its activity at pHs between 3.0 and 10.0. At pHs 5.0 and 9.0, the retained enzymic activity was in the range of 70%. CGTase activity decreased drastically below these pH values. The optimum temperature was 50°C using AS and CS as substrate (**Figure 3B**). Thereafter, the enzymatic activity diminished 60% with values above 50°C and 40% under this temperature.

Kinetic Characterization

The Km, Vmax and Kcat values for partially purified CGTase with AS as substrate were 0.152 mM, 13.4 μM/min and 0.36×10^{-3}/s, respectively (**Figure 3C**).

Cyclodextrin Production

AS was used to synthesize β-CD using a partially purified CGTase obtained previously by *B. megaterium* in a SmF. The comparison of the CDs yields from the AS and CS of the chromatographic assays are shown in **Table 3**. It can be observed that total CDs content obtained with AS was

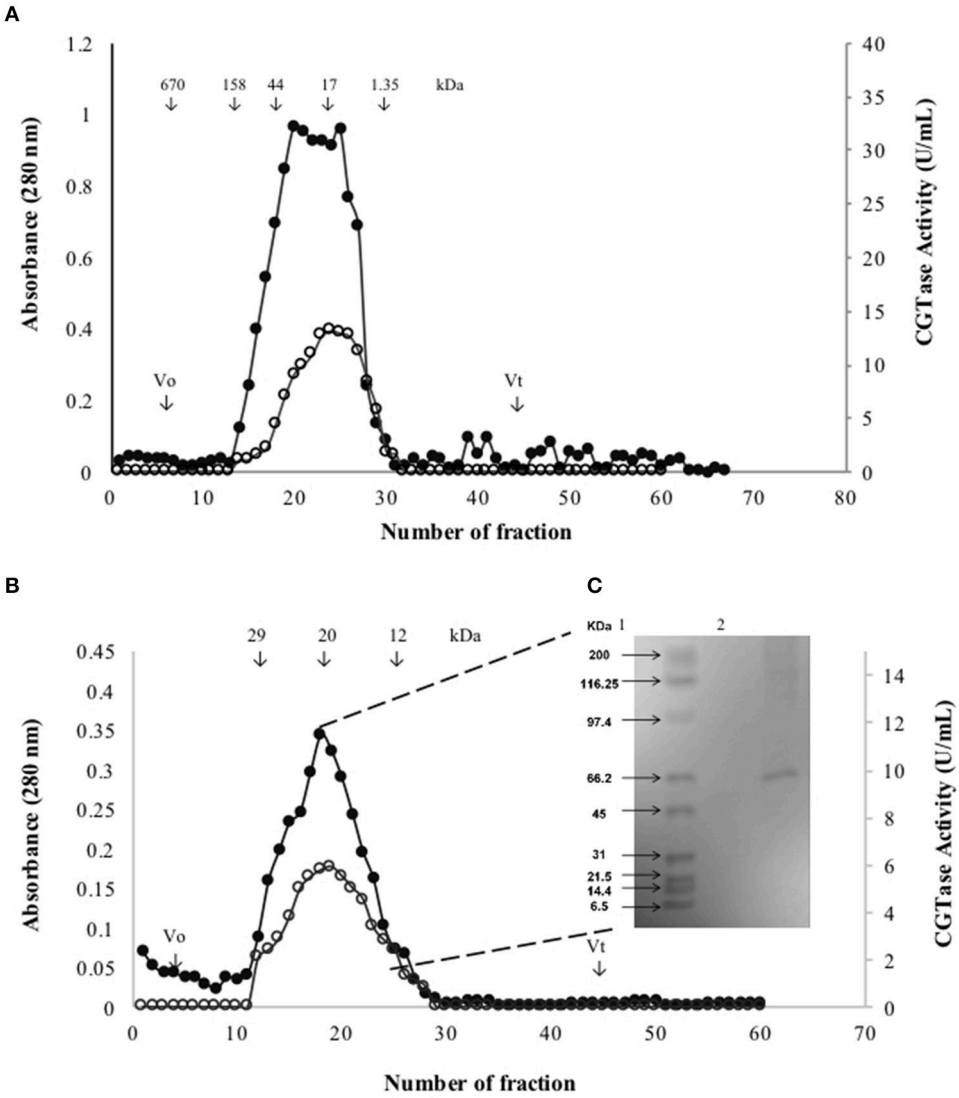


FIGURE 2 | Gel filtration profiles when was used the culture broth of *Bacillus megaterium* grown in SmF when AS was used as substrate. (A) Fractions eluted through Sephadex G-200 column (●) and their CGTase activity (○). **(B)** Fractions eluted through Sephadex G-50 column (●) and their CGTase activity (○). **(C)** Mr of partially purified CGTase by SDS-PAGE; lane 1, Standard markers; lane 2, partially purified CGTase.

TABLE 2 | Purification summary of an CGTase produced by *Bacillus megaterium* in SmF using AS as carbon source.

Purification step	Cyclization activity (U/mL)	Protein (mg/mL)	Specific activity (U/mg)	Yield (%)	Purification fold
Supernatant	57.75 ± 3.3	0.59 ± 0.010	97.88	100	1.00
85% $(NH_4)_2SO_4$ precipitation /dialysis	29.7 ± 1.5	0.13 ± 0.010	228.46	51.43	2.33
Sephadex G-200	13.18 ± 0.94	0.02 ± 0.008	659.00	22.82	6.73
Sephadex G-50	5.92 ± 0.41	0.0015 ± 0.0001	3946.00	10.25	40.32

Data are the mean ± standard deviation of three replicates.

higher (40.73%) than that measured for CS (24.48%). There are also differences in the distribution of the individual CDs. Higher relative proportions of α-CD and β-CD were obtained regardless of the CGTase and starch sources employed (**Table 3**).

DISCUSSION

Recently, it has been reported in some works on production of CGTase in SmF that the lag phase was practically negligible as in this study (Costa et al., 2015; Elbaz et al., 2015). Some authors,

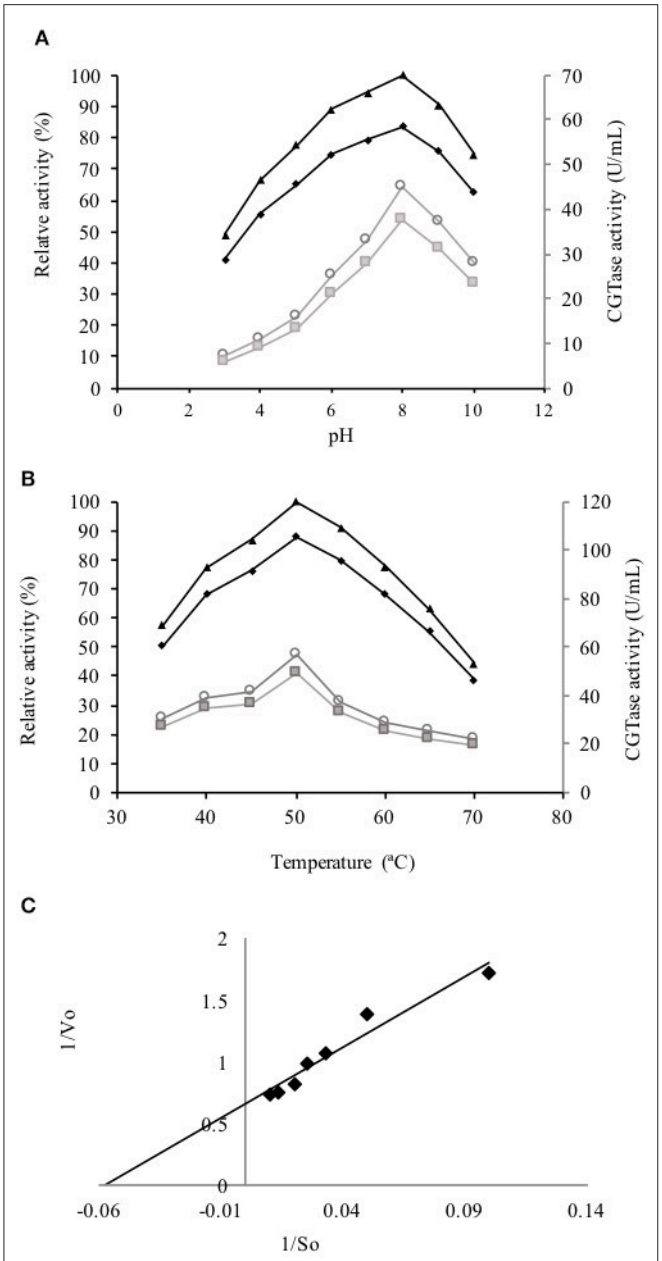


FIGURE 3 | Kinetic curves of the partially purified CGTase. (A) Effect of pH on the CGTase activity of the enzyme obtained from the broth whit AS (♦) and CS (■), as well as, their relative activity using AS (▲) and CS (○). **(B)** Effect of temperature on the CGTase activity of enzyme obtained from the broth whit AS (♦) and CS (■), as well as, their relative activity using AS (▲) and CS (○). **(C)** Lineweaver-Burk plot of partially purified CGTase.

however, have found that it is typical for some alkalophilic bacteria, such as *Bacillus cirulans* var. *alkalophilus,* to have long lag phases, even lasting 30–34 h (Mäkelä et al., 1990). The increase of pH of the culture medium observed in the fermentations using both AS and CS as carbon sources, can be partially explained because the excreted proteins can increase during the first hours of fermentation. These proteins can act as buffers and keep pH levels for up to 60 h. After this time, the gradual increase of pH until 9.0 can be ascribed to the occurrence of peptides produced by protein hydrolysis as a result of cell desintegration (Mäkelä et al., 1990). Sukiminderjit et al. (2014) reported that the optimum pH of the CGTase produced by B. megaterium is roughly 8.0. This pH in a fermentation medium might be beneficial for the enzymatic activity, which is measured by starch cyclization when the reaction occurs with the starch in the culture medium (Ng et al., 2013).

On the other hand, enzyme production can be improved by manipulating fermentation conditions such as pH, temperature, concentrations of nutrients and compositions of the production media (carbon and nitrogen sources). Thus, fermentation conditions may change CGTase yield. Additionally, researchers have been reported recent advances in heterologous expression strategies for improving CGTase production and molecular engineering approaches for enhancing the catalytic properties of CGTases for effective application (Han et al., 2014). It is important to mention that the kinetic growth parameters of *B. megaterium* using AS as substrate in any cultivation conditions have not been previously reported. Mäkelä et al. (1990) observed that CGTase activity appeared in the cultivation broth early in the exponential growth phase, attaining about 65% of the final value at the beginning of the stationary growth phase and during this growth phase, about 20% of the final CGTase activity appeared in the medium as a result of cell desintegration or excretion of CGTase by spore-forming cells. In the death phase, CGTase activity still increased slightly. Costa et al. (2015) claimed that a strain of *Bacillus cirulans* requires the absence of glucose and the presence of starch as carbon source to grow and express the CGTase gene.

The most nutrient-rich culture media increased growth of the strain, but not increased the synthesis of CGTase. Some studies, such as those conducted by de Freitas et al. (2004), have reported the effect of the carbon source on the enzyme synthesis after 48 h of fermentation. According to their results, Bacillus alkalophilic CGH grew very well with higher CGTase specific activities using starch and maltodextrins as carbon sources. Enzyme production was not observed when glucose was added to the medium. Kitahata et al. (1974) reported a CGTase from *Bacillus* sp. that was purified by five steps. The enzyme was 43-fold purified and displayed about 10% its activity. Both values were very similar to those obtained in this study. On the other hand, Ibrahim et al. (2011) reported that the CGTase from *B. agaradhaerens* was purified in three steps, with a recovery of 26% and twice as much specific activity when compared to that observed in this study. After 3 months, the purified CGTase stored at −4°C kept 85% of its biological activity. Covalent immobilization of CGTase on magnetic particles beads promoted a high stabilization of the CGTase against temperature and pH. For example, this technique retained 90% of its initial activity when incubated for 1 h at pH 9.0 and 50°C. The same preparation preserved its high catalytic activity after long-term storage at 4°C (60 days, 80%; Ivanova, 2010).

The CGTase shows a Mr similar to other CGTases such as the produced in SmF by *Bacillus* sp. (69 kDa) and *B. firmus* (80 kDa) using CS as carbon source (Suntinanalert et al., 1997; Pishtiyski et al., 2008; Savergave et al., 2008; Ibrahim et al., 2011). However, there are some reports on CGTases with different Mr, such as that of *Paenibacillus macerans* grown with CS where its Mr

TABLE 3 | CDs yield produced by a partially purified CGTase obtained by *B. megaterium* in SmF using AS as carbon source and compared to that obtained by Urban et al. (2012).

	This work				Previous work[a]			
	AS		CS		AS		CS	
	Amount (g/L)	Yield (%)	Amount (g /L)	Yield (%)	Amount (g /L)	Yield (%)	Amount (g /L)	Yield (%)
α-CD	6.40 ± 0.26[b]	12.81	3.85 ± 0.085	7.70	6.46 ± 0.071	9.23	5.88 ± 0.094	8.4
β-CD	8.97 ± 0.36	17.94	5.39 ± 0.11	10.78	6.13 ± 0.092	8.76	2.84 ± 0.059	4.06
γ-CD	4.98 ± 0.20	9.92	2.99 ± 0.06	5.99	2.98 ± 0.084	4.25	1.47 ± 10.19	2.1
∑CD	20.35	40.73	12.23	24.48	15.57	22.24	10.19	14.56

[a] *In either work, AS was used as substrate for CGTase to synthetize enzymatically CDs and CS was used as control.*
[b] *Data are mean ± standard deviation of three replicates.*

was 114 kDa (Urban et al., 2012). The purified CGTase showed activity at pHs between 3.0 and 10.0, however, its optimum pH was 8.0 using both AS and CS as substrate. There is widespread agreement on the optima pH values (7-12) reported for purified CGTases from *Bacillus* sp. and *B. megaterium*. Most CGTases exhibit optimum pH ranging from 5.0 to 8.0. However, the CGTase with the highest pH (10.0) was reported for the one produced by *Brevibacterium* sp. no. 9605 (Mori et al., 1974; Martínez-Mora et al., 2012). CGTase from *B. agaradhaerens* LS-3C, possesses the widest pH range for stability, specifically pH 5.4-11.0 (Gastón et al., 2009). With respect to the temperature, in this work was observed CGTase activity in all temperatures assayed and the optimum was 50°C, however, previous studies showed that CGTase activity occurs between 23 and 110°C. The enzyme remained active in the tested temperature range from 30 to 70°C (More et al., 2012). Previous reports have shown that the Km values of CGTase from various *Bacillus* using soluble CS, are in the range from 0.05 to 15.54 mM (More et al., 2012). This shows that the partially purified CGTase has a relatively high affinity for AS. Kelly et al. (2008) reported values ranging from 3.0×10^{-3}/s to 329/s for CGTases produced with CS as carbon source. The CGTase from *B. megaterium,* using AS as substrate in this work, is in agreement with the Kcat values published elsewhere (Shahrazi et al., 2013; Usharani et al., 2014). CDs are produced by the catalytic action of CGTase through an intramolecular transglycosylation reaction. The enzyme displays its cyclic action on substrates with α-1,4-glycosyl chains such as starch, amylose, amylopectin, dextrins and glycogen. However, starch is the most commonly used material for CD production (Zhekova et al., 2009). Nevertheless, a complete conversion of starch to CD is not likely, even at optimal reaction conditions. According to published literature, the main limiting factors are inhibition of CGTase by CD and maltoologosaccharides, coupled activity of the enzyme, inability of CGTase to act on α-1,4-linkages of starch and the low molecular mass of the substrate. All known CGTase produces a mixture of α-, β-, and γ-CDs at different ratios. They have been further classified into α-, β-, and γ-CGTases according to their main cyclodextrin products during the initial phase of the reaction (Urban et al., 2012). *B. megaterium* produces all three types of CDs, but the predominant product is β-CD (Pishtiyski et al., 2008). Urban et al. (2012) also observed a greater total CDs production using AS than CS, but the CGTase used in our study was produced by *B. megaterium* using AS as carbon source. Moreover, the CGTase of this study mainly produced β-CD (17.94%) in comparison to that reported by Urban et al. (2012) which was 8.76%. It was also observed that total CDs yield (AS = 40.73%; CS = 24.48%) in this study was roughly twice as much as that obtained previously for AS (22.24%) and CS (14.56%) by Urban et al. (2012). The previous procedure does not produce a good yield of γ-CD. For this purpose, a CGTase that predominantly produces γ-CD can be used (Li et al., 2007). Higher amylopectin content, higher dispersibility, and higher starch-granule susceptibility to amylases can facilitate the CGTase activity to synthesize CDs using the amaranth starch as substrate (Tomita et al., 1981). The influence of various substrates including starchs from corn, potato, sago, rice and tapioca has been assessed. Potato starch seems to give the highest conversion into CDs. Additionally, CDs yield was about 3-fold higher when using gelatinized potato starch in comparison to raw starch (Ibrahim et al., 2011).

CONCLUSION

The amaranth starch displays a higher amylopectin content, higher dispersibility, and higher starch-granule susceptibility to amylases activity than those properties displayed by corn starch. These features can facilitate the CGTase production by a SmF as well as the synthesis of cyclodextrins when the partially purified CGTase is used in the enzymatic reaction. Therefore, amaranth starch might be a good alternative not only to obtain CGTase, but also to produce a higher α-, β-, and γ-cyclodextrins content than that afforded by corn starch. The use of CDs in the pharmaceutical and food industries is limited by high costs. Thus, many efforts have been directed to produce CDs by continuous processes in substitution of the batch process, and immobilized cells have shown higher productivity when used in continuous processes (Moriwaki et al., 2014). Therefore, the high costs could decrease by applying this technique.

AUTHOR CONTRIBUTIONS

This work was carried out in collaboration between all authors. Author JS designed the study, contributed reagents/materials

and supervised work in all its aspects. Author MA carried out trials and prepared the protocol. Author EP managed the literature searches. Authors ED and RP performed the statistical analysis and also supervised this study. Author GD followed and supervised the fermentations performed in this proyect.

ACKNOWLEDGMENTS

We are grateful to Prof. Abraham Avendaño-Martínez for proofreading and translating the manuscript. MA was supported by a CONACYT scholarship (No. 330389).

REFERENCES

AOAC (2000). *Association Official Analytical Chemists. Official Methods of Analyses, 17th Edn*. Washington, DC: Association of Official Analytical Chemists.

Ahmed, E. M., and El-Refai, H. A. (2010). Cyclodextrin glucosyltransferase production by *Bacillus megaterium* NCR: evaluation and optimization of culture conditions using factorial design. *Indian J. Microbiol.* 50, 303–308. doi: 10.1007/s12088-010-0009-x

Anselmi, C., Centini, M., Maggiore, M., Gaggelli, M. A., Buonocore, A., Beretta, G., et al. (2008). Non-covalent inclusion of ferulic acid with α-cyclodextrin improves photo-stability and delivery: NRM and modelling studies. *J. Pharm. Biomed. Analysis* 46, 645–652. doi: 10.1016/j.jpba.2007.11.037

Cheirsilp, B., Kitcha, S., and Maneerat, S. (2010). Kinetic characteristics of -cyclodextrin production by cyclodextrin glycosyltransferase from newly isolated *Bacillus* sp. C26. *Electron. J. Biotechnol.* 13, 4–5. doi: 10.2225/vol13-issue4-fulltext-6

Costa, H., Gastón, J. R., Lara, J., Martinez, C. O., Moriwaki, C., Matioli, G., et al. (2015). Cyclodextrin glycosyltransferase production by free cells of *Bacillus circulans* DF 9R in batch fermentation and by immobilized cells in a semi-continuous process. *Bioprocess Biosyst. Eng.* 38, 1055–1063. doi: 10.1007/s00449-014-1347-6

de Freitas, T. L. D., Monti, R., and Contiero, J. (2004). Production of CGTase by a *Bacillus alkalophilic* CGII strain isolated from wastewater of a manioc flour industry. *Braz. J. Microbiol.* 35, 255–260. doi: 10.1590/S1517-83822004000200015

Elbaz, A. F., Sobhi, A., and ElMekawy, A. (2015). Purification and characterizationof cyclocextrin β-glucanotransferase from novel alkalophilic bacilli. *Bioprocess Biosyst. Eng.* 38, 767–776. doi: 10.1007/s00449-014-1318-y

Gastón, J. A. R., Szerman, N., Costa, H., Krymkiewicz, N., and Ferrarotti, S. A. (2009). Cyclodextrin glycosyltransferase from *Bacillus circulans* DF 9R: activity and kinetic studies. *Enzyme Microb. Technol.* 45, 36–41. doi: 10.1016/j.enzmictec.2009.04.002

Gheetha, R., and More, S. S. (2010). Isolation and characterization of cyclodextrin glucanotransferase from soil bacterium. *Res. J. Biol. Sci.* 5, 699–707. doi: 10.3923/rjbsci.2010.699.707

Han, R., Li, J., Shin, H. D., Chen, R. R., Du, G., Liu, L., et al. (2014). Recent advances in discovery, heterologous expression, and molecular engineering of cyclodextrin glycosyltransferase for versatile applications. *Biotechnol. Adv.* 32, 415–428. doi: 10.1016/j.biotechadv.2013.12.004

Holm, J., Björck, I., Drews, A., and Asp, N. G. (1986). A rapid method for the analysis of starch. *Starch* 38, 224–226. doi: 10.1002/star.19860380704

Ibrahim, A. S. S., El-Tayeb, M. A., Elbadawi, Y. B., and Al-Salamah, A. A. (2011). Effects of substrates and reaction conditions on production of cyclodextrins using cyclodextrin glucanotransferase from newly isolated *Bacillus agaradhaerens* KSU-A11. *Ejbiotechnology* 14. doi: 10.2225/vol14-issue5-fulltext-4

Ivanova, V. (2010). Immobilization of cyclodextrin glucanotransferase from *Paenibacillus macerans* ATCC 8244 on magnetic carriers and production of cyclodextrins. *Biotechnol. Biotec. Equip.* 24, 516–528. doi: 10.1080/13102818.2010.10817893

Kelly, R., Leemhuis, H., Rozeboom, H., van Oosterwijk, N., Dijkstra, B., and Dijkhuizen, L. (2008). Elimination of competing hydrolysis and coupling side reactions of a cyclodextrin glucanotransferase by directed evolution. *Biochem. J.* 413, 517–525. doi: 10.1042/BJ20080353

Kitahata, S., Tsuyama, N., and Okada, S. (1974). Purification and some properties of cyclodextrin glycosyltransferase from a strain of *Bacillus* species. *Agr. Biol. Chem.* 38, 387–393. doi: 10.1080/00021369.1974.10861152

Kong, X., Corke, H., and Bertoft, E. (2009). Fine structure characterization of amylopectins from grain amaranth starch. *Carbohydr. Res.* 344, 1701–1708. doi: 10.1016/j.carres.2009.05.032

Kurkov, S. V., and Loftsson, T. (2013). Cyclodextrins. *Int. J. Pharm.* 453, 167–180. doi: 10.1016/j.ijpharm.2012.06.055

Li, Z., Wang, M., Wang, F., Gu, Z., Du, G., Wu, J., et al. (2007). γ-Cyclodextrin: a review on enzymatic production and applications. *Appl. Microbiol. Biotechnol.* 77, 245–255. doi: 10.1007/s00253-007-1166-7

Mäkelä, M. J., Paavilainen, S. K., and Korpela, T. K. (1990). Growth dynamics of cyclomaltodextrin glucanotransferase producing *Bacillus circulans* var. *alkalophilus. Can. J. Microbiol.* 36, 176–182. doi: 10.1139/m90-031

Martínez-Mora, M., Hernández-Sánchez, K., Villalonga-Santana, R., Pérez-Rojas, A., Ramírez, H. L., and Torres-Labandeira, J. J. (2012). Partial purification and properties of cyclodextrin glycosiltransferase (CGTase) from alkalophilic *Bacillus* species. *SpringerPlus* 1, 1–6. doi: 10.1186/2193-1801-1-61

More, S. S., Niraja, R., Evelyn, C., Byadgi, A. M., Shwetha, V., and Mangaraj, S. D. (2012). Isolation, purification and biochemical characterization of CGTase from *Bacillus halodurans*. *Croatian J. Food Technol. Biotechnol. Nut.* 7, 90–97.

Mori, S., Hirose, S., Oya, T., and Kitahata, S. (1974). Purification and properties of cyclodextrin glucanotrasferase from *Brevibacterium* sp. no. 9605. *Biosci. Biotechnol. Biochem.* 58, 1968–1972. doi: 10.1271/bbb.58.1968

Moriwaki, C., Mangolim, C. S., Ruiz, G. B., de Morais, G. R., Baesso, M. L., and Matioli, G. (2014). Biosynthesis of CGTase by immobilized alkalophilic bacilli and crystallization of beta-cyclodextrin: effective techniques to investigate cell immobilization and the production of cyclodextrins. *Biochem. Eng. J.* 83, 22–32. doi: 10.1016/j.bej.2013.12.004

Ng, H. S., Ooi, C. W., Mokhtar, M. N., Show, P. L., Ariff, A., Tan, J. S., et al. (2013). Extractive bioconversion of cyclodextrins by *Bacillus cereus* cyclodextrin glycosyltransferase in aqueous two-phase system. *Bioresour. Technol.* 142, 723–726. doi: 10.1016/j.biortech.2013.05.087

Pishtiyski, I., Popova, V., and Zhekova, B. (2008). Characterization of cyclodextrin glucanotransferase produced by *Bacillus megaterium*. *Appl. Biochem. Biotechnol.* 144, 263–272. doi: 10.1007/s12010-007-8009-y

Rakmai, J., and Cheirsilp, B. (2016). Continuous production of β-cyclodextrin by cyclodextrin glycosyltransferase immobilized in mixed gel beads: comparative study in continuous stirred tank reactor and packed bed reactor. *Biochem. Eng. J.* 105(Part A), 107–113. doi: 10.1016/j.bej.2015.09.011

Sá Couto, A., Salústio, P., and Cabral-Marques, H. (2015). "Cyclodextrins" in *Polysaccharides Bioactivity and Biotechnology* eds K. G. Ramawat, J.-M. Mérillon (Cham: Springer International Publishing), 263–265.

Savergave, L. S., Dhule, S. S., Jogdand, V. V., Nene, S. N., and Gadre, R. V. (2008). Production and single step purification of cyclodextrin glycosyltransferase from alkalophilic *Bacillus firmus* by ion exchange chromatography. *Biochem. Eng. J.* 39, 510–515. doi: 10.1016/j.bej.2007.09.020

Shahrazi, S., Saallah, S., Mokhtar, M. N., Baharuddin, A. S., and Yunos, K. F. M. (2013). Dynamic mathematical modelling of reaction kinetics for cyclodextrins production from different starch sources using *Bacillus macerans* cyclodextrin glucanotransferase. *Am. J. Biochem. Biotechnol.* 9, 195–205. doi: 10.3844/ajbbsp.2013.195.205

Sivakumar, N., and Shakilabanu, S. (2013). Production of cyclodextrin glycosyl transferase by *Bacillus megaterium*. *Int. J. Curr. Microbiol. Appl. Sci.* 2, 44–55.

Sukiminderjit, K., Simranjeet, K., and Kirandeep, K. (2014). Studies on β-cyclodextrin productos from CGTase producing bacteria and its effect on drug solubility. *Int. J. Pharm. Pharmal.* 6, 383–387.

Suntinanalert, P., Petmaneechote, J., Damnian, N., and Hutadilok, T. N. (1997). Purification and properties of cyclodextrin glycosyltransferase (CGTase) from an alkaline-tolerant *Bacillus* sp. PS304. *J. Sci. Soc. Thail.* 23, 381–388. doi: 10.2306/scienceasia1513-1874.1997.23.381

Tomita, Y., Sugimoto, Y., Sakamoto, S., and Fuwa, H. (1981). Some properties of starches of grain amaranths and several millets. *J. Nutr. Sci. Vitaminol (Tokyo).* 27, 471–484. doi: 10.3177/jnsv.27.471

Urban, M., Beran, M., Adamek, L., Drahorád, J., Molík, P., and Matušová, K. (2012). Cyclodextrin production from amaranth starch by cyclodextrin glycosyltransferase produced by *Paenibacillus macerans* CCM 2012. *Czech. J. Food Sci.* 30, 15–20.

Usharani, L., Prasad, T., Sundar, S., Dhananjaya, K., and Mallesha, H. (2014). Comparative study of cyclodextrin production from the CGTase producing novel strains characterization and hostguest complex formation *J. Drug Deliv. Ther.* 4, 77–81.

Villarreal, M. E., Ribotta, P. D., and Iturriaga, L. B. (2013). Comparing methods for extracting amaranthus starch and the properties of the isolated starches. *LWT-Food Sci. Technol.* 51, 441–447. doi: 10.1016/j.lwt.2012.11.009

Zhekova, B., Dobrev, G., Stanchev, V., and Pishtiyski, I. (2009). Approaches for yield increase of β-cyclodextrin formed by cyclodextrin glucanotransferase from *Bacillus megaterium*. *World J. Microbiol. Biotechnol.* 25, 1043–1049. doi: 10.1007/s11274-009-9985-6

Zhou, J., Liu, H., Du, G., Li, J., and Chen, J. (2012). Production of α-cyclodextrin glycosyltransferase in *Bacillus megaterium* MS941 by systematic codon usage optimization. *J. Agric. Food Chem.* 60, 10285–10292. doi: 10.1021/jf302819h

Conflict of Interest Statement: The authors declare that the research was conducted in the absence of any commercial or financial relationships that could be construed as a potential conflict of interest.

Copyright © 2016 Arce-Vázquez, Ponce-Alquicira, Delgado-Fornué, Pedroza-Islas, Díaz-Godínez and Soriano-Santos. This is an open-access article distributed under the terms of the Creative Commons Attribution License (CC BY). The use, distribution or reproduction in other forums is permitted, provided the original author(s) or licensor are credited and that the original publication in this journal is cited, in accordance with accepted academic practice. No use, distribution or reproduction is permitted which does not comply with these terms.

frontiers in Microbiology

ORIGINAL RESEARCH
published: 25 November 2016
doi: 10.3389/fmicb.2016.01794

Functional Analysis of the Nitrogen Metabolite Repression Regulator Gene *nmrA* in *Aspergillus flavus*

*Xiaoyun Han[1†], Mengguang Qiu[1†], Bin Wang[1†], Wen-Bing Yin[2], Xinyi Nie[1], Qiuping Qin[1], Silin Ren[1], Kunlong Yang[1], Feng Zhang[1], Zhenhong Zhuang[1] and Shihua Wang[1]**

[1] Key Laboratory of Pathogenic Fungi and Mycotoxins of Fujian Province, Key Laboratory of Biopesticide and Chemical Biology of Education Ministry, School of Life Sciences, Fujian Agriculture and Forestry University, Fuzhou, China, [2] State Key Laboratory of Mycology, Institute of Microbiology, Chinese Academy of Sciences, Beijing, China

In *Aspergillus nidulans*, the nitrogen metabolite repression (NMR) regulator NmrA plays a major role in regulating the activity of the GATA transcription factor AreA during nitrogen metabolism. However, the function of *nmrA* in *A. flavus* has not been previously studied. Here, we report the identification and functional analysis of *nmrA* in *A. flavus*. Our work showed that the amino acid sequences of NmrA are highly conserved among *Aspergillus* species and that *A. flavus* NmrA protein contains a canonical Rossmann fold motif. Deletion of *nmrA* slowed the growth of *A. flavus* but significantly increased conidiation and sclerotia production. Moreover, seed infection experiments indicated that *nmrA* is required for the invasive virulence of *A. flavus*. In addition, the Δ*nmrA* mutant showed increased sensitivity to rapamycin and methyl methanesulfonate, suggesting that *nmrA* could be responsive to target of rapamycin signaling and DNA damage. Furthermore, quantitative real-time reverse transcription polymerase chain reaction analysis suggested that *nmrA* might interact with other nitrogen regulatory and catabolic genes. Our study provides a better understanding of NMR and the nitrogen metabolism network in fungi.

Keywords: ***Aspergillus flavus*, nitrogen metabolism, *nmrA*, aflatoxins, AreA**

OPEN ACCESS

Edited by:
Maria De Lourdes Teixeira De Moraes Polizeli, University of São Paulo, Brazil

Reviewed by:
Fernando Segato, University of São Paulo, Brazil
André Ricardo Lima Damásio, University of Campinas, Brazil
Maria Celia Bertolini, Instituto de Química, Brazil

****Correspondence:***
Shihua Wang
wshyyl@sina.com

[†] These authors have contributed equally to this work.

Specialty section:
This article was submitted to Microbial Physiology and Metabolism, a section of the journal Frontiers in Microbiology

Received: *31 July 2016*
Accepted: *25 October 2016*
Published: *25 November 2016*

Citation:
Han X, Qiu M, Wang B, Yin W-B, Nie X, Qin Q, Ren S, Yang K, Zhang F, Zhuang Z and Wang S (2016) Functional Analysis of the Nitrogen Metabolite Repression Regulator Gene nmrA in Aspergillus flavus. Front. Microbiol. 7:1794. doi: 10.3389/fmicb.2016.01794

INTRODUCTION

Aspergillus flavus is ubiquitous in soil and can infect or contaminate a wide range of organic nutrient sources, such as economically important commodities, insects, animal carcasses, and even immunocompromised humans and animals (Amaike and Keller, 2011; Yu, 2012; Zhang et al., 2014; Bai et al., 2015a,b; Zhang et al., 2015). Aflatoxins (AFs), mainly produced by *A. flavus* and *A. parasiticus*, have been identified as a class of the most toxic and carcinogenic secondary metabolites of fungi. AF contamination of agricultural grains is not only a significant food safety concern but also an economic concern for the agricultural industry worldwide (Yu, 2012; Amaike et al., 2013; Yang et al., 2015). To develop effective and novel strategies against AF contamination, it is a necessity to investigate the molecular mechanisms by which AF biosynthesis is regulated in *A. flavus*.

It has been proposed that nitrogen limitation induces the expression of infection-related genes in plant pathogenic fungi (Snoeijers et al., 2000; López-Berges et al., 2010). Microorganisms can use a great many nitrogen sources, and it has become widely accepted that glutamine is a key effector

of nitrogen metabolite repression (NMR), a regulatory circuit in filamentous fungi that ensures the preferential use of superior nitrogen sources such as ammonium and glutamine over a broad array of non-preferred compounds (Caddick et al., 1994; Magasanik and Kaiser, 2002; Wong et al., 2008; Wiemann and Tudzynski, 2013; Tudzynski, 2014). The signaling pathway that orchestrates NMR is complex and refined. The positive-acting GATA family transcription factor AreA functions in NMR to allow utilization of preferred nitrogen sources ammonium and glutamine (Wong et al., 2008; Fernandez et al., 2012; Tudzynski, 2014). However, AreA loss-of-function mutants are unable to use non-preferential nitrogen sources other than ammonium and glutamine (Arst and Cove, 1973; Marzluf, 1997). In the presence of ammonium and glutamine, the nitrogen metabolite repressor NmrA interacts with AreA to prevent nitrogen catabolic gene expression; however, in the presence of less preferred nitrogen sources such as nitrate, NmrA dissociates from AreA, allowing AreA to activate the expression of genes involved in alternative nitrogen source usage (Caddick et al., 1994; Andrianopoulos et al., 1998; Wilson and Arst, 1998; Fernandez et al., 2012; Tudzynski, 2014).

The function of NmrA in nitrogen source metabolism in *A. flavus* has not been well characterized (Andrianopoulos et al., 1998; Schönig et al., 2008; Wagner et al., 2010; Zhao et al., 2010). In this study, we identified and cloned the *nmrA* gene from *A. flavus* and characterized *nmrA* deletion and complementation mutants. We demonstrate that *nmrA* plays a negative role in NMR and nitrogen metabolism. Furthermore, *nmrA* appears to be involved in AF biosynthesis, conidiation, sclerotia formation, invasive virulence, and stress responses.

MATERIALS AND METHODS

Fungal Strains and Growth Conditions

Fungal strains and plasmids used in this study are listed in Supplementary Table S1. The *A. flavus* strain PTSΔ*ku70*Δ*pyrG* (Chang et al., 2010), a uracil auxotroph, was purchased from the Fungal Genetics Stock Center (School of Biological Sciences, University of Missouri, Kansas City, MO, USA) and used for gene deletion (Yang et al., 2016). Wild-type (WT) *A. flavus* and the transformants generated in this study were grown on yeast extract–sucrose (YES) agar, yeast extract–glucose agar, or yeast extract–glucose agar with trace elements, uracil, and uridine (Yang et al., 2016). YES medium, potato dextrose agar (PDA, Bai and Shaner, 1996), Czapek agar (CA, Becton Dickinson), and glucose minimal medium (GMM, Shimizu and Keller, 2001) were used for mycelial growth assays, sporulation analysis, and AF analysis. All experiments included four replicate plates and were performed at least three times with similar results, and the error was expressed as the standard deviation.

Sequence Analysis of NmrA

The NmrA sequence (EED47920) from *A. flavus* was originally identified in the NCBI Protein database using BLAST. To verify the existence and the size of the exon in *nmrA*, we cloned the coding sequence into the pET-28a(+) expression vector and sequenced it. The obtained sequence was compared with that reported in the NCBI database. The protein domains were analyzed using InterPro[1]. A phylogenetic tree based on NmrA sequences from *A. clavatus* (UniProt: A1C544), *A. flavus* (UniProt: B8NR87), *A. fumigatus* (UniProt: Q4WEG4), *A. nidulans* (UniProt: Q5AU62), *A. niger* (G3XN01), *A. oryzae* (GenBank: XP_001822655.2), and *A. terreus* (UniProt: Q0CAL7) was constructed with DNAMAN 6.0 software using the neighbor-joining method.

Targeted Deletion and Complementation of the *nmrA* Gene

To create an *nmrA* deletion mutant, we constructed an AP-pyrG-BP vector by inserting upstream and downstream flanking sequences of the *nmrA* gene on either side of the *pyrG* gene. The upstream and downstream flanking sequences of *nmrA* were amplified from genomic DNA of *A. flavus* WT with primer pairs *nmrA*-P1/*nmrA*-P2 and *nmrA*-P3/*nmrA*-P4, respectively (Supplementary Table S2). The *nmrA* deletion mutant (Δ*nmrA*) was complemented with a full-length *nmrA* gene, a 2869 bp fragment, spanning from 1069 bp upstream of the WT *A. flavus nmrA* translation initiation codon to 681 bp downstream of the translation termination codon, to confirm that the phenotype of the Δ*nmrA* mutant was due to deletion of the *nmrA* gene. The full-length *nmrA* gene was amplified from genomic DNA of *A. flavus* WT using the primer pair *nmrA*-CF/*nmrA*-CR (Supplementary Table S2), and it contained a constitutive promoter, which controlled *nmrA* gene expression. The complementation plasmid (pPTR I-*nmrA*) was constructed using the backbone of the chromosomal integrating shuttle vector pPTR I DNA (Takara, Japan, Kubodera et al., 2000), which contained the same restriction enzyme recognition sites as the full-length *nmrA* gene and could integrate into *A. flavus* genome randomly. Six out of 15 pyrithiamine resistance transformants were selected for their wild-type growth phenotype in the presence of GMM supplementing ammonium as the sole nitrogen source. We concluded that these transformants had integrated an intact copy of the *A. flavus nmrA* gene into the genome after the *A. flavus nmrA* gene in this plasmid was sequenced to ensure flawlessness of the sequence.

Mycelial Growth and Stress Assays

Mycelial growth assays were performed on YES medium, PDA, and GMM supplemented with 50 mM glutamine, ammonium, proline, alanine, or sodium nitrite ($NaNO_2$). For the stress assays, rapamycin, methyl methanesulfonate (MMS), NaCl, and sorbitol were added to YES medium at the concentrations indicated in the figure legends (Yang et al., 2016). Each plate was inoculated with 1 μL of conidial suspension (4×10^4 conidia/mL) and incubated at 28°C for 4–7 days in the dark. The assays were carried out in triplicate and were repeated three times.

Observation and Counting of Conidia

Glucose minimal medium agar and PDA were point-inoculated with 1 μL of conidial suspension (4×10^4 conidia/mL) and

[1]http://www.ebi.ac.uk/interpro/

incubated at 28°C for 5 days in the dark. Three plugs were removed from each plate and the conidia produced by *A. flavus* were suspended in a solution of 0.05% Tween 20 and 7% dimethylsulfoxide (DMSO), and counted in a hemocytometer. Conidial suspensions were viewed with an inverted microscope (Leica Microsystems, Germany).

Analysis of AF Production

For analysis of AF production, 1 mL of spore suspension (1×10^6 spores/mL) was inoculated in YES, PDA or GMM supplemented with 50 mM glutamine, ammonium, proline, alanine, or sodium nitrite and incubated in the dark at 28°C for 7 days. AFs were extracted from 500 μL of culture filtrate with an equal volume of chloroform. The chloroform layer was transferred to a new 1.5 mL tube and evaporated to dryness at 70°C. Thin-layer chromatography was used to identify AFs. A solvent system consisting of acetone and chloroform (1:9, v/v) was used, and the plates were observed under UV light at 365 nm. For quantitative analysis of AF production, GeneTools image analysis software was used.

Sclerotia Assays

Sclerotia formation was measured as previously described (Amaike and Keller, 2011). Briefly, GMM supplemented with the indicated nitrogen sources, 2% agar, and 2% sorbitol was overlaid with 1×10^4 spores/plate. Cultures were grown at 37°C in complete darkness for 7–10 days. Plates were sprayed with 70% ethanol to kill and wash away conidia and exposed sclerotia. The sclerotia were collected from 10 mm cores and counted in triplicate. Experiments were repeated three times.

Seed Infection

Mature live peanut seeds were used to measure the pathogenicity of the WT, Δ*nmrA*, and complementation (Δ*nmrA*::*nmrA*) strains (Duran et al., 2007; Amaike and Keller, 2011). Plates were cultured in the dark at 28°C for 5 days, and the filter paper was moistened daily. Inoculated peanut cotyledons were processed to count conidia and extract AFs, and the methodology of counting conidia and extracting AFs was the same as above described.

Real-Time Quantitative Reverse Transcription Polymerase Chain Reaction (RT-qPCR)

Aspergillus flavus mycelia from the WT, Δ*nmrA*, and Δ*nmrA*::*nmrA* strains were harvested after 48 h of growth. RNA was extracted with TRIzol reagent (Biomarker Technologies, Beijing, China), and then a Nano Drop 2000 and Agilent 2100 were used to evaluate the quality of RNA after total RNA extraction and DNase I treatment. TransScript® All-in-One First-Strand cDNA Synthesis SuperMix was used to synthesize cDNA, and RT-qPCR was performed on a PikoReal™ Real-Time PCR System (Thermo Scientific Inc.) with PikoReal™ 2.2 software using TransStart Top Green qPCR SuperMix (TransGen Biotech, Beijing, China). The RT-qPCR conditions were as follows: 95°C for 7 min and 40 cycles of 95°C for 5 s and 60°C for 30 s. The *A. flavus actin* gene was used as an reference gene to normalize the expression data. The relative expression of genes was calculated using the $2^{-\Delta\Delta Ct}$ method, and standard deviation was calculated from three biological replicates (Livak and Schmittgen, 2001). The gene-specific primers are shown in Supplementarey Table S3.

RESULTS

Sequence Analysis of NmrA in *Aspergillus*

In *A. nidulans*, NmrA can bind nicotinamide dinucleotides and may have a redox-sensing function, since NmrA is bound with NAD^+ and $NADP^+$ preferentially to NADH and NADPH. In addition, NmrA interacts directly with AreA zinc fingers (Stammers et al., 2001; Kotaka et al., 2008; Zhao et al., 2010). The *A. flavus nmrA* ORF consists of 1,119 bp with one introns, and encodes a putative NMR regulator NmrA with 351 amino acids. *A. flavus* NmrA might function similarly to its ortholog in *A. nidulans*, since the two protein sequences have a similarity of 88.07%. We downloaded the NmrA protein sequences of seven representative *Aspergillus* species (*A. clavatus*, *A. flavus*, *A. fumigatus*, *A. nidulans*, *A. niger*, *A. oryzae*, and *A. terreus*) from FungiDB[2] and aligned using DNAMAN software version 6.0.3.99 (**Figure 1**). The sequence similarity was as high as 94.81%, demonstrating a highly conserved nature of NmrA in *Aspergillus*. For instance, the NmrA protein sequences in *A. flavus* and *A. oryzae* are only differed at one amino acid between the proteins of, reflecting the evolutionary similarity between them. We also identified a canonical Rossmann fold motif in *A. flavus* NmrA.

Radial Growth on Various Nitrogen Sources

A targeted gene deletion strategy was employed to determine the roles of *nmrA* in *A. flavus* (Supplementary Figure S1A). The *nmrA* gene was successfully replaced with the *pyrG* cassette (Supplementary Figure S1B), indicating that the *nmrA* deletion mutant (Δ*nmrA*) was successfully constructed. The Δ*nmrA* strain was complemented by introducing a construct consisting of the *nmrA* open reading frame in the pPTR I vector, which generated the complementary strain Δ*nmrA*::*nmrA*. The Δ*nmrA* and Δ*nmrA*::*nmrA* strains were verified by RT-PCR and RT-qPCR (Supplementary Figures S1B,C). The growth rate of the Δ*nmrA* strain consistently matched that of the WT and Δ*nmrA*::*nmrA* strains on YES medium and PDA, but the growth rate was slower than that of the WT and Δ*nmrA*::*nmrA* strains on GMM supplemented with glutamine, ammonium, proline, alanine, or sodium nitrite as the sole nitrogen source (the usual nitrogen source in GMM is sodium nitrate, $NaNO_3$) (**Figures 2A,B**). The edges of the mycelial colonies of the Δ*nmrA* strain were more irregular on glutamine, ammonium, and proline than on the other nitrogen sources (**Figure 2A**). It should be mentioned that *A. flavus* strains could not grow

[2]http://fungidb.org/fungidb/

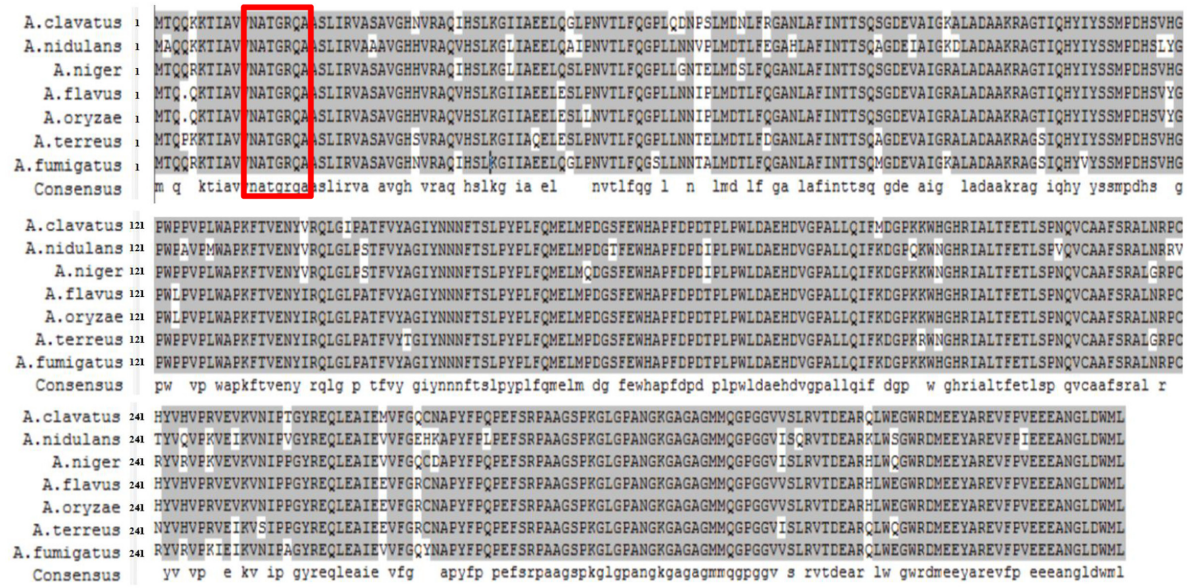


FIGURE 1 | Sequence alignment of nitrogen metabolite repressor NmrA proteins in *Aspergillus clavatus*, *A. flavus*, *A. fumigatus*, *A. nidulans*, *A. niger*, *A. oryzae,* and *A. terreus*. DNAMAN 6.0.3.99 software was used for the alignment and presentation. Residues boxed in red mark the Rossmann fold motif.

normally on sodium nitrate because of a deficiency of the nitrate reductase gene *niaD*. Therefore, sodium nitrite was used in place of sodium nitrate; however, the deletion strain showed retarded growth on this nitrogen source as well. These results suggested that *nmrA* could regulate nitrogen utilization and metabolism.

Colony Morphology and Conidiation of the Δ*nmrA* Mutant

There was little difference in conidia production among strains when they were germinated on PDA, but the Δ*nmrA* strain produced more spores than the WT and Δ*nmrA*::*nmrA* strains when germination occurred on GMM with ammonium (**Figures 2A** and **3A**). The Δ*nmrA* mutant also produced more conidiophores than the WT and Δ*nmrA*::*nmrA* strains on GMM with ammonium (**Figure 3B**). To gain further insight into the role of NmrA in conidiation, we performed RT-qPCR analysis. The results showed that transcript levels of the conidiation-related genes *abaA* (AFLA_029620) and *brlA* (AFLA_082850) were higher in Δ*nmrA* than in WT *A. flavus* and Δ*nmrA*::*nmrA* when the strains were germinated on GMM with ammonium (Kato et al., 2003; Son et al., 2013), while there was little difference among strains when germination occurred on PDA (**Figure 3C**). Collectively, these results indicated that *nmrA* was likely involved in the regulation of conidiation in *A. flavus*.

AF Production by the Δ*nmrA* Mutant

Next, we assessed the production of AFs by the WT, Δ*nmrA*, and Δ*nmrA*::*nmrA* strains on the media described in **Figure 2**. Like the growth rate, AF production was similar among the WT, Δ*nmrA*, and Δ*nmrA*::*nmrA* strains when they were grown on YES or PDA plates (**Figure 4**). However, there were significant decrease in AF production among the strains when they were germinated on GMM supplemented with glutamine and alanine (**Figures 4A,B**). We concluded that *nmrA* might participate in the regulation of AF biosynthesis in *A. flavus*.

Sclerotia Production by the *nmrA* Deletion Strain

We found that in addition to suppressing AF biosynthesis, *nmrA* deletion resulted in a concomitant increase in sclerotia production. The Δ*nmrA* strain displayed a more compact and intensive distribution of sclerotia on the plate than the WT and Δ*nmrA*::*nmrA* strains (**Figure 5A**). To some extent, sclerotia production by the Δ*nmrA* mutant was greater on glutamine than on ammonium (**Figure 5B**), indicating that it could be affected by the quality of the nitrogen source. In summary, the effect of the *nmrA* gene on sclerotia production by *A. flavus* was modulated by the nitrogen source.

Requirement of *nmrA* for Virulence of *A. flavus*

Although Wilson examined the role of three NmrA orthologs in *Magnaporthe oryzae* during infection of rice (Wilson et al., 2010), there has been no report on the role of NmrA in infection by *A. flavus*. To dissect the role of NmrA in invasive growth, we assessed the growth of *A. flavus* on peanut seeds. **Figure 6A** shows that the Δ*nmrA* strain was crippled in its ability to colonize and sporulate on host seeds compared with WT *A. flavus* and Δ*nmrA*::*nmrA*. Deletion of *nmrA* also led to statistically significant reductions in conidia production and AF biosynthesis

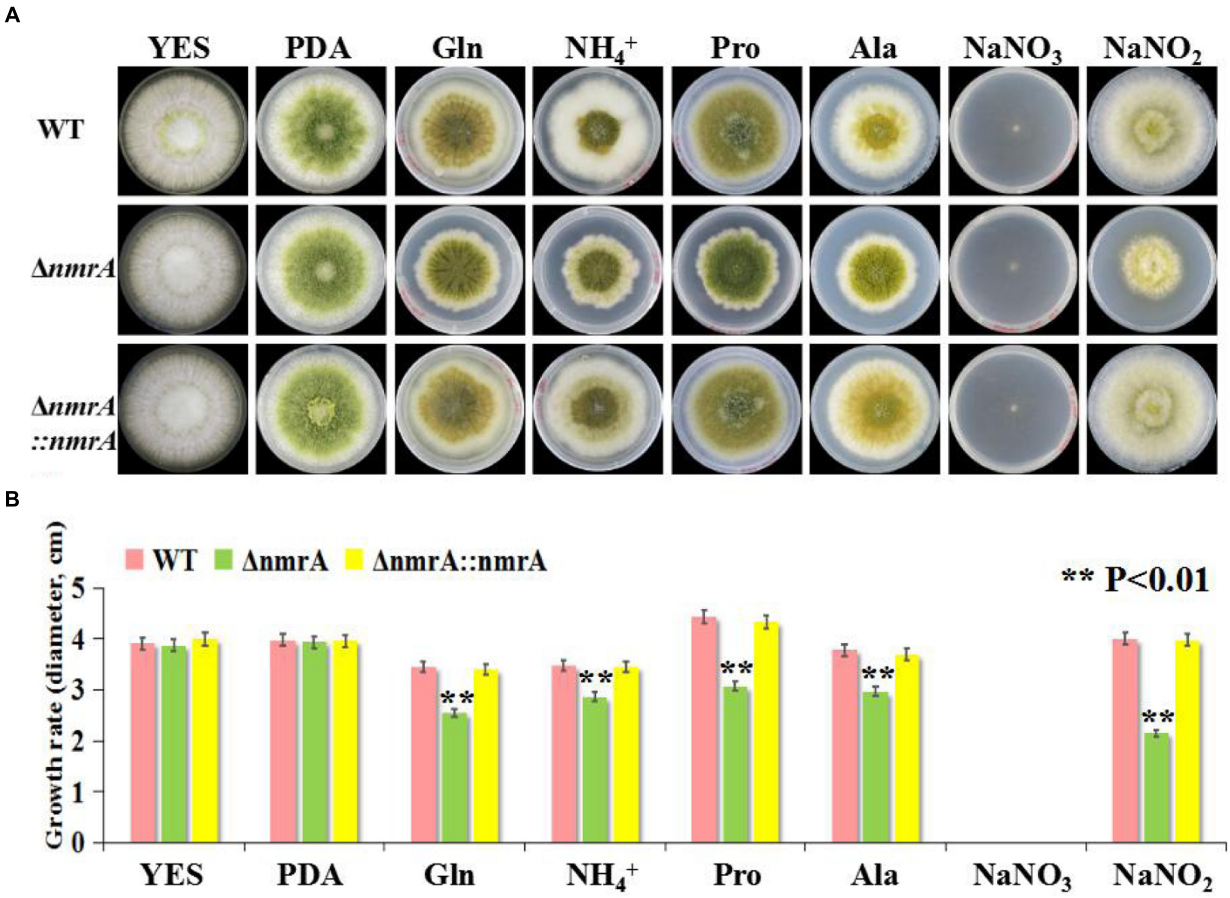


FIGURE 2 | Utilization of *A. flavus* Δ*nmrA* mutant on different nitrogen sources. (A) Radial growth of mycelia on YES, PDA, and GMM supplemented with 50 mM glutamine, ammonium, proline, alanine, sodium nitrate, and sodium nitrite, respectively, as a sole nitrogen source for 7 days at 28°C in the darkness. The photographs were taken on the 5th day. **(B)** Growth rate of WT, Δ*nmrA* and Δ*nmrA*::*nmrA* strains vegetated on YES, PDA, and GMM supplemented with different nitrogen sources on the 5th day at 28°C in the dark. Asterisk indicated statistical significance at $P < 0.01$.

(**Figures 6B,C**), which resulted in the decrease in virulence. These data suggested that *nmrA* deletion reduced the virulence of *A. flavus*.

Responses of the Δ*nmrA* Mutant to Multiple Stressors

To explore the potential roles of NmrA in responses to environmental stressors, we tested fungal sensitivity to the target of rapamycin (TOR) inhibitor rapamycin, the alkylating agent MMS, and the osmotic stressors NaCl and sorbitol. Previous research has shown that TOR-mediated repression of nitrogen catabolic genes and virulence occurs through MeaB-dependent and MeaB-independent mechanisms in *Fusarium oxysporum* (López-Berges et al., 2010), so it seemed possible that an interaction between NmrA and TOR might be involved in nitrogen metabolism regulation in *A. flavus*. The assay results showed that the Δ*nmrA* mutant was more sensitive to rapamycin and MMS than WT *A. flavus* or Δ*nmrA*::*nmrA*. However, the Δ*nmrA* mutant was not more sensitive to the osmotic stressors (**Figures 7A,B**). Overall, these results indicated that NmrA is associated with the TOR pathway.

Possible Crosstalk between NmrA and Other Nitrogen Regulatory Genes

The potential interactive partners of NmrA were identified using the SMART analysis service[3]. The identified partners included the GATA transcriptional activator AreA (AFLA_049870), the bZIP transcription factor MeaB (AFLA_031790), the GATA transcription factor AreB (AFLA_136100), the siderophore transcription factor SreA (AFLA_132440), the nitrate reductase NiaD (AFLA_018810), and the C6 transcription factor NirA (AFLA_093040) (**Figure 8A**). Nitrite reductase NiiA (AFLA_018800) was also analyzed. The possible interactions were analyzed by real-time qRT-PCR. The transcript levels of *areA*, *areB*, *nmrA*, *meaB*, *sreA*, and *nirA* on ammonium were

[3]http://smart.embl-heidelberg.de/

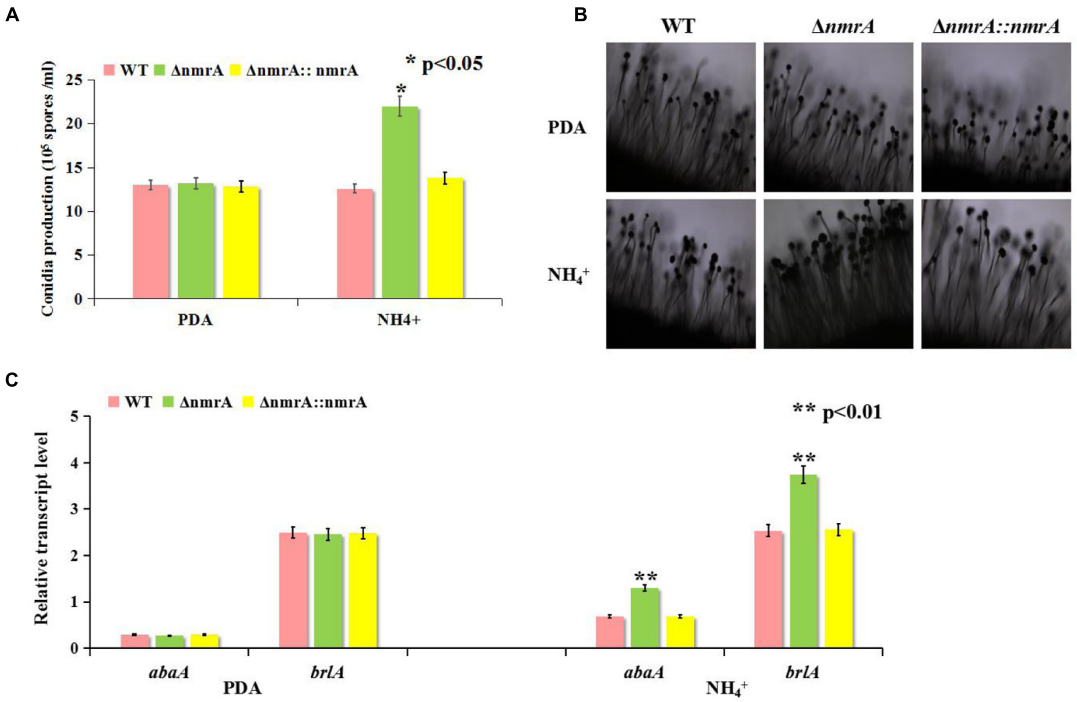


FIGURE 3 | Deletion of *nmrA* affected conidia production. Bars represent SE from three independent experiments with three replicates. **(A)** Deletion of *nmrA* resulted in conidiation augment on GMM supplemented with ammonium. Asterisk indicated statistical significance at $P < 0.05$. **(B)** Conidiophores were observed under a light microscope at 12 h after induction with illumination. Scale bar: 200 μm. **(C)** RT-qPCR analysis was performed in the indicated strains germinated on media as described in **(A)**. The asterisks represented a significant difference level of $P < 0.01$.

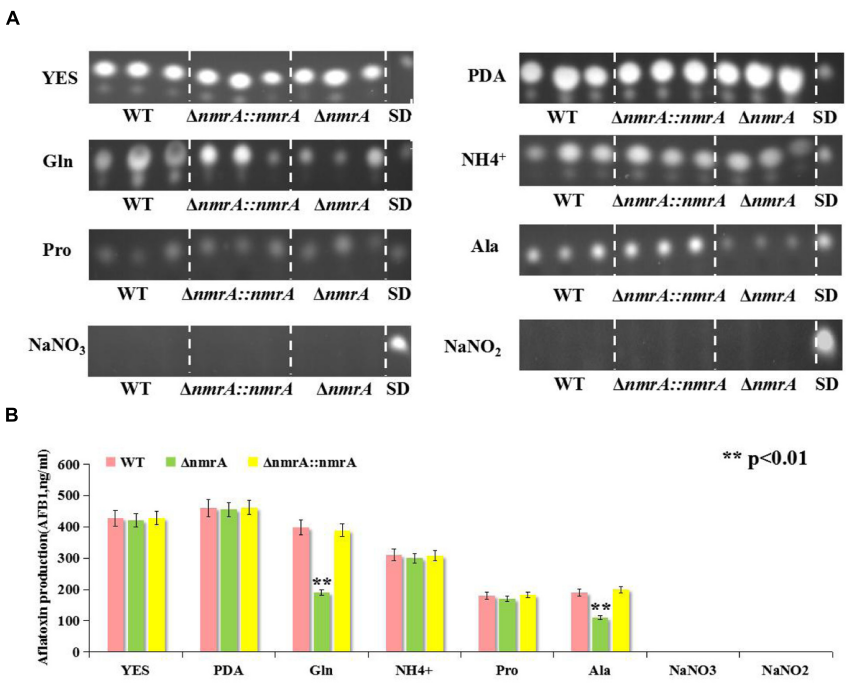


FIGURE 4 | Aflatoxin (AFB1) assessment of WT, Δ*nmrA* and Δ*nmrA*::*nmrA* strains grown on different culture media. (A) Aflatoxin production of WT, Δ*nmrA* and Δ*nmrA*::*nmrA* strains grown on media as described in **Figure 2**. **(B)** Quantification results of AFB1 of WT, Δ*nmrA* and Δ*nmrA*::*nmrA* strains grown on as **(A)** by Gene Tools analysis system software. SD means standard AFB1. The asterisks represented a significant difference level of $P < 0.01$.

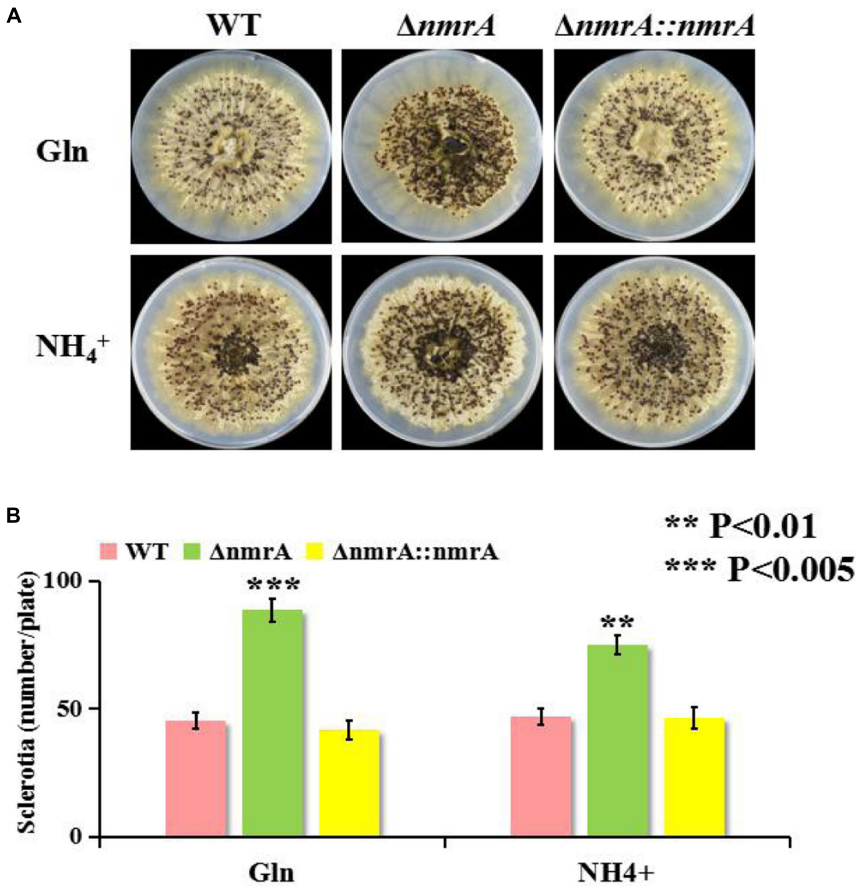


FIGURE 5 | Sclerotia production of Δ*nmrA* mutant. (A) One representative plate for the WT, Δ*nmrA* and Δ*nmrA*::*nmrA* strains grown on GMM supplemented with 50 mM glutamine and ammonium plus 2% sorbitol to induce sclerotia production at 37°C for 7 days in dark condition. **(B)** Quantity analysis of sclerotia among the strains listed. Asterisks indicated significant differences between each depletion strain relative to the WT and Δ*nmrA*::*nmrA* strains as determined by a Student *T*-test, with $^{**}P < 0.01$, $^{***}P < 0.005$.

higher than those on nitrite, suggesting that these genes are likely involved in NMR. The finding that the *areA* expression level on ammonium exceeded that on nitrite was unexpected and was probably correlated with nitrate reductase deficiency and the relative richness of the nitrogen sources. However, transcript levels of *niaD* and *niiA* on ammonium were lower than those on nitrite (**Figure 8B**). Furthermore, on ammonium, all transcript levels except that of *sreA* were higher in the Δ*nmrA* strain than in the WT and Δ*nmrA*::*nmrA* strains. In contrast, on nitrite, *areA*, *meaB*, *sreA*, and *nirA* transcript levels were downregulated in the Δ*nmrA* mutant, while *areB*, *niaD*, and *niiA* transcript levels were upregulated, which was consistent with the postulated reverse roles of *areA* and *areB*. Importantly, the finding that the *areA*, *areB*, and *meaB* transcript levels on ammonium were higher in the Δ*nmrA* mutant than in the WT and Δ*nmrA*::*nmrA* strains indicates that the roles of these genes in nitrogen repression might be related to *nmrA*. Moreover, the observation that *niaD* and *niiA* transcript levels on nitrite were significantly higher in the Δ*nmrA* mutant than in WT *A. flavus* and Δ*nmrA*::*nmrA* demonstrates that NmrA strictly repressed transcriptional activation of genes encoding enzymes required for utilization of less favored nitrogen sources. In conclusion, these findings shed light on the complexity and sophistication of the regulatory mechanisms of NMR.

DISCUSSION

The protein NmrA was defined as a repressor of the GATA transcription factor AreA, which regulates several genes required for utilization of less preferred nitrogen sources (Caddick et al., 1986; Andrianopoulos et al., 1998; Tudzynski, 2014), and the bZIP protein MeaB was proposed to activate NmrA in *A. nidulans* (Wong et al., 2007; López-Berges et al., 2010; Amaike et al., 2013). AreA, MeaB, and NmrA and are conserved in filamentous fungi (Wagner et al., 2010). In this study, we established that NmrA is highly conserved among *Aspergillus* species at the amino acid sequence level, and NmrA of *A. flavus* has a canonical Rossmann fold motif. We then investigated the roles of NmrA in *A. flavus*.

Our work showed that *nmrA* deletion reduced the growth of *A. flavus*, suggesting that *nmrA* participated in nitrogen source metabolism and utilization. Moreover, we also found

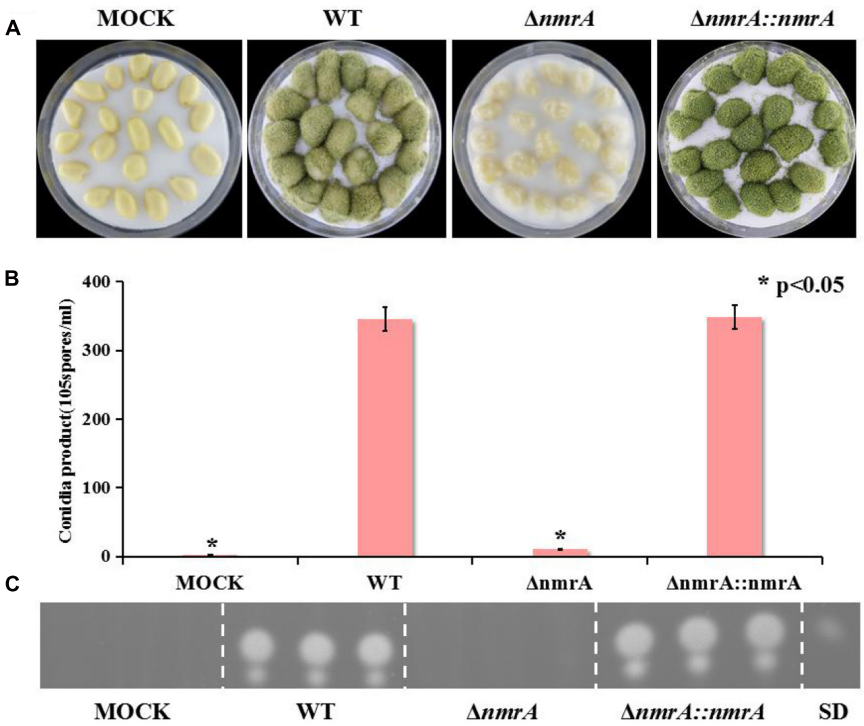


FIGURE 6 | Pathogenicity assay of Δ*nmrA* mutant. (A) Growth of *A. flavus* WT, Δ*nmrA* and Δ*nmrA*::*nmrA* strains on living peanut cotyledons after 5 days of inoculation. **(B)** Conidia production on peanut cotyledons after inoculation of 5 days. Asterisk indicates statistical significance at $P < 0.05$. **(C)** TLC measurements of aflatoxin (AFB1) extracted from seed in **(A)**. SD means standard AFB1.

that there was no difference in mycelial growth among the WT, Δ*nmrA* and Δ*nmrA*::*nmrA* strains grown on Czapek Dox media (carbon source is sucrose), regardless of the nitrogen source (Supplementary Figure S2), which was different from the results of GMM (carbon source is glucose), we speculated that NmrA might also participate in carbon catabolite repression (CCR). It has been shown that deletion of *nmr* (an *nmrA* homolog) in *F. graminearum* had little effect on growth or toxin production in the presence of sucrose (Giese et al., 2013). Furthermore, NmrA was suggested to play a role in carbon metabolism (Macios et al., 2012). Therefore, further investigation of the connections of NmrA with nitrogen and carbon metabolism should be carried out. Interestingly, *A. flavus* WT (functional mutations of nitrate reductase) was incapable of growth on culture medium with nitrate instead of nitrite, but *A. flavus* NRRL3357 was incapable of growth on culture medium with nitrite (data not shown). Therefore, we doubted that there was preferential utilization of nitrate over nitrite.

Aspergillus flavus differentiates to produce asexual dispersing spores (conidia) or overwintering survival structures called sclerotia (Diener et al., 1987; Horowitz Brown et al., 2008). However, sclerotia are also hypothesized to be degenerate sexual structures and may represent a vestige of cleistothecium production (Geiser et al., 1996; Chang et al., 2001). In this study, *nmrA* deletion resulted in significant increases in conidiation and sclerotia production compared with the WT and Δ*nmrA*::*nmrA* strains. Asexual and sexual processes in filamentous fungi are likely to be oppositely regulated by coordinate mechanisms (Horowitz Brown et al., 2008; Chang et al., 2013; Sarikaya-Bayram et al., 2014), so it was surprising that *nmrA* deletion stimulated both conidiation and sclerotia production. These results indicate that NmrA is likely involved in asexual and sexual development.

Aflatoxins, the most deleterious of natural products, are biosynthesized through an extremely refined and sophisticated pathway. This pathway could be affected by many biotic and abiotic factors, including nutritional factors such as carbon and nitrogen sources and environmental factors such as water activity and temperature (Yu, 2012; Amare and Keller, 2014; Zhang et al., 2014, 2015; Bai et al., 2015a,b). In this study, deletion of *nmrA* resulted in reduced AF production only in the presence of glutamine or alanine, suggesting that the effect of *nmrA* on AF biosynthesis is mediated by nitrogen sources and that additional factors must be involved in nitrogen regulation, particularly in the regulation of AF biosynthesis. Although the influence of *nmrA* deletion on secondary metabolism has not been studied in filamentous fungi, the Δ*nmrA* strain of *F. fujikuroi* did not display differential expression of the gibberellic acid biosynthetic gene (Schönig et al., 2008; Tudzynski, 2014). This was not the case in our study and likely reflected the different expression patterns of Nmr1/NmrA in the regulation of secondary metabolism in *Fusarium* and *Aspergillus*.

In some plant pathogenic fungi, AreA is required for full virulence and contributes to pathogenicity, probably because

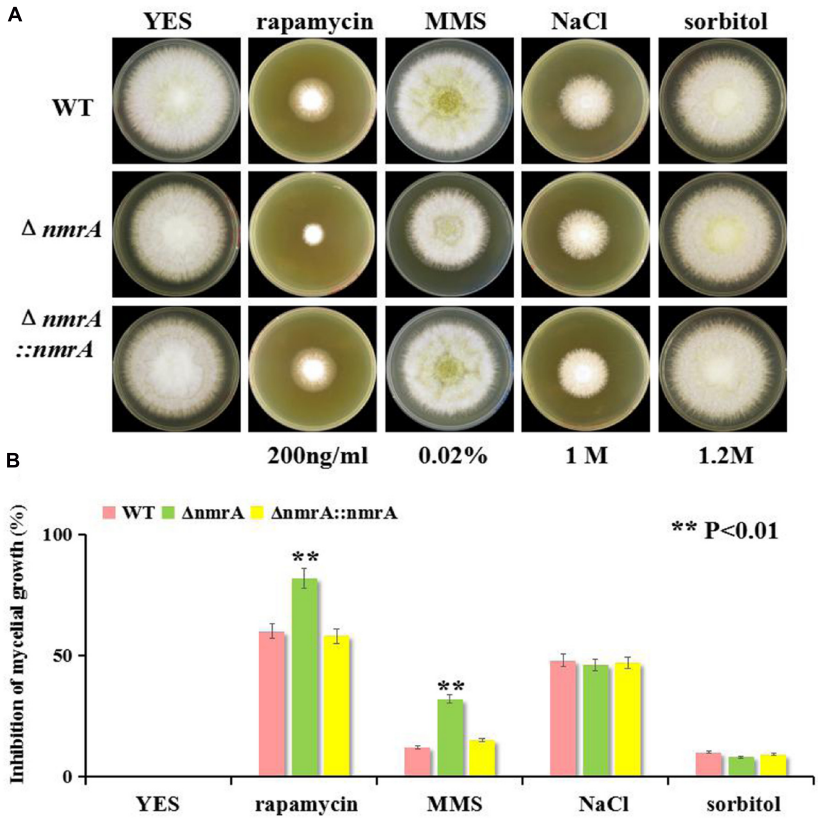


FIGURE 7 | Sensitivity of the Δ*nmrA* strain to multiple stress reagents. (A) Sensitivity of WT, Δ*nmrA* and Δ*nmrA*::*nmrA* strains to 200 ng/mL rapamycin (specific inhibitor of TOR, Target of Rapamycin), 0.02% MMS (methyl methanesulfonate), 1 M NaCl and 1.2 M sorbitol added in YES agar. **(B)** Inhibition of mycelial growth in the Δ*nmrA* strain to multiple stress reagents. Asterisk indicates statistical significance at $P < 0.01$.

of the failure of mutants to fully adapt to poor nitrogen conditions during infection (Min et al., 2012; Tudzynski, 2014). Deletion of *nmrA* in this study decreased the virulence of *A. flavus* on peanut seeds, resulting in decreased colonization as reflected by lower conidia production and AF production. This indicates that NmrA could also contribute to virulence and pathogenicity. As far as we know, this is the first report of the role of NmrA in the virulence and pathogenicity of *A. flavus.*

We examined the sensitivity of the Δ*nmrA* strain to several stressors to dissect the role of NmrA in stress responses. The Δ*nmrA* mutant showed increased sensitivity to rapamycin and MMS, indicating that *nmrA* might be responsive to TOR signaling and DNA damage. Besides the TOR cascade, other signaling components seem to be involved in nitrogen sensing and subsequent regulation of secondary metabolism (Tudzynski, 2014), so it was not surprising that NmrA might be responsive to TOR. However, deletion of the *nmr1* gene in *F. fujikuroi* resulted in increased rapamycin resistance (Teichert et al., 2006), which was the opposite of what we observed. Therefore, we suspect that the roles of Nmr1/NmrA in nitrogen regulation are regulated differently by TOR signaling in *Fusarium* and *Aspergillus*. Zhao et al. (2010) reported that NmrA could discriminate between oxidized and reduced dinucleotides and was positioned close to the GATA motif in DNA, so NmrA might play a role in DNA protection.

In *A. nidulans*, *nmrA* transcription is partially regulated by the bZIP transcription factor MeaB (Wong et al., 2007). However, recent studies showed that *nmrA* expression in *A. nidulans* and *F. fujikuroi* is not MeaB-dependent (Wagner et al., 2010; Amaike et al., 2013), and MeaB and AreA mediate nitrogen repression coordinately while also functioning independently (Wong et al., 2007; Wagner et al., 2010). Moreover, the ability of AreA and AreB to respond to carbon status probably depends on NmrA rather than the transcription factor CreA, which mediates CCR in *A. nidulans* (Macios et al., 2012). Similarly, the sugar sensor Tps1 and the inhibitor proteins Nmr1–3 (orthologs of NmrA) are all regulators of CCR in *Magnaporthe oryzae* (Fernandez et al., 2012), again illustrating how carbon and nitrogen metabolism are intimately linked. Furthermore, AreA, AreB, MeaB, and Nmr (a homolog of NmrA) have been implicated in the regulation of secondary metabolite production in *F. fujikuroi* (Andrianopoulos et al., 1998; Mihlan et al., 2003; Schönig et al., 2008; Wagner et al., 2010). Nevertheless, for most nitrogen-regulated secondary metabolites in fungi, the molecular mechanism of the nitrogen dependency is not well understood (Tudzynski, 2014). So we attempted to find links between NmrA and other interactive partners in the study. We searched for possible interactions

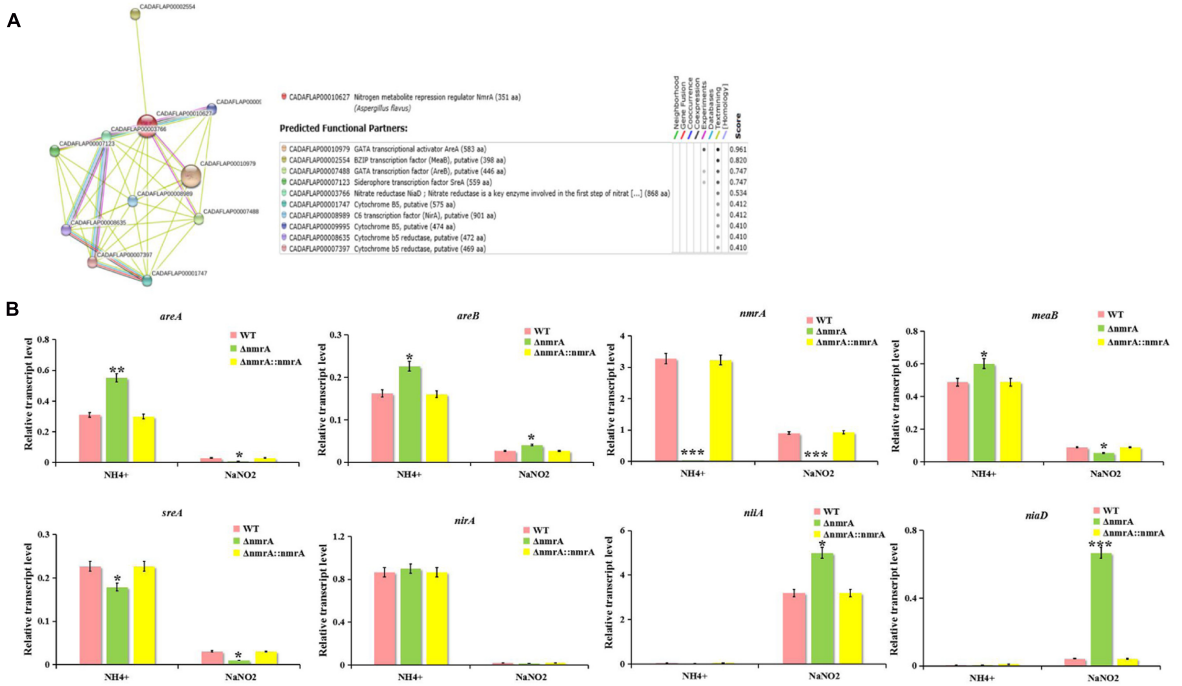


FIGURE 8 | Effect of nitrogen source and Δ*nmrA* on transcript levels of nitrogen regulatory and catabolic genes. (A) Interaction network analyzed by SMART website. **(B)** RT-qPCR analysis was performed in the indicated strains germinated 30 h on GMM supplemented with 50 mM ammonium or NaNO2 as the sole nitrogen source. Transcript levels of nitrogen regulatory genes *areA*, *areB*, *nmrA*, *meaB*, *sreA,* and *nirA* as well as nitrogen catabolic genes *niaD* and *niiA* in Δ*nmrA* strain (light-green columns) were expressed compared to transcript levels of the WT (pink columns), and Δ*nmrA*::*nmrA* strains (yellow columns). The *A. flavus actin* gene was used as an internal control to normalize the expression data. Bars represent SE from three independent experiments with four replicates each. Asterisks indicated significant differences between each depletion strain relative to the WT and Δ*nmrA*::*nmrA* strains as determined by a Student *T*-test, with $^{*}P < 0.05$, $^{**}P < 0.01$, $^{***}P < 0.005$.

between *nmrA* and other nitrogen regulatory and catabolic genes using the SMART website. RT-qPCR showed that the expression of these interactive partners was up- or down-regulated in the Δ*nmrA* mutant compared with the WT and Δ*nmrA*::*nmrA* strains in the presence of ammonium and nitrite. However, the detailed interaction networks of NmrA and its interactive partners are still unknown. Therefore, further investigation of the interaction networks of nitrogen regulatory and catabolic genes should be undertaken.

In this study, the *nmrA* gene was identified in *A. flavus*, and characterization of *nmrA* mutants revealed that NmrA plays crucial roles in radial growth, conidia and sclerotia formation, AF production, virulence, and stress responses. *nmrA* may also interact with other nitrogen regulatory and catabolic genes. To our knowledge, this is the first report of the function of NmrA in *A. flavus*. Our study provides new insights into the role of NmrA in regulating nitrogen source metabolism and AF biosynthesis in *A. flavus*.

AUTHOR CONTRIBUTIONS

XH, BW, and SW conceived and designed the experiments. XH and W-BY wrote the manuscript. XH and MQ performed the experiments. XH and BW analyzed the data. XN, QQ, SR, KY, FZ, and ZZ contributed reagents/materials/analysis tools. SW supported financially and administratively, final approval of manuscript.

FUNDING

This research was supported by the National 973 Program (No. 2013CB127802) from the Ministry of Science, Technology of China and by grants (No. 31172297, 31000961 and 31400100) from the National Natural Science Foundation of China (NSFC), and Foundation of The Education Department of Fujian Province for Young and Middle-aged Researchers (JA14115).

ACKNOWLEDGMENT

We are grateful to Prof. Zhumei He (Sun Yat-sen University, Guangzhou, China) provide the strain *A. flavus* NRRL3357.

SUPPLEMENTARY MATERIAL

The Supplementary Material for this article can be found online at: http://journal.frontiersin.org/article/10.3389/fmicb.2016.01794/full#supplementary-material

REFERENCES

Amaike, S., Affeldt, K. J., Yin, W. B., Franke, S., Choithani, A., and Keller, N. P. (2013). The bZIP protein MeaB mediates virulence attributes in *Aspergillus flavus*. *PLoS ONE* 8:e74030. doi: 10.1371/journal.pone.0074030

Amaike, S., and Keller, N. P. (2011). *Aspergillus flavus*. *Annu. Rev. Phytopathol.* 49, 107–133. doi: 10.1146/annurev-phyto-072910-095221

Amare, M. G., and Keller, N. P. (2014). Molecular mechanisms of *Aspergillus flavus* secondary metabolism and development. *Fungal Genet. Biol.* 66, 11–18. doi: 10.1016/j.fgb.2014.02.008

Andrianopoulos, A., Kourambas, S., Sharp, J. A., Davis, M. A., and Hynes, M. J. (1998). Characterization of the *Aspergillus nidulans* nmrA gene involved in nitrogen metabolite repression. *J. Bacteriol.* 180, 1973–1977.

Arst, H. N. Jr., and Cove, D. J. (1973). Nitrogen metabolite repression in *Aspergillus nidulans*. *Mol. Gen. Genet.* 126, 111–141. doi: 10.1007/BF00330988

Bai, G. H., and Shaner, G. (1996). Variation in *Fusarium graminearum* and cultivar resistance to wheat scab. *Plant Dis.* 80, 975–979. doi: 10.1094/PD-80-0975

Bai, Y., Lan, F., Yang, W., Zhang, F., Yang, K., Li, Z., et al. (2015a). sRNA profiling in *Aspergillus flavus* reveals differentially expressed miRNA-like RNAs response to water activity and temperature. *Fungal Genet. Biol.* 81, 113–119. doi: 10.1016/j.fgb.2015.03.004

Bai, Y., Wang, S., Zhong, H., Yang, Q., Zhang, F., Zhuang, Z., et al. (2015b). Integrative analyses reveal transcriptome-proteome correlation in biological pathways and secondary metabolism clusters in *A. flavus* in response to temperature. *Sci. Rep.* 5:14582. doi: 10.1038/srep14582

Caddick, M. X., Arst, H. N. Jr., Taylor, L. H., Johnson, R. I., and Brownlee, A. G. (1986). Cloning of the regulatory gene *areA* mediating nitrogen metabolite repression in *Aspergillus nidulans*. *EMBO J.* 5, 1087–1090.

Caddick, M. X., Peters, D., and Platt, A. (1994). Nitrogen regulation in fungi. *Antonie Van Leeuwenhoek* 65, 169–177. doi: 10.1007/BF00871943

Chang, P. K., Bennett, J. W., and Cotty, P. J. (2001). Association of aflatoxin biosynthesis and sclerotial development in *Aspergillus parasiticus*. *Mycopathologia* 153, 41–48. doi: 10.1023/A:1015211915310

Chang, P. K., Scharfenstein, L. L., Li, P., and Ehrlichet, K. C. (2013). *Aspergillus flavus* VelB acts distinctly from VeA in conidiation and may coordinate with FluG to modulate sclerotial production. *Fungal Genet. Biol.* 58–59, 71–79. doi: 10.1016/j.fgb.2013.08.009

Chang, P. K., Scharfenstein, L. L., Wei, Q., and Bhatnagar, D. (2010). Development and refinement of a high-efficiency gene-targeting system for *Aspergillus flavus*. *J. Microbiol. Methods* 81, 240–246. doi: 10.1016/j.mimet.2010.03.010

Diener, U. L., Cole, R. J., Sanders, T. H., Payne, G. A., Lee, L. S., and Klich, M. A. (1987). Epidemiology of aflatoxin formation by *Aspergillus flavus*. *Annu. Rev. Phytopathol.* 25, 249–270. doi: 10.1146/annurev.py.25.090187.001341

Duran, R. M., Cary, J. W., and Calvo, A. M. (2007). Production of cyclopiazonic acid, aflatrem, and aflatoxin by *Aspergillus flavus* is regulated by *veA*, a gene necessary for sclerotia formation. *Appl. Microbiol. Biotechnol.* 73, 1158–1168. doi: 10.1007/s00253-006-0581-5

Fernandez, J., Wright, J. D., Hartline, D., Quispe, C. F., Madayiputhiya, N., and Wilson, R. A. (2012). Principles of carbon catabolite repression in the rice blast fungus: Tps1, Nmr1-3, and a MATE–family pump regulate glucose metabolism during infection. *PLoS Genet.* 8:e1002673. doi: 10.1371/journal.pgen.1002673

Geiser, D. M., Timberlake, W. E., and Arnold, M. L. (1996). Loss of meiosis in Aspergillus. *Mol. Biol. Evol.* 13, 809–817. doi: 10.1093/oxfordjournals.molbev.a025641

Giese, H., Sondergaarda, T. E., and Sørensenaet, J. L. (2013). The AreA transcription factor in *Fusarium graminearum* regulates the use of some nonpreferred nitrogen sources and secondary metabolite production. *Fungal Biol.* 117, 814–821. doi: 10.1016/j.funbio.2013.10.006

Horowitz Brown, S., Zarnowski, R., Sharpee, W. C., and Keller, N. P. (2008). Morphological transitions governed by density dependence and lipoxygenase activity in *Aspergillus flavus*. *Appl. Environ. Microbiol.* 74, 5674–5685. doi: 10.1128/AEM.00565-08

Kato, N., Brooks, W., and Calvo, A. M. (2003). The expression of sterigmatocystin and penicillin genes in *Aspergillus nidulans* is controlled by *veA*, a gene required for sexual development. *Eukaryot. Cell* 2, 1178–1186. doi: 10.1128/EC.2.6.1178-1186.2003

Kotaka, M., Johnson, C., Lamb, H. K., Hawkins, A. R., Ren, J., and Stammers, D. K. (2008). Structural analysis of the recognition of the negative regulator NmrA and DNA by the zinc finger from the GATA-type transcription factor AreA. *J. Mol. Biol.* 381, 373–382. doi: 10.1016/j.jmb.2008.05.077

Kubodera, T., Yamashita, N., and Nishimura, A. (2000). Pyrithiamine resistance gene (*ptrA*) of *Aspergillus oryzae*: cloning, characterization and application as a dominant selectable marker for transformation. *Biosci. Biotechnol. Biochem.* 64, 1416–1426. doi: 10.1271/bbb.64.1416

Livak, K. J., and Schmittgen, T. D. (2001). Analysis of relative gene expression data using real time quantitative PCR and the $2^{-\Delta\Delta Ct}$ Method. *Methods* 25, 402–408. doi: 10.1006/meth.2001.1262

López-Berges, M. S., Rispail, N., Prados-Rosales, R. C., and Di Pietro, A. (2010). A nitrogen response pathway regulates virulence functions in *Fusarium oxysporum* via the protein kinase TOR and the bZIP protein MeaB. *Plant Cell* 22, 2459–2475. doi: 10.1105/tpc.110.075937

Macios, M., Caddick, M. X., Weglenski, P., Scazzocchio, C., and Dzikowska, A. (2012). The GATA factors AREA and AREB together with the co-repressor NMRA, negatively regulate arginine catabolism in *Aspergillus nidulans* in response to nitrogen and carbon source. *Fungal Genet. Biol.* 49, 189–198. doi: 10.1016/j.fgb.2012.01.004

Magasanik, B., and Kaiser, C. A. (2002). Nitrogen regulation in *Saccharomyces cerevisiae*. *Gene* 290, 1–18. doi: 10.1016/S0378-1119(02)00558-9

Marzluf, G. A. (1997). Genetic regulation of nitrogen metabolism in the fungi. *Microbiol Mol Biol Rev* 61, 17–32.

Mihlan, M. V., Homann, V., Liu, T. W., and Tudzynski, B. (2003). AREA directly mediates nitrogen regulation of gibberellin biosynthesis in *Gibberella fujikuroi*, but its activity is not affected by Nmr. *Mol. Microbiol.* 47, 975–991. doi: 10.1046/j.1365-2958.2003.03326.x

Min, K., Min, K., Shin, Y., Son, H., Lee, J., Kim, J. C., et al. (2012). Functional analyses of the nitrogen regulatory gene areA in *Gibberella zeae*. *FEMS Microbiol. Lett.* 334, 66–73. doi: 10.1111/j.1574-6968.2012.02620.x

Sarikaya-Bayram, O., Bayram, O., Feussner, K., Kim, J. H., Kim, H. S., Kaever, A., et al. (2014). Membrane-bound methyltransferase complex VapA-VipC-VapB guides epigenetic control of fungal development. *Dev. Cell* 29, 406–420. doi: 10.1016/j.devcel.2014.03.020

Schönig, B., Brown, D. W., Oeser, B., and Tudzynski, B. (2008). Cross-species hybridization with *Fusarium verticillioides* microarrays reveals new insights into *Fusarium fujikuroi* nitrogen regulation and the role of AreA and Nmr. *Eukaryot Cell* 7, 1831–1846. doi: 10.1128/EC.00130-08

Shimizu, K., and Keller, N. P. (2001). Genetic involvement of a cAMP-dependent protein kinase in a G protein signaling pathway regulating molphological and chemical transitions in *Aspergillus nidulans*. *Genetics* 157, 591–600.

Snoeijers, S. S., Perez-Garcia, A., Joosten, M. H. A. J., and de Wit, P. J. G. M. (2000). The effect of nitrogen on disease development and gene expression in bacterial and fungal plant pathogens. *Eur. J. Plant Pathol.* 106, 493–506. doi: 10.1023/A:1008720704105

Son, H., Kim, M. G., Min, K., Seo, Y. S., Lim, J. Y., Choi, G. J., et al. (2013). AbaA regulates conidiogenesis in the Ascomycete Fungus *Fusarium graminearum*. *PLoS ONE* 8:e72915. doi: 10.1371/journal.pone.0072915

Stammers, D. K., Ren, J., Leslie, K., Nichols, C. E., Lamb, H. K., Cocklin, S., et al. (2001). The structure of the negative transcriptional regulator NmrA reveals a structural superfamily which includes the short-chain dehydrogenase/ reductases. *EMBO J.* 20, 6619–6626. doi: 10.1093/emboj/20.23.6619

Teichert, S., Wottawa, M., Schönig, B., and Tudzynski, B. (2006). Role of the *Fusarium fujikuroi* TOR kinase in nitrogen regulation and secondary metabolism. *Eukaryot. Cell* 5, 1807–1819. doi: 10.1128/EC.00039-06

Tudzynski, B. (2014). Nitrogen regulation of fungal secondary metabolism in Fungi. *Front. Microbiol.* 5:656. doi: 10.3389/fmicb.2014.00656

Wagner, D., Schmeinck, A., Mos, M., Morozov, I. Y., Caddick, M. X., and Tudzynski, B. (2010). The bZIP transcription factor MeaB mediates nitrogen

metabolite repression at specfic loci. *Eukaryot. Cell* 9, 1588–1601. doi: 10.1128/EC.00146-10

Wiemann, P., and Tudzynski, B. (2013). "The nitrogen regulation network and its impact on secondary metabolism and pathogenicity," in *Fusarium: Genomics, Molecular and Cellular Biology*, eds D. W. Brown and R. H. Proctor (Norwich: Caister Academic Press), 111–142.

Wilson, R. A., and Arst, H. N. Jr. (1998). Mutational analysis of AREA, a transcriptional activator mediating nitrogen metabolite repression in *Aspergillus nidulans* and a member of the "streetwise" GATA family of transcription factors. *Microbiol. Mol. Biol. Rev.* 62, 586–596.

Wilson, R. A., Gibson, R. P., Quispe, C. F., Littlechild, J. A., and Talbot, N. J. (2010). An NADPH-dependent genetic switch regulates plant infection by the rice blast fungus. *Proc. Natl. Acad. Sci. U.S.A.* 107, 21902–21907. doi: 10.1073/pnas.1006839107

Wong, K. H., Hynes, M. J., Todd, R. B., and Davis, M. A. (2007). Transcriptional control of *nmrA* by the bZIP transcriptional factor MeaB reveals a new level of nitrogen regulation in *Aspergillus nidulans*. *Mol. Microbiol.* 66, 534–551. doi: 10.1111/j.1365-2958.2007.05940.x

Wong, K. H., Hynes, M. J., and Davis, M. A. (2008). Recent advances in nitrogen regulation: a comparison between *Saccharomyces cerevisiae* and filamentous fungi. *Eukaryot. Cell* 7, 917–925. doi: 10.1128/EC.00076-08

Yang, K., Liang, L., Ran, F., Liu, Y., Li, Z., Lan, H., et al. (2016). The DmtA methyltransferase contributes to *Aspergillus flavus* conidiation, sclerotial production, aflatoxin biosynthesis and virulence. *Sci. Rep.* 6:23259. doi: 10.1038/srep23259

Yang, K., Zhuang, Z., Zhang, F., Song, F., Zhong, H., Ran, F., et al. (2015). Inhibition of aflatoxin metabolism and growth of *Aspergillus flavus* in liquid culture by a DNA methylation inhibitor. *Food Addit. Contam. A* 32(4), 554–563. doi: 10.1080/19440049.2014.972992

Yu, J. (2012). Current understanding on aflatoxin biosynthesis and future perspective in reducing aflatoxin contamination. *Toxins (Basel)* 4(11), 1024–1057. doi: 10.3390/toxins4111024

Zhang, F., Guo, Z., Zhong, H., Wang, S., Yang, W., Liu, Y., et al. (2014). RNA-Seq-based transcriptome analysis of aflatoxigenic *Aspergillus flavus* in response to water activity. *Toxins (Basel)* 6, 3187–3207. doi: 10.3390/toxins6113187

Zhang, F., Zhong, H., Han, X., Guo, Z., Yang, W., Liu, Y., et al. (2015). Proteomic profile of *Aspergillus flavus* in response to water activity. *Fungal Biol.* 119, 114–124. doi: 10.1016/j.funbio.2014.11.005

Zhao, X., Hume, S. L., Johnson, C., Thompson, P., Huang, J., Gray, J., et al. (2010). The transcription repressor NmrA is subject to proteolysis by three *Aspergillus nidulans* proteases. *Protein Sci.* 19, 1405–1419. doi: 10.1002/pro.421

Conflict of Interest Statement: The authors declare that the research was conducted in the absence of any commercial or financial relationships that could be construed as a potential conflict of interest.

The reviewer FS and handling Editor declared their shared affiliation, and the handling Editor states that the process nevertheless met the standards of a fair and objective review.

Copyright © 2016 Han, Qiu, Wang, Yin, Nie, Qin, Ren, Yang, Zhang, Zhuang and Wang. This is an open-access article distributed under the terms of the Creative Commons Attribution License (CC BY). The use, distribution or reproduction in other forums is permitted, provided the original author(s) or licensor are credited and that the original publication in this journal is cited, in accordance with accepted academic practice. No use, distribution or reproduction is permitted which does not comply with these terms.

frontiers in Microbiology

ORIGINAL RESEARCH
published: 29 November 2016
doi: 10.3389/fmicb.2016.01899

Structural Elucidation and Molecular Docking of a Novel Antibiotic Compound from Cyanobacterium *Nostoc* sp. MGL001

Niveshika[1], Ekta Verma[1], Arun K. Mishra[1], Angad K. Singh[2] and Vinay K. Singh[3]*

[1] Laboratory of Microbial Genetics, Department of Botany, Banaras Hindu University, Varanasi, India, [2] Department of Chemistry, Banaras Hindu University, Varanasi, India, [3] Centre for Bioinformatics, School of Biotechnology, Banaras Hindu University, Varanasi, India

Cyanobacteria are rich source of array of bioactive compounds. The present study reports a novel antibacterial bioactive compound purified from cyanobacterium *Nostoc* sp. MGL001 using various chromatographic techniques *viz*. thin layer chromatography (TLC) and high performance liquid chromatography (HPLC). Further characterization was done using electrospray ionization mass spectroscopy (ESIMS) and nuclear magnetic resonance (NMR) and predicted structure of bioactive compound was 9-Ethyliminomethyl-12-(morpholin - 4 - ylmethoxy) -5, 8, 13, 16–tetraaza–hexacene - 2, 3 dicarboxylic acid (EMTAHDCA). Structure of EMTAHDCA clearly indicated that it is a novel compound that was not reported in literature or natural product database. The compound exhibited growth inhibiting effects mainly against the gram negative bacterial strains and produced maximum zone of inhibition at 150 μg/mL concentration. The compound was evaluated through *in silico* studies for its ability to bind 30S ribosomal fragment (PDB ID: 1YRJ, 1MWL, 1J7T, and 1LC4) and OmpF porin protein (4GCP, 4GCQ, and 4GCS) which are the common targets of various antibiotic drugs. Comparative molecular docking study revealed that EMTAHDCA has strong binding affinity for these selected targets in comparison to a number of most commonly used antibiotics. The ability of EMTAHDCA to bind the active sites on the proteins and 30S ribosomal fragments where the antibiotic drugs generally bind indicated that it is functionally similar to the commercially available drugs.

Keywords: ***Nostoc*** **sp. MGL001, novel bioactive compound, antibacterial agent, molecular docking, RNA fragments, OmpF porin protein**

OPEN ACCESS

Edited by:
Bhim Pratap Singh, Mizoram University, India

Reviewed by:
Gerard Abraham, Indian Agricultural Research Institute, India
Herdayanto Sulistyo Putro, Institut Teknologi Sepuluh Nopember, Indonesia

****Correspondence:***
Arun K. Mishra
akmishraau@rediffmail.com; akmishraau@hotmail.com

Specialty section:
This article was submitted to Microbial Physiology and Metabolism, a section of the journal Frontiers in Microbiology

Received: *18 September 2016*
Accepted: *11 November 2016*
Published: *29 November 2016*

Citation:
Niveshika, Verma E, Mishra AK, Singh AK and Singh VK (2016) Structural Elucidation and Molecular Docking of a Novel Antibiotic Compound from Cyanobacterium Nostoc sp. MGL001. Front. Microbiol. 7:1899. doi: 10.3389/fmicb.2016.01899

INTRODUCTION

High proportion of drug resistance in bacterial pathogens indicated loss of efficacy of conventional antibiotics as only one third of the diseases could be cured by currently available drugs (Karchmer, 2004; Reynolds et al., 2004; Paterson, 2006). Thus, screening of new biologically active compounds are major thrust area at the present moment (Lahlou, 2013). To date, modern scientific advances in drug discovery could not enable the pace of newer drug development because of very little exploration of natural resources especially microbial metabolites (Cragg and Newman, 2013). Actinomycetes, fungi, unicellular bacteria along with cyanobacteria contributed about 45, 38,

and 17%, respectively, in producing bioactive metabolites (Berdy, 2005; El-Elimat et al., 2012). Of these organisms, cyanobacteria are photoautotrophic in nature and can grow in presence of small amount of nutrients (Bullerjahn and Post, 2014; Dias et al., 2015). Due to these reasons, utilization of cyanobacteria in scientific studies will be a cost effective approach. Cyanobacteria constitute a rich source of unprecedented novel biologically active metabolites (Singh et al., 2005; Sivonen and Börner, 2008; Prasanna et al., 2010), such as peptides, macrolides, phenolic dilactones, polyketides, and alkaloids each of which originate from different pathway and show a broad spectrum of biological activities (Namikoshi and Rinehardt, 1996; Clardy and Walsh, 2004; Kim and Lee, 2006). Estimate proclaim regarding bioactive compounds in fresh water cyanobacteria shown to exhibit antimicrobial, antifungal, antiviral, antitumor, anticancer, and other pharmacological activities (Gul and Hamam, 2005; Mayer and Hamann, 2005; Singh et al., 2005). Extensive screening programme of cyanobacterial bioactive compounds for antibiotics, pharmaceutical and agricultural application has received considerable attention during the past few decades (Patterson et al., 1994; Khairy and El-Kassas, 2010; Kumar et al., 2010).

Among the cyanobacterial genera screened, *Nostoc* sp. are distributed throughout tropical and subtropical regions and proved as prodigious procedure of secondary metabolites. Genus *Nostoc* is highly diversified and reported from various terrestrial and aquatic habitats, and also able to form stable cyanobiont in various symbiosis (Dodds et al., 1995). *Nostoc* species attracted much attention as number of secondary metabolites were isolated, examined and found to have antiviral and antitumor properties (Dembitsky and Rezanka, 2005). Novel antimitotic compound namely Nostodione A has been reported from *Nostoc commune* (Kobayashi et al., 1994). *Nostoc commune* produced novel extracellular diterpenoid having antibacterial activity (Jaki et al., 1999). Potent antitumor agent and antifungal peptolides *viz*. Cryptophycins which is a cyclic depsipeptides isolated from *Nostoc* sp. showing excellent activity against broad spectrum of drug sensitive and drug resistant solid tumors, implanted in mice (Trimurtulu et al., 1994). An antiviral compound Cyanovirin-N has been isolated from *Nostoc ellipsosporum*. Freshwater *Nostoc spongiaeforme* produced Nostocine A exhibiting adverse effect on growth of microorganisms, algae, cultured plants and animal cell lines as well (Hirata et al., 2003). Boron containing metabolite, Borophycin isolated from marine strains *viz. Nostoc linckia* and *N spongiaeforme* var. *tenue*, and cryptophycin from *Nostoc* sp. ATCC 53789 and GSV 224 has been found to exhibit potent cytotoxicity against human tumor cell lines (Burja et al., 2001).

Therefore, in the present study cyanobacterium *Nostoc* sp. MGL001 isolated from fresh water body was used for the screening of antibacterial bioactive compound. Various chromatographic techniques like thin layer chromatography (TLC) and high performance liquid chromatography (HPLC) were performed for purification and purified compound were then subjected to electrospray ionization mass spectrometry (ESIMS) and nuclear magnetic resonance (NMR) spectroscopic analysis for identification and structure elucidation. Additionally, the design approaches mentioned above coupled with the *in silico* computational toolkit for optimizing interactions between ligand (bioactive compound) and receptor molecules. Here, 30S ribosomal fragment (1YRJ, 1MWL, 1J7T, and 1LC4) (Vicens and Westhof, 2001, 2002, 2003; Han et al., 2005) as well as OmpF porin protein (4GCP, 4GCQ and 4GCS) (Ziervogel and Roux, 2013) was selected as target receptors for molecular docking with ligand.

MATERIALS AND METHODS

Isolation and Identification of Cyanobacterium

The experimental organism cyanobacterium *Nostoc* sp. MGL001 was collected from local fresh water pond (Kardmeshwar pond) Chitaipur, Varanasi, India (25.2719° N, 82.9676° E). Pond has an area 5012 m^2 with the mean depth approximately 10.3 m. This pond is present in vicinity of the adjacent temples and not connected to any river.

Sample was washed several times with sterile water and unialgal population of cyanobacterial strain was obtained by serially diluting the source inocula and subsequently streaking it on the solidified BG-11 agar medium. The purity of culture was routinely checked by streaking cyanobacterial culture on nutrient agar plates containing 0.5% of the glucose (w/v) incubated for 24 h. This process was repeated multiple times until pure micro-colonies were obtained. Further cyanobacterial culture was grown in 500 mL Erlenmeyer flasks containing BG11 medium (Rippka et al., 1979). The flasks were kept at 25 ± 2°C under white cool fluorescent light at an intensity of 95 μmol m^{-2} s^{-1}, with a 14/10 h light/dark cycle. Identification of axenic cyanobacterial strain was based on the morphological features (Desikachary, 1959; Komarek, 2013) as well as 16S ribosomal gene amplification (Nübel et al., 1997). The light microscope (Dewinter) attached with a camera was used to study the morphology of filaments and cells. The cell dimensions were measured using software (Dewinter Biowizard 4.1).

To amplify the 16S ribosomal gene segment, DNA was extracted from the exponentially grown cyanobacterial culture growing on BG11 media using Himedia Bacterial DNA purification kit (MB505). Concentration of DNA was measured using Bio Spec Nano Spectrophotometer Life Science (Shimadzu Biotech). Eluted DNA was stored in −20°C. Amplification of 16S rDNA gene was performed using 16S rDNA bacteria specific primers 27F forward (5′-AGAGTTTGATCCTGGCTCAG-3′) and 1492R reverse (5′-TACGGTTACCTTGTTACGACTT-3′) (Weisburg et al., 1991). The PCR amplification (BioRad, DNA Engine, Peltier Thermal Cycler) of 16S rDNA was performed using 25 μl aliquots containing 20–50 μg DNA template, 0.4 μM of each primers, 1.5 μM $MgCl_2$, 200 μM dNTPs, and 1 U/μl Taq Polymerase. Program followed for PCR amplification was: initial denaturation at 95°C for 3 min, 30 cycles of 30 s denaturation at 94°C, 40 s annealing at 55°C, and 50 s extension at 72°C and final extension at 72°C for 20 min (Singh et al., 2015). The amplified product was analyzed on a 1.2% agarose gel stained with ethidium bromide in 1X TBE buffer and then visualized

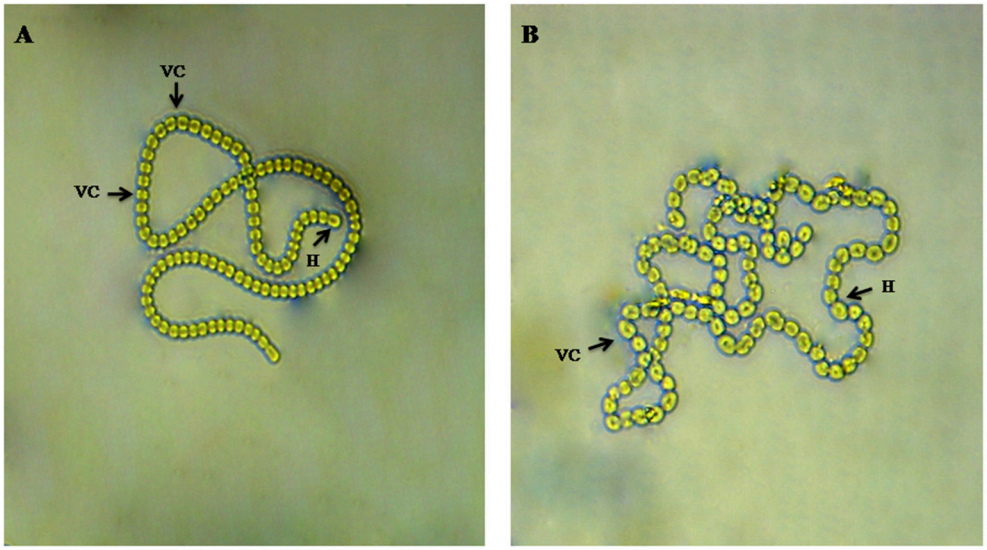


FIGURE 1 | Microphotographs of *Nostoc* sp. MGL001. (A) and **(B)** showing filament with vegetative cell (VC) and heterocysts (H).

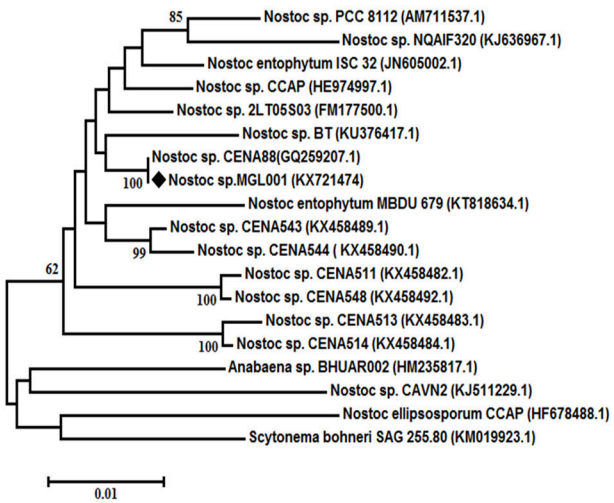


FIGURE 2 | Neighbor-joining tree of *Nostoc* sp MGL001 with reference strains using 16S rDNA gene sequences. Bootstrap values (%) are based on 1000 replicates and shown at the branch point with more than 50% bootstrap values. ♦ Representing the cyanobacteriaum *Nostoc* sp. MGL001 used in the present study.

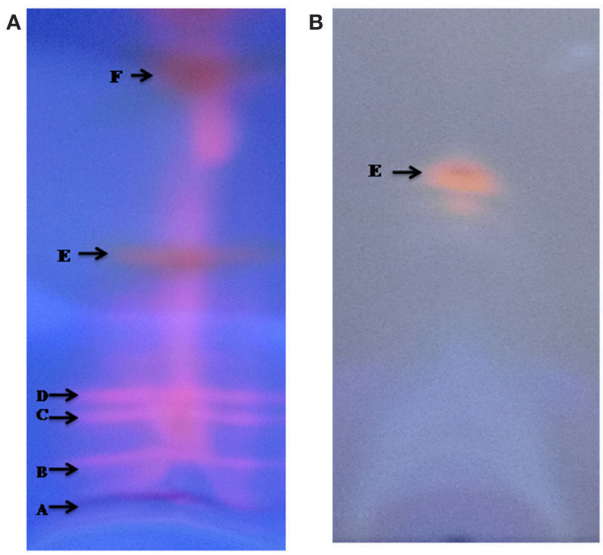


FIGURE 3 | TLC pattern of methanolic crude extract from *Nostoc* sp. MGL001 (A) using carbon tetrachloride and methanol (9:1) as mobile solvent. **(B)** TLC pattern of 2nd TLC spot using ethyl acetate and hexane (1:1) as mobile solvent.

under gel documentation system. The obtained bands were further cut down and eluted using Qiagen quick Gel Extraction kit. The eluted amplified products were finally sent to Sci Genome Cochin, Kerala, India for sequencing.

Nucleotide Sequence Analysis and Construction of Phylogenetic Tree

The partial 16S rDNA sequence obtained from DNA sequencing was then subjected to NCBI sequence database *viz.* nucleotide basic local alignment search tool (Blastn) (http://blast.ncbi.nlm.nih.gov/Blast.cgi) and aligned with the already existing gene sequences of different cyanobacterial species. Furthermore, the partial 16S rDNA sequence of the experimental organism was submitted to the NCBI database using the Sequin submission tool version 15.10. Evolutionary history of closely related sequence in a BLAST search was inferred by neighbor joining algorithm method for construction

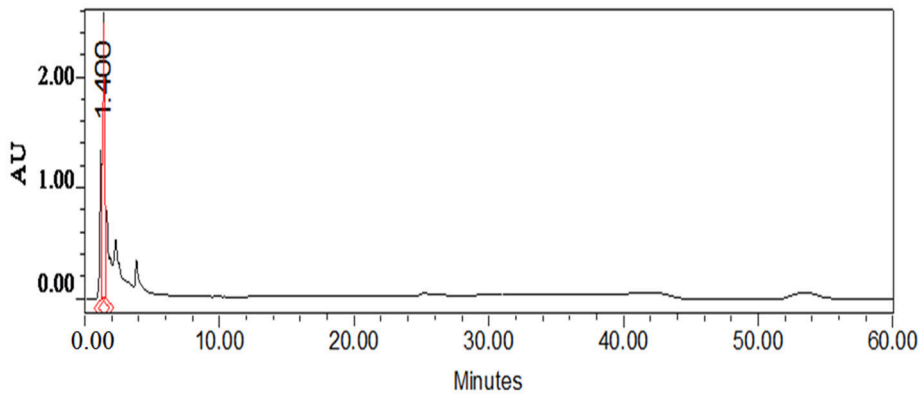


FIGURE 4 | HPLC chromatogram of the spot "E" fraction of the *Nostoc* sp. MGL001 crude extract obtained from TLC.

TABLE 1 | Antibacterial activity of the EMTAHDCA compound against gram negative bacteria.

Test organism	Inhibition zone (mm) at different concentrations of EMTAHDCA (μg/mL)			
	100	150	200	250
E. coli	4.78 ± 0.324	**11.15 ± 0.117**	11.13 ± 0.123	11.15 ± 0.133
P. vulgaris	5.22 ± 0.221	**10.17 ± 0.235**	10.16 ± 0.353	10.16 ± 0.271
P. aeruginosa	4.11 ± 0.356	**9.16 ± 0.211**	9.15 ± 0.233	9.15 ± 0.279

of phylogenetic tree (Saitou and Nei, 1987). Evolutionary analysis was performed using MEGA 6 software (Tamura et al., 2013).

Preparation of Crude Extract

For the preparation of crude extract 40–45 days old cyanobacterial culture was used based on the method of Doan et al. (2000). Cyanobacterial cells (10 g fresh weight) were harvested by centrifugation at 10,000 rpm for 15 min (Remi, India) and then lyophilized (Christ-Alpha 1-2, Germany). Lyophilized cyanobacterial biomass (5 g) was extracted twice or thrice in 300 mL methanol (100%) by keeping it on shaker (150 rpm for 48 h) and centrifuged at 10,000 rpm (15 min). Supernatant was evaporated to dryness using rotary vacuum evaporator (Perfit, India) at 40°C and redissolved in 5 mL of 100% methanol for further use.

Thin Layer Chromatography (TLC)

Dried crude extract of *Nostoc* sp. MGL001 was dissolved in methanol and purified by TLC (TLC silica gel 60, Merck, Darmstadt, Germany). In this process, carbon tetrachloride: methanol (9:1) was used as the mobile phase and silica was used as the stationary phase. The UV-illuminated orange bands on the TLC plate were designated as A, B, C, D, E, and F, which were dissolved separately in 100% methanol (1 mL). Further each elute was then subjected to TLC purification using ethyl acetate: n-hexane (1:1). Only the potent designated bands of the first step were subjected to the second step.

Purification of the Antibacterial Compound Produced by *Nostoc* sp. MGL001 by High Performance Liquid Chromatography (HPLC) Fractionation

Potent band elute after second step of TLC was dissolved in HPLC grade methanol. Separation was achieved using HPLC (Waters, USA) equipped photodiode array (PDA) detector and inline degasser. The reverse phase Nova pack C_{18} Spherisorb S10 ODS column (4.6 × 150 mm, 5 mm particle size) was used and temperature maintained at 40°C. Mobile phase consists of Milli-Q water (A) and acetonitrile (B), containing 0.05% trifluoroacetic acid. All solvents used in study were HPLC grade and filtered through a 0.22 μm membrane filter. For mobile phase, linear gradient programme was: 0 min 25% B, 35 min 70% B, 37 min 70% B, 38 min 25% B, 60 min 25% B (Lawton et al., 1994). Flow rate of 1 ml min^{-1} was maintained for sample run and separation was monitored at 200–300 nm (Harada et al., 1999) having 1.2 nm resolution. Empower2 software was used for instrumentation and data acquisition.

Antibacterial Assay

Pure fraction of bioactive compound was collected through HPLC and concentrated using rotary vacuum evaporator. Concentrated solid mass of pure bioactive compound were weigh. In order to perform antibacterial assay different concentrations of pure bioactive compound were prepared *viz.* 100, 150, 200, and 250 μg/mL in the volume of 1% methanol separately. Antibacterial activity was tested by agar disc diffusion

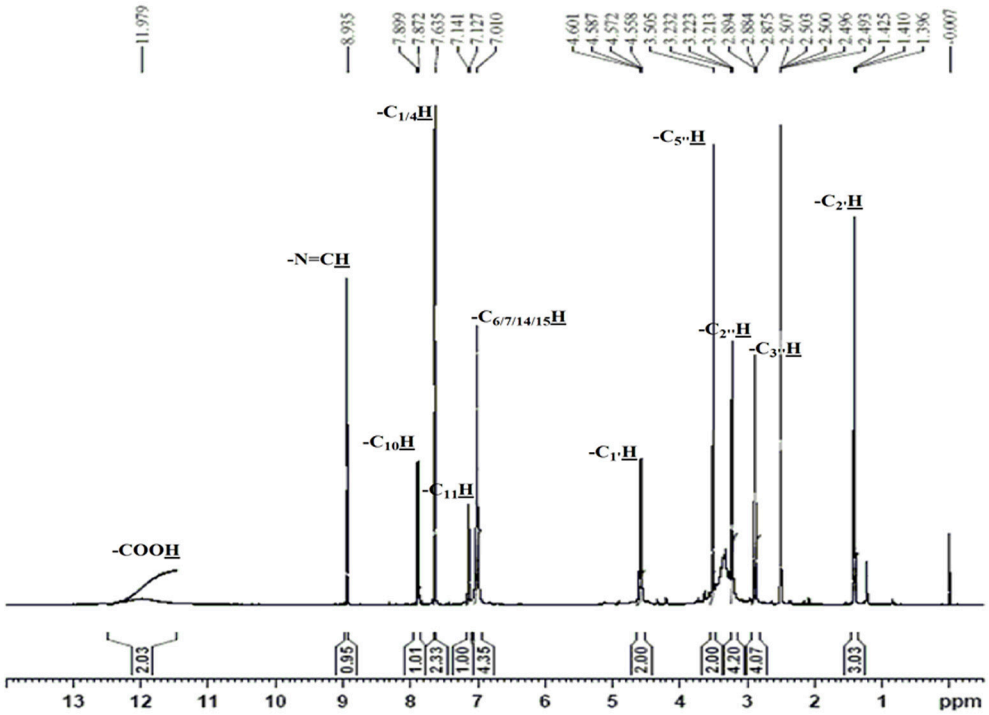


FIGURE 5 | ^{1}H NMR spectrum of the bioactive compound (spot "E" eluate) derived from *Nostoc* sp. MGL001.

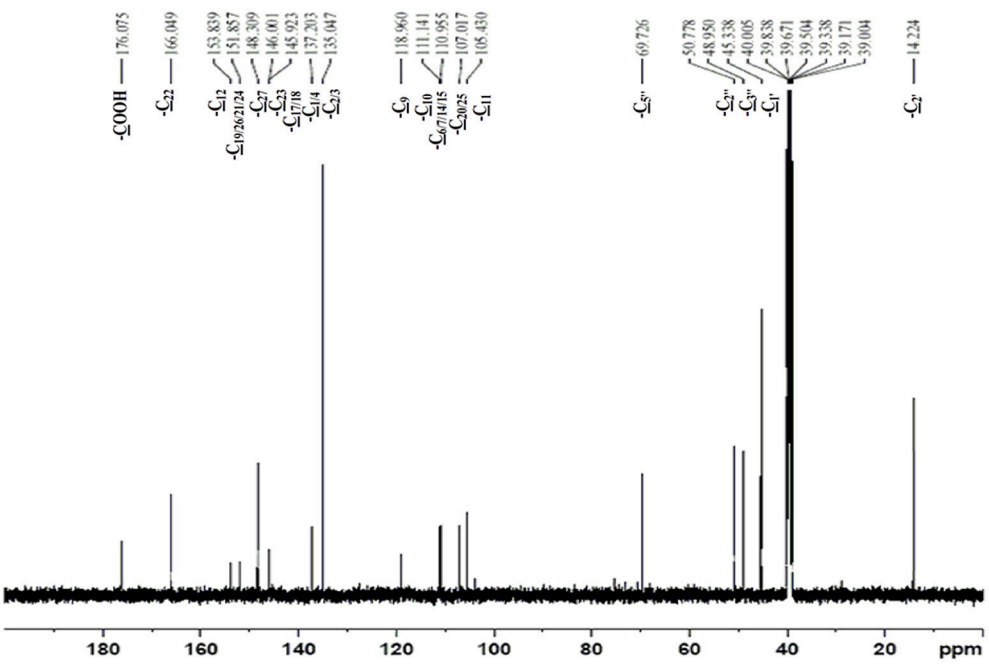


FIGURE 6 | ^{13}C NMR spectrum of the bioactive compound (spot "E" eluate) derived from *Nostoc* sp. MGL001.

method using 5 mm diameter filter paper discs. Agar was inoculated with a standardized quantity of the suspension of the test organisms. Known amount of pure bioactive compound were loaded on filter paper discs. Control discs received only the solvent (1% methanol). Discs were allowed to remain at room temperature until complete solvent evaporation and then placed

on the seeded agar plates. The diameter of the inhibition zone (from periphery of disc to periphery of zone) was measured in mm after 24 h incubation at 37°C.

ESI-MS and NMR Studies

Electrospray ionization (ESI) equipped with time of flight mass spectrometer were recorded on Bruker daltonics AmaZon SL. Capillary voltage 3500 V in positive ion mode was set having 20 μL/min flow rate. The ^{1}H, H-H COSY, ^{13}C{^{1}H}, DEPT-135, and DEPT-90 NMR spectra were recorded on a Bruker AVANCE III HD-500 MHz multinuclear FTNMR spectrometer at 25°C.

Optimization of Isolated Bioactive Compound and Docking Study

For visualization of isolated compound Discovery Studio 3.0 tool was used (Gao and Huang, 2011).

TABLE 2 | NMR Spectral data of EMTAHDCA.

S. No.	^{1}H/^{13}C{^{1}H} (Multiplicity)	No. of proton	Peak position (δ)	Coupling constant $^{3}J_{H-H}$(Hz)
1	-COOH (s)	02	11.979	–
2	-N = CH (s)	01	8.935	–
3	-C_{10}H (d)	01	7.899–7.872	13.50
4	-$C_{1/4}$H(s)	02	7.635	–
5	-C_{11}H(d)	01	7.141–7.127	7.0
6	-$C_{6/7/14/15}$H (s)	04	7.010	–
7	-$C_{1'}$H (q)	02	4.601–4.558	7.5/7.5
8	-$C_{5''}$H (s)	02	3.505	–
9	-$C_{2''}$H (t)	04	3.232–3.213	5.0
10	-$C_{3''}$H (t)	04	2.894–2.875	5.0
11	-$C_{2'}$H (t)	03	1.425–1.396	7.0
12	-COOH	–	176.08	–
13	-C_{22}	–	166.05	–
14	-C_{12}	–	153.84	–
15	-$C_{19/26/21/24}$	–	151.86	–
16	-C_{27}	–	148.31	–
17	-C_{23}	–	146.00	–
18	-$C_{17/18}$	–	145.92	–
19	-$C_{1/4}$	–	137.20	–
20	-$C_{2/3}$	–	135.05	–
21	-C_{9}	–	118.96	–
22	-C_{10}	–	111.14	–
23	-$C_{6/7/14/15}$	–	110.96	–
24	-$C_{20/25}$	–	107.02	–
25	-C_{11}	–	105.43	–
26	-$C_{5''}$	–	69.73	–
27	-$C_{2''}$	–	50.78	–
28	-$C_{3''}$	–	48.95	–
29	-$C_{1'}$	–	45.34	–
30	-$C_{2'}$	–	14.22	–

s, singlet; q, quartet; d, doublet; t, triplet.

Selection of Target Structures

The small ribosomal subunit (30S) fragment and protein structures were selected for interaction with isolated bioactive compound (ligand). The 3-D crystal structure of the target *viz.* the RNA fragments (1YRJ, 1MWL, 1J7T, and 1LC4) (Vicens and Westhof, 2001, 2002, 2003; Han et al., 2005) and OmpF porin structures (4GCP, 4GCQ, and 4GCS) (Ziervogel and Roux, 2013) were retrieved from the protein databank (PDB) (www.rcsb.org/pdb) and further used for interaction calculation using YASARA software (Krieger and Vriend, 2014). Active site of the targeted protein was predicted using MetaPocket 2.0 (http://projects.biotec.tu-dresden.de/metapocket/) (Huang, 2009; Zhang et al., 2011).

Receptor Preparation and Docking

The complexes of RNA fragments and porin protein with heteroatom, water molecules and ligands were taken for receptor preparation. The heteroatom, water molecules and ligands were removed using Discovery Studio 3.1 before docking. The Docking calculation was performed for RNA fragments and porin protein with ligand (bioactive compound). The target protein was set in YASARA to run macro file (dock_run.mcr). The YASARA structure provides Autodock and VINA tools to dock ligands with proteins at the touch of a button (Morris et al., 1998; Trott and Olson, 2010).

RESULTS

Isolation and Identification

The morphological study of the cyanobacterium *Nostoc* sp. MGL001 showed that it contains squarish to cylindrical vegetative cells (**Figure 1**). *Nostoc* sp. MGL001 (GenBank, accession no. KX721474) and other close homologs for the cyanobacterium can be found from the alignment view tree (**Figure 2**).

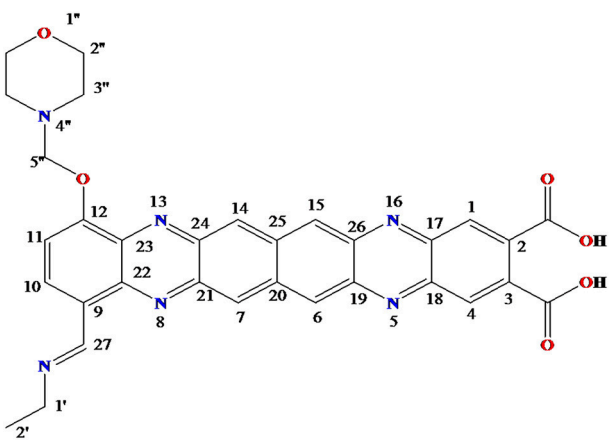


FIGURE 7 | Proposed structure of bioactive compound was 9-Ethyliminomethyl-12-(morpholin - 4 - ylmethoxy) - 5, 8, 13, 16 - tetraaza - hexacene - 2, 3 dicarboxylicacid (EMTAHDCA).

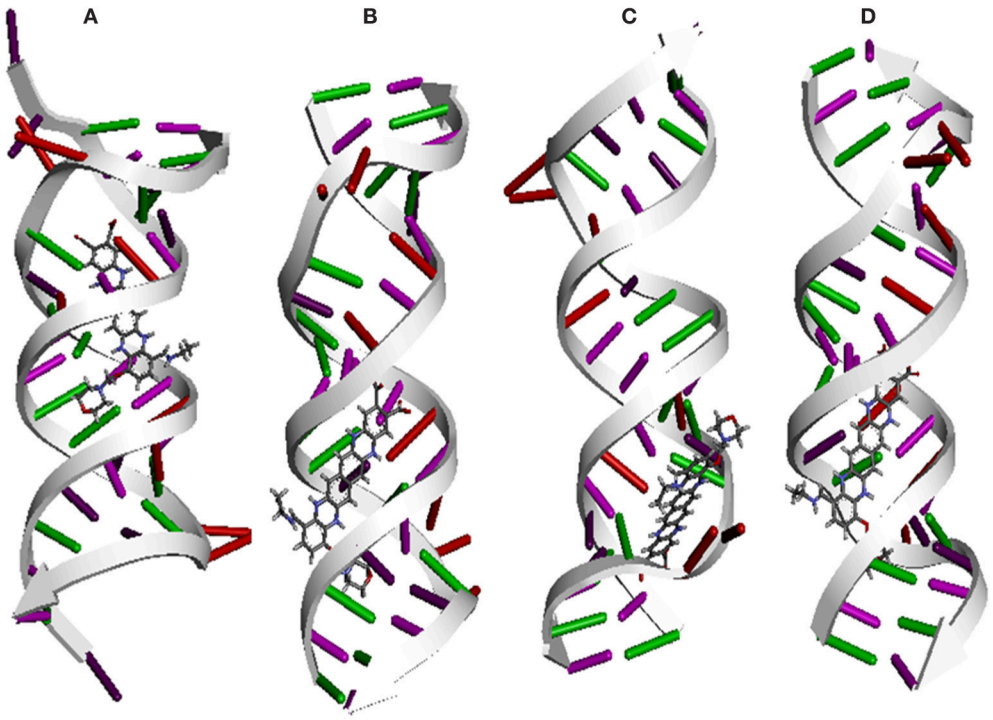


FIGURE 8 | *In silico* interaction between selected ligand (EMTAHDCA) and target RNA fragment (A) 1YRJ **(B)** 1MWL, **(C)** 1J7T, **(D)** 1LC4.

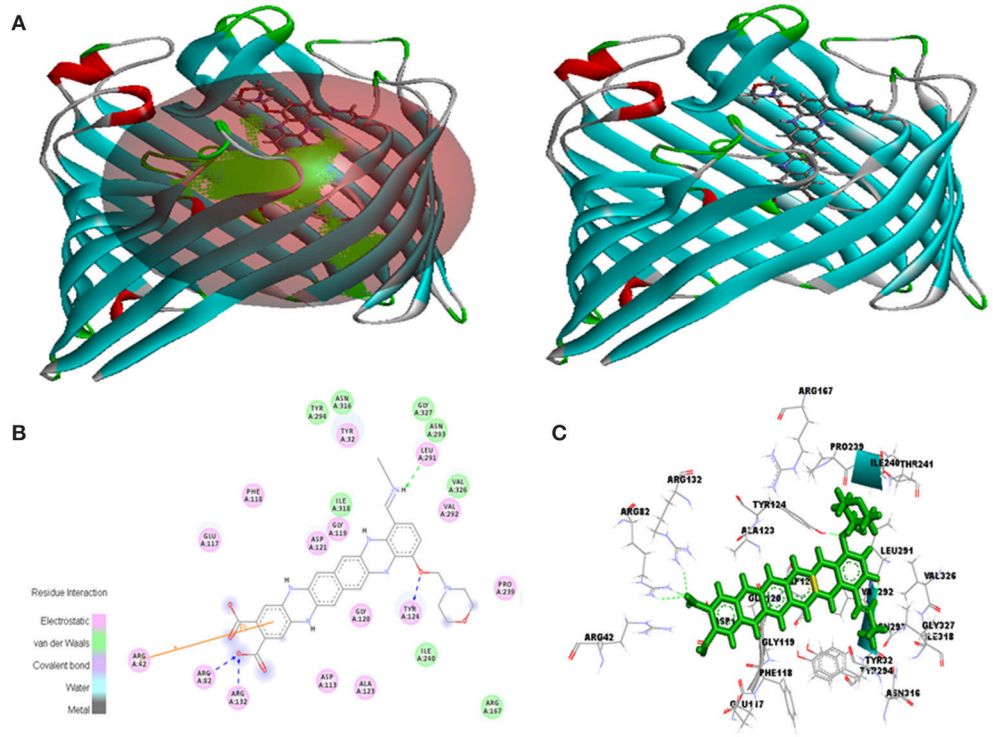


FIGURE 9 | *In silico* interaction between selected ligand (EMTAHDCA) and target OmpF porin protein (4GCP). (A) Poses of docked complexes, green color in sphere indicates prominent active site where the ligand interacted, **(B)** 2D level interaction, **(C)** 3D level interaction.

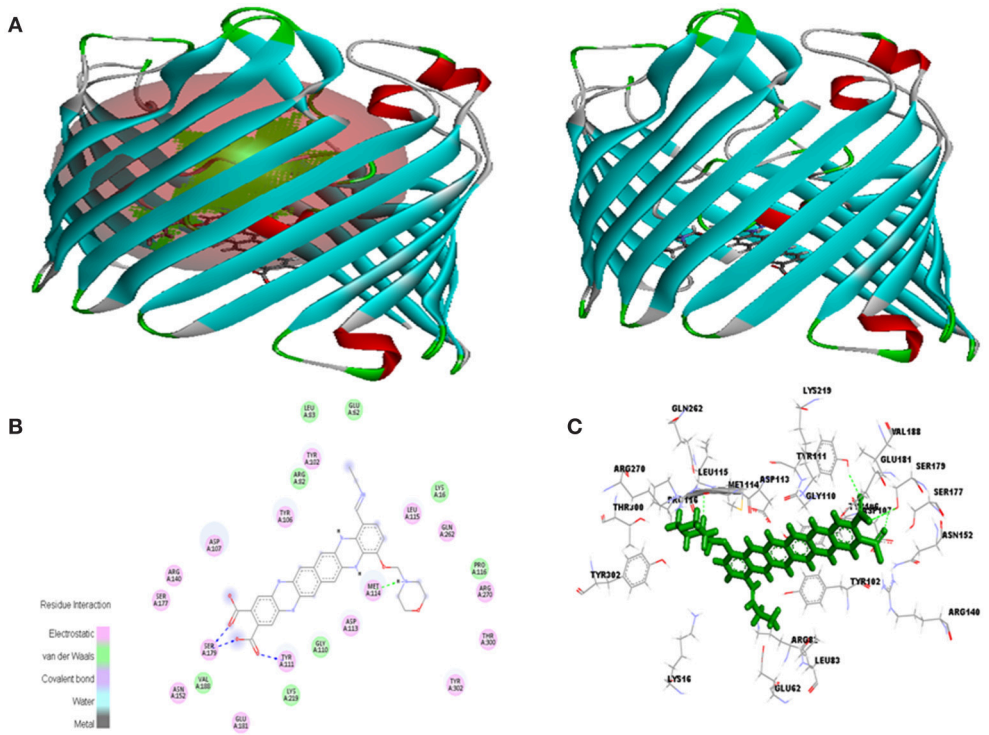


FIGURE 10 | *In silico* interaction between selected ligand (EMTAHDCA) and target OmpF porin protein (4GCQ). (A) Poses of docked complexes, green color in sphere indicates prominent active site where the ligand interacted, **(B)** 2D level interaction, **(C)** 3D level interaction.

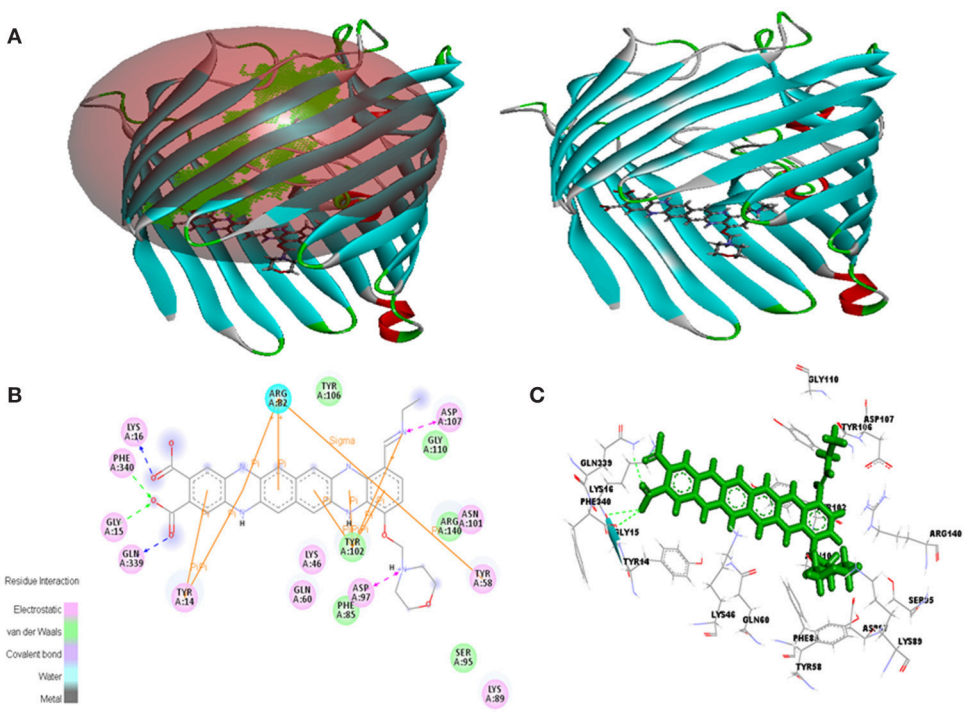


FIGURE 11 | *In silico* interaction between selected ligand (EMTAHDCA) and target OmpF porin protein (4GCS). (A) Poses of docked complexes, green color in sphere indicates prominent active site where the ligand interacted, **(B)** 2D level interaction, **(C)** 3D level interaction.

TLC and HPLC Analysis

Thin layer chromatography (TLC) of the crude extract of cyanobacterium produced five bands A, B, C, D, E, and F (**Figure 3**). Only band E showed potent antibacterial property. Further band E was purified by HPLC, the individual peak with retention time (Rt) of 1.40 min (**Figure 4**) were collected.

Antibacterial Bioassay

This purified compound shows extensive antimicrobial activity against various gram negative bacterial strains chosen, such as *Escherichia coli* (KX758560), *Proteus vulgaris* (KX758561), and *Pseudomonas aeruginosa* (KX758562). Maximum zone of inhibition at a concentration of 150 μg/mL of pure compound isolated from *Nostoc* sp. MGL001 was observed *viz.* 11.15 ± 0.117, 10.17 ± 0.235, and 9.16 ± 0.211 mm against *Escherichia coli, Proteus vulgaris* and *Pseudomonas aeruginosa*, respectively (**Table 1**). Upon further increasing the concentration upto 250 μg/mL, no further increase in the size of zone was observed.

ESI and NMR

The obtained whitish powder compound was used for the analysis through ESI and NMR. The ^{1}H NMR (500.30 MHz;) δ ppm w.r.t. DMSO-d_6(2.500) (**Figure 5**) and ^{13}C{^{1}H} NMR (125.80 MHz) δ ppm w.r.t. DMSO-d_6(39.51) (**Figure 6**) in DMSO-d_6 at 25°C spectral data are given in **Table 2**. Therefore, on the basis of NMR, proposed structure of bioactive compound was 9-Ethyliminomethyl-12-(morpholin - 4 - ylmethoxy) -5, 8, 13, 16–tetraaza–hexacene - 2, 3- dicarboxylic acid (EMTAHDCA) (**Figure 7**). High resolution ESI-MS was operated in positive ion mode revealed an m/z at 591.02 ($M+H^+$) corresponding to the molecular formula $C_{32}H_{26}N_6O_6$ (Molecular weight-590.59) assigned in full agreement with NMR spectral data.

Molecular Docking

Molecular docking was successfully performed between selected ligand (EMTAHDCA) and target receptor RNA fragments (PDB ID: 1YRJ, 1MWL, 1J7T, and 1LC4) (**Figure 8**) and OmpF porin protein (4GCP, 4GCQ, and 4GCS) (**Figures 9**, **10**, **11**) using YASARA software. The active site of OmpF was determined using Metapocket and results are represented in **Table 3**. Summary of molecular docking results of selected ligand with drug target RNA fragment and OmpF porin protein are represented in **Table 4**. The binding energy was found to be 000011.1450, 000010.0550, 000009.8620, and 000009.9690 for 1YRJ, 1MWL, 1J7T, and 1LC4 RNA fragments, respectively. Dissociation constant [pM] was found to be 00000000006770.2808, 00000000042617.4336, 00000000059028.0117, and 00000000059028.0117 for 1YRJ, 1MWL, 1J7T, and 1LC4 RNA fragments, respectively (**Table 4**). Contacting receptor residues were identified through YASARA software and found that G^{A5}, U^{A6}, A^{A8}, A^{A10}, A^{B33}, G^{B39}, and U^{A15} were common active site residues between reported 1YRJ complex with Apramycin and selected ligand.

In case of 1MWL RNA fragment bases C^{A10}, C^{A11}, G^{A12}, G^{A13}, U^{A14}, C^{A20}, G^{B26}, U^{B27}, C^{B28}, C^{B30}, A^{B31}, C^{B32}, C^{B33}, and G^{B34} were involved in interaction between ligand and 1MWL RNA fragment, in which G^{B26}, U^{B27}, C^{B28}, and C^{B30} bases were common active site residues between reported Geneticin antibiotic complex (1MWL) and ligand.

The ligand and 1J7T RNA fragment interacted with the following binding residues C^{A10}, C^{A11}, G^{A12}, G^{A13}, U^{A14}, G^{A18}, U^{A19}, C^{A20}, C^{B25}, G^{B26}, U^{B27}, C^{B28}, A^{B29}, C^{B30}, A^{B31}, C^{B32}, C^{B33}, and G^{B34} in which G^{A18}, U^{A19}, G^{B26}, U^{B27}, C^{B28}, A^{B29}, and C^{B30} bases were common between reported paromomycin antibiotic complex (1J7T) and ligand (**Table 4**).

Active site residues *viz.* U^{A15}, G^{A16}, A^{A17}, A^{A18}, G^{A19}, U^{A20}, C^{A21}, C^{B27}, G^{B28}, U^{B29}, C^{B30}, A^{B31}, C^{B32}, A^{B33}, and C^{B34} were involved in interaction with 1LC4 RNA fragment and ligand in which G^{A16}, A^{A18}, G^{A19}, U^{A20}, C^{B27}, G^{B28}, C^{B30}, and A^{B31} bases were common binding residues between reported tobramycin antibiotic complex (1LC4) and ligand.

In case of 4GCP porin protein docking results, site 1 residues Tyr^{32}, Arg^{42}, Arg^{82}, Asp^{113}, Glu^{117}, Phe^{118}, Gly^{119}, Gly^{120}, Asp^{121}, Ala^{123}, Tyr^{124}, Arg^{132}, Arg^{167}, Pro^{239}, Ile^{240}, Thr^{241}, Leu^{291}, Val^{292}, Asn^{293}, Tyr^{294}, Asn^{316}, Ile^{318}, Val^{326}, and Gly^{327} were involved in interaction with good positive energies and dissociation constant. The site 1 is the major prominent site for interaction of any compound. The residues of site 1 (Tyr^{32}, Phe^{118}, Gly^{119}, Gly^{120}, Asp^{121}, Tyr^{124}, Leu^{291}, Val^{292}, Asn^{316}, and Val^{326}) are common to the reported active site known against ampicillin antibiotics (**Figure 9**, **Table 4**). The 2D and 3D view of interacted residues also mentioned in **Figure 9**. In residue interaction electrostatic bond, van der waals, covalent bond and hydrogen bond were involved.

Molecular docking between 4GCQ porin protein and ligand indicates that active site 1 residues Lys^{16}, Glu^{62}, Arg^{82}, Leu^{83}, Tyr^{102}, Tyr^{106}, Asp^{107}, Gly^{110}, Tyr^{111}, Asp^{113}, Met^{114}, Leu^{115}, Pro^{116}, Glu^{181}, Val^{188}, Lys^{219}, Gln^{262}, Arg^{270}, Thr^{300}, and Tyr^{302} were involved in interaction, whereas only Arg^{82} are common to the reported active site known against Carbenicillin antibiotics (**Figure 10**, **Table 4**). The electrostatic bond, van der waals, covalent bond and hydrogen bond were involved in residues interaction could be clearly visible in 2D and 3D view in **Figure 10**.

TABLE 3 | Prominent active site residues identification of selected Omp porin protein models (4GCP, 4GCQ, and 4GCS).

S.No.	Target	PDB ID	Common active site 1 residues
1.	OmpF porin protein	4GCP	Arg^{42}, Arg^{82}, Tyr^{32}, Leu^{291}, Val^{292}, Asn^{293}, Tyr^{294}, Asn^{316}, Ile^{318}, Val^{326}, Asp^{121}, Gly^{327}, Tyr^{124}, Pro^{239}, Ile^{240}, Thr^{241}, Phe^{118}, Gly^{119}, Gly^{120}, Arg^{167}, Glu^{117}, Ala^{123}, Asp^{113}, Arg^{132}
2.		4GCQ	Lys^{16}, Arg^{82}, Pro^{116}, Tyr^{302}, Thr^{300}, Leu^{115}, Tyr^{102}, Asp^{113}, Met^{114}, Arg^{270}, Tyr^{106}, Gln^{262}, Glu^{62}, Leu^{83}, Gly^{110}, Asp^{107}, Tyr^{111}, Arg^{140}, Lys^{219}, Glu^{181}, Ser^{179}, Val^{188}, Asn^{152}, Ser^{177}
3.		4GCS	Lys^{89}, Ser^{95}, Arg^{140}, Tyr^{58}, Asp^{97}, Asp^{107}, Phe^{85}, Asn^{101}, Gln^{60}, Tyr^{106}, Lys^{46}, Tyr^{102}, Gly^{110}, Tyr^{14}, Lys^{16}, Phe^{340}, Gln^{339}, Gly^{15}

TABLE 4 | Summary of molecular docking results of selected ligand with drug target RNA fragment and OmpF porin protein.

S.No.	Ligand	Target	PDB ID	Binding energy [kcal/mol]	Dissociation constant [pM]	Contacting receptor residues	Reported active site residues	Common
1.	EMTAHDCA	RNA Fragment	1YRJ	000011.1450	00000000006770.2808	G^{A5}, U^{A6}, C^{A7}, A^{A8}, A^{A10}, C^{A11}, C^{A12}, G^{A13}, U^{A15}, A^{B33}, C^{B34}, C^{B35}, G^{B37}, U^{B38}, G^{B39}	C^{A4}, G^{A5}, U^{A6}, A^{A8}, A^{A10}, U^{A15}, C^{A4}, G^{A5}, U^{A6}, A^{A8}, A^{A10}, U^{A15}, G^{A16}, A^{A17}, A^{A18}, G^{A19}, U^{A20}, U^{B25}, A^{B31}, C^{B32}, A^{B33}, G^{B39}, A^{B40}, A^{B41}	G^{A5}, U^{A6}, A^{B33}, G^{B39}, A^{A8}, A^{A10}, U^{A1}, U^{A15}, A^{B33}, G^{B39}
2.	EMTAHDCA	RNA Fragment	1MWL	000010.0550	00000000042617.4336	C^{A10}, C^{A11}, G^{A12}, G^{A13}, U^{A14}, C^{A20}, G^{B26}, U^{B27}, C^{B28}, C^{B30}, A^{B31}, C^{B32}, C^{B33}, G^{B34}	A^{B33}, G^{B39}, G^{A4}, U^{A5}, A^{A6}, C^{A7}, C^{A7}, C^{A8}, G^{A15}, A^{A16}, A^{A17}, G^{A18}, U^{A19}, C^{B25}, G^{B26}, U^{B27}, C^{B28}, A^{B29}, C^{B30}, G^{B37}, A^{B38}, A^{B39}, G^{B40}, U^{B41}	G^{B26}, U^{B27}, C^{B28}, C^{B30}
3.	EMTAHDCA	RNA Fragment	1J7T	000009.8620	00000000059028.0117	C^{A10}, C^{A11}, G^{A12}, G^{A13}, U^{A14}, G^{A18}, U^{A19}, C^{A20}, C^{B25}, G^{B26}, U^{B27}, C^{B28}, A^{B29}, C^{B30}, A^{B31}, C^{B32}, C^{B33}, G^{B34}	G^{A4}, U^{A5}, C^{A6}, A^{A7}, U^{A17}, G^{A15}, A^{A16}, A^{A17}, G^{A18}, U^{A19}, G^{B26}, U^{B27}, C^{B28}, A^{B29}, C^{B30}, U^{B36}, G^{B37}, A^{B38}, A^{B39}, G^{B40}	G^{A18}, U^{A19}
4.	EMTAHDCA	RNA Fragment	1LC4	000009.9690	00000000049274.9414	U^{A15}, G^{A16}, A^{A17}, A^{A18}, G^{A19}, U^{A20}, C^{A21}, C^{B27}, G^{B28}, U^{B29}, C^{B30}, A^{B31}, C^{B32}, A^{B33}, C^{B34}	C^{A4}, G^{A5}, C^{A7}, G^{A16}, A^{A18}, G^{A19}, U^{A20}, C^{B27}, G^{B28}, C^{B30}, A^{B31}, G^{B39}, A^{B41}, G^{B42}, U^{B43}	G^{A16}, A^{A18}, G^{A19}, U^{A20}, C^{B27}, G^{B28}, C^{B30}, A^{B31}
5.	EMTAHDCA	OmpF Porin protein	4GCP	000009.8890	00000000056398.4141	Tyr^{32}, Arg^{42}, Arg^{82}, Asp^{113}, Glu^{117}, Phe^{118}, Gly^{119}, Gly^{120}, Asp^{121}, Ala^{123}, Tyr^{124}, Arg^{132}, Arg^{167}, Pro^{239}, Ile^{240}, Thr^{241}, Leu^{291}, Val^{292}, Asn^{293}, Tyr^{294}, Asn^{316}, Ile^{318}, Val^{326}, Gly^{327}	Ser^{31}, Tyr32, Gly^{33}, Phe^{118}, Gly^{119}, Gly^{120}, Asp^{121}, Tyr^{124}, Lys^{243}, Leu^{291}, Val^{292}, Asn^{316}, Val^{326}, Gly^{327}	Tyr^{32}, Phe^{118}, Gly^{119}, Gly^{120}, Asp^{121}, Tyr^{124}, Leu^{291}, Val^{292}, Asn^{316}, Val^{326}, Gly^{327}
6.	EMTAHDCA	OmpF porin protein	4GCQ	000009.9500	00000000050880.7266	Lys^{16}, Glu^{62}, Arg^{82}, Leu^{83}, Tyr^{102}, Tyr^{106}, Asp^{107}, Gly^{110}, Tyr^{111}, Asp^{113}, Met^{114}, Leu^{115}, Pro^{116}, Glu^{181}, Val^{188}, Lys^{219}, Gln^{262}, Arg^{270}, Thr^{300}, Tyr^{302}	Tyr^{22}, Tyr^{32}, Gly^{33}, Arg^{42}, Arg^{82}, Glu^{117}, Phe^{118}, Gly^{119}, Gly^{120}, Asp121 Arg^{132}, Val ^{292}	Arg^{82}
7.	EMTAHDCA	OmpF porin protein	4GCS	000008.6880	00000000428165.4063	Tyr^{14}, Gly^{15}, Lys^{16}, Lys^{46}, Tyr^{58}, Gln^{60}, Phe^{85}, Lys^{89}, Ser^{95}, Asp^{97}, Asn^{101}, Tyr^{102}, Tyr^{106}, Asp^{107}, Gly^{110}, Arg^{140}, Gln^{339}, Phe^{340}	Thr^{165}, Arg^{168}, Ser^{248}	

Active site 1 residues involved in interaction were Phe^{85}, Ser^{95}, Asn^{101}, Tyr^{102}, Tyr^{106}, Gly^{110}, and Arg^{140} in case of 4GCS porin protein and ligand docking through van der waals bonding, Residues like Tyr^{14}, Lys^{16}, Gly^{15}, Phe^{34}, Gly^{15}, Gln^{339}, Asp^{97}, Lys^{46}, Lys^{89}, Tyr^{58}, Asn^{101}, and Asp^{107} involved in electrostatic bonding whereas Arg^{82} involved in hydrogen bond interaction (**Figure 11**, **Table 4**).

DISCUSSION

Cyanobacteria are known to produce a wide variety of biologically active compounds. To the best of our knowledge, this type of new bioactive compound EMTAHDCA is first time reported from fresh water cyanobacterium *Nostoc* sp. MGL001. In order to isolate EMTAHDCA various chromatographic techniques were tested but TLC was found to be most useful tool to achieve the separation of complex mixtures of organic molecules. Competition between solute and the mobile phase is responsible for the separation of compounds through TLC (Kumar et al., 2013). In order to separate unknown bioactive compounds, different gradients of solvents were tested and ultimately carbon tetrachloride: methanol in 9:1 ratio was found to be best for separation point of view. Same solvent composition was also used by Srivastava et al. (2015) to separate bioactive compound from fresh water cyanobacteria *Geitlerinema* sp. CCC728 and *Arthrospira* sp. CCC729.

Liquid chromatography is one of the most efficient and powerful separation methods for the preparative purification and isolation of biological substances (Nikitas and Pappa-Louisi, 2009). A number of different chromatographic methods were considered for purification of bioactive compounds but reason behind selection of HPLC technique was its reproducibility, sensitivity, high resolution, and absence of extensive sample preparation or derivatization (Quilliam, 2003; Snyder and Dolan, 2006). Water is the weakest eluent for reverse phase HPLC so; its eluent strength is then modified by adding methanol or acetonitrile which are less polar but miscible solvents. After testing methanol and acetonitrile based systems acetonitrile was selected as mobile phase because it gave better peak shapes, stable baselines and sharper resolution as compared to methanol.

The use of ESI-MS systems when coupled with a HPLC-system increases their selectivity and benefits from both techniques (Vishwakarma and Rai, 2013). For the structure elucidation of newly isolated compounds NMR methods have been used as it is very much capable of elucidating intact biomaterials nondestructively without any preceding derivatization (Willmann et al., 2011). Due to the simplicity of sample preparation and ease of interpretation of characteristic signals, NMR was favored as natural products are closely related and difficult to separate. The ^{1}H and $^{13}C\{^{1}H\}$ NMR spectral data of EMTAHDCA has already been presented and interpreted in result section. The proton NMR spectrum of the EMTAHDCA (**Figure 5**), as per the structure, is expected to show a broad peak at δ 11.979 (due to presence two acidic proton of –COO<u>H</u> groups), two doublet [at δ 7.899–7.872 (due to presence of one aromatic proton, such as C_{10}<u>H</u>) and at δ 7.141–7.127 (due to presence of one aromatic proton, such as C_{11}<u>H</u>)], four singlet [at δ 8.935 (due to presence of one proton –N = C<u>H</u> group), δ

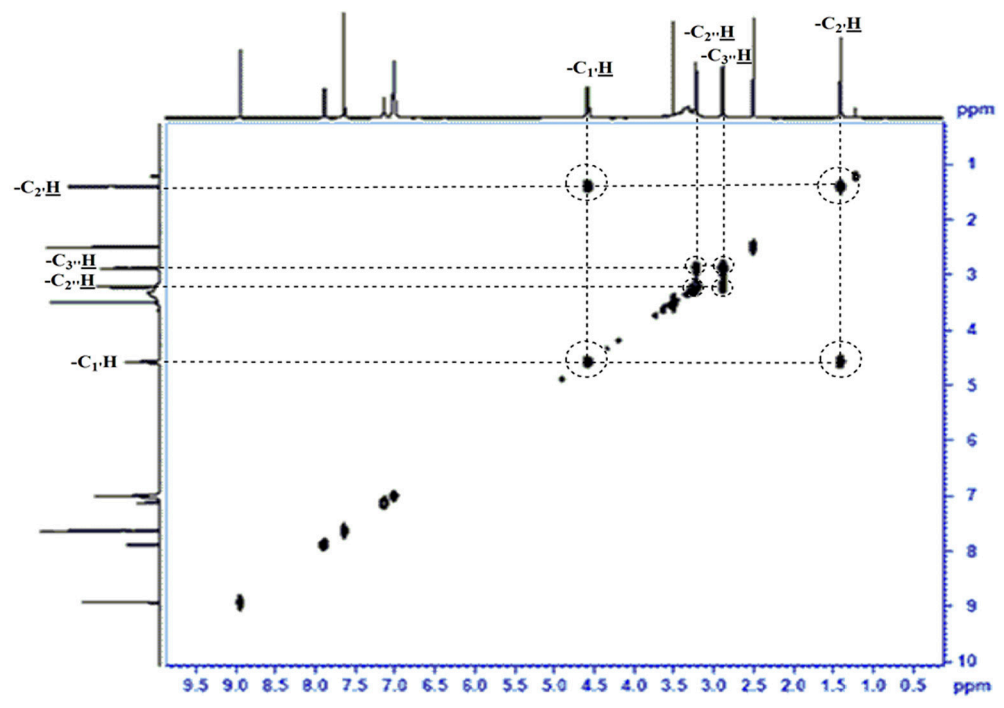


FIGURE 12 | H-H COSY NMR spectrum of EMTAHDCA.

7.635 (due to presence of two aromatic protons, such as $C_1\underline{H}$ and $C_4\underline{H}$), δ 7.010 (due to presence of four aromatic protons, such as C_6H, C_7H, $C_{14}H$, and $C_{15}H$) and at δ 3.505 (due to presence of two protons of methylene group, such as $C_{5''}\underline{H}$)], one quartet at δ 4.601–4.558 (due to presence of two protons of methylene group, such as $C_{1'}\underline{H}$) and three triplets [at δ 3.232–3.213(due to presence of two protons of methylene group, such as $C_{2''}\underline{H}$), δ 2.894–2.875(due to presence of two proton of methylene group, such as $C_{3''}\underline{H}$) and at δ 1.425–1.396 (due to presence of three protons of methyl group, such as $C_{2'}\underline{H}$)]. The splitting pattern of different type of protons of aliphatic region also confirmed by H-H COSY spectrum (**Figure 12**), in this spectrum the methylene group protons ($C_{1'}\underline{H}$) coupled with the methyl group protons ($C_{2'}\underline{H}$) and other methylene group protons ($C_{2'}\underline{H}$) coupled with another methylene group protons ($C_{3'}\underline{H}$). In the $^{13}C\{^1H\}$ NMR spectrum (**Figure 6**), 19 carbon signals were observed, including carbonyl carbon (δ 176.08), one imine carbon (δ 148.31), four aromatic carbons (δ 137.20, 111.14, 110.96, and 105.43), eight different type quaternary aromatic carbons (δ 166.05, 153.84, 151.86, 146.00, 145.92, 135.05, 118.96, and 107.02), four different type methylene carbons (δ 69.73, 50.78, 48.95, and 45.34), and one methyl carbon (δ 14.22). The different type of carbon interpreted with help of DEPT-90 and DEPT-135 NMR spectral technique, in DEPT-135 spectrum (**Figure 13**), carbon with one hydrogen (four type aromatic carbons and one imine carbon) and three hydrogens (one methyl carbon) shows positive peak, whereas carbon has two hydrogens (four different type of methylene carbons) shows negative peak and in DEPT-90 spectrum (**Figure 14**), carbon with one hydrogen (four type aromatic carbons and one imine carbon) shows only positive peak. The spectrum consists of all the expected signals as shown in spectral data of NMR section. The predicted structure of EMTAHDCA using ESI-MS and NMR spectra were verified by subjecting predicted structure on Pubchem (https://pubchem.ncbi.nlm.nih.gov/) and PubMed NCBI https://www.ncbi.nlm.nih.gov/pubmed) and by comparing experimental data with published literature on bioactive compounds of cyanobacteria but structure of EMTAHDCA clearly indicated that it is a novel compound that was not reported earlier in any literature or natural product database.

The ESI-MS and NMR spectra were verified by comparing experimental data with published literature on bioactive compounds but structure of EMTAHDCA clearly indicated that it is a novel compound that was not reported in literature or natural product database.

Also EMTAHDCA identified as an antibacterial agent through *in vitro* and *in silico* approaches. The present work based on *in silico* preclinical evaluation of novel isolated compound EMTAHDCA to proceed ahead for further drug trials. Structure elucidation of bioactive compound EMTAHDCA (Ethyliminomethyl-12-(morpholin - 4 - ylmethoxy) -5, 8, 13, 16 - tetraaza - hexacene - 2, 3 dicarboxylic acid) was done through NMR already mentioned in results section. This compound contain morpholin moiety that is rare in nature. The 2-hydroxymorpholine moiety was also observed in bacilosarcins A isolated from marine-derived bacterium *Bacillus subtilis* TP-B0611 showed growth inhibition against barnyard millet (Azumi

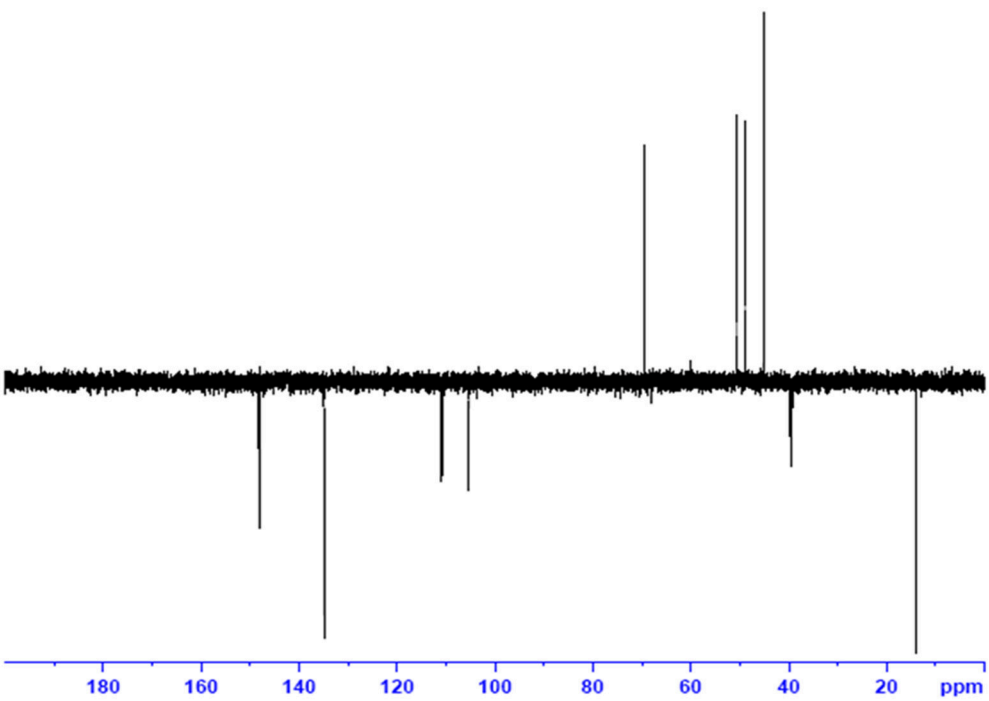


FIGURE 13 | DEPT-135 NMR spectrum of EMTAHDCA.

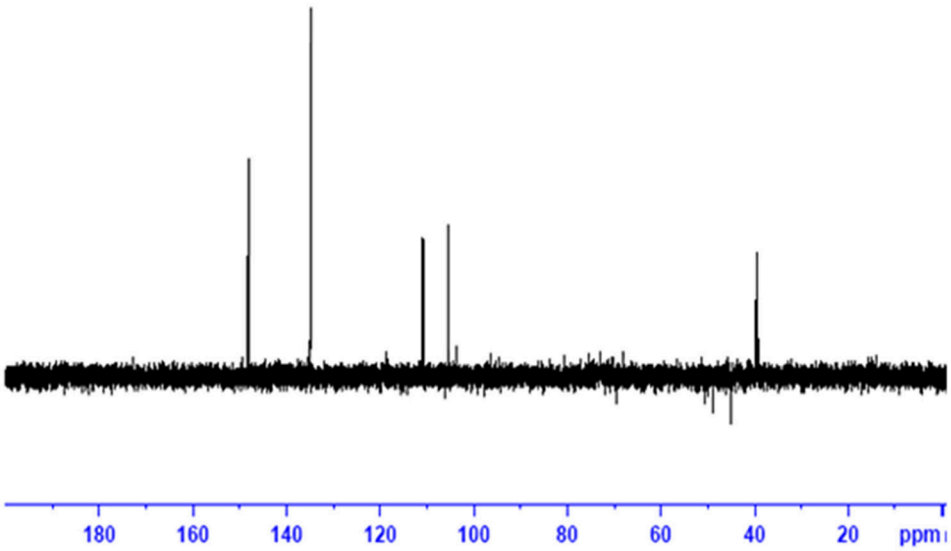


FIGURE 14 | DEPT-90 NMR spectrum of EMTAHDCA.

et al., 2008). Morpholin is commonly used in organic synthesis. It acts as a building block in the preparation of the anticancer agent gefitinib (Iressa), the antibiotic linezolid and the analgesic dextromoramide (Fung et al., 2001; McKillop et al., 2005). Presence of morpholin moiety in the bioactive compound EMTAHDCA is likely to be responsible for its antibiotic activity. Pure bioactive compound EMTAHDCA (150 μg/mL) possessed antibacterial activity against gram negative bacterial strains *viz. E. coli, P. vulgaris,* and *P. aeruginosa.* These strains were tested in laboratory and found multi drug resistant (MDR) to erythromycin, imipenem, ciprofloxacin and vancomycin (data not shown). Bacterial adaptation to antibiotics generated serious medical problem (Chalasani et al., 2015). This finding gives an idea that EMTAHDCA compound could be used as an alternative antibiotic against such resistant bacterial strains. In order to prove its antibiotic potential *in silico* technique was performed to know the interaction of selected bioactive compound EMTAHDCA with small ribosomal subunit (30S) (PDBID: 1YRJ, 1MWL, 1J7T, and 1LC4) fragment and OmpF porin protein (PDBID: 4GCP, 4GCQ, and 4GCS).

Protein synthesis is a fundamental process performed by ribosome. More than half of the total number of clinically used antibiotics exerts their antibiotic effects on the bacterial ribosomes by binding to several sites of 30 and 50S subunits ultimately blocking protein synthesis (Franceschi and Duffy, 2006). Both the 30S and the 50S ribosomal subunits provide functionally relevant active site pockets considered as ribofunctional loci where antibiotics do act (Wilson, 2014). The ribosomes are highly conserved organelles having precise conformational variation which facilitates drug selectivity for clinical use (Hermann, 2005).

The outer membrane (OM), unique to gram negative bacteria acts as selective barrier by providing an extra protective layer against a harsh environment. OM provides passage for nonspecific charged and zwitterionic nutrient molecules (Delcour, 2009). Three major general diffusion porins found in *E.coli* are OmpF, OmpC, and PhoE. In several reports, loss of OmpF, and OmpC porins are linked to antibiotic resistance, especially for *Escherichia coli* and *Salmonella typhimurium* (Nikaido, 2003). Therefore, a better understanding of how modification of membrane permeability triggers bacterial resistance to antibiotics is necessary for the development of new antibiotic therapy strategies.

Molecular docking calculation between EMTAHDCA and target receptor molecule (RNA fragment) showed good binding affinity with best positive energies for selected compound EMTAHDCA. More positive energies indicates stronger binding, and negative energies mean no binding (Krieger and Vriend, 2014). Bases involved in interaction between ligand and ribosomal fragment resides at the prominent active site of ribosomal fragment. Similar type of interaction was observed in the case of EMTAHDCA docking with OmpF porin protein. The crystal structures of OmpF in complex with ampicillin, carbenicillin and ertapenem (4GCP, 4GCQ, and 4GCS) have been already reported. Residues involved in interaction between selected ligand and OmpF porin proteins was found in prominent active site (site 1) predicted by Metapocket. Therefore, with the help of emerging molecular docking tools, we could able to prove that isolated compound EMTAHDCA have ability to work as an antibiotic agent and also recognize their precise mode of action against targeted host. This study suggested that selected compound EMTAHDCA could better act in comparison with reported antibiotics and able to serve as clinical candidate.

CONCLUSION

Novel bioactive compound EMTAHDCA isolated from *Nostoc* sp. MGL001 has antibacterial activity against multi drug resistant

bacterial strains *viz. E coli, P vulgaris,* and *P aeruginosa* through *in vitro* and *in silico* studies. Therefore, it is worth mentioning that EMTAHDCA could serve as potential antibiotic drug.

AUTHOR CONTRIBUTIONS

Niveshika and AM designed the experiments. Niveshika performed the experiments. Niveshika, EV, AM, AS, and VS analyzed the data. Niveshika and EV wrote the manuscript and AM critically reviewed the paper.

ACKNOWLEDGMENTS

The Head and coordinator CAS, Department of Botany, Banaras Hindu University, Varanasi, India is gratefully acknowledged for providing laboratory facilities. We are thankful to Central Instrumentation Facility, Department of Botany BHU for HPLC. We are grateful to Indian Institute of Technology (IIT) Central Instrumentation Facility, BHU for NMR. We are also grateful to Interdisciplinary School of Life Sciences (ISLS), BHU for ESIMS. Two of us (Niveshika and EV) are thankful to the UGC, New Delhi for financial support in the form of JRF.

REFERENCES

Azumi, M., Ogawa, K., Fujita, T., Takeshita, M., Yoshida, R., Furumai, T., et al. (2008). Bacilosarcins A and B, novel bioactive isocoumarins with unusual heterocyclic cores from the marine-derived bacterium *Bacillus subtilis*. *Tetrahedron* 64, 6420–6425. doi: 10.1016/j.tet.2008.04.076

Berdy, J. (2005). Bioactive microbial metabolites. *J. Antibiot.* 58, 1–26. doi: 10.1038/ja.2005.1

Bullerjahn, G. S., and Post, A. F. (2014). Physiology and molecular biology of aquatic cyanobacteria. *Front. Microbiol.* 5:359. doi: 10.3389/fmicb.2014.00359

Burja, A. M., Banaigs, B., Abou-Mansour, E., Burgess, J. G., and Wright, P. C. (2001). Marine cyanobacteria—a prolific source of natural products. *Tetrahedron* 57, 9347–9377. doi: 10.1016/S0040-4020(01)00931-0

Chalasani, A. G., Dhanarajan, G., Nema, S., Sen, R., and Roy, U. (2015). An antimicrobial metabolites from *Bacillus* sp.: significant activity against pathogenic bacteria including multidrug resistant clinical strains. *Front. Microbiol.* 6:1335. doi: 10.3389/fmicb.2015.01335

Clardy, J., and Walsh, C. (2004). Lessons from natural molecules. *Nature* 432, 829–837. doi: 10.1038/nature03194

Cragg, G. M., and Newman, D. J. (2013). Natural products: a continuing source of novel drug leads. *Biochim. Biophys. Acta* 1830, 3670–3695. doi: 10.1016/j.bbagen.2013.02.008

Delcour, A. H. (2009). Outer membrane permeability and antibiotic resistance. *Biochim. Biophys. Acta* 1794, 808–816. doi: 10.1016/j.bbapap.2008.11.005

Dembitsky, V. M., and Rezanka, T. (2005). Metabolites produced by nitrogen fixing Nostoc species. *Folia Microbiol. (Praha).* 50, 363–391. doi: 10.1007/BF02931419

Desikachary, T. V. (1959). *Cyanophyta*. New Delhi: Indian Council of Agricultural Research 700.

Dias,. E., Oliveira, M., Jones-Dias, D., Vasconcelos, V., Ferreira, E., Manageiro, V., et al. (2015). Assessing the antibiotic susceptibility of freshwater *Cyanobacteria* spp. *Front. Microbiol.* 6:799. doi: 10.3389/fmicb.2015.00799

Doan, N. T., Rickards, R. W., Rothschild, J. M., and Smith, G. D. (2000). Allelopathic actions of alkaloids 12-epi-hapalindole E isonitrile and calothrixin A from cyanobacteria of the genera *Fischerella* and *Calothrix*. *J. Appl. Phycol.* 12, 409–416. doi: 10.1023/A:1008170007044

Dodds, W. K., Gudder, D. A., and Mollenhauer, D. (1995). The ecology of *Nostoc*. *J. Phycol.* 31, 2–18. doi: 10.1111/j.0022-3646.1995.00002.x

El-Elimat, T., Zhang, X., Jarjoura, D., Moy, F. J., Orjala, J., Kinghorn, A. D., et al. (2012). Diversity of *Metabolites* from *Fungi*, Cyanobacteria, and Plants Relative to FDA-approved anticancer agents. *ACS Med. Chem. Lett.* 3, 645–649. doi: 10.1021/ml300105s

Franceschi, F., and Duffy, E. M. (2006). Structure based drug design meets the ribosome. *Biochem. Pharmacol.* 71, 1016–1025. doi: 10.1016/j.bcp.2005.12.026

Fung, H. B., Kirschenbaum, H. L., and Ojofeitimi, B. O. (2001). Linezolid: an oxazolidinone antimicrobial agent. *Clin. Ther.* 23, 356–391. doi: 10.1016/S0149-2918(01)80043-6

Gao, Y. D., and Huang, J. F. (2011). An extension strategy of Discovery Studio 2.0 for non-bonded interaction energy automatic calculation at the residue level (in Chinese). *Zool. Res.* 32, 262–266. doi: 10.3724/SP.J.1141.2011.03262

Gul, W., and Hamam, M. J. (2005). Indole alkaloid marine natural products: an established source of cancer drug leads with considerable promise for the control of parasitic, neurological and other diseases. *Life Sci.* 78, 442–453. doi: 10.1016/j.lfs.2005.09.007

Han, Q., Zhao, Q., Fish, S., Simonsen, K. B., Vourloumis, D., Froelich, J. M., et al. (2005). Molecular recognition by glycoside pseudo base pairs and triples in an apramycin-RNA complex. *Angew. Chem. Int. Ed Engl.* 44, 2694–2700. doi: 10.1002/anie.200500028

Harada, K. I., Kondo, F., and Lawton, L. (1999). "Laboratory analysis of cyanotoxins," in *Toxic Cyanobacteria in Water*, eds I. Chorus and J. Bartram (London: E & F.N Spoon and WHO), 369–405.

Hermann, T. (2005). Drugs targeting the ribosome. *Curr. Opin. Struct. Biol.* 15, 355–366. doi: 10.1016/j.sbi.2005.05.001

Hirata, K., Yoshitomi, S., Dwi, S., Iwabe, O., Mahakhant,. A., Polchai, J., et al. (2003). Bioactivities of nostocine A produced by a freshwater cyanobacterium *Nostoc* spongiaeforme TISTR 8169. *J. Biosci. Bioeng.* 95, 512–517. doi: 10.1016/S1389-1723(03)80053-1

Huang, B. (2009). MetaPocket: a meta approach to improve protein ligand binding site prediction. *OMICS* 13, 325–330. doi: 10.1089/omi.2009.0045

Jaki, B., Orjala, J., and Sticher, O. (1999). A novel extracellular diterpenoid with antibacterial activity from the Cyanobacterium *Nostoc* commune. *J. Nat. Prod.* 62, 502–503. doi: 10.1021/np980444x

Karchmer, A. W. (2004). Increased antibiotic resistance in respiratory tract pathogens: PROTEKT US- an update. *Clin. Infect. Dis.* 39, 142–150. doi: 10.1086/421352

Khairy, H. M., and El-Kassas, H. Y. (2010). Active substance from some blue green algal species used as antimicrobial agents. *Afr. J. Biotechnol.* 9, 2789–2800. doi: 10.5897/AJB2010.000-3104

Kim, J. D., and Lee, C. G. (2006). Diversity of heterocystous filamentous cyanobacteria (blue-green algae) from rice paddy fields and their differential susceptibility to ten fungicides used in Korea. *J. Microbiol. Biotechnol.* 16, 240–246.

Kobayashi, A., Kajiyama, S., Inawaka, K., Kanzaki, H., and Kawazu, K. (1994). Nostodione, A. A novel mitotic spindle poison from a blue-green alga *Nostoc* commune. *J. Biosci.* 49, 464–470.

Komarek, J. (2013). "Cyanoprokaryota. 3. Heterocytous genera," in *Suswasserflora von Mitteleuropa/Freshwater flora of Central Europe*, ed B. Budel, G. Gartner, L. Krienitz, and M. Schagerl (Heidelberg: Springer Spektrum), 1130.

Krieger, E., and Vriend, G. (2014). YASARA View—molecular graphics for all devices—from smartphones to workstations. *Bioinformatics* 30, 2981–2982. doi: 10.1093/bioinformatics/btu426

Kumar, R. S., Thajuddin, N., and Venkateswari, C. (2010). Antibacterial activity of cyanolichen and symbiotic cyanobacteria against some selected microorganisms. *Afr. J. Microbiol. Res.* 4, 1408–1411.

Kumar, S., Jyotirmayee, K., and Sarangi, M. (2013). Thin layer chromatography: a tool of biotechnology for isolation of bioactive compounds from medicinal plants. *Int. J. Pharm. Sci. Rev. Res.* 18, 126–132.

Lahlou, M. (2013). The success of natural products in drug discovery. *Pharmacol. Pharm.* 4, 17–31. doi: 10.4236/pp.2013.43A003

Lawton, L. A., Edwards, C., and Codd, G. A. (1994). Extraction and high performance liquid chromatographic method for the determination of microcystins in raw and treated waters. *Analyst* 119, 1525–1530. doi: 10.1039/an9941901525

Mayer, A. M. S., and Hamann, M. T. (2005). Marine Pharmacology in 2001–2002. Marine compounds with anthelmintic, antibacterial, anticoagulant, antidiabetic, antifungal, anti-inflammatory, antimalarial, antiplatelet, antiprotozoal, antituberculosis and antiviral activities, affecting the cardiovascular, immune and nervous systems and other miscellaneous mechanisms of action. *Comp. Biochem. Physiol.* 140, 265–286. doi: 10.1016/j.cca.2005.04.004

McKillop, D., Partridge, A. E., Kemp, J. V., Spence, M. P., Kendrew, J., Wood, P. G., et al. (2005). Tumor penetration of gefitinib (Iressa), an epidermal growth factor receptor tyrosine kinase inhibitor. *Mol. Cancer Ther.* 4, 641–649. doi: 10.1158/1535-7163.MCT-04-0329

Morris, G. M., Goodsell, D. S., Halliday, R. S., Huey, R., Hart, W. E., Belew, R. K., et al. (1998). Automated docking using a Lamarckian genetic algorithm and an empirical binding free energy function. *J. Comput. Chem.* 19, 1639–1662. doi: 10.1002/(SICI)1096-987X(19981115)19:14<1639::AID-JCC10>3.0.CO;2-B

Namikoshi, M., and Rinehardt, K. L. (1996). Bioactive compounds produced by cyanobacteria. *J. Ind. Microbiol. Biotechnol.* 17, 373–384. doi: 10.1007/BF01574768

Nikaido, H. (2003). Molecular basis of bacterial outer membrane permeability revisited. *Microbiol. Mol. Biol. Rev.* 67, 593–656. doi: 10.1128/MMBR.67.4.593-656.2003

Nikitas, P., and Pappa-Louisi, A. (2009). Retention models for isocratic and gradient elution in reverse phase liquid chromatography. *J. Chromatogr. A* 1216, 1737–1755. doi: 10.1016/j.chroma.2008.09.051

Nübel, U., Garcia-Pichel, F., and Muyzer, G. (1997). PCR primers to amplify 16S rRNA genes from Cyanobacteria. *Appl. Environ. Microbiol.* 63, 3327–3332.

Paterson, D. L. (2006). The epidemiological profile of infections with multidrug-resistant *Pseudomonas aeruginosa* and *Acinetobacter* species. *Clin. Infect. Dis.* 43, S43–S48. doi: 10.1086/504476

Patterson, G. M. L., Larsen, L. K., and Moore, R. E. (1994). Bioactive natural products from blue-green algae. *J. Appl. Phycol.* 6, 151–157. doi: 10.1007/BF02186069

Prasanna, R., Sood, A., Jaiswal, P., Nayak, S., Gupta, V., Chaudhary, V., et al. (2010). Rediscovering cyanobacteria as valuable sources of bioactive compounds. *Appl. Biochem. Microbiol.* 46, 119–134. doi: 10.1134/S0003683810020018

Quilliam, M. A. (2003). The role of chromatography in the hunt for red tide toxins. *J. Chromatogr. A* 1000, 527–548. doi: 10.1016/S0021-9673(03)00586-7

Reynolds, R., Potz, N., Colman, M., Williams, A., Livermore, D., and MacGowan, A. (2004). Antimicrobial susceptibility of the pathogens of bacteraemia in the UK and Ireland 2001–2002: the BSAC bacteraemia resistance surveillance programme. *J. Antimicrob. Chemother.* 53, 1018–1032. doi: 10.1093/jac/dkh232

Rippka, R., Deruelles, J., Waterbury, J. B., Herdman, M., and Stanier, R. Y. (1979). Generic assignments, strain histories and properties of pure cultures of cyanobacteria. *J. Gen. Microbiol.* 111, 1–61. doi: 10.1099/00221287-111-1-1

Saitou, N., and Nei, M. (1987). The neighbor-joining method: a new method for reconstructing phylogenetic trees. *Mol. Biol. Evol.* 4, 406–425.

Singh, P., Singh, S. S., Aboal, M., and Mishra, A. K. (2015). Decoding cyanobacterial phylogeny and molecular evolution using an evonumeric approach. *Protoplasma* 252, 519–535. doi: 10.1007/s00709-014-0699-8

Singh, S., Kate, B. N., and Banerjee, U. C. (2005). Bioactive compounds from cyanobacteria and microalgae: an overview. *Crit. Rev. Biotechnol.* 25, 73–95. doi: 10.1080/07388550500248498

Sivonen, K., and Börner, T. (2008). "Bioactive compounds produced by cyanobacteria," in *The Cyanobacteria; Molecular Biology, Genomics and Evolution*, eds A. Herrero and E. Flores (Norflok: Caster Academic Press), 159–197.

Snyder, L. R., and Dolan, J. W. (2006). Initial experiments in high-performance liquid chromatographic method development I. Use of a starting gradient run. *J. Chromatogr. A* 721, 3–14. doi: 10.1016/0021-9673(95)00770-9

Srivastava, A., Tiwari, R., Srivastava, V., Singh, T. B., and Asthana, R. K. (2015). Fresh water *cyanobacteria Geitlerinema* sp. CCC728 and *Arthrospira* sp. CCC729 as an anticancer drug resource. *PLoS ONE* 10:e0136838. doi: 10.1371/journal.pone.0136838

Tamura, K., Stecher, G., Peterson, D., Filipski, A., and Kumar, S. (2013). MEGA6: molecular evolutionary genetics analysis version 6.0. *Mol. Biol. Evol.* 30, 2725–2729. doi: 10.1093/molbev/mst197

Trimurtulu, G., Ohtani, I., Patterson, G. M. L., Moore, R. E., Corbett, T. H., Valeriote, F. A., et al. (1994). Total structures of cryptophycins, potent antitumor depsipeptides from the blue-green alga *Nostoc* sp. strain GSV 224. *J. Am. Chem. Soc.* 116, 4729–4737. doi: 10.1021/ja00090a020

Trott, O., and Olson, A. J. (2010). AutoDock VINA: improving the speed and accuracy of docking with a new scoring function, efficient optimization and multithreading. *J. Comput. Chem.* 31, 455–461. doi: 10.1002/jcc.21334

Vicens, Q., and Westhof, E. (2001). Crystal structure of paromomycin docked into the eubacterial ribosomal decoding A site. *Structure* 9, 647–658. doi: 10.1016/S0969-2126(01)00629-3

Vicens, Q., and Westhof, E. (2002). Crystal structure of a complex between the aminoglycoside tobramycin and an oligonucleotide containing the ribosomal decoding a site. *Chem. Biol.* 9, 747–755. doi: 10.1016/S1074-5521(02)00153-9

Vicens, Q., and Westhof, E. (2003). Crystal structure of geneticin bound to a bacterial 16S ribosomal RNA A site oligonucleotide. *J. Mol. Biol.* 326, 1175–1188. doi: 10.1016/S0022-2836(02)01435-3

Vishwakarma, R., and Rai, A. K. (2013). Separation of bioactive metabolites from *Aphanothece halophytica* through HPLC and characterization of the analytes through ESI-MS and NMR. *J. Nat. Prod.* 3, 151–157. doi: 10.2174/2210315511303020010

Weisburg, W. G., Barns, S. M., Pelletier, D. A., and Lupski, J. R. (1991). 16S Ribosomal DNA amplification for phylogenetic study. *J. Bacteriol.* 173, 697–703. doi: 10.1128/jb.173.2.697-703.1991

Willmann, J., Thiele, H., and Leibfritz, D. (2011). Combined reversed phase HPLC, mass spectrometry and NMR spectroscopy for a fast separation and efficient identification of phosphatidylcholines. *J. Biomed. Biotechnol.* 2001:385786. doi: 10.1155/2011/385786

Wilson, D. N. (2014). Ribosome-targeting antibiotics and mechanisms of bacterial resistance. *Nat. Rev. Microbiol.* 12, 35–48. doi: 10.1038/nrmicro3155

Zhang, Z., Li, Y., Lin, B., Schroeder, M., and Huang, B. (2011). Identification of cavities on protein surface using multiple computational approaches for drug binding site prediction. *Bioinformatics* 21, 2083–2088. doi: 10.1093/bioinformatics/btr331

Ziervogel, B. K., and Roux, B. (2013). The binding of antibiotics in OmpF porin. *Structure* 21, 76–87. doi: 10.1016/j.str.2012.10.014

Conflict of Interest Statement: The authors declare that the research was conducted in the absence of any commercial or financial relationships that could be construed as a potential conflict of interest.

Copyright © 2016 Niveshika, Verma, Mishra, Singh and Singh. This is an open-access article distributed under the terms of the Creative Commons Attribution License (CC BY). The use, distribution or reproduction in other forums is permitted, provided the original author(s) or licensor are credited and that the original publication in this journal is cited, in accordance with accepted academic practice. No use, distribution or reproduction is permitted which does not comply with these terms.

frontiers in Microbiology

ORIGINAL RESEARCH
published: 06 December 2016
doi: 10.3389/fmicb.2016.01921

Isolation, Screening, and Identification of Novel Isolates of Actinomycetes from India for Antimicrobial Applications

Vineeta Singh[1,2]*, *Shafiul Haque*[3,4], *Harshita Singh*[1], *Jyoti Verma*[1], *Kumari Vibha*[1], *Rajbir Singh*[5], *Arshad Jawed*[4,6] and *C. K. M. Tripathi*[4,7]

[1] Microbiology Division, Council of Scientific and Industrial Research—Central Drug Research Institute, Lucknow, India, [2] Department of Biotechnology, Institute of Engineering and Technology, Lucknow, India, [3] Department of Biosciences, Jamia Millia Islamia (A Central University), New Delhi, India, [4] Research and Scientific Studies Unit, College of Nursing and Allied Health Sciences, Jazan University, Jazan, Saudi Arabia, [5] Fermentation Technology Division, Council of Scientific and Industrial Research—Central Drug Research Institute, Lucknow, India, [6] Department of Biotechnology, Himachal Pradesh University, Shimla, India, [7] Department of Biotechnology, Shri Ramswaroop Memorial University, Lucknow, India

OPEN ACCESS

Edited by:
Vijai Kumar Gupta, National University of Ireland, Ireland

Reviewed by:
Alok Kumar Pandey, International Centre for Genetic Engineering and Biotechnology, India
Praveen Chandra Verma, Council of Scientific and Industrial Research-National Botanical Research Institute, India

***Correspondence:**
Vineeta Singh
vscdri@gmail.com

Specialty section:
This article was submitted to Microbiotechnology, Ecotoxicology and Bioremediation, a section of the journal Frontiers in Microbiology

Received: *09 July 2016*
Accepted: *15 November 2016*
Published: *06 December 2016*

Citation:
Singh V, Haque S, Singh H, Verma J, Vibha K, Singh R, Jawed A and Tripathi CKM (2016) Isolation, Screening, and Identification of Novel Isolates of Actinomycetes from India for Antimicrobial Applications. Front. Microbiol. 7:1921. doi: 10.3389/fmicb.2016.01921

The search for novel bioactive compounds from the natural environment has rapidly been gaining momentum with the increase in multi-drug resistant (MDR) pathogens. In the present study, the antimicrobial potential of novel actinomycetes has been evaluated by initial screening of six soil samples. Primary and secondary screening was performed against *Bacillus subtilis, Staphylococcus aureus, Escherichia coli*, *Candida albicans*, *Candida tropicalis*, *Trichophyton rubrum,* and other MDR bacterial and fungal test strains, thirteen active isolates were selected for further study. Microbial strains were identified on the basis of growth conditions and other biochemical characters. Five most active microbial strains were identified using 16S rRNA sequence homology and designated as *Streptomyces xanthophaeus* MTCC 11938, *Streptomyces variabilis* MTCC 12266, *Streptomyces xanthochromogenes* MTCC 11937, *Streptomyces levis* EU 124569, and *Streptomyces* sp. NCIM 5500. Four antibacterial and three antifungal compounds isolated from the above five isolates were purified and partially characterized using UV absorption and IR spectra. Two antibacterial metabolites, belong to chromone and peptide antibiotic, respectively. The antifungal compounds were found to be of non-polyene nature. In conclusion, we study the isolation of novel bacterial strains of actinomycetes for producing novel compounds having antibacterial and antifungal activities from the unexplored agro-ecological niches of India. Also, this study paves the way for further characterization of these isolates of *Streptomyces* sp. for their optimum utilization for antimicrobial purposes.

Keywords: antibiotic production, antimicrobial activity, *Streptomyces* sp., chromone antibiotics, non-polyenes

INTRODUCTION

The search for bioactive metabolites including novel antibiotic compounds from microbial sources for potential use in agricultural, pharmaceutical, and industrial applications has become more important due to the development of drug/multi-drug resistance in most of the pathogenic microbes. Researchers across the globe are aggressively searching for new,

potent, sustainable, and broad-spectrum antimicrobial compounds from various sources including microbes (Berdy, 2005; Hayakawa, 2008; Praveen et al., 2008; Singh and Tripathi, 2011). In natural soil habitat, *Streptomyces* are usually a major proportion of the total actinomycetes population and recognized as prolific producers of useful bioactive compounds (Tanaka and Omura, 1990; Kekuda et al., 2014).

Traditional screening methods have led to the isolation of common microorganisms capable of producing metabolites, which have already been extensively studied and established (Okami and Hotta, 1988; Kurtböke et al., 1992). Among the current strategies of natural-product screening, improved methodologies for isolating the uncommon and less studied rare actinomycetes are required to avoid the repeated isolation of the strains that produce known bioactive metabolites, and to improve the quality of the screened natural products (Takahashi and Omura, 2003; Berdy, 2005; Singh et al., 2009).

Likewise, the traditional methods of species classification and the identification of the organism(s) are mainly based on morphological, physiological, biochemical, developmental, and nutritional characters, and it is not adequate, and warrants for the use of molecular level approaches for assigning accurate taxonomic classification. Hence, precise assignment of taxonomic status to the novel bioactive microbial isolates through existing predictive bioinformatics methods and tools are very essential and aid in chemical characterization of the active molecules.

India has a unique asset of biodiversity, which can be used as a treasure for the search of novel isolates. With the variation of type of soil, according to the geographical changes, soil provide very complex habitat to the microbes residing in it. Due to this intricate environment, the soil microbes play an important role in the isolation of novel drugs. Among soil microbes, the members of *Streptomyces* sp. of actinomycetes, have been widely exploited for the production of commercially important secondary metabolites and enzymes. In the present study, the soil samples from six different unexplored agro-ecological niches of India have been screened-out to isolate *Streptomyces* sp. possessing antibacterial and antifungal activities.

MATERIALS AND METHODS

Collection of Soil Samples

The soil samples were collected from six diverse habitats of India (Lucknow, Uttar Pradesh: 26.7°N, 80.9°E; Badrinath, Uttarakhand: 30.7440°N, 79.4930°E; Delhi, New Delhi: 28.6100°N, 77.2300°E; Bhatinda, Punjab: 30.2300° N, 74.9519° E; Haryana: 28.04°N 76.11°E; Thinmala range, Kerala: 8.5074°N, 76.9730°E) for the isolation of microbes. These habitats included rhizosphere of the plants, agricultural soil, hospital surroundings, river mud, and preserved areas of forest soils. The samples were collected from upto 20 cm depth after the removal of ∼3.0 cm of the soil from the surface. The soil samples were collected in polyethylene bags, sealed, and stored in a refrigerator. All chemicals, media, media components, and other reagents were purchased from Sigma-Aldrich (USA), Merck (USA), HiMedia Laboratories (India) etc.

Pre-treatment of Soil Samples and Isolation of Cultures

The soil samples collected from different geographical areas were pre-treated to eliminate the commonly found microbes using physico-chemical methods. For the physico-chemical treatment of the soil samples, one gram of each soil sample was suspended in 10 ml of normal saline and distributed in aliquots. One aliquot of the soil sample was treated with heat for 1 h at 120°C and the other was treated with 1.5% phenol for 30 min at 30°C as described by Hayakawa et al. (1991). Afterwards, the physico-chemically treated soil samples were vortexed and left for 30 min, there after soil samples were serially diluted and 100 μl of each "dilution" was plated on nutrient agar (NA), actinomycetes isolation agar (AIA), yeast malt glucose agar (M6), antibiotic assay agar, starch casein agar, and Czapek Dox agar.

Screening of Microbial Cultures

Primary screening for evaluating the antimicrobial potential of the axenic cultures was performed by perpendicular streak method of Madigan et al. (1997) against the bacterial strains of *Bacillus subtilis* MTCC 441, *Staphylococcus aureus* MTCC 96, *Escherichia coli* MTCC 64, and *Candida albicans* MTCC 183. Isolates were screened for antagonism studies by inoculating a single streak of the pure producer organism in the middle of the assay media plate. The plates were incubated for 4 days at 28°C and subsequently seeded with "test" organism by a single streak at a 90° angle to the streak of the "producer strain" and finally the plates were incubated for 1–2 days at 28°C. The microbial interactions were analyzed by determining the distance of inhibition measured in mm.

Microbial strains showing "moderate" to "good" inhibition activity were selected for secondary screening, which was performed by agar well method (Wu, 1984), using 100 μl of their fermented broth against *B. subtilis* MTCC 441, *B. subtilis* MTCC 121, *B. pumilus* MTCC 1607, *S. aureus* MTCC 902, *S. aureus* MTCC 96, *E. coli* MTCC 1304, *Salmonella typhi* MTCC 734, *Pseudomonas aeruginosa* MTCC 741, *Proteus vulgaris* MTCC 426, *C. albicans* MTCC 3017, *C. albicans* MTCC 183, *C. tropicalis* MTCC 184, *Saccharomyces cerevisiae* MTCC 170, *Cryptococcus terreus* MTCC 1716, *Aspergillus niger* MTCC 1344, *Trichophyton rubrum* MTCC 296, *Penicillium chrysogenum* MTCC 2725, and *Beauveria bassiana* MTCC 4564. All the experiments were performed in triplicate and the average values were considered for analysis.

Characterization of Microbial Strain(s) from the Selected Cultures

The cultural characteristics of the producer strains were studied according to the method of Shirling and Gottlieb (1966) based upon their intensity of growth, growth pattern, colony color along with the color of aerial and substrate mycelia, and the formation of soluble pigments on oat meal agar (ISP-3), inorganic salt starch agar (ISP-4), glycerol asparagine agar (ISP-5), peptone yeast extract iron agar (ISP6), and tyrosine agar (ISP-7). The strains were characterized by streaking the culture(s) on the

above mentioned medium plates and observed after 7–10 days of incubation at 28°C for the given characteristics.

Physiological and biochemical tests were performed as described by Williams et al. (1989) and Bergey's manual (Holt et al., 1994), and results were observed after 10 days of incubation of plates at 28°C. In addition, the strains were tested for nitrate reduction, tolerance to NaCl, decomposition of citrate, tartrate, acetate and pyruvate, and pH and temperature tolerance. The enzymatic activity assays of urease, amylase, protease and catalase were performed as suggested by Hopwood and Wright (1973). Finally, on the basis of macroscopic, biochemical and physiological characteristics hierarchical cluster analysis was performed by using PASW Statistics (formerly SPSS Statistics) Version 18 software program and dendrogram was generated based on the average linkage between the groups.

Metabolite Production

Pure and active cultures of microbial strains selected from the secondary screening experiments were grown in X-medium (g/l: Soybean meal, 10; $CaCO_3$, 3; $MgSO_4.7H_2O$, 0.5; $(NH_4)_2HPO_4$, 0.5; NaCl, 3; K_2HPO_4, 1; glycerol, 15 ml; DW 1, pH 6.9–7.0), and incubated at 28°C for 3–5 days and cellular growth was confirmed by visible pellets, clumps, aggregates or turbidity in the culture broth. The culture broths were centrifuged separately and filtrates were used to evaluate the antimicrobial activity against the above mentioned test microorganisms. Antibiotic activities of the strains were compared with that of known commercially available erythromycin (E^{15}) and amphotericin B (AmB^{100}).

Extraction, Purification, and Partial Characterization of the Active Compounds

Fermented culture was centrifuged at 10,000 rpm for 20 min to separate the biomass. The active metabolite was recovered from the fermented broth using two phase solvent extraction system with organic solvent. Solvents containing the active compounds were concentrated under vacuum to get "dried crude." The obtained "crude" was treated with non-polar solvents like hexane or chloroform to separate the polar and non-polar components. The active components were purified by adsorption chromatography using silica gel (pore size 60 Å, mesh size: 230–400, particle size 40–63 μm) as a stationary phase and gel filtration chromatography using sephadex LH-20. The eluted fractions were assayed for their bioactivity against *B. subtilis* ATCC 6633 and *C. albicans* ATCC 24433 by disc diffusion method (Wu, 1984). The purity of the active fractions was further checked by high pressure liquid chromatography (HPLC) using reverse phase silica column (RP18). Finally, the UV spectra (Perkin Elmer Lambda-25 UV spectrophotometer) of various antibacterial and antifungal compounds were determined in methanol at 200–500 nm wave length.

RESULTS

Screening of the Active Strains

During the screening, thirty six actinomycetes were isolated from six different stressed agro-ecological niches of India.

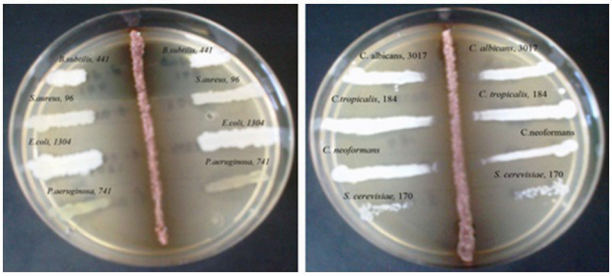


FIGURE 1 | Primary screening using perpendicular streak method for antibacterial and antifungal activity of the soil isolate (ZA25).

Microbial colonies showing distinct morphological characters were selected for the primary screening (**Figure 1**). Out of 36 total actinomycetes isolates, 15 showed moderate to strong antimicrobial activity against gram positive (*B. subtilis* MTCC6633, *S. aureus* MTCC 6538), gram negative (*E. coli* MTCC 1304) and fungal strain (*C. albicans* MTCC 1346). The active strains (actinomycetes) were further subjected to the secondary screening against some multi-drug resistant (MDR) bacterial as well as fungal test strains (**Tables 1, 2**). The screening results suggested that most of the isolates were active against gram positive bacteria in comparison with gram negative bacteria (**Figures 2A,B**). Out of 15 active isolates, 13 showed strong antimicrobial activity and were selected for detailed taxonomic, physiological, and biochemical studies.

Characterization of the Strains

The cultural characteristics, such as microbial growth along with its pattern and pigment formation were studied on International *Streptomyces* Project (ISP) media and their results are summarized in **Table 3**. All the selected actinomycetes isolates showed moderate to heavy growth on nitrate agar, urease agar and inorganic salt starch agar medium, which suggests their capability of breaking down the above complexes. Heavy growth and color change (from green to blue) of Simmons' Citrate Agar (SCA) medium provide the evidence of citrate utilizing ability of the actinomycetes strains YE21, YE22, and YE23. Likewise, melanin formation was demonstrated by the presence of brown to black patches on inorganic salt starch agar (ISP4) and YMG (yeast extract 4 g, malt extract 10 g, glucose 4 g, agar 20 g, water 1 L) medium as a result of the growth of the active strains. This was observed in almost all the selected strains.

All the strains were capable of reducing nitrate salts but they demonstrated some differences against the decomposition of starch and urea. The production of amylase, urease and protease enzymes by the actinomycetes strains was endorsed by their growth on ISP4, urease agar and ISP3 mediums. Except the actinomycetes strains ZA25, ZA26, and YE22, the most favorable temperature range for the growth of strains was 27–37°C. Interestingly, none of the selected strains were able to grow at 50°C or above. All the selected actinomycetes strains possessed the ability to tolerate 3% NaCl in the medium with the exception of strains ZE18 and ZA25.

TABLE 1 | Secondary screening (antibacterial activity).

Sr. No	Test strains	Soil isolates (zone of Inhibition in mm)															PC
		ZE 18	ZE 19	YE 21	YE 22	YE 23	ZA 25	ZA 26	YD 28	RS 25	XD1	H1	V1	N1	S1	K1	E^{15}
1	*Bacillus subtilis* MTCC 441	16	16	13	27	22	23	21	–	–	20	17	25	12	13	11	30
2	*Bacillus subtilis* MTCC 121	16	16	–	17	16	19	19	–	–	17	16	25	–	12	–	30
3	*Bacillus pumilus* MTCC 1607	21	21	18	25	21	26	15	13	–	–	17	30	–	–	–	–
4	*Staphylococcus aureus* MTCC 96	23	17	–	20	17	25	24	–	24	24	20	21	–	13	11	25
5	*Staphylococcus aureus*, MTCC 902	–	–	–	14	17	–	–	12	25	20	15	30	–	14	11	17
6	*Escherichia coli* MTCC 1304	–	–	–	–	12	16	–	–	–	19	17	–	–	–	–	20
7	*Pseudomonas aeruginosa* MTCC 741	–	–	13	27	15	18	27	–	20	20	15	28		–	–	37
8	*Proteus vulgaris* MTCC 426	16	16	–	15	18	–	–	14	–	14	18	30	–	12	–	12
9	*Salmonella typhi* MTCC 581	–	–	–	15	15	18	17	12	–	16	16	29	–	–	–	13
10	*Klebsiella pneumonia* MTCC 13883	15	14	–	16	17	18	–	12	23	17	15	25	–	–	–	–

(–), not active; PC, Positive Control; E^{15}, Erythromycin and well diameter = 10 mm.

TABLE 2 | Secondary screening (antifungal activity).

Sr. No	Test strains	Soil isolates (zone of inhibition in mm)															PC
		ZE 18	ZE 19	YE 21	YE 22	YE 23	ZA 25	ZA 26	YD 28	RS 25	XD1	H1	V1	N1	S1	K1	AmB
1.	*Candida albicans* MTCC 183	16	15	–	–	–	–	–	11	12	–	12	–	12	–	–	25
2.	*Candida albicans* MTCC 3017	30	30	15	14	–	27	19	18	11	–	18	–	–	–	–	25
3.	*Candida tropicalis* MTCC 184	14	11	–	–	–	13	–	18	–	–	21	–	–	–	–	20
4.	*Cryptococcus terreus* MTCC 1716	25	25	–	–	–	19	–	15	–	–	16	–	–	–	–	12
5.	*Saccharomyces cerevisiae* MTCC 170	21	23	–	–	–	25	28	20	–	–	23	–	11	11	–	20
6.	*Kluyveromyces lactis* MTCC32	27	24	–	–	21	21	31	20	–	–	29	–	13	13	–	12
8.	*Penicillium chrysogenum* MTCC 2725	19	11	–	–	–	–	–	–	–	–	20	–	–	–	13	–
9.	*Aspergillus niger* MTCC 1344	–	12	12	–	–	12	13	–	–	–	14	–	–	–	15	–
11.	*Trichophyton rubrum* MTCC 296	–	–	–	–	18	16	14	12	–	–	20	–	–	13	12	32
12.	*Beauveria bassiana* MTCC 4564	16	20	20	11	–	–	19	–	–	–	–	–	–	–	–	–

(–), not active; PC, positive control; AmB, Amphotericin B and well diameter = 10 mm.

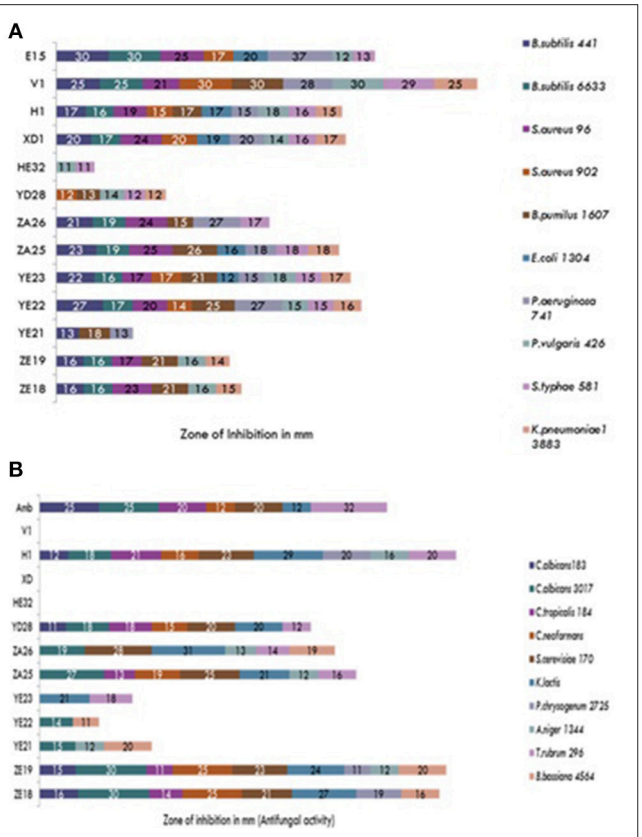


FIGURE 2 | (A) Secondary screening of the soil isolates for the antibacterial activities. **(B)** Secondary screening of the soil isolates for the antifungal activities.

Hierarchical Cluster Analysis

Strains found to be active in primary and secondary screening were subjected to hierarchical cluster analysis based on 49 macroscopic, biochemical and physiological characters. The dendrograms based on the average linkage between the groups were generated by PASW Statistics (formerly SPSS Statistics) Version 18 software. Two broad clusters were generated (**Figure 3**). The first cluster contained four (ZE18, ZE19, ZA25, and ZA26) and the second cluster contained nine actinomycetes (YE23, RS25, H1, V1, N1, S1, YE22, YE21, and K1) isolates. The first cluster was further divided into two sub cluster sub-clad 1.1 and 1.2. The sub-clad 1.1 leaded ZA25 alone whereas sub-clad 1.2 further divided into 1.2.1 and 1.2.2 and so on, and ultimately formed a branched group of three isolates (ZE18, ZE19, and ZA26). Similarly, the second cluster was divided into sub-clad 2.1 and 2.2. The sub-clad 2.1 was further divided into 2.1.1 and 2.1.2 (YE21 and YE2,), whereas sub-clad 2.2 was further divided into 2.2.1 and 2.2.2 and so on, and ultimately formed a branched group of seven isolates (YE23, RS25, H1, V1, N1, S1, and K1).

Based upon the potential antimicrobial activities shown in the primary and secondary screenings, five out of thirteen strains were finally selected for further characterization using 16S rRNA homology studies. The generated dendrogram showed that all the five strains (H1, V1, S1, RS25, and ZA25) were evolutionary far away from each other and displayed varying biochemical characteristics along with excellent antimicrobial activity. The diversity was maintained when we compared the antimicrobial activity data and the UV spectra of the metabolites. Strains, ZA25 and H1 belong to the main cluster I and II, respectively, found to produce both antibacterial and antifungal compounds having different UV absorbance. Similarly, H1, V1, and S1 produce antibacterial compounds and belong to the same cluster II; but their sub-clad were different. Variations in the UV absorbance of the metabolites supported the positional difference of the strains in the dendrogram. The 16S rRNA study for the strains H1, V1, and S1 were performed at Microbial Type Culture Collection (MTCC), Chandigarh, Punjab (India), and identified and submitted to MTCC as - *Streptomyces xanthophaeus* MTCC 11938, *Streptomyces variabilis* MTCC 12266, and *Streptomyces xanthochromogenes* MTCC 11937, respectively. Whereas, the 16S rRNA homology sequence study for the strain RS25 and ZA25 was done at Genomebio Technologies Pvt. Ltd., Pune, Maharashtra (India) and identified and submitted to National Collection of Industrial Microorganisms (NCIM), CSIR-NCL, Pune, Maharashtra (India) as *Streptomyces levis* EU 124569 and *Streptomyces* sp. NCIM 5500, respectively.

Partial Chemical Characterization of the Active Compounds

The bioactive compounds were purified from the selected actinomycetes strains using silica column, with methanol:chloroform gradient as an eluting solvent system. The purified fractions were partially characterized by observing under UV absorbance (λ_{max}) and their absorption pattern to gather some preliminary information regarding the structure of the compound(s) (**Table 4**). Absorbance within UV range confirmed the presence of "*unsaturation*" in all the bioactive compounds. All the active metabolites except from the strain RS25 contained either carboxyl or peptide moiety in their structure. Absorbance band near 253 nm indicated the presence of benzene moiety in H1F2 (antifungal; AF), H1F1 (antibacterial; AB) and ZA25 AF strains. Among antifungal compounds, absence of conjugated absorption suggested non-polyene nature of H1F1 and ZA25 AF. The presence of carboxyl or peptide moieties was further confirmed by IR spectra of the compounds. Hydroxyl and conjugated carbonyl functional moiety in the compound were confirmed by the presence of absorption bands at 3425 and 1648 cm^{-1}, respectively. The absorption bands detected at 3020 and 2927 cm^{-1} correspond to aromatic C-H and alkyl C-H stretching, respectively, and suggested the presence of aromatic ring in the antibacterial compound isolated from ZA25 and absence in the compound isolated from V1. Further, presence of aromatic ring was verified by the absorption bands at 1602 and 1504 cm^{-1} attributed to C=C ring stretching.

DISCUSSION

During the screening of rare actinomycetes, fast growing bacterial colonies inhibits the colonization of actinomycetes on the isolation medium, hence in order to isolate actinomycetes, the growth of these bacteria should be inhibited. Pre-treatment of the soil samples reduced the growth of ubiquitous microbial species,

TABLE 3 | Cultural and Biochemical characteristics of the producer strains.

		Producer strains												
Characteristics		**H1**	**N1**	**S1**	**K1**	**V1**	**ZE 18**	**ZE 19**	**YE 21**	**YE 22**	**YE 23**	**ZA 25**	**ZA 26**	**RS25**
Growth on	ISP2	2+	+	2+	2+	2+	+	2+	3+	3+	2+	3+	–	3+
	ISP3	2+	+	2+	2+	2+	2+	2+	2+	3+	3+	–	2+	2+
	ISP4	3+	2+	2+	3+	3+	2+	3+	+	2+	3+	–	3+	3+
	ISP5	2+	2+	+	2+	+	+	2+	+	+	2+	–	2+	2+
	ISP6	3+	2+	2+	3+	2+	+	+	+	2+	2+	+	+	2+
	ISP7	+	2+	+	+	+	+	3+	2+	3+	2+	+	–	+
Utilization of	Citrate	–	–	–	+	+	–	–	2+	2+	2+	–	–	–
	Asparagine	3+	2+	+	–	2+	–	–	+	+	+	+	–	–
	Oat meal	2+	+	2+	–	2+	2+	2+	2+	3+	3+	–	2+	2+
	Tributyrin	2+	2+	2+	2+	3+	+	–	–	–	+	–	+	+
Enzyme production	Urease	–	–	–	–	–	+	–	2+	–	+	–	–	+
	Amylase	3+	2+	2+	2+	3+	2+	3+	+	2+	3+	–	3+	3+
	Tyrosinase	3+	2+	–	+	+	+	3+	2+	3+	2+	+	–	+
	Chitinase	3+	2+	2+	2+	+	–	–	3+	+	+	–	–	+
	Heparinase	–	–	–	–	3+	–	–	–	–	–	–	–	–
	Protease	2+	2+	2+	2+	2+	+	2+	3+	3+	2+	3+	+	3+
	Catalase	2+	2+	2+	2+	2+	+	+	2+	2+	3+	2+	+	+
pH tolerance	5	3+	3+	2+	3+	3+	3+	3+	3+	3+	2+	2+	2+	3+
	7	3+	2+	3+	3+	3+	+	2+	3+	3+	3+	+	+	3+
	9	2+	3+	+	3+	3+	+	+	3+	3+	2+	2+	+	3+
	11	–	2+	+	2+	3+	+	+	3+	3+	2+	+	+	2+
NaCl tolerance	1%	3+	3+	3+	3+	3+	+	3+	3+	3+	2+	2+	+	3+
	3%	+	2+	2+	3+	3+	–	+	3+	3+	3+	–	+	+
	5%	–	–	+	2+	2+	–	–	3+	3+	2+	–	–	+
	7%	–	–	+	+	+	–	–	+	3+	+	–	–	–
Growth at	28°C	3+	2+	3+	3+	2+	+	2+	3+	+	3+	+	+	3+
	37°C	3+	3+	2+	3+	3+	2+	2+	3+	+	3+	+	–	3+
	47°C	–	–	–	–	+	–	–	–	–	–	–	–	–

(–), No growth; (+1), Poor growth; (+2), Moderate growth; (+3), Heavy growth.

thereby facilitated the recovery of less-abundant microorganisms. The spores of actinomycetes and fungi generally resist desiccation and show slightly higher resistance toward wet or dry heat than other microbes (Hopwood and Wright, 1973). Pre-treatment of the soil suspension with 1.5% phenol (30°C for 30 min) lowered the number of bacteria, fungi, and other common actinomycetes by denaturing their proteins or by disrupting their cell membrane, however phenol-resistant actinomycetes were less affected during this process (Hayakawa et al., 1991). Earlier, Hayakawa et al. (1991) and Kim et al. (1995) reported the use of above mentioned pre-treatment of the soil samples for the isolation of actinomycetes, and they reported similar results, when the soil samples were pre-treated.

A total of 15 isolated strains were subjected to antimicrobial screening and it was found that most of the isolates were active against gram positive bacteria. This was majorly attributed to the presence of lipopolysaccharide (LPS), a major structural unit of gram negative bacterial cell wall. LPS is hydrophobic in nature and makes the cell wall impermeable to lipophilic solutes, whereas in absence of LPS in the cell wall of gram positive bacteria, they become susceptible to the metabolites (Kim et al., 1994).

Out of 15 strains, thirteen showed strong antimicrobial activity and were selected for detailed microbial characterization studies. Melanin formation was also observed in almost all the selected strains, which is a main diagnostic feature of *Streptomyces* sp. (Singh et al., 2009). Further, five strains were characterized by using nucleotide sequencing and designated as H1: *S. xanthophaeus* MTCC 11938, V1: *S. variabilis* MTCC 12266, S1: *S. xanthochromogenes* MTCC 11937, RS25: *S. levis* EU124569, and ZA 25: *Streptomyces* sp. NCIM 5500.

Evolutionary distance of the above five strains (H1, V1, S1, RS25, and ZA 25) was also analyzed by measuring their positions in the dendrogram. Based upon the diversity achieved by the morphological, biochemical, and the phylogenetic characteristics in the selected strains, we can speculate the possibility of involvement/role of diverse bioactive compounds from these strains, responsible for their broad-spectrum antimicrobial properties.

During the purification of the metabolites from ultra violet spectra, maximum absorbance between 205 and 216 nm suggested the presence of carboxyl or peptide moiety in the structure of all the active metabolites except from the strain RS25 (Singh et al., 2009; Kang et al., 2010). However, absorbance at 240–250 and at 332 nm predicted the presence of chromone like nucleus in strain RS25 (Griffiths and Ellis, 1972).

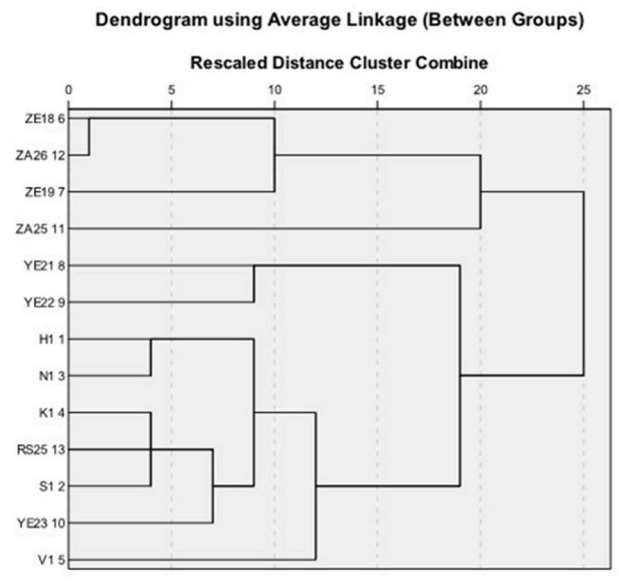


FIGURE 3 | Phylogenetic tree showing evolutionary relationship of the soil isolates.

Pertinent literature about the producer strains were searched using SciFinder software program and it was found that *S. xanthophaeus* is known to produce diverse array of metabolites including Postproline endopeptidase, Benarthin, β-galactosidase-inhibiting isoflavonoids and geomycins (Brockmann and Musso, 1954; Hazato et al., 1979; Aoyagi et al., 1992; Shibamoto et al., 1993). *S. xanthochromogenes* are also known to produce diverse array of chemical compounds such as Diastereoisomeric I-Na, Nitropeptin, xanthicin (I), Pravastatin, reductiomycin, alkaloid AM-6201 (Arishima et al., 1956; Onda et al., 1982; Ohba et al., 1987; Otake et al., 1988; Cho et al., 1993; Zhang et al., 2008). Eleven compounds having same molecular formula have been reported from *S. levis*. Those were oleandomycin, 2-piperidinone and derivatives of either erythromycin or tylonolide. *S. variabilis* is reported for the production of L-Glutaminase, imunosuppresive, clavulanic acid, glycoside antibiotic and 1-hydroxy-1-norresistomycin (Abd-Alla et al., 2013, 2016; Marques et al., 2014; Ramalingam and Rajaram, 2016).

To the best of our knowledge, this is very first time we are reporting the antifungal activity of *S. xanthophaeus* and *S. xanthochromogenes.* Similarly, the compounds reported from *S. levis* didn't show the presence of chromone like structure. Also, the antifungal compound purified from *S. xanthochromogenes* was confirmed as chitinase by performing enzyme assay.

In conclusion, the results of morphological and biochemical characterization and the nature of compounds produced by the microbes established the diversity among the member of actinomycetes. The antimicrobial activities achieved in this study indicate that the isolated strains of *Streptomyces* sp. from different geographical niches of India have potential to produce diverse array of antimicrobial compounds that can be useful for many great applications and must be explored extensively. Currently, our research group and collaborators are actively involved in the chemical characterization of the active compounds identified in this study. In addition, *in silico* predictive studies for target prediction are under progress with our collaborator group. Hopefully, in our successive publication we would be reporting the complete information regarding the chemical characteristics of the

TABLE 4 | IR spectra of bioactive compounds isolated from the selected actinomycetes strains.

Strains	Identification	Nature of purified compound	UV absorbance	IR frequency
H1F1	*Streptomyces xanthophaeus*	Antibacterial	201, 260	3409, 3019, 2400, 1658, 1402, 1384, 1215, 1053, 948, 758, 668
ZA25F1	*Streptomyces* sp.	Antibacterial	264, 495	3411, 3019, 2400, 1647, 1403, 1070, 928, 669
V1	*Streptomyces variabilis*	Antibacterial	210	3412, 2928, 1646, 1215, 1070,
RS25	*Streptomyces levis*	Antibacterial	240-250 and 332	3425 and 1648, 3020 and 2927, 1602 and 1504 cm^{-1}
S1	*Streptomyces xanthochromogenes*	Antifungal	205, 490	3411, 3020, 1646, 1403, 1385, 1216, 1069, 769
H1F2	*Streptomyces xanthophaeus*	Antifungal	201, 265	3850, 3431, 3020, 2399, 2110, 1637, 1403, 1385, 1017, 669
ZA25F2	*Streptomyces* sp.	Antifungal	205, 248, 263,	3850, 3366, 2945, 2833, 2518, 2042, 1638, 1449, 1218, 1113, 757, 666

"*actives*" identified in this study and their targets predicted through *in silico* binding studies and their experimental validation.

AUTHOR CONTRIBUTIONS

Conceived and designed the study and experiments: VS, SH, HS, JV, KV, RS, AJ, CT. Performed the experiments: VS, HS, JV, KV, RS. Analyzed the data: VS, SH, AJ. Contributed reagents/materials/analysis tools: VS, SH, AJ, CT. Wrote the paper: VS, SH, AJ, CT. All authors reviewed the manuscript.

FUNDING

The financial support for this study was available from the Department of Science and Technology, Ministry of Science and Technology, Government of India, New Delhi, under Fast Track Fellowship awarded to VS (Grant No. SR/FT/LS-190/2009).

ACKNOWLEDGMENTS

The authors are grateful to acknowledge the laboratory facility provided by the CSIR-CDRI, Lucknow, UP, India for this study.

REFERENCES

Abd-Alla, M. H., El-Sayed, E. S. A., and Rasmey, A. H. M. (2013). Biosynthesis of L-glutaminase by *Streptomyces variabilis* ASU319 isolated from rhizosphere of triticum vulgaris. *Univ. J. Microbiol. Res.* 1, 27–35. doi: 10.13189/ujmr.2013.010301

Abd-Alla, M. H., Rasmey, A. H. M., El-Sayed, E. S. A., El-Kady, I. A., and Yassin, I. M. (2016). Biosynthesis of anti-inflammatory immunosuppressive metabolite by *Streptomyces variabilis* ASU319. *Eur. J. Biol. Res.* 6, 152–169. Available online at: http://www.journals.tmkarpinski.com/index.php/ejbr/article/view/455

Aoyagi, T., Hatsu, M., Kojima, F., Hayashi, C., Hamada, M., and Takeuchi, T. (1992). Benarthin: a new inhibitor of pyroglutamyl peptidase. i taxonomy, fermentation isolation and biological activities. *J. Antibiot.* 45, 1079–1083. doi: 10.7164/antibiotics.45.1079

Arishima, M., Sakamoto, J., and Sato, T. (1956). An antibiotic *Streptomyces* no. 689 strain. I. Taxonomic studies. *Nippon Nogei Kagaku Kaishi* 30, 469–471. doi: 10.1271/nogeikagaku1924.30.8_469

Berdy, J. (2005). Bioactive microbial metabolites, a personal view. *J. Antibiot.* 58, 1–26. doi: 10.1038/ja.2005.1

Brockmann, H., and Musso, H. (1954). Antibiotics from actinomycetes. XXIX. Geomycin 2. *Chem. Ber.* 87, 1779–1799. doi: 10.1002/cber.19540871128

Cho, H., Beale, J. M., Graff, C., Mocek, U., Nakagawa, A., Omura, S., et al. (1993). Studies on the biosynthesis of the antibiotic reductiomycin in *Streptomyces xanthochromogenus*. *J. Am. Chem. Soc.* 115, 12296–12304. doi: 10.1021/ja00079a009

Griffiths, P. J. F., and Ellis, G. P. (1972). Benzopyrones—VI1: the ultraviolet absorption spectra of chromone and 2-substituted chromones. *Spectrochim. Acta A Mol. Spectros.* 28, 707–713. doi: 10.1016/0584-8539(72)80039-4

Hayakawa, M. (2008). Studies on the isolation and distribution of rare actinomycetes in soil. *Actinomycetologica* 22, 12–19. doi: 10.3209/saj.SAJ220103

Hayakawa, M., Sadakata, T., Kajiura, T., and Nonomura, H. (1991). New methods for the highly selective isolation of Micromonospora and Microbispora from soil. *J. Fermen. Bioeng.* 72, 320–326. doi: 10.1016/0922-338X(91)90080-Z

Hazato, T., Naganawa, H., Kumagai, M., Aoyagi, T., and Umezawa, H. (1979). Beta-Galactosidase-inhibiting new isoflavonoids produced by actinomycetes. *J. Antibiot.* 32, 217–222. doi: 10.7164/antibiotics.32.217

Holt, J. G., Krieg, N. R., Sneath, P. H. A., Staley, J. T., and Williams, S. T. (1994). *Bergey's Manual of Determinative Bacteriology, 9th Edn.* Baltimore, MD; Philadelphia; Hong Kong; London; Munch; Sydney; Tokyo: William and Wilkins.

Hopwood, D. A., and Wright, H. M. (1973). A plasmid of *Streptomyces* coelicolor carrying a chromosomal locus and its inter-specific transfer. *J. Gen. Microbiol.* 79, 331–342. doi: 10.1099/00221287-79-2-331

Kang, M. J., Strap, J. L., and Crawford, D. L. (2010). Isolation and characterization of potent antifungal strains of the *Streptomyces* violaceusniger clade active against *Candida albicans*. *J. Ind. Microbiol. Biotechnol.* 37, 35–41. doi: 10.1007/s10295-009-0641-9

Kekuda, P. T. R., Onkarappa, R., and Jayanna, N. D. (2014). Characterization and antibacterial activity of a glycoside antibiotic from *Streptomyces variabilis* PO-178. *Sci. Technol. Arts Res. J.* 3, 116–121. doi: 10.4314/star.v3i4.17

Kim, C., Lee, K., Kwon, O., Park, D., and Shimazu, A. (1995). Isolation of rare actinomycetes on various types of soil. *Kor. J. Appl. Microbiol. Biotechnol.* 23, 36–42.

Kim, C., Lee, K., Kwon, O., Yoo, I., and Shimazu, A. (1994). Selective isolation of actinomycetes by physical pretreatment of soil sample. *Kor. J. Appl. Microbiol. Biotechnol.* 22, 222–225.

Kurtböke, D. I., Chen, C. F., and Williams, S. T. (1992). Use of polyvalent phage for reduction of streptomycetes on soil dilution plates. *J. Appl. Bacteriol.* 72, 103–111. doi: 10.1111/j.1365-2672.1992.tb01810.x

Madigan, M. T., Martiko, J. M., and Parker, J. (1997). "Antibiotics: isolation and characterization," in *Brock Biology of Microorganisms*, *8th Edn.,* ed M. T. Madigan (New Jersey: Prentice-Hall International Inc.), 440–442.

Marques, D. A. V., Santos-Ebinuma, V. D. C., de Oliveira, P. M. S., de Souza Lima, G. M., Araújo, J. M., Lima-Filho, J. L., et al. (2014). Screening of wild type *Streptomyces* isolates able to overproduce clavulanic acid. *Braz. J. Microbiol.* 45, 919–928. doi: 10.1590/S1517-83822014000300022

Ohba, K., Nakayama, H., Furihata, K., Shimazu, A., Endo, T., Seto, H., et al. (1987). Nitropeptin, a new dipeptide antibiotic possessing a nitro group. *J. Antibiot.* 40, 709–713.

Okami, Y., and Hotta, K. (1988). "Search and discovery of new antibiotics," in *Actinomycetes in Biotechnology,* eds M. Goodfellow, S. T. Williams, and M. Mordarski (London: Academic Press), 37–67.

Onda, M., Konda, Y., Hinotozawa, K., and Omura, S. (1982). The alkaloid AM-6201 from *Streptomyces* xanthochromogenus. *Chem. Pharmaceut. Bull.* 30, 1210–1214. doi: 10.1248/cpb.30.1210

Otake, N., Seto, H., Nakayama, H., Endo, T., Oba, K., Iwata, M., et al. (1988). Antibiotic 6257 manufacture with Streptomyces for *Pyricularia oryzae* infection control in rice. *Jpn. Kokai Tokkyo Koho.* JP 63126495 (Accessed May 30, 1988).

Praveen, V., Tripathi, D., Tripathi, C. K. M., and Bihari, V. (2008). Nutritional regulation of actinomycin-D production by a new isolate of *Streptomyces* sindenensis using statistical methods. *Indian J. Exp. Biol.* 46, 138–144.

Ramalingam, V., and Rajaram, R. (2016). Antioxidant activity of 1-hydroxy-1-norresistomycin derived from *Streptomyces variabilis* KP149559 and evaluation of its toxicity against zebra fish *Danio rerio*. *RSC Adv.* 6, 16615–16623. doi: 10.1039/C5RA22558B

Shibamoto, N., Terasawa, T., Okamoto, R., Shin, T., and Murao, S. (1993). Novel postproline endopeptidase and its manufacture with Streptomyces species. *Jpn. Kokai Tokkyo Koho.* Patent No. JP 05244947, Indexing: Fermentation and Bioindustrial Chemistry (Section 16-4).

Shirling, E. B., and Gottlieb, D. (1966). Methods for characterization of *Streptomyces* sp. *Int. J. Syst. Bacteriol.* 16, 313–340. doi: 10.1099/00207713-16-3-313

Singh, V., and Tripathi, C. K. M. (2011). Olivanic acid production in fed batch cultivation by Streptomyces olivaceus MTCC 6820. *Res. J. Pharmaceut. Biol. Chem. Sci.* 2, 726–731.

Singh, V., Praveen, V., Banga, J., and Tripathi, C. K. M. (2009). Antimicrobial activities of microbial strains isolated from soil of stressed ecological

niches of Eastern Uttar Pradesh, India. *Indian J. Exp. Biol.* 47, 298–303.

Takahashi, Y., and Omura, S. (2003). Isolation of new actinomycete strains for the screening of new bioactive compounds. *J. Gen. Appl. Microbiol.* 49, 141–154. doi: 10.2323/jgam.49.141

Tanaka, Y., and Omura, S. (1990). Metabolism and products of actinomycetes. An introduction. *Actinomycetolgica* 4, 13–14. doi: 10.3209/saj.4_13

Williams, S. T., Goodfellow, M., and Alderson, G. (1989). "Bergey's manual of systematic bacteriology," in *Genus Streptomyces Waksman and Henrici 1943, 339AL, Vol. 4*, eds S. T. Williams, M. E. Sharpe, and J. G. Holt (Baltimore, MD: Williams and Wilkins), 2452–2492

Wu, R. Y. (1984). Studies on the Streptomyces SC4. II Taxonomic and biological characteristics of Streptomyces strain SC4. *Bot. Bull. Acad. Sin.* 25, 111–123.

Zhang, L., Zhang, J., Yang, W., and Bai, G. (2008). Classification of Streptomyces strain Z314 and purification of its product pravastatin. *Wei Sheng Wu Xue Bao* 48, 33–37.

Conflict of Interest Statement: The authors declare that the research was conducted in the absence of any commercial or financial relationships that could be construed as a potential conflict of interest.

The reviewer PCV declared a shared affiliation, though no other collaboration, with the authors to the handling Editor, who ensured that the process nevertheless met the standards of a fair and objective review.

Copyright © 2016 Singh, Haque, Singh, Verma, Vibha, Singh, Jawed and Tripathi. This is an open-access article distributed under the terms of the Creative Commons Attribution License (CC BY). The use, distribution or reproduction in other forums is permitted, provided the original author(s) or licensor are credited and that the original publication in this journal is cited, in accordance with accepted academic practice. No use, distribution or reproduction is permitted which does not comply with these terms.

frontiers in Microbiology

MINI REVIEW
published: 16 January 2017
doi: 10.3389/fmicb.2016.02161

Essential Oils: Sources of Antimicrobials and Food Preservatives

Abhay K. Pandey[1], *Pradeep Kumar*[2]*, *Pooja Singh*[1]*, *Nijendra N. Tripathi*[1] and *Vivek K. Bajpai*[3]*

[1] Bacteriology and Natural Pesticide Laboratory, Department of Botany, Deen Dayal Upadhyay Gorakhpur University, Gorakhpur, India, [2] Department of Forestry, North Eastern Regional Institute of Science and Technology, Nirjuli, India, [3] Department of Applied Microbiology and Biotechnology, School of Biotechnology, Yeungnam University, Gyeongsan, South Korea

Aromatic and medicinal plants produce essential oils in the form of secondary metabolites. These essential oils can be used in diverse applications in food, perfume, and cosmetic industries. The use of essential oils as antimicrobials and food preservative agents is of concern because of several reported side effects of synthetic oils. Essential oils have the potential to be used as a food preservative for cereals, grains, pulses, fruits, and vegetables. In this review, we briefly describe the results in relevant literature and summarize the uses of essential oils with special emphasis on their antibacterial, bactericidal, antifungal, fungicidal, and food preservative properties. Essential oils have pronounced antimicrobial and food preservative properties because they consist of a variety of active constituents (e.g., terpenes, terpenoids, carotenoids, coumarins, curcumins) that have great significance in the food industry. Thus, the various properties of essential oils offer the possibility of using natural, safe, eco-friendly, cost-effective, renewable, and easily biodegradable antimicrobials for food commodity preservation in the near future.

Keywords: essential oils, antibacterial, antifungal, food preservative properties, bioactivity

OPEN ACCESS

Edited by:
Bhim Pratap Singh, Mizoram University, India

Reviewed by:
Jayanta Kumar Patra, Dongguk University, South Korea
Jay Prakash Verma, Banaras Hindu University, India
Pawan Kumar Maurya, Amity University, India

***Correspondence:**
Pradeep Kumar
pkbiotech@gmail.com
Pooja Singh
pooja.ddu@gmail.com
Vivek K. Bajpai
vbiotech04@gmail.com

Specialty section:
This article was submitted to Microbiotechnology, Ecotoxicology and Bioremediation, a section of the journal Frontiers in Microbiology

Received: *01 September 2016*
Accepted: *22 December 2016*
Published: *16 January 2017*

Citation:
Pandey AK, Kumar P, Singh P, Tripathi NN and Bajpai VK (2017) Essential Oils: Sources of Antimicrobials and Food Preservatives. Front. Microbiol. 7:2161. doi: 10.3389/fmicb.2016.02161

INTRODUCTION

Since ancient times, commercial antimicrobial agents have been applied as a way to manage food deterioration or contamination. Nowadays, user concerns toward synthetic preservatives have resulted in increasing attention on various natural antimicrobials such as essential oils. Aromatic and medicinal plant essential oils and their components demonstrate antibacterial, antifungal, and food preservative activities against a wide range of microbial pathogens (Basim et al., 2000; Iacobellis et al., 2004; Tripathi and Kumar, 2007; Pandey et al., 2014b; Sonker et al., 2015; Gormez et al., 2016; **Figure 1**). These essential oils are hydrophobic liquids of aromatic compounds that are volatile and oily in nature and present in various plant parts such as twig, flower, leaf, bark, seed, and root. Many plant essential oils are useful as a flavor or aroma enhancer in cosmetics, food additives, soaps, plastics resins, and perfumes. Moreover, curiosity about essential oil applications that can act as antimicrobial agents is growing because of the broad range of activities, natural origins, and generally recognized as safe (GRAS) status of essential oils. Currently, essential oils are frequently studied for their antimicrobial (Cowan, 1999; Burt, 2004; Nedorostova et al., 2009), antifungal (Singh and Tripathi, 1999), antiulcer (Dordevic et al., 2007), antihelminthic

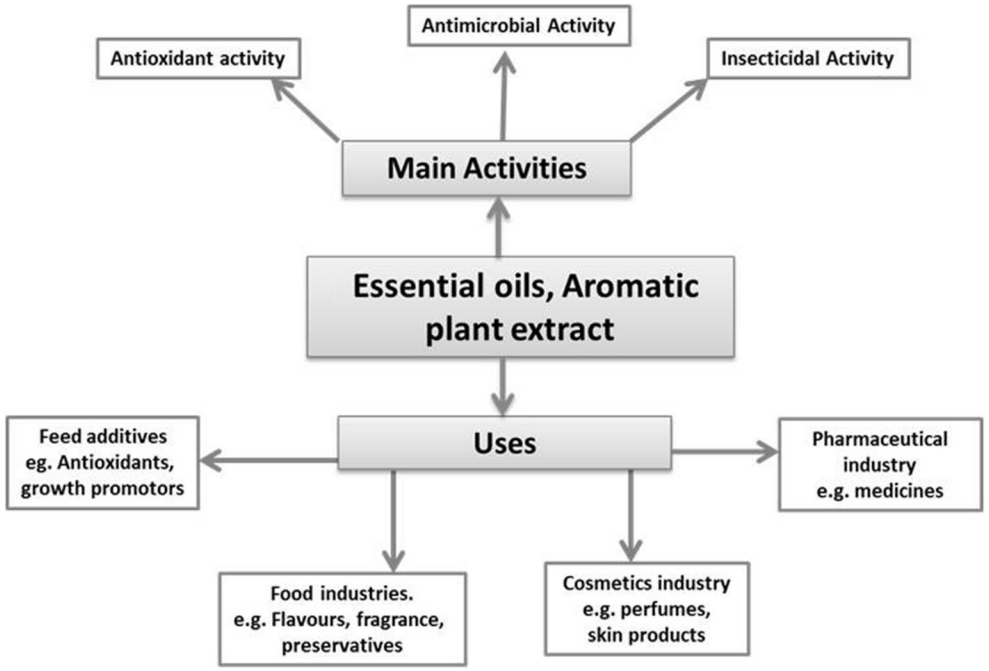


FIGURE 1 | Different activities and uses of essential oils.

(Inouye et al., 2001), antioxidant (Mimica-Dukic et al., 2003), anti-inflammatory (Singh et al., 1996), repellent, insecticidal, antifeedant (Isman et al., 1990; Pandey et al., 2014a), cytotoxic (Sylvestre et al., 2007), antiviral (Maurya et al., 2005), ovicidal (Pandey et al., 2011b), anesthetic (Ghelardini et al., 2001), molluscicidal (Fico et al., 2004), immunomodulatory (Mediratta et al., 2002), antinociceptive (Abdollahi et al., 2003), and larvicidal (Jantan et al., 2003) properties as well as for their use as food preservatives (Ukeh and Mordue, 2009; Pandey et al., 2014c).

Essential oils of aromatic and medicinal plants are reported to be effective against agents affecting stored products such as insects, human pathogenic fungi, and bacteria. Essential oils of *Chenopodium ambrosioides*, *Clausena pentaphylla*, *Mentha arvensis*, and *Ocimum sanctum* are contact-sensitive and act as fumigant toxicants against *Callosobruchus chinensis* and *C. maculatus* (Pandey et al., 2011a) associated with pigeon pea seeds. Similarly, the essential oil of *Tanacetum nubigenum* exhibit significant repellent and fumigant toxicity against *Tribolium castaneum*, which affects wheat during storage (Haider et al., 2015). *Eucalyptus globulus* essential oil has antibacterial activity against *Escherichia coli* and *Staphylococcus aureus,* thus, it is effective against both Gram-positive and Gram-negative bacteria (Bachir and Benali, 2012). In addition, other bacterial pathogens such as *Haemophilus influenzae, S. aureus, S. pneumonia*, and *S. pyogenes* were inhibited by *Eucalyptus odorata* essential oil under *in vitro* conditions (Posadzki et al., 2012). This review highlights the use of essential oils and their antifungal, fungicidal and food preservative properties in controlling fungi associated with food commodities. Additional emphasis has been given on the efficacy of essential oils against plant pathogenic bacteria as antibacterial and bactericidal.

ESSENTIAL OILS AND FUNCTIONS OF THEIR ACTIVE CONSTITUENTS

The majority of aromatic plants retain a volatile odoriferous mixture of compounds which can be extracted as an essential oil. Generally, aromatic and medicinal plants produce a wide range of secondary metabolites *viz*., terpenoids, alcoholic compounds (e.g., geraniol, menthol, linalool), acidic compounds (e.g., benzoic, cinnamic, myristic acids), aldehydes (e.g., citral, benzaldehyde, cinnamaldehyde, carvone camphor), ketonic bodies (e.g., thymol, eugenol), and phenols (e.g., ascaridole, anethole). Among those, terpenes (e.g., pinene, myrcene, limonene, terpinene, *p*-cymene), terpenoids (e.g., oxygen-containing hydrocarbons), and aromatic phenols (e.g., carvacrol, thymol, safrole, eugenol) are found to have major roles in the composition of various essential oils (**Figure 2**) (Koul et al., 2008). Derivatives of terpenoids and aromatic polyterpenoids are synthesized by the mevalonic acid and shikimic acid pathways, respectively (Bedi et al., 2008). Terpenoids are among an immense pool of secondary compounds produced by aromatic and medicinal plants, and they have an important role in providing resistance to pathogens. Monoterpenoids are antimicrobial in nature, result in disruptive multiplication and development of microorganisms, and interfere in physiological and biochemical processes of

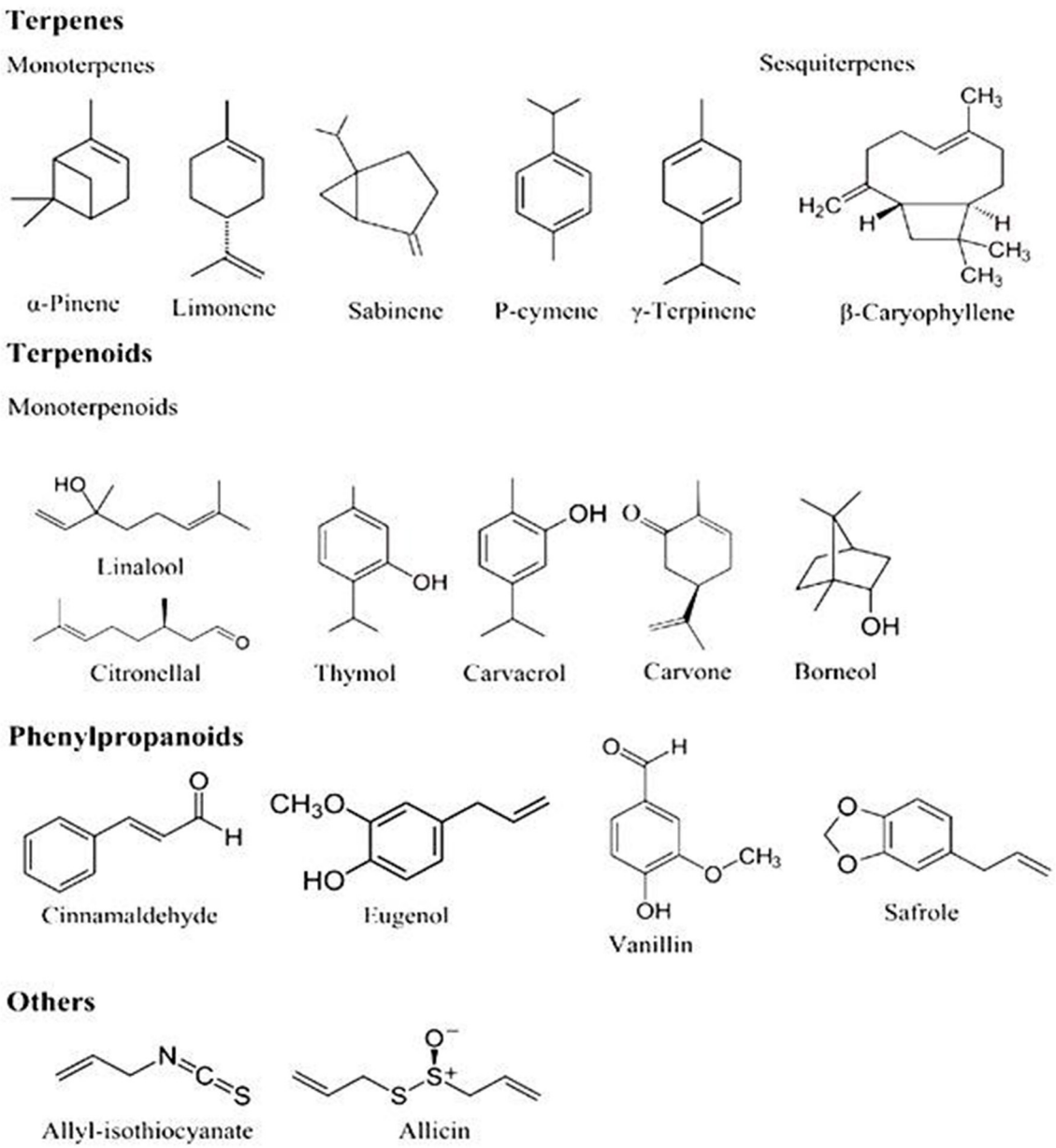


FIGURE 2 | Actives compounds of essential oils. Figure as originally published in Hyldgaard et al. (2012).

microorganisms (Burt, 2004). Some botanical constituents such as azadirachtin, carvone, menthol, ascaridol, methyl eugenol, toosendanin, and volkensin have reported potential to act against several bacterial and fungal pathogens as well as against insect pests (Isman, 2006; Pandey et al., 2012, 2016). Moreover, many of them have powerful bactericidal, fungicidal, and insecticidal activities and can be responsible for improved taste or toxic properties.

Fungi such as *Aspergillus flavus, Neurospora sitophila*, and *Penicillium digitatum* are completely inhibited by *Cymbopogon citratus* essential oil (Shukla, 2009; Sonker et al., 2015). Essential oils from *Nigella sativa*, *Cymbopogon citratus*, and *Pulicaria undulata* inhibit the growth of *Bacillus subtilis, Staphylococcus aureus, Pseudomonas aeruginosa* and *Escherichia coli* (El-Kamali et al., 1998). Essential oils from *Acorus, Artemisia, Chenopodium, Clausena, Curcuma, Cinnamon, Cymbopogon, Eupatorium, Foeniculum, Hyptis, Lippia, Ocimum, Putranjiva, Syzygium,* and *Vitex* are known for their pronounced antimicrobial properties (Pandey et al., 2012, 2013b, 2014c; Sonker et al., 2015). The antibacterial properties of essential oils and their several active natural compounds against foodborne bacteria and their applications in food (Burt, 2004) could provide alternatives to conventional bactericides and fungicides (Perricone et al., 2015).

POTENCY OF ESSENTIAL OILS AGAINST PHYTOPATHOGENIC BACTERIA

In cereals, pulses, fruits, and vegetables, bacterial species can cause major loss of plant quality and quantity during cultivation, transit, and storage by 20–40% of the total harvest per year. The bacterial species responsible for many diseases and loss of crops include *Clavibacter michiganensis, Pseudomonas syringae* pv. *tomato*, *P. solanacearum, P. cichorii, P. syringae* pv. *syringae*, *P. putida, Erwinia carotovora, E. amylovora, E. carotovora* subsp. *atroceptica, E. chrysanthemi, E. herbicola*, *Xanthomonas citri, X. campestris, X. axanopodis* pv. *malvacearum, X. axanopodis* pv. *vesicatoria*, *X. axanopodis* pv. *campestris*, *X. campestris* pv. *raphani, X. axanopodis* pv. *vitians,* and *X. campestris* pv. *zinnia*. Such bacteria cause substantial losses in many crops of national and international significance (Agrios, 2005). There are many essential oils that have been evaluated for their potential for antibacterial activity against these phytopathogenic bacteria under *in vitro* and *in vivo* conditions (Dorman and Deans, 2000; Iscan et al., 2003; Kotan et al., 2013). The methods used to assess the actions of essential oils against phytopathogenic bacteria include disc diffusion, agar dilution, agar well, and broth dilution (Perricone et al., 2015). Antimicrobial studies of essential oil constituents and their mode of actions more have been extensively undertaken on bacteria; however, there is limited information available about their actions on yeasts and molds.

Generally, Gram-negative bacteria are less susceptible to essential oils than Gram-positive bacteria. The outer membrane of Gram-negative bacteria contains hydrophilic lipopolysaccharides (LPS) that acts as a barrier to macromolecules and hydrophobic compounds, thus providing increased tolerance to hydrophobic antimicrobial compounds such as those found in essential oils (Nikaido, 1994, 2003; Trombetta et al., 2005). Therefore, it is difficult to predict the susceptibility of microorganisms to essential oils due to the breadth of genetic variations among species. Antibacterial activities of essential oils against a variety of phytopathogenic bacteria are summarized in **Table 1**.

POTENCY OF ESSENTIAL OILS AGAINST STORAGE FUNGI

Fungi can act as major destroyers of food commodities, including cereals, pulses, fruits, and vegetables, through the production of mycotoxins and render food unhealthy for human consumption by adversely affecting their nutritional value (Paranagama et al., 2003; Pandey et al., 2016). During storage, spoilage of stored food commodities is a chronic problem in tropical hot and humid climates. According to the FAO, foodborne fungal pathogens and their toxic metabolites can produce qualitative and quantitative losses of up to 25% of total agricultural food commodities throughout the world (Agrios, 2005). Fungal infection in food commodities results in a reduction of food quality, color, and texture as well as a reduction in nutrients present and physiological properties of food commodities (Dhingra et al., 2001). During infection, fungi can also produce mycotoxins, which can lead to famines in developing countries (Wagacha and Muthomi, 2008). With regard to molds, food contamination by *Alternaria, Aspergillus, Penicillium, Fusarium,* and *Rhizopus* spp. is of great significance because of the related health hazards and foodborne infections (Pandey and Tripathi, 2011). Hence, during storage and transit, prevention of fungal growth by essential oils could be a cost-effective approach to combat food losses. In recent years, throughout the world, the antifungal potential of essential oils is being considered significantly important (Baruah et al., 1996; Arras and Usai, 2001; Lalitha and Raveesha, 2006; Bosquez-Molina et al., 2010). The antifungal activities of essential oils are related to the associated disintegration of fungal hyphae due to the mono- and sesquiterpene compounds present in the essential oils. Moreover, essential oils amplify membrane permeability; as such compounds can dissolve in cell membranes and cause membrane swelling, thereby reducing membrane function (Dorman and Deans, 2000). Additionally, the lipophilic property of essential oils is responsible for their antifungal activity as that property gives them the ability to penetrate cell walls and affect enzymes involved in cell-wall synthesis, thus altering the morphological characteristics of the fungi (Cox et al., 2000). The present account summarizes the investigations into essential oils tested for their antifungal activity against fungi affecting food storage (**Table 2**).

POTENCY OF ESSENTIAL OILS IN FOOD PRESERVATION

Research into the utility of essential oils in the preservation of food commodities in order to enhance shelf-life has been successfully carried out in recent years. Various investigators have used essential oils, either in pure or formulation forms, to enhance the shelf-life of food commodities in different storage containers such as those made of cardboard, tin, glass, polyethylene, or natural fabrics and have observed significant enhancement of shelf-life (Tripathi and Kumar, 2007; Pandey et al., 2014a). An earlier study reported that some essential oil constituents such as citral, citronella, citronellol, eugenol, farnesol, and nerol could protect chili seeds and fruits from fungal infection for up to 6 months (Tripathi et al., 1984). Essential oil from *Ageratum conyzoides* successfully controlled rotting of mandarins by blue mold and increased mandarin shelf-life by up to 30 days (Dixit et al., 1995). Anthony et al. (2003) investigated essential oils from *Cymbopogon nardus, C. flexuosus,* and *Ocimum basilicum* and observed that they could significantly control anthracnose in banana and increased banana shelf-life by up to 21 days. *Cymbopogon flexuosus* essential oil (20 μL/mL) is capable of protecting against rotting of *Malus pumilo* fruits for up to 3 weeks (Shahi et al., 2003). An fumigant application of essential oils from *Putranjiva roxburghii* was effective against *A. flavus* and *A. niger* infecting groundnuts during storage and enhanced the shelf-life of groundnut from fungal biodeterioration for up to 6 months (Tripathi and Kumar, 2007). The use of *Cymbopogon pendulous* essential oil as a fumigant increased groundnut shelf-life by 6–12 months (Shukla, 2009), thus proving to be more effective than *P. roxburghii*

TABLE 1 | Antibacterial investigations of essential oils against phytopathogenic bacteria.

Plant species (essential oil) tested	Plant pathogenic bacteria	Remarks	Investigators
1	2	3	4
Curcuma longa	*Erwinia carotovora, Pseudomonas solanacearum, Xanthomons citri, Xa. malvacearum*	Oil exhibited efficacy to all bacteria at 1:10 dilution than 1:1000 dilution.	Banerjee and Nigam, 1978
Carum copticum	5 Bacteria	Oils exhibited variable degree of efficacy to test bacteria. Dethymolysed oil of *Carum copticum* was found to be most potent bacteriotoxicant.	Pandey et al., 1981
Origanum vulgare, *Satureja hortensis*, *Thymus vulgaris*	*Erwinia amylovora*	The test bacterium was found to be susceptible toward all the tested oils.	Scortichini and Rossi, 1989
Ocimum basilicum	*Pseudomonas putida*	Resistant to the bacteria.	Lachowicz et al., 1998
Artemisia afra, Pteronia incana, Rosmarinus officinalis	*Erwinia carotovora, Erw. chrysanthemi*	All three oils showed variable range of zone of inhibition.	Mangena and Muyima, 1999
Thymbra spicata	6 Bacteria	The oil showed variable MIC and MBC values against all test bacteria in contact and volatile phase.	Basim et al., 2000
Thymus vulgaris, Pelarogonium graveolens	*Erwinia carotovora*	*Thymus vulgaris* showed highest zone of inhibition, while *Pelarogonium graveolens* showed no inhibition against test bacteria.	Dorman and Deans, 2000
Cinnamomum zeylanicum, Cymbopogon citratus	*Erwinia amylovora, Erw. herbicola*	*Cinnamomum zeylanicum* showed highest toxicity against both bacteria, while *Cymbopogon citratus* was found to be least toxic.	Vanneste and Boyd, 2002
Rosa damascena	*Xanthomonas vesicatoria* XV(88.5, 56, 97.2)	Remarkably inhibited tested strains of *Xa. vesicatoria.*	Basim and Basim, 2003
Satureja hortensis	*Clavibacter michiganensis, Pseudomonas syringae* pv. *tomato, Xa. campestris* subsp. *campestris*	Oil was effective against all three tested organisms.	Gulluce et al., 2003
Heracleum sphondylium sub sp. *ternatum*	5 Bacteria	The MIC of oil was least against 3 bacteria (*Xa. compestris* pv. *phaseoli, Xa. compestris, Ps. syringae* pv. *syringae*) while higher against *Ps*. pv. *phasiolicola* and *Ps. syringae* pv. *tomato*).	Iscan et al., 2003
Thymol oil, Palmerosa oil, Lemongrass oil, Tea tree oil	*Ralstonia solanacearum*	In all the oil tested, 3 oils remarkably inhibited the growth of the test bacteria except Tea tree oil.	Pradhanang et al., 2003
Rosa damascene, Thymbra spicata	*Erwinia amylovora*	*R. damascene* oil was least effective with MBC value 1386.5 μg/m than *T. spicata* oil (500μg/m).	Basim and Basim, 2004
Coriandrum sativum, Foeniculum vulgare	27 Bacteria	A significant antibacterial activity was observed by agar diffusion method with *C. sativum* oil whereas a much reduced effect was observed for *F. vulgare* oil.	Cantore et al., 2004
Coriandrum sativum, Foeniculum vulgare, Cuminum cyminum, Carum carvi	29 Bacteria	A significant antibacterial activity was observed against Gram+ and Gram –ve bacteria. A much reduced effect was observed for the wild fennel.	Iacobellis et al., 2004
Cuminum cyminum, Carum carvi	31 Bacteria	The activity was particularly high against the genera *Clavibacter*, *Curtobacterium, Rhodococcus, Erwinia*, *Xanthomonas, Ralstonia* and *Agrobacterium* while lower activity was observed against *Pseudomonas* sp.	Iacobellis et al., 2005
Thymol, Palmarosa oil	*Ralstonia solanacearum*	Both Thymol and Palmarosa oil during soil treatment reduced bacterial wilt significantly.	Ji et al., 2005
Artemisia absinthium, A. dracunculus, A. santonicum, A. spicigera	16 Bacteria	Among all the 4 oils, *A. santonicum* and *A. spicigera* oils showed antibacterial activities over a very wide spectrum, ineffective against *Ps. syringae* pv. *populans.*	Kordali et al., 2005
Ocimum gratissimum, Thymus vulgaris, Cymbopogon citratus, Zingiber officinale, *Monodora myristica*	5 Bacteria	The essential oils from *Ocimum gratissimum* and *Thymus vulgaris* were highly effective against all bacteria tested, *Cymbopogon citratus* and *Zingiber officinale* were moderate effective while *Monodora myristica* was least effective.	Nguefack et al., 2005

(Continued)

TABLE 1 | Continued

Plant species (essential oil) tested	Plant pathogenic bacteria	Remarks	Investigators
1	2	3	4
Artemisia turanica	*Agrobacterium tumifacience*	The oil did not exhibit any antibacterial effect on test strains.	Behravan et al., 2006
Thymbra spicata, Thymus kotschyanus, Origanum onites, Satureja hortensis	*Clavibacter michiganensis* sub. sp. *michiganensis, Pseudomonas syringae* pv. *tomato, Xanthomonas campestris* pv. *malvacearum*	All the essential oils exhibited antibacterial activity against all pathogens except *Xa. campestris* pv. *malvacearum*. Gram+ve bacteria were more sensitive than Gram -ve bacteria.	Kizil and Uyar, 2006
Ziziphora persica	5 Bacteria	The oil showed variable range of zone of inhibition against *Ps. syringae* and *Erw. caratovora* while ineffective against other three bacteria.	Ozturk and Ercisli, 2006
Origanum vulgare, Carum carvi	6 Bacteria	*Origanum vulgare* exhibited highest effectiveness against all tested bacteria, *Xa. vesicatoria* 67 was the most sensitive to the essential oil extracted from *Carum carvi.*	Vasinauskiene et al., 2006
Rosa brunonii	*Xanthomonas campestris*	20% dilution of essential oil was found to be most effective.	Jangwan et al., 2007
24 Plants	*Xanthomonas axonopodis* pv. *vesicatoria*	Of 24 plant samples, 7 essential oils were highly active showing inhibition zone in range of 22–46.3mm and MIC of 25–200μl/ml in range.	Kotan et al., 2007
Russowia sogdiana	*Erwinia carotovora* var. *carotovora, Pseudomonas lachrymans, Xanthomonas vesicatoria, Agrobacterium tumifacience*	The oil exhibited a broad spectrum of antibacterial activity against all test bacteria with MIC values ranging from 0.2 mg/ml to 0.8 mg/ml.	Tan et al., 2007
Satureja thymbra	*Pseudomonas putida*	The treatment resulted in log reduction at the level below the detection limit formed for either 60 or 18 min.	Chorianopoulos et al., 2008
Mentha arvensis, *Citrus limonum*, *Tagetes bipinata*, *Lavandula latifolia*	*Clavibacter michiganensis* sub. sp. *sepedonicus* (cms), *C. michiganensis* sub. sp. *insidiosus* (cmi)	*Mentha arvensis* and *Citrus limonum* were effective against cms and *Tagetes bipinata* and *Lavandula latifolia* were effective against cmi.	Pouvova et al., 2008
13 Plants	*Agrobacterium tumefaciens, Erwinia carotovora* var. *carotovora*	All the oils exhibited variable degree of toxicity toward both bacteria.	Saad et al., 2008
Teucrium montanum	5 Bacteria	Oil exhibited toxicity. The diameters of zone of inhibition ranged from (10–18 mm) with the highest zone of inhibition were observed against *Azotobacter chlorococcum. Agrobacterium tumifaciens* and *Erwinia carotovora* showed higher level of resistant.	Vukovic et al., 2008
Satureja hortensis	*Erwinia amylovora*	The MIC and MBC of oil against *Erw. amylovora* were found to be 0.025 and 0.05 μl/ml respectively.	Mihajilov-Krstev et al., 2009
Metasequoia glyptostroboides	*Xanthomonas campestris* pv. *campestris* KC94-17, *Xa. campestris* pv. *vesicatoria* YK93-4, *Xa. oryzae* pv. *oryzae* KX019, *Xanthomonas* sp. SK12	The minimum inhibitory concentration (MIC) and minimum bactericidal concentration (MBC) values of oil and the extract were ranged from 125 to 250 μl/ml and 125–500 μg/ml and 250–1000 μl/ml and 250–2000 μg/ml respectively.	Bajpai et al., 2010a
Cleistocalyx operculatus	*Xanthomonas campestris* pv. *campestris* KC94-17, *Xa. campestris* pv. *vesicatoria* YK93-4, *Xa. oryzae* pv. *oryzae* KX019, *Xanthomonas* sp. SK12	The MIC and MBC values of the oil and extract against the tested *Xanthomonas* spp. ranged from 31.25 to 125 μl/ml and 62.5 to 250 μg/ml respectively.	Bajpai et al., 2010b
Satureja hortensis, Thymus vulgaris	*Erwinia amylovora*	20 μl dose of both oil exhibited 25mm zone of inhibition.	Karami-Osboo et al., 2010
Origanum sp., *Thymus* sp., *Mellisa* sp., *Mentha* sp. and *Nepeta* sp	*Erwinia amylovora, Pseudomonas syringae* pv. *syringae*	1 μl dose of all the oils exhibited maximum efficacy and *Origanum* sp. oil was found to be more potent.	Kokoskova et al., 2011
Chenopodium ambrosioides	*Erwinia herbicola, P. putida*	The MIC and MBC of the oil were 0.25 and 2.0 μl/ml for *Erw. herbicola,* and 0.12 and 1.0 μl/ml for *Ps. putida,* respectively.	Pandey et al., 2012

(Continued)

TABLE 1 | Continued

Plant species (essential oil) tested	Plant pathogenic bacteria	Remarks	Investigators
1	2	3	4
Satureja hortensis	*Clavibacter michiganensis* ssp. *michiganensis, Erwinia amylovora, Erw. carotovora* subsp. *atroceptica, Erw. chrysanthemi, Pseudomonas cichorii, Ps. syringae* pv. *syringae*, *Ps. syringae* pv. *tomato, Xanthomonas axanopodis* pv. *malvacearum, Xa. axanopodis* pv. *vesicatoria, Xa. axanopodis* pv. *campestris, Xa. campestris* pv. *raphani, Xa. axanopodis* pv. *vitians, Xa. campestris* pv. *zinnia, Xa. axanopodis* pv. *pelargonii*	12.5 μl dose of essential oil gave maximum zone of inhibition against *Xanthomonas axanopodis* pv. *vitians* (50 mm) followed by *Xanthomonas axanopodis* pv. *campestris* (45 mm), *Xanthomonas axanopodis* pv. *pelargonii, Xanthomonas axanopodis* pv. *malvacearum* (42 mm), *Erwinia carotovora* subsp. *atroceptica* (41mm) while zone of inhibition was <40 mm for other bacterial species.	Kotan et al., 2013
Eupatorium adenophorum	*Erw. herbicola Ps. putida*	The MIC and MBC values were ranges of 0.25–4.0 μl/ml for the both bacterial species.	Pandey et al., 2014b
Nepeta hindostana	*Erw. herbicola Ps. putida*	The MIC and MBC values were 2 and 8 μl/ml for *Erw. herbicola* and 4 and >16 for *Ps. putida.*	Pandey et al., 2015
Origanum rotundifolium	20 plant pathogenic bacteria	The essential oil exhibits significant antibacterial effect against the test bacteria.	Gormez et al., 2016

essential oil. These differences in efficacy of essential oils may be related to the use of oils from different plant species, as well as to their chemical composition, dose level, and storage container type.

Thyme (*Thymus capitata*) (0.1%) and maxican lime (*Citrus aurantifolia*) (0.5%) oil reduced disease incidence in papaya fruit (Bosquez-Molina et al., 2010), while cinnamon (0.3%) oil extended the storage life of banana by up to 28 days and reduced fungal disease incidence in banana (Maqbool et al., 2010). Seed dressing and fumigation of *Ocimum cannum* oil (1 μL/mL) enhanced the self-life of *Bhuchanania* (Singh et al., 2011). *Clausena pentaphylla* and *Chenopodium ambrosioides* oils, when used as fumigants in glass containers and natural fabric bags were able to protect pigeon pea seeds from *A. flavus, A. niger, A. ochraceus,* and *A. terreus* infection for up to 6 months (Pandey et al., 2013a,b). Powder-based formulations of *C. pentaphylla* and *C. ambrosioides* oils were also able to preserve pigeon pea seeds for up to 6 months (Pandey et al., 2014c). *Artemisia nilagirica* oil as a fumigant in cardboard improved the shelf-life of table grapes by up to 9 days (Sonker et al., 2015). Similarly, *Lippia alba* oil when used as an air dosage treatment in glass containers inhibited fungal proliferation and aflatoxin production in green gram (*Vigna radiata*) and enhanced its shelf-life by up to 6 months (Pandey et al., 2016).

CONCLUSION AND FUTURE PROSPECTS

Worldwide investigations carried out on essential oils have motivated researchers to focus their interest toward the study of botanical antimicrobials. It is apparent that the use of essential oils and their derivatives has been widely described, and essential oils have been used against a wide range of pathogens. Accordingly, this review provides a brief overview of essential oils, their active constituents, and their potential as sources of antibacterials, antifungals, and food preservatives. The relevant literature summary shows that essential oils exhibit a diverse range of antimicrobial properties, and indicates their natural sustainability when used as potential biocontrol agents against fungal and bacterial pathogens. Hence, we conclude from this review that essential oils are potential sources of biocontrol products that should be further explored due to their potential to protect food commodities. Also, an essential oil-based fumigant having antimicrobial activity should have a promising GRAS status in mammalian systems. The LD_{50} values of some botanicals like azadirachtin and carvone are found to be high in rat and are reportedly nontoxic for human consumers. Additionally, several essential oils and their constituents (e.g., carvone, carvacrol, cinnamaldehyde, thymol, linalool, citral, limonene, eugenol, limonene, and menthol) are reported by the United States Food and Drug Administration to have a GRAS status and are approved as flavor or food additives.

Essential oil applications are evolving as a means of integrating pathogens into food containers; for example, fumigants that can be useful in natural fabric and cardboard containers, and even containers made of wooden boards. Some oils can be used as light sprays and integrated as a fumigant into the commodity itself. Many essential oils and their active constituents are active against bacteria and fungi, and they can be produced from commonly available raw materials; perhaps in many cases right at the site of use so as to be rather low-cost treatments. Based on this review, it can be summarized that it is possible to develop techniques for food commodity protection without the use, or with reduced use, of commercial bactericides and fungicides. Although the available literature indicates that essential oils are host specific, biodegradable, have limited effect on non-target organisms, have low levels of mammalian toxicity. There, sustainable and commercial uses have some drawbacks, such as their cost effectiveness. Regardless, there are innumerable

TABLE 2 | Antifungal investigations of essential oils against fungi infecting food commodities during postharvest.

Plant species (essential oil) tested	Postharvest fungi	Remarks	Investigators
1	2	3	4
Raphanus sativus	*Alternaria brassicae*, *Fusarium avenaceum*, *Phoma* spp.	The oil was active at 1:250 to 1:1000000 dilutions.	Nehrash, 1961
Juniperus communis	*Aspergillus niger*	Exhibited toxicity.	Slavenas and Razinskaite, 1962
Eugenia bracteata, E. heyneana	*Cephalosporium sacchri, Curvularia lunata, Fusarium moniliforme*	Both the oils were toxic toward test fungi.	Rao and Joseph, 1971
Cymbopogon citratus, *Mentha arvensis*, Sweet basil	*Penicillium italicum*	*Mentha* oil was most toxic during both *in vitro* and *in vivo* testing.	Arora and Pandey, 1977
Curcuma aromatica, C. caesia, Myristica fragrans	15 Storage fungi	*Myristica fragrans* was most toxic.	Kher and Chaurasia, 1978
Trachyspermum ammi, Oenanthera stalonifera, Anethum graveolens, Apium graveolens, Parthenium histerophorus and *Psoralea corylifolia*	16 Fungal species	The essential oils exhibited significant antimycotic activity.	Sharma and Singh, 1979
Cestrum diurnum	39 Storage fungi	The oil inhibited mycelial growth of all test fungi at 0.7% concentration.	Renu et al., 1980
Ageratum conyzoides	*Colletotricum capsici, Penicillium italicum*	The oil was found to be toxic at its MIC of 0.5% and 0.2% against *C. capsici* and *P. italicum* respectively.	Chandra and Dixit, 1981
Ageratum conyzoides, Cymbopogon martini var. *motia*, *Eupatorium capillifolium, Ocimum adscendens,*	*Helminthosporium oryzae*	The oil of *Ocimum adscendens* was found most effective at 200 μl/l conc.	Asthana et al., 1982
Citrus medica, Ocimum canum	*Aspergillus flavus, A. versicolor*	Oils completely inhibited the mycelial growth of test fungi at 2000 ppm.	Dubey et al., 1983
Alpinia galanga	24 Storage fungi	The oil showed broad antifungal spectrum at 0.4% and 0.6% conc.	Tripathi et al., 1983
Lemon grass, *Mentha* sp., Palmarosa, *Zingiber* sp.	*Aspergillus parasiticus*	*Mentha* oil was most potent control the growth of *A. parasiticus* and aflatoxin production.	Kala et al., 1984
Citrus aurantifolia	20 Storage fungi	Fungitoxic at 2000 ppm.	Upadhyay et al., 1985
Ocimum adscendens	30 Storage fungi	Fungicidal at 400 ppm.	Asthana et al., 1986
Anisomeles ovata	*Aspergillus flavus*	Effective at 2000 ppm.	Upadhyay et al., 1987
Eucalyptus sp.	*Aspergillus niger*	Checked mycelial growth at 1000 ppm.	Tiwari et al., 1988
Thyme, Cumin, Clove, Caraway, Rosemary, Sage	*Aspergillus parasiticus*	All the oils exhibited broad range of fungitoxicity.	Farag et al., 1989
Amomum subulatum	*A. flavus*	Fungitoxic at 3000 ppm.	Mishra and Dubey, 1990
Daucus carota	*A. flavus*	Exhibited antifungal activity at 2000 ppm.	Dwivedi et al., 1991
Cinnamomum camphora	*A. flavus*	Fungitoxic at 400 ppm.	Mishra et al., 1991
Ocimum gratissimum	*A. flavus, A. niger*	MIC of oil was 100 ppm against *A. flavus* and 900 ppm against *A. niger.*	Dixit and Shukla, 1992
Hyptis suaveolens	21 Storage fungi	Exhibited mycelial inhibition at 2000 ppm.	Singh et al., 1992
Mixture of *Apium graveolens* and *Cuminum cyminum*	29 Storage fungi	Mixture showed antifungal activity at the conc. of 1:1 ratio.	Mishra et al., 1993
14 Plant essential oils	47 Storage fungi	*Cymbopogon citratus* oil was found to be fungistatic in nature at 1500ppm concentration against all test fungi.	Mishra and Dubey, 1994
Cinnamomum zeylanicum	35 Storage fungi	Showed strongest activity at 400 ppm.	Tiwari et al., 1994
Nardostachys jatmansi	*A. flavus, A. niger, F. oxysporum*	Completely inhibited mycelial growth of all test fungi at 1.0 × 1000 μl/l.	Mishra et al., 1995
Cymbopogon martini, Eucalyptus citriodora, Cinnamomum tamala, *Mentha piperita*	*F. moniliforme*	Mycotoxic activity of oils increased with increase concentration of oil.	Baruah et al., 1996
Monarda citriodora, Melaleuca alternifolia	15 Post-harvest fungi	Exhibited absolute toxicity.	Bishop and Thornton, 1997
Thymus vulgaris	*Botrytis cinerea, Rhizopus stolonifer*	Absolutely inhibited the mycelial growth of test fungi.	Reddy et al., 1998

(Continued)

TABLE 2 | Continued

Plant species (essential oil) tested	Postharvest fungi	Remarks	Investigators
1	2	3	4
Cedrus deodara, Tracchispermum ammi	*A. niger*, *Curvularia ovoidea*	The MIC of oils was found to be 1000 and 500 ppm respectively.	Singh and Tripathi, 1999
Ocimum gratissimum, Zingiber cassumunar and *Cymbopogon citratus*	*A. flavus*	Oils exhibited antimycotic activity at its MIC ranging from 500 to 1300 ppm.	Dubey et al., 2000
Thymus capitatus	*Alternaria citri, Botrytis cinerea, Penicillium digitatum*, *P. italicum*	Oil was effective against all test fungi at 250 ppm conc.	Arras and Usai, 2001
Caesulia axillaris	*A. flavus, A. niger*	MIC of oil against test fungi was 1000 ppm.	Dubey et al., 2002
Putranjiva roxburghii	15 Storage fungi	The MIC and MFC of the oil were 400 and 600 ppm respectively.	Kumar and Tripathi, 2002
Cinnamon and Clove oil	*C. musae, F. proliferatum, Lasiodiplodia theobromae*	The oils were effective at 500 ppm concentration.	Ranasinghe et al., 2002
Acorus calamus, Hedychium spicatum	*Helminthosporium oryzae, F. moniliforme*	The oil inhibited growth of test fungi at 0.5 $\times$ 10^3ml/l and 1.0 $\times$ 10^3ml/l respectively.	Mishra et al., 2003
Cymbopogon citratus	*A. flavus*	Oil was fungistatic and fungicidal nature at 0.60 and 1.0mg/ml concentration respectively.	Paranagama et al., 2003
Cymbopogon flexuosus	25 Fungi	Oil showed absolute toxicity against all fungi at 0.3 μl/ml conc.	Shahi et al., 2003
Curcuma longa	10 Storage fungi	The oil exhibited 10% toxicity at 3000 ppm.	Singh et al., 2003
Chrysanthemum viscidehirtum	*Botrytis cinerea, Phytophthora citrophthora*	*Chrysanthemum viscidehirtum* exhibited strong activity at 150 ppm.	Chebli et al., 2004
Mentha piperita	*P. digitatum*	*M. piperita* caused 100% inhibition at 1000 μg/ml conc.	Dhaliwal et al., 2004
9 Plant essential oils	*P. expansum*	All oils were found to be effective.	Neri et al., 2005
Thymus vulgaris and *T. copticum*	*Alternaria citri, Penicillium italicum, P. digitatum*	Out of 5 oils, *Thymus vulgaris* and *T. copticum* were absolutely fungitoxic at 500 mg/l conc.	Azizi et al., 2006
15 Plant essential oils	10 Fungi	13 essential oils were found to be effective inhibited mycelial growth of all test fungi at 3.0% (v/v).	Lalitha and Raveesha, 2006
Epicarp of *Citrus sinensis*	10 Post-harvest fungi	Oil exhibited absolute toxicity toward test fungi.	Sharma and Tripathi, 2006
Mentha arvensis	9 Post-harvest fungi	Oil exhibited absolute mycelial inhibition against *Aspergillus flavus, A. fumigatus, Helminthosporium oryzae* and *Sclerotium rolfsii* at 0.10 mg/ml.	Kumar et al., 2007
Satureja hortensis	*A. flavus*	Oil exhibited toxicity.	Dikbas et al., 2008
Lippia scaberrima	*Botryosphaeria parva, C. gloeosporioides*	Oil was found to be effective, absolutely inhibited the mycelial growth of test fungi.	Regnier et al., 2008
Mentha arvensis	*A. flavus*	The MIC of *Mentha* oil against *A. flavus* was recorded at 400μl/l and it exhibited broad fungitoxic activity against other 14 storage fungi.	Kumar et al., 2009
Satureja hortensis, Thymus vulgaris	*Botrytis cinerea*	Oil was found to be toxic and significantly inhibited the growth of test fungi	Abdollahi et al., 2010
Thyme and Mexican lime	*C. gloeosporioides, Rhizopus stolonifer*	0.060% concentration of thyme oil stopped the mycelial growth of both test fungi	Bosquez-Molina et al., 2010
Cinnamon oil	*C. musae*	0.4% concentration of oil suppressed mycelial growth	Maqbool et al., 2010
Mentha arvensis, Ocimum canum	*A. flavus, A. ochraceus, A. niger, A. terreus*	Both the oils exhibited significant growth of all the test fungi at 500 ppm concentration.	Pandey and Tripathi, 2011

(Continued)

TABLE 2 | Continued

Plant species (essential oil) tested	Postharvest fungi	Remarks	Investigators
1	2	3	4
Eucalyptus, Clove, Cinnamon, Nutmeg, Neem, Nirgudi, Karanj, Sesame	*A. flavus, A. niger, A. terreus, A. oryzae, A. fumigatus, Fusarium moniliforme, F. solani* and *Penicillium* sp.	At 50 μl concentration of Eucalyptus, Clove, Cinnamon, Nutmeg oils were more potent against these fungi and among these cinnamon was most potent where zone of inhibition observed was in range of 22.5–67.5 mm.	Shirurkar and Wahegaonkar, 2012
Clausena pentaphylla	*A. flavus, A. ochraceus, A. niger, A. terreus*	Oil exhibited absolute mycelial inhibition at 0.36 μl/ml and MIC and MFC values were 0.07 μl/ml against all the test fungi	Pandey et al., 2013a
Chenopodium ambrosioides	*A. flavus, A. ochraceus, A. niger, A. terreus*	Absolute mycelia inhibition for all the test fungi was found at 0.36 μl/ml	Pandey et al., 2013b
Cymbopogon citratus	*A. flavus, A. niger, A. ochraceus*	A 0.33 μl/ml dose of the oil caused 100% mycelial inhibition and MIC was reported to be 0.29 μl/ml against all the test fungi	Sonker et al., 2014
Artemisia nilagirica	*A. flavus, A. niger, A. ochraceus*	Oil showed absolute mycelial inhibition of all the test fungi at 0.33 μl/ml, and MIC and MFC reported were 0.29 and 0.58 μl/ml, respectively for all *Aspergillus* species.	Sonker et al., 2015
Lippia alba	*A. flavus*	Absolute mycelial inhibition was observed at 0.28 μl/ml. Oil was fungicidal (MIC) at 0.14 μl/ml, and fungistatic at 0.28 μl/ml.	Pandey et al., 2016

potential uses of essential oils and more research is needed to meet the needs of a food industry shifting toward the use of green technology.

AUTHOR CONTRIBUTIONS

AP, PS, and NT conceived and designed the experiments. AP performed the experiments. AP and PK write the manuscript and PK and VB did the editing. All the authors read and approved the final manuscript.

ACKNOWLEDGMENTS

The authors (AP, PS, and NT) would like to thanks the Head, Department of Botany, DDU Gorakhpur University, Gorakhpur for providing the necessary facilities. AP is grateful to CST UP, Lucknow for financial assistance (Grant no. CST/AAS, D-09, April 3, 2007). PK thankful to Director and Head, Department of Forestry, NERIST, Nirjuli, Arunachal Pradesh, India. VB sincerely thankful to Yeungnam University, Republic of Korea.

REFERENCES

Abdollahi, A., Hassani, A., Ghosta, Y., Bernousi, I., and Meshkatalsadat, M. H. (2010). Study on the potential use of essential oils for decay control and quality preservation of Tabarzeh table grapes. *J. Plant Prot. Res.* 50, 45–52. doi: 10.2478/v10045-010-0008-2

Abdollahi, M., Karimpour, H., and Monsef-Esfehani, H. R. (2003). Antinociceptive effects of *Teucrium polium* L. total extract and essential oil in mouse writhing test. *Pharmacol. Res.* 48, 31–35. doi: 10.1016/s1043-6618(03)00059-8

Agrios, G. N. (2005). *Plant Pathology, 5th Edn.* Oxford: Elsevier Academic Press.

Anthony, S., Abeywickrama, K., and Wijeratnam, S. W. (2003). The effect of spraying essential oils *Cymbopogon nardus*, *C. flexuosus* and *Ocimum basilicum* on post-harvest diseases and storage life of Embul banana. *J. Hort. Sci. Biotech.* 78, 780–785. doi: 10.1080/14620316.2003.11511699

Arora, R., and Pandey, G. N. (1977). The application of essential oils and their isolates for blue mould decay control in *Citrus reticulata*. *J. Food Sci. Technol.* 14, 14–16.

Arras, G., and Usai, M. (2001). Fungitoxic activity of 12 essential oils against four post-harvest *Citrus* pathogens, chemical analysis of *Thymus capitatus* oil and its effect in sub-atmospheric pressure conditions. *J. Food Protect.* 64, 1025–1029. doi: 10.4315/0362-028X-64.7.1025

Asthana, A., Chandra, H., Dikshit, A., and Dixit., S. N. (1982). Volatile fungitoxicants from leaves of some higher plants against *Helminthosporium oryzae*. *Z. Pflanzenkr. Pflanzenschutz* 89, 475–479.

Asthana, A., Tripathi, N. N., and Dixit, S. N. (1986). Fungitoxic and phytotoxic studies with essential oil of *Ocimum adscendens*. *J. Phytopathol.* 117, 152–159. doi: 10.1111/j.1439-0434.1986.tb00639.x

Azizi, M., Farzad, S., Jafarpour, B., Rastegar, M. F., and Jahanbakhsh, V. (2006). Inhibitory effect of some medicinal plants essential oils on post-harvest fungal disease of *Citrus* fruits. *Acta. Hortic.* 768, 279–286.

Bachir, R. G., and Benali, M. (2012). Antibacterial activity of the essential oils from the leaves of *Eucalyptus globulus* against *Escherichia coli* and *Staphylococcus aureus*. *Asian Pac. J. Trop. Biomed.* 2, 739–742. doi: 10.1016/S2221-1691(12)60220-2

Bajpai, V. K., Cho, M. J., and Kang, S. C. (2010a). Control of plant pathogenic bacteria of *Xanthomonas* spp. by the essential oil and extract of *Metasequoia* glyptostroboides Miki ex Hu *In vitro* and *In vivo*. *J. Phytopathol.* 158, 479–486. doi: 10.1111/j.1439-0434.2009.01646.x

Bajpai, V. K., Dung, N. T., Suh, H., and Kang., S. C. (2010b). Antibacterial activity of essential oil and extract of Cleistocalyx operculatus buds against the bacteria of *Xanthomonas* spp. *J. Am. Oil. Chem. Soc.* 87, 1341–1349.

Banerjee, A., and Nigam, S. S. (1978). Antimicrobial efficacy of essential oil of *Curcuma longa*. *Ind. J. Med. Res.* 68, 864–866.

Baruah, P., Sharma, R. K., Singh, R. S., and Ghosh, A. C. (1996). Fungicidal activity of some naturally occurring essential oils against *Fusarium moniliforme*. *J. Essent. Oil. Res.* 8, 411–414. doi: 10.1080/10412905.1996.9700649

Basim, E., and Basim, H. (2003). Antibacterial activity of *Rosa damascena* essential oil. *Fitoterapia* 74, 394–396. doi: 10.1016/S0367-326X(03)00044-3

Basim, E., and Basim, H. (2004). Evaluation of antibacterial activity of essential oil of Rosa damascena on *Erwinia amylovora*. *Phytoparasitica* 32, 409–412. doi: 10.1007/BF02979853

Basim, H., Yegen, O., and Zeller, W. (2000). Antibacterial effect of essential oil of *Thymbra spicata* L. var. spicata on some plant pathogenic bacteria. *Zeitschrift fur Pflanzenkr. Pflanzenschutz* 107, 279–284.

Bedi, S., Tanuja, and Vyas, S. P. (2008). *A Hand Book of Aromatic and Essential Oil Plants Cultivation, Chemistry, Processing and Uses.* Jodhpur: AGROBIOS Publishers.

Behravan, J., Ramenzani, M., Hassanzadeh, M. K., Eliaspour, N., and Zahra, S. (2006). Cytotoxic and antimicrobial activities of essential oil of *Artemisia turanica* Krasch from Iran. *J. Essent. Oil Bear. Plants* 9, 196–203. doi: 10.1080/0972060X.2006.10643492

Bishop, C. D., and Thornton, L. B. (1997). Evaluation of antifungal activity of the essential oils of *Monarda citriodora* var. *citriodora* and *Melaleuca alternifolia* on post-harvest pathogens. *J. Essent. Oil Res.* 9, 77–82. doi: 10.1080/10412905.1997.9700718

Bosquez-Molina, E., Jesus, E. R., Bautista-Banos, S., Verde-Calvo, J. R., and Morales-Lopez, J. (2010). Inhibitory effect of essential oils against *Colletotrichum gloeosporioides* and *Rhizopus stolonifer* in stored papaya fruits and their possible application in coatings. *Postharvest Biol. Technol.* 57, 132–137. doi: 10.1016/j.postharvbio.2010.03.008

Burt, S. (2004). Essential oils: their antibacterial properties and potential applications in food – A review. *Int. J. Food Microbiol.* 94, 223–253. doi: 10.1016/j.ijfoodmicro.2004.03.022

Cantore, P. L., Iacobellis, N. S., Marco, A. D., Capasso, F., and Senatore, F. (2004). Antibacterial activity of *Coriandrum sativum* L. and *Foeniculum vulgare var. vulgare* (Miller) essential oils. *J. Agric. Food Chem.* 52, 7862–7866. doi: 10.1021/jf0493122

Chandra, H., and Dixit, A. (1981). Volatile fungitoxicant from the leaves of *Ageratum conyzoides* against *Colletotrichum capsici* and *Penicillium italicum*. *J. Ind. Bot. Soc.* 60(Suppl.):13.

Chebli, B., Hmamouchi, M., Achouri, M., and Hassani, L. M. I. (2004). Composition and *in-vitro* fungitoxic activity of 19 essential oils against two post-harvest pathogens. *J. Essent. Oil. Res.* 16, 507–511. doi: 10.1080/10412905.2004.9698783

Chorianopoulos, N. G., Giaouris, E. D., Skandamis, P. N., Haroutounian, S. A., and Nychas, G. J. E. (2008). Disinfectant test against monoculture and mixed-culture biofilm composed of technological, spoilage and pathogenic bacteria: bactericidal effect of essential oil and hydrosol of *Satureja thymbra* and comparison with acid-base sanitizers. *J. Appl. Microbiol.* 104, 1586–1596. doi: 10.1111/j.1365-2672.2007.03694.x

Cowan, M. M. (1999). Plant products as antimicrobial agents. *Clin. Microbiol. Rev.* 12, 564–582.

Cox, S. D., Mann, C. M. I., Markham, J. L., Bell, H. C., Gustafson, J. E., Warmington, J. R., et al. (2000). The mode of antimicrobial action of the essential oil of *Melaleuca alternifolia* (tea tree oil). *J. Appl. Microbiol.* 88, 170–175. doi: 10.1046/j.1365-2672.2000.00943.x

Dhaliwal, H. J. S., Thind, T. S., and Mohan, C. (2004). Relative activity of essential oils from plants against *Penicillium digitatum* causing post-harvest fruit rot of kinnow mandarin. *Plant Dis. Res.* 19, 140–143.

Dhingra, O. D., Mizubuti, E. S. G., Napoleao, I. T., and Jham, G. (2001). Free fatty acid accumulation and quality loss of stored soybean seeds invaded by *Aspergillus ruber*. *Seed Sci. Technol.* 29, 193–203.

Dikbas, N., Kotan, R., Dadasoglu, F., and Sahin, F. (2008). Control of *Aspergillus flavus* with essential oil and methanol extract of *Satureja hortensis*. *Int. J. Food Microbiol.* 124, 179–182. doi: 10.1016/j.ijfoodmicro.2008.03.034

Dixit, S. N., Chandra, H., Tiwari, R., and Dixit, V. (1995). Development of botanical fungicide against blue mould of mandarins. *J. Stored Prod. Res.* 31, 165–172. doi: 10.1016/0022-474X(94)00041-Q

Dixit, V., and Shukla, K. (1992). Evaluation of essential oil of *Ocimum gratissimum* against storage fungi. *Ind. Perf.* 36, 277–283.

Dordevic, S., Petrovic, S., Dobric, S., Milenkovic, M., Vucicevic, D., Zizic, S., et al. (2007). Antimicrobial, anti-inflammatory, anti-ulcer and antioxidant activities of *Carlina acanthifolia* root essential oil. *J. Ethnopharmacol.* 109, 458–463. doi: 10.1016/j.jep.2006.08.021

Dorman, H. J. D., and Deans, S. G. (2000). Antibacterial agents from plants: antibacterial activity of plant volatile oils. *J. Appl. Microbiol.* 88, 308–316. doi: 10.1046/j.1365-2672.2000.00969.x

Dubey, A. K., Kumar, N., and Tripathi, N. N. (2002). *Caesulia axillaris*-Volatile herbal fungitoxicants. *J. Basic. Appl. Mycol.* 1, 68–73.

Dubey, N. K., Bhargava, K. S., and Dixit, S. N. (1983). Protection of some stored food commodities from fungi by essential oils of *Ocimum canum* and *Citrus* medica. *Int. J. Trop. Plant Dis.* 1, 177–179.

Dubey, N. K., Tripathi, P., and Singh, H. B. (2000). Prospects of some essential oils as antifungal agents. *J. Med. Aroma. Plant. Sci.* 22, 354.

Dwivedi, S. K., Pandey, V. N., and Dubey, N. K. (1991). Effect of essential oils of some higher plants on *Aspergillus flavus*, infesting stored seeds of gaur (*Cyamopsis tetragonoloba* L.). *Flavour Frag. J.* 6, 295–297. doi: 10.1002/ffj.2730060410

El-Kamali, H. H., Ahmed, A. H., Mohammed, A. S., Yahia, A. A. M., El-Tayeb, I. H., and Ali, A. A. (1998). Antibacterial properties of essential oils from *Nigella sativa* seeds, *Cymbopogon citratus* leaves and *Pulicaria undulata* aerial parts. *Fitoterapia.* 69, 7–12.

Farag, R. S., Daw, Z. Y., and Abo-Raya, S. H. (1989). Influence of some spice essential oils on *Aspergillus parasiticus* growth and production of aflatoxin in a synthetic medium. *J. Food Sci.* 54, 74–76. doi: 10.1111/j.1365-2621.1989.tb08571.x

Fico, G., Panizzi, L., Flamini, G., Braca, A., Morelli, I., Tome, F., et al. (2004). Biological screening of *Nigella elamascena* for antimicrobial and molluscicidal activities. *Phytother. Res.* 18, 468–470. doi: 10.1002/ptr.1454

Ghelardini, C., Galeotti, N., and Mazzanti, G. (2001). Local anesthetic activity of monoterpenes and phenylpropanes of essential oils. *Planta Med.* 67, 564–566. doi: 10.1055/s-2001-16475

Gormez, A., Bozari, S., Yanmis, D., Gulluce, M., Agar, G., and Sahin, F. (2016). The use of essential oils of *Origanum rotundifolium* as antimicrobial agent against plant pathogenic bacteria. *J. Essent. Oil Bear. Plants* 19, 656–663. doi: 10.1080/0972060X.2014.935052

Gulluce, M., Sokmen, M., Daferera, D., Agar, G., Ozakan, H., Kartal, N., et al. (2003). *In-vitro* antibacterial, antifungal and antioxidant activities of the essential oil and methanol extract of herbal parts and callus culture of *Satureja hortensis* L. *J. Agric. Food. Chem.* 51, 3958–3965. doi: 10.1021/jf0340308

Haider, S. Z., Mohan, M., Pandey, A. K., and Singh, P. (2015). Repellent and fumigant activities of *Tanacetum nubigenum* Wallich. Ex DC essential oils against *Tribolium castaneum (Herbst) (Coleoptera: Tenebrionidae). J. Oleo Sci.* 64, 895–903. doi: 10.5650/jos.ess15094

Hyldgaard, M., Mygind, T., and Meyer, R. L. (2012). Essentials oils in food preservation: mode of action, synergies and interactions with food matrix components. *Front. Microbiol.* 3:12. doi: 10.3389/fmicb.2012.00012

Iacobellis, N. S., Cantore, P. L., Caepasso, F., and Senatore, F. (2005). Antibacterial activity of *Cuminum cyminum* L. and *Carum carvi* L. essential oils. *J. Agric. Food. Chem.* 53, 57–61. doi: 10.1021/jf0487351

Iacobellis, N. S., Cantore, P. L., Marco, A. D., Caepasso, F., and Senatore, F. (2004). Antibacterial activity of some essential oils. Management of plant diseases and arthropod pests by BCAs IOBC/wprs. *Bulletin* 27, 223–226.

Inouye, S., Takizawa, T., and Yamaguchi, H. (2001). Antibacterial activity of essential oils and their major constituents against respiratory tract pathogens by gaseous contact. *J. Antimicrob. Chemother.* 47, 565–573. doi: 10.1093/jac/47.5.565

Iscan, G., Demirci, F., Kurkcuoglu, M., Kivanc, M., and Baser, K. H. C. (2003). The bioactive essential oil of *Heracleum sphondylium* L. subsp. ternatum *(Velen.) Brummitt. Z. Naturforsch.* 58, 195–200.

Isman, M. B. (2006). Botanical insecticides, deterrents and repellents in modern agriculture and an increasingly regulated world. *Annu. Rev. Entomol.* 51, 45–66. doi: 10.1146/annurev.ento.51.110104.151146

Isman, M. B., Koul, O., and Luezynski, N. (1990). Insecticidal and antifeedant bioactivity of neem oil and their relationship to azadirachtin content. *J. Agric. Food Chem.* 38, 1406–1411. doi: 10.1021/jf00096a024

Jangwan, J. S., Painuly, A. M., Joshi, V. P., and Chamoli, R. P. (2007). Chemical composition and antimicrobial activity of essential oil of *Rosa brunonii* L. *Ind. Perf.* 51, 53–55.

Jantan, I., Ping, W. O., Visuvalingam, S. D., and Ahmad., N. W. (2003). Larvicidal activity of the essential oils and methanolic extracts of Malaysian plants on *Aedes aegypti*. *Pharma. Biol.* 41, 234–236. doi: 10.1076/phbi.41.4.234.15665

Ji, P., Momol, M. T., Olson, S. M., Pradhanang, P. M., and Jones, J. B. (2005). Evaluation of Thymol as biofumigant for control of bacterial wilt of tomato under field conditions. *Plant Dis.* 89, 497–500. doi: 10.1094/PD-89-0497

Kala, P. K., Tripathi, R. K., Gupta, K. C., and Singh, A. K. (1984). Effect of some essential oils on growth and aflatoxin production by *Aspergillus parasiticus* in stored grains. *Pesticides* 18, 43–46.

Karami-Osboo, R., Khodaverdi, M., and Ali-Akbari, F. (2010). Antibacterial effect of effective compounds of *Satureja hortensis* and *Thymus vulgaris* essential oils against *Erwinia amylovora*. *J. Agr. Sci. Technol.* 12, 35–45

Kher, A., and Chaurasia, S. C. (1978). Antifungal activity of essential oils of three medicinal plants. *Ind. Drugs* 14, 41–42.

Kizil, S., and Uyar, F. (2006). Antimicrobial activities of some Thymes *Thymus, Satureja, Origanum* and *Thymbra* species against important plant pathogens. *Asian J. Chem.* 18, 1455–1461.

Kokoskova, B., Pouvova, D., and Pavela, R. (2011). Effectiveness of plant essential oils against *Erwinia amylovora*, *Pseudomonas syringae* pv. *syringae* and associated saprophytic bacteria on/in host plants. *J. Plant Pathol.* 93, 133–139.

Kordali, S., Kotan, R., Mavi, A., Cakir, A., Ala, A., and Yildirim, A. (2005). Determination of the chemical composition and antioxidant activity of the essential oil of *Artemisia dracunculus* and of the antifungal and antibacterial activities of Turkish *Artemisia absinthium*, *A. dracunculus, A. santonicum* and *A. spicigera* essential oils. *J. Agric. Food Chem.* 53, 9452–9458. doi: 10.1021/jf0516538

Kotan, R., Dadaşğolu, F., Karagoz, K., Cakir, A., Ozer, H., Kordali, S., et al. (2013). Antibacterial activity of the essential oil and extracts of *Satureja hortensis* against plant pathogenic bacteria and their potential use as seed disinfectants. *Sci. Hortic.* 153, 34–41. doi: 10.1016/j.scienta.2013.01.027

Kotan, R., Dadasoglu, F., Kordali, S., Cakir, A., Dikbas, N., and Cakmaker, R. (2007). Antibacterial activity of essential oils extracted from some medicinal plants, carvacrol and thymol on *Xanthomonas axonopodis* pv. *vesicatoria* (Doidge) Dye causes bacterial spot disease on pepper and tomato. *J. Agric. Technol.* 3, 299–306.

Koul, O., Walia, S., and Dhaliwal, G. S. (2008). Essential oils as green pesticides: potential and constraints. *Biopestic. Int.* 4, 63–84.

Kumar, A., Shukla, R., Singh, P., Singh, A. K., and Dubey, N. K. (2009). Use of essential oil from *Mentha arvensis* L. to control storage moulds and insects in stored chickpea. *J. Sci. Food Agric.* 89, 2643–2649. doi: 10.1002/jsfa.3768

Kumar, N., and Tripathi, N. N. (2002). Fungal infestation in groundnut seeds during storage and their control by essential oil of Putranjiva roxburghii Wall. *J. Indian Bot. Soc.* 81, 127–132.

Kumar, R., Dubey, N. K., Tiwari, O. P., Tripathi, Y. B., and Sinha, K. K. (2007). Evaluation of some essential oils as botanical fungitoxicants for the protection of stored food commodities from fungal infestation. *J. Sci. Food Agric.* 87, 1737–1742. doi: 10.1002/jsfa.2906

Lachowicz, K. J., Jones, G. P., Briggs, D. R., Bienvenu, F. E., Wan, J., Wilcock, A., et al. (1998). The synergistic preservative effects of the essential oils of sweet basil (*Ocimum basilicum* L.) acid tolerant food microflora. *Lett. Appl. Microbiol.* 26, 209–214. doi: 10.1046/j.1472-765X.1998.00321.x

Lalitha, V., and Raveesha, K. A. (2006). Fungitoxicity of some essential oils against important seed-borne pathogens of paddy. *Plant Dis. Res.* 21, 155–157.

Mangena, T., and Muyima, N. Y. O. (1999). Comparative evaluation of the antimicrobial activities of essential oils of *Artemisia afra*, *Pteronia incana* and *Rosmarinus officinalis* on selected bacteria and yeast strains. *Lett. Appl. Microbiol.* 28, 291–296. doi: 10.1046/j.1365-2672.1999.00525.x

Maqbool, M., Ali, A., and Alderson, P. G. (2010). Effect of cinnamon oil on incidence of anthracnose disease and post-harvest quality of bananas during storage. *Int. J. Agric. Biol.* 12, 516–520.

Maurya, S., Marimuthu, P., Singh, A., Rao, G. P., and Singh, G. (2005). Antiviral activity of essential oils and acetone extracts of medicinal plants against papaya ring spot virus. *J. Essent. Oil Bear. Plants* 8, 233–238. doi: 10.1080/0972060x.2005.10643452

Mediratta, P. K., Sharma, K. K., and Singh, S. (2002). Evaluation of immunomodulatory potential of *Ocimum sanctum* seeds oil and its possible mechanism of action. *J. Ethnopharmacol.* 80, 15–20. doi: 10.1016/S0378-8741(01)00373-7

Mihajilov-Krstev, T., Radnovic, D., Kitic, D., Stojanovic-Radic, Z., and Zlatkovic, B. (2009). Antimicrobial activity of *Satureja hortensis* L. essential oil against pathogenic microbial strains. *Biotechnol. Biotechnol.* 4, 1492–1496. doi: 10.2478/V10133-009-0018-2

Mimica-Dukic, N., Bozin, B., Sokovic, M., Mihajlovic, B., and Matavulj, M. (2003). Antimicrobial and antioxidant activities of three *Mentha* species essential oils. *Planta Med.* 69, 413–419. doi: 10.1055/s-2003-39704

Mishra, A. K., and Dubey, N. K. (1990). Fungitoxicity of essential oil of *Amomum subulatum* against *Aspergillus flavus*. *Econ. Bot.* 44, 530–533.

Mishra, A. K., and Dubey, N. K. (1994). Evaluation of some essential oils for their toxicity against fungi causing deterioration of stored food commodities. *Appl. Environ. Microbiol.* 60, 1101–1105.

Mishra, A. K., Dwivedi, S. K., Kishore, N., and Dubey, N. K. (1991). Fungistatic properties of essential oil of Cinnamomum camphora. *Int. J. Pharmacogn.* 29, 259–262.

Mishra, D., Chaturvedi, R. V., and Tripathi, S. C. (1995). The fungitoxic effect of essential oil of the herb *Nardostachys jatamansi* DC. *Trop. Agric.* 72, 48–52.

Mishra, D., Samuel, C. O., and Tripathi, S. C. (1993). Synergistic antifungal activity of essential oils of *Apium graveolens* and *Cuminum cyminum*. *Ind. Perf.* 37, 134–140.

Mishra, D., Samuel, C. O., and Tripathi, S. C. (2003). Evaluation of some essential oils against seed borne pathogens of rice. *Ind. Phytopathol.* 56, 212–213.

Nedorostova, L., Kloucek, P., Kokoska, L., Stolcova, M., and Pulkrabek, J. (2009). Antimicrobial properties of selected essential oils in vapour phase against food borne bacteria. *Food Control* 20, 157–160. doi: 10.1016/j.foodcont.2008.03.007

Nehrash, A. K. (1961). The antimicrobial properties of cultivated reddish I. the antimicrobial activity of extracts and essential oils from cultivated and wild radish. *J. Microbiol. Kiev.* 23, 32–37.

Neri, F., Mari, M., and Brigati, S. (2005). Control of *Penicillium expansum* by plant volatile compounds. *Plant Pathol.* 55, 100–105. doi: 10.1111/j.1365-3059.2005.01312.x

Nguefack, J., Somda, I., Mortensen, C. N., and Zollo, P. H. A. (2005). Evaluation of five essential oils from aromatic plants of Cameroon for controlling seed-borne bacteria of rice (*Oryza sativa*). *Seed Sci. Technol.* 33, 397–407. doi: 10.15258/sst.2005.33.2.12

Nikaido, H. (1994). Prevention of drug access to bacterial targets: permeability barriers and active efflux. *Science* 264, 382–388. doi: 10.1126/science.8153625

Nikaido, H. (2003). Molecular basis of bacterial outer membrane permeability revisited. *Microbiol. Mol. Biol. Rev.* 67, 593–656. doi: 10.1128/MMBR.67.4.593-656.2003

Ozturk, S., and Ercisli, S. (2006). The chemical composition of essential oil and *in vitro* antibacterial activities of essential oil and methanol extract of *Ziziphora persica* Bunge. *J. Ethnopharmacol.* 106, 372–376. doi: 10.1016/j.jep.2006.01.014

Pandey, A. K., Mohan, M., Singh, P., Palni, U. T., and Tripathi, N. N. (2014b). Chemical composition, antibacterial and antioxidant activity of essential oil of *Eupatorium adenophorum* Spreng from Eastern Uttar Pradesh, India. *Food Biosci.* 7, 80–87. doi: 10.1016/j.fbio.2014.06.001

Pandey, A. K., Palni, U. T., and Tripathi, N. N. (2013a). Evaluation of *Clausena pentaphylla* (Roxb.) DC oil as fungitoxicant against storage mycoflora of pigeon pea seeds). *J. Sci. Food Agric.* 93, 1680–1686. doi: 10.1002/jsfa.5949

Pandey, A. K., Palni, U. T., and Tripathi, N. N. (2014a). Repellent activity of some essential oils against two stored product beetles *Callosobruchus chinensis* L. and *C. maculates* F. (Coleoptera: Bruchidae) with reference to *Chenopodium ambrosioides* L. for the safety of pigeon pea seeds). *J. Food Sci. Technol.* 51, 4066–4071. doi: 10.1007/s13197-012-0896-4

Pandey, A. K., Singh, P., Mohan, M., and Tripathi, N. N. (2015). Chemical composition and antimicrobial activity of *Nepeta hindostana* (Roth) Haines from India. *Rec. Nat. Prod.* 9, 224–233.

Pandey, A. K., Singh, P., Palni, U. T., and Tripathi, N. N. (2012). *In-vitro* antibacterial activity of essential oils of aromatic plants against *Erwinia herbicola* (Lohnis) and *Pseudomonas putida* (Krish Hamilton). *J. Serb. Chem. Soc.* 77, 313–323. doi: 10.2298/JSC110524192P

Pandey, A. K., Singh, P., Palni, U. T., and Tripathi, N. N. (2011a). Use of essential oils of aromatic plants for the management of pigeon pea

infestation by pulse bruchids during storage. *Int. J. Agric. Technol.* 7, 1615–1624.

Pandey, A. K., Singh, P., Palni, U. T., and Tripathi, N. N. (2013b). Application of *Chenopodium ambrosioides* Linn. essential oil as botanical fungicide for the management of fungal deterioration in pulse. *Biol. Agric. Hort*ic. 29,197–208. doi: 10.1080/01448765.2013.822828

Pandey, A. K., Singh, P., Palni, U. T., and Tripathi, N. N. (2014c). *In vivo* evaluation of two essential oil based botanical formulations (EOBBF) for the use against stored product pests, *Aspergillus* and *Callosobruchus* (Coleoptera: Bruchidae) species. *J. Stored Prod. Res.* 59, 285–291. doi: 10.1016/j.jspr.2014.09.001

Pandey, A. K., Singh, P., and Tripathi, N. N. (2011b). Impact of essential oils on eggs hatchability and feeding activity of pulse beetles. *J. Entomol. Res.* 35, 221–225.

Pandey, A. K., Sonker, N., and Singh, P. (2016). Efficacy of some essential oils against *Aspergillus flavus* with special reference to *Lippia alba* oil an inhibitor of fungal proliferation and aflatoxin b1 production in green gram seeds during storage. *J. Food Sci.* 81, 928–934. doi: 10.1111/1750-3841.13254

Pandey, A. K., and Tripathi, N. N. (2011). Post- harvest fungal and insect deterioration of pigeon pea seeds and their management by plant volatiles. *J. Ind. Bot. Soc.* 90, 326–331.

Pandey, D. K., Asthana, A., Tripathi, N. N., and Dixit, S. N. (1981). Volatile plant products vis-à-vis potato pathogenic bacteria. *Ind. Perf.* 25, 10–14.

Paranagama, P. A., Abeysekera, K. H. T., Abeywickrama, K., and Nugaliyadde, L. (2003). Fungicidal and anti-aflatoxigenic effects of the essential oil of *Cymbopogon citratus* (DC.) Stapf. (lemongrass) against *Aspergillus flavus* Link. isolated from stored rice. *Lett. Appl. Microbiol.* 37, 86–90. doi: 10.1046/j.1472-765X.2003.01351.x

Perricone, M., Arace, E., Corbo, M. R., Sinigaglia, M., and Bevilacqu, A. (2015). Bioactivity of essential oils: a review on their interaction with food components. *Front. Microbiol.* 6:76. doi: 10.3389/fmicb.2015.00076

Posadzki, P., Alotaibi., A., and Ernst, E. (2012). Adverse effects of aromatherapy: a systematic review of case reports and case series. *Int. J. Risk Saf. Med.* 24, 147–161. doi: 10.3233/JRS-2012-0568

Pouvova, D., Kokoskova, B., Pavela, R., and Rysanek, P. (2008). Effectivity of plant essential oils against *Clavibacter michiganensis*, *in-vitro*. *Zemdirbyste- Agric.* 95, 440–446.

Pradhanang, P. M., Momol, M. T., Olson, S. M., and Jones, J. B. (2003). Effect of plant essential oils on *Ralstonia solanacearum* population density and bacterial wilt incidence in tomato. *Plant Dis.* 87, 423–427. doi: 10.1094/PDIS.2003.87.4.423

Ranasinghe, L., Jayawardena, B., and Abeywickrama, K. P. (2002). Fungicidal activity of essential oils of *Cinnomomum zeylanicum* L. and *Syzygium aromaticum* (L.) Merr et M Perry against crown rot and anthracnose pathogens isolated form banana. *Lett. Appl. Microbiol.* 35, 208–211. doi: 10.1046/j.1472-765X.2002.01165.x

Rao, B. G. V. N., and Joseph, P. L. (1971). Activity of some essential oils towards phytopathogenic fungi. *Riechest Aromas Koer.* 21, 405–410.

Reddy, B. M. V., Angers, P., Gosselin, A., and Arul, J. (1998). Characterization and uses of essential oil from *Thymus vulgaris* against *Botrytis cinerea* and *Rhizopus stolonifer* in strawberry fruits. *Phytochemistry* 47, 1515–1520. doi: 10.1016/S0031-9422(97)00795-4

Regnier, T., DuPlooy, W., Combrinck, S., and Botha, B. (2008). Fungitoxicity of *Lippia scaberrima* essential oil and selected terpenoid components on two mango post-harvest spoilage pathogens. *Postharvest Biol. Technol.* 48, 254–258. doi: 10.1016/j.postharvbio.2007.10.011

Renu, K., Tripathi, R. D., and Dixit, S. N. (1980). Fungitoxic properties of *Cestrum diurnum*. *Naturwissenschaften* 67, 150–151. doi: 10.1007/BF01073626

Saad, R. E., Mohamed, A. R., Shady, A., E., M., and Sheb, M. S. (2008). Antibacterial screening of some essential oils, monoterpenoids and novel N-methyl carbamates based on monoterpenoids against *Agrobacterium tumefaciens* and *Erwinia carotovora*. *Arc. Phytopathol. Plant Protect.* 41, 451–461. doi: 10.1080/03235400600833696

Scortichini, M., and Rossi, M. P. (1989). *In vitro* activity of some essential oils towards *Erwinia amylovora* (Burill) Winslow et al. *Acta. Phytopathol. Entomol. Hung.* 4, 423–431.

Shahi, S. K., Patra, M., Shukla, A. C., and Dikshit, A. (2003). Use of essential oil as botanical-pesticide against post-harvest spoilage in *Malus pumilo* fruits. *BioControl.* 48, 223–232. doi: 10.1023/A:1022662130614

Sharma, N., and Tripathi, A. (2006). Fungitoxicity of the essential oil of *Citrus sinensis* on post harvest pathogens. *World J. Microbiol. Biotechnol.* 22, 587–593. doi: 10.1007/s11274-005-9075-3

Sharma, S. K., and Singh, V. P. (1979). Antifungal activity of essential oils. *Ind. Drugs Pharm. Ind.* 14, 3–6.

Shirurkar, D. D., and Wahegaonkar, N. K. (2012). Antifungal activity of selected plant derived oils and some fungicides against seed borne fungi of maize. *Eur. J. Exp. Biol.* 2, 1693–1696.

Shukla., A. C. (2009). Volatile oil of *Cymbopogon pendulus* as an effective fumigant pesticide for the management of storage-pests of food commodities. *Nat. Acad. Sci. Lett.* 32, 51–59.

Singh, G., Kapoor, I. P. S., Pandey, S. K., and Singh, O. P. (2003). *Curcuma longa*-Chemical, antifungal and antibacterial investigation of rhizome oil. *Ind. Perf.* 47, 173–178.

Singh, G., Upadhyay, R. K., and Rao, G. P. (1992). Fungitoxic activity of the volatile oil of *Hyptis suaveolens*. *Fitoterapia* 63, 462–465.

Singh, J., and Tripathi, N. N. (1999). Inhibition of storage fungi of black gram (*Vigna mungo* L) by some essential oils. *Flavour. Frag. J.* 14, 1–4. doi: 10.1002/(SICI)1099-1026(199901/02)14:1<1::AID-FFJ735>3.0.CO;2-R

Singh, P., Pandey, A. K., Sonker, N., and Tripathi, N. N. (2011). Preservation of *Buchnania lanzan* Spreng. seeds by *Ocimum canum* Sims. Essential oil. *Ann. Plant Protect.* 19, 407–410.

Singh, S., Majumdar, D. K., and Rehan, H. M. S. (1996). Evaluation of anti-inflammatory potential of fixed oil of *Ocimum sanctum* (Holybasil) and its possible mechanism of action. *J. Ethnopharmacol.* 54, 19–26. doi: 10.1016/0378-8741(96)83992-4

Slavenas, J., and Razinskaite, D. (1962). Some studies on phytocidal substances of *Juniperus* oil from common *Juniper*. *Leit TSR Moks Acad. Darbai Ser.* 4, 63–64.

Sonker, N., Pandey, A. K., and Singh, P. (2015). Efficiency of *Artemisia nilagirica* (Clarke) Pamp essential oil as a mycotoxicant against postharvest mycobiota of table grapes. *J. Sci. Food Agric.* 95, 1932–1939. doi: 10.1002/jsfa.6901

Sonker, N., Pandey, A. K., Singh, P., and Tripathi, N. N. (2014). Assessment of *Cymbopogon citratus* (DC.) Stapf essential oil as herbal preservatives based on antifungal, antiaflatoxin and antiochratoxin activities and *in vivo* efficacy during storage. *J. Food Sci.* 79, M628–M634. doi: 10.1111/1750-3841.12390

Sylvestre, M., Pichette, A., Lavoie, S., Longtin, A., and Legault, J. (2007). Composition and cytotoxic activity of the leaf essential oil of *Comptonia peregrine* (L). Coulter. *Phytother. Res.* 21, 536–540. doi: 10.1002/ptr.2095

Tan, M., Zhou, L., Qin, M., Li, D., Jiang, W., Wang, Y., et al. (2007). Chemical composition and antimicrobial activity of the flower oil of *Russowia sogdiana* (Bunge) B. *Fedtsch*. (Asteraceae) from China. *J. Essent. Oil Res.* 19, 197–200. doi: 10.1080/10412905.2007.9699258

Tiwari, R., Dixit, V., and Dixit, S. N. (1994). Studies on fungitoxic properties of essential oil of *Cinnamomum zeylanicum* Breyn. *Ind. Perf.* 38, 98–104.

Tiwari., R., Mishra, D. N., and Upadhyay, P. S. (1988). Efficacy of some plant volatiles for the control of black mould of onion caused by *Aspergillus niger* Van.Teigh during storage. *Nat. Acad. Sci. Lett.* 11, 345–347.

Tripathi, N. N., Asthana, A., and Dixit, S. N. (1984). Toxicity of some terpenoids against fungi infesting fruits and seeds of *Capsicum annum* L. during storage. Phytopathol. Z. 110, 328–335. doi: 10.1111/j.1439-0434.1984.tb00072.x

Tripathi, N. N., Dubey, N. K., Dixit, A., Tripathi, R. D., and Dixit, S. N. (1983). Fungitoxic properties of *Alpinia galanga* oil. *Trop. Plant. Sci. Res.* 1, 49–52.

Tripathi, N. N., and Kumar, N. (2007). *Putranjiva roxburghii* oil- A potential herbal preservative for peanuts during storage. *J. Stored Prod. Res.* 43, 435–442. doi: 10.1016/j.jspr.2006.11.005

Trombetta, D., Castelli, F., Sarpietro, M. G., Venuti, V., Cristani, M., Daniele, C., et al. (2005). Mechanisms of antibacterial action of three monoterpenes. *Antimicrob. Agents Chemother.* 49, 2474–2478. doi: 10.1128/AAC.49.6.2474-2478.2005

Ukeh, D. A., and Mordue, A. J. (2009). Plant based repellents for the control of stored product insect pests. *Biopestic. Int.* 5, 1–23.

Upadhyay, P. S., Dixit, K., and Asthana, A. (1985). Fungitoxic and phytotoxic properties of leaves of *Citrus aurantifolia*. *Res. J. Plant Environ.* 3, 17–19.

Upadhyay, P. S., Mall, H. V., Renu, and Tripathi, N. N. (1987). "Fungitoxic and phytotoxic properties of essential oil of *Anisomeles indica*," in *Proceedings 72nd Indian Science Congress Association*, 110–111.

Vanneste, J. L., and Boyd, R. J. (2002). Inhibition of *Erwinia amylovora* and potential antagonistic bacteria by essential oils and natural

compounds. *Acta Hortic.* 590, 315–317. doi: 10.17660/ActaHortic.2002.590.46

Vasinauskiene, M., Radusiene, J., Zitikaite, I., and Surviliene, E. (2006). Antibacterial activities of essential oils from aromatic and medicinal plants against growth of phytopathogenic bacteria. *Agron. Res.* 4, 437–440.

Vukovic, N., Milosevic, T., Sukdolak, S., and Solujic, S. (2008). The chemical composition of the essential oil and the antibacterial activities of the essential oil and methanol extract of *Teucrium montanum*. *J. Serb. Chem. Soc.* 73, 299–305. doi: 10.2298/JSC0803299V

Wagacha, J. M., and Muthomi, J. W. (2008). Mycotoxin problem in Africa: current status, implications to food safety and health and possible management strategies. *Int. J. Food Microbiol.* 124, 1–12. doi: 10.1016/j.ijfoodmicro.2008.01.008

Conflict of Interest Statement: The authors declare that the research was conducted in the absence of any commercial or financial relationships that could be construed as a potential conflict of interest.

Copyright © 2017 Pandey, Kumar, Singh, Tripathi and Bajpai. This is an open-access article distributed under the terms of the Creative Commons Attribution License (CC BY). The use, distribution or reproduction in other forums is permitted, provided the original author(s) or licensor are credited and that the original publication in this journal is cited, in accordance with accepted academic practice. No use, distribution or reproduction is permitted which does not comply with these terms.

frontiers in Microbiology

REVIEW
published: 17 January 2017
doi: 10.3389/fmicb.2016.02170

Aflatoxins: A Global Concern for Food Safety, Human Health and Their Management

Pradeep Kumar[1], Dipendra K. Mahato[2], Madhu Kamle[1]*, Tapan K. Mohanta[3]* and Sang G. Kang[3]**

[1] Department of Forestry, North Eastern Regional Institute of Science and Technology, Nirjuli, India, [2] Division of Food Science & Postharvest Technology, Indian Agricultural Research Institute, New Delhi, India, [3] Department of Biotechnology, Yeungnam University, Gyeongsan, South Korea

The aflatoxin producing fungi, *Aspergillus spp.*, are widely spread in nature and have severely contaminated food supplies of humans and animals, resulting in health hazards and even death. Therefore, there is great demand for aflatoxins research to develop suitable methods for their quantification, precise detection and control to ensure the safety of consumers' health. Here, the chemistry and biosynthesis process of the mycotoxins is discussed in brief along with their occurrence, and the health hazards to humans and livestock. This review focuses on resources, production, detection and control measures of aflatoxins to ensure food and feed safety. The review is informative for health-conscious consumers and research experts in the fields. Furthermore, providing knowledge on aflatoxins toxicity will help in ensure food safety and meet the future demands of the increasing population by decreasing the incidence of outbreaks due to aflatoxins.

Keywords: aflatoxins, health issues, *Aspergillus* sp., secondary metabolites, food contamination

OPEN ACCESS

Edited by:
Bhim Pratap Singh, Mizoram University, India

Reviewed by:
Giuseppe Spano, University of Foggia, Italy
Mohd Adil, Dalhousie University, Canada

****Correspondence:***
Pradeep Kumar
pkbiotech@gmail.com
Madhu Kamle
madhu.kamle18@gmail.com
Tapan K. Mohanta
nostoc.tapan@gmail.com
Sang G. Kang
kangsg@yu.ac.kr

Specialty section:
This article was submitted to Microbiotechnology, Ecotoxicology and Bioremediation, a section of the journal Frontiers in Microbiology

Received: *07 October 2016*
Accepted: *23 December 2016*
Published: *17 January 2017*

Citation:
Kumar P, Mahato DK, Kamle M, Mohanta TK and Kang SG (2017) Aflatoxins: A Global Concern for Food Safety, Human Health and Their Management. Front. Microbiol. 7:2170. doi: 10.3389/fmicb.2016.02170

INTRODUCTION

Aflatoxins are one of the highly toxic secondary metabolites derived from polyketides produced by fungal species such as *Aspergillus flavus, A. parasiticus*, and *A. nomius* (Payne and Brown, 1998). These fungi usually infect cereal crops including wheat, walnut, corn, cotton, peanuts and tree nuts (Jelinek et al., 1989; Severns et al., 2003), and can lead to serious threats to human and animal health by causing various complications such as hepatotoxicity, teratogenicity, and immunotoxicity (**Figure 1**) (Amaike and Keller, 2011; Kensler et al., 2011; Roze et al., 2013). The major aflatoxins are B1, B2, G1, and G2, which can poison the body through respiratory, mucous or cutaneous routes, resulting in overactivation of the inflammatory response (Romani, 2004).

Food safety is one of the major problems currently facing the world; accordingly, a variety of studies have been conducted to discuss methods of addressing consumer concerns with various aspects of food safety (Nielsen et al., 2009). Since 1985, the United States Food and Drug Administration (USFDA) has restricted the amount of mycotoxins permitted in food products. The USDA Grain and Plant Inspection Service (GPIS) have implemented a service laboratory for inspection of mycotoxins in grains. Additionally, the Food and Agricultural Organization (FAO) and World Health Organization (WHO) have recognized many toxins present in agricultural products. When mycotoxins are contaminated into foods, they cannot be destroyed by normal cooking processes. However, there have been many recent advances in food processing developed

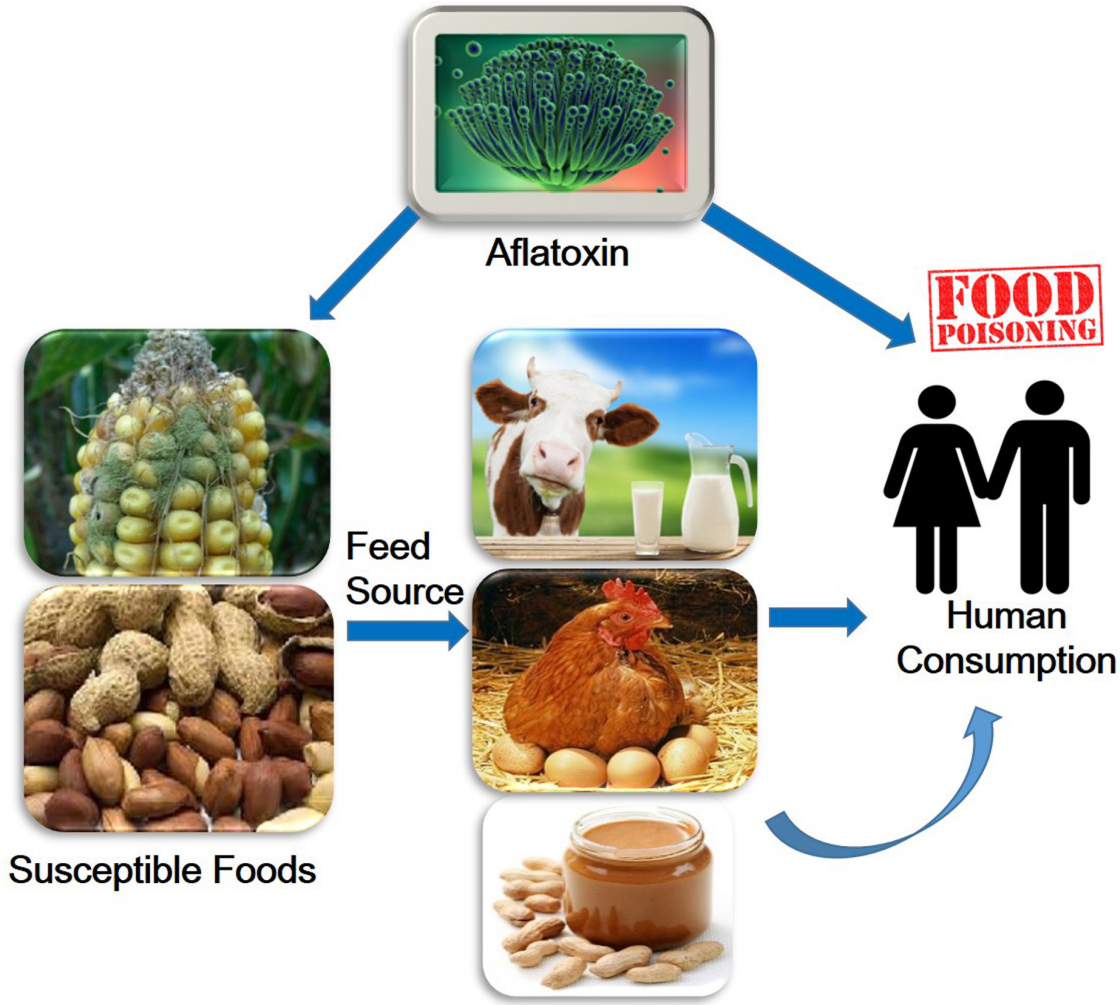


FIGURE 1 | Overview of aflatoxin effects on humans.

to keep final food products safe and healthy, such as hazard analysis of critical control points (HACCP) and good manufacturing practices (GMP; Lockis et al., 2011; Cusato et al., 2013; Maldonado-Siman et al., 2014). Moreover, several physical, chemical and biological methods can be applied to partially or completely eliminate these toxins from food and guarantee the food safety and health concerns of consumers. This review provides an overview of aflatoxigenic fungi, chemistry and biosynthesis of aflatoxins, along with their diversity in occurrence, and their health related risks to humans and livestock. Moreover, the effects of processing techniques on aflatoxins and various physical, chemical and biological methods for their control and management in food are discussed briefly.

OUTBREAKS DUE TO AFLATOXINS

In 1974, a major outbreak of hepatitis due to aflatoxin was reported in the states of Gujrat and Rajasthan in India, resulting in an estimated 106 deaths (Krishnamachari et al., 1975). The outbreak lasted for 2 months and was confined to tribal people whose main staple food, maize, was later confirmed to contain aflatoxin. The preliminary analysis confirmed that consumption of *A. flavus* had occurred (Krishnamachari et al., 1975; Bhatt and Krishnamachari, 1978). Another outbreak of aflatoxin affecting both humans and dogs was reported in northwest India in 1974 (Tandon et al., 1977; Bhatt and Krishnamachari, 1978; Reddy and Raghavender, 2007). A major aflatoxin exposure outbreak was subsequently documented in Kenya in 1981 (Ngindu et al., 1982). Since 2004, multiple aflatoxicosis outbreaks have been reported worldwide, resulting in 500 acute illness and 200 deaths (Centers for Disease Control and Prevention [CDCP], 2004; Azziz-Baumgartner et al., 2005). Most outbreaks have been reported from rural areas of the East Province of Kenya in 2004 and occurred because of consumption of home grown maize contaminated with molds. Preliminary testing of food from affected areas revealed the presence of aflatoxin as reported in 1981 (Ngindu et al., 1982).

In 2013, countries in Europe including Romania, Serbia, and Croatia reported the nationwide contamination of milk with aflatoxin[1].

MAJOR SOURCE OF AFLATOXIN

The major sources of aflatoxins are fungi such as *A. flavus, A. parasiticus,* and *A. nomius* (Kurtzman et al., 1987), although they are also produced by other species of *Aspergillus* as well as by *Emericella* spp. (Reiter et al., 2009). There are more than 20 known aflatoxins, but the four main ones are aflatoxin B1 (AFB1), aflatoxin B2 (AFB2), aflatoxin G1 (AFG1), and aflatoxin G2 (AFG2; Inan et al., 2007), while aflatoxin M1 (AFM1) and M2 (AFM2) are the hydroxylated metabolites of AFB1 and AFB2 (Giray et al., 2007; Hussain and Anwar, 2008).

Aspergillus spp.

The *Aspergillus* species are an industrially important group of microorganisms distributed worldwide. *A. niger* has been given Generally Recognized as Safe (GRAS) status by the USFDA (Schuster et al., 2002). However, some species have negative impacts and cause diseases in grape, onion, garlic, peanut, maize, coffee, and other fruits and vegetables (Lorbeer et al., 2000; Magnoli et al., 2006; Waller et al., 2007; Rooney-Latham et al., 2008). Moreover, *Aspergillus* section *nigri* produces mycotoxins such as ochratoxins and fumonisins in peanut, maize, and grape (Astoreca et al., 2007a,b; Frisvad et al., 2007; Mogensen et al., 2009).

Plant–pathogen interactions have been studied using molecular markers such as green fluorescent protein (GFP) isolated from *Aequorea victoria* (Prasher et al., 1992). The GFP gene has been successfully inserted into *Undifilum oxytropis* (Mukherjee et al., 2010), *Fusarium equiseti* (Macia-Vicente et al., 2009), and *Muscodor albus* (Ezra et al., 2010) and utilized to study the expression of different proteins and production of mycotoxins. *A. flavus* and *A. parasiticus* infect many crops in the field, during harvest, in storage, and during processing. *A. flavus* is dominant in corn, cottonseed, and tree nuts, whereas *A. parasiticus* is dominant in peanuts. *A. flavus* consists of mycelium, conidia, or sclerotia and can grow at temperatures ranging between 12 and 48°C (Hedayati et al., 2007). *A. flavus* produces AFBI and AFB2, whereas *A. parasiticus* isolates produce AFGI, AFG2, AFM1, AFBI, and AFB2. *A. flavus* produces a number of airborne conidia and propagules that infect plants such as cotton (Lee et al., 1986). A high number of propagules was reported in soil, air, and on cotton leaves during mid- to late August, while soilborne inoculum increased drastically between April and December in cotton fields in Arizona (Ashworth et al., 1969). This fungus can even colonize moribund rye cover crop and peanut fruit debris (Griffin and Garren, 1976).

[1]https://en.wikipedia.org/wiki/2013_European_aflatoxin_contamination

AFLATOXIN (AFT)

Among the mycotoxins affecting food and feed, aflatoxin is the major one in food that ultimately harms human and animal health (Boutrif, 1998). The level of toxicity associated with aflatoxin varies with the types present, with the order of toxicity being AFTs-B_1 > AFTs-G_1 > AFTs-B_2 > AFTs-G_2 (Jaimez et al., 2000).

CHEMISTRY AND BIOSYNTHESIS OF AFLATOXINS

Chemically, aflatoxins (AFTs) are difuranocoumarin derivatives in which a bifuran group is attached at one side of the coumarin nucleus, while a pentanone ring is attached to the other side in the case of the AFTs and AFTs-B series, or a six-membered lactone ring is attached in the AFTs-G series (Bennett and Klich, 2003; Nakai et al., 2008). The physical, biological and chemical conditions of *Aspergillus* influence the production of toxins. Among the 20 identified AFTs, AFT-B_1, and AFT-B_2 are produced by *A. flavus,* while AFT-G_1 and AFT-G_2 along with AFT-B_1 and AFT-B_2 are produced by *A. parasiticus* (Bennett and Klich, 2003). AFT-B_1, AFT-B_2, AFT-G_1, and AFT-G_2 are the four major naturally produced aflatoxins (Pitt, 2000). AFTs-M_1 and AFTs-M_2 are derived from aflatoxin B types through different metabolic processes and expressed in animals and animal products (Weidenborner, 2001; Wolf-Hall, 2010). AFT-B_1 is highly carcinogenic (Squire, 1981), as well as heat resistant over a wide range of temperatures, including those reached during commercial processing conditions (Sirot et al., 2013).

The biosynthetic pathway of aflatoxins consists of 18 enzymatic steps for conversion from acetyl-CoA, and at least 25 genes encoding the enzymes and regulatory pathways have been cloned and characterized (Yu et al., 2002; Yabe and Nakajima, 2004). The gene comprises 70 kb of the fungal genome and is regulated by the regulatory gene, *aflR* (Yabe and Nakajima, 2004; Yu et al., 2004; Price et al., 2006). The metabolic grid involved in the aflatoxin biosynthesis (Yabe et al., 1991, 2003). Hydroxyversicolorone (HVN) is converted to versiconal hemiacetal acetate (VHA) by a cytosol monooxygenase, in which NADPH is a cofactor (Yabe et al., 2003). Monooxygenase is encoded by the *moxY* gene, which catalyzes the conversion of HVN to VHA and the accumulation of HVN and versicolorone (VONE) occurs in the absence of the *moxY* gene (Wen et al., 2005).

GENE RESPONSIBLE FOR AFLATOXIN PRODUCTION

Various genes and their enzymes are involved in the production of sterigmatocystin (ST) dihydrosterigmatocystin (DHST), which are the penultimate precursors of aflatoxins (Cole and Cox, 1987). The aflatoxin biosynthesis gene *nor-1*, which was first cloned in *A. Parasiticus*, is named after the product formed by the gene during biosynthesis (Chang et al., 1992).

These genes named according to substrate and the product formed *nor-1* (norsolorinic acid [NOR]), *norA*, *norB, avnA* (averanti [AVN]), *avfA* (averufin [AVF]), *ver-1* (versicolorin A [VERA]), *verA* and *verB* while those based on enzyme functions *fas-2* (FAS alpha subunit), *fas-1* (FAS beta subunit), *pksA* (PKS), *adhA* (alcohol dehydrogenase), *estA* (esterase), *vbs* (VERB synthase), *dmtA* (mt-I; *O*-methyltransferase I), *omtA* (*O*-methyltransferase A), *ordA* (oxidoreductase A), *cypA* (cytochrome P450 monooxygenase), *cypX* (cytochrome P450 monooxygenase), and *moxY* (monooxygenase). Initially, the aflatoxin regulatory gene was named *afl-2* in *A. flavus* (Payne et al., 1993) and *apa-2* in *A. parasiticus* (Chang et al., 1993). However, it was subsequently referred to as *aflR* in *A. flavus, A. parasiticus*, and *A. nidulans* because of its role as a transcriptional activator. Previous studies have shown that *aflA* (fas-2), *aflB* (*fas-1*), and *aflC* (*pksA*) are responsible for the conversion of acetate to NOR (Townsend et al., 1984; Brown et al., 1996). Moreover, the *uvm8* gene was shown to be essential for NOR biosynthesis as well as aflatoxin production in *A. parasiticus.* The amino acid of sequence of the gene is similar to that of the beta subunit of FASs *(FAS1)* from *Saccharomyces cerevisiae* (Trail et al., 1995a,b). FAS forms the polyketide backbone during aflatoxin synthesis; hence, the *uvm8* gene was named *fas-1* (Mahanti et al., 1996). Fatty acid syntheses (FASs) is responsible for sterigmatocystin (ST) biosynthesis in *A. nidulans* and further identified two genes viz., *stcJ* and *stcK* that encode FAS and FAS subunits (FAS-2 and FAS-1; Brown et al., 1996).

OCCURRENCE IN FOOD

Aflatoxins are found in various cereals, oilseeds, spices, and nuts (Lancaster et al., 1961; Weidenborner, 2001; Reddy, 2010; Iqbal et al., 2014). These *Aspergillus* colonize among themselves and produce aflatoxins, which contaminate grains and cereals at various steps during harvesting or storage. Fungal contamination can occur in the field, or during harvest, transport and storage (Kader and Hussein, 2009). Aflatoxins contamination of wheat or barley is commonly happen by the result of inappropriate storage (Jacobsen, 2008). In milk, aflatoxins is generally at 1–6% of the total content in the feedstuff (Jacobsen, 2008). AFTs infect humans following consumption of aflatoxins contaminated foods such as eggs, meat and meat products, milk and milk products, (Bennett and Klich, 2003; Piemarini et al., 2007).

EFFECTS ON AGRICULTURE AND FOOD

Mycotoxins, including aflatoxin, have affected most crops grown worldwide; however, the extent of aflatoxin toxicity varies according to the commodities (Abbas et al., 2010). Aflatoxin can infect crops during growth phases or even after harvesting (Kumar et al., 2008). Exposure to this toxin poses serious hazards to human health (Umoh et al., 2011). Commodities such as corn, peanuts, pistachio, Brazil nuts, copra, and coconut are highly prone to contamination by aflatoxin (Idris et al., 2010; Cornea et al., 2011), whereas wheat, oats, millet, barley, rice, cassava, soybeans, beans, pulses, and sorghum are usually resistant to aflatoxin contamination. However, agricultural products such as cocoa beans, linseeds, melon seeds and sunflower seeds are seldom contaminated (Bankole et al., 2010). Aflatoxin was on the Rapid Alert System for Food and Feed (RASFF) of the European Union in 2008 because of its severe effects (European Commission, 2009), and the International Agency for Research on Cancer (IARC) later categorized AFB1 as a group I carcinogen for humans (Seo et al., 2011). Despite several research and control measures, aflatoxin is still a major threat to food and agricultural commodities.

MECHANISM OF TOXICITY AND HEALTH EFFECTS BY AFLATOXIN

Aflatoxin are specifically target the liver organ (Abdel-Wahhab et al., 2007). Early symptoms of hepatotoxicity of liver caused by aflatoxins comprise fever, malaise and anorexia followed with abdominal pain, vomiting, and hepatitis; however, cases of acute poisoning are exceptional and rare (Etzel, 2002). Chronic toxicity by aflatoxins comprises immunosuppressive and carcinogenic effects. Evaluation of the effects of AFT-B_1 on splenic lymphocyte phenotypes and inflammatory cytokine expression in male F344 rats have been studied (Qian et al., 2014). AFT-B_1 reduced anti-inflammatory cytokine IL-4 expression, but increased the pro-inflammatory cytokine IFN-γ and TNF-α expression by NK cells. These findings indicate that frequent AFT-B_1 exposure accelerates inflammatory responses via regulation of cytokine gene expression. Furthermore, Mehrzad et al. (2014) observed that AFT-B_1 interrupts the process of antigen-presenting capacity of porcine dendritic cells, suggested this perhaps one of mechanism of immunotoxicity by AFT-B_1.

Aflatoxins cause reduced efficiency of immunization in children that lead to enhanced risk of infections (Hendrickse, 1997). The hepatocarcinogenicity of aflatoxins is mainly due to the lipid peroxidation and oxidative damage to DNA (Verma, 2004). AFTs-B_1 in the liver is activated by cytochrome p450 enzymes, which are converted to AFTs-B1-8, 9-epoxide, which is responsible for carcinogenic effects in the kidney (Massey et al., 1995). Among all major mycotoxins, aflatoxins create a high risk in dairy because of the presence of their derivative, AFTs-M_1, in milk, posing a potential health hazard for human consumption (Van Egmond, 1991; Wood, 1991). AFTs-B_1 is rapidly absorbed in the digestive tract and metabolized by the liver, which converts it to AFT-M_1 for subsequent secretion in milk and urine (Veldman et al., 1992). Although AFTs-M_1 is less mutagenic and carcinogenic than AFTs-B_1, it exhibits high genotoxic activity. The other effects of AFTs-M_1 include liver damage, decreased milk production, immunity suppression and reduced oxygen supply to tissues due to anemia (Aydin et al., 2008), which reduces appetite and growth in dairy cattle (Akande et al., 2006). Several studies have shown the detrimental effects of aflatoxins exposure on the liver (Sharmila Banu et al., 2009), epididymis (Agnes and Akbarsha, 2001), testis (Faisal et al., 2008),

kidney and heart (Mohammed and Metwally, 2009; Gupta and Sharma, 2011). It has been found that aflatoxin presences in post-mortem brain tissue (Oyelami et al., 1995), suggested that its ability to cross the blood brain barrier (Qureshi et al., 2015). AFTs also cause abnormalities in the structure and functioning of mitochondrial DNA and brain cells (Verma, 2004). The effects of aflatoxin on brain chemistry have been reviewed in details by Bbosa et al. (2013). Furthermore, few reports have described the effects of AFTs-B_1 administration on the structure of the rodent central nervous system (Laag and Abdel Aziz, 2013).

The liver toxicology of aflatoxin is also a critical issue (IARC, 2002; Iqbal et al., 2014). Limited doses are not harmful to humans or animals; however, the doses that do cause-effects diverse among Aflatoxin groups. The expression of aflatoxin toxicity is regulated by factors such as age, sex, species, and status of nutrition of infected animals (Williams et al., 2004). The symptoms of acute aflatoxicosis include oedema, haemorrhagic necrosis of the liver and profound lethargy, while the chronic effects are immune suppression, growth retardation, and cancer (Gong et al., 2004; Williams et al., 2004; Cotty and Jaime-Garcia, 2007).

EFFECTS OF PROCESSING ON AFLATOXIN

Techniques to eliminate aflatoxin may be either physical or chemical methods. Removing mold-damaged kernels, seeds or nuts physically from commodities has been observed to reduce aflatoxins by 40–80% (Park, 2002). The fate of aflatoxin varies with type of heat treatment (e.g., cooking, drying, pasteurization, sterilization, and spray drying; Galvano et al., 1996). Aflatoxins decompose at temperatures of 237–306°C (Rustom, 1997); therefore, pasteurization of milk cannot protect against AFM1 contamination. Awasthi et al. (2012) reported that neither pasteurization nor boiling influenced the level of AFM1 in bovine milk. However, boiling corn grits reduced aflatoxins by 28% and frying after boiling reduced their levels by 34–53% (Stoloff and Trucksess, 1981). Roasting pistachio nuts at 90°C, 120°C, and 150°C for 30, 60 and 120 min was found to reduce aflatoxin levels by 17–63% (Yazdanpanah et al., 2005). The decrease in aflatoxin content depends on the time and temperature combination. Moreover, alkaline cooking and steeping of corn for the production of tortillas reduces aflatoxin by 52% (Torres et al., 2001). Hameed (1993) reported reductions in aflatoxin content of 50–80% after extrusion alone. When hydroxide (0.7 and 1.0%) or bicarbonate (0.4%) was added, the reduction was enhanced to 95%. Similar results were reported by Cheftel (1989) for the extrusion cooking of peanut meal. The highest aflatoxin reduction was found to be 59% with a moisture content of 35% in peanut meal, and the extrusion variables non-significantly affected its nutritional composition (Saalia and Phillips, 2011a). Saalia and Phillips (2011b) reported an 84% reduction in aflatoxin of peanut meal when cooked in the presence of calcium chloride.

EFFECTS OF ENVIRONMENTAL TEMPERATURE ON AFLATOXIN PRODUCTION

Climate change plays a major role in production of aflatoxin from *Aspergillus* in food crops (Paterson and Lima, 2010, 2011; Magan et al., 2011; Wu F. et al., 2011; Wu S. et al., 2011). Climate change affects the interactions between different mycotoxigenic species and the toxins produced by them in foods and feeds (Magan et al., 2010; Paterson and Lima, 2012). Changes in environmental temperature influence the expression levels of regulatory genes (*aflR* and *aflS*) and aflatoxin production in *A. flavus* and *A. parasiticus* (Schmidt-Heydt et al., 2010, 2011). A good correlation between the expression of an early structural gene (*aflD*) and AFB1 has been reported by Abdel-Hadi et al. (2010). Temperature interacts with water activity (a_w) and influences the ratio of regulatory genes (*aflR*/*aflS*), which is directly proportional to the production of AFB1 (Schmidt-Heydt et al., 2009, 2010). The interactions between water activity and temperature have prominent effect on *Aspergillus* spp. and aflatoxin production (Sanchis and Magan, 2004; Magan and Aldred, 2007). Increasing the temperature to 37°C and water stress significantly reduces the production of AFB1 produced, despite the growth of *A. flavus* under these conditions. The addition of CO_2 under the same temperature and water activity enhances AFB1 production (Medina et al., 2014). According to Gallo et al. (2016), fungal biomass and AFB1 production were reported to be highest at 28°C and 0.96 a_w, while no fungal growth or AFB1 production was seen at 20°C with a_w values of 0.90 and 0.93. There was also no AFB1 production observed at 37°C. Reverse transcriptase quantitative PCR also revealed that the regulatory genes *aflR* and *aflS* were highly expressed at 28°C, while the lowest expression was observed at 20 and 37°C, suggesting that temperature plays a significant role in gene expression and aflatoxin production (Gallo et al., 2016).

DETECTION TECHNIQUES

The detection and quantification of aflatoxin in food and feed is a very important aspect for the safety concerns. Aflatoxins are usually detected and identified according to their absorption and emission spectra, with peak absorbance occurring at 360 nm. B toxins exhibit blue fluorescence at 425 nm, while G toxins show green fluorescence at 540 nm under UV irradiation. This florescence phenomenon is widely accepted for aflatoxins. Thin layer chromatography (TLC) is among one of the oldest techniques used for aflatoxin detection (Fallah et al., 2011), while high performance liquid chromatography (HPLC), liquid chromatography mass spectroscopy (LCMS), and enzyme linked immune-sorbent assay (ELISA) are the methods most frequently used for its detection (Tabari et al., 2011; Andrade et al., 2013; Sulyok et al., 2015). ELISA can be used to identify aflatoxins based on estimation of AfB1-lysine (metabolite of AFB1 toxin) concentration in the blood. Specifically, the test detects levels of AfB1 in blood as low as 5 pg/mg albumin, making it a

cost effective method for routine monitoring that can also be utilized for the detection of hepatitis B virus. Room temperature phosphorescence (RTP) in aflatoxigenic strains grown on media is commonly used in food mycology. Aflatoxins immobilized on resin beads can induce RTP in the presence or absence of oxygen and heavy atoms (Costa-Fernandez and Sanz-Medel, 2000) and also have high sensitivity and specificity (Li et al., 2003). Moreover, several biosensors and immunoassays have been developed to detect ultra-traces of aflatoxins to ensure the food safety.

DEGRADATION KINETICS

Various treatments including chemical, physical, and biological methods are routinely utilized for effective degradation, mitigation and management of aflatoxin (Shcherbakova et al., 2015). The aflatoxins AFB1 and AFG1 are completely removed by ozone treatment at 8.5–40 ppm at different temperatures, but AFB2 and AFG2 are not affected by this method. The degradation of aflatoxin followed first order kinetic equation. However, microbial and enzymatic degradation is preferred for the biodegradation of aflatoxin due to its eco-friendly nature (Agriopoulou et al., 2016). The bacterium *Flavobacterium aurantiacum* reportedly removes AFM1 from milk and *Nocardia asteroides* transforms AFB1 to fluorescent product (Wu et al., 2009). *Rhodococcus* species are able to degrade aflatoxins (Teniola et al., 2005) and their ability to degrade AFB1 occurs in the following order: *R. ruber* < *R. globerulus* < *R. coprophilus* < *R. gordoniae* < *R. pyridinivorans* and < *R. erythropolis* (Cserhati et al., 2013). Fungi such as *Pleurotus ostreatus, Trametes versicolor, Trichosporon mycotoxinivorans, S. cerevisiae, Trichoderma* strains, and *Armillariella tabescens* are known to transform AFB1 into less toxic forms (Guan et al., 2008). Zhao et al. (2011) reported purification of extracellular enzymes from the bacterium *Myxococcus fulvus* ANSM068 with a final specific activity of 569.44 × 103 U/mg. The pure enzyme (100 U/mL) had a degradation ability of 96.96% for AFG1 and 95.80% for AFM1 after 48 h of incubation. Moreover, the recombinant laccase produced by *A. niger* D15-Lcc2#3 (118 U/L) was found to lead to a decrease in AFB1 of 55% within 72 h (Alberts et al., 2009).

MANAGEMENT AND CONTROL STRATEGIES

The biocontrol principle of competitive exclusion of toxigenic strains of *A. flavus* involves the use of non-toxigenic strains to reduce aflatoxin contamination in maize (Abbas et al., 2006). The use of biocontrol agents such as *Bacillus subtilis*, *Lactobacillus* spp., *Pseudomonas* spp., *Ralstonia* spp., and *Burkholderia* spp. are effective at control and management of aflatoxins (Palumbo et al., 2006). Several strains of *B. subtilis* and *P. solanacearum* isolated from the non-rhizosphere of maize soil have been reported to eliminate aflatoxin (Nesci et al., 2005). Biological control of aflatoxin production in crops in the US has been approved by the Environmental Protection Agency and two commercial products based on atoxigenic *A. flavus* strains are being used (Afla-guard® and AF36®) for the prevention of aflatoxin in peanuts, corn, and cotton seed (Dorner, 2009). Good agricultural practices (GAPs) also help control the toxins to a larger extent, such as timely planting, providing adequate plant nutrition, controlling weeds, and crop rotation, which effectively control *A. flavus* infection in the field (Ehrlich and Cotty, 2004; Waliyar et al., 2013).

Biological control is emerging as a promising approach for aflatoxin management in groundnuts using *Trichoderma* spp, and significant reductions of 20–90% infection of aflatoxin have been recorded (Anjaiah et al., 2006; Waliyar et al., 2015). Use of inbred maize lines resistant to aflatoxin has also been employed. Potential biochemical markers and genes for resistance in maize against *Aspergillus* could also be utilized (Chen et al., 2007). Additionally, biotechnological approaches have been reviewed for aflatoxin management strategies (Yu, 2012). Advances in genomic technology based research and decoding of the *A. flavus* genome have supported identification of the genes responsible for production and modification of the aflatoxin biosynthesis process (Bhatnagar et al., 2003; Cleveland, 2006; Holbrook et al., 2006; Ehrlich, 2009). In addition, Wu (2010) suggested that aflatoxin accumulation can be reduced by utilizing transgenic *Bt* maize with insect resistance traits as the wounding caused by insects helps penetrate the *Aspergillus* in kernels.

CONCLUSION

Aflatoxins are a major source of disease outbreaks due to a lack of knowledge and consumption of contaminated food and feed worldwide. Excessive levels of aflatoxins in food of non-industrialized countries are of major concern. Several effective physical, chemical, biological, and genetic engineering techniques have been employed for the mitigation, effective control and management of aflatoxins in food. However, developing fungal resistant and insect resistant hybrids/crops to combat pre-harvest infections and their outcome is a major issue of concern. Post-harvest treatments to remove aflatoxins such as alkalization, ammonization, and heat or gamma radiation are not generally used by farmers. However, some of the microorganisms naturally present in soil have the ability to degrade and reduce the aflatoxin contamination in different types of agricultural produce. Therefore, methods of using these organisms to reduce aflatoxin are currently being focused on. Moreover, application of genetic recombination in *A. flavus* and other species is being investigated for its potential to mitigate aflatoxins to ensure the safety and quality of food.

AUTHOR CONTRIBUTIONS

PK and DM designed and conceived the experiments and wrote the manuscript. MK, TM, and SK edited and helped in finalizing the manuscript.

ACKNOWLEDGMENTS

PK and MK highly grateful to the Director and Head, Department of Forestry, NERIST (Deemed University), Arunachal Pradesh, India. This research was supported by the Basic Science Research Program through the National Research Foundation of Korea (NRF) funded by the Ministry of Education (NRF-2009-0070065).

REFERENCES

Abbas, H. K., Reddy, K. R. N., Salleh, B., Saad, B., Abel, C. A., and Shier, W. T. (2010). An overview of mycotoxin contamination in foods and its implications for human health. *Toxin Rev.* 29, 3–26. doi: 10.3109/15569541003598553

Abbas, H. K., Zablotowicz, R. M., Bruns, H. A., and Abel, C. A. (2006). Biocontrol of aflatoxin in corn by inoculation with non-aflatoxigenic *Aspergillus flavus* isolates. *Biocontrol Sci. Technol.* 16, 437–449. doi: 10.1080/09583150500532477

Abdel-Hadi, A., Carter, D., and Magan, N. (2010). Temporal monitoring of the nor-1 (aflD) gene of *Aspergillus flavus* in relation to aflatoxin B1 production during storage of peanuts under different environmental conditions. *J. Appl. Microbiol.* 109, 1914–1922. doi: 10.1111/j.1365-2672.2010.04820.x

Abdel-Wahhab, M. A., Abdel-Galil, M. M., Hassan, A. M., Hassan, N. H., Nada, S. A., Saeed, A., et al. (2007). Zizyphus spina-christi extract protects against aflatoxin B1-intitiated hepatic carcinogenicity. *Afr. J. Tradit. Complement. Altern. Med.* 4, 248–256.

Agnes, V. F., and Akbarsha, M. A. (2001). Pale vacuolated epithelial cells in epididymis of aflatoxin-treated mice. *Reproduction* 122, 629–641. doi: 10.1530/rep.0.1220629

Agriopoulou, S., Koliadima, A., Karaiskakis, G., and Kapolos, J. (2016). Kinetic study of aflatoxins' degradation in the presence of ozone. *Food Control* 61, 221–226. doi: 10.1016/j.foodcont.2015.09.013

Akande, K. E., Abubakar, M. M., Adegbola, T. A., and Bogoro, S. E. (2006). Nutritional and health implications of mycotoxin in animal feed. *Pak. J. Nutr.* 5, 398–403. doi: 10.3923/pjn.2006.398.403

Alberts, J. F., Gelderblom, W. C. A., Botha, A., and van Zyl, W. H. (2009). Degradation of aflatoxin B1 by fungal laccase enzymes. *Int. J. Food Microbiol.* 135, 47–52. doi: 10.1016/j.ijfoodmicro.2009.07.022

Amaike, S. A., and Keller, N. P. (2011). *Aspergillus flavus*. *Annu. Rev. Phytopathol.* 49, 107–133. doi: 10.1146/annurev-phyto-072910-095221

Andrade, P. D., da Silva, J. L. G., and Caldas, E. D. (2013). Simultaneous analysis of aflatoxins B1, B2, G1, G2, M1 and ochratoxin A in breast milk by high-performance liquid chromatography/fluorescence after liquid-liquid extraction with low temperature purification (LLE-LTP). *J. Chromatogr. A* 1304, 61–68. doi: 10.1016/j.chroma.2013.06.049

Anjaiah, V., Thakur, R. P., and Koedam, N. (2006). Evaluation of bacteria and Trichoderma for biocontrol of pre-harvest seed infection by *Aspergillus flavus* in groundnut. *Biocontrol Sci. Technol.* 16, 431–436. doi: 10.1080/09583150500532337

Ashworth, L. J. Jr., McMeans, J. L., and Brown, C. M. (1969). Infection of cotton by *Aspergillus flavus*: epidemiology of the disease. *J. Stored Prod. Res.* 5, 193–202. doi: 10.1016/0022-474X(69)90033-2

Astoreca, A., Magnoli, C., Barberis, C., Chiacchiera, S. M., Combina, M., and Dalcero, A. (2007a). Ochratoxin A production in relation to ecophysiological factors by *Aspergillus* section Nigri strains isolated from different substrates in Argentina. *Sci. Total Environ.* 388, 16–23. doi: 10.1016/j.scitotenv.2007.07.028

Astoreca, A., Magnoli, C., Ramirez, M. L., Combina, M., and Dalcero, A. (2007b). Water activity and temperature effects on growth of *Aspergillus niger*, *A. awamori* and *A. Carbonarius* isolated from different substrates in Argentina. *Int. J. Food Microbiol.* 119, 314–318.

Awasthi, V., Bahman, S., Thakur, L. K., Singh, S. K., Dua, A., and Ganguly, S. (2012). Contaminants in milk and impact of heating: an assessment study. *Indian J. Public Health* 56, 95–99. doi: 10.4103/0019-557X.96985

Aydin, A., Gunsen, U., and Demirel, S. (2008). Total aflatoxin B1 and ochratoxin A levels in Turkish wheat flour. *J. Food Drug Anal.* 16, 48–53.

Azziz-Baumgartner, E., Lindblade, K., Gieseker, K., Rogers, H. S., Kieszak, S., Njapau, H., et al. (2005). Case–control study of an acute aflatoxicosis outbreak, Kenya, 2004. *Environ. Health Perspect.* 113, 1779–1783.

Bankole, S. A., Adenusi, A. A., Lawal, O. S., and Adesanya, O. O. (2010). Occurrence of aflatoxin B1 in food products derivabl e from 'egusi' melon seeds consumed in southwestern Nigeria. *Food Control* 21, 974–976. doi: 10.1016/j.foodcont.2009.11.014

Bbosa, G. S., Kitya, D., Lubega, A., Ogwal-Okeng, J., Anokbonggo, W. W., and Kyegombe, D. B. (2013). "Review of the biological and health effects of aflatoxins on bodyorgans and body systems," in *Aflatoxins – Recent Advances and Future Prospects*, ed. M. Razzaghi-Abyaneh (Rijeka: InTech), 239–265.

Bennett, J. W., and Klich, M. (2003). Mycotoxins. *Clin. Microbiol. Rev.* 16, 497–516. doi: 10.1128/CMR.16.3.497-516.2003

Bhatnagar, D., Ehrlich, K. C., and Cleveland, T. E. (2003). Molecular genetic analysis and regulation of aflatoxin biosynthesis. *Appl. Microbiol. Biotechnol.* 61, 83–93. doi: 10.1007/s00253-002-1199-x

Bhatt, R. V., and Krishnamachari, K. A. V. R. (1978). Food toxins and disease outbreaks in India. *Arogya J. Health Sci.* 4, 92–100.

Boutrif, E. (1998). Prevention of aflatoxin in pistachios. *Food Nutr. Agric.* 21, 32–38.

Brown, D. W., Adams, T. H., and Keller, N. P. (1996). *Aspergillus* has distinct fatty acid synthases for primary and secondary metabolism. *Proc. Natl. Acad. Sci. U.S.A.* 19, 14873–14877. doi: 10.1073/pnas.93.25.14873

Centers for Disease Control and Prevention [CDCP] (2004). *Outbreak of Aflatoxin Poisoning — Eastern and Central Provinces, Kenya, January—July 2004*. Available at: https://www.cdc.gov/mmwr/preview/mmwrhtml/mm5334a4.htm [accessed October 10, 2016]

Chang, P. K., Cary, J. W., Bhatnagar, D., Cleveland, T. E., Bennett, J. W., Linz, J. E., et al. (1993). Cloning of the *Aspergillus parasiticus* apa-2 gene associated with the regulation of aflatoxin biosynthesis. *Appl. Environ. Microbiol.* 59, 3273–3279.

Chang, P. K., Skory, C. D., and Linz, J. E. (1992). Cloning of a gene associated with aflatoxin B1 biosynthesis in *Aspergillus parasiticus*. *Curr. Genet.* 21, 231–233. doi: 10.1007/BF00336846

Cheftel, J. C. (1989). "Extrusion cooking and food safety," in *Extrusion Cooking*, eds C. Mercier, P. Linko, and J. M. Harper (Eagan, MN: American Association of Cereal Chemists), 435–461.

Chen, Z. Y., Brown, R. L., Damann, K. E., and Cleveland, T. E. (2007). Identification of maiz kernel endosperm proteins associated with resistance to aflatoxin contamination by *Aspergillus flavus*. *Phytopathology* 97, 1094–1103. doi: 10.1094/PHYTO-97-9-1094

Cleveland, T. E. (2006). "The use of crop proteomics and fungal genomics inelucidating fungus–crop interactions," in *Proceedings of the Myco-Globe Conference*, Bari, 32.

Cole, R. J., and Cox, E. H. (1987). *Handbook of Toxic Fungal Metabolites*. New York, NY: Academic Press.

Cornea, C. P., Ciuca, M., Voaides, C., Gagiu, V., and Pop, A. (2011). Incidence of fungal contamination in a Romanian bakery: a molecular approach. *Rom. Biotechnol. Lett.* 16, 5863–5871.

Costa-Fernandez, J. M., and Sanz-Medel, A. (2000). Room temperature phosphorescence biochemical sensors. *Quim. Anal.* 19, 189–204.

Cotty, P. J., and Jaime-Garcia, R. (2007). Influences of climate on aflatoxin producing fungi and aflatoxin contamination. *Int. J. Food Microbiol.* 119, 109–115. doi: 10.1016/j.ijfoodmicro.2007.07.060

Cserhati, M., Kriszt, B., Krifaton, C., Szoboszlay, S., Hahn, J., Toth, S., et al. (2013). Mycotoxin-degradation profile of *Rhodococcus* strains. *Int. J. Food Microbiol.* 166, 176–185. doi: 10.1016/j.ijfoodmicro.2013.06.002

Cusato, S., Gameiro, A. H., Corassin, C. H., Sant'Ana, A. S., Cruz, A. G., Faria, J. D. A. F., et al. (2013). Food safety systems in a small dairy factory: implementation, major challenges, and assessment of systems' performances. *Foodborne Pathog. Dis.* 10, 6–12. doi: 10.1089/fpd.2012.1286

Dorner, J. W. (2009). Development of biocontrol technology to manage aflatoxin contamination in peanuts. *Peanut Sci.* 36, 60–67. doi: 10.3146/AT07-002.1

Ehrlich, K. C. (2009). Predicted roles of uncharacterized clustered genes in aflatoxin biosynthesis. *Toxins* 1, 37–58. doi: 10.3390/toxins1010037

Ehrlich, K. K., and Cotty, P. J. (2004). An isolate of *Aspergillus flavus* used to reduce aflatoxin contamination in cottonseed has a defective polyketide synthase gene. *Appl. Microbiol. Biotechnol.* 65, 473–478. doi: 10.1007/s00253-004-1670-y

Etzel, R. A. (2002). Mycotoxins. *JAMA* 287, 425–427. doi: 10.1001/jama.287.4.425

European Commission (2009). *The Rapid Alert System for Food and Feed (RASFF) Annual Report 2008*. Luxembourg: European Communities.

Ezra, D., Skovorodnikova, J., Kroitor-Keren, T., Denisov, Y., and Liarzi, O. (2010). Development of methods for detection and *Agrobacterium*-mediated transformation of the sterile, endophytic fungus *Muscodor albus*. *Biocontrol Sci. Technol.* 20, 83–97. doi: 10.1080/09583150903420049

Faisal, K., Periasamy, V. S., Sahabudeen, S., Radha, A., Anandhi, R., and Akbarsha, M. A. (2008). Spermatotoxic effect of aflatoxin B1 in rat: extrusion of outer densefibres and associated axonemal microtubule doublets of sperm flagellum. *Reproduction* 135, 303–310. doi: 10.1530/REP-07-0367

Fallah, A. A., Rahnama, M., Jafari, T., and Saei-Dehkordi, S. S. (2011). Seasonal variation of aflatoxin M1 contamination in industrial and traditional Iranian dairy products. *Food Control* 22, 1653–1656. doi: 10.1016/j.foodcont.2011.03.024

Frisvad, J. C., Smedsgaard, J., Samson, R. A., Larsen, T. O., and Thrane, U. (2007). Fumonisin B2 Production by *Aspergillus niger*. *J. Agric. Food Chem.* 55, 9727–9732. doi: 10.1021/jf0718906

Gallo, A., Solfrizzo, M., Epifani, F., Panzarini, G., and Perrone, G. (2016). Effect of temperature and water activity on gene expression and aflatoxin biosynthesis in *Aspergillus flavus* on almond medium. *Int. J. Food Microbiol.* 217, 162–169. doi: 10.1016/j.ijfoodmicro.2015.10.026

Galvano, F., Galofaro, V., and Galvano, G. (1996). Occurrence and stability of aflatoxin M1 in milk and milk products. A worldwide review. *J. Food Prot.* 59, 1079–1090. doi: 10.4315/0362-028X-59.10.1079

Giray, B., Girgin, G., Engin, A. B., Aydın, S., and Sahin, G. (2007). Aflatoxin levels in wheat samples consumed in some regions of Turkey. *Food Control* 18, 23–29. doi: 10.1016/j.foodcont.2005.08.002

Gong, Y., Hounsa, A., Egal, S., Turner, P. C., Sutcliffe, A. E., Hall, A. J., et al. (2004). Postweaning exposure to aflatoxin results in impaired child growth: a longitudinal study in Benin, West Africa. Environ. *Health Perspect.* 112, 1334–1338. doi: 10.1289/ehp.6954

Griffin, G. J., and Garren, K. H. (1976). Colonization of rye green manure and peanut fruit debris by *Aspergillus flavus* and *Aspergillus niger* group in field soils. *Appl. Environ. Microbiol.* 32, 28–32.

Guan, S., Ji, C., Zhou, T., Li, J., Ma, Q., and Niu, T. (2008). Aflatoxin B1 degradation by *Stenotrophomonas maltophilia* and other microbes selected using coumarin medium. *Int. J. Mol. Sci.* 9, 1489–1503. doi: 10.3390/ijms9081489

Gupta, R., and Sharma, V. (2011). Ameliorative effects of tinospora cordifolia root extracton histopathological and biochemical changes induced by aflatoxin-b (1) in mice kidney. *Toxicol. Int.* 18, 94–98. doi: 10.4103/0971-6580.84259

Hameed, H. G. (1993). *Extrusion and Chemical Treatments for Destruction of Aflatoxin in Naturally-Contaminated Corn*. Ph.D. thesis, University of Arizona, Tucson, AZ.

Hedayati, M. T., Pasqualotto, A. C., Warn, P. A., Bowyer, P., and Denning, D. W. (2007). *Aspergillus flavus*: human pathogen, allergen and micotoxin producer. *Microbiology* 153, 1677–1692. doi: 10.1099/mic.0.2007/007641-0

Hendrickse, R. G. (1997). Of sick Turkeys, Kwashiorkor, malaria, perinatal mortality, Herion addicts and food poisoning: research on influence of aflatoxins on child health in the tropics. *J. Trop. Med. Parasitol.* 91, 87–93.

Holbrook, C. C. Jr., Guo, B., Wilson, D. M., and Timper, P. (2006). "The U.S. breeding program to develop peanut with drought tolerance and reduced aflatoxin contamination [abstract]," in *Proceedings of the International Conference on Groundnut Aflatoxin Management and Genomics*, Guangzhou.

Hussain, I., and Anwar, J. (2008). A study on contamination of aflatoxin M1 in raw milk in the Punjab province of Pakistan. *Food Control* 19, 393–395. doi: 10.1016/j.foodcont.2007.12.002

IARC (2002). *Monographs on the Evaluation of Carcinogenic Risks to Humans*, Vol. 82. Lyon: International Agency for Cancer Research.

Idris, Y. M. A., Mariod, A. A., Elnour, I. A., and Mohamed, A. A. (2010). Determination of aflatoxin levels in Sudanese edible oils. *Food Chem. Toxicol.* 48, 2539–2541. doi: 10.1016/j.fct.2010.05.021

Inan, F., Pala, M., and Doymaz, I. (2007). Use of ozone in detoxification of aflatoxin B1 in red pepper. *J. Stored Prod. Res.* 43, 425–429. doi: 10.1016/j.jspr.2006.11.004

Iqbal, S. Z., Mustafa, H. G., Asi, M. R., and Jinap, S. (2014). Variation in vitamin E level and aflatoxins contamination in different rice varieties. *J. Cereal Sci.* 60, 352–355. doi: 10.1016/j.jcs.2014.05.012

Jacobsen, B. J. (2008). "Predicting the Incidence of Mycotoxins," in *Proceeding of 26th Annual International Symposium on Man and His Environment in Health and Disease: Molds & Mycotoxins, Hidden Connections for Chronic Diseases*, (Dallas, TX: American Environmental Health Foundation), 13–17.

Jaimez, J., Fente, C. A., Vazquez, B. I., Franco, C. M., Cepeda, A., Mahuzier, G., et al. (2000). Application of the assay of aflatoxins by liquid chromatography with fluorescence detection in food analysis. *J. Chromatogr. A* 882, 1–10. doi: 10.1016/S0021-9673(00)00212-0

Jelinek, C. F., Pohland, A. E., and Wood, G. E. (1989). Worldwide occurrence of mycotoxins in foods and feeds – an update. *J. Assoc. Off. Anal. Chem.* 72, 223–230.

Kader, A. A., and Hussein, A. M. (2009). *Harvesting and Postharvest Handling of Dates*. Aleppo: ICARDA.

Kensler, T. W., Roebuck, B. D., Wogan, G. N., and Groopman, J. D. (2011). Aflatoxin: a 50-year odyssey of mechanistic and translational toxicology. *Toxicol. Sci.* 120, 28–48. doi: 10.1093/toxsci/kfq283

Krishnamachari, K. A. V. R., Bhat, R. V., Nagarajan, V., and Tilak, T. B. G. (1975). Hepatitis due to aflatoxicosis-An outbreak in western India. *Lancet* 1, 1061–1063. doi: 10.1016/S0140-6736(75)91829-2

Kumar, V., Basu, M. S., and Rajendran, T. P. (2008). Mycotoxin research and mycoflora in some commercially important agricultural commodities. *Crop Prot.* 27, 891–905. doi: 10.1016/j.cropro.2007.12.011

Kurtzman, C. P., Horn, B. W., and Hesseltine, C. W. (1987). *Aspergillus* nomius, a new aflatoxin-producing species related to *Aspergillus flavus* and *Aspergillus parasiticus*. *Antonie Van Leeuwenhoek* 53, 147–158. doi: 10.1016/S0168-6496(03)00154-5

Laag, E. M., and Abdel Aziz, H. O. (2013). Effect of aflatoxin-B1 on rat cerebellar cortex: light and electron microscopic study. *Egypt. J. Histol.* 36, 601–610. doi: 10.1097/01.EHX.0000432619.75801.15

Lancaster, M. C., Jenkins, F. P., and Philip, J. M. C. (1961). Toxicity associated with certain samples of ground nuts. *Nature* 12, 1095–1096. doi: 10.1038/1921095a0

Lee, L. S., Goynes, W. R., and Lacey, P. E. (1986). Aflatoxin in Arizona cottonseed: simulation of insect vectored infection of cotton bolls by *Aspergillus flavus*. *J. Am. Oil Chem. Soc.* 63:468.

Li, G. R., Wu, J. J., Jin, W. J., and Xie, J. W. (2003). Antioxygen quenching room temperature phosphorescence stabilized by deoxycholate aggregate. *Talanta* 60, 552–562. doi: 10.1016/S0039-9140(03)00185-1

Lockis, V. R., Cruz, A. G., Walter, E. H., Faria, J. A., Granato, D., and Sant'Ana, A. S. (2011). Prerequisite programs at schools: diagnosis and economic evaluation. *Foodborne Pathog. Dis.* 8, 213–220. doi: 10.1089/fpd.2010.0645

Lorbeer, J. W., Ransom, V. E., and Tuffley, J. J. (2000). *Nature and source of Inoculums of Aspergillus niger Causing the Aspergillus Black Mold Disease of Onions in New York*. Geneva, NY: New York State Integrated Pest Management Grants Program, 1–6.

Macia-Vicente, J. G., Jansson, H. B., Talbot, N. J., and Lopez-Llorca, L. V. (2009). Real-time PCR quantification and live-cell imaging of endophytic colonization of barley (Hordeumvulgare) roots by *Fusarium equiseti* and Pochonia chlamydosporia. *New Phytol.* 182, 213–228. doi: 10.1111/j.1469-8137.2008.02743.x

Magan, N., and Aldred, D. (2007). Post-harvest control strategies: minimizing mycotoxins in the food chain. *Int. J. Food Microbiol.* 119, 131–139. doi: 10.1016/j.ijfoodmicro.2007.07.034

Magan, N., Aldred, D., Hope, R., and Mitchell, D. (2010). Environmental factors and interactions with mycoflora of grain and grapes: effects on growth and deoxynivalenol and ochratoxin production by *Fusarium culmorum* and *Aspergillus carbonarius*. *Toxins* 2, 353–366. doi: 10.3390/toxins2030353

Magan, N., Medina, A., and Aldred, D. (2011). Possible climate change effects on mycotoxin contamination of food crops pre- and post-harvest. *Plant Pathol.* 60, 150–163. doi: 10.1111/j.1365-3059.2010.02412.x

Magnoli, C., Astoreca, A., Ponsone, L., Fernandez-Juri, M. G., Chiacchiera, S., and Dalcero, A. (2006). Ochratoxin A and the occurrence of ochratoxin A-producing black aspergilla in stored peanut seeds from Cordoba, Argentina. *J. Sci. Food Agric.* 86, 2369–2373. doi: 10.1002/jsfa.2625

Mahanti, N., Bhatnagar, D., Cary, J. W., Joubran, J., and Linz, J. E. (1996). Structure and function of fas-1A, a gene encoding a putative fatty acid synthetase directly

involved in aflatoxin biosynthesis in *Aspergillus parasiticus*. *Appl. Environ. Microbiol.* 62, 191–195.

Maldonado-Siman, E., Bai, L., Ramírez-Valverde, R., Gong, S., and Rodríguez-de Lara, R. (2014). Comparison of implementing HACCP systems of exporter Mexican and Chinese meat enterprises. *Food Control* 38, 109–115. doi: 10.1016/j.foodcont.2013.10.017

Massey, T. E., Stewart, R. K., Daniels, J. M., and Liu, L. (1995). Biochemical and molecular aspects of mammalian susceptibility to aflatoxin B-1 Carcinogenicity. *Proc. Soc. Exp. Biol. Med.* 208, 213–227. doi: 10.3181/00379727-208-43852A

Medina, A., Rodriguez, A., and Magan, N. (2014). Effect of climate change on aspergillus flavus and aflatoxin B1 production. *Front. Microbiol.* 5:348. doi: 10.3389/fmicb.2014.00348

Mehrzad, J., Devriendt, B., Baert, K., and Cox, E. (2014). Aflatoxin B1 interferes with the antigen-presenting capacity of porcine dendritic cells. *Toxicol. Vitro* 28, 531–537. doi: 10.1016/j.tiv.2013.11.015

Mogensen, J. M., Frisvad, J. C., Thrane, U., and Nielsen, K. F. (2009). Production of fumonisin B2 and B4 by *Aspergillus niger* on grapes and raisins. *J. Agric. Food Chem.* 58, 954–958. doi: 10.1021/jf903116q

Mohammed, A. M., and Metwally, N. S. (2009). Antiaflatoxicogenic activities of someaqueous plant extracts against AFB1 induced renal and cardiac damage. *J. Pharmacol. Toxicol.* 4, 1–16. doi: 10.3923/jpt.2009.1.16

Mukherjee, S., Dawe, A. L., and Creamer, R. (2010). Development of a transformation system in the swainsonine producing, slow growing endophytic fungus, Undifilum oxytropis. *J. Microbiol. Methods* 81, 160–165. doi: 10.1016/j.mimet.2010.02.015

Nakai, V. K., Rocha, L. O., Goncalez, E., Foneseca, H., Ortega, E. M., and Correa, B. (2008). Distribution of fungi and aflatoxins in stored peanut variety. *Food Chemistry* 106, 190–285. doi: 10.1016/j.foodchem.2007.05.087

Nesci, A. V., Bluma, R. V., and Etcheverry, M. G. (2005). In vitro selection of maize rhizobac-teria to study potential bio- logical control of *Aspergillus* section Flavi and aflatoxin production. *Eur. J. Plant Pathol.* 113, 159–171. doi: 10.1007/s10658-005-5548-3

Ngindu, A., Kenya, P. R., and Ocheng, D. M. (1982). Outbreak of acute hepatitis by aflatoxin poisoning in Kenya. *Lancet* 319, 1346–1348. doi: 10.1016/S0140-6736(82)92411-4

Nielsen, H. B., Sonne, A. M., Grunert, K. G., Banati, D., Pallak-Toth, A., Lakner, Z., et al. (2009). Consumer perception of the use of high-pressure processing and pulsed electric field technologies in food production. *Appetite* 52, 115–126. doi: 10.1016/j.appet.2008.09.010

Oyelami, O. A., Maxwell, S. M., Adelusola, K. A., Aladekoma, T. A., and Oyelese, A. O. (1995). Aflatoxins in the autopsy brain tissue of children in Nigeria. *Mycopathology* 132, 35–38. doi: 10.1007/BF01138602

Palumbo, J. D., Baker, J. L., and Mahoney, N. E. (2006). Isolation of bacterial antagonists of *Aspergillus flavus* from almonds. *Microb. Ecol.* 52, 45–52. doi: 10.1007/s00248-006-9096-y

Park, D. L. (2002). Effect of processing on aflatoxin. *Adv. Exp. Med. Biol.* 504, 173–179. doi: 10.1007/978-1-4615-0629-4_17

Paterson, R., and Lima, N. (2010). How will climate change affect mycotoxins in food? *Food Res. Int.* 43, 1902–1914. doi: 10.1016/j.foodres.2009.07.010

Paterson, R., and Lima, N. (2011). Further mycotoxin effects from climate change. *Food Res. Int.* 44, 2555–2566. doi: 10.1016/j.foodres.2011.05.038

Paterson, R., and Lima, N. (2012). "Climate change, fumonisins and animal feed," in *Nutrieconomics: Balancing Global Nutrition and Productivity*, ed. E. M. Binder (Tulln: BiominWorld Nutrition Forum), 241–247.

Payne, G. A., and Brown, M. P. (1998). Genetics and physiology of aflatoxin biosynthesis. *Annu. Rev. Phytopathol.* 36, 329–362. doi: 10.1146/annurev.phyto.36.1.329

Payne, G. A., Nystrom, G. J., Bhatnagar, D., Cleveland, T. E., and Woloshuk, C. P. (1993). Cloning of the afl-2 gene involved in aflatoxin biosynthesis from *Aspergillus flavus*. *Appl. Environ. Microbiol.* 59, 156–162.

Piemarini, S., Micheli, L., Ammida, N. H. S., Palleschi, G., and Moscone, D. (2007). Electrical immunosensor array using a 96-well screen-printed microplate for aflatoxin B1 detection. *Biosens. Bioelectron.* 22, 1434–1440. doi: 10.1016/j.bios.2006.06.029

Pitt, J. I. (2000). Toxigenic fungi and mycotoxins. *Br. Med. Bull.* 56, 184–192. doi: 10.1258/0007142001902888

Prasher, D. C., Eckenrode, V. K., Ward, W. W., Prendergast, F. G., and Cormier, M. J. (1992). Primary structure of the *Aequorea victoria* green-fluorescent protein. *Gene* 111, 229–233. doi: 10.1016/0378-1119(92)90691-H

Price, M. S., Yu, J., Nierman, W. C., Kim, H. S., Pritchard, B., Jacobus, C. A., et al. (2006). The aflatoxin pathway regulator AflR induces gene transcription inside and outside of the aflatoxin biosynthetic cluster. *FEMS Microbiol. Lett.* 255, 275–279. doi: 10.1111/j.1574-6968.2005.00084.x

Qian, G., Tang, L., Guo, X., Wang, F., Massey, M. E., Su, J., et al. (2014). Aflatoxin B1 modulates the expression of phenotypic markers and cytokines by splenic lymphocytes of male F344 rats. *J. Appl. Toxicol.* 34, 241–249. doi: 10.1002/jat.2866

Qureshi, H., Hamid, S. S., Ali, S. S., Anwar, J., Siddiqui, A. A., and Khan, N. A. (2015). Cytotoxic effects of aflatoxin B1 on human brain microvascular endothelial cells of the blood–brain barrier. *Med. Mycol.* 53, 409–416. doi: 10.1093/mmy/myv010

Reddy, B. N., and Raghavender, C. N. (2007). Outbreaks of aflatoxicoses in India. *Afr. J. Food Agric. Nutr. Dev.* 7, 1–15.

Reddy, K. R. N. (2010). An overview of mycotoxin contamination in foods and itsimplications for human health. *Toxin Rev.* 29, 3–26. doi: 10.3109/15569541003598553

Reiter, E., Zentek, J., and Razzazi, E. (2009). Review on sample preparation strategies and methods used for the analysis of aflatoxins in food and feed. *Mol. Nutr. Food Res.* 53, 508–524. doi: 10.1002/mnfr.200800145

Romani, L. (2004). Immunity to fungal infections. *Nat. Rev. Immunol.* 4, 1–23. doi: 10.1038/nri1255

Rooney-Latham, S., Janousek, C. N., Eskalen, A., and Gubler, W. D. (2008). First report of *Aspergillus carbonarius* causing sour rot of table grapes (*Vitisvinifera*) in California. *Plant Dis.* 92:651. doi: 10.1094/PDIS-92-4-0651A

Roze, L. V., Hong, S. Y., and Linz, J. E. (2013). Aflatoxin biosynthesis: current frontiers. *Annu. Rev. Food Sci. Technol.* 4, 293–311. doi: 10.1146/annurev-food-083012-123702

Rustom, I. Y. S. (1997). Aflatoxin in food and feed: occurence, legislation and inactivation by physical methods. *Food Chem.* 59, 57–67. doi: 10.1016/S0308-8146(96)00096-9

Saalia, F. K., and Phillips, R. D. (2011a). Degradation of aflatoxins by extrusion cooking: effects on nutritional quality of extrudates. *LWT Food Sci. Technol.* 44, 1496–1501. doi: 10.1016/j.lwt.2011.01.021

Saalia, F. K., and Phillips, R. D. (2011b). Reduction of aflatoxins in peanut meal by extrusion cooking in the presence of nucleophiles. *LWT Food Sci. Technol.* 44, 1511–1516. doi: 10.1016/j.lwt.2011.02.012

Sanchis, V., and Magan, N. (2004). "Environmental profiles for growth and mycotoxin production, Chapter 8," in *Mycotoxins in Food: Detection and Control*, eds N. Magan and M. Olsen (Cambridge, MA: Woodhead Publishing Ltd), 174–189.

Schmidt-Heydt, M., Abdel-Hadi, A., Magan, N., and Geisen, R. (2009). Complex regulation of the aflatoxin biosynthesis gene cluster of *A. flavus* in relation to various combinations of water activity and temperature. *Int. J. Food Microbiol.* 135, 231–237. doi: 10.1016/j.ijfoodmicro.2009.07.026

Schmidt-Heydt, M., Parra, R., Geisen, R., and Magan, N. (2011). Modelling the relationship between environmental factors, transcriptional genes and deoxynivalenol mycotoxin production by two *Fusarium* species. *J. R. Soc. Interface* 8, 117–126. doi: 10.1098/rsif.2010.0131

Schmidt-Heydt, M., Rufer, C. E., Abdel-Hadi, A., Magan, N., and Geisen, R. (2010). The production of aflatoxin B1 or G1 by *Aspergillus parasiticus* at various combinations of temperature and water activity is related to the ratio of aflS to aflR expression. *Mycotoxin Res.* 26, 241–246. doi: 10.1007/s12550-010-0062-7

Schuster, E., Dunn, C., van Frisvad, J., and Dijck, P. W. (2002). On the safety of *Aspergillus niger*: a review. *Appl. Microbiol. Biotechnol.* 59, 426–435. doi: 10.1007/s00253-002-1032-6

Seo, J. H., Min, W. K., Kweon, D. H., Park, K., and Park, Y. C. (2011). Characterization of monoclonal antibody against aflatoxin B (1) produced in hybridoma 2C12 and its single-chain variable fragment expressed in recombinant *Escherichia coli*. *Food Chem.* 126, 1316–1323. doi: 10.1016/j.foodchem.2010.11.088

Severns, D. E., Clements, M. J., Lambert, R. J., and White, D. G. (2003). Comparison of *Aspergillus* ear rot and aflatoxin contamination in grain of high-oil and normal oil corn hybrids. *J. Food Prot.* 66, 637–643. doi: 10.4315/0362-028X-66.4.637

Sharmila Banu, G., Kumar, G., and Murugesan, A. G. (2009). Ethanolic leaves extract of *Trianthema portulacastrum* L. ameliorates aflatoxin B(1) induced hepaticdamage in rats. *Indian J. Clin. Biochem.* 24, 250–256. doi: 10.1007/s12291-009-0074-2

Shcherbakova, L., Statsyuk, N., Mikityuk, O., Nazarova, T., and Dzhavakhiya, V. (2015). Aflatoxin B1 degradation by metabolites of *Phoma glomerata* PG41 isolated from natural substrate colonized by aflatoxigenic *Aspergillus flavus*. *Jundishapur J. Microbiol.* 8:e24324. doi: 10.5812/jjm.24324

Sirot, V., Fremy, J. M., and Leblanc, J. C. (2013). Dietary exposure to mycotoxins and health risk assessment in the second French total diet study. *Food Chem. Toxicol.* 52, 1–11. doi: 10.1016/j.fct.2012.10.036

Squire, R. A. (1981). Ranking animal carcinogens: a proposed regulatory approach. *Science* 214, 877–880. doi: 10.1126/science.7302565

Stoloff, L., and Trucksess, M. W. (1981). Effect of boiling, frying, and baking on recovery of aflatoxin from naturally contaminated corn grits or cornmeal. *J. Assoc. Off. Anal. Chem.* 64, 678–680.

Sulyok, M., Beed, F., Boni, S., Abass, A., Mukunzi, A., and Krska, R. (2015). Quantitation of multiple mycotoxins and cyanogenic glucosides in cassava samples from Tanzania and Rwanda by an LC-MS/MS-based multi-toxin method. *Food Addit. Contam. Part A Chem. Anal. Control, Expo. Risk Assess.* 32, 488–502.

Tabari, M., Karim, G., Ghavami, M., and Chamani, M. (2011). Method validation for aflatoxin M1 determination in yoghurt using immunoaffinity column clean-up prior to high-performance liquid chromatography. *Toxicol. Ind. Health* 27, 629–635. doi: 10.1177/0748233710394236

Tandon, B. N., Krishnamurthy, L., Koshy, A., Tandon, H. D., Ramalingaswamy, V., Bhandari, J. R., et al. (1977). Study of an epidemic of jaundice presumably due to toxic hepatitis in North-West India. *Gastroenterology* 72, 488–494.

Teniola, O. D., Addo, P. A., Brost, I. M., Farber, P., Jany, K. D., Alberts, J. F., et al. (2005). Degradation of aflatoxin B1 by cell-free extracts of *Rhodococcus erythropolis* and *Mycobacterium fluoranthenivorans* sp. nov. DSM44556T. *Int. J. Food Microbiol.* 105, 111–117. doi: 10.1016/j.ijfoodmicro.2005.05.004

Torres, P., Guzman-Ortiz, M., and Ramirez-Wong, B. (2001). Revising the role of pH and thermal treatments in aflatoxin content reduction during the tortilla and deep frying processes. *J. Agric. Food Chem.* 49, 2825–2829. doi: 10.1021/jf0007030

Townsend, C. A., Christensen, S. B., and Trautwein, K. (1984). Hexanoate as a starter unit in polyketide synthesis. *J. Am. Chem. Soc.* 106, 3868–3869. doi: 10.1021/ja00325a031

Trail, F., Manhanti, N., and Linz, J. (1995a). Molecular biology of aflatoxin biosynthesis. *Microbiology* 141, 755–765. doi: 10.1099/13500872-141-4-755

Trail, F., Mahanti, N., Rarick, M., Mehigh, R., Liang, S. H., Zhou, R., et al. (1995b). Physical and transcriptional map of an aflatoxin gene cluster in Aspergillus parasiticus and functional disruption of a gene involved early in the aflatoxin pathway. *Appl. Environ. Microbiol.* 61, 2665–2673.

Umoh, N. J., Lesi, O. A., Mendy, M., Bah, E., Akano, A., Whittle, H., et al. (2011). Aetiological differences in demographical, clinical and pathological characteristics of hepatocellular carcinoma in The Gambia. *Liver Int.* 31, 215–221. doi: 10.1111/j.1478-3231.2010.02418.x

Van Egmond, H. P. (1991). Mycotoxins. *Int. Dairy Fed. Spec. Issue* 101, 131–135.

Veldman, A., Meijs, J. A. C., Borggreve, G. J., and Heeres van der Tol, J. J. (1992). Carryover of aflatoxin from cows' food to milk. *Animal Production* 55, 163–168. doi: 10.1017/S0003356100037417

Verma, R. J. (2004). Aflatoxin causes DNA damage. *Int. J. Hum. Genet.* 4, 231–236.

Waliyar, F., Osiru, M., Ntare, B. R., Vijay, K. K., Sudini, H., Traore, A., et al. (2015). Aflatoxins in maize and other crops. *World Mycotoxin J.* 8, 245–252. doi: 10.3920/WMJ2014.1766

Waliyar, F., Osiru, M., Sudini, H., and Njoroge, S. (2013). "Reducing aflatoxins in groundnuts through integrated management and biocontrol," in *Aflatoxins – Finding Solutions for Improved Food Safety*, eds L. J. Unnevehr and D. Grace (Washington, DC: International Food Policy Research Institute), 1–2.

Waller, J. M., Bigger, M., and Hillocks, R. A. (2007). *Coffee Pests, Diseases and Their Management*. Cambridge, MA: CAB International.

Weidenborner, M. (2001). *Encyclopedia of Food Mycotoxins*. New York, NY: Springer-Verlag.

Wen, Y., Hatabayashi, H., Arai, H., Kitamoto, H. K., and Yabe, K. (2005). Function of the cypX and moxY genes in aflatoxin biosynthesis in *Aspergillus parasiticus*. *Appl. Environ. Microbiol.* 71, 3192–3198. doi: 10.1128/AEM.71.6.3192-3198.2005

Williams, J. H., Phillips, T. D., Jolly, P. E., Stiles, J. K., Jolly, C. M., and Aggarwal, D. (2004). Human aflatoxicosis in developing countries: a review of toxicology, exposure, potential health consequences, and interventions. *Am. J. Clin. Nutr.* 80, 1106–1122.

Wolf-Hall, C. (2010). "Fungal and mushroom toxins," in *Pathogens and Toxins in Foods: Challenges and Interventions*, eds V. K. Juneja and J. N. Sofos (Washington, DC: ASM Press), 275–285.

Wood, G. E. (1991). *Aflatoxin M1, Mycotoxins and Phytoalexins*. London: CRC Press, 145–163.

Wu, F. (2010). *The Global Burden of Disease Caused by Foodborne Aflatoxin*. WHO Commissioned Report. Geneva: World Health Organization Food Borne Disease Burden Epidemiology Reference Group.

Wu, F., Bhatnagar, D., Bui-Klimke, T., Carbone, I., Hellmich, R., and Munkvold, G. (2011). Climate change impacts on mycotoxin risks in US maize. *World Mycotoxin J.* 4, 79–93. doi: 10.3920/WMJ2010.1246

Wu, S., Duan, N., Zhu, C., Ma, X., Wang, M., and Wang, Z. (2011). Magnetic nanobead-based immunoassay for the simultaneous detection of aflatoxin B1 and ochratoxin A using upconversion nanoparticles as multicolor labels. *Biosens. Bioelectron.* 30, 35–42. doi: 10.1016/j.bios.2011.08.023

Wu, Q., Jezkova, A., Yuan, Z., Pavlikova, L., Dohnal, V., and Kuca, K. (2009). Biological degradation of aflatoxins. *Drug Metab. Rev.* 41, 1–7. doi: 10.1080/03602530802563850

Yabe, K., Ando, Y., and Hamasaki, T. (1991). A metabolic grid among versiconal hemiacetal acetate, versiconol acetate, versiconol and versiconal during aflatoxin biosynthesis. *J. Gen. Microbiol.* 137, 2469–2475. doi: 10.1099/00221287-137-10-2469

Yabe, K., Chihaya, N., Hamamatsu, S., Sakuno, E., Hamasaki, T., Nakajima, H., et al. (2003). Enzymatic conversion of averufin to hydroxyversicolorone and elucidation of a novel metabolic grid involved in aflatoxin biosynthesis. *Appl. Environ. Microbiol.* 69, 66–73. doi: 10.1128/AEM.69.1.66-73.2003

Yabe, K., and Nakajima, H. (2004). Enzyme reactions and genes in aflatoxin biosynthesis. *Appl. Microbiol. Biotechnol.* 64, 745–755. doi: 10.1007/s00253-004-1566-x

Yazdanpanah, H., Mohammadi, T., Abouhossain, G., and Cheraghali, A. M. (2005). Effect of roasting on degradation of aflatoxins in contaminated pistachio nuts. *Food Chem. Toxicol.* 43, 1135–1139. doi: 10.1016/j.fct.2005.03.004

Yu, J. (2012). Current understanding on aflatoxin biosynthesis and future perspective in reducing aflatoxin contamination. *Toxins* 4, 1024–1057. doi: 10.3390/toxins4111024

Yu, J., Bhatnagar, D., and Ehrlich, K. C. (2002). Aflatoxin biosynthesis. *Revista Iberoam.Micol.* 19, 191–200.

Yu, J., Chang, P. K., Ehrlich, K. C., Cary, J. W., Bhatnagar, D., Cleveland, T. E., et al. (2004). Clustered pathway genes in aflatoxin biosynthesis. *Appl. Environ. Microbiol.* 70, 1253–1262. doi: 10.1128/AEM.70.3.1253-1262.2004

Zhao, L. H., Guan, S., Gao, X., Ma, Q. G., Lei, Y. P., and Bai, X. M. (2011). Preparation, purification and characteristics of an aflatoxin degradation enzyme from *Myxococcus fulvus* ANSM068. *J. Appl. Microbiol.* 110, 147–155. doi: 10.1111/j.1365-2672.2010.04867.x

Conflict of Interest Statement: The authors declare that the research was conducted in the absence of any commercial or financial relationships that could be construed as a potential conflict of interest.

Copyright © 2017 Kumar, Mahato, Kamle, Mohanta and Kang. This is an open-access article distributed under the terms of the Creative Commons Attribution License (CC BY). The use, distribution or reproduction in other forums is permitted, provided the original author(s) or licensor are credited and that the original publication in this journal is cited, in accordance with accepted academic practice. No use, distribution or reproduction is permitted which does not comply with these terms.

frontiers in Microbiology

ORIGINAL RESEARCH
published: 30 January 2017
doi: 10.3389/fmicb.2017.00023

Sigma Factor Regulated Cellular Response in a Non-solvent Producing *Clostridium beijerinckii* Degenerated Strain: A Comparative Transcriptome Analysis

*Yan Zhang[1†], Shengyin Jiao[2†], Jia Lv[2], Renjia Du[2], Xiaoni Yan[2], Caixia Wan[3], Ruijuan Zhang[2] and Bei Han[2]**

[1] School of Medicine, Institute for Genome Sciences, University of Maryland, Baltimore, MD, USA, [2] School of Public Health, Health Science Center, Xi'an Jiaotong University, Xi'an, China, [3] Department of Bioengineering, University of Missouri, Columbia, MO, USA

Clostridium beijerinckii DG-8052, derived from NCIMB 8052, cannot produce solvent or form spores, a phenomenon known as degeneration. To explore the mechanisms of degeneration at the gene level, transcriptomic profiles of the wild-type 8052 and DG-8052 strains were compared. Expression of 5168 genes comprising 98.6% of the genome was assessed. Interestingly, 548 and 702 genes were significantly up-regulated in the acidogenesis and solventogenesis phases of DG-8052, respectively, and mainly responsible for the phosphotransferase system, sugar metabolic pathways, and chemotaxis; meanwhile, 699 and 797 genes were significantly down-regulated, respectively, and mainly responsible for sporulation, oxidoreduction, and solventogenesis. The functions of some altered genes, including 286 and 333 at the acidogenesis and solventogenesis phases, respectively, remain unknown. Dysregulation of the fermentation machinery was accompanied by lower transcription levels of glycolysis rate-limiting enzymes (*pfk* and *pyk*), and higher transcription of cell chemotaxis genes (*cheA*, *cheB*, *cheR*, *cheW*, and *cheY*), controlled mainly by σ^{54} at acidogenesis. Meanwhile, abnormal spore formation was associated with repressed *spo0A*, *sigE*, *sigF*, *sigG*, and *sigK* which are positively regulated by σ^{70}, and correspondingly inhibited expression of CoA-transferase at the solventogenesis phase. These findings indicated that morphological and physiological changes in the degenerated *Clostridium* strain may be related to altered expression of sigma factors, providing valuable targets for strain development of *Clostridium* species.

Keywords: *Clostridium beijerinckii* NCIMB8052, strain degeneration, transcriptome analysis, microarray, sigma factor

OPEN ACCESS

Edited by:
Wen-Jun Li,
Sun Yat-sen University, China

Reviewed by:
Pablo Ivan Nikel,
National Center for Biotechnology (CSIC), Spain
Hongxia Wang,
University of Alabama at Birmingham, USA

****Correspondence:***
Bei Han
hanbei@mail.xjtu.edu.cn

† These authors have contributed equally to this work.

Specialty section:
This article was submitted to Microbial Physiology and Metabolism, a section of the journal Frontiers in Microbiology

Received: *29 November 2016*
Accepted: *04 January 2017*
Published: *30 January 2017*

Citation:
Zhang Y, Jiao S, Lv J, Du R, Yan X, Wan C, Zhang R and Han B (2017) Sigma Factor Regulated Cellular Response in a Non-solvent Producing Clostridium beijerinckii Degenerated Strain: A Comparative Transcriptome Analysis. Front. Microbiol. 8:23. doi: 10.3389/fmicb.2017.00023

INTRODUCTION

Solventogenic *Clostridium* species are unique microorganisms due to their natural ability to use a wide range of substrates as carbon sources to produce large amounts of bio-butanol, a process termed acetone-butanol-ethanol (ABE) fermentation (Lee et al., 2008). ABE fermentation is a biphasic process in which solventogenic *Clostridium* species produce acetic and butyric acids

intracellularly, and concomitantly release them into the fermentation broth during the exponential growth or acidogenic phase. This is followed by the solventogenic or stationary growth phase, when the acids are re-assimilated into cells and converted to ABE (Ezeji et al., 2010). Butanol, the major ABE fermentation product, is of remarkable interest, since it can be used as alternative fuel due to desirable fuel characteristics and compatibility with gasoline (Bankar et al., 2013). However, solventogenic *Clostridium* species frequently lose their ability to achieve solventogenesis and accumulate excessive amounts of acetic and butyric acids in the fermentation medium after repeated vegetative subculture or during continuous fermentation, a process called strain degeneration (Kashket and Cao, 1995; Sillers et al., 2008).

While degeneration of *Clostridium acetobutylicum* ATCC 824 is caused by the loss of the mega-plasmid pSOL1 that harbors the *sol* operon expressing alcohol/aldehyde dehydrogenase and CoA transferase genes, responsible for acid re-assimilation (Cornillot et al., 1997); degeneration of *C. saccharoperbutylacetonicum* is caused by deficient formation of NADH from pyruvate (Hayashida and Yoshino, 1990). Since *Clostridium beijerinckii* NCIMB 8052 has no mega-plasmid, with solventogenic genes located in the 6.7-Mbp single circular chromosomal DNA (Chen and Blaschek, 1999), this microorganism undergoes degeneration different from *C. acetobutylicum* ATCC 824. Studies applying proteomics and DNA microarrays have been carried out to generate industrially valuable *Clostridia* strains (Tomas et al., 2003; Alsaker and Papoutsakis, 2005; Wang et al., 2012, 2013; Han et al., 2013; Zhang and Ezeji, 2013); however, no genome wide transcriptomic analysis for strain degeneration has been reported.

We recently obtained a degenerated *C. beijerinckii* strain from NCIMB 8052, which only produces 0.58 g/L butanol and 0.87 g/L total ABE at maximum OD_{600} of 2.21. In addition, at the protein level, *C. beijerinckii* 8052 shows lower expression levels of proteins responsible for the disruption of RNA secondary structures, DNA repair, sporulation, signal transduction, transcription regulation, and membrane transport (Lv et al., 2016). Transcriptional profiling of fermentation culture for the degenerated strain may provide more biological evidence and unveil the molecular basis for strain degeneration in this group of microorganisms, especially *C. beijerinckii* NCIMB 8052, whose solventogenic genes are located in the chromosome.

The objective of this study was to explore the molecular basis of degeneration in *C. beijerinckii* NCIMB 8052 by applying genome-wide transcriptional analysis of the WT-8052 and its degenerated strain DG-8052. Comparison of transcriptome profiles associated with ABE production would provide valuable insights regarding potential targets for metabolic engineering of *C. beijerinckii* NCIMB 8052, to prevent strain degeneration and develop robust industrial butanol producing bacteria.

MATERIALS AND METHODS

Bacterial Strains and Culture Conditions

Clostridium beijerinckii NCIMB 8052 and its degenerate strain *C. beijerinckii* DG-8052 were used in this study. *C. beijerinckii* DG-8052 is a non-ABE producing strain, and was generated as described previously (Lv et al., 2016). Tryptone–Glucose–Yeast Extract medium was used to culture *C. beijerinckii* NCIMB 8052 and DG-8052 cells, in an anaerobic chamber.

Batch Fermentation

To perform transcriptional analyzes of *C. beijerinckii* WT-8052 and DG-8052, 6% (v/v), actively growing pre-cultures were sub-cultured into the P2 fermentation medium; unless otherwise stated, all experiments were carried out in triplicate, and temperature was maintained at 35 ± 1°C without shaking or pH control. The pH profile of cultures was monitored on a Beckman Φ500 pH meter. Growth of *C. beijerinckii* strains was estimated at OD_{600} on a F-7000 spectrophotometer (Ezeji et al., 2004; Han et al., 2011).

Total RNA Isolation and Purification

After 12 and 24 h of fermentation, 10 mL of *C. beijerinckii* (WT-8052 and DG-8052) culture were centrifuged at 5000 g and 4°C for 10 min. The resulting cell pellets were kept for total cellular RNA extraction with RiboPure™ bacteria RNA Purification Kit (Ambion®, Life Technologies, Inc., USA) according to the manufacturer's instructions. RNA concentration was measured on a NanoDrop 1000 (NanoDrop Technologies, Wilmington, DE, USA). RNA quality was assessed by 1.2% denatured formaldehyde gel electrophoresis. RNA samples for microarrays had 23S:16S rRNA ≥ 2:1, and A260:A280 ≥ 1.80.

Comparative Microarray Hybridization

Complementary DNA (cDNA) synthesis and amino-allyl labeling were performed as described previously (Almeida et al., 2006). Using the crystal Core® cDNA amplified RNA labeling kit (CapitalBio, Beijing, China), 1 μg of total RNA was reverse transcribed into cDNA and labeled with 100 μM each dATP, dTTP, and dGTP, and 25 μM Cy3- or Cy5-labeled dCTP. For two-color microarray hybridization, Cy5 labeled DG-8052 cDNA and Cy3 labeled WT-8052 cDNAs from samples collected at both acidogenic (12 h, three samples) and solventogenic (24 h, three samples) growth phases were used. Microarray probes were designed with the Agilent eArray software[1], based on the genomic sequence of *C. beijerinckii* NCIMB 8052. Hybridization was performed by CapitalBio corporation (Beijing, China) and Agilent Technologies (Beijing, China) using a custom-made Agilent chip (15000 probes/array). To reduce technical variations, three identical replicates of each *C. beijerinckii* probe (60mer) with 60 negative and positive control probes were included in each array. The 12 and 24 h triplicate samples were hybridized to six arrays; the hybridized slides were scanned on an Agilent G2565CA Microarray Scanner, and the GenePix® Pro 7 Microarray Acquisition and Analysis Software (Molecular Devices, Sunnyvale, CA, USA) was used for data extraction.

[1]https://earray.chem.agilent.com/earray/

Microarray Data Analysis

The extracted images were analyzed with Molecular Annotation System V4.0 (CapitalBio, Beijing, China). Since normalization of signal intensities is needed to render gene expression levels measured by two different dyes comparable, raw signal intensities of messenger RNAs (genes) were normalized with LOWESS (Locally Weighted Scatterplot Smoothing) as described previously (Berger et al., 2004). For each array, gene expression ratios were calculated by dividing Cy5 intensities (DG-8052 signals) by those of Cy3 (WT-8052 signals). The expression ratio for each gene was the average expression ratio of the three replicates. To identify differentially expressed (up- and down-regulated) genes and facilitate a fair comparison between WT-8052 and DG-8052 genes, fold changes were calculated as previously proposed; a cut-off of 2 was set to define differential expression (Quackenbush, 2002). Gene expression profiles of DG-8052 and WT-8052 were analyzed by pairwise and point-by-point comparisons using SAM (Significant Analysis of Microarrays) version 2.23b. To reduce false positives, *p*-value was adjusted to *q*-value. Therefore, genes with greater than twofold change and q-value < 0.05 were considered to be significantly regulated. Gene Ontology enrichment and Kyoto Encyclopedia of Genes and Genomes (KEGG) analyses were performed to elucidate the functions of differentially expressed messenger RNAs (molecular function). Using DAVID Functional Annotation Bioinformatics Microarray Analysis, further functional enrichment analyses were performed to identify cellular and metabolic pathways, especially the statistically overrepresented groups (Zhang and Ezeji, 2013).

Microarray Data Accession Number

All protocols associated with the development of this microarray platform, including but not limited to information regarding probe sequences and synthesis, labeling, hybridization and scan protocols, as well as microarray data have been submitted to NCBI's Gene Expression Omnibus database at http://www.ncbi.nlm.nih.gov/geo/ (GEO accession number GSE63671).

Quantitative Real-Time PCR (qRT-PCR)

To validate microarray data, 10 up-regulated (Cbei_4123, Cbei_0411, Cbei_0311, Cbei_3120, Cbei_0441, Cbei_0331, Cbei_4824, Cbei_2740, Cbei_4871, and Cbei_3356) and 10 down-regulated (Cbei_3835, Cbei_1930, Cbei_0677, Cbei_2826, Cbei_2600, Cbei_1583, Cbei_1079, Cbei_0284, Cbei_3832, and Cbei_2261) genes were randomly selected for qRT-PCR. *C. beijerinckii* (WT-8052 and DG-8052) cultures were grown anaerobically, and cells were harvested after 12 and 24 h of fermentation as described above. RNA was isolated and quantitated as described above. For qRT-PCR, primers specific to the 20 selected genes were designed (Supplementary Table S1). The 16S rRNA gene of *C. beijerinckii* 8052 was used as internal control. Specifically, total RNA (2 μg) was reverse transcribed into cDNA with the SuperScript^{TM} III reverse transcriptase (Invitrogen Corporation, Carlsbad, CA, USA). The expression levels of all tested genes were normalized to the amounts of the internal control gene 16S rRNA (Han et al., 2013).

Cellular Aging and Scavenging Ability of Reactive Oxygen Species

Given that total oxygen species (ROS) are continually generated and possibly degraded under normal physiological conditions, and considering their roles in cell signaling, homeostasis and aging (Kohanski et al., 2008), ROS (·OH), generated by100 μM of ferrous perchlorate (II) and 1 mM of H_2O_2 in *C. beijerinckii* DG-8052 and WT-8052 during ABE fermentation were assessed. Briefly, 12 and 24 h *C. beijerinckii* DG-8052 (100 ml) and WT-8052 cultures (100 ml) grown in P2 medium were used for analyses. About 1 ml culture was centrifuged at 5000 g for 5 min, with the resulting cell pellet suspended in 500 μl of 1 × PBS buffer (pH 7.2) followed by addition of 100 μM ferrous perchlorate (II) (50 μl) and 1 mM H_2O_2 (38 μl) to generate hydroxyl radical. About 1 μl of the cell-permeable fluorogenic probe aminophenyl fluorescein (APF, Molecular Probes^{TM}, Invitrogen, Life Technology; 10 μM), a fluorescent reporter dye, was added to the mixture for 30 min at 35°C. Then, the cells were washed three times with P2 medium to remove excess APF probe. Fluorescence (intracellular ROS levels) was measured at excitation/emission wavelengths of 490/515 nm on a microplate reader (Synergy HT, BioTek, USA) (Liu et al., 2013). The produced .OH were toxic to *C. beijerinckii* cells. In *C. acetobutylicum*, cells could detoxify by specific pathway (Riebe et al., 2009). Higher levels of fluorescence indicated lower scavenging ability of ROS in *C. beijerinckii* DG-8052 and WT-8052 cells. And this experiment could investigate the differences in cell aging between DG-8052 and WT-8052.

Statistical Analysis

Data were analyzed by ANOVA, with $p < 0.05$ considered statistically significant. Unless otherwise stated, all data were expressed as mean ± SD ($n \geq 3$). All analyses were performed using the General Linear Model (GLM) procedure of SAS Version 9.1.3 (SAS Institute Inc., Cary, NC, USA).

RESULTS

Growth of Degenerated Strain *C. beijerinckii* DG-8052

In solventogenic *Clostridium* species, the spore development (sporulation) usually accompanies with the production of solvents. Electron microscopy showed the typical vegetative cells of WT-8052 and DG-8052, and were rod shaped at 12 h (8–10 μm × 0.8 μm, **Figures 1A,C**). At 24 h, WT-8052 cells were in the stationary phase and started to produce solvents, and were rod-shaped with a round end (**Figure 1B**), indicating the developing of pre-endospores. While DG-8052 showed a large proportion of non-split and elongated rod cells (8–12 μm × 0.8 μm, **Figure 1D**). Fermentation results also verified that DG-8052 lost the solvent producing ability, with reduced cell optical density (**Figure 2**).

Overall Gene Transcription Dynamics

Total RNA was isolated from DG-8052 and WT-8052 cell specimens, at 12 and 24 h, separately. Then, transcriptome

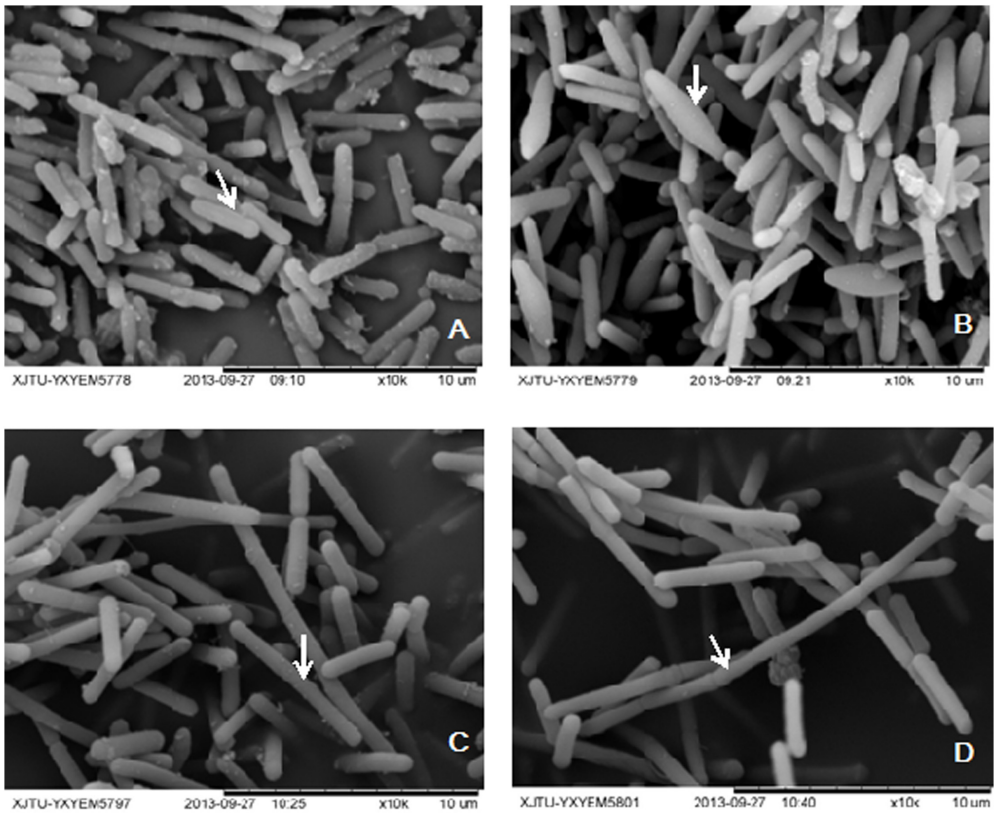


FIGURE 1 | Electron micrograph of *Clostridium beijerinckii* NCIMB 8052 WT-8052 and DG-8052 cells. WT-8052 cells were taken at 12 h **(A)** and 24 h **(B)**; DG-8052 cells were taken at 12 h **(C)** and 24 h **(D)**. WT-8052 cells at 12 h were in rod-shape, and in rod-shape with a rounded end at 24 h, which indicating the developing of pre-endospores; DG-8052 cells were all in non-split and elongated rod-shape both at 12 and 24 h, which were disable to produce solvents and form spores. The typical cells were indicated by white arrows.

profiles of WT-8052 and DG-8052 were assessed by microarrays. This study examined the expression of 5168 genes representing 98.6% of the *C. beijerinckii* NCIMB 8052 genome (Supplementary Tables S3 and S4). DG-8052 showed 548 and 702 genes significantly up-regulated in the acidogenic and solventogenic phases, respectively. According to pathway enrichment and Gene Ontology terms, these genes were significantly overrepresented in cellular functions such as sugar transport system, sugar metabolic pathways, and bacterial chemotaxis. Meanwhile, there were 699 and 797 genes significantly down-regulated in the acidogenic and solventogenic phases, respectively. The repressed genes were mainly enriched in functions, such as sporulation-related biosynthesis, oxidoreduction, and solvent production (**Figures 3** and **4**; **Table 1**). Not all the regulated genes had known function, and COG analysis revealed that 286 and 333 regulated genes in the acidogenesis and solventogenesis phases, respectively, had unspecified functions.

Sugar Phosphotransferase System (PTS) and Sugar Metabolism Related Genes

At the vegetative growth stage of DG-8052, expression of phosphotransferase system (PTS) operons was significantly elevated. The main sugar families affected by altered PTS expression were mannose/fructose/sorbose (Man), lactose/cellobiose (Lac), mannitol (Fru), sucrose/glucoside (Glc), and glucitol/sorbitol (Gut) families (**Figure 2**; Supplementary Table S5a). The sigma-54 dependent PTS operon of the Lac family was characterized in *Listeria monocytogenes*; it regulates the *lpo* operon associated with a cognate activator LacR and positive regulated the sugar transporter (Dalet et al., 2003). In DG-8052, sigma 54 (Cbei_0595) showed an increased expression with 5.75 fold change at 12 h. Four sigma-54 dependent PTS lactose operons (Cbei_0220-0222, Cbei_0950-0953, Cbei_4684-4685, and Cbei_4639-4640) had significantly higher expression levels in DG-8052 (**Figure 3A**). In the Man family operons (Cbei_0953-0959, Cbei_0962-0967, and Cbei_4555-4560), the sigma 54 factor interaction domains (Cbei_0953, 0954, 0962, 4555, 3875, and 4915) were all up-regulated with fold changes of +2.68, +2.38, +2.17, +6.36, +2.64, +2.87, respectively (**Figure 3A**). Beside Sigma-54 factor, several operons were found with elevated expression levels in other families positively regulated by the transcriptional anti-terminator *bglG* (**Figure 3**). Such operons include Fru family Cbei_0239–0245 and Cbei_2739-2741, Gut (Glucitol) family Cbei_0333–0340, and Glc family Cbei_2833. The BglG near

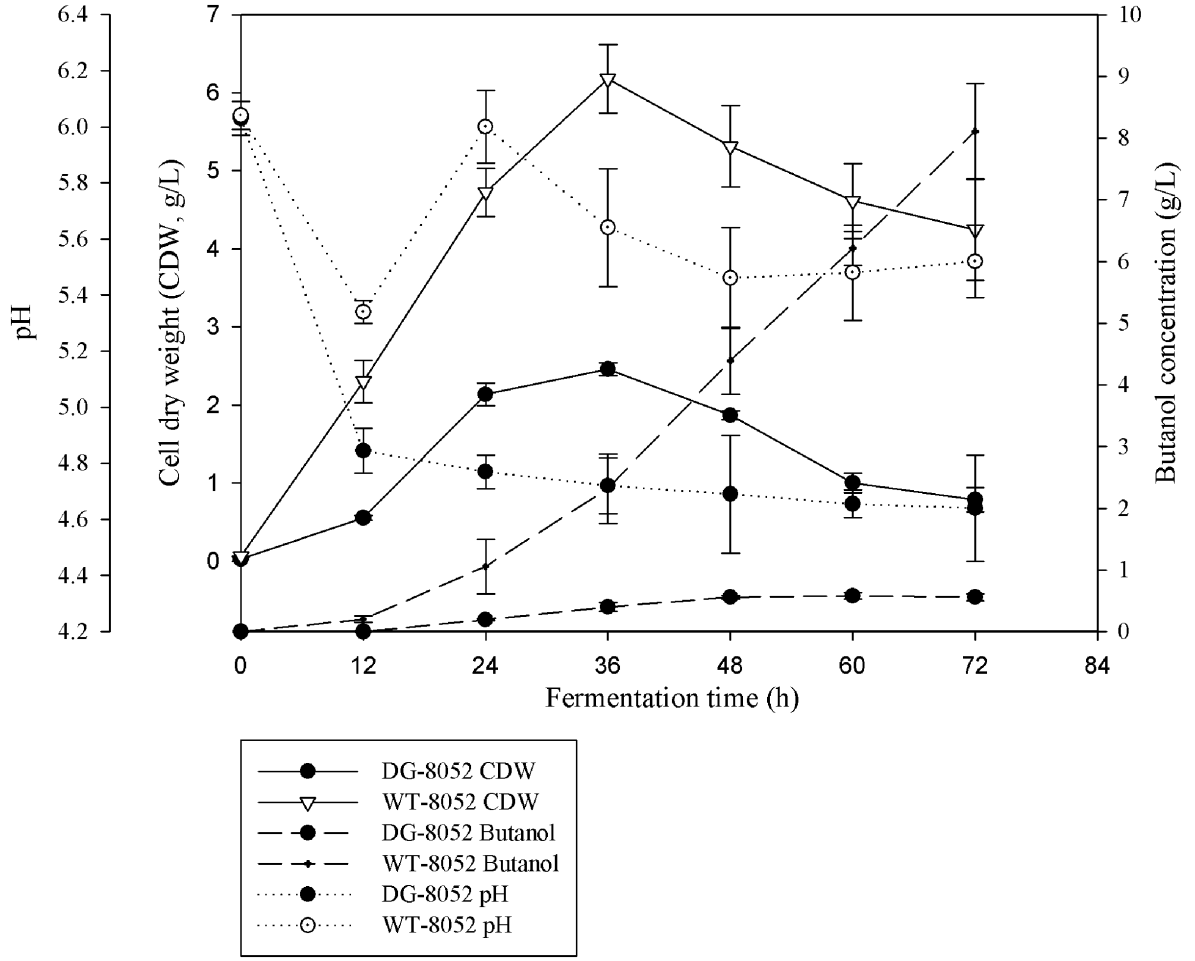


FIGURE 2 | Fermentation profiles for *C. beijerinckii* NCIMB 8052 and its degenerate stain DG-8052 in P2 medium.

the operons showed high expression level, including Cbei_0242 (+6.34), Cbei_2738 (+19.95), Cbei_0334 (+2.63), Cbei_2834 (+2.67).

Beside sugar transporter genes, genes related to sugar metabolic pathways were up-regulated as well in DG-8052, including glycolysis, pentose phosphate pathway, starch and sucrose metabolic pathway, galactose metabolic pathway, and inositol phosphate metabolic pathway (**Figure 3B**; Supplementary Table S5b). In DG-8052, the glycolysis rate-limiting enzymes *pfk* (Cbei_0998, −2.15, −3.61; Cbei_4852, −2.69, −2.48), *pyk* (Cbei_4851, −2.22, −1.73; Cbei_1412, −1.43, −3.16) and *pgam* (Cbei_3168, −8.02, −9.44) were all down-regulated (**Figures 3B** and **4B**). Lower transcription of rate-limiting enzymes in the glycolytic pathway – *pfk* and *pyk* may cause decreased expression of phosphofructokinase and pyruvate kinase, yielding less ATP during glycolysis. This may explain the poor growth and slow metabolism using carbon source in DG-8052 cells. SigE (Cbei_1120, 1.99, −9.81) was down-regulated significantly at 24 h. There may be a similar positive regulation by SigE in degenerated clostridia.

Sigma Factors and Sporulation Genes

In this study, transcription levels of sporulation factors were reduced in the solventogenesis phase, such as YlmC/YmxH (Cbei_1122, −28.65), YunB (Cbei_4229, −4.51), and YtfJ (Cbei_1877, −2.98); sporulation stage II, protein E (Cbei_0097, −21.02), protein R (Cbei_0395, −2.51), protein D (Cbei_0422, −20.31), and protein P (Cbei_0832, −11.68); stage III, protein AA (Cbei_1692, 21.72), protein SpoAB (Cbei_1693, 12.98), protein AC (Cbei_1694, 4.40), protein AD (Cbei_1695, 26.32), protein AE (Cbei_1696, 16.05), protein AG (Cbei_1697, 13.58), protein AH (Cbei_1698, 27.17), and transcription regulator SpoIIID (Cbei_0424, −33.32); stage IV, protein A(Cbei_1136, −8.57) and protein B(Cbei_1711, −6.00); stage V sporulation, protein E (Cbei_1583, −2.21). Sporulation is generally regulated by the transcription factor Spo0A and other sigma factors, such as SigH, SigF, SigE, and SigG, in gram-positive bacteria (Li and McClane, 2010; Kirk et al., 2014). Compared with WT-8052, DG-8052 had the decreased transcription of SigH (sigma 70, Cbei_0135, −2.06, −1.79), Spo0A (Cbei_1712, −3.16, −5.35), SigE (Cbei_1120, 1.99, −9.81), and SigG (Cbei_1121,

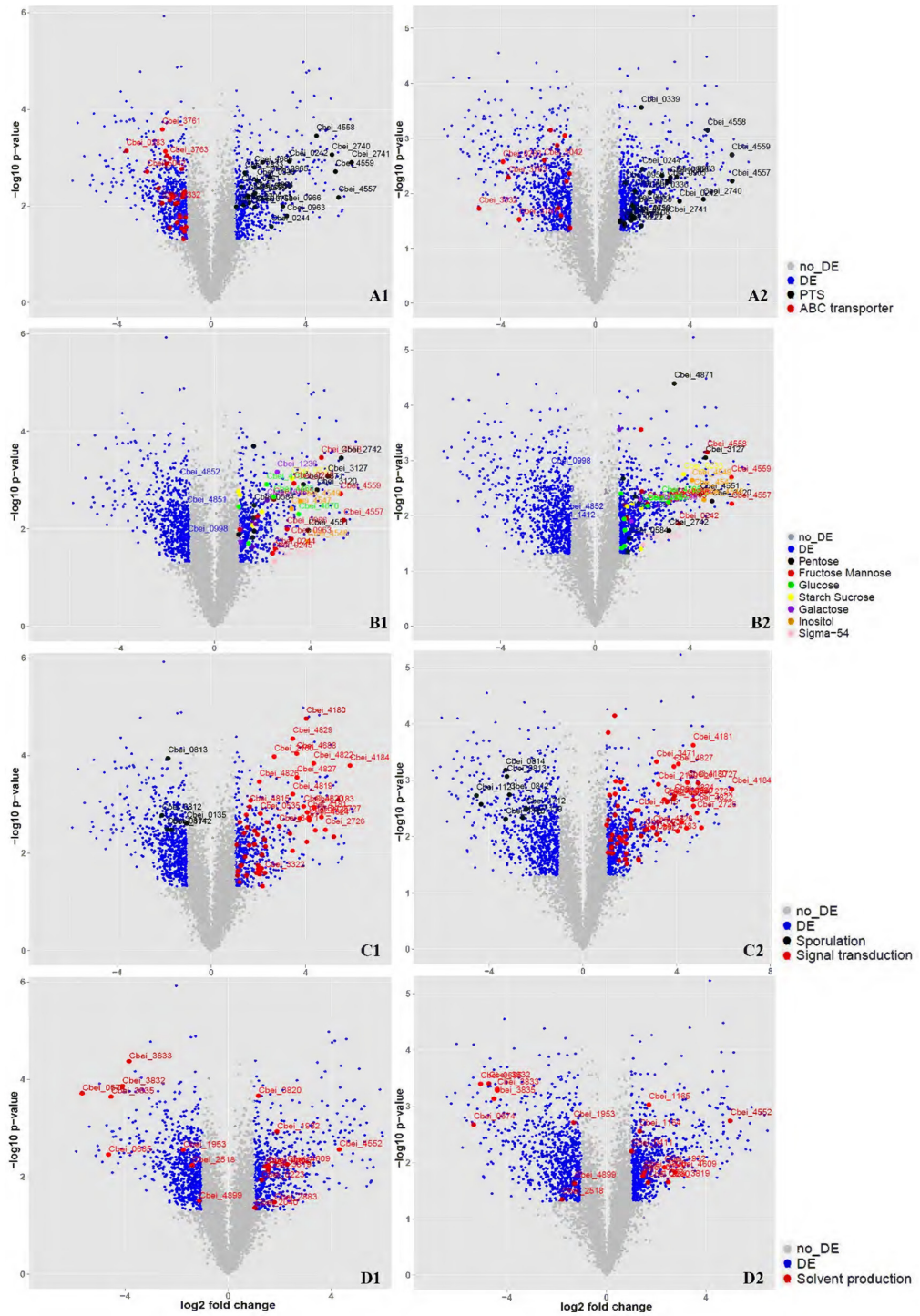


FIGURE 3 | Overview of the related genes expressed significantly at DG-8052 compared with WT-8052. Cell samples from both strains were taken at 12 and 24 h to compare transcriptome profiles at acidogenic and solventogenic phases, respectively. Genes with significantly differential expression (fold change > 2 and *p*-value < 0.05) between the two strains were shown in blue while the others with non-significantly differential expression were shown in gray. Sugar transporter (12 h, **A1**; 24 h, **A2**), Sigma-54 and sugar metabolism (12 h, **B1**; 24 h, **B2**), Sporulation and signal transduction (12 h, **C1**; 24 h, **C2**), Solvent production (12 h, **D1**; 24 h, **D2**). DE, differential expression; no_DE, no differential expression; PTS: phosphotransferase system; ABC transporter: ATP-binding cassette transporters; Pentose: pentose phosphate pathway; Fructose Mannose: fructose and mannose metabolism; Glucose: glycolysis/gluconeogenesis; Starch sucrose: starch and sucrose metabolism; Galactose: galactose metabolism; Inositol: inositol phosphate metabolism; Signal transduction: including chemotaxis, two-component signal transduction system and sensor proteins.

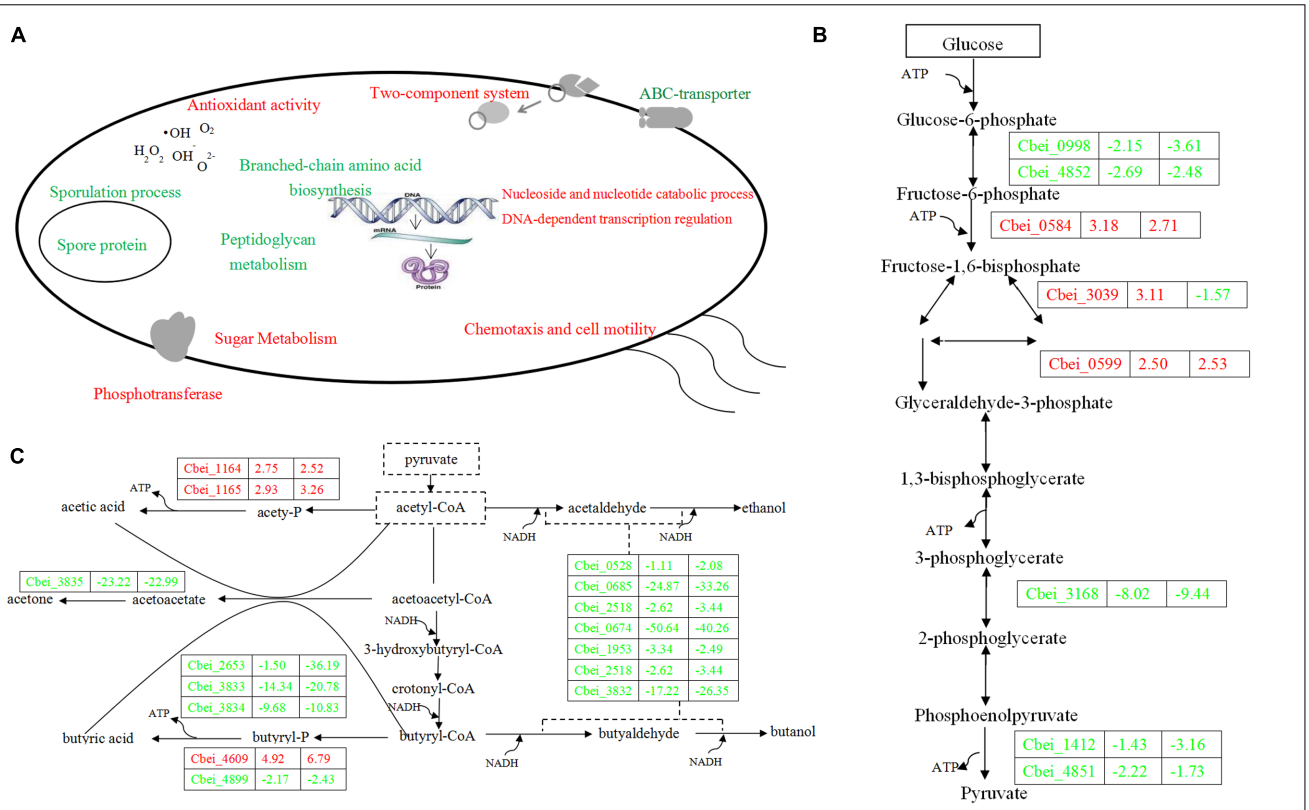


FIGURE 4 | Sketch map of *C. beijerinckii* NCIMB DG-8052 cell metabolic processes (A), glycolysis pathway **(B)** and solventogenic pathway **(C)**. Blue color indicates the down-regulated function/gene; red color indicates the up-regulated function/gene.

−1.02, −23.22) both in the acidogenic and solventogenic phases (**Figure 3C**; Supplementary Table S5c).

Chemotaxis

This study showed that bacterial chemotaxis was one of the most enriched pathways (p-value < 0.01) up-regulated in DG-8052 at both 12 and 24 h. There were 19 chemotaxis genes up-regulated at 12 h, and induced at 24 h including all the 19 above genes, which encompassed genes encoding methyl-accepting chemotaxis sensory transducer (MCP), auto-phosphorylable sensory histidine kinase CheA, adaptor protein CheW, methyltransferase CheR, methylesterase CheB, and response regulator CheY, with up-regulation fold changes from +2.01 to +82.01 (**Figure 3C**; Supplementary Table S5d).

Solvent Producing Pathway

During acidogenesis, genes encoding acid producing enzymes showed higher expression levels in DG-8052 than in WT-8052, e.g., acetate kinase (Cbei_1165, +2.93), phospho-trans-acetylase (Cbei_1164, +2.75), and butyrate kinase (Cbei_4609, +4.92) (**Figure 3D**; Supplementary Table S5). When acids accumulate to a certain level, CoA-transferase begins to re-assimilate them into cells (Millat et al., 2014). In *C. beijerinckii* 8052, a *sol* operon organized in order of *ald* (aldehyde dehydrogenase, Cbei_3832)-*ctfA* (CoA-transferase subunit A, Cbei_3833)-*ctfB* (CoA-transferase subunit B, Cbei_3834); In DG-8052, the coordinated expression was observed for the *sol* operon genes, Cbei_3832-Cbei_3833-Cbei_3834) were all down-regulated at fold changes from −17.22, −14.34, −9.68 (acidogenesis) to −4.91, −20.78, −10.83 (solventogenesis), respectively. In DG-8052, there had several *aldA* copes (aldehyde dehydrogenase, Cbei_1953, Cbei_3832, Cbei_0674, and Cbei_2518), which probes were all down-regulated, especially Cbei_0674 (−50.64, −40.26) (Supplementary Table S5f). In addition, acetoacetate decarboxylase (Cbei_3835, −23.22, −22.99) was greatly down-regulated as well. While there had no obvious changes between DG-8052 and WT-8052 in enzymes, which including acetyl-CoA acetyltransferase (Cbei_0411, Cbei_3630) catalyzing acetyl-CoA into acetoacetyl-CoA; 3-hydroxybutyryl-CoA dehydrogenase (Cbei_0324, Cbei_0325, Cbei_2037) catalyzing acetoacetyl-CoA into 3-hydroxybutyryl-CoA; Enoyl-CoA hydratase (Cbei_2231, Cbei_2230) catalyzing 3-hydroxybutyryl-CoA into crotonyl-CoA; butyryl-CoA dehydrogenase (Cbei_0322, Cbei_2035, Cbei_2883) catalyzing crotonyl-CoA into butyryl-CoA (**Figures 3D** and **4C**; Supplementary Table S5f).

Cellular Aging and Scavenging Ability of Reactive Oxygen Species

To investigate the differences in cell aging between DG-8052 and WT-8052, the concentration of total reactive oxygen species (ROS) were measured. ·OH was generated by100 μM of ferrous

TABLE 1 | Kyoto Encyclopedia of Genes and Genomes (KEGG) pathway showing significant changes in *Clostridium beijerinckii* DG-8052.

Culture	KEGG ID	Pathway definition	*p*-value	Benjamini*	Count**
Up-regulated					
12 h	cbe02030	Bacterial chemotaxis	2.0E−4	1.0E−1	19
	cbe00051	Fructose and mannose metabolism	4.0E−4	1.1E−2	17
	cbe02060	Phosphotransferase system (PTS)	5.3E−4	9.3E−3	24
	cbe00040	Pentose and glucuronate interconversions	8.0E−4	1.0E−2	12
	cbe00562	Starch and sucrose metabolism	3.1E−2	2.4E−1	10
	cbe00030	Pentose phosphate pathway	3.8E−2	2.6E−1	11
	cbe00052	Galactose metabolism	4.3E−2	2.5E−1	8
24 h	cbe02030	Bacterial chemotaxis	1.3E−5	7.7E−4	24
	cbe02060	PTS	2.1E−4	6.2E−3	29
	cbe00051	Fructose and mannose metabolism	6.9E−4	1.4E−2	19
	cbe00040	Pentose and glucuronate interconversions	1.6E−3	2.4E−2	13
	cbe00562	Starch and sucrose metabolism	7.3E−3	8.4E−2	13
	cbe00030	Pentose phosphate pathway	1.4E−2	1.1E−1	14
	cbe00052	Galactose metabolism	1.8E−2	1.3E−1	10
	cbe02020	Two-component system	3.8E−2	2.3E−1	17
	cbe00010	Glycolysis/gluconeogenesis	5.5E−2	2.9E−1	13
	cbe00520	Amino sugar and nucleotide sugar metabolism	5.6E−2	2.7E−1	15
Down-regulated					
12 h	cbe02010	ABC transporters	3.8E−5	2.1E−3	32
	cbe00290	Valine, leucine, and isoleucine biosynthesis	8.6E−4	2.3E−2	9
	cbe00240	Pyrimidine metabolism	7.8E−2	7.7E−1	10
24 h	cbe00633	Trinitrotoluene degradation	4.2E−4	2.2E−2	5
	cbe00680	Methane metabolism	8.2E−3	2.0E−1	4
	cbe00290	Valine, leucine, and isoleucine biosynthesis	1.3E−2	2.1E−1	7
	cbe00340	Pyrimidine metabolism	2.1E−2	2.4E−1	11
	cbe00051	Fructose and mannose metabolism	2.3E−2	2.2E−1	11
	cbe00260	Glycine, serine, and threonine metabolism	4.9E−2	3.6E−1	6
	cbe00230	Purine metabolism	5.3E−2	3.4E−1	11

*Significant groups were selected based upon Benjamini (<0.05). **Number of genes within the given KEGG ID showing a significant change in their expression level.

perchlorate (II) and 1 mM of H_2O_2, and the produced ·OH were toxic to *C. beijerinckii* cells. *C. beijerinckii* could detoxify by the similar pathway (NADH oxidase). In DG-8052, a higher fluorescence signal was detected indicating higher amount of ROS residues than that of DG-8052 (**Figure 5**). It was also observed at the same fermentation time, DG-8052 cells had less viability than WT-8052 cells, which may result from the high cellular oxidative stress in DG-8052.

Validation of Gene Expression Data from Microarray Analysis by Q-RT-PCR

To validate microarray data, Q-RT-PCR was applied to quantify gene expression levels in triplicate cultures of WT-8052 and DG-8052 in the same conditions used for the microarray analysis. A total of 14 and six genes were selected in the acidogenic (12 h) and solventogenic (24 h) phases, respectively for evaluation. The results from both expression assays, microarrays and Q-RT-PCR, showed that gene expression levels in WT-8052 vs DG-8052 had a high correlation at both 12 h ($R = 0.96$) and 24 h ($R = 0.93$) (**Figure 6**, Supplementary Figure S1; Supplementary Table S1).

DISCUSSION

This study showed a dysfunction in spore formation and solvent production in DG-8052, which was similar to degenerated *C. acetobutylicum* M5, a strain with loss of the mega-plasmid pSOL1 containing the key solvent formation genes under the *sol* operon (*aad-ctfA-ctfB*) and *adc* gene (Sillers et al., 2008), as well as degenerated *C. acetobutylicum* SKO1, a strain with inactivated *spo0A* gene (Tomas et al., 2003). In *C. beijerinckii* NCIMB 8052, however, no mega-plasmid has ever been found, and therefore its degeneration could not be ascribed to the loss of key genes on the mega-plasmid, leaving the mechanism largely unclear.

Compared with WT-8052, genome resequencing of DG-8052 (SRP082285) showed no general regulator mutated. As we reported recently (Jiao et al., 2016), a total of 20 SNPs (17 non-synonymous, two premature stop, and one intergenic) and 16 InDels (10 coding and six non-coding) were found in the DG-8052 genome; among them, eight SNPs were effected by strain degeneration (Supplementary Table S2), and no transcription change was observed in the remaining 12 DG-8052 mutations. The transcriptional analysis suggested there's little doubt that *C. beijerinckii* 8052 degeneration drastically altered

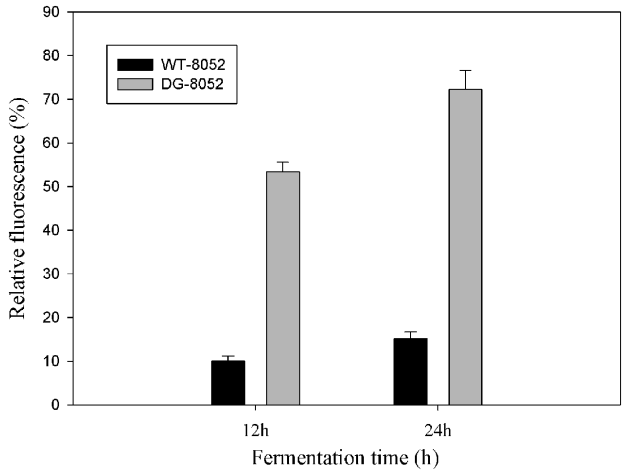


FIGURE 5 | Comparison of the reactive oxygen species produced and accumulated in DG-8052 and WT-8052. 100 μM of ferrous perchlorate (II) and 1 mM of H_2O_2 was used to generate hydroxyl radical, and it was mixed with aminophenyl fluorescein (APF). The green fluorescence was used as positive control. The fluorescence signal of mixture (WT-8052 and DG-8052 cells culture in 12 and 24 h with APF separately) were compared with positive control to get the relative fluorescence (%).

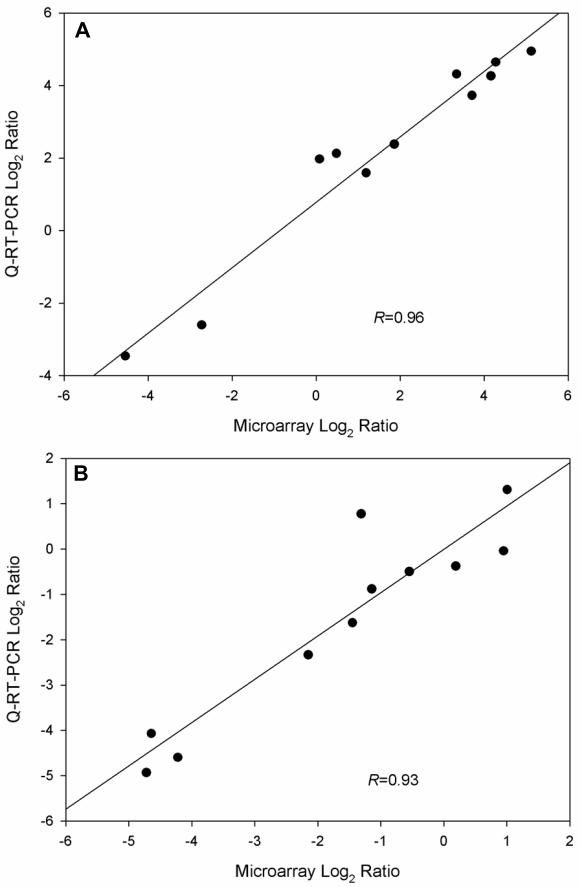


FIGURE 6 | Validation of microarray data from *C. beijerinckii* DG-8052 at two growth stages using Q-RT-PCR. (A) Acidogenic phase and **(B)** solventogenic phase.

gene regulation, resulting in corresponding morphological and physiological changes. At the proteomic level, 3% of proteins were shown to be differentially expressed in DG-8052, resulting in the corresponding morphological and physiological changes (Lv et al., 2016). At the transcriptomic level, further mining of the current data will help reveal the regulatory mechanisms and sensitive gene targets for developing degenerated *Clostridium* strains.

Transcriptional analysis of degenerated *C. beijerinckii* strain DG-8052 suggests morphological and physiological changes were related to the disturbed expression of sigma factors, from aspects of sugar transport and metabolism, sporulation, chemotaxis, and solventogenic pathway.

The sigma-54 dependent PTS operon of the Lac family was characterized in *Listeria monocytogenes*; it regulates the *lpo* operon associated with a cognate activator LacR and positive regulated the sugar transporter (Dalet et al., 2003). In our study, four sigma-54 dependent PTS lactose operons, three sigma-54 dependent Man family operons were all up-regulated in DG-8052. Beside Sigma-54 factor, several operons were found with elevated expression levels in other families positively regulated by the transcriptional anti-terminator *bglG*. These findings suggested that PTS operons for sugar families may be regulated by sigma-54 and/or *bglG*, which deserves further experimental verification.

Beside sugar transporter genes, genes related to sugar metabolic pathways were up-regulated as well in DG-8052, including glycolysis, pentose phosphate pathway, starch and sucrose metabolic pathway, galactose metabolic pathway, and inositol phosphate metabolic pathway. Lower transcription of rate-limiting enzymes in the glycolytic pathway – *pfk* and *pyk* may cause decreased expression of phosphofructokinase and pyruvate kinase, yielding less ATP during glycolysis. This may explain the poor growth and slow metabolism using carbon source in DG-8052 cells. In *Cyanobacterium synechocystis* sp. PCC 6803, sugar catabolic pathways were positively regulated by SigE. Indeed, *sigE* mutation in *C. synechocystis* causes reduced transcription of these genes, including *pfkA*, *gap*, *pyk*, *zwf*, *opcA*, *gnd*, *tal*, *glgX*, and *glgp* (Osanai et al., 2005). In DG-8052, the down-regulated SigE may work as a similar positive regulator.

Sporulation is generally regulated by the transcription factor Spo0A and other sigma factors, such as SigH, SigF, SigE, and SigG, in gram-positive bacteria (Li and McClane, 2010; Kirk et al., 2014). *Spo0A* gene inactivation resulted in the degenerated *C. acetobutylicum* SKO1 strain, which shows an asporogenous, filamentous and largely deficient solventogenic phenotype (Tomas et al., 2003). In *B. subtilis*, the sigma factor SigH (*spo0H*) regulates *spo0A* (Saujet et al., 2011); SigH and Spo0A regulate SigE, which in turn induces the transcription of SigK; SigF controls SigG; SigH and Spo0A may also bind to the promoter region of the *sigF* operon and positively regulate the anti-anti-sigma factors SpoIIAA, SpoIIAB, and SigF (Sierro et al., 2008). In DG-8052, the repressed SigH and Spo0Adecreased the

transcription levels of SigE, SpoIIAA, SpoIIAB and SigF, both in the acidogenic and solventogenic phases; meanwhile, down-regulated SigF positively regulated SigG. SpoIIGA is required for intermembrane proteolytic cleavage of pro-SigE pro-sequences (Dougan, 2013). The *Bacillus* SpoIIGA protein is involved in sporulation and septum formation (Fawcett et al., 2000). The reduced expression of SpoIIGA and other proteolysis genes such as sporulation protease and peptidase overtly hindered spore formation, since intermembrane proteolytic regulation is crucial during this stage. RNA polymerase factor sigma-70 (SigH), appeared to be the key regulatory switch, acting in the acidogenic phase. It may be a potential target gene for decreasing or preventing strain degeneration.

During acidogenesis, genes encoding acid producing enzymes showed higher expression levels in DG-8052. When acids accumulate to a certain level, CoA-transferase begins to re-assimilate them into cells and prepare solvent production. Indeed, decreased expression of CoA-transferase suppresses re-assimilation of acetic and butyric acids in *C. acetobutylicum* (Millat et al., 2014). The *sol* operon *ald-ctfA-ctfB*, *aadc* genes, were all down-regulated in DG-8052. The aldehyde dehydrogenase *aldA* gene is essential for the catabolism of alcohols, and regulated by sigma-54 in *Azotobacter vinelandii* (Gama-Castro et al., 2001). While, in *Clostridium kluyveri*, it was reported that acetoacetyl-CoA, 3-hydroxybutyryl-CoA and crotonyl-CoA are downregulated by Sigma-L, a member of the sigma54 family (Söhling and Gottschalk, 1996). In this study, a non-significant transcription level change of SigL may explain the similar transcription levels of acetoacetyl-CoA, 3-hydroxybutyryl-CoA and crotonyl-CoA in DG-8052.

Spore development (sporulation) is usually accompanied with solvent production in solventogenic *Clostridium* species (Lee et al., 2008). The sporulation associated sigma factors SigH, SigF, Sig K, SpoIIGA, SigE, and SigG were all down-regulated in DG-8052, leading to failed sporulation process. Since solventogenic genes are transcribed and expressed in the sporulation growth stage, uncompleted sporulation may result in reduced transcription of such genes. Therefore, the sigma-70 factor regulated spore formation may contribute to the lost capability of producing solvents in DG-8052 cells; CoA-transferase genes may be the main targets. Chemotaxis is a bacterial response to environmental stimuli. Motile bacteria migrate in smooth and straight lines toward attractants (positive chemotaxis) and tumble to avoid repellents (negative chemotaxis) (Gutierrez and Massox, 1987). The question raised by up-regulated chemotaxis genes in DG-8052 was how to identify potential attractants or repellents. In our previous report, fermentation of DG-8052 resulted in elevated concentrations of acetic and butyric acids as well as impaired production of acetone, butanol, and ethanol (Lv et al., 2016). Chemotaxis assays have shown that undissociated forms of acetic and butyric acids are attractants for *C. acetobutylicum*, with low pH alone not able to induce positive chemotaxis; meanwhile, acetone, butanol, ethanol, and dissociated acetate and butyrate were shown to be repellents (Gutierrez and Massox, 1987). The current findings are not only in line with previous reports, but also validate their conclusion at the mRNA level. In addition, the notion that undissociated acetic and butyric acids result in positive chemotaxis is also supported by another independent study demonstrating that *C. beijerinckii* challenged with furfural accumulates acetic and butyric acids and up-regulates chemotaxis genes (Zhang and Ezeji, 2013). The association of Spo0A and chemotaxis has been demonstrated by many studies. Overexpression of Spo0A in *C. acetobutylicum* results in decreased cell motility and chemotaxis (Alsaker et al., 2004); meanwhile, Spo0A inactivation in *C. acetobutylicum* SKO1 increases cell motility and chemotaxis genes (Tomas et al., 2003), corroborating this study that Spo0A down-regulation leads to increased transcription of chemotaxis genes.

DG-8052 cells could not complete the typical fermentation process, and died rapidly. It is possible that high concentrations of acetate and butyrate in the medium caused stress to DG-8052 cells. Such stress could induce weak metabolism and cause cell death in an early stage (Kohanski et al., 2008). ROS are formed when molecular oxygen diffuses into cells and is adventitiously reduced at the active sites of redox enzymes containing flavins or quinones. There is a pathway for H_2O_2 and O_2 detoxification in *C. acetobutylicum* that includes NADH peroxidase and NADH oxidase, with detoxification activity depending on cell viability (Riebe et al., 2009). APF, a new ROS indicator, is non-fluorescent until it reacts with hydroxyl radicals, peroxynitrite anion or hypochlorite anion. Upon oxidation, APF exhibits bright green fluorescence, and was used to detect the hypochlorite anion generated by activated neutrophils (Setsukinai et al., 2003). Our findings on the decreased ability of ROS scavenging in DG-8052 could explain this phenomenon. DG-8052 cells had reduced viability compared with WT-8052 cells may also result from high oxidative stress. This suggests that ROS generation, bacterial cell morphology changes and cell degeneration are closely related. However, further study is needed to assess the effects of sigma factors on cell aging regulation.

During the growth of *C. beijerinckii* DG-8052, the accumulation of acetic and butyric acid led to the decreasing of pH ($<$5.5), and provided stress to the cell, which may cause the cell to die rapidly. The transcriptional analysis of non-solvent producing strain DG-8052 suggests morphological and physiological changes are related to altered expression of sigma factors. Dysregulation of the fermentation machinery which mainly including glycolysis to solvent/acid production, solventogenesis and sporulation, Chemotaxis, was accompanied by reduced transcription of rate-limiting enzymes *pfk* and *pyk* in glycolysis, and higher transcription of the cell chemotaxis genes *cheA*, *cheB*, *cheR*, *cheW*, and *cheY*, controlled mainly by σ^{54} in the acidogenesis phase. Meanwhile, abnormal spore formation was associated with repressed *spo0A*, *sigE*, *sigF*, *sigG*, and *sigK,* which were positively regulated by σ^{70} (*sigH*), with corresponding inhibited expression of CoA-transferase in the solventogenesis phase. And the specific gene targets need more experiment verification. These findings provide valuable targets for engineered strain development of *Clostridium* species.

AUTHOR CONTRIBUTIONS

BH, YZ, SJ, JL, and RD conducted the work presented here, performed data analysis and drafted the manuscript. All authors contributed to data interpretation, wrote and revised various parts of the paper. YZ, CW, RZ, and BH revised the overall paper; YZ and BH supervised the work. All authors read and approved the final manuscript.

FUNDING

This work was financially supported by the National Natural Science Foundation of China (31200031, 81673199), and China Postdoctoral Science Foundation funded project (2014M56 2427).

ACKNOWLEDGMENT

We are very grateful to Professor Thaddeus Ezeji for the suggestion in experiment design, data analysis, and manuscript.

SUPPLEMENTARY MATERIAL

The Supplementary Material for this article can be found online at: http://journal.frontiersin.org/article/10.3389/fmicb.2017.00023/full#supplementary-material

REFERENCES

Almeida, J. S., Chen, C., Gorlitsky, R., Stanislaus, R., Aires-de-Sousa, M., Eleutério, P., et al. (2006). Replacing cRNA targets with cDNA reduces microarray cross- hybridization. *Nat. Biotechnol.* 24, 1071–1073. doi: 10.1038/nbt0906-1071

Alsaker, K. V., and Papoutsakis, E. T. (2005). Transcriptional program of early sporulation and stationary-phase events in *Clostridium acetobutylicum*. *J. Bacteriol.* 187, 7103–7118. doi: 10.1128/JB.187.20.7103-7118.2005

Alsaker, K. V., Spitzer, T. R., and Papoutsakis, E. T. (2004). Transcriptional analysis of spo0A overexpression in *Clostridium acetobutylicum* and its effect on the cell's response to butanol stress. *J. Bacteriol.* 186, 1959–1971. doi: 10.1128/JB.186.7.1959-1971.2004

Bankar, S. B., Survase, S. A., Ojamo, H., and Granstrom, T. (2013). The outlook of an academic and industrialist. *RSC Adv.* 3, 24734–24757. doi: 10.4161/gmcr.19264

Berger, J. A., Hautaniemi, S., Järvinen, A. K., Edgren, H., Mitra, S. K., and Astola, J. (2004). Optimized LOWESS normalization parameter selection for DNA microarray data. *BMC Bioinformatics* 5:194. doi: 10.1186/1471-2105-5-194

Chen, C. K., and Blaschek, H. P. (1999). Effect of acetate on molecular and physiological aspects of *Clostridium beijerinckii* NCIMB8052 solvent production and strain degeneration. *Appl. Environ. Microbiol.* 65, 499–505.

Cornillot, E., Nair, R. V., Papoutsakis, E. T., and Soucaille, P. (1997). The genes for butanol and acetone formation in *Clostridium acetobutylicum* ATCC 824 reside on a large plasmid whose loss leads to degeneration of the strain. *J. Bacteriol.* 179, 5442–5447. doi: 10.1128/jb.179.17.5442-5447.1997

Dalet, K., Arous, S., Cenatiempo, Y., and Héchard, Y. (2003). Characterization of unique sigma54-dependent PTS operon of the lactose family in *Listeria monocytogenes*. *Biochime* 85, 633–638. doi: 10.1016/S0300-9084(03)00134-2

Dougan, D. A. (2013). *Regulated Proteolysis in Microorganisms*. Dordrecht: Springer, 89.

Ezeji, T., Milne, C., Price, N. D., and Blaschek, H. P. (2010). Achievements and perspectives to overcome the poor solvent resistance in acetone and butanol producing microbiologisms. *Appl. Microbiol. Biotechnol.* 85, 1697–1712. doi: 10.1007/s00253-009-2390-0

Ezeji, T. C., Qureshi, N., and Blaschek, H. P. (2004). Acetone butanol ethanol (ABE) production from concentrated substrate: reduction in substrate inhibition by fed-batch technique and product inhibition by gas stripping. *Appl. Microbiol. Biotechnol.* 63, 653–658. doi: 10.1007/s00253-003-1400-x

Fawcett, P., Eichenberger, P., Losick, R., and Youngman, P. (2000). The transcriptional profile of early to middle sporulation in *Bacillus subtilis*. *Proc. Natl. Acad. Sci. U.S.A.* 97, 8063–8068. doi: 10.1073/pnas.140209597

Gama-Castro, S., Núñez, C., Segura, D., Moreno, S., Guzmán, J., and Espín, G. (2001). *Azotobacter vinelandii* aldehyde dehydrogenase regulated by δ54: role in alcohol catabolism and encystment. *J. Bacteriol.* 183, 6169–6174. doi: 10.1128/JB.183.21.6169-6174.2001

Gutierrez, N. A., and Massox, I. S. (1987). Role of chemotaxis in solvent production by *Clostridium acetobutylicum*. *Appl. Environ. Microbiol.* 53, 1924–1927.

Han, B., Gopalan, V., and Ezeji, T. C. (2011). Acetone production in solventogenic *Clostridium* species: new insights from non-enzymatic decarboxylation of acetoacetate. *Appl. Microbiol. Biotechnol.* 91, 565–576. doi: 10.1007/s00253-011-3276-5

Han, B., Ujor, V., Lai, L. B., Gopalan, V., and Ezeji, T. C. (2013). Use of proteomic analysis to elucidate the role of calcium on acetone-butanol-ethanol (ABE) fermentation in *Clostridium beijerinckii* NCIMB 8052. *Appl. Environ. Microbiol.* 79, 282–293. doi: 10.1128/AEM.02969-12

Hayashida, S., and Yoshino, S. (1990). Degeneration of solventogenic *Clostridium* caused by a defect in NADH generation. *Agric. Biol. Chem.* 54, 427–435. doi: 10.1080/00021369.1990.10869976

Jiao, S. Y., Zhang, Y., Wan, C. X., Lv, J., Du, R. J., Zhang, R. J., et al. (2016). Transcriptional analysis of degenerate strain *Clostridium beijerinckii* DG-8052 reveals a pleiotropic response to CaCO3-associated recovery of solvent production. *Sci. Rep.* 6:38818. doi: 10.1038/srep38818

Kashket, E. R., and Cao, Z. Y. (1995). Clostridial strain degeneration. *FEMS Microbiol. Rev.* 17, 305–315. doi: 10.1111/j.1574-6976.1995.tb00214.x

Kirk, D. G., Zhang, Z., Korkeala, H., and Lindström, M. (2014). Alternative sigma factors SifF, SigE, and SigG are essential for sporulation in *Clostridium botunium* ATCC 3502. *Appl. Environ. Microbiol.* 80, 5141–5150. doi: 10.1128/AEM.01015-14

Kohanski, M. A., Dwyer, D. J., Wierzbowski, J., Cottarel, G., and Collins, J. J. (2008). Mistranslation of membrane proteins and two-component system activation trigger antibiotic-mediated cell death. *Cell* 135, 679–690. doi: 10.1016/j.cell.2008.09.038

Lee, S. Y., Park, J. H., Jang, S. H., Nielsen, L. K., Kim, J., and Jung, K. S. (2008). Fermentative butanol production by Clostridia. *Biotechnol. Bioeng.* 101, 209–228. doi: 10.1002/bit.22003

Li, J., and McClane, B. A. (2010). Evaluating the involvement of alternative sigma factor SigF and SigG in *Clostridium* perfringens sporulation and enterotoxin synthesis. *Infect. Immun.* 78, 4286–4293. doi: 10.1128/IAI.00528-10

Liu, W., Dong, S. L., Xu, F., Wang, X. Q., Withers, T. R., Yu, H. D., et al. (2013). Effect of intracellular expression of antimicrobial peptide LL-37 on growth of *Escherichia coli* strain TOP10 under aerobic and anaerobic conditions. *Antimicrob. Agents Chemother.* 57, 4707–4716. doi: 10.1128/AAC.00825-13

Lv, J., Jiao, S. Y., Du, R. J., Zhang, R. J., Zhang, Y., and Han, B. (2016). Proteomic analysis to elucidate degeneration of *Clostridium beijerinckii* NCIMB 8052 and role of Ca2+ in strain recovery from degeneration. *J. Ind. Microbiol. Biotechnol.* 43, 741–750. doi: 10.1007/s10295-016-1754-6

Millat, T., Voigt, C., Janssen, H., Coolsley, C. M., Winzer, K., Minton, N. P., et al. (2014). Coenzyme A-transferase-independent butyrate re-assimilation in *Clostridium acetobutylicum*-evidence from a mathematical model. *Appl. Microbiol. Biotechnol.* 98, 9059–9072. doi: 10.1007/s00253-014-5987-x

Osanai, T., Kanesaki, Y., Nakano, T., Takahashi, H., Asayama, M., Shirai, M., et al. (2005). Positive regulation of sugar catabolic pathways in the Cyanobacterium

synechocystis sp. PCC 6803 by the group 2 sigma factor sigE. *J. Biol. Chem.* 280, 30653–30659. doi: 10.1074/jbc.M505043200

Quackenbush, J. (2002). Microarray data normalization and transformation. *Nat. Genet.* 32, 496–501. doi: 10.1038/ng1032

Riebe, O., Fischer, R. J., Wampler, D. A., Kurtz, D. M. Jr., and Bahl, H. (2009). Pathway for H2O2 and O2 detoxification in *Clostridium acetobutylicum*. *Microbiology* 155, 16–24. doi: 10.1099/mic.0.022756-0

Saujet, L., Monot, M., Dupuy, B., Soutourina, O., and Martin-Verstraete, I. (2011). The key sigma factor of transition phase, SigH, control sporulation, metabolism, and virulence factor in *Clostridium diffcile*. *J. Bacteriol.* 193, 3186–3196. doi: 10.1128/JB.00272-11

Setsukinai, K., Urano, Y., Kakinuma, K., Majima, H. J., and Nagano, T. (2003). Development of novel fluorescence probes that can be reliably detect reactive oxygen species and distinguish specific species. *J. Biol. Chem.* 278, 3170–3175. doi: 10.1074/jbc.M209264200

Sierro, N., Makita, Y., de Hoon, M. J. L., and Nakai, K. (2008). DBTBS: a database of transcriptional regulation in *Bacillus subtilis* containing upstream intergenic conservation information. *Nucleic Acids Res.* 36, 93–96. doi: 10.1093/nar/gkm910

Sillers, R., Chow, A., Tracy, B., and Papoutsakis, E. T. (2008). Metabolic engineering of the non-sporulating, non-solventogenic *Clostridium acetobutylicum* strain M5 to produce butanol without acetone demonstrate the robustness of the scid-formation pathways and the importance of the electron balance. *Metab. Eng.* 10, 321–332. doi: 10.1016/j.ymben.2008.07.005

Söhling, B., and Gottschalk, G. (1996). Molecular analysis of the anaerobic succinate degradation pathway in *Clostridium kluyveri*. *J. Bacteriol.* 178, 871–880. doi: 10.1128/jb.178.3.871-880.1996

Tomas, C., Alsaker, K. V., Bonarius, H. P. J., Hendriksen, W. T., Yang, H., Beamish, J. A., et al. (2003). DNA array-based transcriptional analysis of asporogenous, nonsolventogenic *Clostridium acetobutylicum* strain SKO1 and M5. *J. Bacteriol.* 185, 4539–4547. doi: 10.1128/JB.185.15.4539-4547.2003

Wang, Q. H., Venkataramanan, K. P., Huang, H. Z., Papoutsakis, E. T., and Wu, C. H. (2013). Transcription factors and genetic circuits orchestrating the complex, multilayered response of *Clostridium acetobutylicum* to butanol and butyrate stress. *BMC Syst. Biol.* 7:120. doi: 10.1186/1752-0509-7-120

Wang, Y., Li, X., Mao, Y., and Blaschek, H. P. (2012). Genome-wide dynamic transcriptional profiling in *Clostridium beijerinckii* NCIMB 8052 using single-nucleotide resolution RNA-seq. *BMC Genomics* 13:102. doi: 10.1186/1471-2164-13-102

Zhang, Y., and Ezeji, T. C. (2013). Transcriptional analysis of *Clostridium beijerinckii* NCIMB8052 to elucidate role of furfural stress during acetone butanol ethanol fermentation. *Biotechnol. Biofuels* 6, 66–83. doi: 10.1186/1754-6834-6-66

Conflict of Interest Statement: The authors declare that the research was conducted in the absence of any commercial or financial relationships that could be construed as a potential conflict of interest.

Copyright © 2017 Zhang, Jiao, Lv, Du, Yan, Wan, Zhang and Han. This is an open-access article distributed under the terms of the Creative Commons Attribution License (CC BY). The use, distribution or reproduction in other forums is permitted, provided the original author(s) or licensor are credited and that the original publication in this journal is cited, in accordance with accepted academic practice. No use, distribution or reproduction is permitted which does not comply with these terms.

frontiers in Microbiology

ORIGINAL RESEARCH
published: 27 February 2017
doi: 10.3389/fmicb.2017.00289

Antagonistic Activity and Mode of Action of Phenazine-1-Carboxylic Acid, Produced by Marine Bacterium *Pseudomonas aeruginosa* PA31x, Against *Vibrio anguillarum In vitro* and in a Zebrafish *In vivo* Model

Linlin Zhang[1,2,3], Xueying Tian[4], Shan Kuang[1,2], Ge Liu[1,2,3], Chengsheng Zhang[4] and Chaomin Sun[1,2]**

[1] Key Laboratory of Experimental Marine Biology, Institute of Oceanology, Chinese Academy of Sciences, Qingdao, China, [2] Laboratory for Marine Biology and Biotechnology, Qingdao National Laboratory for Marine Science and Technology, Qingdao, China, [3] College of Earth Science, University of Chinese Academy of Sciences, Beijing, China, [4] Tobacco Pest Integrated Management Key Laboratory of China, Tobacco Research Institute of Chinese Academy of Agricultural Sciences, Qingdao, China

OPEN ACCESS

Edited by:
Susana Rodriguez-Couto, Ikerbasque, Spain

Reviewed by:
Henry Mueller, Graz University of Technology, Austria
Mehdi Razzaghi-Abyaneh, Pasteur Institute of Iran, Iran

***Correspondence:**
Chaomin Sun
sunchaomin@qdio.ac.cn
Chengsheng Zhang
zhangchengsheng@caas.cn

Specialty section:
This article was submitted to Microbial Physiology and Metabolism, a section of the journal Frontiers in Microbiology

Received: *02 November 2016*
Accepted: *13 February 2017*
Published: *27 February 2017*

Citation:
Zhang L, Tian X, Kuang S, Liu G, Zhang C and Sun C (2017) Antagonistic Activity and Mode of Action of Phenazine-1-Carboxylic Acid, Produced by Marine Bacterium Pseudomonas aeruginosa PA31x, Against Vibrio anguillarum In vitro and in a Zebrafish In vivo Model. Front. Microbiol. 8:289. doi: 10.3389/fmicb.2017.00289

Phenazine and its derivatives are very important secondary metabolites produced from *Pseudomonas* spp. and have exhibited broad-spectrum antifungal and antibacterial activities. However, till date, there are few reports about marine derived *Pseudomonas* and its production of phenazine metabolites. In this study, we isolated a marine *Pseudomonas aeruginosa* strain PA31x which produced natural product inhibiting the growth of *Vibrio anguillarum* C312, one of the most serious bacterial pathogens in marine aquaculture. Combining high-resolution electro-spray-ionization mass spectroscopy and nuclear magnetic resonance spectroscopy analyses, the functional compound against *V. anguillarum* was demonstrated to be phenazine-1-carboxylic acid (PCA), an important phenazine derivative. Molecular studies indicated that the production of PCA by *P. aeruginosa* PA31x was determined by gene clusters *phz1* and *phz2* in its genome. Electron microscopic results showed that treatment of *V. anguillarum* with PCA developed complete lysis of bacterial cells with fragmented cytoplasm being released to the surrounding environment. Additional evidence indicated that reactive oxygen species generation preceded PCA-induced microbe and cancer cell death. Notably, treatment with PCA gave highly significant protective activities against the development of *V. anguillarum* C312 on zebrafish. Additionally, the marine derived PCA was further found to effectively inhibit the growth of agricultural pathogens, *Acidovorax citrulli* NP1 and *Phytophthora nicotianae* JM1. Taken together, this study reveals that marine *Pseudomonas* derived PCA carries antagonistic activities against both aquacultural and agricultural pathogens, which broadens the application fields of PCA.

Keywords: antagonistic, phenazine-1-carboxylic acid, marine, *Pseudomonas aeruginosa*, *Vibrio anguillarum*

INTRODUCTION

There is a perpetual need for novel antibiotics to combat pathogens in the fields of public health, agriculture and aquaculture. Microorganisms are a major resource for the discovery of new drugs. The majority of microbial natural products have been isolated from terrestrial-borne microbes (Berdy, 2005), and the importance of terrestrial microbes as sources of valuable bioactive metabolites has been well established for more than half a century. However, with the fast development in marine related fields, recent trends in drug discovery emphasize that marine microorganisms are a potentially productive source of novel secondary metabolites and have great potential to increase the number of marine microbial natural products (Waters et al., 2010). Metabolically marine strains are different from their terrestrial counterparts, and thereby, they may produce unique bioactive compounds, which are not found in their terrestrial counterparts (Jensen and Fenical, 1994; Feling et al., 2003).

Pseudomonas aeruginosa is a ubiquitous Gram-negative bacterium having a versatile metabolic potential and great ecological and clinical significance. The geographical distribution of *P. aeruginosa* has revealed the existence of an unbiased genetic arrangement in terrestrial isolates. In contrast, there are very few reports about *P. aeruginosa* strains from marine environments. Phenazine and its derivatives are very important secondary metabolites produced from *Pseudomonas* spp. and have exhibited broad-spectrum antifungal and antibacterial activities (Lee et al., 2003; Kumar et al., 2005; Morales et al., 2010). Furthermore, it is reported that phenazine and its derivative also have the function of inhibiting cancer cells and inducing the programmed cell death in some cancer cell lines (Lee et al., 2003; McGuigan and Li, 2014). Among the phenazine compounds, phenazine-1-carboxylic acid (PCA) is confirmed an important metabolic precursor for other phenazine derivatives and also have the antifungal and antibacterial activities (Lee et al., 2003; Pierson and Pierson, 2010; Abraham et al., 2015). In China, PCA named Shenqinmycin has received a Pesticide Registration Certification from the Ministry of Agriculture, and widespreadly used against the plant pathogens in the land agriculture related fields because of its high fungicidal efficiency, low toxicity to humans and animals, environmental compatibility, and improvement of crop production (Su et al., 2010).

Up to now, the phenazine compounds and their hosts are mainly isolated from the rhizosphere of terrestrial plants, however, the same kind of compounds from marine environment and their potential applications in aquaculture are still needed to elucidate. Notably, in addition to the land agriculture, marine aquaculture plays important roles for China's economic development. There are about 1.33 million hectares of marine cultivable areas in China, including shallow seas, mudflats and bays. However, sudden outbreak of diseases in marine aquaculture leads to high mortality and severe economic loss (Yang and Sun, 2016). Marine *Vibrio* species are associated with large-scale losses of penaeids and also cause diseases to fish (Letchumanan et al., 2015). *Vibrio anguillarum* is the causative agent of vibriosis, a deadly haemorrhagic septicaemic disease affecting various marine and fresh/brackish water fish, bivalves and crustaceans (Yu et al., 2012). To find novel antibiotics against *V. anguillarum* is urgently needed. Preetha et al. (2015) reported that brackish water derived *Pseudomonas* sp. was antagonistic to a wide range of pathogenic vibrios, which indicates that marine derived *Pseudomonas* sp. is potential to be antagonistic probiotics in aquaculture.

In this study, a marine *Pseudomonas aeruginosa* strain PA31x isolated from the sediments in China Yellow Sea showed strong inhibitory activity against *V. anguillarum* C312. The active compound was further purified and determined as PCA by HR-ESI-MS and NMR spectroscopic analyses. Finally, the possible inhibitory mechanisms of PCA acted on *V. anguillarum*, and the prevention of zebrafish embryos from the infection of *V. anguillarum* by PCA were also investigated.

MATERIALS AND METHODS

Bacterial Strains Isolation, Identification, and Culture Conditions

The marine bacteria strains used in this study were isolated from the sediments of China Yellow Sea and cultured in marine broth 2216E (5 g/L tryptone, 1 g/L yeast extract, one liter filtered seawater, pH adjusted to 7.4–7.6) or Luria Bertani (LB) medium (10 g/L peptone, 5 g/L yeast extract, 10 g/L NaCl, pH adjusted to 7.0) (Ausubel et al., 1992), and incubated at 28°C. Genomic DNA was extracted from the isolate, and PCR (polymerase chain reaction) was performed to amplify the 16S rDNA gene sequence with universal primers 27F (AGAGTTTGATCCTGGCTCAG) and 1541R (AAGGAGGTGATCCACCC). The 16S rDNA gene sequence was compared with the public databases by the NCBI-BLAST program[1]. Phylogenetic tree was constructed with the MEGA version 6 with the method of maximum likelihood to determine the phylogenetic position of the strain PA31x (Tamura et al., 2013). The pathogen *V. anguillarum* C312 was cultured in 2216E or LB medium at 28°C (Yu et al., 2012).

Antagonistic Assay of Marine Bacterial Strains against *V. anguillarum* C312

Standard agar plate bioassay was followed to test the marine bacteria for growth suppression of *V. anguillarum* (Kumar et al., 2005). Briefly, *V. anguillarum* C312 was cultivated in 2216E broth at 28 °C overnight, and the overnight culture was diluted with 2216E broth to 1×10^6 cfu/mL. Thereafter, the diluted suspension was spread evenly on the surface of 2216E agar plate. After incubation for 30 min, the fresh colonies of marine bacterial strains were seeded on the plate and incubated at 28°C for 2 days. The antagonistic effects of marine bacterial strains against *V. anguillarum* C312 were checked and recorded.

Culture Conditions for Antibiotic Production

Active compound production by marine *P. aeruginosa* PA31x was compared in different media. Four different media containing

[1]http://www.ncbi.nlm.nih.gov/BLAST

various carbon and nitrogen source were used for culture in 250 mL flasks at 28°C for 3 days with 50 mL fermentation scale. The four media include LB broth, marine 2216E broth, modified King's medium B (glycerol 30 mL, peptone 10 g, K_2HPO_4 0.5 g, $MgSO_4.7H_2O$ 0.5 g in 1 L filtered seawater, pH 7.6) and modified liquid PPM medium (peptone 10 g, glycerol 10 mL, yeast extract 10 g, dissolved in 1000 ml filtered seawater) (Kumar et al., 2005). To test the active compound production of different medium, the same volume supernatant was collected and filtrated with 0.22-μm pore size filter. Then 150 μL filtrated supernatant was added into the Oxford cup which was put on the surface of LB agar medium covered with *V. anguillarum* C312 for evaluation of the antibiotic activity.

Purification and Identification of the Anti-*V. anguillarum* Compound from *P. aeruginosa* PA31x

To obtain the active compound against *V. anguillarum* C312, marine bacterium *P. aeruginosa* PA31x was cultured on modified liquid PPM medium in 250 mL glass flasks. The purification was executed as previously described (Kumar et al., 2005). The fermentation was carried out for 2 days at 28°C on a rotary shaker at 160 rpm. The liquid culture (67 L) was centrifuged with 8,000 rpm for 10 min and the cell-free culture supernatant was collected and mixed with equal volume of ethyl acetate. The combined organic layer was concentrated under reduced pressure and 28.6 g crude extract was obtained from 67 L PPM fermentation medium. The crude extract was then mixed with slurry of silica gel (200–400 meshes) and the mixtures were loaded in the glass column (1000 mm × 30 mm), which was successively eluted with gradient from 100% dichloromethane to 100% methanol. The antibacterial activity of individual fraction was monitored by using *V. anguillarum* C312 as the indicator bacterium following the filter paper disk assay with minor modification (Jain and Pandey, 2016). Firstly, the LB plates spread with *V. anguillarum* C312 cell suspensions were prepared as above. Then the sterile filter paper disks (diameter 6 mm) containing eluded fractions dissolved in CH_2Cl_2 were put on the surface of plates and inoculated at 28 C for 2 days. Lastly, the corresponding effective antibacterial fractions were collected and dissolved in dichloromethane-methanol mixtures (9: 1) and crystallized under reduced pressure.

The antibacterial substances were subsequently analyzed by analytical HPLC system (Agilent 1260 series) with a linear gradient from 10 to 100% MeOH containing water on a C18 reversed-phase column (ZORBAX SB-C18, 5 μm, 4.6 mm × 150mm, Agilent) and collected by semi-preparative with solvent (water : MeOH = 1:1). All the HPLC grade mobile phase solvents were filtered (0.22-μm pore size) and degassed under reduced pressure before using (Lee et al., 2003). The active compound obtained from semi-preparative HPLC system was further analyzed by HR-ESI-MS and NMR. NMR spectra were recorded on a Bruker Avance-500 Hz NMR spectrometer. ^1H NMR and ^{13}C NMR spectra were measured in deuterated chloroform ($CDCl_3$) at room temperature.

Antagonistic Assay of Purified PCA against *V. anguillarum* C312

Antimicrobial activity of the PCA was evaluated by the paper filter paper disk assay as described previously (Raio et al., 2011). Briefly, the test plate with *V. anguillarum* C312 was prepared as above. The sterile filter paper disks (diameter 6 mm) containing PCA dissolved in CH_2Cl_2 were put on the plates for inoculation at 28°C for 2 days. The antagonistic effects of *P. aeruginosa* PA31x against *V. anguillarum* C312 were checked and recorded. The minimal inhibitory concentration (MIC) of PCA to *V. anguillarum* C312 was determined according to (Wiegand et al., 2008) with minor modification. Briefly, the OD_{600} of exponential-phase cells of *V. anguillarum* C312 was adjusted to 0.01with Mueller-Hinton broth (MHB). Thereafter, 100 μL *V. anguillarum* C312 cells suspension was transferred into the wells of 96-well microplate with different concentration of PCA. DMSO (1%, v/v) was used as solvent to dissolve PCA and served as the negative control. The microplate was incubated at 28°C for 18 h and checked under absorbance at 600 nm after incubation. In the present study, the MIC was defined as the lowest PCA concentration which inhibited *V. anguillarum* C312 or (OD_{600} < 0.05). The IC_{50} was defined as the concentration of PCA required for the half maximal inhibitory growth of pathogens. All the treatments were executed three times independently.

Scanning Electron Microscopy (SEM)

Microbial morphology analyses by SEM were performed to investigate the morphological changes of pathogens treated with PCA. Briefly, *V. anguillarum* C312 was incubated on the 2216E as described above, and the sterile filter paper disks (diameter 10 mm) impregnated with 100 μg purified PCA was put on the medium and incubated at 28°C for 2–7 days (Kumar et al., 2005; Xu et al., 2014). The cells from the periphery of the inhibition zone and control plates were collected for SEM assay, respectively. The samples were analyzed with a SEM (Hitachi, S-3400N) operated at 5 kV.

Transmission Electron Microscopy (TEM)

The samples for TEM were prepared as described previously with minor modification (Feng et al., 2000). Briefly, *V. anguillarum* C312 was cultivated at 28°C in liquid LB medium at 150 rpm with shaking for 16 h, then the cells were cultivated for another 12 h in the absence or presence of 5 μg/mL PCA. The culture broth was centrifuged and washed with PBS (pH 7.2–7.4). The collected cells were fixed with 2.5% glutaraldehyde. The samples treated with or without 5 μg/mL PCA were fixed as described previously (Mei et al., 2015). All the samples were analyzed with a TEM (HT7700, Hitachi, Japan) operated at 120 kV.

Reactive Oxygen Species (ROS) Accumulation in *V. anguillarum* C312 and Human A549 Cells as Affected by PCA

The reactive oxygen species (ROS) accumulation of *V. anguillarum* C312 was measured with the fluorescent probe 2′,7′-dichlorodihydrofluorescein diacetate (DCFH-DA) as

previously described (Xu et al., 2015) with minor modification as follows. In brief, *V. anguillarum* C312 was inoculated with 2216E broth for 4–6 h and the bacterial cells whose concentration reaching approximately 1×10^8 cfu/mL were collected by centrifugation (5,000 rpm, 10 min, room temperature). Then the pellet was resuspended in 1 mL DCFH-DA solution (10 μM DCFH-DA in PBS buffer pH 7.4). The cell resuspensions were added into the 2 mL centrifuge tubes and incubated at 37°C for 30 min with rotation. After washed with PBS three times, 200 μL cell resuspensions were added to microplates. Thereafter, PCA dissolved in the DMSO were added into the wells with a final concentration of 0, 1, or 2 μg/mL, respectively. The PBS buffer with 3 μg/mL Rosup (a positive compound provided by the assay kit) or without any reagent (DMSO, PCA, or Rosup) was regarded as positive or negative control. The microplates were kept at 28°C, and a fluorescence microplate reader (TECAN, M1000Pro) was used to record the fluorescence values for 120 min at every 10 min with an excitation wavelength of 488 nm and an emission wavelength of 525 nm. Each treatment was represented by three replicates, and the experiment was conducted three times.

Determination of cellular ROS for A549 lung cancer cells was performed according to the method described previously (Hao et al., 2014), and the culture of A549 cells was carried out in accordance with the ethical guidelines of Chinese Academy of Sciences. The generation of intracellular ROS was detected with the probe DCFH-DA. Briefly, A549 cells treated with a final concentration of 0, 2, 10, or 50 μg/mL of PCA for 1 hour were incubated with 10 μM $DCFH_2$-DA for 30 min at 37°C in a humidified atmosphere at 5% CO_2. Then labeled cells were washed with PBS, trypsinized, and resuspended in PBS. To quantify ROS, the fluorescence intensity was measured by flow cytometry (FACS Aria II, BD Biosciences). All the experiments were carried out three times.

Inhibitory Activities of PCA on *V. anguillarum* C312 Infection toward Zebrafish Embryos

Wild type zebrafishes were housed in mixed-sex low density tanks at 28°C on a timer-controlled 14:10 light/dark cycle. The male and female zebrafishes (3–12 months old) from the same tank were selected to generate zebrafish embryos as described (Westerfield, 1994). Ten transparent and healthy embryos were transferred into the wells of 24-well microplate containing 1 mL water and incubated at 28°C. Different concentrations of PCA (0 μg/mL, 2 μg/mL, and 3 μg/mL) dissolved in DMSO was added into per well, and 20 μL of *V. anguillarum* C312 culture adjusted to the concentration of 2×10^8 cfu/mL was added into each well at the same time. The treatment containing DMSO without adding PCA and *V. anguillarum* C312 was regarded as control. The maximal level of DMSO in experimental media was 0.1% (v/v). All the embryos were incubated at 28°C, and the hatching ratio of embryos in each group was investigated. The embryos were observed with a stereo microscope (ZEISS Stemi 2000C, German) equipped with a digital camera after 48 h post-fertilization (hpf). All animal experiments were conducted in accordance with the ethical guidelines of Chinese Academy of Sciences.

Statistical Analyses

The results were shown as the mean ± SD (standard deviations) and the statistical differences were detected with independent sample *t*-tests ($^*P < 0.05$; $^{**}P < 0.01$). All the measurements were executed with three independent experiments.

RESULTS

Anti-*V. anguillarum* Activity of Marine Bacterium PA31x

In order to obtain potential anti-*V. anguillarum* compounds, over 400 bacterial strains isolated from marine sediments were evaluated by their abilities to inhibit the growth of *V. anguillarum* by antagonistic experiment. As shown in **Figure 1A**, the bacterium strain 31x in this study showed strong inhibitory activity against the growth of *V. anguillarum*. Therefore, the bacterium strain 31x was used for further study. The 16S rDNA gene of strain 31x was sequenced and aligned with other bacterial species from NCBI. Based on the alignment result, the 16S rDNA gene sequence (Accession No. KX455116) of 31x shared 99% identity with *P. aeruginosa* M18 which was isolated from terrestrial plant rhizosphere (Supplementary Figure S1). Thus, the bacterial strain 31x was identified to one member of *P. aeruginosa* and designated as PA31x.

Purification and Characterization of Active Component from *P. aeruginosa* PA31x

To purify the active compound inhibiting growth of *V. anguillarum* from *P. aeruginosa* PA31x, the purification was performed as described in Supplementary Figure S2. The filter paper disk assay was carried out to follow the trail of active compound by using *V. anguillarum* C312 as the indicator bacterium. 26.8 g crude extract from 67 L liquid fermentation medium was mixed with same mass of silica gel and eluted. The eluted active components were further analyzed with analytical HPLC. The sole peak appeared at a retention time of 12.11 min was collected and used for anti-*V. anguillarum* assay on the 2216E plate. As expected, the purified compound showed remarkably inhibitory activity against *V. anguillarum* C312 (**Figure 1B**), which further confirmed that we successfully obtained the active component against *V. anguillarum* in *P. aeruginosa* PA31x.

Structure Elucidation of the Antagonistic Compound

To elucidate the chemical structure of the active compound derived from *P. aeruginosa* PA31x, the HR-ESI-MS and NMR spectral data of this compound were analyzed. The HR-ESI-MS spectrum displayed a strong molecular ion peak at m/z 247.0282 (M + Na) (**Figure 2**). The GC-MS Library search result proposed the molecular formula as $C_{13}H_8N_2O_2$.

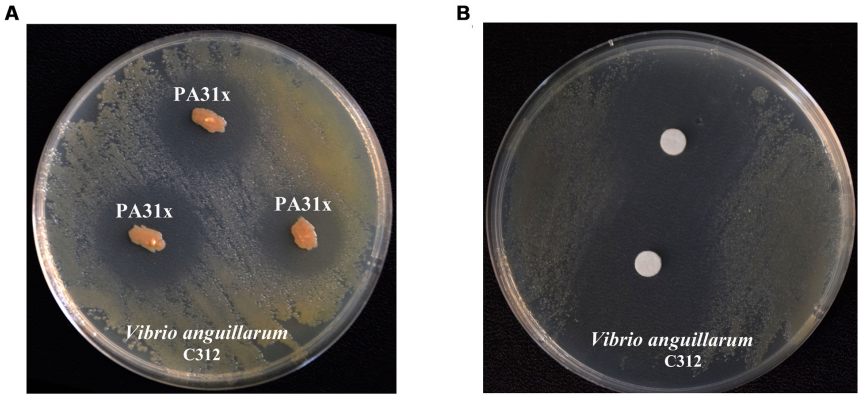


FIGURE 1 | Anti-*Vibrio anguillarum* C312 activity assays of marine bacterium PA31x (A) and its purified active compound **(B)**. Sterile filter paper disks (diameter 10 mm) impregnated with active compound were applied in panel **B**.

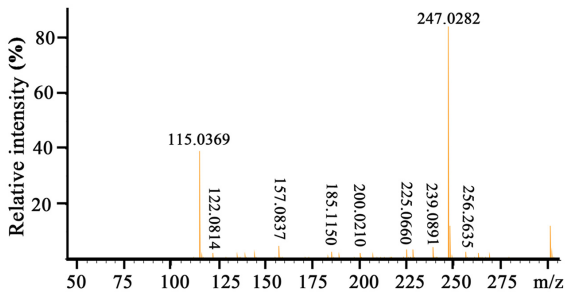


FIGURE 2 | HR-ESI-MS spectrum of the active compound produced by *Pseudomonas aeruginosa* PA31x.

Moreover, ^{1}H NMR and ^{13}C NMR spectroscopy were performed to clarify the exact structure of this active compound (**Figure 3**), which confirmed that eight protons (**Figure 3A**) and 13 carbons (**Figure 3B**) were present in the molecule of this compound. In the^{1}H NMR spectrum, 7 methine groups and a carboxylic acid group were present at δ 8.00–8.99 and 15.55, respectively (**Figure 3A** and Supplementary Table S1). The proton at the position 2 resonated at δ 8.52–8.54. The resonance at δ 8.34 belongs to the proton at the position 3 and at the similar position in the phenazine ring, position 4 resonated at δ 8.97–8.99. Position 6 resonated at δ 8.28–8.29 and the remaining three protons at the positions 7, 8, and 9 were δ 8.00–8.04. The proton singlet at δ 15.55 was in accordance with the hydrogen-bonded carboxylic acid proton. A carbonyl group and aromatic rings at δ 166.0 and 125.1–144.2, respectively, were present in the ^{13}C NMR spectrum of the active compound (**Figure 3B** and Supplementary Table S2). The resonance peak at the position 1 was δ 125.1. The resonances at δ 140.0-144.2 belong to the carbons at the positions 4a, 5a, 9a, and 10a (**Figure 3B**). The remaining resonance peaks at δ 128.1–137.5 were distributed to the carbons at positions 2, 3, 4, 6, 7, 8, and 9 of the phenazine ring (**Figure 3B**). Collectively, based on the HR-ESI-MS and NMR spectral data, the active compound derived from PA31x was characterized as PCA. In addition, antagonistic activities of PCA was dose-dependent, and the MIC of PCA for *V. anguillarum* C312 was measured. The results showed that the MIC of PCA against *V. anguillarum* C312 was 50 μg/mL. The IC_{50} of PCA against *V. anguillarum* C312 was 39.02 μg/mL.

Cloning, Sequencing, and Alignment of Genes Involved in PCA Production

It was documented that the phenazine gene cluster *phz* had a conserved seven-gene operon, *phzABCDEFG*, which was responsible for the synthesis of PCA. Moreover, there were two nearly identical core biosynthetic gene clusters, *phz1* and *phz2*, in *P. aeruginosa* (Mavrodi et al., 2006). To investigate the genes involved in PCA production in *P. aeruginosa* PA31x, the specific primers were used to detect, clone and sequence the gene clusters, *phz1* (Supplementary Table S3) and *phz2* (Supplementary Table S4). The results showed that two gene clusters, *phz1* and *phz2*, existed in the genome of *P. aeruginosa* PA31x (**Table 1**). To further disclose the conservation of genes involved in PCA production between marine and terrestrial derived *Pseudomonas*, gene clusters *phz1* and *phz2* from *P. aeruginosa* PA31x were compared with those of *P. aeruginosa* M18 (Su et al., 2010), the typical terrestrial bacterium producing PCA. The alignment results showed that the gene clusters in *P. aeruginosa* PA31x shared high homology with those in *P. aeruginosa* M18. The identity ratio of different gene in *phz1* varied from 98.23 to 100% (**Table 1**), and the identity ratio of different gene in *phz2* varied from 98.83 to 100% when compared with those genes in *P. aeruginosa* M18 (**Table 1**).

Additionally, PCA was an important precursor which could be converted into other phenazine active compound, like PCN and PYO, with some other phenazine genes (Kerr et al., 1999). The gene *phzH* was considered to be involved in the conversion of PCA to PCN and the proteins encoded by genes *phzS* and *phzM* could transfer PCA into PYO (Kerr et al., 1999). Correspondingly, these three genes, *phzS, phzM* and *phzH* which could transform PCA to antibiotics PYO and PCN, were also

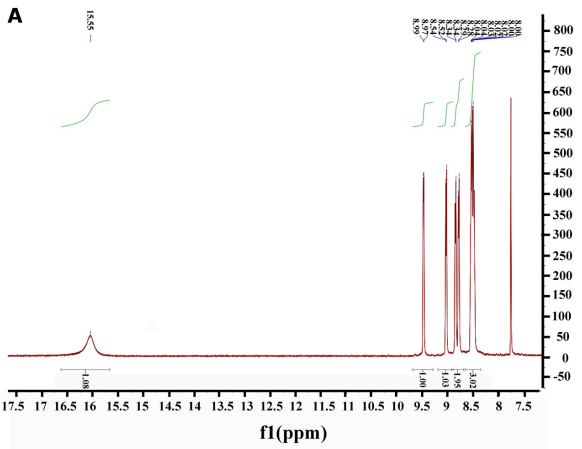


FIGURE 3 | Structure determination of active compound produced by *P. aeruginosa* PA31x by ^{1}H spectral (A) and ^{13}C spectral **(B)**. The chemical structure of phenazine-1-carboxylic acid (PCA) was imbedded in the panel **B**.

TABLE 1 | The identity comparison of antibiotic genes related to PCA biosynthesis from *Pseudomonas aeruginosa* PA31x and *P. aeruginosa* M18.

Genes	Identity (%)	Genes	Identity (%)	Genes	Identity (%)
phzA1	100	*phzA2*	99.80	*phzM*	99.50
phzB1	98.23	*phzB2*	100	*phzS*	99.67
phzC1	99.58	*phzC2*	99.56	*phzH*	99.45
phzD1	99.73	*phzD2*	99.36		
phzE1	99.73	*phzE2*	98.83		
phzF1	99.40	*phzF2*	99.16		
phzG1	99.38	*phzG2*	99.41		

detected in *P. aeruginosa* PA31x with the primers showed in Supplementary Table S5. The sequence of these three genes including *phzM*, *phzH*, and *phzS* were highly homologous to the phenazine genes from *P. aeruginosa* M18, and the identity ratio varied from 99.45 to 99.67% (**Table 1**). Thus, the genes involved in the production and modification of PCA are highly homologous between terrestrial and marine derived *Pseudomonas* sp..

Morphological Changes of *V. anguillarum* C312 Cells Treated with PCA

Scanning electron microscopy is recognized as an attractive and powerful method to determine morphological changes in biological samples owing to its high-resolution imaging capability. SEM can be used to demonstrate significant alterations in cell morphology after treatment with PCA. In the present study, the pathogen *V. anguillarum* C312 was treated with the purified PCA and thereafter checked by SEM to investigate how does PCA act on the bacterium. Morphological changes of *V. anguillarum* C312 treated with PCA or DMSO were shown in **Figures 4A,B**. The surfaces of the cells in the control group were smooth and the bacteria cells were plump and round. On the contrary, the cell membranes became coarse and emerged one to several cystic bulges, and distorted with deeper grooves and corrugations after treatment with PCA (**Figures 4A,B**).

By using a transmission electron microscope, morphological material changes in the pathogenic cells following PCA treatment were further determined. It is believed that structures internal or external to the cells were altered following PCA treatment, since this treatment caused cells death. The cells of *V. anguillarum* C312 in the control group were rod-shaped with a densely-stained cytoplasm, and they were uniformly distributed (**Figure 4C**). On the contrary, the cells in the treatment group were highly variable in structure and almost devoid of nucleic acids. In addition, some cells were split open after treatment with PCA, as evident in **Figure 4D**, which indicate the presence of internal cell contents and the leakage and damage of cytoplasm. It can be concluded that the cytoplasmic content of the cells was affected and at least partially lost in the presence of PCA. The TEM images suggest that the mechanism of bacterial inactivation is mainly via the decomposition of cytoplasm. The degree of damage depends mainly on the concentration of PCA that penetrates the cell.

ROS Accumulation in *V. anguillarum* and Human A549 Cells Treated with PCA

It is known that intracellular ROS are generated in cellular response to exogenous sources such as xenobiotics compounds and pathogen invasion as well as during mitochondrial oxidative metabolism (Ray et al., 2012). To examine the intracellular ROS change by PCA, *V. anguillarum* C312 and A549 cells were treated with PCA, and ROS levels were measured by the cell-permeable substrate DCFH-DA. As evident from **Figure 5A**, the intracellular ROS accumulation in *V. anguillarum* C312 was obviously affected by PCA. It was shown that ROS product differed in the presence of PCA (0–2 μg/mL) and there was a significant increase in the intracellular fluorescence compared to the control, indicating a higher ROS production in the group treated with PCA. As a contrast, the accumulation of ROS in the negative control or DMSO treatment was much lower than those of treated with PCA or Rosup, which indicated that PCA could generate ROS in *V. anguillarum*. On the other

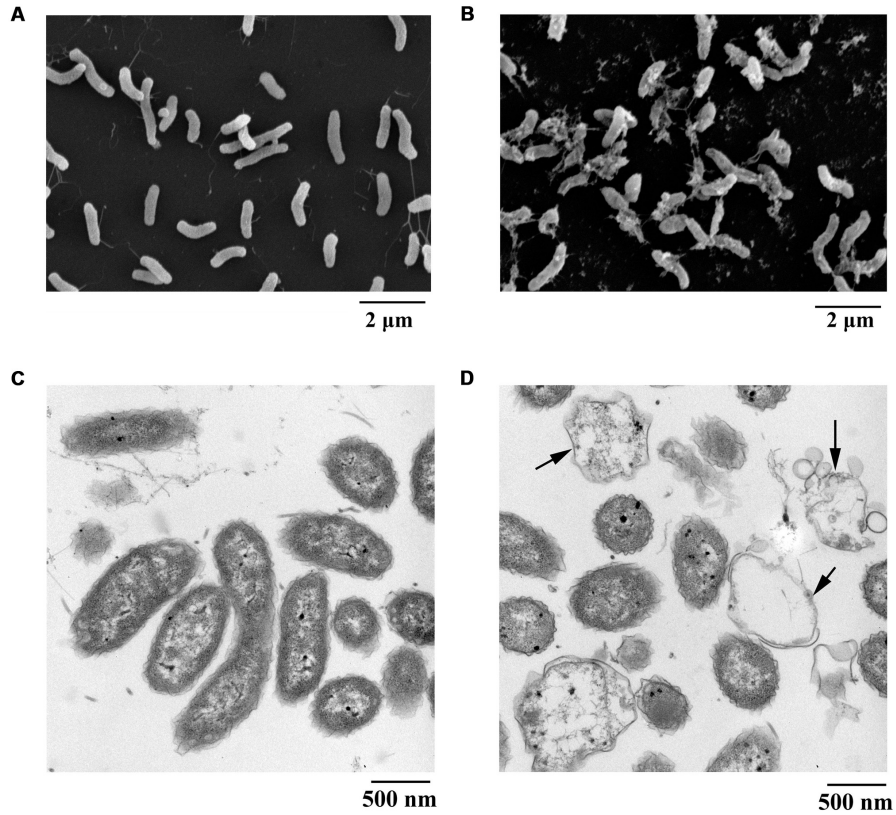


FIGURE 4 | Electron microscopic observation of morphological changes of *V. anguillarum* C312 cells following the treatment of PCA. SEM images of *V. anguillarum* C312 cells without **(A)** or with the treatment of PCA **(B)**. TEM images of *V. anguillarum* C312 cells without **(C)** or with the treatment of PCA **(D)**.

hand, it was reported that PCA showed an antitumor activity in prostate cancer cells by ROS production and mitochondrial-related apoptotic pathway (Karuppiah et al., 2016). To examine the ROS generation by PCA in human cancer cell line, A549 cells treated with PCA were incubated with DCFH-DA. As illustrated in **Figure 5B**, A549 cells treated with PCA showed comparatively higher ROS generation than control cells. Altogether, we concluded that PCA could induce the accumulation of ROS both in *V. anguillarum* and human A549 cells.

Inhibitory Activities of PCA on *V. anguillarum* Infection to Zebrafish Embryos

Based on our above results, PCA could effectively inhibit the growth of *V. anguillarum*. To investigate whether PCA could be applied as antibiotics in aquaculture, zebrafish was used as a model for studying the infection prevention from *V. anguillarum*. The protective assay of PCA for zebrafish embryos was performed and the hatching percent of each group embryos was calculated. As shown in **Figure 6A**, the hatching percent of embryos infected with *V. anguillarum* C312 was lowest in the groups, which was only 3.8%. However, the hatching percent of zebrafish embryos apparently raised to 42.3 or 84.62%, respectively, when 2 μg/mL and 3 μg/mL of PCA was co-incubated with *V. anguillarum* C312. With the observation of microscope, the zebrafish embryos treated with DMSO and PCA could develop normally after 48 h post-fertilization (hpf) (**Figure 6B**). However, the zebrafish embryos infected with *V. anguillarum* C312 developed abnormally and couldn't grow to mature form (**Figure 6B**). Together, it was concluded that PCA could weaken *V. anguillarum* infection to zebrafish embryos in the water environment and would be applied as a protective agent in the aquacultural production.

DISCUSSION

It is reported that over 120 of the most important medicines in use today are obtained from terrestrial microorganisms. Meanwhile, the marine environment has been a source of more than 20,000 inspirational natural products discovered over the past 50 years. From these efforts, more than 22,000 discrete marine metabolites have been isolated and structurally characterized, and a significant percentage has been evaluated for some level of biological activity, such as antimicrobial effects or mammalian cell toxicity (Gerwick and Fenner, 2013). Therefore, many exciting discoveries await a more comprehensive biological evaluation of these known compounds as well as those still left to discover.

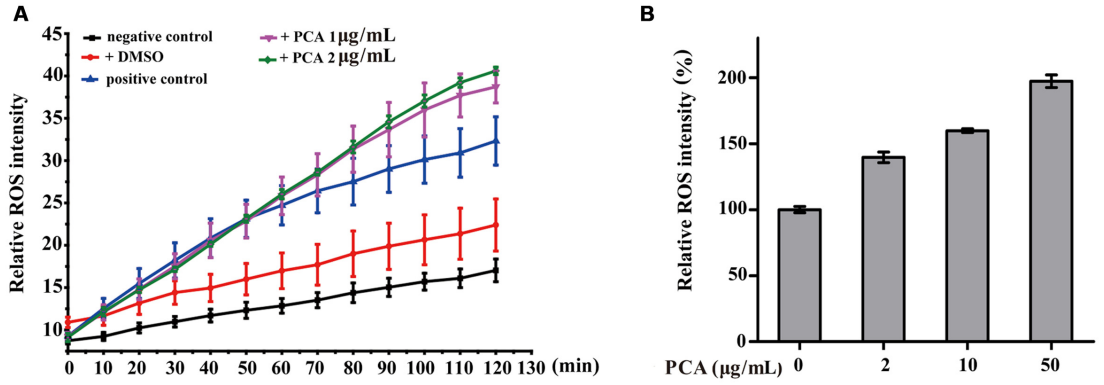


FIGURE 5 | Reactive oxygen species (ROS) accumulation in *V. anguillarum* C312 (A) and A549 lung cancer cells **(B)** as affected by PCA. For the assay in panel **A**, the treatments included PCA in DMSO, DMSO alone (a negative control), Rosup (positive control), or none of these agents (a negative control). Values are means and standard deviations from three independent experiments.

Phenazines are bacterial secondary metabolites that have long been recognized for their broad-spectrum antibiotic activity and been widely used in the biological control of arrange of bacterial and fungal pathogens (Pierson and Pierson, 2010). So far, phenazine compounds are mainly isolated from terrestrial *Pseudomonas* spp. and *Streptomyces* sp., and the marine microbe derived phenazine compounds are still rarely reported. In the present study, in a search program for microorganisms producing bioactive antimicrobial secondary metabolites effective on aquaculture diseases, the bacterial strain PA31x, which showed strong *in vitro* antibacterial and antifungal activities against some aquaculture (**Figure 1**) and plant pathogens (Supplementary Figure S3), was isolated from sediments of China Yellow Sea. The morphological, biochemical and physiological characteristics confirmed that the strain belongs to *Pseudomonas aeruginosa*. The active compound derived from *P. aeruginosa* PA31x was finally identified as PCA combining the analyses of HR-ESI-MS and NMR spectrum (**Figures 2**, **3**). As noted earlier, the antibiotic PCA belongs to the phenazine family of compounds, which have been reported to be effective against many fungi and Gram-positive bacteria but only against very few Gram-negative bacteria (Xu et al., 2015). The marine microbe derived PCA showed significant antagonistic activity against the Gram-negative bacterium *V. anguillarum*, which is consistent with the report that marine *Pseudomonas* sp. could be used as probiotics in aquaculture against *V. harveyi* (Preetha et al., 2015).

It is well known that *V. anguillarum* could cause great economic losses in the marine culture industry worldwide (Toranzo et al., 1996). More than 50 fresh and salt-water species, including some important economic species of the aquaculture industry, could be infected by *V. anguillarum* (Frans et al., 2011). To control the serious vibriosis, one of the solutions is to look for novel antimicrobial substances from natural metabolites which inhibit *V. anguillarum*. Based on our results, PCA could effectively prevent the zebrafish from *V. anguillarum* infection (**Figure 6**). Therefore, PCA would be also used as antibiotics in aquaculture fields because of its low toxicity to humans, and environmental compatibility (Yuan et al., 2008). Notably, the marine microbe derived actinonin was reported to effectively inhibit the growth of *V. anguillarum* (Yang and Sun, 2016), which indicates that it might be a good idea to try the aquatic diseases control with the reported terrestrial derived antibiotics.

Phenazine compounds have been recognized for a wide range of antimicrobial for plant pathogens and induce systemic resistance of plants (Audenaert et al., 2002; Bloemberg and Lugtenberg, 2003). Among the phenazine derivants, PCA had been used as biofungicide reagent against various phytopathogens in China (Zhou et al., 2010). In this study, marine microbial derived PCA showed significant antagonistic activity against terrestrial pathogens *Acidovorax citrulli* NP1 and *Phytophthora nicotianae* JM1 (Supplementary Figures S3–S6). *A. citrulli* causes serious seedling blight and bacterial fruit blotch of cucurbits (Bahar et al., 2011). *Phytophthora nicotianae* is a common plant pathogenic fungus infecting many important plants including tobacco, onion and strawberries (Han et al., 2016). Altogether, our results indicate that PCA has potentials to be as a biopesticide applied in both agricultural and aquacultural fields. Recently, scientists used a combined method involving gene, promoter, and protein engineering to modify the central biosynthetic and secondary metabolic pathways in the PCA-producing *Pseudomonas aeruginosa* strain PA1201 (Jin et al., 2015). The PCA yield of the resulting strain PA-IV was increased 54.6-fold and could produce 9882 mg/L PCA in fed-batch fermentation (Jin et al., 2015). Therefore, PCA has enormous potential to be applied in the aquaculture fields.

Understanding the biological effects of PCA on pathogens is essential to develop corresponding antibiotics. In the present study, on the one hand, morphologic change observed by SEM or TEM was used for studying the action mechanisms of PCA against *V. anguillarum*. It is noted that the membrane surface of *V. anguillarum* C312 emerged one to multiple protrusion of vesicles, however, the cellular contents of *A. citrulli* NP1 were released to the environment and only shaft substances of the cell were left after PCA treatment (Supplementary Figure S4), which indicated that the action mechanisms of PCA on *V. anguillarum* C312 and *A. citrulli* NP1 might be different.

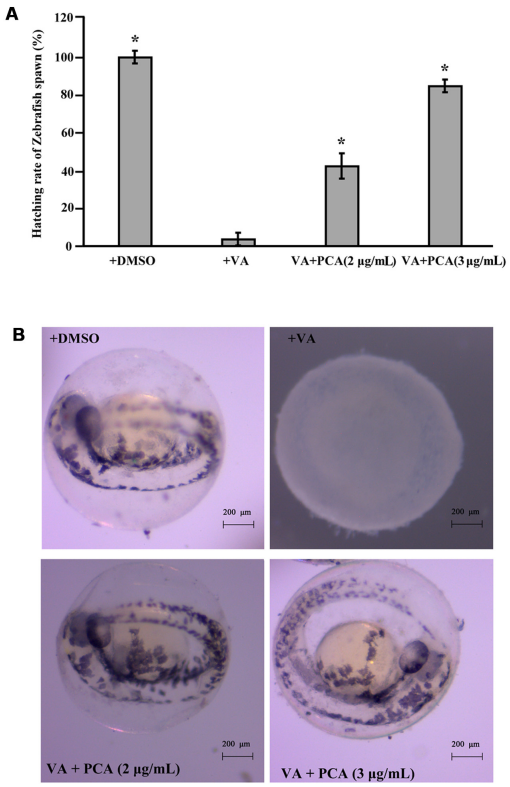


FIGURE 6 | Inhibitory activities of PCA against *V. anguillarum* C312 infection to zebrafish embryos. (A) PCA inhibits *V. anguillarum* C312 infection to zebrafish embryos. Zebrafish embryos were infected with *V. anguillarum* C312 in the absence or presence of different concentrations of PCA and the relative hatching percent of zebrafish embryos was calculated after 48 h infection. Error bars indicate the standard deviations of three measurements. $^*P < 0.05$. The error bars (SD) from the mean for three replicates are shown. **(B)** The typical hatching pictures of zebrafish embryos infected with *V. anguillarum* C312 in the absence or presence of different concentrations of PCA. All the pictures were taken with stereo microscope (ZEISS Stemi 2000C, German).

Additionally, PCA showed effective disease control on tobacco infected with *Phytophthora nicotianae* JM1 (Supplementary Figure S6) via distorting the mycelia of *Phytophthora nicotianae* JM1 (Supplementary Figure S5), which is consistent with the report that deformed mycelia of *Macrophomina phaseolina* appeared when this fungus was treated by phenazine compounds (Kumar et al., 2005). On the other hand, PCA is a redox-cycling agent that can be reduced both *in vitro* and *in vivo*. The reduced form PCA reacts with O_2 and generates ROS, which would damage the cell (Xu et al., 2015). In this study, substantial ROS was accumulated in *V. anguillarum* when treated with PCA (**Figure 5A**). This result indicated that marine derived PCA, like other phenazine compounds, generates ROS in *V. anguillarum* and that ROS generation is likely to be an important mechanism of PCA action, as is the case with PCA acts on *Xanthomonas oryzae* (Xu et al., 2015).

In general, the production of specific antibiotics *in vitro* is closely correlated with their antagonism and disease control efficacy *in vivo* (Lee et al., 2003), although discrepancies exist between *in vitro* antagonistic effect and the corresponding *in vivo* efficacy in some cases. In the present study, we ascertained not only the *in vitro* antibacterial and antifungal activities of PCA against some aquaculture and plant pathogens, but also its *in vivo* antibacterial and antifungal activities in the host animal or plants. Further studies of the effectiveness of PCA for diseases control and the design of practical applications should be carried out under field conditions. Additionally, recent isolation of *P. aeruginosa* strains from an open-ocean site has shown that they possess a unique genotype (Nonaka et al., 2010), which suggests that the geographical origin of the strains is reflected in their phylogeny. Thus, it will be very interesting to investigate that the biosynthesis differences between the marine and terrestrial derived PCA in the future.

ETHICS STATEMENT

For the human cell experiments, this study was carried out in accordance with the recommendations of ethical guidelines of Chinese Academy of Sciences with written informed consent from all subjects. All subjects gave written informed consent in accordance with the Declaration of Helsinki. The protocol was approved by the Chinese Academy of Sciences. For the zebrafish experiments, this study was carried out in accordance with the recommendations of ethical guidelines of Chinese Academy of Sciences. The protocol was approved by the ethical guidelines of Chinese Academy of Sciences.

AUTHOR CONTRIBUTIONS

LZ, CZ, and CS conceived and designed the experiments. LZ performed most of the experiments. XT finished the activity assay of PCA in greenhouse. SK did the ROS accumulation assay of PCA in A549 cells. GL helped to do antagonistic assay of marine bacterial strains. LZ, CZ, and CS analyzed the data. LZ and CS prepared the figures and wrote the paper. All authors reviewed the manuscript.

ACKNOWLEDGMENTS

This work was supported by Natural science outstanding youth fund of Shandong Province (JQ201607), Taishan Young Scholar Program of Shandong Province, AoShan Talents Program supported by Qingdao National Laboratory for Marine Science and Technology (No.2015ASTP), Scientific and Technological Innovation Project of Qingdao National Laboratory for Marine Science and Technology (No.2015ASKJ02-3), "100-Talent Project" of Chinese Academy of Sciences for CS.

SUPPLEMENTARY MATERIAL

The Supplementary Material for this article can be found online at: http://journal.frontiersin.org/article/10.3389/fmicb.2017.00289/full#supplementary-material

REFERENCES

Abraham, A., Philip, S., Jacob, M. K., Narayanan, S. P., Jacob, C. K., and Kochupurackal, J. (2015). Phenazine-1-carboxylic acid mediated anti-oomycete activity of the endophytic *Alcaligenes* sp. EIL-2 against *Phytophthora meadii*. *Microbiol. Res.* 170, 229–234. doi: 10.1016/j.micres.2014.06.002

Audenaert, K., Pattery, T., Cornelis, P., and Höfte, M. (2002). Induction of systemic resistance to *Botrytis cinerea* in tomato by *Pseudomonas aeruginosa* 7NSK2: role of salicylic acid, pyochelin, and pyocyanin. *Mol. Plant Microbe Interact.* 15, 1147–1156.

Ausubel, F. M., Brent, R., Kingston, R. E., Moore, D. D., Seidman, J., Smith, J. A., et al. (eds). (1992). *Short Protocols in Molecular Biology*, 5th Edn. New York, NY: Wiley.

Bahar, O., Levi, N., and Burdman, S. (2011). The cucurbit pathogenic bacterium *Acidovorax citrulli* requires a polar flagellum for full virulence before and after host-tissue penetration. *Mol. Plant Microbe Interact.* 24, 1040–1050. doi: 10.1094/Mpmi-02-11-0041

Berdy, J. (2005). Bioactive microbial metabolites - a personal view. *J. Antibiot.* 58, 1–26.

Bloemberg, G. V., and Lugtenberg, B. J. (2003). Phenazines and their role in biocontrol by *Pseudomonas* bacteria. *New Phytol.* 157, 503–523.

Feling, R. H., Buchanan, G. O., Mincer, T. J., Kauffman, C. A., Jensen, P. R., and Fenical, W. (2003). Salinosporamide A: a highly cytotoxic proteasome inhibitor from a novel microbial source, a marine bacterium of the new genus *Salinospora*. *Angew. Chem. Int. Ed. Engl.* 42, 355–357. doi: 10.1002/anie.200390115

Feng, Q., Wu, J., Chen, G., Cui, F., Kim, T., and Kim, J. (2000). A mechanistic study of the antibacterial effect of silver ions on *Escherichia coli* and *Staphylococcus aureus*. *J. Biomed. Mater. Res. A* 52, 662–668.

Frans, I., Michiels, C. W., Bossier, P., Willems, K., Lievens, B., and Rediers, H. (2011). *Vibrio anguillarum* as a fish pathogen: virulence factors, diagnosis and prevention. *J. Fish Dis.* 34, 643–661. doi: 10.1111/j.1365-2761.2011.01279.x

Gerwick, W. H., and Fenner, A. M. (2013). Drug discovery from marine microbes. *Microb. Ecol.* 65, 800–806. doi: 10.1007/s00248-012-0169-9

Han, T., You, C., Zhang, L., Feng, C., Zhang, C., Wang, J., et al. (2016). Biocontrol potential of antagonist *Bacillus subtilis* Tpb55 against tobacco black shank. *Biocontrol* 61, 195–205.

Hao, W., Zhang, X., Zhao, W., and Chen, X. (2014). Psoralidin induces autophagy through ROS generation which inhibits the proliferation of human lung cancer A549 cells. *PeerJ* 2:e555. doi: 10.7717/peerj.555

Jain, R., and Pandey, A. (2016). A phenazine-1-carboxylic acid producing polyextremophilic *Pseudomonas chlororaphis* (MCC2693) strain, isolated from mountain ecosystem, possesses biocontrol and plant growth promotion abilities. *Microbiol. Res.* 190, 63–71. doi: 10.1016/j.micres.2016.04.017

Jensen, P. R., and Fenical, W. (1994). Strategies for the discovery of secondary metabolites from marine-bacteria - ecological perspectives. *Annu. Rev. Microbiol.* 48, 559–584. doi: 10.1146/annurev.mi.48.100194.003015

Jin, K. M., Zhou, L. A., Jiang, H. X., Sun, S., Fang, Y. L., Liu, J. H., et al. (2015). Engineering the central biosynthetic and secondary metabolic pathways of *Pseudomonas aeruginosa* strain PA1201 to improve phenazine-1-carboxylic acid production. *Metab. Eng.* 32, 30–38. doi: 10.1016/j.ymben.2015.09.003

Karuppiah, V., Alagappan, K., Sivakumar, K., and Kannan, L. (2016). Phenazine-1-carboxylic acid-induced programmed cell death in human prostate cancer cells is mediated by reactive oxygen species generation and mitochondrial-related apoptotic pathway. *J. Appl. Biomed.* 14, 199–209. doi: 10.1016/j.jab.2016.01.003

Kerr, J. R., Taylor, G. W., Rutman, A., Hoiby, N., Cole, P. J., and Wilson, R. (1999). *Pseudomonas aeruginosa* pyocyanin and 1-hydroxyphenazine inhibit fungal growth. *J. Clin. Pathol.* 52, 385–387.

Kumar, R. S., Ayyadurai, N., Pandiaraja, P., Reddy, A. V., Venkateswarlu, Y., Prakash, O., et al. (2005). Characterization of antifungal metabolite produced by a new strain *Pseudomonas aeruginosa* PUPa3 that exhibits broad-spectrum antifungal activity and biofertilizing traits. *J. Appl. Microbiol.* 98, 145–154. doi: 10.1111/j.1365-2672.2004.02435.x

Lee, J. Y., Moon, S. S., and Hwang, B. K. (2003). Isolation and in vitro and in vivo activity against *Phytophthora capsici* and *Colletotrichum orbiculare* of phenazine-1-carboxylic acid from *Pseudomonas aeruginosa* strain GC-B26. *Pest Manag. Sci.* 59, 872–882. doi: 10.1002/ps.688

Letchumanan, V., Pusparajah, P., Tan, L. T. H., Yin, W. F., Lee, L. H., and Chan, K. G. (2015). Occurrence and antibiotic resistance of *Vibrio parahaemolyticus* from shellfish in Selangor, Malaysia. *Front. Microbiol.* 6:1417. doi: 10.3389/fmicb.2015.01417

Mavrodi, D. V., Blankenfeldt, W., and Thomashow, L. S. (2006). Phenazine compounds in fluorescent *Pseudomonas* spp. Biosynthesis and regulation. *Annu. Rev. Phytopathol.* 44, 417–445. doi: 10.1146/annurev.phyto.44.013106.145710

McGuigan, C. F., and Li, X. F. (2014). Cytotoxicity and genotoxicity of phenazine in two human cell lines. *Toxicol. In Vitro* 28, 607–615. doi: 10.1016/j.tiv.2013.12.007

Mei, Y. X., Dai, X. Y., Yang, W., Xu, X. W., and Liang, Y. X. (2015). Antifungal activity of chitooligosaccharides against the dermatophyte *Trichophyton rubrum*. *Int. J. Biol. Macromol.* 77, 330–335. doi: 10.1016/j.ijbiomac.2015.03.042

Morales, D. K., Jacobs, N. J., Rajamani, S., Krishnamurthy, M., Cubillos-Ruiz, J. R., and Hogan, D. A. (2010). Antifungal mechanisms by which a novel *Pseudomonas aeruginosa* phenazine toxin kills *Candida albicans* in biofilms. *Mol. Microbiol.* 78, 1379–1392. doi: 10.1111/j.1365-2958.2010.07414.x

Nonaka, L., Inubushi, A., Shinomiya, H., Murase, M., and Suzuki, S. (2010). Differences of genetic diversity and antibiotics susceptibility of *Pseudomonas aeruginosa* isolated from hospital, river and coastal seawater. *Environ. Microbiol. Rep.* 2, 465–472. doi: 10.1111/j.1758-2229.2010.00178.x

Pierson, L. S., and Pierson, E. A. (2010). Metabolism and function of phenazines in bacteria: impacts on the behavior of bacteria in the environment and biotechnological processes. *Appl. Microbiol. Biotechnol.* 86, 1659–1670. doi: 10.1007/s00253-010-2509-3

Preetha, R., Vijayan, K. K., Jayapraksh, N. S., Alavandi, S. V., Santiago, T. C., and Singh, I. S. B. (2015). Optimization of culture conditions for mass production of the probiotics *Pseudomonas* MCCB 102 and 103 antagonistic to pathogenic *Vibrios* in aquaculture. *Probiotics Antimicrob.* 7, 137–145. doi: 10.1007/s12602-015-9185-7

Raio, A., Puopolo, G., Cimmino, A., Danti, R., Della Rocca, G., and Evidente, A. (2011). Biocontrol of cypress canker by the phenazine producer *Pseudomonas chlororaphis* subsp. aureofaciens strain M71. *Biol. Control* 58, 133–138.

Ray, P. D., Huang, B. W., and Tsuji, Y. (2012). Reactive oxygen species (ROS) homeostasis and redox regulation in cellular signaling. *Cell. Signal.* 24, 981–990. doi: 10.1016/j.cellsig.2012.01.008

Su, J.-J., Zhou, Q., Zhang, H.-Y., Li, Y.-Q., Huang, X.-Q., and Xu, Y.-Q. (2010). Medium optimization for phenazine-1-carboxylic acid production by a gacA qscR double mutant of *Pseudomonas* sp. M18 using response surface methodology. *Bioresour. Technol.* 101, 4089–4095. doi: 10.1016/j.biortech.2009.12.143

Tamura, K., Stecher, G., Peterson, D., Filipski, A., and Kumar, S. (2013). MEGA6: molecular evolutionary genetics analysis version 6.0. *Mol. Biol. Evol.* 30, 2725–2729. doi: 10.1093/molbev/mst197

Toranzo, A., Santos, Y., and Barja, J. (1996). Immunization with bacterial antigens: *Vibrio* infections. *Dev. Biol. Stand.* 90, 93–105.

Waters, A. L., Hill, R. T., Place, A. R., and Hamann, M. T. (2010). The expanding role of marine microbes in pharmaceutical development. *Curr. Opin. Biotechnol.* 21, 780–786. doi: 10.1016/j.copbio.2010.09.013

Westerfield, M. (1994). *The Zebrafish Book: A Guide for the Laboratory Use of Zebrafish Danio (Brachydanio Rerio)*. Eugene, OR: University of Oregon Press.

Wiegand, I., Hilpert, K., and Hancock, R. E. (2008). Agar and broth dilution methods to determine the minimal inhibitory concentration (MIC) of antimicrobial substances. *Nat. Protoc.* 3, 163–175. doi: 10.1038/nprot.2007.521

Xu, H. M., Rong, Y. J., Zhao, M. X., Song, B., and Chi, Z. M. (2014). Antibacterial activity of the lipopetides produced by *Bacillus amyloliquefaciens* M1 against multidrug-resistant *Vibrio* spp. isolated from diseased marine animals. *Appl. Microbiol. Biotechnol.* 98, 127–136. doi: 10.1007/s00253-013-5291-1

Xu, S., Pan, X., Luo, J., Wu, J., Zhou, Z., Liang, X., et al. (2015). Effects of phenazine-1-carboxylic acid on the biology of the plant-pathogenic bacterium *Xanthomonas oryzae* pv. oryzae. *Pestic. Biochem. Physiol.* 117, 39–46. doi: 10.1016/j.pestbp.2014.10.006

Yang, N., and Sun, C. M. (2016). The inhibition and resistance mechanisms of actinonin, isolated from marine *Streptomyces* sp NHF165, against *Vibrio anguillarum*. *Front. Microbiol.* 7:1467. doi: 10.3389/fmicb.2016.01467

Yu, L. P., Hu, Y. H., Sun, B. G., and Sun, L. (2012). C312M: an attenuated *Vibrio anguillarum* strain that induces immunoprotection as an oral and immersion vaccine. *Dis. Aquat. Organ.* 102, 33–42. doi: 10.3354/dao02544

Yuan, L. L., Li, Y. Q., Wang, Y., Zhang, X. H., and Xu, Y. Q. (2008). Optimization of critical medium components using response surface methodology for phenazine-1-carboxylic acid production by *Pseudomonas* sp M-18Q. *J. Biosci. Bioeng.* 105, 232–237. doi: 10.1263/jbb.105.232

Zhou, Q., Su, J., Jiang, H., Huang, X., and Xu, Y. (2010). Optimization of phenazine-1-carboxylic acid production by a gacA/qscR-inactivated *Pseudomonas* sp. M18GQ harboring pME6032Phz using response surface methodology. *Appl. Microbiol. Biotechnol.* 86, 1761–1773. doi: 10.1007/s00253-010-2464-z

Conflict of Interest Statement: The authors declare that the research was conducted in the absence of any commercial or financial relationships that could be construed as a potential conflict of interest.

Copyright © 2017 Zhang, Tian, Kuang, Liu, Zhang and Sun. This is an open-access article distributed under the terms of the Creative Commons Attribution License (CC BY). The use, distribution or reproduction in other forums is permitted, provided the original author(s) or licensor are credited and that the original publication in this journal is cited, in accordance with accepted academic practice. No use, distribution or reproduction is permitted which does not comply with these terms.

frontiers in Microbiology

ORIGINAL RESEARCH
published: 28 February 2017
doi: 10.3389/fmicb.2017.00307

Fungal Root Microbiome from Healthy and Brittle Leaf Diseased Date Palm Trees (*Phoenix dactylifera* L.) Reveals a Hidden Untapped Arsenal of Antibacterial and Broad Spectrum Antifungal Secondary Metabolites

*Fedia B. Mefteh[1], Amal Daoud[1], Ali Chenari Bouket[2,3], Faizah N. Alenezi[2], Lenka Luptakova[2,4], Mostafa E. Rateb[5], Adel Kadri[1,6], Neji Gharsallah[1] and Lassaad Belbahri[2,7]**

[1] Laboratory of Plant Biotechnology, Faculty of Science, University of Sfax, Sfax, Tunisia, [2] Biotechnology, NextBiotech, Agareb, Tunisia, [3] Graduate School of Life and Environmental Sciences, Osaka Prefecture University, Sakai, Japan, [4] Department of Biology and Genetics, Institute of Biology, Zoology and Radiobiology, University of Veterinary Medicine and Pharmacy, Kosice, Slovakia, [5] School of Science and Sport, University of the West of Scotland, Paisley, UK, [6] College of Science and Arts in Baljurashi, Al Baha University, Al Bahah, Saudi Arabia, [7] Laboratory of Soil Biology, University of Neuchâtel, Neuchâtel, Switzerland

OPEN ACCESS

Edited by:
Dietmar Schlosser,
Helmholtz Centre for Environmental Research (UFZ), Germany

Reviewed by:
Giuseppe Spano,
University of Foggia, Italy
Maria Lurdes Inacio,
Instituto Nacional de Investigação Agrária e Veterinária, Portugal

***Correspondence:**
Lassaad Belbahri
lassaad.belbahri@unine.ch

Specialty section:
This article was submitted to Microbiotechnology, Ecotoxicology and Bioremediation, a section of the journal Frontiers in Microbiology

Received: 08 January 2017
Accepted: 14 February 2017
Published: 28 February 2017

Citation:
Mefteh FB, Daoud A, Chenari Bouket A, Alenezi FN, Luptakova L, Rateb ME, Kadri A, Gharsallah N and Belbahri L (2017) Fungal Root Microbiome from Healthy and Brittle Leaf Diseased Date Palm Trees (Phoenix dactylifera L.) Reveals a Hidden Untapped Arsenal of Antibacterial and Broad Spectrum Antifungal Secondary Metabolites. Front. Microbiol. 8:307. doi: 10.3389/fmicb.2017.00307

In this study, we aimed to explore and compare the composition, metabolic diversity and antimicrobial potential of endophytic fungi colonizing internal tissues of healthy and brittle leaf diseased (BLD) date palm trees (*Phoenix dactylifera* L.) widely cultivated in arid zones of Tunisia. A total of 52 endophytic fungi were isolated from healthy and BLD roots of date palm trees, identified based on internal transcribed spacer-rDNA sequence analysis and shown to represent 13 species belonging to five genera. About 36.8% of isolates were shared between healthy and diseased root fungal microbiomes, whereas 18.4 and 44.7% of isolates were specific to healthy and BLD root fungal microbiomes, respectively. All isolates were able to produce at least two of the screened enzymes including amylase, cellulase, chitinase, pectinase, protease, laccase and lipase. A preliminary screening of the isolates using disk diffusion method for antibacterial activity against four Gram-positive and three Gram-negative bacteria and antifungal activities against three phytopathogenic fungi indicated that healthy and BLD root fungal microbiomes displayed interesting bioactivities against examined bacteria and broad spectrum bioactivity against fungal pathogens. Some of these endophytic fungi (17 isolates) were fermented and their extracts were evaluated for antimicrobial potential against bacterial and fungal isolates. Results revealed that fungal extracts exhibited antibacterial activities and were responsible for approximately half of antifungal activities against living fungi. These results suggest a strong link between fungal bioactivities and their secondary metabolite arsenal. EtOAc extracts of *Geotrichum candidum* and *Thielaviopsis punctulata* originating from BLD microbiome gave best results against *Micrococcus luteus* and *Bacillus subtilis* with minimum inhibitory concentration

(MIC, 0.78 mg/mL) and minimum bactericidal concentration (6.25 mg/mL). *G. candidum* gave the best result against *Rhizoctonia solani* with MIC 0.78 mg/mL and minimum fungicidal concentration (MFC, 6.25 mg/mL). In conclusion, using plant microbiomes subjected to biotic stresses offers new endophytes with different bioactivities than those of healthy plants. Therefore, date palm endophytic fungi represent a hidden untapped arsenal of antibacterial and broad spectrum antifungal secondary metabolites and could be considered promising source of bioactive compounds with industrial and pharmaceutical applications.

Keywords: endophytic fungi, secondary metabolites, brittle leaf disease, antimicrobial activity, date palm, enzymes

INTRODUCTION

The recent development of antimicrobial resistance by pathogenic microorganisms intimidates the current treatment and prevention of ever-increasing range of infections by bacteria and fungi and leads to new microorganisms that cannot be controlled by the drugs that referred to as "superbugs" (Vargiu et al., 2016). Reports on superbugs such as MRSA (methicillin-resistant *Staphylococcus aureus*) and NDM-1 (New Delhi metallo-beta-lactamase 1) strains are rising terrifyingly nowadays and represent a serious threat to public health (Khan and Khan, 2016). The most important causes that favored antibiotic resistance include, excessive and inappropriate antibiotic use among humans and animals (Kaye, 2016), environmental contamination with antibiotics (Lammie and Hughes, 2016), poor hygienic conditions (Senn et al., 2016), global trade and travel (Riddle and Connor, 2016), medical tourism (Saliba et al., 2016), and a decline in new antibiotic development (Marston et al., 2016).

Therefore, there is an increasing demand for new bioactive, cost-effective and sustainable antimicrobial molecules in medicine, industry and agriculture that prompted the development of diverse programs such as screening for new plants or fungal species with antimicrobial activities from unexplored ecological niches and habitats (Lugtenberg et al., 2016). Historically, plants were considered potential source of drugs for treatment of many human diseases. Certain endophytes could also produce the same or similar compounds as their host plants (Xu et al., 2009). Since the discovery of the billion-dollar anticancer drug Taxol from the endophytic fungus of *Taxus brevifolia* namely *Taxomyces andreanae*, endophytes have gained increasing interest of mycologists, botanists, pharmacologists, and even plant pathologists (Stierle et al., 1993; Venugopalan and Srivastava, 2015; Gouda et al., 2016; Newman and Cragg, 2016). Recently, considerable knowledge has accumulated about endophytes, defined as a community of microorganisms that colonize all plant species tissues without causing any apparent symptoms (Petrini et al., 1992). Endophytic microorganisms offer many ecological and physiological benefits to their host plants including adaptability to different kinds of stress, growth promotion and resistance against plant pests and pathogens (Jia et al., 2016).

Therefore, several attempts have been made to study the biology of endophytic microorganisms and to exploit the untapped potential of their bioactive compounds (Mousa and Raizada, 2013). Consequently, numerous endophytes including bacteria, fungi, and actinomycetes had been recovered and characterized from approximately 300,000 plant species (Strobel and Daisy, 2003). Accordingly, recent studies have shown that endophytic fungi represent a promising resource of novel natural products with biological importance such as antidiabetic, anticancer, antioxidant, antimicrobial, antiviral, and immunosuppressive activities (Katoch et al., 2015; Chen et al., 2016; Monggoot et al., 2016; Rathna et al., 2016). These bioactive compounds may be classified as alkaloids, steroids, terpenoids, flavonoids, benzopyranones, quinones, isocumarins, phenolics, tetralones, lactones, peptides, and many other subclasses (Xu et al., 2008; Kaul et al., 2012). The discovery of novel antimicrobial compounds from endophytic fungi constitutes an important alternative to overcome numerous recent problems such as the insufficiency of current antibiotics against human pathogens, the wider range of infections and the low rate of new antimicrobial agent discovery (Strobel et al., 2001; Marston et al., 2016). Antimicrobial compounds could also be used as food preservatives among other biotechnological applications (Haque et al., 2015).

Different environmental factors in addition to biotic and abiotic stresses are considered the main drivers of plant fungal endophyte diversity and believed to shape their communities. Although endophyte characterization in healthy tissues have been extensively studied, few reports addressed such communities in plants under abiotic or biotic stresses (Douanla-Meli et al., 2013). Additionally, Date palm trees, extensively used in folk medicine, have been shown to be rich with numerous secondary metabolites with interesting pharmacological and antimicrobial activities (Abdennabi et al., 2016). Therefore, endophytes of this plant species were the main focus of this study, with a double objective. First, endophytes from healthy and brittle leaf diseased (BLD) root tissues have been recovered and identified. Second, endophyte communities have been compared in terms of metabolic potential by testing enzyme activities of amylase, cellulase, chitinase, pectinase, protease, laccase and lipase and antimicrobial bioactivities against four Gram-positive and three Gram-negative bacterial species and antifungal activities against three phytopathogenic fungi. Contribution of

secondary metabolites to the bioactivities of endophytes is then screened using their EtOAc culture extracts.

MATERIALS AND METHODS

Isolation of Root Fungal Endophytes from Healthy and BLD Date Palm Trees

Roots of healthy and BLD adult date palm trees variety Deglet Ennour were collected from groves located in Nefta Oasis, near to Algerian-Tunisian border and just at the north of Chott Djerid (Latitude: 33° 52′ 23.12″ N, Longitude: 7° 52′ 39.54″ E). Numerous samples from roots and leaves were collected ($n = 20$). Plant materials were transferred to the laboratory in sterile bags and stored at 4°C until processing. Endophytic fungi were isolated from the internal tissues of date palm roots, as described by Hallmann et al. (2007). Briefly, samples were washed with tap water for 30 min and surface sterilized by sequential washes in 70% ethanol followed by 3% NaClO for 3 min. Finally, the sterile plant material was washed several times with sterilized distilled water and cut into small fragments (0.5–1 cm) under sterile conditions using a sterile scalpel. In total, 103 root fragments were used for fungal isolation. Surface sterilized plant material was placed on potato dextrose agar (PDA) media supplemented with 100 μg/mL streptomycin for bacterial growth inhibition. The plates were incubated for 3–5 days at 30°C until fungal mycelia were observed. Single fungal isolates have been obtained by sub-culturing emergent hyphal tips. Cultures were preserved on PDA slants for subsequent morphological and molecular identification and biochemical characterization.

Fungal DNA Extraction and Amplification

Pure cultures of the isolates on PDA slant vials were selected for DNA extraction. Mycelia were excised from 5 days old plates. The extraction was processed using the DNA-Easy Plant Mini kit (QIAGEN, Basel, Switzerland) following manufacturer's protocol. The quantity and quality of the genomic DNA were evaluated by a NanoDrop NT-100 UV spectrophotometer (Witec AG, Switzerland) and by visual observation through 1.5% agarose gel electrophoresis. The molecular identification of the endophytic fungi isolated from the roots of healthy and BLD date palm trees was carried out as described by Paul et al. (2008). The internal transcribed spacer (ITS) of rDNA was amplified by the polymerase chain reaction using primers, ITS1 (TCCGTAGGTGAACCTGCGG) and ITS4 (TCCTCCGCTTATTGATATGC) (White et al., 1990). All reactions were carried out in a total volume of 50 μL, containing 5 μL 10x Ex Taq buffer (20 mM Tris–HCl, pH 8.0, 100 mM KCl), 4 μL 2.5 mM dNTP mixture, 0.5 μM of each primer, 1.25 units Taq DNA polymerase (Takara Bio, Ohtsu, Japan) and 10 ng DNA. The amplifications were performed using a master gradient thermal cycler (Eppendorf, Basel, Switzerland) with the following cycling profile: Denaturation step at 95°C for 2 min followed by 30 cycles including denaturation at 94°C for 20 s, annealing at 55°C for 25 s and extension at 72°C for 15 s and final extension step at 72°C for 10 min. PCR amplicons were purified with Minelute PCR purification kit (Qiagen, Basel, Switzerland) according to the manufacturer's specifications (Belbahri et al., 2006).

DNA Sequencing and Phylogenetic Analysis

The purified amplicons were sequenced in both directions using the same PCR primers and BigDye® Terminator v. 3.1 cycle sequencing kit. Sequencing reactions were resolved on an ABI 3130 XL available at the iGE3 [Institute of Genetics and Genomics in Geneva, University of Geneva Medical Center (CMU), Switzerland]. Raw sequence files were manually edited using SeqMan™II (DNASTAR, Madison, WI, USA) and a consensus sequence was generated for each sequence. The consensus sequence for genomic region was blasted against the NCBI's GenBank sequence database using megablast to identify their closest species relatives. For the gene region, the retrieved sequences from GenBank together with sequences generated in this study, were aligned using the multiple sequence alignment web-based MAFFT program (Katoh and Toh, 2008). Phylogenetic trees were constructed based on the maximum-likelihood (ML) algorithm (Felsenstein, 1981) using MEGA6 (Tamura et al., 2013), with evolutionary distances computed using the Kimura 2-parameter model (Kimura, 1980). Validity of branches in the resulting trees was evaluated by bootstrap resampling support of the data sets with 1000 replications.

Screening for Extracellular Enzymes

Screening for Amylase Activity

Amylase-producing fungi were characterized using glucose-yeast-peptone (GYP) medium containing (g/L): glucose (1), yeast extract (0.5), peptone (0.5), agar (15), and supplemented with 0.2% of starch. The pH of the medium was adjusted to 6.0. Mycelia of each endophytic fungus were placed in the center of the plates and incubated at 30°C for 72 h. After incubation, an iodine solution ($I_2 = 1$ g, KI = 2 g/300 ml) was poured on the plates. The appearance of clear zones around the colonies indicated the presence of amylase activity (Saleem and Ebrahim, 2014).

Screening for Cellulolytic Activity

Cellulolytic activity from endophytic fungi was characterized by inoculating GYP agar supplemented with 0.5% carboxymethyl cellulose (CMC). After incubation for 72 h at 30°C, the plates were overlaid with 1% red congo and distained with 1 M NaCl. Strains with clear zones around the colonies were mentioned as cellulolytic enzyme producers (Shahriarinour et al., 2011).

Screening for Chitinase Activity

A minimum medium containing (g/L): colloidal chitin (10 g), $(NH4)_2SO_4$ (2 g), KH_2PO_4 (0.7 g), $HgSO_4$.7 H_2O (0.5 g), $FeSO_4$. $7H_2O$ (0.01 g), agar (15 g) was used for chitinase screening (Jenifer et al., 2014). Colloidal chitin was prepared following the protocol described by Nagpure and Gupta (2012).

Screening for Pectinase Activity

Pectinolytic activity of recovered endophytic fungi were evaluated on the medium based on the method described by

Nitinkumar and Bhushan (2010). After incubation of inoculated plates for 72 h at 30°C, cetrimonium bromide (CTAB) solution (1%) was poured onto colonies for detection of pectinase producing fungi.

Screening for Laccase Activity

The fungal isolates were inoculated on malt extract medium with the following composition (g/L): malt extract (30), agar (20) supplemented with 2 mM ABTS (2,2′-azino-di-3-ethylbenzotiazol-6-sulfonate acid) and incubated at 30°C. Positive laccase activity was recorded by the appearance of reddish brown halo around the inoculated strains indicating the presence of laccase activity (Gnanasalomi and Gnanadoss, 2013).

Screening for Lipase Activity

Lipase activity was assessed using the protocol described by Thota et al. (2012). The endophytic fungi were inoculated on medium containing (g/L): 8 nutrient broth, 4 sodium chloride, 10 agar supplemented after autoclaving with olive oil (16.34 mL), Tween 80 (250 μL) and Rhodamine solution (10 μg/mL). After incubation at 30°C, lipase activity was detected by irradiating the plates with Ultra Violet light at 350 nm.

Screening for Protease Activity

Protease activity was checked using a simple medium containing (g/L): yeast extract (3), casein peptone (5), agar (15) supplemented after autoclave with 250 mL of sterile skimmed milk (Mohanasrinivasan et al., 2012). The fungal isolates were inoculated on the center of plates. After incubation for 72 h at 30°C, the appearance of clear zones around them indicated the ability of the isolates to produce and secrete protease in the medium.

Screening for Secondary Metabolites Production

Assay of Microorganisms

Among microorganisms used for antimicrobial assay, seven were bacteria including four Gram-positive bacteria (*Bacillus cereus* 'Bc' JN 934390, *B. subtilis* 'Bs' JN 934392, *Staphylococcus aureus* 'Sa' ATCC 6538 and *Micrococcus luteus* 'Ml') and three Gram-negative bacteria (*Salmonella enteritidis* 'Se' ATCC 43972, *Escherichia coli* 'Ec' ATCC 25922, and *Klebsiella pneumonia* 'Kp'). Bacterial cultures were prepared in 10 mL of Mueller-Hinton broth (MHB) (Mueller and Hinton, 1941) and maintained at 30°C with constant shaking (180 rpm). For the studied bacteria, the optical density at 600 nm of overnight cultures was adjusted to 0.1 corresponding to 3.2×10^6 CFU/mL.

Antifungal activity was conducted using three phytopathogenic fungi including *Rhizoctonia solani* 'Rs,' *Fusarium oxysporum* 'Fo' AB586994 and *Pythium catenulatum* 'Pc' AY598675. The examined fungi were inoculated on PDA plates and incubated for 7 days at 30°C.

In vitro Antimicrobial (Antagonistic) Assay

The endophytic fungi were subjected to antimicrobial assays that allows rapid but qualitative selection of the bioactive isolates. For antibacterial activity, the disk diffusion method was carried out as described by Ezra et al. (2004). Briefly, plugs from 5-days-old pure culture of each endophytic fungi (6 mm diameter) were cut using sterile Pasteur pipette and placed onto the periphery of Mueller-Hinton agar (MHA) plates initially inoculated with 100 μL of culture of the tested bacteria. Diffusion was carried out for 2 h at 4°C. After incubation of plates for 24 h at 30°C, the antibacterial activity was expressed by measuring the diameters of inhibition zones around the fungal plugs.

The antifungal activity of the isolated fungal endophytes was assessed by dual culture method according to Alenezi et al. (2016). A dual culture was conducted on PDA plates with plugs from pure culture (10 mm in diameter) from the two partners, endophytic fungus and tested phytopathogenic fungi. The control plates were inoculated only with the phytopathogenic fungi. The plates were incubated for 72 h at 30°C and the percentage of inhibition (IP) of each isolate was recorded. All experiments were conducted in triplicates. The percentage of inhibition was calculated as the following formula (A: radial diameter of phytopathogenic fungus in control plate, B: radial diameter of phytopathogenic fungus in dual culture plate)

$$IP = [(A - B) \div A] \times 100$$

Secondary Screening: Fermentation in Liquid Medium and Antimicrobial Activity

The endophytic isolates from healthy and BLD date palm roots that exhibited inhibitory activity against the largest number of examined bacteria and fungi were selected for secondary screening of bioactive metabolites production (Santos et al., 2015). Endophytic fungi were cultured on PDA plates for 5 days at 30°C. Then, three plugs (5 mm × 5 mm) with fungal culture were transferred to 300 mL flasks containing 150 mL of autoclaved potato dextrose broth (PDB). The cultures were incubated in a shaker at 30°C, 150 rpm for 21 days until stationary phase reached. Afterward, the fungal mycelia were separated from culture by filtration. The resulting filtrates from each endophytic fungus were extracted with equal volume of EtOAc. The organic solvent was evaporated under reduced pressure using rotary evaporator. The fungal extracts were then dissolved in DMSO or double distilled water to obtain final concentration of 100 μg/μL. Finally, the concentrated fungal extracts were passed through 0.2 μm filtration membrane and assayed for their antimicrobial activity by agar diffusion method. Briefly, 100 μL of freshly prepared culture for bacteria or spore suspension (10^6 spores/mL) for fungi were seeded onto agar plates surface using a sterile swab cotton. Each well was then filled with 60 μL of endophytic fungi extracts. The plates were kept for 2 h at 4°C to facilitate the diffusion of fungal filtrate. Afterward, they were incubated at 37°C for 24 h for bacteria and at 30°C for 3–5 days for fungal strains. Antimicrobial activity was evaluated by measuring the diameter of inhibition zones around the wells. All experiments were carried out in duplicate.

Determination of Minimum Inhibitory Concentration (MIC), Minimum Bactericidal Concentration (MBC), and Minimum Fungicidal Concentration (MFC) of Endophytic Fungal Extracts

The minimum bactericidal concentration (MBC) and minimum fungicidal concentration (MFC) were determined using broth micro-dilution method in a sterile 96 well micro plate, as described by Gulluce et al. (2007). Serial dilution of each fungal extract was prepared to get final concentrations ranging from 0.781 to 100 μg/μL. Each well was supplemented with 10 μL of bacterial or fungal suspension, 90 μL of liquid culture broth and 100 μL of fungal extract. The last well containing the above-cited components without addition of the fungal extract was considered as positive control. The one containing DMSO without extract was the negative control. Plates were incubated at 37°C for 24 h for bacterial strains and for 3 days at 30°C for fungal strains. Afterward, 25 μL of MTT (3-(4,5-dimethylthiazol-2-yl)-2,5-diphenyltetrazolium bromide] was added to each well for evaluation of the microorganisms viability. After incubation of plates for 30 min at 37°C, the clear wells indicated the inhibition of cell growth. The MIC is defined as the lowest concentration of extract that inhibit the growth of microorganisms. The MBC values were determined after incubation of plates for 48 h at 37°C as the highest dilution of extract that completely inhibit the growth of bacteria. MFC was considered as the first well with no visible growth of the test fungi. It was determined by inoculating the PDA plates with 10 μL of the well content followed by incubation for 3–5 days at 30°C. The MFC values were interpreted as the lowest concentration of endophytic fungal extract that inhibits fungal growth.

Statistical Analysis

Data were analyzed using IBM SPSS statistics by one-way analysis of variance (ANOVA) and independent-samples *T*-test. The level of significance used for all statistical tests is 5% ($p < 0.05$).

RESULTS

Phylogenetic Affinities of Endophytic Fungi

Endophytic fungi ITS-rDNA sequence analysis revealed diverse taxonomic affinities among the isolates (**Figures 1A,B**). In total, 52 ascomycetes were obtained in the present study. About 21 of them were isolated from healthy date palm roots, the remaining isolates were recovered from BLD roots (**Figures 1A,B**). Isolates belonged to Eurotiomycetes ($n = 38$), Sordariomycetes ($n = 11$) and Saccharomycetes ($n = 3$). Isolates comprised six genera with highest abundance of *Penicillium* (26 isolates) and *Aspergillus* (12 isolates). Among *Penicillium* species isolated, 12 isolates were identified as *P. bilaiae*, nine as *P. citrinum*, three as *P. citreonigrum,* one as *P. steckii*, and one as *P. cordubense*. The 12 *Aspergillus* species comprised one isolate of *A. quadrilineatus*, nine as *A. flavus*, and two as *A. niger*. Eight *Fusarium* were isolated from roots of date palm including six *Fusarium* sp. and two *F. oxysporum*. In Addition, two, three and one isolate of *Thielaviopsis punctulata, G. candidum and Thielavia arenaria,* respectively, were isolated only from BLD date palm roots (**Figures 1B,C**).

Screening for Enzyme Production

All 52 isolates were evaluated for their enzymatic activity with plate clearing assay for amylase, cellulase, chitinase, pectinase, protease, laccase, and lipase production. The results are presented in **Figure 2**.

Amylase Activity

Amylase activity has been studied in either healthy or BLD date palm roots fungal isolates. The results revealed a relevant capacity of the examined fungi to secrete these enzymes (**Figure 2**). Most of amylase producing fungi belonged to *Penicillium* followed by *Aspergillus* and *Fusarium* genera (**Figures 2A,B**). Mean amylase activity of all isolates of healthy roots was not significantly different from mean amylase activity of BLD isolates (**Figure 2C**).

Cellulase Activity

Figure 2A shows that among the recovered endophytic fungi, only 34 isolates displayed cellulase activity (**Figures 2A,B**). *Penicillium* species were able to degrade CMC at high percentage followed by *Aspergillus* and *Fusarium*. Among *Geotrichum* species, only *G. candidum* TDPEF 19 exhibited cellulase activity with halo diameter between 15 and 25 mm. Mean cellulase activity of all isolates of healthy roots was not significantly different from mean cellulase activity of BLD isolates (**Figure 2C**).

Chitinase Activity

All the isolated genera were able to grow on colloidal chitin agar plates reflecting their ability to produce extracellular chitinase (**Figure 2A**). Among the examined fungi, 25 chitinase-producing isolates belonged to Eurotiomycetes including *Penicillium* and *Aspergillus* species followed by nine Sordariomycetes and two *Geotrichum* species (**Figure 2B**). Mean chitinase activity of all isolates of healthy roots was not significantly different from mean chitinase activity of BLD isolates (**Figure 2C**).

Pectinase Activity

The findings revealed that the highest percentage of the isolated endophytic fungi (84.61%) exhibited pectinase activity (**Figure 2A**). The ability to degrade pectin substrates were detected mainly in endophytic fungi belonging to *Penicillium* species within *Thielavia* and *Thielaviopsis* genera (**Figure 2B**). Almost all of the isolated fungi showed halos diameter between 15 and 25 mm. Mean pectinase activity of all isolates of healthy roots were not significantly different from mean pectinase activity of BLD isolates (**Figure 2C**).

Protease Activity

As shown in **Figure 2A**, proteolytic activity was present in 59.61% of isolated endophytic fungi. Among the analyzed strains, 31 fungi showed degradation halos of casein on solid medium reflecting their ability to produce extracellular proteases. *Penicillium*, *Aspergillus,* and *Fusarium* are among the genera able to degrade casein (**Figure 2B**). Mean protease

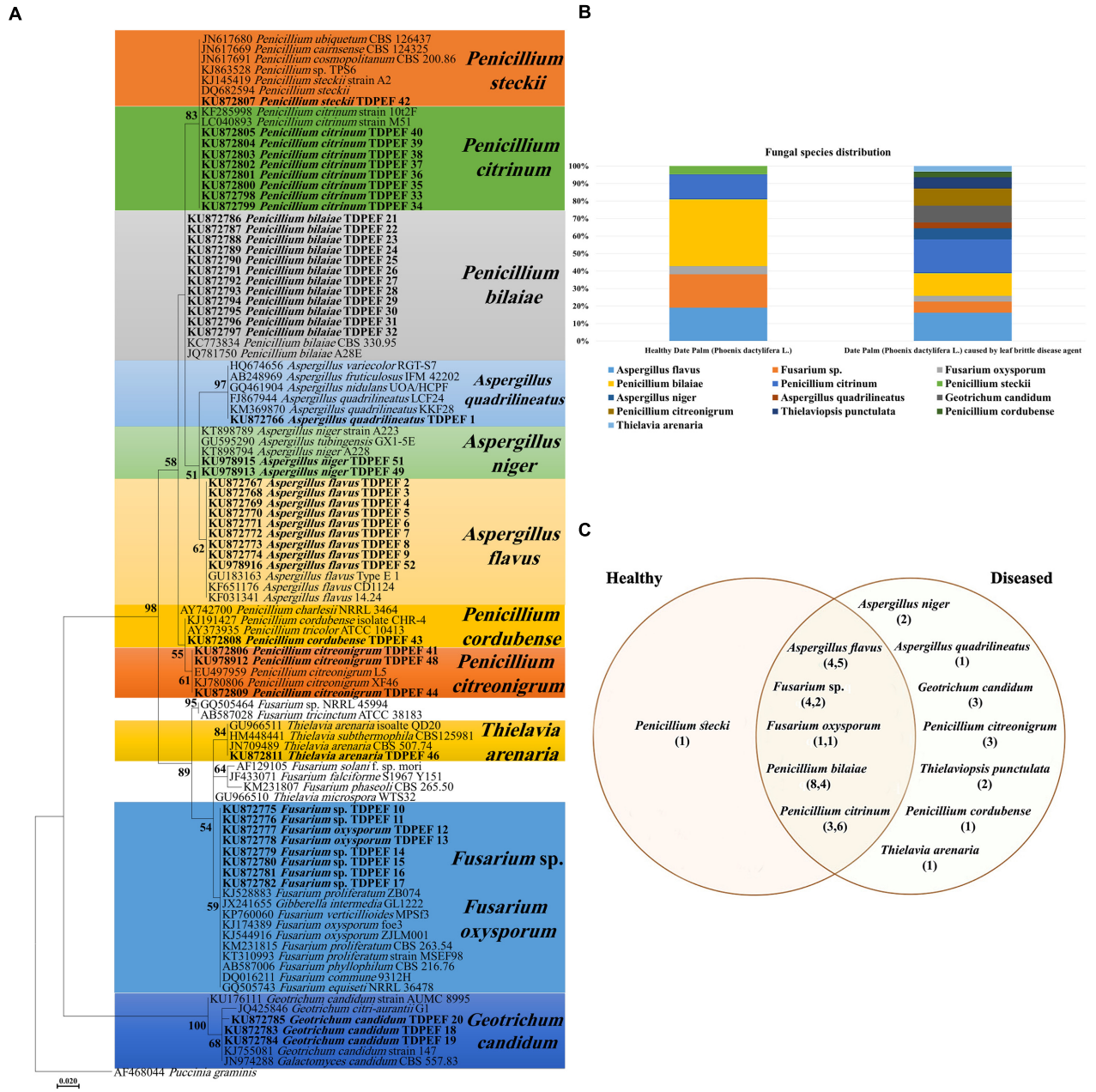


FIGURE 1 | (A) Maximum Likelihood phylogenetic tree of fungal endophytes recovered from healthy and brittle leaf diseased (BLD) diseased date palm roots. **(B)** Fungal species composition in healthy and BLD roots. **(C)** Venn diagram showing the distribution of endophytic isolates in plants roots (the first number between brackets represents the number of isolates recovered from healthy roots and the second number represents that recovered from roots of LBD roots).

activity of all isolates of healthy roots was not significantly different from mean protease activity of BLD isolates (**Figure 2C**).

Laccase Activity

Half of isolated endophytic fungi from healthy and BLD date palm roots showed positive results for laccase screening on solid medium (**Figure 2A**). As shown in **Figure 2B**, fungal species belonged to Eurotiomycetes class that showed ability to produce this type of enzyme. Mean laccase activity of all isolates of healthy roots were not significantly different from mean protease activity of BLD isolates (**Figure 2C**).

Lipase Activity

The lipolytic activity of the fungal isolates are presented in **Figure 2A**. After irradiation with UV light of plates, 28 endophytic fungal strains showed fluorescent halos around their mycelia reflecting their ability to produce extracellular

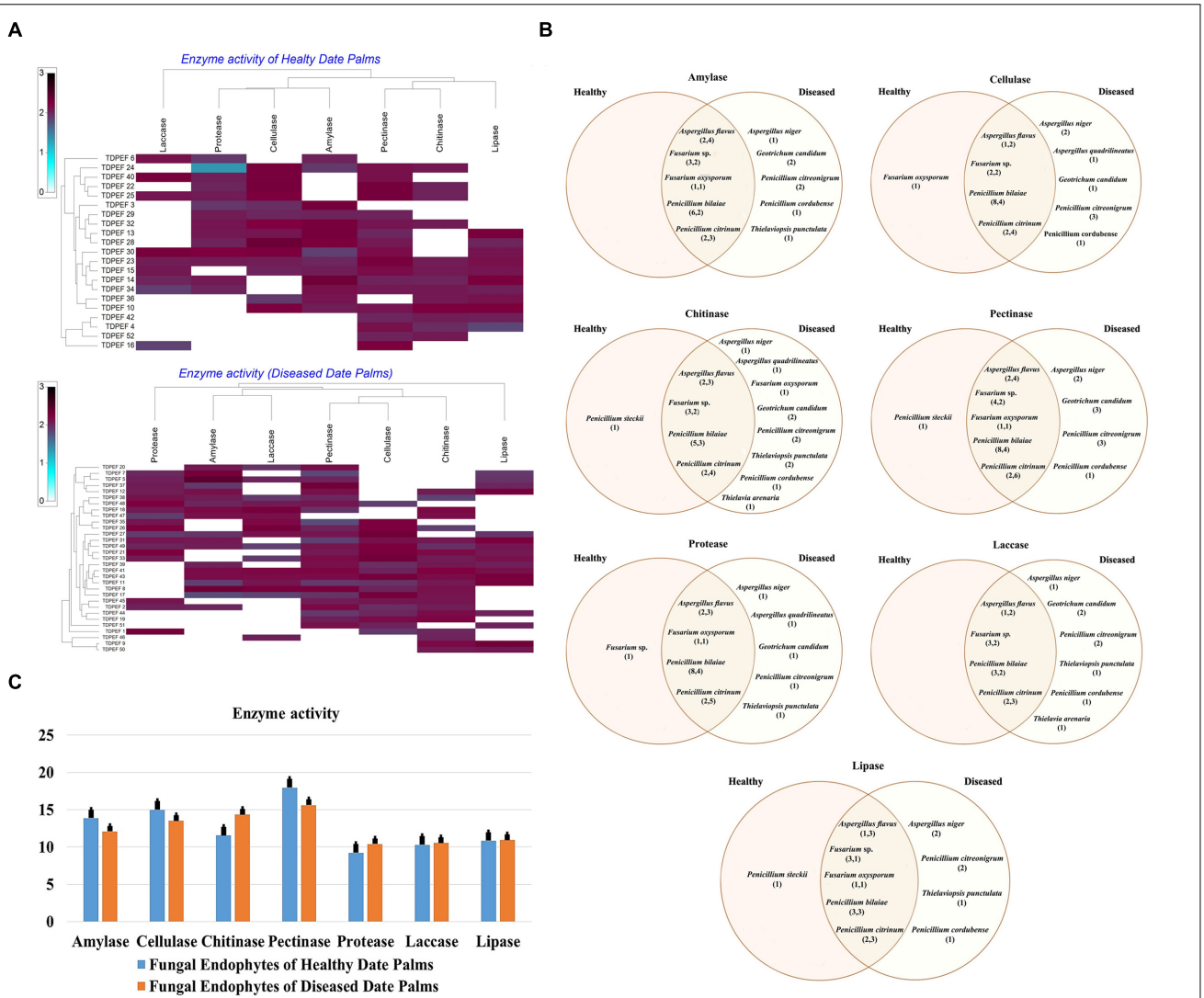


FIGURE 2 | (A) Heat map of enzyme activity of fungal endophytes recovered from both of healthy and BLD date palm roots. **(B)** Venn diagram showing the distribution of endophytic fungal isolates in different enzyme activities including amylase, cellulose, chitinase, pectinase, protease, laccase, and lipase (the first number between brackets represents the number of isolates recovered from healthy roots and the second number represents that recovered from BLD roots). **(C)** Enzyme activity of fungal endophytes isolated from both of healthy and BLD diseased. Data presents mean ± standard error.

lipase. The lipase producing fungi were detected in *Penicillium* and within *Geotrichum* and *Thielavia* species (**Figure 2B**). Mean lipase activity of all isolates of healthy roots was not significantly different from mean lipase activity of BLD isolates (**Figure 2C**).

In vitro Antimicrobial (Antagonistic) Assay of Date Palm Endophytes

The isolated date palm healthy and BLD root endophytic fungi were examined against several pathogenic bacteria and phytopathogenic fungi to assess their antimicrobial activities. The results are presented in **Figures 3–5**. All isolates showed antimicrobial activity at least against two pathogenic microorganisms (**Figures 3**, **4**). For antibacterial activity, the average of the inhibition halo diameter was between 9.3 and 26.6 mm. The highest halo diameter was against *B. cereus* and *M. luteus* with *G. candidum* TDPEF 18 and *T. punctulata* TDPEF 47, respectively (**Figure 3A**). Only three endophytic fungi exhibited antibacterial activity against all tested bacteria including, *Fusarium* sp. TDPEF 11 and two *T. punctulata* species TDPEF 47 and TDPEF 50 (**Figures 3A,B**, **4A,B**). The Gram-negative bacteria *K. pneumoniae* was more sensitive than the other pathogenic bacteria. Among 52 isolates, 22 (42.30%) and 23 (44.23%) displayed antibacterial activity against both *B. cereus* and *B. subtilis*, respectively (**Figures 4A,B**). Furthermore, 20 (38.46%) and 27 (51.9%) endophytic fungi were able to inhibit the Gram-positive bacteria *S. aureus* and *M. luteus*, while 19 (36.53%) and 15 (28.84%) isolates could inhibit *S. enteritidis* and *E. coli*, respectively (**Figures 3A**, **4A**). Concerning antifungal activity, the percentage of inhibition

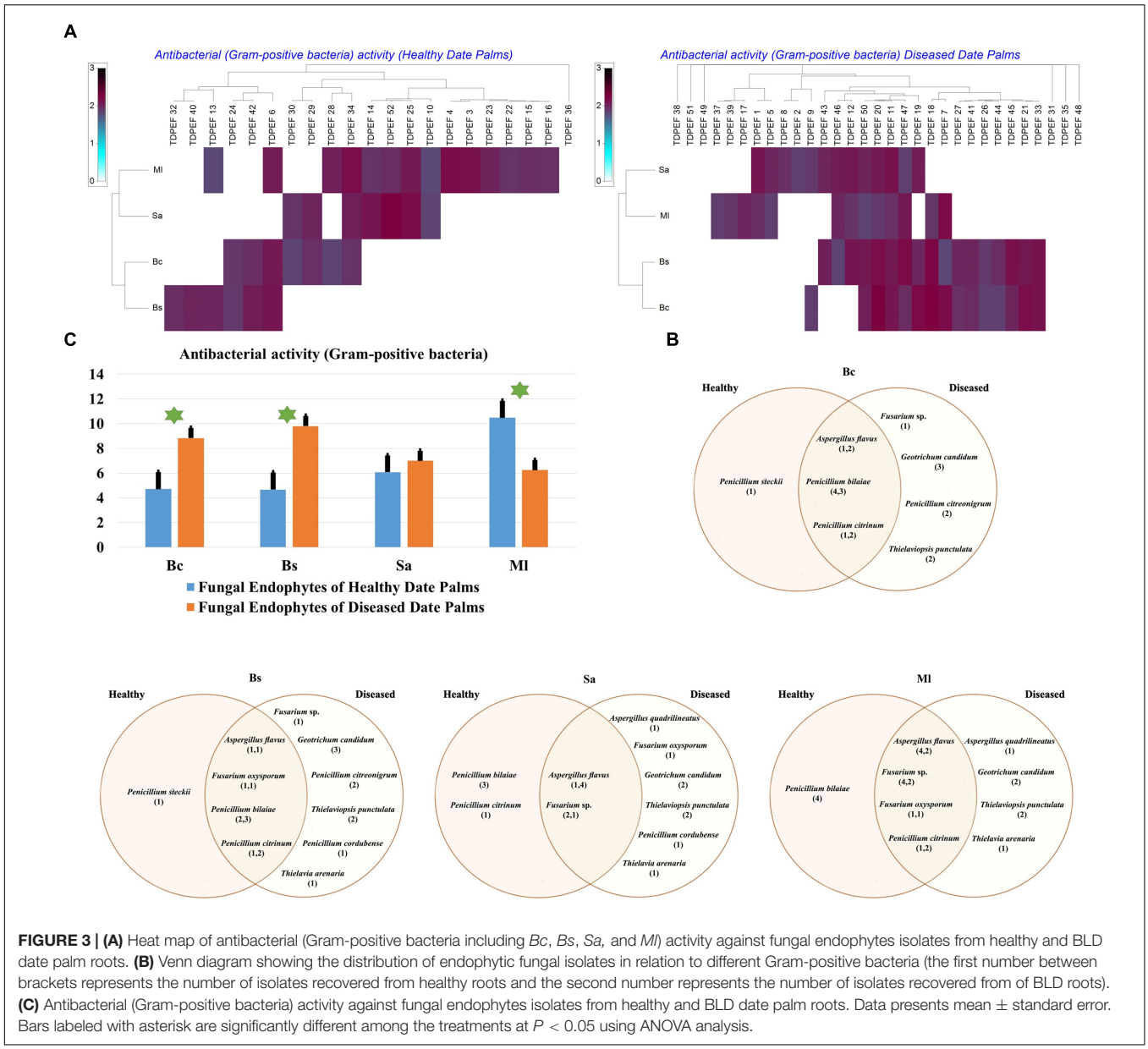


FIGURE 3 | (A) Heat map of antibacterial (Gram-positive bacteria including *Bc*, *Bs*, *Sa,* and *Ml*) activity against fungal endophytes isolates from healthy and BLD date palm roots. **(B)** Venn diagram showing the distribution of endophytic fungal isolates in relation to different Gram-positive bacteria (the first number between brackets represents the number of isolates recovered from healthy roots and the second number represents the number of isolates recovered from of BLD roots). **(C)** Antibacterial (Gram-positive bacteria) activity against fungal endophytes isolates from healthy and BLD date palm roots. Data presents mean ± standard error. Bars labeled with asterisk are significantly different among the treatments at $P < 0.05$ using ANOVA analysis.

was between 10.3 and 72 mm (**Figure 5A**). The best percentage of inhibition was obtained with *A. flavus* TDPEF 2 against *F. oxysporum*. The endophytic isolates were more active against pathogenic fungi than bacteria, as shown in **Figures 5A,B**. Only 18 isolates of date palm endophytes were unable to inhibit all the tested fungi. *F. oxysporum* was the most sensitive phytopathogenic fungus to date palm endophytic isolates. Among 52 endophytic fungi, 39 (75%) displayed antifungal activity against *P. catenulatum* (**Figure 5B**). A high number of isolates (85%) were able to inhibit the growth of both phytopathogenic fungi *F. oxysporum* and *R. solani* with wide spectrum activity (**Figures 5A,B**). Mean antibacterial activity against *B. cereus* and *B. subtilis* and antifungal activity against *F. oxysporum* of all isolates of healthy roots were significantly different from mean antibacterial activity of BLD isolates that have higher activities (**Figures 3C**, **5C**). Mean antibacterial activity against *S. aureus* and antifungal activity against *R. solani* and *P. catenulatum* show non-significant difference between healthy and BLD endophytic fungi, whereas, healthy date palm roots endophytes show significantly higher antimicrobial activities against *Ml* than BLD derived root endophytes (**Figures 3C**, **4C**, **5C**).

Antimicrobial Assay of Date Palm Endophyte Extracts

The EtOAc extracts of 17 endophytic fungi were evaluated for their antibacterial and antifungal activity using agar-well diffusion method (**Figures 6–8**). Among the examined fungal extracts, only five originated from the isolates of healthy date

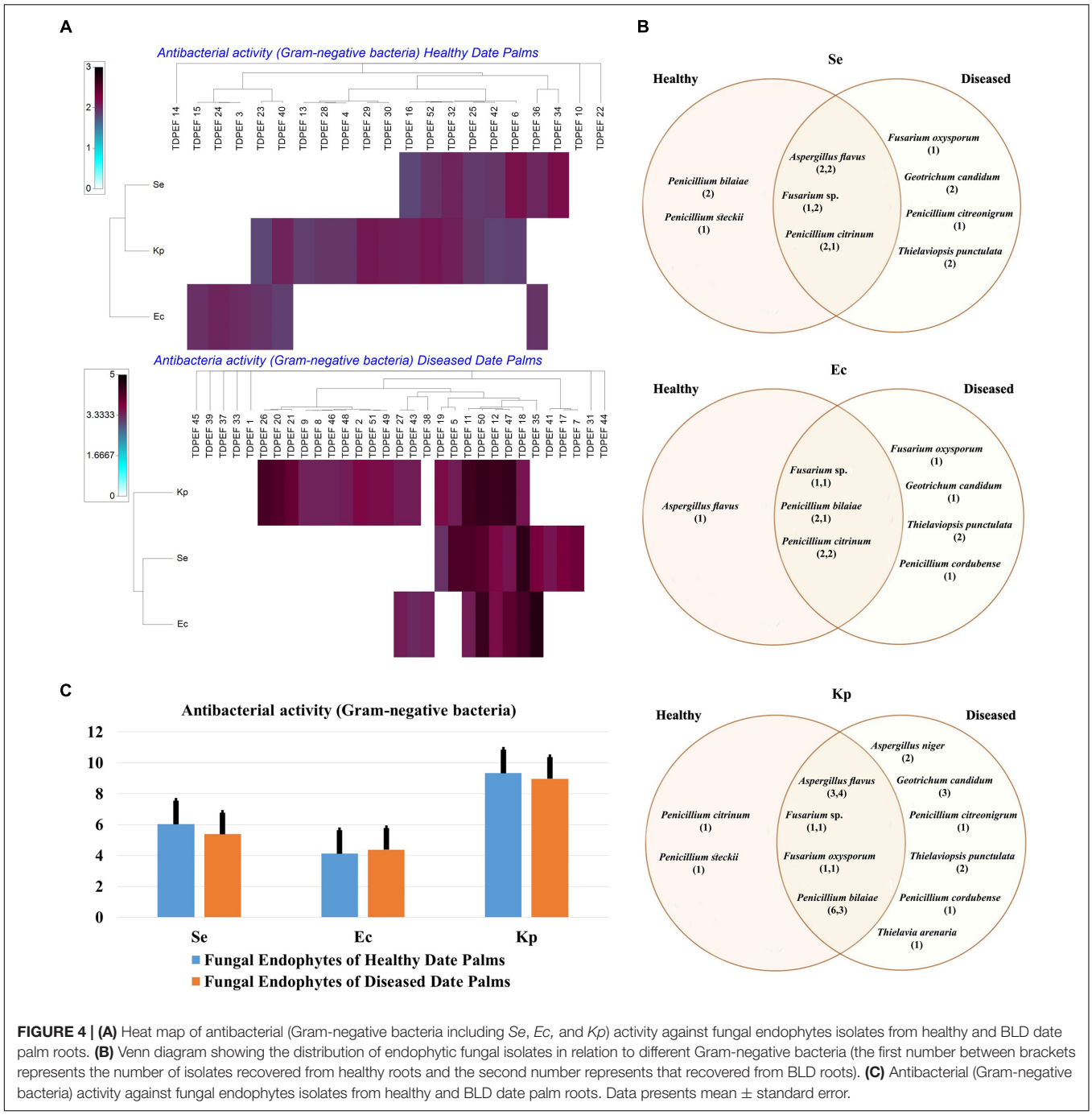


FIGURE 4 | (A) Heat map of antibacterial (Gram-negative bacteria including *Se*, *Ec*, and *Kp*) activity against fungal endophytes isolates from healthy and BLD date palm roots. **(B)** Venn diagram showing the distribution of endophytic fungal isolates in relation to different Gram-negative bacteria (the first number between brackets represents the number of isolates recovered from healthy roots and the second number represents that recovered from BLD roots). **(C)** Antibacterial (Gram-negative bacteria) activity against fungal endophytes isolates from healthy and BLD date palm roots. Data presents mean ± standard error.

palm roots. The 17 isolates submitted to fermentation assay were composed of four *Aspergillus*, two *Fusarium*, three *Geotrichum*, two *Thielaviopsis*, five *Penicillium* species, and *T. arenaria* TDPEF46. The inhibitory activity of fungal extracts expressed in term of diameter of inhibition zones were presented in **Figures 6A**, **7A**, **8A**. The halo inhibition diameter ranged from 12.6 to 28.6 mm for antibacterial activity, while for antifungal activity the inhibition diameter was between 13.6 and 30 mm. Among the 17 fungal extracts, 11 showed promising growth inhibitory activity against *B. cereus*. A high number of EtOAc extracts were able to inhibit the growth of *B. subtilis* with halo diameter ranging from 14.3 to 28 mm (**Figure 6B**). Nine extracts of date palm endophytic fungi exhibited significant inhibitory activity against *S. enteritidis*, *E. coli*, and *K. pneumoniae* (**Figure 7B**). Furthermore, all the examined extracts displayed antagonistic activity against *F. oxysporum* (**Figure 8B**). The EtOAc extracts of *G. candidum* and the two strains of *T. punctulata* exhibited the highest levels of antagonistic activity thanks to their ability to inhibit the growth of six test bacteria and three phytopathogenic fungi.

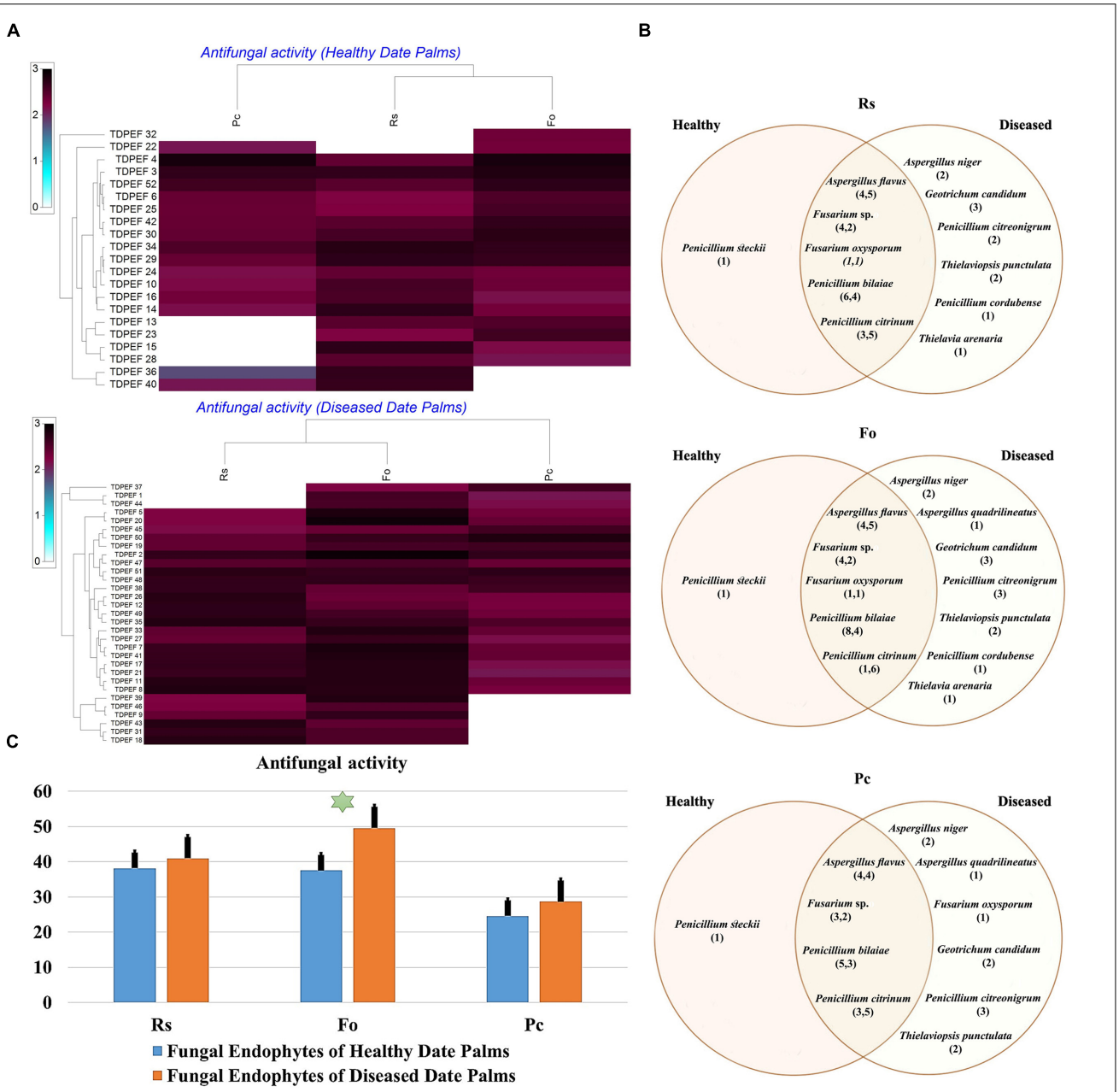


FIGURE 5 | (A) Heat map of antifungal (fungal isolates including *Rs*, *Fo,* and *Pc*) activity against fungal endophytes isolates from healthy and BLD date palm roots. **(B)** Venn diagram showing the distribution of endophytic fungal isolates in relation to different fungal isolates (the first number between brackets represents the number of isolates recovered from healthy roots and the second number represents that recovered from BLD roots). **(C)** Antifungal activity against fungal endophytes isolates from healthy and BLD date palm roots. Data presents mean ± standard error. Bars labeled with asterisk are significantly different among the treatments at $P < 0.05$ using ANOVA analysis.

Concerning antibacterial activity, the highest halo diameter was recorded with the extract of *P. bilaiae* TDPEF 25 against the Gram-positive bacteria *M. luteus* (**Figure 6B**). In addition, the EtOAc extract of *G. candidum* TDPEF 19 displayed the highest level of antifungal activity with halo diameter of 30 mm against *P. catenulatum* (**Figure 8B**). Mean antibacterial activity against *Bs* and *Ec* and antifungal activity against *Rs* of all isolates of healthy roots were significantly different from mean lipase activity of BLD isolates that have higher activities (**Figures 6C**, **7C**, **8C**). Mean antibacterial activity against *Bc*, *Sa,* and *Se* and antifungal activity against *Fo* and *Pc* show non-significant difference between healthy and BLD endophytic fungi, whereas, healthy date palm roots endophytes show significantly higher antimicrobial activities against *Ml* and *Kp* than BLD derived root endophytes (**Figures 6C**, **7C**).

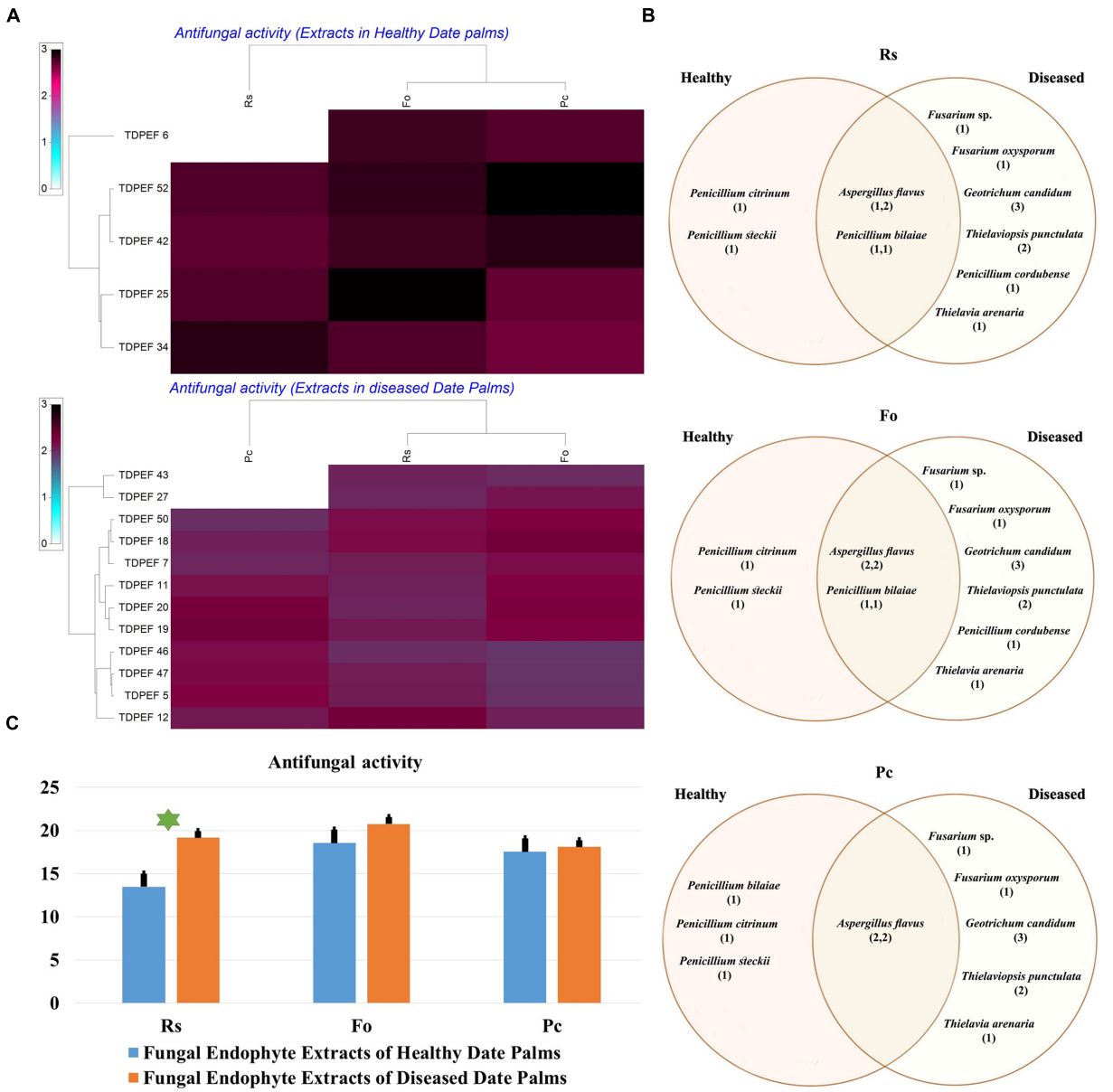


FIGURE 6 | (A) Heat map of antifungal (fungal isolates including *Rs*, *Fo,* and *Pc*) activity against fungal endophytes extracts from healthy and BLD date palm roots. **(B)** Venn diagram showing the distribution of endophytic fungal isolates extracts in relation to different fungal isolates (the first number between brackets represents the number of isolates recovered from healthy roots and the second number represents that recovered from BLD roots). **(C)** Antifungal activity against fungal endophytes extracts from healthy and BLD date palm roots. Data presents mean ± standard error. Bars labeled with asterisk are significantly different among the treatments at $P < 0.05$ using ANOVA analysis.

Date Palm Endophytes versus Endophyte Extracts Antimicrobial Activities

Comparison between mean antimicrobial activity against Gram-positive and Gram-negative bacteria and phytopathogenic fungi and antimicrobial activity of fungal endophytes extracts are reported in **Figure 9**. Results clearly suggest that endophytic root fungal extracts account for all the observed antimicrobial activity when using endophytes themselves. However, extracts from endophytes significantly account approximately for half of the antimicrobial activity obtained when using endophytes *in vitro* assays against fungal phytopathogens ($p < 0.01$).

Determination of MIC, MBC, and MFC of Endophytic Fungal Extracts

The EtOAc extract of the endophytic fungi *G. candidum* TDPEF20 and *T. punctulata* TDPEF47 were subjected to micro-

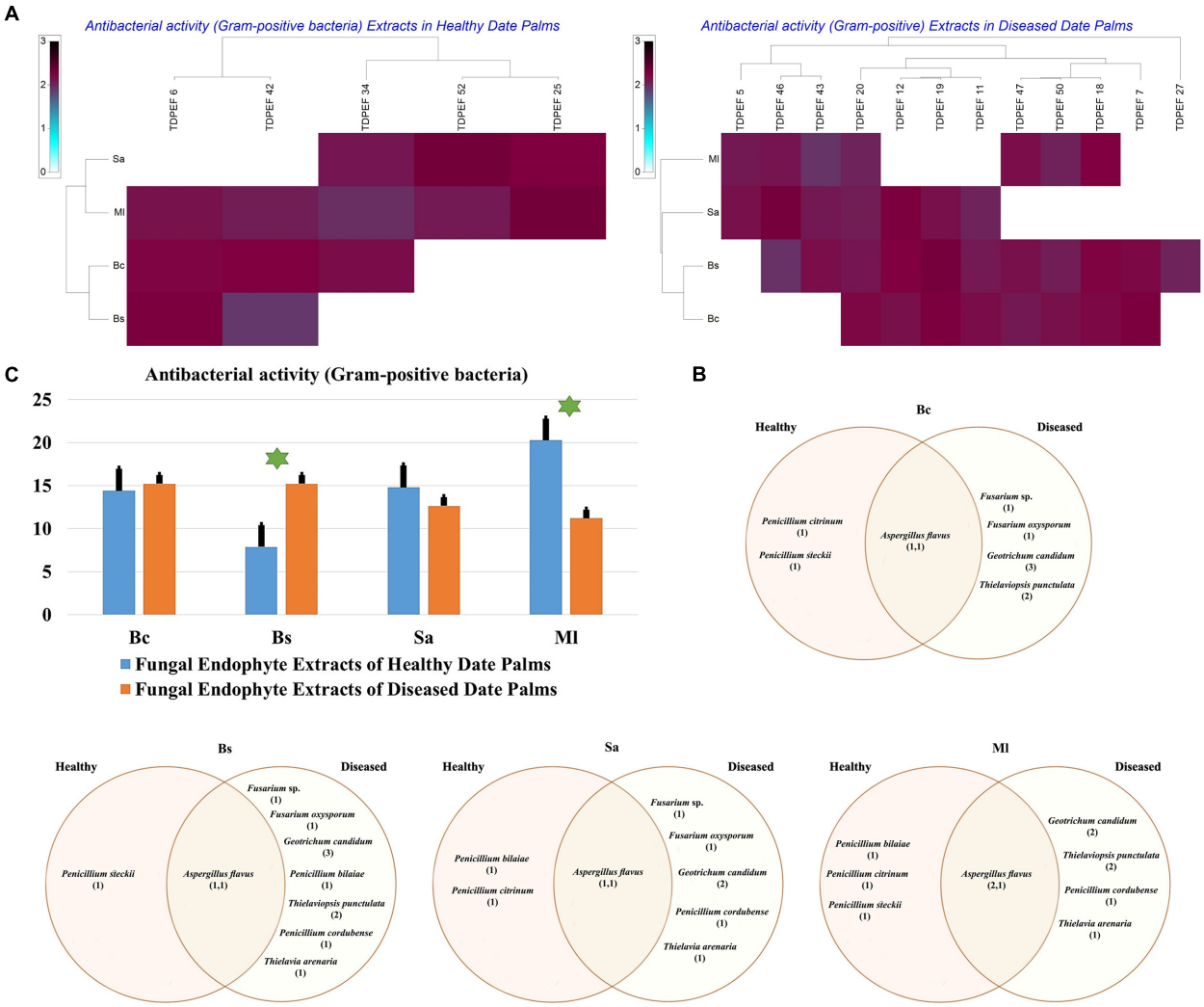


FIGURE 7 | (A) Heat map of antibacterial (Gram-positive bacteria including *Bc*, *Bs*, *Sa,* and *Ml*) activity against fungal endophytes extracts from healthy and BLD date palm roots. **(B)** Venn diagram showing the distribution of endophytic fungal isolates extracts in relation to different Gram-positive bacteria (the first number between brackets represents the number of isolates recovered from healthy roots and the second number represents that recovered from BLD roots). **(C)** Antibacterial activity against fungal endophytes extracts from healthy and BLD date palm roots. Data presents mean ± standard error. Bars labeled with asterisk are significantly different among the treatments at $P < 0.05$ using ANOVA analysis.

dilution plate in order to determine their MIC, MBC, and MFC values. As shown in **Table 1**, the EtOAc extract of *G. candidum* was more active against *Bc*, *Ml,* and *Rs* (MIC of 0.56 μg/μL), followed by *Bs*, *Ec,* and *Fo*. In addition, *Geotrichum* extract exhibited both bacteriostatic and fungistatic effects (MBC/MIC and MFC/MIC ≥4). Concerning *Thielaviopsis* extract, its MIC values ranged from 0.78 to 6.25 μg/μL. However, *Thielaviopsis* extract exhibited the best inhibitory activity against *Bs* and *Kp*. The recorded MBC values indicated the bacteriostatic actions of *Thielaviopsis* extract. It could predominantly inhibit completely the fungal growth (MFC/MIC ≥4) in exception of *Pc.* The results obtained in terms of MIC, MBC, and MFC indicated that *G. candidum* extract displayed a higher bactericidal and fungicidal effect than *T. punctulata* extract.

DISCUSSION

Endophytes especially fungi produce an impressive myriad of bioactive molecules and enzymes that cope with pathogen infection of plants (Newman and Cragg, 2016; Vasundhara et al., 2016). Natural compounds produced by endophytic fungi have been shown to interfere with key host and pathogen processes required for successful infection of the host and to mitigate the adverse effects of broad variety of animal and plant pathogens (Stierle and Stierle, 2015; Mousa et al., 2016; Tanney et al., 2016). Endophytic fungi have tremendous impacts on their host plants inducing their tolerance to biotic and abiotic stresses, promoting their growth and the production of wide variety of secondary metabolites (Jia et al., 2016). Therefore, it is believed that some bioactive compounds produced by some medicinal plants are

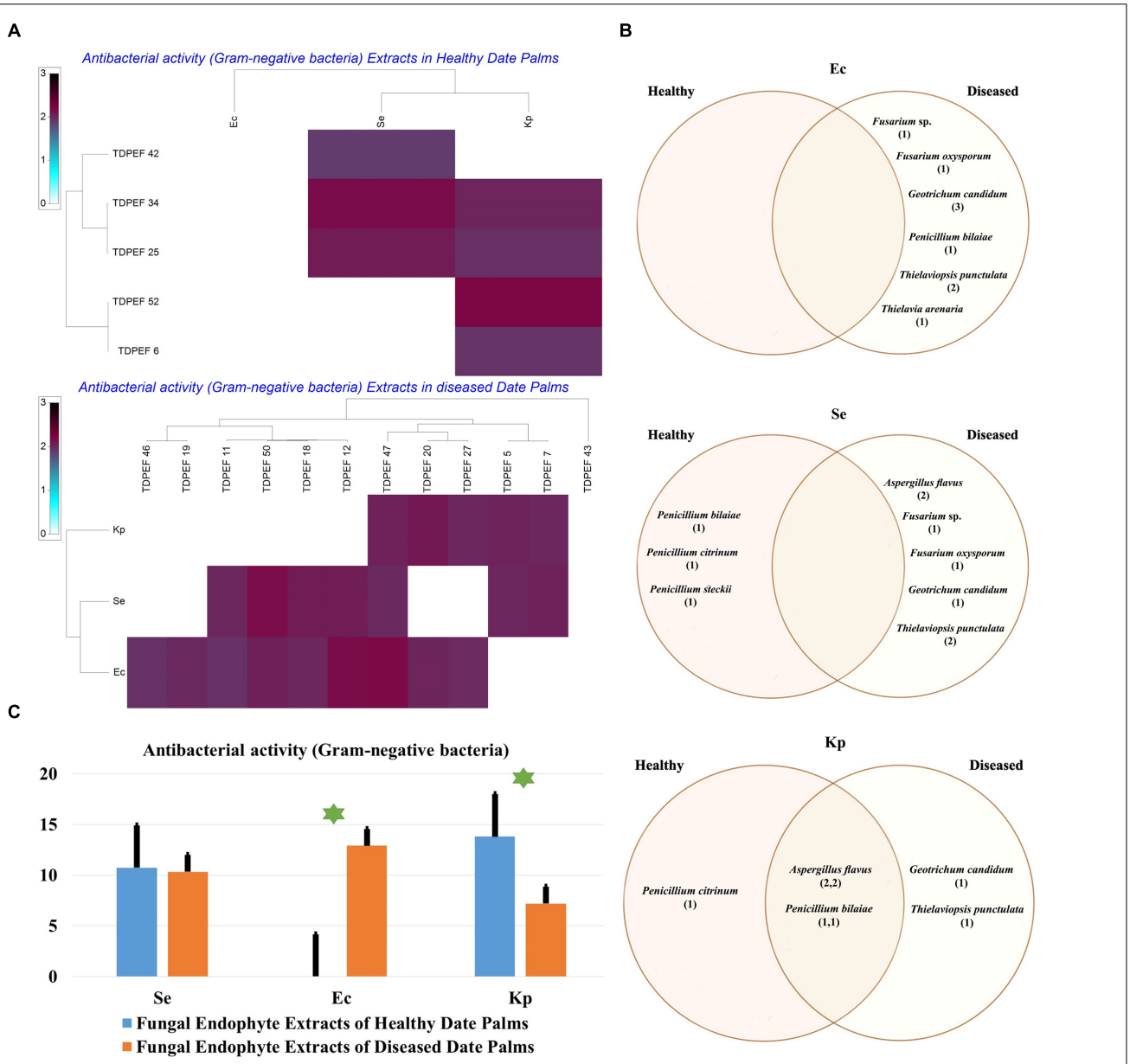


FIGURE 8 | (A) Heat map of antibacterial (Gram-negative bacteria including *Se*, *Ec,* and *Kp*) activity against fungal endophytes extracts from healthy and BLD diseased date palm roots. **(B)** Venn diagram showing the distribution of endophytic fungal isolates extracts in relation to different Gram-negative bacteria (the first number between brackets represents the number of isolates recovered from healthy roots and the second number represents the number of isolates recovered from roots of BLD plant). **(C)** Antibacterial activity against fungal endophytes extracts from healthy and BLD date palm roots. Data presents mean ± standard error. Bars labeled with asterisk are significantly different among the treatments at $P < 0.05$ using ANOVA analysis.

actually the result of the secondary metabolite biosynthesis by their endophytes. This is the case of the highly oxygenated diterpenoid natural product Taxol, one of the most widely used anticancer drugs, first isolated from the pacific yew tree (*Taxus brevifolia*) and then attributed to its endophyte *Taxomyces andreanae* (Stierle et al., 1993).

Geographic locality, host identity, developmental stage, and biotic and abiotic stresses are considered the main drivers of plant fungal endophyte diversity and believed to shape their communities. While fungal endophyte characterization in healthy tissues have been extensively studied, few reports addressed these communities in plants subjected to abiotic or biotic stresses (Douanla-Meli et al., 2013). In the current study, endophytic fungi from healthy and BLD roots of date palm trees widely cultivated in many tropical and subtropical regions worldwide were studied for their phylogenetic affinities

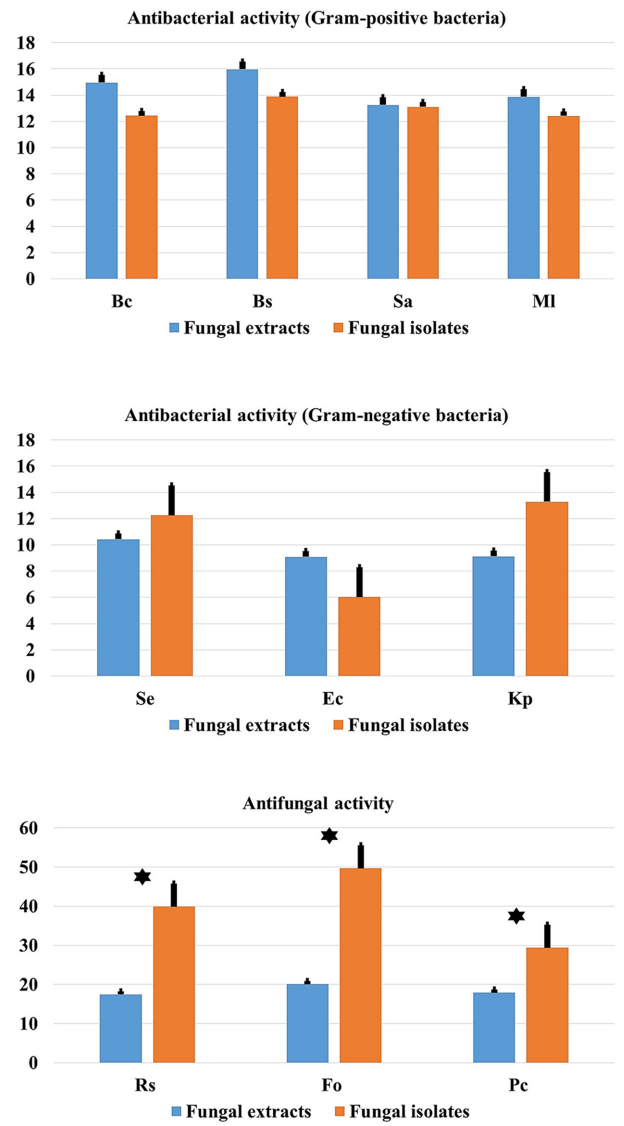


FIGURE 9 | Comparison of antibacterial (Gram-positive and Gram-negative) and antifungal activity in relation to endophytic fungal isolates and extracts. Data presents mean ± standard error. Bars labeled with asterisk are significantly different among the treatments at $P < 0.05$ using ANOVA analysis.

TABLE 1 | Minimum inhibitory, minimum bactericidal and minimum fungicidal concentrations of extracts of *G. candidum* TDPEF 20 and *T. punctulata* TDPEF 47 against human bacterial pathogens and fungal phytopathogens.

	TDPEF 20		TDPEF 47	
	Concentration (μ g/μ L)			
	MIC	MBC	MIC	MBC
Gram-positive bacteria				
Bacillus subtilis	1.56	6.25	0.78	6.25
Bacillus cereus	0.78	12.5	1.56	12.5
Staphylococcus aureus	3.12	12.5	–	–
Micrococcus luteus	0.78	6.25	1.56	6.25
Gram-negative bacteria				
Salmonella enteric serotype enteritidis	–	–	6.25	50
Escherichia coli	1.56	6.25	3.12	25
Klebsiella pneumoniae	6.25	25	3.12	12.5
Phytopathogen fungi	**MIC**	**MFC**	**MIC**	**MFC**
Rhizoctonia solani	0.78	6.25	3.12	12.5
Fusarium oxysporum	1.56	6.25	6.25	25
Pythium catenulatum	3.12	25	3.12	6.25

and bioactive potential. Date palm tree was favored because of its wide use in folk medicine mainly for its antioxidant, wound healing and antimicrobial activities (Abdennabi et al., 2016). Furthermore, extracts of different parts of date palm trees including fruits and pollen showed potential inhibitory activity against several pathogens (Saleh and Otaibi, 2013; Daoud et al., 2015). In addition, Siala et al. (2016) reported the potential of endophytic bacteria isolated from healthy date palm (*P. dactylifera* L.) against phytopathogenic fungi namely *F. oxysporum* f. sp. *albedinis*, the causal agent of bayoud disease. Date palms have the ability to survive in arid regions for several years, therefore, their endophytic community may produce wide range of bioactive components during various stages of their life cycle. Roots of date palm were chosen for isolation of endophytic fungi owing to their significant content of endophytic communities (Wearn et al., 2012). In addition, previous researches have revealed that most of endophytes isolated from foliar tissues were already known to occur commonly in the roots of the host plants (Moricca et al., 2012). A total of 52 endophytic fungi was isolated from roots of date palm (*P. dactylifera* L.). These isolates were identified on the basis of their 18S rDNA sequences analysis and shown to represent 13 species belonging to five genera. Some of isolates (36.8%) were shared between healthy and diseased root fungal microbiomes, whereas 18.4 and 44.7% of the isolates were specific to healthy and BLD root fungal microbiomes, respectively (**Figures 1A–C**). Shared species found to belong to genera *Penicillium*, *Fusarium,* and *Aspergillus*. *Penicillium stecki* was specific to healthy tissues, whereas *A. niger*, *A. quadrilineatus*, *P. citreonigrum*, *P. cordubense*, *G. candidum*, *T. punctulata,* and *T. arenaria* were specific to BLD root fungal microbiome (**Figure 1C**).

Our results disagree with those of Ben Chobba et al. (2013) who recorded the dominance of *Alternaria*, *Pythium,* and *Curvularia* genera in roots of date palm belonging to the same variety Deglet Ennour. However, many factors such as time of sampling, age of host plant, soil conditions as well as dynamics of soil mycobiota may have influence on endophytes of date palm trees and can explain therefore this discrepancy. Variations in fungal endophytes and their frequency of isolation have been reported for many host plants (Collado et al., 2001; Nalini et al., 2014). Most of our isolates have been reported as endophytes in other plants, including mangrove, *Catharanthus roseus*, *Moringa oleifera*, *Paspalum maritimum, Pinus thunbergii,* and *Coffee*

arabica (Vega et al., 2006; Correa et al., 2011; Elavarasi et al., 2012; Kumar et al., 2013; Rajeswari et al., 2016). Moreover, *Fusarium* and *Aspergillus* genera were also previously isolated as endophytic fungi from the plants of *Opuntia dillenii* that survive in arid regions (Ratnaweera et al., 2015).

One of the most abundant genera in the roots of date palm was *Penicillium*, which have been isolated as endophyte from different photosynthetic plants such as *Nicotiana* spp., *Pasania edulis* Makino and *Vigna radiata* L. Recent research excluded the pathogenicity of *Penicillium* species in symbiotic lifestyle with plant tissues (Diaz et al., 2011). In our study, only two species of *Penicillium* were isolated from either healthy and/or BLD roots of date palm trees, including *P. bilaiae* and *P. citrinum*. These two species are ubiquitous saprobes that promote seedling and plant growth (Mushtaq et al., 2012). However, *G. candidum* is known as pathogenic fungus of citrus, tomato, cucumber, grapefruit, and carrot causing sour rot disease (Suprapta et al., 1995). We believe that the isolation of *G. candidum* in the oasis of Nefta might be related to the cooled system of geothermal water used for irrigation of greenhouse cultures (Ben Mohamed and Said, 2008). The project of greenhouses was recently established in south regions of Tunisia and the crops produced were composed of tomatoes, cucumber, melons and watermelons. Among the endophytic fungi from BLD roots of date palm, *T. punctulata* was isolated for the first time in North Africa and never described to date as endophyte. This fungus, previously known as *Ceratocystis radicicola*, is the responsible agent of several date palm disorders called black scorched leaves (Al-Naemi et al., 2014). Recent reports revealed that *T. punctulata* occur especially on stressed date palm trees in areas where salinity and drought are preponderating (Zaid et al., 2002). Greenhouse cultures around Nefta oasis are irrigated using a slightly saline water, which could provide additional clues to explain the presence of *T. punctulata*. We therefore recommend strict control of salinity of irrigation water in the oasis in order to avoid stress of date palm trees.

Any speculation about putative involvement of *G. candidum* or *T. punctulata* in the development of BLD in date palm trees needs additional investigations. Several studies have shown the detection and isolation of pathogenic fungi in endophytic communities of diverse host plants (Sun et al., 2012; Wearn et al., 2012). This confirm the observation of Pawłowska et al. (2014) which suggested that endophytism is a period in the life cycle of pathogenic microorganisms (Schulz and Boyle, 2005).

Recently, the endophytes isolated from arid zones are becoming increasingly recognized as potential source for new enzymes and secondary metabolites. Our findings revealed that endophytic fungi of date palm are able to produce a broad range of valuable enzymes including amylase, cellulase, chitinase, pectinase, protease, laccase, and lipase. In the present study, all endophytic fungi were able to produce at least two of the seven evaluated enzymes, attesting the metabolic diversity within date palm endophytes (**Figures 2A,B**). Jrad et al. (2014) reported the potentiality of both healthy and BLD date palm bacteria to produce diverse hydrolytic enzymes. In line with our findings *Fusarium*, *Penicillium,* and *Aspergillus* genera have been reported to produce an extensive range of extracellular enzymes (Kwon et al., 2007; Alp and Arikan, 2008; Park et al., 2016). Additionally, almost all of the assayed enzymes in the current study were known to be produced by endophytic microorganisms and are needed for both colonization of host plant and decomposition of dead tissues (Saikkonen et al., 2004). There was no statistical support for a higher mean activity of the different enzymes in BLD endophytes compared to healthy roots fungal endophytes (**Figure 2C**).

All endophytic fungi recovered in this study were screened for their antibacterial and antifungal potential on solid media. Preliminary screening allows the detection of the microorganisms that possess interesting antimicrobial activity. Almost all isolates exhibited antimicrobial activity against at least two of the test microorganisms, including 7 Gram-positive and Gram-negative bacteria and three fungi, on solid media (**Figures 3A,B**, **4A,B**, **5A,B**). In total, 17 (32.69%) isolates among endophytic fungi exhibited potential antimicrobial activity and were further subjected to fermentation assay. This percentage is comparable to the percentage recovered in the study of Santos et al. (2015) using *Indigofera suffruticosa* Miller (33.6%). This result highlight the enormous capacity of bioactive molecules production of these endophytes as suggested by Santos et al. (2015). Comparing mean antimicrobial activities between healthy and BLD root endophytes revealed that no clear tendency suggests superior activity of one group to the others. Therefore, we can conclude that using stressed roots for recovery of isolates offers new different endophytes than normal roots but does not provide isolates with higher antimicrobial activities (**Figures 3C**, **4C**, **5C**).

The 17 most active isolates have been selected and were submitted to fermentation in liquid medium, extraction of bioactive secondary metabolites using EtOAc and subsequent test of their antimicrobial activities using agar diffusion method. EtOAc was chosen for its ability to extract both polar and non-polar bioactive metabolites present in the fungal mycelia. All extracts were very efficient in inhibiting both Gram-positive and Gram-negative bacteria and fungi (**Figures 6A,B**, **7A,B**, **8A,B**). Interestingly, these fungal endophyte extracts proved effective against the three fungal pathogens used. Comparing mean antimicrobial activities between healthy and BLD root endophytes extracts revealed also that no clear tendency suggests superior activity of one group to the other (**Figures 6C**, **7C**, **8C**).

Comparison between mean antimicrobial activity against Gram-positive and Gram-negative bacteria and phytopathogenic fungi and antimicrobial activity of fungal endophytes extracts, (**Figure 9**) clearly suggest that endophytic fungal extracts responsible for all the observed antimicrobial activity when using endophytes themselves. However, extracts from endophytes significantly account for approximately half of the antimicrobial activity obtained when using endophytes as *in vitro* assays against fungal phytopathogens ($p < 0.01$). This finding suggests that mechanisms other than the production of secondary metabolites account for the remaining 50% of the antifungal activity observed by living endophytes. We speculate that this could be related to the presence of alternative biocontrol strategies such as the production of chitinases for example that are known to inhibit the growth of fungal phytopathogens (Da Silva et al., 2016).

However, more detailed research work is required to confirm this hypothesis.

The two most active isolates *G. candidum* and *T. punctulata* were submitted to the microdilution method to evaluate precisely their MIC, MBC, and MFC. Extract of *G. candidum* was more active against *B. cereus*, *M. luteus,* and *R. solani* (MIC of 0.56 μg/μL). *Thielaviopsis* extract exhibited the best inhibitory activity against *B. subtilis* and *K. pneumoniae*. In line with our findings, endophytes from *Geotrichum* genus have been reported as source of nematicidal, antituberculosis, antifungal, and antimalarial compounds (Kongsaeree et al., 2003; Li et al., 2007). Most of the compounds isolated from the endophytes of *Geotrichum* sp. are almost isocumarin and triterpenoids. Production of such compounds by endophytic fungi has been reported by recent review (Mousa and Raizada, 2013). No previous researches have isolated *Thielaviopsis* as an endophyte which warrants serious investigation to study its full antimicrobial potential. Our results indicate that endophytic fungi of healthy and BLD roots of date palm constitute a potent source of useful antibacterial and antifungal compounds. The next step will be to establish a strain collection bank with high throughput antibacterial and antifungal screening in addition to performing large scale fermentation of the potential microbial hits to identify the bioactive metabolites responsible for such activities in these extracts.

AUTHOR CONTRIBUTIONS

Conceived and designed the experiments: FM, AD, LB, and NG. Performed the experiments: FM, LB, AD, ACB, LL, FA, and MR. Analyzed the data: FM, LB, AD, ACB, LL, MR, and NG. Contributed reagents/materials/analysis tools: LB, LL, FA, and NG. Wrote and enriched the literature: LB, FM, AD, ACB, LL, FA, AK, MR, and NG.

ACKNOWLEDGMENTS

Financial support of the Tunisian Ministry of Higher Education and Scientific Research is gratefully acknowledged. LL is indebted to the Ministry of Education, Science, Research and Sport of the Slovak Republic for financial support in the frame of the project "VEGA 1/0061/16."

REFERENCES

Abdennabi, R., Bardaa, S., Mehdi, M., Rateb, M. E., Raab, A., Alenezi, F. N., et al. (2016). *Phoenix dactylifera* L. sap enhances wound healing in Wistar rats: phytochemical and histological assessment. *Int. J. Biol. Macromol.* 88, 443–450. doi: 10.1016/j.ijbiomac.2016.04.015

Alenezi, F. N., Rekik, I., Belka, M., Ibrahim, A. F., Luptakova, L., Jaspars, M., et al. (2016). Strain-level diversity of secondary metabolism in the biocontrol species *Aneurinibacillus migulanus*. *Microbiol. Res.* 182, 116–124. doi: 10.1016/j.micres.2015.10.007

Al-Naemi, F. A., Nishad, R., and Ahmed, T. A. (2014). First report of *Thielaviopsis punctulata* causing black scorch disease on date palm in Qatar. *Plant Dis.* 98, 1437. doi: 10.1094/PDIS-04-14-0424-PDN

Alp, S., and Arikan, S. (2008). Investigation of extracellular elastase, acid proteinase and phospholipase activities as putative virulence factors in clinical isolates of *Aspergillus* species. *J. Basic Microbiol.* 48, 331–337. doi: 10.1002/jobm.200700349

Belbahri, L., Moralejo, E., Calmin, G., Oszako, T., Garcia, J. A., Descals, E., et al. (2006). *Phytophthora polonica*, a new species isolated from declining *Alnus glutinosa* stands in Poland. *FEMS Microbiol. Lett.* 261, 165–174. doi: 10.1111/j.1574-6968.2006.00349.x

Ben Chobba, I., Elleuch, A., Ayadi, I., Khannous, L., Namsi, A., Cerqueira, F., et al. (2013). Fungal diversity in adult date palm (*Phoenix dactylifera* L.) revealed by culture-dependent and culture-independent approaches. *J. Zhejiang Univ. Sci. B* 14, 1084–1099. doi: 10.1631/jzus.B1200300

Ben Mohamed, M., and Said, M. (2008). "Geothermal energy development in Tunisia: present status and future outlook," in *Proceedings 30th Anniversary Workshop*, Reykjavik, 12.

Chen, L., Zhang, Q., Jia, M., Ming, Q. L., Yue, W., Rahman, K., et al. (2016). Endophytic fungi with antitumor activities: their occurrence and anticancer compounds. *Crit. Rev. Microbiol.* 42, 454–473. doi: 10.3109/1040841X.2014.959892

Collado, J., Platas, G., and Pelaez, F. (2001). Identification of an endophytic *Nodulisporium* sp. from *Quercus ilex* in central Spain as the anamorph of *Biscogniauxia mediterranea* by rDNA sequence analysis and effect of different ecological factors on distribution of the fungus. *Mycologia* 93, 875–886. doi: 10.2307/3761753

Correa, M. J. C., Nunes, F. M., Bitencourt, H. R., Borges, F. C., Guilhon, G. M. S. P., Arruda, M. S. P., et al. (2011). Biotransformation of chalcones by the endophytic fungus *Aspergillus flavus* isolated from *Paspalum maritimum* trin. *J. Braz. Chem. Soc.* 22, 1333–1338. doi: 10.1590/S0103-50532011000700019

Da Silva, J. A. T., de Medeiros, E. V., da Silva, J. M., Tenorio, D. D., Moreira, K. A., Nascimento, T. C. E. D., et al. (2016). *Trichoderma aureoviride* URM 5158 and *Trichoderma hamatum* URM 6656 are biocontrol agents that act against cassava root rot through different mechanisms. *J. Phytopathol.* 164, 1003–1011. doi: 10.1111/jph.12521

Daoud, A., Drira, M., Bakari, S., Hfaieth, N., Manfgui, K., Kadri, A., et al. (2015). Assessment of polyphenol composition, antioxidant and antimicrobial properties of various extracts of date palm pollen (DPP) from two Tunisian cultivars. *Arabian J. Chem.* (in press). doi: 10.1016/j.arabjc.2015.07.014

Diaz, G. A., Yanez, L., and Latorre, B. A. (2011). Low occurrence of patulin-producing strains of *Penicillium* in grapes and patulin degradation during winemaking in Chile. *Am. J. Enol. Vitic.* 62, 542–546. doi: 10.5344/ajev.2011.11034

Douanla-Meli, C., Langer, E., and Mouafo, F. T. (2013). Fungal endophyte diversity and community patterns in healthy and yellowing leaves of *Citrus limon*. *Fungal Ecol.* 6, 212–222. doi: 10.1016/j.funeco.2013.01.004

Elavarasi, A., Sathiya Rathna, G., and Kalaiselvam, M. (2012). Taxol producing mangrove endophytic fungi *Fusarium oxysporum* from *Rhizophora annamalayana*. *Asian Pac. J. Trop. Biomed.* 2, S1081–S1085. doi: 10.1016/S2221-1691(12)60365-7

Ezra, D., Hess, W. M., and Strobel, G. A. (2004). New endophytic isolates of *Muscodor albus*, a volatile-antibiotic-producing fungus. *Microbiology* 150, 4023–4031. doi: 10.1099/mic.0.27334-0

Felsenstein, J. (1981). Evolutionary trees from DNA sequences: a maximum likelihood approach. *J. Mol. Evol.* 17, 368–376. doi: 10.1007/BF01734359

Gnanasalomi, V. D. V., and Gnanadoss, J. J. (2013). Laccases from fungi and their applications: recent developments. *Asian J. Exp. Biol. Sci.* 4, 581–590. doi: 10.1016/j.cbpa.2015.06.009

Gouda, S., Das, G., Sen, S. K., Shin, H. S., and Patra, J. K. (2016). Endophytes: a treasure house of bioactive compounds of medicinal importance. *Front. Microbiol.* 7:1538. doi: 10.3389/fmicb.2016.01538

Gulluce, M., Sahin, F., Sokmen, M., Ozer, H., Daferera, D., Sokmen, A., et al. (2007). Antimicrobial and antioxidant properties of the essential oils and methanol extract from *Mentha longifolia* L. ssp. *longifolia*. *Food Chem.* 103, 1449–1456. doi: 10.1016/j.foodchem.2006.10.061

Hallmann, J., Berg, G., and Schulz, B. (2007). *Isolation Procedures for Endophytic Microorganisms*. Berlin: Springer.

Haque, M. A., Lee, J. H., and Cho, K. M. (2015). Endophytic bacterial diversity in Korean kimchi made of Chinese cabbage leaves and their antimicrobial activity against pathogens. *Food Control* 56, 24–33. doi: 10.1016/j.foodcont.2015.03.006

Jenifer, S., Jeyasree, J., Laveena, D. K., and Manikandan, K. (2014). Purification and characterization of chitinase from *Trichoderma viride* n9 and its antifungal activity against phytopathogenic fungi. *World J. Pharm. Pharm. Sci.* 3, 1604–1611.

Jia, M., Chen, L., Xin, H. L., Zheng, C. J., Rahman, K., Han, T., et al. (2016). A friendly relationship between endophytic fungi and medicinal plants: a systematic review. *Front. Microbiol.* 7:906. doi: 10.3389/fmicb.2016.00906

Jrad, M., Fendri, I., Ben Choba, I., Drira, N., Kadri, A., and Gharsallah, N. (2014). Enzymatic activities in different strains isolated from healthy and brittle leaf disease affected date palm leaves: study of amylase production conditions. *Appl. Biochem. Biotechnol.* 175, 2075–2086. doi: 10.1007/s12010-014-1409-x

Katoch, M., Khajuria, A., Sharma, P. R., and Saxena, A. K. (2015). Immunosuppressive potential of *Botryosphaeria dothidea*, an endophyte isolated from Kigelia Africana. *Pharm. Biol.* 53, 85–91. doi: 10.3109/13880209.2014.910673

Katoh, K., and Toh, H. (2008). Recent developments in the MAFFT multiple sequence alignment program. *Brief. Bioinf.* 9, 286–298. doi: 10.1093/bib/bbn013

Kaul, S., Ahmed, M., Zargar, K., Sharma, P., and Dhar, M. K. (2012). Prospecting endophytic fungal assemblage of *Digitalis lanata* Ehrh. (foxglove) as a novel source of digoxin: a cardiac glycoside. *3 Biotech* 3, 335–340. doi: 10.1007/s13205-012-0106-0

Kaye, D. (2016). Unregulated antibiotic sales may increase risk of "Superbugs" – UK review. *Clin. Infect. Dis.* 62, 1–2.

Khan, S. N., and Khan, A. U. (2016). Breaking the spell: combating multidrug resistant 'Superbugs'. *Front. Microbiol.* 7:174. doi: 10.3389/fmicb.2016.00174

Kimura, M. (1980). A simple method for estimating evolutionary rates of base substitutions through comparative studies of nucleotide sequences. *J. Mol. Evol.* 16, 111–120. doi: 10.1007/BF01731581

Kongsaeree, P., Prabpai, S., Sriubolmas, N., Vongvein, C., and Wiyakrutta, S. (2003). Antimalarial Dihydroisocoumarins produced by *Geotrichum* sp., an endophytic fungus of *Crassocephalum crepidioides*. *J. Nat. Prod.* 66, 709–711. doi: 10.1021/np0205598

Kumar, A., Patil, D., Rajamohanan, P. R., and Ahmad, A. (2013). Isolation, purification and characterization of vinblastine and vincristine from endophytic fungus *Fusarium oxysporum* isolated from *Catharanthus roseus*. *PLoS ONE* 8:e71805. doi: 10.1371/journal.pone.0071805

Kwon, H. W., Yoon, J. H., Kim, S. H., Hong, S. B., Cheon, Y., and Ko, S. J. (2007). Detection of extracellular enzymes activities in various *Fusarium* spp. *Microbiology* 35, 162–165. doi: 10.4489/MYCO.2007.35.3.162

Lammie, S. L., and Hughes, J. M. (2016). Antimicrobial resistance, food safety, and one health: the need for convergence. *Annu. Rev. Food Sci. Technol.* 7, 287–312. doi: 10.1146/annurev-food-041715-033251

Li, G. H., Yu, Z. F., Li, X., Wang, X. B., Zheng, L. J., and Zhang, K. Q. (2007). Nematicidal metabolites produced by the endophytic fungus *Geotrichum* sp. AL4. *Chem. Biodivers.* 4, 1520–1524. doi: 10.1002/cbdv.200790131

Lugtenberg, B. J., Caradus, J. R., and Johnson, L. J. (2016). Fungal endophytes for sustainable crop production. *FEMS Microbiol. Ecol.* 92:fiw194. doi: 10.1093/femsec/fiw194

Marston, H. D., Dixon, D. M., Knisely, J. M., Palmore, T. N., and Fauci, A. S. (2016). Antimicrobial resistance. *JAMA* 316, 1193–1204. doi: 10.1001/jama.2016.11764

Mohanasrinivasan, V., Shankar, V., Elizabeth, R., Soumya, A. R., and Devi, C. S. (2012). Isolation, screening and identification of protease producing fungi from rhizosphere soil and optimization of pH, incubation time and inducer concentration for enhanced protease production. *Int. J. Pharm. Biol. Sci.* 3, 784–793.

Monggoot, S., Burawat, J., and Pripdeevech, P. (2016). Antibacterial activities of endophytic fungi isolated from *Mentha cordifolia* leaves and their volatile constituents. *Nat. Prod. Commun.* 11, 1349–1351.

Moricca, S., Ginetti, B., and Ragazzi, A. (2012). Species- and organ-specificity in endophytes colonizing healthy and declining Mediterranean oaks. *Phytopatol. Mediterr.* 51, 587–598.

Mousa, W. K., and Raizada, M. N. (2013). The diversity of antimicrobial secondary metabolites produced by fungal endophytes: an interdisciplinary perspective. *Front. Microbiol.* 4:65. doi: 10.3389/fmicb.2013.00065

Mousa, W. K., Schwan, A. L., and Raizada, M. N. (2016). Characterization of antifungal natural products isolated from endophytic fungi of finger millet (*Eleusine coracana*). *Molecules* 21:E1171. doi: 10.3390/molecules21091171

Mueller, J. H., and Hinton, J. (1941). Protein-free medium for primary isolation of gonococcus and meningococcus. *Proc. Soc. Exp. Biol. Med.* 48, 330–333. doi: 10.3181/00379727-48-13311

Mushtaq, S., Nasim, G., Khokhar, I., and Mukhtar, I. (2012). Effects of *Penicillium* extracts on germination vigour in subsequent seedling growth of tomato (*Solanum lycopersicum* L.). *Arch. Phytopathol. Plant Protect.* 45, 932–937. doi: 10.1080/03235408.2011.603965

Nagpure, A., and Gupta, R. K. (2012). Purification and characterization of an extracellular chitinase from antagonistic *Streptomyces violaceusniger*. *J. Basic Microbiol.* 52, 1–11. doi: 10.1002/jobm.201100648

Nalini, M. S., Sunayana, N., and Prakash, H. S. (2014). Endophytic fungal diversity in medicinal plants of Western Ghats, India. *Int. J. Biodivers.* 2014:494213. doi: 10.1155/2014/494213

Newman, D. J., and Cragg, G. M. (2016). Natural products as sources of new drugs from 1981 to 2014. *J. Nat. Prod.* 79, 629–661. doi: 10.1021/acs.jnatprod.5b01055

Nitinkumar, P. P., and Bhushan, L. C. (2010). Production and purification of Pectinase by soil isolate *Penicillium* sp. and search for better agroresidue for its SSF. *Recent Res. Sci. Tech.* 2, 36–42.

Park, M. S., Lee, S., Oh, S. Y., Cho, G. Y., and Lim, Y. W. (2016). Diversity and enzyme activity of *Penicillium* species associated with macroalgae in Jeju Island. *J. Microbiol.* 54, 646–654. doi: 10.1007/s12275-016-6324-0

Paul, B., Mathew, R., Kanak, B., Paul, A., Henry, M., Lefort, F., et al. (2008). Morphology, taxonomy, and phylogenetic analysis of a new species of *Pythium* isolated from France. *Fungal Divers.* 28, 55–63.

Pawłowska, J., Wilk, M., Śliwińska-Wyrzychowska, A., Mętrak, M., and Wrzosek, M. (2014). The diversity of endophytic fungi in the above-ground tissue of two *Lycopodium* species in Poland. *Symbiosis* 63, 87–97. doi: 10.1007/s13199-014-0291-1

Petrini, O., Sieber, T. N., Toti, L., and Viret, O. (1992). Ecology, metabolite production and substrate utilization in endophytic fungi. *Nat. Toxins* 1, 185–196. doi: 10.1002/nt.2620010306

Rajeswari, S., Umamaheswari, S., Arvind Prasanth, D., and Rajamanikandan, K. C. P. (2016). Bioactive potential of endophytic fungi *Aspergillus flavus* (SS03) against clinical isolates. *Int. J. Pharm. Pharm. Sci.* 8, 37–40. doi: 10.22159/ijpps.2016.v8i9.11466

Rathna, J., Yazhini, K. B., Ajilda, A. A. K., Prabu, H. G. M., and Pandian, S. K. (2016). Production of naphthoquinones and phenolics by a novel isolate *Fusarium solani* PSC-R of Palk Bay and their industrial applications. *Bioresour. Technol.* 213, 289–298. doi: 10.1016/j.biortech.2016.04.050

Ratnaweera, P. B., De Silva, E. D., Williams, D. E., and Andersen, R. J. (2015). Antimicrobial activities of endophytic fungi obtained from the arid zone invasive plant *Opuntia dillenii* and the isolation of equisetin from endophytic *Fusarium* sp. *BMC Complement Altern. Med.* 15:220. doi: 10.1186/s12906-015-0722-4

Riddle, M. S., and Connor, B. A. (2016). The traveling microbiome. *Curr. Infect. Dis. Rep.* 18:29. doi: 10.1007/s11908-016-0536-7

Saikkonen, K., Wälli, P., Helander, M., and Faeth, S. H. (2004). Evolution of endophyte-plant symbioses. *Trends Plant Sci.* 9, 275–280. doi: 10.1016/j.tplants.2004.04.005

Saleem, A., and Ebrahim, M. K. H. (2014). Production of amylase by fungi isolated from legume seeds collected in Almadinah Almunawwarah, Saudi Arabia. *J. Taibah Univ. Sci.* 8, 90–97. doi: 10.1016/j.jtusci.2013.09.002

Saleh, F. A., and Otaibi, M. M. (2013). Antibacterial activity of date palm (*Phoenix dectylifera* L.) fruit at different ripening stages. *J. Food Process. Technol.* 4:285. doi: 10.4172/2157-7110.1000285

Saliba, V., Washer, P., Pett, P., Kakkar, M., Abbas, S., Raghuvanshi, B., et al. (2016). Comparative analysis of how the media in the United Kingdom and India represented the emergence of NDM-I. *J. Public Health Policy* 37, 1–19. doi: 10.1057/jphp.2015.30

Santos, I. P., Silva, L. C. N., Silva, M. V., Araújo, J. M., Cavalcanti, M. S., and Lima, V. L. M. (2015). Antibacterial activity of endophytic fungi from leaves of *Indigofera suffruticosa* Miller (Fabaceae). *Front. Microbiol.* 6:350. doi: 10.3389/fmicb.2015.00350

Schulz, B., and Boyle, C. (2005). The endophytic continuum. *Mycol. Res.* 109, 661–686. doi: 10.1017/S095375620500273X

Senn, L., Clerc, O., Zanetti, G., Basset, P., Prodhom, G., Gordon, N. C., et al. (2016). The stealthy superbug: the role of asymptomatic enteric carriage in maintaining a long-term hospital outbreak of ST228 methicillin-resistant *Staphylococcus aureus*. *MBio* 7, e02039-15. doi: 10.1128/mBio.02039-15

Shahriarinour, M., Wahab, M. N. A., Ariff, A. B., Rosfarizan, M., and Shuhaimi, M. (2011). Screening, isolation and selection of cellulolytic fungi from oil palm empty fruit bunch fibre. *Biotechnology* 10, 108–113. doi: 10.3923/biotech.2011.108.113

Siala, R., Ben Chobba, I., Vallaeys, T., Triki, M. A., Jrad, M., Cheffi, M., et al. (2016). Analysis of the cultivable endophytic bacterial diversity in the date palm (*Phoenix dactylifera* L.) and evaluation of its antagonistic potential against pathogenic *Fusarium* species that cause date palm bayound disease. *J. Appl. Environ. Microbiol.* 4, 93–104. doi: 10.12691/jaem-4-5-2

Stierle, A., Strobel, G. A., and Stierle, D. B. (1993). Taxol and taxane production by *Taxomyces andreanae*, an endophytic fungus of Pacific yew. *Science* 260, 214–216. doi: 10.1126/science.8097061

Stierle, A. A., and Stierle, D. B. (2015). Bioactive secondary metabolites produced by the fungal endophytes of conifers. *Nat. Prod. Commun.* 10, 1671–1682.

Strobel, G., and Daisy, B. (2003). Bioprospecting for microbial endophytes and their natural products. *Microbiol. Mol. Biol. Rev.* 67, 491–502. doi: 10.1128/MMBR.67.4.491-502.2003

Strobel, G. A., Dirksie, E., Sears, J., and Markworth, C. (2001). Volatile antimicrobials from *Muscodor albus*, a novel endophytic fungus. *Microbiology* 147, 2943–2950. doi: 10.1099/00221287-147-11-2943

Sun, X., Ding, Q., Hyde, K. D., and Guo, L. D. (2012). Community structure and preference of endophytic fungi of three woody plants in a mixed forest. *Fungal Ecol.* 5, 624–632. doi: 10.1016/j.funeco.2012.04.001

Suprapta, D. N., Arai, K., and Iwai, H. (1995). Distribution of *Geotrichum candidum* citrus race in citrus groves and non-citrus fields in Japan. *Mycoscience* 36, 277–282. doi: 10.1007/BF02268602

Tamura, K., Stecher, G., Peterson, D., Filipski, A., and Kumar, S. (2013). MEGA 6: molecular evolutionary genetics analysis version 6.0. *Mol. Biol. Evol.* 30, 2725–2729. doi: 10.1093/molbev/mst197

Tanney, J. B., Mcmullin, D. R., Green, B. D., Miller, J. D., and Seifert, K. A. (2016). Production of antifungal and anti-insectan metabolites by the *Picea* endophyte *Diaporthe maritima* sp. nov. *Fungal Biol.* 120, 1448–1457. doi: 10.1016/j.funbio.2016.05.007

Thota, P., Bhogavalli, P. K., Vallem, P. R., and Sreerangam, V. (2012). Screening and identification of potential fungal strains for the production of extracellular lipase from soil. *Plant Sci. Fd.* 2, 79–84.

Vargiu, A. V., Pos, K. M., Poole, K., and Nikaido, H. (2016). Editorial: bad bugs in the XXIst century: resistance mediated by multi-drug efflux pumps in gram-negative bacteria. *Front. Microbiol.* 7:833. doi: 10.3389/fmicb.2016.00833

Vasundhara, M., Kumar, A., and Reddy, M. S. (2016). Molecular approaches to screen bioactive compounds from endophytic fungi. *Front. Microbiol.* 7:1774. doi: 10.3389/fmicb.2016.01774

Vega, F. E., Posada, F., Peterson, S. W., Gianfagna, T. J., and Chaves, F. (2006). *Penicillium* species endophytic in coffee plants and ochratoxin A production. *Mycologia* 98, 31–42. doi: 10.3852/mycologia.98.1.31

Venugopalan, A., and Srivastava, S. (2015). Endophytes as in vitro production platforms of high value plant secondary metabolites. *Biotechnol. Adv.* 33, 873–887. doi: 10.1016/j.biotechadv.2015.07.004

Wearn, J. A., Sutton, B. C., Morley, N. J., and Gange, A. C. (2012). Species and organ specificity of fungal endophytes in herbaceous grassland plants. *J. Ecol.* 100, 1085–1092. doi: 10.1111/j.1365-2745.2012.01997.x

White, T. J., Bruns, T., Lee, S., and Taylor, J. (1990). "Amplification and direct sequencing of fungal ribosomal RNA genes for phylogenetics," in *PCR Protocols, a Guide to Methods and Applications*, eds M. A. Innis, D. H. Gelfand, J. J. Sninsky, and T. J. White (San Diego, CA: Academic Press), 315–322.

Xu, L., Zhou, L., Zhao, J., and Jiang, W. (2008). Recent studies on the antimicrobial compounds produced by plant endophytic fungi. *Nat. Prod. Res. Dev.* 20, 731–740.

Xu, L. L., Han, L., Wu, J. Z., Zhang, Q. Y., Zhang, H., Huang, B. K., et al. (2009). Comparative research of chemical constituents, antifungal and antitumor properties of ether extracts of *Panax ginseng* and its endophytic fungus. *Phytomedicine* 16, 609–616. doi: 10.1016/j.phymed.2009.03.014

Zaid, A., de Wet, P. F., Djerbi, M., and Oihabi, A. C. (2002). "Diseases and pests of date palm," in *Date Palm Cltivation. FAO Plant Production and Protection Paper No. 156*, eds A. Zaid and E. Arias-Jimenez (Rome: FAO), 227–281.

Conflict of Interest Statement: The authors declare that the research was conducted in the absence of any commercial or financial relationships that could be construed as a potential conflict of interest.

Copyright © 2017 Mefteh, Daoud, Chenari Bouket, Alenezi, Luptakova, Rateb, Kadri, Gharsallah and Belbahri. This is an open-access article distributed under the terms of the Creative Commons Attribution License (CC BY). The use, distribution or reproduction in other forums is permitted, provided the original author(s) or licensor are credited and that the original publication in this journal is cited, in accordance with accepted academic practice. No use, distribution or reproduction is permitted which does not comply with these terms.

frontiers in Microbiology

ORIGINAL RESEARCH
published: 14 March 2017
doi: 10.3389/fmicb.2017.00430

Cold Stress and Nitrogen Deficiency Affected Protein Expression of Psychrotrophic *Dyadobacter psychrophilus* B2 and *Pseudomonas jessenii* MP1

*Deep C. Suyal[1], Saurabh Kumar[1], Amit Yadav[2], Yogesh Shouche[2] and Reeta Goel[1]**

[1] *Department of Microbiology, College of Basic Sciences and Humanities, G. B. Pant University of Agriculture and Technology, Pantnagar, India,* [2] *Microbial Culture Collection, National Centre for Cell Science, Pune University Campus, Pune, India*

Nitrogen (N) deficiency and low temperature conditions are the prominent facet of Western Himalayan agro-ecosystems. A slight change in the environment alters the protein expression of the microorganisms. Therefore, proteomes of the two psychrotrophs *Dyadobacter psychrophilus* B2 and *Pseudomonas jessenii* MP1 were analyzed using two dimensional electrophoresis and MALDI–TOF–MS, to determine the physiological response of altitudinally different but indigenous microorganisms in response to cold stress under N depleting conditions. Functional assessment of 150 differentially expressed proteins from both the psychrotrophs revealed several mechanisms might be involved in cold stress adaptation, protein synthesis/modifications, energy metabolism, cell growth/maintenance, etc. In both the proteomes, abundance of the proteins related to energy production and stress were significantly increased while, proteins related to biosynthesis and energy consuming processes decreased. *ATP synthase subunit alpha, beta, ATP-dependent Clp protease, Enolase, groL HtpG* and *N(2)-fixation sustaining protein CowN* proteins were found to be expressed in both B2 and MP1, similarly to previously studied diazotrophs under low temperature N_2 fixing conditions and therefore, can be considered as a biomarker for monitoring the nitrogen fixation in cold niches. Nevertheless, in both the diazotrophs, a good fraction of the proteins were related to hypothetical proteins which are still uncharacterized, thereby, suggesting the need for in-depth studies on cold adapted diazotrophs and their adaptive mechanisms.

Keywords: differential proteomics, Western Indian Himalaya, nitrogen fixation, cold diazotrophy, psychrotrophs, 2-D gel electrophoresis

OPEN ACCESS

Edited by:
Bhim Pratap Singh, Mizoram University, India

Reviewed by:
Christophe Nguyen-The, Institut National de la Recherche Agronomique (INRA), France
Anita Pandey, G. B. Pant National Institute of Himalayan Environment and Sustainable Development, India

****Correspondence:***
Reeta Goel
rg55@rediffmail.com

Specialty section:
This article was submitted to Microbial Physiology and Metabolism, a section of the journal Frontiers in Microbiology

Received: *27 October 2016*
Accepted: *28 February 2017*
Published: *14 March 2017*

Citation:
Suyal DC, Kumar S, Yadav A, Shouche Y and Goel R (2017) Cold Stress and Nitrogen Deficiency Affected Protein Expression of Psychrotrophic Dyadobacter psychrophilus B2 and Pseudomonas jessenii MP1. Front. Microbiol. 8:430. doi: 10.3389/fmicb.2017.00430

INTRODUCTION

Microorganisms need to adapt constantly to different environmental changes *viz.* availability of nutrients and oxygen, osmotic stress and temperature changes. To survive these conditions bacteria need to develop unique survival strategies enabling them to persist in the environment until stress is alleviated. Nitrogen depletion at low temperature creates environmental stress as

well as oligotrophic conditions along with oxidative stress which is reported to be induced by cold and therefore, impose multiple stress conditions (MSC) on the microorganisms. Very few reports are available on bacterial adaptive responses under oligotrophic and low temperature conditions including *Rhodococcus biphenylivorans* (Su et al., 2015) which was found to enter the viable but non-culturable state (VBNC) state under oligotrophic and low temperature conditions. This behavior is also very common in natural environments in which bacteria remain alive with slight metabolic modifications but are difficult to be cultured in lab. Moreover, bacteria can alter their protein expression to thrive under MSC as revealed by differential proteomic analysis of psychrophilic diazotroph *Pseudomonas migulae* S10724 (Suyal et al., 2014) and psychrotrophic diazotroph *P. palleroniana* N26 (Soni et al., 2015). However, multiple studies are needed to unravel the untouched facet of multiple stress biology induced by cold stress N depleting conditions as many key issues are still unanswered. In this context, differential proteomic analysis of psychrotrophic diazotrophs *Dyadobacter psychrophilus* B2 and *Pseudomonas jessenii* MP1 strain was carried out using two dimensional gel electrophoresis (2-DE) and MALDI–TOF–MS. This study can be explored for identifying the novel proteins/peptides and/or associated biomarkers.

MATERIALS AND METHODS

Bacterial Strain and Growth Conditions

Dyadobacter psychrophilus B2 (JX233788) and *P. jessenii* MP1 (JX310329) were originally isolated from the agriculture field from WIH hill, Bhowali (1654 m; 29.22°N, 79.31°E) and Munsyari (2200 m; 30.60°N, 80.20°E). Both were grown aerobically in Burk medium (Rennie, 1981; Soni et al., 2015) at 28°C. Further, both the cultures were investigated for their growth in nitrogen deficient medium at 10°C followed by *nif*H gene amplification as described earlier (Suyal et al., 2014). Bacterium was identified using 16S rDNA sequencing as described previously (Suyal et al., 2014).

Protein Extraction, Two Dimensional Gel Electrophoresis and Gel Image Analysis

Bacterial proteins were extracted at mid log phase as described earlier (Soni et al., 2015) (Supplementary Material). Lyophilized protein samples were sent to Sandor Proteomics Pvt. Ltd., Hyderabad for 2-DE analysis. *In silico* study of 2-DE gel was carried out as reported earlier (Suyal et al., 2014; Soni et al., 2015) (Supplementary Material). The experiment was performed in triplicates.

MALDI–TOF–MS Analysis and MASCOT Database Searches

MALDI–TOF analysis was done at Sandor Proteomics Pvt. Ltd., Hyderabad as per the previous studies (Soni et al., 2015). The data that were obtained were used in the determination of the identity of the proteins using the Mascot search tool[1] .

RESULTS

Differential Proteomics of Psychrotrophs *D. psychrophilus* B2 and *P. jessenii* MP1 Strain in Response to Cold Stress Nitrogen Depleting Conditions

Both, B2 and MP1 strains showed luxuriant growth on N deficient Burk medium, indicating their ability to fix atmospheric N_2. Moreover, both were positive for *nif*H amplification too. *nif* genes are often used as a biomarker in diazotroph's identification (Suyal et al., 2014; Soni et al., 2015). 2-DE was used to compare the protein expression patterns of both the bacteria B2 and MP1 separately, under two different conditions – low temperature nitrogen supplemented medium (NSM) and low temperature nitrogen deficient medium (NFM) (**Figure 1**). A pH gradient from 4 to 7 was used to analyze bacterial protein expression under NSM and NFM. A total of 82 protein spots were differentially expressed in B2, out of which 31 were found to be upregulated, while 51 were downregulated under NFM (**Figures 1A,B**). Similarly, in case of MP1, 22 proteins were upregulated while, 46 proteins were found to downregulate under NFM (**Figures 1C,D**).

A total of 12 randomly selected protein spots (6 from each bacterium) were analyzed through MALDI–TOF–MS analysis based on their expression level and molecular weight. Remaining protein spots were analyzed by analyzing 2D gel images manually (Jain et al., 2010; Suyal et al., 2014). All the spots are summarized below with their pI and Mw (Supplementary Table SM 1).

Functional Assessment of Identified Protein Spots

A closer look at the differentially expressed proteins in psychrotolerant B2 strain indicates that major fraction of upregulated proteins was related to energy production (17%) (**Figure 2A**) *viz. ATP synthase subunit c, subunit E, ATP-dependent Clp protease ATP-binding subunit ClpX, ATP synthase subunit alpha, beta, Enolase* followed by stress response (12%) *viz. 60 kDa chaperonin, Chaperone protein HtpG, Chaperone protein ClpB*. However, in case of MP1 strain stress response related proteins (15%) *viz. Chaperone protein DnaK, Chaperone protein HscA homolog, 60 kDa chaperonin, Chaperone protein TorD* were more expressed than proteins related to energy production (6%) *viz. ATP synthase subunit alpha, beta, Enolase* (**Figure 2B**). Furthermore, in both B2 and MP1 strains, nitrogen fixation related proteins (1 and 3%, respectively) were also found to upregulate *viz. N(2)-fixation sustaining protein CowN, Iron-sulfur cluster repair protein YtfE,* and *Ferredoxin-like protein in nif region*. These proteins may assist the bacteria to fix the atmospheric N through diverse strategies. Furthermore, MALDI-TOF based identification of 12 randomly

[1]www.matrixscience.com

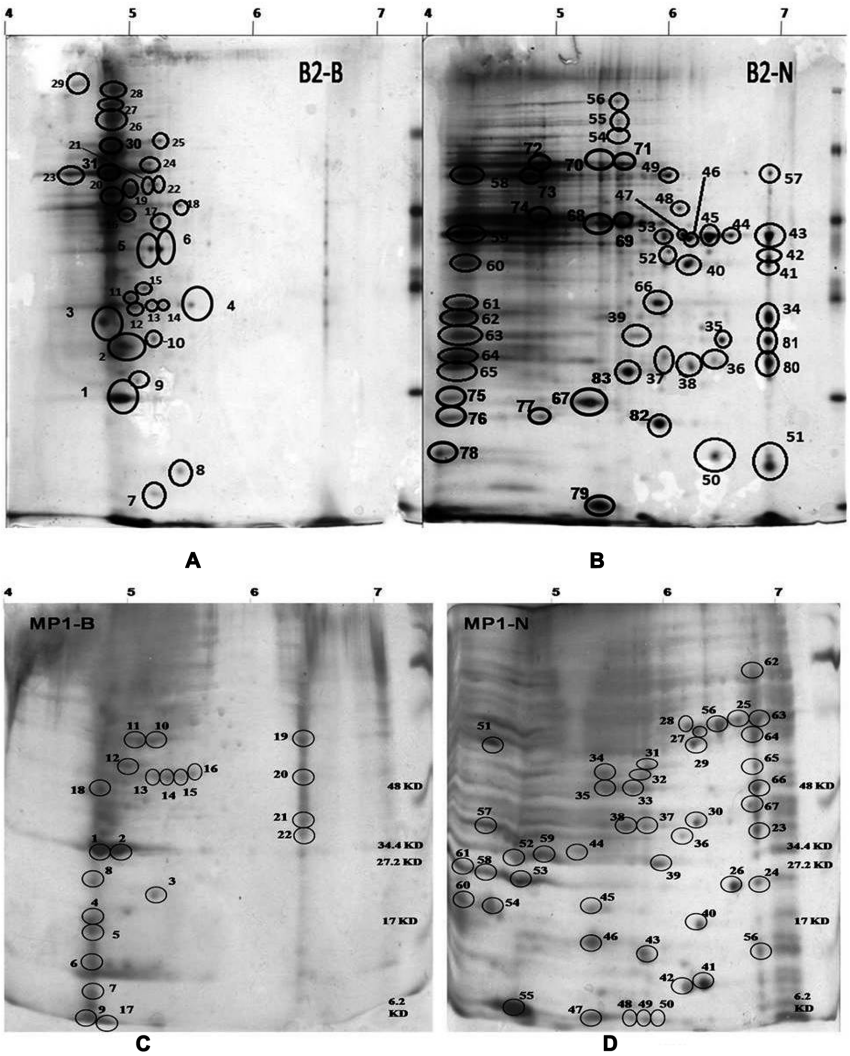


FIGURE 1 | 2D profile of *Dyadobacter psychrophilus* B2 and *Pseudomonas jessenii* MP1 cultured in the absence (**A**, B2-B and **C**, MP1-B; respectively) and in the presence of external nitrogen source (**B**, B2-N and **D**, MP1-N; respectively) in growth medium. Cells were harvested at mid-logarithmic phase.

selected protein spots encountered several important proteins *viz. Protein mrp homolog, Protein SlyX homolog, Aspartate carbamoyltransferase, Probable NADP-dependent dehydrogenase, Tail Sheath protein* and *Enolase* in B2 and *2-octaprenyl-6-methoxyphenyl hydroxylase, Phenylalanyl-tRNA synthetase alpha chain, Glycine cleavage H-protein, Dephospho-CoA kinase* as well as two uncharacterized proteins *UPF0260 protein ycgN* and *hypothetical protein SSON_1170* in MP1 subsequently.

Among the downregulated proteins, B2 and MP1 showed similar distribution pattern of the proteins related to biosynthesis (26 and 28%, respectively) and energy consuming processes (20 and 28%, respectively) (**Figure 3**). Nonetheless, B2 showed the downregulation of the proteins related to RNA modifications *viz. tRNA 2-thiocytidine biosynthesis protein TtcA* while, MP1 downregulated the expression of the proteins related to gene regulation/transcription *viz. N utilization substance protein B homolog* under NFM. Nevertheless, in both the cases, a good fraction of the upregulated proteins (7 and 9%, respectively) as well as downregulated proteins (11 and 9%, respectively) showed no resemblance with existing database and designated as Hypothetical/Uncharacterized proteins.

DISCUSSION

In nature, microorganisms adopt distinct strategies to cope with N depleting conditions *viz.* diazotrophs can fix atmospheric N_2 while other microorganisms assimilate nitrate or ammonia to fulfill their needs. Both, B2 and MP1 strains showed luxuriant growth on N deficient Burk medium and thereby indicating toward their ability to fix N_2. Similar protein expression patterns were observed under NFM conditions with slight variation in their percent distribution. In our previous studies, differential

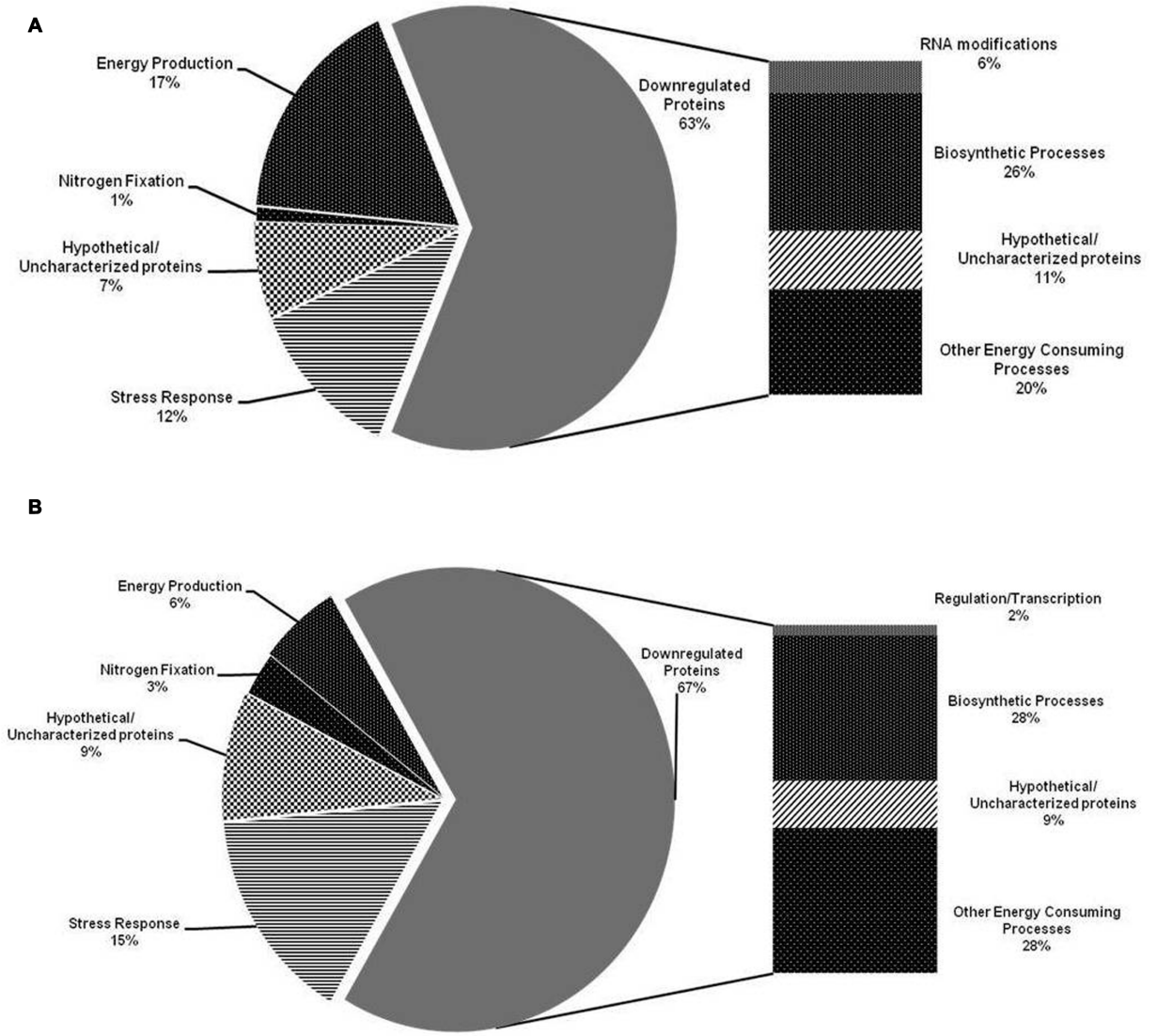


FIGURE 2 | Distribution pattern of the identified proteins upregulated and downregulated in *Dyadobacter psychrophilus* B2 (A) and *Pseudomonas jessenii* MP1 **(B)** under low temperature N_2 depleting conditions, according to their biological function.

proteomic analysis of the psychrophilic diazotroph *p. migulae* S10724 (Suyal et al., 2014) and psychrotrophic diazotroph *P. Palleroniana* N26 (Soni et al., 2015) was carried out to investigate the cold adaptive nitrogen fixation and associated mechanisms. When compared to these studies, the proteins related to stress response, nitrogen fixation, and energy production were found to be upregulated in each and every case, while energy consuming processes and biosynthetic processes were always downregulated (**Figure 3**). These proteins need a detailed investigation as they can be targeted for identifying the adaptive mechanisms of N_2 fixation in cold habitats.

ATP synthase subunit alpha, beta, ATP-dependent Clp protease and *Enolase* were the common energy production related proteins upregulated under NFM. *Atp-dependent Clp protease* was the proteolytic subunit and found to involve in the stress response in *Salmonella enterica* (Thomsen et al., 2002). Moreover, it is very critical for low temperature nitrogen fixation as revealed by our previous studies (Suyal et al., 2015). The differential expression of energy related proteins indicates toward the energy requirement of organisms under cold diazotrophy conditions. N_2 fixation is an energetically costly process in terms of reducing equivalents and ATP. Their activities may therefore, mainly be related to electron transfer reactions required to provide reducing equivalents to nitrogenase and respiratory electron transport (Varley et al., 2015).

Another aspect of cold diazotrophy was to respond the stress produced by low temperature and nitrogen deprived conditions. Under normal conditions, several stress related proteins are found to present at lower levels and contributing to cellular homoeostasis under both optimal and adverse growth conditions

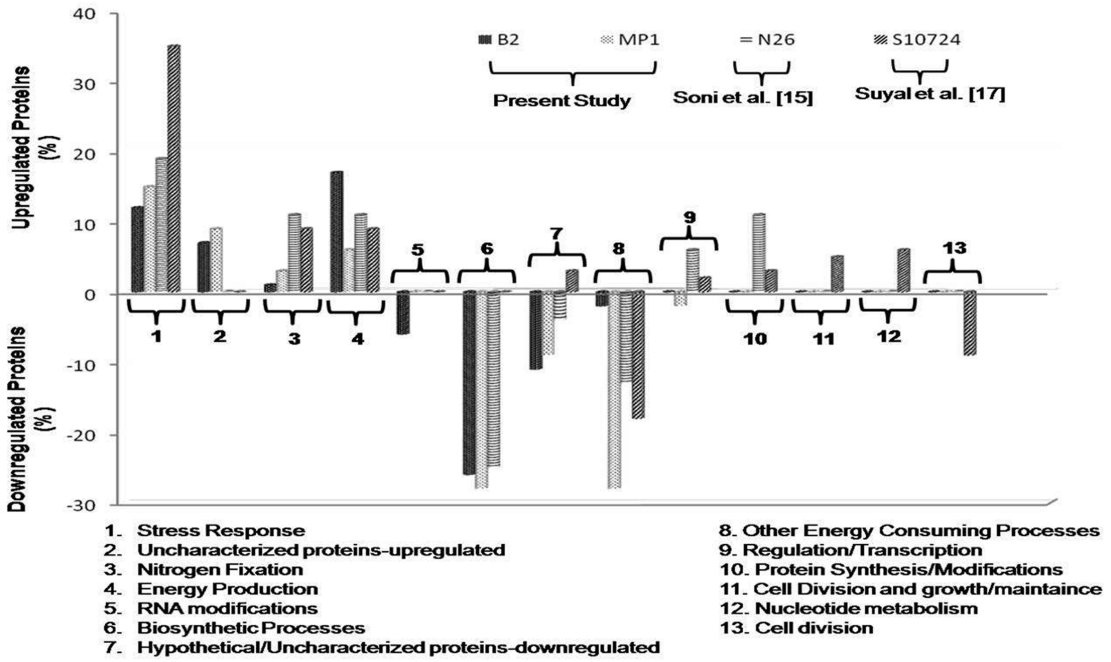


FIGURE 3 | Comparison of the identified proteins in *Dyadobacter psychrophilus* B2 and *Pseudomonas jessenii* MP1 with that of *P. palleroniana* N26 (Soni et al., 2015) and *P. migulae* S10724 (Suyal et al., 2014) under low temperature N depleting conditions, according to their biological function.

(Prema et al., 2009; Oh et al., 2015). *60 kDa chaperonin groL* and *chaperone protein HtpG* was commonly expressed proteins in both B2 and MP1 strains under NFM. *GroL* and *Htpg* both promote the proper assembly of misfolded polypeptides under stress conditions. *HtpG* has also been observed to enhance thermotolerance in the nitrogen fixing cyanobacteria (Jae-Sung et al., 2012). Besides them, *P. jessenii* MP1 also expressed *chaperone protein TorD* which involved in the biogenesis of *TorA* and probably favors a confirmation of the apoenzyme that is competent for acquiring the cofactor and *chaperone protein HscB* homolog which is a co-chaperone involved in the maturation of iron–sulfur cluster-containing proteins. These two chaperons was also observed in psychrophilic diazotroph *P. migulae* S10724 (Suyal et al., 2014), thereby, suggesting their crucial role under low temperature N_2 fixing conditions.

The expression of *N(2)-fixation sustaining protein CowN* in all the cold adapted diazotrophs including B2, MP1 and previously studied N26 (Soni et al., 2015) and S10724 (Suyal et al., 2014) reveals its importance for cold diazotrophy. This protein protects the N_2 fixation ability of the nitrogenase complex from the carbon monoxide (CO) which is supposed to increase in cold conditions (Kourtelesis et al., 2015). It has been observed that under low temperature conditions iron–sulfur clusters of nitrogenase are highly susceptible to oxidative damage (Takahashi and Tokumoto, 2002). Therefore, *iron–sulfur cluster repair protein YtfE* was observed to be overexpressed in B2 and may be involved in the repair of iron–sulfur clusters of nitrogenase damaged by cold induced oxidative stress (Vinella et al., 2013). Nevertheless, *Ferredoxin-like protein in nif region* was found to upregulate in MP1 under NFM. It was also expressed in psychrophilic *P. migulae* S10724 exclusively under low temperature nitrogen fixing conditions (Suyal et al., 2014). However, its exact role under cold diazotrophy needs to be further validated.

MALDI–TOF based identification of the expressed proteins in B2 revealed the expression of *Iron–sulfur cluster carrier protein mrp* which probably helps in the proper functioning of nitrogenase complex. Further, the upregulation of *protein SlyX homolog* and *Tail Sheath protein* under NFM is not clearly understood. They may help in protein folding and perhaps showed chaperon like activities. *Aspartate carbamoyltransferase, NADP-dependent dehydrogenase* and *Enolase* are known to catalyze the pyrimidine biosynthetic pathway, pyruvate metabolism and glycolysis, respectively (Rangeshwaran et al., 2013). These proteins might be crucial for DNA synthesis/repair and energy generation processes. In contrast to B2, MP1 upregulate the protein *2-octaprenyl-6-methoxyphenyl hydroxylase* which is crucial against oxidative stress (Ammerman et al., 2008). Moreover, *Phenylalanyl-tRNA synthetase, Glycine cleavage H-protein,* and *Dephospho-CoA kinase* were also identified which are responsible for biosynthesis processes as well in protection against oxidative stress (Fan et al., 2015).

A major fraction of the downregulated proteins in B2 and MP1 was related to energy consuming processes along with biosynthetic proteins *viz. Isocitrate dehydrogenase kinase/phosphatase, Anthranilate phosphoribosyltransferase,* and *Argininosuccinate synthase*. Moreover, the downregulation of the proteins related to cell division *viz. ZipA* and *SepF* and stress response *viz. protein GrpE* and *10 kDa chaperonin* were also in agreement with the previous studies (Soni et al., 2015). The functions of these proteins might be performed by some

multipurpose proteins and/or other energetically favorable alternatives, to bring down the energy requirements of the cells so that it could be utilized for nitrogen fixation. Similarly, Karas et al. (2015) studied the dual functions of the *tDNA-binding protein* from starved cells to defend cells against multiple stresses.

CONCLUSION

The experimental findings provide important clues on the bacterial adaptive response to nitrogen depleting conditions in cold which will be useful in filling knowledge gaps of associated mechanisms. The common upregulated N_2 fixation related protein *N(2)-fixation sustaining protein CowN* needs detail study to unravel its role in cold diazotrophy. This study is a step forward to reveal different enzymes/proteins involved during low temperature nitrogen fixation. However, the adaptations to protein architecture and metabolic pathways are still not well understood, hence, in depth analysis to unlock these adaptations and regulatory mechanisms could be an active area of investigation.

AUTHOR CONTRIBUTIONS

DS: Design of the work, experimental work, first draft of manuscript. SK: Experimental work, analysis work. AY: Analysis, manuscript drafting. YS: Sequence analysis, provided research facilities. RG: Idea of the work, manuscript checking, provide all laboratory facilities.

ACKNOWLEDGMENTS

This work is funded by the Science and Engineering Research Board (SERB) Grant No. YSS/2015/001214 to DS. DS acknowledge SERB fellowship under young scientist scheme during the course of this study.

SUPPLEMENTARY MATERIAL

The Supplementary Material for this article can be found online at: http://journal.frontiersin.org/article/10.3389/fmicb.2017.00430/full#supplementary-material

REFERENCES

Ammerman, N. C., Rahman, M. S., and Azad, A. F. (2008). Characterization of sec-translocon-dependent extracytoplasmic proteins of *Rickettsia typhi*. *J. Bacteriol.* 190, 6234–6242. doi: 10.1128/JB.00794-08

Fan, Y., Wu, J., Ung, M. H., Lay, N. D., and Cheng, C. (2015). Protein mistranslation protects bacteria against oxidative stress. *Nucleic Acids Res.* 43, 1740–1748. doi: 10.1093/nar/gku1404

Jae-Sung, R., Ki, J. S., Kim, B. M., Hwang, S. J., Choi, I. Y., and Lee, J. S. (2012). HspA and HtpG enhance thermotolerance in the Cyanobacterium, *Microcystis aeruginosa* NIES-298. *J. Microbiol. Biotechnol.* 22, 118–125. doi: 10.4014/jmb.1108.08001

Jain, S., Rani, A., Marla, S. S., and Goel, R. (2010). Differential proteomic analysis of psychrotolerant *Pseudomonas putida* 710A and alkaliphilic *Pseudomonas monteilli* 97AN for cadmium stress. *Int. J. Biol. Med. Res.* 1, 234–241.

Karas, V. O., Westerlaken, I., and Meyer, A. S. (2015). The DNA-binding protein from starved cells (Dps) utilizes dual functions to defend cells against multiple stresses. *J. Bacteriol.* 197, 3206–3215. doi: 10.1128/JB.00475-15

Kourtelesis, M., Panagiotopoulou, S., and Verykios, X. E. (2015). Influence of the support on the reaction network of ethanol steam reforming at low temperatures over pt catalysts. *Top. Catal.* 58, 1202–1217. doi: 10.1007/s11244-015-0485-7

Oh, E., McMullen, L., and Jeon, B. (2015). Impact of oxidative stress defense on bacterial survival and morphological change in *Campylobacter jejuni* under aerobic conditions. *Front. Microbiol.* 6:295. doi: 10.3389/fmicb.2015.00295

Prema, L. K., Soni, R., Khan, M., Marla, S. S., and Goel, R. (2009). Exploration of Csp genes from temperate and glacier soils of the Indian Himalayas and in silico analysis of encoding proteins. *Curr. Microbiol.* 58, 343–348. doi: 10.1007/s00284-008-9344-0

Rangeshwaran, R., Ashwitha, K., Sivakumar, G., and Jalali, S. K. (2013). Analysis of proteins expressed by an abiotic stress tolerant *Pseudomonas putida* (NBAII-RPF9) isolate under saline and high temperature conditions. *Curr. Microbiol.* 67, 659–667. doi: 10.1007/s00284-013-0416-4

Rennie, R. J. (1981). A single medium for the isolation of acetylene reducing (dinitrogen-fixing) bacteria from soils. *Can. J. Microbiol.* 27, 8–14. doi: 10.1139/m81-002

Soni, R., Suyal, D. C., Agrawal, K., Yadav, A., Souche, Y., and Goel, R. (2015). Differential proteomic analysis of Himalayan psychrotolerant diazotroph *Pseudomonas palleroniana* N26 strain under low temperature diazotrophic conditions. *CryoLetters* 36, 74–82.

Su, X., Sun, F., Wang, Y., Hashmi, M. Z., Guo, L., Ding, L., et al. (2015). Identification, characterization and molecular analysis of the viable but nonculturable *Rhodococcus biphenylivorans*. *Sci. Rep.* 5:18590. doi: 10.1038/srep18590

Suyal, D. C., Yadav, A., Shouche, Y., and Goel, R. (2014). Differential proteomics in response to low temperature diazotrophy of Himalayan psychrophilic nitrogen fixing Pseudomonas migulae S10724 strain. *Curr. Microbiol.* 68, 543–550. doi: 10.1007/s00284-013-0508-1

Suyal, D. C., Yadav, A., Shouche, Y., and Goel, R. (2015). Bacterial diversity and community structure of Western Indian Himalayan red kidney bean (*Phaseolus vulgaris* L.) rhizosphere as revealed by 16S rRNA gene sequences. *Biologia* 7, 305–313. doi: 10.1515/biolog-2015-0048

Takahashi, Y., and Tokumoto, U. (2002). A third bacterial system for the assembly of iron-sulfur clusters with homologs in archaea and plastids. *J. Biol. Chem.* 277, 28380–28383. doi: 10.1074/jbc.C200365200

Thomsen, L. E., Olsen, J. E., Foster, J. W., and Ingmer, H. (2002). ClpP is involved in the stress response and degradation of misfolded proteins in *Salmonella enterica* serovar Typhimurium. *Microbiology* 148, 2727–2733. doi: 10.1099/00221287-148-9-2727

Varley, J. B., Wang, Y., Chan, K., Studtac, F., and Norskov, J. K. (2015). Mechanistic insights into nitrogen fixation by nitrogenase enzymes. *Phys. Chem. Chem. Phys.* 17, 29541–29547. doi: 10.1039/c5cp04034e

Vinella, D., Loiseau, L., Ollagnier-de-Choudens, S., Fontecave, M., and Barras, F. (2013). In vivo [Fe-S] cluster acquisition by IscR and NsrR, two stress regulators in *Escherichia coli*. *Mol. Microbiol.* 87, 493–508. doi: 10.1111/mmi.12135

Conflict of Interest Statement: The authors declare that the research was conducted in the absence of any commercial or financial relationships that could be construed as a potential conflict of interest.

Copyright © 2017 Suyal, Kumar, Yadav, Shouche and Goel. This is an open-access article distributed under the terms of the Creative Commons Attribution License (CC BY). The use, distribution or reproduction in other forums is permitted, provided the original author(s) or licensor are credited and that the original publication in this journal is cited, in accordance with accepted academic practice. No use, distribution or reproduction is permitted which does not comply with these terms.

frontiers in Microbiology

MINI REVIEW
published: 15 March 2017
doi: 10.3389/fmicb.2017.00394

Cloning and Heterologous Expression of a Large-sized Natural Product Biosynthetic Gene Cluster in *Streptomyces* Species

Hee-Ju Nah, Hye-Rim Pyeon, Seung-Hoon Kang, Si-Sun Choi and Eung-Soo Kim *

Department of Biological Engineering, Inha University, Incheon, South Korea

Actinomycetes family including *Streptomyces* species have been a major source for the discovery of novel natural products (NPs) in the last several decades thanks to their structural novelty, diversity and complexity. Moreover, recent genome mining approach has provided an attractive tool to screen potentially valuable NP biosynthetic gene clusters (BGCs) present in the actinomycetes genomes. Since many of these NP BGCs are silent or cryptic in the original actinomycetes, various techniques have been employed to activate these NP BGCs. Heterologous expression of BGCs has become a useful strategy to produce, reactivate, improve, and modify the pathways of NPs present at minute quantities in the original actinomycetes isolates. However, cloning and efficient overexpression of an entire NP BGC, often as large as over 100 kb, remain challenging due to the ineffectiveness of current genetic systems in manipulating large NP BGCs. This mini review describes examples of actinomycetes NP production through BGC heterologous expression systems as well as recent strategies specialized for the large-sized NP BGCs in *Streptomyces* heterologous hosts.

Keywords: *Streptomyces*, natural product, biosynthetic gene cluster, heterologous expression, large-sized

OPEN ACCESS

Edited by:
Wen-Jun Li,
Sun Yat-sen University, China

Reviewed by:
Shawn Chen,
Revive Genomics Inc., USA
Jiangxin Wang,
Shenzhen University, China

***Correspondence:**
Eung-Soo Kim
eungsoo@inha.ac.kr

Specialty section:
This article was submitted to Microbiotechnology, Ecotoxicology and Bioremediation, a section of the journal Frontiers in Microbiology

Received: *31 December 2016*
Accepted: *24 February 2017*
Published: *15 March 2017*

Citation:
Nah H-J, Pyeon H-R, Kang S-H, Choi S-S and Kim E-S (2017) Cloning and Heterologous Expression of a Large-sized Natural Product Biosynthetic Gene Cluster in Streptomyces Species. Front. Microbiol. 8:394. doi: 10.3389/fmicb.2017.00394

INTRODUCTION

Natural products (NPs) and their derivatives lead a huge pharmaceutical market share comprising 61% of anticancer drugs and 49% of anti-infection medicine in the past 30 years (Newman and Cragg, 2012). Especially, actinomycetes NPs are a major resource for drug discovery and development, mainly due to their structural novelty, diversity, and complexity (Donadio et al., 2007). Isolation and characterization of NP biosynthetic gene clusters (BGCs) have further accelerated our understanding of their molecular biosynthetic mechanisms, leading to the rational redesign of novel NPs through BGC manipulation (Fischer et al., 2003; Castro et al., 2015).

Some of these potentially valuable BGCs are, however, derived from non-culturable metagenomes or genetically recalcitrant microorganisms. Moreover, many of these BGCs are expressed poorly or not at all under laboratory culture conditions, which makes it challenging to characterize the target NPs (Galm and Shen, 2006). Since efficient expression of actinomycetes NP BGCs present a major bottleneck for novel NP discovery, various cryptic BGC awakening strategies such as regulatory genes control, ribosome engineering, co-culture fermentation, and heterologous expression have been pursued for NP development (Tang et al., 2000; Flinspach et al., 2014; Martinez-Burgo et al., 2014; Miyamoto et al., 2014).

A traditional method for BGC cloning involves cosmid library construction by partial digestion or random shearing of chromosomal DNA. A typical size of NP BGC is usually larger than 20 kb (sometimes over 100 kb), and a cosmid vector system can only accept a relatively small BGC (up to 40 kb) or only a part of a large BGC. Therefore, cloning and efficient overexpression of an entire BGC still remains challenging due to the ineffectiveness of current host cells including the genetic and metabolic characteristics in manipulating large BGCs for heterologous expression. This mini review summarizes the list of the actinomycetes NP BGCs that have been successfully cloned and expressed in *Streptomyces* heterologous hosts (**Table 1**). In addition, three cloning and heterologous expression systems, which are quite suitable for large NP BGCs, such as transformation-associated recombination (TAR) system, integrase-mediated recombination (IR) system, and plasmid *Streptomyces* bacterial artificial chromosome (pSBAC) system are introduced (**Figure 1**).

TRADITIONAL METHOD FOR HETEROLOGOUS EXPRESSION OF NP BGCS

We summarized about 90 actinomycetes NP BGCs that have been successfully expressed in *Streptomyces* heterologous hosts from the last several decades (**Table 1**). Relatively small BGCs encoding Type II polyketide were first to be isolated at the beginning of heterologous expression research. Many of the listed BGCs (about 83%) were isolated by cosmid/fosmid library construction and some of these BGCs were cloned into replicative or integrative vector by linear-plus-linear (recombination between two linear DNAs) or linear-plus-circular (recombination between linear and replicating circular DNA) homologous recombination. Approximately 60% of BGCs were integrated into the heterologous host chromosome and only 37% of BGCs existed in the heterologous host via replicative plasmid. Cosmid vectors such as pOJ446 and SuperCos1 were used to be replicative or integrative in the heterologous host, so the production level of the heterologously expressed NP BGC varied significantly. Some BGCs were isolated with two different vector systems, followed by heterologous expression via both integrative and replicative systems. For example, the epothilone BGC was expressed by both pSET152-based integration vector and SCP2*-based replication vectors, so that its expression level was increased from 0.1 mg/L in the original *Sorangium cellulosum* system to 20 mg/L in the epothilone BGC-expressing *Streptomyces* host (Tang et al., 2000). *S. coelicolor* and *S. lividans* were two major strains for heterologous expression, thanks to their well-characterized genetic and biochemical properties. About 12% BGCs were expressed in another popular heterologous host, *S. albus*, which has fast growth and an efficient genetic system (Zaburannyi et al., 2014). Comparing with the original NP producing strains, approximately 14% of NPs had a higher expression level and 12% lower when they were expressed in the heterologous hosts. When bernimamycin BGC was heterologously expressed both in *S. lividans* and *S. venezuelae*, its production yield was increased 2.4-fold in *S. lividans* with no production in *S. venezuelae* (Malcolmson et al., 2013).

CLONING SYSTEMS OF LARGE NP BGCS FOR HETEROLOGOUS EXPRESSION IN *STREPTOMYCES*

TAR System

The TAR system takes advantage of the natural *in vivo* homologous recombination of *Saccharomyces cerevisiae* (Larionov et al., 1994). It has also been applied to capture and express large biosynthetic gene clusters from environmental DNA samples (Feng et al., 2010; Kim et al., 2010). Yamanaka and colleagues designed TAR cloning vector, pCAP01, which consists of three elements, one from each of yeast, *E. coli*, and actinobacteria (Yamanaka et al., 2014). The target BGC can be directly captured and manipulated in yeast background, and the captured BGC can be shuttled between *E. coli* and actinobacteria species. It also has a pUC *ori* that could stably carry an over 50 kb insert in *E. coli* hosts. The pCAP01 vector contains *oriT* and *attP-int* that can transfer the target BGC by conjugation, and the DNA stability can be maintained by insertion into heterologous host chromosomes. To generate a capturing vector, both flanking homologous arms of the target BGC were PCR-amplified and cloned into the pCAP01. The linearized capturing vector and the restriction enzyme digested genomic DNA were co-transformed into yeast, then the target BGC was captured by yeast recombination activities (**Figure 1A**). The marinopyrrole BGC (30 kb) and the taromycin A BGC (67 kb) were captured by this TAR system, and functionally expressed in *Streptomyces coelicolor* (Yamanaka et al., 2014).

IR System

Most cloning systems to clone a large DNA fragment directly from bacterial genome are based on different site-specific recombination systems that consist of a specialized recombinase and its target sites. The IR system is based on ΦBT1 integrase-mediated site-specific recombination and simultaneous *Streptomyces* genome engineering (Du et al., 2015). The actinorhodin BGC, the napsamycin BGC and the daptomycin BGC were successfully isolated by the IR system (Du et al., 2015). pUC119-based suicide vector and pKC1139 carrying mutated *attP* or *attB*, respectively, and an integrative plasmid containing the ΦBT1 integrase gene were used for the system (**Figure 1B**). The pUC119-based plasmid carrying mutated *attB* and a homologous region to 5′ end of the target BGC was introduced into the chromosome by single crossover. The pKC1139 carrying mutated *attP* and a homologous region to 3′ end of the BGC was transferred and integrated into chromosome by conjugation and single crossover through cultivation at high temperature above 34°C. Expression of ΦBT1 integrase leads to excision of the pKC1139 containing the target BGC. The pKC1139 containing BGC from original producing *Streptomyces* was extracted and transferred into *E. coli* for recovery. The IR system was only expressed in parental strain not heterologous

TABLE 1 | Heterologous expression of NP BGCs.

NP name (Class)	Original host	BGC size (kb)	Expression method	Heterologous host	WT titer (mg/L)	HH titter (mg/L)	References
A201A (Nucleoside)	*Sacchaothrix mutabilis* subsp. Capreolus	34	PAC Integrative	*S. coelicolor S. lividans*	12	8	Saugar et al., 2016
A54145 (NRPS)	*S. fradiae* NRRL 18160	~60	BAC Integrative	*S. ambofaciens S. roseosporus*	NR	100 ~ 385	Alexander et al., 2010
Actinorhodin (PKS II)	*S. coelicolor* M145	33	LLHR Integrative	*Streptomyces*	NR	NR	Chen and Qin, 2011
Amicetin (NRPS)	*S. vinaceusdrappus* NRRL 2363	37.3	Cosmid Replicative	*S. lividans*	NR	NR	Zhang et al., 2012
Ammosamides A-C (Alkaloid)	*S.* sp. CNR-698	35	TAR Integrative	*S. coelicolor*	4 ~ 6	17	Jordan and Moore, 2016
Anthracimycin (PKS I)	*S.* sp. T676	53.2	PAC Integrative	*S. coelicolor*	NR	8.6 ~ 13.8	Alt and Wilkinson, 2015
Aristeromycin (Nucleoside)	*S. citricolor*	37.5	Cosmid Replicative	*S. albus*	NR	ND	Kudo et al., 2016
Aureothin (PKS I)	*S. thioluteus* HKI-227	27	Cosmid Integrative	*S. lividans*	NR	NR	He and Hertweck, 2003
Barbamide (PKS-NRPS)	*Moorea producens*	26	LCHR Replicative	*S. venezuelae*	NR	ND*	Kim et al., 2012
Bernimamycin (Thiopeptide)	*S. bernensis* UC5144	12.9	LLHR Integrative	*S. lividans S. venezuelae*	NR	NR	Malcolmson et al., 2013
Blasticidin S (Nucleoside)	*S. griseochromogenes*	20	Cosmid Replicative	*S. lividans*	NR	NR	Cone et al., 2003
Cacibiocin (Aminocoumarin)	*Catenulispora acidiphila*	20	LLHR Integrative	*S. coelicolor*	4.9	60	Zettler et al., 2014
Caerulomycin (PKS-NRPS)	*Actinoalloteichus cyanogriseus* WH1-2216-6	44.6	Cosmid Replicative	*S. coelicolor*	NR	NR	Zhu et al., 2012
Cephamycin C (NRPS)	*S. clavuligerus* ATCC 27064	35.6	Cosmid Integrative	*S. flavogriseus S. coelicoor S. albus*	3640	8 ~ 300#	Martinez-Burgo et al., 2014
Chalcomycin (PKS I)	*S. bikiniensis*	80	LLHR Integrative	*S. fradiae*	NR	NR	Ward et al., 2004
Chaxamycin (PKS I)	*S. leeuwenhoekii*	80.2	PAC Integrative	*S. coelicolor*	NR	NR	Castro et al., 2015
Chloramphenicol (PKS-NRPS)	*S. venezuelae* ATCC10712	NR	Cosmid Integrative	*S. coelicolor*	NR	1.6 ~ 26.23	Gomez-Escribano and Bibb, 2011
Chlorizidine A (PKS I)	*S.* sp. CNH-287	42.4	Fosmid Integrative	*S. coelicolor*	NR	NR	Mantovani and Moore, 2013
Chrysomycin (PKS II)	*S. albaduncus* AD0819	34.65	Cosmid Replicative	*S. lividans*	NR	ND	Kharel et al., 2010
Clavulanic acid (β-lactam)	*S. clavuligerus* ATCC27064	20	Cosmid Integrative	*S. flavogriseus S. coelicolor*	164.50	0.6	Alvarez-Alvarez et al., 2013
Complestatin (Glycopeptide)	*S. chartreusis* AN1542	54.5	LLHR Integrative	*S. lividans*	5.57	0.24	Park et al., 2016
Congocidine (NRPS)	*S. ambofaciens* ATCC23877	NR	Cosmid Integrative	*S. coelicolor*	NR	NR	Gomez-Escribano and Bibb, 2011
Coumermycin A1 (Aminocoumarin)	*S. rishiriensis* DSM40489	38.6	Cosmid Integrative	*S. coelicolor*	0.002 ~ 0.005	0.01	Wolpert et al., 2008
Cremeonycin (Diazoquinone)	*S. cremeus* NRRL3241	18	BAC Integrative	*S. lividans*	NR	NR	Waldman et al., 2015
Cyclothiazomycin (Thiopeptide)	*S. hygroscopicus* 10-22	22.7	LLHR Integrative	*S. lividans*	NR	NR	Wang et al., 2010
Daptomycin (NRPS)	*S. roseosporus* NRRL 11379	128	BAC Integrative	*S. lividans*	900	18	Miao et al., 2005
Desotamide (NRPS)	*S. scopuliridis* SCSIO	39	Cosmid Integrative	*S. coelicolor*	NR	ND*	Li et al., 2015
Epothilone (PKS-NRPS)	*Sorangium cellulosum* SHP44	56	LLHR Replicative & Integrative	*S. coelicolor*	0.05 ~ 0.1	20	Tang et al., 2000
FK506 (PKS I)	*S.* sp. KCCM11116P	120	LCHR Integrative	*S. albus*	NR	NR	Chen et al., 2014
	S. tsukubaensis	83.5	PAC Integrative	*S. coelicolor*	1.20	5.50	Jones et al., 2013
Flustatin (PKS II)	*Micromonospora* SCSIO N160	40	Cosmid Replicative	*S. coelicolor*	NR	NR	Yang et al., 2015

(Continued)

TABLE 1 | Continued

NP name (Class)	Original host	BGC size (kb)	Expression method	Heterologous host	WT titer (mg/L)	HH titter (mg/L)	References
Fostriecin PKS (PKS I)	*S. pulveraceus* ATCC31906	48.6	LLHR Replicative & Integrative	*S. coelicolor S. lividans*	NR	ND	Su et al., 2015
Galbonolide B (PKS I)	*S.* sp. L235	12.1	LLHR Integrative	*S. coelicolor*	NR	NR[†]	Liu et al., 2015
GE2270 (Thiopeptide)	*Planobispora rosea* ATCC53733	21.4	LLHR Integrative	*S. coelicolor*	NR	0.08	Flinspach et al., 2014
GE37468 (Thiazolyl peptide)	*S.* ATCC 55365	17.1	LLHR Integrative	*S. lividans*	5 ∼ 7	2 ∼ 3	Young and Walsh, 2011
Gilvocarcin V (PKS II)	*S. griseoflavus* Gö 3592	32.9	Cosmid Replicative	*S. lividans*	20 ∼ 30	NR	Fischer et al., 2003
Goadsporin (Azole)	*S.* sp. TP-A0584	14	LLHR Integrative	*S. lividans*	126.3	342.7	Haginaka et al., 2014
Gougerotin (Nucleoside)	*S. graminearus*	28.7	LCHR Integrative	*S. coelicolor*	NR	NR	Niu et al., 2013
Granaticin (PKS II)	*S. violaceoruber* Tü22	39	Cosmid Replicative	*S. coelicolor*	NR	NR	Ichinose et al., 1998
Grecocycline (PKS II)	*S.* sp. Acta 1362	36	TAR Integrative	*S. albus*	NR	ND*	Bilyk et al., 2016
Grincamycin (PKS II)	*S. lusitanus* SCSIO LR32	37	LCHR Integrative	*S. coelicolor*	NR	ND*	Zhang et al., 2013
Holomycin (NRPS)	*S. clavuligerus* ATCC27064	24	LLHR Integrative	*S. coelicolor*	NR	NR	Robles-Reglero et al., 2013
Kanamycin (Aminoglycoside)	*S. kanamyceticus* ATCC12853	32	Cosmid Replicative	*S. venezuelae*	1.80	0.50	Thapa et al., 2007
Kinamycin (PKS II)	*S. murayamaensis*	40	Cosmid Replicative	*S. lividans*	NR	ND	Gould et al., 1998
Lincomycin (Lincosamide)	*S. lincolnensis* ATCC25466	35	Cosmid Integrative	*S. coelicolor*	50.1	0.66 ∼ 1.49	Koberska et al., 2008
Lyngbyatoxin A (NRPS)	*Moorea products*	11.3	LLHR Replicative	*S. coelicolor*	NR	NR	Jones et al., 2012
Lysolipin (PKS II)	*S. tendae* Tü 4042	43.2	Cosmid Replicative	*S. albus*	NR	NR	Lopez et al., 2010
Macrotetrolide (PKS II)	*S. griseus* DSM40695	25	LLHR Integrative	*S. lividans*	40	10	Kwon et al., 2001
Marineosin (Oligopyrrole)	*S.* sp. CNQ-617	32	Cosmid Integrative	*S. venezuelae*	0.5	5	Salem et al., 2014
Medermycin (PKS II)	*S.* sp. AM7161	30	LLHR Integrative	*S. coelicolor S. lividans*	NR	NR	Ichinose et al., 2003
	S. sp. K73	36.2	Cosmid Replicative	*S. coelicolor*	NR	NR	Ichinose et al., 2003
Mensacarcin (PKS II)	*S. bottropensis*	40	Cosmid Integrative	*S. albus*	NR	ND*	Yan et al., 2012
Meridamycin (PKS-NRPS)	*S.* sp. NRRL 30748	90	pSBAC Integrative	*S. lividans*	NR	0.1[#]	Liu et al., 2009
Merochlorin A-D (PKS-terpenoid)	*S.* sp. CNH-189	57.6	Fosmid Integrative	*S. coelicolor*	10.0	NR	Kaysser et al., 2012
Mycosperine	*Actinosynnema mirum* DSM43827	6.3	LLHR Integrative	*S. avermitilis*	NR	NR[#]	Miyamoto et al., 2014
Naphthocyclinone (PKS II)	*S. arenae* DSM40737	12	Cosmid Replicative	*S. coelicolor*	NR	NR	Brunker et al., 1999
Nataxazole (PKS I)	*S.* sp. Tü6176	44.1	TAR Integrative	*S. lividans*	NR	ND*	Cano-Prieto et al., 2015
Neocarzilin (PKS I)	*S. carzinostaticus* var. F-41	33	Cosmid Integrative	*S. lividans*	NR	NR	Otsuka et al., 2004
Nogalamycin (PKS II)	*S. nogalater*	20	Cosmid Replicative	*S. lividans*	NR	NR	Ylihonko et al., 1996
		29	LLHR Replicative	*S. lividans S. galilaeus S. peucetius*	NR	NR	Torkkell et al., 2001
Novobiocin (Aminocoumarin)	*S. spheroides*	25.6	Cosmid Replicative	*S. lividans*	NR	NR[†]	Steffensky et al., 2000
Oleandomycin (PKS I)	*S. antibiticus*	65	LLHR Replicative	*S. lividans*	NR	NR[†]	Shah et al., 2000
Oxytetracycline (PKS II)	*S. rimosus* M4018	29	Cosmid Integrative	*S. venezuelae*	75	431	Yin et al., 2016
	S. rimosus	34	Cosmid Replicative	*S. lividans*	NR	20	Binnie et al., 1989

(Continued)

TABLE 1 | Continued

NP name (Class)	Original host	BGC size (kb)	Expression method	Heterologous host	WT titer (mg/L)	HH titter (mg/L)	References
Phosphinothricin (NRPS)	*S. viridochromogenes* DSM 40736	40	Fosmid Integrative	*S. lividans*	NR	NR	Blodgett et al., 2005
Puromycin (Nucleoside)	*S. alboniger*	13	Cosmid Replicative	*S. lividans S. griseofuscus*	150.00	4 ∼ 15	Lacalle et al., 1992
R1128 (PKS II)	*S.* sp. R1128	17	Cosmid Replicative	*S. lividans*	NR	1.00	Marti et al., 2000
Ravidomycin PKS II	*S. ravidus*	33.28	Cosmid Replicative	*S. lividans*	NR	NR	Kharel et al., 2010
Rebeccamycin (Indolocarbazole)	*Saccharothrix aerocolonigenes* ATCC 39243	25.6	Cosmid Replicative	*S. albus*	NR	NR	Sanchez et al., 2002
Resorcinomycin	*Streptorerticilium roseoverticillatum*	11	LLHR Replicative	*S. lividans*	NR	ND*	Ooya et al., 2015
Rimosamide (NRPS-PKS)	*S. rimosus* NRRL B-2659	30.5	Fosmid Integrative	*S. lividans*	NR	NR	McClure et al., 2016
Rishirilide A (PKS II)	*S. bottropensis*	50	Cosmid Integrative	*S. albus, S. lividans*	NR	NR	Yan et al., 2012
Salinomycin (PKS I)	*S. albus* DSM41398	106	LLHR Integrative	*S. coelicolor*	NR	NR	Yin et al., 2015
Sparsomycin (NRPS)	*S. sparsogenes*	30	TAR Integrative	*S. lividans*	NR	NR	Rui et al., 2015
Staurosporine (Indolocarbazole)	*S. sanyensis* FMA	34.6	Cosmid Integrative	*S. coelicolor*	NR	NR	Li T. et al., 2013
	S. sp. TP-A0274	20	Cosmid Integrative	*S. lividans*	10.5	2.6	Onaka et al., 2002
Streptocolin (Lanthipeptide)	*S. colimus* Tü365	6	Cosmid Integrative	*S. coelicolor*	NR	5.4 ∼ 110	Iftime et al., 2015
Streptothricin (NRPS)	*S. sp.* TP-A0356	41	Cosmid Replicative	*S. coelicolor*	NR	NR	Li J. et al., 2013
Tautomycetin (PKS I)	*S.* sp. CK4412	80	pSBAC Integrative	*S. coelicolor S. lividans*	3.10	3.91 ∼ 4.05	Nah et al., 2015
Tetracenomycin C (PKS II)	*S. glaucescens*	24	LLHR Replicative	*S. lividans*	NR	NR	Motamedi and Hutchinson, 1987
Tetrangulol (PKS II)	*S.* sp. WP4669 *S. rimosus* NRRL3016	40	Cosmid Replicative	*S. lividans*	NR	NR	Hong et al., 1997
Thioriridamide (Ribosomal peptide)	*S. olivoriridis* NA05001	14.5	LLHR Replicative	*S. lividans*	NR	NR	Izawa et al., 2013
		70	BAC Integrative	*S. avermitilis*	NR	2.5	Izumikawa et al., 2015
TP-1161 (Thiopeptide)	*Nocardiopsis* sp. TFS65-07	16	Cosmid Replicative	*S. coelicolor*	NR	ND	Engelhardt et al., 2010
Undecylprodigiosin (NRPS)	*S. coelicolor* M145	38	LLHR Replicative	*S. parvulus*	NR	NR	Malpartida et al., 1990
Validamycin (Pseudosaccharide)	*S. hygroscopicus* var. limoneus KTCC 1715	37	Cosmid Replicative	*S. lividans S. albus*	NR	NR	Singh et al., 2006
Venemycin (PKS I)	*S. venezuelae*	29.5	Cosmid Integrative	*S. coelicolor*	NR	ND	Thanapipatsiri et al., 2016
Versipelostatin (PKS I)	*S. versipellis* 4083	108	BAC Integrative	*S. albus*	1.5	21.0	Hashimoto et al., 2015
YM-216391 (NRPS)	*S. nobilis*	<40	Cosmid Replicative	*S. lividans*	NR	0.18	Jian et al., 2012

*PKS, polyketide synthase; NRPS, non-ribosomal peptide synthase; S, Streptomyces; sp, species; TAR, transformation-associated recombination; PAC, phage P1 artificial chromosome; BAC, bacterial artificial chromosome; LLHR, linear-plus-linear homologous recombination; LCHR, linear-plus-circular homologous recombination; NR, not reported (but produced); ND, not detected (not produced); WT, wild type; HH, heterologous host; *intermediate produced only; †expressed part of gene cluster; #produced by gene cluster modification (e.g., Promoter substitution).*

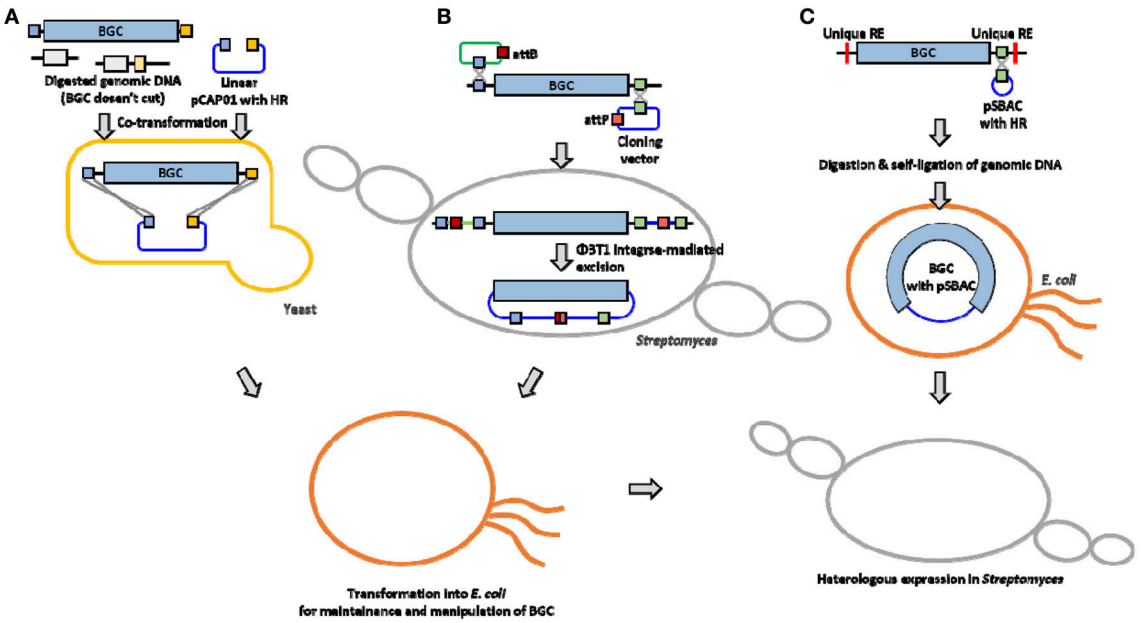


FIGURE 1 | Overview of large BGC cloning system (A) TAR system **(B)** IR system **(C)** pSBAC system. HR, Homologous region; RE, restriction enzyme.

host, but it was presumed to be transferred and maintained by replication in heterologous host (Du et al., 2015).

pSBAC Vector System

In the early 1990s, Bacterial Artificial Chromosomes (BAC) was reported to carry inserts approaching 200 kb in length emerged (Shizuya et al., 1992). Various BAC vectors have been used extensively for construction of DNA libraries to facilitate physical genomic mapping and DNA sequencing efforts (Sosio et al., 2000; Martinez et al., 2004; Fuji et al., 2014; Varshney et al., 2014). Several *E. coli-Streptomyces* shuttle BAC vectors have been developed to carry the large-sized NP BGCs such as pStreptoBAC V and pSBAC (Miao et al., 2005; Liu et al., 2009). The utility of pSBAC was demonstrated through the precise cloning and heterologous expression of the tautomycetin BGC and the pikromycin BGC of the type I PKS biosynthetic pathway, as well as the meridamycin BGC of the PKS-NRPS hybrid biosynthetic pathways (Liu et al., 2009; Nah et al., 2015). Unique restriction enzyme recognition sites naturally existing or artificially inserted into both flanking regions of the entire BGC were used for capturing the BGCs. The pSBAC vector was also inserted within the unique restriction enzyme site by homologous recombination. And then the entire target BGC was captured in a single pSBAC through straightforward single restriction enzyme digestion and self-ligation (**Figure 1C**). The pSBAC contains two replication origins, *ori2* and *oriV*, for DNA stability in *E. coli*, and *oriT* and ΦC31 *attP-int* for BGC integration into the surrogate host chromosome through intergenic conjugation. The recombinant pSBAC containing the large BGCs of varied length from 40 kb to over 100 kb have been successfully cloned and conjugated from *E. coli* to *S. coelicolor* and *S. lividans* (Liu et al., 2009; Nah et al., 2015), implying that the pSBAC system seems to be the most suitable for large BGC cloning comparing with TAR and IR systems.

Recently, a new cloning method named CATCH (Cas9-Assisted Targeting of Chromosome) based on the *in vitro* application of RNA-guided Cas9 nuclease was developed (Jiang and Zhu, 2016). The Cas9 nuclease cleaves target DNA *in vitro* from intact bacterial chromosomes embedded in agarose plugs, which can be subsequently ligated with cloning vector through Gibson assembly. Jiang and colleagues cloned the 36-kb jadomycin BGC from *S. venezuelae* and the 32-kb chlortetracycline BGC from *S. aureofaciens* by CATCH (Jiang et al., 2015).

STREPTOMYCES HETEROLOGOUS EXPRESSION OF NP BGCS

The *Streptomyces* genus is suitable for heterologous expression of large NP BGCs due to its intrinsic ability to produce various valuable secondary metabolites. Well-studied *Streptomyces* strains such as *S. coelicolor, S. lividans,* and *S. albus* have been mainly used as heterologous expression surrogate hosts (**Table 1**). The regulatory networks of secondary metabolite production have been well characterized in these strains, and thus several NP high-level producing strains have been constructed (Baltz, 2010; Gomez-Escribano and Bibb, 2011). In addition, some of these *Streptomyces* host genomes have been further engineered to eliminate precursor-competing biosynthetic BGCs, so that the extra precursors such as malonyl-CoA and acetyl-CoA could be funneled into the target polyketide NP biosynthesis (Gomez-Escribano and Bibb, 2011).

As shown in **Table 1**, most of the heterologously expressed NPs were detected as a final product, but some were detected as an intermediate due to their partial BGC expression. The NP production yield was similar to or slightly lower than that in WT. To increase the production level in heterologous hosts, it was devised to substitute with strong promoters or to increase the copy number of BGCs (Montiel et al., 2015; Nah et al., 2015). In case of pSBAC system, the tautomycetin production yield in the heterologous hosts was similar to that in the original producing strain. The selection marker on the tautomycetin BGC was changed and re-introduced into the heterologous host by tandem repeat, resulting in further yield increase from 3.05 to 13.31 mg/L in comparison with the heterologous host harboring only single copy of tautomycetin BGC. The heterologous host harboring tandem copies of tautomycetin BGC was proved to stably maintain two BGCs in the presence of appropriate antibiotic selection (Nah et al., 2015).

Meanwhile, the TAR system used yeast homologous recombination-based promoter engineering for the activation of silent natural product BGCs (Montiel et al., 2015). Bi-directional promoter cassettes were generated by PCR amplification of varied yeast selectable markers, which contains promoter-insulator-RBS combinations, and they were co-transformed with the cosmid or BAC clone harboring the target BGC into yeast. The rebeccamycin BGC was used as a model BGC. The promoter-replaced rebeccamycin BGC was transferred into *S. albus* by conjugation, and the production of rebeccamycin was examined in the heterologous host (Montiel et al., 2015). Using the TAR-based promoter engineering strategy, multiple promoter cassettes could be inserted simultaneously into the target BGC, thereby expediting the re-engineering process. The TAR-based promoter engineering strategy was also used to capture the silent tetarimycin BGC and the silent, cryptic pseudogene-containing, environmental DNA-derived lazarimide BGC (Montiel et al., 2015).

In conclusion, *Streptomyces* heterologous expression systems have been proved to be a very attractive strategy to awaken cryptic NP BGCs, and could also be applied to overexpression of a variety of large NP BGCs in actinomycetes.

AUTHOR CONTRIBUTIONS

HN, SK, SC, and EK planned, outlined, and revised the manuscript. HN, HP, and EK wrote and revised the manuscript.

ACKNOWLEDGMENTS

This research was supported by "National Research Foundation of Korea (NRF)" (Project No. NRF-2014R1A2A1A11052236 & NRF-2016K2A9A2A10005545).

REFERENCES

Alexander, D. C., Rock, J., He, X., Brian, P., Miao, V., and Baltz, R. H. (2010). Development of a genetic system for combinatorial biosynthesis of lipopeptides in *Streptomyces fradiae* and heterologous expression of the A54145 biosynthesis gene cluster. *Appl. Environ. Microbiol.* 76, 6877–6887. doi: 10.1128/AEM.01248-10

Alt, S., and Wilkinson, B. (2015). Biosynthesis of the novel macrolide antibiotic anthracimycin. *ACS Chem. Biol.* 10, 2468–2479. doi: 10.1021/acschembio.5b00525

Alvarez-Alvarez, R., Martinez-Burgo, Y., Perez-Redondo, R., Brana, A. F., Martin, J. F., and Liras, P. (2013). Expression of the endogenous and heterologous clavulanic acid cluster in *Streptomyces flavogriseus*: why a silent cluster is sleeping. *Appl. Microbiol. Biotechnol.* 97, 9451–9463. doi: 10.1007/s00253-013-5148-7

Baltz, R. H. (2010). *Streptomyces* and *Saccharopolyspora* hosts for heterologous expression of secondary metabolite gene clusters. *J. Ind. Microbiol. Biotechnol.* 37, 759–772. doi: 10.1007/s10295-010-0730-9

Bilyk, O., Sekurova, O. N., Zotchev, S. B., and Luzhetskyy, A. (2016). Cloning and heterologous expression of the grecocycline biosynthetic gene cluster. *PLoS ONE* 11:e0158682. doi: 10.1371/journal.pone.0158682

Binnie, C., Warren, M., and Butler, M. J. (1989). Cloning and heterologous expression in *Streptomyces lividans* of *Streptomyces rimosus* genes involved in oxytetracycline biosynthesis. *J. Bacteriol.* 171, 887–895. doi: 10.1128/jb.171.2.887-895.1989

Blodgett, J. A., Zhang, J. K., and Metcalf, W. W. (2005). Molecular cloning, sequence analysis, and heterologous expression of the phosphinothricin tripeptide biosynthetic gene cluster from *Streptomyces viridochromogenes* DSM 40736. *Antimicrob. Agents Chemother.* 49, 230–240. doi: 10.1128/AAC.49.1.230-240.2005

Brunker, P., McKinney, K., Sterner, O., Minas, W., and Bailey, J. E. (1999). Isolation and characterization of the naphthocyclinone gene cluster from *Streptomyces arenae* DSM 40737 and heterologous expression of the polyketide synthase genes. *Gene* 227, 125–135. doi: 10.1016/S0378-1119(98)00618-0

Cano-Prieto, C., Garcia-Salcedo, R., Sanchez-Hidalgo, M., Brana, A. F., Fiedler, H. P., Mendez, C., et al. (2015). Genome mining of *Streptomyces* sp. Tu 6176: characterization of the nataxazole biosynthesis pathway. *Chembiochem* 16, 1461–1473. doi: 10.1002/cbic.201500153

Castro, J. F., Razmilic, V., Gomez-Escribano, J. P., Andrews, B., Asenjo, J. A., and Bibb, M. J. (2015). Identification and heterologous expression of the chaxamycin biosynthesis gene cluster from *Streptomyces leeuwenhoekii*. *Appl. Environ. Microbiol.* 81, 5820–5831. doi: 10.1128/AEM.01039-15

Chen, C., Zhao, X., Jin, Y., Zhao, Z. K., and Suh, J. W. (2014). Rapid construction of a bacterial artificial chromosomal (BAC) expression vector using designer DNA fragments. *Plasmid* 76, 79–86. doi: 10.1016/j.plasmid.2014.10.002

Chen, W., and Qin, Z. (2011). Development of a gene cloning system in a fast-growing and moderately thermophilic *Streptomyces* species and heterologous expression of *Streptomyces* antibiotic biosynthetic gene clusters. *BMC Microbiol.* 11:243. doi: 10.1186/1471-2180-11-243

Cone, M. C., Yin, X., Grochowski, L. L., Parker, M. R. and Zabriskie, T. M. (2003). The blasticidin S biosynthesis gene cluster from *Streptomyces griseochromogenes*: sequence analysis, organization, and initial characterization. *ChemBioChem* 4, 821–828. doi: 10.1002/cbic.200300583

Donadio, S., Monciardini, P., and Sosio, M. (2007). Polyketide synthases and nonribosomal peptide synthetases: the emerging view from bacterial genomics. *Nat. Prod. Rep.* 24, 1073–1109. doi: 10.1039/b514050c

Du, D., Wang, L., Tian, Y., Liu, H., Tan, H., and Niu, G. (2015). Genome engineering and direct cloning of antibiotic gene clusters via phage ΦBT1 integrase-mediated site-specific recombination in *Streptomyces*. *Sci. Rep.* 5:8740. doi: 10.1038/srep08740

Engelhardt, K., Degnes, K. F., and Zotchev, S. B. (2010). Isolation and characterization of the gene cluster for biosynthesis of the thiopeptide antibiotic TP-1161. *Appl. Environ. Microbiol.* 76, 7093–7101. doi: 10.1128/AEM.01442-10

Feng, Z., Kim, J. H., and Brady, S. F. (2010). Fluostatins produced by the heterologous expression of a TAR reassembled environmental DNA derived type II PKS gene cluster. *J. Am. Chem. Soc.* 132, 11902–11903. doi: 10.1021/ja104550p

Fischer, C., Lipata, F., and Rohr, J. (2003). The complete gene cluster of the antitumor agent gilvocarcin V and its implication for the biosynthesis of the gilvocarcins. *J. Am. Chem. Soc.* 125, 7818–7819. doi: 10.1021/ja034781q

Flinspach, K., Kapitzke, C., Tocchetti, A., Sosio, M., and Apel, A. K. (2014). Heterologous expression of the thiopeptide antibiotic GE2270 from *Planobispora rosea* ATCC 53733 in *Streptomyces coelicolor* requires deletion of ribosomal genes from the expression construct. *PLoS ONE* 9:e90499. doi: 10.1371/journal.pone.0090499

Fuji, K., Koyama, T., Kai, W., Kubota, S., Yoshida, K., Ozaki, A., et al. (2014). Construction of a high-coverage bacterial artificial chromosome library and comprehensive genetic linkage map of yellowtail *Seriola quinqueradiata*. *BMC Res. Notes* 7:200. doi: 10.1186/1756-0500-7-200

Galm, U., and Shen, B. (2006). Expression of biosynthetic gene clusters in heterologous hosts for natural product production and combinatorial biosynthesis. *Expert Opin. Drug Discov.* 1, 409–437. doi: 10.1517/17460441.1.5.409

Gomez-Escribano, J. P., and Bibb, M. J. (2011). Engineering *Streptomyces coelicolor* for heterologous expression of secondary metabolite gene clusters. *Microb. Biotechnol.* 4, 207–215. doi: 10.1111/j.1751-7915.2010.00219.x

Gould, S. J., Hong, S. T., and Carney, J. R. (1998). Cloning and heterologous expression of genes from the kinamycin biosynthetic pathway of *Streptomyces murayamaensis*. *J. Antibiot. (Tokyo)* 51, 50–57. doi: 10.7164/antibiotics.51.50

Haginaka, K., Asamizu, S., Ozaki, T., Igarashi, Y., Furumai, T., and Onaka, H. (2014). Genetic approaches to generate hyper-producing strains of goadsporin: the relationships between productivity and gene duplication in secondary metabolite biosynthesis. *Biosci. Biotechnol. Biochem.* 78, 394–399. doi: 10.1080/09168451.2014.885824

Hashimoto, T., Hashimoto, J., Teruya, K., Hirano, T., Shin-ya, K., Ikeda, H., et al. (2015). Biosynthesis of versipelostatin: identification of an enzyme-catalyzed [4+2]-cycloaddition required for macrocyclization of spirotetronate-containing polyketides. *J. Am. Chem. Soc.* 137, 572–575. doi: 10.1021/ja510711x

He, J., and Hertweck, C. (2003). Iteration as programmed event during polyketide assembly; molecular analysis of the aureothin biosynthesis gene cluster. *Chem. Biol.* 10, 1225–1232. doi: 10.1016/j.chembiol.2003.11.009

Hong, S. T., Carney, J. R., and Gould, S. J. (1997). Cloning and heterologous expression of the entire gene clusters for PD 116740 from *Streptomyces* strain WP 4669 and tetrangulol and tetrangomycin from *Streptomyces rimosus* NRRL 3016. *J Bacteriol.* 179, 470–476. doi: 10.1128/jb.179.2.470-476.1997

Ichinose, K., Bedford, D. J., Tornus, D., Bechthold, A., Bibb, M. J., Revill, W. P., et al. (1998). The granaticin biosynthetic gene cluster of *Streptomyces violaceoruber* Tu22: sequence analysis and expression in a heterologous host. *Chem. Biol.* 5, 647–659. doi: 10.1016/S1074-5521(98)90292-7

Ichinose, K., Ozawa, M., Itou, K., Kunieda, K., and Ebizuka, Y. (2003). Cloning, sequencing and heterologous expression of the medermycin biosynthetic gene cluster of Streptomyces sp. AM-7161: towards comparative analysis of the benzoisochromanequinone gene clusters. *Microbiology* 149, 1633–1645. doi: 10.1099/mic.0.26310-0

Iftime, D., Jasyk, M., Kulik, A., Imhoff, J. F., Stegmann, E., Wohlleben, W., et al. (2015). Streptocollin, a Type IV lanthipeptide produced by *Streptomyces collinus* Tu 365. *Chembiochem* 16, 2615–2623. doi: 10.1002/cbic.201500377

Izawa, M., Kawasaki, T., and Hayakawa, Y. (2013). Cloning and heterologous expression of the thioviridamide biosynthesis gene cluster from *Streptomyces olivoviridis*. *Appl. Environ. Microbiol.* 79, 7110–7113. doi: 10.1128/AEM.01978-13

Izumikawa, M., Kozone, I., Hashimoto, J., Kagaya, N., Takagi, M., Koiwai, H., et al. (2015). Novel thioviridamide derivative–JBIR-140: heterologous expression of the gene cluster for thioviridamide biosynthesis. *J. Antibiot. (Tokyo)* 68, 533–536. doi: 10.1038/ja.2015.20

Jian, X. H., Pan, H. X., Ning, T. T., Shi, Y. Y., Chen, Y. S., Li, Y., et al. (2012). Analysis of YM-216391 biosynthetic gene cluster and improvement of the cyclopeptide production in a heterologous host. *ACS Chem. Biol.* 7, 646–651. doi: 10.1021/cb200479f

Jiang, W., Zhao, X., Gabrieli, T., Lou, C., Ebenstein, Y., and Zhu, T. F. (2015). Cas9-assisted targeting of chromosome segments CATCH enables one-step targeted cloning of large gene clusters. *Nat. Commun.* 6:9101. doi: 10.1038/ncomms9101

Jiang, W., and Zhu, T. F. (2016). Targeted isolation and cloning of 100-kb microbial genomic sequences by Cas9-assisted targeting of chromosome segments. *Nat. Protoc.* 11, 960–975. doi: 10.1038/nprot.2016.055

Jones, A. C., Gust, B., Kulik, A., Heide, L., Buttner, M. J., and Bibb, M. J. (2013). Phage p1-derived artificial chromosomes facilitate heterologous expression of the FK506 gene cluster. *PLoS ONE* 8:e69319. doi: 10.1371/journal.pone.0069319

Jones, A. C., Ottilie, S., Eustaquio, A. S., Edwards, D. J., Gerwick, L., Moore, B. S., et al. (2012). Evaluation of *Streptomyces coelicolor* A3(2) as a heterologous expression host for the cyanobacterial protein kinase C activator lyngbyatoxin A. *FEBS J.* 279, 1243–1251. doi: 10.1111/j.1742-4658.2012.08517.x

Jordan, P. A., and Moore, B. S. (2016). Biosynthetic pathway connects cryptic ribosomally synthesized posttranslationally modified peptide genes with pyrroloquinoline alkaloids. *Cell Chem. Biol.* 23, 1504–1514. doi: 10.1016/j.chembiol.2016.10.009

Kaysser, L., Bernhardt, P., Nam, S. J., Loesgen, S., Ruby, J. G., Skewes-Cox, P., et al. (2012). Merochlorins, A.-D., cyclic meroterpenoid antibiotics biosynthesized in divergent pathways with vanadium-dependent chloroperoxidases. *J. Am. Chem. Soc.* 134, 11988–11991. doi: 10.1021/ja305665f

Kharel, M. K., Nybo, S. E., Shepherd, M. D., and Rohr, J. (2010). Cloning and characterization of the ravidomycin and chrysomycin biosynthetic gene clusters. *Chembiochem* 11, 523–532. doi: 10.1002/cbic.200900673

Kim, E. J., Lee, J. H., Choi, H., Pereira, A. R., Ban, Y. H., Yoo, Y. J., et al. (2012). Heterologous production of 4-O-demethylbarbamide, a marine cyanobacterial natural product. *Org. Lett.* 14, 5824–5827. doi: 10.1021/ol302575h

Kim, J. H., Feng, Z., Bauer, J. D., Kallifidas, D., Calle, P. Y., and Brady, S. F. (2010). Cloning large natural product gene clusters from the environment: piecing environmental DNA gene clusters back together with TAR. *Biopolymers* 93, 833–844. doi: 10.1002/bip.21450

Koberska, M., Kopecky, J., Olsovska, J., Jelinkova, M., Ulanova, D., Man, P., et al. (2008). Sequence analysis and heterologous expression of the lincomycin biosynthetic cluster of the type strain *Streptomyces lincolnensis* ATCC 25466. *Folia Microbiol. (Praha)* 53, 395–401. doi: 10.1007/s12223-008-0060-8

Kudo, F., Tsunoda, T., Takashima, M., and Eguchi, T. (2016). Five-membered cyclitol phosphate formation by a myo-inositol phosphate synthase orthologue in the biosynthesis of the carbocyclic nucleoside antibiotic aristeromycin. *Chembiochem* 17, 2143–2148. doi: 10.1002/cbic.201600348

Kwon, H. J., Smith, W. C., Xiang, L., and Shen, B. (2001). Cloning and heterologous expression of the macrotetrolide biosynthetic gene cluster revealed a novel polyketide synthase that lacks an acyl carrier protein. *J. Am. Chem. Soc.* 123, 3385–3386. doi: 10.1021/ja0100827

Lacalle, R. A., Tercero, J. A., and Jimenez, A. (1992). Cloning of the complete biosynthetic gene cluster for an aminonucleoside antibiotic, puromycin, and its regulated expression in heterologous hosts. *EMBO J.* 11, 785–792.

Larionov, V., Kouprina, N., Eldarov, M., Perkins, E., Porter, G., and Resnick, M. A. (1994). Transformation-associated recombination between diverged and homologous DNA repeats is induced by strand breaks. *Yeast* 10, 93–104. doi: 10.1002/yea.320100109

Li, J., Guo, Z., Huang, W., Meng, X., Ai, G., Tang, G., et al. (2013). Mining of a streptothricin gene cluster from *Streptomyces* sp. TP-A0356 genome via heterologous expression. *Sci. China Life Sci.* 56, 619–627. doi: 10.1007/s11427-013-4504-2

Li, Q., Song, Y., Qin, X., Zhang, X., Sun, A., and Ju, J. (2015). Identification of the biosynthetic gene cluster for the anti-infective desotamides and production of a new analogue in a heterologous host. *J. Nat. Prod.* 78, 944–948. doi: 10.1021/acs.jnatprod.5b00009

Li, T., Du, Y., Cui, Q., Zhang, J., Zhu, W., Hong, K., et al. (2013). Cloning, characterization and heterologous expression of the indolocarbazole biosynthetic gene cluster from marine-derived *Streptomyces sanyensis* FMA. *Mar. Drugs* 11, 466–488. doi: 10.3390/md11020466

Liu, C., Zhang, J., Lu, C., and Shen, Y. (2015). Heterologous expression of galbonolide biosynthetic genes in *Streptomyces coelicolor*. *Antonie Van Leeuwenhoek* 107, 1359–1366. doi: 10.1007/s10482-015-0415-5

Liu, H., Jiang, H., Haltli, B., Kulowski, K., Muszynska, E., Feng, X., et al. (2009). Rapid cloning and heterologous expression of the meridamycin biosynthetic gene cluster using a versatile *Escherichia coli-Streptomyces* artificial chromosome vector, pSBAC. *J. Nat. Prod.* 72, 389–395. doi: 10.1021/np8006149

Lopez, P., Hornung, A., Welzel, K., Unsin, C., Wohlleben, W., Weber, T., et al. (2010). Isolation of the lysolipin gene cluster of *Streptomyces tendae* Tu. *Gene* 461, 5–14. doi: 10.1016/j.gene.2010.03.016

Malcolmson, S. J., Young, T. S., Ruby, J. G., Skewes-Cox, P., and Walsh, C. T. (2013). The posttranslational modification cascade to the thiopeptide berninamycin generates linear forms and altered macrocyclic scaffolds. *Proc. Natl. Acad. Sci. U.S.A.* 110, 8483–8488. doi: 10.1073/pnas.1307111110

Malpartida, F., Niemi, J., Navarrete, R., and Hopwood, D. A. (1990). Cloning and expression in a heterologous host of the complete set of genes for biosynthesis of the *Streptomyces coelicolor* antibiotic undecylprodigiosin. *Gene* 93, 91–99. doi: 10.1016/0378-1119(90)90141-D

Mantovani, S. M., and Moore, B. S. (2013). Flavin-linked oxidase catalyzes pyrrolizine formation of dichloropyrrole-containing polyketide extender unit in chlorizidine A. *J. Am. Chem. Soc.* 135, 18032–18035. doi: 10.1021/ja409520v

Marti, T., Hu, Z., Pohl, N. L., Shah, A. N., and Khosla, C. (2000). Cloning, nucleotide sequence, and heterologous expression of the biosynthetic gene cluster for R1128, a non-steroidal estrogen receptor antagonist. Insights into an unusual priming mechanism. *J. Biol. Chem.* 275, 33443–33448. doi: 10.1074/jbc.M006766200

Martinez, A., Kolvek, S. J., Tiong Yip, C. L., Hopke, J., Brown, K. A., MacNeil, I. A., et al. (2004). Genetically modified bacterial strains and novel bacterial artificial chromosome shuttle vectors for constructing environmental libraries and detecting heterologous natural products in multiple expression hosts. *Appl. Environ. Microbiol.* 70, 2452–2463. doi: 10.1128/AEM.70.4.2452-2463.2004

Martinez-Burgo, Y., Alvarez-Alvarez, R., Perez-Redondo, R., and Liras, P. (2014). Heterologous expression of *Streptomyces clavuligerus* ATCC 27064 cephamycin C gene cluster. *J. Biotechnol.* 186, 21–29. doi: 10.1016/j.jbiotec.2014.06.002

McClure, R. A., Goering, A. W., Ju, K. S., Baccile, J. A., Schroeder, F. C., Metcalf, W. W., et al. (2016). Elucidating the rimosamide-detoxin natural product families and their biosynthesis using metabolite/gene cluster correlations. *ACS Chem. Biol.* 11, 3452–3460. doi: 10.1021/acschembio.6b00779

Miao, V., Coeffet-LeGal, M., Brian, P., Brost, R., Penn, J., Whiting, A., et al. (2005). Daptomycin biosynthesis in *Streptomyces roseosporus*: cloning and analysis of the gene cluster and revision of peptide stereochemistry. *Microbiology* 151(Pt 5), 1507–1523. doi: 10.1099/mic.0.27757-0

Miyamoto, K. T., Komatsu, M., and Ikeda, H. (2014). Discovery of gene cluster for mycosporine-like amino acid biosynthesis from Actinomycetales microorganisms and production of a novel mycosporine-like amino acid by heterologous expression. *Appl. Environ. Microbiol.* 80, 5028–5036. doi: 10.1128/AEM.00727-14

Montiel, D., Kang, H. S., Chang, F. Y., Charlop-Powers, Z., and Brady, S. F. (2015). Yeast homologous recombination-based promoter engineering for the activation of silent natural product biosynthetic gene clusters. *Proc. Natl. Acad. Sci. U.S.A.* 112, 8953–8958. doi: 10.1073/pnas.1507606112

Motamedi, H., and Hutchinson, C. R. (1987). Cloning and heterologous expression of a gene cluster for the biosynthesis of tetracenomycin C, the anthracycline antitumor antibiotic of *Streptomyces glaucescens*. *Proc. Natl. Acad. Sci. U.S.A.* 84, 4445–4449. doi: 10.1073/pnas.84.13.4445

Nah, H. J., Woo, M. W., Choi, S. S., and Kim, E. S. (2015). Precise cloning and tandem integration of large polyketide biosynthetic gene cluster using *Streptomyces* artificial chromosome system. *Microb. Cell Fact.* 14, 140. doi: 10.1186/s12934-015-0325-2

Newman, D. J., and Cragg, G. M. (2012). Natural products as sources of new drugs over the 30 years from 1981 to 2010. *J. Nat. Prod.* 75, 311–335. doi: 10.1021/np200906s

Niu, G., Li, L., Wei, J., and Tan, H. (2013). Cloning, heterologous expression, and characterization of the gene cluster required for gougerotin biosynthesis. *Chem. Biol.* 20, 34–44. doi: 10.1016/j.chembiol.2012.10.017

Onaka, H., Taniguchi, S., Igarashi, Y., and Furumai, T. (2002). Cloning of the staurosporine biosynthetic gene cluster from *Streptomyces* sp. TP-A0274 and its heterologous expression in *Streptomyces lividans*. *J. Antibiot. (Tokyo)* 55, 1063–10671. doi: 10.7164/antibiotics.55.1063

Ooya, K., Ogasawara, Y., Noike, M., and Dairi, T. (2015). Identification and analysis of the resorcinomycin biosynthetic gene cluster. *Biosci. Biotechnol. Biochem.* 79, 1833–1837. doi: 10.1080/09168451.2015.1050992

Otsuka, M., Ichinose, K., Fujii, I., and Ebizuka, Y. (2004). Cloning, sequencing, and functional analysis of an iterative type I polyketide synthase gene cluster for biosynthesis of the antitumor chlorinated polyenone neocarzilin in "*Streptomyces carzinostaticus*." *Antimicrob. Agents Chemother.* 48, 3468–3476. doi: 10.1128/AAC.48.9.3468-3476.2004

Park, O. K., Choi, H. Y., Kim, G. W., and Kim, W. G. (2016). Generation of new complestatin analogues by heterologous expression of the complestatin biosynthetic gene cluster from *Streptomyces chartreusis* AN1542. *Chembiochem* 17, 1725–1731. doi: 10.1002/cbic.201600241

Robles-Reglero, V., Santamarta, I., Alvarez-Alvarez, R., Martin, J. F., and Liras, P. (2013). Transcriptional analysis and proteomics of the holomycin gene cluster in overproducer mutants of *Streptomyces clavuligerus*. *J. Biotechnol.* 163, 69–76. doi: 10.1016/j.jbiotec.2012.09.017

Rui, Z., Huang, W., Xu, F., Han, M., Liu, X., Lin, S., et al. (2015). Sparsomycin biosynthesis highlights unusual module architecture and processing mechanism in non-ribosomal peptide synthetase. *ACS Chem. Biol.* 10, 1765–1769. doi: 10.1021/acschembio.5b00284

Salem, S. M., Kancharla, P., Florova, G., Gupta, S., Lu, W., and Reynolds, K. A. (2014). Elucidation of final steps of the marineosins biosynthetic pathway through identification and characterization of the corresponding gene cluster. *J. Am. Chem. Soc.* 136, 4565–4574. doi: 10.1021/ja411544w

Sanchez, C., Butovich, I. A., Brana, A. F., Rohr, J., Mendez, C., and Salas, J. A. (2002). The biosynthetic gene cluster for the antitumor rebeccamycin: characterization and generation of indolocarbazole derivatives. *Chem. Biol.* 9, 519–531. doi: 10.1016/S1074-5521(02)00126-6

Saugar, I., Molloy, B., Sanz, E., Blanca Sanchez, M., Fernandez-Lobato, M., and Jimenez, A. (2016). Characterization of the biosynthetic gene cluster (ata) for the A201A aminonucleoside antibiotic from *Saccharothrix mutabilis* subsp. capreolus. *J. Antibiot. (Tokyo).* doi: 10.1038/ja.2016.123. [Epub ahead of print].

Shah, S., Xue, Q., Tang, L., Carney, J. R., Betlach, M., and McDaniel, R. (2000). Cloning, characterization and heterologous expression of a polyketide synthase and P-450 oxidase involved in the biosynthesis of the antibiotic oleandomycin. *J. Antibiot. (Tokyo)* 53, 502–508. doi: 10.7164/antibiotics.53.502

Shizuya, H., Birren, B., Kim, U. J., Mancino, V., Slepak, T., Tachiiri, Y., et al. (1992). Cloning and stable maintenance of 300-kilobase-pair fragments of human DNA in *Escherichia coli* using an F-factor-based vector. *Proc. Natl. Acad. Sci. U.S.A.* 89, 8794–8797. doi: 10.1073/pnas.89.18.8794

Singh, D., Seo, M. J., Kwon, H. J., Rajkarnikar, A., Kim, K. R., Kim, S. O., et al. (2006). Genetic localization and heterologous expression of validamycin biosynthetic gene cluster isolated from *Streptomyces hygroscopicus* var. limoneus KCCM 11405 (IFO 12704). *Gene* 376, 13–23. doi: 10.1016/j.gene.2005.12.035

Sosio, M., Giusino, F., Cappellano, C., Bossi, E., Puglia, A. M., and Donadio, S. (2000). Artificial chromosomes for antibiotic-producing actinomycetes. *Nat. Biotechnol.* 18, 343–345. doi: 10.1038/73810

Steffensky, M., Muhlenweg, A., Wang, Z. X., Li, S. M., and Heide, L. (2000). Identification of the novobiocin biosynthetic gene cluster of *Streptomyces spheroides* NCIB 11891. *Antimicrob. Agents Chemother.* 44, 1214–1222. doi: 10.1128/AAC.44.5.1214-1222.2000

Su, C., Zhao, X., Qiu, R., and Tang, L. (2015). Construction of the co-expression plasmids of fostriecin polyketide synthases and heterologous expression in *Streptomyces*. *Pharm. Biol.* 53, 269–274. doi: 10.3109/13880209.2014.914956

Tang, L., Shah, S., Chung, L., Carney, J., Katz, L., Khosla, C., et al. (2000). Cloning and heterologous expression of the epothilone gene cluster. *Science* 287, 640–642. doi: 10.1126/science.287.5453.640

Thanapipatsiri, A., Gomez-Escribano, J. P., Song, L., Bibb, M. J., Al-Bassam, M., Chandra, G., et al. (2016). Discovery of unusual biaryl polyketides by activation of a silent *Streptomyces venezuelae* biosynthetic gene cluster. *Chembiochem* 17, 2189–2198. doi: 10.1002/cbic.201600396

Thapa, L. P., Oh, T. J., Lee, H. C., Liou, K., Park, J. W., Yoon, Y. J., et al. (2007). Heterologous expression of the kanamycin biosynthetic gene cluster (pSKC2) in *Streptomyces venezuelae* YJ003. *Appl. Microbiol. Biotechnol.* 76, 1357–1364. doi: 10.1007/s00253-007-1096-4

Torkkell, S., Kunnari, T., Palmu, K., Mantsala, P., Hakala, J., and Ylihonko, K. (2001). The entire nogalamycin biosynthetic gene cluster of *Streptomyces nogalater*: characterization of a 20-kb DNA region and generation of hybrid structures. *Mol. Genet. Genomics* 266, 276–288. doi: 10.1007/s0043801 00554

Varshney, R. K., Mir, R. R., Bhatia, S., Thudi, M., Hu, Y., Azam, S., et al. (2014). Integrated physical, genetic and genome map of chickpea (*Cicer arietinum* L.). *Funct. Integr. Genomics* 14, 59–73. doi: 10.1007/s10142-014-0363-6

Waldman, A. J., Pechersky, Y., Wang, P., Wang, J. X., and Balskus, E. P. (2015). The cremeomycin biosynthetic gene cluster encodes a pathway for diazo formation. *Chembiochem* 16, 2172–2175. doi: 10.1002/cbic.201500407

Wang, J., Yu, Y., Tang, K., Liu, W., He, X., Huang, X., et al. (2010). Identification and analysis of the biosynthetic gene cluster encoding the thiopeptide antibiotic cyclothiazomycin in *Streptomyces hygroscopicus* 10-22. *Appl. Environ. Microbiol.* 76, 2335–2344. doi: 10.1128/AEM.01790-09

Ward, S. L., Hu, Z., Schirmer, A., Reid, R., Revill, W. P., Reeves, C. D., et al. (2004). Chalcomycin biosynthesis gene cluster from *Streptomyces bikiniensis*: novel features of an unusual ketolide produced through expression of the chm polyketide synthase in *Streptomyces fradiae*. *Antimicrob. Agents Chemother.* 48, 4703–4712. doi: 10.1128/AAC.48.12.4703-4712.2004

Wolpert, M., Heide, L., Kammerer, B., and Gust, B. (2008). Assembly and heterologous expression of the coumermycin A1 gene cluster and production of new derivatives by genetic engineering. *Chembiochem* 9, 603–612. doi: 10.1002/cbic.200700483

Yamanaka, K., Reynolds, K. A., Kersten, R. D., Ryan, K. S., Gonzalez, D. J., Nizet, V., et al. (2014). Direct cloning and refactoring of a silent lipopeptide biosynthetic gene cluster yields the antibiotic taromycin A. *Proc. Natl. Acad. Sci. U.S.A.* 111, 1957–1962. doi: 10.1073/pnas.1319584111

Yan, X., Probst, K., Linnenbrink, A., Arnold, M., Paululat, T., Zeeck, A., et al. (2012). Cloning and heterologous expression of three type II PKS gene clusters from *Streptomyces bottropensis*. *Chembiochem* 13, 224–230. doi: 10.1002/cbic.201100574

Yang, C., Huang, C., Zhang, W., Zhu, Y., and Zhang, C. (2015). Heterologous expression of fluostatin gene cluster leads to a bioactive heterodimer. *Org. Lett.* 17, 5324–5327. doi: 10.1021/acs.orglett.5b02683

Yin, J., Hoffmann, M., Bian, X., Tu, Q., Yan, F., Xia, L., et al. (2015). Direct cloning and heterologous expression of the salinomycin biosynthetic gene cluster from *Streptomyces albus* DSM41398 in *Streptomyces coelicolor* A3(2). *Sci. Rep.* 5:15081. doi: 10.1038/srep15081

Yin, S., Li, Z., Wang, X., Wang, H., Jia, X., Ai, G., et al. (2016). Heterologous expression of oxytetracycline biosynthetic gene cluster in *Streptomyces* venezuelae WVR2006 to improve production level and to alter fermentation process. *Appl. Microbiol. Biotechnol.* 100, 10563–10572. doi: 10.1007/s00253-016-7873-1

Ylihonko, K., Hakala, J., Kunnari, T., and Mantsala, P. (1996). Production of hybrid anthracycline antibiotics by heterologous expression of *Streptomyces nogalater* nogalamycin biosynthesis genes. *Microbiology* 142(Pt 8), 1965–1972. doi: 10.1099/13500872-142-8-1965

Young, T. S., and Walsh, C. T. (2011). Identification of the thiazolyl peptide GE37468 gene cluster from *Streptomyces* ATCC 55365 and heterologous expression in *Streptomyces lividans*. *Proc. Natl. Acad. Sci. U.S.A.* 108, 13053–13058. doi: 10.1073/pnas.1110435108

Zaburannyi, N., Rabyk, M., Ostash, B., Fedorenko, V., and Luzhetskyy, A. (2014). Insights into naturally minimised *Streptomyces albus* J1074 genome. *BMC Genomics* 15:97. doi: 10.1186/1471-2164-15-97

Zettler, J., Xia, H., Burkard, N., Kulik, A., Grond, S., Heide, L., et al. (2014). New aminocoumarins from the rare actinomycete *Catenulispora acidiphila* DSM 44928: identification, structure elucidation, and heterologous production. *Chembiochem* 15, 612–621. doi: 10.1002/cbic.201300712

Zhang, G., Zhang, H., Li, S., Xiao, J., Zhang, G., Zhu, Y., et al. (2012). Characterization of the amicetin biosynthesis gene cluster from *Streptomyces vinaceusdrappus* NRRL 2363 implicates two alternative strategies for amide bond formation. *Appl. Environ. Microbiol.* 78, 2393–2401. doi: 10.1128/AEM.07185-11

Zhang, Y., Huang, H., Chen, Q., Luo, M., Sun, A., Song, Y., et al. (2013). Identification of the grincamycin gene cluster unveils divergent roles for GcnQ in different hosts, tailoring the L-rhodinose moiety. *Org. Lett.* 15, 3254–3257. doi: 10.1021/ol401253p

Zhu, Y., Fu, P., Lin, Q., Zhang, G., Zhang, H., Li, S., et al. (2012). Identification of caerulomycin A gene cluster implicates a tailoring amidohydrolase. *Org. Lett.* 14, 2666–2669. doi: 10.1021/ol300589r

Conflict of Interest Statement: The authors declare that the research was conducted in the absence of any commercial or financial relationships that could be construed as a potential conflict of interest.

Copyright © 2017 Nah, Pyeon, Kang, Choi and Kim. This is an open-access article distributed under the terms of the Creative Commons Attribution License (CC BY). The use, distribution or reproduction in other forums is permitted, provided the original author(s) or licensor are credited and that the original publication in this journal is cited, in accordance with accepted academic practice. No use, distribution or reproduction is permitted which does not comply with these terms.

frontiers in Microbiology

ORIGINAL RESEARCH
published: 07 April 2017
doi: 10.3389/fmicb.2017.00517

Increased Biological Activity of *Aneurinibacillus migulanus* Strains Correlates with the Production of New Gramicidin Secondary Metabolites

*Faizah N. Alenezi[1,2], Imen Rekik[2], Ali Chenari Bouket[2,3], Lenka Luptakova[2,4], Hedda J. Weitz[1], Mostafa E. Rateb[5], Marcel Jaspars[6], Stephen Woodward[1] and Lassaad Belbahri[2,7]**

[1] Institute of Biological and Environmental Sciences, University of Aberdeen, Aberdeen, UK, [2] NextBiotech, Rue Ali Belhouane, Agareb, Tunisia, [3] Graduate School of Life and Environmental Sciences, Osaka Prefecture University, Sakai, Japan, [4] Department of Biology and Genetics, Institute of Biology, Zoology and Radiobiology, University of Veterinary Medicine and Pharmacy, Košice, Slovakia, [5] School of Science and Sport, University of the West of Scotland, Paisley, UK, [6] Marine Biodiscovery Centre, Department of Chemistry, University of Aberdeen, Aberdeen, UK, [7] Laboratory of Soil Biology, University of Neuchatel, Neuchatel, Switzerland

OPEN ACCESS

Edited by:
Peter Neubauer,
Technische Universität Berlin,
Germany

Reviewed by:
Sanna Sillankorva,
University of Minho, Portugal
Jian Li,
University of Northwestern – St. Paul,
USA
Maria Lurdes Inacio,
Instituto Nacional de Investigação
Agrária e Veterinária, Portugal

***Correspondence:**
Lassaad Belbahri
lassaad.belbahri@unine.ch

Specialty section:
This article was submitted to
Microbiotechnology, Ecotoxicology
and Bioremediation,
a section of the journal
Frontiers in Microbiology

Received: 08 January 2017
Accepted: 13 March 2017
Published: 07 April 2017

Citation:
Alenezi FN, Rekik I,
Chenari Bouket A, Luptakova L,
Weitz HJ, Rateb ME, Jaspars M,
Woodward S and Belbahri L (2017)
Increased Biological Activity
of Aneurinibacillus migulanus Strains
Correlates with the Production of New
Gramicidin Secondary Metabolites.
Front. Microbiol. 8:517.
doi: 10.3389/fmicb.2017.00517

The soil-borne gram-positive bacteria *Aneurinibacillus migulanus* strain *Nagano* shows considerable potential as a biocontrol agent against plant diseases. In contrast, *A. migulanus NCTC 7096* proved less effective for inhibition of plant pathogens. *Nagano* strain exerts biocontrol activity against some gram-positive and gram-negative bacteria, fungi and oomycetes through the production of gramicidin S (GS). Apart from the antibiotic effects, GS increases the rate of evaporation from the plant surface, reducing periods of surface wetness and thereby indirectly inhibiting spore germination. To elucidate the molecular basis of differential biocontrol abilities of *Nagano* and *NCTC 7096*, we compared GS production and biosurfactant secretion in addition to genome mining of the genomes. Our results proved that: (i) Using oil spreading, blood agar lysis, surface tension and tomato leaves wetness assays, *Nagano* showed increased biosurfactant secretion in comparison with *NCTC 7096*, (ii) Genome mining indicated the presence of GS genes in both *Nagano* and *NCTC 7096* with two amino acid units difference between the strains: T342I and P419S. Using 3D models and the DUET server, T342I and P419S were predicted to decrease the stability of the *NCTC 7096* GS synthase, (iii) *Nagano* produced two additional GS-like molecules GS-1155 (molecular weight 1155) and GS-1169 (molecular weight 1169), where one or two ornithine residues replace lysine in the peptide. There was also a negative correlation between surface tension and the quantity of GS-1169 present in *Nagano*, and (iv) the *Nagano* genome had a full protein network of exopolysaccharide biosynthesis in contrast to *NCTC 7096* which lacked the first enzyme of the network. *NCTC 7096* is unable to form biofilms as observed for *Nagano*. Different molecular layers, mainly gramicidin secondary metabolite production, account for differential biocontrol abilities of *Nagano* and

NCTC 7096. This work highlighted the basis of differential biological control abilities between strains belonging to the same species and demonstrates techniques useful to the screening of effective biocontrol strains for environmentally friendly secondary metabolites that can be used to manage plant pathogens in the field.

Keywords: secondary metabolism, bioinformatics, genome mining, *Aneurinibacillus migulanus*, biocontrol bacteria, gramicidin S, biosurfactant

INTRODUCTION

Plant diseases are responsible for many economic losses in landscape, agriculture and forest settings through negative impacts on yields, quality of crops and visual amenity. Huge losses can occur in crops, in certain instances between 25 and 100% (Ghai et al., 2007). Affected food may also contain pathogen-produced toxins that can cause poisoning or death in humans and other animals. Nowadays, the application of widely used xenobiotic chemicals (pesticides) to crops is expensive, potentially resulting in toxicity to other biota; moreover, chemical residues may present a hazard to animals and humans consuming the food (Yánez-Mendizábal et al., 2011). Producing pesticide-free food and maintaining a healthy environment are the main reasons to promote the development of environmentally sound approaches of disease control. Therefore, biological control agents (BCAs) that can suppress pathogen activities with less damage to the wider environment are increasingly used in agriculture (Roberts and Lohrke, 2003; Mefteh et al., 2017).

Numerous *Bacillus* species have been tested as BCAs against plant pathogens with some showing promising activities in trials (Ghai et al., 2007; Jamalizadeh et al., 2008; Chandel et al., 2010; Yánez-Mendizábal et al., 2011). BCAs are antagonistic to plant pathogens through antibiosis, competition for nutrients and infection sites on the plant surface, hyperparasitism and by induction of host resistance (Kim et al., 2008; Chandel et al., 2010; Alenezi et al., 2016b). An additional advantage of *Bacillus* species is their ability to produce highly resilient endospores during unfavorable environmental conditions, allowing efficient storage of *Bacillus*-based BCA preparations (Piret and Demain, 1982). Biofilm formation, the predominant lifestyle of many bacteria in natural environments, is well known in *Bacillus* spp. and is increasingly studied in closely related genera to understand the development of this life strategy. Bacteria within a biofilm resist a wide range of environmental stresses mainly through the action of the extracellular matrix of the biofilm, generally composed of exopolysaccharide (Mielich-Süss and Lopez, 2015). Biofilm formation is considered an important means of attachment to plant roots or other plant surfaces such as leaves, that correlates with the protection of plants against plant disease development (Beauregard et al., 2013; Yaron and Römling, 2014). Better knowledge of the mechanisms of action of BCAs is urgently required to improve the efficiency of these methods in combating plant diseases in the field.

The soil-borne species, *Aneurinibacillus migulanus* (syn. *Bacillus brevis*; *Brevibacillus brevis*) controls plant disease development through production of the cyclic peptide GS (Edwards and Seddon, 2001; Belbahri et al., 2015). *A. migulanus* strain *Nagano* shows considerable potential as a biocontrol agent (Edwards and Seddon, 2001; Schmitt and Seddon, 2005; Chandel et al., 2010; Alenezi et al., 2016a). Apart from the direct antibiosis effect, *A. migulanus Nagano* GS biosurfactant activity increases the rate of evaporation from the plant surface, reducing periods of surface wetness and thereby indirectly inhibiting spore germination (Seddon et al., 1997, 2000). The combination of the direct action of GS on pathogens and biosurfactant reduction of periods of surface wetness in a single BCA increases the potential for biocontrol activity and has been considered as an advantageous approach to managing disease, avoiding the development of pathogen resistance to a control agent, common when pesticides are being used (Seddon et al., 2000; Schmitt and Seddon, 2005). Strain-level diversity in the biocontrol ability of *A. migulanus* has been described between strains *Nagano* and *NCTC 7096* (Alenezi et al., 2016b). The secondary metabolite arsenal was also shown to be different between the two strains, highlighting the importance of unique genes in the pan genome of *A. migulanus* strains (Alenezi et al., 2016b). Therefore, the identification of molecular determinants that could account for differential biocontrol ability is crucial to deliver efficient BCAs.

The aim of this work was to compare the biocontrol abilities of *A. migulanus* strains *Nagano* and *NCTC 7096* and examine the roles of GS production and biosurfactant secretion in the two strains in order to unravel the mechanisms behind these differential biocontrol abilities.

MATERIALS AND METHODS

Growth Conditions for Bacteria

Two strains of *A. migulanus* were used in this work: *Nagano* obtained from the culture collection of the Institute of Biological and Environmental Sciences (University of Aberdeen) and *NCTC 7096* obtained from the National Collection of Type Cultures (NCTC, Porton Down, Salisbury, UK). Both strains were maintained on tryptone soya agar (TSA; Oxoid, Basingstoke, Hants, UK). For the production of cell suspensions, cells from these cultures were used to inoculate 20 mL of tryptone soya broth (TSB; Oxoid, Basingstoke, Hants, UK) and incubated at 37°C for 16 h, with shaking at 180 rpm.

Growth Curves for Bacteria

One milliliter of an overnight culture of the bacterial strain studied was transferred to 100 mL TSB in 250 mL Erlenmeyer flasks and incubated at 37°C, with shaking at 180 rpm. One milliliter of the resulting culture was sampled periodically for optical density measurement (OD) at 600 nm using a

spectrophotometer (CECIL, CE1010, Cecil Instruments, UK) and to estimate the numbers of colony forming units (CFU). CFU enumeration was carried out on TSA after serial dilution in sterile 1/4 strength Ringer's solution. Ten microliter of each dilution was placed on TSA in triplicate and incubated at 37°C for 3 days. After appearance of bacterial colonies, CFU were counted.

Culture Conditions for Fungi and Oomycetes

Fusarium oxysporum f. sp. *lycopersici SW1* (obtained from Dr. Steve Rossall, University of Nottingham), *Heterobasidion annosum O27_21* (isolated from a severely infected Sitka spruce in Bennachie forest, Aberdeenshire, Scotland: 57°162433N; 2°302573W), *Phytophthora plurivora MKDF-179* and *Rhizoctonia solani MB 140731* were from the culture collection of the Institute of Biological and Environmental Sciences (University of Aberdeen). *Pythium ultimum DSM 62987* and *Botrytis cinerea DSM 4709* were obtained from the German Collection of Microorganisms and Cell Cultures (DSMZ). All strains were maintained on potato dextrose agar (PDA; Oxoid, Basingstoke, Hants, UK) at 25°C for 10 days, with routine sub culturing at 15 days intervals.

Inhibition of *Botrytis cinerea* DSM 4709 Spore Germination

Botrytis cinerea DSM 4709 was cultured on malt extract agar (MEA; Oxoid, Hants, UK) and incubated at 25°C for 28 days. Ten milliliter of sterile distilled water containing 0.025% Tween 80 was poured into the *B. cinerea* culture and a sterile loop used to gently agitate the colony surface to dislodge conidia. The suspension was passed through sterilized nylon mesh (50 μm) to eliminate mycelial fragments (Govrin and Levine, 2000). The spore density was determined using replicate haemocytometer counts and adjusted to 1×10^6 per mL.

Spore germination was tested with increasing concentrations (0, 1, 5, 10, 20, 40, 50, 80, 100, 150, 200, 250, 300, 350 μM) of commercial GS hydrochloride (Sigma-Aldrich, UK), prepared according to Edwards and Seddon (2001). Different concentrations of washed cells of both *A. migulanus Nagano* and *NCTC 7096* were tested against fungal spores. A range of washed bacterial cell concentrations of both *A. migulanus Nagano* and *NCTC 7096* were prepared (10^2, 10^3, 10^4, 10^5, 10^6 cell/ml). Five hundred microliter *B. cinerea* spore suspension were added to 500 μL of the different concentrations of GS tested or washed bacterial cells of *A. migulanus Nagano* and *NCTC 7096* in 1.5 mL Eppendorf tubes, followed by incubation at 25°C for 24 h. Each GS concentration or washed bacteria cell suspension was tested in triplicate. Percentage spore germination was calculated by counting 100 (germinated and non-germinated) *B. cinerea* spores (Edwards and Seddon, 2001).

Co-cultivation of *A. migulanus* and Plant Pathogens

A dual culture method was used to test the antifungal activity of *A. migulanus Nagano* and *NCTC 7096* against a range of plant pathogens. Bacterial suspension was streaked onto the left side of PDA in a 9 cm diameter Petri plate and incubated at 37°C for 3 days. A disk of *F. oxysporum* f. sp. *lycopersici SW1*, *Heterobasidion annosum O27_21*, *Phytophthora plurivora MKDF-179*, *Rhizoctonia solani MB 140731*, *Botrytis cinerea DSM 4709* or *Pythium ultimum DSM 62987* on PDA, cut using a 6 mm diameter Cork borer, was placed on the right hand side of the plate, and the dual cultures incubated in darkness at 25°C for 10 days. Fungal growth was measured at 24 h intervals; inhibition of fungal growth (%) by the bacteria was calculated using the formula: $\left(C - T/C\right) \times 100$, where C is the diameter growth of the pathogen in control cultures, and T the diameter growth of the pathogen in dual cultures with the bacteria.

Effects of *A. migulanus* Treatment on *B. cinerea* Disease Severity on Tomato Leaves

One milliliter of overnight culture of *A. migulanus Nagano* or *A. migulanus NCTC 7096* was transferred to 100 mL TSB in 250 ml conical flasks and incubated for 3 days at 37°C with shaking at 180 rpm. The bacterial culture was harvested by centrifugation at 3500 rpm for 30 min at 4°C. The supernatant was discarded and the cells washed by replacing the supernatant with 100 mL sterile distilled water. The centrifugation and resuspension steps were repeated three times.

Sterilized Whatman No.1, 140 mm diameter filter paper (Whatman, UK) was placed in the bottom of a 145 mm diameter Petri dish and moistened with sterile distilled water. Second or third true leaves of tomato cultivar Craigella were removed from 12-week-old plants and the terminal leaflet, plus two additional leaflets excised before immersing in 100 mL of washed bacterial cells of *A. migulanus Nagano* or *NCTC 7096* for 3 min. Leaf portions were transferred to the 145 mm diameter Petri dishes and left in the laminar flow cabinet at 25°C for 24 h to dry. Six drops (5 μL each) of *B. cinerea DSM4709* spore suspension were placed on the abaxial surface of each leaflet and the Petri dishes incubated at (25°C, 9 h daylight) for 5 days (Nafisi et al., 2014). Ten Petri dishes containing leaflets were treated with sterile distilled water as a negative control; a further 10 dishes containing leaflets were initially treated with sterile distilled water before inoculating with *B. cinerea DSM4709* spore suspension as a positive control. Disease symptoms were recorded 7 days after inoculation using a categorical scale, where 0 = healthy and 5 = presence of severe symptoms (**Figure 1B**).

Screening for Biosurfactant Activity

Surface Tension Method

Surface tension measurements were carried out on a White's Tensiometer using the Du Nouy ring method (Pornsunthorntawee et al., 2008). Four milliliter *A. migulanus Nagano* or *A. migulanus NCTC 7096* bacterial suspension from a 16 h culture was transferred to 400 mL TSB in 1 L conical flasks and incubated at 37°C, with shaking at 180 rpm for 48 h. One milliliter of the culture was centrifuged for 2 min at 10,000 × *g* in a microcentrifuge and the cell free supernatant used to measure surface tension. One milliliter TSB or cell free supernatant was placed in a 5 cm diameter concave glass dish and allowed to

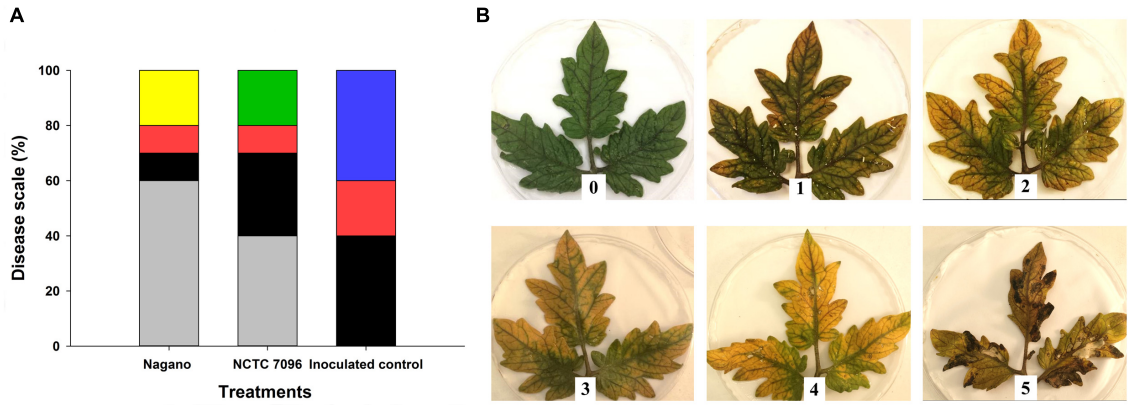


FIGURE 1 | Severity of *Botrytis cinerea* infection on detached tomato leaves treated with *A. migulanus Nagano* or *NCTC 7096*. (A) Disease symptoms on detached leaves following treatment with *A. migulanus*. Disease scale is represented as follows: (■) 0, (■) 1, (■) 2, (■) 3, (■) 4 and (■) 5. Negative control detached tomato leaves were treated with sterilized distilled water. Each treatment was replicated 10 times. **(B)** 0–5 visual scale used to rate the severity of *B. cinerea* infection on detached tomato leaves.

equilibrate for 5 min. Pure water and TSB were used as controls. A thin ring was immersed into the sample and pulled out, the maximum force required to remove the ring was recorded at the instant the ring separated from the surface of the liquid, and expressed in mNm^{-1}. Three replicate measurements of surface tension were taken from each culture.

Blood Agar Method

Ten milliliter fluid was removed from *A. migulanus Nagano* or *A. migulanus NCTC 7096* cultures after 16 h incubation, and three drops placed on sheep blood agar (Oxoid, UK) containing 7% (v/v) sheep blood in 9 cm diameter Petri dishes. Following incubation for 48 h at 37°C, dishes were inspected visually for zones of clearing around the bacterial colonies. Clearing zones were considered to indicate biosurfactant production and GS haemolytic activity (Youssef et al., 2004; Plaza et al., 2006; Jazeh et al., 2012).

Oil Spreading Method

Twenty-five milliliter distilled water was added to a 9-cm diameter Petri dish and 10 μL crude oil applied to the surface of the water. Ten microliter of *A. migulanus Nagano* or *A. migulanus NCTC 7096* bacterial suspension from a 48 h old culture (37°C, 180 rpm) was placed gently on the surface of the oil (Morikawa et al., 2000; Youssef et al., 2004). The diameter of the clear zone on the oil surface was measured. All tests were made in triplicate.

Calibration and Quantification of Gramicidin S by HPLC

Preparation of Gramicidin S Standard Curve

Gramicidin S hydrochloride (Sigma-Aldrich; 1 mM) was prepared by dissolving commercial GS in 10 mL sterile distilled water and passing the solution through a 0.22 μm membrane filter (Millipore, UK). This stock solution was used to prepare the following concentrations of GS: 10, 30, 50, 100, 300, 500 and 700 μM. One milliliter of each concentration was submitted to LC-MS analysis (see below) and peak areas obtained by the total ion chromatogram (TIC) calculated. Samples were analyzed in triplicate, and a calibration curve prepared.

Extraction of Gramicidin S from *A. migulanus* Cultures

One milliliter of overnight cultures of *A. migulanus Nagano* or *NCTC 7096* was transferred to 100 mL TSB in 250 mL Erlenmeyer flasks and incubated at 37°C, with shaking at 180 rpm for 48 h. One milliliter of this culture was centrifuged at 3000 × *g* for 10 min and the supernatant discarded. One milliliter of absolute ethanol was added to the cells, the tubes shaken, covered with a marble to reduce ethanol evaporation and placed in water bath at 70°C for 15 min. After cooling, the tubes were centrifuged again at 3000 × *g* for 10 min. One milliliter of ethanol extract was transferred to a fresh tube and the ethanol evaporated to dryness at room temperature by rotary evaporation at 45°C. The residue was re-dissolved in 1 mL methanol prior to LC-MS analysis. GS production was quantified 0, 12, 24, 36 and 48 h after sub-culture.

LC-MS Analysis

HPLC analyses were carried out on a reversed-phase column (Pursuit XRs ULTRA 2.8, C18, 100 mm × 2 mm, Agilent Technologies, UK). Sample injection volume was 20 μL. The column temperature was set at 30°C. Mobile phases consisted of 0.1% formic acid in water (A) and 0.1% formic acid in MeOH (B). A gradient program was used for separation at a flow rate of 1 mL/min. Initial composition of the mobile phases was 100% solvent A, with a gradient to 100% solvent B over 20 min, hold on 100% solvent B for 5 min. Drying gas flow rate was 1 mL/min at 320°C. MS was operated in the positive ion mode in a mass range of *m/z* 100–2000. High resolution mass spectral data were obtained on a Thermo Instruments ESI-MS system (LTQ XL/LTQ Orbitrap Discovery, UK) connected to a Thermo Instruments HPLC system (Accela PDA detector, Accela PDA autosampler and Accela Pump). The percentage of each gramicidin in both strains was calculated and compared

to commercial GS using the standard curve. All concentrations calculated were within the linear region of the calibration curve.

Chromatographic Purification of Exopolysaccharides and Gramicidin

After bacterial fermentation, *A. migulanus Nagano* culture was centrifuged at 3000 × *g* for 10 min and the supernatant discarded. The cell mass was extracted twice in absolute ethanol, the extracts combined and evaporated *in vacuo* to dryness. The dry *A. migulanus Nagano* bacterial extract was dissolved in 80% aqueous MeOH and loaded on a 40+M reversed phase C18 flash column connected to Biotage SP1 flash system and eluted in a gradient of 10–100% MeOH over 30 min followed by isocratic elution (100% MeOH) for 10 min at a 40 mL/min flow rate, using UV detector at 250 and 220 nm as monitoring and collection wavelengths.

Genome Sequence and Genome Mining of *A. migulanus* Strains *Nagano* and *NCTC 7096*

All genome sequencing experiments were performed at the iGE3 genomics platform of the University of Geneva[1]. The annotated draft genomes of *A. migulanus Nagano* and *NCTC 7096* were previously reported (Alenezi et al., 2015a,b). The nucleotide as well as the amino acids sequences of the whole genomes and the deduced coding sequences were retrieved from the GenBank DNA database for *A. migulanus Nagano* (accession no. JYBN00000000.1) and *A. migulanus NCTC 7096* (accession no. JYBO00000000.1) and detailed gene content comparisons performed manually (**Supplementary Table S1**). The bioinformatic tools Spine and AGEnt (Ozer et al., 2014) as implemented in Omic tools website, were used to estimate the core genome and unique genes of *A. migulanus* (Henry et al., 2014).

Identification and Annotation of Gramicidin Synthase Genes in *A. migulanus* Genomes

Genes related to GS biosynthesis, were identified using CLC software with appropriate template sequences. The identified genes were annotated by BLASTX search of UniProtKB/TrEMBL, with an *E*-value < 10−5. Three dimensional models of gramicidin synthase genes were determined using sequences of GS synthases of both *A. migulanus Nagano* and *NCTC 7096* as an input to the Swiss model server[2]. Stability of GS synthases was estimated using 3D models and the DUET server (Pires et al., 2014) with default parameters.

Statistical Analysis

Data were analyzed using IBM SPSS statistics by one-way analysis of variance (ANOVA) and independent-samples *T*-test. The groups were compared using a *post hoc* Tukey's HSD test. The level of significance used for all statistical tests was 5% ($p < 0.05$).

[1]http://www.ige3.unige.ch/genomics-platform.php

[2]http://swissmodel.expasy.org/

RESULTS

Effect of *A. migulanus* on *B. cinerea* Symptoms in Tomato

Treatments with *A. migulanus Nagano* and *NCTC 7096* had significant effects on the incidence of gray mold on excised tomato leaves after 5 days of incubation ($p < 0.05$, **Figures 1A,B**). Forty percent of positive control leaves, inoculated with the pathogen, but not pre-treated with the bacteria, displayed maximum disease severity (**Figure 1A**). Disease severity was less on leaves treated with *Nagano* and *NCTC 7096*, with the *Nagano* treatment showing the greatest reduction in disease. Disease incidence and severity on leaves treated with *A. migulanus NCTC 7096* was significantly greater than that observed on *A. migulanus Nagano* treated foliage (**Figure 1A**). The highest disease severity on *Nagano* treated foliage was 3, compared with 4 on *NCTC 7096* treated leaves (**Figure 1A**).

Growth Characteristics of *A. migulanus Nagano* and *NCTC 7096*

Aneurinibacillus migulanus Nagano and *NCTC 7096* grew rapidly in TSB, exponential growth began within 2 h of sub-culture. The maximum number of CFU was attained after incubation for 48 h (data not shown), with a density of 10^8 mL^{-1}. Both CFU counts and OD measurements indicated that cultures entered the stationary phase at approximately 8 h after sub-culturing. There was no significant difference between growth of the *Nagano* and *NCTC 7096* strains ($p > 0.05$).

Comparison of Biosurfactant Activity of *A. migulanus* Strains

Blood Agar and Oil Spreading Methods

Although both strains were able to spread oil on the surface of water, the diameter of oil spread was greater for *A. migulanus Nagano* than for *NCTC 7096* ($p = 0.00$; two-sample *t*-test). No spreading of the oil occurred when TSB was applied (**Figures 2A,B**). Culture fluids of *A. migulanus Nagano* hydrolyzed red blood cells within 48 h incubation, whereas those of *NCTC 7096* did not (**Figure 2C**).

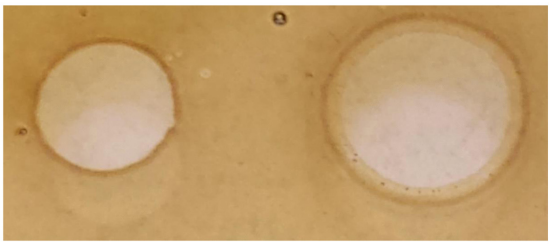
Effect on Surface Tension

For *A. migulanus Nagano*, surface tension of the culture fluids began to decline 5 h after sub-culture (**Figure 3A**), stabilizing at approximately 34 mNm^{-1} after 12–24 h growth. In contrast, surface tension of the culture fluids of *NCTC 7096* strain did not begin to decline until 12 h after sub-culture and the final reduction, to approximately 44 mNm^{-1}, was significantly less than that of *Nagano* culture fluids at the same time ($p < 0.05$). The *A. migulanus Nagano* dried significantly faster on the tomato leaf surface than *A. migulanus NCTC 7096* as shown in **Figure 3B**.

Genome Mining of Gramicidin Synthase Genes in *A. migulanus*

Genome mining showed that GS genes occurred in both *Nagano* and *NCTC 7096* with two amino acid changes between the gramicidin synthase sequences of the two strains, designated

A



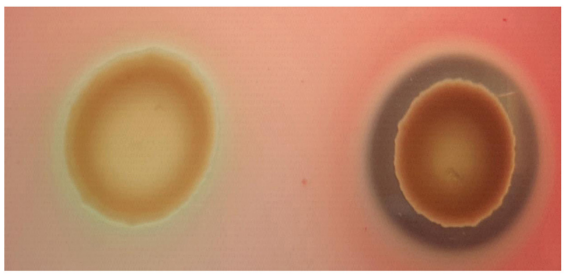
NCTC 7096 Nagano

B

Method	*A. migulanus* NCTC 7096	*A. migulanus* Nagano
Oil spreading	7.2±0.3	16.4±0.9

[b] Results for oil spreading (mm) represent mean ± standard error of at least three replicates

C



NCTC 7096 Nagano

FIGURE 2 | *Aneurinibacillus migulanus Nagano* and *NCTC 7096* biosurfactant production estimated based on lysis of hemoglobin and spread of oil assays. (A) Oil spreading assay. **(B)** Hemoglobin lysis assay. **(C)** Quantification of oil spreading abilities of *Nagano* and *NCTC 7096*.

T342I and P419S. Using 3D models and the DUET server, the substitutions T342I and P419S were predicted to decrease the stability of the *A. migulanus NCTC 7096* GS synthase protein (**Supplementary Figures S1–S3**). Detection of gramicidin in both strains showed that they are equally able to produce equivalent amount (**Figure 4**).

Effect of GS on *Botrytis cinerea* Spore Germination

In the absence of GS, 74% of *B. cinerea* spores germinated and formed branched, septate hyphae within 24 h of treatment. Germination of *B. cinerea* spores was markedly reduced at 10 μM GS, and complete inhibition of germination occurred at approximately 100 μM GS (**Figure 5A**). In the presence of 10 μM GS, the germinated conidia produced short, swollen germ tubes (data not shown). Washed *A. migulanus* cells were also effective in inhibiting germination of *B. cinerea* spores (**Figure 5B**): *Nagano* washed cells were more effective than *NCTC 7096* in inhibiting *B. cinerea* spore germination.

Structures of Gramicidins from *A. migulanus Nagano* and *NCTC 7096*

Gramicidins are linear pentadecapeptides produced by *Brevibacillus parabrevis* ATCC 10068 and 8185 or DSMZ 5618 and DSMZ 362. Genome mining proved that both *A. migulanus Nagano* and *NCTC 7096* produce a molecular species matching the structure of commercial GS, hereafter designated gramicidin S-1141 (**Figure 6B**). *A. migulanus Nagano* produced two additional molecular species, gramicidin S-1155 and gramicidin S-1169 (**Figure 6A**). In addition, the different molecular species of GS were confirmed by MS^n analysis (**Supplementary Tables S1, S2**) and simulation of their isotope patterns compared to those acquired using Thermo Xcalibur 3.1 software (**Figure 6C** and **Supplementary Table S3**).

Comparison of GS Production by *A. migulanus* Nagano and NCTC 7096

Concentrations of each GS produced by *A. migulanus Nagano* and *NCTC 7096*, and in the commercial GS-1141 preparation are shown in **Figure 7**. The commercial preparation of GS contained 95.16% GS-1141, along with 4.40% GS-1155 and 0.44% GS-1169. In *A. migulanus NCTC 7096*, GS concentration increased rapidly in cultures between sub-culture and 12 h later (**Figure 7B**), after which the concentration remained stable. Differences in GS-1141 production between *Nagano* and *NCTC 7096* were not significant ($P > 0.05$). A Pearson test showed a strong positive association (0.995; $p < 0.05$) between the number of bacterial cells and concentration of GS-1141. Changes in the percentage of each gramicidin in the two strains are shown in **Figures 7A,B**.

Correlation between Surface Tension and Production of Gramicidin-1169

A negative correlation was found between surface tension and the amount of GS-1169 present in culture fluids over time (**Figure 7B**). Pearson correlation tests suggested that with *A. migulanus Nagano* a strong negative relationship between reduction in surface tension and increasing production of GS-1169 ($p = 0.015$); no relationships between surface tension and concentrations of GS-1155 or GS-1141 was found ($p > 0.05$).

Protein Interaction Network of the Exopolysaccharide Biosynthetic Pathway

Ten genes showing strong homology with bacterial genes responsible for exopolysaccharide biosynthesis and biofilm formation abilities were identified in the strain *Nagano*. The genes were envisioned into an interaction network using STRING and GeneMANIA server (**Supplementary Figure S4A**). The unique genes of *A. migulanus* strains *Nagano* and *NCTC 7096* showed the presence of exopolysaccharide biosynthesis polyprenyl glycosylphosphotransferase enzyme in *Nagano* and its absence in *NCTC 7096* (**Supplementary Table S4**).

Chromatographic Purification of Exopolysaccharides and Gramicidin

After fermentation and bacterial extraction, the total extract was injected to the Biotage SP1 flash reversed phase (RP-C18) column and exopolysaccharides extracted as the polar earlier fraction, gramicidins as the non-polar later eluting fraction (**Supplementary Figure S4B**). Due to structural similarity, multiple attempts to separate the GS analogs by HPLC using different columns and varied solvent systems under different

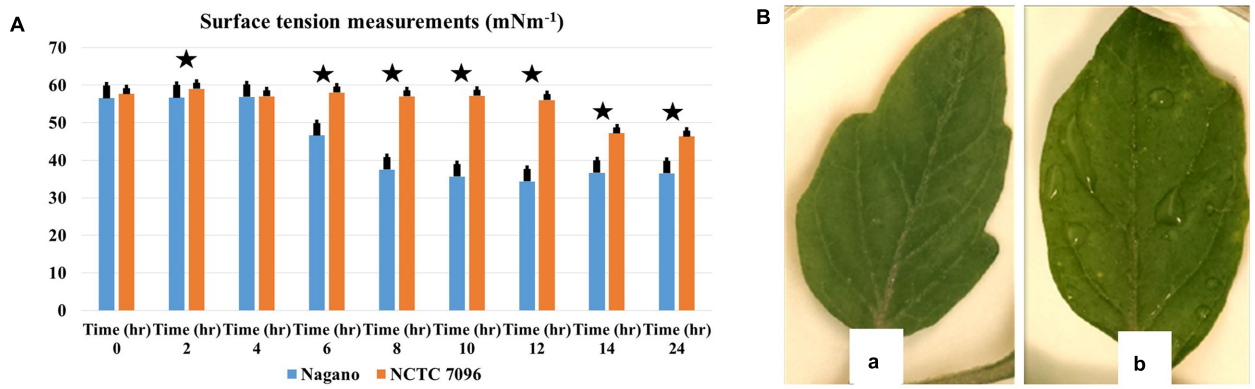


FIGURE 3 | *Aneurinibacillus migulanus* biosurfactant effects on surface tension of culture fluids and wetness of tomato leaves. (A) Time course of changes in surface tension of (■) *A. migulanus Nagano* and (■) *A. migulanus NCTC 7096* culture fluids. Vertical bars represent standard errors of the means, ($N = 3$). **(B)** Effects of *A. migulanus Nagano* (a) and *NCTC 7096* (b) on surface wetness of tomato leaves. Data presents mean ± standard error. Bars labeled with asterisk are significantly different among the treatments at $P < 0.05$ using ANOVA analysis.

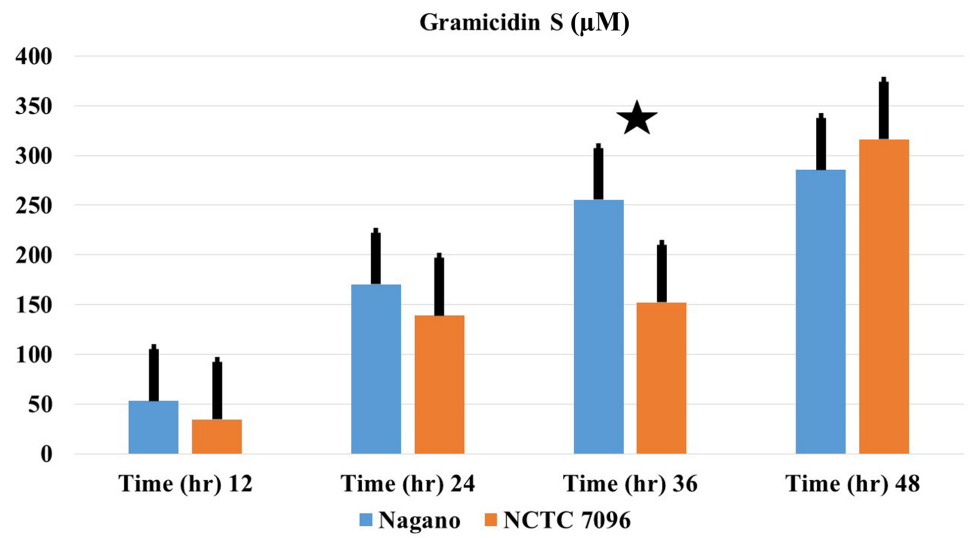


FIGURE 4 | Production of GS-1141 by *A. migulanus Nagano* (■) and *A. migulanus NCTC 7096* (■). Vertical bars represent standard errors of the means, ($N = 3$). Data presents mean ± standard error. Bars labeled with asterisk are significantly different among the treatments at $P < 0.05$ using ANOVA analysis.

conditions were not successful. The purity of the acquired fractions was confirmed by LC-MS analysis before use in biological screening.

Biofilm Formation by *A. migulanus*

Aneurinibacillus migulanus Nagano formed biofilms in TSB in 12 well plates and attached efficiently the plant surface around *B. cinerea* spores, whereas *NCTC 7096* did not (**Supplementary Figure S4C**).

DISCUSSION

Using *in vitro* assays, *A. migulanus* proved effective against various plant pathogens known to cause serious diseases, such as *F. oxysporum*, *B. cinerea* and Oomycete species (Alenezi et al., 2016b). Our results confirmed previous findings suggesting that *A. migulanus Nagano* has potential as a BCA against plant diseases (Edwards and Seddon, 2001; Schmitt and Seddon, 2005; Chandel et al., 2010; Alenezi et al., 2016a). These results indicated clearly that selection of an appropriate strain of *A. migulanus* for use as a BCA is crucial in obtaining successful disease management. In the present study, inhibition of pathogen growth by *A. migulanus Nagano* was greater than that in dual cultures with *A. migulanus NCTC 7096*. Moreover, *A. migulanus Nagano* proved more effective than *NCTC 7096* in reducing the severity of gray mold caused by *B. cinerea* on inoculated tomato leaves. As these two strains of *A. migulanus* grew at a similar rate, factors other than growth of the two strains were clearly responsible for the differences in the biocontrol

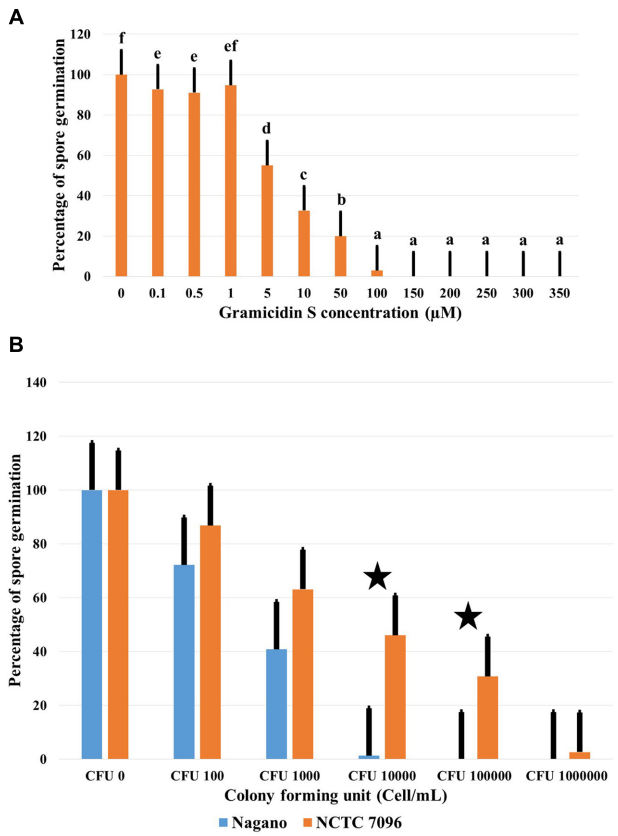


FIGURE 5 | Effect of commercial GS and *A. migulanus* cells on *B. cinerea* conidiospore germination. (A) Effect of increasing GS concentrations on germination of *B. cinerea* DSM 4709 spores after 24 h exposure to the treatment. Vertical bars represent standard errors of the means of three independent replicates. Data presents mean ± standard error. Bars labeled with different letters are significantly different among the treatments at $P < 0.05$ using Tukey's HSD test. In each bar group, bars labeled with the same letter are not significantly different from each other according to Tukey's HSD at $p < 0.05$. **(B)** Reduction of *B. cinerea* DSM 4709 spore germination (%) caused by washed cells of *A. migulanus* (■) *Nagano* or (■) *NCTC 7096*. Bars labeled with asterisk are significantly different among the treatments at $P < 0.05$ using ANOVA analysis.

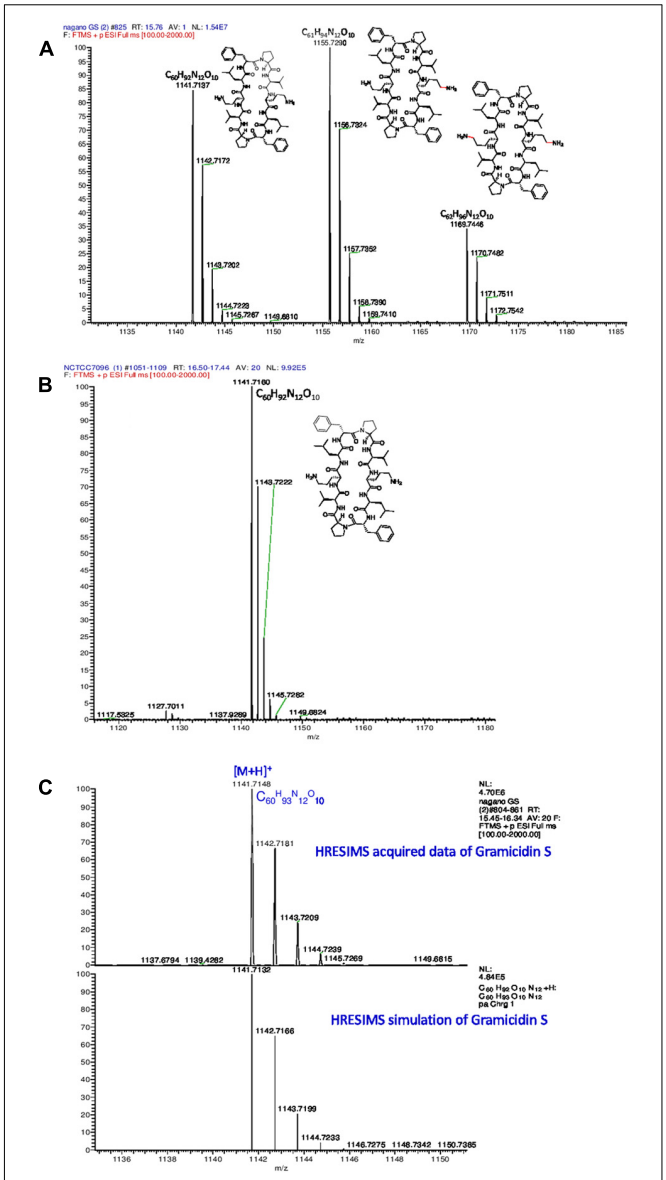


FIGURE 6 | High resolution electrospray ionisation mass spectrometry (HRESIMS) analysis of gramicidin S molecular species from (A) *A. migulanus Nagano*; **(B)** *A. migulanus NCTC 7096*; **(C)** Analysis of gramicidin S-1141 and its simulated isotope pattern.

potential (Data not shown). Since all studies of the biocontrol potential of *A. migulanus* have been conducted using strain *Nagano* (Edwards and Seddon, 2001; Schmitt and Seddon, 2005; Chandel et al., 2010), the present work highlighted a strain level biocontrol ability in *A. migulanus*, confirming the results of Alenezi et al. (2016b). It was previously suggested that the biocontrol potential of *A. migulanus Nagano* was due to the production of GS (Seddon et al., 1997), along with its associated biosurfactant activity, acting at the plant surface (Seddon et al., 1997, 2000). In the present work, GS production by the two strains of *A. migulanus* was demonstrated and quantified using liquid chromatography coupled to high resolution electrospray ionisation mass spectrometry (LC-HRESIMS). There was no difference in the quantities of GS-1141 produced by the two strains but *Nagano* exhibited higher biosurfactant activity than *NCTC 7096*.

A commercial preparation of GS inhibited germination of *B. cinerea* conidiospores with distinct antifungal activity at 10 µM GS and complete inhibition of spore germination at 100 µM, similar to the results reported previously (Edwards and Seddon, 2001; Troskie et al., 2012). The direct application of *A. migulanus* cells to suspensions of *B. cinerea* spores proved that the strain *Nagano* was more effective than *NCTC 7096* at reducing germination of *B. cinerea* spores, suggesting that factors other than quantities of GS-1141 produced were responsible for the antimicrobial effects observed.

Genome mining of the two draft genome sequences of *A. migulanus Nagano* and *NCTC 7096* (Alenezi et al.,

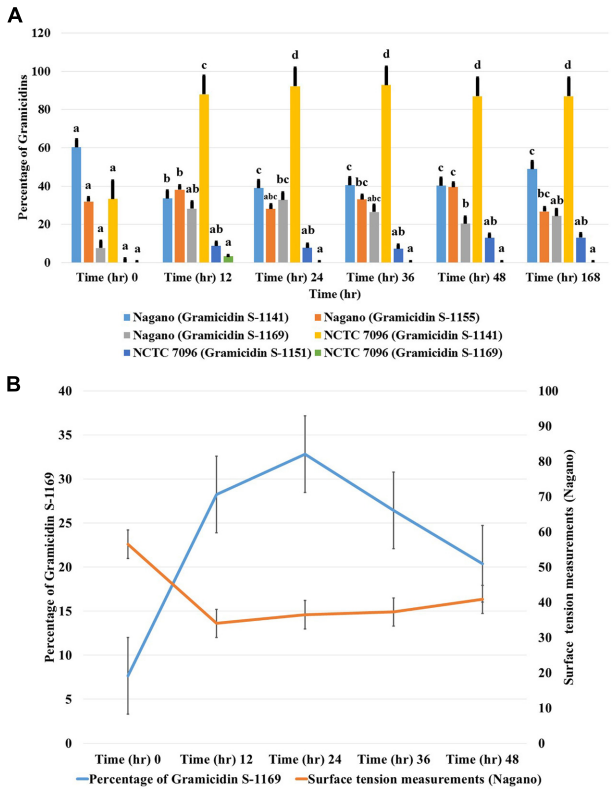


FIGURE 7 | Relative concentrations of gramicidin-1141, gramicidin-1155 and gramicidin-1169 produced by (A) *A. migulanus Nagano* and *NCTC 7096* determined using LC-MS. **(B)** Relationship between changes in surface tension of *A. migulanus Nagano* culture fluids and production of GS-1169. Vertical bars represent standard errors of the means, $N = 3$. Error bars represent standard error of three independent replicates for each gramicidin (1141, 1155 and 1169). Data presents mean ± standard error. Bars labeled with different letters are significantly different among the treatments at $P < 0.05$ using the Tukey's HSD test. In each bar groups, bars labeled with the same letter are not significantly different from each other according to Tukey's HSD at $p < 0.05$.

2015a,b) suggested two amino acid unit differences between the gramicidin synthase sequences of the two strains, designed as T342I and P419S. Using sequences of GS synthases of both strains as an input to the Swiss model server[3] 3D models of the proteins were generated. Using 3D models and the DUET server (Pires et al., 2014), the T342I and P419S substitutions should decrease the stability of the GS synthase protein synthesized by *A. migulanus NCTC 7096*. This suggestion requires verification through purification of the *Nagano* and *NCTC 7096* GS synthases and testing stability *in vitro*. An alternative explanation would be that the T342I and P419S substitutions direct the synthesis of the two-different gramicidin homologs in Nagano, although additional experiments are needed to confirm this assumption. Further experiments are also required to test whether differences at the amino acid sequence level of *A. migulanus Nagano* and *NCTC 7096* could explain the observed differences in their respective biocontrol abilities. LC-MS studies of GS structures showed that, although both strains produced a molecular species matching the structure of commercial GS, here designated as GS-1141, *A. migulanus Nagano* produced two additional molecular species, GS-1155 and GS-1169 which were confirmed by HRESIMS analysis. Additionally, the gramicidin isotope pattern was confirmed by matching the simulated pattern. In GS-1155 and GS-1169 lysine replaced one or two ornithine residues in the cyclic peptide structure of the molecule. Quantification of the different GS and GS-like compounds showed that GS-1155 and GS-1169 accumulated at similar levels to GS-1141 in *A. migulanus Nagano*. Due to structural similarity, identical polarity and very similar molecular weights, numerous different attempts to separate these GS analogs chromatographically were not successful, using HPLC equipped with different normal phase columns, reversed phase columns with a range C-8 to C-18 packing material in addition to size-exclusion Sephadex LH20 column and different solvent systems under different conditions. The significance of this finding remains unclear and further work is needed to clarify the role and function of the newly discovered GS-1155 and GS-1169 in the biocontrol ability of *Nagano*.

Production of a biosurfactant by *A. migulanus Nagano*, which increases the rate of evaporation from the plant surface, thereby reducing periods of surface wetness and indirectly inhibiting spore germination, was reported previously (Seddon et al., 1997, 2000). The standard tests for biosurfactant activity used here – surface tension, blood agar and oil spreading methods – clearly demonstrated that, although *A. migulanus Nagano* excreted biosurfactant activity into culture fluids, *A. migulanus NCTC 7096* was less effective in exerting a biosurfactant activity. The present work also revealed a strong negative correlation between surface tension and the quantity of GS-1169 present in culture fluids with time. More in-depth investigation to ascertain the link between the biosynthesis of the newly recognized gramicidins, the production of biosurfactant and the biocontrol ability of *A. migulanus Nagano* is required.

Genome mining of whole genome sequences of *A. migulanus Nagano* and *NCTC 7096* detected 10 genes showing strong homology with bacterial genes responsible for exopolysaccharide biosynthesis and biofilm formation abilities. The gene encoding the first step of exopolysaccharide biosynthesis, exopolysaccharide biosynthesis polyprenyl glycosylphosphotransferase, was present in the genome of *Nagano* and absent in the genome of *NCTC 7096*. This exopolysaccharide biosynthetic gene is a promising candidate for the generation of knock-out mutants in *Nagano* that would enable the testing of the importance of the exopolysaccharides in biocontrol ability of *Nagano*. Similar mechanisms have been described in *B. subtilis* strain 6051 (Kinsinger et al., 2003; Bais et al., 2004). The prediction of presence of exopolysaccharides genes by genome-mining approach was confirmed by preliminary purification of the polar exopolysaccharide fraction from the non-polar gramicidin fraction, after injection of the total *Nagano* bacterial extract to the RP-C18 flash chromatographic system, followed by MS analysis. Exopolysaccharides have been linked to biofilm formation in bacteria

[3]http://swissmodel.expasy.org/

(Mielich-Süss and Lopez, 2015). Therefore, biofilm formation by the *Nagano* and *NCTC 7096* strains of *A. migulanus* at the medium-air interface were tested. The results presented here, while preliminary, clearly showed that *Nagano* was able to form a biofilm, in contrast to *NCTC 7096* in which no biofilm developed. Biofilm formation has also been proposed as a mean of providing efficient attachment of bacteria to plant surfaces (Yaron and Römling, 2014). Moreover, *Nagano* showed strong attachment to pine needles whereas *NCTC 7096* showed only a weak attachment ability (Alenezi et al., 2016a). *Nagano* was able to persist after infection with *Dothistroma septosporum*. The presence of the exopolysaccharide cluster suggested that biofilm formation could be an important mechanism used by *A. migulanus Nagano* to interact with plant roots and therefore provide biocontrol ability. The use of knock-out mutants, as described above, would answer this question. The genome mining approach also yielded a list of candidate proteins present only in one of the two strains which could be a starting point for additional studies. Therefore, the work presented here greatly increased understanding of the biocontrol ability of *A. migulanus* at the strain level, providing a model for further similar investigations in closely related genera.

ETHICS STATEMENT

This research did not involve any work with human participants or animals by any of the authors.

AUTHOR CONTRIBUTIONS

Conceived and designed the experiments: FA, LB, MJ, and SW. Performed the experiments: FA, LB, LL, HW, and MR. Analyzed the data: FA, LB, ACB, IR, MR, and SW. Contributed reagents/materials/analysis tools: LB, SW, MR, and MJ. Wrote and enriched the literature: LB, FA, and AC. Corrected the manuscript: MR, MJ, SW, and ACB.

FUNDING

This project was funded by the Government of Kuwait (to FA) and the European Union Seventh Framework Programme under grant agreement 245268 (ISEFOR; to LB and SW). Further support came from the SwissBOL project, financed by the Swiss Federal Office for the Environment (grant holder LB) and the Sciex–Scientific Exchange Programme NMS.CH (to LL and LB). LL is indebted to the Ministry of Education, Science, Research and Sport of the Slovak Republic for financial support in the frame of the project "VEGA 1/0061/16."

ACKNOWLEDGMENTS

This project was funded by the Government of Kuwait (to FA) and the European Union Seventh Framework Programme under grant agreement 245268 (ISEFOR; to LB and SW). Further support came from the SwissBOL project, financed by the Swiss Federal Office for the Environment (grant holder LB) and the Sciex–Scientific Exchange Programme (http://nms.ch/) (NMS.CH; to LL and LB). LL is indebted to the Ministry of Education, Science, Research and Sport of the Slovak Republic for financial support in the frame of the project "VEGA 1/0061/16" and "VEGA 1/0046/16".

SUPPLEMENTARY MATERIAL

The Supplementary Material for this article can be found online at: http://journal.frontiersin.org/article/10.3389/fmicb.2017.00517/full#supplementary-material

FIGURE S1 | Predicted gramicidin S synthases protein sequences alignment.

FIGURE S2 | Predicted 3D structure of gramicidin S synthase of *Aneurinibacillus migulanus* and Mg^{2+}, dAMP and phenylalanine (PHE) molecule binding sites. (A) 3D structure of the protein, showing the binding site. **(B)** Critical residues for binding of dAMP. **(C)** Critical residues for binding of Mg^{2+}. **(D)** Critical residues for binding of PHE. The proposed binding modes of Mg^{2+}, dAMP and PHE molecules are shown in stick format and non-carbon atoms are colored by atom type. Green balls correspond to Mg^{2+} ions, dAMP molecules are pink in color and PHE is blue. Hydrogen bonds are shown with dotted lines.

FIGURE S3 | DUET prediction of gramicidin S synthase of *Aneurinibacillus migulanus* for mutations T342I (I) and P419S (II). The results display the predicted change in folding free energy upon mutation (G in kcal/mol). A negative value (and red lettering) corresponds to a mutation predicted as destabilizing. The information displayed includes the mCSM and SDM individually predicted protein stability changes, the combined DUET prediction, a structural summary of the mutation highlighting the wild-type (*Nagano*) residue and position number, the mutation and its 3D environment.

FIGURE S4 | Exopolysaccharide production by *A. migulanus*. (A) Protein interaction network of the exopolysaccharide biosynthetic pathway of *A. migulanus*. **(B)** RP-C18 flash chromatographic system purification of the polar exopolysaccharide fraction from the non-polar gramicidin fraction of exopolysaccharide. **(C)** Biofilm formation as suggested by the floating pellicles that form at the liquid-air interface of standing cultures in 12 well plates (left) and efficient attachment to pine needles infected with *Dothistroma septosporum*.

TABLE S1 | *Nagano* Gramicidins MS^n fragmentation.

TABLE S2 | *NCTC 7096* Gramicidins MS^n fragmentation.

TABLE S3 | High resolution electrospray ionisation mass spectrometry (HRESIMS) analysis of the GS novel analogs.

TABLE S4 | Differences between genes and gene families of *A. migulanus Nagano* and *A. migulanus NCTC 7096.*

REFERENCES

Alenezi, F. N., Fraser, S., Bełka, M., Doğmuş, T. H., Hečkova, Z., Oskay, F., et al. (2016a). Biological control of *Dothistroma* needle blight on pine with *Aneurinibacillus migulanus*. *For. Pathol.* 46, 555–558. doi: 10.1111/efp.12237

Alenezi, F. N., Rekik, I., Belka, M., Ibrahim, A. F., Luptakova, L., Woodward, S., et al. (2016b). Strain-level diversity of secondary metabolism in the biocontrol species *Aneurinibacillus migulanus*. *Microbiol. Res.* 182, 116–124. doi: 10.1016/j.micres.2015.10.007

Alenezi, F. N., Weitz, H. J., Belbahri, L., Nidhal, J., Luptakova, L., Jaspars, M., et al. (2015a). Draft genome sequence of *Aneurinibacillus migulanus*

NCTC 7096. *Genome Announc.* 3:e00234-15. doi: 10.1128/genomeA.00234-15

Alenezi, F. N., Weitz, H. J., Belbahri, L., Ben Rebah, H., Luptakova, L., Jaspars, M., et al. (2015b). Draft genome sequence of *Aneurinibacillus migulanus* strain nagano. *Genome Announc.* 3:e00232-15. doi: 10.1128/genomeA.00232-15

Bais, H. P., Park, S. W., Weir, T. L., Callaway, R. M., and Vivanco, J. M. (2004). How plants communicate using the underground information superhighway. *Trends Plant Sci.* 9, 26–32. doi: 10.1016/j.tplants.2003.11.008

Beauregard, P. B., Chai, Y., Vlamakis, H., Losick, R., and Kolter, R. (2013). *Bacillus subtilis* biofilm induction by plant polysaccharides. *Proc. Natl. Acad. Sci. U.S.A.* 110, E1621–E1630. doi: 10.1073/pnas.1218984110

Belbahri, L., Alenezi, F. N., Luptakova, L., Rateb, M. E., and Woodward, S. (2015). Complete genome sequence of *Aneurinibacillus migulanus* E1, a gramicidin S- and D-phenylalanyl-L-propyl diketopiperazine-deficient mutant. *Genome Announc.* 3:e01441-15. doi: 10.1128/genomeA.01441-15

Chandel, S., Allan, E. J., and Woodward, S. (2010). Biological control of *Fusarium oxysporum* f.sp. *lycopersici* on tomato by *Brevibacillus brevis*. *J. Phytopathol.* 158, 470–478. doi: 10.1111/j.1439-0434.2009.01635.x

Edwards, S. G., and Seddon, B. (2001). Mode of antagonism of *Brevibacillus brevis* against *Botrytis cinerea* in vitro. *J. Appl. Microbiol.* 91, 652–659. doi: 10.1046/j.1365-2672.2001.01430.x

Ghai, S., Sood, S. S., and Jain, R. K. (2007). Antagonistic and antimicrobial activities of some bacterial isolates collected from soil samples. *Ind. J. Microbiol.* 47, 77–80. doi: 10.1007/s12088-007-0014-x

Govrin, E. M., and Levine, A. (2000). The hypersensitive response facilitates plant infection by the necrotrophic pathogen *Botrytis cinerea*. *Curr. Biol.* 10, 751–757. doi: 10.1016/S0960-9822(00)00560-1

Henry, V. J., Bandrowski, A. E., Pepin, A. S., Gonzalez, B. J., and Desfeux, A. (2014). OMICtools: an informative directory for multi-omic data analysis Database. *Database* 2014:bau069. doi: 10.1093/database/bau069

Jamalizadeh, M., Etebarian, H. R., Alizadeh, A., and Aminian, H. (2008). Biological control of grey mold on apple fruits by *Bacillus licheniformis* (EN74-1). *Phytoparasitica* 36, 23–29. doi: 10.1007/BF02980744

Jazeh, M. G., Forghani, F., and Oh, D. H. (2012). Biosurfactant production by *Bacillus* sp. isolated from petroleum contaminated soils of Sirri Island. *Am. J. Appl. Sci.* 9, 1–6. doi: 10.3844/ajassp.2012.1.6

Kim, W. G., Weon, H. Y., Seok, S. J., and Lee, K. H. (2008). In vitro antagonistic characteristics of bacilli isolates against *Trichoderma* spp. and three species of mushrooms. *Mycobiology* 36, 266–269. doi: 10.4489/MYCO.2008.36.4.266

Kinsinger, R. F., Shirk, M. C., and Fall, R. (2003). Rapid surface motility in *Bacillus subtilis* is dependent on extracellular surfactin and potassium ion. *J. Bacteriol.* 185, 5627–5631. doi: 10.1128/JB.185.18.5627-5631.2003

Mefteh, F. B., Daoud, A., Chenari Bouket, A., Alenezi, F. N., Luptakova, L., Rateb, M. E., et al. (2017). Fungal root microbiome from healthy and brittle leaf diseased date palm trees (*Phoenix dactylifera* L.) reveals a hidden untapped arsenal of antibacterial and broad spectrum antifungal secondary metabolites. *Front. Microbiol.* 8:307. doi: 10.3389/fmicb.2017.00307

Mielich-Süss, B., and Lopez, D. (2015). Molecular mechanisms involved in *Bacillus subtilis* biofilm formation. *Environ. Microbiol.* 17, 555–565. doi: 10.1111/1462-2920.12527

Morikawa, M., Hirata, Y., and Imanaka, T. (2000). A study on the structure–function relationship of the lipopeptide biosurfactants. *Biochim. Biophys. Acta* 1488, 211–218. doi: 10.1016/S1388-1981(00)00124-4

Nafisi, M., Stranne, M., Zhang, L., van Kan, J., and Sakuragi, Y. (2014). The endo-arabinanase BcAra1 is a novel host-specific virulence factor of the necrotic fungal phytopathogen *Botrytis cinerea*. *Mol. Plant Microbe Interact.* 27, 781–792. doi: 10.1094/MPMI-02-14-0036-R

Ozer, E. A., Allen, J. P., and Hauser, A. R. (2014). Characterization of the core and accessory genomes of *Pseudomonas aeruginosa* using bioinformatic tools Spine and AGEnt. *BMC Genomics* 15:737. doi: 10.1186/1471-2164-15-737

Pires, D. E., Ascher, D. B., and Blundell, T. L. (2014). DUET: a server for predicting effects of mutations on protein stability using an integrated computational approach. *Nucleic Acids Res.* 42, W314–W319. doi: 10.1093/nar/gku411

Piret, J. M., and Demain, A. L. (1982). Germination initiation and outgrowth of spores of *Bacillus brevis* strain Nagano and its gramicidin S-negative mutant. *Arch. Microbiol.* 133, 3843.

Plaza, G. A., Zjawiony, I., and Banat, I. M. (2006). Use of different methods for detection of thermophilic biosurfactant-producing bacteria from hydrocarbon-contaminated and bioremediated soils. *J. Petrol. Sci. Eng.* 50, 71–77. doi: 10.1016/j.petrol.2005.10.005

Pornsunthorntawee, O., Arttaweeporn, N., Paisanjit, S., Somboonthanate, P., Abe, M., Rujiravanit, R., et al. (2008). Isolation and comparison of biosurfactants produced by *Bacillus subtilis* PT2 and *Pseudomonas aeruginosa* SP4 for microbial surfactant-enhanced oil recovery. *Biochem. Eng. J.* 42, 172–179. doi: 10.1016/j.bej.2008.06.016

Roberts, D. P., and Lohrke, S. M. (2003). United States Department of Agriculture-agricultural research service research programs in biological control of plant diseases. *Pest Manag. Sci.* 59, 654–664. doi: 10.1002/ps.613

Schmitt, A., and Seddon, B. (2005). "Biocontrol of plant pathogens with microbial BCAs and plant extracts–advantages and disadvantages of single and combined use," in *Proceedings of the 14th International Reinhardbrunn Symposium: Modern Fungicides and Antifungal Compounds IV*, eds H. W. Dehne, U. Gisi, K. H. Kuck, P. E. Russell, and H. Lyr (Alton: BCPC), 205–225.

Seddon, B., Edwards, S. G., Markellou, E., and Malathrakis, N. E. (1997). "Bacterial antagonist-fungal pathogen interactions on the plant aerial surface," in *Multitrophic Interactions Interrestrial Systems*, eds A. C. Grange and V. K. Brown (Oxford: Blackwell Science Ltd), 5–25.

Seddon, B., McHugh, R. C., and Schmitt, A. (2000). "*Brevibacillus brevis* – a novel candidate biocontrol agent with broad-spectrum antifungal activity," in *Proceedings of the Brighton Crop Protection Conference Pests and Diseases*, Brighton, 563–572.

Troskie, A. M., Vlok, N. M., and Rautenbach, M. J. (2012). A novel 96-well gel-based assay for determining antifungal activity against filamentous fungi. *Microbiol. Methods* 91, 551–558. doi: 10.1016/j.mimet.2012.09.025

Yánez-Mendizábal, V., Usall, J., Vinas, I., Casals, C., Marın, S., Solsona, C., et al. (2011). Potential of a new strain of *Bacillus subtilis* CPA-8 to control the major post-harvest diseases of fruit. *Biocontrol Sci. Technol.* 21, 409–426. doi: 10.1080/09583157.2010.541554

Yaron, S., and Römling, U. (2014). Biofilm formation by enteric pathogens and its role in plant colonization and persistence. *Microb. Biotechnol.* 7, 496–516. doi: 10.1111/1751-7915.12186

Youssef, N. H., Duncan, K. E., Nagle, D. P., Savage, K. N., Knapp, R. M., and McInerney, M. J. (2004). Comparison of methods to detect biosurfactant production. *J. Microbiol. Methods* 56, 339–347. doi: 10.1016/j.mimet.2003.11.001

Conflict of Interest Statement: The authors declare that the research was conducted in the absence of any commercial or financial relationships that could be construed as a potential conflict of interest.

Copyright © 2017 Alenezi, Rekik, Chenari Bouket, Luptakova, Weitz, Rateb, Jaspars, Woodward and Belbahri. This is an open-access article distributed under the terms of the Creative Commons Attribution License (CC BY). The use, distribution or reproduction in other forums is permitted, provided the original author(s) or licensor are credited and that the original publication in this journal is cited, in accordance with accepted academic practice. No use, distribution or reproduction is permitted which does not comply with these terms.

frontiers in Microbiology

ORIGINAL RESEARCH
published: 19 April 2017
doi: 10.3389/fmicb.2017.00678

Discovery of Antimycin-Type Depsipeptides from a *wbl* Gene Mutant Strain of Deepsea-Derived *Streptomyces somaliensis* SCSIO ZH66 and Their Effects on Pro-inflammatory Cytokine Production

*Huayue Li[1], Huiming Huang[1], Lukuan Hou[1], Jianhua Ju[2] and Wenli Li[1,3]**

[1] Key Laboratory of Marine Drugs, Ministry of Education, School of Medicine and Pharmacy, Ocean University of China, Qingdao, China, [2] CAS Key Laboratory of Marine Bio-resources Sustainable Utilization, Guangdong Key Laboratory of Marine Materia Medica, RNAM Center for Marine Microbiology, South China Sea Institute of Oceanology, Chinese Academy of Sciences, Guangzhou, China, [3] Laboratory for Marine Drugs and Bioproducts of Qingdao National Laboratory for Marine Science and Technology, Qingdao, China

OPEN ACCESS

Edited by:
Wen-Jun Li,
Sun Yat-sen University, China

Reviewed by:
Yanqing Tian,
South University of Science and Technology of China, China
Lijiang Song,
University of Warwick, UK

***Correspondence:**
Wenli Li
liwenli@ouc.edu.cn

Specialty section:
This article was submitted to Microbial Physiology and Metabolism, a section of the journal Frontiers in Microbiology

Received: *09 October 2016*
Accepted: *03 April 2017*
Published: *19 April 2017*

Citation:
Li H, Huang H, Hou L, Ju J and Li W (2017) Discovery of Antimycin-Type Depsipeptides from a wbl Gene Mutant Strain of Deepsea-Derived Streptomyces somaliensis SCSIO ZH66 and Their Effects on Pro-inflammatory Cytokine Production. Front. Microbiol. 8:678. doi: 10.3389/fmicb.2017.00678

Deepsea microbes are a rich source of novel bioactive compounds, which have developed unique genetic systems as well as biosynthetic pathways compared with those of terrestrial microbes in order to survive in extreme living environment. However, a large variety of deepsea-microbial secondary metabolic pathways remain "cryptic" under the normal laboratory conditions. Manipulation of global regulators is one of the effective approaches for triggering the production of cryptic secondary metabolites. In this study, by combination of various chromatographic purification process, we obtained somalimycin (**1**), a new antimycin-type depsipeptide, with an unusual substitution of 3-aminosalicylate instead of conserved 3-formamidosalicylate moiety, along with two known (**2** and **3**) analogs from the Δ*wblA*$_{SO}$ mutant strain of deepsea-derived *Streptomyces somaliensis* SCSIO ZH66. The structures of **1–3** were elucidated on the basis of extensive spectroscopic analyses including LC-MS and NMR. In the evaluation of potent anti-inflammatory activity, compound **2** exhibited strong inhibitory activity on the IL-5 production in ovalbumin-stimulated splenocytes with IC_{50} value of 0.57 μM, while **1** and **3** displayed mild effect (>10 μM), which might be attributed to their different side-chain substitutions. Moreover, compounds **1–3** showed very weak cytotoxicity against human umbilical vein endothelial cells with LD_{50} values of 62.6, 34.6, and 192.9 μM, respectively, which were far over their IL-5 inhibitory activity. These results indicated that these compounds have good potential for further use in anti-inflammatory drug development.

Keywords: antimycin-type depsipeptides, deepsea-derived bacteria, regulatory gene, anti-inflammatory, IL-5 production

INTRODUCTION

Marine natural products are a rich source of drug candidates, an increasing number of which have been approved to the market or are currently in clinical trials (Newman and Cragg, 2004; Salomon et al., 2004; Kollar et al., 2014; Rangel and Falkenberg, 2015). In the expanding search for sources of new chemical and bioactivity diversity, the exploration of deepsea microbes has emerged as a new frontier in drug discovery and development. Deepsea microbes live in a biologically competitive environment with unique conditions of temperature, pressure, oxygen, light, salinity, and nutrients. In the long process of evolution, deepsea microbes developed unique genetic systems as well as different biosynthetic pathways compared with those of terrestrial microbes for good adaption to extreme living environment, which enables them to produce a large diversity of structurally novel and biologically active secondary metabolites (Skropeta, 2008; Skropeta and Wei, 2014).

Historically, the exploration of novel bioactive compounds was mostly "grind and find" mode, which frequently get half the result with twice the effort. The microbial secondary metabolites that have been reported by traditional methods are just the tip of the ice berg. A large variety of the biosynthetic pathways still remain "cryptic" under the normal laboratory conditions. With the recent advances in genomics and bioinformatics analytical techniques, genome-guided compound mining, the key point of which is to find ways to turn on or turn up the expression of cryptic or poorly expressed pathways to trigger novel compound production, has been used as a more efficient approach compared to those traditional methods for novel bioactive compound discovery (Challis, 2008; Lane and Moore, 2011; Bachmann et al., 2014).

Manipulation of global regulators is one of the effective strategies for triggering the production of cryptic secondary metabolites (Baltz, 2016). In our previous study, we inactivated the negative global regulatory gene *wblA*$_{so}$ in deepsea-derived *Streptomyces somaliensis* SCSIO ZH66, and it led to significant changes of secondary metabolites production in the Δ*wblA*$_{so}$ mutant strain, from which a series of anti-MRSA (methicillin-resistant *Staphylococcus aureus*) α-pyrone compounds (violapyrones A-C, H, and J) were isolated and identified (Huang et al., 2016).

In the continuing study of the same mutant strain, we found that, in addition to violapyrones, the production of several other secondary metabolites were notably increased as well compared to those in the wild-type strain. With the subsequent UV-spectrum-guided separation, we obtained a new antimycin-type depsipeptide, namely somalimycin (**1**), and two known analogs, USF-19A (**2**) and urauchimycin D (**3**) (**Figure 1**). The current paper deals with the isolation, structural elucidation, and biological evaluation of the compounds from the Δ*wblA*$_{so}$ mutant strain of deepsea-derived *S. somaliensis* SCSIO ZH66. Moreover, on the inhibitory effect of IL-5 cytokine production, the structure–activity relationship (SAR) study of compounds **1–3** with reported antimycin analogs were also performed.

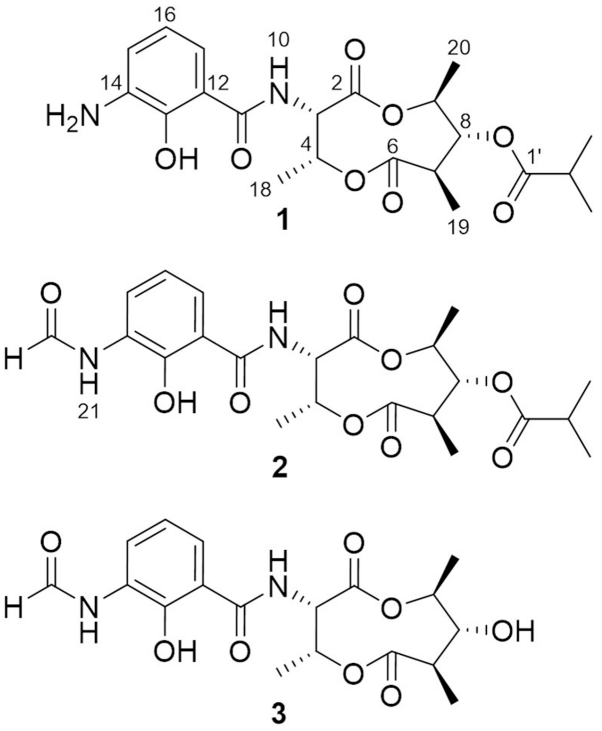


FIGURE 1 | Structures of compounds 1–3.

MATERIALS AND METHODS

Bacterial Strains and Culture Conditions

The *S. somaliensis* SCSIO ZH66 (CGMCC NO.9492) wild-type strain was isolated from the deepsea sediment collected at a depth of 3536 m of the South China Sea (120° 0.250′E; 20° 22.971′N; Zhang et al., 2015). The Δ*wblA*$_{so}$ mutant strain was constructed in our previous study (Huang et al., 2016). The strains were grown at 30°C on MS medium for sporulation, and were fermented as previously described (Huang et al., 2016).

Isolation and Purification

The fermentation broth (50 mL) of the wild-type and the Δ*wblA*$_{so}$ mutant strains was extracted with EtOAc, respectively, and was subsequently subjected to HPLC analysis (Agilent 1260 Infinity equipment). Analytical HPLC was performed with a linear gradient from 10 to 100% B/A in 50 min (mobile phase A: H_2O + 0.1% HCOOH; phase B: 100% MeOH + 0.1% HCOOH; YMC-Pack ODS-A column 150 mm × 4.6 mm, i.d. 5 μm; wavelength: 220 nm) to analyze the production changes between the wild-type and mutant strains (**Figure 2**). The combined culture broth of the Δ*wblA*$_{so}$ mutant strain (20 L) was extracted with EtOAc at room temperature, which was partitioned between 90% MeOH and *n*-hexane to remove non-polar components. Then the MeOH layer was subjected to a stepped-gradient open column (ODS-A, 120 Å, S-30/50 mesh) eluting with 20–100% MeOH to yield five fractions. Each fraction was subjected to the HPLC to confirm the notably enhanced products in the mutant

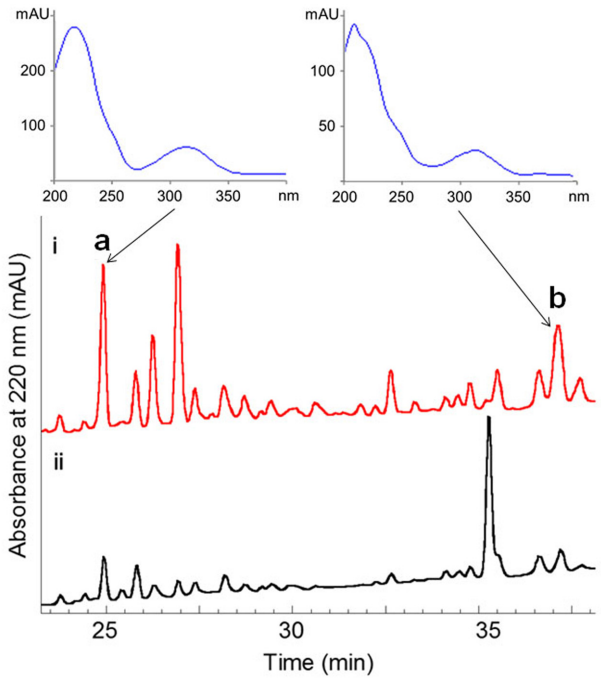


FIGURE 2 | Comparative HPLC analysis of secondary metabolites in the culture extracts of wild-type *S. somaliensis* SCSIO ZH66 and its Δ*wblAso* mutant strain. The notably enhanced production displaying similar UV-spectra in the Δ*wblAso* mutant strain were marked with a and b. Compounds **1** and **2** were purified from peak b, and compound **3** was obtained from the enhanced peak a.

strain by their retention time and UV spectra. Compounds **1** (5.1 mg) and **2** (1.8 mg) were obtained by further purification of the enhanced peak **b** in fraction 4 on a reversed-phase HPLC (YMC-Pack ODS-A column 250 mm × 10 mm, i.d. 5 μm; wavelength: 220 nm) eluting with 85% MeOH + 0.2% HCOOH (v/v) (1 mL/min). Compound **3** (6.5 mg) was obtained from the enhanced peak **a** in fraction 3 eluting with 75% MeOH + 0.2% HCOOH (v/v) (1 mL/min). The structures of compounds **1–3** are shown in **Figure 1**.

Somalimycin ***(1)***: dark brown, amorphous solid; CD (*c* 1.15×10^{-3} M, MeOH) λ_{max} ($\Delta\varepsilon$) 228 (1.23), 245.5 (0.63), 262.5 (1.35) nm, 350 (−0.24) nm (Supplementary Figures S2, S3); ^{1}H and ^{13}C NMR data, see **Table 1**; HR-ESIMS *m/z* 437.1931 $[M + H]^+$ (calcd for $C_{21}H_{29}O_8N_2$, 437.1918).

Structure Elucidation

The structures of compounds **1–3** were elucidated by combination of extensive spectroscopic analysis. 1D and 2D NMR spectra were recorded on Bruker Avance III 600 or Agilent DD2-500 spectrometers at 25°C. Chemical shifts were reported with reference to the respective solvent peaks and residual solvent peaks (δ_H 2.50 and δ_C 39.5 ppm for DMSO-d_6; and δ_H 7.26 and δ_C 77.1 ppm for $CDCl_3$). The molecular weight of each compound was determined using a Q-TOF Ultima Global GAA076 LC-MS spectrometer. CD spectra were recorded on a JASCO J-715 spectropolarimeter, using MeOH as solvent.

Marfey's Analysis of Compound 1

Compound **1** (200 μg) was dissolved in 1 mL of 6 N HCl and hydrolyzed at 110°C for 24 h, and the HCl was then removed by evaporation under the N_2 gas. The hydrolysate was dissolved in 100 μL of H_2O and added 200 μL of Marfey's reagent (1-fluoro-2,4-dinitrophenyl-5-L-alanine amide, FDAA; 1 mg/mL in acetone) together with 50 μL of 1 M $NaHCO_3$. Then, the mixture was reacted at 50°C for 60 min. After cooling to room temperature, the mixture was neutralized with 2 N HCl (25 μL). The reaction mixture was subjected to a reversed-phase HPLC (YMC-Pack ODS-A column 150 mm × 4.6 mm, i.d. 5 μm; wavelength: 340 nm) with a linear gradient elution (30–80% solvent B in 50 min; solvent A: H_2O + 0.1% TFA, solvent B: 90% ACN + 0.1% TFA). Derivatization of L- or D-threonine with FDAA was carried out in the similar manner.

Mouse Immunization, Cell Culture, and Cytokine (IL-5) Measurement

The inhibitory effects of the compounds **1–3** on the pro-inflammatory cytokine production were determined by the method previously described by Strangman et al. (2009). The experiment was carried out in strict ethical guidelines of Institutional Animal Care and Use Committee. Female BALB/c mice aged 6–8 weeks (Shanghai Laboratory Animal Center, Chinese Academy of Sciences, China), were immunized subcutaneously with ovalbumin (OVA, 25 μg) allergen adsorbed to alum adjuvant (1 mg) in the phosphate-buffered saline (200 μL) weekly for 4 weeks. Then, the mice were sacrificed and their spleens were surgically removed. The

TABLE 1 | ^{1}H and ^{13}C NMR chemical shifts of 1 in DMSO-d_6.

	1	
Position	**δ_H (*J* in Hz)**	**δ_C**
2		169.9
3	5.28 (1H, t, 7.8)	54.1
4	5.54 (1H, quin, 6.6)	71.8
6		174.5
7	2.65 (1H, m)	43.5
8	4.83 (1H, t, 10.2)	76.3
9	4.92 (1H, m)	73.9
10-NH	9.26 (1H, d, 8.4)	
11		170.2
12		115.0
13		151.4
14		129.1
15	7.20 (1H, d, 7.8)	123.7
16	6.87 (1H, t, 7.8)	119.1
17	7.74 (1H, d, 7.8)	122.4
18	1.31 (3H, d, 6.6)	15.4
19	1.02 (3H, d, 6.6)	14.0
20	1.21 (3H, d, 6.6)	18.0
1′		175.9
2′	2.67 (1H, m)	33.7
3′/4′	1.14 (3H, d, 7.2)	19.1

splenocytes were separated and suspended in RPMI-1640 media (1.3×10^6 cells/mL) and then were aliquoted into 96 well plates (100 μL/well). Compounds **1–3** (in DMSO) and an aliquot of stimulating OVA allergen were added to the well containing splenocytes, and were incubated for 48 h. The supernatants were then collected and assayed for the cytokine IL-5 production using mouse ELISA kit (R&D Systems Inc.). Absorbance was measured at 450 nm. The wells containing DMSO + OVA allergen were plated as a negative control, and dexamethasone was used as a positive control.

Cell Viability Assay

Cell viability of human umbilical vein endothelial cells (HUVEC) was measured by MTT assay (Liu G. et al., 2016). The cells seeded into 96-well plate were cultured at 37°C for 24 h, and were treated with various concentrations of SPS (0, 0.2, 0.3, 0.4, 0.5, 0.6, 0.7, 0.8, 0.9, 1.0, and 1.5 mg/mL) for 12 and 24 h. Then MTT solution (5 mg/mL, 20 μL) was added to each well, and were incubated for 4 h. After that, the medium was removed and DMSO (150 μL) was added to each well to dissolve purple crystals of formazan at 260 rpm for 10 min. Absorbance was measured with TECAN infinite M1000 Pro multi-detection microplate reader at 490 nm and relative cell viability was presented as a percentage relative to the control group. The LD_{50} value was determined as the concentration that caused 50% inhibition of cell proliferation.

Antibacterial Activity Assay

The antibacterial activity against five multi-drug resistant (MDR) strains (*S. aureus* CCARM 3090, *Escherichia coli* CCARM 1009, *Enterococcus faecalis* CCARM 5172, *Enterococcus faecium* CCARM 5203, *Salmonella typhimurium* CCARM 8250) was tested by the radial diffusion assay. Each bacterial strain was grown overnight at 37°C in LB media and diluted to 1/100. A gel solution containing 2.5% (w/v) of powdered LB medium and 1.5% agar was prepared and autoclaved. Then, 0.15 mL of the diluted bacterial culture was added to 15 mL of the gel solution at 40–50°C. Once the bacteria were adequately dispersed, the gel was poured into a plate (90 mm × 15 mm). After solidification, wells were made using a 2 mm punch. Each sample (30 mg/mL, 10 μL) was added to the well, and the plates were incubated for 18 h at 37°C. Tetracycline (≥98%, 30 μg/well) was used as a positive control. The diameters of the inhibition zones surrounding the wells were measured in millimeters.

RESULTS

Isolation and Purification of the Compounds

The Δ*wblA*$_{so}$ mutant strain of *S. somaliensis* SCSIO ZH66 was obtained as described in our previous study (Huang et al., 2016). The fermentation broths of the wild-type and the Δ*wblA*$_{so}$ mutant strains were extracted with EtOAc, respectively, and were subsequently subjected to HPLC analysis, in which we observed a series of peak changes (**Figure 2**). The enhanced peaks of **a** and **b** in Δ*wblA*$_{so}$ strain displayed similar UV spectra with characteristic UV absorption around 230 and 320 nm, indicating them likely to be the same class of compounds. With the large scale fermentation of the Δ*wblA*$_{so}$ mutant strain and further UV-spectrum-guided separation, we isolated a major compound **1** together with a small amount of compound **2** from peak **b**, and compound **3** from peak **a**.

Structural Identification of Compounds 1–3

Compound **1** was isolated as a brown, amorphous solid. The molecular formula of **1** was established as $C_{21}H_{28}O_8N_2$ on the basis of HR-ESIMS data ($[M + H]^+$ at *m/z* 437.1931; Supplementary Figure S4). The planar structure of **1** was determined by 1D (^{1}H, ^{13}C) and 2D NMR (COSY, HSQC, and HMBC) data (Supplementary Figures S5–S10). The structure elucidation step was first started with a secondary amide proton NH-10 (δ_H 9.26), which acts as a connection bridge between two parts of substructures. In the ^{1}H-^{1}H COSY spectrum, we observed two proton spin systems that consist of NH-10/H-3 (δ_H 5.28)/H-4 (δ_H 5.54)/H-18 (δ_H 1.31), and H-19 (δ_H 1.02)/H-7 (δ_H 2.65)/H-8 (δ_H 4.83)/H-9 (δ_H 4.92)/H-20 (δ_H 1.21), respectively (**Figure 3**). The ^{13}C chemical shifts of C-2 (δ_C 169.9), C-4 (δ_C 71.8), C-6 (δ_C 174.5), and C-9 (δ_C 73.9), as well as the ^{1}H chemical shifts of H-4 and H-9 revealed the existence of two ester groups. Additionally, the HMBC correlations (**Figure 3**) from H-3 and H-9 to C-2, and from H-4, H-7, and H-8 to C-6 finally assigned the substructure as a nine-membered *bis*-lactone ring. The HMBC correlations from NH-10 and H-17 (δ_H 7.74) to the carbonyl carbon C-11 (δ_C 170.2) allowed further assignment of the substructure located on the other side of the amide group. The ^{1}H-^{1}H COSY correlations between H-15 (δ_H 7.20), H-16 (δ_H 6.87) and H-17, together with the HMBC correlations from these protons to three quaternary carbons C-12 (δ_C 115.0), C-13 (δ_C 151.4), and C-14 (δ_C 129.1) revealed that a trisubstituted aromatic ring connected to the amide group. The downfielded ^{13}C chemical shift value of C-13 compared to other aromatic carbons proved it to be a hydroxylated carbon. The HMBC correlations from H-8, H-2′ (δ_H 2.67), H-3′/H-4′ (δ_H 1.14) to C-1′ (δ_C 175.9) revealed an isobutyrate moiety was attached to

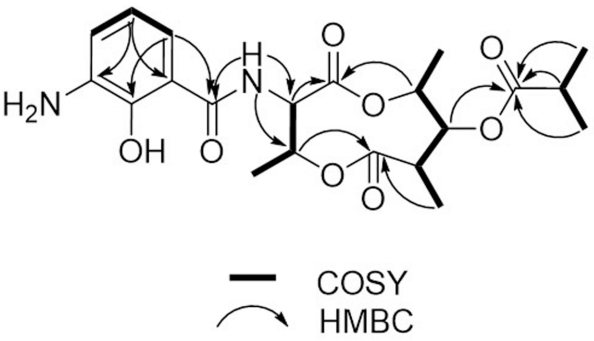


FIGURE 3 | ^{1}H-^{1}H COSY and key HMBC correlations of 1.

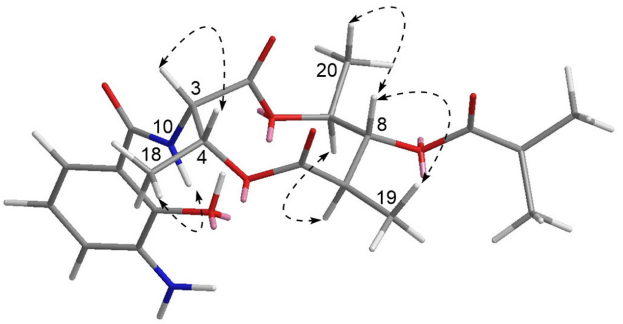


FIGURE 4 | Key NOESY correlations of 1. The 3D structure is the conformer with the lowest energy.

C-8 of the *bis*-lactone ring. Based on the HR-ESIMS data of **1**, we finally confirmed that C-14 was an aminated aromatic carbon, thus assigning the planar structure of **1** as an antimycin-type depsipeptide.

Compound **1** has five chiral carbons (C-3, C-4, C-7, C-8, and C-9), all of which are located on the *bis*-lactone ring. The strong NOE correlations of H-18/NH-10 and H-3/H-4 (**Figure 4**), as well as small *J* value (7.2 Hz) between H-3 and H-4 provided credible evidence for the assignment of *syn* configuration between C-3 and C-4. Furthermore, C-3 and C-4 are part of the threonine residue (C^{α} and C^{β}, respectively) embedded in **1**. Therefore, we performed acid-catalyzed hydrolysis followed by Marfey's analysis to determine their absolute configurations (Supplementary Figure S1). According to the result, the threonine residue in **1** was identified to be L-amino acid; hence the absolute configurations of C-3 and C-4 were assigned to be *S*- and *R*-, respectively. In the ^{1}H NMR spectrum, H-8 showed a triplet signal pattern with the *J* value of 10.2 Hz, indicative of the *anti*-configurations between C-7, C-8, and C-9. The NOE correlations of H-7/H-9, H-8/H-19 and H-8/H-20 further supported this assignment (**Figure 4**). In our attempt to determine the absolute configurations of C-7, C-8, and C-9 using ECD calculation, it was failed because of the high structural flexibility. Nevertheless, the ^{1}H and ^{13}C chemical shifts of *bis*-lactone ring in **1** showed almost identical values with those of the reported antimycin-type depsipeptide USF-19A (**2**) (Komoda et al., 1995), in which the 3-aminosalicylate of **1** is replaced by a 3-formamidosalicylate moiety. The chemical shifts similarity of C-7, C-8, and C-9 in two compounds indicated that these chiral carbons in **1** share the same absolute configurations with those in USF-19A, which were determined as *7R*, *8R*, and *9S*, respectively. The ^{1}H and ^{13}C NMR chemical shift values of **1** are summarized in **Table 1**.

Compound **2** was isolated as a white, amorphous solid. The molecular formula of **2** was established as $C_{22}H_{28}O_9N_2$ on the basis of HR-ESIMS data ($[M + H]^+$ at *m/z* 465.1869) (Supplementary Figure S11). Analysis of its NMR data recorded in DMSO-d_6 (Supplementary Figures S12–S19 and Table S1) revealed that its structure resembles that of **1** except for the amide linkage of a formyl group at C-14 (δ_C 127.4), which was determined by the HMBC correlations from H-22 (δ_H 8.34) to C-14 and from NH-21 (δ_H 9.85) to C-22 (δ_C 160.8) (Supplementary Figure S15). Thus, **2** was identified as USF-19A, that was further collaborated by comparison of ^{1}H and ^{13}C NMR data (in $CDCl_3$) with those reported (Komoda et al., 1995).

Compound **3** was isolated as a white, amorphous solid. The molecular formula of **3** was established as $C_{18}H_{22}O_8N_2$ on the basis of HR-ESIMS data ($[M + H]^+$ at *m/z* 395.1441) (Supplementary Figure S20). Compound **3** has a free hydroxyl group at C-8 (δ_C 77.2) instead of an isobutyrate moiety in **1** and **2**. Compound **3** was identified as urauchimycin D by NMR assignment with further comparison of ^{1}H and ^{13}C NMR data (Supplementary Figures S21–S25 and Table S1) with those reported (Yao et al., 2006).

Inhibitory Activity on IL-5 Production

To investigate the potent anti-inflammatory activity of the compounds **1–3**, the inhibitory effect of each compound on the cytokine (IL-5) production was tested dose dependently. According to **Figure 5**, compound **2** exhibited up to 80% of inhibition on IL-5 production in the OVA-stimulated splenocytes at the concentration of 1 μM, the IC_{50} value of which was further determined as 0.57 μM; however, **1** and **3** showed only less than 20% and null activity, respectively, in the concentration ranging from 0.001 to 1 μM.

Cytotoxicity Assay

To evaluate the cytotoxicity of compounds **1–3** toward human normal cells, the cell viability assay was performed, in which compounds **1–3** showed very weak cytotoxicity toward HUVEC with LD_{50} values of 62.6, 34.6, and 192.9 μM, respectively (Supplementary Table S2).

Antibacterial Activity Assay

In the antibacterial activity evaluation, compounds **1–3** exhibited null inhibition zones against five MDR strains (*S. aureus* CCARM 3090, *E. coli* CCARM 1009, *E. faecalis* CCARM 5172, *E. faecium* CCARM 5203, *S. typhimurium* CCARM 8250) at the treating amount of 300 μg/well (data not shown).

DISCUSSION

Antimycin-type compounds are a class of depsipeptides sharing a nine-membered *bis*-lactone ring with a conserved substitution of 3-formamidosalicylic acid, which exhibited a wide range of bioactivities including antifungal, insecticidal, antiviral, anticancer, and anti-inflammatory (Hosotani et al., 2005; Shiomi et al., 2005; Raveh et al., 2013; Liu J. et al., 2016). Antimycins are generated from a hybrid NRPS (non-ribosomal peptide synthetase)–PKS (polyketide synthase) assembly line in various *Streptomyces* species with the 3-formamidosalicylate substitution as a starter unit.

In the present study, we isolated an unusual 3-aminosalicylate substituted somalimycin (**1**) from the Δ*wblA*$_{so}$ mutant strain of *S. somaliensis* SCSIO ZH66, which was accumulated after the disruption of the negative global regulatory gene

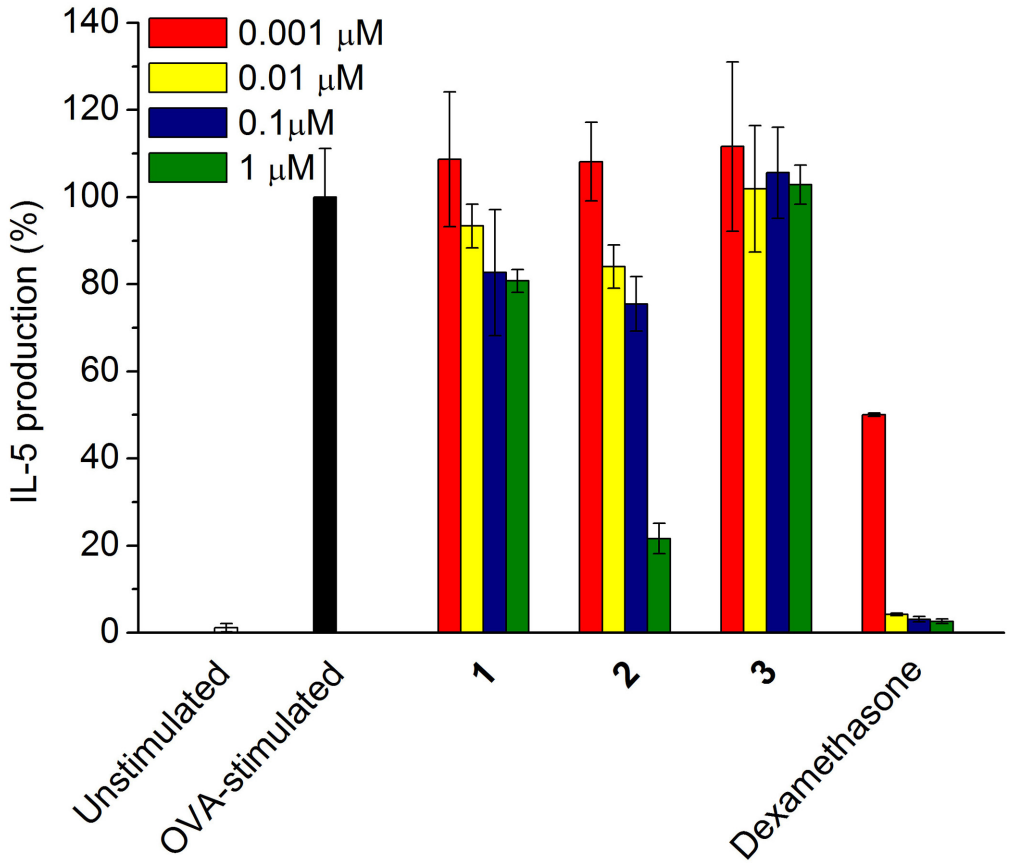


FIGURE 5 | Inhibitory effect of compounds 1–3 on the pro-inflammatory cytokine IL-5 production. OVA-stimulated splenocytes were incubated with each sample from 0.001 to 1.0 μM, respectively. Dexamethasone was used as a positive control.

wblA$_{so}$. Recently, Zhang and colleagues reconstituted the 3-formamidosalicylate moiety in *E. coli*, revealing that it is generated from anthranilic acid by the action of the multicomponent oxygenase AntHIJKL and the formyltransferase AntO on the carrier protein AntG. The intermediates during this process, including anthraniloyl-*S*-AntG and 3-aminosalicyloyl-*S*-AntG, could be recognized by the following hybrid NRPS–PKS assembly line to yield shunt products with anthranilate and 3-aminosalicylate substitution, respectively (Liu et al., 2015). The significantly increased production of 3-aminosalicylate substituted somalimycin (**1**) might be the result of the accumulation of 3-aminosalicyloyl-*S*-AntG, which could be explained by the up-regulation of AntHIJKL in the *wblA*$_{so}$ mutant.

In our investigation for potent anti-inflammatory activity of the compounds **1–3**, USF-19A (**2**) exhibited highest inhibition on IL-5 production in the OVA-stimulated splenocytes (IC_{50} = 0.57 μM); however, somalimycin (**1**) and urauchimycin D (**3**) showed only less than 20% and null activity, respectively, up to the concentration of 1 μM (**Figure 5**). Fenical and colleagues reported that splenocins A–J, a subfamily of antimycin-type depsipeptides, exhibited strong inhibition against IL-5 production, some of which are comparable to that of the corticosteroid drug dexamethasone (Strangman et al., 2009). Among them, splenocin B exhibited the strongest inhibition with IC_{50} value of 1.8 nM, while splenocin J showed the weakest activity (IC_{50} = 1022.7 nM). The activity gap between splenocins B and J is over 500-fold, and somalimycin (**1**) and urauchimycin D (**3**) showed even much lower activity (IC_{50} > 10 μM) than splenocin J. From a structural point of view, compounds **1–3** and splenocins share a common structural skeleton: a nine-membered *bis*-lactone ring with an amide linkage (C-3) connecting to a salicylic acid. The structural differences among these compounds are substitutions at C-7, C-8, and C-14. By comparable analysis of the bioactivity results in this study with those of splenocins (Strangman et al., 2009), we came to a conclusion that (i) the ester linkage to the hydroxyl group at C-8 plays the most important role in the inhibition of IL-5 production; (ii) and the longer alkyl group at C-7 displays the stronger activity; (iii) furthermore, the formylation of the amine group at C-14 is also essential for enhancement of IL-5 inhibition. Compounds **1–3** showed very weak cytotoxicity against HUVEC (Supplementary Table S2), which were far over their IL-5 inhibitory activity. Thus, these compounds may have good potential for further use in the development of anti-inflammatory drugs. Furthermore, the SAR study of

the antimycin-type depsipeptides on the IL-5 production in this study may provide useful information for searching or synthesizing novel antimycin-based anti-inflammatory lead compounds.

CONCLUSION

We isolated a new (**1**) and two known (**2** and **3**) antimycin-type depsipeptides from the $\Delta wblA_{so}$ mutant strain of deepsea-derived *S. somaliensis* SCSIO ZH66. USF-19A (**2**) exhibited strong inhibition against IL-5 production (IC_{50} = 0.57 μM), while somalimycin (**1**) and urauchimycin D (**3**) showed much weaker activity (IC_{50} > 10 μM), which might be attributed to their different side-chain substitutions at C-8 and C-14. All of these three compounds showed very low cytotoxicity against HUVEC, which provided the possibility for their further use in anti-inflammatory drug development.

ETHICS STATEMENT

This study was carried out in accordance with the recommendations of the Animal Research and Ethics Committee of Ocean University of China. The protocol was approved by the Animal Research and Ethics Committee of Ocean University of China.

AUTHOR CONTRIBUTIONS

HL was involved in the NMR assignment and wrote the manuscript. HH and LH performed experiments. JJ provided *S. somaliensis* SCSIO ZH66. WL supervised the whole work and revised and edited the manuscript. All authors read and approved the final manuscript.

FUNDING

This work was supported by grants from the National Natural Science Foundation of China (21502180, 81561148012, and 41506157), the NSFC-Shandong Joint Fund for Marine Science Research Centers (U1606403), the National High Technology Research and Development Program of China (2012AA092104), the Shandong Provincial Natural Science Foundation of China (ZR2014HQ053), the Scientific and Technological Innovation Project Financially Supported by Qingdao National Laboratory for Marine Science and Technology (2015ASKJ02), and Qingdao Research Program of Application Foundation (15-9-1-110-jch).

ACKNOWLEDGMENTS

We would like to thank Dr. Chaomin Sun (The Institute of Oceanology, Chinese Academy of Sciences) for his help in cytotoxicity evaluation, and Dr. Jing Li (School of Medicine and Pharmacy, Ocean University of China) for the measurement of cytokine IL-5.

SUPPLEMENTARY MATERIAL

The Supplementary Material for this article can be found online at: http://journal.frontiersin.org/article/10.3389/fmicb.2017.00678/full#supplementary-material

REFERENCES

Bachmann, B. O., Van Lanen, S. G., and Baltz, R. H. (2014). Microbial genome mining for accelerated natural products discovery: Is a renaissance in the making? *J. Ind. Microbiol. Biotechnol.* 41, 175–184. doi: 10.1007/s10295-013-1389-9

Baltz, R. H. (2016). Genetic manipulation of secondary metabolite biosynthesis for improved production in *Streptomyces* and other actinomycetes. *J. Ind. Microbiol. Biotechnol.* 43, 343–370. doi: 10.1007/s10295-015-1682-x

Challis, G. L. (2008). Mining microbial genomes for new natural products and biosynthetic pathways. *Microbiology* 154, 1555–1569. doi: 10.1099/mic.0.2008/018523-0

Hosotani, N., Kumagai, K., Nakagawa, H., Shimatani, T., and Saji, I. (2005). Antimycins A10 approximately A16, seven new antimycin antibiotics produced by *Streptomyces* spp. SPA-10191 and SPA-8893. *J. Antibiot.* 58, 460–467. doi: 10.1038/ja.2005.61

Huang, H., Hou, L., Li, H., Qiu, Y., Ju, J., and Li, W. (2016). Activation of a plasmid-situated type III PKS gene cluster by deletion of a wbl gene in deepsea-derived *Streptomyces somaliensis* SCSIO ZH66. *Microb. Cell Fact.* 15:116. doi: 10.1186/s12934-016-0515-6

Kollar, P., Rajchard, J., Balounova, Z., and Pazourek, J. (2014). Marine natural products: bryostatins in preclinical and clinical studies. *Pharm. Biol.* 52, 237–242. doi: 10.3109/13880209.2013.804100

Komoda, T., Morimitsu, Y., Hirota, H., and Hirota, A. (1995). USF-19A, a new lipoxygenase inhibitor from *Streptomyces* sp. *Biosci. Biotechnol. Biochem.* 59, 924–926. doi: 10.1271/bbb.59.924

Lane, A. L., and Moore, B. S. (2011). A sea of biosynthesis: marine natural products meet the molecular age. *Nat. Prod. Rep.* 28, 411–428. doi: 10.1039/C0NP90032J

Liu, G., Kuang, S., Wu, S., Jin, W., and Sun, C. (2016). A novel polysaccharide from *Sargassum integerrimum* induces apoptosis in A549 cells and prevents angiogensis *in vitro* and *in vivo*. *Sci. Rep.* 6:26722. doi: 10.1038/srep26722

Liu, J., Zhu, X., Kim, S. J., and Zhang, W. (2016). Antimycin-type depsipeptides: discovery, biosynthesis, chemical synthesis, and bioactivities. *Nat. Prod. Rep.* 33, 1146–1165. doi: 10.1039/c6np00004e

Liu, J., Zhu, X., Seipke, R. F., and Zhang, W. (2015). Biosynthesis of antimycins with a reconstituted 3-formamidosalicylate pharmacophore in *Escherichia coli*. *ACS Synth. Biol.* 4, 559–565. doi: 10.1021/sb5003136

Newman, D. J., and Cragg, G. M. (2004). Marine natural products and related compounds in clinical and advanced preclinical trials. *J. Nat. Prod.* 67, 1216–1238. doi: 10.1021/np040031y

Rangel, M., and Falkenberg, M. (2015). An overview of the marine natural products in clinical trials and on the market. *J. Coast. Life Med.* 3, 421–428. doi: 10.12980/JCLM.3.2015JCLM-2015-0018

Raveh, A., Delekta, P. C., Dobry, C. J., Peng, W., Schultz, P. J., Blakely, P. K., et al. (2013). Discovery of potent broad spectrum antivirals derived from marine actinobacteria. *PLoS ONE* 8:e82318. doi: 10.1371/journal.pone.0082318

Salomon, C. E., Magarvey, N. A., and Sherman, D. H. (2004). Merging the potential of microbial genetics with biological and chemical diversity: an even brighter future for marine natural product drug discovery. *Nat. Prod. Rep.* 21, 105–121. doi: 10.1039/B301384G

Shiomi, K., Hatae, K., Hatano, H., Matsumoto, A., Takahashi, Y., Jiang, C. L., et al. (2005). A new antibiotic, antimycin Ag, produced by *Streptomyces* sp. K01-0031. *J. Antibiot.* 58, 74–78. doi: 10.1038/ja.2005.10

Skropeta, D. (2008). Deep-sea natural products. *Nat. Prod. Rep.* 25, 1131–1166. doi: 10.1039/b808743a

Skropeta, D., and Wei, L. (2014). Recent advances in deep-sea natural products. *Nat. Prod. Rep.* 31, 999–1025. doi: 10.1039/c3np70118b

Strangman, W. K., Kwon, H. C., Broide, D., Jensen, P. R., and Fenical, W. (2009). Potent inhibitors of pro-inflammatory cytokine production produced by a marine-derived bacterium. *J. Med. Chem.* 52, 2317–2327. doi: 10.1021/jm801110j

Yao, C. B. F., Schiebel, M., Helmke, E., Anke, H., and Laatsch, H. (2006). Prefluostatin and new urauchimycin derivatives produced by *Streptomycete* isolates. *Z. Naturforsch.* 61, 320–325.

Zhang, Y., Huang, H., Xu, S., Wang, B., Ju, J., Tan, H., et al. (2015). Activation and enhancement of fredericamycin A production in deepsea-derived *Streptomyces somaliensis* SCSIO ZH66 by using ribosome engineering and response surface methodology. *Microb. Cell Fact.* 14:64. doi: 10.1186/s12934-015-0244-2

Conflict of Interest Statement: The authors declare that the research was conducted in the absence of any commercial or financial relationships that could be construed as a potential conflict of interest.

Copyright © 2017 Li, Huang, Hou, Ju and Li. This is an open-access article distributed under the terms of the Creative Commons Attribution License (CC BY). The use, distribution or reproduction in other forums is permitted, provided the original author(s) or licensor are credited and that the original publication in this journal is cited, in accordance with accepted academic practice. No use, distribution or reproduction is permitted which does not comply with these terms.

frontiers in Microbiology

ORIGINAL RESEARCH
published: 05 May 2017
doi: 10.3389/fmicb.2017.00813

The Biosynthetic Gene Cluster for Andrastin A in *Penicillium roqueforti*

*Juan F. Rojas-Aedo[1†], Carlos Gil-Durán[1†], Abdiel Del-Cid[1], Natalia Valdés[1], Pamela Álamos[1], Inmaculada Vaca[2], Ramón O. García-Rico[3], Gloria Levicán[1], Mario Tello[1] and Renato Chávez[1]**

[1] Departamento de Biología, Facultad de Química y Biología, Universidad de Santiago de Chile, Santiago, Chile, [2] Departamento de Química, Facultad de Ciencias, Universidad de Chile, Santiago, Chile, [3] GIMBIO Group, Department of Microbiology, Faculty of Basic Sciences, Universidad de Pamplona, Pamplona, Colombia

Penicillium roqueforti is a filamentous fungus involved in the ripening of several kinds of blue cheeses. In addition, this fungus produces several secondary metabolites, including the meroterpenoid compound andrastin A, a promising antitumoral compound. However, to date the genomic cluster responsible for the biosynthesis of this compound in *P. roqueforti* has not been described. In this work, we have sequenced and annotated a genomic region of approximately 29.4 kbp (named the *adr* gene cluster) that is involved in the biosynthesis of andrastin A in *P. roqueforti*. This region contains ten genes, named *adrA*, *adrC*, *adrD*, *adrE*, *adrF*, *adrG*, *adrH*, *adrI*, *adrJ* and *adrK*. Interestingly, the *adrB* gene previously found in the *adr* cluster from *P. chrysogenum*, was found as a residual pseudogene in the *adr* cluster from *P. roqueforti*. RNA-mediated gene silencing of each of the ten genes resulted in significant reductions in andrastin A production, confirming that all of them are involved in the biosynthesis of this compound. Of particular interest was the *adrC* gene, encoding for a major facilitator superfamily transporter. According to our results, this gene is required for the production of andrastin A but does not have any role in its secretion to the extracellular medium. The identification of the *adr* cluster in *P. roqueforti* will be important to understand the molecular basis of the production of andrastin A, and for the obtainment of strains of *P. roqueforti* overproducing andrastin A that might be of interest for the cheese industry.

Keywords: *Penicillium roqueforti*, fungal secondary metabolism, andrastin A, gene cluster, RNA-mediated gene silencing

OPEN ACCESS

Edited by:
Mostafa Rateb,
University of the West of Scotland, UK

Reviewed by:
Antje Labes,
University of Applied Sciences Flensburg, Germany
Giovanna Cristina Varese,
University of Turin, Italy

****Correspondence:***
Renato Chávez
renato.chavez@usach.cl

† These authors have contributed equally to this work.

Specialty section:
This article was submitted to Microbiotechnology, Ecotoxicology and Bioremediation, a section of the journal Frontiers in Microbiology

Received: *01 February 2017*
Accepted: *20 April 2017*
Published: *05 May 2017*

Citation:
Rojas-Aedo JF, Gil-Durán C, Del-Cid A, Valdés N, Álamos P, Vaca I, García-Rico RO, Levicán G, Tello M and Chávez R (2017) The Biosynthetic Gene Cluster for Andrastin A in Penicillium roqueforti. Front. Microbiol. 8:813. doi: 10.3389/fmicb.2017.00813

INTRODUCTION

Andrastin A is a meroterpenoid compound produced by several fungi from the genus *Penicillium* (Nielsen et al., 2005; Sonjak et al., 2005; Visagie et al., 2014). This metabolite has interesting biological activities that make it a promising antitumoral compound. Andrastin A inhibits the farnesyltransferase activity of the oncogenic Ras proteins, and also promotes the intracellular accumulation of anticancer compounds in tumoral cells (Uchida et al., 1996; Rho et al., 1998).

Regarding the biosynthesis of andrastin A by fungi, early studies (Uchida et al., 1996) suggested that this compound is derived from a farnesyl pyrophosphate and, at that time, an unknown tetraketide (later known as 3,5-dimethylorsellinic acid, DMOA). More recently, a genomic cluster (the *adr* cluster) that is responsible for the andrastin A biosynthesis in *Penicillium chrysogenum*, was identified (Matsuda et al., 2013). The *adr* cluster from *P. chrysogenum* contains eleven genes

named *adrA* (encoding a cytochrome P450 monooxygenase), *adrB* (encoding a protein with unknown function), *adrC* (encoding a putative major facilitator superfamily (MSF) transporter), *adrD* (encoding a polyketide synthase, PKS), *adrE* (encoding a ketoreductase), *adrF* (encoding a short chain dehydrogenase/reductase), *adrG* (encoding a prenyltransferase), *adrH* (encoding a FAD-dependent monooxygenase), *adrI* (encoding a terpene cyclase), *adrJ* (encoding an acetyl transferase) and *adrK* (encoding a methyl transferase) (Matsuda et al., 2013).

Based on the fact that *adrD*, *adrG*, *adrK*, and *adrH* have high similarity to their respective homologous genes of the austinol and terretonin biosynthetic gene clusters, Matsuda et al. (2013) hypothesized the four first putative steps of the andrastin A biosynthesis in *P. chrysogenum*. They proposed that the four enzymes encoded by *adrD*, *adrG*, *adrK* and *adrH* would act consecutively to produce epoxyfarnesyl-DMOA methyl ester from the primary metabolites acetyl CoA, malonyl CoA and *S*-adenosylmethionine. From this point, and by using the heterologous co-expression of *adrI*, *adrF*, *adrE*, *adrJ,* and *adrA* in a strain of *Aspergillus oryzae* that produces epoxyfarnesyl-DMOA methyl ester, they were able to experimentally reconstitute the rest of the pathway until the formation of andrastin A (Matsuda et al., 2013). Thus, currently five out of the eleven *adr* genes from *P. chrysogenum* (*adrI*, *adrF*, *adrE*, *adrJ,* and *adrA*) have been experimentally shown to be involved in andrastin A biosynthesis, whereas other four genes (*adrD*, *adrG*, *adrK,* and *adrH*) are probably involved in the biosynthesis of this compound, but this has not been experimentally demonstrated yet. Finally, the putative roles of the *adrB* and *adrC* genes in andrastin A biosynthesis pathway remain as unknown.

Penicillium roqueforti is a filamentous fungus widely used in the production of blue-veined cheeses, such as Roquefort, Stilton, and others (Fernández-Bodega et al., 2009). In addition, and like other filamentous fungi, *P. roqueforti* is an active producer of secondary metabolites. Thus, this species produces mycotoxins (such as roquefortine C and PR-toxin), and bioactive compounds such as mycophenolic acid and andrastin A (García-Estrada and Martín, 2016). In *P. roqueforti*, the gene clusters responsible for the biosynthesis of roquefortine C, PR-toxin and mycophenolic acid have been recently identified (Kosalková et al., 2015; Del-Cid et al., 2016; Hidalgo et al., 2016). However, to date the genes responsible for the biosynthesis of andrastin A in this fungus remain as unknown. Interestingly, *P. roqueforti* produces andrastin A during cheese ripening (Nielsen et al., 2005; Fernández-Bodega et al., 2009). Taking into account the potential positive effects of andrastin A on human health, it has been proposed that strains of *P. roqueforti* overproducing this compound might be of interest for the future production of "functionalized cheeses" with higher quantities of andrastin A (Albillos et al., 2011). For these purposes, the knowledge of the genes involved in the biosynthesis of andrastin A in *P. roqueforti* would be very useful.

In the present work, we have sequenced and annotated a genomic region containing the biosynthetic gene cluster for andrastin A in *P. roqueforti*. In addition, we performed the functional characterization of each gene of that cluster by using RNA interference.

MATERIALS AND METHODS

Fungal Strains and Culture Media

Penicillium roqueforti strain CECT 2905 (ATCC 10110) was used in this work. This strain and all the transformants obtained in this work were kept on Potato dextrose agar (Merck, Germany), excepting when andrastin A production was required. In these cases, the strains were grown on YES agar [Bacto Yeast Extract (Difco, USA) 20 g/L, sucrose (Merck, Germany, biochemical grade) 150 g/L and Bacto Agar (Difco, USA) 20 g/L].

Sequencing and Identification of the Andrastin A Gene Cluster of *P. roqueforti* CECT 2905

DNA from *P. roqueforti* CECT 2905 was obtained as described before (Gil-Durán et al., 2015). This DNA was used to perform the sequencing of the *P. roqueforti* CECT 2905 genome, by using Illumina technology. This genome was assembled in several contigs and currently is under annotation (unpublished data). We take advantage of this genome sequence to identify the *adr* cluster from *P. roqueforti* CECT 2905 as follows: the *adrD* gene from *P. chrysogenum* (7,930 nucleotides) encoding the putative PKS, was used to scan all the contigs from *P. roqueforti* CECT 2905 by BlastN. One contig containing a gene with very high similarity to *adrD* (coverage 99%, identity 84%, and *E*-value closer to zero) was obtained. Then, the vicinities of this gene were compared to the rest of the *adr* cluster from *P. chrysogenum* by BlastX, BlastP, and BlastN, revealing the presence of the rest of the *adr* genes, excepting *adrB* (see Results). All the genes were manually analyzed, delimited, and annotated using a combination of the Blast tools, multiple alignments by Clustal Omega, and the Translate Tool from Expasy web interface[1].

The nucleotide sequence of the *adr* gene cluster from *P. roqueforti* CECT 2905 described in this work has been deposited in the GenBank database under accession number KY349137.

Construction of RNA-Silencing Plasmids and Transformation of *P. roqueforti*

To silence the ten genes of the *adr* cluster of *P. roqueforti,* RNA-mediated gene silencing technology was used. The strategy was essentially the same described by Del-Cid et al. (2016). Briefly, a small sequence of each gene was amplified by PCR using suitable primers (Supplementary Table S1). Each amplicon was digested with *Nco*I and then, ligated into plasmid pJL43-RNAi (Ullán et al., 2008) previously digested with the same restriction enzyme, thus giving rise to ten RNAi-silencing constructs (pJL-RNAi-adrA to pJL-RNAi-adrK, Supplementary Table S1 and Figure S1). These constructs were then used to transform *P. roqueforti*, exactly as was described before (Gil-Durán et al., 2015).

[1]http://web.expasy.org/translate/

RT-qPCR Experiments

For RT-qPCR experiments, total RNA was purified as described previously (Gil-Durán et al., 2015) and quantified in a MultiSkan GO quantification system (Thermo Scientific, Germany). Two μg of RNA were used to synthesize cDNA using RevertAid Reverse Transcriptase (Thermo Scientific, Germany). For each RT-qPCR reaction (20 μl) the following conditions were set: 10 μl of KAPA SYBR Fast qRT-PCR Master Mix 2x (Kapa Biosystems, USA), 0.4 μl of each primer (at a concentration of 10 μM each), 0.4 μl de 50x ROX High/Low, 6.8 μl of water and 2 μl of the cDNA previously synthesized. RT-qPCR reactions were carried out in the StepOne Real-Time PCR System (Applied Biosystems, USA). Amplification conditions were 20 s at 95°C and 40 cycles of 3 s at 95°C and 30 s at 50°C. Three replicates were performed for each analysis and suitable negative controls were included. Relative gene expression values were determined by the comparative Ct (ΔΔCt) method using β-tubulin gene expression as a normalization control. The sequences of the primer sets used in RT-qPCR experiments are described in the Supplementary Table S2.

Extraction of Andrastin A and HPLC Analysis

The extraction of andrastin A was done using the same method described by Del-Cid et al. (2016). Briefly, the fungal strains were grown on YES agar for 7 days at 28°C. The selected sample (mycelium or triturated agar) was extracted overnight with 50 mL of an ethyl acetate: dichloromethane: methanol (3:2:1) mixture containing formic acid (1%). After that, the mixtures were sonicated during 30 min and filtered through a 0.45 μm Millex-HV hydrophilic PVDF syringe filter (Merck Millipore). The filtrated was evaporated to dryness in a rotary evaporator, resuspended in 500 μl of methanol (HPLC grade) and submitted to HPLC analysis. The HPLC equipment used consists in a Waters 1525 HPLC system (Waters, Ireland) equipped with a Waters 1525 Binary HPLC pump, a Waters 2996 Photodiode Array (PDA) Detector and a 4.6 × 250 mm (5 μm) SunFire C18 column. HPLC runs were performed as was described by Del-Cid et al. (2016): samples (20 μL) were injected into the HPLC using water (solvent A) and acetonitrile (solvent B), both acidified with 0.02% trifluoroacetic acid. The elution gradient was as follows: 15% solvent B to 68% solvent B linear over 25 min, 68% solvent B to 100% solvent B linear over 2 min, isocratic for 5 min and 100% solvent B to 15% solvent B linear over 2 min. The flow used was 1.2 mL/min and the column was held at 35°C.

Under the HPLC conditions described above, andrastin A was identified by the "spiking" technique. Briefly, known amounts of pure andrastin A (Santa Cruz Biotechnology, Dallas, TX, USA) were added to the samples (spiked samples). As control, non-spiked samples were used. In all the spiked samples, a single peak (with retention time of 24.72 min) increased its size. The increase of the peak size was proportional to the amount of pure andrastin A added. No increase of the peak size was observed in non-spiked samples and no new chromatographic peaks or "shoulder peaks" were seen in the spiked samples. Moreover, the identity of the peak was confirmed by UV-Vis absorption spectrum (200–600 nm). Both the UV-Vis spectrum and the retention time of the peak were identical to those observed for the pure andrastin A.

Finally, the quantity of andrastin A of each sample was obtained from a calibration curve constructed with the pure compound as standard and the UV detector set at 254 nm. The quantity of andrastin A obtained was normalized to the dry weight of the fungal mycelia. For this purpose, the mycelium of each *P. roqueforti* strain was dried as described before (García-Rico et al., 2009).

RESULTS

Identification and Bioinformatics Analysis of the Andrastin A Gene Cluster in *Penicillium roqueforti* CECT 2905

To find the *adr* gene cluster in *P. roqueforti* CECT 2905, we sequenced and scanned its genome as was described in Material and Methods. As a result, a genomic region of approximately 29.4 kbp containing 10 genes was identified (**Figure 1**). This region has high similarity (84% overall identity) to the *adr* gene cluster from *P. chrysogenum* (Matsuda et al., 2013). Thus, according to the nomenclature of their orthologs in *P. chrysogenum*, the genes found in the *P. roqueforti adr* cluster were named *adrA*, *adrC*, *adrD*, *adrE*, *adrF*, *adrG*, *adrH*, *adrI*, *adrJ,* and *adrK* (**Figure 1**). At this point, it should be noted that recently, the genome of another *P. roqueforti* strain (named FM164) was sequenced and annotated (Cheeseman et al., 2014). We also analyzed this genome and as expected, we found the *adr* cluster. The *adr* clusters from both *P. roqueforti* strains have identical size, contain the same 10 genes with identical organization, and are almost identical at nucleotide level (only 75 nucleotide differences in 29,321 total nucleotides, representing 99% overall identity, 100% coverage and no gaps). In **Table 1**, the correspondence between each *adr* gene from strain CECT 2905 and the respective ORF from the genome of strain FM164 is described.

Despite several efforts, we did not found any ORF with similarity to the *adrB* gene from *P. chrysogenum* in the *P. roqueforti* genome. Specifically, we used the *adrB* gene from *P. chrysogenum* and its deduced protein to exhaustively scan the whole genome of *P. roqueforti* CECT 2905 using several bioinformatics analysis (BlastN, BlastX, tBlastN) with no positive results. It should be noted that this gene was not found either in the genome of *P. roqueforti* strain FM164 (Cheeseman et al., 2014), suggesting that its absence is a common fact in *P. roqueforti* strains.

Recently, it has been suggested that some fungal gene clusters can suffer reorganization processes leading to the total or partial loss of some genes (Martín and Liras, 2016). In accordance with this suggestion, it can be hypothesized that the *adrB* gene originally present in *P. chrysogenum* was entirely or partially

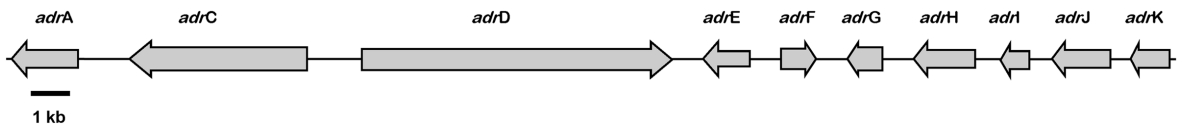


FIGURE 1 | Schematic organization of the *adr* gene cluster in *P. roqueforti* CECT 2905. The arrows represent the genes and the direction of their transcription. The organization of the *adr* cluster in *P. roqueforti* FM164 (Cheeseman et al., 2014) is identical (data not shown).

TABLE 1 | Analysis of the deduced proteins encoded by the *adr* cluster of *P. roqueforti* CECT 2905.

Gene name in *P. roqueforti*				
Strain CECT 2905[a]	**Strain FM164[b]**	**Size of the deduced protein[c] (aminoacids)**	**Putative function in andrastin A biosynthesis[d]**	**Identity (%) with orthologous proteins of the *P. chrysogenum adr* cluster**
adrA	Proq04g062820	508	Cytochrome P450 monooxygenase	94
adrC	Proq04g062830	1,452	MFS transporter	83
adrD	Proq04g062840	2,495	Polyketide synthase	83
adrE	Proq04g062850	336	Ketoreductase	89
adrF	Proq04g062860a	256	Short chain dehydrogenase	91
adrG	Proq04g062870	316	Prenyltransferase	87
adrH	Proq04g062880a	476	FAD-dependent monooxygenase	83
adrI	Proq04g062890	245	Terpene cyclase	94
adrJ	Proq04g062900	496	Acetyltransferase	85
adrK	Proq04g062910	278	Methyltransferase	94

[a]*The adr gene cluster from P. roqueforti CECT 2905 can be found at GenBank under accession number KY349137.* [b]*Gene nomenclature according to the original annotation of the genome of strain FM164 (Cheeseman et al., 2014). In this genome, the adr gene cluster is contained in the genomic scaffold ProqFM164S01 (GenBank accession number HG792015).* [c]*The sizes of the deduced proteins in strains CECT 2905 and FM164 are identical.* [d]*Putative functions of the orthologous proteins of the P. chrysogenum adr cluster (Matsuda et al., 2013).*

lost in the *adr* cluster from *P. roqueforti*. To address this hypothesis, we take the region comprising the intergenic zone between *adrA* and *adrC* in *P. roqueforti* and we compared it with the syntenic region from the *P. chrysogenum* genome. A first interesting observation was that the intergenic zone between *adrA* and *adrC* in *P. roqueforti* is 1,444 nucleotides shorter that the syntenic region from *P. chrysogenum* (1,218 bp vs. 2,662 bp; **Figure 2A**), supporting the possibility that the *adrB* gene was total or partially lost in *P. roqueforti*. Using these regions, we performed several alignments using nucleotide and protein sequences, and we found that the *adrB* gene in *P. roqueforti* was partially lost and is found as a residual pseudogene (**Figure 2B**). In this pseudogene, the first 10 aminoacids almost exactly match to the first 10 aminoacids of the AdrB protein from *P. chrysogenum* (**Figure 2B**). However, from this point, a deletion of 49 nucleotides (and other minor insertion/deletion events) changes the sequence and produces in-frame stop codons in all the frame shifts (**Figure 2B**). Finally, and due to additional four consecutive deletion events in the pseudogene, the similarity between these sequences is entirely lost.

Finally, regarding the deduced proteins encoded by the *adr* genes from *P. roqueforti*, **Table 1** summarizes the sizes and putative functions of these proteins. As can be observed, all the deduced proteins have high similarity to their respective orthologs from *P. chrysogenum* (between 83 and 94% identities), suggesting that in *P. roqueforti*, these proteins should perform the same function assigned in *P. chrysogenum*.

RNA-Mediated Silencing of the Ten Genes of the *adr* Cluster from *Penicillium roqueforti* CECT 2905

To test the participation of each gene of the *adr* cluster from *P. roqueforti* CECT 2905 in andrastin A biosynthesis, we employed RNA-mediated gene-silencing technology. This technology has been widely used to demonstrate the functionality of several biosynthetic gene clusters in *P. roqueforti* (Kosalková et al., 2015; Del-Cid et al., 2016; Hidalgo et al., 2016). For this purpose, ten suitable plasmids were constructed and used to transform *P. roqueforti* CECT 2905 (see Material and Methods for details).

In each transformation event, around 40–50 phleomycin-resistant transformants were obtained. From each transformation event, fifteen transformants were chosen randomly and submitted to preliminary RT-PCR analysis (data not shown). Those two transformants showing the most significant decrease in the mRNA level were selected for further quantification of the down-regulation using RT-qPCR (**Figure 2**). The results indicate that depending on the gene, the transformants selected exhibited between 1.4- and 10- fold of decrease in mRNA levels compared with the wild-type strain of *P. roqueforti* (**Figure 3**), confirming the successful knock-down of all the genes of the *adr* cluster. Additionally, in all cases the presence of the full silencing cassette was confirmed (Supplementary Figure S1). The transformants selected were used for further analysis.

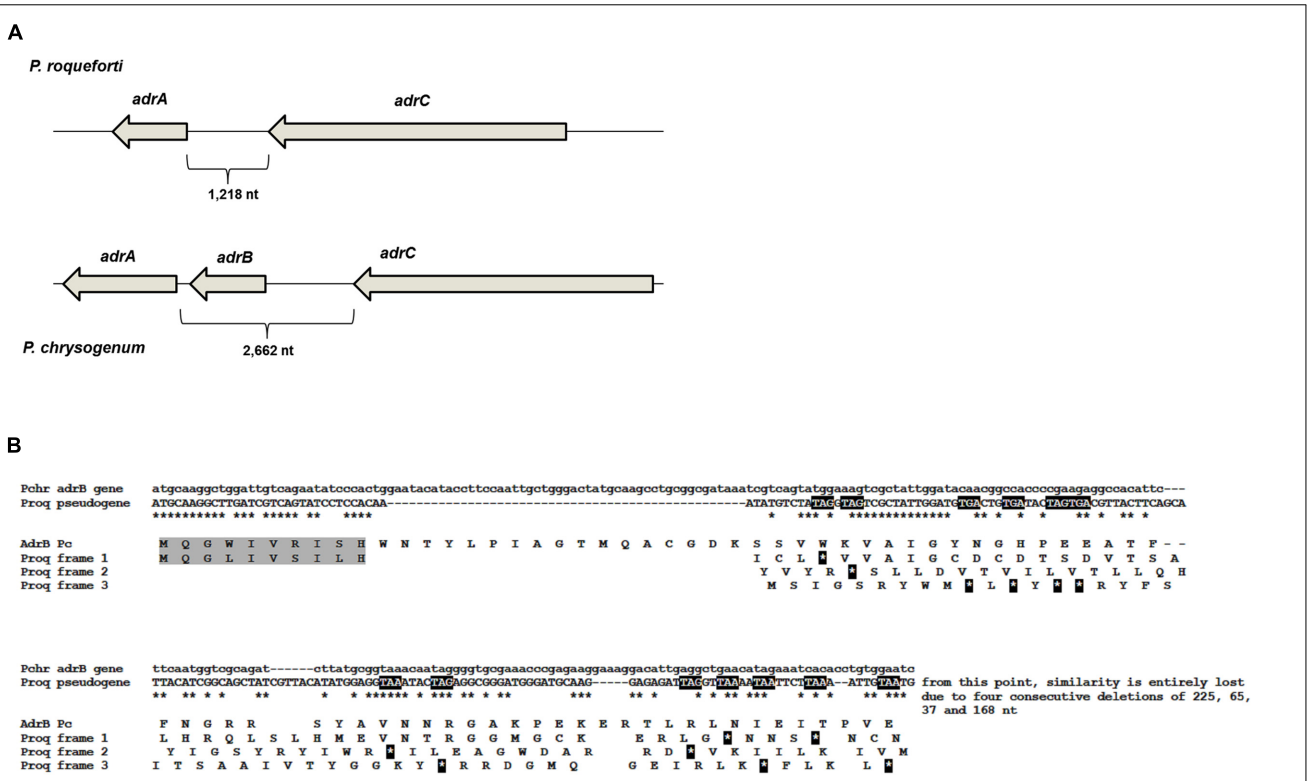


FIGURE 2 | Comparison between the zones comprising *adrA* to *adrC* in *P. roqueforti* and *P. chrysogenum*. (A) Schematic comparison between these zones. The drawings are at scale. In *P. chrysogenum*, the *adrB* gene is included. Please note the difference in the size of these regions between *P. roqueforti* and *P. chrysogenum*. **(B)** Alignment of the nucleotide sequence (5′ end) of the *adrB* gene from *P. chrysogenum* (PchradrB gene) and the pseudogene found in *P. roqueforti* (Proq pseudogene). The first 30 nucleotides (and their 10 deduced aminoacids, highlighted in gray box) show high similarity. However, a deletion of 49 nucleotides in the pseudogene (plus other minor deletion/insertion events) results in several in-frame translations stop codons (highlighted in black boxes). As a consequence, after translation, protein fragments resulting show very low similarity to AdrB from *P. chrysogenum* in the three reading frames. The sequence of the pseudogene shown is the only part that shows some degree of similarity. After this sequence, and due to four consecutive deletions in the pseudogene, the similarity between these regions is entirely lost.

Effect of *adrI*, *adrF*, *adrE*, *adrJ,* and *adrA* Silencing on Andrastin A Production in *Penicillium roqueforti* CECT 2905

Previously, the participation of *adrI*, *adrF*, *adrE*, *adrJ* and *adrA* genes in the biosynthesis of andrastin A in the fungus *P. chrysogenum* was experimentally demonstrated (Matsuda et al., 2013). Therefore, as first approach, we tested if their orthologs in *P. roqueforti* are effectively involved in the andrastin A biosynthesis. For this purpose, RNA-mediated silenced transformants were obtained (see above) and they were used to evaluate the production of andrastin A by HPLC (**Figure 4**). As control, *P. roqueforti* CECT 2905 (wild-type strain) and a strain harboring empty plasmid pJL43-RNAi were used.

Silencing of the five genes aforementioned drastically reduced the production of andrastin A by *P. roqueforti* CECT 2905 (**Figure 4**). Specifically, transformants with attenuated levels of *adrI*, *adrF*, *adrE*, *adrJ* and *adrA* transcripts produced between 14 and 57.7% of the andrastin A produced by the wild-type strain, depending on the gene and the transformant analyzed (**Figure 4**). These results experimentally confirm the participation of these genes in the production of andrastin A by *P. roqueforti*.

Effect of *adrD*, *adrG*, *adrK*, and *adrH* Silencing on Andrastin A Production in *Penicillium roqueforti* CECT 2905

It has been hypothesized that *adrD*, *adrG*, *adrK* and *adrH* encode for four enzymes that would act consecutively in the four first putative steps of the andrastin A biosynthesis (Matsuda et al., 2013). However, to the best of our knowledge, the role of these genes has not been experimentally tested yet. Therefore, it was of great interest to address the participation of these genes in the biosynthesis of andrastin A in *P. roqueforti*.

Silencing of the *adrD*, *adrG*, *adrK*, and *adrH* genes drastically reduced the production of andrastin A by *P. roqueforti* CECT 2905 (**Figure 4**). Specifically, transformants with attenuated levels of *adrD*, *adrG*, *adrK*, and *adrH* transcripts produced between 8.6 and 56.7 % of the andrastin A produced by the wild-type strain, depending on the gene and the transformant analyzed (**Figure 4**). These results provide the first experimental support for the participation of *adrD*, *adrG*, *adrK* and *adrH* in the *in vivo* production of andrastin A by fungi.

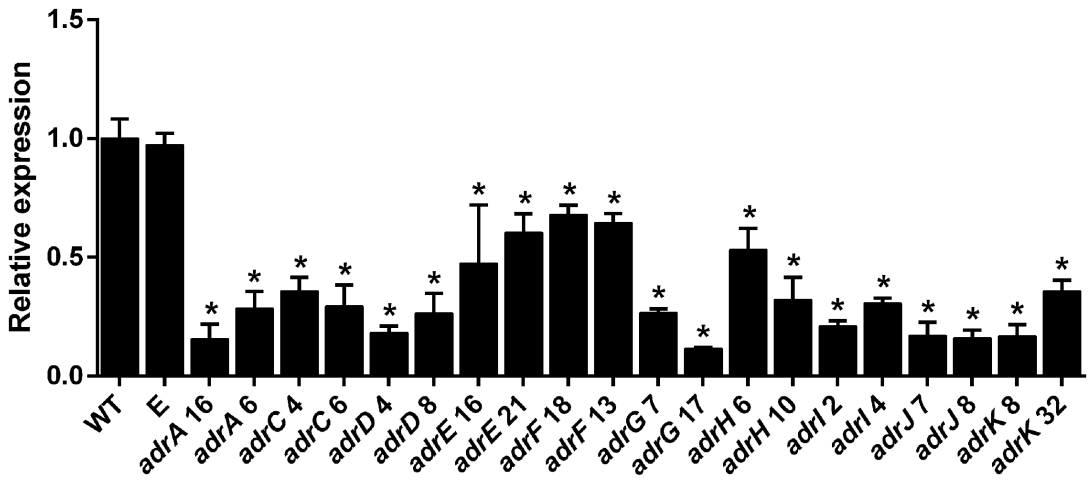


FIGURE 3 | qRT-PCR analysis of the expression of *adr* genes in the RNAi-silenced transformants of *P. roqueforti* CECT 2905. Two transformants were selected for each gene. They were adrA6, adrA16, adrC4, adrC6, adrD4, adrD8, adrE16, adrE21, adrF13, adrF18, adrG7, adrG17, adrH6, adrH10, adrI2, adrI4, adrJ7, adrJ8, adrK 8 and adrK 32. As controls, *P. roqueforti* CECT 2905 (WT) and *P. roqueforti* CECT 2905 containing empty pJL43-RNAi vector (E) were used. Error bars represent the standard deviation of three replicates in three different experiments. The symbol *indicates that reductions in the expression of the genes in RNAi-silenced transformants were statistically significant ($P < 0.05$ using Student's *t*-test) respect to the wild-type strain and *P. roqueforti* CECT 2905 containing empty pJL43-RNAi.

The *adrC* Gene, Encoding for a MFS Transporter, Is Required for the Production of Andrastin A But Does Not Have a Significant Role in Its Secretion

The protein encoded by *adrC* has high similarity with MFS transporters proteins (**Table 1**). MSF proteins are ubiquitous membrane proteins that are responsible for the movement of a wide range of substrates across biological membranes (Quistgaard et al., 2016). In the case of genes encoding for MSF proteins located into fungal biosynthetic gene clusters, it has been suggested that these proteins could be involved in the secretion of the secondary metabolites produced (Martín et al., 2005; Martín and Liras, 2016). Therefore, we tested if *adrC* could influence andrastin A production and/or secretion. Interestingly, the silencing of *adrC* drastically reduced the production of andrastin A by *P. roqueforti* CECT 2905 (**Figure 3**). The transformants with attenuated levels of *adrC* transcripts produced between 15.2 and 18.7 % of the andrastin A produced by the wild-type strain (**Figure 4**), suggesting that *adrC* is necessary for the production of andrastin A.

Regarding a putative role of *adrC* in andrastin A secretion, we compared the quantity (μg) of the compound found in mycelium and agar medium (**Figure 5A**). The result, expressed as the percentage of the total andrastin A produced by the strain, indicates that the quantity of andrastin A found in agar and mycelium is similar in the wild type strain and the transformants with attenuated levels of *adrC* transcripts. The same result was obtained when all the rest of strains with *adr* genes attenuated were analyzed (**Figure 5A**). In addition, in order to assess a putative effect of the volume of the sample used (agar or mycelium) we also compared the concentrations (μg/mL) of andrastin A in these samples. Our results indicate that the concentrations of andrastin A in the cells of the transformants with attenuated levels of *adrC* transcripts are around three times higher than those found in agar (**Figure 5B**). However, this effect was not specific to *adrC* and was observed in all the strains, including the wild-type strain (**Figure 5B**). Taken together, these results suggest that *adrC* (or any other gene from the *adr* cluster) has no specific role in andrastin A secretion.

DISCUSSION

Penicillium roqueforti strain CECT 2905 produces several secondary metabolites and currently, the gene clusters responsible for the biosynthesis of three of them, namely roquefortine C, PR-toxin and mycophenolic acid, have been identified (Kosalková et al., 2015; Del-Cid et al., 2016; Hidalgo et al., 2016). Here we describe the gene cluster responsible for the biosynthesis of another secondary metabolite from this fungus, andrastin A, a promising antitumoral compound. In *P. roqueforti* CECT 2905, the *adr* gene cluster comprises a genomic region of approximately 29.4 kbp and contains ten genes. More interesting, the silencing of all of them resulted in significant reductions in andrastin A production, confirming their involvement in the biosynthesis of this compound.

As was stated before (see Introduction), Matsuda et al. (2013) experimentally reconstituted the last steps in the formation of andrastin A from the intermediate epoxyfarnesyl-DMOA methyl ester, by using the heterologous co-expression of *adrI*, *adrF*, *adrE*, *adrJ* and *adrA* genes from *P. chrysogenum* in an *A. oryzae* strain that produces the mentioned

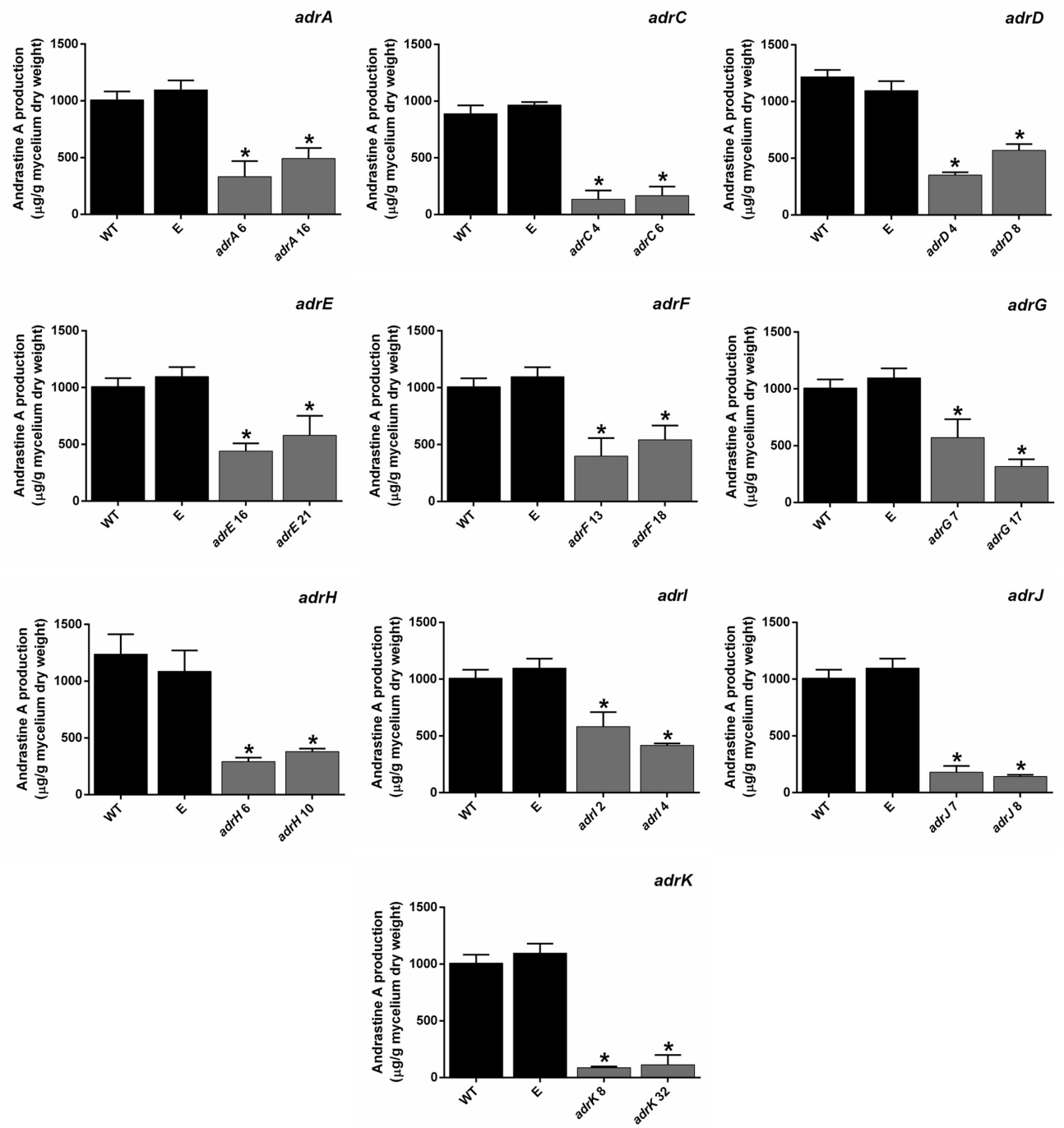


FIGURE 4 | Production of andrastin A by *P. roqueforti* strains. For a best comparison, data for each gene is shown separately. RNAi-silenced transformants are the same described in **Figure 3**. Metabolites were extracted, quantified and normalized by the dry weight of the fungal mycelia as described in Section "Materials and Methods." Error bars represent the standard deviation of three replicates in three independent experiments. The symbol *indicates that reductions in andrastin A production by RNAi-silenced transformants were statistically significant ($P < 0.05$ using Student's *t*-test). As can be observed, production of andrastin A by *P. roqueforti* CECT 2905 containing empty pJL43-RNAi vector was statistically indistinguishable from the wild-type strain.

intermediate. In agreement with these results, here we show the participation of their orthologous genes in the biosynthesis of andrastin A by *P. roqueforti*. In *P. chrysogenum*, *adrI*, *adrF*, *adrE*, *adrJ,* and *adrA* encode for a terpene cyclase, a short chain dehydrogenase/reductase, a ketoreductase, an acetyl transferase and a cytochrome P450 monooxygenase,

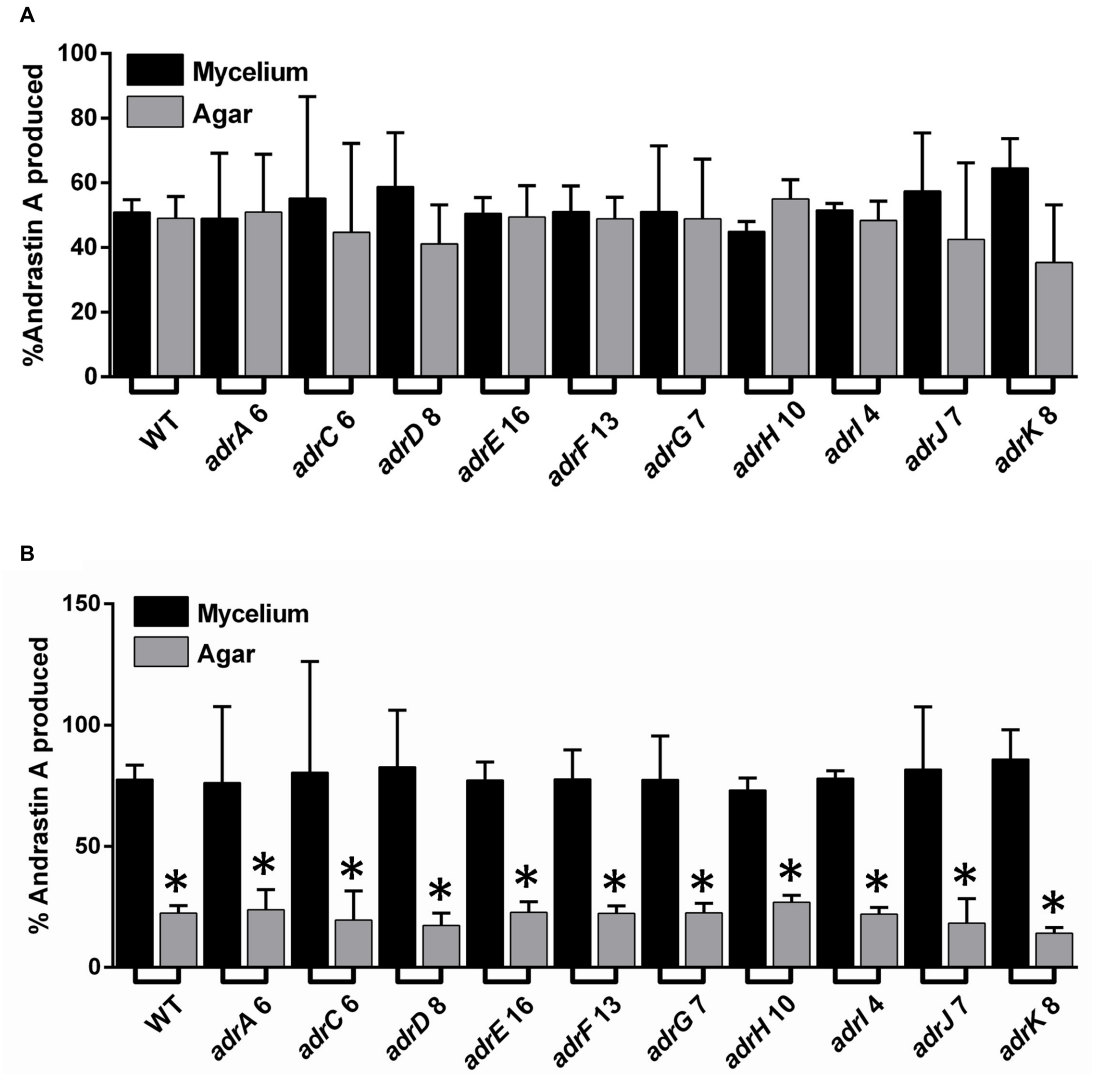


FIGURE 5 | Comparison of the levels of andrastin A found in mycelium and agar in *P. roqueforti* strains. (A) Comparison of the quantity (μg) of andrastin A found in mycelium and agar. For simplicity, only one transformant is shown for each gene. Each strain was grown on solid YES medium for 7 days, and andrastin A was extracted separately from both the mycelium and agar as described in Section "Materials and Methods." In each case, the quantity (μg) of andrastin A found in mycelium and agar is shown as percentage (%) of the total quantity of andrastin A produced by the strain. Error bars represent the standard deviation of three replicates in three independent experiments. As can be observed, in all cases no significant differences were found between the percentage of andrastin A in the mycelium and the agar (Student's *t*-test, $P < 0.05$). **(B)** Comparison of the concentrations (μg/mL) of andrastin A in mycelium and agar. Andrastin A was quantified as above, and in each case, the volume of the mycelium or agar was used to calculate concentration. Results are shown as percentages. Error bars represent the standard deviation of three replicates in three different experiments. The symbol *indicates that the differences in andrastin A concentration between mycelium and the agar were statistically significant ($P < 0.05$ using Student's *t*-test).

respectively. All these proteins from *P. chrysogenum* have very high similarity to their orthologs from *P. roqueforti* (**Table 1**), strongly suggesting that they may catalyze the same reactions in the biosynthetic pathway of andrastin A in *P. roqueforti*.

Regarding the four enzymes encoded by *adrD*, *adrG*, *adrK* and *adrH*, it has been hypothesized that they would act consecutively in the four first steps of the andrastin A biosynthesis (Matsuda et al., 2013). However, to the best of our knowledge, the participation of these genes in the biosynthesis of andrastin A has not been experimentally tested thus far in any fungus. Our results provide the first experimental support for the participation of these genes in the *in vivo* production of andrastin A by fungi.

Compared with *P. roqueforti*, the *adr* cluster from *P. chrysogenum* contains one additional gene named *adrB*, which was found as a residual pseudogene in the *P. roqueforti adr* cluster (**Figure 2**). Recently, Martín and Liras (2016) have suggested that during their evolutionary formation, some fungal gene clusters can suffer drastic reorganization processes. As a

product of this reorganization, some genes could be entirely lost, whereas other genes could be partially lost and found as residual pseudogenes. In accordance with this proposal, our results suggest that the *adrB* gene originally present in *P. chrysogenum* was partially lost in the *adr* cluster from *P. roqueforti*. The loss of genes in a *P. roqueforti* gene cluster, compared with the respective *P. chrysogenum* cluster, has been observed before in the roquefortine C/ meleagrin gene cluster. In *P. chrysogenum*, this cluster contains seven genes, whereas in *P. roqueforti* it is shorter and contains four genes (Kosalková et al., 2015). In this case, the evolutionary reorganization of the cluster produced that two genes present in *P. chrysogenum* were entirely lost in *P. roqueforti*, whereas a third gene was partially lost and now is found as a residual pseudogene (Kosalková et al., 2015; Martín and Liras, 2016). These data and our observation about the pseudogenization of *adrB* in the *adr* cluster suggest that the evolutionary reorganization in clusters from *P. chrysogenum* and *P. roqueforti* may be a common and extended process.

Taking into account the pseudogenization of *adrB* in *P. roqueforti*, an interesting question arises: is *adrB* a functional gene in *P. chrysogenum*? In the *P. chrysogenum* genome (GenBank accession number AM920437), the *adrB* gene corresponds to ORF Pc22g22830 of 1,162 bp, encoding a protein of 232 aminoacids annotated as "hypothetical protein." In accordance with that, Matsuda et al. (2013) did not assign any function to the *adrB* gene in the andrastin A biosynthetic pathway in *P. chrysogenum*. We performed our own BlastP search using the deduced AdrB protein, and we did not found similarity with any protein in the whole GenBank database (data not shown). In a first view, these data suggest that *adrB* may represent an ORF defined by *in silico* annotation, but it may not be a functional gene from *P. chrysogenum*. However, some evidences call into question this explanation. Specifically, two transcriptomic assays by microarray performed on *P. chrysogenum* have found expression of mRNAs from ORF Pc22g22830 (van den Berg et al., 2008; Becker et al., 2016), indicating that *adrB* is actively transcribed in *P. chrysogenum*. Thus, taking into account that at least at transcriptional level, *adrB* seems to be a functional gene in *P. chrysogenum*, in the future it would be interesting to test if *adrB* has any role in andrastin A biosynthesis in this fungus.

Our results suggest that the *adrC* gene encoding for a putative MSF transporter is necessary for the production of andrastin A by *P. roqueforti*. In literature, there are other cases where genes encoding MSF proteins are necessaries for the production of secondary metabolites by fungi. For example, in *Cercospora kikuchii* and *Fusarium fujikuroi*, the disruption of genes encoding MSF transporters leads to drastic reductions in the production of cercosporin and bikaverin, respectively (Callahan et al., 1999; Wiemann et al., 2009). Currently, it remains unclear how the disruption of genes encoding for MSF proteins can reduce the levels of production of fungal secondary metabolites. Callahan et al. (1999) suggested that the lack of MSF protein leads to the accumulation of the secondary metabolite above a critical threshold, producing the inhibition of biosynthetic enzymes or the down-regulation of the transcription of the biosynthetic genes. Another possibility is that these MSF proteins be intracellular transporters involved in the traffic of some intermediates of the biosynthesis (Martín and Liras, 2016). The absence of these transporters could be interfering in the normal intracellular transport of these intermediates, hence decreasing the production of the final secondary metabolite.

Interestingly, despite the *adrC* gene is required for the production of andrastin A, it does not have any role in the secretion of the compound to the extracellular medium. Although there are several cases where MSF transporters are clearly linked to the secretion of a given fungal secondary metabolite (see reviews of Martín et al., 2005; Martín and Liras, 2016), there are several other cases where the MSF transporters does not have role in the secretion of secondary metabolites. For example, when the *aflT* gene (encoding for a MFS transporter within the aflatoxin gene cluster in *A. parasiticus*) was disrupted, the deleted mutants secreted aflatoxins at similar levels to the wild type strain (Chang et al., 2004). Similarly, when the *mfsA* gene from *A. carbonarius* (encoding a MFS transporter in the ochratoxin A gene cluster) was deleted, ochratoxin A was found at similar levels both in mycelia and extracellular medium in all the strains analyzed (Crespo-Sempere et al., 2014). The same was observed in the case of the *roqT* gene from the roquefortine C/meleagrin cluster in *P. chrysogenum*: mutants disrupted in this MSF-encoding gene were still able to secrete roquefortine C, indicating that the protein encoded by *roqT* is not involved in the secretion of this compound (Ali et al., 2013).

According to our results, none of the *adr* genes from *P. roqueforti* is in charge of the secretion of andrastin A to the extracellular medium, so the secretion of this compound must to proceed by other mechanism. The simplest mechanism is passive diffusion across the plasmatic membrane. However, other active mechanisms cannot be ruled out. Chanda et al. (2009) showed that once synthesized, aflatoxin is exported to the extracellular medium by an exocytosis process leading by specialized vesicles, named aflatoxisomes. On the other hand, in *P. roqueforti* it has been suggested that the secretion of roquefortine C could be performed by additional redundant MSF transporters (the so-named "surrogate transporters," Kosalková et al., 2015). In the future, it will be very interesting to investigate whether any of these mechanisms may be responsible of andrastin A secretion in *P. roqueforti*.

AUTHOR CONTRIBUTIONS

IV, RG-R, GL, MT, and RC conceived and designed the experiments, contributed reagents/materials, analyzed the data and supervised work. JR-A, CG-D, AD-C, PA and IV carried out the experiments and analyzed the data. NV, IV, and MT performed genome sequencing, assembly, annotation, and genome analysis. JR-A, CG-D, AD-C, PA, and RC performed bioinformatics analysis. PA, IV, GL, and RC drafted the manuscript. All authors have read and approved the manuscript.

FUNDING

This work was supported by grants Fondecyt 1120833 and Proyectos Basal USA 1555-VRIDEI 021743CR_PUBLIC, Universidad de Santiago de Chile. MT and NV were supported by grant Basales USA1555 USACH-MECESUP. PA and GL were supported by grant Proyecto Basal USA1498. JR-A and CG-D have received doctoral fellowships CONICYT-PFCHA/DoctoradoNacional/2013-21130251 and CONICYT-PFCHA/Doctorado Nacional/2014-63140056, respectively.

ACKNOWLEDGMENT

The support of VRIDEI-USACH is acknowledged.

SUPPLEMENTARY MATERIAL

The Supplementary Material for this article can be found online at: http://journal.frontiersin.org/article/10.3389/fmicb.2017.00813/full#supplementary-material

REFERENCES

Albillos, S. M., García-Estrada, C., and Martín, J. F. (2011). "Spanish blue cheeses: functional metabolites," in *Cheese: Types, Nutrition and Consumption*, ed. R. D. Foster (New York, NY: Nova Science Publishers, Inc), 89–105.

Ali, H., Ries, M. I., Nijland, J. G., Lankhorst, P. P., Hankemeier, T., Bovenberg, R. A., et al. (2013). A branched biosynthetic pathway is involved in production of roquefortine and related compounds in *Penicillium chrysogenum*. *PLoS ONE* 8:e65328. doi: 10.1371/journal.pone.0065328

Becker, K., Ziemons, S., Lentz, K., Freitag, M., and Kück, U. (2016). Genome-wide chromatin immunoprecipitation sequencing analysis of the *Penicillium chrysogenum* Velvet protein PcVelA identifies methyltransferase PcLlmA as a novel downstream regulator of fungal development. *mSphere* 1:e00149-16. doi: 10.1128/mSphere.00149-16

Callahan, T. M., Rose, M. S., Meade, M. J., Ehrenshaft, M., and Upchurch, R. G. (1999). CFP, the putative cercosporin transporter of *Cercospora kikuchii*, is required for wild type cercosporin production, resistance, and virulence on soybean. *Mol. Plant Microbe Interact.* 12, 901–910. doi: 10.1094/MPMI.1999.12.10.901

Chanda, A., Roze, L. V., Kang, S., Artymovich, K. A., Hicks, G. R., Raikhel, N. V., et al. (2009). A key role for vesicles in fungal secondary metabolism. *Proc. Natl. Acad. Sci. U.S.A.* 106, 19533–19538. doi: 10.1073/pnas.0907416106

Chang, P.-K., Yu, J., and Yu, J.-H. (2004). *aflT*, a MFS transporter-encoding gene located in the aflatoxin gene cluster, does not have a significant role in aflatoxin secretion. *Fungal Genet. Biol.* 41, 911–920. doi: 10.1016/j.fgb.2004.06.007

Cheeseman, K., Ropars, J., Renault, P., Dupont, J., Gouzy, J., Branca, A., et al. (2014). Multiple recent horizontal transfers of a large genomic region in cheese making fungi. *Nat. Commun.* 5:2876. doi: 10.1038/ncomms3876

Crespo-Sempere, A., Martínez-Culebras, P. V., and González-Candelas, L. (2014). The loss of the inducible *Aspergillus carbonarius* MFS transporter MfsA leads to ochratoxin A overproduction. *Int. J. Food Microbiol.* 181, 1–9. doi: 10.1016/j.ijfoodmicro.2014.04.014

Del-Cid, A., Gil-Durán, C., Vaca, I., Rojas-Aedo, J. F., García-Rico, R. O., Levicán, G., et al. (2016). Identification and functional analysis of the mycophenolic acid gene cluster of *Penicillium roqueforti*. *PLoS ONE* 11:e0147047. doi: 10.1371/journal.pone.0147047

Fernández-Bodega, M. A., Mauriz, E., Gómez, A., and Martín, J. F. (2009). Proteolytic activity, mycotoxins and andrastin A in *Penicillium roqueforti* strains isolated from Cabrales, Valdeón and Bejes-Tresviso local varieties of blue-veined cheeses. *Int. J. Food Microbiol.* 136, 18–25. doi: 10.1016/j.ijfoodmicro.2009.09.014

García-Estrada, C., and Martín, J. F. (2016). Biosynthetic gene clusters for relevant secondary metabolites produced by *Penicillium roqueforti* in blue cheeses. *Appl. Microbiol. Biotechnol.* 100, 8303–8313. doi: 10.1007/s00253-016-7788-x

García-Rico, R., Chávez, R., Fierro, F., and Martín, J. F. (2009). Effect of a heterotrimeric G protein α subunit on conidia germination, stress response, and roquefortine C production in *Penicillium roqueforti*. *Int. Microbiol.* 12, 123–129.

Gil-Durán, C., Rojas-Aedo, J. F., Medina, E., Vaca, I., García-Rico, R. O., Villagrán, S., et al. (2015). The *pcz1* gene, which encodes a Zn(II)2Cys6 protein, is involved in the control of growth, conidiation, and conidial germination in the filamentous fungus *Penicillium roqueforti*. *PLoS ONE* 10:e0120740. doi: 10.1371/journal.pone.0120740

Hidalgo, P. I., Poirier, E., Ullán, R. V., Piqueras, J., Meslet-Cladière, L., Coton, E., et al. (2016). *Penicillium roqueforti* PR toxin gene cluster characterization. *Appl. Microbiol. Biotechnol.* 101, 2043–2056. doi: 10.1007/s00253-016-7995-5

Kosalková, K., Domínguez-Santos, R., Coton, M., Coton, E., García-Estrada, C., Liras, P., et al. (2015). A natural short pathway synthesizes roquefortine C but not meleagrin in three different *Penicillium roqueforti* strains. *Appl. Microbiol. Biotechnol.* 99, 7601–7612. doi: 10.1007/s00253-015-6676-0

Martín, J. F., Casqueiro, J., and Liras, P. (2005). Secretion systems for secondary metabolites: how producer cells send out messages of intercellular communication. *Curr. Opin. Microbiol.* 8, 282–293. doi: 10.1016/j.mib.2005.04.009

Martín, J. F., and Liras, P. (2016). Evolutionary formation of gene clusters by reorganization: the meleagrin/roquefortine paradigm in different fungi. *Appl. Microbiol. Biotechnol.* 100, 1579–1587. doi: 10.1007/s00253-015-7192-y

Matsuda, Y., Awakawa, T., and Abe, I. (2013). Reconstituted biosynthesis of fungal meroterpenoid andrastin A. *Tetrahedron* 69, 8199–8204. doi: 10.1016/j.tet.2013.07.029

Nielsen, K. F., Dalsgaard, P. W., Smedsgaard, J., and Larsen, T. O. (2005). Andrastins A-D, *Penicillium roqueforti* metabolites consistently produced in blue-mold-ripened cheese. *J. Agric. Food Chem.* 53, 2908–2913. doi: 10.1021/jf047983u

Quistgaard, E. M., Löw, C., Guettou, F., and Nordlund, P. (2016). Understanding transport by the major facilitator superfamily (MFS): structures pave the way. *Nat. Rev. Mol. Cell Biol.* 17, 123–132. doi: 10.1038/nrm.2015.25

Rho, M. C., Toyoshima, M., Hayashi, M., Uchida, R., Shiomi, K., Komiyama, K., et al. (1998). Enhancement of drug accumulation by andrastin A produced by *Penicillium* sp. FO-3929 in vincristine-resistant KB cells. *J. Antibiot.* 51, 68–72. doi: 10.7164/antibiotics.51.68

Sonjak, S., Frisvad, J. C., and Gunde-Cimerman, N. (2005). Comparison of secondary metabolite production by *Penicillium crustosum* strains, isolated from Arctic and other various ecological niches. *FEMS Microbiol. Ecol.* 53, 51–60. doi: 10.1016/j.femsec.2004.10.014

Uchida, R., Shiomi, K., Inokoshi, J., Sunazuka, T., Tanaka, H., Iwai, Y., et al. (1996). Andrastins A-C, new protein farnesyltransferase inhibitors produced by *Penicillium* sp. FO-3929 II. Structure elucidation and biosynthesis. *J. Antibiot.* 49, 418–424. doi: 10.7164/antibiotics.49.418

Ullán, R. V., Godio, R. P., Teijeira, F., Vaca, I., García-Estrada, C., Feltrer, R., et al. (2008). RNA-silencing in *Penicillium chrysogenum* and *Acremonium chrysogenum*: validation studies using β-lactam genes expression. *J. Microbiol. Methods* 75, 209–218. doi: 10.1016/j.mimet.2008.06.001

van den Berg, M. A., Albang, R., Albermann, K., Badger, J. H., Daran, J. M., Driessen, A. J., et al. (2008). Genome sequencing and analysis of the filamentous fungus *Penicillium chrysogenum*. *Nat. Biotechnol.* 26, 1161–1168. doi: 10.1038/nbt.1498

Visagie, C. M., Houbraken, J., Frisvad, J. C., Hong, S.-B., Klaassen, C. H. W., Perrone, G., et al. (2014). Identification and nomenclature of the genus *Penicillium*. *Stud. Mycol.* 78, 343–371. doi: 10.1016/j.simyco.2014.09.001

Wiemann, P., Willmann, A., Straeten, M., Kleigrewe, K., Beyer, M., Humpf, H. U., et al. (2009). Biosynthesis of the red pigment bikaverin in *Fusarium fujikuroi*: genes, their function and regulation. *Mol. Microbiol.* 72, 931–946. doi: 10.1111/j.1365-2958.2009.06695.x

Conflict of Interest Statement: The authors declare that the research was conducted in the absence of any commercial or financial relationships that could be construed as a potential conflict of interest.

Copyright © 2017 Rojas-Aedo, Gil-Durán, Del-Cid, Valdés, Álamos, Vaca, García-Rico, Levicán, Tello and Chávez. This is an open-access article distributed under the terms of the Creative Commons Attribution License (CC BY). The use, distribution or reproduction in other forums is permitted, provided the original author(s) or licensor are credited and that the original publication in this journal is cited, in accordance with accepted academic practice. No use, distribution or reproduction is permitted which does not comply with these terms.

frontiers in Microbiology

ORIGINAL RESEARCH
published: 17 May 2017
doi: 10.3389/fmicb.2017.00887

Detection of Androgenic-Mutagenic Compounds and Potential Autochthonous Bacterial Communities during *In Situ* Bioremediation of Post-methanated Distillery Sludge

Ram Chandra and Vineet Kumar*

Department of Environmental Microbiology, School for Environmental Sciences, Babasaheb Bhimrao Ambedkar University, Lucknow, India

Sugarcane-molasses-based post-methanated distillery waste is well known for its toxicity, causing adverse effects on aquatic flora and fauna. Here, it has been demonstrated that there is an abundant mixture of androgenic and mutagenic compounds both in distillery sludge and leachate. Gas chromatography-mass spectrometry (GC-MS) analysis showed dodecanoic acid, octadecanoic acid, *n*-pentadecanoic acid, hexadecanoic acid, β-sitosterol, stigmasterol, β-sitosterol trimethyl ether, heptacosane, dotriacontane, lanosta-8, 24-dien-3-one, 1-methylene-3-methyl butanol, 1-phenyl-1-propanol, 5-methyl-2-(1-methylethyl) cyclohexanol, and 2-ethylthio-10-hydroxy-9-methoxy-1,4 anthraquinone as major organic pollutants along with heavy metals (all mg kg^{-1}): Fe (2403), Zn (210.15), Mn (126.30, Cu (73.62), Cr (21.825), Pb (16.33) and Ni (13.425). In a simultaneous analysis of bacterial communities using the restriction fragment length polymorphism (RFLP) method the dominance of *Bacillus* sp. followed by *Enterococcus* sp. as autochthonous bacterial communities growing in this extremely toxic environment was shown, indicating a primary community for bioremediation. A toxicity evaluation showed a reduction of toxicity in degraded samples of sludge and leachate, confirming the role of autochthonous bacterial communities in the bioremediation of distillery waste *in situ*.

Keywords: distillery sludge, toxicity, β-sitosterol, *Bacillus* sp., *Enterococcus* sp., RFLP

OPEN ACCESS

Edited by:
Bhim Pratap Singh,
Mizoram University, India

Reviewed by:
Maulin P. Shah,
Enviro Technology Limited, India
Luiz Fernando Romanholo Ferreira,
Universidade Tiradentes, Brazil

****Correspondence:***
Ram Chandra
rc_microitrc@yahoo.co.in;
prof.chandrabbau@gmail.com

Specialty section:
This article was submitted to Microbiotechnology, Ecotoxicology and Bioremediation, a section of the journal Frontiers in Microbiology

Received: *26 December 2016*
Accepted: *02 May 2017*
Published: *17 May 2017*

Citation:
Chandra R and Kumar V (2017) Detection of Androgenic-Mutagenic Compounds and Potential Autochthonous Bacterial Communities during In Situ Bioremediation of Post-methanated Distillery Sludge. Front. Microbiol. 8:887. doi: 10.3389/fmicb.2017.00887

INTRODUCTION

Various forms of industrial waste are major sources of environmental pollution due to the release of several unidentified toxic pollutants. The majority of agro-based industries, i.e., distilleries, tanneries, and pulp paper are major sources of aquatic and soil pollution. Due to the release of huge amounts of waste water and sludge, sugarcane-molasses-based distilleries are among the most polluting industries in India. Distilleries release 12 to 15 l of spent wash per liter of alcohol produced. Currently, there are more than 319 distilleries in India, reflecting the magnitude of the problem due to the presence of various complex pollutants in post-methanated distillery effluent (PMDE) and post-methanated distillery sludge (PMDS). The detection and detoxification

of distillery waste is a challenge for the safe disposal of effluent and sludge. Safe disposal of PMDS in the environment is of paramount importance currently due to the presence of various unidentified complex organic and inorganic pollutants (melanoidins, phenolics, and sulfur compounds as well as heavy metals) (Chandra and Kumar, 2017a). These complex pollutants in PMDS are generated during the process of the distillation of fermented molasses slurry and the subsequent methanogenesis of the spent wash. The toxicity of PMDS and PMDE to the terrestrial and aquatic environment are well documented due to the presence of heavy metals and organic compounds (Bharagava and Chandra, 2010). The seed germination (SG) test has indicated stunted stem growth and reduced root systems in *Phaseolus mungo* at higher concentrations of sludge-amended soil (Chandra et al., 2008).

Microbial communities are fundamental components of any ecosystem, playing a primary and critical role in the metabolism of organic matter to maintain biogeochemical cycles in various critical environments (Fuhrman, 2009). They are predominantly involved in the bioremediation of contaminated sites, and several microorganisms, which degrade a wide range of pollutants have been described (Loviso et al., 2015). A detailed knowledge of microbial communities at any polluted site not only reflects their relationships with pollutants, but also reflects information with respect to the bioremediation potential of microbes on specific pollutants. This may indicate a direction of the bio-stimulation or bio-augmentation for the restoration of any polluted ecosystem.

However, recent progress in molecular microbial ecology has shown that traditional culturing methods are insufficient to allow detailed analysis of the microbial diversity at any contaminated site. This is because only a small proportion of viable microorganisms from a sample are recovered by culturing techniques. So, to show the full extent of microbial diversity various molecular techniques have been applied (Zhongtang and Mohn, 2001). The study of pollutants and their influence on the microbial communities of WWTPs can provide useful information for solving the problem of fluctuation in WWTPs. The study has also demonstrated that different configurations of treatment plants influence the structures of microbial communities (Gich et al., 2000).

Some significant research has been carried out on the analysis of bacterial communities derived from the activated sludge of wastewater treatment processes and bioreactors, which was designed to evaluate the process performance of treatment plants for the biodegradation of hazardous chemicals (Whiteley and Bailey, 2000; Forney et al., 2001). For the assessment of the biodegradability of toxic compounds and the measurement of whole bacterial communities, substrate utilization has been reported using phospholipid fatty acid (PLFA) analysis and fluorescence *in situ* hybridization (FISH) techniques (Maharana and Patel, 2014). Rapid community fingerprinting by the polymerase chain reaction (PCR)-based denaturing gradient electrophoresis (DGGE) of 16S rDNA also indicated highly structured bacterial communities growing in treatment plants and different classes of bacteria were detected (γ-*Proteobacteria, Firmicutes,* etc.; Kapley et al., 2015). Some gene probes have also been used as a tool to detect the degradation of phenolic compounds in wastewater treatment systems (Purohit et al., 2003). A few studies have been published in the literature on microbial community indices using fatty acid or phospholipid analysis as a tool for the assessment of bioremediation of pollutants and eco-restoration of contaminated sites (Maharana and Patel, 2014). Detailed knowledge regarding organic pollutants and the growth of autochthonous bacterial communities at several complex polluted industrial waste sites is lacking. These recalcitrant pollutants persist in the environment and cause adverse effects on aquatic and soil ecosystems, and on flora and fauna, as well as on humans due to the presence of some unidentified mutagenic and androgenic compounds, which have, so far, not been isolated. So, the extraction of organic pollutants from PMDS using appropriate solvents would allow the extraction of the maximum number of toxic organic pollutants present in sludge. Their further detection by gas chromatography-mass spectrometry (GC-MS) will show the properties of the pollutants that challenge safe disposal, while simultaneously investigating the autochthonous bacterial communities present in disposed PMDS that mediate the bioremediation of toxic compounds *in situ*. Hence, an analysis of the growing autochthonous bacterial communities present in PMDS after 90 days of *in situ* bioremediation would not only provide information on the bacterial communities, it will also highlight a prerequisite step for the monitoring of polluting discharges from sugarcane-molasses-based distillery waste. Furthermore, the characterization of metabolic products will also provide important information about the environmental fate of these pollutants. The *in situ* bioremediation of organochlorine-pesticides-contaminated soil by using gene probes has been reported, but there is no knowledge of the chemical properties of pollutants present in complex industrial sludge discharge from sugarcane-molasses-based distillery waste after bio-methanogenesis. Furthermore, the autochthonous bacterial communities growing in sludge, which have potential capabilities for *in situ* and *ex situ* bioremediation remain unidentified.

In the present study, we have detected organic pollutants by GC-MS extracted with organic solvents to ensure the extraction of the majority of pollutants from disposed sludge. Energy dispersed spectroscopy (EDS) of sludge was also carried out for qualitative and quantitative analysis of heavy metals and of various salts. Potential autochthonous bacterial communities have also been detected using culture-independent methods, i.e., restriction fragment length polymorphism (RFLP) during *in situ* bioremediation to show the relationship between pollutants and the potential autochthonous bacterial communities responsible for biodegradation of PMDS. These findings will allow exploration of the potential autochthonous bacterial communities existing in the extreme environment of PMDS, which are capable of the bioremediation of inorganic and organic pollutants that are rich with phenolic and melanoidin compounds. Such bioremediation currently poses a challenge for the safe disposal of PMDS in the environment due to its complex structural and recalcitrant properties and its toxic effects on ecosystems.

MATERIALS AND METHODS

Site Description, Sample Collection, and Preparation of Sludge Leachate

The fresh PMDS sample was collected in clean pre-sterilized polythene bags from the effluent treatment plant (ETP) of M/s Unnao Distillery and Breweries Limited, located in Unnao (26°320" N, 80°30′0"E) Uttar Pradesh, India. The plant has a capacity for 9000 kL of alcohol production and generates ∼800 tons of sludge annually (All India Distillers Association [AIDA], 2004). After 90 days of *in situ* bioremediation the degraded sludge sample was collected from the sludge dumping site of the distillery plant, which is located inside the premises. All the sludge samples collected were transported to the laboratory and used for the analysis of physicochemical parameters, detection of organic pollutants, detection of bacterial communities and preparation of leachate. The sludge leachate was prepared by stirring it in distilled water (1:1 w/v) for approximately 48 h and allowing the sludge suspension to stand still for 6 h in an Erlenmeyer flask. Clear supernatant was pumped out and filtered by passing through Whatman filter paper 42. Newly prepared sludge leachate was taken as 100%, with different concentrations prepared from it by adding distilled water to a final concentration of 1.0, 2.5, 5, and 10% for the analysis of various physicochemical parameters, detection of organic pollutants, phytotoxicty, and genotoxicity assays.

Chemicals and Reagents

The organic solvents, *n*-hexane (C_6H_{14}), was procured from Merck (Merck KGaA, Darmstadt, Germany) and used for the extraction of organic compounds from distillery sludge. The following derivatizing reagents were obtained from Sigma-Aldrich (Saint Louis, MO, United States): pyridine, BSTFA [*N*,*O*-bis (trimethylsilyl) trifluoroacetamide] and TMCS (trimethylchlorosilane). All the chemicals and reagents used in this study were of HPLC grade.

Physicochemical Analysis of Distillery Sludge and Sludge Leachate

The physicochemical parameters of fresh distillery sludge and sludge leachate samples, i.e., pH, electrical conductivity (EC), salinity, chloride, sodium, nitrate, ammonical nitrogen were estimated according to the method of Kalra and Maynard (1991). The pH and EC of sludge samples (1:1 sludge:water) and leachate were measured using an Orion meter (Model-960, Thermo Scientific, United States) and an Orion conductivity meter (Model-150, Thermo Scientific, United States), respectively. The heavy metals in the sludge and leachate samples were analyzed with standard methods (American Public Health Association [APHA], 2012) by atomic absorption spectrophotometry (AAS) (ZEEnit 700, Analytic Jena, Germany) after nitric acid-perchloric acid digestion method no. 3030H. Elemental analysis was performed for total C, N_2, H_2, and O_2 by using an elemental analyzer (EuroVector EA 3000, University of AL-al-Bayt, Jordan). In addition, the SEM-EDS analysis of PMDS was performed using a scanning electron microscope (JEOL JSM-6490LV, Peabody, MA, United States). Operating conditions were: accelerating voltage 20 kV, probe current 45 nA and counting time 60 s. The physicochemical parameters were also analyzed in the degraded sample after 90 days of bioremediation of sludge *in situ*.

Extraction and Identification of Various Organic Compounds from Fresh and Degraded Sludge

Solid Liquid Extraction of PMDS and Liquid–Liquid Extraction of Distillery Leachate

The fresh PMDS sample (5.0 g) was weighed and put into an Erlenmeyer flask (250 ml); 5 ml of *n*-hexane was added and it was mixed vigorously. Further, the samples were processed by vortex agitation (2 min), sonication (2 min on and 30 s off, ×3) and centrifuged (15 min 10,000 × *g*). In order to extract organic pollutants from distillery leachate, a fixed volume (10 ml) of sludge leachate was acidified with 35% (v/v) hydrochloric acid (HCl) and placed in a separating funnel (100 ml), after which an equal volume of *n*-hexane was added and the mixture was shaken continuously for 5 h with intermittent rests for liquid–liquid extraction. The extraction was repeated successively three times to complete the extraction of organic pollutants. Subsequently, the organic layer was collected from the sludge and leachate, dehydrated over anhydrous sodium sulfate (Na_2SO_4) and dried under a stream of N_2 gas. A similar process was followed for the extraction of metabolic products from a degraded sludge sample after bioremediation *in situ*. The dry residue obtained was dissolved in 1.0 ml ethyl acetate and filtered through 0.22 μm syringe filters (Millipore Ltd., Bedford, MA, United States) and used for further Fourier transform-infrared spectrophotometry (FTIR) and GC-MS analysis.

Fourier Transform-Infrared Spectrophotometry

Fourier transform-infrared spectrophotometry analysis of purified extract was performed using a spectrophotometer (Nexus-890, Thermo Electron Co., Yokohama, Japan) in order to reveal the chemical nature of sludge and leachate. The purified samples were dispersed in spectral-grade KBr (Merck, Darmstadt, Germany) and made into pellets by applying 5–6 tons cm^{-2} of pressure for 10 min using a hydraulic pressure (Specac, United Kingdom) instrument. The spectrum was generated in the range of 400 to 4,000 cm^{-1} with a resolution of 4 cm^{-1} for all samples (fresh sludge, fresh sludge leachate, and degraded leachate).

Gas Chromatography-Mass Spectrometry (GC-MS) Analysis

In GC-MS analysis, the extracted PMDS and leachate samples were derivatized with trimethylsilyl (TMS) as described by Minuti et al. (2006). In this method, 50 μl pyridine and 80 μl TMS BSTFA, and TMCS were added to 300 μl samples. The mixture was heated at 70°C for 30 min, with periodic shaking to dissolve residues. An aliquot (2.0 μl) of silylated sample was automatically injected into a GC-MS (Thermo Scientific Trace GC Ultra Gas Chromatograph) equipped with a TriPlus

auto sampler coupled to TSQ Quantum XLS triple quadrupole mass spectrometer (Thermo Scientific, Miami, FL, United States). Separation was carried out on a DB-5MS capillary column [30 m length × 0.25 μm I.D. × 0.25 mm film thickness of 5% phenyl and 95% methylpolysiloxane (v/v)]. The flow rate of carrier gas (He) was maintained at 1.1 ml/min, GC oven temperature was started at 65°C (held for 2 min), increased to 230°C at a rate of 6°C/min and finally reached 290°C (held for 20 min) at a rate of increase of 10°C/min (Chandra and Kumar, 2017b). Transfer line temperature and ion source temperature were kept at 290 and 220°C, respectively. The mass spectrometer was operated in the positive electron ionization (+EI) mode at an electron energy of 70 eV with a solvent delay of 7 min. Initially, to confirm the derivatization of organic compounds, full scanning mode was used in the mass range of 45–800 amu. Similar methods were also followed for other samples. The organic compounds were identified by comparing their mass spectra with that of the National Institute of Standards and Technology (NIST) library available with the instrument and by comparing the retention times with those of available standard compounds.

Analysis of Uncultured Bacterial Communities Growing in PMDS

Genomic DNA Extraction and Purification

The total genomic DNA from degraded PMDS samples after 90 days of *in situ* bioremediation was extracted following the protocol of Berthelet et al. (1996). An aliquot (2.0 g) of sludge sample was mixed with 5.0 ml of 0.1 M sodium phosphate buffer (pH 8.0) in screw-capped polypropylene micro-centrifuge tubes (10 ml capacity) containing 5.0 g silica beads (0.1 mm diameter) followed by addition of 500 mM Tris-HCl (pH 8.0) and 10% sodium dodecyl sulfate (SDS). The tubes were shaken for 5 min at high speed on a Mini-Bead beater to lyse the cells. After lyses, the lysate was centrifuged (15,000 × *g*; 10 min; 4°C) in a microfuge and the supernatant obtained was mixed with double the volume of 7.5 M ammonium acetate and incubated on ice for 10 min. The samples were then centrifuged (15,000 × *g*; 10 min; 4°C) in a microfuge and aliquots of 300–500 μl supernatant were purified by centrifugation (1,000 × *g*; 2 min) through a spin column (Bangalore Genei, India), which was previously equilibrated and slurried with 20 mM potassium phosphate buffer (pH 7.4).

PCR Amplification of 16S rRNA Genes

The PCR amplification of 16S rDNA genes derived from degraded PMDS was performed with universal eubacterial primers (27F) 5′ AGAGTTTGATCMTGGCTCAG 3′ and (1492R) 5′ TACGGYTACCTTGTTACGACTT 3′ using a Thermocycler (Sure Cycler-8800, Agilent Technologies, United States). The reaction mixture contained 5 μl of template DNA (1 × PCR buffer, 10 mM of each: dNTP, 3.0 mM $MgCl_2$, 10 pmol of primer and 2.5 U of *Taq* DNA polymerase. Bangalore Genei, India) in a final volume of 50 μl reaction mixture. As a negative control, reactions without DNA were carried out. The complete reaction mixture was overlaid with mineral oil and incubated in a thermal cycler (Sure Cycler-8800, Agilent Technologies, United States). The cycling program was as follows: initial denaturation at 94°C for 1 min, primer annealing at 55°C for 1 min, a final extension at 72°C for 3 min with an additional extension time of 10 min added to the final cycle, for a total of 35 cycles. The PCR products (amplicon) were electrophoresed through 1.2 % (w/v) agarose gel in 1× TAE buffer using a 1 Kb DNA ladder (Bangalore Genei, India) as molecular weight markers and visualized by staining with ethidium bromide. The amplified 16S rDNA gene products were gel purified by using a PCR-Clean-up kit (Bangalore Genei, India) and used for the clone library preparation.

Cloning of 16S rDNA PCR Products

For cloning, 10 μl purified PCR products were made blunt-ended by treatment with 10 U of the large (Klenow) fragment of DNA polymerase I, after which the 5′ end was phosphorylated with 10 U of T4 polynucleotide kinase (Promega, Madison, WI, United States). The reaction mixture, also contained 10 μl 10 × Klenow buffer [0.5 M Tris HCl (pH 7.5 at 25°C), with 10 mM $MgCl_2$, 10 mM dithiothreitol, 0.5 mg bovine serum albumin per ml, 1 mM ATP, 200 μM DdATP, 200 μM dCTP, 200 μM dGTP and 200 μM dTTP also present]; the total volume was 100 μl and the prepared solution was incubated at 37°C for 1.0 h (Moyer et al., 1994). The blunt-ended PCR-amplified 10S rDNA gene products were again purified with Quiaex and ligated into a SmaI-digested dephosphorylated pUC18 vector (Promega, Madison, WI, United States). Competent *Escherichia coli* XL1 blue MRF′ cells (Stratagene) were transformed using the method described by Morrison (1977). The positive recombinants were screened for α-complementation with X-Gal (5-bromo-4-chloro-3-indoyl-β-D-galactopyranosides) as a substrate on solid agar medium plates supplemented with ampicillin (150 μg/ml).

16S rDNA RFLP Analysis

Recombinant plasmids were isolated from overnight cultures by alkaline lysis. The cloned 16S rDNA gene fragments were then digested with the restriction enzymes, *Taq*I and *Sau*3AI, either separately or together (Merck Biosciences, Maharashtra, India). Restriction digestion was performed at 37°C for 2 h in a 50 μl reaction mixture containing 12 μl (∼200 ng) of PCR-amplified 16S rRNA gene product, 0.5 μl (5U) of restriction endonucleases (*Taq*I/*Sau*3AI; Merck Biosciences, Maharashtra, India), 5 μl of reaction buffer and 32.5 μl of autoclaved Milli-Q water. The restriction digestion process was repeated twice in order to establish the reproducibility of results. The resulting RFLP products were separated by gel electrophoresis in 1.8% (w/v) agarose gel and Tris-borate-EDTA buffer at 75 V for 5 h. Next, gels were stained with EtBr (1.0 μg/ml) and DNA bands were visualized using the Gel Documentation System (Syngene, United States). The DNA fragments were compared with a 100 and 500 bp DNA ladder (Merck Biosciences, Maharashtra, India) to determine molecular weights and sizes.

Sequencing of Cloned 16S rDNA PCR Fragments

Based on differences in the RFLP profiles generated, 10 bands generated by digestion of DSW by *Taq*I and *Sau*3AI were selected for sequence analysis. Selected bands were gel purified using gel extraction kits (Merck Biosciences, Maharashtra, India) and sequenced using the M13 forward

(5′-GTAAAACGACGGCCAGT-3′) and reverse universal primers (5′-CAGGAAACAGCTATGAC-3′) and an ABI PRISM® BigDye™ Terminator Cycle Sequencing Ready Reaction Kit (Applied Biosystems, Waltham, MA, United States). The samples were then sequenced using an automatic DNA sequencer (ABI PRISM® 310 Genetic Analyzer, United States). The partial sequences obtained were subjected to BLAST analysis using the online option available at http://blast.ncbi.nlm.nih.gov/Blast.cgi (Altschul et al., 1997).

Phylogenetic Analysis and Nucleotide Sequence Accession Number

A phylogenetic tree was generated using MEGA-6.0 software (Tamura et al., 2013). All query sequences and other homologous sequences available online in the NCBI (National Centre for Biotechnology Information)[1] nucleotide database were saved in a single FASTA file format after retrieval. Furthermore, all sequences were saved in one FASTA format file and then subjected to multiple sequence alignment using MEGA-6.0, which was subsequently used to reconstruct phylogenetic trees by the Neighbor-Joining method using the MEGA-6.0 Draw Tree tool (Larkin et al., 2007) with a bootstrap value of 1,000 replicates. Nucleotide sequences were deposited in the GenBank Nucleotide database under accession numbers from FJ227523 – FJ227532.

Toxicity Assessment of Sludge

Phytotoxicity Assay

The toxicity of the fresh and *in situ*-degraded sludge leachate was assessed by measuring the phytotoxicity effect on the germination of seeds of *Phaseolus mungo* L. using the Petri dish method (Santal et al., 2011). Prior to preparation of various concentrations of distillery leachate, the pH was adjusted to 7.0 with 1 M NaOH. For the SG experiment, distillery leachate was applied at 1.0, 2.5, 5, and 10% (v/v). The surfaces of the seeds were sterilized with 0.1% $HgCl_2$ for 2 min to remove any fungal contamination, after which they were subjected to repeated washings with sterilized distilled water. Subsequently, 10 seeds of *P. mungo* L. were placed separately in sterilized glass Petri dishes of uniform size lined with two Whatman No. 1 filter paper disks. Disks were then moistened with 10 ml tap water for controls and with the same volume of distillery leachate, after which they were incubated at 25°C for a period of two consecutive days. The bioassay was performed on three replicate samples. The percentage SG and the percentage phytotoxicity (RI) was calculated with the formula previously described (Oleszczuk et al., 2012):

$$\mathrm{SG/RI} = \frac{(A - B)}{A} \times 100$$

Where, *A* is mean SG and root length in controls, *B* is mean SG and root length in test experiments.

Other SG parameters such as the germination index (GI), relative percentage toxicity, percentage phytotoxicity, and the stress tolerance index were calculated using the formula described by David Noel and Rajan (2015).

[1]http://ncbi.nlm.nih.gov/

Genotoxicity Assay

The root tip cells of onion, *Allium cepa*, were used to test the genotoxic effects of fresh and degraded sludge leachate. The test was carried out as described by Fiskesjo (1985). The onion bulbs were previously germinated in tap water at room temperature. When the seeds reached about 2.0 cm in length, they were transferred to test tubes containing different concentrations of distillery sludge leachate (1%, 2.5%, 5% and 10%), while one tube with distilled water was used as a control. After 24 h of treatment, the root tips were collected and fixed in Carnoy's fluid (ethanol-glacial acetic acid 3:1; v/v) for 24 h at 4°C, in order to arrest mitosis (Fiskesjo, 1993, 1997). Afterward, they were washed with distilled water and placed in 70% (v/v) ethanol for 24 h at room temperature. The root tips of bulbs were hydrolyzed with 1 M HCl at 60°C for 4–5 min to dissolve cell walls. After hydrolysis, the roots were washed with distilled water and approximately 1–2 mm of root tips were cut off and processed for staining with hematoxylin. Five slides were prepared for each concentration and for the control, out of which five (at 500 cells per slide) were analyzed with a light microscope (Leica Microsystem, Germany; ×1000). A total of 2500 cells were evaluated for each concentration. In the analysis, the following chromosomal and nuclear aberrations were considered: chromosome adherence, c-mitosis, chromosome bridges, vagrant chromosomes, disordered metaphase and anaphase, lagging chromosomes, multipolarity, and polyploidy. Mitotic index (MI) and mitotic inhibition were also an indication of cytotoxicity. In this study, MI and mitotic inhibition % was determined with the following formula, as described by Fiskesjo (1997):

$$\text{Mitotic index (\%)} = \frac{\text{Total number of cells in division}}{\text{Total cell number of cells observed}} \times 100$$

$$\text{Mitotic inhibition (\%)} = \frac{\text{Mitotic index in Control group} - \text{Mitotic index in test group}}{\text{Mitotic index in control group}} \times 100$$

RESULTS

Physicochemical Analysis of the Distillery Sludge and Leachate

The physicochemical properties of PMDS and its leachate are shown in **Table 1**. The value of pH and EC were higher in the sludge. In addition, the sludge showed high concentrations of ions, e.g., Na^+, Cl^-, NO_3^-, and NH_4^+ (**Table 1**). It also had a high content of various heavy metals, where the highest content was noted for Fe followed by Mn, Zn, Cu, Cr, Pb, Ni, and Cd. Leachate analysis also demonstrated high values for pH and EC, BOD, COD, TDS, and various heavy metals (**Table 1**). This indicated the high leaching properties of the pollutants present in PMDS. However, the leachate obtained after 90 days of *in situ* bioremediation of PMDS had lower values of various physiochemical parameters (**Table 1**). This indicates that the biodegradation of various

organic and inorganic content by autochthonous bacterial communities growing in PMDS had occurred. The SEM-EDS analysis of PMDS also showed heterogenous morphology (See Supplementary Figure 1), and its elemental composition included C (24.10%), O (50.08), Si (8.67%), Al (5.22%), and Fe (4.27%) as the main elements (See Supplementary Table 1).

Characterization of Organic Compounds

FTIR Analysis

Fourier transform-infrared spectrophotometry analysis showed that there are significant differences between the spectra of PMDS, fresh sludge leachate and degraded sludge leachate obtained after *in situ* bioremediation by potential autochthonous bacterial communities (**Figure 1**). The infrared spectra (500–4000 cm^{-1}) of distillery sludge were similar to the spectra obtained with distillery leachate. The FTIR spectra were analyzed based on the peak in control sludge, sludge leachate solution and in the treated samples, indicating the presence of different chemical bonds and various organic pollutants. The control region, as well as the degraded leachate at between 3200 and 3600 cm^{-1} represented broad peaks of stretching vibration indicative of O-H of COOH and the N-H stretching of amides. The peak values of 3425.9, 3450.3, and 3408.8 represented the O-H vibrational stretching present in acids, alcohols, and phenols. The region between 2800 and 3000 cm^{-1} exhibited C-H stretching due to the presence of $-CH_3$ in hydrocarbon chains (de Oliveira Silva et al., 2012; Kadam et al., 2013). The controls and degraded samples showed peaks at 2854.5, 2854.6, 2855.5, 2922.6, 2923.3, 2923.5, 2956.0, and 2957.1 cm^{-1} of the C-H asymmetric stretching vibration of -CH, $-CH_2$, and $-CH_3$ functional groups. In untreated distillery sludge and leachate, the broad stretching adsorption band peaks at 2019.4 and 1998.8 cm^{-1} could be assigned to C=C stretching vibrations. The band peak at 1081.0, 1081.1, and 1080.3 cm^{-1} was attributable to an O-H stretching vibration of the COOH band present in acids. A very strong band at 1,660.9, 1,667.4, 1,708.6, 1,709.0, 1,783.4, and 1,606 cm^{-1} was indicative of the C=O carbonyl stretching of secondary amides (Narain et al., 2012; Yang et al., 2015). There is a medium band at 1,396.4, 1,368.1, 1,365.3, 1,302.8 cm^{-1}, which represents the C-H deformation of a $-CH_2$, or CH_3 group, while a band at 1,032.3 cm^{-1} indicates the presence of C-O stretching in polysaccharides. The spectrum region between 1,100 and 1,200 cm^{-1} of controls and degraded samples showed peaks at 1,188.2, 1,187.1, and 1,189.9 cm^{-1}, which represents the S=O stretching in sulfone groups, while a band at 969.1, 968.7, and 970.4 indicates the presence of the C-O stretching of polysaccharides or an Si-O-asymmetric stretch. The band at 891.6, 891.1, 832.8, 824.3, 823.9, and 832.8 cm^{-1}

TABLE 1 | Physico-chemical analysis of disposed distillery sludge and leachate.

S. No.	Physico-chemical Parameters	Distillery sludge	Distillery sludge leachate	Sludge leachate after *in situ* remediation	% Reduction of sludge leachate
1	pH	8.00 ± 0.21	7.99 ± 0.10	7.114 ± 0.21[a]	10.96
2	EC	4.1 ± 2.11	3.9 ± 1.14	2.4 ± 1.34[a]	38.46
3	Sodium (Na^+)	56 ± 1.31	55.108 ± 0.97	13.352 ± 0.80[a]	75.77
4	Chloride (Cl^-)	1825 ± 0.10	7034.6. ± 0.89	6878.674 ± 129.45[ns]	83.14
5	Nitrate (NO_3^-)	110 ± 3.14	109.916 ± 1.30	46.295 ± 0.90[a]	57.88
6	Ammonical nitrogen (NH_4^+)	190 ± 1.24	187.794 ± 0.94	85.594 ± 0.71[a]	54.42
7	TDS	–	16550.4 ± 2.07	2406 ± 89.19[a]	85.56
8	BOD	–	11050.2 ± 2.28	2555.698 ± 1.78[a]	76.87
9	COD	–	22421 ± 1.58	4512.934 ± 1.90[a]	79.87
10	Total organic carbon	17.318 ± 0.21	16.404 ± 0.28	7.407 ± 1.09[a]	66.48
11	Total nitrogen	2.463 ± 0.01	2.084 ± 0.04	1.982 ± 0.05[c]	57.29
12	Total hydrogen	4.013 ± 0.04	3.668 ± 0.38	2.93 ± 0.05[c]	69.41
13	Total oxygen	36.251 ± 1.11	35.408 ± 0.58	26.039 ± 3.52[b]	9.42
14	Trace elements				
a	Iron (Fe)	2403 ± 3.11	1401.22 ± 1.86	852.528 ± 2.05[a]	39.15
b	Zinc (Zn)	210.15 ± 2.14	95.273 ± 0.68	21.463 ± 1.67[a]	77.47
c	Copper (Cu)	73.62 ± 1.14	62.928 ± 1.20	11.526 ± 1.02[a]	81.68
d	Chromium (Cr)	21.825 ± 0.41	18.447 ± 0.60	9.140 ± 0.49[a]	50.45
e	Cadmium (Cd)	1.440 ± 0.12	1.166 ± 0.15	0.94 ± 0.05[c]	19.38
f	Manganese (Mn)	126.30 ± 0.94	94.602 ± 1.13	45.105 ± 0.72[a]	52.32
g	Nickel (Ni)	13.425 ± 0.21	8.302 ± 0.31	2.250 ± 0.20[a]	72.89
h	Lead (Pb)	16.33 ± 1.11	14.311 ± 1.65	7.222 ± 0.38[a]	49.53

All values are mean of three replicate ± SD and presented in mg kg^{-1} and ml L^{-1} for distillery sludge and distillery leachate, respectively, except electrical conductivity (μS cm^{-1}), total carbon, total nitrogen, total hydrogen, and total oxygen (%). EC, electric conductivity; BOD, biological oxygen demand; COD, chemical oxygen demand; TDS, total dissolved solids; t-test (two-tailed as compared to fresh distillery leachate). [a]*Highly significant at $p < 0.001$.* [b]*Significant at $p < 0.01$.* [c]*Less significant at $p < 0.05$.* [ns]*Non significant at $p > 0.05$.*

represents the hydrogen-bonded OH- deformation in carboxyl groups (Kadam et al., 2013). Some peaks were also detected below 700 cm^{-1} due to the presence of multiple functional groups/compounds such as sulfates, carbohydrates, alkyl halides, nitro groups, and C-S bonds (Yang et al., 2015). The peaks at 702.0, 719.9, and 720.2 cm^{-1} were usually weak and due to the C-H bending vibrations of methyl groups. The absorption bands at 642.6 and 602.5 cm^{-1} were indicative of the S-O stretching vibration of sulfate compounds. The region in between 500 and 600 cm^{-1} represents the stretching vibration peaks of C-Cl, indicating the presence of alkyl chlorides. However, the sharpness of all the peaks diminished over time with *in situ* bioremediation, indicating the degradation of distillery leachate molecules into smaller ones and an overall decrease in organic compounds.

GC-MS Analysis

The GC-MS chromatogram of compounds extracted from PMDS and leachate with n-hexane is shown in **Figure 2** and organic compounds have been identified in detail at various retention times based upon mass to charge ratios (m/z). The results show that fresh PMDS and leachate contained large numbers of organic compounds as identified by GC-MS (**Table 2**). The major compounds were identified as saturated fatty acids (propanoic acid, dodecanoic acid, tetradecanoic acid, *n*-pentadecanoic acid, octadecanoic acid, and hexadecanoic acid). Other compounds were also identified as stigmasta-5, 22-dien-3-ol(3 β,22E), stigmasterol and β-sitosterol. Other compounds such as 1-propanol, 3-(octadecycloxy), D-lactic acid, TMS ether, TMS ester, 2-methyl-4-keto-pentan-2-ol, 1-methylene-3-methyl-butanol, benzene, 1,3-bis (1,1-dimethylethyl), phosphoric acid, 1-phenyl 1-propanol, 2-isoropyl-5-methyl-1-heptanol, 5-methyl-2-(1-methylethyl) cyclohexanol, 2-ethylthio-10-hydroxy-9-methoxy-1,4 anthraquinone, tert-hexadecanethiol and 2,6,10,14,18,22-tetracosahexane 2,6,10,18,19,23-hexamethyl were detected in sludge as well as sludge leachate samples.

However, in the GC-MS chromatogram of the n-hexane extract obtained from the degraded sludge sample after 90 days of *in situ* bioremediation the disappearance of several peaks and generation of some new peaks was clear. This indicated the degradation of major toxic organic compounds had occurred (mutagens, carcinogens, and environmental endocrine disrupters) along with the simultaneous biotransformation of some new compounds (**Figure 2** and **Table 2**).

Characterization of Bacterial Communities Using 16S rRNA Gene Analysis

The restriction digestion of the 16S rDNA genes derived from the bulk DNA from the uncultured bacterial community growing in PMDS with *Taq*1 and *Sau*3A1 restriction enzymes demonstrated the presence of 10 clones of uncultured bacterial species (**Figure 3**) Specifically, fragments of 1503, 1496, 1515, 1519, 1515, 1521, 1515, 1500, and 1513 bp were observed. RFLP analysis indicated that clones of uncultured *Bacillus* sp. (9) were dominant in degraded PMDS followed by clones of *Enterococcus* sp. (1). On the basis of phylogenetic relationships, the dominant bacterial species identified belong to the phylum *Firmicutes* (See Supplementary Figure 2). Disposed PMDS might be a major source of microbial nutrients (nitrogen, phosphate, and carbon sources). The results indicate that the *Firmicutes* might have wide ranging metabolic capabilities, such that they are able to utilize various fatty acids, sugars and organic compounds as a sole carbon source. This ability would create a specific niche for these autochthonous bacterial communities, which may allow *in situ* bioremediation of pollutants.

Phytotoxicity Assay

The SG test of green gram (*P. mungo* L.) showed inhibitory effects of fresh and degraded sludge leachate at different concentrations in terms of SG and growth parameters of seedlings (**Figure 4** and **Table 3**). Seeds germinated at rate of 100% with a 1% (v/v) concentration of fresh leachate, as the concentration increased the percent germination decreased, with 2.5 and 5% (v/v) resulting in 90 and 78% germination, respectively. There was no SG at a concentration of 10% (v/v) fresh sludge leachate after 24 h. However, in degraded sludge leachate 85% germination was recorded in up to a 10% (v/v) concentration, which was higher than with untreated leachate. With respect to the seedling growth (radical length), the radical length of seeds exposed to fresh (control) and degraded sludge leachate varied from 1.9 to 0.50 cm and 2.0 to 1.1 cm, respectively. When the seeds had been exposed to 10% (v/v) untreated leachate they showed no root development, but after treatment seeds showed development of a radical (1.1 cm). Inhibition of radical length was considered to be the first evidence of an effect of organic pollutants and of metal toxicity in plants. The germination percentage and the radical length were combined to give a comprehensive interpretation of leachate toxicity in terms of the GI. The GI values of untreated and treated leachate ranged between 0.19 to 0.95 and 1.0 to 0.46, respectively. The GI decreased with increasing concentrations of leachate. The maximum relative toxicity of control and degraded sludge leachate was noted as 22% at a concentration of 5% (v/v) and 15% at an 85% (v/v) concentration, respectively. The control sludge leachate showed greater relative toxicity. The percentage phytotoxicity analysis of the leachate obtained from controls revealed that phytotoxicity increased with increases in leachate concentrations, but in degraded leachate it gradually decreased. However, the extent of toxicity was found to be higher [75% at a 5% (v/v) concentration] of fresh sludge (control) leachate, while at the same concentration only 5% toxicity was noted in the degraded sludge leachate. The stress tolerance index of seedlings was at a minimum at a 5% (v/v) concentration of treated leachate. These results clearly indicate that the toxicity of sludge leachate was reduced significantly after *in situ* bioremediation.

Genotoxicity Assay

The results of genotoxic studies showed a concentration dependent reduction of the MI of root tip meristem cells of *Allium cepa*, after 24 h of treatment with different concentrations of distillery sludge leachate (**Table 4**). It was found that MI decreased with increasing concentrations (as percentages) of fresh sludge leachate compared to degraded sludge leachate and the decrease in MI was in the order 1% > 2.5% > 5% > 10%,

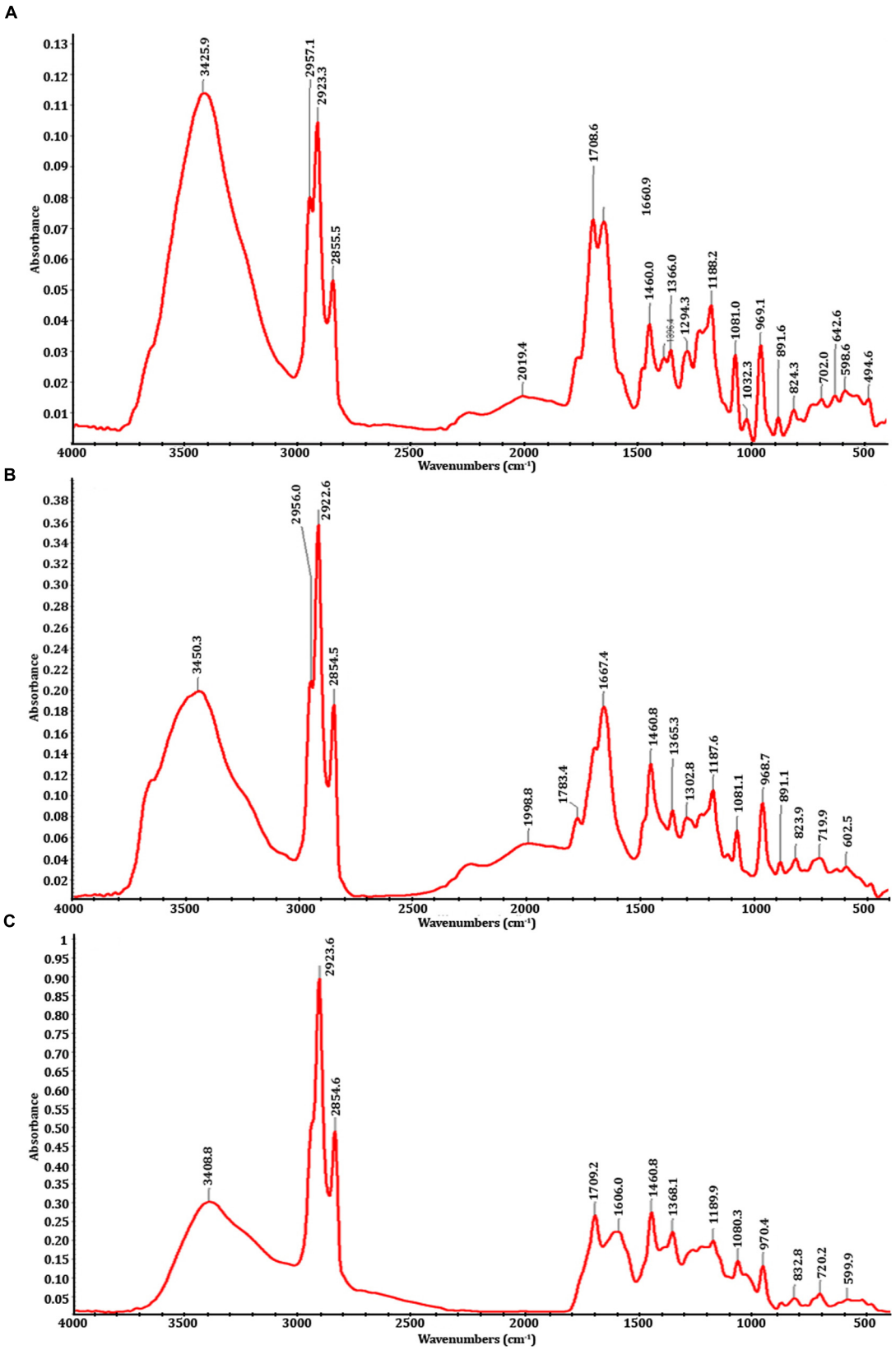


FIGURE 1 | FTIR spectra; (A) fresh distillery sludge, **(B)** fresh distillery sludge leachate, **(C)** biodegraded distillery sludge leachate after 90 days of *in situ* bioremediation.

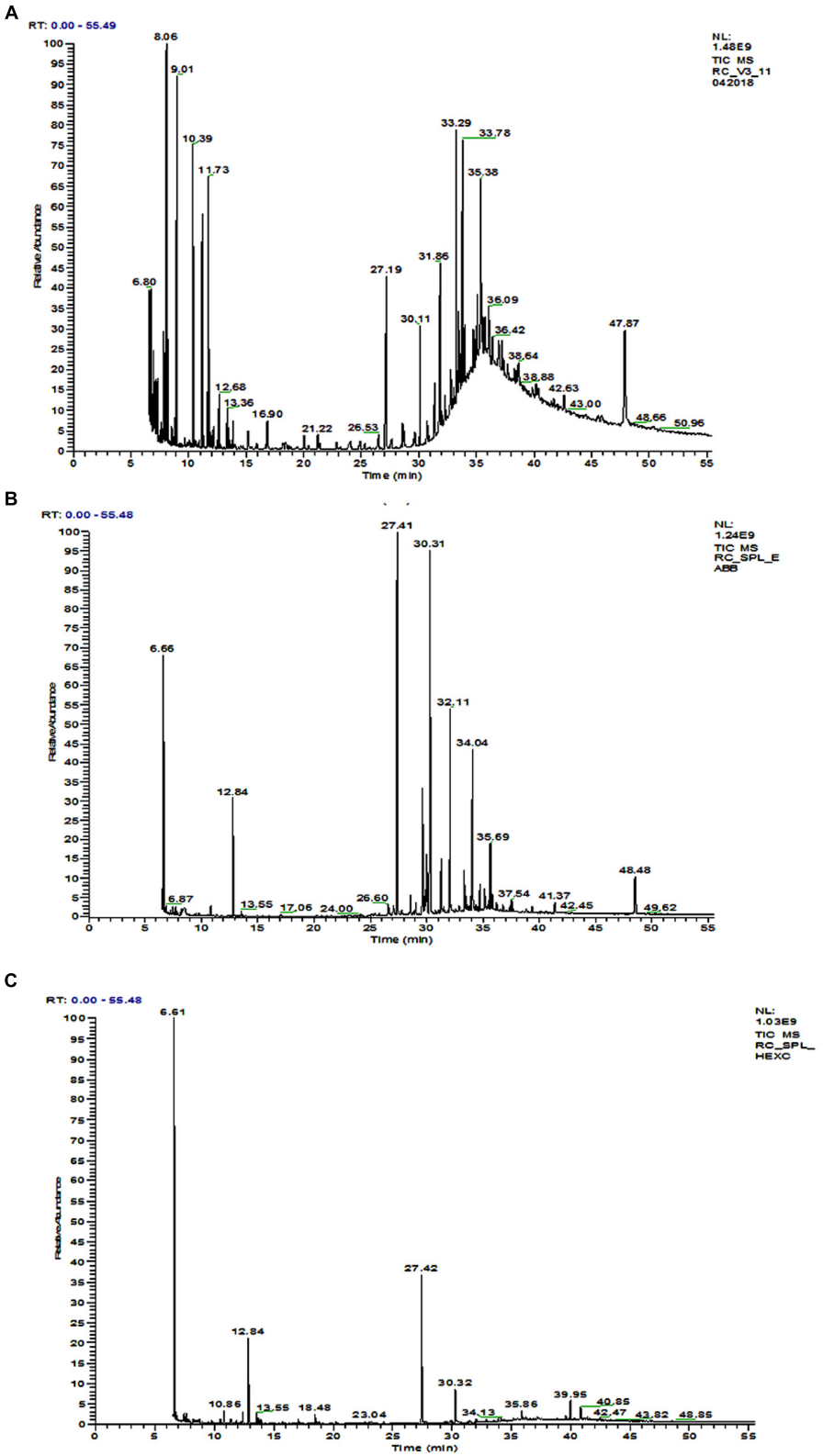


FIGURE 2 | GC-MS chromatogram of organic compounds extracted with *n*-hexane from; (A) fresh distillery sludge, **(B)** fresh distillery leachate, **(C)** distillery leachate after 90 days of *in situ* bioremediation.

which produced MI values of 16.6, 10.32, 6.68, 3.0, respectively. All tested samples induced chromosome abnormalities at all concentrations of fresh sludge leachate. Maximal chromosomal aberrations were recorded at a 10% concentration, showing 165% aberration and a total of 124 aberrant cells. The chromosomal aberrations observed included morphologically altered cells with losses of genetic material, disturbed metaphase, c-mitosis, chromosome bridges, sticky chromosomes, laggard chromosomes, polyploidy cells and apoptotic bodies (**Figure 5** and Supplementary Table 2). Exposure to distillery sludge leachate adversely affected the shape of cells of *A. cepa*. The percentage of morphologically altered cells was higher during treatment with different concentrations of leachate. Our study showed the presence of both c-mitosis (c-metaphase) and polyploid cells after treatment with distillery leachate exposure for 24 h. The frequency of cells with laggard and sticky chromosomes significantly increased with increasing distillery leachate concentrations (See Supplementary Table 2). These were seen mostly in anaphase-telophase aberration tests. In our study, the significant decrease in the MI and chromosome abnormalities observed after *in situ* bioremediation, indicated the detoxification of distillery leachate (**Table 4** and Supplementary Table 2). The

TABLE 2 | Identified organic compounds by GC-MS present in *n*-hexane extract of distillery sludge and leachate.

S. No.	RT	Name of compound	DS	DSLC	DSLD
1	7.33	1-Propanol, 3-(octadecycloxy)	−	+	+
2	8.15	2-Methyl-4-keto pentan-2-OL	+	+	−
3	8.16	D-Lactic acid, TMS ether, TMS ester	+	+	+
5	10.41	Trisiloxane, 1,1,1,5,5,5-hexamethyl-3,3-bis[(trimethylsilyl)oxy]-(CAS)	−	+	−
6	11.13	1-Methylene-3-methyl-butanol	+	−	−
7	12.46	Benzene, 1,3-bis(1,1-dimethylethyl)	+	+	−
8	12.86	Phosphoric acid	+	+	−
9	12.68	3,7-Dioxa-2,8-disilanonane, 2,2,8,8-tetramethyl-5-[(TMS)oxy	−	−	+
10	13.55	Docosanoic acid, docosyl ester	−	+	+
11	13.74	2-Isoropyl-5-methyl-1-heptanol	+	−	
12	14.84	1-Phenyl-1-propanol	+	+	−
13	15.70	Tetradecane	+	−	−
14	16.69	Tert-Hexadecanethiol	−	−	+
15	17.23	Decane, 2,3,5,8-tetramethyl	+	+	−
16	17.50	Propanoic acid	+	+	−
17	18.47	Benzoic acid, 3,5-bis(1,1-dimethylethyl)-4-hydroxy ethyl ester	−	−	+
18	19.12	1-Dodecanol	+	−	−
19	19.73	Docosane	+	+	−
20	20.73	Dodecanoic acid	+	−	−
21	21.62	Heptacosane	+	+	−
22	22.13	Dotriacontane	+	+	−
23	22.63	1-Hexadecanol, 2-methyl	−	−	+
24	23.01	Tert-Hexadecanethiol	+	−	−
25	24.24	Tetradecanoic acid	+	+	−
26	25.28	*n*-Pentadecanoic acid	+	+	−
27	27.15	Hexadecanoic acid, TMS ester	+	+	−
28	28.63	Palmidrol	−	−	+
29	30.34	Octadecanoic acid	+	+	−
30	31.85	Hexanedioic acid, bis(2-ethylhexyl ester)	−	+	+
31	34.71	Quercetin 7,3',4'-trimethoxy	−		+
32	35.08	1H-Purin-6-amine, [(fluorophenyl)methyl	−	+	+
33	35.09	2-Monostearin TMS ether	−	−	+
34	35.91	2,6,10,14,18,22-Tetracosahexane 2,6,10,18,19,23-hexamethyl	+	+	−
35	37.41	Butyl 11-eicosenoate	−	−	+
36	41.33	Stigmasta-5,22-dien-3-ol(3β,22E)	+	+	−
37	41.55	Stigmasterol	+	+	−
38	42.14	Lanosta-8, 24 dien-3-one	+	+	−
39	42.61	1-Monolinoleoylglycerol TMS ether	−	−	+
40	42.40	Spirostan-3-one (5α, 20β, 25R)	+	−	+
41	42.66	β-Sitosterol trimethyl ether	+	+	−

DS, distillery sludge; DSLC, distillery sludge leachate control; DSLD, distillery sludge leachate degraded after 90 days in situ bioremediation.

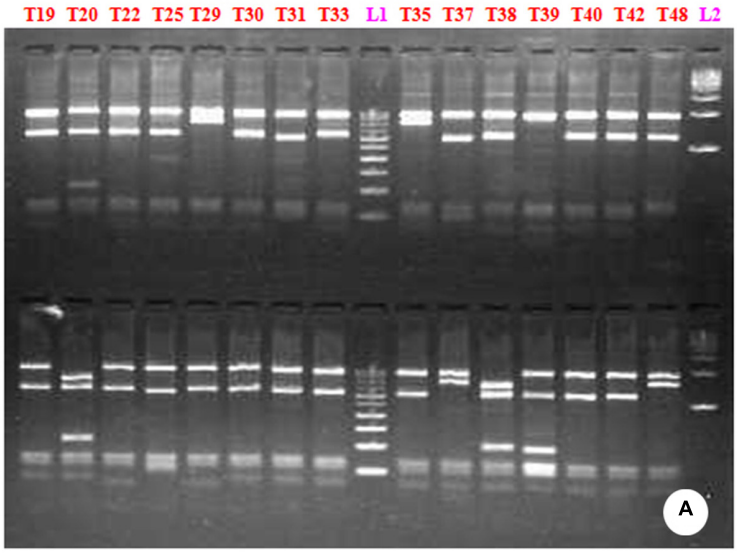
most likely reason for the high genotoxicity and cytotoxicity of these industrial water samples is the complex assortment of organic pollutants produced during the sugarcane molasses distillation process. In summary, genotoxicity results indicate that distillery sludge and leachate produce genotoxicity and may exert potentially harmful effects on flora and fauna, however, this toxicity was reduced after 90 days of *in situ* bioremediation.

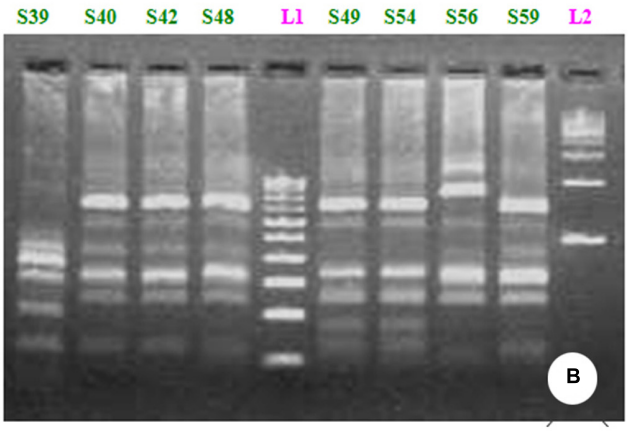
DISCUSSION

Physicochemical analysis showed that sludge and leachate both have a high pH. This may be due to the presence of large amounts of salt, but the slight reduction in various physicochemical properties, as measured for leachate, was due to bioremediation by autochthonous bacterial communities; this alters the original chemical structure and properties of various organic constituents and salts in the sludge (Chandra and Kumar, 2017b). The alkalinity of the waste arises from the combined residual effect of carbonates, bicarbonates, and hydroxides, which are used in a distillery for pH adjustment during the fermentation process and the washing of fermentation products (Tiwari et al., 2013). While the EC of sludge and leachate was found to be 4.1 and 3.9, respectively, the high values of EC indicated the role of various cations and anions, such as sodium, chloride, nitrate, and ammonium ions, which are present in both fresh distillery sludge and leachate. The high pH and EC of sludge could be due to the presence of high concentrations of soluble salts. Several authors have also reported higher values of these cations and anions in distillery waste (Chandra et al., 2008; Chandra and Kumar, 2017b). Furthermore, in the present study the presence of various heavy metals along with melanoidins has also been shown. Heavy metals have a strong tendency to bind to melanoidins (Migo et al., 1997). The high content of heavy metals in distillery sludge could be due to the corrosive effect of sugarcane juice during the sugar manufacturing process. Metals may be added further during the fermentation and distillation processes of sugarcane molasses in distilleries, as it is finally discharged as a spent wash under highly acidic conditions and again, undergoes treatment in an anaerobic reactor and all of these processes potentially induce metal corrosion of metal pipes. This may be the main source of the heavy metal content of distillery sludge. The high concentrations of heavy metals and salts in PMDS are due to the condensation process that takes place during sugar manufacturing and alcohol production. Our findings corroborated well with earlier data (Chandra and Kumar, 2017b). The high levels of organic and inorganic parameters in PMDS are also concordant with previous reports (Chandra et al., 2008). The high content of several heavy metals is an environmental health hazard because they are known to be damaging to humans and animals due to their persistence and accumulation in the environment from contaminated sites. They are known to cause neural toxicity, renal disorders, asthma, and carcinogenic effects in humans and animals (Barakat, 2011). Therefore, the sludge has toxic properties and apparently does not degrade. There was a subsequent reduction in various physicochemical parameters of the distillery leachate after 90 days of *in situ* bioremediation; possibly due to the action of the microbial community resulting in the mineralization of complex compounds. The majority of bacteria, actinomycetes and fungi are saprophytes and so they decompose organic matter. They hydrolyze and oxidize various complex organic and inorganic compounds through enzymic processes, resulting in the reduction in some physicochemical parameters following *in situ* bioremediation.

Fourier transform-infrared spectrophotometry spectroscopy is an extensively used method for the determination of the functional groups present in organic compounds. The observed change in the peaks in FTIR spectra analysis of control and degraded sludge leachate suggests degradation of organic compounds has occurred after 90 days of bioremediation *in situ*. This indicated the conversion of complex toxic compounds into simpler, non-toxic molecules. The autochthonous bacterial communities employed during *in situ* remediation during the investigation potentially resulted in the cleavage of various chemical linkages.

Gas chromatography-mass spectrometry is a good technique for determining the organic pollutants in the environment. In our study, the majority of the organic compounds detected in distillery sludge and leachate posing a threat to the environment and human health are substances derived from biochemical processes at the various stages of sugar and alcohol production, and of effluent treatment. GC-MS analysis of organic extracts in the sample identified more than 35 organic compounds some of which were mutagens, carcinogens, and environmental endocrine disrupters. Octadecanoic acid and hexadecanoic were detected in our study, which have been reported to be anti-quorum sensing molecules in bacterial products (Singh et al., 2013). However, in some studies octadecanoic acid has also been reported to be a toxic compound in aquatic systems (Kamaya et al., 2003), while hexadecanoic acid has been reported to be a DNA fragmentation inducer in a human melanoma cell line (de Sousa Andrade et al., 2005). Similar compounds have been reported by various researchers, and so our data support results reported previously (González et al., 2000; Quinn et al., 2007). This finding also corroborated previous studies (Kaushik et al., 2010). These organic compounds constitute the main components of wastewater and discharge in sludge from yeast or original sugarcane molasses, which remains after the secondary treatment of distillery effluent. Apart from this, other compounds were also identified as stigmasta-5, 22-dien-3-ol(3 β,22E), stigmasterol and β-sitosterol. These are major phytosterols (plant sterol) with a chemical structure similar to cholesterol, soluble in water at all pH values and previously reported to be present in sugarcane (*Saccharum officinarum* L.) and the wastewater from sugarcane molasses. These compounds are screened under the list of environmental endocrine-disrupting chemicals (EDCs; as in USEPA, 2012). In a previous study, it was reported that in nature, aerobic, and/or anaerobic microorganisms may transform β-sitosterol and other sterols into androgenic hormones such as 5-β-androstan 3, 17-dione and androstan 4-en-3, 17-dion (Taylor et al., 1981). Such androstan derivatives of sterols may ultimately interfere with endocrine systems and produce hermaphroditism or other morphological defects. A role of these compounds in masculinizing the fish





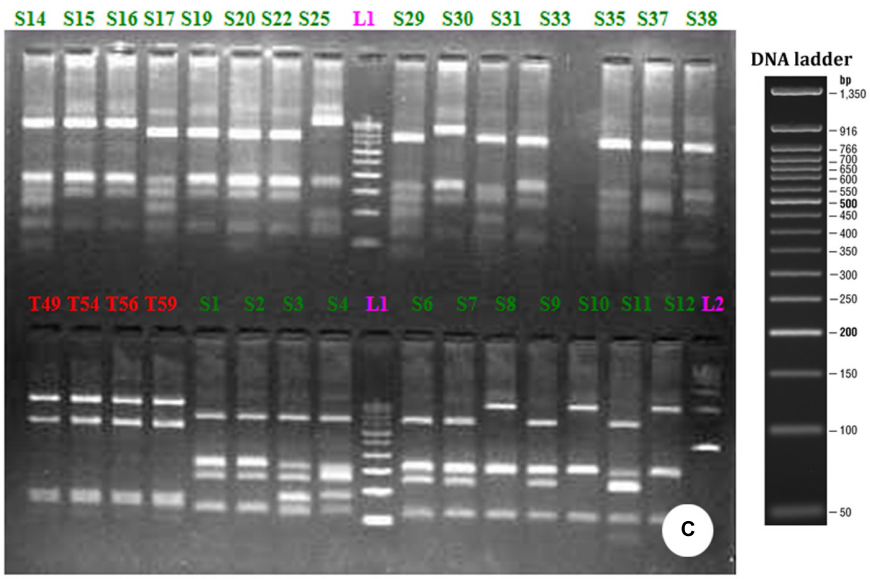


FIGURE 3 | RFLP profile generated by the restriction digestion of 16S rRNA gene derived from bacterial community growing on distillery sludge using *Taq* 1 (A) *Sau*3AI **(B)** and *Taq* 1 and *Sau*3AI restriction endonuclease together **(C)**. The above picture shows the clones, labeled from T1-T48 **(A)** S39-S59 **(B)** T49-T59 are PCR positive products **(C)** L1-100 bp ladder; L2-500 bp ladder.

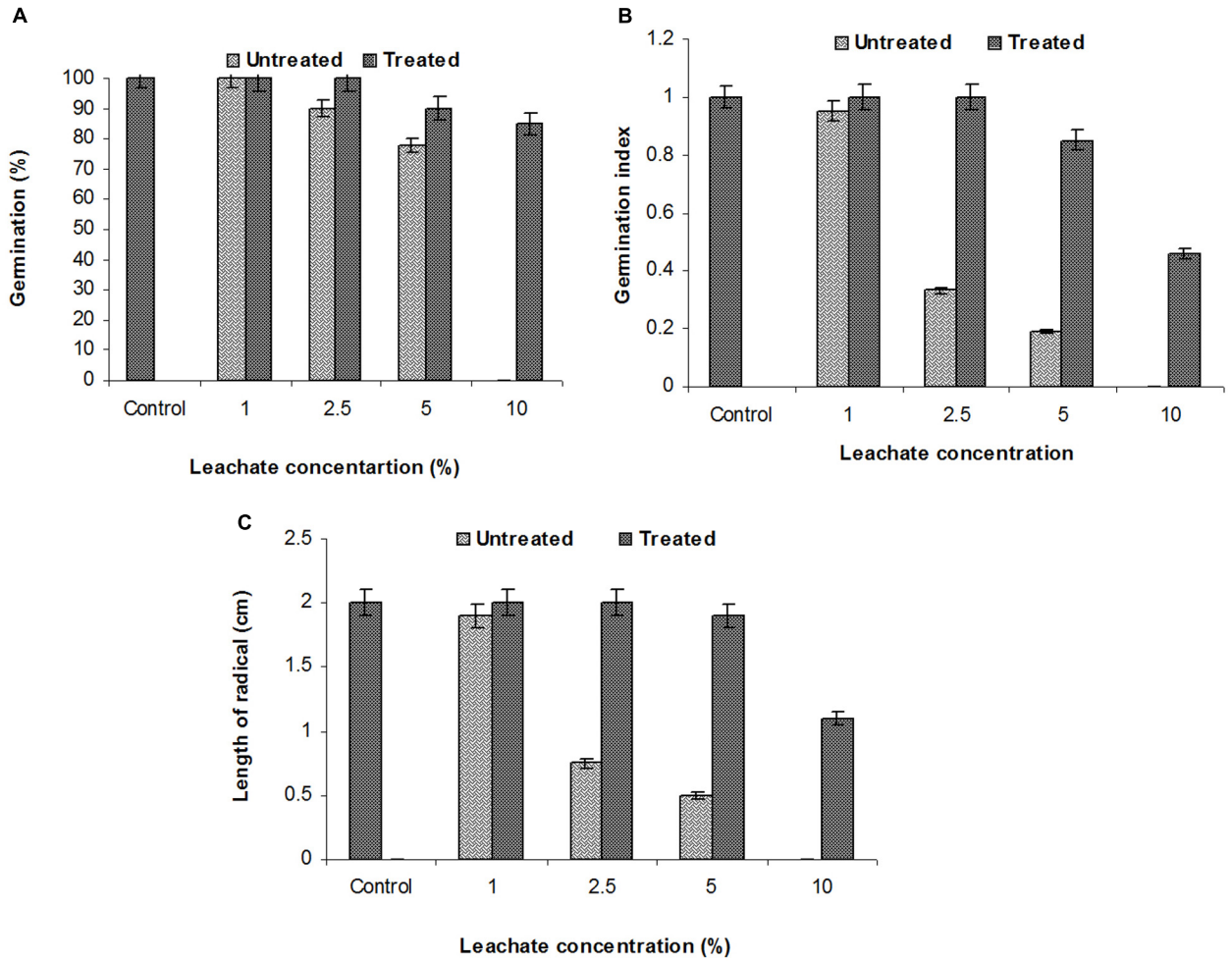


FIGURE 4 | Effects of various concentrations of sludge leachate on *Phaseolus mungo* L. vs. control (tap water); (A) percent germination, **(B)** germination index, **(C)** radical length.

population and reducing fish numbers has been suggested (Jenkins et al., 2003). However, tetradecane and other similar phyo hydrocarbons (heptacosane dotriacontane, lanosta-8, 24 dien-3-one) have also been identified, and reported as key constituents of environmental pollutants responsible for dermal irritation (Muhammad et al., 2005). We have also detected several other organic compounds in control and degraded sludge leachates. This might occur as a residual fraction of the distillation process during ethanol production from fermented molasses slurry by yeast cells. However, the role of several other organic compounds detected in the environment is still of interest and requires detailed investigation for environmental safety.

Sequence analysis of the 16S rRNA genes of bacteria and archaea has been frequently used to characterize the taxonomic composition and phylogenetic diversity of environmental samples (Langille et al., 2013). In the present work, the RFLP technique was used to divulge phylogenetic relatedness among uncultured bacterial clones. RFLP analysis disclosed the presence of the major phyla *Bacillus*, followed by *Enterococcus*. The genus *Bacillus* is also characterized by its cellular properties, which are Gram-positive, have a low G+C content, are mostly straight rod shaped, and occur singly, in pairs, or chains. They also form endospores and grow aerobically. So, in the presence of organic compounds under anaerobic conditions they could grow slowly or are in the inactive phase and become viable after the discharge of sludge (Whitman, 2009). The heat resistant nature of the endospores accounts for the presence of *Bacillus* sp. in cooling tower water, as the heat-exchange process selects for heat resistant microorganisms that become even more dominant as water is recycled (Sharmin et al., 2013). Also, Park et al. (2007) reported the dominance of *Bacillus* sp. growing on a Rotating Activated *Bacillus* Contactor Biofilm (RABCS) as used for advanced wastewater treatment by culture-dependent methods. The second member of the phylum *Firmicutes* noted in this study was *Enterococcus* sp. These bacteria are characterized as being Gram-positive, cocci-shaped, often occurring in pairs (diplococci) or short chains, non-endospore forming, aerobic or facultative anaerobes, capable of the fermentation of sugars and

TABLE 3 | Effect of different concentration of distillery sludge leachate on seedling growth of *Phaseolus mungo* L.

Concentration (%)	Germination (%)		Relative toxicity (%)		Radical length (cm)		Germination index		Phytotoxicity (%)		Stress tolerance index	
	Untreated	Treated	Untreated	Treated	Untreated	Treated	Untreated	Treated	Untreated	Treated	Untreated	Treated
1	100 ± 0.00	100 ± 0.00	00 ± 00	00 ± 0.00	1.9 ± 0.04	2.00 ± 0.01[a]	0.95 ± 0.10	1.0 ± 0.08[a]	5.0 ± 0.01	00 ± 00[ns]	0.95 ± 0.02	1.00 ± 0.01[ns]
2.5	90 ± 0.00	100 ± 0.00	10 ± 0.00	00 ± 00	0.75 ± 0.02	2.00 ± 0.02[a]	0.33 ± 0.02	1.0 ± 0.01[a]	62.50 ± 2.77	00 ± 00[a]	0.37 ± 0.01	1.00 ± 0.04[a]
5.0	78 ± 0.00	90 ± 0.00	22 ± 0.00	10 ± 0.00	0.50 ± 0.04	1.9 ± 0.02[a]	0.19 ± 0.00	0.85 ± 0.00[a]	75 ± 2.98	5.0 ± 1.4[a]	0.25 ± 0.03	0.95 ± 0.00[a]
10	NG	85 ± 0.00	NG	15 ± 0.00	NG	1.1 ± 0.01[a]	NG	0.46 ± 0.00[a]	NG	45 ± 1.2[a]	NG	0.55 ± 0.00[a]
Control	100 ± 00	100 ± 00	00 ± 00	00 ± 00	2.00 ± 0.10	2.00 ± 0.18[ns]	00 ± 00	00 ± 00	00 ± 00	00 ± 00	00 ± 00	00 ± 00

NG, no germination was observed; All the values are means of triplicate (n = 3) ± SD. The statistical significance between the values of untreated to their respective treated samples was evaluated by one-way ANOVA.
[a]*Significant level $p < 0.001$.* [ns]*Non-significant level $p > 0.05$. Control; tap water.*

of producing lactic acid or other acidic products. One study has also revealed the presence of *Bacillus* and *Enterococcus* sp. (España-Gamboa et al., 2012) in the anaerobic sludge of an upflow anaerobic sludge blanket (UASB) reactor for the treatment of distillery spent wash. This indicated that bacteria are able to exploit carbon compounds from spent wash as a necessary source of energy, and can adapt to this environment by using their endogenous enzymatic systems. This corroborates our results.

Based on sequence analyses recovered from the clone libraries, the phyla *Firmicutes* represented the dominant group of bacteria. PhyloChip analysis has also been used to assess the dominance of *Firmicutes* growing within sugarcane processing plants (Sharmin et al., 2013). Acharya et al. (2011) also studied the dynamics of the microbial communities within anaerobic biphasic fixed film bioreactor treatment distillery spent wash, showing the clear dominance by *Firmicutes* in a methanogenic bioreactor, which indicates the high degree of diversity of this phylum. The presence of *Firmicutes* as a dominant group is quite rare for natural samples. However, lignocellulosic material, such as sugarcane molasses/sugarcane bagasse represents an abundant, inexpensive source of organic material, which can be a carbon source for a growing bacterial population. Hence, the results of the current study agree with previously reported data from autochthonous bacterial communities in similar environments (Ch]andra et al., 2012). PMDS contains much more various organic and inorganic complex pollutants at much greater concentrations, but the autochthonous bacterial communities identified were specific and capable of growing in this environment.

The SG test is a common and basic tool used for toxicity evaluations of the environmental safety of industrial waste (OECD, 2003). A SG rate of 100% occurred with a 1% (v/v) concentration of fresh leachate and as the concentration increased, so the percent germination decreased. The promotion of seedling growth by lower concentrations of leachate might be due to the presence of lower concentrations of toxicant in samples tested. While the suppression of germination at high concentrations of leachate might be due to the presence of highly toxic organic compounds and dissolved solid, which were absorbed by the seeds before germination and affected various physiological and biochemical processes of SG (Bharagava and Chandra, 2010). Increases in the percentage germination in degraded sludge leachate may be due to the presence of less organic compounds, so creating a favorable environment for germination and utilization of nutrients present in the leachate prepared from the degraded sludge. Different concentrations of leachate and the different degrees of seed coat permeability led to different degrees of inhibition of germination. The inhibitory effect of the fresh sludge leachate on SG and seedling growth might be attributed to the high salt load and metal content, which induces both a high osmotic pressure and anaerobic conditions. It has also been reported that a high salt load and metal content acts as an inhibitor of plant hormones (amylases, auxins, gibberellins, and cytokinins), which are required mainly for SG, seedling growth and plant development, respectively (Ahsan et al., 2007). One study showed that distillery-sludge-amended soil delayed flowering and reduced pod formation in *P. mungo* L., which

TABLE 4 | Mitotic index and mitotic inhibition at different concentration of distillery sludge leachate.

PMDS leachate concentration (%)	Total no. of cells		Total no. of dividing cell		Mitotic index (%)		Mitotic inhibition (%)	
	Untreated	Treated	Untreated	Treated	Untreated	Treated	Untreated	Untreated
1.0	2500	2500	415 ± 20.75	551 ± 19.28[a]	16.6 ± 0.74	22.04 ± 0.90[a]	28.93 ± 1.27	5.65 ± 0.19[a]
2.5	2500	2500	258 ± 12.38	475 ± 18.05[a]	10.32 ± 0.36	19.00 ± 0.86[a]	55.82 ± 1.95	18.66 ± 0.55[a]
5.0	2500	2500	167 ± 8.14	315 ± 35.12[a]	6.68 ± 0.24	12.6 ± 0.44[a]	71.40 ± 3.28	46.06 ± 1.42[a]
10	2500	2500	75 ± 2.25	269 ± 9.14[a]	3.0 ± 0.12	10.76 ± 0.40[a]	87.15 ± 4.00	53.93 ± 1.94[a]
Control	2500	2500	584 ± 28.61	584 ± 27.51[ns]	23.36 ± 0.93	23.36 ± 1.14[ns]	–	–

All the values are means of triplicate (n = 5) ± SD. The statistical significance between the values of untreated to their respective treated samples was evaluated by one-way ANOVA. [a]*Significant level p < 0.001.* [ns]*Non-significant level p > 0.05. Control; tap water.*

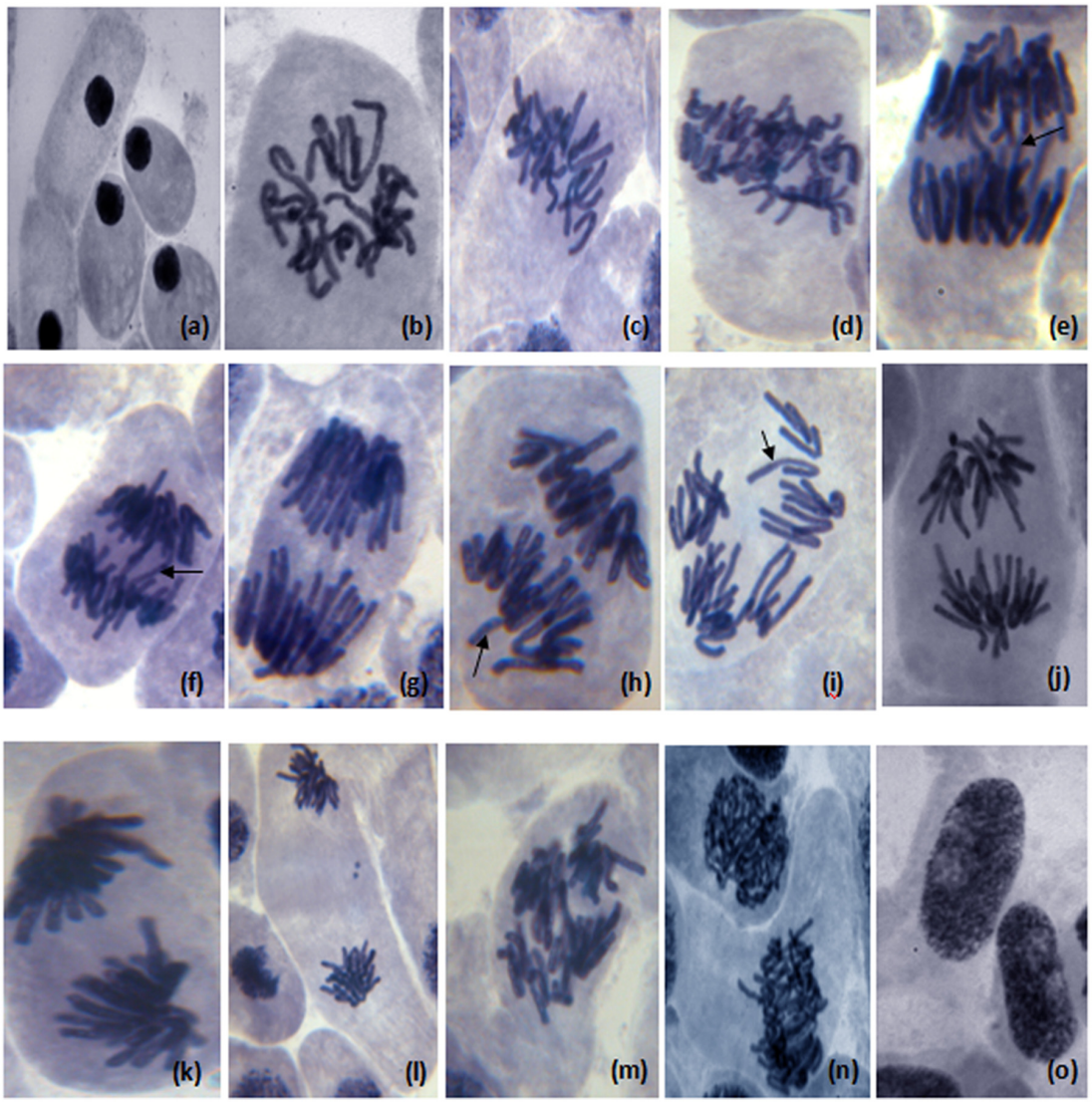


FIGURE 5 | Different chromosome aberration observed in meristematic cells of *Allium cepa* (2*n* = 16) treated with distillery sludge leachate; (a) change in nucleus position in morphological altered cell, **(b)** prophase with genetic material loss, **(c,d)** disturb metaphase, **(e)** disturb anaphase, (c-mitosis) **(e,f)** chromosome bridge in anaphase, **(g)** sticky chromosome in anaphase, **(h,i)** laggard chromosome with diagonal anaphase, **(j)** disturb chromosome in anaphase, **(k)** sticky chromosome in anaphase, **(l,m)** sticky chromosome in telophase (chromosome adherence), **(n)** polyploidy cell, **(o)** apoptotic bodies (Magnification:1000×).

apparently provides evidence for the suppression of reproductive hormones by the toxicants present in distillery sludge (Chandra et al., 2008). These findings support the presence of high levels of EDCs plus other toxic compounds in distillery sludge.

Many national and international studies have focused on genotoxicity evaluation of industrial wastewater in different test models (Hemavanthi et al., 2015; Kumari et al., 2016). We selected the *A. cepa* assay due to its sensitivity and effectiveness in assessing effluent pollutants. The assay demonstrated that untreated samples were more toxic than the respective treated samples. The results of genotoxicity tests showed that MI decreased with increasing concentrations of fresh sludge leachate as compared to degraded sludge leachate. Trace metals and other organic pollutants have been considered responsible for diminishing the MI of *A. cepa* exposed to industrial wastewater (Chandra et al., 2005; Carita and Marin-Morales, 2008). A cytogenic effect was also observed that might be due to the presence of genotoxic compounds within the PMDS. We observed various chromosomal aberrations including morphologically altered cells with loss of genetic material, disturbed metaphase, c-mitosis, chromosome bridges, laggard chromosomes, sticky chromosomes, polyploidy cells, and apoptotic bodies. The reason for such effects could be due to the presence of toxic substances in the liquid medium, which may disturb division, causing a relatively high number of aberrations. c-Metaphase may result from the action of aneurogenic agents on the cell; compounds that promote complete inactivation of the mitotic spindle (Fiskesjo, 1993; Fernandes et al., 2007). Such alterations may generate other types of cell abnormalities, such as polyploid cells (Odeigah et al., 1997). The presence of chromosomal adherence reinforces the evidence of the aneugenic action of organic pollutants present in distillery leachate. However, organic pollutants disturb the balance in the quantity of histones or other proteins responsible for controlling the proper structure of nuclear chromatin. Chromosome stickiness reflects a highly toxic effect, which probably leads to cell death (Fiskesjo, 1997). Similar observations have been reported in *A. cepa* root after treatment with distillery effluent (Hemavanthi et al., 2015). This increased stickiness also leads to the formation of chromosome bridges. However, the frequency of cells with chromosome bridges significantly increased with increases in the concentration of distillery sludge leachate, indicating a clastogenic effect of leachate (Lerne and Marin-Morales, 2009) involving one or more chromosomes. Chromosome bridges were observed here, and may have occurred due to the misrepair of DNA, telomere end fusions or even from chromosome adherence. Our findings are well corroborated with earlier studies (Hemavanthi et al., 2015).

CONCLUSION

This study has revealed that PMDS and its leachate contain several residual recalcitrant organic pollutants plus heavy metals, the majority of which are environmental toxicants (i.e., octadecanoic acid), endocrine disrupting chemicals (i.e., β-sitosterol) and also DNA fragmentation inducers (i.e., tetradecanoic acid), which are still fairly unknown. During bioremediation of PMDS *in situ*, *Bacillus* sp., and *Enterococcus* sp., were noted growing dominantly as autochthonous bacterial communities of the phylum *Firmicutes*. This showed a capability to degrade the toxic pollutants present in PMDS. This bacterial community also demonstrated a special niche in high concentrations of Fe, Zn, Cu, Mn, and Pb, and an environment rich in complex organic compounds containing mutagenic molecules and EDCs. The findings of the present study will be useful for monitoring and managing distillery waste environmentally and for the eco-restoration of polluted sites.

AUTHOR CONTRIBUTIONS

RC did leading role for designing of experiments, analysis of pollutants, and bacterial community. While, VK played role as team member and supported in experimental work and data arrangement. Further, the co-author also supported to corresponding author, i.e., RC for manuscript formatting and phytotoxicity and genotoxicity assay and graph preparation. Thus, both authors justified their role for manuscript preparation and communication.

FUNDING

This work was supported by Department of Biotechnology (DBT), Govt. of India funded project (No. BT/PR/11978/BCE/08/744/2009).

ACKNOWLEDGMENT

The authors are grateful to acknowledge the laboratory facility provided by the CSIR-IITR, Lucknow, UP, India for this study.

SUPPLEMENTARY MATERIAL

The Supplementary Material for this article can be found online at: http://journal.frontiersin.org/article/10.3389/fmicb.2017.00887/full#supplementary-material

REFERENCES

Acharya, B. K., Pathaka, H., Mohana, S., Shouche, Y., Singh, V., and Madamwara, D. (2011). Kinetic modelling and microbial community assessment of anaerobic biphasic fixed film bioreactor treating distillery spent wash. *Wat. Res.* 45, 4248–4259. doi: 10.1016/j.watres.2011.05.048

Ahsan, N., Lee, S. H., Lee, D. G., Lee, H., Lee, S. W., Bahk, J. D., et al. (2007). Physiological and protein profiles alternation of germinating rice seedlings exposed to acute cadmium toxicity. *C. R. Biol.* 330, 735–746. doi: 10.1016/j.crvi.2007.08.001

All India Distillers Association [AIDA] (2004). *All India Distillers Association and Sugar Technologists of India*. New Delhi: All India Distillers Association.

Altschul, S. F., Madden, T. L., Schaffer, A. A., Zhang, J., Zhang, Z., Miller, W., et al. (1997). Gapped BLAST and PSIBLAST: s new generation of protein database search programs. *Nucl. Acids Res.* 25, 3389–3402. doi: 10.1093/nar/25.17.3389

American Public Health Association [APHA] (2012). *Standard Method for Examination of Water and Wastewater*, 22nd Edn. Washington, DC: American Public Health Association.

Barakat, M. A. (2011). New trends in removing heavy metals from industrial wastewater. *Arab. J. Chemis.* 4, 361–377. doi: 10.1098/rsif.2010.0270

Berthelet, M., Whyte, L. G., and Greer, C. W. (1996). Rapid, direct extraction of DNA from soils for PCR analysis using polyvinylpolypyrrolidone spin columns. *FEMS Microbiol. Lett.* 138, 17–22. doi: 10.1111/j.1574-6968.1996.tb08128.x

Bharagava, R. N., and Chandra, R. (2010). Effect of bacteria treated and untreated post-methanated distillery effluent (PMDE) on seed germination, seedling growth and amylase activity in *Phaseolus mungo* L. *J. Hazard. Mater.* 180, 730–734. doi: 10.1016/j.jhazmat.2010.04.100

Carita, R., and Marin-Morales, M. A. (2008). Induction of chromosome aberrations in the *Allium cepa* test system caused by the exposure of seed to industrial effluent contaminated with azo dye. *Chemosphere* 72, 722–725. doi: 10.1016/j.chemosphere.2008.03.056

Chandra, R., Bharagava, R. N., Kapley, A., and Purohit, H. J. (2012). Characterization of *Phragmites cummunis* rhizosphere bacterial communities and metabolic products during the two stage sequential treatment of post methanated distillery effluent by bacteria and wetland plants. *Bioresour. Technol.* 103, 78–86. doi: 10.1016/j.biortech.2011.09.132

Chandra, R., and Kumar, V. (2017a). Detection of *Bacillus* and *Stenotrophomonas* species growing in an organic acid and endocrine-disrupting chemical-rich environment of distillery spent wash and its phytotoxicity. *Environ. Monit. Assess.* 189, 26. doi: 10.1007/s10661-016-5746-9

Chandra, R., and Kumar, V. (2017b). Phytoextraction of heavy metals by potential native plants and their microscopic observation of root growing on stabilised distillery sludge as a prospective tool for in-situ phytoremediation of industrial waste. *Env. Sci. Pollut. Res.* 24, 2605–2619. doi: 10.1007/s11356-016-8022-1

Chandra, R., Yadav, S., and Mohan, D. (2008). Effect of distillery sludge on seed germination and growth parameters of green gram (*Phaseolus mungo* L.). *J. Hazard. Mater.* 152, 431–439. doi: 10.1016/j.jhazmat.2007.06.124

Chandra, S., Chauhan, L. K., Murthy, R. C., Saxena, P. N., Pande, P. N., and Gupta, S. K. (2005). Comparative biomonitoring of leachates from hazardous solid waste of two industries using the *Allium* test. *Sci. Total Environ.* 347, 46–52. doi: 10.1016/j.scitotenv.2005.01.002

David Noel, S., and Rajan, M. R. (2015). Phytotoxic effect of dyeing industry effluent on seed germination and early growth of lady's finger. *J. Pollut. Eff. Contr.* 2:126. doi: 10.4172/2375-4397.1000128

de Oliveira Silva, J., Filho, G. R., da Silva Meireles, C., Ribeiro, S. D., Vieira, J. G., da Silva, C. V., et al. (2012). Thermal analysis and FTIR studies of sewage sludge produced in treatment plant. The case of sludge in the city of Uberlandia-MG. Brazil. *Thermochimica Acta* 528, 72–75. doi: 10.1016/j.tca.2011.11.010

de Sousa Andrade, L. N., De Lima, T. M., Curi, R., and de Lauro Castrucci, A. M. (2005). Toxicity of fatty acids on murine and human melanoma cell lines. *Toxicol. In Vitro* 19, 553–560. doi: 10.1016/j.tiv.2005.02.002

España-Gamboa, E. I., Mijangos-Cortés, J. O., Hernández-Zárate, G., Maldonado, J. A. D., and Alzate-Gaviria, L. M. (2012). Methane production by treating vinasses from hydrous ethanol using a modified UASB reactor. *Biotechnol. Biofuels* 5:82. doi: 10.1186/1754-6834-5-82

Fernandes, T. C. C., Mazzeo, D. E. C., and Marin-Morales, M. A. (2007). Mechanism of micronuclei formation in polyploidizated cells of *Allium cepa* exposed to trifluralin. *Pesti. Biochem. Physiol.* 88, 252–259. doi: 10.1016/j.pestbp.2006.12.003

Fiskesjo, G. (1985). The Allium as a standard en environmental monitoring. *Hereditas* 102, 99–102. doi: 10.1111/j.1601-5223.1985.tb00471.x

Fiskesjo, G. (1993). "The *Allium* test-A potential standard protocol of assessment of environmental toxicity," in *Environmental Toxicology and Risk Assessment*, eds J. W. Gorusch, F. J. Dwyner, C. D. Ingorsoll, and T. W. La Pount (Philadelphia, PA: American Society For Testing and Materials).

Fiskesjo, G. (1997). "Allium test for screening chemicals: evaluation of cytological parameters," in *Plants for Environmental Studies*. eds W. Wang, J. W. Gorsuch, and J. S. Hughes (Boca Raton, NY: CRC Lewis Publishers).

Forney, L. J., Liu, W. T., Guckert, J. B., Kumagai, Y., Namkung, E., Nishihara, T., et al. (2001). Structure of microbial communities in activated sludge: potential implications for assessing the biodegradability of chemicals. *Ecotoxicol. Environ. Saf.* 49, 40–53. doi: 10.1006/eesa.2001.2034

Fuhrman, J. A. (2009). Microbial community structure and its functional implications. *Nature* 459, 193–199. doi: 10.1038/nature08058

Gich, F. B., Amer, E., Figueras, J. B., Abella, C. A., Balaguer, M. D., and Poch, M. (2000). Assessment of microbial community structure gene by amplified ribosomal DNA restriction analysis. *Int. Microbiol.* 3, 103–106. doi: 10.1128/AEM.01719-07

González, T., Terrón, M. C., Yagüe, S., Zapico, E., Galletti, G. C., and González, A. E. (2000). Pyrolysis/gas chromatography/mass spectrometry monitoring of fungal-biotreated distillery wastewater using *Trametes* sp. I-62 (CECT 20197). *Rapid Commun. Mass Spectrom.* 14, 1417–1424. doi: 10.1002/1097-0231(20000815)14:15<1417::AID-RCM41>3.0.CO;2-I

Hemavanthi, K. L., Kumar, N. K. H., and Jagannath, S. (2015). Gentotoxic effect of distillery effluent on root tip cells of *Allium sativum* L. *J. Appl. Biol. Biotechnol.* 3, 038–041. doi: 10.7324/JABB.2015.3308

Jenkins, R., Wilson, E. M., Angus, R. A., Howell, W. M., and Kirk, M. (2003). Androstenedione and progesterone in the sediment of a river receiving paper mill effluent. *Toxicol. Sci.* 73, 53–59. doi: 10.1093/toxsci/kfg042

Kadam, A. A., Kamatkar, J. D., Khandare, R. V., Jadhav, J. P., and Govindwar, S. P. (2013). Solid-state fermentation: tool for bioremediation of adsorbed textile dyestuff on distillery industry waste-yeast biomass using isolated *Bacillus cereus* strain EBT1. *Environ. Sci. Pollut. Res.* 20, 1009–1020. doi: 10.1007/s11356-012-0929-6

Kalra, Y. P., and Maynard, D. G. (1991). *Methods Manual for Forest Soil and Plant Analysis*. Information Report NOR-X-319 Forestry Canada. Edmonton, AB: Northern Forest Centre.

Kamaya, Y., Kurogi, Y., and Suzuki, K. (2003). Acute toxicity of fatty acids to the freshwater green alga *Selenastrum capricornutum*. *Environ. Toxicol.* 18, 289–294. doi: 10.1002/tox.10127

Kapley, A., Liu, R., Jadeja, N. B., Zhang, Y., Yang, M., and Purohit, H. J. (2015). Shift in microbial community and its correlation with degradative efficiency in a wastewater treatment plant. *Appl. Biochem. Biotechnol.* 176, 2131–2143. doi: 10.1007/s12010-015-1703-2

Kaushik, G., Gopal, M., and Thakur, I. S. (2010). Evaluation of performance and community dynamics of microorganisms during treatment of distillery spent wash in a three stage bioreactor. *Bioresour. Technol.* 101, 4296–4305. doi: 10.1016/j.biortech.2010.01.046

Kumari, V., Yadav, A., Haq, I., Kumar, S., Bharagava, R. N., Singh, S. K., et al. (2016). Genotoxicity evaluation of tannery effluent treated with newly isolated hexavalent chromium reducing *Bacillus cereus*. *J. Environ. Manag.* 183, 204e211. doi: 10.1016/j.jenvman.2016.08.017

Langille, M. G. I., Zaneveld, J., Caporaso, J. G., McDonald, D., Knights, D., Reyes, J. A., et al. (2013). Predictive functional profiling of microbial communities using 16S rRNA marker gene sequences. *Nat. Biotechnol.* 31, 814–821. doi: 10.1038/nbt.2676

Larkin, M. A., Blackshields, G., Brown, N. P., Chenna, R., McGettigan, P. A., McWilliam, H., et al. (2007). Clustal W and Clustal X version 2.0. *Bioinformatics* 23, 2947–2948. doi: 10.1093/bioinformatics/btm404

Lerne, D. M., and Marin-Morales, M. A. (2009). *Allium cepa* test in environmental monitoring: a review on its application. *Mutat. Res.* 682, 71–81. doi: 10.1016/j.mrrev.2009.06.002

Loviso, C. L., Lozada, M., Guibert, L. M., Musumeci, M. A., Sarango Cardenas, S., Kuin, R. V., et al. (2015). Metagenomics reveals the high polycyclic aromatic hydrocarbon-degradation potential of abundant uncultured bacteria from chronically polluted subantarctic and temperate coastal marine environments. *J. Appl. Microbiol.* 119, 411–424. doi: 10.1111/jam.12843

Maharana, J. K., and Patel, A. K. (2014). Microbial community PLFA responses to ecosystem restoration in a chronosequence coal mine overburden spoil and implications of soil quality. *Int. J. Curr. Microbial. App. Sci.* 3, 45–71.

Migo, V. P., Del Rosario, E. J., and Matsumura, M. (1997). Flocculation of melanoidins induced by inorganic ions. *J. Ferment. Bioeng.* 83, 287–291. doi: 10.1016/S0922-338X(97)80994-4

Minuti, L., Pellegrino, R. M., and Tesei, I. (2006). Simple extraction method and gas chromatography-mass spectrometry in the selective ion monitoring mode for the determination of phenols in wine. *J. Chromatogr.* 1114, 263–268. doi: 10.1016/j.chroma.2006.02.068

Morrison, D. A. (1977). Transformation in *Escherichia coli*. *J. Bacteriol.* 132, 349–351.

Moyer, C. L., Dobbs, F. C., and Karl, D. M. (1994). Estimation of diversity and community structure through restriction fragment length polymorphism distribution analysis of bacterial 16S rRNA genes from a microbial mat at an active, hydrothermal vent system, Loihi Seamount, Hawaii. *Appl. Environ. Microbiol.* 60, 871–879.

Muhammad, F., Monteiro-Riviere, N. A., and Riviere, J. E. (2005). Comparative in vivo toxicity of topical JP-8 jet fuel and its individual hydrocarbon components: identification of tridecane and tetradecane as key constituents responsible for dermal irritation. *Toxicol. Pathol.* 33, 258–266. doi: 10.1080/01926230590908222

Narain, K., Yazdani, T., Bhat, M. M., and Yunus, M. (2012). Effect on physico-chemical and structural properties of soil amended with distillery effluent and ameliorated by cropping two cereal plant spp. *Environ. Earth Sci.* 66, 977–987. doi: 10.1007/s12665-011-1344-x

Odeigah, P. G. C., Nurudeen, O., and Amund, O. O. (1997). Genotoxicity of oil field wastewater in Nigeria. *Hereditas* 126, 161–167. doi: 10.1111/j.1601-5223.1997.00161.x

OECD (2003). *OECD Guideline for Testing of Chemicals. Terrestrial Plant Tests: 208: Seedling Emergence and Seedling Growth Test*. Paris: OECD, 1–19.

Oleszczuk, P., Malara, A., Jośko, I., and Lesiuk, A. (2012). The phytotoxicity changes of sewage sludge-amended soils. *Water Air Soil Pollut.* 223, 4937–4948. doi: 10.1007/s11270-012-1248-8

Park, S. J., Yoon, J. C., Shin, K., Kim, E. H., Yim, S., Cho, Y. J., et al. (2007). Dominance of endospore-forming bacteria on a rotating activated *Bacillus* contactor biofilm for advanced wastewater treatment. *J. Microbiol.* 45, 113–121.

Purohit, H. J., Raje, D. V., Kapley, A., Padmanabhan, P., and Singh, R. N. (2003). genomics tools in environmental impact assessment. *Environ. Sci. Technol.* 37, 356A–363A. doi: 10.1021/es032594m

Quinn, B. P., Bernier, U. R., Geden, C. J., Hogsette, J. A., and Carlson, D. A. (2007). Analysis of extracted and volatile components in blackstrap molasses feed as candidate house fly attractants. *J. Chromatogr.* 1139, 279–284. doi: 10.1016/j.chroma.2006.11.039

Santal, A. R., Singh, N. P., and Saharan, B. S. (2011). Biodegradation and detoxification of melanoidin from distillery effluent using an aerobic bacterial strain SAG5 of *Alcaligenes faecalis*. *J. Hazard. Mater.* 193, 319–324. doi: 10.1016/j.jhazmat.2011.07.068

Sharmin, F., Wakelin, S., Huygens, F., and Hargreaves, M. (2013). Firmicutes dominate the bacterial taxa within sugar-cane processing plants. *Sci. Rep.* 3:3107. doi: 10.1038/srep03107

Singh, V. K., Kavita, K., Prabhakaran, R., and Jha, B. (2013). Cis-9-octadecenoic acid from the rhizospheric bacterium *Stenotrophomonas maltophilia* BJ01 shows quorum quenching and anti-biofilm activities. *Biofouling* 29, 855–867. doi: 10.1080/08927014.2013.807914

Tamura, K., Stecher, G., Peterson, D., Filipski, A., and Kumar, S. (2013). MEGA6: molecular evolutionary genetics analysis version 6.0. *Mol. Biol. Evol.* 30, 2725–2729. doi: 10.1093/molbev/mst197

Taylor, C. D., Smith, O. S., and Gagosian, R. (1981). Use of microbial enrichments for the study of anaerobic degradation of cholesterol. *Geochim. Coscochim. Acta* 45, 2161–2168. doi: 10.1016/0016-7037(81)90068-5

Tiwari, S., Rai, P., Yadav, S. K., and Gaur, R. (2013). A novel thermotolerant *Pediococcus acidilactici* B-25 strain for color, COD, and BOD reduction of distillery effluent for end use applications. *Environ. Sci. Pollut. Res. Int.* 20, 4046–4058. doi: 10.1007/s11356-012-1339-5

USEPA (2012). *U.S. Environmental Protection Agency Endocrine Disruptor Screening Program Universe of Chemicals*. Washington, DC: United States Environmental Protection Agency.

Whiteley, A. S., and Bailey, M. J. (2000). Bacterial community structure and physiological state within an industrial phenol bioremediation system. *Appl. Environ. Microbiol.* 66, 2400–2407. doi: 10.1128/AEM.66.6.2400-2407.2000

Whitman, W. B. (ed.) (2009). *Bergey's Manual of Systematic Bacteriology*, 2nd Edn, Vol. 3. New York, NY: Springer.

Yang, L., Han, D. H., Lee, B., and Hur, J. (2015). Characterizing treated wastewater of different industries using clustered fluorescence EEM-PARAFAC and FT-IR spectroscopy: implication for downstream impact and source identification. *Chemosphere* 127, 222–228. doi: 10.1016/j.chemosphere.2015.02.028

Zhongtang, Y., and Mohn, W. W. (2001). Bacterial diversity and community structure in an aerated lagoon revealed by ribosomal intergenic spacer analyses and 16S ribosomal DNA sequencing. *Appl. Environ. Microbiol.* 67, 1565–1574. doi: 10.1128/AEM.67.4.1565-1574.2001

Conflict of Interest Statement: The authors declare that the research was conducted in the absence of any commercial or financial relationships that could be construed as a potential conflict of interest.

Copyright © 2017 Chandra and Kumar. This is an open-access article distributed under the terms of the Creative Commons Attribution License (CC BY). The use, distribution or reproduction in other forums is permitted, provided the original author(s) or licensor are credited and that the original publication in this journal is cited, in accordance with accepted academic practice. No use, distribution or reproduction is permitted which does not comply with these terms.

frontiers in Microbiology

ORIGINAL RESEARCH
published: 16 June 2017
doi: 10.3389/fmicb.2017.01112

Optimum O_2:CH_4 Ratio Promotes the Synergy between Aerobic Methanotrophs and Denitrifiers to Enhance Nitrogen Removal

*Jing Zhu, Xingkun Xu, Mengdong Yuan, Hanghang Wu, Zhuang Ma and Weixiang Wu **

Institute of Environmental Science and Technology, Zhejiang University, Hangzhou, China

The O_2:CH_4 ratio significantly effects nitrogen removal in mixed cultures where aerobic methane oxidation is coupled with denitrification (AME-D). The goal of this study was to investigate nitrogen removal of the AME-D process at four different O_2:CH_4 ratios [0, 0.05, 0.25, and 1 (v/v)]. In batch tests, the highest denitrifying activity was observed when the O_2:CH_4 ratio was 0.25. At this ratio, the methanotrophs produced sufficient carbon sources for denitrifiers and the oxygen level did not inhibit nitrite removal. The results indicated that the synergy between methanotrophs and denitrifiers was significantly improved, thereby achieving a greater capacity of nitrogen removal. Based on thermodynamic and chemical analyses, methanol, butyrate, and formaldehyde could be the main trophic links of AME-D process in our study. Our research provides valuable information for improving the practical application of the AME-D systems.

Keywords: aerobic methane oxidation, denitrification, O_2:CH_4 ratio, intermediate accumulation, thermodynamics

OPEN ACCESS

Edited by:
Wen-Jun Li,
Sun Yat-sen University, China

Reviewed by:
Binbin Liu,
Centre of Agricultural Resources Research (CAS), China
Sung-Woo Lee,
Oregon Health & Science University, United States

****Correspondence:***
Weixiang Wu
weixiang@zju.edu.cn

Specialty section:
This article was submitted to Microbiotechnology, Ecotoxicology and Bioremediation, a section of the journal Frontiers in Microbiology

Received: *25 December 2016*
Accepted: *31 May 2017*
Published: *16 June 2017*

Citation:
Zhu J, Xu X, Yuan M, Wu H, Ma Z and Wu W (2017) Optimum O_2:CH_4 Ratio Promotes the Synergy between Aerobic Methanotrophs and Denitrifiers to Enhance Nitrogen Removal. Front. Microbiol. 8:1112. doi: 10.3389/fmicb.2017.01112

INTRODUCTION

Biological denitrification, following nitrification, is widely used to remove nitrogen from wastewater. It includes four reduction steps: (1) from nitrate (NO_3^-) to nitrite (NO_2^-), (2) from NO_2^- to nitric oxide (NO), (3) from NO to nitrous oxide (N_2O) and (4) from N_2O to dinitrogen (N_2) (Zumft, 1997). Theoretically, NO_3^- and NO_2^- can be completely reduced to N_2 in the presence of enough carbon sources if the microbes are equipped with full set of denitrification genes (Rittmann and McCarty, 2001). Among the four steps of denitrification, the reduction of soluble nitrite by nitrite reductase into gas is the key step and considered as the symbol of permanent removal of nitrogen from the aquatic ecosystem (Saunders and Kalff, 2001; Philippot and Hallin, 2005). Currently, carbons in the forms of methanol, ethanol and acetate are frequently supplemented for complete denitrification in wastewater treatment systems. However, the addition of external carbon sources inevitably increases the operational cost of wastewater treatment. Methane (CH_4), a greenhouse gas, is readily available in many wastewater treatment plants and landfills and has a potential as an electron donor to replace traditional carbon sources for denitrification in nitrate-contaminated wastewater treatment (Modin et al., 2007). It was successfully demonstrated as a carbon source for denitrification in the presence of oxygen for the first time in 1978 (Rhee and Fuhs, 1978). This process was defined as aerobic methane oxidation coupled with denitrification (AME-D) (all the following discussions about this process are based on wastewater treatment systems). The AME-D process is a promising and realistic alternative to conventional biological treatment of nitrate-rich wastewaters. However, the nitrogen removal performance of AME-D systems is

required to be higher than conventional systems for practical applications. Basic knowledge regarding operational parameters that affect the AME-D process is highly needed for the system process design.

The AME-D process is a synergistic collaboration between aerobic methanotrophs and denitrifying bacteria. Aerobic methanotrophs are a group of microorganisms capable of utilizing CH_4 as a carbon and energy source. These microbes can oxidize CH_4 to carbon dioxide (CO_2) in the presence of oxygen (O_2). Metabolic pathways of methane oxidation in aerobic methanotrophs are comprehensively summarized by other researchers (Trotsenko and Murrell, 2008; Zhu et al., 2016; **Figure 1**). Briefly, CH_4 is initially catalyzed by methane monooxygenase (MMO), soluable MMO (sMMO) or particulate MMO (pMMO), to produce methanol as the first intermediate. Afterwards, methanol is transformed into formaldehyde by methanol dehydrogenase. Formaldehyde may be assimilated into biomass through the ribulose monophosphate pathway or the serine pathway, releasing multi-carbon intermediates such as acetate and citrate. Alternatively, formaldehyde can be dissimilated to CO_2 via formate for energy production. It was demonstrated that dissolved organic intermediates, such as methanol (Meschner and Hamer, 1985), formaldehyde (Liu et al., 2014), acetate (Costa et al., 2000), which were released during aerobic methane oxidation, could be used as carbon sources for co-existing denitrifiers. On the metabolic pathways, denitrification in the AME-D process consists of two critical steps that may occur simultaneously or sequentially. The first is methane oxidation to release carbon sources, and the second is the use of these carbon compounds for denitrification (i.e., nitrate or nitrite removal). Therefore, operational parameters that affect the organic carbons excreted by methanotrophs for denitrification would have a critical impact on the nitrogen removal of AME-D process. Because of the well-known inhibition of excessive O_2 on denitrification (Zumft, 1997), supply of enough electron donors and well-control of O_2 level are two critical strategies to improve nitrogen removal and promote complete denitrification (NO_3^--NO_2^--NO-N_2O-N_2) in the AME-D systems.

It has been demonstrated that the O_2:CH_4 ratio is an essential parameter to regulate the carbon flow from CH_4 to biomass and CO_2, which impacts the production of carbon sources for nitrogen removal in the AME-D process. Morinaga et al. (1979) and Costa et al. (2000) discovered that methanotrophic strains could excrete formaldehyde and acetate, when the O_2:CH_4 ratio was lower than 1.0 (i.e., oxygen-limited). In contrast, no organic metabolites were detected when O_2:CH_4 ratio was higher than 1.0 (i.e., methane-limited). Kalyuzhnaya et al. (2013) further studied the pathway of intermediates production by aerobic methanotrophs under oxygen-limited conditions and discovered that acetate, lactate, and even hydrogen could be released during novel fermentation-related methanotrophy. Besides, oxygen is another critical factor to influence nitrogen removal in the AME-D process. Aerobic methanotrophs require enough O_2 to utilize CH_4, whereas excessive O_2 will inhibit denitrifiers to reduce nitrogen (Modin et al., 2007). To date, environmental conditions that are favorable for both aerobic methanotrophs and denitrifiers are still unclear. Determination of an optimal O_2:CH_4 ratio which balances the requirements of carbon source and O_2 could be an effective way for improving denitrifying performance in the AME-D process.

The aim of this research was to investigate the impact of the O_2:CH_4 ratio on nitrogen removal in the AME-D process and to determine the optimal ratio resulting in the highest nitrogen removal performance. It was hypothesized that intermediates released by methanotrophs primarily control nitrogen removal when O_2:CH_4 ratio is below the optimal value, whereas O_2 level mainly controls nitrogen removal when O_2:CH_4 ratio is over the optimal. According to the stoichiometric (Equations 1 and 2) of the AME-D process (Zhu et al., 2016), the O_2:CH_4 ratio should be maintained below 1.1:1 (more specifically 0, 0.05, 0.25, and 1.0 in this study) to avoid excessive O_2 inhibition on denitrification.

$$CH_4 + 1.1O_2 + 0.72NO_3^- + 0.72H^+ = 0.36N_2 + CO_2 + 2.36H_2O \quad (1)$$

$$CH_4 + 1.1O_2 + 1.2NO_2^- + 1.2H^+ = 0.6N_2 + CO_2 + 2.6H_2O \quad (2)$$

MATERIALS AND METHODS

Sludge Preparation

The sludge used in this study was collected from an AME-D culture that was enriched for more than 1 year in a batch bioreactor with continuous CH_4 supply. The sludge was pre-incubated in a nitrite-containing medium under anoxic conditions in the dark at 25°C for 3 days to eliminate residual organic carbon sources. Then the sludge was centrifuged at 3,300 g for 5 min and the supernatant was discarded. The sludge pellet was resuspended and washed in sterile phosphate buffer solution (pH = 6.8) for three times to further remove extracellular organic carbons. Subsequently, it was centrifuged at higher speed of 14,000 g for 10 min to ensure complete precipitation of suspended cells. The experiments were initiated when no organic carbon was present in the supernatant. The organic carbon was determined with a Total Organic Carbon (TOC) analyzer (MultiN/C3100, Analytikjena, Germany). After all residual organics were removed, the sludge was re-suspended in the basal medium (Liu et al., 2014) at a mixed liquor suspended solid (MLSS) concentration of 17,735 mg/L. The basal medium contained the following components in 1 liter (L) distilled water: 1,250 mg $KHCO_3$, 50 mg KH_2PO_4, 300 mg $CaCl_2{\cdot}2H_2O$, 200 mg $MgSO_4{\cdot}7H_2O$, 345 mg $NaNO_2$, 1.0 mL acidic trace element solution and 1.0 mL alkaline trace element solution. Constituents of the acidic and alkaline trace element solution were described by Liu et al. (2014). Inorganic nitrogenous compounds were prepared from $NaNO_2$ to result in a concentration of NO_2^--N in the basal medium of 70 mg/L. Ammonium (NH_4^+) and NO_3^- were also supplied at low concentrations, 0.07 and 3.82 mg/L, respectively, to serve as nitrogen sources for microbes in the AME-D system. The pH of the medium was 7.2.

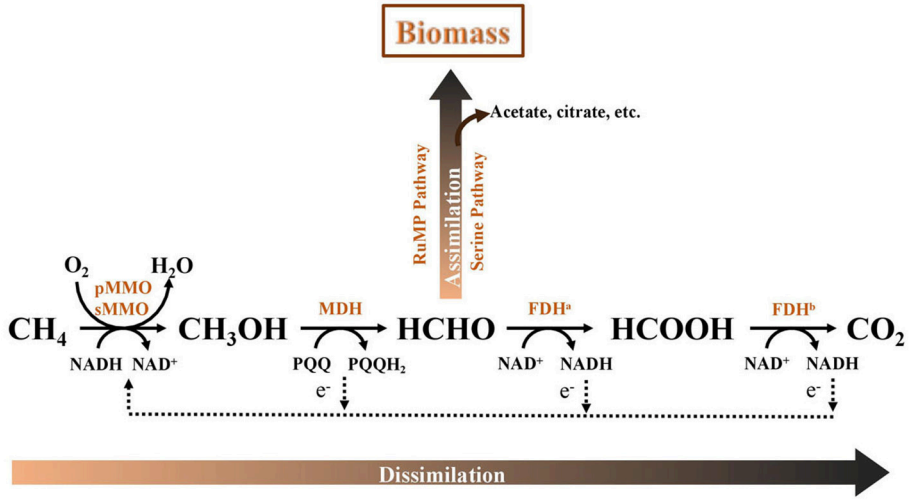


FIGURE 1 | Traditional metabolism of methane in aerobic methanotrophs (modified from Zhu et al., 2016). pMMO, particulate methane monooxygenase; sMMO, soluble methane monooxygenase; MDH, methanol dehydrogenase; FDH^a, formaldehyde dehydrogenase; FDH^b, formate dehydrogenase; RuMP, ribulose monophosphate pathway. PQQ, pyrroloquinolinequinone; NAD^+, oxidized form of nicotinamide-adenine dinucleotide; NADH, reduced form of nicotinamide-adenine dinucleotide.

Batch Experiment

Batch experiment was conducted using 10 mL of the prepared sludge and 20 mL of the basal medium in a 150 mL glass vial. Freshly prepared mixture of the basal medium and the sludge was sparged with CH_4 (99.99%) for 5 min. The vial was crimp-sealed with a butyl rubber stopper. Different volumes of CH_4 (0, 6, 24, and 60 mL) were withdrawn from the headspace of the vials with a gas-lock syringe. Afterwards, the same volume of pure O_2 (99.99%) was injected into the headspace of vials. The final compositions of O_2 and CH_4 in the gas mixtures of each treatment were shown in **Table 1**. Un-inoculated media was used as blank controls to test for leakage and non-biological chemical transformations. Triplicate samples were incubated at 28°C in shaking incubator at 180 rpm in the dark for 60 h. CH_4 and nitrogen (NO_3^--N, NO_2^--N and NH_4^+-N) consumptions and intermediate production were monitored in each treatment.

Chemical Analysis

The NO_3^--N, NO_2^--N, and NH_4^+-N concentrations were determined by ultraviolet spectrophotometry (UV-5300PC, METASH, China). The measurement of volatile suspended solid (VSS) was performed according to standard methods (American Public Health Association, American Water Works Association, Water Pollution Control Federation, 1989). In this study, nitrite removal expressed as mmol nitrite consumed per gram of biomass per day i.e., mmol NO_2^--N/gVSS/d. To quantify CH_4 content in the headspace of each vial, a sample of 0.5 mL was removed from the headspace of the vial with a gas-lock syringe. The sample was analyzed with a gas chromatograph (GC) equipped with a thermal conductivity detector under the conditions previously described by Zhang et al. (2014). Methane oxidation activity was expressed as CH_4 consumed per gram of biomass per day i.e., mmol CH_4/gVSS/d (Wang et al., 2008). NO concentration was measured by GC-mass spectrometry (6890N GC-5973MS, Agilent, USA) with the methods described by Leone et al. (1994). N_2O concentration in the vial headspace was determined by a GC (GC-14B, Shimadzu, Japan) equipped with an electron capture detector and a Porapak Q column maintained at 330 K. Intermediate (methanol, formaldehyde, formate, acetate, and other potential organics) concentrations were determined with a high performance liquid chromatograph using the methods described by Thalasso et al. (1997).

DNA Extraction

Sludge samples were analyzed for DNA before and after incubation. Three independent DNA extractions of each treatment were performed from 30 mg of sludge using a FastDNA SPIN Kit for Soil (MP Biomedical, LLC, Ohio, USA). The extraction was performed according to the manufacturer's instructions. The concentrations and the quality of DNA samples were measured with a Nanodrop analyzer (Thermo Scientific, Wilmington, DE, USA). Extracted DNA was stored at −20°C prior to subsequent analyses.

Quantification of Functional Genes

The abundance of aerobic methanotrophs and denitrifiers was estimated through quantitative PCR (q-PCR). Due to the low level of *mmoX*-harboring methanotrophs in the enrichment and high enough Cu concentration (2 μM) in the medium to inhibit the expression of *mmoX* gene (Takeguchi et al., 1997), the function of sMMO encoded by *mmoX* gene was considered to be negligible. Therefore, only *pmoA* gene encoding a subunit of pMMO was used to investigate the abundance variation of aerobic methanotrophs in this study. For denitrifiers, the *nirK* gene encoding copper nitrite reductase and the *nirS* gene encoding cytochrome cd_1-containing nitrite reductase were used

TABLE 1 | Experimental set up for aerobic methane oxidation coupled with denitrification (AME-D) process.

Treatment	Volume of the sludge (mL)	Volume of the deionized water (mL)	Volume of the basal medium (mL)	Volume of gas in the headspace		Percentage of gas in the headspace	
				O_2 (mL)	CH_4 (mL)	O_2 (%)	CH_4 (%)
Treatment 1 (O_2: CH_4 = 0)	10	–	20	0	120	0	100
Un–inoculated control 1	–	10	20	0	120	0	100
Treatment 2 (O_2: CH_4 = 0.05)	10	–	20	6	114	5	95
Un–inoculated control 2	–	10	20	6	114	5	95
Treatment 3 (O_2: CH_4 = 0.25)	10	–	20	24	96	20	80
Un–inoculated control 3	–	10	20	24	96	20	80
Treatment 4 (O_2: CH_4 = 1.0)	10	–	20	60	60	50	50
Un–inoculated control 4	–	10	20	60	60	50	50

as the biomarkers. The quantification was based on the intensity of SYBR Green dye fluorescence, which can bind to double-stranded DNA. Standard curve for each gene were generated using a 10-fold dilution series of the linearized plasmid standard (10^{-1}–10^{-6} ng) ranging from 10^8 to 10^3 copies. Each qPCR assay (25 μL) included 12.5 μL of 2 × SYBR Premix Ex Taq (Takara, Dalian, China), 1 μL of each forward and reverse primer (20 μM), either 1 μL of template DNA or the standard vector plasmid of the clones grown as single cellular suspension. The optimized thermal conditions and primers used for each gene can be viewed in the Supplementary Table 1. All real-time PCR assays were performed in triplicate for each sample in a Bio-Rad CFX1000 Thermal Cycler. All PCR runs included negative controls that did not contain DNA templates. The gene copy numbers were determined by comparing threshold cycles obtained in each PCR run with those of known standard DNA concentrations. Standard curves were obtained using serial dilutions of linearized plasmids containing cloned *pmoA*, *nirK,* and *nirS* genes.

Statistical Analysis

All data are presented as means and standard deviations. Analysis of variance and least significant difference (LSD) tests at the 5% level were used to determine the statistical significance of different treatments. Any differences with $p \geq 0.05$ were not considered as statistically significant. The relationships between *nirK/nirS* gene copies and the nitrite removals at four treatments were tested with linear regression analyses using SPSS 20.0 for Windows (SPSS Inc., Chicago, IL).

RESULTS

Methane Oxidation Activity and Intermediates Accumulation at Different O_2:CH_4 Ratios

Methane oxidation activity and concentrations of extracellular metabolites (methanol, formaldehyde, formate, and acetate, etc.) were determined under four different O_2:CH_4 ratios. As shown in **Figure 2**, methane oxidation activity substantially decreased from 277.80 mmol/gVSS/d to 21.06 mmol/gVSS/d when the O_2:CH_4 ratio was increased from 0 to 1 ($p < 0.05$). With the exception of treatment 1 at an O_2:CH_4 ratio of 0, a similar trend was observed for qPCR data of the *pmoA* gene. The *pmoA* gene abundance decreased almost an order of magnitude (from 9.36 × 10^9 to 1.63 × 10^9 copies per g dry biomass) when the O_2:CH_4 ratio was increased from 0.05 to 1 (**Figure 2**). The three primary metabolites observed in the bulk media were formaldehyde, acetate and citrate. Their concentrations went up from 42 to 76 μg/L (formaldehyde), 11 to 45 μg/L (acetate) and 0 to 28 μg/L (citrate), respectively, when O_2:CH_4 ratio was increased from 0 to 1 (**Figure 3**). Methanol, formate and butyrate were considered as three trace metabolites and their concentrations were lower than 1.20 μg/L (Supplementary Figure 1). However, methanol were not detected in the treatment 1 in the absence of O_2.

Nitrite Removal at Different O_2:CH_4 Ratios

The concentrations of NO_2^--N, NH_4^+-N and NO_3^--N were measured at the beginning and the end of incubation. Results showed that concentrations of NH_4^+-N and NO_3^--N decreased slightly by the end of the experiment and were detected in all final samples (Supplementary Table 2). There was a jump in the nitrite removal from 0.53 mmol NO_2^--N/gVSS/d to 7.32 mmol NO_2^--N/gVSS/d when the O_2:CH_4 ratio was increased from 0 to 0.25 (**Figure 4**). However, the nitrite removal decreased by 53.8% as the O_2:CH_4 ratio was increased from 0.25 to 1 ($p < 0.05$). The amount of reduced nitrogen released as NO was very low (0.13–0.32 μM; **Table 2**). In addition, the percentage of the reduced nitrogen emitted as N_2O decreased from 37.96 to 12.30% when the O_2:CH_4 ratio increased from 0 to 0.25 (**Table 2**). This percentage at the O_2:CH_4 ratio of 1 was about 2 times higher than that at the O_2:CH_4 ratio of 0.25, while this difference was insignificant ($p > 0.05$; **Table 2**). The highest nitrite removal and the low percentage of NO-N and N_2O-N in total reduced nitrogen were observed at the O_2:CH_4 ratio of 0.25. Based on the results, the O_2:CH_4 ratio of 0.25 was proposed as the optimal ratio for this AME-D system.

Nitrite reduction is catalyzed by nitrite reductase which are found in two different forms: copper nitrite reductase encoded by *nirK* gene and cytochrome cd_1-containing nitrite reductase encoded by *nirS* gene (Wang et al., 2014). Investigating the difference in *nirK* and *nirS* gene abundance might provide further evidences for the variation of nitrite removal. The

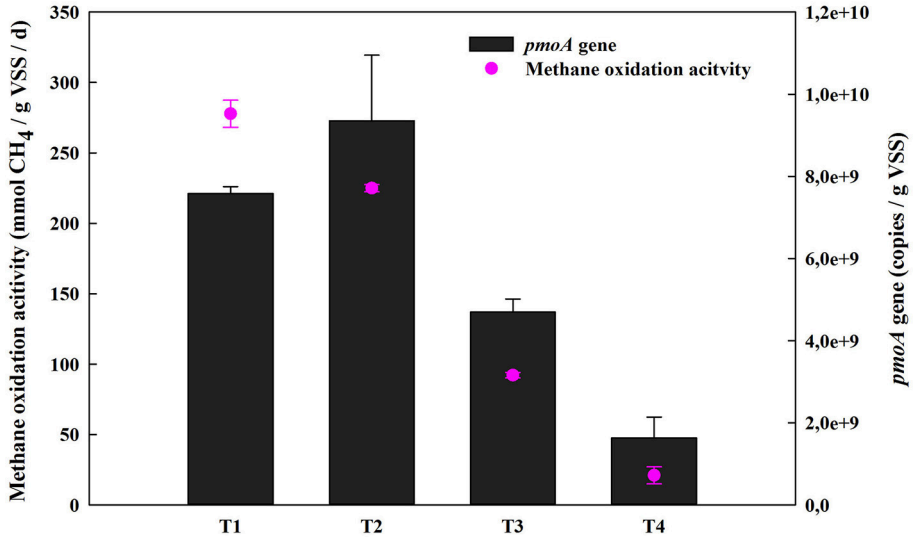


FIGURE 2 | Methane oxidation activities of the consortia and the abundance of *pmoA* gene at different O_2:CH_4 ratios in aerobic methane oxidation coupled with denitrification (AME-D) process. T1, Treatment 1 (0% O_2 and 100% CH_4); T2, Treatment 2 (5% O_2 and 95% CH_4); T3, Treatment 3 (20% O_2 and 80% CH_4); T4, Treatment 4 (50% O_2 and 50% CH_4).

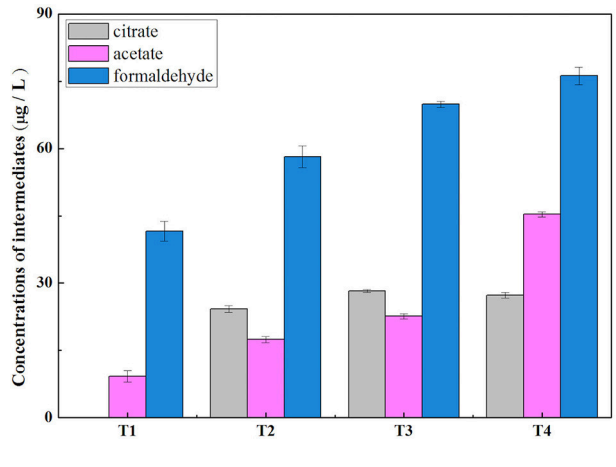


FIGURE 3 | Accumulation of acetate, citrate and formaldehyde in the liquid at different O_2:CH_4 ratios in aerobic methane oxidation coupled with denitrification (AME-D) process. T1, Treatment 1 (0% O_2 and 100% CH_4); T2, Treatment 2 (5% O_2 and 95% CH_4); T3, Treatment 3 (20% O_2 and 80% CH_4); T4, Treatment 4 (50% O_2 and 50% CH_4).

abundance of *nirK* gene was more than doubled as the O_2:CH_4 ratio was increased from 0 to 0.25 (from 3.47×10^{10} copies/gVSS up to 7.91×10^{10} copies/gVSS). However, it descended to 6.23×10^{10} copies/gVSS as the O_2:CH_4 ratio was further raised to 1. In contrast, copy numbers of *nirS* gene displayed no significant change (a slight increase from 1.82 copies/gVSS to 2.34×10^{11} copies/gVSS) when O_2:CH_4 ratio was increased from 0 to 0.25. However, it went down significantly to 7.10×10^{10} copies/gVSS at higher O_2:CH_4 ratio of 1. In addition, the linear correlation analysis revealed that *nirK* gene copies were positively correlated with nitrite removal ($r^2 = 0.8639$, $p = 0.0707$), whereas *nirS* gene copies had a slightly negative correlation with the nitrite removal ($r^2 = 0.0121$, $p = 0.8899$; **Figure 5**). If the nitrite removal was considered as the representation of the denitrifying conditions in the corresponding treatment, the higher nitrite removal indicated the better denitrifying conditions in this treatment. Thereby, the linear coorelation analyses suggest that *nirK*-type denitrifiers might be more responsive to the denitrifying conditions than *nirS*-type denitrifiers (Yoshida et al., 2010).

DISCUSSION

The Optimal O_2:CH_4 Ratio with Highest Nitrite Removal of AME-D Process

The results from the batch experiment showed that the peak nitrite removal (7.32 mmol NO_2^--N/gVSS/d) was obtained at an O_2:CH_4 ratio of 0.25. As NH_4^+-N and NO_3^--N are the preferred microbial nitrogen sources (Modin et al., 2007), their presence throughout the incubation period (Supplementary Table 2) indicated that nitrite was negligibly consumed as a nitrogen source for assimilation. Therefore, nitrite removal from the media was through dissimilatory, i.e., denitrification. Additionally, the low percentage of the consumed NO_2^--N emitted as N_2O-N (12.30%) and NO-N (0.20%, **Table 2**) at the O_2:CH_4 ratio of 0.25 indicated that enough carbon sources provided by the methanotrophs may allow denitrifiers to reduce almost 87.5% of NO_2^--N through complete denitrification. At a lower O_2:CH_4 ratio of 0.25, it was consistent with our hypothesis that nitrite removal were not inhibited by O_2, and were stimulated by the increased carbon provided by methanotrophic metabolism. However, nitrite removal was less effective at higher O_2:CH_4 ratios with higher oxygen concentrations, which was corroborated by the lower abundance of denitrifying genes (**Figure 4**).

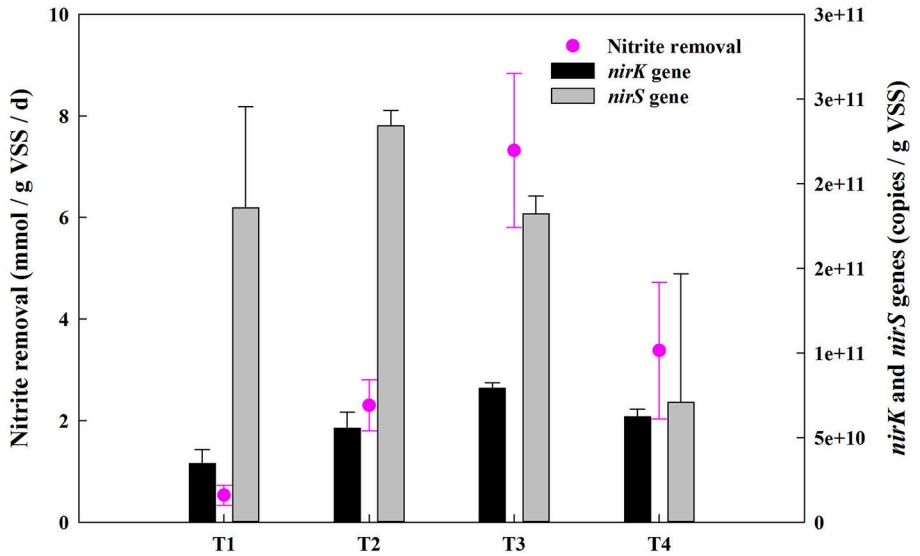


FIGURE 4 | Nitrite removal of the consortia and the abundance of functional genes at different O_2:CH_4 ratios in aerobic methane oxidation coupled with denitrification (AME-D) process. T1, Treatment 1 (0% O_2 and 100% CH_4); T2, Treatment 2 (5% O_2 and 95% CH_4); T3, Treatment 3 (20% O_2 and 80% CH_4); T4, Treatment 4 (50% O_2 and 50% CH_4).

TABLE 2 | Reduction of NO_2^--N and accumulation of NO-N and N_2O-N at different O_2:CH_4 ratios in aerobic methane oxidation coupled with denitrification (AME-D) process.

O_2/CH_4 ratio	0[a]	0.05[b]	0.25[c]	1[d]
Reduced NO_2^--N (μmol)	5.06 ± 1.88	21.87 ± 4.74	69.54 ± 14.37	32.11 ± 12.78
Accumulated NO-N (μmol)	0.18 ± 0.03	0.24 ± 0.03	0.14 ± 0.03	0.32 ± 0.03
Accumulated N_2O-N (μmol)	1.82 ± 0.27	3.58 ± 0.23	8.24 ± 0.71	7.17 ± 0.47
Accumulated NO-N/ Reduced NO_2^--N	3.96 ± 1.50%	1.14 ± 0.18%	0.20 ± 0.03%	1.17 ± 0.68%
Accumulated N_2O-N/ Reduced NO_2^--N	37.96 ± 9.13%	16.78 ± 3.06%	12.30 ± 3.27%	26.11 ± 14.34%

[a] *(0% O_2; 100% CH_4).*
[b] *(5% O_2; 95% CH_4).*
[c] *(20% O_2; 80% CH_4).*
[d] *(50% O_2; 50% CH_4).*

The conclusion that nitrite removal was stimulated by carbon sources released from aerobic methane oxidation at a O_2:CH_4 ratio lower than or equal to 0.25 could be supported by the variation of intermediate concentrations among four treatments. Concentrations of accumulated intermediates were higher and higher in the bulk media with the O_2:CH_4 ratios increasing from 0 to 0.25 (**Figure 3**). It may be attributed to the increased O_2 concentration in these treatments. Morinaga et al. (1979) and Costa et al. (2001) demonstrated that the O_2 level would significantly impact the consumption and production of metabolites in methane metabolism. However, the effect was not unambiguously determined. Morinaga et al. (1979) observed formaldehyde accumulation under oxygen-limited conditions, whereas Costa et al. (2001) discovered that formaldehyde accumulated under oxygen-excessive conditions. Our results indicated that the increased oxygen level promoted intermediates accumulation in methane metabolism. Low level of available carbon sources for denitrifiers in Treatment 1 resulted in the lowest nitrite removal. Once O_2 was largely induced in the headspace in Treatment 2 and 3, concentrations of intermediates increased in the liquid bulk. The observation of simultaneous higher nitrite removal and lower ratio of accumulated N_2O-N:consumed NO_2^--N indicated that complete denitrifying activity was improved by these accumulated intermediates.

The ability of denitrifiers to resist the inhibition of O_2 at the optimal O_2:CH_4 ratio may be due to two reasons. Firstly, the abundance of *nirK*-harboring denitrifiers was the highest among the four treatments and these denitrifiers are able to tolerate higher O_2 levels (Desnues et al., 2007). Secondly, the sludge aggregation/granulation in anoxic micro-environments can lessen the O_2 exposure of the denitrifiers. As shown in **Figure 6**, at the O_2:CH_4 ratio of 0.25, suspended biomass formed granule-like agglomerates with an average diameter of about 2 mm, while such effect did not occur for the O_2:CH_4 ratios of 0, 0.05, and 1. Sludge aggregation has also been observed in an AME-D system with an optimized O_2 level that had the highest nitrogen removal rate (Thalasso et al., 1997). It can be therefore concluded that sludge aggregation at an optimal O_2:CH_4 ratio

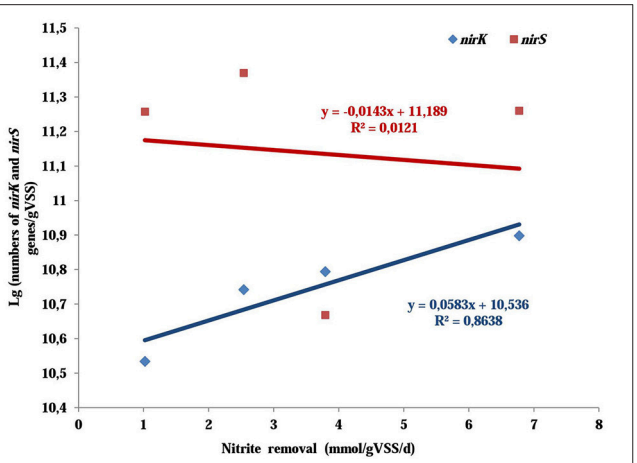


FIGURE 5 | The relationships between nitrite removal and the abundance of *nirK*/*nirS* genes in aerobic methane oxidation coupled with denitrification (AME-D) process. Linear regressions were used to test the correlation between nitrite removal and the abundance of *nirK*/*nirS* genes.

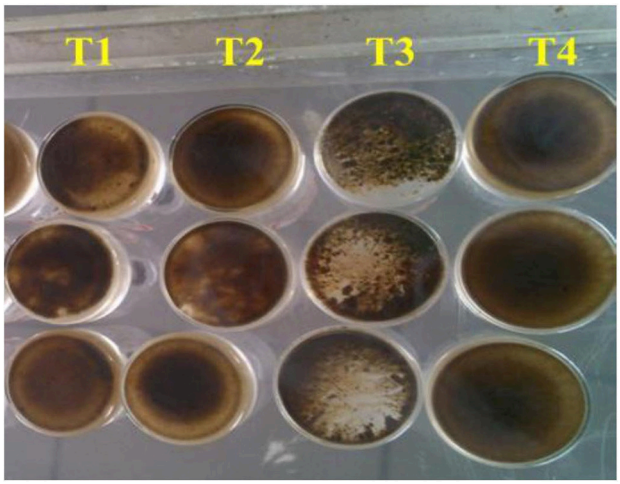


FIGURE 6 | Configuration of activated sludge in four treatments at the end of incubation during aerobic methane oxidation coupled with denitrification (AME-D) process. The phenomenon of aggregation is apparent in treatment 3 (T3) while activated sludge in other treatments were dispersive. T1, Treatment 1 (0% O_2 and 100% CH_4); T2, Treatment 2 (5% O_2 and 95% CH_4); T3, Treatment 3 (20% O_2 and 80% CH_4); T4, Treatment 4 (50% O_2 and 50% CH_4).

could improve nitrite removal. The spatial distribution of microorganisms and O_2 level within the aggregates should be investigated in the future.

With regard to the effect of the O_2:CH_4 ratio on denitrification, Sun et al. (2013) observed a similar phenomenon that the O_2:CH_4 ratio affected nitrogen removal of AME-D process in a membrane biofilm bioreactor (MBfR). Their optimal O_2:CH_4 ratio of 1.5 was considerably higher than the one in this study. It is likely that the spatial arrangement of the microbial community within a well-developed biofilm would allow for greater tolerance to O_2, as compared to a suspended culture. They speculated that greater metabolite excretion by the methanotrophs improved nitrate removal performance initially, and that excessive O_2 caused the significant drop in the denitrifying rate when O_2:CH_4 ratio increased to 2.0. The results from this study corroborate the trend that Sun et al. (2013) observed.

Methane oxidation activity dramatically decreased when O_2:CH_4 ratio increased from 0 to 1 (**Figure 2**). It was probably due to the large change in methane availability. Li et al. (2014) observed a similar trend with methanotrophic activity of landfill cover soils. The methane oxidation activity at O_2:CH_4 ratio of 0.25 (4×10^4 ppmv O_2/2×10^5 ppmv CH_4) was almost 4-fold higher than that at O_2:CH_4 ratio of 4.00 (2×10^5 ppmv O_2/5×10^4 ppmv CH_4) (Supplementary Table 3). In their research, methane oxidation activity was much more sensitive to CH_4 than O_2, and a drop of CH_4 concentration would result in a simultaneous decrease of methane oxidation activity. Additionally, copy numbers of the *pmoA* gene decreased as the methane concentration decreased (Baani and Liesack, 2008; Li et al., 2014). In the current research, CH_4 concentration declined from 100 to 50% and O_2 concentrations rose from 0 to 50% for the ratios tested. This suggests that a decrease in methane oxidation activity with a substantial increase in O_2:CH_4 ratio is plausible. However, it is unexpected that the high *pmoA* gene copy numbers and methane oxidation activity were observed in Treatment 1 in the absence of O_2. Rechecking the gaseous composition of the headspace in this treatment at the beginning of the incubation, it was discovered that trace amount (0.012%) of O_2 can still be detected after the sludge was sparged with pure CH_4 (99.99%). This trace level of O_2 may result in the observed CH_4 consumption. However, further investigations are still required to focus on examining if anaerobic methane oxidation contributed to CH_4 consumption when this trace amount of O_2 was depleted.

Thermodynamic Speculation for Metabolic Pathways of AME-D Process

Acetate, citrate, and formaldehyde were detected as three primary compounds detected during the AME-D process, while methanol, formate, and butyrate occurred in trace quantities. It is difficult to postulate which were the main substrates for the denitrifiers as their levels of consumption relative to production were not known. However, thermodynamic analysis of AME-D process may provide useful information for speculating the actual metabolic pathway (all of the following thermodynamic analyses are based on aerobic methane oxidation coupled with complete denitrification).

Methanol is considered as the most effective intermediate for denitrification according to the review of the AME-D process (Zhu et al., 2016). The reactions (Equations 3–5) related to energy production contained in AME-D process using NO_2^- as the denitrifying electron acceptor were shown in **Table 3**. These equations are based on one electron equivalent (eeq). Assuming that at least X (<1) mol of methanol is needed by aerobic methanotrophs for their requirement of cell synthesis and maintenance when one mole of CH_4 is oxidized to methanol, the remaining part of methanol can be used for denitrification as

TABLE 3 | Stoichiometric equations in aerobic methane oxidation coupled with denitrification (AME-D) process based on theoretical hypotheses.

Equation	Stoichiometric equation	$\Delta G^{0'}$
(3)	$\frac{1}{2}CH_4+\frac{1}{4}O_2=\frac{1}{2}CH_3OH$	−62.34 kJ/eeq
(4)	$\frac{1}{6}CH_3OH+\frac{1}{4}O_2=\frac{1}{6}CO_2+\frac{1}{3}H_2O$	−115.56 kJ/eeq
(5)	$\frac{1}{6}CH_3OH+\frac{1}{3}NO_2^-+\frac{1}{3}H^+=\frac{1}{6}N_2+\frac{1}{6}CO_2+\frac{1}{2}H_2O$	−129.40 kJ/eeq

the electron donor. An energy-balanced equation for the AME-D process can be described as Equation (6).

$$6\cdot\ \Delta G_{Eq.(4)}\cdot\varepsilon\cdot X+2\cdot\left[\Delta G_{Eq.(3)}-0.5\cdot\Delta G_{xy}\right]+\Delta G_m=0 \quad (6)$$

Where ε, is the energy transfer efficiency a value of 0.37 (McCarty, 2007). $[\Delta G_{Eq.(3)} - 0.5\Delta G_{xy}]$ denotes the net energy production for the oxidation from CH_4 to methanol after considering the energy input for the mono-oxygenase and the required reducing equivalent, which equals to 47.26 kJ/eeq. ΔG_m represents the minimum maintenance energy requirement with a value of about 8.1 kJ/mol oxidized CH_4 (Modin et al., 2007). The exhaustive description of calculation processes for $[\Delta G_{Eq.(3)} - 0.5\Delta G_{xy}]$ and ΔG_m is presented by Zhu et al. (2016). From Equation (6), the value derived for X is 0.40. Because the energy required by cell synthesis has not been considered during the above calculation, the theoretical maximum quantity of methanol used by denitrifiers was 0.60 mol. This means that the maximum proportion of methanol that can be captured by denitrifiers is 60%. The overall reaction of AME-D process in the presence of NO_2^- was described as Equation (7), a combination of the proposed value and Equations (3–5).

$$CH_4+\frac{11}{10}O_2+\frac{6}{5}NO_2^-+\frac{6}{5}H^+=\frac{3}{5}N_2+CO_2+\frac{13}{5}H_2O$$
$$\Delta G^{0'}=-867.86\,\mathrm{kJ/mol\,CH_4} \quad (7)$$

All six substrates detected in this study were potential carbon sources for denitrifiers. In order to understand which substrates were likely the functional intermediates, thermodynamic analysis was performed based on the chemical data associated with the O_2:CH_4 ratio of 0.25. During the process of thermodynamic derivation, all of organics detected in the bulk liquid were individually chosen as the trophic link of aerobic methane oxidation and denitrification. After several iterations, the same general equation (Equation 8) for the AME-D process, which was in agreement with CH_4 and NO_2^- consumption was obtained through three different approaches:

(1) 4.34% of consumed CH_4-C flowed to denitrifiers using methanol as the trophic link;
(2) 5.22% of consumed CH_4-C flowed to denitrifiers using butyrate as the trophic link;
(3) 6.52% of consumed CH_4-C flowed to denitrifiers using formaldehyde as the trophic link. This means that methanol, butyrate and formaldehyde released by aerobic methanotrophs were three possible intermediates that could be used as carbon sources by denitrifiers at an O_2:CH_4 ratio of 0.25. However, acetate could not be an active carbon source under this condition in our study, although it was a feasible electron donor with highest denitrifying potential (Hallin and Pell, 1998). This conclusion is further supported by the increased copy numbers of *nirK* genes, which would have decreased if acetate was the main active electron donor for denitrifiers (Li et al., 2015).

$$CH_4+\frac{89}{46}O_2+\frac{2}{23}NO_2^-+\frac{2}{23}H^+=\frac{1}{23}N_2+CO_2+\frac{47}{23}H_2O$$
$$\Delta G^{0'}=-821.65\,\mathrm{kJ/mol\,CH_4} \quad (8)$$

Based on the above analysis, it was evident that the percentage of carbon flow from methane to denitrification (4.34–6.52%) was much lower than the ideal flow (60%). Further improvement in the carbon flow is vital to enhance the AME-D denitrification rates.

Implication of O_2:CH_4 Ratio Control for Nitrogen Removal in AME-D Process

The effect of the O_2:CH_4 ratio was demonstrated to significantly impact nitrogen removal during the AME-D process through contribution of the carbon metabolites generated by the methanotrophs and oxygen inhibition. To date, most studies have considered only the individual impact of O_2 on the apparent nitrogen removal rate of the AME-D process (Werner and Kayser, 1991; Thalasso et al., 1997; Modin et al., 2010), whereas the combined effect of O_2 and CH_4 and associated mechanisms are rarely investigated. It is necessary to address the impact of O_2:CH_4 ratio on CH_4 and NO_3^-/NO_2^- metabolism in the AME-D process, rather than the tendency of methane oxidation rates and denitrifying activities under different gaseous environments. The knowledge will allow a better understanding of the specific roles of the O_2:CH_4 ratio in CH_4 and NO_3^-/NO_2^- metabolism. It is expected that this will contribute to well-founded strategies that will improve nitrogen removal, one of bottle-necks in the application of the AME-D process.

In this study, the optimal O_2:CH_4 ratio for denitrification was found to be 0.25. At this point, denitrifying activity reached the highest level of 7.32 mmol NO_2^--N/gVSS/d. When the O_2:CH_4 ratio was below the optimal ratio, nitrite removal was improved with the increased O_2:CH_4 ratio, presumably due to an increase in available substrates released by aerobic methanotrophs. Methanol, butyrate and formaldehyde were thermodynamically speculated as the main active intermediates of the AME-D process. When the O_2:CH_4 ratio was above the optimal ratio, nitrite removal was presumably inhibited by the excessive O_2. These results indicate that adjusting the O_2:CH_4 ratio can improve the cooperation between aerobic methanotrophs and denitrifiers to obtain better nitrogen removal performance using the AME-D process.

AUTHOR CONTRIBUTIONS

JZ: contributed to the conception, experimental design, acquisition, analysis, and interpretation of data, and article drafting; XX, MY: analyzed and interpreted data; HW, ZM: contributed to data acquisition; WW: supervised the student and revised the article.

ACKNOWLEDGMENTS

We would like to express our appreciation to Dr. P. J. Strong from the Centre for Solid Waste Bioprocessing in the University of Queensland, Prof. Jiayang Cheng from Biological and Agricultural Engineering Department of North Carolina State University, Dr. Faqian sun, Dr. Cheng Wang, Dr. Pengfei Liu, PhD student Xingguo Han and Christina Horn for their help to improve the quality of this manuscript. We additionally thank the reviewers for their valuable suggestions. This work was supported by the China National Critical Project for Science and Technology on Water Pollution and Control under No. 2014ZX07101-012.

SUPPLEMENTARY MATERIAL

The Supplementary Material for this article can be found online at: http://journal.frontiersin.org/article/10.3389/fmicb.2017.01112/full#supplementary-material

REFERENCES

American Public Health Association, American Water Works Association, Water Pollution Control Federation (1989). *Standard Methods for the Examination of Water and Wastewater, 17th Edn.* Washington, D. C: American Water Works Association, Water Pollution Control Federation.

Baani, M., and Liesack, W. (2008). Two isozymes of particulate methane monooxygenase with different methane oxidation kinetics are found in *Methylocystis* sp. strain SC2. *Proc. Natl. Acad. Sci. U.S.A.* 105, 10203–10208. doi: 10.1073/pnas.0702643105

Costa, C., Dijkema, C., Friedrich, M., Garcia-Encina, P., Fernandez-Polanco, F., and Stams, A. J. (2000). Denitrification with methane as electron donor in oxygen-limited bioreactors. *Appl. Microbiol. Biotechnol.* 53, 754–762. doi: 10.1007/s002530000337

Costa, C., Vecherskaya, M., Dijkema, C., and Stams, A. J. M. (2001). The effect of oxygen on methanol oxidation by an obligate methanotrophic bacterium studied by *in vivo*13C nuclear magnetic resonance spectroscopy. *J. Ind. Microbiol. Biot.* 26, 9–14. doi: 10.1038/sj.jim.7000075

Desnues, C., Michotey, V. D., Wieland, A., Zhizang, C., Fourcans, A., Duran, R., et al. (2007). Seasonal and diel distributions of denitrifying and bacterial communities in a hypersaline microbial mat (Camargue, France). *Water Res.* 41, 3407–3419. doi: 10.1016/j.watres.2007.04.018

Hallin, S., and Pell, M. (1998). Metabolic properties of denitrifying bacteria adapting to methanol and ethanol in activated sludge. *Water Res.* 32, 13–18. doi: 10.1016/S0043-1354(97)00199-1

Kalyuzhnaya, M. G., Yang, S., Rozova, O. N., Smalley, N. E., Clubb, J., Lamb, A., et al. (2013). Highly efficient methane biocatalysis revealed in a methanotrophic bacterium. *Nat. Commun.* 4:2785. doi: 10.1038/ncomms3785

Leone, A. M., Gustafsson, L. E., Francis, P. L., Persson, M. G., Wiklund, N. P., and Moncada, S. (1994). Nitric oxide is present in exhaled breath in humans: direct GC-MS confirmation. *Biochem. Bioph. Res. Commun.* 201, 883–887. doi: 10.1006/bbrc.1994.1784

Li, C., Cao, J. S., Ren, H. Q., Li, Y., and Tang, S. Y. (2015). Comparison on kinetics and microbial community among denitrification process fed by different kinds of volatile fatty acids. *Process Biochem.* 50, 447–455. doi: 10.1016/j.procbio.2015.01.005

Li, H., Chi, Z., Lu, W., and Wang, H. (2014). Sensitivity of methanotrophic community structure, abundance, and gene expression to CH_4 and O_2 in simulated landfill biocover soil. *Environ. Pollut.* 184, 347–353. doi: 10.1016/j.envpol.2013.09.002

Liu, J., Sun, F., Wang, L., Ju, X., Wu, W., and Chen, Y. (2014). Molecular characterization of a microbial consortium involved in methane oxidation coupled to denitrification under micro-aerobic conditions. *Microb. Biotechnol.* 7, 64–76. doi: 10.1111/1751-7915.12097

McCarty, P. L. (2007). Thermodynamic electron equivalents model for bacterial yield prediction: modifications and comparative evaluations. *Biotechnol. Bioeng.* 97, 377–388. doi: 10.1002/bit.21250

Meschner, K. L., and Hamer, G. (1985). "Denitrification by methanotrophic/metylotrophic bacterial associations in aquatic environments," in *Denitrification in the Nitrogen Cycle,* ed H. L. Golterman (New York, NY: Plenum Press), 257–271.

Modin, O., Fukushi, K., Nakajima, F., and Yamamoto, K. (2010). Aerobic methane oxidation coupled to denitrification: kinetics and effect of oxygen supply. *J. Environ. Eng-Asce.* 136, 211–219. doi: 10.1061/(ASCE)EE.1943-7870.0000134

Modin, O., Fukushi, K., and Yamamoto, K. (2007). Denitrification with methane as external carbon source. *Water Res.* 41, 2726–2738. doi: 10.1016/j.watres.2007.02.053

Morinaga, Y., Yamanaka, S., Yoshimura, M., Takinami, K., and Hirose, Y. (1979). Methane metabolism of the obligate methane-utilizing bacterium, Methylomonas Flagellata, in methane-limited and oxygen-limited chemostat culture. *Agric. Biol. Chem. Tokyo* 43, 2453–2458.

Philippot, L., and Hallin, S. (2005). Finding the missing link between diversity and activity using denitrifying bacteria as a model functional community. *Curr. Opin. Microbiol.* 8, 234–239. doi: 10.1016/j.mib.2005.04.003

Rhee, G. Y., and Fuhs, G. W. (1978). Wastewater denitrification with one-carbon compounds as energy-source. *J. Water Pollut. Control Fed.* 50, 2111–2119.

Rittmann, B. E., and McCarty, P. L. (2001). *Environmental Biotechnology: Principles and Applications*. New York, NY: McGraw-Hill Book Co.

Saunders, D. L., and Kalff, J. (2001). Nitrogen Retention in Wetlands, Lakes and Rivers. *Hydrobiologia* 443, 205–212. doi: 10.1023/A:1017506914063

Sun, F. Y., Dong, W. Y., Shao, M. F., Lv, X. M., Li, J., Peng, L. Y., et al. (2013). Aerobic methane oxidation coupled to denitrification in a membrane biofilm reactor: treatment performance and the effect of oxygen ventilation. *Bioresour. Technol.* 145, 2–9. doi: 10.1016/j.biortech.2013.03.115

Takeguchi, M., Furuto, T., Sugimori, D., and Okura, I. (1997). Optimization of methanol biosynthesis by *Methylosinus trichosporium* OB3b: an approachto improve methanol accumulation. *Appl. Biochem. Biotech.* 68, 143–152. doi: 10.1007/BF02785987

Thalasso, F., Vallecillo, A., GarciaEncina, P., and FdzPolanco, F. (1997). The use of methane as a sole carbon source for wastewater denitrification. *Water Res.* 31, 55–60. doi: 10.1016/S0043-1354(96)00228-X

Trotsenko, Y. A., and Murrell, J. C. (2008). Metabolic aspects of aerobic obligate methanotrophy. *Adv. Appl. Microbiol.* 63, 183–229. doi: 10.1016/S0065-2164(07)00005-6

Wang, Y. L., Wu, W. X., Ding, Y., Liu, W., Perera, A., Chen, Y. X., et al. (2008). Methane oxidation activity and bacterial community composition in a simulated landfill cover soil is influenced by the growth of *Chenopodium album* L. *Soil Biol. Biochem.* 40, 2452–2459. doi: 10.1016/j.soilbio.2008.06.009

Wang, Z., Zhang, X. X., Lu, X., Liu, B., Li, Y., Long, C., et al. (2014). Abundance and diversity of bacterial nitrifiers and denitrifiers and their functional genes in tannery wastewater treatment plants revealed by high-throughput sequencing. *PLoS ONE* 9:0113603. doi: 10.1371/journal.pone.0113603

Werner, M., and Kayser, R. (1991). Denitrification with biogas as external carbon source. *Water Sci. Technol.* 23, 701–708.

Yoshida, M., Ishii, S., Otsuka, S., and Senoo, K. (2010). nirK-harboring denitrifiers are more responsive to denitrification-inducing conditions in rice paddy soil than nirS-harboring bacteria. *Microbes Environ.* 25, 45–48. doi: 10.1264/jsme2.ME09160

Zhang, X., Kong, J. Y., Xia, F. F., Su, Y., and He, R. (2014). Effects of ammonium on the activity and community of methanotrophs in landfill biocover soils. *Syst. Appl. Microbiol.* 37, 296–304. doi: 10.1016/j.syapm.2014.03.003

Zhu, J., Wang, Q., Yuan, M. D., Tan, G. Y., Sun, F., Wang, C., et al. (2016). Microbiology and potential applications of aerobic methane oxidation coupled to denitrification (AME-D) process: a review. *Water Res.* 90, 203–215. doi: 10.1016/j.watres.2015.12.020

Zumft, W. G. (1997). Cell biology and molecular basis of denitrification. *Microbiol. Mol. Biol. Rev.* 61, 533–616.

Conflict of Interest Statement: The authors declare that the research was conducted in the absence of any commercial or financial relationships that could be construed as a potential conflict of interest.

Copyright © 2017 Zhu, Xu, Yuan, Wu, Ma and Wu. This is an open-access article distributed under the terms of the Creative Commons Attribution License (CC BY). The use, distribution or reproduction in other forums is permitted, provided the original author(s) or licensor are credited and that the original publication in this journal is cited, in accordance with accepted academic practice. No use, distribution or reproduction is permitted which does not comply with these terms.

frontiers in Microbiology

ORIGINAL RESEARCH
published: 19 June 2017
doi: 10.3389/fmicb.2017.01126

Induction of Cryptic and Bioactive Metabolites through Natural Dietary Components in an Endophytic Fungus *Colletotrichum gloeosporioides* (Penz.) Sacc.

*Vijay K. Sharma[1], Jitendra Kumar[1], Dheeraj K. Singh[1], Ashish Mishra[1], Satish K. Verma[1], Surendra K. Gond[2], Anuj Kumar[3], Namrata Singh[1] and Ravindra N. Kharwar[1]**

[1] Mycopathology and Microbial Technology Laboratory, Centre of Advanced Study in Botany, Department of Botany, Institute of Science, Banaras Hindu University, Varanasi, India, [2] Botany Section, Mahila Maha Vidyalaya, Banaras Hindu University, Varanasi, India, [3] Department of Botany, Buddha PG College, Kushinagar, India

OPEN ACCESS

Edited by:
Bhim Pratap Singh, Mizoram University, India

Reviewed by:
M. Sudhakara Reddy, Thapar University, India
Joao Lucio Azevedo, University of São Paulo, Brazil

***Correspondence:**
Ravindra N. Kharwar
rnkharwar@gmail.com

Specialty section:
This article was submitted to Microbiotechnology, Ecotoxicology and Bioremediation, a section of the journal Frontiers in Microbiology

Received: *06 January 2017*
Accepted: *01 June 2017*
Published: *19 June 2017*

Citation:
Sharma VK, Kumar J, Singh DK, Mishra A, Verma SK, Gond SK, Kumar A, Singh N and Kharwar RN (2017) Induction of Cryptic and Bioactive Metabolites through Natural Dietary Components in an Endophytic Fungus Colletotrichum gloeosporioides (Penz.) Sacc. Front. Microbiol. 8:1126. doi: 10.3389/fmicb.2017.01126

Grape skin and turmeric extracts having the major components resveratrol and curcumin, respectively, were used for the induction of cryptic and bioactive metabolites in an endophytic fungus *Colletotrichum gloeosporioides* isolated from *Syzygium cumini.* The increase in total amount of crude compounds in grape skin and turmeric extract treated cultures was 272.48 and 174.32%, respectively, compared to the untreated control. Among six human pathogenic bacteria tested, the maximum inhibitory activity was found against *Aeromonas hydrophila* IMS/GN11 while no inhibitory activity was observed against *Enterococcus faecalis* IMS/GN7. The crude compounds derived from turmeric extract treated cultures showed the highest DPPH free radicals scavenging activity (86.46% inhibition) followed by compounds from grape skin treated cultures (11.80% inhibition) and the control cultures (1.92% inhibition). Both the treatments significantly ($p \leq 0.05$) increased the antibacterial and antioxidant activities of crude metabolites compared to the control. HPLC profiling of crude compounds derived from grape skin and turmeric extract treated cultures revealed the presence of additional 20 and 14 cryptic compounds, respectively, compared to the control. These findings advocate the future use of such dietary components in induced production of cryptic and bioactive metabolites.

Keywords: endophytic fungi, epigenetic modulation, HPLC, metabolites, *Syzygium cumini*, *Colletotrichum gloeosporioides*

INTRODUCTION

The term endophytes was coined by the German scientist de Bary (1866) for any organism (bacteria, fungi, actinomycetes, etc.) that inhabit healthy plant tissues internally, without causing any identifiable disease symptoms to the host. Normally, endophytes obtain nutrients and protection from their host and in turn significantly contribute to enhance the defense mechanism of host against pathogens, herbivores, and abiotic stresses. Until 1990, endophyte researches, were mainly confined to the diversity, distribution, ecology and host health, but a new avenue opens up

and got the momentum after the synthesis of host mimetic billion dollar anticancer compound taxol by *Taxomyces andreanae*, an endophytic fungus of *Taxus brevifolia* (Stierle et al., 1993; Kharwar et al., 2011). The success of obtaining fungal taxol has initiated a paradigm for the search of still other bioactive compounds to be found in endophytic microbes. Later several other host mimetic compounds were reported from endophytic fungi such as, camptothecine, vincristine, vinblastine, rohitukine, azadirachtine, and piperine. Such alternative potential fungal sources may reduce the prices of host mimetic compounds and over exploitation of host plants (Verma et al., 2009; Kusari et al., 2012; Chithra et al., 2014; Su et al., 2014; Monggoot et al., 2017). Endophytic fungi are also well known producer of other potential natural compounds of agricultural, industrial and pharmaceutical interest. Some recent reviews have thoroughly discussed the considerable numbers of antibacterial compounds isolated from endophytic microbes and their efficacy and probable usages (Mishra et al., 2012, 2016; Deshmukh et al., 2015; Rao et al., 2017). More than 100 anticancer compounds have been reported alone from fungal endophytes between the period of 1990–2010 (Kharwar et al., 2011).

Colletotrichum gloeosporioides (Penz.) Sacc., is known to produce several biologically active compounds such as 10-hydroxy camptothecine, aspergillomarasmine A and B and highly antimicrobial gloeosporone. This fungus also produces some host mimetic anticancer compounds like taxol, piperine, and rohitukine (Senthilkumar et al., 2013; Chithra et al., 2014; Kumara et al., 2014; Su et al., 2014). One novel compound viz. 2-phenylethyl 1*H*-indol-3-yl-acetate, and seven known compounds viz. uracil, cyclo-(*S**-Pro-*S**-Tyr), cyclo-(*S**-Pro-*S**-Val), 2(2-aminophenyl) acetic acid, 2(4-hydroxyphenyl) acetic acid, 4-hydroxy-benzamide, and 2(2-hydroxyphenyl) acetic acid with antifungal, anticancer and acetylcholinesterase (AChE) inhibitory activities have also been reported from *C. gloeosporioides* (Chapla et al., 2014). Gloeosporone, a self conidial germination inhibitory compound and ferricrocin, a phytotoxin, have been isolated from *C. gloeosporioides* (Meyer et al., 1983; Ohra et al., 1995). Highly functional antibacterial compounds azaphilones and colletotric acid and a ring B aromatic steroid are also known to be produced by endophytic *C. gloeosporioides* (Zhang et al., 2009; Wang et al., 2016).

Syzygium cumini (Syn. *Eugenia jambolana* Lam.) has great economic importance as its most parts like bark, leaf, seed, and fruits are used in alternative medicine to treat various diseases. This plant was selected to isolate the endophytic fungi in anticipation of receiving the potential strain because of its various medicinal properties like antimicrobial, antiviral, anti-genotoxic, anti-inflammatory, anti-ulcerogenic, anti-allergic, cardio protective, anticancer, chemo preventive, radio protective, antioxidant, hepatoprotective, anti-diarrheal, hypoglycemic, and anti-diabetic activities (Baliga et al., 2011). *S. cumini* also contains various important phytochemicals like tannins, terpenoids, gallic acid, glycoside jambolin, anthocyanins, and various minerals (Chaudhary and Mukhopadhyay, 2012). In filamentous fungi, the biosynthetic genes for secondary metabolites are typically arranged in cluster (Keller and Hohn, 1997; Walton, 2000). Generally, in optimum laboratory conditions, many gene clusters responsible for the biosynthesis of secondary metabolites remains silent and cryptic (Rutledge and Challis, 2015). These cryptic or silent genes can also be induced through epigenetic modulations. A recent review reported that the endophytes can produce even more compounds with far greater potential by using epigenetic modulations (Fischer et al., 2016). Epigenetics is the study of changes in the expression and regulation of the genes that are not dependent on DNA sequences. The idea of epigenetics was introduced by Waddington (1942) for the development of specific traits by interaction of genes and its environmental factors. The two broad mechanisms of epigenetic modulation are the DNA methylation and histone modifications. The fungal treatment with DNA methyltransferase (DNMT) inhibitors like 5-azacytidine, 5-aza-2′-deoxycytidine, hydralazine, procaine, procainamide and/or histone deacetylase (HDAC) inhibitors like sodium butyrate, suberoylanilide hydroxamic acid (SAHA), valproic acid are effective in facilitating the activation of biosynthetic pathways of secondary metabolites that are dormant under regular conditions. However, some recent studies have suggested that various components of dietary items like turmeric, grapes, green tea, soybean, and cruciferous vegetables can also bring epigenetic changes (vel Szic et al., 2010; Hardy and Tollefsbol, 2011; Abdulla et al., 2013). These bioactive dietary components alter the DNA methylation and histone modifications requisite for gene activation the same way as the chemical epigenetic modifiers (Meeran et al., 2010). Folate, methionine, betaine, choline, and vitamin B-12, alters the 1-carbon metabolism that influences DNA and histone methylation (Choi and Friso, 2010). Catechins, the phenolic compounds of natural origin found in tea, are effective inhibitors of human DNMT-mediated DNA methylation in cultured cancer cells (Fang et al., 2003). Curcumin, a component of *Curcuma longa* (turmeric), has recently been determined to induce epigenetic changes by regulating histone acetyltransferases, histone deacetylases DNA methyltransferase I, and miRNAs activities (Reuter et al., 2011). Epigenetic influences of intake of the dietary nutrients and bioactive food components have been much studied in the field of environmental and cancer research (Su et al., 2012). But the influence of natural dietary components on the induction of secondary metabolites is not studied till date. Considering the above facts present study has been designed to assess the effects of grape skin and turmeric extract on the production of cryptic and antimicrobial rich compounds by endophytic fungus *C. gloeosporioides* (Penz.) Sacc.

MATERIALS AND METHODS

Plant Sample Collection, Surface Sterilization, Isolation and Identification of Endophytic Fungi

Mature healthy, asymptomatic leaves were collected from the tree of *Syzygium cumini* from botanical garden of BHU (Banaras Hindu University) campus, Varanasi. The collected leaves were placed in polythene bags and were stored at 4°C. The leaf samples were washed thoroughly in running tap water for 30 min and then

rinsed with double distilled water to remove the debris adhered. Methodology given by Petrini et al. (1992) was adopted for the surface sterilization of leaves and its effectiveness was checked following leaf imprint method (Schulz et al., 1993). Epiphytic microbes were eradicated by immersing the tissues in 90% ethanol for ∼1 min and in aqueous sodium hypo chlorite solution (2% available chlorine) for ∼2 min, followed by washing with 70% ethanol for ∼10 s. The leaf tissues were then rinsed in sterile distilled water and allowed to surface dry in sterile condition. After surface treatment the samples were then carefully dissected into small pieces of approximately 0.5 mm^2 × 0.5 mm^2 size. The 4–5 small pieces were placed in Petri dishes containing potato dextrose agar (PDA) medium supplemented with streptomycin (250 mg/l) and were incubated for 21 days at 26 ± 2°C in a BOD cum humidity incubator (Caltan Super Deluxe, NSW, New Delhi).

Molecular Characterization of Endophytic Fungal Isolate

Genomic DNA of the endophytic fungus *C. gloeosporioides* was extracted following the modified protocol of Sim et al. (2010). The universal primers ITS-1: 5′TCCGTAGGTGAACCTGCGG3′ and ITS-4: 5′TCCTCCGCTTATTGATATGC3′ (Metabion International, Martinsried, Germany), were used to amplify the 5.8S rDNA and two ITS regions between 18S and 28S rDNA. Total PCR mixture of 25 μl, containing 1 μl (100 ng/μl) DNA template, 1 μl each primer, 0.33 μl (3 units/μl) *Taq* polymerase, 0.5 μl dNTPs, 2.5 μl 10× PCR buffer with 25 mM $MgCl_2$ and 18.67 μl milli Q water was used for the PCR. PCR was performed in Mycycler (BioRad, Hercules, CA, United States) under the following conditions: pre-denaturation at 94°C for 4 min; 35 cycles of each denaturation at 94°C for 1 min, annealing at 55°C for 1 min, extension at 72°C for 1 min; and then a final extension at 72°C for 5 min. Amplified PCR products were resolved by electrophoresis on a 1.5% (w/v) agarose gel stained with ethidium bromide (0.5 μg/ml) for visual examination. PCR amplified DNA was purified using HiYield PCR DNA mini kit from Real Biotech Corporation (RBC, India) through gel excision method. Purified DNA was sequenced by Amnion Biosciences Pvt. Ltd, India. The ITS rDNA sequences obtained were used to retrieve similar sequences from the NCBI GenBank sequence database using the NCBI nBLAST program. The rDNA sequence was submitted to NCBI GenBank database for identification and accession number.

Preparation of Extracts from Turmeric and Grape Skin for Epigenetic Treatment

One gram of each grape skin and turmeric was separately crushed in 100 ml methanol with the help of mortar and pestle and left overnight at 4°C followed by filtration with Whatman no. 1 filter paper. Filtrates were vacuum evaporated with the help of rotary evaporator (IKA, Germany). Dried crude extract were weighted and dissolved in a concentration of 10 mg/ml in milli Q water as stock solutions, and were then filtered with 0.20 μm filter paper for removal of any contaminant. PDB medium amended with 10 μg/ml of crude extract in each case was prepared. Finally test culture was inoculated and incubated at 26 ± 2°C. The treatments were done in triplicate for reproducibility.

Isolation of Secondary Metabolites

After 21 days of incubation, the broth cultures were filtered by Whatman filter paper and filtrates were subjected to extraction thrice with the equal volume of ethyl acetate. The extracted secondary metabolites were concentrated and evaporated by rotary vacuum evaporator (IKA, Germany). The total amount of the secondary metabolites obtained from different treatments were measured and dissolved in methanol to the final concentration of 1 mg/5 μl.

Antibacterial Activity

The metabolites, extracted after different treatments of endophytic fungi, were screened for antibacterial activity against the six human bacterial pathogens using disk diffusion method. To the sterilized filter paper disks, 5 μl (1 mg) of crude extract was loaded aseptically and air dried. Antibacterial test was performed against the following gram positive and gram negative bacteria – *Aeromonas hydrophila* IMS/GN11, *Shigella boydii* IMS/GN17, *Salmonella typhi* MTCC 3216, *Staphylococcus aureus* ATCC 25923, *Escherichia coli* IMS/GN19, and *Enterococcus faecalis* IMS/GN7. The lawn of test bacterial culture was prepared with cotton swab on the surface of solidified Mueller-Hinton agar Petri plates. The paper disks containing 1 mg crude extract were placed on the surface of the Mueller-Hinton medium seeded with test bacterium in Petri plate. The paper disk dried after impregnating 5 μl methanol was placed as positive control. Plates were incubated for 24 h at 35 ± 2°C and then were analyzed for antibacterial activity by observing the zone of inhibition. Each test was done in triplicates and the means of the diameter of the inhibition zones with standard deviation were presented in the results.

Antioxidant Assay

The scavenging activity of the secondary metabolites of different treatments and control was measured on DPPH radicals following the method devised by Shen et al. (2010) with minor modifications. An aliquot of 1 ml of 0.2 mM DPPH radical (Sigma) in methanol was added to a test tube containing 3 ml of methanolic solution of crude extract (1 mg/3 ml). The reaction mixture was vortex mixed at room temperature and the absorbance (Abs) was taken at 517 nm after 30 min of incubation at room temperature in the dark. The ascorbic acid was used as standard antioxidant and the methanol as control. The % inhibition was calculated against control as $[(Abs_{control} - Abs_{test\ sample}) \div Abs_{control} \times 100]$.

All the data were statistically analyzed by analysis of variance (ANOVA) and means were compared by Tukey's honestly significant differences (HSD) test. All the analyses were performed using Graph pad prism 5.1 software.

HPLC Profiling of Crude Compounds

HPLC analysis of crude compounds was done on RP-C18 column using Photodiode Array Detectors (PDA). The injection volume

and flow rate used were 20 µl and 0.50 ml/min, respectively. Acetonitrile along with double distilled water were used as mobile solvent. Elution program of compounds started with 15% acetonitrile reaching up to 100% in 40 min with a hold on this condition for 5 min, and again gradient coming down to 15% acetonitrile in 8 min which was finally held for 5 min. The samples and mobile phase were filtered through 0.2 µm nylon membrane filter before applying into the column. All samples were analyzed at 254 nm wavelength.

RESULTS

Isolation and Identification of Endophytic *Colletotrichum gloeosporioides*

In present study, an endophytic fungus was isolated from the surface sterilized leaves of *Syzygium cumini* growing in the botanical garden of BHU campus, Varanasi. On the basis of ITS rDNA gene sequencing, it was identified as *C. gloeosporioides* with GenBank accession number JN692296 (**Figure 1**).

Crude Metabolites and Antibacterial Activity of Treated Cultures

The amount of crude secondary metabolite extracted was highest (406 ± 3.46 mg/500 ml of broth) from the cultures of *C. gloeosporioides* treated with grape skin extract followed by the cultures treated with turmeric extract (299 ± 9.07 mg/500 ml of broth) and the lowest (109 ± 9.54 mg/500 ml of broth) in the control cultures. Thus, in contrast to control the amount of secondary metabolites secreted was 272.48 and 174.32% more in the cultures treated with grape skin and turmeric extracts, respectively.

The crude compounds when screened for antibacterial activity against six human pathogenic bacteria showed a high antibacterial activity against *A. hydrophila* IMS/GN11, *Shigella boydii* IMS/GN17, *Salmonella typhi* MTCC 3216, *Staphylococcus aureus* ATCC 25923, and *Escherichia coli* IMS/GN19 (**Figure 2** and **Table 1**). Contrarily, *Enterococcus faecalis* IMS/GN7, was not at all susceptible to the secondary metabolites of the any treatment or control. The zone of inhibition against *A. hydrophila* was found maximum (27 mm) by the metabolites extracted from the grape skin treated culture followed by turmeric extract treated culture (25 mm) and the control culture (23 mm). Similar trend in the zone of inhibition was also recorded against *S. boydii, S. typhi, S. aureus,* and *E. coli* for the metabolites extracted from the cultures treated with grape skin extract, turmeric extract and control (**Figure 2** and **Table 1**). Both the treatments showed significant ($p \leq 0.05$) increase in antibacterial activity of metabolites compared to control.

Antioxidant Assay

The scavenging activity of different crude metabolites against the DPPH radical in terms of % inhibition is given in **Figure 3**. Like the standard ascorbic acid antioxidant activity (97.85% inhibition), the near similar antioxidant activity (86.46% inhibition) was observed by the secondary metabolites of the culture treated with turmeric extract. However, metabolites from the culture treated with grape skin extract showed lower antioxidant activity (11.80% inhibition) even though it was multifold higher than the untreated control culture (1.92% inhibition). Antioxidant activity of treatments significantly differed ($p \leq 0.05$) with one another and that of the control (**Figure 3**).

HPLC Analysis of Crude Compounds

HPLC analysis of the crude compounds derived from differently treated cultures revealed that the treatment of *C. gloeosporioides* by grape skin and turmeric extracts activated the secretion of many cryptic compounds that were not observed in the untreated samples (**Figures 4a–d** and Supplementary Table 1). This analysis clearly demonstrated that the crude secondary metabolites of the grape skin treated culture produced 37 compounds while turmeric extract treated culture showed 35 compounds and the untreated control culture displayed 34 compounds. The number of cryptic compounds was more in the secondary metabolites extracted from the culture treated with the grape skin extract (20) as compared to those in the culture treated with turmeric extract (14). Although in the treated cultures many cryptic compounds were encountered, but at the same time certain compounds which were present in the control were found missing in the treated ones. The number of common compounds present in the treated as well as control samples were detected more in the culture treated with turmeric extract (21) as compared to those (17) in the culture treated with the grape skin extract (**Table 2**).

DISCUSSION

Initially most of the epigenetic studies, were confined to the developmental and clinical biology particularly for the treatment of various life threatening diseases, but in the last few decades, researchers from other fields of biology, including the endophytic microbiology, also showed interest in this fascinating area of research (Brueckner and Lyko, 2004; Feinberg and Tycko, 2004; Chen et al., 2013; Kumar et al., 2016). *Colletotrichum,* the present study material was isolated from the healthy leaf segments of *Syzygium cumini. C. gloeosporioides* has also been reported from a vast range of host plants including *Artemisia mongolica, Artemisia annua, Justicia gendarussa, Theobroma cacao, Vitex negundo*, and *Buxus sinica* (Lu et al., 2000; Zou et al., 2000; Gangadevi and Muthumary, 2008; Mejía et al., 2008; Arivudainambi et al., 2011; Wang et al., 2016).

In this study, the secondary metabolites of *C. gloeosporioides*, extracted with ethyl acetate showed significant antibacterial activity against five human pathogenic bacteria *viz. A. hydrophila*, *S. boydii*, *S. typhi*, *S. aureus,* and *E. coli.* No inhibitory activity was registered against *E. faecalis* (**Figure 2** and **Table 1**). A number of bioactive compounds have been reported from *C. gloeosporioides s*upporting our finding. Previously, *C. gloeosporioides*, an endophytic fungus isolated from the stem of *Artemisia mongolica*, was found to produce new antimicrobial metabolite, named colletotric acid in broth culture

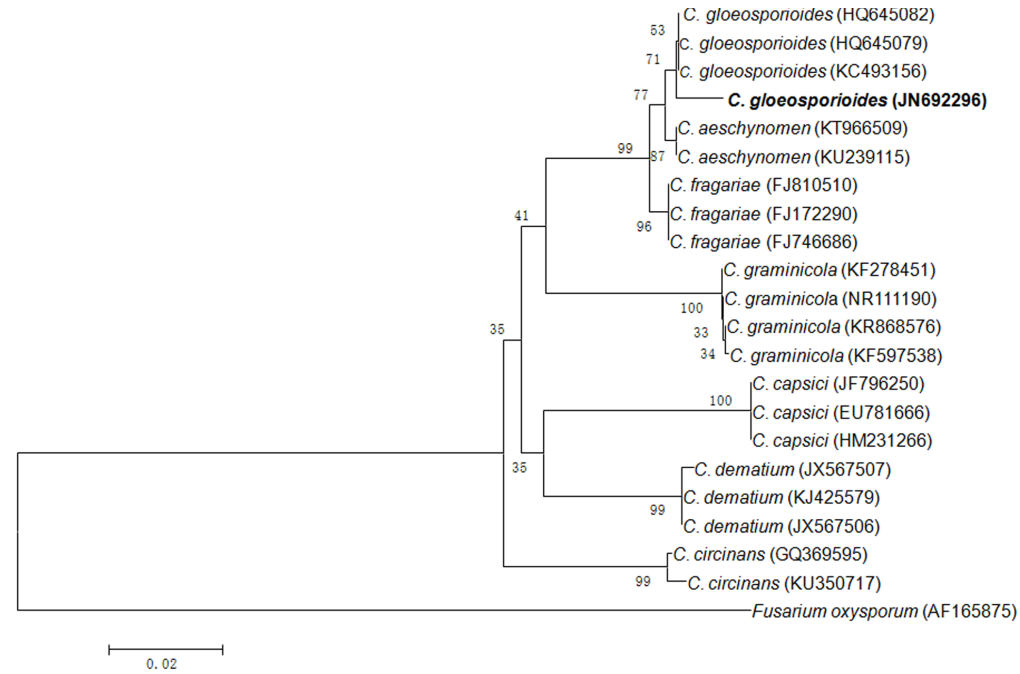


FIGURE 1 | Neighbor-joining tree from ITS sequences showing the relationship between *Colletotrichum* species of the present study and other closely related *Colletotrichum* species retrieved from the GenBank. Bootstrap values (1000 replicates) are shown on the branches. Bar = 2 nucleotide substitutions per 100 nucleotides.

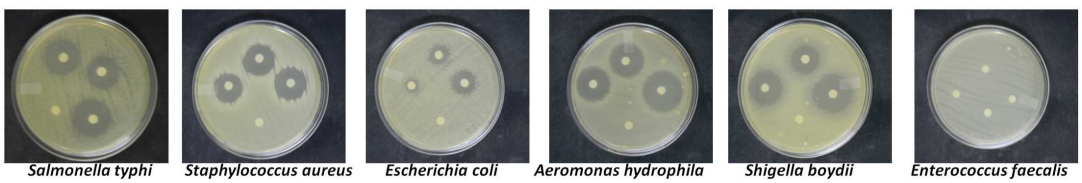


FIGURE 2 | Antibacterial activity of crude compounds isolated from treated and untreated control cultures of *Colletotrichum gloeosporioides*.

TABLE 1 | Antibacterial activity of crude metabolites of different treatments.

Treatments	Inhibition zone (mm)					
	Staphylococcus aureus	***Enterococcus faecalis***	***Shigella boydii***	***Salmonella typhi***	***Aeromonas hydrophila***	***Escherichia coli***
Control	19.0 ± 1.7^{c}	0 ± 0^{a}	18.3 ± 0.6^{c}	19.0 ± 2.0^{b}	23.0 ± 1.0^{b}	8.0 ± 0.0^{c}
Grape skin extract	20.3 ± 0.6^{bc}	0 ± 0^{a}	25.3 ± 0.6^{a}	22.0 ± 1.7^{a}	27.3 ± 1.5^{a}	16.3 ± 0.6^{a}
Turmeric extract	22.0 ± 1.0^{a}	0 ± 0^{a}	22.0 ± 1.7^{b}	20.0 ± 1.0^{ab}	25.3 ± 0.6^{ab}	11.7 ± 1.2^{b}

Values (Mean ± SD) sharing a common letter within the column is not significant at $p \leq 0.05$.

(Zou et al., 2000). In another report endophytic *Colletotrichum* sp., isolated from *Artemisia annua* stem was shown to produce three novel and seven known compounds, out of which all novel and only three known compounds exhibited antibacterial activity against tested bacteria (Lu et al., 2000). The metabolites of endophytic *C. gloeosporioides* were also reported to have anticancer activity. *C. gloeosporioides* (JGC-9) isolated from *Justicia gendarussa*, was reported to secrete 163.4 μg/L of taxol in liquid culture which showed strong cytotoxic activity toward BT 220, H116, Int 407, HL 251, and HLK 210 human cancer cells *in vitro* (Gangadevi and Muthumary, 2008). The treatment of *Theobroma cacao* with its own endophyte *C. gloeosporioides* significantly reduced pod loss due to *Moniliophthora roreri* (frosty pod rot) and *Phytophthora palmivora* (black pod rot) in field trials, suggesting the biocontrol potential of fungal endophytes (Mejía et al., 2008). Novel bioactive metabolites from this endophytic fungus isolated from the medicinal plant *Vitex negundo* L. registered effective antimicrobial activity together

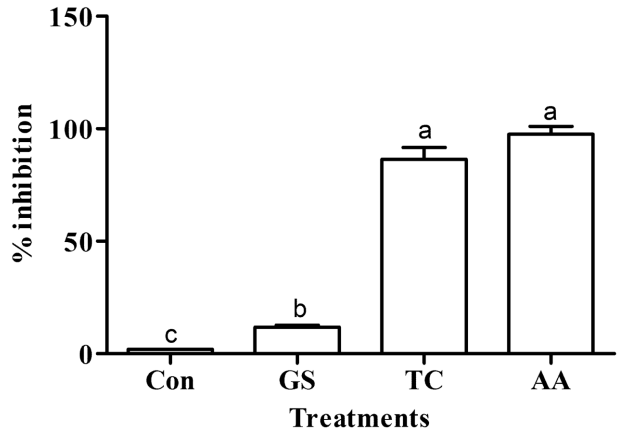


FIGURE 3 | Effect of grape skin (GS) and turmeric (TC) extracts on the antioxidant activity. Error bars represent ± Standard deviation. AA represents ascorbic acid (100 μg ml^{-1}) used as a positive control. Bars sharing a common letter(s) are not significant at $P < 0.05$.

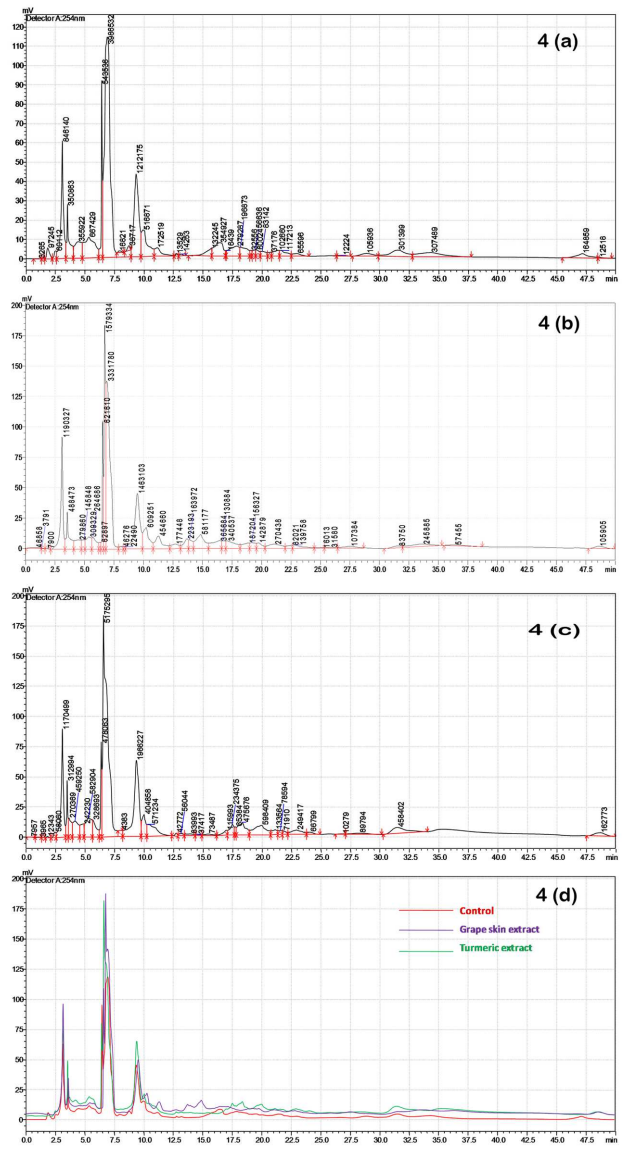


FIGURE 4 | HPLC profiles of secondary metabolites isolated after grape skin and turmeric extract treatments of *C. gloeosporioides* at 254 nm; **(a)** HPLC chromatogram of the untreated control; **(b)** HPLC chromatogram of grape skin extract; **(c)** HPLC chromatogram of turmeric extract; **(d)** overlay of control, grape skin extract and turmeric extract.

with strong activity against multidrug-resistant *Staphylococcus aureus* indicating that these metabolites can be a potential source of new antibiotics (Arivudainambi et al., 2011). In a recent study an endophytic fungus, *Colletotrichum* sp. (BS4), isolated from the leaves of *Buxus sinica* was reported to produce three novel compounds, colletotrichones A–C, and one known compound, chermesinone B having antibacterial properties (Wang et al., 2016).

The cultures treated with the grape skin and turmeric extracts showed increased antibacterial activity against the tested human bacterial pathogens. Resveratrol is main component of the grape skin extract while curcumin is the main component of turmeric extract. Both of these compounds are known to have potential to bring epigenetic changes required for gene expression. Resveratrol, a polyphenolic compound commonly found in grapes, berries, and peanuts, is used in the epigenetic alteration for gene expression for therapeutic uses. But the use of resveratrol in epigenetic activation of the silent gene clusters for secondary metabolites production in fungi is not common. Resveratrol prevents epigenetic silencing of BRCA-1 protein which is tumor suppressor and is involved in the repair of DNA damage through aromatic hydrocarbon receptor in human breast cancer cells (Papoutsis et al., 2010). Resveratrol, which binds and activates estrogen receptors, are important factor in the regulation of transcription of estrogen-responsive target genes and increases expression of BRCA1 and BRCA2 mRNA in breast tumor cell lines (Fustier et al., 2003). Resveratrol also increases the expression of native estrogen-regulated genes, and stimulates the proliferation of estrogen-dependent T47D breast cancer cells. It also acts as an agonist for the estrogen receptor (Gehm et al., 1997). Just like resveratrol, the curcumin is also not frequently used in the epigenetic induction of silent genes for cryptic metabolites in fungal systems. Curcumin is also a polyphenolic compound that is well known as an inhibitor of DNA methyltransferase, beside its interaction together with microRNAs, reestablishes the balance between histone acetyl transferase and HDAC activity to selectively regulate the expression of genes concerned with human cancer (Fu and Kurzrock, 2010; Teiten et al., 2013). Wilken et al. (2011) discussed the anticancer property of the curcumin.

Through HPLC we have recorded the increase in the number of cryptic metabolites after successful induction by the grape skin and turmeric extract (**Figure 4**). The increased number of cryptic compounds can be related with the enhanced antibacterial activity of the secondary metabolites isolated from

TABLE 2 | Different category of compounds based on the HPLC profile of the total metabolite of *Colletotrichum gloeosporioides* from different treatments.

	Control	Grape skin extract	Turmeric extract
Total number of compounds detected	34	37	35
Number of common compounds detected in treated and control		17	21
Number of cryptic compounds detected in treated cultures		20	14
Number of compounds missing in treated cultures		17	13

the treated cultures of an endosymbiotic fungus *C. gloeosporioides* (**Table 2**). Though some compounds were found missing in the treated cultures, in most probability, due to epigenetic silencing of gene(s) associated with the biosynthetic pathways of these compounds, the basic aim of the present study to increase the number of compounds with improved bioactivity by treating the cultures with the grape skin and turmeric extracts seems to be fulfilled with significant ($p \leq 0.05$) increase in DPPH radical scavenging and antibacterial activities (**Figure 3**).

Epigenetic modulations in the endophytic fungus not only improve the production of cryptic metabolites, but it also opens a new possibility for the regulation of secondary metabolites synthesis and the illustration of metabolite pathways of the cryptic natural compounds. In a recent study an endophytic actinomycetes, *Streptomyces coelicolor* strain AZRA 37 horbouring *Azadirachta indica* A. Juss., when treated with 5-azacytidine (25 μM) increased the number of compounds in the crude metabolite and its effectiveness against pathogenic bacteria, with an induced protein porin (Kumar et al., 2016). Successful attempts of epigenetic modulation have been made earlier using both the types of modifiers, i.e., 5-azacytidine as a DNMT inhibitor and sodium butyrate as a HDAC inhibitor in marine fungus *Leucostoma persoonii* for the increased production of known cytosporones B (360%), C (580%) and E (890%), and a new cytosporone R (Beau et al., 2012). Epigenetic induction of fusaric acid derivatives 5-butyl-6-oxo-1,6-dihydropyridine-2-carboxylic acid and 5-(but-9-enyl)-6-oxo-1,6-dihydropyridine-2-carboxylic acid were done using SAHA an HDAC inhibitor, in the culture medium of endophytic fungus isolated from Indian medicinal plant *Datura stramonium* (Chen et al., 2013). Three novel aromatic compounds, viz., 2′-hydroxy-6′-hydroxymethyl-4′-methylphenyl-2,6-dihydroxy-3-(2-isopentenyl) benzoate, 4,6-dihydroxy-7-hydroxymethyl-3-methylcoumarin, 4,6-dihydroxy-3,7-dimethylcoumarin and some known polyketides, endocrocin, pestalotiollide B, pestalotiopyrone G, scirpyrone A, and 7-hydroxy-2-(2-hydroxypropyl)-5-methylchromone were isolated from epigenetically induced endophytic *Pestalotiopsis acaciae* using 5-azacytidine and SAHA (Yang et al., 2013). Addition of 5-azacytidine, and/or SAHA, to the culture medium of endophytic fungus *Alternaria* sp. from *Datura stramonium* induced the production of mycotoxins, like alternariol, alternariol-5-*O*-methyl ether, 3′-hydroxyalternariol-5-*O*-methyl ether, altenusin, tenuazonic acid, and altertoxin II (Sun et al., 2012).

In a mycodiesel-producing endophyte *Hypoxylon* sp. (CI-4), 5-azacytidine treatment increased the ratio of ethanol to the total mass of all other ionizable volatile organic compounds (VOCs), from ∼0.6 to ∼0.8 while several other compounds like terpenes such as α-thujene, sabinene, γ-terpinene, α-terpinolene and β-selinene, several primary and secondary alkanes, alkenes, organic acids and derivatives of benzene that were not previously observed in the untreated culture were also observed in variable amounts with 5-azacytidine and SAHA treatments (Ul-Hassan et al., 2012). These studies clearly demonstrate that fungi like other eukaryotic microbes have genes for a wide range of potential bioactive metabolites, which remain silent/or unexpressed under normal conditions. Further, recent advancement in the next generation sequencing approaches like expression of PKS, NRPS, terpene synthase, or dimethylallyl-tryptophan synthase can be used to get the required information regarding biosynthetic gene clusters and prediction of the secondary metabolites (Cacho et al., 2014).

CONCLUSION

Both, grape skin extract and turmeric extract were found effective in inducing the endophytic fungus *C. gloeosporioides* for isolation of bioactive cryptic metabolites and thereby increasing the antibacterial and antioxidant activities in the treated cultures. This study successfully establishes the importance of active dietary components which also interact with the epigenetic targets and can significantly induce the production of cryptic metabolites in the endophytic fungus. However, the evaluation of pure resveratrol and curcumin, the key components of the grape skin extract and turmeric extract, respectively, for their direct role in the epigenetic modulation needs to be elucidated further. The protein level changes brought out by the treatment of these extracts will further help explore the exact mechanisms/pathway involved.

AUTHOR CONTRIBUTIONS

Conceived and designed the experiments: VS, JK, and RK. Performed the experiments: VS, JK, NS, DS, and AM. Analyzed the data: VS, AM, SG, SV, and AK. Contributed reagents/materials/analysis tools: VS and RK. Wrote the paper: VS, JK, RK, AM, and SV.

FUNDING

This work was supported by UGC, New Delhi [RFSMS to VS]; Department of Science and Technology, New Delhi [Project SB/EMEQ-121/2014 to RK] and DST-PURSEUGC-UPE, BHU, Varanasi, India.

ACKNOWLEDGMENTS

Authors are thankful to the Head and Coordinator, CAS and DST-FIST in Botany, Institute of Science, BHU, Varanasi, India, for providing essential research facilities and technical supports. Authors appreciably acknowledge the helps of ISLS, UGC-UPE, DST-PURSE, BHU, Varanasi, India for HPLC analysis and Prof. Gopal Nath, Institute of Medical Sciences, BHU, Varanasi, India for antibacterial assay facility. RK expresses his thanks to DST, New Delhi for the project (SB/EMEQ-121/2014).

SUPPLEMENTARY MATERIAL

The Supplementary Material for this article can be found online at: http://journal.frontiersin.org/article/10.3389/fmicb.2017.01126/full#supplementary-material

REFERENCES

Abdulla, A., Zhao, X., and Yang, F. (2013). Natural polyphenols inhibit lysine-specific demethylase-1 in vitro. *J. Biochem Pharmacol. Res.* 1, 56–63.

Arivudainambi, U. E., Anand, T. D., Shanmugaiah, V., Karunakaran, C., and Rajendran, A. (2011). Novel bioactive metabolites producing endophytic fungus *Colletotrichum gloeosporioides* against multidrug-resistant *Staphylococcus aureus*. *FEMS Immunol. Med. Microbiol.* 61, 340–345. doi: 10.1111/j.1574-695X.2011.00780.x

Baliga, M. S., Bhat, H. P., Baliga, B. R. V., Wilson, R., and Palatty, P. L. (2011). Phytochemistry, traditional uses and pharmacology of *Eugenia jambolana* Lam. (black plum): a review. *Food Res. Int.* 44, 1776–1789. doi: 10.1016/j.foodres.2011.02.007

Beau, J., Mahid, N., Burda, W. N., Harrington, L., Shaw, L. N., Mutka, T., et al. (2012). Epigenetic tailoring for the production of anti-infective cytosporones from the marine fungus *Leucostoma persoonii*. *Mar. Drug* 10, 762–774. doi: 10.3390/md10040762

Brueckner, B., and Lyko, F. (2004). DNA methyltransferase inhibitors: old and new drugs for an epigenetic cancer therapy. *Trends Pharmacol. Sci.* 25, 551–554. doi: 10.1016/j.tips.2004.09.004

Cacho, R. A., Tang, Y., and Chooi, Y. H. (2014). Next-generation sequencing approach for connecting secondary metabolites to biosynthetic gene clusters in fungi. *Front. Microbiol.* 5:774. doi: 10.3389/fmicb.2014.00774

Chapla, V. M., Zeraik, M. L., Leptokarydis, I. H., Silva, G. H., Bolzani, V. S., Young, M. C., et al. (2014). Antifungal compounds produced by *Colletotrichum gloeosporioides*, an endophytic fungus from *Michelia champaca*. *Molecules* 19, 19243–19252. doi: 10.3390/molecules191119243

Chaudhary, B., and Mukhopadhyay, K. (2012). *Syzygium cumini* (L.) skeels: a potential source of nutraceuticals. *Int. J. Pharm. Biol. Sci.* 2, 46–53.

Chen, H. J., Awakawa, T., Sun, J. Y., Wakimoto, T., and Abe, I. (2013). Epigenetic modifier-induced biosynthesis of novel fusaric acid derivatives in endophytic fungi from *Datura stramonium* L. *Nat. Prod. Bioprospect.* 3, 20–23. doi: 10.1007/s13659-013-0010-2

Chithra, S., Jasim, B., Sachidanandan, P., Jyothis, M., and Radhakrishnan, E. K. (2014). Piperine production by endophytic fungus *Colletotrichum gloeosporioides* isolated from *Piper nigrum*. *Phytomedicine* 21, 534–540. doi: 10.1016/j.phymed.2013.10.020

Choi, S. W., and Friso, S. (2010). Epigenetics: a new bridge between nutrition and health. *Adv. Nutr.* 1, 8–16. doi: 10.3945/an.110.1004

de Bary, A. (1866). *Morphologie und Physiologie der Pilze, Flechtem, und Myxomycelen*, Vol. 2. Leipzig: Holfmeister's Handbook of Physiological Botany. doi: 10.5962/bhl.title.120970

Deshmukh, S. K., Verekar, S. A., and Bhave, S. V. (2015). Endophytic fungi: a reservoir of antibacterials. *Front. Microbiol.* 5:715. doi: 10.3389/fmicb.2014.00715

Fang, M. Z., Wang, Y., Ai, N., Hou, Z., Sun, Y., Lu, H., et al. (2003). Tea polyphenol ()-epigallocatechin-3-gallate inhibits DNA methyltransferase and reactivates methylation-silenced gene in cancer cell lines. *Cancer Res.* 63, 7563–7570.

Feinberg, A. P., and Tycko, B. (2004). The history of cancer epigenetics. *Nat. Rev. Cancer* 4, 143–153. doi: 10.1038/nrc1279

Fischer, J., Schroeckh, V., and Brakhage, A. A. (2016). "Awakening of fungal secondary metabolite gene clusters," in *Gene Expression Systems in Fungi: Advancements and Applications*, eds M. Schmoll and C. Dattenböck (Cham: Springer International Publishing), 253–273. doi: 10.1007/978-3-319-27951-0_11

Fu, S., and Kurzrock, R. (2010). Development of curcumin as an epigenetic agent. *Cancer* 116, 4670–4676. doi: 10.1002/cncr.25414

Fustier, P., Le Corre, L., Chalabi, N., Vissac-Sabatier, C., Communal, Y., Bignon, Y. J., et al. (2003). Resveratrol increases BRCA1 and BRCA2 mRNA expression in breast tumour cell lines. *Br. J. Cancer* 89, 168–172. doi: 10.1038/sj.bjc.6600983

Gangadevi, V., and Muthumary, J. (2008). Isolation of *Colletotrichum gloeosporioides*, a novel endophytic taxol-producing fungus from the leaves of a medicinal plant, *Justicia gendarussa*. *Mycol. Balc.* 5, 1–4.

Gehm, B. D., McAndrews, J. M., Chien, P. Y., and Jameson, J. L. (1997). Resveratrol, a polyphenolic compound found in grapes and wine, is an agonist for the estrogen receptor. *Proc. Natl. Acad. Sci. U.S.A.* 94, 14138–14143. doi: 10.1073/pnas.94.25.14138

Hardy, T. M., and Tollefsbol, T. O. (2011). Epigenetic diet: impact on the epigenome and cancer. *Epigenomics* 3, 503–518. doi: 10.2217/epi.11.71

Keller, N., and Hohn, T. (1997). Metabolic pathway gene clusters in filamentous fungi. *Fung. Genet. Biol.* 21, 17–29. doi: 10.1006/fgbi.1997.0970

Kharwar, R. N., Mishra, A., Gond, S. K., Stierle, A., and Stierle, D. (2011). Anticancer compounds derived from fungal endophytes: their importance and future challenges. *Nat. Prod. Rep.* 28, 1208–1228. doi: 10.1039/c1np00008j

Kumar, J., Sharma, V. K., Singh, D. K., Mishra, A., Gond, S. K., Verma, S. K., et al. (2016). Epigenetic activation of antibacterial property of an Endophytic *Streptomyces coelicolor* strain AZRA 37 and identification of the induced protein using MALDI TOF MS/MS. *PLoS ONE* 11:e0147876. doi: 10.1371/journal.pone.0147876

Kumara, P. M., Soujanya, K. N., Ravikanth, G., Vasudeva, R., Ganeshaiah, K. N., and Uma Shaanker, R. (2014). Rohitukine, a chromone alkaloid and a precursor of flavopiridol, isproduced by endophytic fungi isolated from *Dysoxylum binectariferum* Hook.f and *Amoora rohituka* (Roxb).Wight & Arn. *Phytomedicine* 21, 541–546. doi: 10.1016/j.phymed.2013.09.019

Kusari, S., Verma, V. C., Lamshoeft, M., and Spiteller, M. (2012). An endophytic fungus from *Azadirachta indica* A. Juss. that produces azadirachtin. *World. J. Microbiol. Biotechnol.* 28, 1287–1294. doi: 10.1007/s11274-011-0876-2

Lu, H., Zou, W. X., Meng, J. C., Hu, J., and Tan, R. X. (2000). New bioactive metabolites produced by *Colletotrichum* sp., an endophytic fungus in *Artemisia annua*. *Plant Sci.* 151, 67–73. doi: 10.1016/S0168-9452(99)00199-5

Meeran, S. M., Ahmed, A., and Tollefsbol, T. O. (2010). Epigenetic targets of bioactive dietary components for cancer prevention and therapy. *Clin. Epigenetics* 1, 101–116. doi: 10.1007/s13148-010-0011-5

Mejía, L. C., Rojas, E. I., Maynard, Z., Van Bael, S., Arnold, A. E., Hebbar, P., et al. (2008). Endophytic fungi as biocontrol agents of *Theobroma cacao* pathogens. *Biol. Control* 46, 4–14. doi: 10.1016/j.funbio.2010.08.006

Meyer, W. L., Lax, A. R., Templeton, G. E., and Brannon, M. J. (1983). The structure of gloeosporone, a novel germination self-inhibitor from conidia of *Colletotrichum gloesporioides*. *Tetrahedron Lett.* 24, 5059–5062. doi: 10.1016/S0040-4039(00)94040-1

Mishra, A., Gond, S. K., Kumar, A., Sharma, V. K., Verma, S. K., and Kharwar, R. N. (2012). "Sourcing the fungal endophytes: a beneficial transaction of biodiversity, bioactive natural products, plant protection and nanotechnology," in *Microorganisms in Sustainable Agriculture and Biotechnology*, eds T. Satyanarayana, B. N. Johri, and A. Prakash (Dordrecht: Springer), 581–612.

Mishra, V. K., Singh, G., Passari, A. K., Yadav, M. K., Gupta, V. K., and Singh, B. P. (2016). Distribution and antimicrobial potential of endophytic fungi associated with ethnomedicinal plant *Melastoma malabathricum* L. *J. Environ. Biol.* 37, 229–237.

Monggoot, S., Popluechai, S., Gentekaki, E., and Pripdeevech, P. (2017). Fungal endophytes: an alternative source for production of volatile compounds from agarwood oil of *Aquilaria subintegra*. *Microb. Ecol.* doi: 10.1007/s00248-016-0908-4

Ohra, J., Morita, K., Tsujino, Y., Tazaki, H., Fujimori, T., Goering, M., et al. (1995). Production of the phytotoxin metabolite, ferricrocin, by the fungus *Colletotrichum gloeosporioides*. *Biosci. Biotechnol. Biochem.* 59, 113–114. doi: 10.1271/bbb.59.113

Papoutsis, A. J., Lamore, S. D., Wondrak, G. T., Selmin, O. I., and Romagnolo, D. F. (2010). Resveratrol prevents epigenetic silencing of BRCA-1 by the aromatic hydrocarbon receptor in human breast cancer cells. *J. Nutr.* 140, 1607–1614. doi: 10.3945/jn.110.123422

Petrini, O., Sieber, T. N., Toti, L., and Viret, O. (1992). Ecology, metabolite production and substrate utilization in endophytic fungi. *Nat. Toxins* 1, 185–196. doi: 10.1002/nt.2620010306

Rao, H. C. Y., Rakshith, D., Harini, B. P., Gurudatt, D. M., and Satish, S. (2017). Chemogenomics driven discovery of endogenous polyketide anti-infective compounds from endosymbiotic *Emericella variecolor* CLB38 and their RNA secondary structure analysis. *PLoS ONE* 12:e0172848. doi: 10.1371/journal.pone.0172848

Reuter, S., Gupta, S. C., Park, B., Goel, A., and Aggarwal, B. B. (2011). Epigenetic changes induced by curcumin and other natural compounds. *Genes Nutr.* 6, 93–108. doi: 10.1007/s12263-011-0222-1

Rutledge, P. J., and Challis, G. L. (2015). Discovery of microbial natural products by activation of silent biosynthetic gene clusters. *Nat. Rev. Microbiol.* 13, 509–523. doi: 10.1038/nrmicro3496

Schulz, B., Wanke, U., Draeger, S., and Aust, H. J. (1993). Endophytes from herbaceous plants and shrubs: effectiveness of surface sterilization methods. *Mycol. Res.* 97, 1447–1450. doi: 10.1016/S0953-7562(09)80215-3

Senthilkumar, N., Murugesthan, S., Mohan, V., and Muthumury, J. (2013). Taxol producing fungal endophyte, *Colletotrichum gloeosporioides* (Penz) from *Tectona grandis* L. *Curr. Biotica* 7, 3–15.

Shen, Q., Zhang, B., Xu, R., Wang, Y., Ding, X., and Li, P. (2010). Antioxidant activity in vitro of the selenium-contained protein from the Se-enriched Bifidobacterium animalis 01. *Anaerobe* 16, 380–386. doi: 10.1016/j.anaerobe.2010.06.006

Sim, J. H., Khoo, C. H., Lee, L. H., and Cheah, Y. K. (2010). Molecular diversity of fungal endophytes isolated from *Garcinia mangostana* and *Garcinia parvifolia*. *J. Microbiol. Biotechnol.* 20, 651–658. doi: 10.4014/jmb.0909.09030

Stierle, A., Strobel, G., and Stierle, D. (1993). Taxol and taxane production by *Taxomyces andreanae*, an endophytic fungus of Pacific yew. *Science* 260, 214–216. doi: 10.1126/science.8097061

Su, H., Kang, J., Cao, J., Mo, L., and Hyde, K. D. (2014). Medicinal plant endophytes produce analogous bioactive compounds. *Chiang Mai J. Sci.* 41, 1–13. doi: 10.1007/s00284-010-9685-3

Su, L. J., Mahabir, S., Ellison, G. L., McGuinn, L. A., and Reid, B. C. (2012). Epigenetic contributions to the relationship between cancer and dietary intake of nutrients, bioactive food components, and environmental toxicants. *Front. Genet.* 2:91. doi: 10.3389/fgene.2011.00091

Sun, J., Awakawa, T., Noguchi, H., and Abe, I. (2012). Induced production of mycotoxins in an endophytic fungus from the medicinal plant *Datura stramonium* L. *Bioorg. Med. Chem. Lett.* 22, 6397–6400. doi: 10.1016/j.bmcl.2012.08.063

Teiten, M. H., Dicato, M., and Diederich, M. (2013). Curcumin as a regulator of epigenetic events. *Mol. Nutr. Food Res.* 57, 1619–1629. doi: 10.1002/mnfr.201300201

Ul-Hassan, S. R., Strobel, G. A., Booth, E., Knighton, B., Floerchinger, C., and Sears, J. (2012). Modulation of volatile organic compound formation in the Mycodiesel-producing endophyte Hypoxylon sp. *CI*-4. *Microbiology* 158, 465–473. doi: 10.1099/mic.0.054643-0

vel Szic, K. S., Ndlovu, M. N., Haegeman, G., and Berghe, W. V. (2010). Nature or nurture: let food be your epigenetic medicine in chronic inflammatory disorders. *Biochem. Pharmacol.* 80, 1816–1832. doi: 10.1016/j.bcp.2010.07.029

Verma, V. C., Kharwar, R. N., and Strobel, G. A. (2009). Chemical and functional diversity of natural products from plant associated endophytic fungi. *Nat. Prod. Commun.* 4, 1511–1532.

Waddington, C. H. (1942). The epigenotype. *Endeavour* 1, 18–20.

Walton, J. D. (2000). Horizontal gene transfer and the evolution of secondary metabolite gene clusters in fungi: an hypothesis. *Fung. Genet. Biol.* 30, 167–171. doi: 10.1006/fgbi.2000.1224

Wang, W. X., Kusari, S., Laatsch, H., Golz, C., Kusari, P., Strohmann, C., et al. (2016). Antibacterial azaphilones from an Endophytic Fungus, *Colletotrichum* sp. BS4. *J. Nat. Prod.* 79, 407–410. doi: 10.1021/acs.jnatprod.5b00436

Wilken, R., Veena, M. S., Wang, M. B., and Srivatsan, E. S. (2011). Curcumin: a review of anti-cancer properties and therapeutic activity in head and neck squamous cell carcinoma. *Mol. Cancer* 10, 12. doi: 10.1186/1476-4598-10-12

Yang, X. L., Awakawa, T., Wakimoto, T., and Abe, I. (2013). Induced production of novel prenyldepside and coumarins in endophytic fungi *Pestalotiopsis acaciae*. *Tetrahed. Lett.* 54, 5814–5817. doi: 10.1016/j.tetlet.2013.08.054

Zhang, W., Draeger, S., Schulz, B., and Krohn, K. (2009). Ring B aromatic steroid from endophytic fungus *Colletotrichum* sp. *Nat. Prod. Commun.* 4, 1449.

Zou, W. X., Meng, J. C., Lu, H., Chen, G. X., Shi, G. X., Zhang, T. Y., et al. (2000). Metabolites of *Colletotrichum gloeosporioides*, an endophytic fungus in *Artemisia mongolica*. *J. Nat. Prod.* 63, 1529–1530. doi: 10.1021/np000204t

Conflict of Interest Statement: The authors declare that the research was conducted in the absence of any commercial or financial relationships that could be construed as a potential conflict of interest.

Copyright © 2017 Sharma, Kumar, Singh, Mishra, Verma, Gond, Kumar, Singh and Kharwar. This is an open-access article distributed under the terms of the Creative Commons Attribution License (CC BY). The use, distribution or reproduction in other forums is permitted, provided the original author(s) or licensor are credited and that the original publication in this journal is cited, in accordance with accepted academic practice. No use, distribution or reproduction is permitted which does not comply with these terms.

frontiers in Microbiology

REVIEW
published: 22 June 2017
doi: 10.3389/fmicb.2017.01113

Fungal and Bacterial Pigments: Secondary Metabolites with Wide Applications

*Manik Prabhu Narsing Rao[1†], Min Xiao[1†] and Wen-Jun Li[1,2]**

[1] State Key Laboratory of Biocontrol and Guangdong Provincial Key Laboratory of Plant Resources, School of Life Sciences, Sun Yat-sen University, Guangzhou, China, [2] Key Laboratory of Biogeography and Bioresource in Arid Land, Xinjiang Institute of Ecology and Geography, Chinese Academy of Sciences, Ûrúmqi, China

The demand for natural colors is increasing day by day due to harmful effects of some synthetic dyes. Bacterial and fungal pigments provide a readily available alternative source of naturally derived pigments. In contrast to other natural pigments, they have enormous advantages including rapid growth, easy processing, and independence of weather conditions. Apart from colorant, bacterial and fungal pigments possess many biological properties such as antioxidant, antimicrobial and anticancer activity. This review outlines different types of pigments. It lists some bacterial and fungal pigments and current bacterial and fungal pigment status and challenges. It also focuses on possible fungal and bacterial pigment applications.

Keywords: color, pigments, synthetic dye, microbial pigments, secondary metabolites

OPEN ACCESS

Edited by:
Peter Neubauer, Technische Universität Berlin, Germany

Reviewed by:
Antti Ilmari Vasala, BioSilta Oy, Finland
Michael Craig Crampton, Council for Scientific and Industrial Research, South Africa

***Correspondence:**
Wen-Jun Li
liwenjun3@mail.sysu.edu.cn; liact@hotmail.com

[†]These authors have contributed equally to this work.

Specialty section:
This article was submitted to Microbiotechnology, Ecotoxicology and Bioremediation, a section of the journal Frontiers in Microbiology

Received: *23 December 2016*
Accepted: *31 May 2017*
Published: *22 June 2017*

Citation:
Narsing Rao MP, Xiao M and Li W-J (2017) Fungal and Bacterial Pigments: Secondary Metabolites with Wide Applications. Front. Microbiol. 8:1113. doi: 10.3389/fmicb.2017.01113

INTRODUCTION

Color affects every bit of life, including the clothes we wear, the furniture in our home, and the allure of food (Downham and Collins, 2000; Manikprabhu and Lingappa, 2013). Just think, for instance, how plants could prepare their own food without chlorophyll or how oxygen could be carried in the body without hemoglobin. It can be said that life on earth depends on pigments (Britton, 1995).

The use of pigments as coloring agents has been practiced since prehistoric times. Archaeologists have uncovered evidence that early humans used paint for aesthetic purposes. The use of pigment in prehistoric times was further proven when pigments and grinding equipments, which were between 350,000 and 400,000 years old, were found in a cave at Twin Rivers, near Lusaka, Zambia (Kassinger, 2003). Pigments were used in different parts of the world. In Europe, it was practiced during the Bronze Age. In China, dyeing with plants, barks, and insects has been traced back more than 5,000 years. In India, it occurred during the Indus Valley period (2500 BC) (Gokhale et al., 2004; Aberoumand, 2011). Henna was used before 2500 BC, while saffron has been mentioned in the Bible (Gulrajani, 2001). In Egypt, mummies have been found wrapped in colored cloth, which showed the presence of alizarin.

The addition of color to food started in Egypt when candy makers added natural extracts to their candy. Similarly, the use of natural colorants in food was seen in Japan in the shosoin text of the Nara period (8th century) that contains references to coloring soybean and adzuki-bean cakes (Aberoumand, 2011).

The first synthetic color, mauvine, was developed by Sir William Henry Perkin in 1856 and this development started a revolution in the history of synthetic colorants (Walford, 1980).

Since then, the synthetic color industrial revolution has rapidly proceeded (Downham and Collins, 2000). Synthetic color captured the market due to ease of production, less expensive, no unwanted flavors imparted to food, superior coloring properties, and only tiny amounts are needed to color anything. Sellers at the time offered more than 80 artificial coloring agents. Many color additives at that time had never been tested for their toxicity or other adverse effects, which ultimately led to adverse effects on the health and environment (Downham and Collins, 2000).

Dyes such as tartrazine, cochineal red, and sunset yellow provoke allergies either on their own or in combination with other colorants. Although, some synthetic colorants that had been approved by the Food and Drug Administration (FDA) for use in foods, pharmaceuticals, and cosmetic preparations were later found to promote cancer. Some synthetic dyes have even been withdrawn from external use due to their apparent hazards. For example, benzidine dyes cause bowel cancer, while carbon black (widely used as printing ink pigment) is thought to be a potential carcinogen. From the environmental point of view, unethical discharge of untreated industrial dye effluents produce toxins and persist for long time due to long periods of stability (Babitha, 2009). The drawbacks of synthetic color have increased the global demand for natural pigments (Manikprabhu and Lingappa, 2013).

The main sources for natural pigments are plants or microorganisms. The use of plant pigments has many drawbacks such as non-availability throughout the year and pigment stability and solubility. Large scale plant use may lead to loss of valuable species. For these reasons, the process may not consider viable (Downham and Collins). Microorganisms such as fungi and bacteria provide a readily available alternate source of naturally derived pigments (Arulselvi et al., 2014). Bacterial and fungal pigments have extensive applications (**Table 1**) and have an enormous advantage over plant pigments, including easy and rapid growth in low cost medium, easy processing, and growth that is independent of weather conditions (Manikprabhu and Lingappa, 2013).

Market Trend

There are no reliable published statistics on the size of the color market (Babitha, 2009); however, according to global industry analysts, the demand for organic pigments and dyes is expected to reach almost 10 million tons by 2017. Among the various available pigments, the carotenoids alone are estimated to reach $1.4 billion by 2018 (Venil et al., 2014).

Microbial production of β-carotene costs approximately US$1000/kg versusUS$500/kg for synthetic means. Though microbial pigments are several times more expensive, they still can compete with synthetic dyes for being natural and safe (Venil et al., 2013). There is an increased push to reduce the production costs for microbial pigments by using low cost substrates or strain improvements, and in the near future, there may be a monopoly market for microbial pigments.

Textile industries remains the largest consumer of organic pigments and dyes, while faster growth is expected to occur in other industrial sector such as printing inks, paints, and coating agents. The value of the international food colorant market, which was estimated at around $1.15 billion USD in 2007 (Mapari et al., 2010), may also increase in the future due to food coloring approval for use in the food industry (Aberoumand, 2011).

Fungal Pigments

Filamentous fungi are known to produce an extraordinary range of pigments such as carotenoids, melanins, flavins, phenazines, quinones, monascins, violacein, and indigo (Dufosse et al., 2014). The use of *Monascus* for ang-kak (red mold rice) production is the oldest recorded use of fungal pigment. *Monascus* produce yellow (ankaflavine, monascine), orange (rubropunctatine, monascorubrine), and purple (rubropunctamine, monascorubramine) pigments which are often encountered in Oriental foods, especially in Southern China, Japan and Southeast Asia. Currently, more than 50 *Monascus* pigments have been identified and studied. More than 50 patents around the globe have been issued concerning the use of *Monascus* pigments in food (Dufosse et al., 2005). *Monascus* pigments possess antimicrobial, anticancer, anti-mutagenic, and anti-obesity properties (Feng et al., 2012).

There are more than 200 fungal species reported for carotenes production (Dufosse et al., 2005). Carotenes production was often found in zygomycetes from the order Mucorales, which includes *Phycomyces*, *Blakeslea,* and *Mucor*. In addition to Mucorales, carotene production has been reported in the basidiomycetes genera such as *Rhodosporidium*, *Sclerotium*, *Sclerotinia*, *Sporidiobolus,* and *Ustilago.* Ascomycetes such as *Aspergillus*, *Cercospora*, *Penicillium,* and *Aschersonia* have also been reported for carotenes production (Avalos and Carmen Limon, 2015).

Pigments such as anthraquinones, naphthaquinones, dihydroxy naphthalene melanin, flavin, anthraquinone, chrysophanol, cynodontin, helminthosporin, tritisporin, and erythroglaucin were reported by genera such as *Eurotium*, *Fusarium Curvularia* and *Drechslera* (Babitha, 2009).

Recent literature extensively has reported the interest in marine organisms with respect to the production of new molecules, including new pigments. Indeed, many marine ecological niches are still unexplored. Marine environments have unique features such as low temperatures, absence of light and high pressure and salinity. These conditions induce marine microorganisms to produce unique substances (Dufosse et al., 2014). Genera such as *Aspergillus* (He et al., 2012), *Penicillium* (Dhale and Vijay Raj, 2009), *Trichoderma* (Blaszczyk et al., 2014), and *Eurotium* (Smetanina et al., 2007) have been reported for pigment production. Marine derived fungal pigments are quite similar to terrestrial derived fungal pigments (Capon et al., 2007); however, some pigments were obtained only from marine fungi. Yellow pigment (anthracene-glycoside asperflavin-ribofuranoside) produced by *Microsporum* sp. appears only in marine-derived fungus (Li et al., 2006).

Several marine-derived endophytic fungi such as *Eurotium rubrum* (Li et al., 2009), *Halorosellinia* (Xia et al., 2007), *Hortaea*, *Phaeotheca,* and *Trimmatostroma* have been reported for pigment production (Dufosse et al., 2014). Apart from plants, marine fungi also make associations with algae and corals. Reports suggest that marine endophytic fungi produce pigments

TABLE 1 | Fungal and bacterial pigments and their applications.

Fungi/Bacteria	Pigment	Application	Reference
Bacteria			
Micromonospora lupine	Anthraquinone	Antitumor agent	Igarashi et al., 2007
Streptomyces sp.	Carotenoid	Food-grade pigment	Dharmaraj et al., 2009
Chromobacterium	Violacein	Anti-tumor, anti-microbial, and anti-parasitic agent	Duran et al., 2007
Chromobacterium sp. NIIST (MTCC 5522)	Violacein	Antifungal agent	Sasidharan et al., 2015
Hymenobacter sp. and *Chryseobacterium* sp.	Carotenoid	Photo-sensitizers in dye sensitized solar cells	Ordenes Aenishanslins et al., 2016
Streptomyces glaucescens NEAE-H	Melanin	Anti-cancer agent and anti-oxidant	El-Naggar and El-Ewasy, 2017
Pseudomonas aeruginosa	Pyocyanin	Anti-microbial agent	El-Fouly et al., 2015
Hahella chejuensis	Prodiginines	Antibiotic	Kim et al., 2007
Pedobacter	Carotenoid	Antioxidant	Correa Llanten et al., 2012
Vogesella indigofera	Blue pigment	Detect heavy metal	Gu and Cheung, 2001
Fungi			
Aspergillus versicolor	Asperversin	Antifungal agent	Miao et al., 2012
Fusarium sp. JN158	Benzoquinon	Anticancer agent	Zheng et al., 2017
Fusarium oxysporum	Anthraquinone	Dyeing of wool fabrics	Nagia and El-Mohamedy, 2007
Talaromyces verruculosus	Red pigment	Dye textile having antimicrobial activity	Chadni et al., 2017
Stemphylium lycopersici	Anthraquinone	Antioxidant	Li et al., 2017

that help to mimic and often increase the beauty of the associated life form (Dufosse et al., 2014). Fungus like *Aspergillus* associates with coral skeleton (*Porites lutea* and *Porites lobata*) and imparts black bands that are quite similar to the coral color (Priess et al., 2000).

Although several fungal pigments have been reported in the literature, they must satisfy several criteria regarding their toxicity, regulatory approval, stability, and capital investment required to bring the products from Petri dish to the market (Malik et al., 2012). Although used for centuries, many microbial pigments are still forbidden in many countries. The best example is the *Monascus* pigment that has been used in Asia for centuries as a food colorant but forbidden in Europe and United States due to the presence of mycotoxin (Dufosse et al., 2005). In this context, methods were developed to avoid toxin productions.

(a) Selection of non-pathogenic strains: to evaluate whether toxin production was strain specific, several strains were screened to check toxicity. The toxin production was observed only in some strains, indicating the toxin production was strain specific.
(b) Through controlling the biosynthesis of the metabolite: toxin production can be controlled through the biosynthesis process; this can be achieved when the metabolic pathway were investigated.
(c) Media selection: researcher observed that the addition or removal of metal ions, carbon sources, and nitrogen sources can affect toxin production (Hajjaj et al., 2000; Dufosse et al., 2005); hence, selection of media plays a crucial role in controlling the toxin production.

Apart from toxin production, microbial pigments should withstand extreme pH and temperature in order to meet industrial standards. Many fungal pigments are stable at a wide pH range.

Pigments produced by *Monascus purpureus, Isaria farinosa, Emericella nidulans, Fusarium verticillioides,* and *Penicillium purpurogenum* showed improved dyeing ability at acidic pH (pH 5) (Velmurugan et al., 2010). Pigment produced by *Thermomyces* was stable from acidic to moderate alkaline conditions (pH 5.1 and 8.0) (Poorniammal and Gunasekaran, 2015). The pigment produced by *Penicillium aculeatum* which is used in soft drink found stable at neutral pH (Mapari et al., 2009). The pigment produced by *Monascus purpureus* was stable even at high alkaline conditions (pH 11) (Huang et al., 2011).

Fungal pigments are stable at various temperatures. Pigments from *Monascus purpureus, Isaria* spp., *Emericella* spp., *Fusarium* spp., and *Penicillium* spp. used for the dyeing pre-tanned leather samples that were found stable at high temperatures (Velmurugan et al., 2010). *Monascus* pigment when added to sausages showed 92% to 98% stability at 4 °C for three months (Fabre et al., 1993).

Though many fungi were reported for non-toxic and stable pigments production, but the development of fermentation derived pigments needs high capital investment in terms of media components. The best example is microbial production of β-carotene. The microbial production of β-carotene cost approximately US$1000/kg versus US$500/kg produced by synthetic means (Venil et al., 2014).

To counter balance the production cost, researchers have shown a great interest in the use of waste or industrial side-streams for the fermentation processes in the development microbial pigments (Panesar et al., 2015). Many fungi were reported for pigment production in low cost substrate. *Monascus ruber* reported for pigment production utilizing corn steep liquor as a nitrogen source instead of yeast extract (Hamano and Kilikian, 2006). Similarly, *Monascus purpureus* produce pigment using grape waste (Silveira et al., 2008). Despite many hurdles, fungal pigments made their way to the market and compete with synthetic colors. Food grade pigments from fungi, including

TABLE 2 | Fungal and bacterial pigments studied or applied for commercial production.

Fungi/Bacteria	Color	Pigment	Status
Fungi			
Monascus spp.	Yellow	Ankaflavin	Industrial production#
Monascus spp.	Orange	Rubropunctatin	Industrial production#
Ashbya gossip	Yellow	Riboflavin	Industrial production#
Cordyceps unilateralis	Deep blood red	Naphtoquinone	Industrial production#
Monascus spp.	Red	Monascorubramin	Industrial production#
Penicillium oxalicum	Red	Anthraquinone	Industrial production#
Blakeslea trispora	Red	Lycopene	Development stage**
Blakeslea trispora	Yellow–orange	ß-carotene	Industrial production**
Mucor circinelloides	Yellow–orange	ß-carotene	Development stage**
Bacteria			
Bradyrhizobium spp.	Orange	Canthaxanthin	Research project#
Streptomyces sp.	Yellow	Carotenoids	Development stage*
Streptomyces echinoruber	Red	Rubrolone	Development stage**
Paracoccus zeaxanthinifaciens	Yellow	Zeaxanthin	Research project**
Paracoccus carotinifaciens	Pink–red	Astaxhantin	Research project**
Bradyrhizobium sp.	Dark-red	Canthaxhantin	Research project**
Pseudomonas spp.	Blue, green	Pyocyanin	Industrial production#
Flavobacterium spp.	Yellow	Zeaxanthin	Development stage#
Agrobacterium aurantiacum	Pink-red	Astaxanthin	Research project#

*Data obtained from # Tuli et al., 2015; *Venil et al., 2013; ** Ahmad et al., 2012.*

Monascus pigments, Arpink red^{TM} from *Penicillium oxalicum*, riboflavin from *Ashbya gossypii*, lycopene, and β-carotene from *Blakeslea trispora* are now available in the market (Dufosse et al., 2014). Many fungal pigments are already used for industrial production, while some are in the development stage (**Table 2**).

Bacterial Pigments

The use of bacteria for pigment production has several advantages over fungi, such as short life cycle and ease for genetic modification (Venil et al., 2013, 2014). However, compared with fungal pigments, most of bacterial pigments are still at the research and development stage (**Table 2**); hence, work on bacterial pigments production should be intensified to make them available on the market. Pigment producing bacteria are ubiquitous and present in various ecological niches, such as soil (Zhu et al., 2007), rhizospheric soil (Peix et al., 2005), desert sand (Liu et al., 2009), fresh water (Asker et al., 2008), and marine samples (Franks et al., 2005). They were reported in low (Nakamura et al., 2003) and high (Manachini et al., 1985) temperature regions, can persist in salt regions (Asker and Ohta, 1999), and even as endophytes (Deng et al., 2011).

Compared with other bacterial groups, the pigment production is more likely to be present in actinobacteria (Marroquin and Zapata, 1954). Various genera such as *Streptomyces, Nocardia, Micromonospora, Thermomonospora, Actinoplanes, Microbispora, Streptosporangium, Actinomadura, Rhodococcus,* and *Kitasatospora* (Rana and Salam, 2014) produce a wide variety of pigments. The genus *Streptomyces* was reported for highest pigment production (Conn and Jean, 1941). Many species of this genus, like *Streptomyces griseus*, *Streptomyces griseoviridis*, *Streptomyces coelicolor* (Darshan and Manonmani, 2015), *Streptomyces cyaneus* (Petinate et al., 1999), *Streptomyces vietnamensis* (Zhu et al., 2007), *Streptomyces peucetius (*Arcamone, 1998), *Streptomyces echinoruber* (Gupta et al., 2011), *Streptomyces shaanxiensis* (Lin et al., 2012), and *Streptomyces caeruleatus* (Zhu et al., 2011) were reported to produce pigments.

Similar to fungi, bacteria also produce a wide range of pigments such as carotenoids, melanin, violacein, prodigiosin, pyocyanin, actinorhodin, and zeaxanthin (Ahmad et al., 2012; Venil et al., 2014).

Two fundamental biotechnological approaches are applied when producing microbial pigments; firstly a search for new sources, and secondly enhancing the yield of already recognized sources either through optimization or strain improvement (Venil et al., 2013). To obtain new sources, several ecological niches were screened, and many pigments producing novel bacterial strains (**Table 3**) were discovered suggesting their vast availability. Strain improvement through chemical and physical mutations significantly varied the pigment production. Strain improvement through ultraviolet (UV) mutation increased prodigiosin production by 2.8-fold when compared with the parent strain (Tao et al., 2005). Employment of UV radiation and ethyl methanesulfonate enhanced pigment production in *Serratia marcescens* (El-Bialy and Abou El-Nour, 2015). Cultural conditions and media optimization showed increased pigment production. *Bacillus* sp. showed significant pigment production when cultivated at pH 7.0 ± 0.1 and a temperature of 34°C (Mondal et al., 2015). Similarly, *Duganella* sp. B2 under optimum pH and nitrogen sources showed increased violacein (4.8-folds) production (Wang et al., 2009).

Recent developments in genetic engineering have made it now possible to modify the bacteria to produce the pigment of interest. *Streptomyces coelicolor,* which produces a blue pigment, can be

TABLE 3 | List of novel bacteria producing pigments.

Bacteria	Gram	Pigment	Isolated from	Reference
Paracoccus haeundaensis	Positive	Orange	Sea water	Lee et al., 2004
Streptomyces vietnamensis	Positive	Violet–blue	Soil	Zhu et al., 2007
Streptomyces shaanxiensis	Positive	Blue	Sewage irrigation soil	Lin et al., 2012
Streptomyces caeruleatus	Positive	Dark blue	Tomato rhizosphere soil	Zhu et al., 2011
*Pseudomonas brassicacearum*subsp. *neoaurantiaca*	Negative	Red–orange	Rhizosphere	Ivanova et al., 2009
Pseudomonas argentinensis	Negative	Yellow	Rhizospheric soil	Peix et al., 2005
Bacillus nakamurai	Positive	Black	Soil	Dunlap et al., 2016
Nubsella zeaxanthinifaciens	Negative	Yellow	Freshwater	Asker et al., 2008
Kineococcus xinjiangensis	Positive	Brown	Desert sand	Liu et al., 2009

genetically modified to produce a bright yellow (kalafungin), orange, or yellow–red (anthraquinones) pigment (Bartel et al., 1990; McDaniel et al., 1993).

TYPES OF PIGMENTS

Carotenoids

Carotenoids were first isolated by Heinrich Wilhelm Ferdinand Wackenroder (Wackenroder, 1831). All carotenoids are tetraterpenoids (Kocher and Muller, 2011) and there are over 600 known carotenoids, which are divided into two classes: xanthophylls (which contain oxygen) and carotenes (which are purely hydrocarbons, and contain no oxygen). Among the various carotenoids, the most important carotenoids (**Figure 1**) are alpha and beta-carotenes, cryptoxanthin, lutein, lycopene, violaxanthin, neoxanthin, zeaxanthin, and canthxanthin (Rymbai et al., 2011).

Commercial carotenoids are either extracted from vegetables or produced through chemical synthesis. Extraction of carotenoids from plants has many drawbacks such as seasonal and geographic variability while chemical synthesis generates hazardous wastes that can affect the environment. In contrast to these methods, the microbial production of carotenoids shows great praise for use of low-cost substrates and safety (Mata Gomez et al., 2014). Microorganisms producing carotenoids are many and include *Flavobacterium multivorum* (Bhosale and Bernstein, 2004), *Rhodobacter sphaeroides* (Chen et al., 2006), *Rhodotorula mucilaginosa* (Aksu and Eren, 2005), *Sphingomonas* sp. (Silva et al., 2004), *Dunaliella* sp., *Blakeslea trispora*, *Phycomyces blakesleeanus*, *Mucor circinelloides*, *Fusarium sporotrichioides*, *Agrobacterium aurantiacum*, *Paracoccus carotinifaciens, Gordonia jacobea* (Dufosse, 2006), *Sporidobolus salmoncolor, Rhodosporium paludigenum,* and *Rhodotorula glutinis* (Panesar et al., 2015).

Carotenoids producing microorganisms are diverse, isolated from soil (Arulselvi et al., 2014), cave (Liu et al., 2015), marine (Lee et al., 2004), and slattern crystallizer pond (Anton et al., 2002) environments.

The most prominent function of carotenoids is their contribution to harvest light energy. They absorb light and pass the excitation energy onto chlorophyll, thereby extending the wavelength range of harvested light (Kocher and Muller, 2011). They protect chlorophyll from photo damage (Armstrong and Hearst, 1996). They are used as vitamin supplements and play an important role in protection from oxidative stress. Their intake can prevent photo-aging and sun burn (Della Penna and Pogson, 2006). Epidemiological studies have shown that people with high β-carotene intake have a reduced risk of lung cancer (Alija et al., 2004). Carotenoids are used commercially as food colorants, as animal feed supplements, and treatment for obesity. More recently they have been used for nutraceutical, cosmetic, and pharmaceutical purposes (Garrido-Fernandez et al., 2010; Jaswir et al., 2011).

Melanin

Melanins are indolic polymers (Surwase et al., 2013) classified as eumelanins, pheomelanins, and allomelanins (Banerjee et al., 2014). Melanin is commonly found in all living systems, and their presence in almost every large taxon suggests evolutionary importance (Plonka and Grabacka, 2006).

Melanin production has been reported by a wide variety of microorganisms such as *Colletotrichum lagenarium*, *Magnaporthe grisea*, *Cryptococcus neoformans*, *Paracoccidioides brasiliensis*, *Sporothrix schenckii*, *Aspergillus fumigates* (Langfelder et al., 2003), *Vibrio cholerae, Shewanella colwelliana, Alteromonas nigrifaciens* (Soliev et al., 2011), and many species of the genus *Streptomyces* (Manivasagan et al., 2013).

Melanin confers resistance to UV light by absorbing a broad range of the electromagnetic spectrum and preventing photo-induced damage (Hill, 1992). Melanin is used for mimicry, and protects against high temperatures and chemical stresses. Melanin is extensively used in cosmetics, photo protective creams, eyeglasses, and immobilization of radioactive waste such as uranium. Bacterial melanin genes have been used as reporter genes to screen recombinant bacterial strains. It has anti-HIV properties and is useful for photo voltage generation and fluorescence studies. Melanin is also used to generate monoclonal antibodies for the treatment of human metastatic melanoma (Plonka and Grabacka, 2006; Surwase et al., 2013).

Prodigiosin

Prodigiosin (**Figure 2**) is a red pigment, first isolated from *Serratia marcescens* (Boger and Patel, 1987).

The name prodigiosin has been attributed to isolation from *Bacillus prodigiosus* which was later renamed as *Serratia*

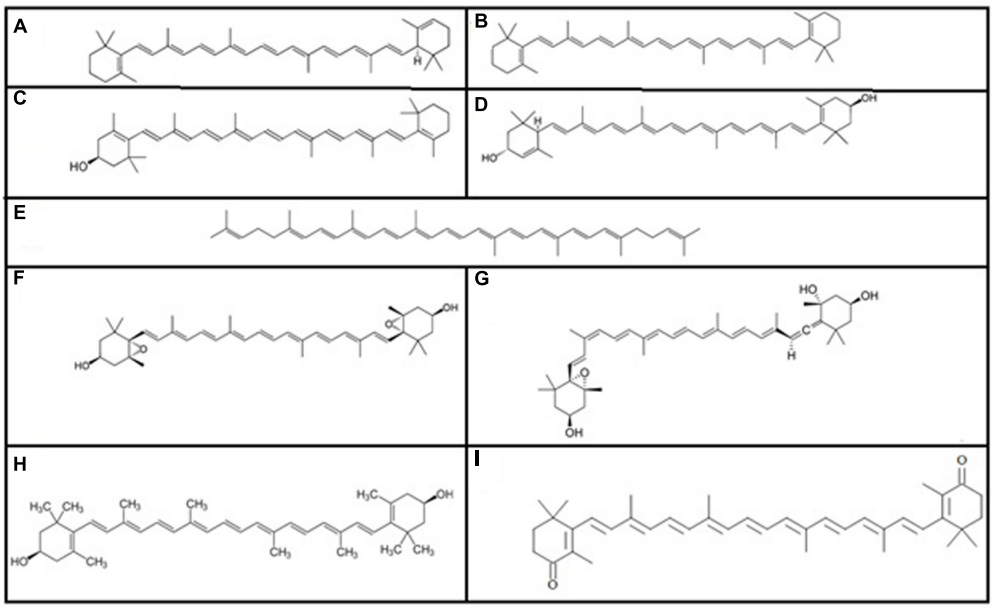


FIGURE 1 | Some important carotenoids: **(A)** alpha carotene, **(B)** beta-carotene, **(C)** cryptoxanthin, **(D)** lutein, **(E)** lycopene, **(F)** violaxanthin, **(G)** neoxanthin, **(H)** zeaxanthin, and **(I)** canthxanthin.

marcescens (Gerber, 1975). Apart from *Serratia marcescens,* prodigiosin production has been reported from *Pseudomonas magneslorubra*, *Vibrio psychroerythrous*, *Vibrio gazogenes*, *Alteromonas rubra*, *Rugamonas rubra,* and *Streptoverticillium rubrireticuli* (Darshan and Manonmani, 2015). Prodigiosin producing microbes are wide spread, and they are isolated from marine samples (Gandhi et al., 1976; Kim et al., 2007), shallow estuarine water (Boric et al., 2011), tidal flat sediment (Yi et al., 2003), and beach sand (Ramaprasad et al., 2015). Prodigiosin acts as a potent therapeutic molecule, especially as an immuno-suppresser and anticancer agents. Prodigiosin also shows insecticidal, antifungal, antibacterial, and anti-malarial activities (Harris et al., 2004; Kamble and Hiwarale, 2012).

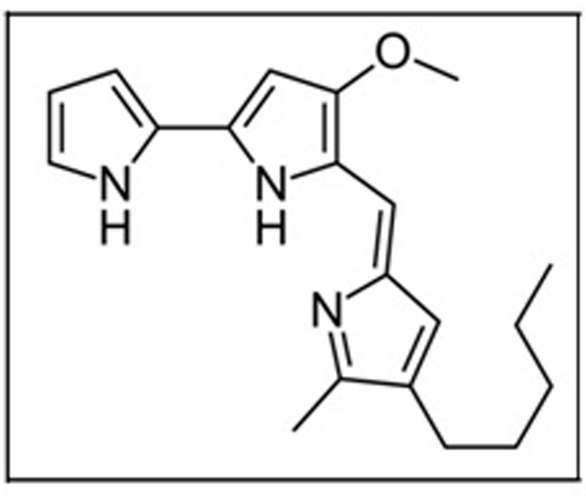


FIGURE 2 | Structure of prodigiosin.

Violacein

Violacein is a violet colored pigment, first described from Gram-negative bacterium *Chromobacterium violaceum* isolated from Amazon River in Brazil. Apart from *Chromobacterium violaceum*, violacein production has been reported from various microorganisms such as *Collimonas* sp., *Duganella* sp., *Janthinobacterium lividum*, *Microbulbifer* sp., *Pseudoalteromonas luteoviolacea*, *Pseudoalteromonas tunicata*, and *Pseudoalteromonas ulvae* inhabiting different environments like soil, marine (Yada et al., 2008; Aranda et al., 2011), glacier (Lu et al., 2009), sea surface (Hakvag et al., 2009), rhizosphere (Aranda et al., 2011), and surface of marine sponge (Yang et al., 2007).

Violacein has been reported for variety of biological activities including antiviral, antibacterial, antiulcerogenic, anti-leishmanial, anticancer, and enzyme modulation properties (Matz et al., 2004; Duran et al., 2007; Soliev et al., 2011)

Riboflavin

Riboflavin (**Figure 3**), also called vitamin B_2 is water soluble pigment that exhibits a strong yellowish-green fluorescence. It was first isolated by the English chemist Alexander Wynter Blyth (Blyth, 1879). The riboflavin structure was confirmed by Kuhn and Weygand, which suggests that it has two distinct parts consisting of a ribose sugar unit and a three-ring flavin structure known as a lumichrome (Kuhn et al., 1933). Riboflavin is an essential vitamin that needs to be supplemented in the human

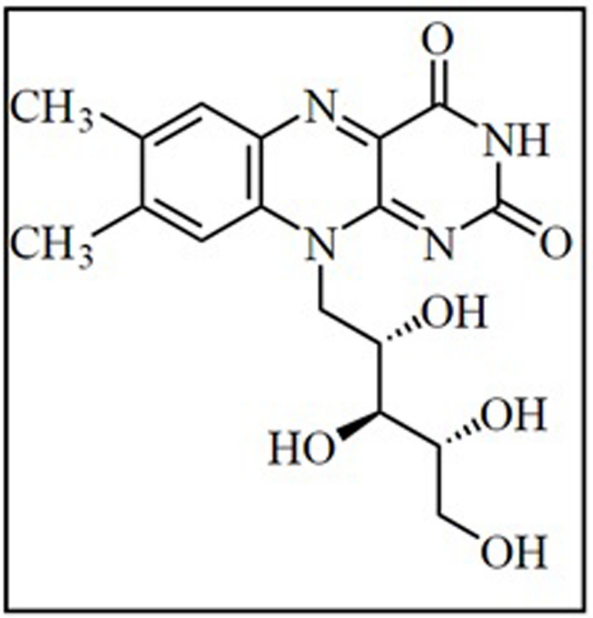


FIGURE 3 | Structure of riboflavin.

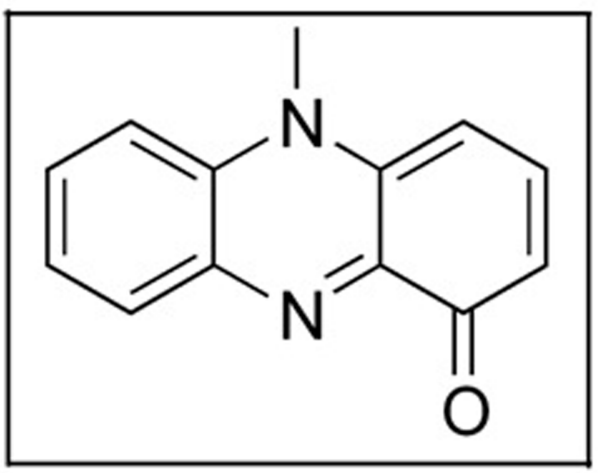


FIGURE 4 | Structure of pyocyanin.

diet at a concentration of 1.1–1.3 mg per day. Riboflavin acts as a structural component of the coenzymes flavin mononucleotide and flavin adenine dinucleotide. Both coenzymes catalyze non-enzymatic oxidation-reduction reactions by functioning as dehydrogenating hydrogen carriers in the transport system involved in ATP production. For over 30 years, riboflavin supplements have been used as part of the phototherapy treatment for neonatal jaundice. Riboflavin co-treatment with β blockers showed improvement against migraine headaches (Kutsal and Ozbas, 1989; Feroz, 2010). Riboflavin in combination with UV light has been shown to be effective in reducing harmful pathogens found in blood products (Goodrich et al., 2006).

Pyocyanin

Pyocyanin (**Figure 4**) is a blue pigment produced by *Pseudomonas aeruginosa* (Hassan and Fridovich, 1980). It is composed of two subunits of *N*-methyl-1-hydroxyphenazine (Norman et al., 2004). To synthesize pyocyanin, specific genes must be functional. *MvfR* is a gene which produces a transcription factor which activates *phnAB* genes. These genes produce the molecule quinolone which then regulates operons 1 and 2 of *phzRABCDEFG* which are the key to the synthesis pyocyanin (Mavrodi et al., 2001). Pyocyanin has been used as bio-control agent and possess anti-bacterial and anti-fungal activity (Jayaseelan et al., 2014).

APPLICATIONS OF PIGMENTS

Pigments in Textile Industry

The textile industry uses approximately 1.3 million tons of synthetic dyes and dye precursors (Venil et al., 2013). About 200,000 tons of dyes are lost as effluents every year during the dyeing and finishing operations. Unfortunately, most of these dyes escape conventional wastewater treatment processes and persist in the environment as a result of their high stability against light, temperatures, water, detergents, chemicals, soap, and other parameters such as bleach and perspiration (Ogugbue and Sawidis, 2011). In this context, there is a great concern about using eco-friendly dyes. Microbial pigments are eco-friendly colorants applicable to dyeing textile fabrics (Chadni et al., 2017). Many microbial pigments were used to dye different types of fabric. Prodigiosin from *Vibrio* spp. can dye wool, nylon, acrylics, and silk. By using tamarind as a mordant, pigment from *Serratia marcescens* can color up to five types of fabric, including acrylic, polyester microfiber, polyester, silk, and cotton (Yusof, 2008). Anthraquinone from *Fusarium oxysporum* can be used to dye wool fabrics (Nagia and El-Mohamedy, 2007). Recently, Sudha, Gupta and Aggarwal (2016) reported dyeing of wet blue goat nappa skin with the *Penicillium minioluteum* pigment. A red pigment from *Talaromyces verruculosus* shows an adequate color tone for cotton fabric without any cytotoxic effect (Chadni et al., 2017).

Microbial pigments produce different color tones in different textiles. Pigment from *Janthinobacterium lividum* show a bluish-purple color tone on silk, cotton, and wool, while dark blue is seen with nylon and vinylon (Shirata et al., 2000). Similarly, the dyeing ability of yellow pigment from *Thermomyces* was evaluated for cotton, silk, and wool fabrics. It was observed that silk fabric showed high affinity for *Thermomyces* pigments when compared with other fabrics (Poorniammal et al., 2013). Deep blue and red pigments from *Streptomyces* strains NP2 and NP4 also showed significant changes in dyeing ability with respect to the material used. Polyamide and acrylic fibers were stained vibrantly, while cotton and cellulosic fibers were stained weakly (Kramar et al., 2014).

In addition, as a colorant, microbial dyed textiles, showed antimicrobial properties. Textile fabric dyed by prodiginines obtained from *Vibrio* sp. showed antibacterial activity against

Staphylococcus aureus and *Escherichia coli* (Alihosseini et al., 2008). In the view of the extensive availability of the microbial pigments, their affinity towards different textiles, cost effectiveness, and nontoxic nature, microbial pigments may increase their market appeal and could replace such synthetic colors which are toxic to mankind and nature.

Pigments as Antimicrobial Agents

The increasing emergence of multidrug resistant bacteria worldwide and the lack of antibiotics to combat such pathogens continue to be a major concern for the medical community (Manikprabhu and Li, 2015). Microbial pigments serve as antimicrobial agents against a wide range of pathogens. Pigments such as carotenoids, melanins, flavins, quinones, monascins, violacein, and indigo have been reported as good antimicrobial agents (Malik et al., 2012). Pigments such as pyocyanin and pyorubin obtained from *Pseudomonas aeruginosa* have shown distinct antibacterial activity against *Citrobacter* sp., which are usually associated with urinary tract and wound infections. Pigments produced from *Micrococcus luteus* KF532949 showed promising antimicrobial activity against wound associated pathogens such as *Staphylococcus* sp., *Klebsiella* sp., and *Pseudomonas* sp. (Umadevi and Krishnaveni, 2013). Pigment obtained from *Streptomyces hygroscopicus*, even showed good antimicrobial activity against drug resistant pathogens such as methicillin and vancomycin resistant strains of *Staphylococcus aureus* and β-lactamase producing strains of *Escherichia coli*, *Pseudomonas aeruginosa,* and *Klebsiella* sp. (Berlanga et al., 2000; Selvameenal et al., 2009). Pigment from *Monascus ruber* showed antimicrobial activity against food borne bacteria (Vendruscolo et al., 2014). Further, inhibition of human pathogenic bacteria such as *Staphylococcus aureus*, *Klebsiella pneumoniae*, and *Vibrio cholera* was observed by the pigment of an endophytic fungal species *Monodictys castaneae* (Visalakchi and Muthumary, 2010).

Efforts in understanding the mechanism of antibacterial activity of some pigments have also been made. The mode of antibacterial action of prodigiosin produced from *Vibrio* sp. DSM 14379 against *Escherichia coli* was evaluated. It was found that the prodigiosin treated *Escherichia coli* cells showed membrane leakage, decreased respiration, and inhibition of protein and RNA synthesis (Danevcic et al., 2016). In view of the above, microbial pigments apart from coloring agents, can be used as novel drugs.

Pigments as Food Colorants

The development of foods with an attractive appearance is an important goal in the food industry. To make the food appealing, either synthetic or natural colors are added. In recent days, food producers are turning from synthetic to natural colors, due to negative health issues associated with some synthetic colors (Aberoumand, 2011; Venil et al., 2013). Natural colorants from microbes play a significant role as food coloring agents, because of its cheap production, easier extraction, high yield, and no lack of raw materials and seasonal variations (Malik et al., 2012). Many pigments from microbial sources such as red pigment from *Monascus* sp., astaxanthin from *Xanthophyllomyces dendrorhous*, Arpink red^{TM} from *Penicillium oxalicum*, riboflavin from *Ashbya gossypii*, β-carotene from *Blakeslea trispora,* and lycopene from *Erwinia uredovora* and *Fusarium sporotrichioides* were added to the food to increase its appeal (Dharmaraj et al., 2009). Pigment like canthaxanthin used in foods, particularly in products such as cheese, candy, fish, meat, fruits, beverages, snacks, beer, and wine. Pigments like riboflavin (i.e., vitamin B2) are used in beverages, instant desserts and ice creams. Carotenoids can act as a sunscreen to maintain the quality of food by protecting them from intense light (Chattopadhyay et al., 2008).

Pigments as Antioxidants

An increase in free radicals in the body enhances the chances of occurrence of chronic diseases such as cancer, diabetes, cardiovascular, and autoimmune disorders (Rankovic et al., 2011). To avoid this, antioxidants are used. Antioxidants are molecules that delay or inhibit cellular damage by donating electrons to a rampaging free radical and neutralizing them via their free radical scavenging properties (Lobo et al., 2010). Microbial pigments such as carotenoid, and naphthaquinone demonstrated antioxidant activities (Tuli et al., 2015). Similarly, anthraquinones from the endophytic fungus *Stemphylium lycopersici* (Li et al., 2017) and melanin from *Streptomyces glaucescens* NEAE-H (El-Naggar and El-Ewasy, 2017) were reported as antioxidants. Pigment like xanthomonadin showed antioxidant activity and protection against photo damage (Tuli et al., 2015). Similarly, the antioxidant activity of carotenoid pigment from an antarctic bacterium *Pedobacter* was evaluated. The pigment possessed strong antioxidant capacity and protected the bacterium against oxidative damage (Correa Llanten et al., 2012). The above reports suggest that microbial pigments used as antioxidants may prevent the incidence of many diseases such as cancer and heart disease.

Pigments as Anticancer Agents

Cancer is one of the most-deadly diseases known to man. The cure for certain types of cancers is considered to be like the Holy Grail since most of the existing treatments are not effective enough to provide full protection (Chakraborty and Rahman, 2012). Efforts to use microbial pigments as anticancer agents have laid the foundation for successful treatments. Many microbial pigments possess anticancer activity. Pigments such as prodigiosin from *Pseudoalteromonas* sp. 1020R have cytotoxicity against U937 leukemia cells (Wang et al., 2012). Melanin from *Streptomyces glaucescens* NEAE-H has been reported for anticancer activity against skin cancer cell line (El-Naggar and El-Ewasy, 2017). Derivatives of anthraquinone from mangrove endophytic fungus *Alternaria* sp. ZJ9-6B has been reported for anti-cancer activity against human breast cancer cell lines (Huang et al., 2011). Pigments obtained from *Monascus* spp. showed remarkable anticancer activity against different cancer cells. Pigments from *Monascus,* such as monascin, showed inhibitory activity against mouse skin carcinogenesis, while ankaflavin showed inhibitory activity against Hep G2 and A549 human cancer cell lines. Similarly, monaphilone A and monaphilone B, exhibits anti-proliferative effect against HEp-2 human laryngeal carcinoma cell lines (Feng et al., 2012). Pigment like prodigiosin has been tested for anticancer activity against more than 60 cancer cell lines and showed a good anticancer activity due to the

presence of multiple cellular targets (Darshan and Manonmani, 2015). In the view of the above, microbial pigments can be a potential therapeutic agents to treat cancer.

Pigments as Bio-indicators

Apart from colorants, antioxidants, antimicrobial agents, and anticancer agents, microbial pigments are used as bio-indicators. Fluorescent pigments from bacteria can be used to check the progress of specific reactions. A key example is phycoerythrin, which is used to predict the rate of peroxy radical scavenging in human plasma. The pigment initially shows fluorescence, however, dark spots appear where the pigment reacts with radicals (Delange and Glazer, 1989).

Pigments are used to detect heavy metals for example, *Vogesella indigofera* produce blue pigment under normal environmental growth condition; however, when exposed to heavy metal like hexavalent chromium, the pigment production did not observed (Gu and Cheung, 2001). Microbial pigments can also be used to monitor temperature variation. *Pantoea agglomerans* produce deep blue pigment only at temperatures of $\geq$10°C and hence can be used as temperature indicator for the low-temperature-storage management of foods and clinical materials (Fujikawa and Akimoto, 2011).

CONCLUSION

Synthetic dyes have caused considerable environmental and health problems. In contrast, microbial pigments are eco-friendly and used in the textile industry, as food colorants, antioxidants, bio-indicators, and antimicrobial and anticancer agents. Though extensive research has been done to bring microbial pigments from the Petri dish to market, still their output cannot fulfill market demand if synthetic dyes withdrawn. Efforts in finding new microbial sources for pigment production and decrease in production cost through optimization, strain improvement and genetic engineering have to be carried out to eradicate toxic synthetic dyes.

AUTHOR CONTRIBUTIONS

All authors listed, have made substantial, direct and intellectual contribution to the work, and approved it for publication.

ACKNOWLEDGMENTS

This work was supported by the Key Project of International Cooperation of Ministry of Science and Technology (MOST) (No. 2013DFA31980), Science and technology infrastructure work project (No. 2015FY110100), and China Postdoctoral Science Foundation Grant No. 2017M612796. W-JL was also supported by Project Supported by Guangdong Province Higher Vocational Colleges and Schools Pearl River Scholar Funded Scheme (2014).

REFERENCES

Aberoumand, A. (2011). A review article on edible pigments properties and sources as natural biocolorants in foodstuff and food industry. *World J. Dairy Food Sci.* 6, 71–78.

Ahmad, W. A., Ahmad, W. Y. M., Zakaria, Z. A., and Yusof, N. Z. (2012). "Application of bacterial pigments as colorant," in *Application of Bacterial Pigments as Colorant: the Malaysian Perspective*, eds W. A. Ahmad, W. Y. M. Ahmad, Z. A. Zakaria, and N. Z. Yusof (Berlin: Springer), 57–74. doi: 10.1007/978-3-642-24520-6_4

Aksu, Z., and Eren, A. T. (2005). Carotenoids production by the yeast *Rhodotorula mucilaginosa*: use of agricultural wastes as a carbon source. *Process Biochem.* 40, 2985–2991. doi: 10.1016/j.procbio.2005.01.011

Alihosseini, F., Ju, K. S., Lango, J., Hammock, B. D., and Sun, G. (2008). Antibacterial colorants: characterization of prodiginines and their applications on textile materials. *Biotechnol. Prog.* 24, 742–747. doi: 10.1021/bp070481r

Alija, A. J., Bresgen, N., Sommerburg, O., Siems, W., and Eckl, P. M. (2004). Cytotoxic and genotoxic effects of β-carotene breakdown products on primary rat hepatocytes. *Carcinogenesis* 25, 827–831. doi: 10.1093/carcin/bgh056

Anton, J., Oren, A., Benlloch, S., Rodriguez-Valera, F., Amann, R., and Rossello-Mora, R. (2002). *Salinibacter ruber* gen. nov., sp. nov., a novel, extremely halophilic member of the Bacteria from saltern crystallizer ponds. *Int. J. Syst. Evol. Microbiol.* 52, 485–491. doi: 10.1099/00207713-52-2-485

Aranda, S., Montes-Borrego, M., and Landa, B. B. (2011). Purple-pigmented violacein-producing *Duganella* spp. inhabit the rhizosphere of wild and cultivated olives in Southern Spain. *Microb. Ecol.* 62, 446–459. doi: 10.1007/s00248-011-9840-9

Arcamone, F. M. (1998). From the pigments of the actinomycetes to third generation antitumor anthracyclines. *Biochimie* 80, 201–206. doi: 10.1016/S0300-9084(98)80003-5

Armstrong, G. A., and Hearst, J. E. (1996). Carotenoids 2: genetics and molecular biology of carotenoid pigment biosynthesis. *FASEB J.* 10, 228–237.

Arulselvi, I. P., Umamaheswari, S., Sharma, R. G., Kartik, C., and Jayakrishna, C. (2014). Screening of yellow pigment producing bacterial isolates from various eco-climatic areas and analysis of the carotenoid produced by the isolate. *J. Food. Process Technol.* 5:292. doi: 10.4172/2157-7110.1000292

Asker, D., Beppu, T., and Ueda, K. (2008). *Nubsella zeaxanthinifaciens* gen. nov., sp. nov., a zeaxanthin-producing bacterium of the family Sphingobacteriaceae isolated from freshwater. *Int. J. Syst. Evol. Microbiol.* 58, 601–606. doi: 10.1099/ijs.0.65493-0

Asker, D., and Ohta, Y. (1999). Production of canthaxanthin by extremely halophilic bacteria. *J. Biosci. Bioeng.* 88, 617–621. doi: 10.1016/S1389-1723(00)87089-9

Avalos, J., and Carmen Limon, M. (2015). Biological roles of fungal carotenoids. *Curr. Genet.* 61, 309–324. doi: 10.1007/s00294-014-0454-x

Babitha, S. (2009). "Microbial pigments," in *Biotechnology for Agro-Industrial Residues Utilisation*, eds P. Singh-Nee Nigam and A. Pandey (Dordrecht: Springer), 147–162. doi: 10.1007/978-1-4020-9942-7_8

Banerjee, A., Supakar, S., and Banerjee, R. (2014). Melanin from the nitrogen-fixing bacterium *Azotobacter chroococcum*: a spectroscopic characterization. *PLoS ONE* 9:e84574. doi: 10.1371/journal.pone.0084574

Bartel, P. L., Zhu, C. B., Lampel, J. S., Dosch, D. C., and Connors, N. C. (1990). Biosynthesis of anthraquinones by interspecies cloning of actinorhodin biosynthesis genes in streptomycetes: clarification of actinorhodin gene functions. *J. Bacteriol.* 172, 4816–4826. doi: 10.1128/jb.172.9.4816-4826.1990

Berlanga, M., Ruiz, N., Hernandez-Borrell, J., Montero, T., and Vinas, M. (2000). Role of the outer membrane in the accumulation of quinolones by *Serratia marcescens*. *Can. J. Microbiol.* 46, 716–722. doi: 10.1139/w00-052

Bhosale, P., and Bernstein, P. S. (2004). β-Carotene production by *Flavobacterium multivorum* in the presence of inorganic salts and urea. *J. Ind. Microbiol. Biotechnol.* 31, 565–571. doi: 10.1007/s10295-004-0187-9

Błaszczyk, L., Siwulski, M., Sobieralski, K., Lisiecka, J., and Jedryczka, M. (2014). *Trichoderma* spp. application and prospects for use in organic farming and industry. *J. Plant Prot. Res.* 54, 309–317. doi: 10.2478/jppr-2014-0047

Blyth, A. W. (1879). The composition of cow's milk in health and disease. *J. Chem. Soc.* 35:530. doi: 10.1039/CT8793500530

Boger, D. L., and Patel, M. (1987). Total synthesis of prodigiosin. *Tetrahedron Lett.* 28, 2499–2502. doi: 10.1021/jo00242a013

Boric, M., Danevcic, T., and Stopar, D. (2011). Prodigiosin from *Vibrio* sp. DSM 14379; a new UV-protective pigment. *Microb. Ecol.* 62, 528–536. doi: 10.1007/s00248-011-9857-0

Britton, G. (1995). Structure and properties of carotenoids in relation to function. *FASEB J.* 9, 1551–1558.

Capon, R. J., Stewart, M., Ratnayake, R., Lacey, E., and Gill, J. H. (2007). Citromycetins and bilains A–C: new aromatic polyketides and diketopiperazines from Australian marine-derived and terrestrial *Penicillium* spp. *J. Nat Prod.* 70, 1746–1752. doi: 10.1021/np0702483

Chadni, Z., Rahaman, M. H., Jerin, I., Hoque, K. M. F., and Reza, M. A. (2017). Extraction and optimisation of red pigment production as secondary metabolites from *Talaromyces verruculosus* and its potential use in textile industries. *Mycology* 8, 48–57. doi: 10.1080/21501203.2017.1302013

Chakraborty, S., and Rahman, T. (2012). The difficulties in cancer treatment. *Ecancermedicalscience.* 6:ed16. doi: 10.3332/ecancer.2012.ed16

Chattopadhyay, P., Chatterjee, S., and Sen, S. K. (2008). Biotechnological potential of natural food grade biocolorants. *Afr. J. Biotechnol.* 7, 2972–2985. doi: 10.5897/AJB08.433

Chen, D., Han, Y., and Gu, Z. (2006). Application of statistical methodology to the optimization of fermentative medium for carotenoids production by *Rhodobacter sphaeroides*. *Process Biochem.* 41, 1773–1778. doi: 10.1016/j.procbio.2006.03.023

Conn, H. J., and Jean, E. C. (1941). Value of pigmentation in classifying actinomycetes. *J. Bacteriol.* 42, 791–799.

Correa Llanten, D. N., Amenabar, M. J., and Blamey, J. M. (2012). Antioxidant capacity of novel pigments from an Antarctic bacterium. *J. Microbiol.* 50, 374–379. doi: 10.1007/s12275-012-2029-1

Danevcic, T., Boric Vezjak, M., Zorec, M., and Stopar, D. (2016). Prodigiosin-a multifaceted *Escherichia coli* antimicrobial agent. *PLoS ONE* 11:e0162412. doi: 10.1371/journal.pone.0162412

Darshan, N., and Manonmani, H. K. (2015). Prodigiosin and its potential applications. *J. Food. Sci. Technol.* 52, 5393–5407. doi: 10.1007/s13197-015-1740-4

Delange, R. J., and Glazer, A. N. (1989). Phycoerythrin fluorescence-based assay for peroxy radicals: a screen for biologically relevant protective agents. *Anal. Biochem.* 177, 300–306. doi: 10.1016/0003-2697(89)90056-0

Della Penna, D., and Pogson, B. J. (2006). Vitamin synthesis in plants: tocopherols and carotenoids. *Annu. Rev. Plant Biol.* 57, 711–738. doi: 10.1146/annurev.arplant.56.032604.144301

Deng, Z. S., Zhao, L. F., Xu, L., Kong, Z. Y., Zhao, P., Qin, W., et al. (2011). *Paracoccus sphaerophysae* sp. nov., a siderophore-producing, endophytic bacterium isolated from root nodules of *Sphaerophysa salsula*. *Int. J. Syst. Evol. Microbiol.* 61, 665–669. doi: 10.1099/ijs.0.021071-0

Dhale, M. A., and Vijay Raj, A. S. (2009). Pigment and amylase production in *Penicillium* sp NIOM-02 and its radical scavenging activity. *Int. J. Food Sci. Technol.* 44, 2424–2430. doi: 10.1111/j.1365-2621.2009.01983.x

Dharmaraj, S., Ashokkumar, B., and Dhevendaran, K. (2009). Food-grade pigments from *Streptomyces* sp. isolated from the marine sponge *Callyspongia diffusa*. *Food. Res. Int.* 42, 487–492. doi: 10.1016/j.foodres.2009.02.006

Downham, A., and Collins, P. (2000). Coloring our foods in the last and next millennium. *Int. J. Food Sci. Technol.* 35, 5–22. doi: 10.1046/j.1365-2621.2000.00373.x

Dufosse, L. (2006). Microbial production of food grade pigments. *Food Technol. Biotechnol.* 44, 313–321.

Dufosse, L., Fouillaud, M., Caro, Y., Mapari, S. A., and Sutthiwong, N. (2014). Filamentous fungi are large-scale producers of pigments and colorants for the food industry. *Curr. Opin. Biotechnol.* 26, 56–61. doi: 10.1016/j.copbio.2013.09.007

Dufosse, L., Galaup, P., Yaron, A., Arad, S. M., Blanc, P., Murthy, K. N. C., et al. (2005). Microorganisms and microalgae as source of pigments for use: a scientific oddity or an industrial reality? *Trends. Food Sci. Technol.* 16, 389–406. doi: 10.1016/j.tifs.2005.02.006

Dunlap, C. A., Saunders, L. P., Schisler, D. A., Leathers, T. D., Naeem, N., and Cohan, F. M. (2016). *Bacillus nakamurai* sp. nov., a black-pigment-producing strain. *Int. J. Syst. Evol. Microbiol.* 66, 2987–2991. doi: 10.1099/ijsem.0.001135

Duran, N., Justo, G. Z., Ferreira, C. V., Melo, P. S., Cordi, L., and Martins, D. (2007). Violacein: properties and biological activities. *Biotechnol. Appl. Biochem.* 48, 127–133. doi: 10.1042/BA20070115

El-Bialy, H. A., and Abou El-Nour, S. A. (2015). Physical and chemical stress on *Serratia marcescens* and studies on prodigiosin pigment production. *Ann. Microbiol.* 65, 59–68. doi: 10.1007/s13213-014-0837-8

El-Fouly, M. Z., Sharaf, A. M., Shahin, A. A. M., El-Bialy, H. A., and Omara, A. M. A. (2015). Biosynthesis of pyocyanin pigment by *Pseudomonas aeruginosa*. *J. Radiat. Res. Appl. Sci.* 8, 36–48. doi: 10.1016/j.jrras.2014.10.007

El-Naggar, N. E., and El-Ewasy, S. M. (2017). Bioproduction, characterization, anticancer and antioxidant activities of extracellular melanin pigment produced by newly isolated microbial cell factories *Streptomyces glaucescens* NEAE-H. *Sci. Rep.* 14:42129. doi: 10.1038/srep42129

Fabre, C. E., Santerre, A. L., Loret, M. O., Baberian, R., Pareilleux, A., Goma, G., et al. (1993). Production and food applications of the red pigments of *Monascus ruber*. *J. Food. Sci.* 58, 1099–1102. doi: 10.1111/j.1365-2621.1993.tb06123.x

Feng, Y., Shao, Y., and Chen, F. (2012). *Monascus* pigments. *Appl. Microbiol. Biotechnol.* 96, 1421–1440. doi: 10.1007/s00253-012-4504-3

Feroz, M. S. (2010). *Optimization of Riboflavin Production by Fungi on Edible oil Effluent*. Master's thesis, Durban University of Technology, Durban.

Franks, A., Haywood, P., Holmstrom, C., Egan, S., Kjelleberg, S., and Kumar, N. (2005). Isolation and structure elucidation of a novel yellow pigment from the marine bacterium *Pseudoalteromonas tunicate*. *Molecules* 10, 1286–1291. doi: 10.3390/10101286

Fujikawa, H., and Akimoto, R. (2011). New blue pigment produced by Pantoea agglomerans and its production characteristics at various temperatures. *Appl. Environ. Microbiol.* 77, 172–178. doi: 10.1128/AEM.00264-10

Gandhi, N. M., Patell, J. R., Gandhi, J., De Souza, N. J., and Kohl, H. (1976). Prodigiosin metabolites of a marine *Pseudomonas* species. *Mar. Biol.* 34, 223–227. doi: 10.1007/BF00388799

Garrido-Fernandez, J., Maldonado-Barragan, A., Caballero-Guerrero, B., Hornero-Mendez, D., and Ruiz-Barba, J. L. (2010). Carotenoid production in *Lactobacillus plantarum*. *Int. J. Food. Microbiol.* 140, 34–39. doi: 10.1016/j.ijfoodmicro.2010.02.015

Gerber, N. N. (1975). Prodigiosin-like pigments. *CRC Crit. Rev. Microbiol.* 3, 469–485. doi: 10.3109/10408417509108758

Gokhale, S. B., Tatiya, A. U., Bakliwal, S. R., and Fursule, R. A. (2004). Natural dye yielding plants in India. *Nat. prod. Radiance* 3, 228–234.

Goodrich, R. P., Edrich, R. A., Li, J., and Seghatchian, J. (2006). The Mirasol PRT system for pathogen reduction of platelets and plasma: an overview of current status and future trends. *Transfus. Apher. Sci.* 35, 5–17. doi: 10.1016/j.transci.2006.01.007

Gu, J. D., and Cheung, K. H. (2001). Phenotypic expression of *Vogesella indigofera* upon exposure to hexavalent chromium, Cr6+. *World. J. Microb. Biot.* 17, 475–480. doi: 10.1023/A:1011917409139

Gulrajani, M. L. (2001). Present status of natural dyes. *Indian J. Fibre Textitle Res.* 26, 191–201.

Gupta, C., Amar, P. G., Prakash, D., Goyal, S., and Gupta, S. (2011). Microbes as potential source of biocolors. *Pharmacologyonline* 2, 1309–1318.

Hajjaj, H., Blanc, P., Groussac, E., Uribelarrea, J. L., Goma, G., and Loubiere, P. (2000). Kinetic analysis of red pigment and citrinin production by *Monascus ruber* as a function of organic acid accumulation. *Enzyme Microb. Technol.* 27, 619–625. doi: 10.1016/S0141-0229(00)00260-X

Hakvag, S., Fjaervik, E., Klinkenberg, G., Borgos, S. E. F., Josefsen, K. D., Ellingsen, T. E., et al. (2009). Violacein-producing *Collimonas* sp. from the sea surface microlayer of costal waters in Trondelag, Norway. *Mar. Drugs* 7, 576–588. doi: 10.3390/md7040576

Hamano, P. S., and Kilikian, B. B. (2006). Production of red pigments by *Monascus ruber* in culture media containing corn steep liquor. *Braz. J. Chem. Eng.* 23, 443–449. doi: 10.1590/S0104-66322006000400002

Harris, A. K., Williamson, N. R., Slater, H., Cox, A., Abbasi, S., Foulds, I., et al. (2004). The *Serratia* gene cluster encoding biosynthesis of the red antibiotic, prodigiosin, shows species and strain-dependent genome context variation. *Microbiology* 150, 3547–3560. doi: 10.1099/mic.0.27222-0

Hassan, H. M., and Fridovich, I. (1980). Mechanism of the antibiotic action pyocyanine. *J. Bacteriol.* 141, 156–163.

He, F., Sun, Y. L., Liu, K. S., Zhang, X. Y., Qian, P. Y., Wang, Y. F., et al. (2012). Indole alkaloids from marine-derived fungus *Aspergillus sydowii* SCSIO 00305. *J. Antibiot.* 65, 109–111. doi: 10.1038/ja.2011.117

Hill, H. Z. (1992). The function of melanin or six blind people examine an elephant. *Bioessays* 14, 49–56. doi: 10.1002/bies.950140111

Huang, C. H., Pan, J. H., Chen, B., Yu, M., Huang, H. B., Zhu, X., et al. (2011). Three bianthraquinone derivatives from the mangrove endophytic fungus *Alternaria* sp. ZJ9-6B from the South China Sea. *Mar. Drugs* 9, 832–843. doi: 10.3390/md9050832

Igarashi, Y., Trujillo, M. E., Martinez-Molina, E., Yanase, S., Miyanaga, S., Obata, T., et al. (2007). Antitumor anthraquinones from an endophytic actinomycete *Micromonospora lupini* sp. nov. *Bioorg. Med. Chem. Lett.* 17, 3702–3705. doi: 10.1016/j.bmcl.2007.04.039

Ivanova, E. P., Christen, R., Bizet, C., Clermont, D., Motreff, L., Bouchier, C., et al. (2009). *Pseudomonas brassicacearum* subsp. *neoaurantiaca* subsp. nov., orange-pigmented bacteria isolated from soil and the rhizosphere of agricultural plants. *Int. J. Syst. Evol. Microbiol.* 59, 2476–2481. doi: 10.1099/ijs.0.009654-0

Jaswir, I., Noviendri, D., Hasrini, R. F., and Octavianti, F. (2011). Carotenoids: sources, medicinal properties and their application in food and nutraceutical industry. *J. Med. Plants Res.* 5, 7119–7131. doi: 10.5897/JMPRx11.011

Jayaseelan, S., Ramaswamy, D., and Dharmaraj, S. (2014). Pyocyanin: production, applications, challenges and new insights. *World. J. Microbiol. Biotechnol.* 30, 1159–1168. doi: 10.1007/s11274-013-1552-5

Kamble, K. D., and Hiwarale, V. D. (2012). Prodigiosin production from *Serratia marcescens* strains obtained from farm soil. *Int. J. Environ. Sci.* 3, 631–638. doi: 10.6088/ijes.2012030131061

Kassinger, R. G. (2003). *Dyes: From Sea Snails to Synthetics*. Minneapolis, MN: Millbrooke Press, Inc.

Kim, D., Lee, J. S., Park, Y. K., Kim, J. F., Jeong, H., Oh, T. K., et al. (2007). Biosynthesis of antibiotic prodiginines in the marine bacterium *Hahella chejuensis* KCTC 2396. *J. Appl. Microbiol.* 102, 937–944. doi: 10.1111/j.1365-2672.2006.03172.x

Kocher, S., and Muller, V. (2011). "The nature and function of carotenoids in the moderately halophilic bacterium *Halobacillus halophilus*," in *Halophiles and Hypersaline Environments*, eds A. Ventosa, A. Oren, and Y. Ma (Berlin: Springer), 303–317.

Kramar, A., Llic Tomic, T., Petkovic, M., Radulovic, N., Kostic, M., Jocic, D., et al. (2014). Crude bacterial extracts of two new *Streptomyces* sp. isolates as bio-colorants for textile dyeing. *World. J. Microbiol. Biotechnol.* 30, 2231–2240. doi: 10.1007/s11274-014-1644-x

Kuhn, R., Gyorgy, P., and Jauregg, T. W. (1933). Uber eine neue klasse von naturfarbstoffen. *Eur. J. Inorg. Chem.* 66, 317–320. doi: 10.1002/cber.19330660244

Kutsal, T., and Ozbas, M. T. (1989). "Microbial production of vitamin B2 (riboflavin)," in *Biotechnology of Vitamins, Pigments and Growth Factors*, ed. E. J. Vandamme (Dordrecht: Springer), 149–166. doi: 10.1007/978-94-009-1111-6_10

Langfelder, K., Streibel, M., Jahn, B., Haase, G., and Brakhage, A. A. (2003). Biosynthesis of fungal melanins and their importance for human pathogenic fungi. *Fungal Genet. Biol.* 38, 143–158. doi: 10.1016/S1087-1845(02)00526-1

Lee, J. H., Kim, Y. S., Choi, T. J., Lee, W. J., and Kim, Y. T. (2004). *Paracoccus haeundaensis* sp. nov., a Gram-negative, halophilic, astaxanthin-producing bacterium. *Int. J. Syst. Evol. Microbiol.* 54, 1699–1702. doi: 10.1099/ijs.0.63146-0

Li, D. L., Li, X. M., and Wang, B. G. (2009). Natural anthraquinone derivatives from a marine mangrove plant-derived endophytic fungus *Eurotium rubrum*: structural elucidation and DPPH radical scavenging activity. *J. Microbiol. Biotechnol.* 19, 675–680. doi: 10.4014/jmb.0805.342

Li, F., Xue, F., and Yu, X. (2017). GC-MS, FTIR and Raman analysis of antioxidant components of red pigments from *Stemphylium lycopersici*. *Curr. Microbiol.* 74, 532–539. doi: 10.1007/s00284-017-1220-3

Li, Y., Li, X., Lee, U., Kang, J. S., Choi, H. D., and Son, B. W. (2006). A new radical scavenging anthracene glycoside, asperflavin ribofuranoside, and polyketides from a marine isolate of the fungus *Microsporum*. *Chem. Pharm. Bull.* 54, 882–883. doi: 10.1002/chin.200647202

Lin, Y. B., Wang, X. Y., Fang, H., Ma, Y. N., Tang, J., Tang, M., et al. (2012). *Streptomyces shaanxiensis* sp. nov., a blue pigment-producing streptomycete from sewage irrigation soil. *Int. J. Syst. Evol. Microbiol.* 62, 1725–1730. doi: 10.1099/ijs.0.029959-0

Liu, L., Zhou, E. M., Jiao, J. Y., Manikprabhu, D., Ming, H., Huang, M. J., et al. (2015). *Hymenobacter mucosus* sp. nov., isolated from a soil sample in karst cave. *Int. J. Syst. Evol. Microbiol.* 65, 4121–4127. doi: 10.1099/ijsem.0.000550

Liu, M., Peng, F., Wang, Y., Zhang, K., Chen, G., and Fang, C. (2009). *Kineococcus xinjiangensis* sp. nov., isolated from desert sand. *Int. J. Syst. Evol. Microbiol.* 59, 1090–1093. doi: 10.1099/ijs.0.004168-0

Lobo, V., Patil, A., Phatak, A., and Chandra, N. (2010). Free radicals, antioxidants and functional foods: impact on human health. *Pharmacogn. Rev.* 4, 118–126. doi: 10.4103/0973-7847.70902

Lu, Y., Wang, L., Xue, Y., Zhang, C., Xing, X. H., Lou, K., et al. (2009). Production of violet pigment by a newly isolated psychrotrophic bacterium from a glacier in Xinjiang, China. *Biochem. Eng. J.* 43, 135–141. doi: 10.1016/j.bej.2008.09.009

Malik, K., Tokkas, J., and Goyal, S. (2012). Microbial pigments: a review. *Int. J. Microb. Res. Technol.* 1, 361–365.

Manachini, P. L., Fortina, M. G., Parini, C., and Craveri, R. (1985). *Bacillus thermoruber* sp. nov., nom. rev., a red-pigmented thermophilic bacterium. *Int. J. Syst. Evol. Microbiol.* 35, 493–496. doi: 10.1099/00207713-35-4-493

Manikprabhu, D., and Li, W. J. (2015). "Antimicrobial agents from actinomycetes Chemistry and applications," in *Antimicrobials Synthetic and Natural Compounds*, eds D. Dhanasekaran, N. Thajuddin, and A. Panneerselvam (Boca Raton, FL: CRC Press), 99–116.

Manikprabhu, D., and Lingappa, K. (2013). γ Actinorhodin a natural and attorney source for synthetic dye to detect acid production of fungi. *Saudi J. Biol Sci.* 20, 163–168. doi: 10.1016/j.sjbs.2013.01.004

Manivasagan, P., Venkatesan, J., Sivakumar, K., and Kim, S. K. (2013). Marine actinobacterial metabolites: current status and future perspectives. *Microbiol. Res.* 168, 311–332. doi: 10.1016/j.micres.2013.02.002

Mapari, S. A., Meyer, A. S., and Thrane, U. (2009). Photostability of natural orange-red and yellow fungal pigments in liquid food model systems. *J. Agric. Food. Chem.* 57, 6253–6261. doi: 10.1021/jf900113q

Mapari, S. A. S., Thrane, U., and Meyer, A. S. (2010). Fungal polyketide azaphilone pigments as future natural food colorants? *Trends Biotechnol.* 28, 300–307. doi: 10.1016/j.tibtech.2010.03.004

Marroquin, A. S., and Zapata, M. (1954). Observations on the pigment of *Streptomyces coelicolor*. *Appl. Microbiol.* 2, 102–107.

Mata Gomez, L. C., Montanez, J. C., Mendez Zavala, A., and Aguilar, C. N. (2014). Biotechnological production of carotenoids by yeasts: an overview. *Microb. Cell Fact.* 13:12. doi: 10.1186/1475-2859-13-12

Matz, C., Deines, P., Boenigk, J., Arndt, H., Eberl, L., Kjelleberg, S., et al. (2004). Impact of violacein-producing bacteria on survival and feeding of bacterivorous nanoflagellates. *Appl. Environ. Microbiol.* 70, 1593–1599. doi: 10.1128/AEM.70.3.1593-1599.2004

Mavrodi, D. V., Bonsall, R. F., Delaney, S. M., Soule, M. J., Phillips, G., and Thomashow, L. S. (2001). Function analysis of genes for biosynthesis of pyocyanin and phenazine -1-carboxamide from *Pseudomonas aeruginosa* PAO1. *J. Bacteriol.* 183, 6454–6465. doi: 10.1128/JB.183.21.6454-6465.2001

McDaniel, R., Ebert-Khosla, S., Hopwood, D. A., and Khosla, C. (1993). Engineered biosynthesis of novel polyketides. *Science* 262, 1546–1550. doi: 10.1126/science.8248802

Miao, F. P., Li, X. D., Liu, X. H., Cichewicz, R. H., and Ji, N. Y. (2012). Secondary metabolites from an algicolous *Aspergillus versicolor* strain. *Mar Drugs* 10, 131–139. doi: 10.3390/md10010131

Mondal, S. K., Samantaray, D. P., and Mishra, B. B. (2015). Optimization of pigment production by a novel *Bacillus* sp. BBMRH isolated from cow dung. *J. Pure Appl. Microbiol.* 9, 2321–2326.

Nagia, F. A., and El-Mohamedy, R. S. R. (2007). Dyeing of wool with natural anthraquinone dyes from *Fusarium oxysporum*. *Dyes Pigments* 75, 550–555. doi: 10.1016/j.dyepig.2006.07.002

Nakamura, Y., Asada, C., and Sawada, T. (2003). Production of antibacterial violet pigment by psychrotropic bacterium RT102 strain. *Biotechnol. Bioprocess Eng.* 8, 37–40. doi: 10.1007/BF02932896

Norman, R. S., Moeller, P., Mc Donald, T. J., and Morris, P. J. (2004). Effect of pyocyanin on a crude oil degrading microbial community. *Appl. Environ. Microbiol.* 70, 4004–4011. doi: 10.1128/AEM.70.7.4004-4011.2004

Ogugbue, C. J., and Sawidis, T. (2011). Bioremediation and detoxification of synthetic wastewater containing triarylmethane dyes by *Aeromonas hydrophila* isolated from industrial effluent. *Biotechnol. Res. Int.* 2011:967925. doi: 10.4061/2011/967925

Ordenes Aenishanslins, N., Anziani-Ostuni, G., Vargas-Reyes, M., Alarcon, J., Tello, A., and Perez-Donoso, J. M. (2016). Pigments from UV-resistant antarctic bacteria as photosensitizers in dye sensitized solar cells. *J. Photochem. Photobiol. B.* 162, 707–714. doi: 10.1016/j.jphotobiol.2016.08.004

Panesar, R., Kaur, S., and Panesar, P. S. (2015). Production of microbial pigments utilizing agro-industrial waste: a review. *Curr. Opin. Food. Sci.* 1, 70–76. doi: 10.1016/j.cofs.2014.12.002

Peix, A., Berge, O., Rivas, R., Abril, A., and Velazquez, E. (2005). *Pseudomonas argentinensis* sp. nov., a novel yellow pigment-producing bacterial species, isolated from rhizospheric soil in Cordoba, Argentina. *Int. J. Syst. Evol. Microbiol.* 55, 1107–1112. doi: 10.1099/ijs.0.63445-0

Petinate, S. D., Martins, R. M., Coelho, R. R., Meirelles, M. N., Branquinha, M. H., and Vermelho, A. B. (1999). Influence of growth medium in proteinase and pigment production by *Streptomyces cyaneus*. *Mem. Inst. Oswaldo Cruz* 94, 173–177. doi: 10.1590/S0074-02761999000200008

Plonka, P. M., and Grabacka, M. (2006). Melanin synthesis in microorganisms–biotechnological and medical aspects. *Acta. Biochim. Pol.* 53, 429–443.

Poorniammal, R., and Gunasekaran, S. (2015). Physical and chemical stability analysis of *Thermomyces* yellow pigment for food application. *Int. J. Food. Ferment. Technol.* 5, 47–52. doi: 10.5958/2277-9396.2015.00006.9

Poorniammal, R., Parthiban, M., Gunasekaran, S., Murugesan, R., and Thilagavathy, R. (2013). Natural dye production from *Thermomyces* sp. fungi for textile application. *Indian J. Fiber Textile Res.* 38, 276–279.

Priess, K., Le Campion-Alsumard, T., Golubic, S., Gadel, F., and Thomassin, B. A. (2000). Fungi in corals: black bands and density-banding of *Porites lutea* and *P. lobata* skeleton. *Mar. Biol.* 136, 19–27. doi: 10.1007/s002270050003

Ramaprasad, E. V., Bharti, D., Sasikala, C. H., and Ramana, C. H. V. (2015). *Zooshikella marina* sp. nov. a cycloprodigiosin- and prodigiosin-producing marine bacterium isolated from beach sand. *Int. J. Syst. Evol. Microbiol.* 65, 4669–4673. doi: 10.1099/ijsem.0.000630

Rana, S., and Salam, M. D. (2014). Antimicrobial potential of actinomycetes isolated from soil samples of Punjab, India. *J. Microbiol. Exp.* 1:00010. doi: 10.15406/jmen.2014.01.00010

Rankovic, B. R., Kosanic, M. M., and Stanojkovic, T. P. (2011). Antioxidant, antimicrobial and anticancer activity of the lichens *Cladonia furcata*, *Lecanora atra* and *Lecanora muralis*. *BMC. Complement. Altern. Med.* 11:97. doi: 10.1186/1472-6882-11-97

Rymbai, H., Sharma, R. R., and Manish, S. (2011). Biocolorants and its implications in Health and Food Industry - a review. *Int. J. PharmTech Res.* 3, 2228–2244.

Sasidharan, A., Sasidharan, N. K., Amma, D. B., Vasu, R. K., Nataraja, A. V., and Bhaskaran, K. (2015). Antifungal activity of violacein purified from a novel strain of *Chromobacterium* sp. NIIST (MTCC 5522). *J. Microbiol.* 53, 694–701. doi: 10.1007/s12275-015-5173-6

Selvameenal, L., Radhakrishnan, M., and Balagurunathan, R. (2009). Antibiotic pigment from desert soil actinomycetes; biological activity, purification and chemical screening. *Indian J. Pharm Sci.* 71, 499–504. doi: 10.4103/0250-474X.58174

Shirata, A., Tsukamoto, T., Yasui, H., Hayasaka, T., Hayasaka, S., Kojima, A., et al. (2000). Isolation of bacteria producing bluish-purple pigment and use for dyeing. *Japan Agric. Res. Q.* 34, 131–140.

Silva, C., Cabral, J. M. S., and Keulen, F. V. (2004). Isolation of a β-total carotenoids over-producing soil bacterium, *Sphingomonas* sp. *Biotechnol. Lett.* 26, 257–262. doi: 10.1023/B:BILE.0000013716.20116.dc

Silveira, S. T., Daroit, D. J., and Brandelli, A. (2008). Pigment production by *Monascus purpureus* in grape waste using factorial design. *LWT Food Sci. Technol.* 41, 170–174. doi: 10.1016/j.lwt.2007.01.013

Smetanina, O. F., Kalinovskii, A. I., Khudyakova, Y. V., Slinkina, N. N., Pivkin, M. V., and Kuznetsova, T. A. (2007). Metabolites from the marine fungus *Eurotium repens*. *Chem. Nat. Compd.* 43, 395–398. doi: 10.1007/s10600-007-0147-5

Soliev, A. B., Hosokawa, K., and Enomoto, K. (2011). Bioactive pigments from marine bacteria: applications and physiological roles. *Evid. Based Complement. Alternat. Med.* 2011:670349. doi: 10.1155/2011/670349

Sudha Gupta, C., and Aggarwal, S. (2016). Dyeing wet blue goat nappa skin with a microbial colorant obtained from *Penicillium minioluteum*. *J. Clean. Prod.* 127, 585–590. doi: 10.1016/j.jclepro.2016.03.043

Surwase, S. N., Jadhav, S. B., Phugare, S. S., and Jadhav, J. P. (2013). Optimization of melanin production by *Brevundimonas* sp. SGJ using response surface methodology. *3 Biotech* 3, 187–194. doi: 10.1007/s13205-012-0082-4

Tao, J., Wang, X., Shen, Y., and Wei, D. (2005). Strategy for the improvement of prodigiosin production by a *Serratia marcescens* mutant through fed-batch fermentation. *World J. Microbiol. Biotechnol.* 21, 969–972. doi: 10.1007/s11274-004-7257-z

Tuli, H. S., Chaudhary, P., Beniwal, V., and Sharma, A. K. (2015). Microbial pigments as natural color sources: current trends and future perspectives. *J. Food. Sci. Technol.* 52, 4669–4678. doi: 10.1007/s13197-014-1601-6

Umadevi, K., and Krishnaveni, M. (2013). Antibacterial activity of pigment produced from *Micrococcus luteus* KF532949. *Int. J. Chem. Anal. Sci.* 4, 149–152. doi: 10.1016/j.ijcas.2013.08.008

Velmurugan, P., Kim, M. J., Park, J. S., Karthikeyan, K., Lakshmanaperumalsamy, P., Lee, K. J., et al. (2010). Dyeing of cotton yarn with five water soluble fungal pigments obtained from five fungi. *Fiber Polym.* 11, 598–605. doi: 10.1007/s12221-010-0598-5

Vendruscolo, F., Tosin, I., Giachini, A. J., Schmidell, W., and Ninow, J. L. (2014). Antimicrobial activity of *Monascus* pigments produced in submerged fermentation. *J. Food Process Preserv.* 38, 1860–1865. doi: 10.1111/jfpp.12157

Venil, C. K., Aruldass, C. A., Dufosse, L., Zakaria, Z. A., and Ahmad, W. A. (2014). Current perspective on bacterial pigments: emerging sustainable compounds with coloring and biological properties for the industry-an incisive evaluation. *RSC Adv.* 4, 39523–39529. doi: 10.1039/c4ra06162d

Venil, C. K., Zakaria, Z. A., and Ahmad, W. A. (2013). Bacterial pigments and their applications. *Process Biochem.* 48, 1065–1079. doi: 10.1016/j.procbio.2013.06.006

Visalakchi, S., and Muthumary, J. (2010). Antimicrobial activity of the new endophytic *Monodictys castaneae* SVJM139 pigment and its optimization. *Afr. J. Microbiol. Res.* 4, 38–44.

Wackenroder, H. (1831). Ueber das Oleum radicis Dauci aetherum, das Carotin, den Carotenzucker und den officinellen succus Dauci; so wie auch über das Mannit, welches in dem Möhrensafte durch eine besondere Art der Gahrung gebildet wird. *Geigers Magazin Pharmazie.* 33, 144–172.

Walford, J. (ed.). (1980). "Historical development of food colouration," in *Developments in Food Colours*, (London: Applied Science publishers).

Wang, H., Jiang, P., Lu, Y., Ruan, Z., Jiang, R., Xing, X. H., et al. (2009). Optimization of culture conditions for violacein production by a new strain of *Duganella* sp. B2. *Biochem. Eng. J.* 44, 119–124. doi: 10.1016/j.bej.2008.11.008

Wang, Y., Nakajima, A., Hosokawa, K., Soliev, A. B., Osaka, I., Arakawa, R., et al. (2012). Cytotoxic prodigiosin family pigments from Pseudoalteromonas sp. 1020R isolated from the Pacific coast of Japan. *Biosci. Biotechnol. Biochem.* 76, 1229–1232. doi: 10.1271/bbb.110984

Xia, X. K., Huang, H. R., She, Z. G., Shao, C. L., Liu, F., Cai, X. L., et al. (2007). 1H and 13C NMR assignments for five anthraquinones from the mangrove endophytic fungus *Halorosellinia* sp. (No. 1403). *Magn. Reson. Chem.* 45, 1006–1009. doi: 10.1002/mrc.2078

Yada, S., Wang, Y., Zou, Y., Nagasaki, K., Hosokawa, K., Osaka, I., et al. (2008). Isolation and characterization of two groups of novel marine bacteria producing violacein. *Mar. Biotechnol.* 10, 128–132. doi: 10.1007/s10126-007-9046-9

Yang, L. H., Xiong, H., Lee, O. O., Qi, S. H., and Qian, P. Y. (2007). Effect of agitation on violacein production in *Pseudoalteromonas luteoviolacea* isolated from a marine sponge. *Lett. Appl. Microbiol.* 44, 625–630. doi: 10.1111/j.1472-765X.2007.02125.x

Yi, H., Chang, Y. H., Oh, H. W., Bae, K. S., and Chun, J. (2003). *Zooshikella ganghwensis* gen. nov., sp. nov., isolated from tidal flat sediments. *Int. J. Syst. Evol. Microbiol.* 53, 1013–1018. doi: 10.1099/ijs.0.02521-0

Yusof, N. Z. (2008). *Isolation and Applications of Red Pigment from Serratia marcescens*. B.Sc. thesis, Universiti Teknologi Malaysia, Johor Bahru.

Zheng, L., Cai, Y., Zhou, L., Huang, P., Ren, X., Zuo, A., et al. (2017). Benzoquinone from *Fusarium* pigment inhibits the proliferation of estrogen receptor-positive

MCF-7 cells through the NF-κB pathway via estrogen receptor signaling. *Int. J. Mol. Med.* 39, 39–46. doi: 10.3892/ijmm.2016.2811

Zhu, H. H., Guo, J., Yao, Q., Yang, S. Z., Deng, M. R., and Li, T. H. (2011). *Streptomyces caeruleatus* sp. nov., with dark blue diffusible pigment. *Int. J. Syst. Evol. Microbiol.* 61, 507–511. doi: 10.1099/ijs.0.017392-0

Zhu, H. H., Guo, J., Yao, Q., Yang, S. Z., Deng, M. R., Phuong le, T. B., et al. (2007). *Streptomyces vietnamensis* sp. nov., a streptomycete with violet blue diffusible pigment isolated from soil in Vietnam. *Int. J. Syst. Evol. Microbiol.* 57, 1770–1774. doi: 10.1099/ijs.0.64774-0

Conflict of Interest Statement: The authors declare that the research was conducted in the absence of any commercial or financial relationships that could be construed as a potential conflict of interest.

Copyright © 2017 Narsing Rao, Xiao and Li. This is an open-access article distributed under the terms of the Creative Commons Attribution License (CC BY). The use, distribution or reproduction in other forums is permitted, provided the original author(s) or licensor are credited and that the original publication in this journal is cited, in accordance with accepted academic practice. No use, distribution or reproduction is permitted which does not comply with these terms.

frontiers in Microbiology

ORIGINAL RESEARCH
published: 28 June 2017
doi: 10.3389/fmicb.2017.01147

Identification, Bioactivity, and Productivity of Actinomycins from the Marine-Derived *Streptomyces heliomycini*

Dongyang Wang[1], Cong Wang[1], Pengyan Gui[1], Haishan Liu[1], Sameh M. H. Khalaf[2], Elsayed A. Elsayed[2,3], Mohammed A. M. Wadaan[2], Wael N. Hozzein[2,4] and Weiming Zhu[1]**

[1] Key Laboratory of Marine Drugs, MEC, School of Medicine and Pharmacy, Ocean University of China, Qingdao, China, [2] Bioproducts Research Chair, Zoology Department, College of Science, King Saud University, Riyadh, Saudi Arabi, [3] Natural and Microbial Products Deptartment, National Research Centre, Dokki, Cairo, Egypt, [4] Botany and Microbiology Department, Faculty of Science, Beni-Suef University, Beni-Suef, Egypt

In the process of profiling the secondary metabolites of actinobacteria isolated from the Saudi coastal habitats for production of antibiotics and anti-cancer drugs, the cultures of strain WH1 that was identified as *Streptomyces heliomycini* exhibited strong antibacterial activity against *Staphylococcus aureus*. By means of MS and NMR techniques, the active compounds were characterized as actinomycins $X_{0\beta}$, X_2, and D, respectively. The research on the productivity of this strain for actinomycins revealed that the highest production of actinomycins $X_{0\beta}$, X_2, and D was reached in the medium MII within 5% salinity and pH 8.5. In this optimized condition, the fermentation titers of actinomycins $X_{0\beta}$, X_2, and D were 107.6 ± 4.2, 283.4 ± 75.3, and 458.0 ± 76.3 mg/L, respectively. All the three actinomycins $X_{0\beta}$, X_2, and D showed potent cytotoxicities against the MCF-7, K562, and A549 tumor cell lines, in which actinomycin X_2 was the most active against the three tumor cell lines with the IC_{50} values of 0.8–1.8 nM. Both actinomycins X_2 and D showed potent antibacterial activities against *S. aureus* and the methicillin-resistant *S. aureus*, *Bacillus subtilis,* and *B. cereus* and the actinomycin X_2 was more potent.

Keywords: marine-derived actinobacteria, *Streptomyces heliomycini* WH1, actinomycins, cytotoxicity, antimicrobial activity

OPEN ACCESS

Edited by:
Mostafa Rateb,
University of the West of Scotland, United Kingdom

Reviewed by:
Khaled Shaaban,
University of Kentucky, United States
Ernani Pinto,
University of São Paulo, Brazil

****Correspondence:***
Wael N. Hozzein
hozzein29@yahoo.com
Weiming Zhu
weimingzhu@ouc.edu.cn

Specialty section:
This article was submitted to Microbial Physiology and Metabolism, a section of the journal Frontiers in Microbiology

Received: *27 March 2017*
Accepted: *07 June 2017*
Published: *28 June 2017*

Citation:
Wang D, Wang C, Gui P, Liu H, Khalaf SMH, Elsayed EA, Wadaan MAM, Hozzein WN and Zhu W (2017) Identification, Bioactivity, and Productivity of Actinomycins from the Marine-Derived Streptomyces heliomycini. Front. Microbiol. 8:1147. doi: 10.3389/fmicb.2017.01147

INTRODUCTION

The actinobacteria have been reported as the producers of two-thirds of the microbially-derived antibiotics known today (Newman et al., 2003). However, the rate for identification of novel compounds has decreased significantly from the widely explored normally terrestrial strains (Lam, 2006; Tiwari et al., 2015). Therefore, the discovery of new strains of actinobacteria may be the first and the key step to obtain novel compounds with bioactivity and subsequently to discover the natural product-based drugs. Increasing number of studies show that unusual and underexplored habitats, such as desert and marine ecosystems, are a rich source of novel actinobacteria with the capacity to produce new compounds with bioactivities (Bister et al., 2004; Bull and Stach, 2007; Fu et al., 2011, 2012, 2014; Wang et al., 2013).

Actinomycins are a class of chromopeptide antibiotics produced by *Streptomyces* sp., most of which share the same phenoxazinone chromophore. Actinomycin D (Act-D) is the most extensively studied example and is widely used as an anti-tumor drug for treatment of childhood rhabdomyosarcoma and Wilms' tumor, etc. The binding of Act-D to DNA is the basis for

the antitumor activity (Koba and Konopa, 2005). This characteristic also makes Act D and 7-aminoactinomycin D as the useful tools for biological investigation (Chen Chiao et al., 1979). Act D also exhibit antiviral activity against coxsackievirus B3 (Saijets et al., 2003) and human immunodeficiency virus HIV-1 (Rill and Hecker, 1996), as well as the enzyme inhibitors against sereine proteinases (Betzel et al., 1993), acid phosphatase (Kapp and Okada, 1972), and tryptophan 2,3-dioxygenase (Killewich et al., 1975). However, its structurally related actinomycins (Acts), Act-X_2 and Act-$X_{0\beta}$, have not been well investigated for their medicinal properties due to the limits of the available amounts (Kurosawa et al., 2006). To discover new actinobacterial strains and optimize their cultural conditions to produce Acts, we carried out screenings of the marine-derived actinobacterial strains from the coastal habitats of Saudi Arabia. A producing strain of Acts, designated WH1, was identified as *Streptomyces heliomycini* whose products showed significant inhibition on the growth of *Staphyloccocus aureus*. A chemical study on the ethyl acetate (EtOAc) extract of the fermentation broth of *S. heliomycini* WH1 resulted in the isolation and identification of three Acts, Act-$X_{0\beta}$ (**1**), Act-X_2 (**2**), and Act-D (**3**) (**Figure 1**). All three Acts exhibited more potent cytotoxicities on the A549, MCF-7 and K562 tumor cell lines than adriamycin in which Act-X_2 is the most active with the IC_{50} values of 0.8–1.8 nM and the lowest toxicity against the human embryo liver cell strand (L02 cells) with the values of the selective index (SI) of 5.2–12.2. Moreover, all the three Acts displayed more active or comparable antibacterial to ciprofloxacin hydrochloride against *Staphylococcus aureus* and the methicillin-resistant *S. aureus* (MRSA), *Bacillus subtilis,* and *Bacillus cereus* with MICs of 0.04–2.48 μM. In addition, the productivity on actinomycins of *S. heliomycini* WH1 under different cultural conditions were investigated.

MATERIALS AND METHODS

General Experimental Procedures

Silica gel (200–300 mesh) and on plates pre-coated with silica gel GF254 (10–40 μm) (Qingdao Marine Chemical Factory, Qingdao, China) were used in vacuum liquid chromatography (VLC) and thin layer chromatography (TLC), respectively. The optical rotation was measured by a Jasco P-1020 digital polarimeter. IR and UV spectra were recorded on a Nicolet Nexus 470 spectrophotometer using KBr discs and on a Hitachi UH5300 UV-Visible spectrophotometer, respectively. NMR spectra of Acts X_2 and D were measured by a JEOL JNM-ECP 600 spectrometer while Act-$X_{0\beta}$ was recorded on a Bruker Avance III 600 spectrometer and the chemical shifts were recorded as δ values using TMS as internal standard. Compounds were separately injected into the Q-TOF Ultima Global GAA076 LC mass spectrometer to obtained mass spectra. The cultures were analyzed over an analyzing YMC-ODS-A chromatographic column (4.6 × 250 mm, 5 μm) eluted with 80% H_2O-MeOH (v/v) at a flow rate of 1 mL/min by a Shimadzu LC-6AD HPLC

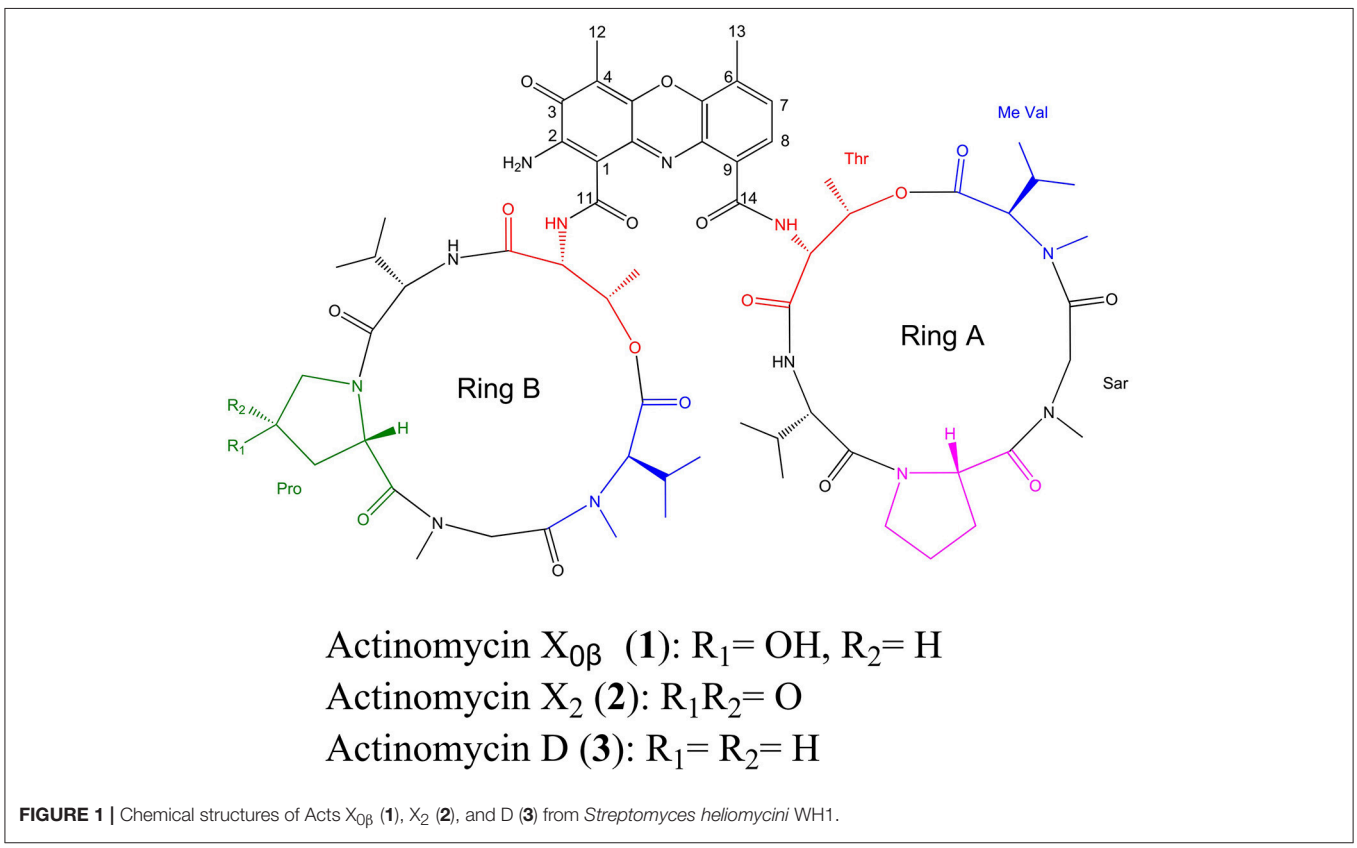


FIGURE 1 | Chemical structures of Acts $X_{0\beta}$ (**1**), X_2 (**2**), and D (**3**) from *Streptomyces heliomycini* WH1.

equipment and detected at λ_{max} 443 nm. The actinomycins were purified over a semi-preparative YMC-ODS-A chromatographic column (10 × 250 mm, 5 μm) eluted with 80% H_2O-MeOH (v/v) at a flow of 4 mL/min by a Waters 1525 HPLC equipment. The RPMI 1640 powder with L-glutamine (Gln) and without $NaHCO_3$ was from Life Technologies Corporation (USA). The ciprofloxacin hydrochloride was from J&K Scientific Ltd. (Beijing, China), and ketoconazole and itraconazole were from Energy Chemical (Shanghai, China). Phosphate Buffer Solution (PBS, 0.01 M, pH 7.2–7.4) and RPMI 1640 liquid medium for cell culture were from Beijing Solarbio Science & Technology Co., Ltd (Beijing, China).

Bacterial Material

The actinobacterial strain WH1 was isolated from a sandy soil sample collected at the coastal region of the Arabian Gulf at Jobail industrial city, in the Eastern Province of Saudi Arabia, and identified as *S. heliomycini* WH1 according to its phenotypic and phylogenetic characters (Figures S1, S2). The strain was deposited in our laboratories in 20% glycerol at −80°C. The working strain was prepared on ISP2 agar slants and stored at 4°C. The human pathogenic bacteria, *B. subtilis* (ATCC 6051), *Escherichia coli* (ATCC 11775), *Pseudomonas aeruginosa* (ATCC 10145), *Staphyloccocus aureus* (ATCC 6538) and MRSA (ATCC 43300), and the pathogenic fungi, *Candida albicans* (ATCC 10231) and *Candida glabrata* (ATCC 2001) were purchased from the Institute of microbiology, Chinese Academy of Sciences. The aquatic pathogenic bacteria, *B. cereus* (ATCC 14579), *Vibrio vulnificus* (ATCC 27562), and *Vibrio parahaemolyticus* (ATCC 17802) were purchased from Guangdong Institute of Microbiology (GIM). *Aspergillus fumigates* AF293 was given by Prof. Ling Lu, Nanjing Normal University, and *Vibrio alginolyticus*, *Vibrio splendidus,* and *Aeromonas hydrophila* were given by Prof. Xiangli Tian, Fisheries College of Ocean University of China.

Isolation and Identification of Strain WH1

The collected sandy soil sample was air dried at room temperature (rt) for 7 days and then serially diluted up to 10^{-4} and inoculated in triplicates onto two selective media recommended for the isolation of actinobacteria, M1 (Mincer et al., 2002) and MM (Hozzein et al., 2008). After incubation at 28°C for 3 weeks, the isolate under study was picked and purified by streaking on the isolation medium twice each for 14 days at 28°C. The pure culture was maintained on slants at 4°C and preserved as a mixture of hyphae and spores in 20% glycerol at −80°C.

The purified isolate was characterized by its morphological characteristics (mycelia, cell morphology, and spore surface) by examining coverslip cultures on ISP2 agar plates grown at 28°C for 14 days by light and scanning electron (JEOL M6060) microscopes as described in the International Streptomyces Project (ISP) (Shirling and Gottlieb, 1966). The isomer type of the diaminopimelic acid in the cell wall and the whole-organism sugars were determined according to the standard methods of Hasegawa et al. (1983) and Staneck and Roberts (1974), respectively. The genomic DNA extraction, PCR amplification of the 16S rRNA gene, and sequencing of the PCR product were carried out as described before (Hozzein and Goodfellow, 2007). The obtained sequence was deposited in Genbank (accession No. AB184712) and compared with available 16S rRNA gene sequences of validly published species from the EzTaxon-e server (http://eztaxon-e.ezbiocloud.net/; Kim et al., 2012).

Cultural Media

The isolation medium was MM agar medium containing 0.05% glucose, 0.05% yeast extract, 0.05% $MgSO_4{\cdot}7H_2O$, 0.05% NaCl, 0.1% K_2HPO_4, 1.8% agar, and 1 L seawater, pH 7.5. The working strain was prepared on ISP2 agar slants composed of 0.4% glucose, 1% malt extract, 0.4% yeast extract, 1.8% agar, and 1 L 50% seawater, pH 7.5. The MM liquid medium, soybean meal medium (2% soybean meal and 1 L seawater, pH 8.0), and the MI–MIV media were used to investigate the productivity of WH1 for actinomycins. MI–MIV media contained 2.0% yeast extract, 0.15% KH_2PO_4, 0.05% $MgSO_4{\cdot}7H_2O$ and 1 L seawater (pH 8.0), 2.0% soybean meal, 0.15% KH_2PO_4, 0.05% $MgSO_4{\cdot}7H_2O$ and 1 L seawater (pH 8.0), 2.25% soluble starch, 0.5% yeast extract, 0.15% KH_2PO_4, 0.05% $MgSO_4{\cdot}7H_2O$ and 1 L seawater (pH 8.0), and 2.25% glucose, 0.5% yeast extract, 0.15% KH_2PO_4, 0.05% $MgSO_4{\cdot}7H_2O$ and 1 L seawater (pH 8.0), respectively. The LB agar medium consisted of 1% tryptone, 0.5% yeast extract, 0.5% NaCl, 1.8% agar, and 1 L tap water (pH 7.4), while the YPD agar medium consisted of 1% yeast extract, 2% peptone, 2% glucose, 1.8% agar, and 1 L tap water (pH 7.0). The 2216E agar medium was prepared by 1% peptone, 0.5% yeast extract powder, 1.8% agar, and 1 L seawater (pH 7.8). The PDA agar medium contained 20% potato, 2% glucose, 1.8% agar, and 1 L tap water.

Fermentation and Extraction

S. heliomycini WH1 was fermented in ten 500-mL Erlenmeyer flasks each containing 150 mL MM liquid medium and was shaken for 10 days at 28°C and 180 rpm. The fermentation broth was extracted three times each with 1,500 mL EtOAc. The EtOAc phase was combined and evaporated to dryness under reduced pressure by a rotary evaporator to give the EtOAc extracts (0.5 g). *S. heliomycini* WH1 was also cultured in different media under different pH and salinity. The chemo-diversity of the EtOAc extracts was investigated by high performance liquid chromatography (HPLC, Figure S3).

Purification and Identification of the Acts

The EtOAc extract (0.5 g) was separated into five fractions on a VLC silica gel column using a step gradient elution with 100:0, 50:1, 30:1, 10:1, and 0:100 (v/v) of CH_2Cl_2-MeOH. Then the fractions 2–4 containing actinomycins were combined and purified by semi-preparative HPLC using YMC-pack semi-preparative chromatographic column (ODS-A) eluted with 80% H_2O-MeOH (v/v) at a flow rate of 4 mL/min to give Act-$X_{0\beta}$ (**1**) (1.0 mg, t_R 9.6 min), Act-X_2 (**2**) (3.7 mg, t_R 11.2 min) and Act-D (**3**) (6.6 mg, t_R 13.0 min). The isolation yields of Acts $X_{0\beta}$, X_2, and D were 0.7, 2.5, and 4.4 mg/L, respectively.

Sample Preparation for Analysis of the Acts Production

The strain WH1 was fermented with three parallels for 10 days at 180 rpm and 28°C in a 500 mL Erlenmeyer flask containing 150 ml of MM liquid, soybean meal, and MI–MIV media, and the pH value was adjusted to a certain value before sterilization. The initial pH values were adjusted by 20% hydrochloric acid (HCl) or 4% sodium hydroxide (NaOH). The 0, 3, 5, and 7% salinity were prepared by tap water, seawater, and sea water supplemented with NaCl, respectively. Each experiment was carried out in three parallel. The fermentation broths were extracted thrice with EtOAc (each 250 mL), and concentrated to dryness *in vacuo* to give the extracts for HPLC analysis.

Analysis of the Acts Production

The production of Acts was estimated by establishing the standard curve between the HPLC peak areas and the concentrations of Acts. The standard curve was established using standard solutions from 0.1 to 10 μg/mL on a YMC-pack C18 analytical column with 1 mL/min of flow rate and detection at λ_{max} 443 nm. Linear curves and their fitting equations were established using Origin 9.0. The production of Acts was calculated according to the fitting equations.

Cytotoxic Assay of the Acts

The cytotoxicities on three human cancer cell lines, nonsmall cell lung cancer cell line (A549), breast cancer cell line (MCF-7), and myelogenous leukemia cell line (K562), along with human embryo liver L02 cell line were assayed. The method for A549, MCF-7 and L02 was the 3-(4,5-Dimethylthiazol-2-yl)-2,5-diphenyltetrazolium bromide (MTT) (Mosmann, 1983), while the one for K562 was the cell counting Kit-8 (CCK-8) (Tominaga et al., 1999). A549, MCF-7, K562, and L02 cell lines were cultured for 3–5 d in the RPMI-1640 liquid medium supplemented with 10% FBS under a humidified atmosphere with 5% CO_2 and 95% air at 37°C. Then 100 μL of the cell suspensions with a density of 3×10^5 cells mL^{-1} was plated in the 96-well microtiter plates and incubated for 12 h. The 200 μM testing DMSO solutions of the samples were diluted into 12.5 and then to 0.012 μM by the continuous 2-fold dilution method with RPMI-1640 medium. Then, the obtained test solutions (100 μL) were added into above wells each containing 100 μL cell suspension and further incubated for 72 h. The 20 μL 0.5% MTT solution (in PBS) was added to each well containing A549, MCF-7, and L02 cell lines and further incubated for 4 h. The culture broth was then gently pipetted and the DMSO (150 μL) was added to dissolve the formed formazan crystals. Absorbance of the solution was determined on a Spectra Max Plus plate reader at 570 nm. The CCK-8 solution was added to each well containing K562 cell and further incubated for 6 h, absorbance was determined on a Spectra Max Plus plate reader at 450 nm. The inhibition rates were calculated as $((A_{blankcontrol} - A_{sample})/A_{blankcontrol} \times 100\%)$. The half-maximal inhibitory concentration (IC_{50}) is defined as the concentration within 50% inhibition. Adriamycin was used as the positive control with the IC_{50} values of 1.30, 0.30, and 1.00 μM for A549, K562, and MCF-7, and the CC_{50} value of 0.40 μM for L02 cell lines, respectively. The selective index (SI) is defined as the value of CC_{50}/IC_{50}.

Antimicrobial Assay of the Acts

The antimicrobial activities against human pathogenic bacteria (*B. subtilis*, *E. coli*, *P. aeruginosa*, *S. aureus*, and MRSA) and pathogenic fungi (*C. albicans*, *C. glabrata*, *Aspergillus fumigatus* AF293) and aquatic pathogenic bacteria (*A. hydrophila*, *B. cereus*, *V. alginolyticus*, *V. parahaemolyticus*, *V. splendidus,* and *V. vulnificus*) were evaluated using the filter paper disc method. The pathogenic strains were cultivated in LB agar plates at 37°C for bacteria and in YPD agar plates at 37°C for fungi. The testing methanol (MeOH) solutions (1 mg/mL) of the samples and positive control (ciprofloxacin hydrochloride for bacteria, and ketoconazole for *C. albicans* and *C. glabrata*) were diluted into 500–1.95 μg/mL by the continuous 2-fold dilution method with MeOH. Then 10 μL of the testing solutions were separately added to the paper disc (5 mm diameter). After evaporation to dryness, the drug paper discs were added into the cultural plates of the pathogenic microorganisms and incubated at 28°C for 12 h. Inhibition zones were then recorded as mm in diameter. The samples were first tested for their inhibitory zone diameters (IZDs) at the concentration of 1 mg/mL. Only those active samples with IZDs ≥14 mm were tested for their minimum inhibitory concentration (MIC) by 2-fold dilution method (Fu et al., 2013). The drug solutions of the three actinomycins, extracts and ciprofloxacin hydrochloride (positive control) were respectively prepared by a serial 2-fold dilution method from 100 to 0.049 μg/mL with the LB liquid medium for *S. aureus* and *B. subtilis* and 2216E liquid medium for *B. cereus*. The pathogenic bacterial colony with 24 h old grown on the LB (*S. aureus* and *B. subtilis*) or 2216E (*B. cereus*) agar plates were transferred into a 50-mL tube containing 30 mL fresh corresponding liquid media and incubated for 12 h at 28°C and 180 rpm. The final bacterial suspension was adjusted to the density of 5×10^5 CFU/mL with fresh corresponding liquid media and was added into the 96-well plates. Each well contains 100 μL bacterial suspension and 100 μL of the testing solution. The medium (100 μL) equipped with 100 μL bacterial suspension was used as the corresponding negative controls and the medium (200 μL) was used as blank controls. Each experiment was carried out in three parallel wells. All plates were stationary incubated for 15 h at 37°C. The minimal inhibitory concentration (MIC) was the lowest drug concentration at which no bacteria were grown, that is, the wells were more transparent than the negative control examined by eyes. In addition, the antifungal activity against *A. fumigatus* AF293 was also assayed. 3-(N-morpholino) propansulfonic acid (MOPS, 6.906 g) and glucose (4 g) were dissolved in 65 mL of deionized water at 60°C and then cooled to rt. And then 2.08 g RPMI 1640 powder with L-Gln and without $NaHCO_3$ was added to the solution. The pH was adjusted to 7.0 with 5.0% NaOH and the solution volume was adjusted to 90 mL by adding deionized water. The *A. fumigatus* was grown on PDA at 28°C for a week and the mature spores were suspended in 0.9% saline and the density was adjusted to 2×10^4 CFU/mL with above fresh-prepared RPMI 1640 medium. The drug solution was

TABLE 1 | ^{1}H (600 MHz) and ^{13}C (150 MHz) NMR Date of Act-$X_{0\beta}$ (**1**) in $CDCl_3$[a].

	Ring-A			Ring-B		
	Position	**δ_C, type**	**δ_H (*J* in Hz)**	**Position**	**δ_C, type**	**δ_H (*J* in Hz)**
Thr	1	168.8, C		1	169.0, C	
	2	55.5, CH	4.81 (dd, 7.0, 2.5)	2	54.9, CH	4.49 (dd, 6.5, 2.8)
	3	74.7, CH	5.24 (m)	3	75.4, CH	5.24 (m)
	4	17.7, CH_3	1.28 (d, 6.3)	4	17.8, CH_3	1.24 (d, 6.0)
	NH		7.44 (d, 6.9)	NH		7.50 (d, 6.4)
Val	1	173.5, C		1	173.3, C	
	2	58.9, CH	3.57 (dd, 10.2, 3.5)	2	58.1, CH	3.55 (dd, 8.9, 4.3)
	3	32.0, CH	2.16 (m)	3	31.9, CH	2.12 (m)
	4	19.2, CH_3	0.75 (d, 2.7)	4	19.2, CH_3	0.74 (d, 2.7)
	5	19.2, CH_3	0.96 (d, 7.4)	5	19.0, CH_3	0.94 (d, 1.6)
	NH		8.17 (d, 6.2)	NH		7.91 (d, 5.5)
Pro	1	173.2, C		1	173.0, C	
	2	57.0, CH	5.97 (d, 9.2)	2	56.5, CH	6.05 (d, 9.6)
	3	31.2, CH_2	1.84 (m), 2.78 (m)	3	31.4, CH_2	4.13 (m), 3.95 (m)
	4	23.0, CH_2	2.06 (m), 2.26 (m)	4	70.0, CH	4.70 (m)
	5	47.6, CH_2	3.85 (m), 3.73 (m)	5	54.7, CH_2	3.56 (m), 3.08 (m)
Sar	1	166.5, C		1	166.5, C	
	2	51.3, CH_2	4.72 (d, 17.4), 3.63 (d, 17.4)	2	51.5, CH_2	4.55 (d, 17.4), 3.59 (d, 17.4)
MeVal	NMe	35.0, CH_3	2.87 (s)	NMe	35.1, CH_3	2.87 (s)
	1	167.6, C		1	167.7, C	
	2	71.3, CH	2.71 (d, 9.3)	2	71. 4, CH	2.67 (d, 9.4)
	3	27.0, CH	2.78 (m)	3	27.0, CH	2.64 (m)
	4	21.7, CH_3	0.96 (m)	4	21.7, CH_3	0.94 (m)
	5	19.4, CH_3	0.75 (d, 2.7)	5	19.2, CH_3	0.74 (d, 3.1)
	NMe	39.5, CH_3	2.95 (s)	NMe	39.3, CH_3	2.94 (s)
chromophore	1	102.7, C				
	2	147.1, C				
	3	179.1, C				
	4	113.6, C				
	4a	145.0, C				
	5a	140.7, C				
	6	128.5, C				
	7	130.4, CH	7.35 (d, 7.8)			
	8	126.2, CH	7.64 (d, 7.8)			
	9	131.3, C				
	9a	129.6, C				
	10a	146.1, C				
	11	166.2, C				
	12	7.9, CH_3	2.22 (s)			
	13	15.3, CH_3	2.54 (s)			
	14	173.0, C				

[a] *Thr, Threonine; Val, Valine; Pro, Proline; Sar, Sarcosine.*

prepared by dissolving extracts (50 mg/mL) or compounds (10 mg/mL) in DMSO and then diluted to 100-fold with the sterile water so that the final concentration of DMSO was less than 1%. One hundred microliters of the drug solution was added into 96-well plates (Costar 3599) that each well contains 100 μL *A. fumigatus* AF293 suspension within the density of

TABLE 2 | ^{1}H (500 MHz) and ^{13}C (125 MHz) NMR Date of Act-X_2 (**2**) in $CDCl_3$[a].

	Ring-A			Ring-B		
	Position	**δ_C, type**	**δ_H (*J* in Hz)**	**Position**	**δ_C, type**	**δ_H (*J* in Hz)**
Thr	1	168.7, C		1	168.8, C	
	2	55.0, CH	4.55 (m)	2	54.8, CH	4.48 (m)
	3	74.7, CH	5.15 (m)	3	74.6, CH	5.24 (m)
	4	17.2, CH_3	1.14 (d, 6.4)	4	17.7, CH_3	1.26 (d, 7.3)
	NH		7.17 (d, 7.2)	NH		7.67 (d, 6.1)
Val	1	173.5, C		1	174.0, C	
	2	58.5, CH	3.57 (dd, 9.3, 6.3)	2	57.2, CH	3.70 (dd, 10.4, 6.3)
	3	31.9, CH	2.10 (m)	3	31.7, CH	2.09 (m)
	4	18.9, CH_3	0.90 (d, 6.8)	4	18.8, CH_3	0.89 (d, 6.8)
	5	19.2, CH_3	1.12 (d,6.8)	5	19.2, CH_3	1.15 (d, 6.8)
	NH		7.68 (d, 6.2)	NH		8.19 (d, 5.9)
Pro	1	173.1, C		1	172.7, C	
	2	56.4, CH	5.95 (d, 8.9)	2	54.3, CH	6.55 (d, 11.0)
	3	31.0, CH_2	1.84 (m), 2.75 (m)	3	41.9, CH_2	3.85 (m), 2.33 (m)
	4	23.0, CH	2.24 (m)	4	208.8, C	
	5	47.4, CH_2	3.91 (m), 3.74 (m)	5	52.9, CH_2	4.55 (m), 3.89 (m)
Sar	1	166.0, C		1	165.9, C	
	2	51.3, CH_2	4.72 (d, 17.3), 3.62 (d, 17.3)	2	51.3, CH_2	4.57 (d, 17.3), 3.62 (d, 17.3)
MeVal	NMe	34.8, CH_3	2.88 (s)	NMe	34.9, CH_3	2.89 (s)
	1	166.5, C		1	166.3, C	
	2	71.3, CH	2.68 (m)	2	71.5 CH	2.68 (m)
	3	26.9, CH	2.68 (m)	3	27.0, CH	2.68 (m)
	4	21.6, CH_3	0.94 (d, 5.8)	4	21.7, CH_3	0.97 (d, 5.5)
	5	19.1, CH_3	0.74 (d, 5.8)	5	19.1, CH_3	0.73 (d, 5.5)
	NMe	31.7, CH_3	2.92 (s)	NMe	31.9, CH_3	2.93 (s)
chromophore	1	101.7, C				
	2	147.4, C				
	3	179.0, C				
	4	113.6, C				
	4a	145.0, C				
	5a	140.5, C				
	6	127.8, C				
	7	130.3, CH	7.35 (d, 7.8)			
	8	126.2, CH	7.60 (d, 7.8)			
	9	132.1, C				
	9a	129.1, C				
	10a	145.9, C				
	11	167.4, C				
	12	7.8, CH_3	2.24 (s)			
	13	15.1, CH_3	2.55 (s)			
	14	172.7, C				

[a] *Thr, Threonine; Val, Valine; Pro, Proline; Sar, Sarcosine.*

2×10^4 CFU/mL. The 96-well plates were incubated in a wet box at 28°C for 4–7 days. Itraconazole, *A. fumigatus* AF293 suspension without drugs and the fresh-prepared RPMI 1640 medium were used as the positive control, growth control, and the negative control, respectively. Each experiment was set in three parallels. The MIC was the lowest drug concentration at which no fungal growth was observed compared to the growth control.

TABLE 3 | ^{1}H (500 MHz) and ^{13}C (125 MHz) NMR Date of Act-D (**3**) in $CDCl_3$[a].

	Ring-A			Ring-B		
	Position	**δ_C, type**	**δ_H (*J* in Hz)**	**Position**	**δ_C, type**	**δ_H (*J* in Hz)**
Thr	1	169.0, C		1	168.5, C	
	2	55.4, CH	4.60 (d, 5.1)	2	55.0, CH	4.48 (d, 5.2)
	3	75.2, CH	5.20 (d, 5.1)	3	75.1, CH	5.16 (d, 5.6)
	4	17.5, CH_3	1.26 (s)	4	18.0, CH_3	1.26 (s)
	NH		7.19 (d, 6.4)	NH		7.81 (d, 5.8)
Val	1	173.8, C		1	173.5, C	
	2	59.0 CH	3.54 (m)	2	58.8, CH	3.55 (m)
	3	31.9, CH	2.16 (m)	3	31.6, CH	2.08 (m)
	4	19.4, CH_3	1.12 (d, 5.7)	4	19.2, CH_3	1.12 (d, 5.7)
	5	19.2, CH_3	0.9 (d, 6.7)	5	19.1, CH_3	0.89 (d, 6.7)
	NH		8.09 (d, 5.3)	NH		7.94 (d, 5.7)
Pro	1	173.4 C		1	173.4, C	
	2	56.4, CH	6.02 (d, 9.0)	2	56.3, CH	5.98 (d, 9.0)
	3	31.1, CH_2	1.88 (m), 2.67 (m)	3	31.4, CH_2	1.87 (m), 2.67 (m)
	4	23.1, CH	2.17 (m), 2.25 (m)	4	23.0, CH_2	2.15 (m), 2.25 (m)
	5	47.7, CH_2	3.72 (m)	5	47.4, CH_2	3.82 (m)
Sar	1	166.4, C		1	166.1, C	
	2	51.5, CH_2	4.76 (d, 17.6), 3.61 (d, 17.6)	2	51.5, CH_2	4.70 (d, 17.4), 3.64 (d, 17.5)
MeVal	NMe	35.0, CH_3	2.88 (s)	NMe	35.0, CH_3	2.88 (s)
	1	167.8, C		1	167.7, C	
	2	71.6, CH	2.67 (m)	2	71.4, CH	2.67 (m)
	3	27.0, CH	2.67 (m)	3	27.0, CH	2.67 (m)
	4	21.8, CH_3	0.96 (d, 7.4)	4	21.7, CH_3	0.95 (d, 6.6)
	5	19.4, CH_3	0.75 (s)	5	19.2, CH_3	0.75 (s)
	NMe	39.4, CH_3	2.90 (s)	NMe	39.3, CH_3	2.94 (s)
chromophore	1	101.8, C				
	2	147.8, C				
	3	179.2, C				
	4	113.6, C				
	4a	145.2, C				
	5a	140.6, C				
	6	127.7, C				
	7	130.4, CH	7.37 (d, 7.7)			
	8	126.0, CH	7.64 (d, 7.7)			
	9	132.7, C				
	9a	129.2, C				
	10a	146.0, C				
	11	169.0, C				
	12	7.9, CH_3	2.25 (s)			
	13	15.2, CH_3	2.56 (s)			
	14	166.6.0, C				

[a] *Thr, Threonine; Val, Valine; Pro, Proline; Sar, Sarcosine.*

RESULTS

Identification of Strain WH1

The observed morphological features of strain WH1 showed that it produced extensively branched hyphae bearing long spore chains with smooth surfaces (Figure S1). The cell walls of the strain WH1 contained LL-DAP as the characteristic amino acid of the peptidoglycan and its whole-organism sugar patter have glucose, galactose, and mannose as the characteristic sugars. These characters indicated that WH1 belongs to genus Streptomyces. The taxonomic position of WH1 and its affiliation to genus Streptomyces was confirmed by the analysis of the

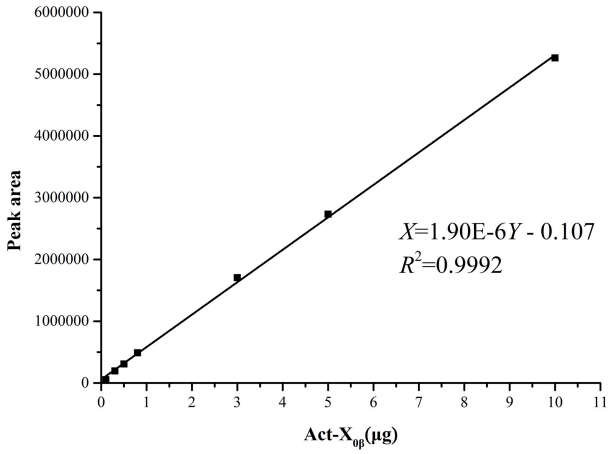


FIGURE 2 | Standard carve of Act-$X_{0\beta}$.

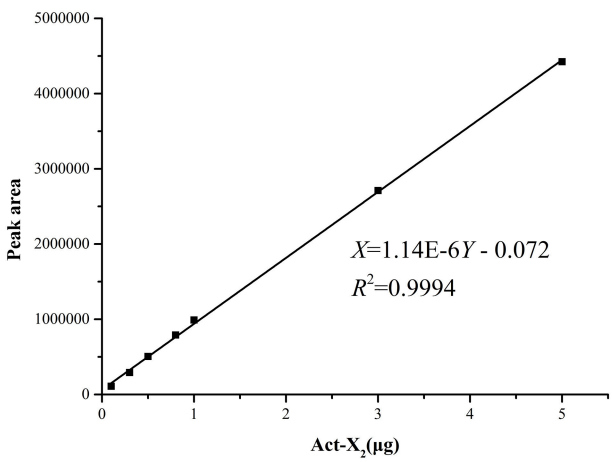


FIGURE 3 | Standard carve of Act-X_2.

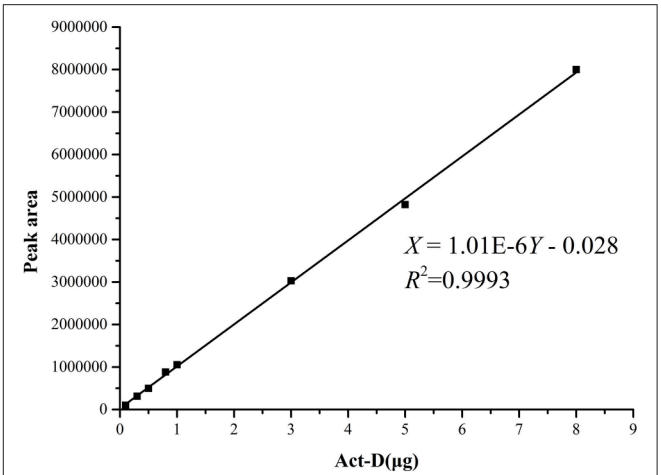


FIGURE 4 | Standard carve of Act-D.

16S rRNA gene sequence against the available validly published species. The sequence analysis using the EzTaxon-e server showed that strain WH1 had 100% similarity to *S. heliomycini* NCBR 15899(T). These results indicated that the strain WH1 under study is a strain of *S. heliomycini*.

The Identification of Acts $X_{0\beta}$, X_2, and D

HPLC analysis revealed that there were three peaks with the typical UV absorption of Acts at λ_{max} 203, 225, and 443 nm in the cultures of *S. heliomycini* WH1 (Wang et al., 2014) (Figure S3). Chemical investigations resulted in the isolation of the three Acts, compounds **1**–**3**, by VLC and semi-preparative HPLC. By means of specific rotation, MS and NMR data, their structures were identified. The ^{13}C NMR spectra of compounds **1**–**3** showed the characteristic skeleton resonances of Acts at δ 34–40 for N-CH_3 (× 4) and δ 165–175 for N-C=O (× 12), further indicating the nature of the Acts of compounds **1**–**3**. All the ^{13}C NMR spectra of compounds **1**–**3** showed 62 carbon signals (Figures S5, S8, S11) and the ESIMS of compounds **1**–**3** showed molecular peaks at *m/z* 1272.06 $[M+H]^+$ (Figure S6), 1270.03 $[M+H]^+$ (Figure S9), and 1256.05$[M+H]^+$ (Figure S12). Their molecular formulas were further determined as $C_{62}H_{86}O_{17}N_{12}$, $C_{62}H_{84}N_{12}O_{17}$, and $C_{62}H_{86}N_{12}O_{16}$ from the HRESIMS peaks at *m/z* 1271.6305$[M+H]^+$ (Figure S6), 1269.6155$[M+H]^+$ (Figure S9), and 1255.6365$[M+H]^+$ (Figure S12), respectively. The differences of ^{13}C NMR spectra of compounds **1**–**3** are that a methylene carbon signal (δ_C 23.0) in **3** is replaced by an oxygenated methine carbon signal (δ_C 70.0) in **1** and a carbonyl signal (δ_C208.8) in **2**, respectively. These data suggested that compounds **1**–**3** might be corresponding to Acts $X_{0\beta}$, X_2, and D. The consistence of NMR (Figures S4, S5, S7, S8, S10, S11, **Tables 1**–**3**) and $[\alpha]_D$ with those reported further supported Acts **1**–**3** were Act-$X_{0\beta}$ (**1**) (Lifferth et al., 1999), Act-X_2 (**2**) (Lifferth et al., 1999) and Act-D (**3**) (Wang et al., 2014), respectively (**Figure 1**).

The Standard Curves for Analysis of the Productions of Acts

The standard curves of Acts $X_{0\beta}$, X_2, and D were established by means of HPLC-UV. The liner regression equations for Acts$X_{0\beta}$, X_2, and D were respectively obtained as X = 1.90E–6Y – 0.107 (R^2 = 0.9992) (**Figure 2**), X = 1.14E–6Y – 0.072 (R^2 = 0.9994) (**Figure 3**), and X = 1.01E–6Y – 0.028 (R^2 = 0.9993) (**Figure 4**), where Y is the weight of Acts (μg) and X is the peak area. All curves showed good linear relationships that could be used to estimate the production of the Acts from the corresponding HPLC peaks' areas.

The Effects of pH, salinity, and Media on Productivity of Acts from *S. heliomycini* WH1

The effect of the initial pH values on the production was studied in the MM liquid medium with 3% salinity (natural seawater), whose initial pH was increased to 9.0 from 4.5 at an interval of

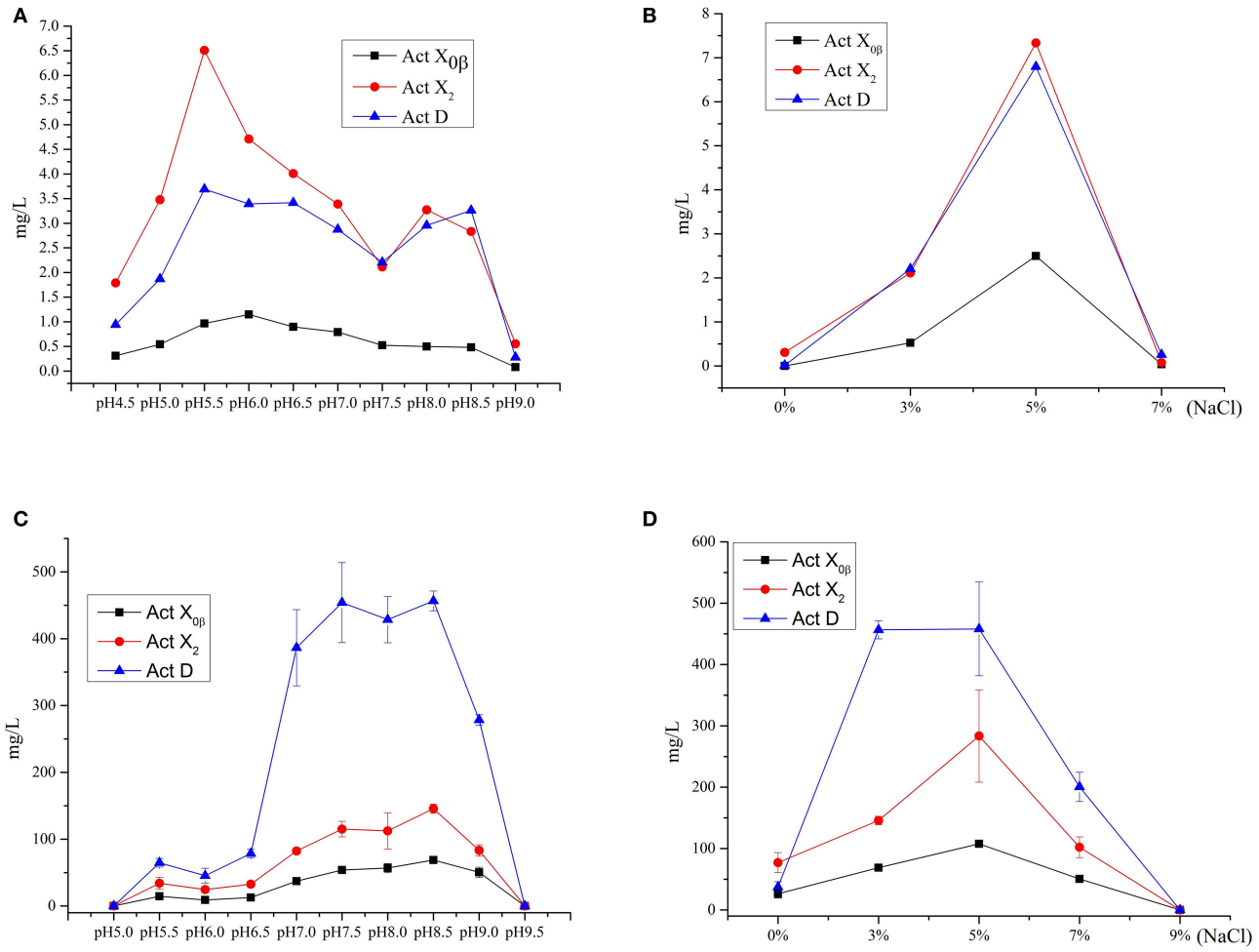


FIGURE 5 | The effect of the initial pH values and salinity on the productions of Acts $X_{0\beta}$, X_2 and D. **(A)** The effect of the initial pH values on the productions of Acts $X_{0\beta}$, X_2 and D in the liquid medium MM. **(B)** The effect of the salinity on the productions of Acts $X_{0\beta}$, X_2 and D in the liquid medium MM. **(C)** The effect of the initial pH values on the productions of Acts $X_{0\beta}$, X_2 and D in the liquid medium MII. **(D)** The effect of the salinity on the productions of Acts $X_{0\beta}$, X_2 and D in the liquid medium MII.

TABLE 4 | The productions of Acts $X_{0\beta}$, X_2, and D in different media (mg/L).

Medium	Act-$X_{0\beta}$	Act-X_2	Act-D
MM	0.7 ± 0.02	2.5 ± 0.2	4.4 ± 0.2
MI	36.0 ± 3.4	34.2 ± 3.5	173.4 ± 20.5
MII	56.8 ± 6.8	112.4 ± 27.2	428.5 ± 34.5
MIII	38.7 ± 1.7	90.7 ± 14.1	162.0 ± 10.3
MIV	53.8 ± 5.4	219.7 ± 23.8	269.7 ± 40.3
Soybean meal	61.5 ± 15.7	121.6 ± 32.0	330.8 ± 64.2

0.5. The results (**Figure 5A**, Table S1) showed that the production of Acts $X_{0\beta}$, X_2, and D reached the highest at pH 6.0, 5.5, and 5.5 in the MM medium, whose yields were 1.2, 6.5 and 3.7 mg/L, respectively. This indicated that 5.5 is the most suitable initial pH value for producing both Acts D and X_2 in MM medium, and is also suitable for producing Act-$X_{0\beta}$ that was 1.0 mg/L only after the production at pH 6.0. The reason is that all the components in the MM liquid medium were completely dissolved at pH 5.5. Only under this pH value, the MM liquid medium is clear and transparent that is easy to be used by microorganisms.

The effect of the salinity on the Acts production was studied in the MM liquid medium at pH 5.5. The salinity of the medium was designed as 0, 3, 5, and 7%, respectively. The results (**Figure 5B**, Table S2) showed that the highest production of Acts $X_{0\beta}$, X_2, and D was under 5% salinity with the yields of 2.5, 7.3, and 6.8 mg/L, respectively, while the corresponding production under 3% salinity was 0.5, 2.1, and 2.2 mg/L, respectively. However, the Acts fermentation titers under these conditions in MM liquid medium are too low to be satisfactory. Therefore, the other media were adopted to improve the productions of the Acts.

The study on the productivity of Acts in the soybean meal and MI–MIV liquid media (**Table 4**) showed that the highest production of all the Acts $X_{0\beta}$, X_2, and D was in the MII liquid medium with the yields of 56.8 ± 6.8, 112.4 ± 27.2,

and 428.5 ± 34.5 mg/L, respectively. The results indicated that the soybean meal supplemented with the minor elements Mg, K, P, and S, that is MII liquid medium, is favorable for the production performance of actinomycins by strain *S. heliomycini* WH1. Therefore, the productivity of Acts was further optimized in the liquid medium MII by investigating the effects of pH values and salinity. The results showed that initial pH 8.5 was the most suitable pH value for production of all the Acts $X_{0\beta}$, X_2, and D in the medium MII with the yields of 68.8 ± 1.2, 145.7 ± 6.8, and 456.5 ± 14.7 mg/L (**Figure 5C**, Table S3) at 3% salinity, respectively. On the basis of initial pH 8.5, the highest productivity of all the Acts $X_{0\beta}$, X_2, and D was obtained in the liquid medium MII with 5% salinity which reached to 107.6 ± 4.2, 283.4 ± 75.3, and 458.0 ± 76.3 mg/L (**Figure 5D**, Table S4), respectively.

The Bioactivities of Acts from *S. heliomycini* WH1

The cytotoxicities of Acts $X_{0\beta}$, X_2, and D on the A549, MCF-7, and K562 and L02 cell lines were examined. The results indicated that all the three Acts exhibited strong cytotoxicities on the three tumor cell lines and the one normal cell line with the IC_{50} and CC_{50} values of 0.8–157.4 nM (**Table 5**). Among them, Act-X_2 displayed the strongest activities on the three human tumor cell lines, A549, MCF-7 and K562, and the lowest toxicity on the human normal embryo liver L02 cell line. Thus, Act-X_2 showed the highest selective index (SI) for the three tested tumor cell lines (10.3, 12.2, and 5.2, respectively), indicating a potential of Act-X_2 as a drug candidate for treatment of human cancers. As far as we known, there were no reports on the cytotoxicity of Acts $X_{0\beta}$ and X_2 on the A549, MCF-7 and K562 tumor cells.

The antimicrobial activities against the human and aquatic pathogenic microbes, *A. hydrophila*, *B. subtilis*, *B. cereus*, *E. coli*, *P. aeruginosa*, *S. aureus*, MRSA, *V. vulnificus*, *V. alginolyticus*, *V. parahaemolyticus*, *V. splendidus*, *C. albicans*, *C. glabrata*, *A. fumigatus* AF293, and were evaluated. The results indicated that both Act-X_2 and Act-D showed comparable or stronger antimicrobial activities against *S. aureus*, MRSA, *B. subtilis,* and *B. cereus* to ciprofloxacin hydrochloride (a positive control, MIC 0.1–12.5 μM) with MIC values of 0.04–0.15 μM (**Table 6**), while Act-$X_{0\beta}$ displayed very weak inhibitions on *S. aureus* and *B. subtilis* (MIC 0.3–2.5 μM). All the three Acts were not active against the tested pathogenic fungi and other bacteria at the concentration of 1 mg/mL. Except for the antibacterial activities of Act-X_2 on the *S. aureus* and *B. cereus* (Xiong et al., 2008) and Act-D on the *S. aureus* (Bian et al., 2003), there were no other reports on the antibacterial activities of Acts D, X_2 and $X_{0\beta}$ against MRSA and *B. subtilis*, the Act-$X_{0\beta}$ against *S. aureus* and *B. cereus*, as well as the Act-D against *B. cereus*. And the Acts D and X_2 were more active. These results revealed the potential use of Act-X_2 and Act-D in the treatment of infectious diseases caused by *S. aureus*, *B. subtilis,* and *B. cereus*, especially by MRSA.

DISCUSSION

Actinomycins were firstly reported in 1940 from *Actinomyces antibioticus* (Waksman and Woodruff, 1940). Since then, more than 30 actinomycins have been discovered from the natural sources including Acts A_I (B_I, X_I), A_{II}, A_{IV} (B_{IV}, D, X_{IV}), A_V (B_V, X_V), and Acts C_1–C_3 (Roussos and Vining, 1956), Acts E_1, E_2, and F_1–F_4 (Brockmann, 1961), Acts G_1–G_6 (Lackner et al., 2000a; Bitzer et al., 2006), $X_{0\alpha}$–$X_{0\delta}$ (Brockmann, 1961), Acts Y_1–Y_5 (Bitzer et al., 2009), and Acts Y_6–Y_9 (Cai et al., 2016), Acts Z_1–Z_5 (Lackner et al., 2000b), and Act Z_p(Cai et al., 2016). To date, there are many *Streptomyces* species capable of producing actinomycins, but few of them were reported to produce relatively large quantities of one or two major actinomycins. *Streptomyces parvulus* (Foster and Katz, 1981), *S. halstedii*, *S. anulatus* (Praveen et al., 2008a), *S. sindenensis* (Praveen et al., 2008b), and *S. griseoruber* (Praveen and Tripathi, 2009) are examples to produce Act D, among which the highest production is 620 mg/L (Praveen et al., 2008a). *Streptomyces nasri* YG62 (Elnaggar et al., 1998) and *S. triostinicus* (Singh et al., 2009) are examples to produce Act X_2 whose production reached to 443 mg/L (Singh et al., 2009). *Streptomyces* sp. MITKK-103 (Kurosawa et al., 2006), *Streptomyces* sp. JAU4234 (Xiong et al., 2008) and *Streptomyces* sp. MS449 (Chen et al., 2012) can simultaneously produce Acts D, $X_{0\beta}$ and X_2 and strain MS449 produced the highest production of Acts D and X_2 with the yields of 1,770 and 1,920 mg/L, respectively. No examples were

TABLE 6 | The MIC values (μM) of Acts $X_{0\beta}$, X_2, and D on the pathogenic bacteria.

Bacteria	Act-$X_{0\beta}$	Act-X_2	Act-D	Ciprofloxacin hydrochloride
S. aureus	0.31	0.15	0.31	0.53
MRSA	2.48	0.15	0.31	12.48
B. subtilis	0.31	0.08	0.04	0.13
B. cereus	1.23	0.04	0.08	8.50

TABLE 5 | The cytotoxicity and selective index (SI) of Acts $X_{0\beta}$, X_2, and D.

Cell lines	Act-$X_{0\beta}$		Act-X_2		Act-D		Adriamycin	
	IC_{50} (nM)	SI	IC_{50} (nM)	SI	IC_{50} (nM)	SI	IC_{50} (nM)	SI
A549	63.8 ± 2.9	2.5 ± 0.3	0.9 ± 0.1	10.4 ± 1.9	3.4 ± 0.1	3.9 ± 0.3	1,300	0.3
MCF-7	85.2 ± 12.2	1.9 ± 0.4	0.8 ± 0.1	12.2 ± 1.8	2.6 ± 0.1	4.9 ± 0.4	1,000	0.4
K562	128.3 ± 6.1	1.2 ± 0.2	1.8 ± 0.1	5.2 ± 0.5	3.3 ± 0.3	4.0 ± 0.5	300	1.3
L02 (CC_{50})	157.4 ± 14.7		9.3 ± 0.7		13.0 ± 0.5		400	

found to produce Act $X_{0\beta}$ solely. This study identified Acts $X_{0\beta}$, X_2, and D by comparison of ^{13}C NMR data to those reported ones (Lifferth et al., 1999; Wang et al., 2014) with the errors less than 0.5 ppm. And the productions of Acts D, $X_{0\beta}$, and X_2 by the marine-derived *S. heliomycini* WH1 in the optimized fermentation conditions were significantly improved by 100, 110, and 150 folds, respectively, relative to those in the isolation medium (MM medium). Among these actinomycins, Act-D has been extensively studied and widely used in the treatment of malignant tumors, such as Wilms' tumor and childhood rhabdomyosarcoma (Womer, 1997). However, the cytotoxicity of Acts X_2 and $X_{0\beta}$ against the tumor cells and antibacterial activities of Acts D, X_2, and $X_{0\beta}$ against pathogenic bacteria were received very little attention. Compared to Act D, Act X_2 showed stronger cytotoxicity toward HL-60 cells (Kurosawa et al., 2006) and better antibacterial activity against MTB H37Rv (Chen et al., 2012) and *S. aureus* and *B. cereus* (Xiong et al., 2008). Our investigation firstly demonstrated that Act-X_2 displayed the strongest activities against MCF-7, A549, and K562 human tumor cell lines, and the lowest toxicity on L02 human normal embryo liver cell line, indicating the potential use of Act-X_2 as a cancer drug candidate. In addition, our fresh results on the strong antibacterial activity of Acts D and X_2 against MRSA and *B. subtilis* along with Act-D against *B. cereus* indicated the potential use of Act-D and Act-X_2 in the treatment of the infections caused by those human and aquatic pathogenic bacteria, especially by MRSA. Therefore, the present study revealed that actinobacteria from newly-explored, special or extreme environments could be a potential pool for drug discovery.

AUTHOR CONTRIBUTIONS

The authors from China contribute to the isolation and identification of Acts, the optimization of fermentation conditions, as well as the assays of the cytotoxic and antimicrobial activities, and prepared the paper. The authors from Saudi Arabia are responsible for the isolation and identification of the marine-derived actinobacterial strain, *Streptomyces heliomycini* WH1.

ACKNOWLEDGMENTS

This work was supported by grants from the National Natural Science Foundation of China (No. 81561148012) and the National Plan for Science, Technology and Innovation (MAARIFAH), King Abdulaziz City for Science and Technology, Kingdom of Saudi Arabia, Award number (12-BIO2630-02).

SUPPLEMENTARY MATERIAL

The Supplementary Material for this article can be found online at: http://journal.frontiersin.org/article/10.3389/fmicb.2017.01147/full#supplementary-material

DATA SHEET

The colony and micrograph of *Streptomyces heliomycini* WH1 and the MS and NMR spectra of compounds **1**–**3**.

REFERENCES

Betzel, C., Rachev, R., Dolashka, P., and Genov, N. (1993). Actinomycins as proteinase inhibitors. *Biochim. Biophys. Acta* 1161, 47–51. doi: 10.1016/0167-4838(93)90194-V

Bian, Z.-L., Xiong, P.-Y., and Shen, D.-S. (2003). Determination of bactericidal effect of six antitumor antibiotics on five antibiotic-resistant bacteria. *Pharm. Care Res.* 3, 253–255. doi: 10.3969/j.issn.1671-2838.2003.04.014

Bister, B., Bischoff, D., Strobele, M., Riedlinger, J., Reicke, A., Wolter, F., et al. (2004). Abyssomicin C–a polycyclic antibiotic from a marine *Verrucosispora* strain as an inhibitor of the *p*-aminobenzoic acid/tetrahydrofolate biosynthesis pathway. *Angew. Chem. Int. Ed Engl.* 43, 2574–2576. doi: 10.1002/anie.200353160

Bitzer, J., Gesheva, V., and Zeeck, A. (2006). Actinomycins with altered threonine units in the β-peptidolactone. *J. Nat. Prod.* 69, 1153–1157. doi: 10.1021/np060063g

Bitzer, J., Streibel, M., Langer, H., and Grond, S. (2009). First Y-type actinomycins from *Streptomyces* with divergent structure-activity relationships for antibacterial and cytotoxic properties. *Org. Biomol. Chem.* 7, 444–450. doi: 10.1039/B815689A

Brockmann, H. (1961). Chemistry of the actinomycins. *Pure Appl. Chem.* 2, 405–424. doi: 10.1351/pac196102030405

Bull, A. T., and Stach, J. E. M. (2007). Marine actinobacteria: new opportunities for natural product search and discovery. *Trends Microbiol.* 15, 491–499. doi: 10.1016/j.tim.2007.10.004

Cai, W., Wang, X., Elshahawi, S. I., Ponomareva, L. V., Liu, X., McErlean, M. R., et al. (2016). Antibacterial and cytotoxic actinomycins Y_6–Y_9 and Z_p from *Streptomyces* sp. Strain Gö-GS12. *J. Nat. Prod.* 79, 2731–2739. doi: 10.1021/acs.jnatprod.6b00742

Chen Chiao, Y. C., Gurudath Rao, K., Hook, J. W. III, Krugh, T. R., and Sengupta, S. K. (1979). 7-Amino-actinomycin D complexes with deoxynucleotides as model for binding of the drug to DNA. *Biopolymers* 18, 1749–1762. doi: 10.1002/bip.1979.360180712

Chen, C., Song, F., Wang, Q., Abdel-Mageed, W. M., Guo, H., Fu, C., et al. (2012). A marine-derived *Streptomyces* sp. MS449 produces high yield of actinomycin X_2 and actinomycin D with potent anti-tuberculosis activity. *Appl. Microbiol. Biot.* 95, 919–927. doi: 10.1007/s00253-012-4079-z

Elnaggar, M. Y. M., Elaassar, S. A., Hashem, M. A., Stoodley, R. J., Raynor, C. M., and Sigee, D. C. (1998). Production of actinomycin X_2 by immobilized *Streptomyces nasri* YG62 mycelia. *Microbios* 95, 165–179.

Foster, J. W., and Katz, E. (1981). Control of actinomycin D biosynthesis in *Streptomyces parvulus*: regulation of tryptophan oxygenase activity. *J. Bacteriol.* 148, 670–677.

Fu, P., Kong, F., Li, X., Wang, Y., and Zhu, W. (2014). Cyanogramide with a new spiro[indolinone-pyrroloimidazole] skeleton from *Actinoalloteichus cyanogriseus*. *Org. Lett.* 16, 3708–3711. doi: 10.1021/ol501523d

Fu, P., Kong, F., Wang, Y., Wang, Y., Liu, P., Zuo, G., et al. (2013). Antibiotic metabolites from the coral-associated actinomycete *Streptomyces* sp. OUCMDZ-1703. *Chinese J. Chem.* 31, 100–104. doi: 10.1002/cjoc.201201062

Fu, P., Liu, P., Li, X., Wang, Y., Wang, S., Hong, K., et al. (2011). Cyclic bipyridine glycosides from the marine-derived actinomycete *Actinoalloteichus cyanogriseus* WH1-2216-6. *Org. Lett.* 13, 5948–5951. doi: 10.1021/ol202245s

Fu, P., Zhuang, Y., Wang, Y., Liu, P., Qi, X., Gu, K., et al. (2012). New indolocarbazoles from a mutant strain of the marine-derived actinomycete *Streptomyces fradiae* 007M135. *Org. Lett.* 14, 6194–6197. doi: 10.1021/ol302940y

Hasegawa, T., Takizawa, M., and Tanida, S. (1983). A rapid analysis for chemical grouping of aerobic actinomycetes. *J. Gen. Appl. Microbiol.* 29, 319–322. doi: 10.2323/jgam.29.319

Hozzein, W. N., Ali, M. I. A., and Rabei, W. (2008). A new preferential medium for enumeration and isolation of desert actinomycetes. *World J. Microbiol. Biotechnol.* 24, 1547–1552. doi: 10.1007/s11274-007-9641-y

Hozzein, W. N., and Goodfellow, M. (2007). Nonomuraea aegyptia sp. nov., a novel actinomycete isolated from a sand dune. *Antonie van Leeuwenhoek* 92, 165–171. doi: 10.1007/s10482-007-9145-7

Kapp, L. N., and Okada, S. (1972). Actinomycin D induction of acid phosphatase in synchronized L5178Y mouse leukemia cells. *Exp. Cell Res.* 72, 473–479. doi: 10.1016/0014-4827(72)90016-X

Killewich, L., Schutz, G., and Feigelson, P. (1975). Functional level of rat liver tryptophan 2,3-dixoygenase messenger RNA during superinduction of enzyme with actinomycin D. *Proc. Natl. Acad. Sci. U.S.A.* 72, 4285–4287. doi: 10.1073/pnas.72.11.4285

Kim, O. S., Cho, Y. J., Lee, K., Yoon, S. H., Kim, M., Na, H., et al. (2012). Introducing EzTaxon-e: a prokaryotic 16S rRNA gene sequence database with phylotypes that represent uncultured species. *Int. J. Syst. Evol. Microbiol.* 62, 716–721. doi: 10.1099/ijs.0.038075-0

Koba, M., and Konopa, J. (2005). Actinomycin D and its mechanisms of action. *Postepy Hig. Med. Dosw.* 59, 290–298. Available online at: http://www.phmd.pl/fulltxt.php?ICID=16586

Kurosawa, K., Bui, V. P., Van Essendelft, J. L., Willis, L. B., Lessard, P. A., Ghiviriga, I., et al. (2006). Characterization of *Streptomyces* MITKK-103, a newly isolated actinomycin X_2-producer. *Appl. Microbiol. Biot.* 72, 145–154. doi: 10.1007/s00253-005-0240-2

Lackner, H., Bahner, I., Shigematsu, N., Pannell, L. K., and Mauger, A. B. (2000b). Structures of five components of the actinomycin Z complex from *Streptomyces fradiae*, two of which contain 4-chlorothreonine. *J. Nat. Prod.* 63, 352–356. doi: 10.1021/np990416u

Lackner, H., Hulsmann, H., Heinze, S., Simon, H., Bar, H., Zimmer, C., et al. (2000a). A new actinomycin-type chromopeptide from *Streptomyces* sp. HKI-0155. *J. Antibiot.* 53, 84–87. doi: 10.7164/antibiotics.53.84

Lam, K. S. (2006). Discovery of novel metabolites from marine actinomycetes. *Curr. Opin. Microbiol.* 9, 245–251. doi: 10.1016/j.mib.2006.03.004

Lifferth, A., Bahner, I., Lackner, H., and Schäfer, M. (1999). Synthesis and structure of proline ring modified actinomycins of the X-type. *Z. Naturforsch. B* 54, 681–691. doi: 10.1515/znb-1999-0518

Mincer, T. J., Gensen, P. R., Kauffman, C. A., and Fenical, W. (2002). Widespread and persistent populations of a major new marine actinomycete taxon in ocean sediments. *Appl. Environ. Microbiol.* 68, 5005–5011. doi: 10.1128/AEM.68.10.5005-5011.2002

Mosmann, T. (1983). Rapid colorimetric assay for cellular growth and survival: application to proliferation and cytotoxicity assays. *J. Immunol. Methods* 65, 55–63. doi: 10.1016/0022-1759(83)90303-4

Newman, D. J., Cragg, G. M., and Snader, K. M. (2003). Natural products as sources of new drugs over the period 1981−2002. *J. Nat. Prod.* 66, 1022–1037. doi: 10.1021/np030096l

Praveen, V., and Tripathi, C. K. M. (2009). Studies on the production of actinomycins D by *Streptomyces griseoruber*—a novel source. *Lett. Appl. Microbiol.* 49, 450–455. doi: 10.1111/j.1472-765X.2009.02689.x

Praveen, V., Tripathi, C. K. M., and Bihari, V. (2008a). Studies on optimum fermentation conditions for actinomycin D production by two new strains of *Streptomyces* spp. *Med. Chem. Res.* 17, 114–112. doi: 10.1007/s00044-007-9042-7

Praveen, V., Tripathi, C. K. M., Bihari, V., and Srivastava, S. C. (2008b). Production of actinomycins D by a new isolate, *Streptomyces sindenensis*. *Ann. Microbiol.* 58, 109–114. doi: 10.1007/BF03179453

Rill, R. L., and Hecker, K. H. (1996). Sequence-specific actinomycins D binding to single-stranded DNA inhibits HIV reverse transcriptase and other polymerases. *Biochemistry* 35, 3525–3533. doi: 10.1021/bi9530797

Roussos, G., and Vining, C. (1956). Isolation and properties of pure actinomycins. *J. Chem. Soc.* 2, 2469–2474. doi: 10.1039/jr9560002469

Saijets, S., Ylipaasto, P., Vaarala, O., Hovi, T., and Roivainen, M. (2003). Enterovirus infection and activation of human umbilical vein endothelial cells. *J. Med. Virol.* 70, 430–439. doi: 10.1002/jmv.10413

Shirling, E. B., and Gottlieb, D. (1966). Methods for characterization of *Streptomyces* species. *Int. J. Syst. Bacteriol.* 16, 313–340. doi: 10.1099/00207713-16-3-313

Singh, V., Khan, M., Khan, S. A., and Tripathi, C. K. M. (2009). Optimization of actinomycin V production by *Streptomyces triostinicus* using artificial neural network and genetic algorithm. *Appl. Microbiol. Biotechnol.* 82, 379–385. doi: 10.1007/s00253-008-1828-0

Staneck, J. L., and Roberts, G. D. (1974). Simplified approach to identification of aerobic actinomycetes by thin-layer chromatography. *Appl. Microbiol.* 28, 226–231.

Tiwari, K., Upadhyay, D. J., Mösker, E., Süssmuth, R., and Gupta, R. K. (2015). Culturable bioactive actinomycetes from the Great Indian Thar Desert. *Ann. Microbiol.* 65, 1901–1914. doi: 10.1007/s13213-014-1028-3

Tominaga, H., Ishiyama, M., Ohseto, F., Sasamoto, K., Hamamoto, T., Suzuki, K., et al. (1999). A water-soluble tetrazolium salt useful for colorimetric cell viability assay. *Anal. Commun.* 36, 47–50. doi: 10.1039/a809656b

Waksman, S. A., and Woodruff, H. B. (1940). Bacteriostatic and bactericidal substances produced by a soil actinomyces. *Exp. Biol. Med.* 45, 609–614. doi: 10.3181/00379727-45-11768

Wang, C., Liu, P.-P., Wang, Y., Sun, K.-L., Jia, H.-J., and Zhu, W.-M. (2014). Optimization of fermentation conditions for production of actinomycin D by marine-derived *Strptomyces parvulus* OUCMDZ-2554. *Chinese J. Mar. Drugs* 33, 34–42. doi: 10.13400/j.cnki.cjmd.2014.03.006

Wang, Z., Fu, P., Liu, P., Wang, P., Hou, J., Li, W., et al. (2013). New pyran-2-ones from alkalophilic actinomycete, *Nocardiopsis alkaliphila* sp. Nov. YIM-80379. *Chem. Biodivers.* 10, 281–287. doi: 10.1002/cbdv.201200086

Womer, B. R. (1997). Soft tissue sarcomas. *Eur. J. Cancer* 33, 2230–2236. doi: 10.1016/S0959-8049(97)00334-1

Xiong, Z., Tu, X., and Tu, G. (2008). Optimization of medium composition for actinomycin X_2 production by *Streptomyces* spp JAU4234 using response surface methodology. *J. Ind. Microbiol. Biotechnol.* 35, 729–734. doi: 10.1007/s10295-008-0339-4

Conflict of Interest Statement: The authors declare that the research was conducted in the absence of any commercial or financial relationships that could be construed as a potential conflict of interest.

Copyright © 2017 Wang, Wang, Gui, Liu, Khalaf, Elsayed, Wadaan, Hozzein and Zhu. This is an open-access article distributed under the terms of the Creative Commons Attribution License (CC BY). The use, distribution or reproduction in other forums is permitted, provided the original author(s) or licensor are credited and that the original publication in this journal is cited, in accordance with accepted academic practice. No use, distribution or reproduction is permitted which does not comply with these terms.

frontiers in Microbiology

ORIGINAL RESEARCH
published: 11 July 2017
doi: 10.3389/fmicb.2017.01284

Dual Induction of New Microbial Secondary Metabolites by Fungal Bacterial Co-cultivation

*Jennifer Wakefield[1], Hossam M. Hassan[2], Marcel Jaspars[1], Rainer Ebel[1] and Mostafa E. Rateb[3]**

[1] Marine Biodiscovery Centre, Department of Chemistry, University of Aberdeen, Aberdeen, United Kingdom, [2] Pharmacognosy Department, Faculty of Pharmacy, Beni-Suef University, Beni Suef, Egypt, [3] School of Science and Sport, University of the West of Scotland, Paisley, United Kingdom

The frequent re-isolation of known compounds is one of the major challenges in drug discovery. Many biosynthetic genes are not expressed under standard culture conditions, thus limiting the chemical diversity of microbial compounds that can be obtained through fermentation. On the other hand, the competition during co-cultivation of two or more different microorganisms in most cases leads to an enhanced production of constitutively present compounds or an accumulation of cryptic compounds that are not detected in axenic cultures of the producing strain under different fermentation conditions. Herein, we report the dual induction of newly detected bacterial and fungal metabolites by the co-cultivation of the marine-derived fungal isolate *Aspergillus fumigatus* MR2012 and two hyper-arid desert bacterial isolates *Streptomyces leeuwenhoekii* strain C34 and strain C58. Co-cultivation of the fungal isolate MR2012 with the bacterial strain C34 led to the production of luteoride D, a new luteoride derivative and pseurotin G, a new pseurotin derivative in addition to the production of terezine D and 11-*O*-methylpseurotin A which were not traced before from this fungal strain under different fermentation conditions. In addition to the previously detected metabolites in strain C34, the lasso peptide chaxapeptin was isolated under co-culture conditions. The gene cluster for the latter compound had been identified through genome scanning, but it had never been detected before in the axenic culture of strain C34. Furthermore, when the fungus MR2012 was co-cultivated with the bacterial strain C58, the main producer of chaxapeptin, the titre of this metabolite was doubled, while additionally the bacterial metabolite pentalenic acid was detected and isolated for the first time from this strain, whereas the major fungal metabolites that were produced under axenic culture were suppressed. Finally, fermentation of the MR2012 by itself led to the isolation of the new diketopiperazine metabolite named brevianamide X.

Keywords: microbial co-cultivation, *Aspergillus fumigatus*, *Streptomyces leeuwenhoekii*, pseurotin G, luteoride D, brevianamide X

OPEN ACCESS

Edited by:
Peter Neubauer, Technische Universität Berlin, Germany

Reviewed by:
Giovanna Cristina Varese, University of Turin, Italy
Tabea Schuetze, Technische Universität Berlin, Germany

****Correspondence:***
Mostafa E. Rateb
mostafa.rateb@uws.ac.uk

Specialty section:
This article was submitted to Microbiotechnology, Ecotoxicology and Bioremediation, a section of the journal Frontiers in Microbiology

Received: *08 March 2017*
Accepted: *27 June 2017*
Published: *11 July 2017*

Citation:
Wakefield J, Hassan HM, Jaspars M, Ebel R and Rateb ME (2017) Dual Induction of New Microbial Secondary Metabolites by Fungal Bacterial Co-cultivation. Front. Microbiol. 8:1284. doi: 10.3389/fmicb.2017.01284

INTRODUCTION

Natural products are considered as specialized metabolites that often appear to play no part in the primary metabolism of the producing organism but instead are thought to confer an evolutionary advantage under specific environmental conditions (Challis and Hopwood, 2003). They occupy a diverse chemical structural space that is unmatched by synthetic compounds and remain an

eminent source for new drug leads. Of the 1562 new chemical entities (NCEs) which were approved by the FDA covering all diseases/sources in the time frame spanning January 1981 until December 2014, about 60% are natural products, their analogs, or mimics (Newman and Cragg, 2016). Additionally, there is a significant number of natural product or natural product-derived drugs currently in development pipeline. For example, between 2008 and 2013, approximately 100 drug candidates based on natural products were in various phases of clinical trials, or in the final stage of registration (Butler et al., 2014).

Microorganisms of both terrestrial and marine origin have a long track record as important sources of novel bioactive natural products. However, the frequent re-isolation of known compounds is one of the major challenges in the process of the discovery of new natural products. Recent advances in microbial genomics have unequivocally demonstrated that the biosynthetic potential of microbes for producing natural products is much higher than currently appreciated (Harvey et al., 2015), but it is commonly believed that a significant number of microbial gene clusters may be silent under standard laboratory fermentation conditions.

In the last decade, several methods have been developed to eventually activate these cryptic biosynthetic pathways and hence, to elicit the production of hitherto unexpressed chemical diversity. Genetic engineering (Bergmann et al., 2007), epigenetic modifiers (Nützmann et al., 2011), and the OSMAC approach (Bode et al., 2002) are currently the most commonly applied strategies to increase chemical diversity in microorganisms through manipulation or activation of biosynthetic genes (Hertweck, 2009; Luo et al., 2013; Bertrand et al., 2014). In addition to this, microbial co-cultivation (also called mixed fermentation), involving the cultivation of two or more microorganisms in the same confined environment, has also successfully been used for the induction of the expression of otherwise cryptic pathways, leading to the production of new microbial natural products. Co-cultivation can be considered an experimental imitation of the competition within natural microbe communities at a laboratory scale which could encourage the production of secondary metabolites, for example *via* signaling molecules (auto-regulator/quorum sensing molecules, siderophores, etc.) in their environment (Bertrand et al., 2014; Marmann et al., 2014). Alternative interpretations suggest that this effect could be related to the production of enzymes that activate the metabolite precursor produced by the producer strain, yielding the active metabolite, or that the inducer strain may induce epigenetic modifications in the producer strain (Abdelmohsen et al., 2015). Even though the precise mechanism behind these microbial interactions may thus not be clear, the advantage of the co-cultivation methodology is that prior knowledge of the signaling mechanism is not required. However, it is worth noting that in many cases, direct contact was necessary between bacteria/fungi to observe such effects (Scherlach and Hertweck, 2009).

There are a number of recent studies which have demonstrated that co-cultivation is a remarkably successful approach for the discovery of new bioactive natural products (Onaka et al., 2011; Rateb et al., 2013; Dashti et al., 2014; Ebrahim et al., 2016), and an overview is provided by Marmann et al. (2014). Moreover, microbial co-cultivation has been shown to increase the titre of a specific metabolite in some cases, for example for the yew tree fungal endophyte *Paraconiothyrium*, responsible for production of the potent anticancer drug paclitaxel. The concentration of this alkaloid was raised to approximately eightfold when the producer strain was co-cultivated with other fungal community members such as the bark-derived fungi *Alternaria* sp. or *Phomopsis* sp. (Soliman and Raizada, 2013). Recently, our group has demonstrated the efficiency of the co-culture approach when investigating hyper-arid desert bacterial isolates (Rateb et al., 2013). In the course of that previous study, when screening a series of fungal isolates, we identified strains of *Aspergillus fumigatus* to be particularly responsive to the presence of other microbes. These results prompted us to investigate further isolates of the same fungal species from other habitats. In the present study, we report on the co-cultivation of the marine-derived fungal isolate *A. fumigatus* MR2012, and our findings indicate for the first time the dual induction of newly detected bacterial and fungal metabolites that were not traced previously.

MATERIALS AND METHODS

General Experimental Procedures

Optical rotations were recorded using a Perkin-Elmer 343 polarimeter. UV and IR spectra were measured on a Perkin-Elmer Lambda 25 UV-vis spectrometer and a Thermo Nicolet IR 100 FT-IR spectrometer, respectively. NMR data were acquired on a Varian VNMRS 600 MHz NMR spectrometer. High resolution mass spectrometric data were obtained using a Thermo LTQ Orbitrap coupled to an HPLC system (PDA detector, PDA autosampler, and pump). The following conditions were used: capillary voltage of 45 V, capillary temperature of 260°C, auxiliary gas flow rate of 10-20 arbitrary units, sheath gas flow rate of 40-50 arbitrary units, spray voltage of 4.5 kV, and mass range of 100-2000 amu (maximal resolution of 30000). For LC/MS, a C18 analytical HPLC column (5 μm, 4.6 mm × 150 mm) was used with a mobile phase of 0 to 100% MeOH over 30 min at a flow rate of 1 mL min^{-1}. A Biotage Flash system (Part No: SP1-XOB1) Charlottesville, WA, United States was used for initial fractionation. Preparative HPLC separations were conducted using a C18 column (5 μm, 100 Å, 10 mm × 250 mm), connected to a binary pump, and monitored using a photodiode array detector.

Microbial Strains

The marine fungal isolate MR2012 used in this study was isolated from a Red Sea sediment in Hurghada, Egypt in September 2011, and taxonomically identified on a molecular basis as *A. fumigatus* (El-Gendy and Rateb, 2015). The two bacterial isolates C34 and C58 were collected from the hyper-arid soil of Laguna de Chaxa, Salar de Atacama, Chile and identified as *Streptomyces*

leeuwenhoekii subspecies C34 and C58, respectively (Okoro et al., 2009).

Fermentation, Extraction, and Isolation

Three different media; ISP2 (Shirling and Gottlieb, 1966), GYE medium composed of (g/L) glucose 10, yeast extract 10, and F-medium (Tian et al., 2017) composed of (g/L) sucrose 100, glucose 10, casamino acids 0.1, yeast extract 5, MOPS (3-*N*-morpholinopropanesulfonic acid) 21, K_2SO_4 0.25 × 10^{-6}, $MgCl_2$ $6H_2O$ 1.0 × 10^{-6}, were used for small scale fermentation to screen for secondary metabolite production. The seed culture of each strain was prepared by inoculating 50 mL of liquid ISP2 medium with a single colony of the bacteria or a small piece (approximately 1 cm^2) of agar containing fungal mycelia, respectively, and incubating for 3 days at 30°C with shaking at 180 rpm. Then, 2.5 mL of the primary culture was used to inoculate 250 mL of each of the three media. To adjust fermentation parameters and ensure reproducibility of secondary metabolite production before commencing large scale cultivation, screening of secondary metabolite profiles was conducted using LC-HRESIMS and LC-UV (in duplicate). The growth of both bacterial and fungal mycelia in their axenic or co-cultures, respectively, was also checked microscopically at different time intervals during the fermentation process (data not shown).

For large scale production, the seed culture of each strain was prepared as described above. Then 200 mL primary seed culture of each of fungal and bacterial isolates were used to inoculate 4 L of ISP2 medium as production medium in duplicate. For co-culture experiments, inoculation of the primary fungal culture was started 2 days before bacterial inoculation. Then, incubation of the secondary culture was conducted for 8 days at 30°C with shaking at 180 rpm as before. At the end of the incubation period, 50 g/L Diaion HP-20 resin was added to the culture media and shaken for 6 h at 180 rpm, then cultures were centrifuged (3000 rpm for 20 min) where the residue composed of cell mass and resin were washed with distilled water twice and extracted with MeOH, and subjected to LC-HRESIMS analysis. This extract was fractionated successively with *n*-hexane (3 mL × 250 mL), CH_2Cl_2 (3 mL × 300 mL), and then EtOAc (3 mL × 250 mL). Each solvent fraction was evaporated *in vacuo* and subjected to LC-HRESIMS and ^{1}H NMR analysis, which revealed that the CH_2Cl_2 fraction was the one of interest for the fungal isolate and both fungal bacterial co-culture experiments. This CH_2Cl_2 fraction for each of the three fermentations was loaded on Flash Biotage using a FLASH 65i cartridge, solvent methanol/water 0–100%, flow rate 60 mL/min over 20 min and UV collection wavelengths 225 and 254 nm to produce six fractions. All of these fractions were monitored by LC-HRESIMS.

For the pure fungal isolate MR2012, fraction 3 was subjected to Sephadex LH-20 column using CH_2Cl_2:MeOH 1:1 as a mobile phase to obtain three subfractions A–C. Further purification of fraction B on Agilent HPLC system using semi-preparative Sunfire C18 column (250 mm × 10 mm, 5 μm) with CH_3CN:H_2O 40–80% over 30 min with a 2 mL/min flow led to the isolation of 0.9 mg of **1**.

For the fungal isolate MR2012/bacterial isolate C34 co-culture experiment, fraction 3 was directly subjected to HPLC using the same column with CH_3CN:H_2O 25–60% over 30 min and 2 mL/min flow which led to the isolation of 1.2 mg of **2**. Additionally, the injection of fraction 5 on HPLC using the same column with CH_3CN:H_2O 40–90% over 30 min and 2 mL/min flow led to the isolation of 0.8 mg of **3**.

Brevianamide X **1**: white amorphous; $[\alpha]^{25}_D$ −86.9 (*c* 0.18, MeOH); UV (MeOH) λ_{max}, nm (log ε) 225 (4.62), 278 (3.90), 285 (2.85), 295 (3.70); IR (KBr) ν_{max} (cm^{-1}) 3275, 1698, 1275, 1126; ^{1}H and ^{13}C NMR data were described in **Table 1**; HRESIMS: *m/z* 350.1470 $[M+Na]^+$ (calcd for $C_{18}H_{21}O_3N_3$, 350.1475).

Luteoride D **2**: white amorphous; $[\alpha]^{25}_D$ −36.3 (*c* 0.12, MeOH); UV (MeOH) λ_{max}, nm (log ε) 212 (4.12), 258 (3.83), 329 (3.64); IR (KBr) ν_{max} (cm^{-1}) 3315, 2950, 1720, 1432, 1340, 1215, 1135; ^{1}H and ^{13}C NMR data were described in **Table 1**; HRESIMS: *m/z* 315.1338 $[M+H]^+$ (calcd for $C_{17}H_{18}N_2O_4$, 315.1339).

Pseurotin G **3**: light yellow amorphous; $[\alpha]^{25}_D$ −11.3 (*c* 0.14, MeOH); UV (MeOH) λ_{max}, nm (log ε) 213 (3.62), 259 (4.12), 285 (3.74); IR (KBr) ν_{max} (cm^{-1}) 3242, 1712, 1681, 1605, 1124; ^{1}H and ^{13}C NMR data were described in **Table 1**;

TABLE 1 | Summary of ^{1}H (600 MHz) and ^{13}C (150 MHz) NMR spectroscopic data for brevianamide X **1** and luteoride D **2** in DMSO at 298 K.

	Brevianamide X 1		Luteoride D 2	
Atom	**δ_C,[1] mult.**	**δ_H, mult. (*J* in Hz)**	**δ_C,[1] mult.**	**δ_H, mult. (*J* in Hz)**
1				6.60 (d, 1.6)
2	127.9, CH	7.28 (s)	80.4, CH	5.03 (d, 1.7)
3	110.0, C		74.8, C	
4	128.2, C		132.3, C	
5	118.8, CH	7.61 (d, 8.1)	122.0, CH	7.02 (d, 7.8)
6	119.0, CH	7.06 (t, 7.9)	117.9, CH	6.63 (t, 7.6)
7	121.3, CH	7.15 (t, 8.1)	125.2, CH	7.31 (d, 7.8)
8	109.8, CH	7.50 (d, 8.2)	118.8, C	
9	135.9, C		147.0, C	
10	25.3, CH_2	3.24 (m), 3.08 (m)		
11	54.9, CH	4.33 (t, 4.9)	143.2, C	
12		7.86 (s)	29.9, CH_2	3.16 (d, 15.7), 2.79 (d, 15.7)
13	168.7, C		155.0, C	
14	58.1, CH	4.07 (t, 8.6)	124.6, CH	6.69 (d, 16.0)
15			129.9, CH	6.80 (d, 16.1)
16	165.2, C		142.4, C	
17	44.4, CH_2	3.40 (m), 3.27 (m)	116.4, CH_2	5.11 (br s), 5.01 (br s)
18	21.5, CH_2	1.70 (m), 1.65 (m)	18.5, CH_3	1.94 (s)
19	27.5, CH_2	2.00 (q), 1.41 (m)		
20	76.1, CH_2	5.46 (s)		
OMe	55.0, CH_3	3.14 (s)	52.6, CH_3	3.61 (s)

[1]*Extracted from HSQC and HMBC.*

HRESIMS: *m/z* 550.2177 $[M+H]^+$ (calcd for $C_{29}H_{31}O_8N_3$, 550.2184).

RESULTS

In our previous work on fungal-bacterial co-culture, it became evident that the addition of the bacterial isolate was the trigger to initiate the production of fungal secondary metabolites (Rateb et al., 2013). In the current study, we aimed to monitor the effects of both bacteria and fungi on the induction of microbial secondary metabolites when inoculated in the same culture vessel. Before conducting microbial co-culture experiments, the chemical profiles of each strain were separately investigated using the OSMAC approach to obtain a maximum number of compounds produced, using a variety of media and both low and high nutrient conditions. Once the metabolite profile for each of these three strains was confirmed, the co-cultivation experiment was conducted.

The axenic marine-derived fungal isolate *A. fumigatus* MR2012 (El-Gendy and Rateb, 2015) was screened using three different media followed by media and mycelia extraction. Fractionation and multiple steps of SiO_2 and Sephadex LH-20 followed by reversed phase semi-preparative HPLC purification led to the isolation and identification of a new metabolite belonging to the diketopiperazine family named brevianamide X **1** (**Figure 1**), in addition to the known metabolites brevianamide F **4**, cyclo(L-pro-L-val), cyclo(L-pro-L-ile), cyclo(L-pro-L-phe), cyclo(L-pro-L-leu), fumitremorgin C, spirotryprostatin A, 6-methoxy-spirotryprostatin C (El-Gendy and Rateb, 2015), pseurotin A (Rateb et al., 2013), *bis*(dethio)*bis*(methylthio)gliotoxin (Afiyatullov et al., 2005), and azaspirofurans A and B (Ren et al., 2010). These metabolites were identified based on comparing their spectral data with published data.

The molecular formula of **1** was established as $C_{18}H_{21}O_3N_3$ based on the HRESIMS analysis which gave an $[M+Na]^+$ quasimolecular ion at *m/z* 350.1470. The analysis of ^1H, ^{13}C and multiplicity-edited HSQC NMR spectral data (**Table 1**) revealed the presence of two amide groups (δ_C 168.7, 165.2), a methoxy group (δ_C 55.0/δ_H 3.14), a methylene group attached to oxygen and nitrogen (δ_C 76.1/δ_H 5.46), a 1,2-disubstituted benzene ring (δ_H 7.61, 7.06, 7.15, 7.50), an olefinic singlet at δ_H 7.3, two α-protons at (δ_C 54.9/δ_H 4.33) and (δ_C 58.1/δ_H 4.07), four methylene groups, and an NH group at δ_H 7.86 (s).

The COSY correlations of H-14 through H_2-17 confirmed the proline ring substructure (**Figure 2**) and that of H-5 through to H-8 established the 1,2-disubstituted benzene ring, along with an olefinic singlet at δ_H 7.28 which indicated an indole

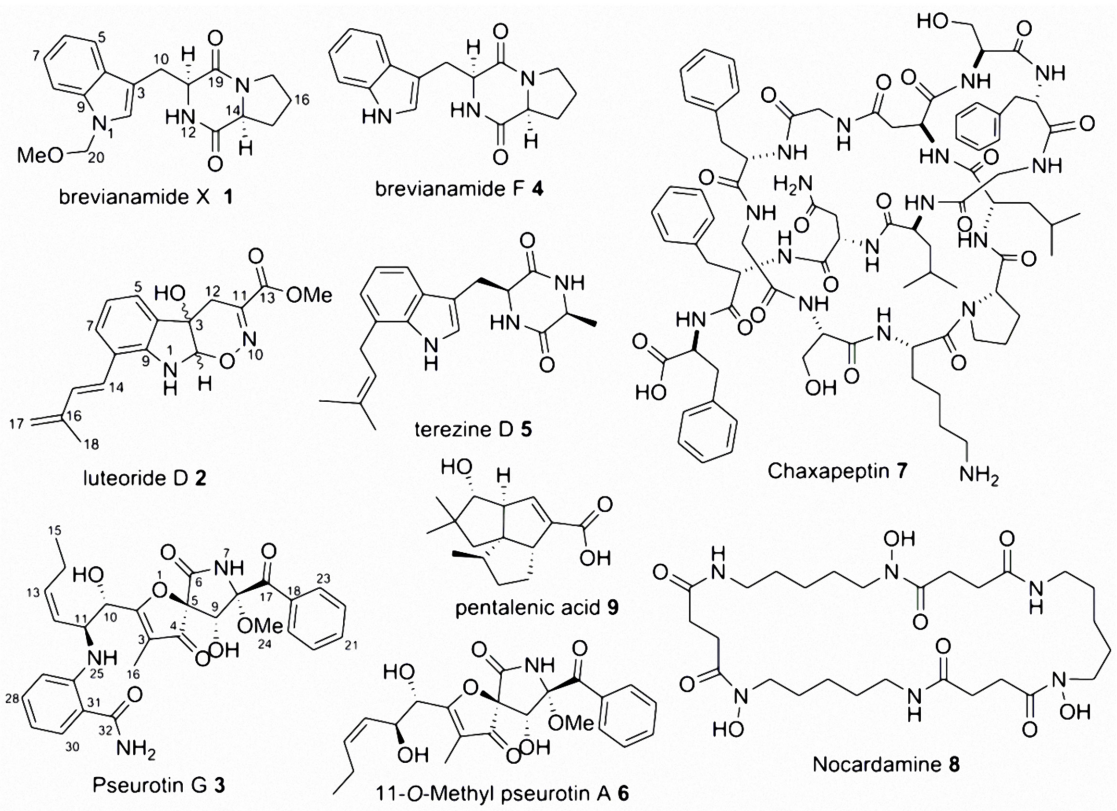


FIGURE 1 | Compounds isolated from the microbial co-culture of *Aspergillus fumigatus* MR2012 and *Streptomyces leeuwenhoekii* strains C34 and C58 in addition to that isolated from the axenic marine-derived *A. fumigatus* MR2012.

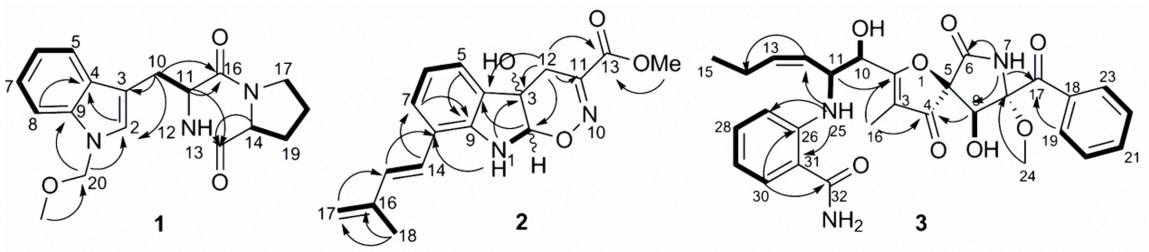


FIGURE 2 | Key COSY correlations in bold and HMBC correlations shown with arrows of compounds **1**–**3**.

moiety. This was confirmed by the HMBC correlations of H-2 to both C-4 and C-9, H-5 to C-3 and H-8 to C-4. The HMBC correlations of H_2-10 to C-2, C-3, C-11 and C-19, H-14 to C-13 and H-11 to both C-13 and C-16 established the presence of an indolyl proline diketopiperazine skeleton which was identical to brevianamide F **4** structure (**Figure 2**) according to spectroscopic data comparison. The HMBC correlations of H_2-20 to C-9, C-2 and C-21 were the key in the determination of the new substructure and its connection to the rest of the brevianamide F **4** structure (**Figure 2**). Since both **4** and **1** shared the same NOESY correlations, virtually identical ^{13}C NMR spectral data and optical rotation values, and are assumed to be formed via a similar non-ribosomal peptide biosynthetic route, we proposed **1** to have the same absolute configuration as brevianamide F (Zhang et al., 2007). Hence, **1** was identified as a new marine fungal metabolite for which we propose the name brevianamide X.

Our previous investigation of the Atacama Desert bacterial isolates *S. leeuwenhoekii* strains C34 and C58 led to the isolation of the ansamycin derivatives, chaxamycins (Rateb et al., 2011a), the macrolactin derivatives, chaxalactins in addition to the sedirophore nocardamine from *S. leeuwenhoekii* C34 (Rateb et al., 2011b), and the lasso peptide chaxapeptin from *S. leeuwenhoekii* C58 (Elsayed et al., 2015). All of these previously described compounds were identified in the current study using LC-HRESIMS analysis (**Figures 3**, **4**). As observed during our previous study, the profile pattern of *S. leeuwenhoekii* strain C34 changed markedly in the OSMAC approach (Rateb

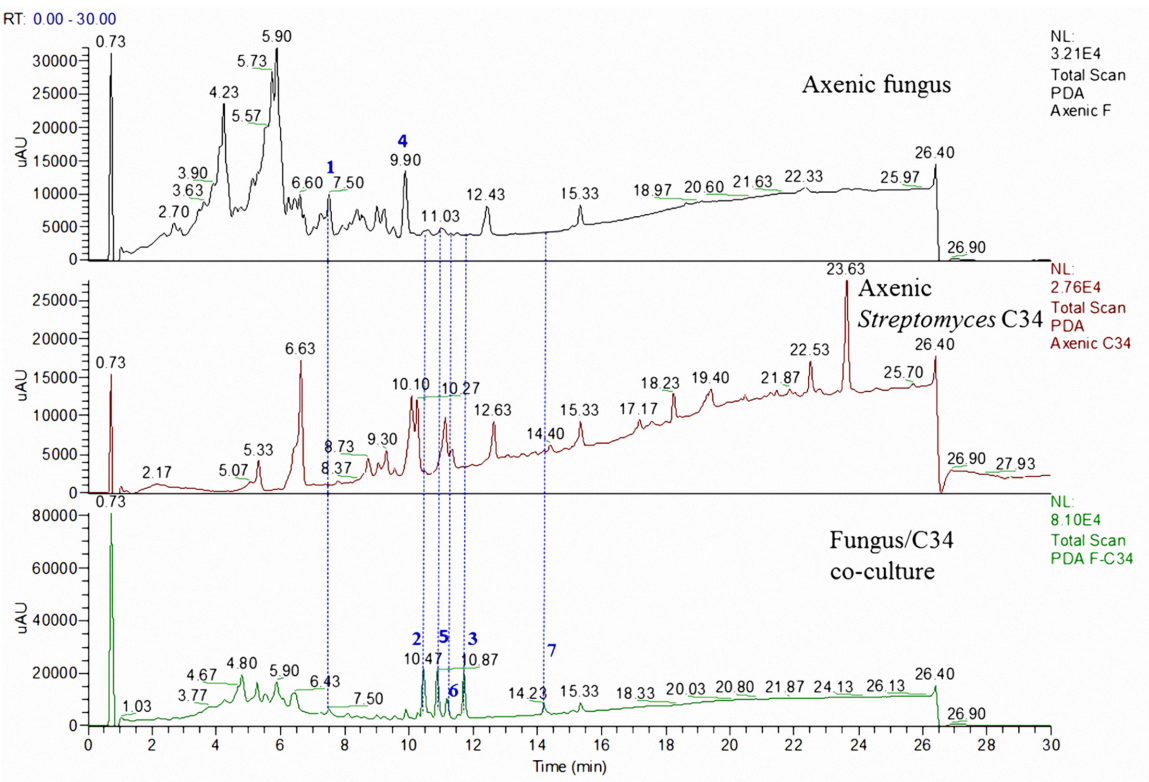


FIGURE 3 | LC comparison of the microbial co-culture of *A. fumigatus* MR2012 and *S. leeuwenhoekii* strain C34 on ISP2 medium.

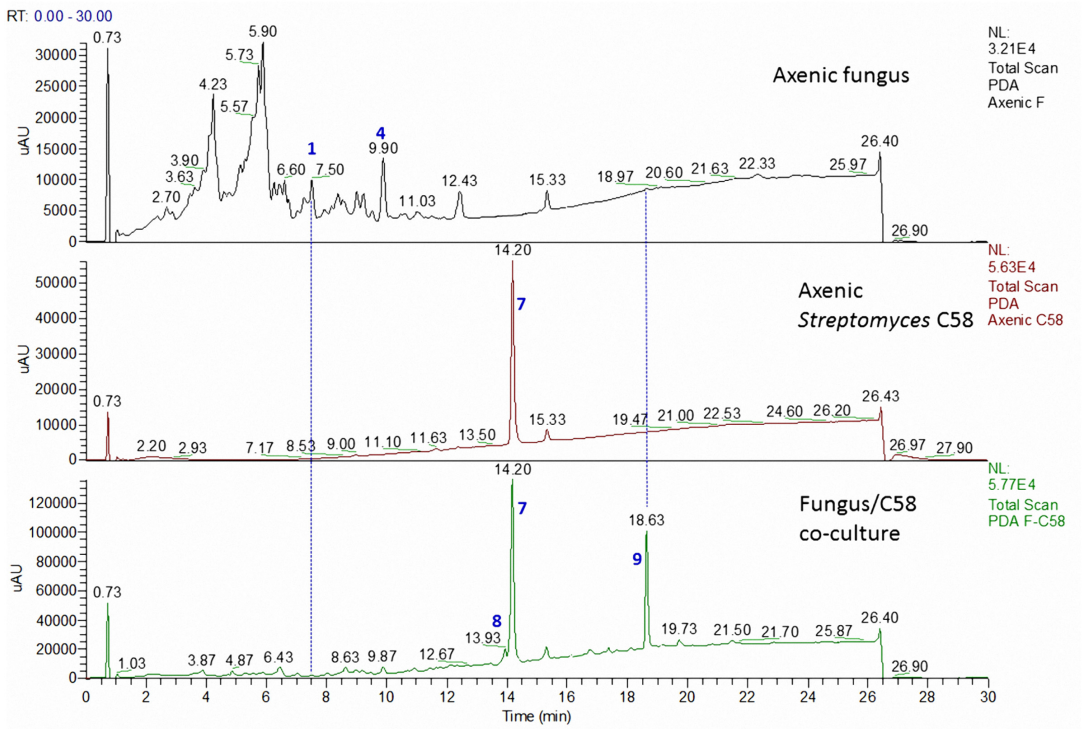


FIGURE 4 | LC comparison of the microbial co-culture of *A. fumigatus* MR2012 and *S. leeuwenhoekii* strain C58 on ISP2 medium.

et al., 2011b), while it was fairly constant for *S. leeuwenhoekii* strain C58.

However, we observed a dramatic change in chemical profiles when each of the two bacteria was separately co-cultured together with the fungus as described in the experimental section. At this stage we carried out large scale co-cultivation, extraction and chromatographic separation, which was guided by focusing on unique peaks with retention times and UV spectra observed in the HPLC profiles which were not present in the profiles of either strain when cultivated on its own. **Table 2** represents all bacterial and fungal metabolites identified in axenic and co-culture flasks of these micro-organisms.

The microbial co-culture of *A. fumigatus* MR2012 and *S. leeuwenhoekii* strain C34 on ISP2 medium (**Figure 3**) led to the production of the bacterial metabolite chaxapeptin **7**, the gene cluster of which is known to be present in the bacterial strain. However, no chaxapeptin production was obtained when the bacterium was fermented using six different media and different cultivation parameters during previous studies (Rateb et al., 2011b; Gomez-Escribano et al., 2015). On the other hand, all other bacterial metabolites that were previously detected were not produced in the current co-culture experiment, except for nocardamine. Interestingly, the HPLC profile of the co-culture was dominated by fungal metabolites, including the known diketopiperazine terezine D **5**, the new luteoride derivative luteoride D **2**, the known 11-*O*-methylpseurotin A **6**, and a new pseurotin derivative, pseurotin G **3**. None of these compounds were observed when the fungus was cultivated on its own.

HRESIMS analysis afforded an $[M+H]^+$ quasimolecular ion at *m/z* 315.1338, establishing the molecular formula of **2** as $C_{17}H_{18}N_2O_4$. The analysis of ^1H, ^{13}C and multiplicity-edited HSQC NMR spectral data (**Table 1**) indicated the presence of a methoxy group (δ_C 52.6/δ_H 3.61), a methyl group connected to a double bond (δ_C 18.5/δ_H 1.94), a methylene group (δ_C 29.9/δ_H 3.16, 2.79), a geminal olefinic methylene group (δ_C 116.4/δ_H 5.11, 5.01), a 1,2,3-trisubstituted benzene ring (δ_H 7.02, 6.63, 7.31), a hemiaminal (δ_C 80.4/δ_H 5.03), and a disubstituted *E*-olefinic moiety [δ_H 6.69 (d, 16.0) and 6.80 (d, 16.1)].

The COSY correlations of H-5 through H-7, 1-NH to H-2, and the HMBC correlations of 1-NH to C-8 and C-3, H-2 to C-9, C-3 and C-12, H-5 to C-3 and C-9 confirmed the presence of indoline ring substructure substituted at position 8 (**Figure 2**). The COSY correlations of H-14 to H-15, H_2-17 to H_3-18 and the HMBC correlations of H_3-18 to C-15, C-16 and C-17, H-15 to C-8 and H-14 to C-7 indicated a 2-methylpenta-1,3-dienyl moiety connected to the indoline ring at position 8. The HMBC correlations of the methyl group at δ_H 3.61 to C-13 indicated a -$COOCH_3$ group. The remaining two double bond equivalents as well as one nitrogen and one oxygen implied by the molecular formula, were attributed by the presence of an oxazine ring connected to the indoline moiety. This was confirmed by the HMBC correlations of H_2-12 to C-2, C-3 and C-11, establishing a dihydro-[1,2]oxazino[6,5-*b*]indol-4a(4H)-ol moiety, and the connection of the -$COOCH_3$ group was corroborated through the HMBC correlations of H_2-12 to C-13. No NOEs for either H-2 or 3-OH were observed in DMSO-d_6 or CD_3OD, so

TABLE 2 | Summary of the metabolites detected by LCMS in bacterial and fungal axenic culture and co-culture experiments.

Media	Strain C34			Strain C58			Fungus MR2012			Fungus/C34	Fungus/C58
Compounds	**ISP2**	**GYE**	**F**	**ISP2**	**GYE**	**F**	**ISP2**	**GYE**	**F**	**ISP2**	**ISP2**
Brevianamide F	−	−	−	−	−	−	+	−	+	−	−
Brevianamide X	−	−	−	−	−	−	−	−	+	−	−
Cyclo(L-pro-L-val)	−	−	−	−	−	−	+	+	−	−	+
Cyclo(L-pro-L-ile)	−	−	−	−	−	−	+	+	−	−	+
Cyclo(L-pro-L-phe)	−	−	−	−	−	−	+	+	−	−	+
Cyclo(L-pro-L-leu)	−	−	−	−	−	−	+	+	+	−	+
Fumitremorgin C	−	−	−	−	−	−	+	−	−	−	−
Spirotryprostatin C	−	−	−	−	−	−	+	−	−	−	−
Pseurotin A	−	−	−	−	−	−	+	+	+	−	−
B*is*(dethio)*bis*(methylthio)gliotoxin	−	−	−	−	−	−	+	−	+	−	−
Azaspirofuran A	−	−	−	−	−	−	+	−	+	−	−
Azaspirofuran B	−	−	−	−	−	−	+	−	+	−	−
Chaxamycins A–D	+	−	+	−	−	−	−	−	−	−	−
Chaxalactins A–C	+	−	−	−	−	−	−	−	−	−	−
Nocardamine	+	+	+	−	−	−	−	−	−	++	++
Chaxapeptin	−	−	−	+	+	+	−	−	−	+	++
Terezine D	−	−	−	−	−	−	−	−	−	+	−
Luteride D	−	−	−	−	−	−	−	−	−	+	−
Methylpseurotin A	−	−	−	−	−	−	−	−	−	+	−
Pseurotin G	−	−	−	−	−	−	−	−	−	+	−
Pentalenic acid	−	−	−	−	−	−	−	−	−	−	+

the relative configuration at these two positions could not be determined. Thus, compound **2** was identified as a new natural product for which the name luteoride D is proposed. Although indoline moieties are frequently encountered in fungal natural products, to the best of our knowledge this is the first report of a oxazino[6,5-*b*]indole nucleus in nature. Based on inspection of its structure, **2** may be formed from the known luteoride A via nucleophilic attack of oxime OH moiety to the olefinic carbon of the indole ring. The latter compound is a prenylated tryptophan analog that was reported recently from the entomopathogenic fungus *Torrubiella luteorostrata* when induced by the histone deacetylase inhibitor suberoyl *bis*-hydroxamic acid (Asai et al., 2011).

The molecular formula $C_{29}H_{31}O_8N_3$ was established for compound **3** based on the HRESIMS a $[M+H]^+$ quasimolecular ion at *m/z* 550.2177. The analysis of the ^1H, ^{13}C, and multiplicity-edited HSQC NMR data of **3** (**Table 3**) indicated the presence of a monosubstituted benzene ring (δ_H 8.27, 7.83, 7.54), a 1,2-disubstituted benzene ring (δ_H 7.96, 7.24, 6.65, 6.52), a disubstituted *Z* double bond ($J = 10.9$ Hz), one aliphatic and one allylic methyl group at $\delta_{C/H}$ 13.7/0.81 and 5.42/1.67, respectively, one O-methyl group at $\delta_{C/H}$ 51.4/3.23, four carbonyls including one α,β-unsaturated ketone at δ_C 196.5, one ketone at δ_C 196.1, and two amide groups at δ_C 171.2 and 171.9, two NH groups (δ_H 8.43 and 9.96), and a oxygenated tetrasubstituted olefinic bond (δ_C 185.8 and 111.5). Comparison with reported data (Wang et al., 2011) indicated that **3** belonged to the pseurotin family of compounds.

The COSY correlations (**Figure 2**) confirmed the location of the two OH groups, confirmed the identity of the two aromatic rings, and established the chain from H-10 through H_3-15. The HMBC correlation from H-19/23 to C-17 confirmed the attachment of the mono-substituted benzene ring to the carbonyl C-17, while the di-substituted benzene ring was identified as part of an anthranilamide moiety on the basis of HMBC correlations of H-30 to C-32 and of NH-25 to both C-27 and C-31. The attachment of the latter to the pseurotin core at position 11 was confirmed through the COSY correlation of NH-25 to H-11 and HMBC correlation of NH-25 to C-12. Furthermore, the mono-substituted benzene ring was connected to the pyrrolidinone moiety through the carbonyl C-17 as evident from HMBC correlations of both NH-7 and H-9 to C-17. The HMBC correlation of H-9 to C-4 confirmed the spirocyclic system, while the furanone ring was established on the basis of correlation between H_3-16 to C-2, C-3, and C-4. Since both pseurotin A and **3** share the same NOESY correlations, displayed virtually identical ^{13}C spectral data and optical rotation values, we assume **3** to have the same absolute configuration as pseurotin A, and propose the name pseurotin G for this new metabolite. A putative biosynthetic route leading to **3** is shown in Supplementary Figure S14 based on the biosynthetic pathway of pseurotin A published by Tsunematsu et al. (2014).

The microbial co-culture of *A. fumigatus* MR2012 and *S. leeuwenhoekii* strain C58 on ISP2 medium (**Figure 4**) led to the production of four simple diketopiperazines assumed to be produced by the fungus, since they were also observed in the axenic culture of the fungus. However, the titre of bacterial metabolite chaxapeptin **7** was dramatically increased, and additionally, the bacterium was induced to produce the known bacterial sesquiterpene pentalenic acid **9**, which had previously

TABLE 3 | Summary of ^{1}H (600 MHz) and ^{13}C (150 MHz) NMR spectroscopic data for pseurotin G **3** in DMSO at 298 K.

	Pseurotin G 3	
Atom	**δ_C,[1] mult.**	**δ_H, mult. (*J* in Hz)**
2	185.8, C	
3	111.5, CH	
4	196.5, C	
5	90.9, C	
6	171.9, C	
8	92.4, C	
9	74.7, CH	4.50 (s)
10	70.6, CH	4.63 (s)
11	52.2, CH	4.50 (s)
12	134.6, CH	5.48 (m)
13	125.3, CH	5.30 (m)
14	20.5, CH_2	2.03 (m), 1.94 (m)
15	13.7, CH_3	0.81 (t, 7.4)
16	5.42, CH_3	1.67 (s)
17	196.1, C	
18	133.3, C	
19/23	130.7, CH	8.27 (d, 7.9)
20/22	128.2, CH	7.54 (t, 7.8)
21	133.7, CH	7.68 (t, 7.3)
24	51.4, CH_3	3.23 (s)
26	148.0, C	
27	111.4, C	6.65 (d, 8.9)
28	132.1, CH	7.24 (t, 7.6)
29	114.5, CH	6.52 (t, 7.6)
30	129.0, CH	7.56 (d, 7.6)
31	114.2, C	
32	171.2, C	
7-NH		9.96 (s)
25-NH		8.43 (d, 8.2)

[1]*Extracted from HSQC and HMBC.*

been isolated from various *Streptomyces* spp. (Takamatus et al., 2011), and the known siderophore, nocardamine **8**. The latter two were not observed in single cultures of the bacterium under different fermentation conditions. Based on inspection of their structures, these three compounds clearly are bacterial metabolites, and additionally, the gene clusters responsible for their biosynthesis were confirmed to be present in the genome of *S. leeuwenhoekii* strain C58 (data not shown). All three bacterial compounds were identified based on their HRESIMS analysis and comparison with the previously reported NMR data (Rateb et al., 2011a; Elsayed et al., 2015).

DISCUSSION

In the past few years, various researchers have established microbial co-cultivation as a powerful tool for mimicking the natural microbial environment and enhancing the production of specific metabolites, or inducing the production of new secondary metabolites not previously observed in the independent strain cultures. Activation of cryptic biosynthetic genes in a second microorganism may be stimulated through microbial crosstalk and may be interpreted as a defense mechanism triggered in response to a chemical signal from the other microorganism (Pettit, 2009; Schroeckh et al., 2009). Ten years ago, the application of co-cultivation (mixed fermentation) was still in its infancy, probably due to the fear of lack of reproducibility (Pettit, 2009) but since then, various studies have demonstrated that this approach is capable of delivering reproducible metabolite patterns, provided relevant fermentation parameters are first established and then carefully maintained.

In the present study, small scale fermentation of axenic cultures of bacteria and fungi, and of their co-cultures was conducted at different conditions, and was carefully monitored by LC-HRESIMS, LC-UV and microscopic analysis (data not shown) to adjust fermentation parameters and ensure reproducibility of secondary metabolite production. Once an optimized set of fermentation parameters was established, a large scale co-culture experiment was conducted at a scale of 4 L for natural product isolation. Chemical profiles observed for small and large scale cultivation were highly comparable (data not shown). Our selection of *A. fumigatus* as the fungal component was established as a results of a broader screening of different fungal strains, which revealed this species to be particularly prone to respond by displaying modified metabolite profiles upon co-cultivation with other microorganisms (data not shown). During the preliminary chemical screening of various isolates of *A. fumigatus*, strain MR2012 which had been obtained from a Red Sea sediment sample caught our attention as it produced a new metabolite, brevianamide X **1**, which was only observed upon fermentation in F-medium, but not in two other culture media. This finding highlights the importance of varying culture conditions and of using a variety of fermentation media for screening (Kang et al., 2013).

To date, co-culture studies reported the effect of one microorganism to affect the metabolite profile of the second microorganism. Our current investigation not only showed that co-culture can induce the production of new metabolites, but highlighted the fact that this may work in both directions. Comparing the chemical profiles of the pure cultures to those from the co-culture, a great diversity was shown (**Figures 3**, **4**). In the microbial co-culture of *A. fumigatus* MR2012 and *S. leeuwenhoekii* C34, the bacterial strain appears to have suppressed the production of most of fungal metabolites detected in the axenic culture. However, it induced the production of two fungal prenylated indole metabolites which were not traced before in the fungus; the known terezine D and the new luteoride D **2** featuring an oxazino[6,5-*b*]indole nucleus that was not previously reported in nature. Additionally, the new compound, pseurotin G **3** was also induced in the fungus. Based on analysis of its structure, **3** is assumed to be of hybrid polyketide and non-ribosomal peptide origin as was demonstrated for pseurotin A (Tsunematsu et al., 2014). A putative biosynthetic route for **3** is provided in Supplementary Figure S14. It is interesting to note that fungi have been found to readily incorporate anthranilamide or anthranilic acid (Xin et al., 2007; Li et al., 2013). Thus, the origin of the respective substructure in **3** which so far has not

been observed for other pseurotin derivatives, i.e., whether it is produced by the fungus itself or by the bacterium, or may be even incorporated from the culture medium, cannot be established at this point.

Surprisingly, in the co-cultivation experiments of *A. fumigatus* MR2012 and *S. leeuwenhoekii* C34, the fungus appears to have suppressed all ansamycin and macrolactin derivatives that previously were observed in axenic cultures of the bacterium (Rateb et al., 2011b), while the lasso peptide chaxapeptin was produced at significant levels. Whereas genome scanning had revealed the presence of the chaxapeptin biosynthetic gene cluster in *S. leeuwenhoekii* C34 (Gomez-Escribano et al., 2015), our previous chemical analysis had failed to detect the expression of this metabolite when the bacterium was fermented using six different media and a variety of cultivation parameters (Rateb et al., 2011b). It is worth noting that the production of antimicrobial lasso peptides could be triggered by competing nutrient scarcity in the culture vessel (Hegemann et al., 2015).

In the microbial co-culture of *A. fumigatus* MR2012 and *S. leeuwenhoekii* C58, the bacterial strain appears to have suppressed the production of the fungal metabolites that were present in the axenic culture. However, the bacterium was induced to produce pentalenic acid and nocardamine, both of which were not observed in the single bacterial culture under different fermentation conditions. Additionally, the titre of the lasso peptide chaxapeptin was greatly increased. It is worth noting that none of these metabolites proved to have antifungal effects when screened in previous studies.

Interestingly, siderophores such as nocardamine have been identified as auto-regulator/quorum sensing molecules (Bertrand et al., 2014). In order to assess whether the effects observed in the present study are due to some metabolites acting as signaling molecules, or may be explained in terms of mere antimicrobial effects, further studies need to be conducted.

In summary, co-cultivation is an ecologically driven approach which has become a powerful method to induce previously unexpressed biosynthetic pathways and increase the metabolic capacity of chemically prolific microorganisms beyond the boundaries that can be reached by routine axenic cultivation. In this current study, a bi-lateral cross talk that led to dual induction of both bacterial and fungal metabolites in the same culture flask was proved for the first time.

AUTHOR CONTRIBUTIONS

Conceived and designed the experiments: JW, HH, MJ, RE, and MR. Performed the experiments: JW, HH, and MR. Analyzed the data: JW, HH, MJ, RE, and MR. Contributed reagents/materials/analysis tools: JW, MJ, RE, and MR. Wrote and enriched the literature: JW, HH, MJ, RE, and MR.

ACKNOWLEDGMENTS

We thank the College of Physical Sciences, University of Aberdeen, for provision of infrastructure and facilities in the Marine Biodiscovery Centre. We acknowledge the receipt of funding from the European Union's Seventh Programme for Research, Technological Development and Demonstration under Grant Agreement No. 312184 (PharmaSea). MR thanks School of Science and Sport, University of the West of Scotland for providing the open-access fees required for the publication.

SUPPLEMENTARY MATERIAL

The Supplementary Material for this article can be found online at: http://journal.frontiersin.org/article/10.3389/fmicb.2017.01284/full#supplementary-material

REFERENCES

Abdelmohsen, U. R., Grkovic, T., Balasubramanian, S., Kamel, M. S., Quinn, R. J., and Hentschel, U. (2015). Elicitation of secondary metabolism in actinomycetes. *Biotechnol. Adv.* 33, 798–811. doi: 10.1016/j.biotechadv.2015.06.003

Afiyatullov, S. S., Kalinovskii, A. I., Pivkin, M. V., Dmitrenok, P. S., and Kuznetsova, T. A. (2005). Alkaloids from the marine isolate of the fungus *Aspergillus fumigatus*. *Chem. Nat. Comp.* 41, 236–238. doi: 10.1007/s10600-005-0122-y

Asai, T., Yamamoto, T., and Oshima, Y. (2011). Histone deacetylase inhibitor induced the production of three novel prenylated tryptophan analogs in the entomopathogenic fungus, *Torrubiella luteorostrata*. *Tetrahed. Lett.* 52, 7042–7045. doi: 10.1016/j.tetlet.2011.10.020

Bergmann, S., Schümann, J. S., Cherlach, K., Lange, C., Brakhage, A. A., and Hertweck, C. (2007). Genomics-driven discovery of PKS-NRPS hybrid metabolites from *Aspergillus nidulans*. *Nat. Chem. Biol.* 3, 213–217. doi: 10.1038/nchembio869

Bertrand, S., Bohni, N., Schnee, S., Schumpp, O., Gindro, K., and Wolfender, J. (2014). Metabolite induction via microorganism co-culture: a potential way to enhance chemical diversity for drug discovery. *Biotechnol. Adv.* 32, 1180–1204. doi: 10.1016/j.biotechadv.2014.03.001

Bode, H. B., Bethe, B., Höfs, R., and Zeeck, A. (2002). Big effects from small changes: possible ways to explore nature's chemical diversity. *Chembiochem* 3, 619–627. doi: 10.1002/1439-7633(20020703)3:7<619::AID-CBIC619>3.0.CO;2-9

Butler, M. S., Robertson, A. A. B., and Cooper, M. A. (2014). Natural product and natural product derived drugs in clinical trials. *Nat. Prod. Rep.* 31, 1612–1661. doi: 10.1039/C4NP00064A

Challis, G. L., and Hopwood, D. A. (2003). Synergy and contingency as driving forces for the evolution of multiple secondary metabolite production by *Streptomyces* species. *Proc. Natl Acad. Sci. U.S.A.* 25, 14555–14561. doi: 10.1073/pnas.1934677100

Dashti, Y., Grkovic, T., Abdelmohsen, U. R., Hentschel, U., and Quinn, R. J. (2014). Production of induced secondary metabolites by a co-culture of sponge-associated actinomycetes, *Actinokineospora* sp. EG49 and *Nocardiopsis* sp. RV163. *Mar. Drugs* 12, 3046–3059. doi: 10.3390/md12053046

Ebrahim, W., El-Neketi, M., Lewald, L. I., Orfali, R. S., Orfali, R. S., Lin, W., et al. (2016). Metabolites from the fungal endophyte *Aspergillus austroafricanus* in axenic culture and in fungal-bacterial mixed cultures. *J. Nat. Prod.* 79, 914–922. doi: 10.1021/acs.jnatprod.5b00975

El-Gendy, B. E., and Rateb, M. E. (2015). Antibacterial activity of diketopiperazines isolated from a marine fungus using t-butoxycarbonyl group as a simple tool for

purification. *Bioorg. Med. Chem. Lett.* 25, 3125–3128. doi: 10.1016/j.bmcl.2015.06.010

Elsayed, S. S., Trusch, F., Deng, H., Raab, A., Prokes, I., Busarakam, K., et al. (2015). Chaxapeptin, a lasso peptide from extremotolerant *Streptomyces leeuwenhoekii* strain C58 from the hyperarid atacama desert. *J. Org. Chem.* 80, 10252–10260. doi: 10.1021/acs.joc.5b01878

Gomez-Escribano, J. P., Castro, J. F., Razmilic, V., Chandra, G., Andrews, B., Asenjo, J. A., et al. (2015). The *Streptomyces leeuwenhoekii* genome: de novo sequencing and assembly in single contigs of the chromosome, circular plasmid pSLE1 and linear plasmid pSLE2. *BMC Genomics* 16:485. doi: 10.1186/s12864-015-1652-8

Harvey, A. L., Edrada-Ebel, R., and Quinn, R. J. (2015). The re-emergence of natural products for drug discovery in the genomics era. *Nat. Rev. Drug Discov.* 14, 111–129. doi: 10.1038/nrd4510

Hegemann, J. D., Zimmermann, M., Xie, X., and Marahiel, M. A. (2015). Lasso peptides: an intriguing class of bacterial natural products. *Acc. Chem. Res.* 48, 1909–1919. doi: 10.1021/acs.accounts.5b00156

Hertweck, C. (2009). Hidden biosynthetic treasures brought to light. *Nat. Chem. Biol.* 5, 450–452. doi: 10.1038/nchembio0709-450

Kang, D., Son, G. H., Park, H. M., Kim, J., Choi, J. N., Kim, H. Y., et al. (2013). Culture condition-dependent metabolite profiling of *Aspergillus fumigatus* with antifungal activity. *Fungal Biol.* 117, 211–219. doi: 10.1016/j.funbio.2013.01.009

Li, C.-S., Li, X.-M., Gao, S.-S., Lu, Y.-H., and Wang, B.-G. (2013). Cytotoxic anthranilic acid derivatives from deep sea sediment-derived fungus *Penicillium paneum* SD-44. *Mar. Drugs* 11, 3068–3076. doi: 10.3390/md11083068

Luo, Y., Huang, H., Liang, J., Wang, M., Lu, L., Shao, Z., et al. (2013). Activation and characterization of a cryptic polycyclic tetramate macrolactam biosynthetic gene cluster. *Nat. Commun.* 4:2894. doi: 10.1038/ncomms3894

Marmann, A., Aly, A. H., Lin, W., Wang, B., and Proksch, P. (2014). Co-cultivation-a powerful emerging tool for enhancing the chemical diversity of microorganisms. *Mar. Drugs* 12, 1043–1065. doi: 10.3390/md12021043

Newman, D. J., and Cragg, G. M. (2016). Natural products as sources of new drugs from 1981 to 2014. *J. Nat. Prod.* 79, 629–661. doi: 10.1021/acs.jnatprod.5b01055

Nützmann, H.-W., Reyes-Dominguez, Y., Scherlach, K., Schroeckh, V., Horn, F., Gacek, A., et al. (2011). Bacteria-induced natural product formation in the fungus *Aspergillus nidulans* requires Saga/Ada-mediated histone acetylation. *Proc. Natl. Acad. Sci. U.S.A.* 108, 14282–14287. doi: 10.1073/pnas.1103523108

Okoro, C. K., Brown, R., Jones, A. L., Andrews, B. A., Asenjo, J. A., Goodfellow, M., et al. (2009). Diversity of culturable actinomycetes in hyper-arid soils of the Atacama Desert, Chile. *Antonie Van Leeuwenhoek* 95, 121–133. doi: 10.1007/s10482-008-9295-2

Onaka, H., Mori, Y., Igarashi, Y., and Furumai, T. (2011). Mycolic acid-containing bacteria induce natural-product biosynthesis in *Streptomyces* species. *Appl. Environ. Microbiol.* 77, 400–406. doi: 10.1128/AEM.01337-10

Pettit, R. K. (2009). Mixed fermentation for natural product drug discovery. *Appl. Microbiol. Biotechnol.* 83, 19–25. doi: 10.1007/s00253-009-1916-9

Rateb, M. E., Hallyburton, I., Houssen, W. E., Bul, A. T., Goodfellow, M., Santhanam, R., et al. (2013). Induction of diverse secondary metabolites in *Aspergillus fumigatus* by microbial co-culture. *RSC Adv.* 3, 14444–14450. doi: 10.1039/C3RA42r378F

Rateb, M. E., Houssen, W. E., Arnold, M., Abdelrahman, M. H., Deng, H., Harrison, W. T., et al. (2011a). Chaxamycins A–D, bioactive ansamycins from a hyper-arid desert *Streptomyces* sp. *J. Nat. Prod.* 74, 1491–1499. doi: 10.1021/np200320u

Rateb, M. E., Houssen, W. E., Harrison, W. T., Deng, H., Okoro, C. K., Asenjo, J. A., et al. (2011b). Diverse metabolic profiles of a *Streptomyces* strain isolated from a hyper-arid environment. *J. Nat. Prod.* 74, 1965–1971. doi: 10.1021/np200470u

Ren, H., Liu, R., Chen, L., Zhu, T., Zhu, W. M., and Gu, Q. Q. (2010). Two new hetero-spirocyclic γ-lactam derivatives from marine sediment-derived fungus *Aspergillus sydowi* D2-6. *Arch. Pharm. Res.* 33, 499–502. doi: 10.1007/s12272-010-0401-4

Scherlach, K., and Hertweck, C. (2009). Triggering cryptic natural product biosynthesis in microorganisms. *Org. Biomol. Chem.* 7, 1753–1760. doi: 10.1039/b821578b

Schroeckh, V., Scherlach, K., Nützmann, H. W., Shelest, E., Schmidt-Heck, W., Schuemann, J., et al. (2009). Intimate bacterial–fungal interaction triggers biosynthesis of archetypal polyketides in *Aspergillus nidulans*. *Proc. Natl. Acad. Sci. U.S.A.* 106, 14558–14563. doi: 10.1073/pnas.0901870106

Shirling, E. B., and Gottlieb, D. (1966). Methods for characterizing *Streptomyces* species. *Int. J. Syst. Bacteriol.* 16, 313–340. doi: 10.1099/00207713-16-3-313

Soliman, S. S., and Raizada, M. N. (2013). Interactions between co-habitating fungi elicit synthesis of Taxol from an endophytic fungus in host Taxus plants. *Front. Microbiol.* 4:3. doi: 10.3389/fmicb.2013.00003

Takamatus, S., Xu, L. H., Fushinobu, S., Shoun, H., Komatsu, M., Cane, D. E., et al. (2011). Pentalenic acid is a shunt metabolite in the biosynthesis of the pentalenolactone family of metabolites: hydroxylation of 1-deoxypentalenic acid mediated by CYP105D7 of *Streptomyces avermitilis*. *J. Antibiot.* 64, 65–71. doi: 10.1038/ja.2010.135

Tian, H., Shafi, J., Ji, M., Bi, Y., and Yu, Z. (2017). Antimicrobial metabolites from *Streptomyces* sp. *SN*0280. *J. Nat. Prod.* 80, 1015–1019. doi: 10.1021/acs.jnatprod.6b01016

Tsunematsu, Y., Fukutomi, M., Saruwatari, T., Noguchi, H., Hotta, K., Tang, Y., et al. (2014). Elucidation of pseurotin biosynthetic pathway points to trans-acting C-methyltransferase: generation of chemical diversity. *Angew. Chem. Int. Ed.* 53, 8475–8479. doi: 10.1002/anie.201404804

Wang, F. Z., Li, D. H., Zhu, T. J., Zhang, M., and Gu, Q. Q. (2011). Pseurotin A1 and A2, two new 1-oxa-7-azaspiro[4.4]non-2-ene-4,6-diones from the holothurian-derived fungus *Aspergillus fumigatus* WFZ-25. *Can. J. Chem.* 89, 72–76. doi: 10.1139/V10-157

Xin, Z. H., Fang, Y., Du, L., Zhu, T., Duan, L., Chen, J., et al. (2007). Aurantiomides A-C, quinazoline alkaloids from the sponge-derived fungus *Penicillium aurantiogriseum* SP0-19. *J. Nat. Prod.* 70, 853–855. doi: 10.1021/np060516h

Zhang, D., Noviendri, D., Nursid, M., Yang, X., and Son, B. W. (2007). 12,13-Dihydroxyfumitremorgin C, Fumitremorgin C, and Brevianamide F, antibacterial diketopiperazine alkaloids from the marine-derived fungus *Pseudallescheria* sp. *Nat. Prod. Sci.* 13, 251–254.

Conflict of Interest Statement: The authors declare that the research was conducted in the absence of any commercial or financial relationships that could be construed as a potential conflict of interest.

The reviewer TS and handling Editor declared their shared affiliation, and the handling Editor states that the process nevertheless met the standards of a fair and objective review.

Copyright © 2017 Wakefield, Hassan, Jaspars, Ebel and Rateb. This is an open-access article distributed under the terms of the Creative Commons Attribution License (CC BY). The use, distribution or reproduction in other forums is permitted, provided the original author(s) or licensor are credited and that the original publication in this journal is cited, in accordance with accepted academic practice. No use, distribution or reproduction is permitted which does not comply with these terms.

frontiers in Microbiology

ORIGINAL RESEARCH
published: 11 July 2017
doi: 10.3389/fmicb.2017.01286

Fungal and Bacterial Diversity Isolated from *Aquilaria malaccensis* Tree and Soil, Induces Agarospirol Formation within 3 Months after Artificial Infection

Hemraj Chhipa and Nutan Kaushik **

Plant Biotechnology, The Energy and Resources Institute, New Delhi, India

Aquilaria malaccensis Lam, commonly known as Agarwood, is a highly valuable species used in production of agar oil from its infected wood, which is utilized in pharmaceutical and perfumery industry. Agar oil formation in agarwood takes years through the natural process which is induced by natural or artificial injury or microbial infection. The role of soil fungi and bacteria in artificial induction is still an unexplored area. In the present study, we isolated the fungal and bacterial community residing inside the stem of *A. malaccensis* tree and circumventing soil, samples collected from 21 different sites of the north-eastern state Assam of India and explored their potential in induction of Agarospirol (2-(6,10-Dimethylspiro[4,5]dec-6-en-2-yl)-2-propanol) production by artificially infecting the trees with these microorganisms. A total 340 fungi and 131 bacteria were isolated from 50 stem samples, and 188 fungi and 148 bacteria were isolated from 50 soil samples. Highest Shannon ($H' = 2.43$) and Fisher ($\alpha = 5.57$) diversity index was observed in the stem isolates. The dominant fungal genus was *Trichoderma* in stem with *Pi* value of 0.18; while in soil, *Aspergillus* showed dominance with *Pi* value 0.73. In bacteria, *Bacillus* genera showed dominance in both stem and soil samples with $Pi = 0.62$ and 0.51, respectively. Forty fungal and bacterial isolates were used to assess their potential to induce formation of agarwood in *A. malaccensis* by artificial infection method. Gas chromatography mass spectroscopy (GC-MS) analysis confirmed development of Agarwood by the presence of Agarospirol compound in samples collected after 3 months of the artificial infection. Only 31% of bacterial and 23% of fungal isolates showed their ability in production of Agarospirol by artificial infection method. Bacteria *Pantoea dispersa* and fungi *Penicillium polonicum* showed the highest production in comparison to other isolates.

Keywords: endophytes, diversity, artificial infection, *Pantoea dispera,* agarwood, agarospirol, GC-MS

OPEN ACCESS

Edited by:
Bhim Pratap Singh, Mizoram University, India

Reviewed by:
Bharath Prithiviraj, Brooklyn College (CUNY) and CUNY Advanced Science Research Center, United States
Azucena Gonzalez Coloma, Instituto de Ciencias Agrarias (CSIC), Spain

***Correspondence:**
Nutan Kaushik
kaushikn@teri.res.in;
kaushikn2008@gmail.com

Specialty section:
This article was submitted to Microbiotechnology, Ecotoxicology and Bioremediation, a section of the journal Frontiers in Microbiology

Received: *12 April 2017*
Accepted: *27 June 2017*
Published: *11 July 2017*

Citation:
Chhipa H and Kaushik N (2017) Fungal and Bacterial Diversity Isolated from Aquilaria malaccensis Tree and Soil, Induces Agarospirol Formation within 3 Months after Artificial Infection. Front. Microbiol. 8:1286. doi: 10.3389/fmicb.2017.01286

INTRODUCTION

Aquilaria malaccensis is an oleoresin-producing tree which occurs in Malaysia, Myanmar, Sumatra, Borneo Island, Philippines, Bangladesh, Vietnam, China, and India (Gibson, 1977; Hai et al., 1999). The oleoresin produced by the tree is a highly valuable component of incense, perfumes, drugs, stimulants, cardiac tonics, and carminatives (Mengling et al., 2005). Further, it is used as an active

ingredient in traditional medicines of China and has also been included in different pharmaceutical products of coughs, acroparalysis, asthma, and anti-histamine (Kim et al., 1997; Bhuiyan and Bhuiyan, 2008). The dark wood of *Aquilaria* tree having oleoresin is known as agarwood, which emits a pleasant smell on burning and is widely used as incense in Islamic, Buddhist, and Hindu ceremonies. The essential oil extracted from agarwood also has antimicrobial properties (Chen et al., 2011). Commercial exploitation and uncontrolled cutting is leading to a decline in number of these trees. Eight species of *Aquilaria* are listed in Appendix II of the Convention on International Trade in Endangered Species (CITES) of wild fauna and flora (CITES, 1994) and are categorized as vulnerable by the International Union for the Conservation of Nature (IUCN, 2009).

Agarwood is the oleoresin containing part of *Aquilaria* tree which is formed after natural and artificial injury and tree produced oleoresin to prevent or recover the injury in response to plant defense mechanism (Zhang et al., 2012). Naturally the wound is produced by microbial invasion, gnawing of insects, lightning strikes and heavy winds (Xu et al., 2013; Zhang et al., 2014). As a defense response to these outbreaks, normal heartwood converts into dark agarwood. Firstly, Bhattacharyya in 1952 reported role of endophytic fungi in inducing agarwood production in the tree trunk. Later many scientists isolated several endophytes from the agarwood tree (Chhipa et al., 2017). Mohamed et al. (2010) showed the presence of *Curvularia, Cunninghamella*, *Trichoderma*, and *Fusarium* species in the agarwood fungal community in Malaysia. Similarly, Tian et al. (2013) reported the presence of *Phomopsis, Botryosphaeria*, *Cylindrocladium*, and *Colletotrichum gloeosporioides* species in wounded *Aquilaria* tree; and the presence of *Alternaria, Mycosphaerella, Phoma*, *Ramichloridium*, and *Sagenomella* species in the non-resinous tree internally. Bhore et al. (2013) demonstrated the presence of endophytic bacteria and reported *Bacillus pumilus* to be a dominating species among 18 different types of bacteria. In another study, Huang et al. (2015) reported the presence of distinct bacterial community in agarwood and non-agarwood plant of *A. sinensis*. It has been reported that local tree environment and wound microclimate also affect the succession pattern of the fungal population (Mohamed et al., 2014). The community of bacterial endophytes are also affected by the formation of agarwood and on metabolic changes in the plant (Huang et al., 2015). It is important to compare the microbial community structure and their association with the artificially induced agarwood formation at different locations for determining responsible microbes in artificial infection.

The natural development of agarwood takes 25–30 years and the yield is less, thus it unable to meet the demand of the growing market (Zhang et al., 2010). The increasing commercial demand has led to forced development of artificial infection methods. Different methods, such as physical, chemical, and biological or combinations have been reported for artificially inducing resinous oil in *Aquilaria* tree (Ito et al., 2005; Pojanagaroon and Kaewrak, 2005; Gong and Guo, 2009; Okudera and Ito, 2009; Kumeta and Ito, 2010; Novriyanti et al., 2010; Chen et al., 2011; Wei et al., 2012; Liu et al., 2013). The physical methods include severe bark removal, inflicting nail and axe wounds, making hole with screws, inflicting wounds with chisels, partial-trunk pruning, burning-chisel-drilling, pin-hole, and agar wit are recently reported (Pojanagaroon and Kaewrak, 2005; Liu et al., 2013; Tian et al., 2013). The biological methods include fungi-based inoculation, introduced by Tunstall (Gibson, 1977). Few fungal isolates, such as *Melanotus flavolivens*, *Phytium sp., Penicillium sp., Diplodia sp., Botryodyplodis sp., Lasiodiplodis sp.*, and *Fusarium sp*. A2, have been used for artificial infection (Gong and Guo, 2009; Zhang et al., 2014). The role of bacteria in artificial inoculation is less explored in comparison to fungi. More research is required to look at microbial strain or consortia that can develop high yield of agarwood by artificial infection. In the present study, microbial diversity residing in *A. malaccensis* tree and surrounding soil of *A. malaccensis* growing in north-eastern region of India was explored and their potential for inducing agarwood production by artificial inoculation method was assessed.

MATERIALS AND METHODS

Sample Collection and Isolation of Microbes

Fifty healthy trees from 21 different sites (**Figure S1**) in Assam, India were identified by the State Forest Research Institute, Itanagar. Stem and soil samples were collected from these sites and transported to the lab in an icebox. Isolation of microbes was done within 48 h of the collection. List of collected samples is provided at **Table S1**. The isolation of stem endophytes was done using surface sterilization according to the method established in our laboratory (Kumar et al., 2011) and the soil microbes were isolated by serial dilution method according to protocol of Kasana et al. (2008). Grouping of these isolates was done on the basis of morphological similarities and agar block of axenic cultures were stored in 15% glycerol stock at −70°C for long-time preservation.

Extraction of DNA, PCR, and Sequencing

The genomic DNA of pure fungal isolates was extracted using DNeasy Plant mini kit (Qiagen GmbH, Hilden Cat. No 69104) by following the manufacture's instruction. Bacterial DNA was isolated using the CTAB method (Nishiguchi et al., 2002). The extracted DNA was used for PCR amplification by primer ITS1 and ITS4 according to Kumar et al. (2011) for fungi and 518F and 1492 R universal primers for bacterial sequence. The Polymerase chain reaction was achieved in 25 μL of reaction mixture, which contained 2.5 μL of 10× PCR Buffer with 15 mM $MgCl_2$ (Applied Biosystem, India), 0.5 μL of dNTP mix (10 mM, Applied Biosystem), 2.5 μL of ITS1, ITS4 for fungi, and 518F and 1492 R primers for bacteria (10 picomole/μL), 1 μL of DNA template, and 0.5 μL of Ampli Teg Gold (5 U/μL). The ITS1, ITS4, 518F, and 1492 R primers were synthesized from Merck nucleotide synthesis services, Bengaluru, India, according ITS1 5′TCCGTAGGTGAACCTGCGG3′, ITS4 5′TCCTCCGCTTATTGATATGC3′, 518F 5′-CCAGCAGCCGCGGTAAT-3′, and 1492R 5′-GGYTACCTTGTTACGACTT-3′ sequence. The Polymerase

Chain Reaction was done on Veriti Thermal Cycler (Applied Biosystem) using following programmes: initial denaturation at 94°C for 2 min; 30 cycles of denaturation, annealing, and elongation at 94°C for 1 minute; 57°C for 1.30 min, and 72°C for 2 min followed by final elongation at 72°C for 4 min. The negative control was also run using sterile water. The amplified product was checked on 1.5% agarose gel by gel electrophoresis. The amplified product was sequenced by Merck sequencing services, Bengaluru, India.

Identification of Microbes and Phylogenetic Evaluation

The sequences were aligned and trimmed by DNA Baser 4.2 software on the basis of quality read values. The identification of microbes was done on the basis of similarity of amplified sequence with NCBI database using Basic Local Alignment Search Tool (nBLAST) of the US National Centre for Biotechnology Information (NCBI), SILVA and UNITE databases. The sequences were submitted to NCBI database. The phylogenetic tree was developed using Neighbor-Joining and Maximum Likelihood method by MEGA 6.0 software using sequence alignment by Clustal W pairwise sequence Alignment tool of the EMBL Nucleotide Sequence Database. The evolutionary distances were computed using the Maximum Composite Likelihood method.

Evaluation of Microbial Diversity

The microbial diversity in the stem and surrounding soil of *A. malaccensis* was determined by the Shannon diversity index, Simpson's index, and Fisher Alpha index. Species richness of the isolated microbes was estimated according to the Menhinick's index (D*mn*) by the following equation (Whittaker, 1972):

$$Dmn = \frac{s}{\sqrt{N}} \quad (1)$$

Where "s" represents the number of different type of species in a sample and "*N*" represents the total number of isolates in a given sample. Simultaneously, dominance of class was also determined by Camargo's index (1/*Dmn*), where "*Dmn*" denotes species richness. A species was explained as dominant if $Pi > 1/Dmn$, where *Pi* represents the relative abundance of a species, *i* explains the total number of competing species in the community (Camargo, 1992). The diversity was also evaluated to understand the distribution of organisms as randomly, aggregated, or uniformly distributed. Shannon diversity index (H'), Simpson's index, and Fisher Alpha index were calculated by SPADE programme version 3.1 (Chao and Shen, 2010). The heat map analysis was also done for soil and stem isolates using online tool Heatmapper[1] (Babicki et al., 2016). The pairwise heat map was generated by average linkage calculation using Euclidean distance measurement method.

[1]http://www.heatmapper.ca.

Agarwood Formation by Artificial Infection Method

Forty microbial isolates selected on the basis of their dominance were screened for their potential to induce agarwood formation by artificial infecting the wood with these micobes. For this, fungal mycelium was grown on PDA media and 5 days old fungal plugs were transferred to 100 ml of potato dextrose broth. The cultures were incubated at 25°C for 7 days. While, bacterial cultures were grown in 100 ml of nutrient broth medium and incubated for 48 h at 37°C. The grown fungal biomass was collected by filtration with Whatman filter paper no 1 and bacterial biomass with centrifugation at 8,000 rpm for 10 min and lyophilized to get powder form. The lyophilized sample was transported in sterile falcon tubes at experimental site. The inoculum was developed in 10 ml of 2% glucose solution. The artificial infection was done in *A. malaccensis* tree in Dergaon, Assam using syringe method. Artificial infection was introduced in 4–5 years old *A. malaccensis* trees. Holes were made in a zigzag manner with a drill machine (5 mm diameter bit size) in the trunk of the tree. The initial hole was made 20 cm above from the ground and next wound was drilled at 10 cm interval and the depth of the drill was 1.5 cm. Around 1 ml of homogenized microbial culture was inoculated in each hole using sterile syringe and hole was covered with para film. Each strain was infected in replicates. A sterilized medium was used as a syringe control.

Gas Chromatography–Mass Spectroscopy Analysis

The wood samples (∼2–3 g) were collected 3 months after inducing artificial infection by drilling the wood around the inoculated hole. The collected of infected wood dust sample (1 g) were extracted in ethyl acetate by the reflux method. Uninoculated wood dust (wood control) and media control wood dust (syringe control) were also treated in similar manner to compare chemical composition with treated wood dust samples. The extract was concentrated in rotary evaporator. The concentrated extract was dissolved in 1 mL of dichloromethane and analyzed by Gas Chromatography-Mass Spectroscopy (GC-MS) (7890A/5975C, Agilent, California, United States) using an DB-WAX capillary column (30 m × 0.25 mm; film thickness 0.25 μm) and using Helium (purity > 99.999%) as the carrier gas with the constant flow rate of 1.0 mL/min. Around 1 μL of injection volume was used. The temperature of injector part was 230°C and oven temperature programing was used. The initial oven temperature was maintained at 80°C for 1 minute, then increased to 150°C @ 10°C/min in 7 min followed by temperature increase to 250°C @ 5°C/min till 22.5 min. The Mass Spectroscopic system was operated in EI mode (70 eV). Mass of the compounds was analyzed in the range of m/z 50–500 amu.

Data Analysis

Unscrambler version 10 (CAMO, USA) was used to perform Principal Component Analysis (PCA) and statistical analysis.

RESULTS

Identification of Fungi and Bacteria and Their Distribution

In all 340 fungi and 131 bacteria were isolated from 50 stem samples, and 188 fungi and 148 bacteria were isolated from 50 soil samples. These isolates were grouped on the basis of similarity of their external morphology and microscopic examination and representative isolates were used for molecular identification by 16s rRNA region amplification using 518F and 1492 R primers for bacteria and ITS region amplification using ITS1 and ITS4 primers for fungi and sequenced using Merck sequencing services, Bengaluru, India. Distribution of fungi and bacteria up to class level is given in **Figure 1** and up to genus level in **Figure 2**. The list of identified strains and their accession number along with % similarity with the best match with different sequence databases is given in supplementary information **Table S2**. The identification based on ITS sequence of fungal strains showed maximum diversity in the stem samples (**Table 3**). It was observed that in the stem five fungal classes viz. Eurotiomycetes, Dothideomycetes, Zygomycetes, Saccharomycetes, and Sordariomycetes represented fungal community, while in the soil samples only four out of the five classes were present. Saccharomycetes were not isolated from stem samples. In the case of bacteria Bacilli class was dominant in the stem and soil samples.Actionbacteria and Alpha Proteobacteria members were obtained only from the stem and Beta Proteobacteria only from the soil samples.

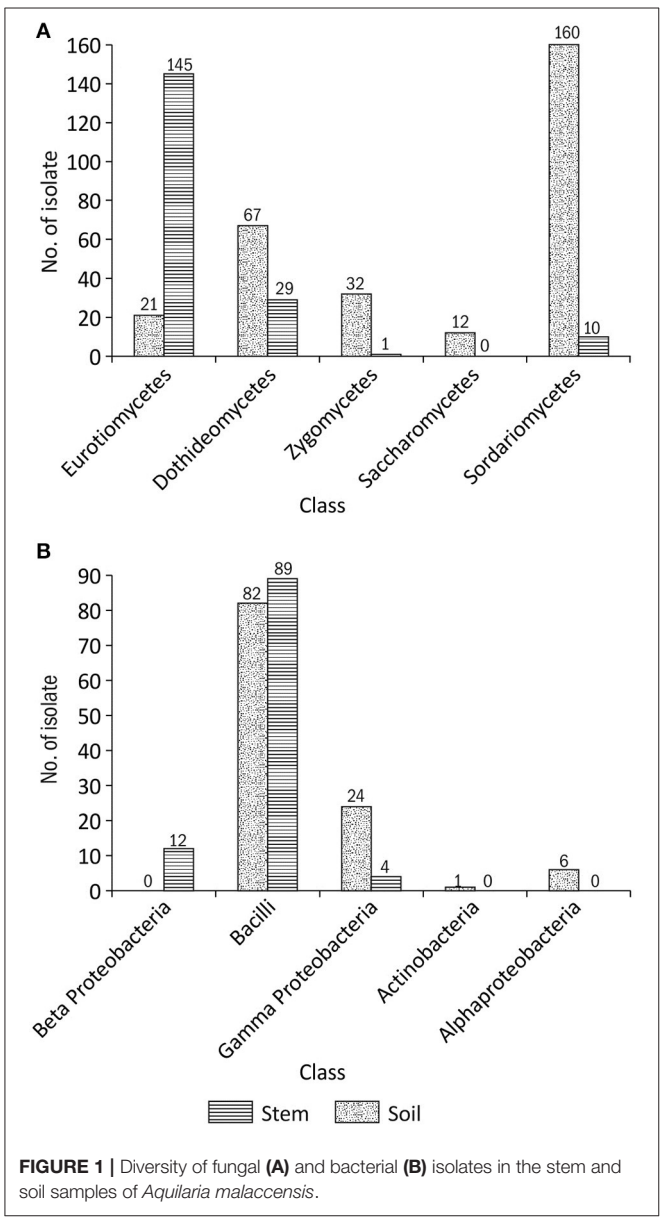


FIGURE 1 | Diversity of fungal **(A)** and bacterial **(B)** isolates in the stem and soil samples of *Aquilaria malaccensis*.

Phylogenetic and Microbial Diversity Analysis

The phylogenetic relation between different morphotypes isolated from stem and soil samples were measured by MEGA version 6.06 using the Neighbor-Joining (N-J) and Maximum Likelihood (M-L) method (**Figures 3**, **4**). Both type of method showed similar type of fungal and bacterial clusters. But in stem fungal isolate, *Meyerozyma guilliermondii* AQGWD10 showed less distant from *Lasiodiplodia* sp. cluster in N-J method while, in M-L method *M. guilliermondii* showed close to *Pichia* sp. (**Figure 3A**). In the case of soil fungal, soil and stem bacterial isolates cluster pattern was similar in both N-J and M-L method. In stem, 19 genera from 11 fungal families were identified using sequence similarity with NCBI database. In the stem, Hypocreaceae family was most dominant contributing 23.8% to richness while *Hypocrea* and *Trichoderma* genera, Botryospaeriaceae and Nectriaceae were second most commonly occurring family with 13.2 and 13.5% richness, having *Microdiplodia*, *Lasiodiplodia, Fusarium*, and *Gibberella* genera (**Table 1**). Pleosporace and Trichocomaceae family contributed only 6.5 and 6.2% richness, but contained 4 and 3 types of genera, including *Cochliobolus, Curvularia, Alterneria,* and *Epicoocum* in Pleosporace family and *Aspergillus, Penicillium,* and *Paecilomyces* in Trichocomaceae family. Around 14.1% of unidentified fungal sp. also contributed in fungal diversity. Likewise, in soil samples Trichocomaceae family showed the highest with 77.1% richness and members of Syncephalastraceae family was only isolated from soil samples.

The phylogenetic relation of these isolates is given in the **Figures 3**, **4**. In the case of bacteria, Bacillaceae is the dominant family in the stem and soil with 62.6 and 59.5% richness, respectively. Various bacterial families were isolated only in stem samples. Xanthomonadaceae showed 10.7% dominance, followed by Acetobacteraceae (4.6%) and Enterobacteriaceae (0.8%), while Alcaligenaceae and Paenibacillaceae showed presence only in the soil samples with 8.11% and 0.7% richness. Debaryomycetaceae, Saccharomycetaceae, Diaporthaceae, Clavicipitaceae, and Trichosphaeriaceae fungal families were exclusively isolated from stem, while Syncephalastraceae from soil samples. Similarly in bacteria, Enterobacteriaceae, Acetobacteraceae, and Xanthomonadaceae family was exclusively isolated from stem.

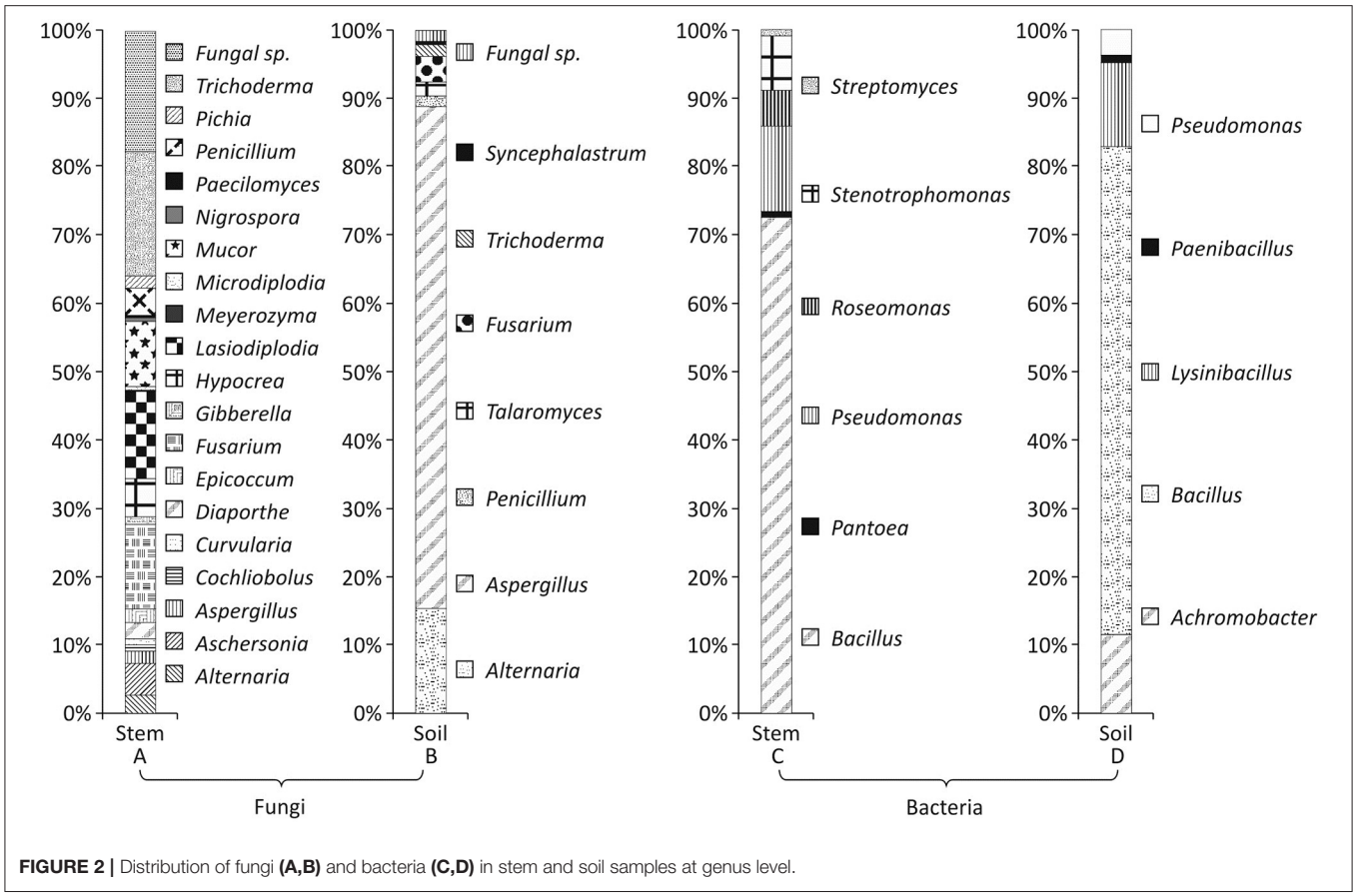


FIGURE 2 | Distribution of fungi **(A,B)** and bacteria **(C,D)** in stem and soil samples at genus level.

The fungal diversity of *A. malaccensis* in the North Eastern part of India was measured using Shannon diversity index (H'), Simpson index (D), and Fisher alpha index (α). Species richness in each source was measured by the Menhinick's diversity index (*Dmn*). The diversity index for all samples were measured by SPADES software and presented in **Table 2**. It was observed that stem were rich in fungal species (*Dmn* =0.034) followed by soil (*Dmn* = 0.02). A similar pattern was measured in bacteria also (stem = 0.03 and soil = 0.02). Source-specific fungal dominance by Camargo's index was the highest measured in soil (47.00) followed by stem (29.57) and bacterial dominance also observed the highest in soil (49.33) than stem (37.43). The dominant genus was *Tricoderma* in stem with their $Pi = 0.18$, while in soil *Aspergillus* showed dominance with $Pi = 0.73$. The next dominance genus was *Lasiodiplodia* ($Pi = 0.13$) and *Fusarium* ($Pi = 0.12$) in stem and *Alternaria* ($Pi = 0.15$) in soil. Rests of fungal species were less dominant <0.09. In bacteria, Bacillus genera showed dominance in both root and soil samples with $Pi = 0.62$ and 0.51, respectively. *Pseudomonas* was dominant in the stem and *Lysinibacillus* in soil with $Pi = 0.10$ and 0.09, respectively. The Pielou's evenness index showed the distribution of fungal and bacterial species evenly in soil ($J' = 0.18$ and 0.25) and stem ($J' = 0.42$ and 0.25). The Maximum Shannon diversity index was observed for stem fungal isolates ($H' = 2.43$) accompanied by soil bacteria ($H' = 1.25$), while the Simpson diversity index was the highest in soil bacteria ($H' = 2.84$) followed by stem bacteria in comparison to fungi. Fisher alpha (α) was measured the highest in fungal stem ($\alpha = 5.57$), followed by fungal soil ($\alpha = 1.70$) samples. The similarity of fungal and bacterial isolates from stem and soil were done using heat map expression. It is observed that stem and bacterial isolates showed less variation at genera level and creating a cluster in heat map (**Figure 5**).

Induction of Artificial Infection

Total 21 fungal and 19 bacterial strains isolated from infectious stem and surrounding soil were screened to assess their potential for induction of artificial infection in *A. malaccensis* tree. It was observed that the color of wood changed from white to brown/black after 3 months of infection in infected trees (**Figure 6**). Wood dust was harvested after 3months of inoculation and subjected to GC-MS analysis for confirmation of artificial infection on the basis of production of compounds presented in agarwood oil. In our previous study on comparison of GC-MS profile of infected and uninfected woods, we identified agarospirol, benzyl acetone and anisyl acetone as marker compounds for infection therefore, these compounds were selected as indicator for agrawood formation. Presence of agarospirol compound in the harvested wood confirmed the initiation of infection in the tree (**Figure S2** and **Table 3**). Other details such as percentage of benzyl acetone and anisyl acetone are provided in **Table S3**.

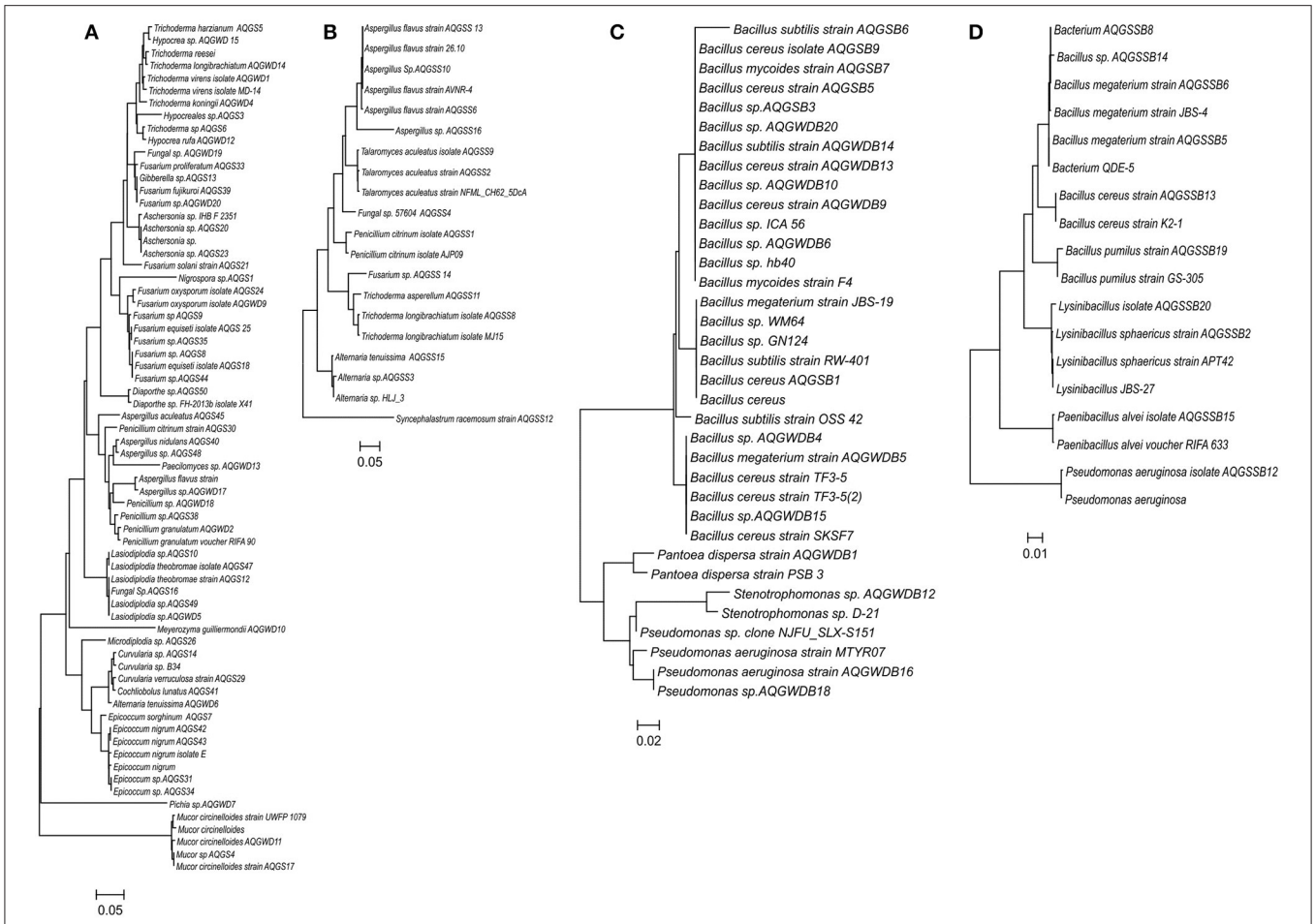


FIGURE 3 | Phylogenetic trees based on Neighbor-Joining method of the r DNA and ITS sequence of different fungi from stem **(A)** and soil **(B)** and bacterial isolates from stem of *Aquilaria malaccensis* **(C)** and soil **(D)**. 1000 replicates were calculated in the bootstrap.

It was noted that in comparison to uninfected wood and experimental control (syringe and wood controls) agarospirol was detected only in artificially infected wood samples. It is reported that the presence of agarospirol is one of the responsible compound for fragrance in agarwood (Kalra and Kaushik, 2017). Highest agarospirol content was measured in wood infected by *Pantoea dispersa* (3.77%), followed by fungi *Penicillium polonicum* (3.33%), *Syncephalastrum racemosum, Penicillium aethiopicum, and Trichoderma asperellum* (**Table 3**). The infection length was measured in the range of 2.00 to 11.83 cm. Strain *Paenibacillus alvei* AQGSSB15 showed the highest infection up to 11.83 cm in length. Although, agarospirol could not be detected in this sample, however, it showed presence of benzyl acetone confirming early stage of infection (**Table S3**). Highest agarospirol was measured in the sample infected by *Pantoea dispersa* AQGWDB1 and length of infection was found only up to 1.26 cm. Therefore, no relation was observed between infection length and agarospirol production. Based on the agarospirol formation, 31% of bacterial and 23% of fungal isolates showed their ability to produce agarospirol in agarwood through artificial infection (**Table 3**). Production of agarospirol was significantly higher with bacterial inoculum than the fungal inoculum with *P*-value 0.0057 (**Figure S3**). Principal component analysis (PCA) also showed two distinct clusters of bacteria and fungi (**Figures S4**, **S5**).

DISCUSSION

Fungi and Bacteria Identification and Their Distribution

Endophytes play an important role in plant physiology. Most of the endophytes are helpful in host plant growth, stress tolerance, and explained as the microorganisms that are not detrimental to the plant (Oses et al., 2008; Huang et al., 2009; Nimnoi et al., 2010). However, some had no beneficial impact and showed latent pathogenicity in plant species (Pojanagaroon and Kaewrak, 2005). Latent pathogenicity of endophytes could be an economical source of local community and *Aquilaria* is a live example in this regard, which produces oleoresin after infection and enhances the value of tree in market (Barden et al., 2000; Pojanagaroon and Kaewrak, 2005; Chhipa et al., 2017). Various studies have been done on isolation of endophytes from

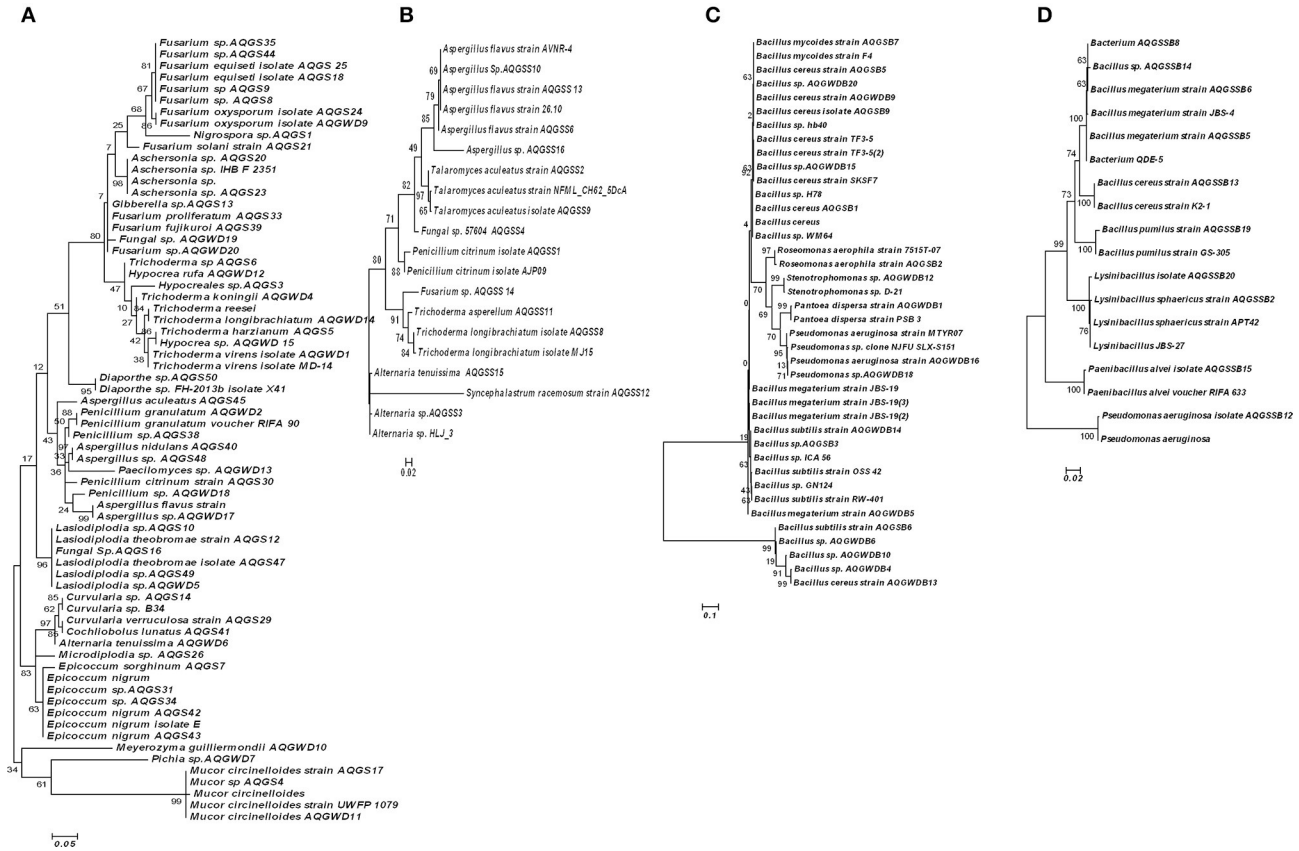


FIGURE 4 | Phylogenetic trees based on Maximum likelihood method of the SSU ribosomal sequence of different fungi from stem **(A)** and soil **(B)** and bacterial isolates from stem of *Aquilaria malaccensis* **(C)** and soil **(D)**.

TABLE 1 | Family dominance of fungus and bacteria isolated from stems and soil samples of *A. malaccensis*.

S. No.	Fungal family	Richness (%)		Bacterial family	Richness (%)	
		Stem	Soil		Stem	Soil
1	Botryosphaeriaceae	13.20	0.0	Acetobacteraceae	4.6	0.0
2	Clavicipitaceae	04.70	0.0	Alcaligenaceae	0.0	8.11
3	Debaryomycetaceae	00.30	0.0	Bacillaceae	62.6	59.5
4	Diaporthaceae	02.40	0.0	Enterobacteriaceae	0.8	0.0
5	Fungal sp	17.60	1.6	Paenibacillaceae	0.0	0.68
6	Hypocreaceae	23.80	1.6	Pseudomonadaceae	10.7	2.7
7	Mucoraceae	09.40	0.0	Xanthomonadaceae	6.9	0.0
8	Nectriaceae	13.50	3.7			
9	Pleosporaceae	06.50	15.4			
10	Saccharomycetaceae	01.80	0.0			
11	Syncephalastraceae	00.00	0.5			
12	Trichocomaceae	06.20	77.1			
13	Trichosphaeriaceae	00.60	0.0			

Aquilaria species, such as Malyasian *A. malaccensis* (Mohamed et al., 2010; Bhore et al., 2013); Chinese *A. sinensis* (Gong and Guo, 2009; Tian et al., 2013); Thai *A. crassna* (Nimnoi et al., 2010); *A. agallocha* (Tamuli et al., 2000), and Indian *A. malaccensis* (Bhore et al., 2013). However, very few reports are available on the development of artificial infection by using these endophytes (Mitra and Gogol, 2001; Mohamed et al., 2014). In the present study endophytic microbes of *Aquilaria* tree, and

soil microbes isolated from circumventing soils of *Aquilaria* tree were successfully utilized for induction of agarospirol formation through artificial inoculation,. *Trichoderma virens* was found as the most abundant fungi in stem followed by *Lasiodiplodia theobromae*, *Lasiodiplodia* sp., and *Fusarium equiseti* (4.9%). While Mohamed et al. (2010) observed a reverse pattern with *Fusarium* sp. as the most dominant and *Trichoderma* sp. as the least dominant in infected and similar fungal strains in non-infected samples of *A. malaccensis* in Malaysia region and suggested that these fungi might have little role in resin formation. Similarly, *Colletotrichum, Botryosphaeria*, *Phomopsis*, *Gloeosporioides,* and *Cylindrocladium* species are reported in wounded *Aquilaria* tree, while *Alternaria, Mycosphaerella, Ramichloridium, Sagenomella*, and *Phoma* species is in non-resinous tree of *A. sinensis* in China (Tian et al., 2013). While in the case of bacteria dominance of *Bacillus*, genus was observed in both soil and stem samples. *Pantoea, Roseomonas, Stenotrophomonas,* and *Streptomyces* genera were only obtained from stem samples, while *Achromobacter, Lysinibacillus,* and *Paenibacillus* were only observed in soil samples. Presence of endophytic actinomycetes including *Streptomyces, Nonomuraea, Actinomadura, Pesudonocardi,* and *Nocardia* genera is also reported in *A. crassna* (Nimnoi et al., 2010). Similarly, Bhore et al. (2013) demonstrated dominance of *Bacillus pumilus* (36.4%) among 18 different bacterial species in *Aquilaria* sp. of Malaysia region.

TABLE 2 | Diversity indexes of fungi and bacteria in the different samples.

Diversity index	Fungi		Bacteria	
	Stem	Soil	Stem	Soil
Shannon (*H'*)	2.43	0.95	1.20	1.30
Simpson index (*D*)	0.10	0.56	0.42	0.40
Simpson Diversity index (1-D)	0.90	0.44	2.35	2.80
Fisher (α)	5.57	1.70	1.58	1.30
Menhinick's Diversity (*Dmn*)	0.034	0.02	0.03	0.02
Pielou's Evenness index (*J'*)	0.42	0.18	0.25	0.25
Camargo's index (1/ *Dmn*)	29.57	47.0	37.43	49.33

Phylogenetic and Microbial Diversity Analysis

In the case of the *Aquilaria* plant, microbial diversity and dominance could be species and region specific. Kusari et al. (2012) observed that 70% of isolates in soil and plant part are common. It suggests that the plant and endophytes association developed after overcoming many physical and chemical barriers and particular fungi established as endophytes in a particular niche or localized in the tissue in a systemic manner (Hyde and Soytong, 2008). Subsequently, pathogenicity is also affected by the surrounding environment as endophytic to host plant in one ecosystem can be pathogenic in another ecological niche. It is reported that endophytic and pathogenic lifestyle are inter convertible due to environmental, chemical, and molecular elicitors (Schulz et al., 2002; Eaton et al., 2011).

In the present study, higher diversity of microbial isolates has been observed in the stem than the soil samples. The Shannon and Fisher alpha diversity index in the stem measured the highest

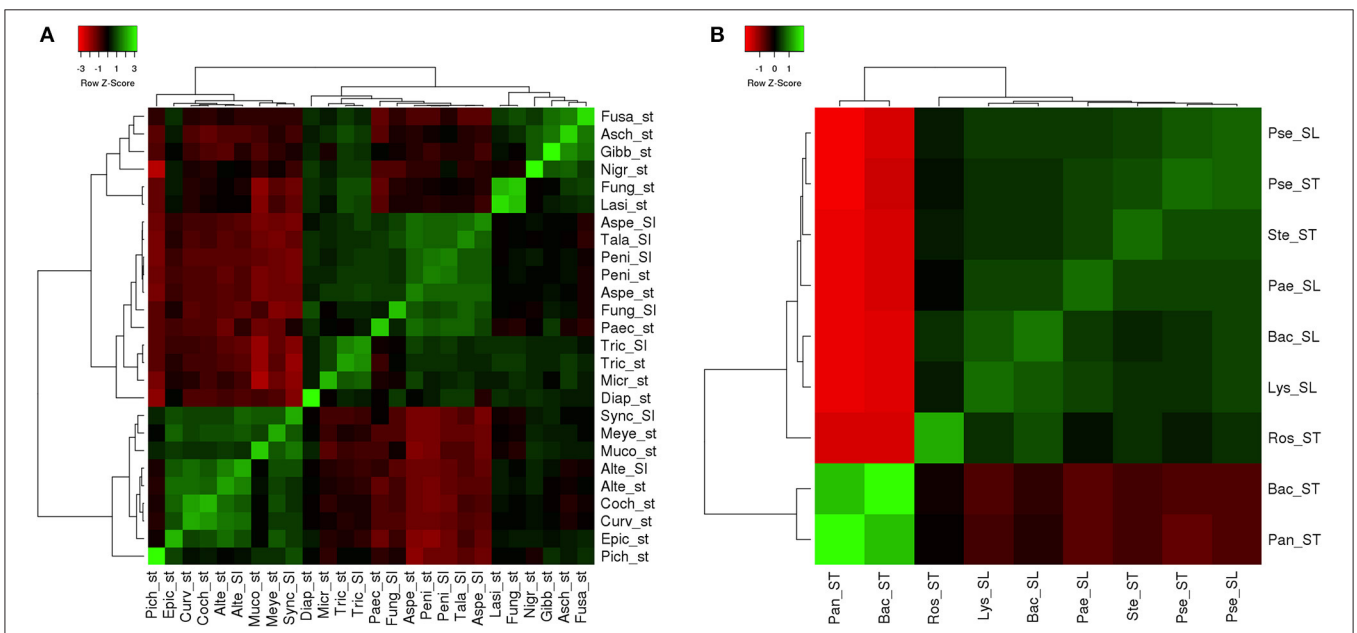


FIGURE 5 | Heat map analysis of **(A)** fungi and **(B)** bacterial isolates from stem and soil samples. St, stem isolate; Sl, Soil isolate; Pich, *Pichia*; Epic, *Epicoccum*; Curv, *Curvularia*; Coch, *Cochliobolus*; Alte, *Alternaria*; Muco, *Mucor*; Meye, *Meyerozyma*; Sync, *Syncephalastrum*; Diap, *Diaporthe*; Micr, *Microdiplodia*; Tric, *Trichoderma*; Pace, *Paecilomyces*; Fung, Fungal; Aspe, *Aspergillus*; Peni, *Penicillium*; Tala, *Talaromyces*; Lasi, *Lasiodiplodia*; Nigr, *Nigrospora*; Gibb, *Gibberella*; Asch, *Aschersonia*; Fusa, *Fusarium*; Pan, *Pantoea*; Bac, *Bacillus*; Ros, Roseomonas; Lys, *Lysinibacillus*; Pae, *Paenibacillus*; Ste, *Stenotrophomonas*; Pse, *Pseudomonas*.



FIGURE 6 | Artificial infection in different *Aquilaria malaccensis* trees after 3 months of inoculation of fungal and bacterial strain: Dark brownish color of wood showing the initiation of artificial infection.

TABLE 3 | Agarospirol content and infection length obtained with different fungal and bacterial strains 3 months after the artificial inoculation in the *A. malaccensis* trees.

S. No.	Species	Type of organism	Source	Agarospirol[*a,b,c] (2-(6,10-Dimethylspiro[4,5]dec-6-en-2-yl)-2-propanol)	Infection
				Content (%)	Length (cm)
1	*Pantoea dispersa* AQGWDB1	Bacteria	Stem	3.77	1.26
2	*Penicillium polonicum AQGGR1.1*	Fungi	Stem	3.33	2.60
3	*Syncephalastrum racemosum AQGSS 12*	Fungi	Soil	1.34	2.60
4	*Penicillium aethiopicum AQGGR1.2*	Fungi	Stem	0.67	3.00
5	*Trichoderma asperellum AQGSS 11*	Fungi	Soil	0.20	3.00
6	*Bacillus cereus AQGWDB9*	Bacteria	Stem	0.09	3.45
7	*Penicillium polonicum AQGGR1.1*	Fungi	Stem	0.08	2.60
8	(Unidentified) AQGSSB23	Bacteria	Soil	0.06	2.00
9	*Bacillus anthricus strain AQGWDB2*	Bacteria	Stem	0.05	2.91
10	*Rhizopus oryzae AQGGR1.3*	Fungi	Stem	0.05	2.00
11	(Unidentified) AQGWDB7	Bacteria	Stem	0.05	3.33
12	*Bacillus megaterium AQGWDB 3*	Bacteria	Stem	0.03	2.35
13	Wood control	Control		0.00	0.00

*Variance comparison at significant level: 0.05.
*[a] Fungi vs. control- P-value < 0.001.
*[b] Bacteria vs. control -P-value < 0.001.
*[c] Bacteria vs. Fungi -P-value = 0.0057231.

value showing diversity and abundance of endophytes in stem comparison to soil samples. The results are similar to previously reported by Kumar and Hyde (2004) in *Tripterigium wilfordii* and Gond et al. (2012) in *Nyctanthes arbortristis* showed the highest Shannon index in stem.

Induction of Artificial Infection

The development of artificial infection method using endophytic and soil microorganisms will provide significant impact on agarwood production. In present study, 31% of bacterial and 23% of fungal isolates showed positive response in agarwood formation by production of agarospirol compound within 3 months of infection. To the best of our knowledge no previous study has reported agarospirol production by artificial infection in 3 months. Zhang et al. (2012) reported agarwood production in 6 months after infection, while Lin et al. (2010) after 12 months. The maximum amount of Agarospirol was induced by *Pantoea dispersa* AQGWDB1 followed by *Penicillium polonicum* AQGGR1.1. Previously, various researchers have used fungi in Agarwood formation (Chhipa et al., 2017). However, this is the first report on use of bacteria in artificial infection and agarospirol production (Bose, 1934; Bhattacharyya et al., 1952; Jalaluddin, 1977; Venkataramanan et al., 1985; Beniwal, 1989; Tamuli et al., 2000; Mitra and Gogol, 2001). Further, Studies on artificial infection have been reported by *Aspergillus* sp., *Lasiodiplodia* sp., *Fusarium* sp., *Penicillium* sp., and *Trichoderma* sp. (Yunita, 2009; Akter et al., 2013). Recently, Mohamed et al. (2014) also reported artificial Agarwood formation in young *A. malaccensis* tree by fungal inoculation. Similarly, Lin et al. (2010) also reported that fungus *Melanotus flavolivence* is also capable of inducing Agarwood formation after 6 months of infection. It has been reported that the accumulation of plant secondary metabolites can be the result of microbial stimulation. Cui et al. (2013) also demonstrated the production of resin-containing organic volatile fatty acid in response to fungal attack. This process is called "tylosis." The resin increases the density and changes the color of the wood from pale to dark brown or black. In present study, it was observed that 41% of stem isolates showed their potential in development of agarospirol while 13.6% soil isolates could induce agarwood infection, confirming the role of endophytes in

agarwood formation. This study is extremely beneficial for local tribes of north-eastern part of India where Agarwood is treated as an economic resource (Lin et al., 2010). Identification of such microbes that can induce agarwood production at short time exposure and validation at field levels has lot of potentials for future research.

CONCLUSION

Endophytes are helpful in plant physiology by producing different compounds, which assist in plant growth, stress tolerance, and plant immunity. Isolation and identification of such microbes are an important aspect for biotechnological applications. In present study, we could isolate total 528 fungi and 279 bacteria from Aquilaria stem and surrounding soil samples collected from different sites of Assam. Bacilli were found most dominant class in the bacteria and Sordariomycetes in fungi. In stem, Hypocreaceae was measured most dominant fungal family with 23.8% richness while Bacileaceae was dominant bacterial family with 62.6 and 59.5% richness in both stem and soil isolates. Maximum Shannon diversity index was measured in stem fungal isolates ($H' = 2.43$). Agarospirol production was induced successfully using bacteria *Pantoea dispersa* (3.77%) and fungi *Penicillium polonicum* (3.33%) within 3 months only, after inducing the infection. The agarospirol is one of the responsible compounds for fragrance in Agarwood. The use of such microbes in artificial production of agarospirol could be source of economic development of villagers of North Eastern part of India.

AUTHOR CONTRIBUTIONS

Conception and designed the experiments: HC and NK. Performed the experiments: HC. Analyzed the data: HC and NK. Contributed reagents/materials/analysis tools: HC and NK. Wrote and enriched the literature: HC and NK. Corrected the manuscript: NK.

FUNDING

This work has been supported by the Department of Biotechnology, Government of India, Research Grant no BT/PR1505/NDB/38/223/2011.

ACKNOWLEDGMENTS

We are highly thankful to Mr. Surjit Bohra, Golaghat, Assam and R. K. Mohsang Society, Jairampur, Arunachal Pradesh for providing *Aquilaria* trees for experimental purpose. We are highly thankful to Dr. L. R. Bhuyan, SFRI, Itanagar, for identification of the *Aquilaria malaccensis* tree.

SUPPLEMENTARY MATERIAL

The Supplementary Material for this article can be found online at: http://journal.frontiersin.org/article/10.3389/fmicb.2017.01286/full#supplementary-material

Figure S1 | Site map of the districts selected for sample collection.

Figure S2 | GC-MS profile of oil extracted from artificial infected wood dust sample inoculated with *Pantoea dispersa* AQGWDB1 **(A)** and *Penicillium aethiopicum* AQGGR1.2 **(B)** showing the presence of the agarospirol compound in gas chromatogram mass spectrum of Agarospirol compound (RT 35.72) **(C)**.

Figure S3 | *F*-test of significance for agarospirol content variation between fungal infected and control wood **(A)**, bacterial infected and control wood **(B)** and fungal and bacterial infected wood **(C)**.

Figure S4 | Bi plot of GC data of bacterial and fungal infected wood samples collected 3 months after artificial inoculation Bacteria Fungi.

Figure S5 | PCA plot of GC data of bacterial and fungal infected wood samples collected 3 months after artificial inoculation Bacteria Fungi.

Table S1 | List of sample collected from different districts of Assam for microbial isolation.

Table S2 | Identification of fungal and bacterial isolates on the basis of sequence similarity with different sequence data base.

Table S3 | Per cent composition of compounds in oleoresin extract identified by gas chromatography mass spectroscopy.

REFERENCES

Akter, S., Islam, M. T., Zulkefeli, M., and Khan, S. I. (2013). Agarwood production-a multidisciplinary field to be explored in Bangladesh. *Int. J. Pharm. Life Sci.* 2, 22–32. doi: 10.3329/ijpls.v2i1.15132

Babicki, S., Arndt, D., Marcu, A., Liang, Y., Grant, J. R., Maciejewski, A., et al. (2016). Heatmapper: web-enabled heat mapping for all. *Nucleic Acids Res.* 44, W147–W153. doi: 10.1093/nar/gkw419

Barden, A., Awang, A., Mulliken, T., and Song, M. (2000). *Heart of the Matter Agarwood Use and Trade and CITES Implementation for Aquilaria Malaccensis.* Cambridge: Traffic International.

Beniwal, B. S. (1989). Silvical characteristics of *Aquilaria agallocha* Roxb. *Indian Forester* 115, 17–21.

Bhattacharyya, B., Datta, A., and Baruah, H. K. (1952). On the formation and development of agaru in *Aquilaria agallocha*. *Sci. Cult.* 18, 240–243.

Bhore, S. J., Preveena, J., and Kandasamy, K. I. (2013). Isolation and identification of bacterial endophytes from pharmaceutical agarwood-producing Aquilaria species. *Pharmacognosy Res.* 5, 134–137. doi: 10.4103/0974-8490.110545

Bhuiyan, M. N., and Bhuiyan, M. N. J. (2008). Analysis of essential oil of eaglewood tree (*Aquilaria agallocha* Roxb.) by gas chromatography mass spectrometry. *Bangladesh J. Pharmacol.* 4, 24–28. doi: 10.3329/bjp.v4i1.851

Bose, S. R. (1934). The nature of agar formation. *Sci. Cult.* 4, 89–91

Camargo, J. A. (1992). Temporal and spatial variations in dominance, diversity and biotic indices along a limestone stream receiving a trout farm effluent. *Water Air Soil Pollut.* 63, 343–359. doi: 10.1007/BF00475501

Chao, A., and Shen, T. J. (2010). *Program SPADE (Species Prediction and Diversity Estimation). Program and User's Guide*. Available online at: http://chao.stat.nthu.edu.tw

Chen, H., Yang, Y., Xue, J., Wei, J., Zhang, Z., and Chen, H.f (2011). Comparison of compositions and antimicrobial activities of essential oils from chemically stimulated agarwood, wild agarwood and healthy *Aquilaria sinensis* (Lour.) Gilg trees. *Molecules* 16, 4884–4896. doi: 10.3390/molecules16064884

Chhipa, H., Chowdhary, K., and Kaushik, N. (2017). Artificial production of agarwood oil in *Aquilaria* sp. by fungi: a review. *Phytochem. Rev.* doi: 10.1007/s11101-017-9492-6. [Epub ahead of print].

CITES (1994). "Resolution of the conference of the parties," in *Ninth Meeting of the Conference of the Parties*, Fort Lauderdale, FL.

Cui, J., Wang, C., Guo, S., Yang, L., Xiao, P., and Wang, M. (2013). Evaluation of fungus-induced agilawood from *Aquilaria sinensis* in China. *Symbiosis* 60, 37–44. doi: 10.1007/s13199-013-0237-z

Eaton, C. J., Cox, M. P., and Scott, B. (2011). What triggers grass endophytes to switch from mutualism to pathogenism? *Plant Sci.* 180, 190–195. doi: 10.1016/j.plantsci.2010.10.002

Gibson, I. A. (1977). The role of fungi in the origin of oleoresin deposits (agaru) in the wood of *Aquilaria agallocha* Roxb. *Bano Biggyan Patrika* 6, 16–26.

Gond, S. K., Mishra, A., Sharma, V. K., Verma, S. K., Kumar, J., Kharwar, R. N., et al. (2012). Diversity and antimicrobial activity of endophytic fungi isolated from nyctanthes arbor-tristis, a well-known medicinal plant of India. *Mycoscience* 53, 113–121. doi: 10.1007/S10267-011-0146-Z

Gong, L., and Guo, S. (2009). Endophytic fungi from *Dracaena cambodiana* and *Aquilaria sinensis* and their antimicrobial activity. *Afr. J. Biotechnol.* 8, 731–736. Available online at: https://www.ajol.info/index.php/ajb/article/view/59937/48209

Hai, L. E., Shyun, C. Y., and Yusoff, A. M., (1999). Early survival and growth in field trials of *Aquilaria malaccensis* (karas) and *Azadirachta excelsa* (sentang). *J. Trop. For. Sci.* 11, 852–854.

Huang, W. Y., Cai, Y. Z., Surveswaran, S., Hyde, K. D., Corke, H., and Sun, M. (2009). Molecular phylogenetic identification of endophytic fungi isolated from three Artemisia species. *Fungal Divers.* 36, 69–88. Available online at: www.fungaldiversity.org/fdp/sfdp/FD36-5.pdf

Huang, Y. L., Kuang, Z. Y., Song, M. W., and Zhang, R. (2015). Community structure and difference of endophtic bacteria in *Aquilaria sinensis* with and without agarwood. *Zhongguo Zhong Yao Za Zhi* 40, 63–67. Available online at: http://europepmc.org/abstract/med/25993789

Hyde, K. D., and Soytong, K. (2008). The fungal endophyte dilemma. *Fungal Divers.* 33, 163–173. Available online at: www.fungaldiversity.org/fdp/sfdp/33-9.pdf

Ito, M., Okimoto, K. I., Yagura, T., Honda, G., Kiuchi, F., and Shimada, Y. (2005). Induction of sesquiterpenoid production by methyl jasmonate in *Aquilaria sinensis* cell suspension culture. *J. Essent. Oil Res.* 17, 175–180. doi: 10.1080/10412905.2005.9698867

IUCN (2009). "Asian Regional Workshop (Conservation & Sustainable Management of Trees, Vietnam) 1998. Aquilaria malaccensis," in *IUCN 2009, IUCN Red List of Threatened Species*, Version 2009.2.2. (Hanoi). Available online at: http://www.iucnredlist.org/details/32056/0

Jalaluddin, M. A. (1977). Useful pathological condition of wood. *Econ. Bot.* 31, 222–224. doi: 10.1007/BF02866592

Kalra, R., and Kaushik, N. (2017). A review of chemistry, quality and analysis of infected agarwood tree (Aquilaria sp.). *Phytochem. Rev.* doi: 10.1007/s11101-017-9518-0. [Epub ahead of print].

Kasana, R. C., Salwan, R., Dhar, H., Dutt, S., and Gulati, A. (2008). A rapid and easy method for the detection of microbial cellulases on agar plates using Gram's iodine. *Curr. Microbiol.* 57, 503–507. doi: 10.1007/s00284-008-9276-8

Kim, Y. C., Lee, E. H., Lee, Y. M., Kim, H. K., Song, B. K., Lee, E. J., et al. (1997). Effect of the aqueous extract of *Aquilaria agallocha* stems on the immediate hypersensitivity reactions. *J. Ethnopharmacol.* 58, 318. doi: 10.1016/S0378-8741(97)00075-5

Kumar, D. S., and Hyde, K. D. (2004). Biodiversity and tissue-recurrence of endophytic fungi in *Tripterygium wilfordii*. *Fungal Divers.* 17, 69–90. Available online at: www.fungaldiversity.org/fdp/sfdp/17-6.pdf

Kumar, S., Kaushik, N., Edrada-Ebel, R., Ebel, R., and Proksch, P. (2011). Isolation, characterization, and bioactivity of endophytic fungi of *Tylophora indica*. *World J. Microbiol. Biotechnol.* 27, 571–577. doi: 10.1007/s11274-010-0492-6

Kumeta, Y., and Ito, M. (2010). Characterization of δ-guaiene synthases from cultured cells of *Aquilaria*, responsible for the formation of the sesquiterpenes in agarwood. *Plant Physiol.* 154, 1998–2007. doi: 10.1104/pp.110.161828

Kusari, S., Hertweck, C., and Spiteller, M. (2012). Chemical ecology of endophytic fungi: origins of secondary metabolites. *Chem. Biol.* 19, 792–798. doi: 10.1016/j.chembiol.2012.06.004

Lin, F., Mei, W. L., Wu, J., and Dai, H. F. (2010). GC-MS analysis of volatile constituents from Chinese eaglewood produced by artificial methods. *Zhong Yao Cai* 33, 222–225.

Liu, Y., Chen, H., Yang, Y., Zhang, Z., Wei, J., Meng, H., et al. (2013). Whole-tree agarwood-inducing technique: an efficient novel technique for producing high-quality agarwood in cultivated *Aquilaria sinensis* trees. *Molecules* 18, 3086–3106. doi: 10.3390/molecules18033086

Mengling, H. E., Shu-yuan, Q. I., and Lan-juan, H. U. (2005). Rapid *in vitro* propagation of medicinally important *Aquilaria agallocha*. *J. Zhejiang Univ. Sci. B* 6, 849–852. doi: 10.1631/jzus.2005.B0849

Mitra, J., and Gogol, P. (2001). "Fungi associated with the diseased wood (agarwood/agaru) of Aquilaria agallocha Roxb. grown in Assam," in *Proceedings of Seminar on Scope and Dimension of Agar Plantation in NE Region of New Delhi, India*, eds M. Ahmed, P. Gogoi, and G. U. Ahmed (Hojai: AATMA), 61–69.

Mohamed, R., Jong, P. L., and Kamziah, A. K. (2014). Fungal inoculation induces agarwood in young *Aquilaria malaccensis* trees in the nursery. *J. Forestry Res.* 25, 201–204. doi: 10.1007/s11676-013-0395-0

Mohamed, R., Jong, P. L., and Zali, M. S. (2010). Fungal diversity in wounded stems of *Aquilaria malaccensis*. *Fungal Divers.* 43, 67–74. doi: 10.1007/s13225-010-0039-z

Nimnoi, P., Pongsilp, N., and Lumyong, S. (2010). Endophytic actinomycetes isolated from *Aquilaria crassna* Pierre ex Lec and screening of plant growth promoters production. *World J. Microbiol. Biotechnol.* 26, 193–203. doi: 10.1007/s11274-009-0159-3

Nishiguchi, M. K., Doukakis, P., Egan, M., Kizirian, D., Phillips, A., Prendini, L., et al. (2002). "DNA isolation procedures," in *Techniques in Molecular Systematics and Evolution*, eds R. DeSalle, G. Giribet, and W. Wheeler (Basel: Springer Science & Business Media), 249–287.

Novriyanti, E., Santosa, E., Syafii, W., Turjaman, M., and Sitepu, I. R. (2010). Anti-fungal activity of wood extract of *Aquilaria crassna* pierre ex lecomte against agarwood-inducing fungi, *Fusarium solani*. *Indones. J. Forestry Res.* 7, 155–165. doi: 10.20886/ijfr.2010.7.2.155-165

Okudera, Y., and Ito, M. (2009). Production of agarwood fragrant constituents in *Aquilaria calli* and cell suspension cultures. *Plant Biotechnol.* 26, 307–315. doi: 10.5511/plantbiotechnology.26.307

Oses, R., Valenzuela, S., Freer, J., Sanfuentes, E., and Rodriguez, J. (2008). Fungal endophytes in xylem of healthy Chilean trees and their possible role in early wood decay. *Fungal Divers.* 33, 77–86. Available online at: www.fungaldiversity.org/fdp/sfdp/33-4.pdf

Pojanagaroon, S., and Kaewrak, C. (2005). "Mechanical methods to stimulate aloes wood formation in *Aquilaria crassna* Pierre ex H. Lec.(Kritsana) trees," in *III WOCMAP Congress on Medicinal and Aromatic Plants-Volume 2: Conservation, Cultivation and Sustainable Use of Medicinal*, eds A. Jatisatienr, T. Paratasilpin, S. Elliott, V. Anusarnsunthorn, D. Wedge, L. E. Craker, and Z. E. Gardner (Chiang Mai: International Society for Horticultural Science) 161–166.

Schulz, B., Boyle, C., Draeger, S., Römmert, A. K., and Krohn, K. (2002). Endophytic fungi: a source of novel biologically active secondary metabolites. *Mycol. Res.* 106, 996–1004. doi: 10.1017/S0953756202006342

Tamuli, P., Boruah, P., Nath, S. C., and Samanta, R. (2000). Fungi from diseased agarwood tree (*Aquilaria agallocha* Roxb.): two new records. *Adv. Forestry Res. India* 22, 182–187. Available online at: https://www.cabdirect.org/cabdirect/abstract/20023060621

Tian, J. J., Gao, X. X., Zhang, W. M., Wang, L., and Qu, L. H. (2013). Molecular identification of endophytic fungi from *Aquilaria sinensis* and artificial agarwood induced by pinholes-infusion technique. *Afr. J. Biotechnol.* 12, 3115–3131. doi: 10.5897/AJB11.3159

Venkataramanan, M. N., Borthakur, R., and Singh, H. D. (1985). Occurrence of endotrophic myccorhizzal fungus in agarwood plant *Aquilaria agallocha* Roxb. *Curr. Sci.* 54, 928.

Wei, J. H., Zhang, Z., Yang, M. H., Gao, Z. H.,Chen, W. P., Feng, J. D., et al. (2012). *Tambac Inducer and Preparation Method*. CN101731282B.

Whittaker, R. H. (1972). Evolution and measurement of species diversity. *Taxonomy* 21, 213–251. doi: 10.2307/1218190

Xu, Y., Zhang, Z., Wang, M., Wei, J., Chen, H., Gao, Z., et al. (2013). Identification of genes related to agarwood formation: transcriptome analysis of healthy and wounded tissues of *Aquilaria sinensis*. *BMC Genomics* 14:227. doi: 10.1186/1471-2164-14-227

Yunita, L. (2009). *Effectivity of Acremonium sp. and Methyl Jasmonate to Improve Agarwood Quality of Aquilaria Microcarpa*. IPB Scientific Repository, Bogor Agricultural University. Available online at: http://repository.ipb.ac.id/handle/123456789/14803

Zhang, X. L., Liu, Y. Y., Wei, J. H., Yang, Y., Zhang, Z., Huang, J. Q., et al. (2012). Production of high-quality agarwood in *Aquilaria sinensis* trees via whole-tree agarwood-induction technology. *Chin. Chem. Lett.* 23, 727–730. doi: 10.1016/j.cclet.2012.04.019

Zhang, Z., Yang, Y., Meng, H., Sui, C. H., Wei, J. H., and Chen, H. Q., (2010). Advances in studies on mechanism of agarwood formation in *Aquilaria sinensis* and its hypothesis of agarwood formation induced by defense response. *Chin. Trad. Herbal Drugs* 41, 156–159. Available online at: http://en.cnki.com.cn/Article_en/CJFDTOTAL-ZCYO201001045.htm

Zhang, Z., Zhang, X., Yang, Y., Wei, J. H., Meng, H., Meng, Z. H., et al. (2014). Hydrogen peroxide induces vessel occlusions and stimulates sesquiterpenes accumulation in stems of *Aquilaria sinensis*. *Plant Growth Regul.* 72, 81–87. doi: 10.1007/s10725-013-9838-z

Conflict of Interest Statement: The authors declare that the research was conducted in the absence of any commercial or financial relationships that could be construed as a potential conflict of interest.

Copyright © 2017 Chhipa and Kaushik. This is an open-access article distributed under the terms of the Creative Commons Attribution License (CC BY). The use, distribution or reproduction in other forums is permitted, provided the original author(s) or licensor are credited and that the original publication in this journal is cited, in accordance with accepted academic practice. No use, distribution or reproduction is permitted which does not comply with these terms.

frontiers in Microbiology

ORIGINAL RESEARCH
published: 20 October 2017
doi: 10.3389/fmicb.2017.02037

In Vivo Study of the Sorbicillinoid Gene Cluster in *Trichoderma reesei*

*Christian Derntl[1], Fernando Guzmán-Chávez[2], Thiago M. Mello-de-Sousa[1], Hans-Jürgen Busse[3], Arnold J. M. Driessen[2], Robert L. Mach[1] and Astrid R. Mach-Aigner[1]**

[1] Research Area Biochemical Technology, Institute of Chemical, Environmental & Biological Engineering, Vienna, Austria, [2] Molecular Microbiology, Groningen Biomolecular Sciences and Biotechnology Institute, University of Groningen, Groningen, Netherlands, [3] Institute of Microbiology, University of Veterinary Medicine, Vienna, Austria

Sorbicillinoids are a diverse group of yellow secondary metabolites that are produced by a range of not closely related ascomycetes, including *Penicillium chrysogenum*, *Acremonium chrysogenum*, and *Trichoderma reesei*. They share a similarity to the name-giving compound sorbicillin, a hexaketide. Previously, a conserved gene cluster containing two polyketide synthases has been identified as the source of sorbicillin, and a model for the biosynthesis of sorbicillin in *P. chrysogenum* has been proposed. In this study, we deleted the major genes of interest of the cluster in *T. reesei*, namely *sor1*, *sor3*, and *sor4*. Sor1 is the homolog of *P. chrysogenum* SorA, which is the first polyketide synthase of the proposed biosynthesis pathway. Sor3 is a flavin adenine dinucleotide (FAD)-dependent monooxygenase, and its homolog in *P. chrysogenum*, SorC, was shown to oxidize sorbicillin and 2′,3′-dihydrosorbicillin to sorbicillinol and 2′,3′-dihydrosorbicillinol, respectively, *in vitro*. Sor4 is an FAD/flavin mononucleotide-containing dehydrogenase with an unknown function. We measured the amounts of synthesized sorbicillinoids throughout growth and could verify the roles of Sor1 and Sor3 *in vivo* in *T. reesei*. In the absence of Sor4, two compounds annotated to dihydrosorbicillinol accumulate in the supernatant and only small amounts of sorbicillinol are synthesized. Therefore, we suggest extending the current biosynthesis model about Sor4 reducing 2′,3′-dihydrosorbicillin and 2′,3′-dihydrosorbicillinol to sorbicillinol and sorbicillinol, respectively. Sorbicillinol turned out to be the main chemical building block for most sorbicillinoids, including oxosorbicillinol, bisorbicillinol, and bisvertinolon. Further, we detected the sorbicillinol-dependent synthesis of 5-hydroxyvertinolide at early time points, which contradicts previous models for biosynthesis of 5-hydroxyvertinolide. Finally, we investigated whether sorbicillinoids from *T. reesei* have a growth limiting effect on the fungus itself or on plant pathogenic fungi or on pathogenic bacteria.

Keywords: sorbicillinoids, sorbicillinol, 5-hydroxyvertinolide, *Trichoderma reesei*, *Acremonium chrysogenum*, *Penicillium chrysogenum*

OPEN ACCESS

Edited by:
Bhim Pratap Singh, Mizoram University, India

Reviewed by:
Roberto Silva, University of São Paulo, Brazil
Chandra Nayak, University of Mysore, India

****Correspondence:***
Astrid R. Mach-Aigner
astrid.mach-aigner@tuwien.ac.at

Specialty section:
This article was submitted to Microbiotechnology, Ecotoxicology and Bioremediation, a section of the journal Frontiers in Microbiology

Received: *31 March 2017*
Accepted: *05 October 2017*
Published: *20 October 2017*

Citation:
Derntl C, Guzmán-Chávez F, Mello-de-Sousa TM, Busse H-J, Driessen AJM, Mach RL and Mach-Aigner AR (2017) In Vivo Study of the Sorbicillinoid Gene Cluster in Trichoderma reesei. Front. Microbiol. 8:2037. doi: 10.3389/fmicb.2017.02037

INTRODUCTION

Sorbicillinoids are a group of yellow secondary metabolites that are produced by a range of ascomycetes, including *Penicillium* (Cram, 1948) and *Trichoderma* (Abe et al., 2000). Many of these hexaketide metabolites are highly oxygenated and have complex bicyclic and tricyclic frameworks (Harned and Volp, 2011). However, their name-giving, common feature is an apparent similarity of

their core structures to sorbicillin (**Figure 1**, compound **1**). Many sorbicillinoids possess interesting bioactive properties. For instance, bisorbicillinoids have been demonstrated to have outstanding radical scavenging properties (Abe and Hirota, 2002). Additionally, trichodimerol was shown to inhibit the tumor necrosis factor-a (TNF-a) via targeting the prostaglandin H synthase-2, and thus to act anti-inflammatorily (Mazzucco and Warr, 1996; Warr et al., 1996). Further, some sorbicillinoids have been demonstrated to show antimicrobial activity (Maskey et al., 2005; Reategui et al., 2006). Zhao et al. (2017) observed anti-HIV and anti-inflammatory activities of sorbicillinoids. For detailed reviews about sorbicillinoids and their bioactive properties refer to (Meng et al., 2016) and (Harned and Volp, 2011).

The proposed biosynthesis pathway of sorbicillin in *P. chrysogenum* includes the consecutive action of the two polyketide synthases (PKS), SorA and SorB, resulting in the release of an aldehyde that undergoes spontaneous cyclization, yielding sorbicillin or 2′,3′-dihydrosorbicillin (**Figure 1**; Fahad et al., 2014). Notably, sorbicillin and 2′,3′-dihydrosorbicillin were isolated and identified from *P. chrysogenum* cultures previously (Trifonov et al., 1983). Fahad et al. (2014) demonstrated that an oxidative dearomatization of sorbicillin and 2′,3′-dihydrosorbicillin (**2**) by the flavin adenine dinucleotide (FAD)-dependent monooxygenase SorC leads to the formation of sorbicillinol (**3**), and 2′,3′-dihydrosorbicillinol (**4**) *in vitro*, respectively (**Figure 1**). Sorbicillinol is highly reactive and therefore considered to be the main building block for the formation of bicyclic sorbicillinoids such as bisorbicillinol and trichodimerol (Harned and Volp, 2011).

In *P. chrysogenum*, the genes encoding for the two PKS, SorA and SorB, and the FAD-dependent monooxygenase SorC are part of a gene cluster (Salo et al., 2016), which is also present in a range of not closely related ascomycetes, including *T. reesei* and *Acremonium chrysogenum* (Martinez et al., 2008; Terfehr et al., 2014; Derntl et al., 2016; **Figure 2**). The core set of the gene cluster consists of genes encoding for two PKS, an FAD-dependent monooxygenase, a transporter, and two Gal4-like transcription factors. Additionally, some auxiliary genes can be present (**Figure 2**). *P. chrysogenum* Pcg21g05110, *T. reesei* protein ID 73631 (*sor4*), and *A. chrysogenum* ACRE_048110 are FAD/flavin mononucleotide (FMN)-containing dehydrogenases containing a "berberine and berberine like" domain according to a NCBI conserved domain search (Marchler-Bauer et al., 2015). Despite the similar domain architecture, only *T. reesei sor4* and *A. chrysogenum* ACRE_048110 appear to be orthologous according to a DELTA-BLAST analysis (Boratyn et al., 2012). Further, the hydrolase ACRE_048140 is only present in *A. chrysogenum*; ACRE_048140 is related to *Monascus ruber ctnB*/*citA* which is considered to support the respective PKS in the citrinin biosynthesis pathway (He and Cox, 2016).

Recently, we verified that the PKS SorA is essential for the sorbicillinoid biosynthesis in *P. chrysogenum* (Salo et al., 2016). In *T. reesei*, which is studied and industrially applied for its outstanding protein secretion capabilities of plant cell wall-degrading enzymes (Peterson and Nevalainen, 2012), we identified the main regulator of the sorbicillinoid gene cluster

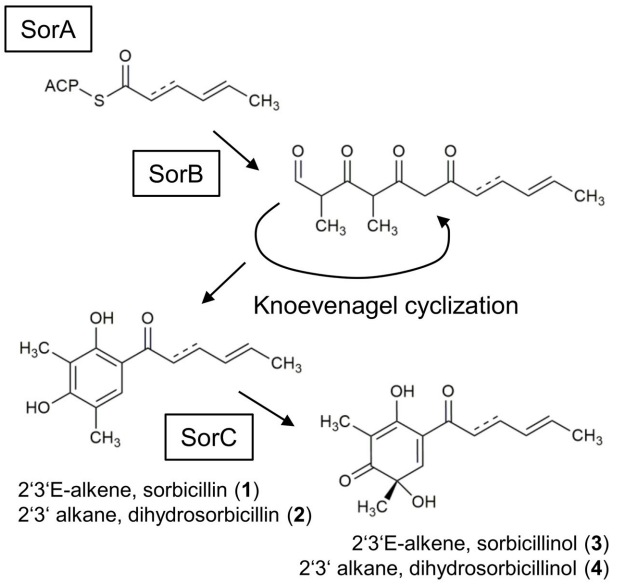


FIGURE 1 | Currently suggested sorbicillinol biosynthesis pathway. The iterative PKS SorA combines three acetyl units, and the growing chain is modified by the ketoacyl reductase subunit, removing the keto-groups. The enoyl reductase subunit might be active in the second cycle, which inserts a single bond. The polyketide is handed over to the PKS SorB, which adds three more acetyl units and two methyl groups. SorB releases an aldehyde, which undergoes spontaneous cyclization, resulting in the formation of sorbicillin (**1**) or 2′,3′-dihydrosorbicillin (**2**), depending on whether the enoyl reductase subunit had been active in SorA or not. Finally, the FAD-dependent monooxygenase SorC transforms sorbicillin or 2′,3′-dihydrosorbicillin to sorbicillinol (**3**) or 2′,3′-dihydrosorbicillinol (**4**).

(Derntl et al., 2016). The deletion of this transcription factor, Yellow pigment regulator 1 (Ypr1, **Figure 2**), abolishes the synthesis of the yellow sorbicillinoids and the expression of all genes of cluster, except of *sor4*.

In this study, we deleted the cluster genes encoding for the first PKS, the FAD-dependent monooxygenase, and the FAD/FMN-containing dehydrogenase in *T. reesei*. Further, we expressed the *citA*/*ctnB*-similar hydrolase from *A. chrysogenum* in *T. reesei*. The strains were investigated together with a *ypr1* deletion strain and a *ypr1* overexpression strain regarding their growth and their yellow pigment synthesis behavior. Further, the presence and the abundance of sorbicillinoids in their supernatants were measured, allowing us to extend the existing model for the biosynthesis pathway of sorbicillinoids. Additionally, we assayed the influence of the sorbicillinoids on the growth of other fungi and bacteria and on the confrontation behavior of *T. reesei* in presence of plant pathogenic fungi.

MATERIALS AND METHODS

Fungal Strains and Cultivation Conditions

All *T. reesei* strains (**Table 1**) were maintained on malt extract agar at 30°C. Uridine was added to a final concentration of

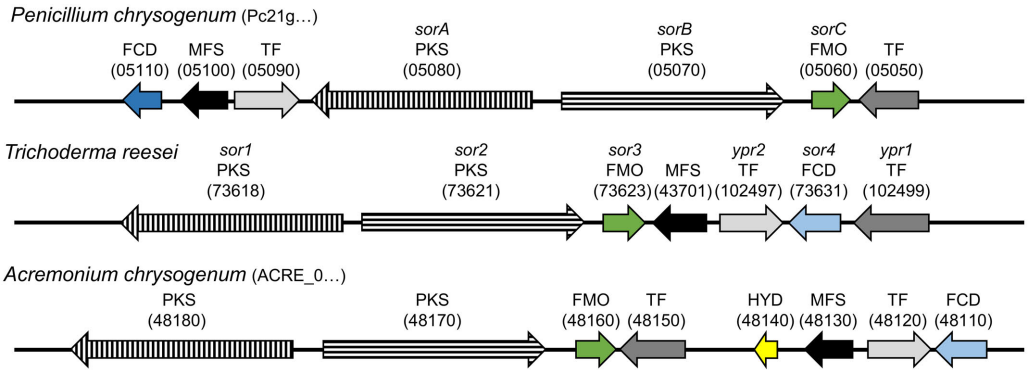


FIGURE 2 | Genomic organization of the sorbicillin cluster in *P. chrysogenum*, *T. reesei*, and *A. chrysogenum*. The arrows indicate the genes belonging to the sorbicillin cluster in the depicted fungi. Arrows with the same filling (color/pattern) represent homologs. The FCD Pc21g05110 shares only the same domain architecture with homologs FCDs *sor4* and ACRE_048110, which is indicated by the distinction between dark and light blue. Orientation, distance, and size are to scale and comparable. The beginning of a protein IDs is given in brackets after the species name and the variable part of the ID in brackets above the respective arrow. FCD, FAD/FMN-containing dehydrogenase; MFS, transporter of the multifacilitator superfamily; TF, transcription factor; PKS, polyketide synthase; FMO, FAD-dependent monooxygenase; HYD, hydrolase.

5 mM if applicable. Mandels–Andreotti (MA) medium (Mandels, 1985) without peptone containing 1% (w/v) D-glucose was used as minimal medium for selections after fungal transformations. For cultivation on D-glucose, *T. reesei* was grown in 300 ml MA medium containing 1% (w/v) D-glucose 30°C on a rotary shaker at 180 rpm. Mycelia and supernatants were separated by filtration through Miracloth (EMD Millipore, part of Merck KGaA, Darmstadt, Germany). Mycelia were dried at 80°C overnight for biomass determination and supernatants were stored at −20°C. Mycelia for RNA isolation and transcript analysis were harvested after 36 h cultivation and stored over liquid nitrogen. *Fusarium oxysporum* Foc4 (TUCIM 4812), *Alternaria alternata* TUCIM 3737, *Rhizoctonia solani* TUCIM 3753, and *Thanatephorus cucumeris* (*Botrytis cinerea*) TUCIM 4679 were maintained on potato dextrose agar at room temperature (approximately 22°C).

Bacterial Strains and Cultivation Conditions

Escherichia coli Top10 (Invitrogen, part of Thermo Fisher Scientific Inc., Waltham, MA, United States) was used for all cloning purposes throughout this study and maintained on LB at 37°C. If applicable, ampicillin was added to a final concentration of 100 μg/ml. *Staphylococcus aureus* DSM 20231^T, a methicillin-resistant *S. aureus* (MRSA) strain, an *E. coli* strain, and a multi-resistant *Acinetobacter baumannii* strain (the latter three are isolates from the clinical diagnostics unit at the Institute of Microbiology, Veterinary University Vienna) were grown on Peptone Yeast Extract (PYE) agar [0.3% (w/v) peptone from casein, 0.3% (w/v) yeast extract, 1.5% (w/v) agar–agar, pH 7.2] and used to test sensibility for sorbicillinoids.

TABLE 1 | *Trichoderma reesei* strains used throughout this study.

Strain	Abbreviation	Source
QM6aΔ*tmus53*	QM6a	Steiger et al., 2011
QM6aΔ*tmus53*Δ*pyr4*	Δ*pyr4*	Derntl et al., 2015
QM6aΔ*tmus53*Δ*ypr1*	Δ*ypr1*	Derntl et al., 2016
QM6aΔ*tmus53*Re*ypr1*	Re*ypr1*	Derntl et al., 2016
QM6aΔ*tmus53*Δ*sor1*	Δ*sor1*	This study
QM6aΔ*tmus53*Δ*sor3*	Δ*sor3*	This study
QM6aΔ*tmus53*Δ*sor4*	Δ*sor4*	This study
QM6aΔ*tmus53*p*sor3*::ACRE_048140 (*pyr4*)	A4814	This study

Plasmid Constructions

Polymerase chain reactions (PCRs) for cloning purposes were performed with Q5 High-Fidelity DNA Polymerase (New England Biolabs, Ipswich, MA, United States) according to the manufacturer's instructions. All used primers are listed in Supplementary Table S1. PCR products were cloned into *Eco*RV-digested pJET1.2 (Thermo Scientific, part of Thermo Fisher Scientific Inc., United States), and after verification of the PCR products by sequencing (Microsynth, Balgach, Switzerland), they were released for subsequent cloning purposes by digestion with suitable restriction endonucleases.

For the construction of the plasmids pCDΔsor1, pCDΔsor3, and pCDΔsor4 the 5′- and 3′-flanking regions of the respective genes were amplified by PCR using chromosomal DNA of *T. reesei* QM6a as template and corresponding primers given in Supplementary Table S1. Consecutively, corresponding flanking regions were inserted into pJET-pyr4 (Derntl et al., 2016) using the restriction enzymes indicated in the primer names.

For the construction of pRP4-ACRE_048140$_{ex}$ the promoter of *sor3* was amplified by PCR using chromosomal DNA of *T. reesei* QM6a as template and the primers P_{sor3}_fwd-BspEI and P_{sor3}_rev-SpeI and inserted into pCD-RPyr4T (Derntl et al., 2015) using *Bsp*EI and *Spe*I. The coding sequence of ACRE_048140 was amplified by PCR using chromosomal DNA of *A. chrysogenum* ATCC 11550 as template and the primers ACRE_048140_fwd-SpeI and ACRE-048140_rev-BamHI and

subsequently inserted into the latter plasmid using *Spe*I and *Bam*HI.

Fungal Transformation

The protoplast transformation of *T. reesei* was performed as described earlier (Gruber et al., 1990). Typically, 30 μg of linearized plasmid DNA of the plasmids pCDΔsor1, pCDΔsor3, pCDΔsor4, or pRP4-ACRE_048140$_{ex}$ (in 15 μl sterile ddH_2O) was used for the transformation of 10^7 protoplasts of the strain Δ*pyr4*. For selection for prototrophy, 100 μl to 2 ml of the transformation reaction were added to 20 ml melted, 50°C warm minimal medium agar containing 1.2 M sorbitol. This mixture was poured into sterile petri dishes. The plates were incubated at 30°C for 3–5 days until colonies were visible. Candidates were subjected to homokaryon selection by spore streak-outs on selection medium plates to obtain stable, homokaryotic strains.

Genotype Testing

Chromosomal DNA was isolated from mycelium by grinding in liquid nitrogen followed by a phenol/chloroform extraction (Gruber et al., 1990). RNA was degraded using RNaseA (Thermo Scientific). DNA was precipitated with isopropanol, washed with 70% ethanol, and dissolved in ddH_2O. For testing the genotype, 10 ng of chromosomal DNA were used as template in a 25-μl PCR using GoTaq® G2 polymerase (Promega, Madison, WI, United States) according to the manufacturer's instructions. All used primers are listed in Supplementary Table S1. For subsequent agarose gel electrophoresis of DNA fragments a GeneRuler 1 kb DNA Ladder (Thermo Scientific, United States) was applied for estimation of the fragment size.

RNA Isolation and RT-PCR

Approximately 20 mg of harvested mycelia were homogenized in 1 ml of peqGOLD TriFast DNA/RNA/protein purification system reagent (PEQLAB Biotechnologie, Erlangen, Germany) using a FastPrep FP120 BIO101 ThermoSavant cell disrupter (Qbiogene, Carlsbad, CA, United States). RNA was isolated according to the manufacturer's instructions, and the concentration was measured using the NanoDrop 1000 (Thermo Scientific). Synthesis of cDNA from mRNA was carried out using the RevertAid^{TM} H Minus First Strand cDNA Synthesis Kit (Thermo Scientific) according to the manufacturer's instructions.

Reverse transcription polymerase chain reactions (RT-PCRs) were performed in a Mastercycler® ep realplex 2.2 system (Eppendorf, Hamburg, Germany). All reactions were performed in triplicates. The amplification mixture (final volume 25 μl) contained 12.5 μl 2 × iQ SYBR Green Mix (Bio-Rad), 100 nM forward and reverse primer, and 2.5 μl cDNA (diluted 1:100) as template. All used primers are listed in Supplementary Table S1. Cycling conditions and control reactions were performed as described earlier (Steiger et al., 2010).

Metabolite Analysis

Culture supernatants were filtered using a 2 μm-pore polytetrafluoroethylene (PTFE) syringe filter. Liquid chromatography–mass spectrometry (LC-MS) analysis was performed in an Accella 1250 LC system coupled with the benchtop ES-MS Orbitrap Exactive (Thermo Fisher Scientific, United States) as described earlier (Salo et al., 2016). Reserpine is used as an internal standard. The differential analysis was done using the Thermo Scientific 205 SIEVE software. The response ratio indicates the fold-change of the compound detected in relation to reserpine. The metabolite analysis was performed from single representative biological samples in technical duplicates. Reserpine (Sigma–Aldrich, United States) was used as internal standard.

Fungal Plate Confrontation Assays

Trichoderma reesei strains were cultivated in MA medium containing 1% (w/v) D-glucose at 30°C at 180 rpm for 48 h. The cultivation supernatant was filtered using a 2-μm-pore syringe filter, mixed 1:1 (v/v) with melted potato dextrose agar that contained additional agar–agar, and poured into sterile petri dishes. The resulting plates were inoculated with agar pieces overgrown with plant pathogenic fungi, which were pre-grown on potato dextrose agar, and were incubated at room temperature. For fungal confrontation assays, all strains were pre-grown on potato dextrose agar at room temperature. Overgrown agar pieces of a *T. reesei* strain and a plant pathogenic strain, respectively, were transferred to opposite sides of a single potato dextrose agar plate and the plates were incubated at room temperature.

Agar Diffusion Assay

Suspensions of the pathogenic bacterial strains were spread on PYE agar plates. Different filter disks each soaked with 30 μl of each supernatant obtained from 48 h of cultivation of *T. reesei* strains and, as control, unconditioned MA medium were placed circularly on each agar plate and incubated at 37°C. The results were evaluated after 12, 36, and 50 h.

RESULTS

Construction of Recombinant *T. reesei* Strains to Characterize the Sorbicillin Cluster

In order to get insights into the biosynthesis of sorbicillinoids in *T. reesei*, we constructed a set of corresponding strains. We deleted the homolog of *sorA*, *sor1* (**Figure 2**), which we expected to result in a complete abolishment of the biosynthesis pathway (**Figure 1**). We also deleted the homolog of *sorC*, *sor3* (**Figure 2**), which we expected to interrupt the pathway prior to the oxidative dearomination of sorbicillin and 2′,3′-dihydrosorbicillin (**Figure 1**). Further, we deleted *sor4*, and inserted ACRE_048140 (**Figure 2**); both genes were not characterized yet. All gene deletions were performed via homologous recombination using reestablishment of *pyr4* as marker (Supplementary Figure S1A). The expression cassette for ACRE_048140 was inserted into the *pyr4* locus as described earlier (Derntl et al., 2015; Supplementary Figure S2A). The genomic manipulations were confirmed by PCR analyses

(Supplementary Figures S1B, S2B). Further, the absence of *sor1*, *sor3*, and *sor4* transcripts in the corresponding deletions strains and the presence of ACRE_048140 transcripts in the strain A4814 were confirmed by RT-PCR. The *ypr1* transcript was used as positive control for expression of the whole cluster (Supplementary Figures S1C, S2C).

Next, we cultivated the obtained strains Δ*sor1*, Δ*sor3*, Δ*sor4*, and A4814 together with the strain QM6a, which contains the wild-type version of the gene cluster, the *ypr1* deletion strain Δ*ypr1*, and the *ypr1* overexpression strain Re*ypr1* on glucose. As Ypr1 is the main regulator of the sorbicillin cluster, Δ*ypr1* is deficient in synthesis of sorbicillinoids, and Re*ypr1* produces high amounts of sorbicillinoids (Derntl et al., 2016). We monitored growth and biosynthesis of the yellow sorbicillinoids by measuring biomass accumulation and absorbance at 370 nm, respectively. As expected, the supernatants of Δ*ypr1*, Δ*sor1*, and Δ*sor3* did not turn yellow (**Figure 3A**), but we could measure high absorbance for Re*ypr1* (**Figure 3A**). A4814 had the same phenotype as QM6a, whereas Δ*sor4* secreted less yellow pigments than QM6a at time points after 36 h (**Figure 3A**). Further, we observed that the strains Δ*ypr1* and Δ*sor1* produced more biomass than all the other strains (**Figure 3B**). *Vice versa*, Re*ypr1* produced the lowest amount of biomass. The remaining strains grew equally well (**Figure 3B**). On a first glance, it appears as if the synthesis of the sorbicillinoids impairs growth of *T. reesei*.

Sorbicillinol Is the Main Product of the Biosynthesis Pathway

We were interested in what kind of sorbicillinoids were produced and accumulated in the recombinant strains. Consequently, we performed an LC-MS analysis of the culture supernatants from the above-described growth experiment on glucose (**Figure 3**). We used samples from early, middle, and late time points (24, 36, and 72 h). All compounds that were detected in the supernatant of any strain that produces sorbicillinoids (QM6a, Re*ypr1*, Δ*sor4*, or A4814), but not in strains that are deficient in sorbicillinoid synthesis (Δ*ypr1* and Δ*sor1*) are listed in **Table 2**. In the supernatant of strain Δ*sor3*, in which biosynthesis is assumed to be interrupted after sorbicillin generation (**Figure 1**), only traces of sorbicillinol were detected (**Table 3**). We consider them to be the result of chemical conversions and not of enzymatic activity. Further, the two compounds J_207 and F193 were also present in Δ*sor3* (**Table 3**). We suggest that J_207 and F193 might be degradation products of sorbicillin or precursors that occur during sorbicillin biosynthesis, because they have lower masses than sorbicillin (**Table 2**). Therefore, we did not include them in further data interpretations. However, we also detected a series of compounds containing up to nine nitrogen atoms in the sorbicillinoid producing strains (**Table 2**). We consider these compounds (D_293, C_309, E_333, M_479, A_556, and S_657) to be the result of a sponanteous chemical reaction of sorbicillinoids with urea and/or ammonium ions in the medium. Therefore, we decided to omit also these compounds in further data interpretations.

Next, we grouped the remaining metabolites (given in bold letters in **Table 2**) into three categories, i.e., (i) metabolites that occur in elevated levels at early time points of cultivation, (ii) metabolites that occur in elevated levels only in Δ*sor4*, and (iii) metabolites that occur in elevated levels at late time points of cultivation.

First, we had a detailed look on the presence and amounts of metabolites in QM6a, which is wild-type regarding the sorbicillinoids synthesis. The main early compound is sorbicillinol (**Figure 4**) or to be more precisely, sorbicillinols, because we detect two compounds with the same mass that have very similar retention times (**Table 2**). We consider them to be identical. Further, we detect small amounts of sorbicillin in the beginning (**Figure 4**). These findings are in concordance with the previously suggested biosynthesis pathway in *P. chrysogenum*, which claims that sorbicillin is oxidized to sorbicillinol (**Figure 1**). Further, we also detected 5-hydroxyvertinolide and the compound K_307 in the early stages of cultivation (**Figure 4**). The strain A4814 produced nearly the same amounts of all the early compounds as QM6a (**Figure 4**). We detected higher amounts of all early metabolites in the *ypr1* overexpression strain Re*ypr1* compared to QM6a (**Figure 4**). In Δ*sor4* we detected substantially lower amounts of sorbicillinols, 5-hydroxyvertinolide, and the compound K_307 than in QM6a, but slightly higher amounts of sorbicillin (**Figure 4**).

Deletion of *sor4* Leads to Accumulation of Dihydrosorbicillinol

In the Δ*sor4* strain, we observed high amounts of two compounds that were annotated to dihydrosorbicillinol (**Table 2**). The compound J_251 was predominantly detected at early time points, while F_251 accumulated throughout growth (**Figure 5**). Notably, these compounds were not detected in any other strain. We also found higher amounts of F_265, which was annotated to oxosorbicillinol or epoxysorbicillinol (**Table 2**), in strain Δ*sor4* compared to the other strains after 24 and 36 h of cultivation (**Figure 5**).

Sorbicillinol Is the Building Block for the Other Sorbicillinoids

Next, we analyzed the abundance and occurrence of the late sorbicillinoids (**Figure 6**). We detected disorbicillinol, bisvertinolon, and two compounds that were annotated to oxosorbicillinol or epoxysorbicillinol, and traces of a dihydrobisvertinolone in QM6a (**Figure 6**). In Re*ypr1*, we measured higher levels of these late sorbicillinoids (**Figure 6**). Notably, Re*ypr1* also produces higher amounts of sorbicillinols at the early and middle time points (**Figure 4**). *Vice versa*, in A4814, lower amounts of sorbicillinols were detected than in QM6a after 36 h (**Figure 4**), and also lower amounts of the late sorbicillinoids (**Figure 6**). In Δ*sor4*, which produces very small amounts of sorbicillinols (**Figure 4**), we detected none of the late sorbicillinoids (**Figure 6**). This suggests that the late sorbicillinoids are the products of chemical and/or enzymatical conversion of sorbicillinol. Interestingly, the late metabolite Q_499 is found in small amounts in all strains (**Figure 6**). Its empirical

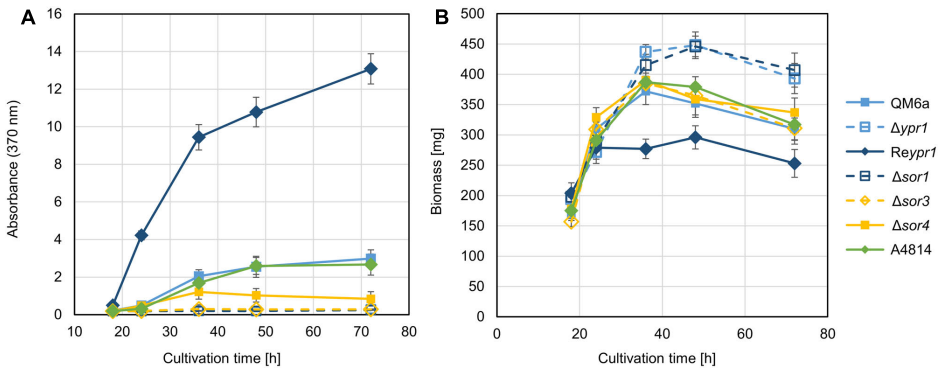


FIGURE 3 | Phenotypic comparison of the recombinant *T. reesei* strains. The indicated *T. reesei* strains were cultivated on glucose for the indicated periods, and absorbance at 370 nm of the supernatants **(A)** and biomass accumulation (dry weight) **(B)** were determined. The gives values are the mean of three replicates. The error bars represent the standard deviations.

formula suggests that is an unknown bicyclic sorbicillinoid (**Table 2**).

The Sorbicillinoids of *T. reesei* Restrict Growth of Pathogenic Fungi But Not of Bacteria

The cultivation experiment on glucose pointed toward a growth limiting effect of sorbicillinoids on *T. reesei*. Consequently, we were interested, whether these metabolites might also influence growth of plant pathogenic fungi. To test this, supernatants from 48 h of cultivation of the *T. reesei* strains QM6a, Δ*ypr1*, Re*ypr1*, and Δ*sor4* were filtered and added to cultivation medium in order to cast plates containing the sorbicillinoids. On these plates, the plant pathogenic fungi *A. alternata*, *B. cinerea*, *F. oxysporum*, and *R. solani* were inoculated. Here we observed a clear growth impairment of all four tested fungi caused by the secreted sorbicillinoids of *T. reesei* (**Figure 7**). On plates containing the supernatant of Δ*ypr1*, the four fungi grew the same as on plates containing medium that was not mixed with any cultivation supernatant (control). All plant pathogenic fungi grew slower on plates containing sorbicillinol

TABLE 2 | Compounds detected in the supernatants of the strains *T. reesei* QM6a, Re*ypr1*, A4814, or Δ*sor4*.

Compound ID	Acquired $[M+H]^+$	RT (min)	Formular	Annotated metabolite(s)
F_193	193.0862	20.41	C11H12O3	Unknown
J_207	207.1017	24.02	C12H14O3	Unknown
N_233[1]	**233.1174**	**32.09**	**C14H16O3**	**Sorbicillin**
G_249	**249.1123**	**20.89**	**C14H16O4**	**Sorbicillinol**[2]
H_249	**249.1123**	**22.19**	**C14H16O4**	**Sorbicillinol**[2]
F_251	**251.1279**	**19.74**	**C14H18O4**	**Dihydrosorbicillinol**
J_251	**251.1279**	**24.07**	**C14H18O4**	**Dihydrosorbicillinol**
F_265	**265.1071**	**19.91**	**C14H16O5**	**Oxosorbicillinol/Epoxysorbicillinol**
L_265	**265.1071**	**26.65**	**C14H16O5**	**Oxosorbicillinol/Epoxysorbicillinol**
B_267	**267.1228**	**15.37**	**C14H18O5**	**5-hydroxyvertinolide**
D_293	293.1495	16.73	C15H20O4N2	Unknown
K_307	**307.1543**	**25.91**	**C17H22O5**	Unknown
C_309	309.1441	15.61	C15H20O5N2	Unknown
E_333	333.1444	18.93	C16H14N9	Unknown
M_479	479.2064	29.54	C27H24O2N7	Unknown
M_497	**497.2166**	**29.63**	**C28H32O8**	**Bisorbicillinol**
R_513	**513.2117**	**34.15**	**C28H32O9**	**Bisvertinolon**
P_515	**515.2274**	**33.16**	**C28H34O9**	**Dihydrobisvertinolone**
B_517	**517.243**	**15.37**	**C28H36O9**	**Tetrahydrobisvertinolone**
A_556	556.1957	14.39	C16H29O13N9	Unknown
S_657	657.2694	36.75	C22H40O15N8	Unknown

[1]*Compounds highlighted in bold were considered for subsequent data interpretations.* [2]*We consider these two compounds to be identical and refer to them as "sorbicillinols".*

TABLE 3 | Abundance of the compounds detected in the supernatant of *T. reesei* Δ*sor3*.

Compound	RR[1] after 24 h	RR after 36 h	RR after 72 h
G_249 + H_249 (sorbicillinols)	0	0.07	0.03
J_207	0.00	0.00	0.02
F_193	0.01	0.43	0.19

[1]*Response ratio (see section "Materials and Methods").*

and the derived sorbicillinoids (i.e., supernatant of cultivation of *T. reesei* strains QM6a and Re*ypr1*). Notably, the growth inhibiting effect seems to be in direct relation to the amount of sorbicillinoids in the plate. We observed a less pronounced inhibition of growth of *A. alternata*, *B. cinerea*, and *R. solani* on plates with the supernatant of Δ*sor4*, which contains dihydrosorbicillinols and only small amounts sorbicillinol and no complex sorbicillinoids (**Figures 4–6**). *F. oxysporum* was not affected by the Δ*sor4* supernatant (**Figure 7**). Interestingly, the mycelium of *R. solani* had a more compact and organized appearance on Δ*sor4* supernatant than on the other plates. The growth of *A. alternata* is only marginally inhibited on Δ*sor4* supernatant, but sporulation is augmented compared to the control plate and Δ*ypr1* (**Figure 7**).

We were also interested, whether the sorbicillinoids might also have antibacterial activities. To this end, we used the supernatants of QM6a, Δ*ypr1*, and Re*ypr1* cultivated for 48 h on glucose in an agar diffusion assay against strains of *E. coli*, *A. baumanii*, *S. aureus*, and MRSA. As control, we used medium, which had not been inoculated with any *T. reesei* strain. None of the culture supernatants had a growth inhibiting effect on any of the tested bacteria (not shown).

Sorbicillinoids Influence the Competition with Plant Pathogenic Fungi

Next, we aimed to test whether the growth limiting properties of the sorbicillinoids might support *T. reesei* in confrontation with other fungi. To this end, we performed confrontation plate assays using the plant pathogenic fungi *A. alternata*, *B. cinerea*, *F. oxysporum*, and *R. solani* and the following *T. reesei* strains: the wild-type QM6a, the sorbicillinoid non-producer Δ*ypr1*, the sorbicillinoid hyper-producer Re*ypr1*, and Δ*sor4* which has a different sorbicillinoid spectrum [i.e., dihydrosorbicillinols, small amounts of sorbicillinol (**Figures 4**, **5**), but no other sorbicillinoids (**Figures 4**, **6**)]. Interestingly, *T. reesei*Δ*sor4* produced as much, or even more, yellow pigments as QM6a on the plates (**Figure 8**), in contrast to liquid cultures (**Figure 3A**). We comment on this in the Section "Discussion." However, we observed no differences at all among the four *T. reesei* strains in confrontation to *A. alternata* (**Figure 8**). In confrontation with the other three fungi, we observed only subtle differences among the four *T. reesei* strains. Against *B. cinerea*, Δ*ypr1* grows weaker in vicinity to *B. cinerea* than the other strains at early time points. In confrontation with *F. oxysporum*, Δ*ypr1* gets stronger overgrown than QM6a, while Re*ypr1* is able to resist *F. oxysporum* better than the other strains. Notably, the

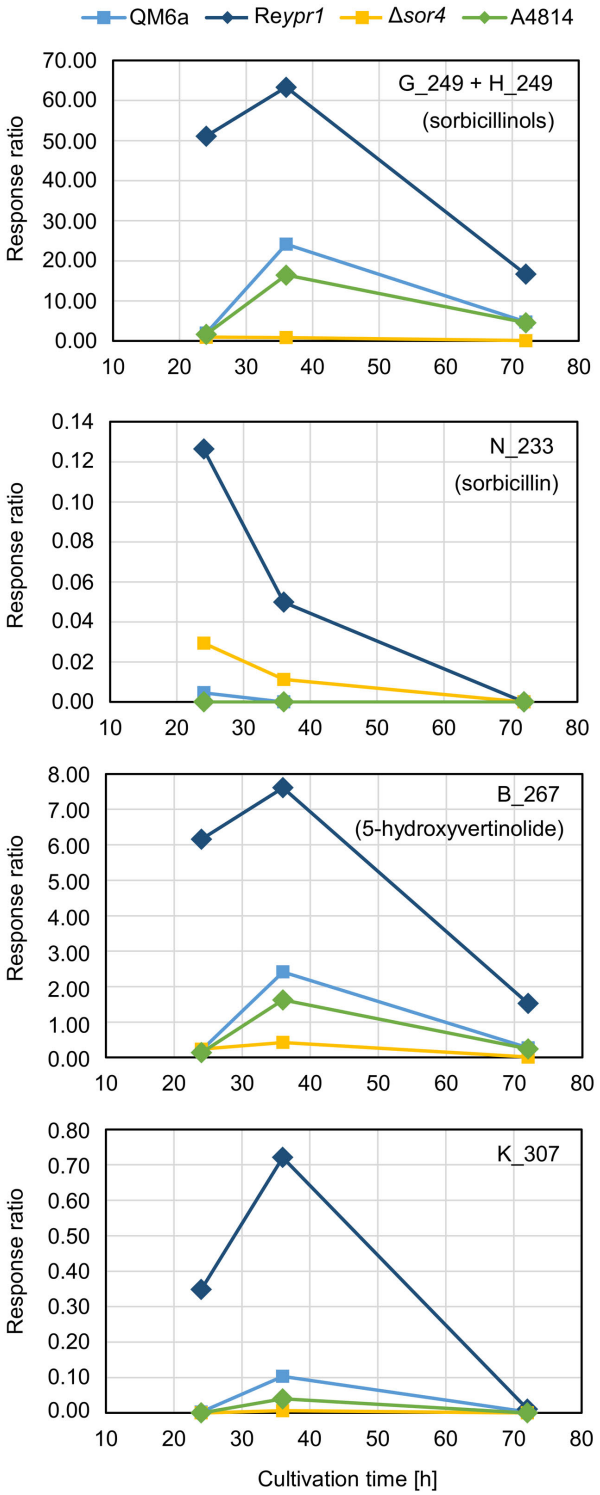


FIGURE 4 | Abundance of compounds that are secreted early into the supernatant. The indicated *T. reesei* strains were cultivated on glucose in three replicates (compare **Figure 3**) for the indicated periods. A representative sample for each time point and strain was analyzed by HPLC-MS in technical duplicates. The quantities of the indicated compounds are given as response ratios (i.e., the fold-change of the compound detected in relation to the internal standard).

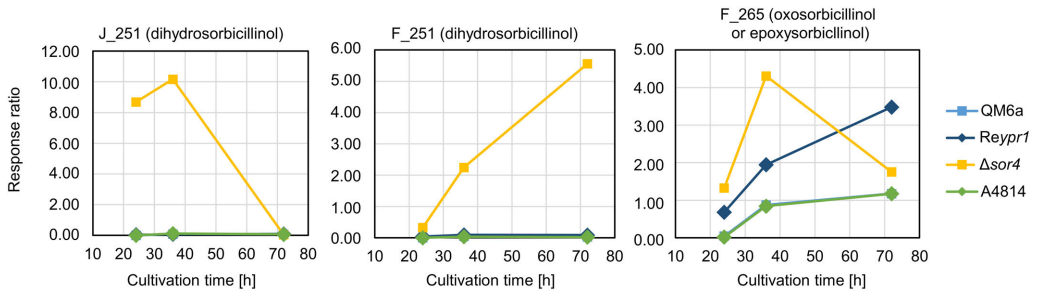


FIGURE 5 | Abundance of compounds that accumulate in the supernatant over time. The indicated *T. reesei* strains were cultivated on glucose in three replicates (compare **Figure 3**) for the indicated periods. A representative sample for each time point and strain was analyzed by LC-MS in technical duplicates. The quantities of the indicated compounds are given as response ratios (i.e., the fold-change of the compound detected in relation to the internal standard).

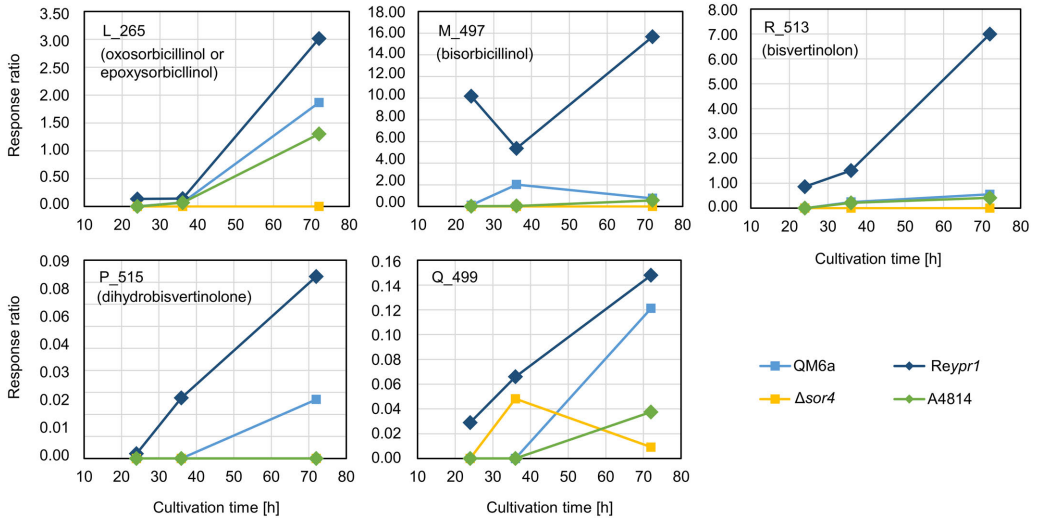


FIGURE 6 | Abundance of compounds that are elevated in the supernatant of strain Δ*sor4*. The indicated *T. reesei* strains were cultivated on glucose in three replicates (compare **Figure 3**) for the indicated periods. A representative sample for each time point and strain was analyzed by LC-MS in technical duplicates. The quantities of the indicated compounds are given as response ratios (i.e., the fold-change of the compound detected in relation to the internal standard).

mycelium of *F. oxysporum* overgrowing Δ*sor4* has a more structured and denser morphology than on the other *T. reesei* strains. Surprisingly, the sorbicillinoid non-producer Δ*ypr1* most strongly overgrows *R. solani* in comparison to the other *T. reesei* strains (**Figure 8**).

DISCUSSION

On the Biosynthesis Pathway of Sorbicillinoids, 5-Hydroxyvertinolide, and the Roles of Sor4 and ACRE_048140

Previously, *P. chrysogenum* SorC was demonstrated to oxidize sorbicillin and 2′,3′-dihydrosorbicillin to sorbicillinol and 2′,3′-dihydrosorbicillinol, respectively, *in vitro* (Fahad et al., 2014). Based on these results, *in silico* analyses of the PKS SorA and SorB, and previous data from metabolite identifications and radio-labeled feed experiments, the authors proposed the model described in **Figure 1**. An earlier model had claimed that oxosorbicillinol was a key intermediate for sorbicillinol synthesis via a hypothetical compound, and that sorbicillin was derived from sorbicillinol (Abe et al., 2002). Our data support the newer model proposed by Fahad et al. (2014), because we detected the highest amounts of sorbicillin at the earliest time point, and because we observed the accumulation of oxosorbicillinol only after sorbicillinol had been built, timely and hierarchically (**Figures 4**, **6**).

The model of Abe et al. (2002) also suggested that 5-hydroxyvertinolide was derived from the same hypothetical compound as sorbicillinol. Another, previous model proposed that epoxysorbicillinol could be converted into 5-hydroxyvertinolide (Sperry et al., 1998). Our observations do not support any of these two models, because we detect 5-hydroxyvertinolide already at early time points in dependence of sorbicillinol (**Figure 4**). We consider 5-hydroxyvertinolide, as well as the unknown, early metabolite K_307 (**Table 2**), to be (chemically and/or enzymatically) derived from sorbicillinol because they are barely present in Δ*sor4* (**Figure 4**).

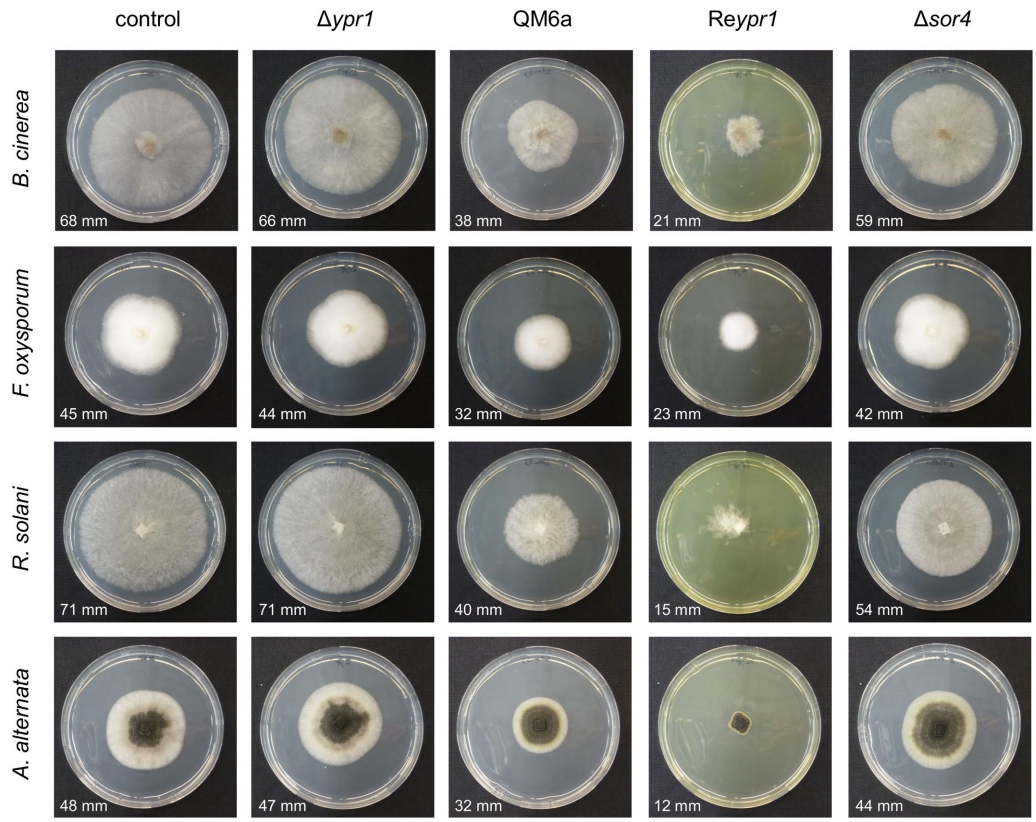


FIGURE 7 | Influence of *T. reesei* sorbicillinoids on growth of plant pathogenic fungi. The *T. reesei* strains (indicated on top) were cultivated on glucose for 48 h and the resulting culture supernatants were filtered, mixed 1:1 (v/v) with potato dextrose agar, and poured into petri dishes. As a control, medium that was not inoculated with any *T. reesei* strain was used. The plant pathogenic fungi (indicated on the left) were inoculated on these plates and incubated at room temperature. Pictures were taken after 3 days in the case of *R. solani* and *B. cinerea*, and after 5 days in the case of *F. oxysporum* and *A. alternata*. The diameters of the growth halos are provided.

However, we would like to extend the model proposed by Fahad et al. (2014) on the biosynthesis of sorbicillinol in *T. reesei*. We observed the accumulation of the two compounds, J_251 and F_251, that were both annotated to dihydrosorbicillinol (**Table 2**), but only small amounts of sorbicillinol in *T. reesei* Δ*sor4* (**Figures 4**, **5**). Notably, we did not detect the dihydrosorbicillinols in any other strain. We speculate, that the early arising compound J_251 might be 2′,3′-dihydrosorbicillinol. This assumption is based on the already existing model, which proposes that 2′,3′-dihydrosorbicillinol is synthesized in parallel to sorbicillinol (Fahad et al., 2014) (**Figure 1**). Sor4 is an FAD-binding dehydrogenase according to a conserved domain analysis. These enzymes are able to reduce alkanes to alkenes, because FAD has such a high reduction potential that it can accept two electrons and two protons simultaneously. The accumulation of dihydrosorbicillinol in the absence of Sor4 suggests that Sor4 might reduce the double-bond in the linear side-chain of 2′,3′-dihydrosorbicillinol (**4**). This implies that the main product of the PKS-cascade and the cyclization reaction is in fact 2′,3′-dihydrosorbicillin (**2**), which is oxidized to 2′,3′-dihydrosorbicillinol (**4**) by Sor3. Finally, Sor4 might reduce 2′,3′-dihydrosorbicillinol (**4**) to sorbicillinol (**3**). Alternatively, Sor4 might as well reduce 2′,3′-dihydrosorbicillin (**2**) to sorbicillin (**1**) before it is oxidized to sorbicillinol (**3**) by Sor3 in a final step (**Figure 9A**). Of course, the two alternative pathways might occur simultaneously.

F_251, the second dihydrosorbicillinol in the Δ*sor4* supernatant (**Figure 5**), could be 2′,5′-dihydrosorbicillinol or 4′,5′-dihydrosorbicillinol or another unknown isomer; 2′,5′-dihydrosorbicillin was previously identified as a product of chemical hydrogenation of sorbicillin (Trifonov et al., 1983). If F_251 was 2′,5′-dihydrosorbicillinol, its occurrence could be explained by a chemical conversion. This speculation is supported by the fact that F_251 accumulates over time (**Figure 5**). Alternatively, it could be another unknown isomer that occurs by chemical isomerization. If F_251 was 4′,5′-dihydrosorbicillinol, its occurrence could be explained by the implied sloppy mode of action of SorA/1, as already discussed by Fahad et al. (2014). The PKS SorA/1 contains, next to the core acyl transferase subunit, a presumably non-functional methyl transferase subunit, a ketoacyl reductase subunit, and an enoyl reductase subunit. The ketoacyl reductase subunit reduces the beta-carbonyl of the growing polyketide to a hydroxyl group. The enoyl reductase subunit reduces a double to single

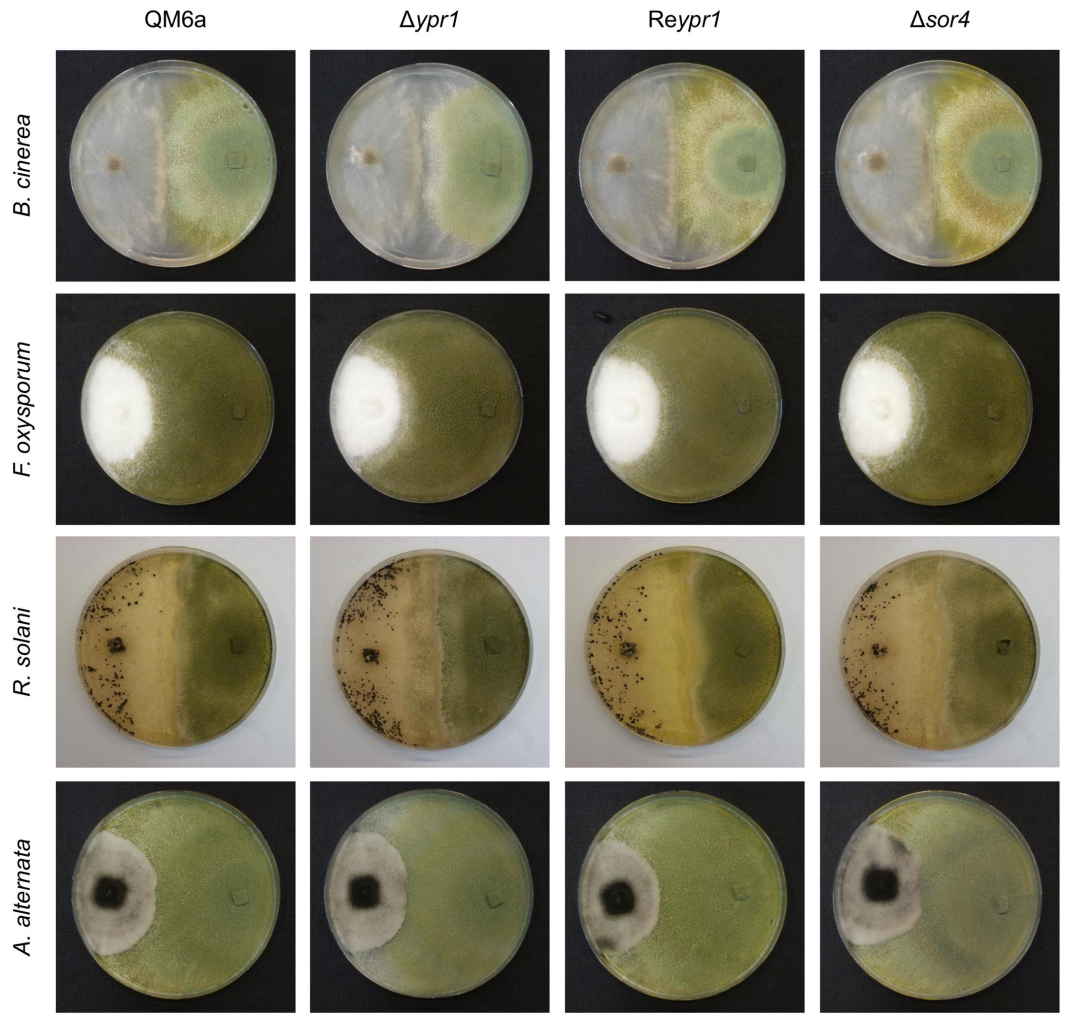


FIGURE 8 | Influence of *T. reesei* sorbicillinoids on direct fungal confrontations. The *T. reesei* strains (indicated on top) and plant pathogenic fungi (indicated on the left) were inoculated on potato dextrose agar plates at opposite sides (*T. reesei* on the right, the plant pathogenic fungi on the left) using equal pieces of overgrown potato dextrose agar, and incubated at room temperature. Pictures were taken after 2 days after initial contact in the case of *B. cinerea*, and after 3 weeks in the case of *F. oxysporum, R. solani*, and *A. alternata*.

bond. Depending on, whether, and during which cycle of chain elongation the enoyl reductase subunit is active, sorbicillinol, 2′,3′- or 4′,5′-dihydrosorbicillinol would be synthesized in the end (compare **Figures 9A,B**, compounds **3**, **4**, and **5**).

Further, if we speculate that the ketoacyl reductase subunit of Sor1 was not active during a cycle of polyketide elongation, a sorbicillinol derivate containing a keto-group would be synthesized ultimately (**Figure 9C**, compound **6**). This hypothetical compound has the same empiric formula as oxosorbicillinol and epoxysorbicillinol, and might be compound F_265 (**Table 2**) that was detected in all sorbicillinoid producing strains (**Figure 5**). Its higher levels in Δ*sor4* could be explained by a feedback of the accumulating dihydrosorbicillinol on Sor1.

The amounts of early metabolites were nearly equal in the wild-type-like QM6a and the strain A4814, which bears the hydrolase ACRE_048140 from *A. chrysogenum* (**Figure 4**). We detected smaller amounts of the late metabolites in A4814 than in QM6a (**Figure 6**), but we consider this to be the result of lower sorbicillinol levels in strain A4814 (**Figure 4**) because these metabolites are derived from sorbicillinol. Therefore, we conclude that the hydrolase ACRE_048140 did not influence the sorbicillinoid biosynthesis in *T. reesei*.

On the Growth-Limiting Properties of Sorbicillinoids

During the growth experiment of the recombinant strains, we observed that the growth rate seems to be negatively related to the biosynthesis of sorbicillinoids (**Figure 3**). The strains, which do not produce sorbicillinoids, Δ*ypr1* and Δ*sor1*, grew better than the wild-type-like strains QM6a and A4814, whereas the sorbicillinoid hyper-producer Re*ypr1* accumulated less biomass. Interestingly, Δ*sor3* and Δ*sor4* grew equally well as the wild-type-like strains, although they do not produce mature sorbicillinoids. In Δ*sor3* the biosynthesis

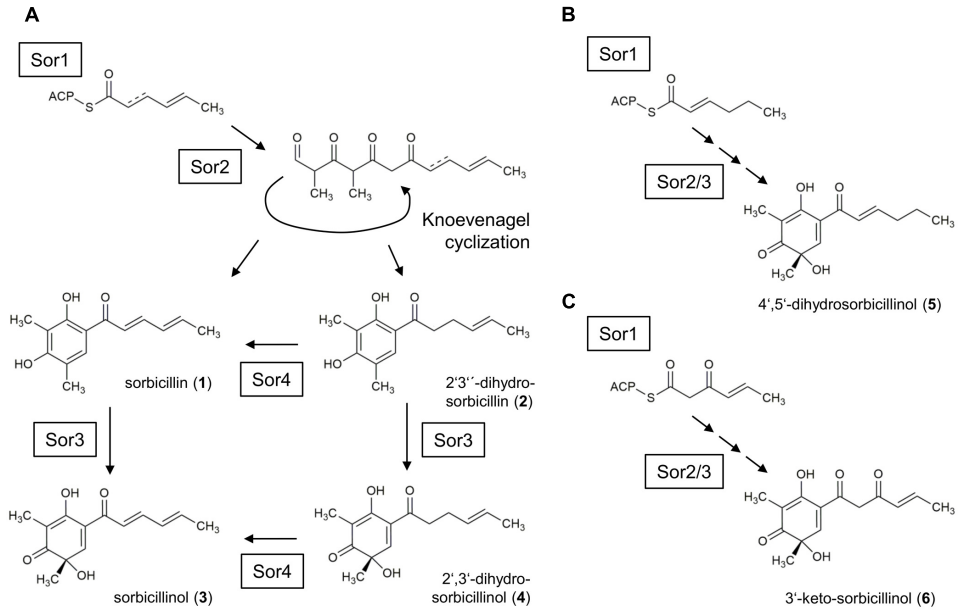


FIGURE 9 | Model for the sorbicillinol biosynthesis pathway in *T. reesei*. **(A)** The basic model is identical to the earlier proposed model by Fahad et al., 2014 (compare **Figure 1**). Briefly, the PKS Sor1 iteratively combines three acetyl units and the growing chain is modified by the ketoacyl reductase subunit, and optional by the enoyl reductase subunit in the second cycle. The polyketide is handed over to the PKS Sor2, which adds three more acetyl units, and two methyl groups. Sor2 releases an aldehyde, which undergoes spontaneous cyclization resulting in the formation of sorbicillin (**1**) or 2′,3′-dihydrosorbicillin (**2**). Next, the FAD-dependent monooxygenase Sor3 transforms sorbicillin or 2′,3′-dihydrosorbicillin to sorbicillinol (**3**) or 2′,3′-dihydrosorbicillinol (**4**). Further, Sor4 might reduce 2′,3′-dihydrosorbicillin (**2**) to sorbicillin (**1**) and/or 2′,3′-dihydrosorbicillinol (**4**) to sorbicillinol (**3**). The obtained data from our study (**Figures 4**–**6**) suggest that the main product of Sor1/2 is in fact 2′,3′-dihydrosorbicillin. **(B)** Assumed that the enoyl reductase subunit of Sor1 was active during the first cycle, 4′,5′-dihydrosorbicillinol (**5**) would have been synthesized by Sor2 and Sor3. **(C)** Assumed that the ketoacyl reductase subunit of Sor1 was not active during the third cycle, Sor2 and Sor3 would have assembled 3′-keto-sorbicillinol (**6**).

pathway is disrupted after the cyclization of the released aldehydes (**Figure 1**), implying that intracellular sorbicillin and dihydrosorbicillin are built. In Δ*sor4* dihydrosorbicillinol accumulates, very small amounts of sorbicillinol are synthesized, and no late sorbicillinoids are produced (**Figure 6**). Therefore, the reason for the growth limitation is likely to be either the metabolic burden or the intracellular presence of sorbicillin and dihydrosorbicillin (**Figure 9**). It cannot be excluded that the extracellular sorbicillinoids also have a growth limiting effect on *T. reesei*. Probably, all three factors contribute to some extents to the observed growth restrictions.

During the confrontation assays on the plates, we observed that Δ*sor4* turned the medium more intensely yellow than the wild-type-like QM6a (**Figure 8**), but it was the opposite in liquid cultures (**Figure 3A**). Generally, we observed that the medium in plates became more yellow than in liquid cultures. We speculate that oxygen and/or light might degrade the sorbicillinoids. The strain Δ*sor4* produces predominantly dihydrosorbicillinols (**Figure 5**), which might be more susceptible to degradation by light and/or oxygen than sorbicillinol and the late sorbicillinoids. The presence of the dihydrosorbicillinols and the lack of the mature sorbicillinoids explain why Δ*sor4* did influence neither the morphology of the other fungi nor their growth rates.

The extracellular sorbicillinol and/or mature sorbicillinoids had a clear influence on the growth of other fungi (**Figure 6**). In direct fungal confrontations, the sorbicillinoids supported growth of *T. reesei* in presence of *B. cinerea* and *F. oxysporum*, however, subtle the effects were. In confrontation against *B. cinerea*, the radical-scavenging properties and/or the chemical reactivity of the sorbicillinoids might protect *T. reesei* from secreted compounds and/or proteins of *B. cinerea*. In confrontation against *F. oxysporum* and *R. solani*, the growth-inhibiting effects pose an obstacle for the stronger fungus. This is, the sorbicillinoids delayed *F. oxysporum* in overgrowing *T. reesei*, but they also hindered *T. reesei* from overgrowing *R. solani*. Taken together, the sorbicillinoids pose a possibility for *T. reesei* to maintain its already claimed territory in confrontation with other fungi, but it has to put up with their growth limiting effects.

AUTHOR CONTRIBUTIONS

CD constructed the plasmids, the deletion strains, performed the growth experiment, and the fungal confrontation assays, performed data analysis, co-drafted the manuscript, and was involved in the study design. FG-C performed the LC-MS analyses and performed data analysis. TM-d-S constructed the strain A4814. H-JB performed the agar diffusion assay. AD performed data analysis. RM was involved in the study design. AM-A co-drafted the manuscript and was involved in the study design.

FUNDING

This work was supported by two grants from the Austrian Science Fund (FWF): [P26733, P29556] given to AM-A and RM, respectively.

ACKNOWLEDGMENTS

We thank Ulrich Kück and Dominik Terfehr for providing chromosomal DNA of *A. chrysogenum* ATCC 11550. We thank Irina S. Druzhinina for providing fungal strains of *Fusarium oxysporum*, *Alternaria alternata*, *Rhizoctonia solani*, and *Botrytis cinerea*, and Oleksandr Salo for assisting in the LC-MS data analysis.

SUPPLEMENTARY MATERIAL

The Supplementary Material for this article can be found online at: https://www.frontiersin.org/articles/10.3389/fmicb.2017.02037/full#supplementary-material

REFERENCES

Abe, N., Arakawa, T., and Hirota, A. (2002). The biosynthesis of bisvertinolone: evidence for oxosorbicillinol as a direct precursor. *Chem. Commun.* 3, 204–205. doi: 10.1039/b109505f

Abe, N., and Hirota, A. (2002). Chemical studies of the radical scavenging mechanism of bisorbicillinol using the 1,1-diphenyl-2-picrylhydrazyl radical. *Chem. Commun.* 6, 662–663. doi: 10.1039/b200039n

Abe, N., Yamamoto, K., and Hirota, A. (2000). Novel fungal metabolites, demethylsorbicillin and oxosorbicillinol, isolated from *Trichoderma* sp. USF-2690. *Biosci. Biotechnol. Biochem.* 64, 620–622. doi: 10.1271/bbb.64.620

Boratyn, G. M., Schaffer, A. A., Agarwala, R., Altschul, S. F., Lipman, D. J., and Madden, T. L. (2012). Domain enhanced lookup time accelerated BLAST. *Biol. Direct* 7:12. doi: 10.1186/1745-6150-7-12

Cram, D. J. (1948). Mold metabolites; the structure of sorbicillin, a pigment produced by the mold *Penicillium notatum*. *J. Am. Chem. Soc.* 70, 4240–4243. doi: 10.1021/ja01192a077

Derntl, C., Kiesenhofer, D. P., Mach, R. L., and Mach-Aigner, A. R. (2015). Novel strategies for genomic manipulation of *Trichoderma reesei* with the purpose of strain engineering. *Appl. Environ. Microbiol.* 81, 6314–6323. doi: 10.1128/AEM.01545-15

Derntl, C., Rassinger, A., Srebotnik, E., Mach, R. L., and Mach-Aigner, A. R. (2016). Identification of the main regulator responsible for synthesis of the typical yellow pigment produced by *Trichoderma reesei*. *Appl. Environ. Microbiol.* 82, 6247–6257. doi: 10.1128/AEM.01408-16

Fahad, A. A., Abood, A., Fisch, K. M., Osipow, A., Davison, J., Avramovic, M., et al. (2014). Oxidative dearomatisation: the key step of sorbicillinoid biosynthesis. *Chem. Sci.* 5, 523–527. doi: 10.1039/c3sc52911h

Gruber, F., Visser, J., Kubicek, C. P., and de Graaff, L. H. (1990). The development of a heterologous transformation system for the cellulolytic fungus *Trichoderma reesei* based on a *pyrG*-negative mutant strain. *Curr. Genet.* 18, 71–76. doi: 10.1007/BF00321118

Harned, A. M., and Volp, K. A. (2011). The sorbicillinoid family of natural products: isolation, biosynthesis, and synthetic studies. *Nat. Prod. Rep.* 28, 1790–1810. doi: 10.1039/c1np00039j

He, Y., and Cox, R. J. (2016). The molecular steps of citrinin biosynthesis in fungi. *Chem. Sci.* 7, 2119–2127. doi: 10.1073/pnas.1201469109

Mandels, M. (1985). Applications of cellulases. *Biochem. Soc. Trans.* 13, 414–416. doi: 10.1042/bst0130414

Marchler-Bauer, A., Derbyshire, M. K., Gonzales, N. R., Lu, S., Chitsaz, F., Geer, L. Y., et al. (2015). CDD: NCBI's conserved domain database. *Nucleic Acids Res.* 43, D222–D226. doi: 10.1093/nar/gku1221

Martinez, D., Berka, R. M., Henrissat, B., Saloheimo, M., Arvas, M., Baker, S. E., et al. (2008). Genome sequencing and analysis of the biomass-degrading fungus *Trichoderma reesei* (syn. *Hypocrea jecorina*). *Nat. Biotechnol.* 26, 553–560. doi: 10.1038/nbt1403

Maskey, R. P., Grun-Wollny, I., and Laatsch, H. (2005). Sorbicillin analogues and related dimeric compounds from *Penicillium notatum*. *J. Nat. Prod.* 68, 865–870. doi: 10.1021/np040137t

Mazzucco, C. E., and Warr, G. (1996). Trichodimerol (BMS-182123) inhibits lipopolysaccharide-induced eicosanoid secretion in THP-1 human monocytic cells. *J. Leukoc. Biol.* 60, 271–277.

Meng, J., Wang, X., Xu, D., Fu, X., Zhang, X., Lai, D., et al. (2016). Sorbicillinoids from fungi and their bioactivities. *Molecules* 21:E715. doi: 10.3390/molecules21060715

Peterson, R., and Nevalainen, H. (2012). *Trichoderma reesei* RUT-C30 - thirty years of strain improvement. *Microbiology* 158(Pt 1), 58–68. doi: 10.1099/mic.0.054031-0

Reategui, R. F., Wicklow, D. T., and Gloer, J. B. (2006). Phaeofurans and sorbicillin analogues from a fungicolous *Phaeoacremonium* species (NRRL 32148). *J. Nat. Prod.* 69, 113–117. doi: 10.1021/np0504199

Salo, O., Guzman-Chavez, F., Ries, M. I., Lankhorst, P. P., Bovenberg, R. A., Vreeken, R. J., et al. (2016). Identification of a polyketide synthase involved in sorbicillin biosynthesis by *Penicillium chrysogenum*. *Appl. Environ. Microbiol.* 82, 3971–3978. doi: 10.1128/AEM.00350-16

Sperry, S., Samuels, G. J., and Crews, P. (1998). Vertinoid polyketides from the saltwater culture of the fungus *Trichoderma longibrachiatum* separated from a *Haliclona* marine sponge. *J. Org. Chem.* 63, 10011–10014. doi: 10.1021/jo9808122

Steiger, M. G., Mach, R. L., and Mach-Aigner, A. R. (2010). An accurate normalization strategy for RT-qPCR in *Hypocrea jecorina* (*Trichoderma reesei*). *J. Biotechnol.* 145, 30–37. doi: 10.1016/j.jbiotec.2009.10.012

Steiger, M. G., Vitikainen, M., Uskonen, P., Brunner, K., Adam, G., Pakula, T., et al. (2011). Transformation system for *Hypocrea jecorina* (*Trichoderma reesei*) that favors homologous integration and employs reusable bidirectionally selectable markers. *Appl. Environ. Microbiol.* 77, 114–121. doi: 10.1128/AEM.02100-10

Terfehr, D., Dahlmann, T. A., Specht, T., Zadra, I., Kurnsteiner, H., and Kuck, U. (2014). Genome sequence and annotation of *Acremonium chrysogenum*, producer of the beta-lactam antibiotic cephalosporin C. *Genome Announc.* 2:e00948-14. doi: 10.1128/genomeA.00948-14

Trifonov, L. S., Bieri, J. H., Prewo, R., Dreiding, A. S., Hoesch, L., and Rast, D. M. (1983). Isolation and structure elucidation of three metabolites from *Verticillium intertextum*: sorbicillin, dihydrosorbicillin and bisvertinoquinol. *Tetrahedron* 39, 4243–4256. doi: 10.1016/S0040-4020(01)88647-6

Warr, G. A., Veitch, J. A., Walsh, A. W., Hesler, G. A., Pirnik, D. M., Leet, J. E., et al. (1996). BMS-182123, a fungal metabolite that inhibits the production of TNF-alpha by macrophages and monocytes. *J. Antibiot.* 49, 234–240. doi: 10.7164/antibiotics.49.234

Zhao, J. L., Zhang, M., Liu, J. M., Tan, Z., Chen, R. D., Xie, K. B., et al. (2017). Bioactive steroids and sorbicillinoids isolated from the endophytic fungus *Trichoderma* sp. Xy24. *J. Asian Nat. Prod. Res.* 19, 1028–1035. doi: 10.1080/10286020.2017.1285908

Conflict of Interest Statement: The authors declare that the research was conducted in the absence of any commercial or financial relationships that could be construed as a potential conflict of interest.

Copyright © 2017 Derntl, Guzmán Chávez, Mello-de-Sousa, Busse, Driessen, Mach and Mach-Aigner. This is an open-access article distributed under the terms of the Creative Commons Attribution License (CC BY). The use, distribution or reproduction in other forums is permitted, provided the original author(s) or licensor are credited and that the original publication in this journal is cited, in accordance with accepted academic practice. No use, distribution or reproduction is permitted which does not comply with these terms.

frontiers in Microbiology

REVIEW
published: 05 January 2018
doi: 10.3389/fmicb.2017.02536

Marine Fungi: A Source of Potential Anticancer Compounds

Sunil K. Deshmukh[1]*, *Ved Prakash*[2] *and Nihar Ranjan*[1]*

[1] TERI–Deakin Nano Biotechnology Centre, The Energy and Resources Institute, New Delhi, India, [2] Department of Biotechnology, Motilal Nehru National Institute of Technology, Allahabad, India

Metabolites from marine fungi have hogged the limelight in drug discovery because of their promise as therapeutic agents. A number of metabolites related to marine fungi have been discovered from various sources which are known to possess a range of activities as antibacterial, antiviral and anticancer agents. Although, over a thousand marine fungi based metabolites have already been reported, none of them have reached the market yet which could partly be related to non-comprehensive screening approaches and lack of sustained lead optimization. The origin of these marine fungal metabolites is varied as their habitats have been reported from various sources such as sponge, algae, mangrove derived fungi, and fungi from bottom sediments. The importance of these natural compounds is based on their cytotoxicity and related activities that emanate from the diversity in their chemical structures and functional groups present on them. This review covers the majority of anticancer compounds isolated from marine fungi during 2012–2016 against specific cancer cell lines.

Keywords: marine fungi, deep sea fungi, cytotoxic compounds, mangroove associated fungi, sponge associated fungi

OPEN ACCESS

Edited by:
Bhim Pratap Singh,
Mizoram University, India

Reviewed by:
Giovanna Cristina Varese,
Università degli Studi di Torino, Italy
Antje Labes,
Fachhochschule Flensburg, Germany

***Correspondence:**
Sunil K. Deshmukh
sunil.deshmukh@teri.res.in
Nihar Ranjan
nihar.ranjan@teri.res.in

Specialty section:
This article was submitted to Microbiotechnology, Ecotoxicology and Bioremediation, a section of the journal Frontiers in Microbiology

Received: *18 April 2017*
Accepted: *06 December 2017*
Published: *05 January 2018*

Citation:
Deshmukh SK, Prakash V and Ranjan N (2018) Marine Fungi: A Source of Potential Anticancer Compounds. Front. Microbiol. 8:2536. doi: 10.3389/fmicb.2017.02536

INTRODUCTION

Marine fungi are important source of secondary metabolites useful for the drug discovery purposes. Even though marine fungi are less explored in comparison to their terrestrial counterparts, a number of useful hits have been obtained from the drug discovery perspective adding to their importance in the natural product discovery (Molinski et al., 2009; Butler et al., 2014), which have yielded a wide range of chemically diverse agents with antibacterial, antiviral and anticancer properties in animal systems. Starting with the celebrated example of cephalosporins, marine fungi have provided unique chemical skeletons that could be used to develop drugs of clinical importance (Bhadury et al., 2006; Saleem et al., 2007; Javed et al., 2011; Sithranga and Kathiresan, 2011). Fungi, in general, have been generous source of drugs as evidenced by the isolation of many drugs in use such as paclitaxel, camptothecin, vincristine, torreyanic acid and cytarabine to name a few. In this light, marine are important not just from the perspective of new drugs but also as a source of new scaffolds that can be modified further to obtain the desired action. Despite significant progress in the drug discovery that has provided treatment for some major ailments, minor infections, and epidemics; new drugs are required to combat global resistance to drugs for existing diseases and new infections that have been reported in recent times (such as SARS, dengue and Zika

viruses). In addition to drug resistance in diseases such as tuberculosis and malaria, cancer & HIV-AIDS (Passaes and Sáez-Cirión, 2014) have been biological targets with limited success toward therapeutics development.

In addition to terrestrial sources, oceans have been a huge reservoir of a variety of biologically active compounds, which have often been the resulting metabolite of marine life (König et al., 2006; Chen G. et al., 2014; Agrawal et al., 2016; Deshmukh et al., 2017). Though, why marine fungi produce such complex and diverse set of metabolites in not fairly understood, it is largely assumed that they play key roles in chemical defense and communication. The biosynthesis of these metabolites in dependent on ecological, physical and biological factors and, therefore, small changes in these conditions can generate entirely new set of metabolites (Pejin and Maja, 2017). The contribution of marine based therapeutics can be gauged from the fact that during 1981–2002, more than half of the FDA approved drugs had originated from marine life. Most of the marine based drugs have come from invertebrates (sponges, tunicates, mollusks, and bryozoans); two-thirds of which, belong to the class of non-ribosomal peptides. Some of these are already in the market (Polymixin B, pristinamycin, gramicidin, vancomycin, bleomycin, actinomycin D) as antibiotic and anti-cancer agents while several others are in clinical trials (Manoalide, discodermolide) (Singh et al., 2008). In this regard, there have not been many reports of drugs from marine fungi that are used clinically which can be partly attributed to lack of systematic and comprehensive approaches as well as lack of optimization which has precluded a large number of potential hits from becoming actual drugs. Therefore, metabolites marine fungi constitute a group of under-represented resource for discovering novel therapeutics (Imhoff, 2016).

Several classes of chemically distinct metabolites from marine fungi have been reported in recent years which have a wide range of activities against different targets (Wu et al., 2015, 2016). From marine fungi alone, over thousand metabolites have been reported to have potential to be developed as drugs (Gomes et al., 2015), with several as anticancer compounds (please also see a detailed review, Bugni and Ireland, 2004 for historical inputs, taxonomy, ecological roles, distribution and chemistry as well biological activities of marine fungi), none of these have reached the market till now. However, for majority of these findings, complete taxonomy studies, biological targets and modes of interaction have not been identified yet. Due to these limitations, in this review, we cover anticancer compounds reported from marine fungi obtained from different sources such as deep-sea sediments, algae, sponge, mangrove endophytic and other marine fungi, discovered during 2012–2016 with a focus on summarizing the important findings and highlighting the lead compounds. Wherever explored, the biological targets and efficacies have been discussed as well. Novel anticancer compounds reported from marine fungi are given in Supplementary Table 1. They are arranged on the basis of sources the fungi isolated.

METABOLITES ISOLATED FROM DEEP-SEA SEDIMENT FUNGI

Deep-sea fungi inhabit at depths of thousand meters or below the surface (Swathi et al., 2013) where the sea environments are extreme; which are typically characterized by the absence of sunlight irradiation, predominantly low temperature, high hydrostatic pressure, and oligotrophy. Many reports indicate abundance and diversity of fungi in these environments (Hua et al., 2011; Mahé et al., 2013). Here, we present an account of metabolites reported from the deep-sea fungi during 2012–2016 that have displayed anticancer activities in various cell lines.

Linear peptides, simplicilliumtides A, E, G, and H (**1–4**; **Figure 1**) were isolated from a culture broth of the deep-sea-derived fungal strain *Simplicillium obclavatum* EIODSF 020e collected in the East Indian Ocean. Simplicilliumtides A and G showed weak cytotoxicity toward human leukemia HL-60 cell line with IC_{50} values of 64.7 and 100 μM, and simplicilliumtides E and H showed weak cytotoxicity toward K562 cell line with IC_{50} values of 39.4 and 73.5 μM (Liang et al., 2016). Using a combination of fermentation and subsequent chromatographic separation, acaromycin A **(5)** and (+)-cryptosporin (**6**; **Figure 1**) were isolated from the deep-sea derived fungus *Acaromyces ingoldii* FS121 which was obtained from the South Sea in China. Using a combinaion of one and two-dimensional NMR as well as mass spectroscopic techniques, the chemical structures were elucidated and the absolute configuration was further determined by circular dichroism (CD) experiments. Compounds **(5)** and **(6)** exhibited considerable growth inhibition against tumor cell lines MCF-7, NCI-H460, SF-268, and HepG-2 with IC_{50} values <10 μM. The inhibitory effect of compound **(5)** against MCF-7 cell line was comparable to cytoxicity of cisplatin which was used as a positive control (Gao et al., 2016a). A new tetranorlabdane diterpenoid, asperolide E (**7**; **Figure 1**) was isolated from the deep sea sediment-derived fungus *Aspergillus wentii* SD-310. The cytotoxicity of compound **(7)** was evaluated against HeLa, MCF-7, and NCI-H446 cell lines which showed IC_{50} values of 10.0, 11.0, and 16.0 μM respectively (Li X.-D. et al., 2016).

Asperethers A-E (**8–12**; **Figure 1**), five new 20-nor-isopimarane diterpenoids having a 14,16-cyclic ether unit and a unique 6/6/6/5 tetracyclic skeleton, were discovered from the culture extract of *Aspergillus wentii* SD-310 from the deep-sea sediment sample. The chemical structure of these compounds was determined by mass spectrometry and NMR techniques (^{1}H NMR, COSY, HSQC, HMBC) and the absolute configurations were supported by NOESY, X-ray crystallography, CD and computational methods. Compounds (**8–12**) displayed cytotoxic activities against A549 cell line with the IC_{50} values of 20, 16, 19, 17, and 20 μM, respectively, which were moderately higher than the positive control Adriamycin (Li X. et al., 2016).

Circumdatin G (**13**; **Figure 1**), was isolated from the culture of the deep-sea fungus *Aspergillus westerdijkiae* SCSIO 05233 which was isolated from a sediment sample in the South China Sea. Spectroscopic analysis using mass spectrometry and a variety of one and two-dimensional NMR techniques (DEPT, HMBC)

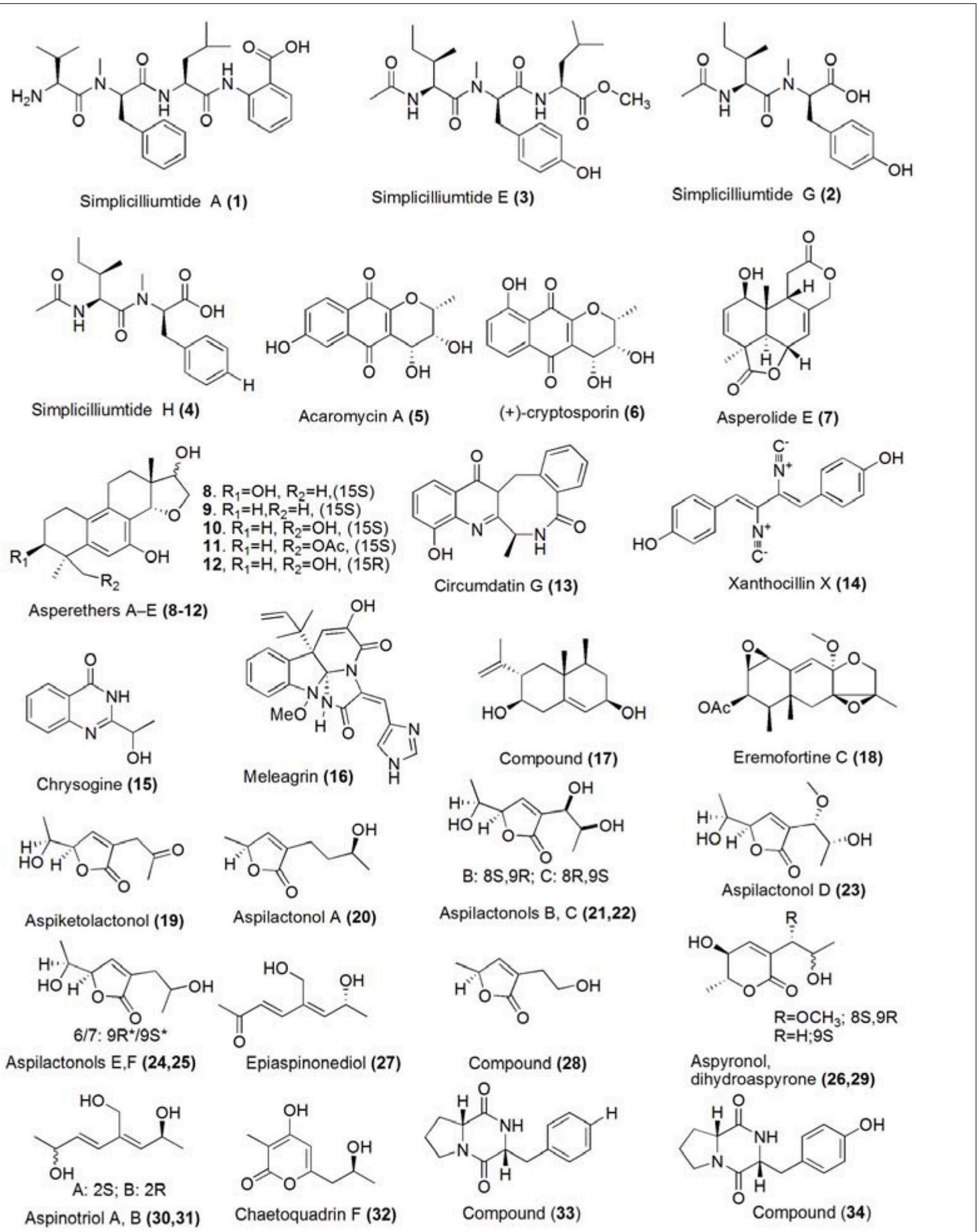


FIGURE 1 | Continued

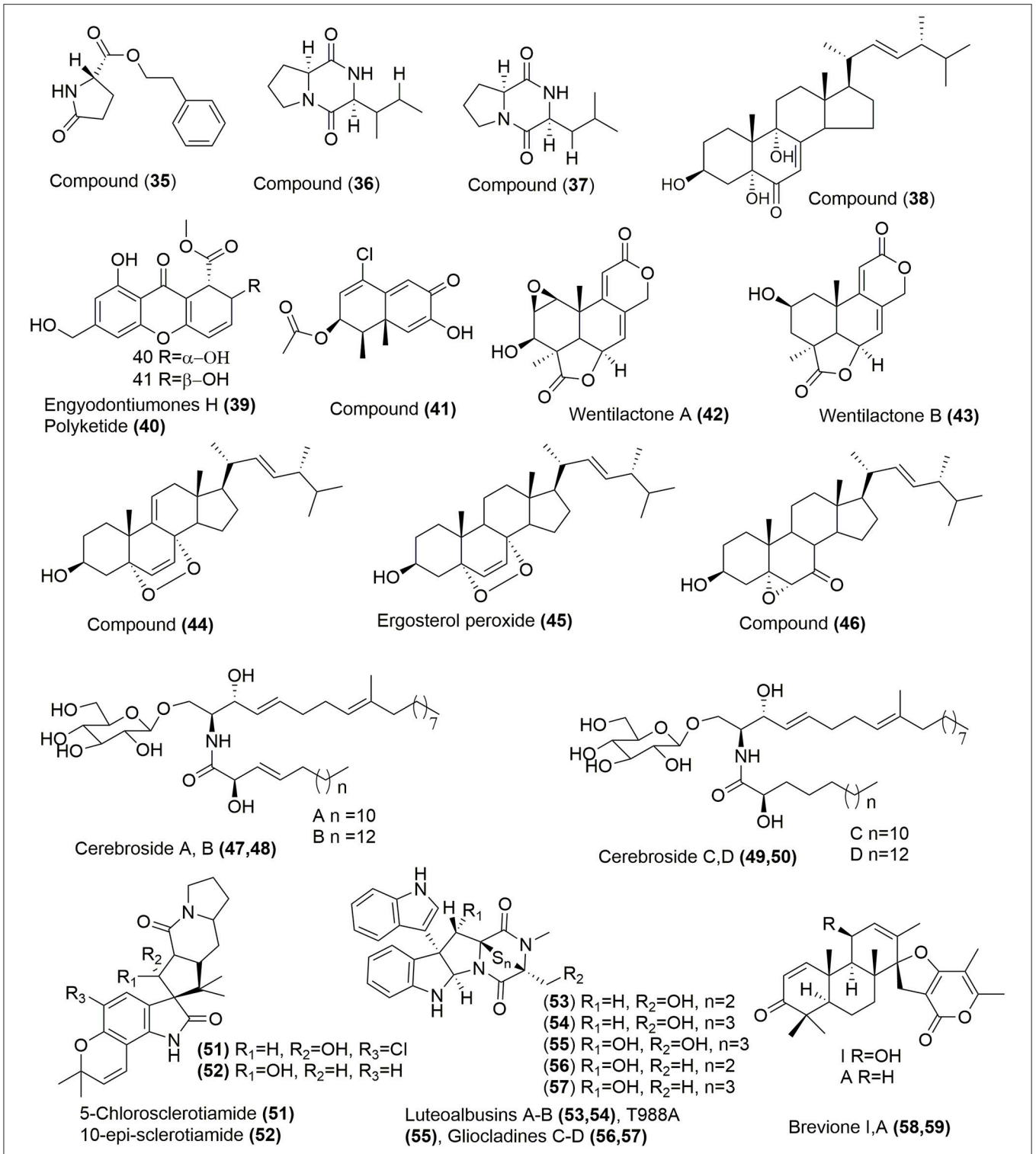


FIGURE 1 | Structures of metabolites obtained from deep sea marine fungi. For complete chemical names, please see Supplementary Table 1.

led to the determination of its chemical structure. Compound (**13**) displayed weak antiproliferation activities toward K562 and promyelocytic HL-6 cell lines with IC_{50} values ranging between 25.8 and 44.9 μM (Fredimoses et al., 2015). Xanthocillin X (**14**), chrysogine (**15**) and meleagrin (**16**; **Figure 1**) were discovered from *Penicillium commune* SD-118. The growth inhibition of

compound **(14)** was evaluated against MCF-7, HepG2, NCI-H460, HeLa, DU145, and MDA-MB- 231 cell lines with the IC_{50} values of 12.0, 7.0, 10.0, 10.0, 8.0, and 8.0 μg/mL respectively. The cytotoxicity of compound **(15)** was moderate against SW1990 cell line with an IC_{50} value of 20.0 μg/mL, whereas compound **(16)** exhibited potent cytotoxicity against DU145 cell line with an IC_{50} value of 5.0 μg/mL. It also showed moderate cytotoxicity toward HepG2, NCIH460, HeLa, and MDA-MB-231 cell lines with IC_{50} values of 12.0, 22.0, 20.0, and 11.0 μg/mL respectively (Shang et al., 2012a; Zhao et al., 2012).

Using a combination of traditional and high-performance liquid chromatography techniques, eremophilane type sesquiterpene (**17**; **Figure 1**) and an analog of one tautomeric form of eremofortine C **(18)** were isolated from the Antarctic deep-sea fungus *Penicillium* sp. PR19 N-. The cytotoxicity studies of compounds **(17)** and **(18)** against HL-60 cells were evaluated which gave IC_{50} values of 45.8, 28.3 μM respectively. The inhibitory concentrations of compounds **(17)** and **(18)** against A-549 cells were found to have IC_{50} values of 82.8, 5.2 μM respectively (Lin et al., 2014). Nine new C_9 polyketides named aspiketolactonol **(19)**, aspilactonols A–F (**20-25**; **Figure 1**), aspyronol **(26)** and epiaspinonediol **(27)** were isolated together with five known polyketides (*S*)-2-(2′-hydroxyethyl)-4-methyl-γ-butyrolactone **(28)**, dihydroaspyrone **(29)**, aspinotriol A **(30)**, aspinotriol B **(31)** and chaetoquadrin F **(32)** from *Aspergillus* sp. 16-02-1, which was collected from a deep-sea sediment at a Lau Basin hydrothermal vent in the southwest of the Pacific Ocean. NMR, mass and CD spectroscopy techniques were used to determine the chemical structure and assign the absolute configuration of these novel molecules. Compounds **(19-32)** exhibited significant cytotoxic activities with inhibitory rate (IR%) values at 100 μg/mL between 10 and 79% against human cancer cell lines K562, HL-60, HeLa, and BGC-823 (Chen X. et al., 2014). Six metabolites, (**33–38**; **Figure 1**) were isolated from a mutated deep-sea fungal strain of *Aspergillus versicolor* ZBY-3. Their inhibitory activities were determined aginst K562 cells at a concentration of 100 μg/mL which showed inhibitory rates of 54.6, 72.9, 23.5, 29.6, 30.9, and 51.1% respectively (Dong et al., 2014). From a deep-sea fungus *Engyodontium album* DFFSCS021, a new chromone engyodontiumones H **(39)** and a known polyketide (**40**; **Figure 1**) were isolated. Their cytotoxcities were determined which showed selectivity against human histiocytic lymphoma U937 cell line with the IC_{50}values of 4.9 and 8.8 μM respectively (Yao et al., 2014).

An Antarctic deep-sea derived fungus *Penicillium* sp. PR19N-1 was the source of compound (**41**; **Figure 1**). Its chemical structures was established using IR, HRMS as well as one and two-dimensional NMR techniques. The cytotoxicity of compound **(41)** was modest against HL-60 and A549 cell lines with IC_{50} values of 11.8 and 12.2 μM respectively (Wu et al., 2013). The deep-sea sediment of the South China Sea was the source of fungus *Aspergillus dimorphicus* SD317 from which, Wentilactone A **(42)** and B (**43**; **Figure 1**) were isolated (Xu et al., 2015). Further exploration of induced apoptosis of Wentilactone A **(42)** displayed G2/M cell cycle arrest of human lung carcinoma cells (Lv et al., 2013). Wentilactone B **(43)** inhibited proliferation and migration of human hepatoma SMMC-7721 cells (Zhang et al., 2013). Seven secondary metabolites including ergosterol peroxide derivative **(44)**, ergosterol peroxide **(45)**, (22*E*,24*R*)-5α,6α-epoxy-3β-hydroxyergosta-22-ene-7-one **(46)**, and cerebroside A-D (**47-50**; **Figure 1**) were reported by Cui and coworkers in 2013 from the deep-sea fungus *Paecilomyces lilacinus* ZBY-1. These compounds exhibit cytotoxic activity against K562, MCF-7, HL-60, and BGC-823 cells with IC_{50} of 22.3–139.0 μM (Cui et al., 2013). The compounds 5-chlorosclerotiamide **(51)** and 10-epi-sclerotiamide **(52)** were the secondary metabolites of the deep-sea fungus *Aspergillus westerdijkiae* DFFSCS013, which showed excellent cytotoxicity against K562 cell line with IC_{50} of 44 and 53 μM respectively (Peng et al., 2013). Another deep-sea sediment in the South China Sea was the source of fungus *Acrostalagmus luteoalbus* SCSIO F457 from which metabolites luteoalbusins A–B **(53, 54)**, T988A **(55)** and gliocladines C–D **(56, 57)** were isolated (**Figure 1**). The cytotoxicity of compound **(53)** was evaluated against SF-268 MCF-7 NCI-H460 HepG-2 cell lines, which gave IC_{50} values of 0.46, 0.233, 1.15, and 0.91 μM respectively. Similarly, the cytotoxicity of compound **(54)** against SF-268 MCF-7 NCI-H460 HepG-2 gave IC_{50} values of 0.59, 0.25, 1.31, 1.29 μM respectively. Compounds **(55–57)** were slightly less cytotoxic against SF-268, MCF-7, NCI-H460, and HepG-2 with IC_{50} values ranging in between 0.91 and 17, 7 μM respectively. The positive control cisplatin, exhibited cytotoxicity against SF-268, MCF-7, NCI-H460, and HepG-2 cell lines with IC_{50} values of 4.7, 3.9, 2.9, and 2.4 μM respectively (Wang et al., 2012). Breviones I and A **(58, 59)** were isolated from the deep-sea fungus *Penicillium* sp. in China (**Figure 1**). The cytotoxicity of compounds **(58)** and **(59)** were determined against MCF-7 cells lines, which gave IC_{50} values of 7.44 and 28.4 μM respectively. The IC_{50} of compound **(58)** against A549 cells was found to be 32.5 μM (cisplatin, the positive control, gave IC_{50} values of 8.0 and 8.9 μM against these two tumor cell lines; Li et al., 2012).

COMPOUNDS FROM ALGAE-ASSOCIATED FUNGI

Marine algae-derived endophytic fungus *Paecilomyces variotii* EN-291 was the source of indole derivatives varioloid A **(60)** and varioloid B (**61**; **Figure 2**). Both compounds were cytotoxic against A549, HCT116, and HepG2 cell lines with IC_{50} values between 2.6 and 8.2 μg/mL (Zhang et al., 2016). Another marine algae-derived fungus *Aspergillus ochraceus* Jcma1F17 gave cinnamolide derivative **(62)** and a known compound insulicolide A **(63)** whose chemical structures are given in **Figure 2**. The cytotoxicity of these compounds was determined against H1975, U937, K562,−823, Molt-4,−7, A549, HeLa, HL60, and Huh-7 human cancer cell lines, which gave IC_{50} values between 1.95 and 6.35 μM (Fang et al., 2014).

Marine red alga *Lomentaria catenata* was collected at Guryongpo, NamGu, PoHang in Republic of Korea. From the surface of this alga, fungus *Microsporum* sp. (MFS-YL) was obtained from which physcion **(64)** was isolated (**Figure 2**). Physcion **(64)** induced apoptosis in HeLa cells and its effect on the expressions of p53, p21, Bax, Bcl-2, caspase-9, and

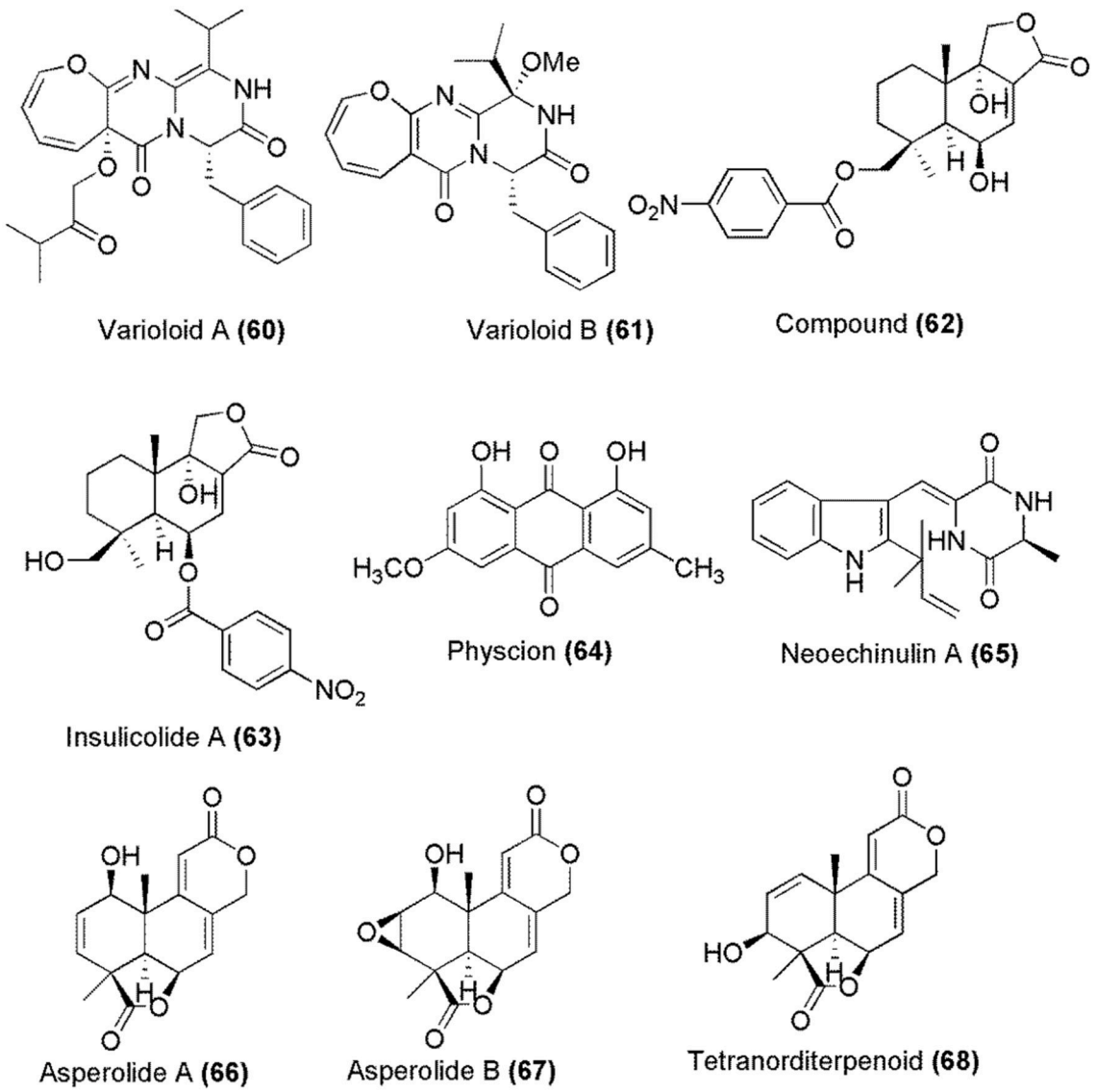


FIGURE 2 | Structures of metabolites obtained from marine algae associated fungi.

caspase-3 proteins were investigated. The western blot analysis revealed that physcion **(64)** induces cell apoptosis through down-regulation of Bcl-2 expression, up-regulation of Bax expression, and activation the caspase-3 pathway. Additionally, physcion **(64)** also induced the formation of reactive oxygen species (ROS) in HeLa cells (Wijesekara et al., 2014). A prenylated indole alkaloid neoechinulin A **(65)** (**Figure 2**) was obtained from a marine-derived fungus, *Microsporum* sp. (MFS-YL), which was isolated from the surface of a marine red alga *Lomentaria catenata*, collected at Guryongpo, NamGu, PoHang in the Republic of Korea. Neoechinulin A **(65)** has shown the cytotoxic effect on human cervical carcinoma HeLa cells and its apoptosis induction in HeLa cells was investigated by the expressions of p53, p21, Bax, Bcl-2, Caspase 9, and Caspase 3 proteins. Western blot analysis revealed that neoechinulin A **(65)** could induce cell apoptosis through down-regulation of Bcl-2 expression, up-regulation of Bax expression and activation the caspase-3 pathway (Wijesekara et al., 2013). Marine alga, *Sargassum* sp. was the source of endophytic fungus *Aspergillus wentii* EN-48 from which asperolides A–B **(66–67)** together with tetranorlabdane diterpenoid derivative **(68)**, wentilactones A **(42)** and B **(43)** were isolated. The cytotoxicity of these compounds **(66–68, 42, 43)** was moderate against HeLa, HepG2, MCF-7, MDA-MB-231, NCI-H460, SMMC-7721 and SW1990 tumor cell lines. Wentilactone B **(43)** was the most potent among the tested compounds ($IC_{50} = 17\ \mu M$) (Sun H.-F. et al., 2012).

COMPOUNDS FROM MANGROVE ENDOPHYTIC FUNGI

Using one strain many compounds (OSMAC) approach, spirobrocazines C **(69)** and brocazine G **(70)** were obtained from mangrove-derived fungus *Penicillium brocae* MA-231 (**Figure 3**). Their chemical structures and absolute stereochemical

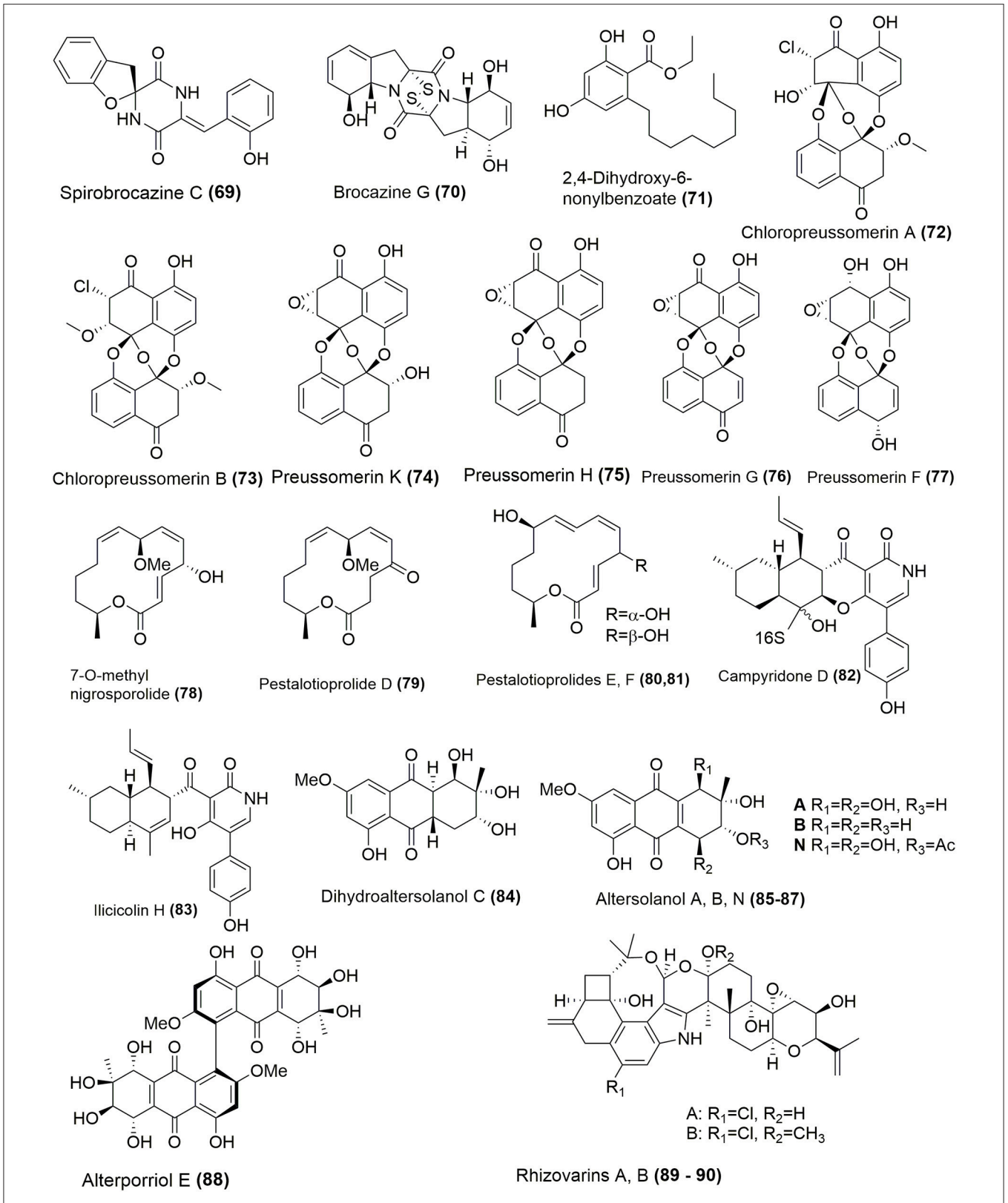


FIGURE 3 | Continued

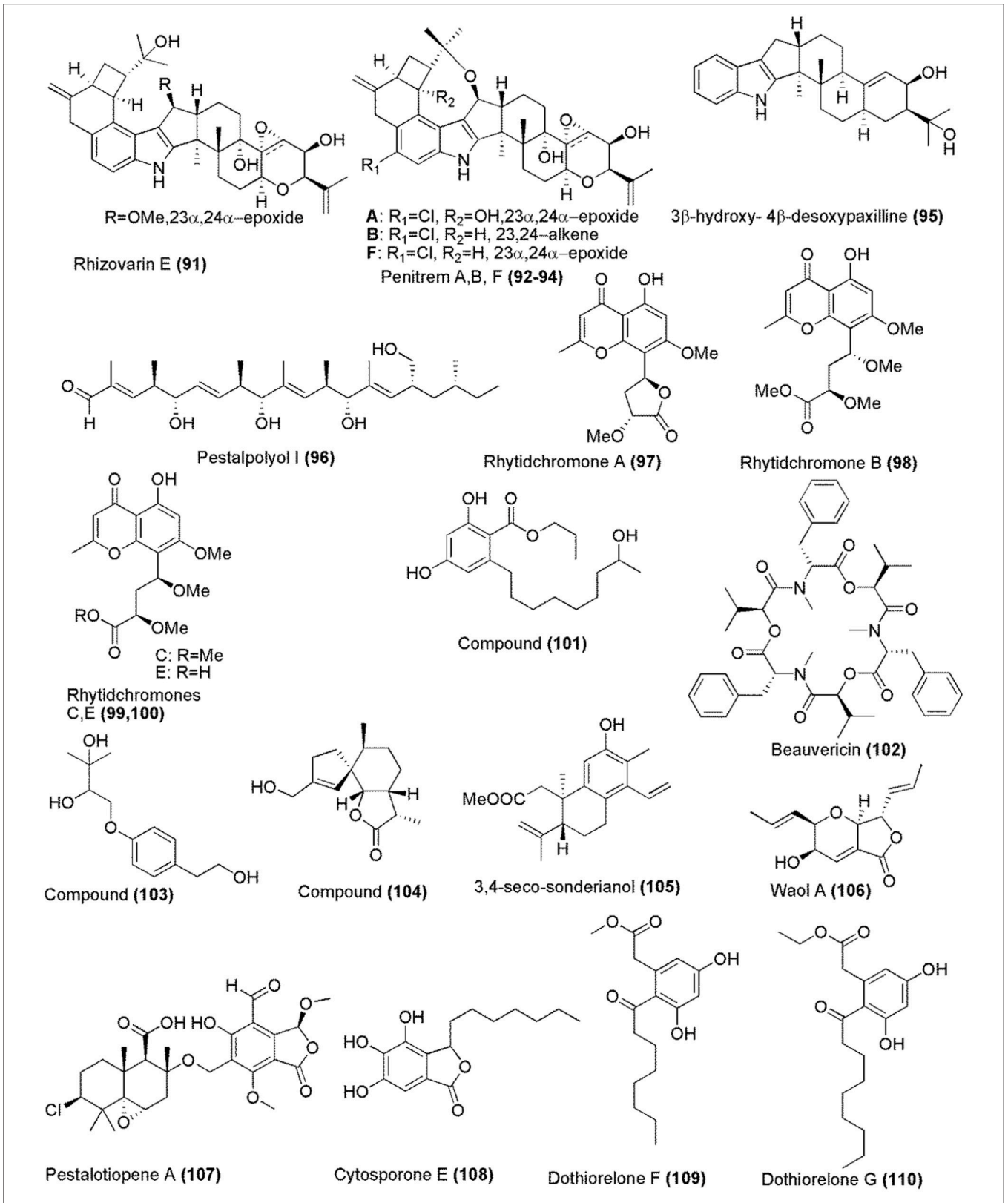


FIGURE 3 | Continued

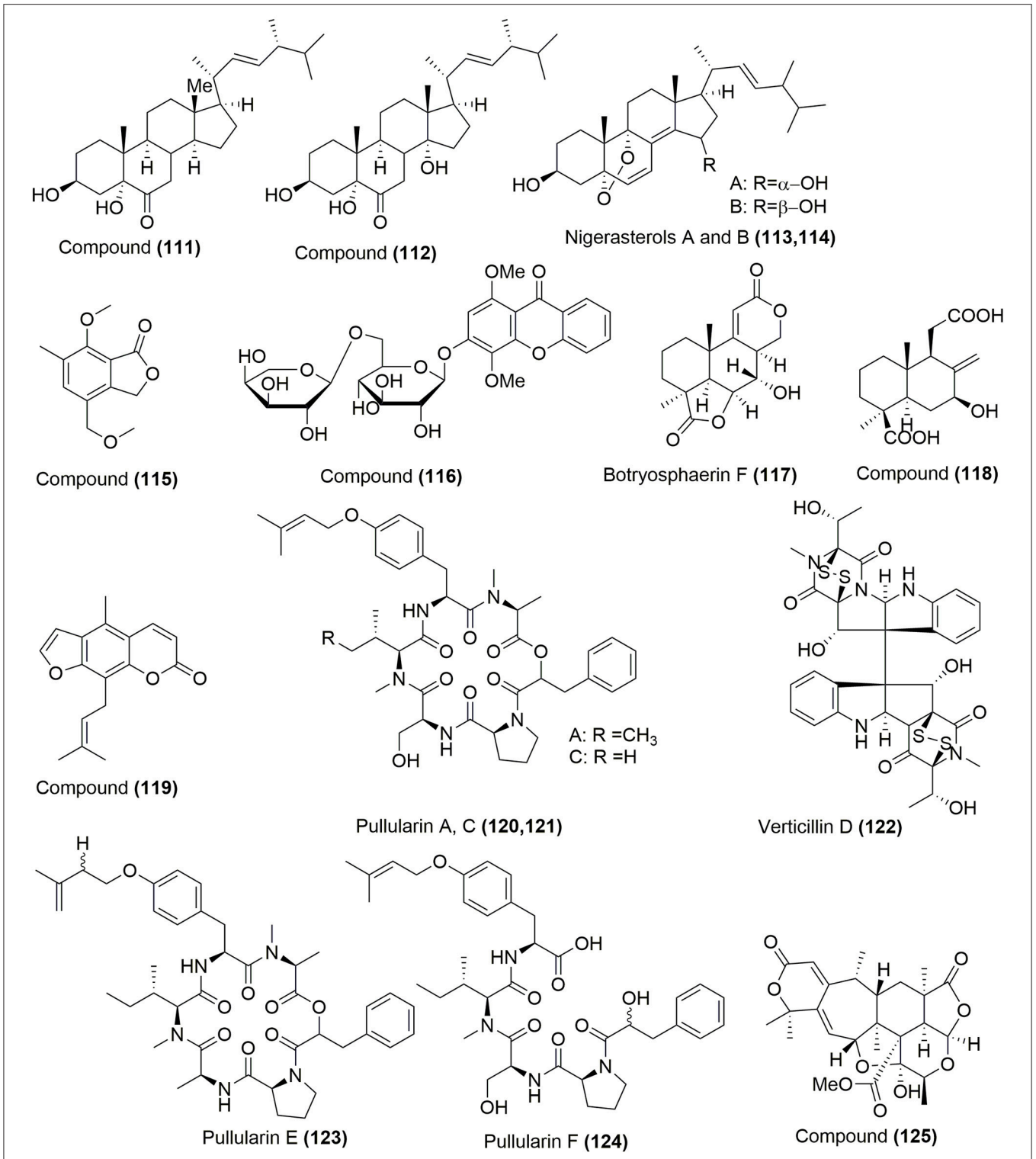


FIGURE 3 | Continued

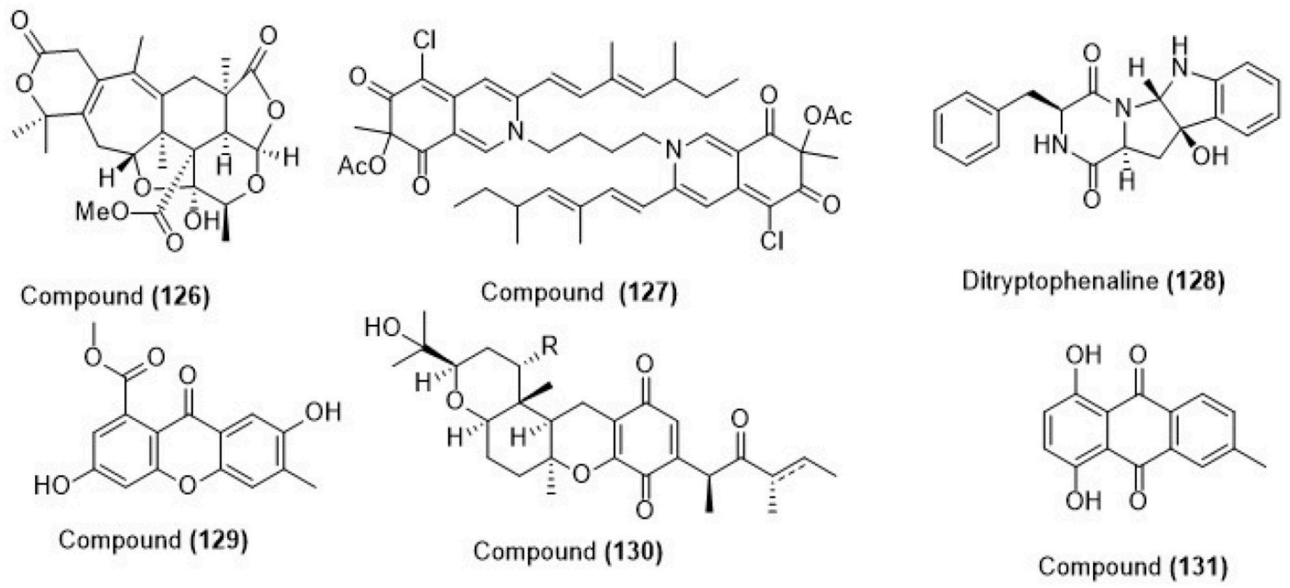


FIGURE 3 | Chemical structures of metabolites associated with marine mangrove endophytic fungi. For complete chemical names, please see Supplementary Table 1.

configurations were determined by spectroscopic analysis, computational calculations and X-ray diffraction. Spirobrocazine C **(69)** showed moderate activity against A2780 cells (IC_{50} 59 μM) while compound **(70)** showed strong activity against A2780 and A2780 CisR cell with the IC_{50} values of 664 and 661 nM respectively, which were much better than that of the positive control cisplatin, which gave IC_{50} values of 1.67 and 12.63 μM respectively (Meng et al., 2016). 2,4-Dihydroxy-6-nonylbenzoate (**71**; **Figure 3**) was isolated from a mangrove endophytic fungus, *Lasiodiplodia* sp. 318, which was collected from *Excoecaria agallocha* in Mangrove National Nature Reserve in Gaoqiao, Zhanjiang city, Guangdong Province, China. Its structure was established by spectroscopic techniques (one and two-dimensional NMR, HR-ESI-MS), and electronic CD experiment. Compound **(71)** exhibited cytotoxicity against MMQ and GH3 cell lines with the IC_{50} values of 5.2 and 13.0 μM respectively (Huang et al., 2017). Endophytic fungus, *Lasiodiplodia theobromae* ZJ-HQ1 was isolated from a healthy leaf of the marine mangrove *A. ilicifolius*, which was collected from Zhanjiang Mangrove Nature Reserve in Guangdong Province, China. This fungus gave two new chlorinated preussomerins, chloropreussomerins A and B **(72, 73)** together with spreussomerin K **(74)**, preussomerin H **(75)**, preussomerin G **(76)**, and preussomerin F **(77)** as their metabolites (**Figure 3**). Their chemical structures were elucidated by a combination of spectroscopic techniques. The absolute configurations of **(72)** and **(73)** were determined by single-crystal X-ray diffraction techniques. Compounds **(72)** and **(73)** were the first chlorinated compounds in the preussomerins family, which showed potent *in vitro* cytotoxicity against A549 and MCF-7 human cancer cell lines with IC_{50} values ranging from 5.9 to 8.9 μM. Compounds **(74–77)** exhibited significant bioactivity against A549, HepG2, and MCF-7 human cancer cell lines with the IC_{50} values of 2.5–9.4 μM (Chen et al., 2016).

7-O-methylnigrosporolide **(78)**, pestalotioprolides D-F **(79–81)** were isolated from mangrove derived endophytic fungus *Pestalotiopsis microspore* (**Figure 3**), which was obtained from fresh healthy fruits of *Drepanocarpus lunatus* (Fabaceae) collected from Douala, Cameroon. Co-culture of *P. microspora* with *Streptomyces lividans* resulted in roughly ten-fold enhancement in the production accumulation of compounds **(80)** and **(81)** compared to axenic fungal control. Their chemical structures were determined by the analysis of NMR and mass spectroscopy data. The cytotoxicity of these compounds **(78-81)** was significant against murine lymphoma cell line L5178Y, which showed IC_{50} values of 0.7, 5.6, 3.4, and 3.9 μM respectively. Compound **(80)** was potent against the human ovarian cancer cell line A2780 with an IC_{50} value of 1.2 μM (Liu et al., 2016). Campyridones D **(82)** and ilicicolin H **(83)** were isolated from *Campylocarpon* sp. HDN13-307 (**Figure 3**), which was obtained from the root of mangrove plant *Sonneratia caseolaris*. Their chemical structures and absolute configurations were determined on the basis of spectroscopic analysis and electronic CD results. Campyridone D **(82)** and ilicicolin H **(83)** were cytotoxic against HeLa cell with the IC_{50} values of 8.8 and 4.7 μM respectively (Zhu et al., 2016).

Dihydroaltersolanol C **(84)**, altersolanols A, B, N **(85-87)**, and alterporriol E **(88)** were isolated from white bean solid culture media of the endophytic fungus, *Stemphylium globuliferum*, collected from the Egyptian mangrove plant *Avicennia marina* (**Figure 3**). Their structures were elucidated using one and two-dimensional NMR spectroscopy as well as high-resolution mass spectroscopy (Moussa et al., 2016). Dihydroaltersolanol C **(84)**, altersolanol A **(85)**, B **(86)**, and alterporriol E **(88)** exhibited

toxicity against L5178Y mouse lymphoma cell line with the IC_{50} values of 3.4, 2.5, 3.7, and 6.9 μM (Liu Y. et al., 2015). Altersolanol N **(87)** also exhibited potent cytotoxicity against L5178Y mouse lymphoma cell line with IC_{50} values in the low micromolar range (Debbab et al., 2012). Altersolanol A **(85)** showed cytotoxic activity against 34 human cancer cell lines *in vitro*, with mean IC_{50} (IC_{70}) values of 0.005 μg/mL (0.024 μg/ml) respectively (Mishra et al., 2015). The cellular activity of altersolanol A **(85)** has been studied in detail, which has shown that it is a kinase inhibitor which induces cell death by apoptosis through caspase dependent pathway. Altersolanol A **(85)** inhibited a variety of kinases, which suggested that the kinase inhibition might be the mechanism for the cytotoxic activity (Debbab et al., 2009). Further studies revealed that its antitumor potential was linked to pro-apoptotic and anti-invasive activity that occurred through the inhibition of NF-κB transcriptional activity (Teiten et al., 2013). *Mucor irregularis* QEN-189, an endophytic fungus obtained from the fresh inner tissue of the marine mangrove plant *Rhizophora stylosa*, collected in Hainan Island, China was the source of rhizovarins A, B, E **(89–91)**, penitrems A, C, F **(92–94)**, and 3β-hydroxy- 4β-desoxypaxilline **(95)** whose chemical structures are shown in **Figure 3**. The structures of these compounds were determined by detailed spectroscopic analysis. Compounds **(89-94)** were cytotoxic against the human A-549 cell lines with IC_{50} values of 11.5, 6.3, 9.2, 8.4, 8.0, 8.2, and 4.6 μM, while compounds **(89, 90, 92–95)** showed cytotoxicity against the human HL-60 cell lines with IC_{50} values of 9.6, 5.0,7.0, 4.7, 3.3, and 2.6 μM respectively. Adriamycin, a positive control, exhibited cytotoxicity with the IC_{50} values of 0.30 and 0.06 μM against A-549 and HL-60 cell lines respectively (Gao et al., 2016b).

Endophytic fungus *Pestalotiopsis clavispora* isolated from the mangrove plant *Rhizophora harrisonii* was the source of a new polyketide derivative pestalpolyol I (**96**; **Figure 3**). The chemical structure of the new compound was determined using one and two-dimensional NMR spectroscopy, as well as by high-resolution mass spectrometry. Compound **(96)** displayed cytotoxicity against the mouse lymphoma cell line L5178Y activity with an IC_{50} value of 4.10 μM (Perez et al., 2016). Four highly oxygenated chromones, rhytidchromone A, B, C, and E **(97–100)** were isolated from the culture broth of a mangrove-derived endophytic fungus, *Rhytidhysteron rufulum,* which was obtained from Thai *Bruguiera gymnorrhiza* (**Figure 3**). Their structures were determined by analysis of 1D and 2D NMR spectroscopic data. The structure of rhytidchromone A **(97)** was further confirmed by single-crystal X-ray diffraction analysis. Compounds **(97–100)** displayed cytotoxicity against Kato-3 cell lines with the IC_{50} values ranging from 16.0 to 23.3 μM, while rhytidchromones A and C were active against MCF-7 cells with the IC_{50} values of 19.3 and 17.7 μM respectively (Chokpaiboon et al., 2016).

Another compound ethyl-2,4-dihydroxy-6-(8′-hydroxynonyl)- benzoate (**101**; **Figure 3**) was isolated from a mangrove endophytic fungus, *Lasiodiplodia* sp. 318# and its complete chemical structure was elucidated by spectroscopic techniques. The compound **(101)** was cytotoxic against several cell lines with the IC_{50} values of 10.1 μM (MDA-MB-435), 12.5 μM (HepG2), 11.9 μM (HCT-116), 13.31 μM (A549), and 39.74 μM (THP1) respectively (Li J. et al., 2016). Mangrove derived endophytic fungus *Fusarium* sp. (No. DZ27) in the South China Sea was the source of beauvericin **(102)**, a cyclic peptide (**Figure 3**), and its chemical structure was deduced by spectroscopic methods and also using the reference data from the literature. Beauvericin **(102)** was potent in the growth inhibition of KB and KBv200 cells with the IC_{50} values of 5.76 and 5.34 μM. Further analysis of beauvericin **(102)** activity was done, which showed that it induced apoptosis through the decrease of reactive oxygen species generation, loss of mitochondrial membrane potential, release of cytochrome C, activation of Caspase-9 and -3, and cleavage of PARP and did not regulate Bcl-2 or Bax expression (Tao et al., 2015).

Mangrove associated endophytic fungus *Penicillium* sp.FJ-1 of *Avicennia marina,* which was collected in Fujian, China was the source of two new metabolites; compounds **(103)** and **(104)** as shown in **Figure 3**. Their chemical structures were determined using NMR and mass spectroscopy. The antiproliferative activity of compound **(103)** was weak against Tca8113 and MG-63 cells with the IC_{50} values of 26 and 35 μM respectively. The positive control, taxol, gave the IC_{50} values of 46 and 10 nM with Tca8113 and MG-63 cell lines respectively. The IC_{50} value of compound **(104)** on Tca8113 and normal liver cell line WRL-68 was 10 and 58 μM respectively. Compound **(104)** also showed anti-tumor effect on MG-63 cells with an IC_{50} value of 55 nM. Compound **(104)** was also tested against nude mice, which showed significant inhibition of tumor growth of human osteosarcoma (Zheng et al., 2014). A known diterpenoid 3,4-seco-sonderianol (**105**; **Figure 3**) was isolated from endophytic fungus J3 of *Ceriops tagal* collected in the mangrove reserve of Dong Zhai Gang, Hainan province, China. Its structure was elucidated using spectroscopic methods including 1D and 2D NMR (HMQC, ^{1}H-^{1}H COSY and HMBC). Compound **(105)** exhibited activities against K562, SGC-7901, and BEL-7402 cell lines with the IC_{50} values of 9.2, 15.7, and 25.4 μg/mL respectively. Paclitaxel was used as the positive control, which displayed the IC_{50} values of 5.1 μg/mL against K562, 1.6 μg/mL against SGC-7901 and 6.3 μg/mL against BEL-7402 cel lines respectively (Zeng et al., 2015). Waol A **(106)**, pestalotiopene A **(107)**, cytosporone E **(108)** were obtained from the endophytic fungus *Acremonium strictum*, isolated from the mangrove tree *Rhizophora apiculata* (**Figure 3**). The chemical structures of the isolated compounds were elucidated on the basis of comprehensive NMR and mass spectrometry analysis. Compounds **(106–108)** showed moderate cytotoxic activity against human cisplatin-sensitive (IC_{50} values 27.1, 76.2, and 8.3 μM respectively) and resistant A2780 cell lines (IC_{50} values 12.6, 30.1, and 19.0 μM respectively) (Hammerschmidt et al., 2014).

Mangrove endophytic fungus *Dothiorella* sp., which was obtained from the bark of the mangrove tree *Aegiceras corniculatum* at the estuary of Jiulong River, Fujian Province of China, was the source of two new polyketides, named dothiorelones F **(109)** and G **(110)** as shown in **Figure 3**. Their chemical structures were determined on the basis of NMR data and mass spectrometry. Dothiorelones F **(109)** and G **(110)** showed significant cytotoxicity against Raji cancer cell line with

an IC_{50} value of 2 μg/mL (Du and Su, 2014). The mangrove endophytic fungus *Aspergillus terreus* (No. GX7-3B), which was obtained from a branch of *Bruguiera gymnoihiza* (Linn.) growing on the coastal salt marsh of the South China Sea was the source of compounds **(111**, **112)** and beauvericin **(102)** as shown in **Figure 3**. Their chemical structures were determined by the analysis of the spectroscopic data. The cytotoxicity of compounds **(111)** and **(102)** ranged from moderate to strong against MCF-7, A549, HeLa, and KB cell lines with the IC_{50} values of 4.98 and 2.02 (MCF-7), 1.95 and 0.82 (A549), 0.68 and 1.14 (HeLa) and 1.50 and 1.10 μM (KB) respectively. The inhibitory activity of compound **(112)** was weak against these tumor cell lines (Deng C. M. et al., 2013). Endophytic fungus *Aspergillus niger* MA-132 was isolated from mangrove plant *Avicennia marina,* which was the source of two sterol derivatives nigerasterols A and B (**113, 114)** as shown in **Figure 3**. The chemical structures and absolute configurations of these compounds were determined using spectroscopic methods. Modified version of Mosher's method was used to confirm the absolute configuration of compound **(113)**. Nigerasterols A and B **(113, 114)**, which represent the first 5,9-epidioxy-sterol compounds of marine origin were evaluated for cytotoxicity. Nigerasterol B **(114)** displayed potent activity against the tumor cell line HL60 with an IC_{50} value of 1.50 μM, while nigerasterol A **(113)** displayed stronger activity with an IC_{50} value of 0.30 μM. Both compounds **(113)** and **(114)** displayed potent activities against A549 cell line with the IC_{50} values of 1.82 and 5.41 μM respectively (Liu et al., 2013).

A new isobenzofuranone, 4-(methoxymethyl)-7-methoxy-6-methyl-1(3H)-isobenzofuranone (**115**; **Figure 3**) was isolated from the mangrove endophytic fungus *Penicillium* sp. ZH58, which was obtained from the South China Sea coast. Its chemical structure was determined by the analysis of spectroscopic data. Compound **(115)** exhibited cytotoxicity against KB and KB_{V200} cells with the IC_{50} values of 6 and 10 μg/mL, respectively (Yang et al., 2013). A new xanthone derivative (**116**; **Figure 3**) was isolated from the culture of mangrove endophytic fungus, *Phomopsis* sp. (ZH76). Its chemical structure was determined on the basis of spectroscopic data. Compound **(116)** inhibited the growth of HEp-2 and HepG2 cells with the IC_{50} values of 9 and 16 μM respectively (Huang et al., 2013). Mangrove fungus *Aspergillus terreus* (No. GX7-3B) led to the production of two metabolites: compound **(117)** and compound **(118)** as shown in **Figure 3**. The chemcial structures of these compounds were determined on the basis of spectroscopic data. Compound **(117)** showed inhibitory activity toward MCF-7 and HL-60 cancer cell lines with the IC_{50} values of 4.4 and 3.4 μM, respectively. The cytotoxicity of compound **(118)** was promising against HL-60 cell line with an IC_{50} value of 0.6 μM (Deng C. et al., 2013). Mangrove endophytic fungus, *Penicillium* sp. ZH16 was obtained from the South China Sea, which produced furanocoumarin derivative **(119)** as shown in **Figure 3**. Its chemical structure was determined by the analysis of NMR and mass spectroscopic data. Compound **(119)** was cytotoxic against KB and KB_V200 cells with the IC_{50} values 5 and 10 μg/mL respectively (Huang Z. et al., 2012). Endophytic fungus *Bionectria ochroleuca,* which was obtained from the inner leaf tissues of the plant *Sonneratia caseolaris* in Hainan island (China) produced pullularin A **(120)**, pullularin C **(121)**, verticillin D **(122)** and pullularins E and F **(123, 124)** as shown in **Figure 3**. Their chemical structures were established using NMR spectroscopy and high-resolution mass spectrometry. Compounds **(120–124)** were cytotoxic against the mouse lymphoma cells (L5178Y) with the EC_{50} values between 0.1 and 6.7 μg/mL (Ebrahim et al., 2012).

Meroterpenes **(125–127)** were isolated from the marine fungus *Penicillium* sp. 303 cultured from sea water samples obtained from Zhanjiang Mangrove National Nature Reserve in Guangdong Province, China (**Figure 3**). The isolated compounds are structurally related to the miniolutelide class of meroterpenoids and were identified as derivatives of miniolutelide B. Compounds **(125)** and **(126)** showed moderate cytotoxic activities against a panel of cancer cell lines including MDA-MB-435, HepG2, HCT-116 and A549 cell lines. Compound **(127)** showed potent cytotoxic activity with IC_{50} values of 7.13 μM against MDA-MB-435 (Li J. et al., 2014). Ditryptophenaline **(128)** was isolated from mangrove endophytic fungus No·Gx-3a in the South China Sea (**Figure 3**). Ditryptophenaline showed strong inhibitory activity on KB and KBv200 cell lines with LD_{50} values of 8.0 and 12.0 μM (Yang et al., 2013b). A marine fungus *Phomopsis* sp. (No. SK7RN3G1) was obtained from mangrove sediment of Shankou in Hainan, China, which led to the production of a new xanthone derivative **(129)** as shown in **Figure 3**. Its chemical structure was determined by spectroscopic methods and it was found to be cytotoxic against HEp-2 and HepG2 cells with the IC_{50} values of 8 and 9 μg/mL (Yang et al., 2013c). The endophytic fungus *Nigrospora* sp. MA75 was obtained from the marine semi-mangrove plant *Pongamia pinnata* that led to the production of a new quinone derivative (**130**; **Figure 3**) which was isolated from *Nigrospora* sp. MA75, an. The chemical structure of compound **(130)** was elucidated by detailed spectroscopic analysis and absolute configuration determination. Compound **(130)** showed potent inhibition growth of MCF-7, SW1990, and SMMC7721 tumor cell lines with the IC_{50} values of 4, 5, and 7 μg/mL respectively (Shang et al., 2012b). Anthracene derivative **(131)** was isolated from mangrove endophytic fungus No.5094 which was collected in the South China Sea as shown in **Figure 3**. The compound was identified on the basis of spectral analysis. Compound **(131)** showed strong inhibitory activity with KB and KBv200 cell lines having the LD_{50} values of 5.5 and 10.2 μM respectively (Yang et al., 2013a).

COMPOUNDS FROM MARINE SEDIMENT-DERIVED FUNGI

Marine sediment-derived fungus *Eutypella* sp. FS46 was obtained from the South China Sea. The culture of this fungus produced a pimarane-type diterpene, scopararane I **(134)** as shown in **Figure 4**. Compound (**132)** showed moderate cytotoxicity against MCF-7, NCI-H460 and SF-268 cell lines with the IC_{50} values 83.9, 13.5, and 25.3 μg/ mL respectively (Liu et al., 2017). Hetero-spirocyclic γ-lactams pseurotin A **(133)**, pseurotin D **(134)**, alkaloids fumitremorgin C **(135)**, and

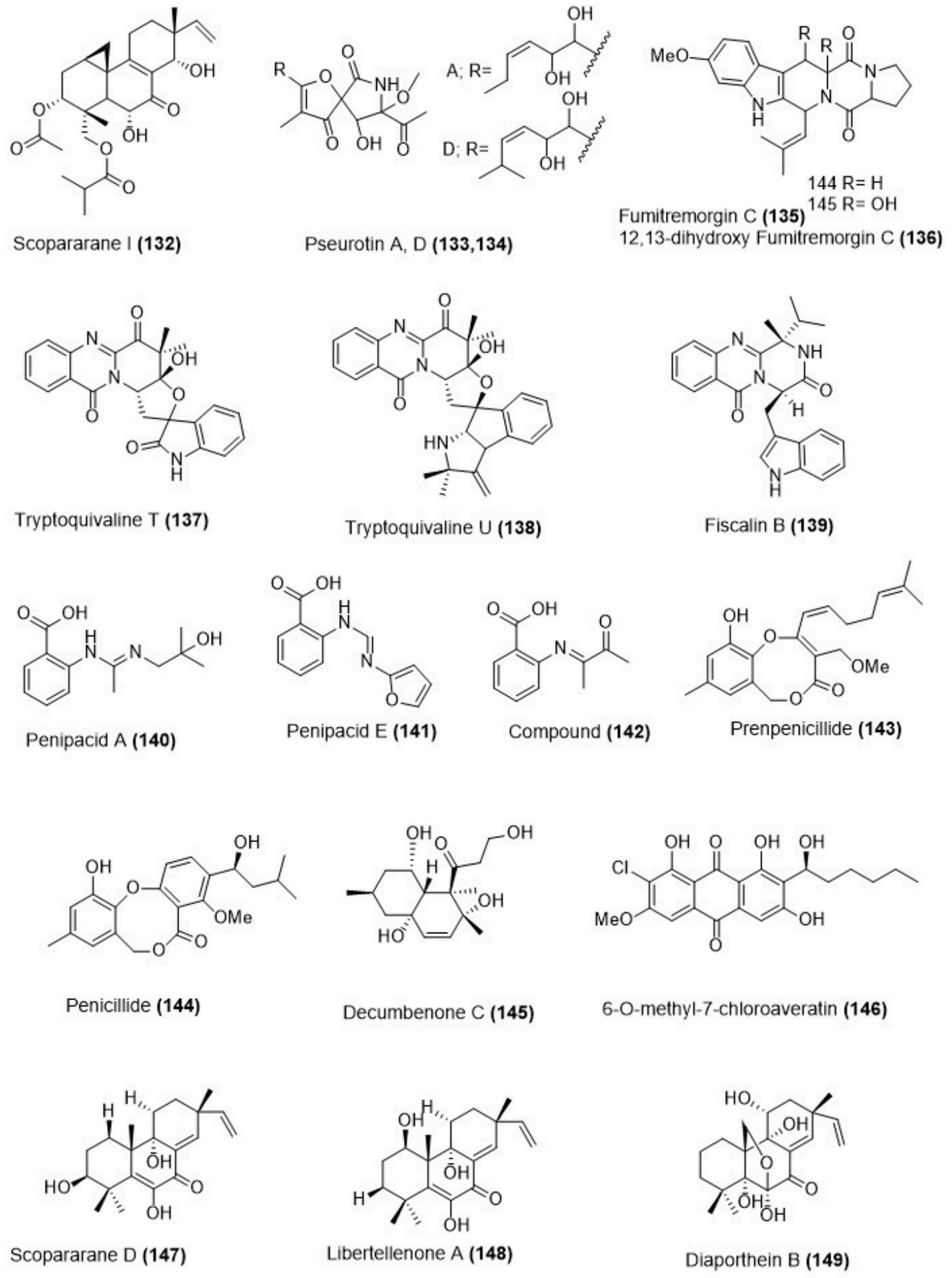


FIGURE 4 | Chemical structures of metabolites obtained from marine sediment derived fungi. For complete chemical names, please see Supplementary Table 1.

12,13-dihydroxy fumitremorgin C (**136**; **Figure 4**) were isolated from *Aspergillus* sp. (BRF 030) which was obtained from the sediments collected on the northeast coast of Brazil. Pseurotin A **(133)**, pseurotin D **(134)**, fumitremorgin C **(135)**, and 12,13-dihydroxy-fumitremorgin C **(136)** showed toxicity against HCT-116 cell line with the IC_{50} values 72.0, 85.0, 15.1, and 4.5 μM (Saraiva et al., 2015). Tryptoquivaline T **(137)**, tryptoquivaline U **(138)**, and fiscalin B **(139)** were isolated from *Neosartorya fischeri* which was obtained from marine mud in the intertidal zone of Hainan Province of China (**Figure 4**). The bioactivity of compounds **(137–139)** toward apoptosis of HL-60 cells were done which showed the IC_{50} values of 82.3, 90.0, and 8.8 μM respectively (Wu et al., 2015). Fungus *Penicillium paneum* SD-44 was obtained from marine sediment sample in the South China Sea which produced anthranilic acid derivatives penipacids A and E (**140, 141**; **Figure 4**) together with one known analog **(142)**. Their chemical structures were deduced using NMR and mass spectrometry analysis. Penipacids A **(140)** and E **(141)** inhibited RKO cell growth with the IC_{50} values of 8.4 and 9.7 μM while compound **(142)** was cytotoxic against HeLa cell line with an IC_{50} value of 6.6 μM, which was better than the positive control fluorouracil (IC_{50} = 25.0 and 14.5 μM against RKO and HeLa cells lines respectively; Li et al., 2013).

Marine-derived fungus *Penicillium* sp. ZLN29 was obtained from the sediments collected in the Jiaozhou Bay of China from which penicillide derivative **(143)** and a known polyketide compound **(144)** were isolated (**Figure 4**). Compounds **(143)** and **(144)** showed weak cytotoxicity against HepG2 cell line with the IC_{50} values of 9.9 and 9.7 μM respectively (Gao et al., 2013a). The marine fungus *Aspergillus sulphureus* KMM 4640 was obtained from marine sediments which produced a new decalin derivative decumbenone C **(145)** as shown in **Figure 4**. Decumbenone C **(145)** was cytotoxic against SK-MEL-5 human melanoma cells with an IC_{50} value of 0.9 μM (Zhuravleva et al., 2012). Marine-derived fungus *Aspergillus* sp. SCSIO F063 was obtained from a marine sediment sample, collected in the South China Sea which produced chloroaveratin derivative **(146)** as shown in **Figure 4**. Chemical structure determination was done by spectroscopic analyses that included mass spectrometry and NMR. Compound **(146)** showed inhibitory activity against three human tumor cell lines; SF-268, MCF-7, and NCI-H460 with the IC_{50} values of 7.1, 6.6, and 7.4 μM respectively (Huang H. et al., 2012).

Marine-derived fungus *Eutypella scoparia* FS26 that had been obtained from the sediment collected in the South China Sea produced scopararane D **(147)**, libertellenone A **(148)** and diaporthein B **(149)** whose structures are depicted in **Figure 4**. All isolated compounds were assessed for their antiproliferative activity using a cytotoxicity (MTT) assay against three different human cancer cell lines: MCF-7 (breast), NCI-H460 (lung), and SF-268 (brain). Compound **(147)** showed only mild antiproliferative activity with the IC_{50} values between 25.6 and 46.0 μM, whereas, libertellenone A **(148)** and diaporthein B **(149)**, revealed potent antiproliferative activities with IC_{50} values ranging from 4.4 to 20.0 μM, compared to cisplatin (IC_{50} = 1.5–9.2 μM) (Sun L. et al., 2012).

COMPOUNDS FROM SPONGE ASSOCIATED FUNGI

Fungus *Arthrinium arundinis* ZSDS1-F3 was collected from sponge *Phakellia fusca* in Xisha Islands of China which led to the isolation of metabolites cytochalasin K **(150)** and compound **(151)** as shown in **Figure 5**. Compounds **(150)** and **(151)** showed cytotoxicity against K562, A549, Huh-7, H1975, HL60, HeLa, and MOLT-4 cell lines with the IC_{50} values ranging between 1.1 and 47.4 μM. Compound **(150)** showed cytotoxicity against K562, A549, Huh-7, H1975, MCF-7, U937, BGC823, HL60, HeLa, and MOLT-4 cell lines, with IC_{50} values of 10.5, 13.7, 10.9, 19.1, 11.1, 47.4, and 11.8 μM respectively while compound **(151)** was cytotoxic against K562, A549, Huh-7, H1975, MCF-7, U937, BGC823, HL60, HeLa MOLT-4 cell lines with IC_{50} values of 6.2, 1.1, >50, 14.2, 18.5, 3.4, 18.8, 6.2, 3.2, and 4.1 μM respectively. The positive control trichostatin A was cytotoxic to the same cell lines with the IC_{50} values of 0.24, 0.05, 0.09, 0.10, 0.08, 0.06, 0.09, 0.09, 0.11, and 0.03 μM respectively (Wang et al., 2015). Coral-derived fungus *Neosartorya laciniosa* (KUFC 7896) which was collected from the coastal forest soil at Samaersarn island, Chonburi Province, Thailand was the source of aszonapyrone A **(152)**, 13-oxofumitremorgin B **(153)**, sartorypyrone A **(154)** and sartorypyrone B **(155)** as shown in **Figure 5**. The chemical structures of the new compounds were determined on the basis of one and two-dimensional NMR spectral analysis as well as HR-ESIMS. Aszonapyrone A **(152)**, 13-oxofumitremorgin B **(153)**, sartorypyrone A **(154)** and sartorypyrone B **(155)** were evaluated for their ability to inhibit the growth of MCF-7, NCI-H460, and A375-C5 cell lines. The cytotoxicity results displayed that, among the meroditerpenes tested, aszonapyrone A **(152)** was the most potent compound showing strong growth inhibitory activity with GI_{50} = 13.6, 11.6 and 10.2 μM for MCF- 7, NCI-H460 and A375-C5 cell lines respectively. Sartorypyrone B **(155)** was also potent in growth inhibition, however, it was less active than aszonapyrone A **(154)** having the GI_{50} values 17.8, 20.5, and 25.0 μM for MCF-7, NCI-H460 and A375- C5 cell lines respectively. Another compound 13-oxofumitremorgin B **(153)** exhibited only weak inhibitory activity against all the three cell lines (GI_{50} = 115.0, 123.3, and 68.6 μM for MCF-7, NCI-H460 and A375-C5 cell lines respectively; Eamvijarn et al., 2013).

The marine-derived fungus *Aspergillus* sp., which was obtained from the sponge *Xestospongia testudinaria,* was collected from the South China Sea that gave two phenolic bisabolane sesquiterpenoid dimers, disydonols A and C **(156, 157)** as shown in **Figure 5**. Their chemical structures were determined on the basis of spectroscopic analysis. Compound **(156)** exhibited *in vitro* moderate cytotoxicity toward HepG-2 and Caski human tumor cell lines with the IC_{50} values of 9.31 and 12.40 μg/mL respectively. Compound **(157)** also displayed selectivity against HepG-2 and Caski human tumor cell lines with the IC_{50} values of 2.91 and 10.20 μg/mL respectively (Sun L.-L. et al., 2012). A new polyacetylene, xestospongiamide **(158)** was obtained from the Red Sea sponge, *Xestospongia* sp. which was collected from deep waters of

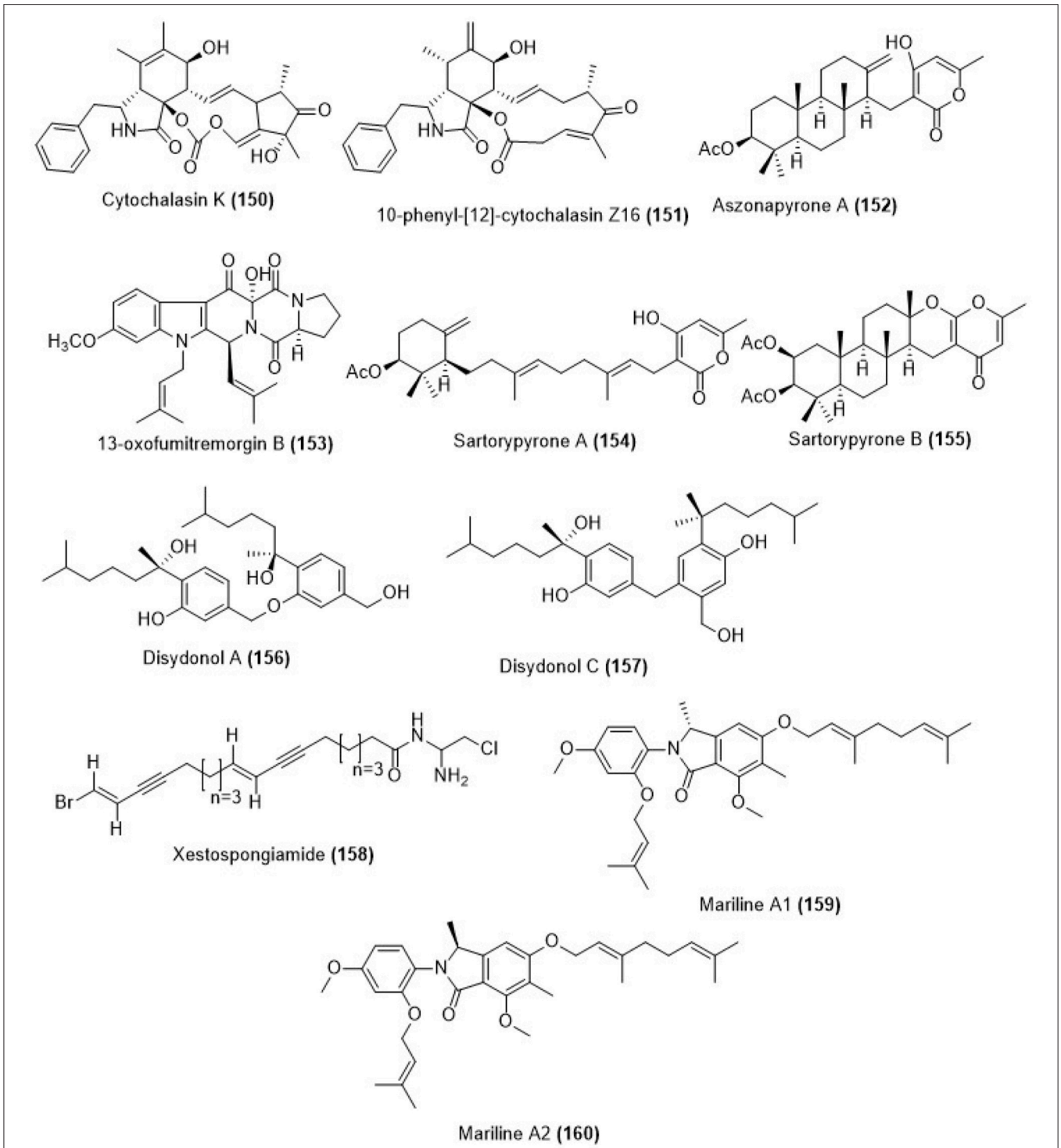


FIGURE 5 | Chemical structures of metabolites obtained from marine sponge associated fungi.

Sharm Obhur, Jeddah, Saudi Arabia (**Figure 5**). Compound **(158)** showed antitumor effect against both Ehrlich ascites carcinoma and lymphocytic leukemia (LD_{50} 5.0 μM each) (Ayyad et al., 2015).

A marine-derived fungus of the genus *Stachylidium* was isolated from the sponge *Callyspongia* cf. *C. flammea*. Chemical investigation of the bioactive fungal extract led to the isolation of the novel phthalimidine derivatives

marilines A1 and A2 **(159, 160)** whose chemical structures are shown in **Figure 5**. The absolute configurations of the enantiomeric compounds **(159)** and **(160)** were assigned using a combination of experimental circular dichroism (CD) investigation and quantum chemical CD calculations. The skeleton of marilines is unusual and its biosynthesis was suggested to require uncommon biochemical reactions in fungal secondary metabolism. Both enantiomers, marilines A1 **(159)** and A2 **(160)** inhibited human leukocyte elastase (HLE) with an IC_{50} value of 0.86 μM (Almeida et al., 2012).

COMPOUNDS FROM OTHER MARINE DERIVED FUNGUS

Aspergillus versicolor Y31-2, which was obtained from seawater samples in the Indian Ocean, gave a quinolinone derivative **(161)** as shown in **Figure 6**. Compound **(161)** was cytotoxic against MCF-7 and SMMC-7721 cell lines with the IC_{50} values of 16.6 and 18.2 μmol/L (Li P. et al., 2016). Fermented products of marine fungus *Penicillium sclerotiorum* M-22 which was isolated from a rotten leaf sample collected on the west coast of Haikou, Hainan province, China gave two azaphilonidal derivatives penicilazaphilones B **(162)** and C **(163)** as shown in **Figure 6**. Cytotoxicity studies revealed that penicilazaphilones B **(162)** and C **(163)** were selective against melanoma cells B-16 and human gastric cancer cells SGC-7901 with the IC_{50} values of 0.29, 0.44 and 0.06, 0.72 μM respectively. The control experiments with normal mammary epithelial cells M10 at the same concentration did not show significant toxicity (Zhou et al., 2016). A furan derivative **(164)** was isolated from marine-derived fungus *Penicillium chrysogenum* HGQ6 which was obtained from Lianyungang sea mud sample (**Figure 6**). The compound **(164)** was active against BGC823 cell line with an IC_{50} value of 0.19 mg/mL, which was lower than that of adriamycin with an IC_{50} value of 0.06 mg/mL (Guo et al., 2016). A mutant from diethyl sulfate (DES) mutagenesis of a marine-derived fungus *Penicillium purpurogenum* G59 produced epiremisporine B **(165)**, epiremisporine B1 **(166)** and isoconiochaetone C **(167)** as shown in **Figure 6**. Epiremisporine B **(165)** exhibited cytotoxicity against K562, HL-60, with the IC_{50} values of 69.0 and 62.9 μg/mL. Similarly epiremisporine B1 **(166)** exhibited cytotoxicity against K562, HL-60 cell lines with the IC_{50} values of 53.1 and 54.7 μg/mL respectively while the percent inhibition rate for isoconiochaetone C **(167)** were 20.4 and 26.0 at 100 μg/ mL against K562 and HL-60 cell lines respectively (Xia et al., 2015). Penicitrinine A **(168)** a novel alkaloid with a unique spiro skeleton was isolated from a marine-derived fungus *Penicillium citrinum* (**Figure 6**). Penicitrinine A **(168)** showed toxicity against A-375, SPC-A1, and HGC-27 cancer cell lines with IC_{50} values of 20.1, 28.6 and 29.4 μM respectively. Morphological evaluation, apoptosis rate analysis, Western blot and real-time quantitative PCR (RT-qPCR) results showed that penicitrinine A could significantly induce A-375 cell apoptosis by decreasing the expression of Bcl-2 and increasing the expression of Bax. Additionally, anti-metastatic effects of penicitrinine A in A-375 cells by wound healing assay, trans-well assay, Western blot and RT-qPCR were also investigated. These results showed penicitrinine A significantly suppressed metastatic activity of A-375 cells by regulating the expression of MMP-9 and its specific inhibitor TIMP-1 (Liu Q. Y. et al., 2015).

Aspergillus sp. was found in the gut of a marine isopod *Ligia oceanica,* which was collected in the seaside of Dinghai in Zhoushan, Zhejiang Province of China, that produced aspochalasin V (**169**; **Figure 6**). Apochalasin V **(169)** showed moderate activity against PC3 and HCT116 cell line with the IC_{50} values of 30.4 and 39.2 μM respectively (Liu et al., 2014). Fungus *Aspergillus terreus* SCSGAF0162 was obtained from the tissue of gorgonian *Echinogorgia aurantiaca* collected in Sanya, Hainan Province, China which produced a cytotoxic and antiviral cyclic tetrapeptide asperterrestide A **(170)** as shown in **Figure 6**. Compound **(170)** was cytotoxic to human carcinoma U937 and MOLT4 cell lines with the IC_{50} values of 6.4 and 6.2 μM respectively (He et al., 2013). Aculeatusquinones B and D **(171, 172)** were produced from marine-derived fungus *Aspergillus aculeatus* (**Figure 6**). The chemical structures of these compounds were determined by spectroscopic methods. Compounds **(171)** and **(172)** were cytotoxic to HL-60, K562, and A-549 cell lines with the IC_{50} values in the range of 5.4–6.1 μM (Chen et al., 2013).

Diorcinol D **(173)** and diorcinol E **(174)** (**Figure 6**) were produced from the marine-derived fungus *Aspergillus versicolor*. Their chemical structures were determined using spectroscopic analysis. Compound **(173)** was moderately cytotoxic against HeLa and K562 cell lines with the IC_{50} values of 31.5 and 48.9 μM respectively while compound **(174)** showed cytotoxicity against only HeLa cell line with the IC_{50} value 36.5 μM (Gao et al., 2013b). A new pyridinone, chaunolidone A (**175**; **Figure 6**) was isolated from marine-derived fungus *Chaunopycnis* sp. (CMB-MF028) which was obtained from the inner tissue of a pulmonate false limpet *Siphonaria* sp. that was collected from rock surfaces in the intertidal zone of Moora Park, Shorncliffe, Queensland, Australia. Chaunolidone A **(175)** was found to be a selective and potent inhibitor of human non-small cell lung carcinoma cell NCI-H460 with the IC_{50} value 0.09 μM (Shang et al., 2015).

Penicimutalidine **(176)** and a known compound oxaphenalenone (**177**; **Figure 6**) were isolated from a fungal mutant generated through the diethyl sulfate (DES) mutagenesis of marine-derived *Penicillium purpurogenum* G59. The IC_{50} values for cytotoxicity of **(176)** and **(177)** on HL-60 cells under the same conditions were determined to be 95.2 μg/ mL (313.2 μM) and 14.0 μg/ mL (56.9 μM). Compounds **(176)** and **(177)** also weakly inhibited the K562 cells with inhibition rate (IR) % values of 20.8 and 28.1% at 100 μg/mL (328.9 μM for **176** and 406.5 μM for **177**). The positive control 5-fluorouracil inhibited K562 cells with an IR% of 40.3% at 100 μg/mL (796.2 μM) (Li C.-W. et al., 2016). A novel cyclic dipeptide, named penicimutide **(178)** was produced from a neomycin-resistant mutant of the marine-derived fungus *Penicillium purpurogenum* G59 (**Figure 6**). Penicimutide **(178)** was selective against the HeLa cells with an inhibition rate (IR%) of 39.4% at 100 μg/mL which was similar to that of the positive control 5-fluorouracil (IR%

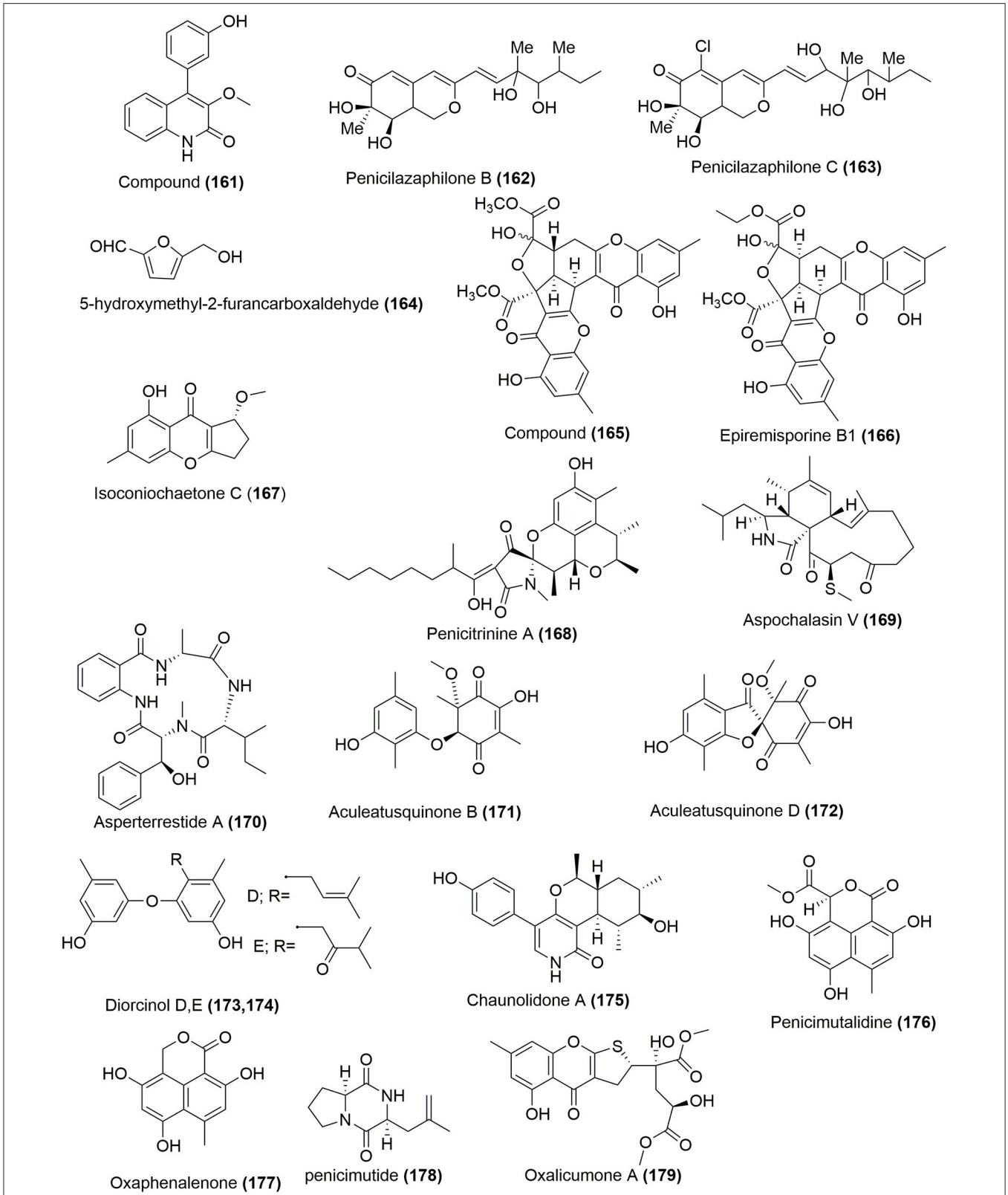


FIGURE 6 | Continued

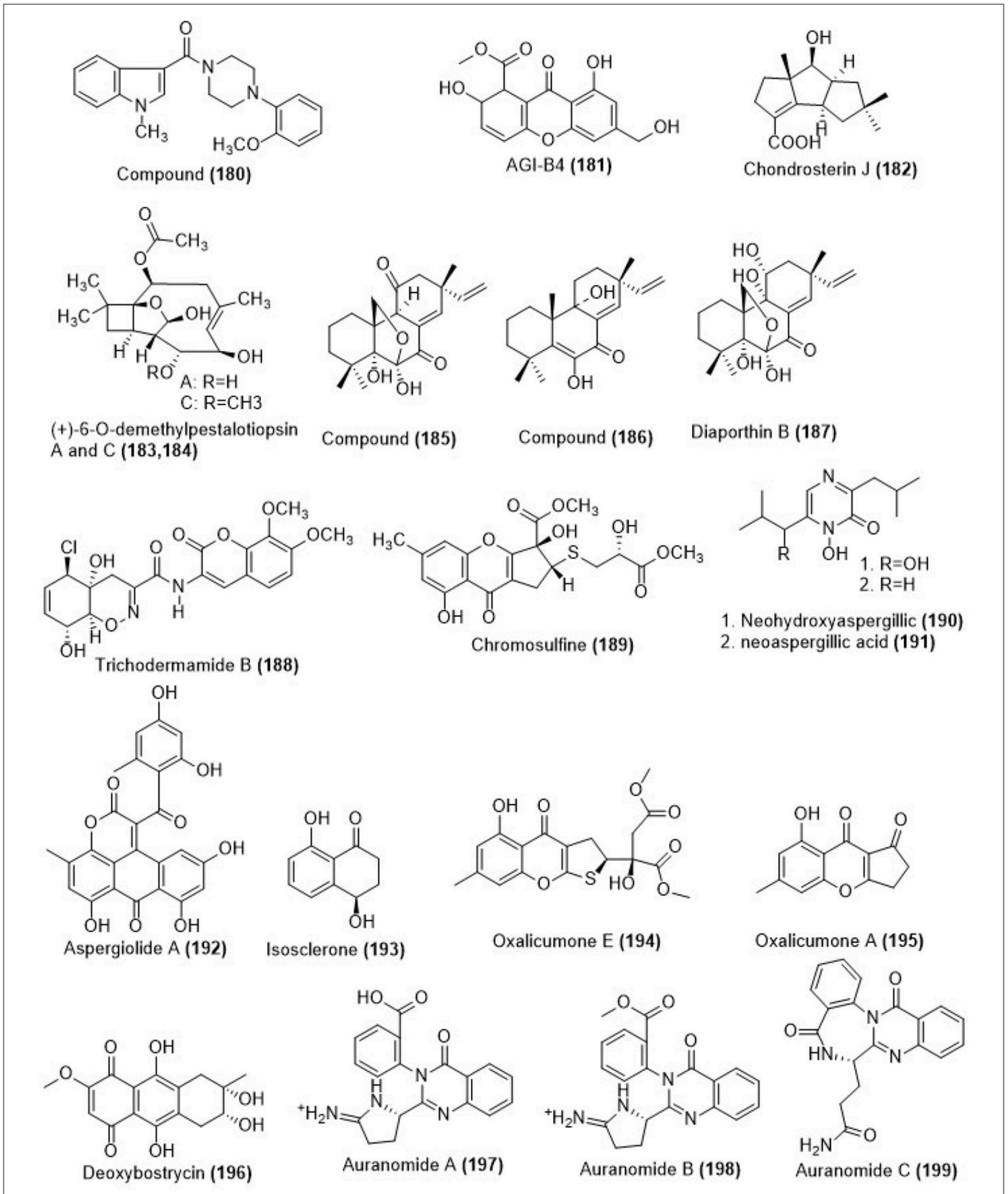


FIGURE 6 | Chemical structures of metabolites isolated from other marine derived fungi. For complete chemical names, please see Supplementary Table 1.

of 41.4% at 100 μg/mL against HeLa cells) (Wang et al., 2016).

Marine-derived fungus *Penicillium oxalicum* SCSGAF 0023, which was isolated from the South China Sea gorgonian *Muricella flexuosa,* produced oxalicumone A **(179**; (**Figure 6**). The compound **(179)** was cytotoxic against A375 and SW-620 cell lines with IC_{50} values of 11.7 and 22.6 μM (Sun et al., 2013). Compound (**180**; **Figure 6**) was isolated from the fungal strain *Aspergillus sydowii* SCSIO 00305 which was collected from a healthy tissue of *Verrucella umbraculum*. The compound **(180)** showed significant cytotoxicity against A375 cell lines with the IC_{50} value of 5.7 μM (He et al., 2012). A cytotoxic compound AGI-B4 (**181**; **Figure 6**) was obtained from the culture of a marine-derived fungus *Neosartorya fischeri* strain 1008F1. The chemical structure of the isolated compound was elucidated on the basis of spectroscopic data. Compound **(181)** showed toxicity aginst human gastric cancer cell line SGC-7901 with an IC_{50} value of 0.29 μM and against hepatic cancer cells BEL-7404 with an IC_{50} value of 0.31 μM (Tan et al., 2012). Fungus *Chondrostereum* sp. which was collected from soft coral *Sarcophyton tortuosum* in Hainan Sanya National Coral Reef Reserve, China produced chondrosterin J (**182**; **Figure 6**). The chemical structure of the compound was determined using NMR, mass spectrometry and single crystal X-ray diffraction techniques. The compound **(182)** was cytotoxic against human nasopharyngeal cancer cell lines CNE-1 and 2 with the inhibitory concentration (IC_{50}) values of 1.32 and 0.56 μM respectively (Li H.-J. et al., 2014). Fungus *Ascotricha* sp. ZJ-M-5 was obtained from a mud sample in Fenghua, China which produced compound **(183)** and (+)-6-O-demethylpestalotiopsin C (**184**; **Figure 6**). Compounds **(183)** and **(184)** were cytotoxic against HL-60 and K562 with the IC_{50} values 6.9 and 12.3 μM respectively (Wang W.-J. et al., 2014).

Fungal strain HS-1 was isolated from the sea cucumber *Apostichopus japonicas* that gave two pimarane diterpenoids **(185, 186)** and a known compound diaporthin B **(187)** as shown in (**Figure 6**). Their chemical structures and absolute configurations were determined using NMR and CD experiments. Compounds **(185-187)** were effective in growth inhibition of KB and KBv200 cell lines with the IC_{50} values of 3.51, 2.34 μg/mL, 20.74, 14.47 μg/mL, and 3.86, 6.52 μg/mL respectively (Xia et al., 2012).

The trichodermamides are modified dipeptides isolated from a wide variety of fungi, including *Trichoderma virens*. Previous studies have reported that trichodermamide B initiated cytotoxicity in HCT-116 colorectal cancer cells. In the present study trichodermamide B (**188**; **Figure 6**) showed an IC_{50} value of 3.1 μM in HeLa cell line. Compound **(189)** caused S-phase accumulation and cell death in HeLa cells, suggesting response to DNA double strand breaks (Jans et al., 2017). Chromosulfine (**189**; **Figure 6**), a novel cyclopentachromone sulfide, was isolated from a neomycin-resistant mutant of the marine-derived fungus, *Penicillium purpurogenum* G59. Its structure, including stereochemistry, was determined using spectroscopic methods using NMR, electronic CD (ECD) analysis and Mosher's method. The compound **(189)** showed toxicity against K562, HL-60, BGC-823, HeLa, and MCF-7 cell lines with IC_{50} values of 60.8, 16.7, 73.8, 75.4, and 59.2 μM (Yi et al., 2016).

Neohydroxyaspergillic **(190)** and neoaspergillic acid **(191)** (**Figure 6**) were isolated from the marine-derived fungus (strain CF07002) of the genus *Aspergillus*. Their structures were determined by the interpretation of NMR spectroscopic data which were corroborated by subsequent synthesis. Compound **(191)** exhibited toxicity against Jurkat, K562, U937, and Raji cell lines with the IC_{50} values of 31.6, 50.1, 42.6, and 54.9 μM respectively. Compound **(190)** was poorly active against Jurkat cell lines with an IC_{50} value of 60.2 μM (Cardoso-Martinez et al., 2015). *Aspergillus glaucus* was obtained from the marine sediment in Fujian province of the People's Republic of China which gave a novel anthraquionone derivative aspergiolide A **(192)**. The active components of this fungus were isolated which resulted in the identification of a novel naphtho[1,2,3-de]chromene-2,7-dione skeleton. Compound **(192)** acts by topoisomerase II inhibition similar to adriamycin activity. Further experiments with BEL-7402 cells showed that **(192)** reduced cancer growth via a caspase dependent pathway (Wang Y. et al., 2014). Marine-derived fungus, *Aspergillus fumigatus* was isolated from marine green algae in Seosaeng-myeon, Ulsan in the Republic of Korea which produced isosclerone **(193)** as shown in **Figure 6**. It showed cytotoxicity toward MCF-7 human breast cancer cells with the IC_{50} value 63 μM after 24 h incubation. Further experiments showed that compound **(193)** inhibited the protein and gene expressions of MMP-2,-9 in MCF-7 human breast cancer cells by altering MAPK signaling pathway (Li Y.-X. et al., 2014). Marine gorgonian-associated fungus *Penicillium oxalicum* SCSGAF 0023 produced oxalicumone E **(194)** and oxalicumone A (**195**; **Figure 6**). The chemical structures of these compounds were determined by spectroscopic analysis. Compounds **(194)** and **(195)** exhibited cytotoxicity against eight cell lines (H1975, U937, K562, BGC823, MOLT-4, MCF-7, HL60, and Huh-7) with the IC_{50} values of < 10 μM respectively (Bao et al., 2014). Deoxybostrycin **(196)** is an anthraquinone compound which was obtained from the marine mangrove fungus *Nigrospora* sp. No. 1403 as shown in **Figure 6**. The *in vitro* cytotoxicity of deoxybostrycin against MDA-MB-435, HepG2, and HCT-116 cancer cell lines were determined with the IC_{50} values of 3.1, 29.9, and 5.6 μM respectively (Chen et al., 2012). Three new alkaloids auranomides A and B **(197**, **198)** and auranomide C **(201)** were isolated from the marine-derived fungus *Penicillium aurantiogriseum* (**Figure 6**). The chemical structures of compounds **(197-199)** were elucidated by using spectroscopic methods such as IR, high-resolution mass spectroscopy and two-dimensional NMR spectroscopy. Auranomides A-C **(197-199)** exhibited moderate cytotoxic activity against K562, ACHN, HEPG2, and A549 cell lines. Auranomide B **(199)** displayed the best activity among them with an IC_{50} value of 0.097 μmol/mL against HEPG2 cells (Song et al., 2012).

AN OVERVIEW OF CYTOTOXICITY RESULTS

As discussed before in different sections in this review article, a total of 199 compounds isolated from marine fungi have

shown considerable promise as cytotoxic agents with potential to be developed as anticancer agents in recent years. About half of these compounds have been known to be isoloated from terrestrial or other natural sources previously but they have been reported to be isolated from the marine soruces for the first time. The Supplementary Table 1 outlines the novelty of these compounds with known previous anticancer acitivities, if any. A number of compounds reported in this review article have shown considerable anticancer activity comparable to positive controls (which are currently used anticancer drugs). Many of these metabolites have displayed inhibitory concentrations in the low micromolar range which obviously mark their potential to be developed as anticancer drugs. However, there is a definite need to improve these inhibitory concentrations since lower dosage would help in eliminating undesired side effects. The exploration in this direction has to be a two pronged approach: one, where the actual cellular targets that lead to cytotoxic effects need to be identified while the other, needs to focus on identifying the structural moieties that are responsible for cytotoxicity. The latter effort would lead to structure-activity based drug design programs to alter chemical functionalities in order to achieve higher efficacy.

Additionally, since several of these metabolites possess structural features (such as compounds **84**, **88**, **116**, **119**, **129**, **131**, **192,** and **196**) that would enable binding to DNA and RNA, cancer targets that involve nucleic acid recognition should be probed. For example, chromosomal DNA ends in humans, which are rich in guanines, have been shown to form a unique four stranded structures called G-quadruplexes. Both *in vitro* and *in vivo* studies have shown the formation of these non-canonical structures which use assembly of four guanines (called G-tetrads), hydrogen bonded in a Hoogsteen fashion (Ranjan et al., 2010). After every cell division, the telomeric DNA gets shortened by certain bases and this process continues until reaching a threshold (called Hayflick limit) where senescence is initiated in a normal cell cycle. However, in the majority of cancer cases, a ribonucleoprotein called telomerase gets activated. The telomerase contains an RNA unit complementary to human telomeric repeat sequence TTAGGG. Binding of this RNA unit of telomerase initiates reverse transcription process to regenerate the curtailed telomere (Camarena et al., 2007; Fakhoury et al., 2007). Many research efforts have, therefore, targeted inhibiting/disrupting telomerase interaction with the telomeric DNA as a means to develop new therapies for cancer treatment (Mergny and Hélène, 1998). One of the ways in which this inhibition can be achieved, is by folding the telomeric ends as stable G-quadruplex structures since telomerase recognizes only the linear form of the telomeric DNA. As a result, small molecules that target these G-quadruplex structures have been tested to see if they could function as inhibitors of telomerase interaction. A number of small molecule inhibitors have been reported that bind to G-quadruplexes and enhance their stability (Xue et al., 2011; Ranjan and Arya, 2013; Ranjan et al., 2013). Such stabilizations are known to disfavor telomerase binding and thereby stopping the telomere regeneration. An important feature of G-quadruplex stabilization by small molecule is making stabilizing interactions with the G-tetrads by means of π-bonding. Some other molecules have shown interactions exclusively with the grooves whereas few have shown interactions both with the tetrads and the grooves. Several of the molecules reported in this review have features that would enable binding both with the G-tetrads and the grooves (for example compound **116**). Furthermore, topoisomerases are enzymes that remove supercoiling in DNA during the replication process and repairs strand breaks (Tse-Dinh, 2009; Pommier, 2013). Human DNA topoisomerase has been an attractive cancer target and anticancer drug camptothecin is known to elicit its effect by forming a ternary complex between the enzyme and the DNA. Some of the molecules reported in this review (e.g., compound **194**) have already shown topoisomerase inhibitory function. Stalling topoisomerase functions by its stabilization with small molecules is another target for anticancer therapy. Since several of these molecules possess structural features that would enable binding to nucleic acids, a screen that targets all forms of nucleic acid structures should be done. This would not only identify the lead compounds for cancer therapy but would also result in identifying the compound that could be of potential use in antibacterial and antiviral therapy.

In addition to this, there are many new discoveries that could have protein targets within the cancer cells. In fact, the majority of FDA approved anticancer drugs target proteins such as cyclin dependent kinases and histone deacytylase. Could these proteins targets be the potential mechanism by which these metabolites induce cytotoxicity? For some of the compounds (**64**, **65**, **168**), Bcl-2 downregulation was established as one factor that led to the apoptosis. Do these metabolites function by upregulation of tumor suppressor proteins such as p53 and Bax? The curiosities can be answered only when all protein targets are screened for binding; at least for the ones whose cellular functioning is fairly understood. This would usher a new beginning in the development of natural product based small molecules and possibly identify structural motifs that target specific regions in the protein binding pockets. Such leads can then be used to launch structure activity relationship programs to improve the potency of these leads whose inhibitory concentrations are mostly in the micromolar range. Overall, the discoveries presented in this review highlights many structural classes including some new skeletons that these metabolites produce, which have potential to be developed as clinically useful anticancer drugs. However, in the absence of more detailed studies that focuses on deciphering the cellular events that lead to cell death, their true potential as an anticancer compound might remain to be under-appreciated.

CONCLUSIONS AND PERSPECTIVES

Marine life has been the source of several clinically useful drugs. The findings covered in this review highlight the discoveries of many new natural small molecules, some of them with novel skeletons, that have anticancer activity against a variety of cancer cell lines. The anticancer activity of these compounds is varied with inhibitory concentrations ranging from low to high micromolar concentrations. Some of these metabolites have

inhibitory concentrations comparable or better than some of the currently used anticancer drugs. Clearly, these leads have not been explored in detail to determine the actual cellular targets that result in the cytotoxicity and that has been an area whose complete exploration may result in a paradigm shift in the current drug discovery efforts. However, other parallel efforts are needed to facilitate and accentuate marine based drug discovery. One such need is setting-up national and international centers for culture collection since many of the new metabolites reported here have been collected from harsh and hostile environments where the human reach is not easily achievable. This would also help not just in retaining these precious cultures but also in allowing wider reach of these metabolites to specialized groups. A major impediment in marine based drug discovery and, in general, natural product based drug discovery has been the lack of centers that foster programs at the interface of chemistry and biology. Clearly, such specialized centers that have expertise both in chemistry and biology could help in realizing true properties of these metabolites. Morever, lack of complete taxonomy details of the new species and bureaucratic difficulties in the implementation of Nagoya protocol hinder smooth access of knowledge and resources. Therefore, international agreements that clearly address these problems and seek solutions to it, could also greatly help in the smooth exchange of resources. Another important improvement in the area would be developing sustainable biochemical production processes of the screening hits as demonstrated in the case of anticancer compounds Scopularide A and B (Yu et al., 2008; Kramer et al., 2014). Additionally, efforts should also be initiated to look beyond anticancer properties of these molecules.

AUTHOR CONTRIBUTIONS

SD, VP, and NR reviewed the contents critically. VP and NR drew chemical structures and assisted in the preparation of Supplementary Table 1. SD and NR wrote the review.

ACKNOWLEDGMENTS

The authors are thankful to Dr. Alok Adholeya, Director, Sustainable Agriculture Division, The Energy and Resources Institute (India) for continuous support.

SUPPLEMENTARY MATERIAL

The Supplementary Material for this article can be found online at: https://www.frontiersin.org/articles/10.3389/fmicb.2017.02536/full#supplementary-material

REFERENCES

Agrawal, S., Adholeya, A., and Deshmukh, S. K. (2016). The pharmacological potential of non-ribosomal peptides from marine sponge and tunicates. *Front. Pharmacol.* 25:333. doi: 10.3389/fphar.2016.00333

Almeida, C., Hemberger, Y., Schmitt, S. M., Bouhired, S., Natesan, L., Kehraus, S., et al. (2012). Marilines A-C: novel phthalimidines from the sponge-derived fungus *Stachylidium* sp. *Chem. Eur. J.* 18, 8827–8834. doi: 10.1002/chem.201103278

Ayyad, S. E., Katoua, D. F., Alarif, W. M., Sobahi, T. R., Aly, M. M., Shaala, L. A., et al. (2015). Two new polyacetylene derivatives from the red sea sponge *Xestospongia* sp. *Z. Naturforsch. C. Bio. Sci.* 70, 297–303. doi: 10.1515/znc-2015-5015

Bao, J., Luo, J. F., Qin, X. C., Xu, X. Y., Zhang, X. Y., Tu, Z. C., et al. (2014). Dihydrothiophene-condensed chromones from a marine-derived fungus *Penicillium oxalicum* and their structure-bioactivity relationship. *Bioorg. Med. Chem. Lett.* 24, 2433–2436. doi: 10.1016/j.bmcl.2014.04.028

Bhadury, P., Mohammad, B. T., and Wright, P. C. (2006). The current status of natural products from marine fungi and their potential as anti-infective agents. *J. Ind. Microbiol. Biotechnol.* 33, 325–337. doi: 10.1007/s10295-005-0070-3

Bugni, T. S., and Ireland, C. M. (2004). Marine-derived fungi: a chemically and biologically diverse group of microorganisms. *Nat. Prod. Rep.* 21, 143–163. doi: 10.1039/B301926H

Butler, M. S., Robertson, A. A., and Cooper, M. A. (2014). Natural product and natural product derived drugs in clinical trials. *Nat. Prod. Rep.* 31, 1612–1661. doi: 10.1039/C4NP00064A

Cardoso-Martinez, F., de la Rosa, J. M., Diaz-Marrero, A. R., Darias, J., D'Croz, L., Cerella, C., et al. (2015). Oximoaspergillimide, a fungal derivative from a marine isolate of *Aspergillus* sp. *Eur. J. Org. Chem.* 10, 2256–2261. doi: 10.1002/ejoc.201403668

Chen, G., Wang, H. F., and Pei, Y. H. (2014). Secondary metabolites from marine-derived microorganisms, *J. Asian. Nat. Prod. Res.* 16, 105–122. doi: 10.1080/10286020.2013.855202

Chen, H., Zhu, X., Zhong, L. L., Yang, B., Li, J., Wu, J. H., et al. (2012). Synthesis and antitumor activities of derivatives of the marine mangrove fungal metabolite deoxybostrycin. *Mar. Drugs* 10, 2715–2728. doi: 10.3390/md10122715

Chen, L., Zhang, W. W., Zheng, Q. H., Liu, Q. Y., Zhong, P., Hu, X., et al. (2013). Aculeatusquinones A-D, novel metabolites from the marine-derived fungus *Aspergillus aculeatus*. *Heterocycles* 87, 861–868. doi: 10.3987/COM-13-12667

Chen, S., Chen, D., Cai, R., Cui, H., Long, Y., Lu, Y., et al. (2016). Cytotoxic and antibacterial preussomerins from the mangrove endophytic fungus *Lasiodiplodia theobromae* ZJ-HQ1. *J. Nat. Prod.* 79, 2397–2402. doi: 10.1021/acs.jnatprod.6b00639

Chen, X. W., Li, C.W., Cui, C. B., Hua, W., Zhu, T. J., and Gu, Q. Q. (2014). Nine new and five known polyketides derived from a deep sea-sourced *Aspergillus* sp., 16-02-1. *Mar. Drugs.* 12, 3116–3137. doi: 10.3390/md12063116

Chokpaiboon, S., Choodej, S., Boonyuen, N., Teerawatananond, T., and Pudhom, K. (2016). Highly oxygenated chromones from mangrove-derived endophytic fungus *Rhytidhysteron rufulum*. *Phytochemistry* 122, 172–177. doi: 10.1016/j.phytochem.2015.12.010

Cui, X., Li, C., Wu, C., and Hua, W. (2013). Metabolites of *Paecilomyces lilacinus* ZBY-1 from deep-sea water and their antitumor activity. *J. Int. Pharm. Res.* 40, 177–186.

Debbab, A., Aly, A. H., Edrada-Ebel, R., Wray, V., Muller, W. E. G., Totzke, F., et al. (2009). Bioactive metabolites from endophytic fungus *Stemphylium globuliferum* isolated from *Mentha pulegium J. Nat. Prod.* 72, 626–631. doi: 10.1021/np8004997

Debbab, A., Aly, A. H., Edrada-Ebel, R., Wray, V., Pretsch, A., Pescitelli, G., et al. (2012). New anthracene derivatives – structure elucidation and antimicrobial activity. *Eur. J. Org. Chem.* 2012, 1351–1359. doi: 10.1002/ejoc.201101442

Deng, C., Huang, C., Wu, Q., Pang, J., and Lin, Y. (2013). A new sesquiterpene from the mangrove endophytic fungus *Aspergillus terreus* (No. GX7-3B). *Nat. Prod. Res.* 27, 1882–1887. doi: 10.1080/14786419.2013.778847

Deng, C. M., Liu, S. X., Huang, C. H., Pang, J. Y., and Lin, Y. C. (2013). Secondary metabolites of a mangrove endophytic fungus *Aspergillus terreus* (No. GX7-3B) from the South China Sea. *Mar. Drugs.* 11, 2616–2624. doi: 10.3390/md11072616

Deshmukh, S. K., Prakash, V., and Ranjan, N. (2017). Recent advances in the discovery of bioactive metabolites from *Pestalotiopsis*. *Phytochem. Rev.* 16, 883–920. doi: 10.1007/s11101-017-9495-3

Dong, Y., Cui, C. B., Li, C. W., Hua, W., Wu, C., Zhu, T. J., et al. (2014). Activation of dormant secondary metabolite production by introducing

neomycin resistance into the deep-sea fungus *Aspergillus versicolor* ZBY-3. *Mar. Drugs* 12, 4326–4352. doi: 10.3390/md12084326

Du, X. P., and Su, W. J. (2014). Two new polyketides from mangrove endophytic fungus *Dothiorella* sp. *Chem. Nat. Compd.* 50, 214–216. doi: 10.1007/s10600-014-0915-y

Eamvijarn, A., Gomes, N. M., Dethoup, T., Buaruang, J., Manoch, L., Silva, A., et al. (2013). Bioactive meroditerpenes and indole alkaloids from the soil fungus *Neosartorya fischeri* (KUFC 6344), and the marine-derived fungi *Neosartorya laciniosa* (KUFC 7896) and *Neosartorya tsunodae* (KUFC 9213). *Tetrahedron* 69, 8583–8591. doi: 10.1016/j.tet.2013.07.078

Ebrahim, W., Kjer, J., El Amrani, M., Wray, V., Lin, W., Ebel, R., et al. (2012). Pullularins E and F, two new peptides from the endophytic fungus *Bionectria ochroleuca* isolated from the mangrove plant *Sonneratia caseolaris*. *Mar. Drugs* 10, 1081–1091. doi: 10.3390/md10051081

Fakhoury, J., Nimmo, G. A., and Autexier, C. (2007). Harnessing telomerase in cancer therapeutics. *Anti Cancer Agents Med. Chem.* 7, 475–483. doi: 10.2174/187152007781058622

Fang, W., Lin, X., Zhou, X., Wan, J., Lu, X., Yang, B., et al. (2014). Cytotoxic and antiviral nitrobenzoyl sesquiterpenoids from the marine-derived fungus *Aspergillus ochraceus* Jcma1F17, *Med.Chem.Comm*. 5, 701–705. doi: 10.1039/c3md00371j

Fredimoses, M., Zhou, X., Ai, W., Tian, X., Yang, B., Lin, X., et al. (2015). Westerdijkin A, a new hydroxyphenylacetic acid derivative from deep sea fungus *Aspergillus westerdijkiae* SCSIO 05233. *Nat. Prod. Res.* 29, 158–162. doi: 10.1080/14786419.2014.968154

Gao, H., Zhou, L., Cai, S., Zhang, G., Zhu, T., Gu, Q., et al. (2013b). Diorcinols B-E, new prenylated diphenyl ethers from the marine-derived fungus *Aspergillus versicolor* ZLN-60, *J. Antibiot.* 66(9), 539–542. doi: 10.1038/ja.2013.40

Gao, H., Zhou, L., Li, D., Gu, Q., and Zhu, T. J. (2013a). New cytotoxic metabolites from the marine-derived fungus *Penicillium* sp. ZLN29. *Helv. Chim. Acta* 96, 514–519. doi: 10.1002/hlca.201200596

Gao, S. S., Li, X. M., Williams, K., Proksch, P., Ji, N. Y., and Wang, B. G. (2016b). Rhizovarins A-F, indole-diterpenes from the mangrove-derived endophytic fungus *Mucor irregularis* QEN-189, *J. Nat. Prod.* 79, 2066–2074. doi: 10.1021/acs.jnatprod.6b00403

Gao, X. W., Liu, H. X., Sun, Z. H., Chen, Y. C., Tan, Y. Z., and Zhang, W. M. (2016a). Secondary metabolites from the deep-sea derived fungus *Acaromyces ingoldii* FS121. *Molecules* 21, 371/1–371/7. doi: 10.3390/molecules21040371

Gomes, N. G., Lefranc, F., Kijjoa, A., and Kiss, R. (2015). Can some marine-derived fungal metabolites become actual anticancer agents? *Mar. Drugs* 13, 3950–3991. doi: 10.3390/md13063950

Guo, L., Huang, T., Hu, B., and Wang, C. (2016). Bioactivity-guided isolation and characterization of antitumor active compound from marine-derived fungus *Penicillium chrysogenum* HGQ6. *Adv. J. Food. Sci. Technol.* 10, 353–355. doi: 10.19026/ajfst.10.2081

Hammerschmidt, L., Debbab, A., Ngoc, T. D., Wray, V., Hemphil, C. P., Lin, W. H., et al. (2014). Polyketides from the mangrove-derived endophytic fungus *Acremonium strictum*. *Tetrahedron Lett.* 55, 3463–3468. doi: 10.1016/j.tetlet.2014.04.063

He, F., Bao, J., Zhang, X. Y., Tu, Z. C., Shi, Y. M., and Qi, S. H. (2013). Asperterrestide A, a Cytotoxic Cyclic Tetrapeptide from the marine-derived fungus *Aspergillus terreus* SCSGAF0162. *J. Nat. Prod.* 76, 1182–1186. doi: 10.1021/np300897v

He, F., Sun, Y. L., Liu, K. S., Zhang, X. Y., Qian, P. Y., Wang, Y. F., et al. (2012). Indole alkaloids from marine-derived fungus *Aspergillus sydowii* SCSIO 00305, *J. Antibiot.* 65, 109–111. doi: 10.1038/ja.2011.117

Hua, W., Chen, X., and Cui, X. (2011). "Preliminary study of deep-sea fungi and their bioactive secondary metabolites," in *Proceedings of the Eleventh National Symposia of Chinese Medicine and Natural Products* (Shenyang), 46.

Huang, H., Wang, F., Luo, M., Chen, Y., Song, Y., Zhang, W., et al. (2012). Halogenated anthraquinones from the marine-derived fungus *Aspergillus* sp. SCSIO F063. *J. Nat. Prod.* 75, 1346–1352. doi: 10.1021/np3002699

Huang, J., Xu, J., Wang, Z., Khan, D., Niaz, S. I., Zhu, Y., et al. (2017). New lasiodiplodins from mangrove endophytic fungus *Lasiodiplodia* sp. 318. *Nat. Prod. Res.* 31, 326–332. doi: 10.1080/14786419.2016.1239096

Huang, Z., Yang, J., Cai, X., She, Z., and Lin, Y. (2012). A new furanocoumarin from the mangrove endophytic fungus *Penicillium* sp. ZH16. *Nat. Prod. Res.* 26, 1291–1295. doi: 10.1080/14786419.2011.569502

Huang, Z., Yang, J., Lei, F., She, Z., and Lin, Y. (2013). A new xanthone O-glycoside from the mangrove endophytic fungus *Phomopsis* sp. *Chem. Nat. Compd.* 49, 27–30. doi: 10.1007/s10600-013-0497-0

Imhoff, J. F. (2016). Natural products from marine fungi-still an underrepresented resource. *Mar. Drugs* 14:19. doi: 10.3390/md14010019

Jans, P. E., Mfuh, A. M., Arman, H. D., Shaffer, C. V., Larionov, O. V., and Mooberry, S. L. (2017). Cytotoxicity and mechanism of action of the marine-derived fungal metabolite trichodermamide B and synthetic analogues. *J. Nat. Prod.* 80, 676–683. doi: 10.1021/acs.jnatprod.6b00963

Javed, F., Qadir, M. I., Janbaz, K. H., and Ali, M. (2011). Novel drugs from marine microorganisms. *Crit. Rev. Microbiol.* 37, 245–249. doi: 10.3109/1040841X.2011.576234

König, G. M., Kehraus, S., Seibert, S. F., Abdel-Lateff, A., and Müller, D. (2006). Natural products from marine organisms and their associated microbes. *Chembiochem* 7, 229–238. doi: 10.1002/cbic.200500087

Kramer, A., Paun, L., Imhoff, J. F., Kempken, F., and Labes, A. (2014). Development and validation of a fast and optimized screening method for enhanced production of secondary metabolites using the marine *Scopulariopsis brevicaulis* strain LF580 producing anti-cancer active scopularide A and B. *PLoS ONE* 9:e103320. doi: 10.1371/journal.pone.0103320

Li, C. S., Li, X. M., Gao, S. S., Lu, Y. H., and Wang, B. G. (2013). Cytotoxic anthranilic acid derivatives from deep sea sediment-derived fungus *Penicillium paneum* SD-44, *Mar. Drugs* 11, 3068–3076. doi: 10.3390/md11083068

Li, C.-W., Xia, M. W., Cui, C. B., Peng, J. X., and Li, D. H. (2016). A novel oxaphenalenone, penicimutalidine: activated production of oxaphenalenones by the diethyl sulphate mutagenesis of marine-derived fungus *Penicillium purpurogenum* G59. *RSC Adv.* 6, 82277–82281. doi: 10.1039/C6RA 17087K

Li, H.-J., Jiang, W. H., Liang, W. L., Huang, J. X., Mo, Y. F., Ding, Y. Q., et al. (2014). Induced marine fungus *Chondrostereum* sp. as a means of producing new sesquiterpenoids chondrosterins I and J by using glycerol as the carbon source. *Mar. Drugs.* 12, 167–175. doi: 10.3390/md12010167

Li, J., Xue, Y., Yuan, J., Lu, Y., Zhu, X., Lin, Y., et al. (2016). Lasiodiplodins from mangrove endophytic fungus *Lasiodiplodia* sp., 318#. *Nat. Prod. Res.* 30, 755–760. doi: 10.1080/14786419.2015.1062762

Li, J., Yang, X., Lin, Y., Yuan, J., Lu, Y., Zhu, X., et al. (2014). Meroterpenes and azaphilones from marine mangrove endophytic fungus *Penicillium 303 #*. *Fitoterapia* 97, 241–246. doi: 10.1016/j.fitote.2014.06.011

Li, P., Fan, Y., Chen, H., Chao, Y., Du, N., and Chen, J. (2016). Phenylquinolinones with antitumor activity from the Indian ocean-derived fungus *Aspergillus versicolor* Y31-2. *Chinese J. Oceanol. Limnol.* 34, 1072–1075. doi: 10.1007/s00343-016-5097-y

Li, X., Li, X. M., Li, X. D., Xu, G. M., Liu, Y., and Wang, B. G. (2016). 20-Nor-isopimarane cycloethers from the deep-sea sediment-derived fungus *Aspergillus wentii* SD-310. *RSC Adv.* 6, 75981–75987. doi: 10.1039/C6RA17638K

Li, X.-D., Li, X., Li, X. M., Xu, G. M., Zhang, P., Meng, L. H., et al. (2016). Tetranorlabdane diterpenoids from the deep sea sediment-derived fungus *Aspergillus wentii* SD-310. *Planta Med.* 82, 877–881. doi: 10.1055/s-0042-102965

Li, Y., Ye, D., Shao, Z., Cui, C., and Che, Y. (2012). A sterol and spiroditerpenoids from a *Penicillium* sp. isolated from a deep sea sediment sample. *Mar. Drugs.* 10, 497–508. doi: 10.3390/md10020497

Li, Y.-X., Himaya, S. W. A., Dewapriya, P., Kim, H. J., and Kim, S. K. (2014). Anti-proliferative effects of isosclerone isolated from marine fungus *Aspergillus fumigatus* in MCF-7 human breast cancer cells. *Process. Biochem.* 49, 2292–2298. doi: 10.1016/j.procbio.2014.08.016

Liang, X., Zhang, X. Y., Nong, X. H., Wang, J., Huang, Z. H., and Qi, S. H. (2016). Eight linear peptides from the deep-sea-derived fungus *Simplicillium obclavatum* EIODSF 020. *Tetrahedron* 72, 3092–3097. doi: 10.1016/j.tet.2016.04.032

Lin, A., Wu, G., Gu, Q., Zhu, T., and Li, D. (2014). New eremophilane-type sesquiterpenes from an Antarctic deep-sea derived fungus *Penicillium* sp. PR19 N-1. *Arch. Pharm. Res.* 37, 839–844. doi: 10.1007/s12272-013-0246-8

Liu, D., Li, X. M., Li, C. S., and Wang, B. G. (2013). Nigerasterols A and B, antiproliferative sterols from the mangrove-derived endophytic fungus *Aspergillus niger* MA-132. *Helv. Chim. Acta* 96, 1055–1061. doi: 10.1002/hlca.201200332

Liu, H., Zhang, L., Chen, Y., Li, S., Tan, G., Sun, Z., et al. (2017). Cytotoxic pimarane-type diterpenes from the marine sediment-derived fungus *Eutypella* sp. FS46. *Nat. Prod. Res.* 31, 404–410, doi: 10.1080/14786419.2016.1169418

Liu, Q. Y., Zhou, T., Zhao, Y. Y., Chen, L., Gong, M. W., Xia, Q. W., et al. (2015). Antitumor effects and related mechanisms of penicitrinine A, a novel alkaloid with a unique spiro skeleton from the marine fungus *Penicillium citrinum*. *Mar. Drugs* 13, 4733–4753. doi: 10.3390/md13084733

Liu, S., Dai, H., Makhloufi, G., Heering, C., Janiak, C., Hartmann, R., et al. (2016). Cytotoxic 14-membered macrolides from a mangrove-derived endophytic fungus *Pestalotiopsis microspore*. *J. Nat. Prod.* 79, 2332–2340. doi: 10.1021/acs.jnatprod.6b00473

Liu, Y., Marmann, A., Abdel-Aziz, M. S., Wang, C. Y., Müller, W. E. G., Lin, W. H., et al. (2015). Tetrahydroanthraquinone derivatives from the endophytic fungus *Stemphylium globuliferum*. *Eur. J. Org. Chem.* 2015, 2646–2653. doi: 10.1002/ejoc.201500079

Liu, Y., Zhao, S., Ding, W., Wang, P., Yang, X., and Xu, J. (2014). Methylthioaspochalasins from a marine-derived fungus *Aspergillus* sp. *Mar. Drugs.* 12, 5124–5131. doi: 10.3390/md12105124

Lv, C., Hong, Y., Miao, L., Li, C., Xu, G., Wei, S., et al. (2013). Wentilactone A as a novel potential antitumor agent induces apoptosis and G2/M arrest of human lung carcinoma cells, and is mediated by HRas-GTP accumulation to excessively activate the Ras/Raf/ERK/p53-p21 pathway. *Cell Death Dis.* 4:e952. doi: 10.1038/cddis.2013.484

Mahé, S., Rédou, V., Calvez, T. L., Vandenkoornhuyse, P., and Burgaud, G. (2013). "Fungi in deep-sea environments and metagenomics," in The *Ecological Genomics of Fungi*, ed F. Martin (Hoboken, NJ: John Wiley & Sons Inc.), 325–354.

Meng, L. H., Wang, C. Y., Mandi, A., Li, X. M., Hu, X. Y., Kassack, M. U., et al. (2016). Three diketopiperazine alkaloids with spirocyclic skeletons and one bisthiodiketopiperazine derivative from the mangrove-derived endophytic fungus *Penicillium brocae* MA-231. *Org. Lett.* 18, 5304–5307. doi: 10.1021/acs.orglett.6b02620

Mergny, J. L., and Hélène, C. (1998). G-quadruplex DNA: a target for drug design. *Nat. Med.* 4, 1366–1367. doi: 10.1038/3949

Mishra, P. D., Verekar, S. A., Deshmukh, S. K., Joshi, K. S., Fiebig, H. H., and Kelter, G. (2015). Altersolanol A: a selective cytotoxic anthraquinone from a *Phomopsis* sp. *Lett. Appl. Microbiol.* 60, 387–391. doi: 10.1111/lam.12384

Molinski, T. F., Dalisay, D. S., Lievens, S. L., and Saludes, J. P. (2009). Drug development from marine natural products. *Nat. Rev. Drug Disc.* 8:69. doi: 10.1038/nrd2487

Moussa, M., Ebrahim, W., El-Neketi, M., Mandi, A., Kurtan, T., Hartmann, R., et al. (2016). Tetrahydroanthraquinone derivatives from the mangrove-derived endophytic fungus *Stemphylium globuliferum*. *Tetrahedron Lett.* 57, 4074–4078. doi: 10.1016/j.tetlet.2016.07.091

Passaes C. P., and Sáez-Cirión, A. (2014). HIV cure research: advances and prospects. *Virology* 454–455, 340–352. doi: 10.1016/j.virol.2014.02.021

Pejin, B., and Maja, K. (2017). "Antitumor natural products of marine-derived fungi," in *Fungal Metab*, eds J. M. Mérillon and K. G. Ramawat (Springer International Publishing), 1–28. doi: 10.1007/978-3-319-19456-1_25-1

Peng, J., Zhang, X. Y., Tu, Z. C., Xu, X. Y., and Qi, S. H. (2013). Alkaloids from the deep-sea-derived fungus *Aspergillus westerdijkiae* DFFSCS013. *J. Nat. Prod.* 76, 983–987. doi: 10.1021/np400132m

Perez, H. C. F., Daletos, G., Liu, Z., Lin, W., and Proksch, P. (2016). Polyketides from the mangrove-derived fungal endophyte *Pestalotiopsis clavispora*. *Tetrahedron Lett.* 57, 2078–2083. doi: 10.1016/j.tetlet.2016.03.101

Pommier, Y. (2013). Drugging topoisomerases: lessons and challenges. *ACS Chem. Biol.* 8, 82–95. doi: 10.1021/cb300648v

Ranjan, N., and Arya, D. P. (2013). Targeting C-myc G-quadruplex: dual recognition by aminosugar-bisbenzimidazoles with varying linker lengths. *Molecules* 18, 14228–40. doi: 10.3390/molecules181114228

Ranjan, N., Andreasen, K. F., Kumar, S., Hyde-Volpe, D., and Arya, D. P. (2010). Aminoglycoside binding to oxytricha nova telomeric DNA. *Biochemistry* 49, 9891–9903. doi: 10.1021/bi101517e

Ranjan, N., Davis, E., Xue, L., and Arya, D. P. (2013). Dual recognition of the human telomeric G-quadruplex by a neomycin-anthraquinone conjugate. *Chem. Commun.* 49, 5796–5798. doi: 10.1039/C3CC42721H

Saleem, M., Ali, M. S., Hussain, S., Jabbar, A., Ashraf, M., and Lee, Y. S. (2007). Marine natural products of fungal origin. *Nat. Prod. Rep.* 24, 1142–1152. doi: 10.1039/b607254m

Sampedro Camarena, F., Cano Serral, G., and Sampedro Santaló, F. (2007). Telomerase and telomere dynamics in ageing and cancer: current status and future directions. *Clin. Transl. Oncol.* 9, 145–154. doi: 10.1007/s12094-007-0028-1

Saraiva, N. N., Rodrigues, B. S., Jimenez, P. C., Guimarães, L. A., Torres, M. C. M., Rodrigues-Filho, E., et al. (2015). Cytotoxic compounds from the marine-derived fungus *Aspergillus* sp. recovered from the sediments of the Brazilian coast. *Nat. Prod. Res.* 29, 1545–1550. doi: 10.1080/14786419.2014.987772

Shang, Z., Li, L., Espósito, B. P., Salim, A. A., Khalil, Z. G., Quezada, M., et al. (2015). New PKS-NRPS tetramic acids and pyridinone from an Australian marine-derived fungus *Chaunopycnis* sp. *Org. Biomol. Chem.* 13, 7795–7802. doi: 10.1039/C5OB01058F

Shang, Z., Li, X. M., Li, C. S., and Wang, B. G. (2012b). Diverse secondary metabolites produced by marine-derived fungus *Nigrospora* sp. MA75 on various vulture media. *Chem. Biodivers.* 9, 1338–1348. doi: 10.1002/cbdv.201100216

Shang, Z., Li, X., Meng, L., Li, C., Gao, S., Huang, C., et al. (2012a). Chemical profile of the secondary metabolites produced by a deep-sea sediment-derived fungus *Penicillium commune* SD-118. *Chin. J. Oceanol. Limnol.* 30, 305–314. doi: 10.1007/s00343-012-1075-1

Singh, R., Sharma, M., Joshi, P., and Rawat, D. S. (2008). Clinical status of anti-cancer agents derived from marine sources. *Anti Cancer Agents Med. Chem.* 8, 603–617. doi: 10.2174/187152061080606O3

Sithranga, N. B., and Kathiresan, K. (2011). Anticancer drugs from marine flora: an overview. *J. Oncol.* 2010:18. doi: 10.1155/2010/214186

Song, F., Ren, B., Yu, K., Chen, C., Guo, H., Yang, N., et al. (2012). Quinazolin-4-one coupled with pyrrolidin-2-iminium alkaloids from marine-derived fungus *Penicillium aurantiogriseum*. *Mar. Drugs.* 10, 1297–1306. doi: 10.3390/md10061297

Sun, H.-F., Li, X. M., Meng, L., Cui, C. M., Gao, S. S., Li, C. S., et al. (2012). Asperolides A-C, tetranorlabdene diterpenoids from the marine alga-derived endophytic fungus *Aspergillus wentii* EN-48. *J. Nat. Prod.* 75, 148–152. doi: 10.1021/np2006742

Sun, L., Li, D., Tao, M., Chem, Y., Dan, F., and Zhang, W. (2012). Scopararanes C-G: new oxygenated pimarane diterpenes from the marine sediment-derived fungus *Eutypella scoparia* FS26. *Mar. Drugs* 10, 539–550. doi: 10.3390/md10030539

Sun, L.-L., Shao, C. L., Chen, J. F., Guo, Z. Y., Fu, X. M., Chen, M., et al. (2012). New bisabolane sesquiterpenoids from a marine-derived fungus *Aspergillus* sp. isolated from the sponge Xestospongia testudinaria. *Bioorg. Med. Chem. Lett.* 22, 1326–1329. doi: 10.1016/j.bmcl.2011.12.083

Sun, Y. L., Bao, J., Liu, K. S., Zhang, X. Y., He, F., Wang, Y. F., et al. (2013). Cytotoxic dihydrothiophene-condensed chromones from the marine-derived fungus *Penicillium oxalicum*. *Planta Med.* 79, 1474–1479. doi: 10.1055/s-0033-1350805

Swathi, J., Narendra, K., Sowjanya, K. M., and Satya, A. K. (2013). Evaluation of biologically active molecules isolated from obligate marine fungi. *Mintage J. Pharm. Med. Sci.* 2, 45–47.

Tan, Q. W., Ouyang, M. A., Shen, S., and Li, W. (2012). Bioactive metabolites from a marine-derived strain of the fungus *Neosartorya fischeri*. *Nat. Prod. Res.* 26, 1402–1407. doi: 10.1080/14786419.2011.592834

Tao, Y. W., Lin, Y. C., She, Z. G., Lin, M. T., Chen, P. X., and Zhang, J. Y. (2015). Anticancer activity and mechanism investigation of beauvericin isolated from secondary metabolites of the mangrove endophytic fungi. *Anticancer. Agents. Med. Chem.* 15, 258–266. doi: 10.2174/1871520614666140825112255

Teiten, M. H., Mack, F., Debbab, A., Aly, A. H., Dicato, M., Proksch, P., et al. (2013). Anticancer effect of altersolanol A, a metabolite produced by the endophytic fungus *Stemphylium globuliferum*, mediated by its proapoptotic and anti-invasive potential via the inhibition of NF-κB activity. *Bioorg. Med. Chem.* 21, 3850–3858. doi: 10.1016/j.bmc.2013.04.024

Tse-Dinh, Y. (2009). Bacterial topoisomerase I as a target for discovery of antibacterial compounds. *Nucleic Acids Res.* 37, 731–737. doi: 10.1093/nar/gkn936

Wang, F. Z., Huang, Z., Shi, X. F., Chen, Y. C., Zhang, W. M., Tian, X. P., et al. (2012). Cytotoxic indole diketopiperazines from the deep sea-derived fungus

Acrostalagmus luteoalbus SCSIO F457. *Bioorg. Med. Chem. Lett.* 22, 7265–7267. doi: 10.1016/j.bmcl.2012.08.115

Wang, J., Wang, Z., Ju, Z., Wan, J., Liao, S., Lin, X., et al. (2015). Cytotoxic cytochalasins from marine-derived fungus *Arthrinium arundinis*. *Planta Med.* 81, 160–166. doi: 10.1055/s-0034-1383403

Wang, N., Cui, C. B., and Li, C. W. (2016). A new cyclic dipeptide penicimutide: the activated production of cyclic dipeptides by introduction of neomycin-resistance in the marine-derived fungus *Penicillium purpurogenum* G59. *Arch. Pharm. Res.* 39, 762–770. doi: 10.1007/s12272-016-0751-7

Wang, W.-J., Li, D. Y., Li, Y. C., Hua, H. M., Ma, E. L., and Li, Z. L. (2014). Caryophyllene sesquiterpenes from the marine-derived fungus *Ascotricha* sp. ZJ-M-5 by the one strain-many compounds strategy. *J. Nat. Prod.* 77, 1367–1371. doi: 10.1021/np500110z

Wang, Y., Qi, X., Li, D., Zhu, T., Mo, X., and Li, J. (2014). Anticancer efficacy and absorption, distribution, metabolism, and toxicity studies of Aspergiolide A in early drug development. *Drug Design Develop. Ther.* 8, 1965–1977. doi: 10.2147/DDDT.S64989

Wijesekara, I., Li, Y. X., Vo, T. S., Van Ta, Q., Ngo, D. H., and Kim, S. K. (2013). Induction of apoptosis in human cervical carcinoma HeLa cells by neoechinulin A from marine-derived fungus *Microsporum* sp. *Process. Biochem.* 48, 68–72. doi: 10.1016/j.procbio.2012.11.012

Wijesekara, I., Zhang, C., Van Ta, Q., Vo, T. S., Li, Y. X., and Kim, S. K. (2014). Physcion from marine-derived fungus *Microsporum* sp. induces apoptosis in human cervical carcinoma HeLa cells. *Microbiol. Res.* 169, 255–261. doi: 10.1016/j.micres.2013.09.001

Wu, B., Chen, G., Liu, Z. G., and Pei, Y. (2015). Two new alkaloids from a marine-derived fungus *Neosartorya fischeri*. *Rec. Nat. Prod.* 9, 271–275.

Wu, B., Wiese, J., Wenzel-Storjohann, A., Malien, S., Schmaljohann, R., and Imhoff, J. F. (2016). Engyodontochones, antibiotic polyketides from the marine fungus *Engyodontium album* strain LF069. *Chemistry* 22, 7452–7462. doi: 10.1002/chem.201600430

Wu, G., Lin, A., Gu, Q., Zhu, T., and Li, D. (2013). Four new chloro-eremophilane sesquiterpenes from an Antarctic deep-sea derived fungus *Penicillium* sp. PR19N-1. *Mar. Drugs* 11, 1399–1408. doi: 10.3390/md11041399

Xia, M. W., Cui, C. B., Li, C. W., Wu, C. J., Peng, J. X., and Li, D. H. (2015). Rare Chromones from a fungal mutant of the marine-derived *Penicillium purpurogenum* G59. *Mar. Drugs* 13, 5219–5236. doi: 10.3390/md13085219

Xia, X., Zhang, J., Zhang, Y., Wie, F., Liu, X., Jia, A., et al. (2012). Pimarane diterpenes from the fungus *Epicoccum* sp. HS-1 associated with *Apostichopus japonicus*. *Bioorg. Med. Chem. Lett.* 22, 3017–3019. doi: 10.3390/md13031124

Xu, R., Xu, G. M., Li, X. M., Li, C. S., and Wang, B. G. (2015). Characterization of a newly isolated marine fungus *Aspergillus dimorphicus* for optimized production of the anti-tumor agent wentilactones. *Mar. Drugs.* 13, 7040–7054. doi: 10.3390/md13117040

Xue, L., Ranjan, N., and Arya, D. P. (2011). Synthesis and spectroscopic studies of the aminoglycoside (neomycin) perylene conjugate binding to human telomeric DNA. *Biochemistry* 50, 2838–2849. doi: 10.1021/bi1017304

Yang, J. X., Qiu, S. X., She, Z. G., and Lin, Y. C. (2013b). Metabolites of mangrove endophytic fungus Gx-3a from the south China sea. *Guangxi Kexue* 20, 168–170.

Yang, J. X., Qiu, S. X., She, Z. G., and Lin, Y. C. (2013a). Metabolites of mangrove endophytic fungus 5094 from the south china sea. *Shizhen Guoyi Guoyao* 24, 1059–1061. doi: 10.3969/j.issn.1008-0805.2013.05.014

Yang, J. X., Qiu, S. X., She, Z. G., and Lin, Y. C. (2013c). A new xanthone derivative from the marine fungus *Phomopsis* sp. (No. SK7RN3G1). *Chem. Nat. Compd.* 49, 246–248. doi: 10.1007/s10600-013-0572-6

Yang, J., Huang, R., Qiu, S. X., She, Z. G., and Lin, Y. C. (2013). A new isobenzofuranone from the mangrove endophytic fungus *Penicillium* sp. (ZH58). *Nat. Prod. Res.* 27, 1902–1905. doi: 10.1080/14786419.2013.784870

Yao, Q., Wang, J., Zhang, X., Nong, X., Xu, X., and Qi, S. (2014). Cytotoxic polyketides from the deep-sea-derived fungus *Engyodontium album* DFFSCS021. *Mar. Drugs* 12, 5902–5915. doi: 10.3390/md12125902

Yi, L., Cui, C. B., Li, C. W., Peng, J. X., and Gu, Q. Q. (2016). Chromosulfine, a novel cyclopentachromone sulfide produced by a marine-derived fungus after introduction of neomycin resistance. *RSC Advances* 6, 43975–43979. doi: 10.1039/C6RA06250D

Yu, Z., Lang, G., Kajahn, I., Schmaljohann, R., and Imhoff, J. F. (2008). Scopularides A and B, cyclodepsipeptides from a marine sponge-derived fungus, *Scopulariopsis brevicaulis*. *J. Nat. Prod.* 71, 1052–1054. doi: 10.1021/np070580e

Zeng, Y. B., Gu, H. G., Zuo, W. J., Zhang, L. L., Bai, H. J., Guo, Z. K., et al. (2015). Two new sesquiterpenoids from endophytic fungus J3 isolated from mangrove plant *Ceriops tagal*. *Arch. Pharm. Res.* 38, 673–676. doi: 10.1007/s12272-014-0448-8

Zhang, P., Li, X. M., Mao, X. X., Mandi, A., Kurtan, T., and Wang, B. G. (2016). Varioloid A, a new indolyl-6,10b-dihydro-5aH-[1]benzofuro[2,3-b]indole derivative from the marine alga-derived endophytic fungus *Paecilomyces variotii* EN-291. *Beilstein J. Org. Chem.* 12, 2012–2018. doi: 10.3762/bjoc.12.188

Zhang, Z., Miao, L., Lv, C., Sun, H., Wei, S., Wang, B., et al. (2013). Wentilactone B induces G2/M phase arrest and apoptosis via the Ras/Raf/MAPK signaling pathway in human hepatoma SMMC-7721 cells. *Cell Death Dis.* 4:e657. doi: 10.1038/cddis.2013.182

Zhao, Y., Chen, H., Shang, Z., Jiao, B., Yuan, B., Sun, W., et al. (2012). SD118-xanthocillin X (1), a novel marine agent extracted from *Penicillium commune*, induces autophagy through the inhibition of the MEK/ERK pathway. *Mar. Drugs* 10, 1345–1359. doi: 10.3390/md10061345

Zheng, C., Chen, Y., Jiang, L. L., and Shi, X. M. (2014). Antiproliferative metabolites from the endophytic fungus *Penicillium* sp. FJ-1 isolated from a mangrove *Avicennia marina*. *Phytochem. Lett.* 10, 272–275. doi: 10.1016/j.phytol.2014.10.011

Zhou, S. L., Wang, M., Zhao, H. G., Huang, Y. H., Lin, Y. Y., Tan, G. H., et al. (2016). Penicilazaphilone C, a new antineoplastic and antibacterial azaphilone from the marine fungus *Penicillium sclerotiorum*. *Arch. Pharm. Res.* 39, 1621–1627. doi: 10.1007/s12272-016-0828-3

Zhu, M., Zhang, X., Feng, H., Che, Q., Zhu, T., Gu, Q., et al. (2016). Campyridones A-D, pyridone alkaloids from a mangrove endophytic fungus *Campylocarpon* sp. HDN13-307. *Tetrahedron* 72, 5679–5683. doi: 10.1016/j.tet.2016.07.080

Zhuravleva, O. I., Afiyatullov, S. S. H., Vishchuk, O. S., Denisenko, V. A., Slinkina, N. N., and Smetanina, O. F. (2012). Decumbenone C, a new cytotoxic decaline derivative from the marine fungus *Aspergillus sulphureus* KMM 4640. *Arch. Pharm. Res.* 35, 1757–1762. doi: 10.1007/s12272-012-1007-9

Conflict of Interest Statement: The authors declare that the research was conducted in the absence of any commercial or financial relationships that could be construed as a potential conflict of interest.

Copyright © 2018 Deshmukh, Prakash and Ranjan. This is an open-access article distributed under the terms of the Creative Commons Attribution License (CC BY). The use, distribution or reproduction in other forums is permitted, provided the original author(s) or licensor are credited and that the original publication in this journal is cited, in accordance with accepted academic practice. No use, distribution or reproduction is permitted which does not comply with these terms.

Advantages of publishing in Frontiers

OPEN ACCESS
Articles are free to read for greatest visibility and readership

FAST PUBLICATION
Around 90 days from submission to decision

HIGH QUALITY PEER-REVIEW
Rigorous, collaborative, and constructive peer-review

TRANSPARENT PEER-REVIEW
Editors and reviewers acknowledged by name on published articles

Frontiers
Avenue du Tribunal-Fédéral 34
1005 Lausanne | Switzerland

Visit us: www.frontiersin.org
Contact us: info@frontiersin.org | +41 21 510 17 00

REPRODUCIBILITY OF RESEARCH
Support open data and methods to enhance research reproducibility

DIGITAL PUBLISHING
Articles designed for optimal readership across devices

FOLLOW US
@frontiersin

IMPACT METRICS
Advanced article metrics track visibility across digital media

EXTENSIVE PROMOTION
Marketing and promotion of impactful research

LOOP RESEARCH NETWORK
Our network increases your article's readership